NUREG/CR-3332
ORNL-5968

Radiological Assessment

A Textbook on Environmental Dose Analysis

Date Published: September 1983

Edited by

John E. Till
Radiological Assessments Corporation
Neeses, South Carolina

and

H. Robert Meyer
Health and Safety Research Division
Oak Ridge National Laboratory
Oak Ridge, Tennessee

Prepared for
Division of Systems Integration
Office of Nuclear Reactor Regulation
U.S. Nuclear Regulatory Commission
Washington, D.C. 20555
NRC FIN B0766

This document was prepared under U.S. Nuclear Regulatory Commission (NRC) Contract No. B-0766. The opinions, findings, conclusions, and recommendations expressed herein are those of the authors and do not necessarily reflect the views of the NRC. The technical contents do not necessarily represent methods and procedures acceptable to the NRC staff for demonstrating compliance with rules, regulations, and staff positions.

Available as NUREG/CR-3332 from
The Superintendent of Documents
U.S. Government Printing Office
P.O. Box 37082
Washington, DC 20013-7082

and

National Technical Information Service
5285 Port Royal Road
Springfield, VA 22161

Printed in the United States of America

September 1983

Contents

Foreword

By S. V. KAYE*

It has often been said that we know more about radiation than any other pollutant known to man. We are at this vantage point now because of an early concern for radiation protection when nuclear programs were developing at U.S. Government and university laboratories. Indeed, the protection of man and his environment from the harmful effects of ionizing radiation came to be known as the field of health physics and benefited from considerable previous experience in medical physics and a vigorous program in radiation biology. To properly appreciate where we are now in our ability to assess radionuclide releases, it is necessary to trace the path of development.

Assessment of radionuclide releases to the environment was first required on a somewhat large scale in the 1940s for the environs of the major nuclear research and production facilities operated for the Federal Government; measurement and assessment of worldwide fallout from nuclear testing required a large effort starting in the 1950s. This early work placed much emphasis on environmental measurements, which frequently were reported as gross beta-gamma or gross alpha because spectrometry systems had not yet reached full versatility. Investigators were usually not able to calculate radionuclide-specific doses because of this restriction, so the early "assessments" were more typically "monitoring" than assessments.

The United States initiated the Plowshare Program in 1957 to use nuclear explosives for peaceful purposes. This program created an immediate need for predicting the dispersion and ultimate fate of radionuclides that might be vented to the atmosphere or enter the groundwater and expose man. Experience from previous assessments related to facility operations and worldwide fallout studies proved very useful and were augmented with new considerations

*Director, Health and Safety Research Division, Oak Ridge National Laboratory, Oak Ridge, Tenn.

of exposures due to resuspension and potential contamination of natural resources such as natural gas, oil, and deep aquifers. Typical assessments involved estimation of annual somatic and 30-year gonadal doses for comparison to limits recommended by the International Commission on Radiological Protection. Improvements in methodology and refinements in data used to implement transport and dosimetry models were made during the relatively short duration of the Plowshare Program. Bioenvironmental data for a large number of radionuclides were compiled by radioecologists, with particularly valuable contributions by Lawrence Radiation Laboratory (now Lawrence Livermore National Laboratory). By the late 1960s engineering systems analysis had been demonstrated in several publications as a useful tool to predict radionuclide movement in environmental exposure pathways by using computer codes developed originally to study reactor dynamics. The Plowshare Program is now gone, but systems analysis remains as a major predictive tool for assessing radionuclide releases.

Several reports published from 1959 to 1962 by special working groups of the Committee on Oceanography of the National Academy of Sciences–National Research Council addressed disposal of radioactive waste in Atlantic and Pacific coastal waters. Maximum permissible specific activities of radionuclides in seawater were the principal numerical guides of the committee's publications.

Both Oak Ridge National Laboratory (ORNL) and the Hanford Works (called Pacific Northwest Laboratory, Battelle-Northwest since takeover by Battelle Memorial Institute in 1965) completed comprehensive bioenvironmental studies to assess the radiological safety of their operations. The Clinch River Study was summarized in a number of documents by ORNL. The study utilized extensive measurements to estimate total releases, pathways resulting in human exposure, and dietary factors contributing to doses received by populations living downstream from the nuclear operations. The Columbia River Study was very comprehensive because it attempted to verify calculations of body burdens in the exposed population by whole-body counting and bioassay measurements. The results of this study were also well documented in the literature.

By the mid- to late 1960s the civilian nuclear power program started to gain momentum and was able to make immediate use of the methodologies developed for assessing radiological releases at the national laboratories and other federally supported institutions. Two example applications sponsored by the U.S. Atomic Energy Commission (AEC) were the Upper Mississippi River Basin Study and the Tennessee Valley Region Study. The National Environmental Policy Act (NEPA) of 1969, which was signed into law in January 1970, required Federal agencies to prepare detailed and comprehensive assessments of all potential environmental impacts resulting from any major project under their charge. In the case of nuclear power stations to be operated by

utilities, the AEC was responsible for preparing an environmental impact statement for each facility seeking a construction permit.

Potential radiological releases from both routine operations and postulated accidents were considered even in the initial environmental impact statements, and actions were taken by the AEC to standardize the radiological assessment methodology. AEC staff met with radiological assessment scientists of Argonne National Laboratory, Pacific Northwest Laboratory, and Oak Ridge National Laboratory to seek mutual agreement on dosimetry models, human dietary factors, energy decay schemes, bioaccumulation factors, etc., to be used in radiological sections of environmental impact statements being prepared by the laboratories for the AEC. These data bases and models established the groundwork for the U.S. Nuclear Regulatory Commission Regulatory Guide 1.109 and other guides which were issued several years later. As a result of the Calvert Cliffs decision in 1971, the AEC was required to consider all environmental issues, whereas previously they had accepted responsibility only for radiological impacts. The U.S. Nuclear Regulatory Commission (NRC) inherited the responsibility for preparing environmental impact statements for utility-operated power stations when it was formed in 1974, simultaneous with abolishment of the AEC. The AEC's successors, the U.S. Energy Research and Development Administration and later the U.S. Department of Energy, continued to have responsibility for preparing such statements on nuclear-fuel-cycle projects that were funded under their budgets for nuclear power development.

Most radiological assessments that antedate NEPA were prepared using conservative methodologies. However, NEPA gave birth to public hearings and reviews by other government agencies and special interest groups. There was pressure to reduce the dose limits for operating nuclear facilities through regulatory changes, and the "as low as practicable" (ALAP) concept [later changed to "as low as reasonably achievable" (ALARA)], as set forth in the *Code of Federal Regulations,* Part 50, Appendix I, was formalized by the NRC and applied to proposed plant designs to further reduce potential exposures. Since Appendix I set forth numerical design objectives which translated into doses that were a small fraction of natural background levels, there was a need to refine the radiological assessment methodologies and eliminate excessive conservatism in the calculations. Some important changes included the use of average rather than maximum values for physical transport and bioaccumulation and consideration of existing pathways in the environs rather than the "fence post cow." Soon some concern was expressed about the uncertainties associated with use of radiological assessment models, and efforts to address that concern were initiated. A historical milestone was the workshop "The Evaluation of Models Used for the Environmental Assessment of Radionuclide Releases" held at Gatlinburg, Tennessee, in September 1977 and sponsored by the newly formed U.S. Department of Energy. The workshop resulted in a series of critiques on the status of various models and components making up

the assessment methodology. Recommendations were made on limitations on their use, uncertainties, and further research that would be required. The NRC responded over the next 2 to 3 years by funding many of the items recommended for research.

Another milestone was the publication of the *Reactor Safety Study* (Report WASH-1400), which was the first comprehensive application of probabilistic risk analysis (PRA) to reactor safety. The performance of some nuclear power stations is now being assessed with PRA techniques, which consider all events involving people, machines, and environmental interactions to arrive at an estimate of the risk to the public from operation of the facility. Is it too unlikely to assume that someday nuclear plants might be licensed principally on the results of PRA?

The progress made in the past decade in assessing radionuclide releases to the environment has been outstanding. Many important decisions continue to be made on the basis of calculational techniques because actual measurements may not be possible. This book fulfills the need to compile and document the current calculational models, data bases, and regulatory standards most widely used for assessing routine and accidental releases of radionuclides to the environment. Further changes are likely, but the numerical values of estimated doses to the public may not change much in the next 5 to 10 years compared to the changes that have advanced us to our present capability. It is hoped that our understanding of what these predictions mean may be advanced considerably through validation studies. We have come a long way, but there is still room for more progress.

Preface

Radiological assessment is the quantitative process of estimating the consequences to humans resulting from the release of radionuclides to the biosphere. It is a multidisciplinary subject requiring the expertise of a number of individuals in order to predict source terms, describe environmental transport, calculate internal and external dose, and extrapolate dose to health effects. Up to this time there has been available no comprehensive book describing, on a uniform and comprehensive level, the techniques and models used in radiological assessment. Because of the increasing importance of this subject, the need for such a book is evident.

Radiological Assessment is based on material presented at the 1980 Health Physics Society Summer School held in Seattle, Washington. The material has been expanded and edited to make it comprehensive in scope and useful as a text. Because the book includes the contributions of a number of individuals, there is some disparity in style and depth among the chapters. In addition, although there is consistency in the use of symbols and units within each chapter, individual chapters may use different systems of measurement: SI alone, dual units, or a composite of SI and conventional units.

A basic understanding of integral calculus, nuclear and radiation physics, statistical methods, and radiation biology is needed to thoroughly comprehend and apply the broad spectrum of concepts discussed in the book. It is written primarily as a graduate-level textbook, incorporating both example problems that illustrate application of specific models and working problems at the end of chapters. It is also intended that the book be a reference manual to explain and assist in the use of models for radiological assessments in the preparation of environmental impact statements, engineering design of facilities, and release of radionuclides from operating facilities. It is emphasized, however, that *Radiological Assessment* is not meant to be a replacement for U.S. Nuclear Regulatory Commission (NRC) guides or other accepted modeling practices, but is rather a supplement to such accepted practices.

This book would not have been possible without the cooperation of many people. Foremost, the authors of individual chapters are recognized for the voluntary contribution of their time, talent, and expertise. Mrs. Ann Ragan, Mr. Charles Hagan, Mr. George Battle, and Mrs. Janice Moody of the Oak Ridge National Laboratory (ORNL) deserve special recognition for their thorough and professional editorial assistance. Also, Mrs. Malinda Hutchinson, Mrs. Karen Galloway, and Mrs. Nancy Hardin of ORNL as well as the members of the Composition Unit of the Technical Publications Department are thanked for typing and retyping the manuscript over many months. We are also indebted to Dr. George Killough of ORNL for the excellence of his contributions to format design. The editors are grateful to the Health Physics Society for support of the 1980 Summer School on which much of the book is based, and to Dr. William A. Mills (NRC) and Dr. William E. Kreger (NRC, retired) for their early encouragement and support. Finally, we are especially appreciative of financial support by the NRC during preparation of this document, and the guidance of Drs. Edward Branagan, Sarbes Acharya, Tin Mo, Walt Pasciak, Frank Congel, and others of the NRC who provided guidance and assistance during preparation of the text.

John E. Till
H. Robert Meyer

Introduction

J. E. Till*
H. R. Meyer†

Because of continued and intense interest in the effects of radioactivity on man and his environment, the transport, uptake, and health impact of radionuclides released to the biosphere have been well studied by scientists. It is certain that the prediction of the impact of radionuclides in the environment is much better understood than that of nonradioactive pollutants. One of the primary purposes of this book is to link, in one document, the models and data most commonly used to simulate the movement and effects of radionuclides in the environment.

The ultimate goal of radiological assessment is to show the relationship between the "source term," or quantity and types of released radionuclides, and the potential effect on human health. The assessment process must proceed in a logical fashion, following the radioactive pollutant of interest from its point of origin along various exit pathways to the environment, then considering its transport in air, water, soil, or food sources to man. Once transport and intake are determined, the dose from radiation and resulting risk to health can be calculated. Figure 1 illustrates the major steps in this process, identifying chapters in which each step is addressed and showing the relationship between calculated results.

Chapter 1 considers the source terms typically encountered in radiological assessment and demonstrates their derivation. The ultimate goal of source term development is to determine, through measurement or theoretical calculation, the type and quantity of radionuclides emitted, in activity per unit time. The chemical and physical form of the releases must also be considered. Unfortunately, in the past too little emphasis was placed on the accurate estimation of source terms, and it is likely that considerable uncertainty still exists in this

*Radiological Assessments Corporation, Neeses, S.C.
†Oak Ridge National Laboratory, Oak Ridge, Tenn.

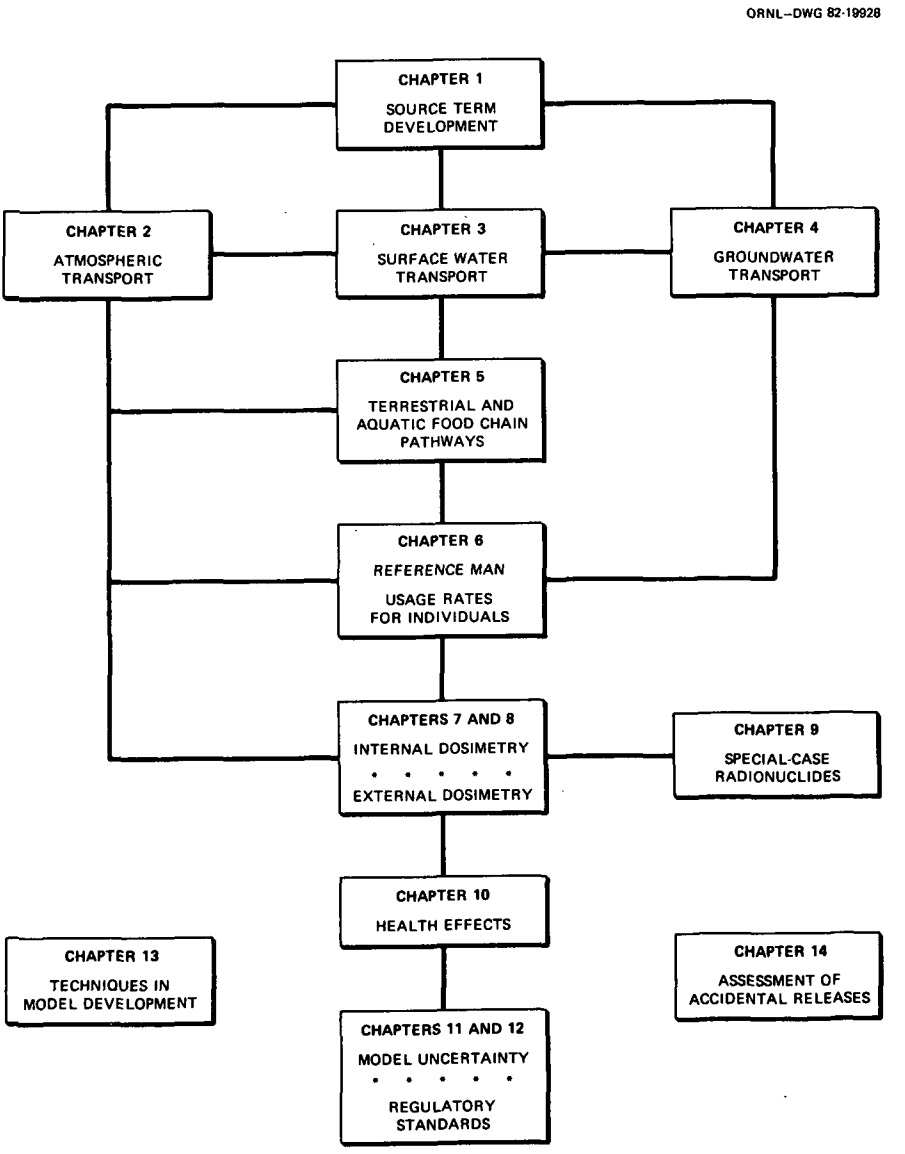

Figure 1. Major steps in radiological assessment and the chapters in which they are addressed.

area for many assessments. This chapter discusses source terms for routine releases, that is, controlled releases of radionuclides during normal operation of a facility over a prolonged period of time.

Chapters 2, 3, and 4 deal with the primary mechanisms of radionuclide transport through air, surface water, and groundwater. The objective here is to predict the concentrations of radionuclides reaching humans directly, or indirectly through the foods they eat. These models simulate physical transport and are generally considered to be element-specific and independent of the particular isotope originally released in the source term. The key product of transport models is an estimate of the activity per unit volume of air or water.

The next step in radiological assessment is to determine the deposition of radionuclides onto terrestrial or aquatic environments and to estimate bioaccumulation. This subject is discussed in Chapter 5. The goal is to quantitatively predict the concentration of radionuclides once they have entered the food chain, in terms of activity per unit mass ingested. Because of the variety of routes and radionuclides to be considered in this phase of the assessment procedure, this chapter presents numerous tabulations of data specific to the variables to be considered.

Chapter 6 deals with rates of intake of various food products, and accepted metabolic parameters for members of the human population. The chapter primarily discusses characteristics of a hypothetical individual rather than a specific person or group of people. The content of Chapter 6 is an important link between the concentrations calculated in Chapters 2 to 5 and the final determination of dose; it is only through the application of these usage factors that one can estimate the quantity of each radionuclide entering the body.

Chapters 7 and 8 concern internal and external dosimetry, respectively. The authors discuss health physics techniques used to estimate the energy to be deposited in various organs of the body via radionuclide inhalation and ingestion or through direct, external exposure. Although these chapters present a detailed review of dose calculation, they also tabulate dose conversion factors for many radionuclides, providing values which can be applied directly in radiological assessments.

Tritium and ^{14}C, because of their tendency to move freely through biological systems, and their association with their abundant stable element counterparts, are treated as special cases. The special case models are addressed in Chapter 9, which also discusses methods used to estimate global circulation and dose for ^{3}H, ^{14}C, ^{85}Kr, and ^{129}I.

Once the absorbed radiation dose is calculated, health detriment can be estimated by applying one or more risk factors based largely on epidemiological data. Determination of the risk from radiation exposure is discussed in Chapter 10. Levels of exposure to radiation are usually very low, and related effects are not observable in the context of the background health effects rate

in the population. Therefore, the estimation of risk from radiation exposure is a difficult process, subject to frequent reevaluation.

The calculation of radiological risk, from source term development to risk extrapolation, is obviously based on numerous sets of data and assumptions of varying levels of accuracy. Chapter 11 discusses approaches to determining the overall level of confidence in radiological assessment calculations, considering the uncertainty associated with each step. It emphasizes the mechanism of determining model uncertainty and reviews procedures for limiting the scope of a problem prior to engaging in formal uncertainty analysis.

Chapter 12 deals with the historical development of regulatory standards and lists the current standards used as the basis for protection of the public from radionuclide releases. The chapter is meant to provide a quick reference to these current standards and a perspective on the evolutionary process producing them.

Given the complexity associated with the calculations necessary to perform a thorough assessment, it is not surprising that a large number of computer codes have been developed by organizations requiring repetitive, reproducible results. Chapter 13 provides a careful look at good modeling techniques and presents examples from models currently being used for assessment purposes.

Chapter 14 considers the assessment of accidental releases, from the standpoint of reactor personnel responsible for developing emergency preparedness programs at a facility. It focuses on modeling and monitoring requirements and on the essential element of communication with outside authorities during an emergency. It is presented in *Radiological Assessment* to acquaint the reader with this rapidly developing branch of the field, and identifies a number of areas, including probabilistic source term development, short-term transport models, and short-term and age-dependent dosimetry, in which research is currently in progress.

In conclusion, the rapid development of radiological assessment as a discipline is worthy of mention. The assessment process has become an essential step in the regulatory preoperational evaluation of discharges of radioactivity to determine important pathways of exposure, key radionuclides in the source term, and critical exposure groups or populations. For planned or operating emission sources, it is relied upon to guide effluent treatment system development and operation. It has become necessary in the guidance of environmental surveillance programs to estimate concentrations in the biosphere that are below detectable limits and to convert measured values of radionuclide intake and exposure into estimates of health effects. It is often the only mechanism we have to analyze the potential impact of radionuclide releases to the biosphere. It is important to understand, however, that even though radiological assessment has developed rapidly, it is still a new field and continued improvement in its data base and methodologies can be expected in the future.

1 Source Terms for Nuclear Facilities, and Medical and Industrial Sites

By G. G. EICHHOLZ*

1.1 INTRODUCTION

Radiological assessment is a linear process; that is, the health effects of radioactive releases to the environment depend directly on the quantity and form of any radionuclide introduced into the sequence of calculations shown in Fig. 1 in the Introduction. This initial quantity, comprising all radionuclides of interest, is referred to as the "source term." The nature of the source term will vary, of course, with the process and facility being considered, but in many cases, once the source term has been defined, most of the subsequent migration paths will be similar, though their relative importance may vary.

Only rarely will there be any direct exposure of the surrounding population by radiation emitted from a nuclear facility; in practice, one is concerned only with the transport of the radioactive materials emitted, usually in trace (ppm or ppb) concentrations, through airborne or liquid pathways. For this reason, any activity contained in the source term is of interest only if it is mobile in the environment, that is, capable of escaping from any containment or encapsulation in a form that would enable it to travel along environmental pathways or be carried as surface contamination on packages, vehicles, or other transported bodies. In examining the source terms, therefore, one must assess the probability of escape from the containment under routine use conditions or in any postulated accident situation. There is little interest in components that are inherently immobile, well fixed in position, so low in activity as to make a

*School of Nuclear Engineering and Health Physics, Georgia Institute of Technology.

negligible contribution under any accident situation envisioned, or so short-lived that they are unlikely to survive any anticipated migration path before reaching the target population.

The environmental impact of nuclear power plants and fuel cycle facilities has been investigated in great detail, and the results indicate that average population exposures to medical and industrial radionuclide applications are substantially greater than average population exposures to nuclear power plant emissions. Again, we eliminate from consideration direct radiation exposure for diagnostic and therapeutic purposes and occupational exposures to industrial sources, such as in radiography or borehole logging. Only those radionuclides that move through the environment in unconfined form are of interest as source terms in estimating environmental impact; a related area not considered here is the impact of commercial transportation of packaged radioisotopes or nuclear materials.

For obvious reasons, predicting the pathways and mode of behavior of gaseous components, especially noble gases and very volatile materials, poses the greatest problem. Gaseous components are also often more difficult to quantify in their chemical form; for instance, it makes a substantial difference whether radioiodine is produced or released in inorganic or organic form, both for purposes of controlling its escape from the facility and for predicting its subsequent pathway through the environment (Eichholz 1977). For this reason, all likely forms and internal pathways, and all processes that may modify the physical or chemical forms of the radionuclide must be included in any reformulation of the source term, leading to a "release source term," which may be substantially different from the "initial source term," especially for nuclear power plants.

1.2 PROPERTIES OF RADIONUCLIDES

As far as the mechanism of movement through plant process equipment and the natural environment is concerned, the activity level of the radionuclides is irrelevant, except in a few cases where recoil processes contribute to release mechanisms. Since radioisotopes have chemical properties identical to those of their stable homologs, their movement will faithfully follow that of the stable element. From the point of view of release and mobility, therefore, the important parameters are the physical state (whether liquid, solid, or gaseous), the type of aggregation if any (e.g., microparticulate, colloidal), the chemical form, solubility in air and water, oxidation states, sorption properties, and volatility. For purposes of radiation protection and the calculation of population dose, one must know the total activity, the specific activity, and the half-lives of all radionuclides comprising the source term.

In industrial and medical applications, typically only a single radionuclide is involved, thus simplifying identification of leakage pathways from encapsulation, from radiotracer tests, and for disposal purposes. However, even there one may encounter more than one radionuclide in a source material because

1. the production process may give rise to more than one reaction, with varying cross sections [e.g., (n,p), (n,d), $(n,2n)$ reactions may give rise to nuclides of comparable half-life that are chemically different];

2. production involves bombardment of target material with more than one activable isotope [e.g., production of ^{124}Sb by the $^{123}Sb(n,\gamma)^{124}Sb$ reaction will be accompanied by ^{122}Sb from $^{121}Sb(n,\gamma)^{122}Sb$];

3. the nuclide of interest is the daughter of a longer-lived parent, and both may be found in various conditions of equilibrium (examples are the ^{99}Mo-^{99m}Tc, ^{90}Sr-^{90}Y, and ^{140}Ba-^{140}La parent-daughter pairs); and

4. a short-lived nuclide of interest may decay or be accompanied by a long-lived daughter or isotope (examples are the ^{129}Te-^{129}I, ^{134}Cs-^{137}Cs, ^{93}Y-^{93}Zr pairs and the ^{210}Pb daughter of radon decay).

Neutron activation, usually involving the (n,γ) thermal neutron capture process, is a particularly convenient method of radioisotope production. Since the product nuclide, in general, will be an isotope of the target element, specific activity will depend on available neutron flux, and product and target isotopes are not readily separable. Among the more important radionuclides in medicine and industry produced by this method are $^{60}Co[^{59}Co(n,\gamma)^{60}Co]$, $^{192}Ir[^{191}Ir(n,\gamma)^{192}Ir]$, and ^{24}Na $[^{23}Na(n,\gamma)^{24}Na]$. If the product nuclide itself is unstable, one may permit it to beta-decay to another daughter, which will then be associated with another element and be chemically separable. This can result in a product of high specific activity, limited only by the need to employ a carrier for more efficient separation. Examples of this method of preparation are ^{131}I, produced by $^{130}Te(n,\gamma)$ $^{131}Te \xrightarrow{\beta} {}^{131}I$ (8 d), or ^{210}Po, produced by $^{209}Bi(n,\gamma)$ ^{210}Bi (5 d) $\xrightarrow{\beta}$ ^{210}Po. In some cases, the intermediate parent activity decays slowly enough to permit shipment to the user in that form. If the parent is adsorbed on an ion-exchange medium, the system can serve as an isotope "cow" by pouring an eluting solution through the column; thus, the short-lived daughter can be removed selectively for immediate use. Such a system is usable until the parent activity decays to a level below the minimum practical amount.

Some radionuclides that are not neutron-abundant or for which no suitable target nuclei exist for neutron activation must be produced by charged-particle reactions in an accelerator. The total activities attainable by this method tend to be lower than those for reactor-produced nuclides, and the cost per curie (or megabecquerel) may be higher. Gallium-67, from the $^{68}Zn(p,2n)^{67}Ga$ reaction, is an example of this type. For some production procedures, the $^{6}Li(n,\alpha)^{3}H$ reaction may be useful as a source of reactor-induced tritons or α particles to initiate (t,p), (α,n), or similar reactions. For example, ^{18}F can be produced by neutron irradiation of lithium carbonate through the two-stage reaction $^{6}Li(n,\alpha)T$ and $^{16}O(t,n)^{18}F$.

One of the major reactions for the production of radionuclides is, of course, the fission process, involving predominantly the $^{235}U(n,f)$ reaction. For ^{235}U,

this results in the production of neutron-abundant fission products; Fig. 1.1 shows the well-known double-humped fission yield curve. Note that the yield (i.e., number of atoms of given mass number produced per fission) applies to the production of nuclides of a certain mass, so decay along an isobaric chain, changing neutrons into protons by beta emission, does not affect that proportion. This is illustrated in Fig. 1.2, where one can see the progression from initial, neutron-abundant, very short-lived fission products by succesive beta decay to the final stable isobar of that mass (e.g., from 0.2-s ^{94}Kr to stable ^{94}Zr) via steadily longer-lived intermediates. Some of the intermediate isobars may be sufficiently long-lived to move freely through the environment before decaying; for instance, in the mass-88 chain, 28-h ^{88}Kr may diffuse through the atmosphere, but it is its ^{88}Rb daughter that may be taken up in plants in water-soluble form. Maximum fission yields are of the order of 6–7% for atomic masses 92–100 and 133–143, falling off rather rapidly on either side of the peaks. Because of the vastly different chemical properties even among isobars of the same decay chain, each fission product must be evaluated separately in terms of its contribution to the source term in a reactor and its subsequent history in any environmental migration.

Finally, it is important to consider the large number of labeled radioisotopes that are widely used in medical, biological, and agricultural research. Those in greatest demand are ^{14}C- and tritium-labeled organic compounds, which are used in research quantities, micro- to millicuries at a time. They are produced by organic synthesis and may be supplied with the labeling atom at a specified structural position at extra cost. Since both ^{14}C and tritium emit only very low-energy beta particles, their handling is considered relatively safe. However, they are encountered widely because of the large number of individual, discrete users of varying quantities of these radioisotopes and other tracer radionuclides, and safe disposal of such materials may present a problem. For instance, many of these isotopes end up in liquid scintillation solutions. This is usually considered a separate problem from the more elaborate scenarios embodied in environmental computer models. Figure 1.3 illustrates an arbitrary selection from a commercial catalog of the type and variety of such labeled compounds that may be encountered. In some cases, the same compound may be obtained either ^{3}H- or ^{14}C-labeled, depending on the subsequent processes to be studied.

1.3 INDUSTRIAL USES OF RADIONUCLIDES

Radioisotopes are much more widely used in industry than is generally recognized and represent a significant component in the man-made radiation environment. The principal applications include industrial radiography, borehole logging, radiation gauging, smoke detectors, and self-luminous materials. Because most of these applications entail the utilization of encapsulated

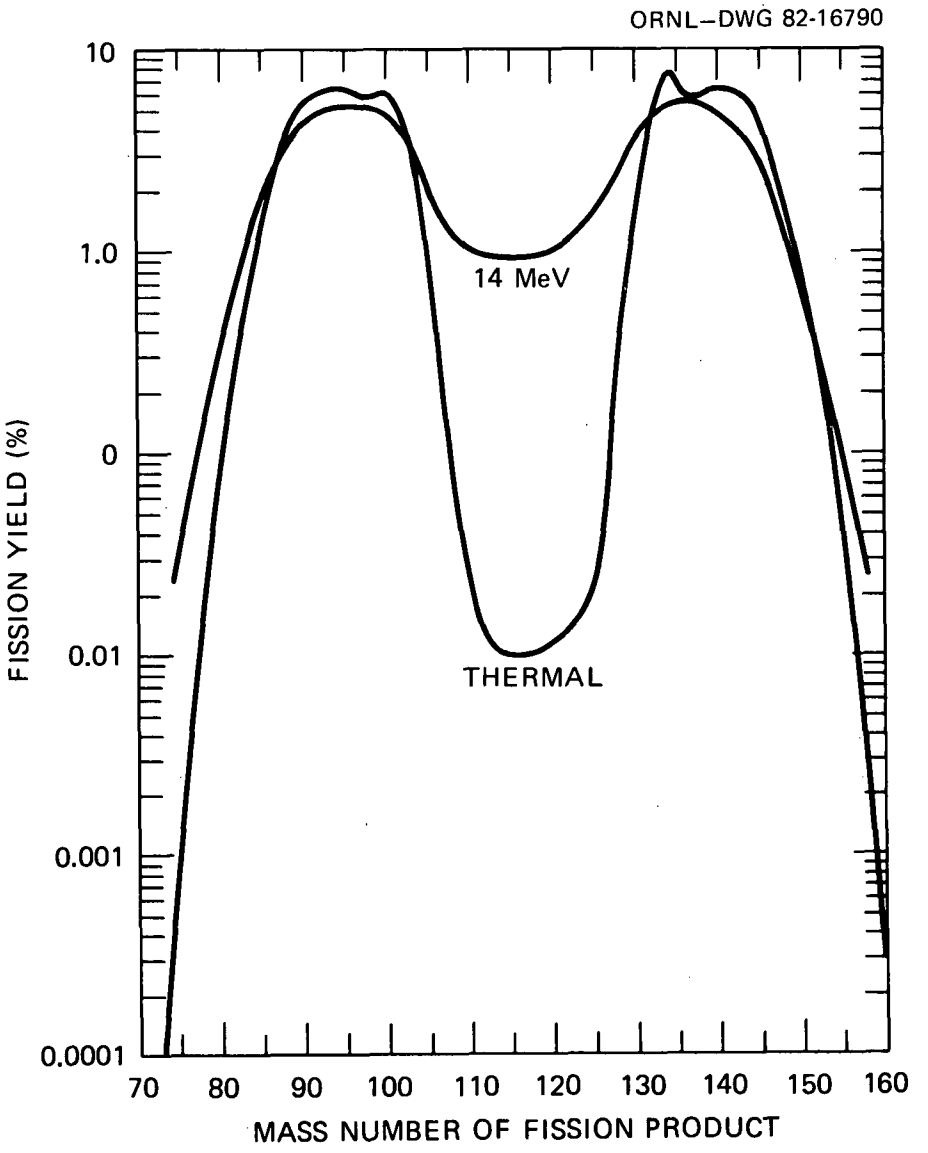

Figure 1.1. Fission yield curve for neutron bombardment of ^{235}U.

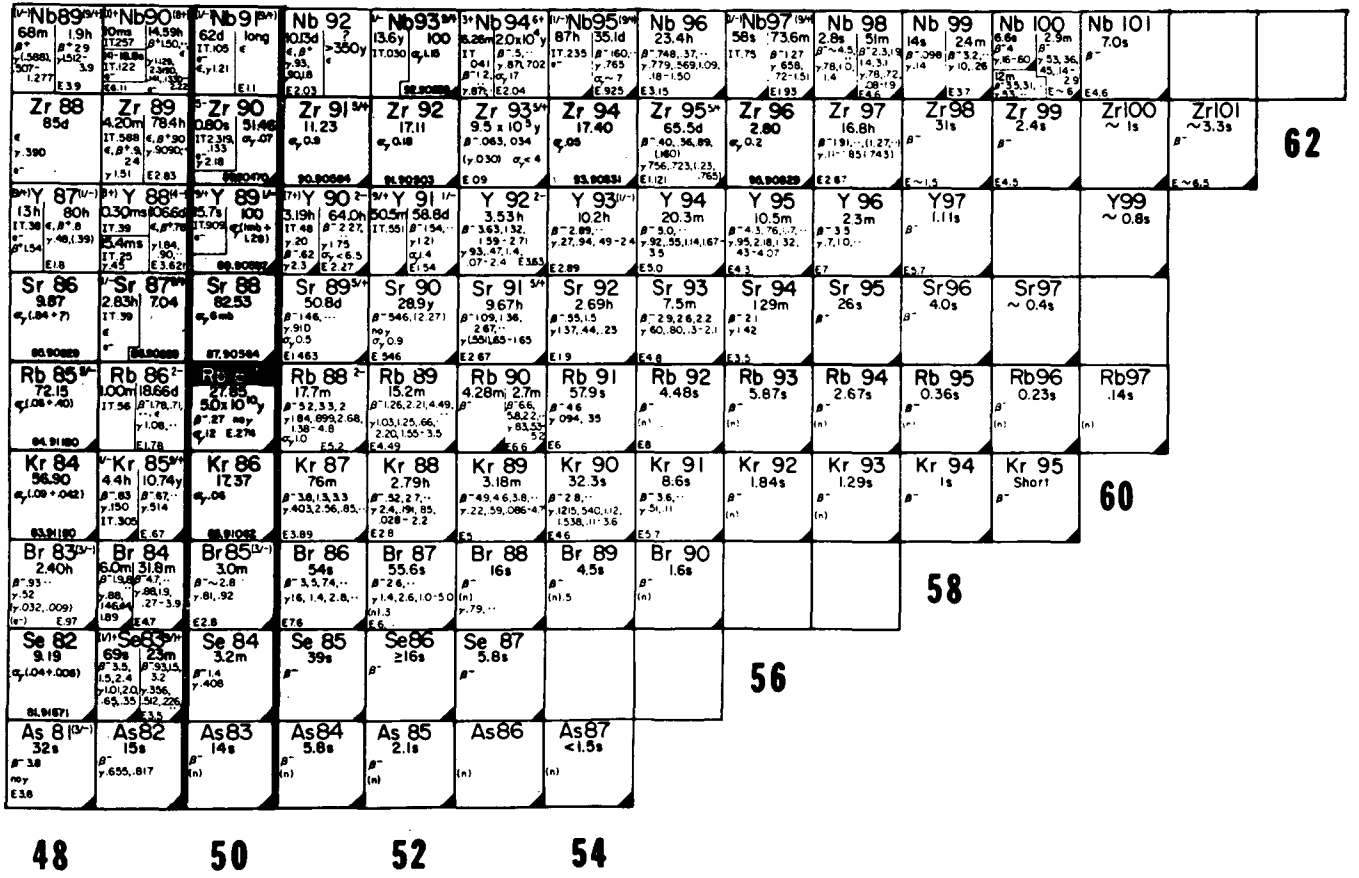

Figure 1.2. Segment of the Chart of the Nuclides. Source: U.S. Department of Health, Education, and Welfare 1970. *Radiological Health Handbook,* rev., Washington, D.C. Reprinted with permission of General Electric Company.

ORNL–DWG 82-16789

COMPOUND	MOLECULAR WEIGHT	STANDARD PACKAGE
CHOLIC ACID [*CARBOXYL*-^{14}C]- SEE STRUCTURAL FORMULA SECTION – STEROIDS 40–60 mCi/mmol ETHANOL	408.6	50 μCi 250 μCi
CHOLIC ACID, [2,4-^{3}H]- SEE STRUCTURAL FORMULA SECTION – STEROIDS 10–25 Ci/mmol ETHANOL	408.6	250 μCi 1 mCi 5 mCi
CHOLINE CHLORIDE, [1, 2-^{14}C]- $HOCH_2CH_2N(CH_3)_3 \cdot Cl$ 2–10 mCi/mmol ETHANOL	139.6	50 μCi 250 μCi
CHOLINE CHLORIDE, [*METHYL*-^{14}C]- $HOCH_2CH_2N(CH_3)_3 \cdot Cl$ 40–60 mCi/mmol ETHANOL	139.6	100 μCi 500 μCi 1 mCi
CHOLINE CHLORIDE, [*METHYL*-^{3}H]- $HOCH_2CH_2N(CH_3)_3 \cdot Cl$ 60–90 Ci/mmol ETHANOL	139.6	250 μCi 1 mCi 5 mCi
CITRIC ACID, [1,5-^{14}C]- $HOOCCH_2C(OH)(COOH)CH_2COOH$ 50–100 mCi/mmol WATER:ETHANOL, 9:1	192.1	50 μCi 250 μCi 500 μCi
CITRIC ACID, [6-^{14}C]- $HOOCCH_2C(OH)(COOH)CH_2COOH$ 1–5 mCi/mmol CRYSTALLINE SOLID IN SCREW-CAP BOTTLE	192.1	50 μCi 250 μCi
CITRULLINE, L-[*UREIDO*-^{14}C]- $H_2NCONH(CH_2)_3CH(NH_2)COOH$ 40–60 mCi/mmol 0.01 N HCl	175.2	50 μCi 250 μCi 1 mCi
COCAINE, *LEVO*-[*BENZOYL*-3,4-^{3}H(N)]- SEE STRUCTURAL FORMULA SECTION – MISCELLANEOUS 25–50 Ci/mmol ETHANOL	303.4	100 μCi 250 μCi
COENZYME A, [^{3}H(G)]- SEE STRUCTURAL FORMULA SECTION – MISCELLANEOUS 0.5–1.5 Ci/mmol AQUEOUS SOLUTION CONTAINING 5 mmol OF DITHIOTHREITOL PER milliliter SHIPPED IN DRY ICE	767.6	50 μCi 250 μCi
COENZYME A, [*ACETYL*-1-^{14}C]- ACETYL SEE STRUCTURAL FORMULA SECTION – MISCELLANEOUS 40–60 mCi/mmol AQUEOUS SOLUTION (pH ~ 5) SHIPPED IN DRY ICE.	809.6	10 μCi 50 μCi

Figure 1.3. Examples of commercial labeled radioactive compounds. Source: Adapted from New England Nuclear Corporation 1980. *Labeled Compounds,* Boston, Mass. Printed with permission.

sources, radiation exposures would be expected to occur mainly externally during shipment, transfer, maintenance, and disposal. In the past decade, radiation exposures in research and industrial applications were roughly half those due to medical occupational exposure; hence, their contribution to the direct population dose is substantial. Although reported exposure levels are probably significantly underestimated, the average dose contribution to the U.S. population was only of the order of 0.2 mrem/y (2 μSv/y). Table 1.1 lists the principal radionuclides involved and typical applications, and Fig. 1.4 shows the source strengths typically encountered.

Table 1.1. Typical uses of radionuclides in industry

Application	Radionuclides	Typical source strengths
	Encapsulated sources	
Industrial radiography	^{192}Ir, ^{137}Cs, ^{170}Tm, ^{60}Co	10—100 Ci (0.4—4 TBq)
Borehole logging	^{137}Cs, ^{60}Co	10 mCi—2 Ci (~0.4—70 GBq)
	Pu-Be, Am-Be	50 mCi—20 Ci (~1.9—700 GBq)
	^{252}Cf	100 μCi (~4 MBq)
Radiation gauges, automatic weighing equipment	^{90}Sr, ^{147}Pm, ^{144}Ce ^{137}Cs, ^{60}Co	5—200 mCi (~0.2—7 GBq)
Smoke detectors	^{241}Am	5 μCi (~200 kBq)
Luminous signs	^{3}H	0.5 Ci (~20 GBq)
Mössbauer analysis	^{57}Fe, ^{57}Co	2—50 μCi (~0.4 MBq)
	Tracer applications	
Hydrological tracers	^{3}H	1—100 Ci (~4 TBq)
	^{82}Br	10—100 mCi (~4 GBq)
Reservoir engineering	^{85}Kr	200 mCi (~7 GBq)

Source: Adapted from U.S. Environmental Protection Agency 1974. *Environmental Radiation Dose Commitment: An Application to the Nuclear Power Industry,* EPA-520/4-73-002, Washington, D.C.

In terms of subsequent movement through the environment, such encapsulated sources obviously do not represent a significant source term. They contribute to specific assessment areas, such as transport and waste disposal, and occasionally cause alarm when one is lost or misdirected or even placed in a municipal garbage dump by mistake.

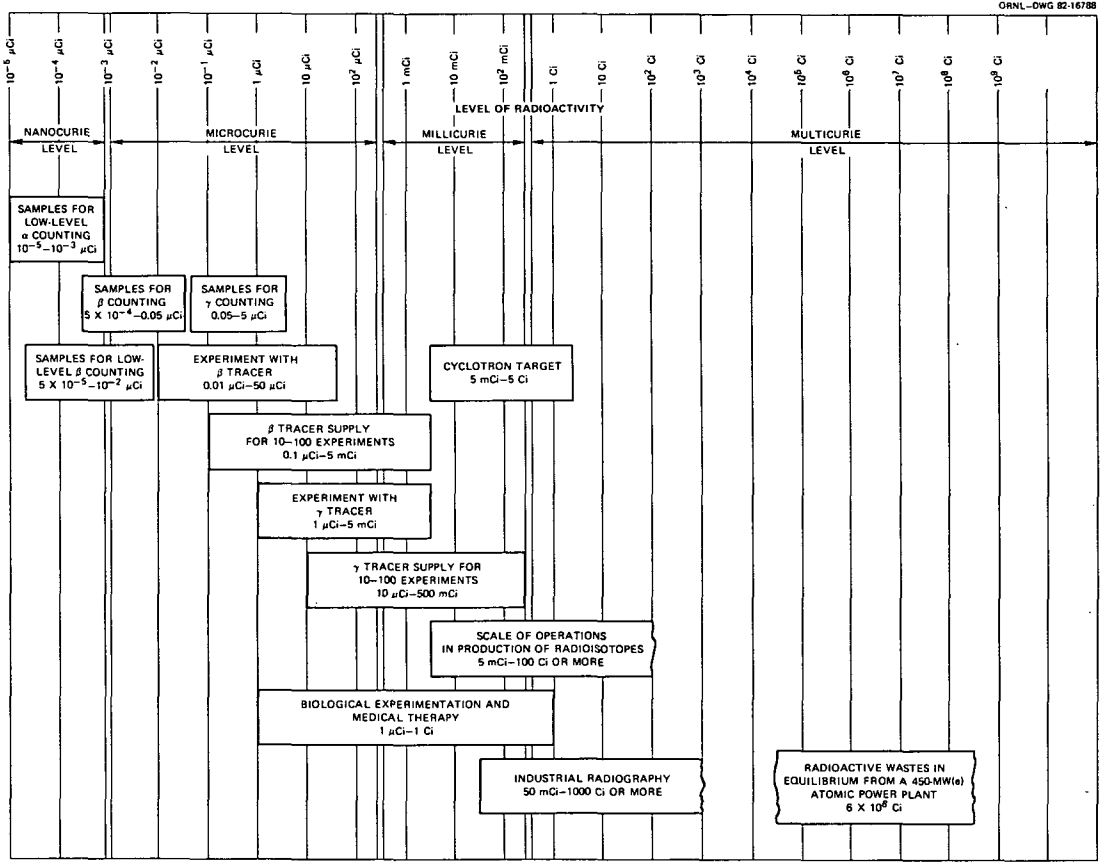

Figure 1.4. Source strengths of radioactive material typically encountered.

Sealed sources for industrial use typically are shipped and installed in the form of doubly encapsulated disks or cylinders. In most cases, the capsule material is stainless steel, ring-welded, and required to be leak-tested at regular intervals. Shipment of radiographic sources and other, less active sources must be done in accordance with the regulations in Title 10, *Code of Federal Regulations,* Parts 20 and 71, and Title 49, *Code of Federal Regulations,* Parts 172 to 177.

Disposal of industrial sources may pose a problem. There is a certain second-hand value associated with cobalt therapy sources and some longer-lived radiography sources. Shorter-lived sources may be stored and allowed to decay, but even then they must be properly accounted for, and the residual active material must be disposed of at a licensed facility. Stronger sources similarly must be shipped to a licensed facility for disposal; finding such a facility is becoming more and more difficult under present conditions.

Increasing attention is being paid to the safe decommissioning and decontamination of industrial sites where radioactive materials have been handled in the past. Most are plants built for processing nuclear materials in the early days, but increasingly other industries have become involved, such as plants making self-luminous tritium-containing signs.

A special problem may exist for long-lived low-level sources that are widely distributed, such as ^{241}Am alpha sources used in smoke detectors. Individually they pose no hazard, and it would require a rather artificial scenario for them to be reconsolidated at a future time in sufficient amounts to pose a problem. Moghissi et al. (1978) have reviewed the impact of radioactive materials in consumer products and the resultant public and occupational exposures.

1.4 MEDICAL USES OF RADIONUCLIDES

The use of radioisotopes in medicine is widespread and may potentially have significant radiological impact. These applications can be classified as (1) diagnostic uses, (2) therapy, (3) analytical procedures, and (4) pacemakers and similar portable sources.

Both sealed sources and a wide variety of radioactive tracers are used in diagnostic applications; medical institutions usually distinguish carefully between these two applications as Radiology and Nuclear Medicine, respectively. X-ray fluoroscopy is a well-known diagnostic radiographic procedure, typically employing an X-ray tube as a source; however, there is a variety of isotopic source applications for medical radiography, employing gamma sources, beta sources, bremsstrahlung sources and, experimentally, neutron sources for image formation under conditions where X-ray units would be inconvenient, inappropriate, or might cause operational hazards. Environmentally, radiographic sources are negligible as source terms as long as they remain accountable and are disposed of properly. In that respect, the history of radium sources, radon needles, and radium-containing luminescent compounds

has not been encouraging. Occupational exposures from work on radium-containing watch dials and tritiated luminous signs have been substantial (Moghissi and Carter 1975; USEPA 1977), and radium-contaminated rooms and buildings, many of them dating to the early decades of this century, are being found from time to time all over the world. In the United States, this situation was accentuated by the fact that radium uses were specifically exempted from the control and licensing provisions of the Atomic Energy Control Act.

The emergence of ^{252}Cf as a portable neutron source has made neutron radiography more widely available, although generally the method is still heavily dependent on nuclear reactors as sources. There are also a number of routine applications for ^{90}Sr- or ^{147}Pm-based bremsstrahlung sources (Cameron and Clayton 1971).

The major potential environmental impact arises from the use of radioactive tracers in nuclear medicine, a field that has grown enormously in recent years. Figure 1.5 illustrates this growth. Nuclear medicine exposures can be classified as (1) exposure of the patient, (2) exposure of hospital personnel, (3) exposure during transport of radiopharmaceuticals, (4) exposure during manufacture, and (5) exposure from radioactive waste.

Patient exposure varies with the type of examination and the procedure. Administered doses of ^{99m}Tc, for instance, may range from 600 to 15,000 μCi per examination for brain scans (UNSCEAR 1977). The range of exposures for the most common examinations may be substantial, with thyroid doses from ^{131}I scans up to 100 to 200 rad per examination. Developments in recent years have tended to reduce patient exposure through the introduction of short-lived isotopes of higher specific activity and the use of more highly localized preparations. The shorter half-life also simplifies the impact of radioactive waste, since most of the longer-lived activity is usually eliminated through the kidneys into the sanitary waste system. The environmental impact of the release of radiopharmaceuticals has been analyzed by Leventhal et al. (1980). Figure 1.6 shows the flow of radioisotopes in a nuclear medicine department of a hospital. Presumably, the environmental impact, via the sewers, of any excreted material is the same for in-patients or out-patients. Although most of the excreted radioactivity is likely to be short-lived, the aggregate environmental impact from this source probably greatly exceeds that of all nuclear power plants from routine effluents. This can be seen in Table 1.2, which gives the quantities produced at just one hospital (Leventhal et al. 1980). As a rough assumption, 50% of the administered dose of soluble iodine will be eliminated through the kidney during the first 48 h; colloidal gold and technetium will mostly decay in situ in the organ of interest and not be eliminated rapidly.

Leventhal et al. (1980) have reported on tests to trace the excreted activities. Table 1.3 illustrates the data obtained for a flush release of a sample containing active pertechnetate. Concern about such radioactive releases has

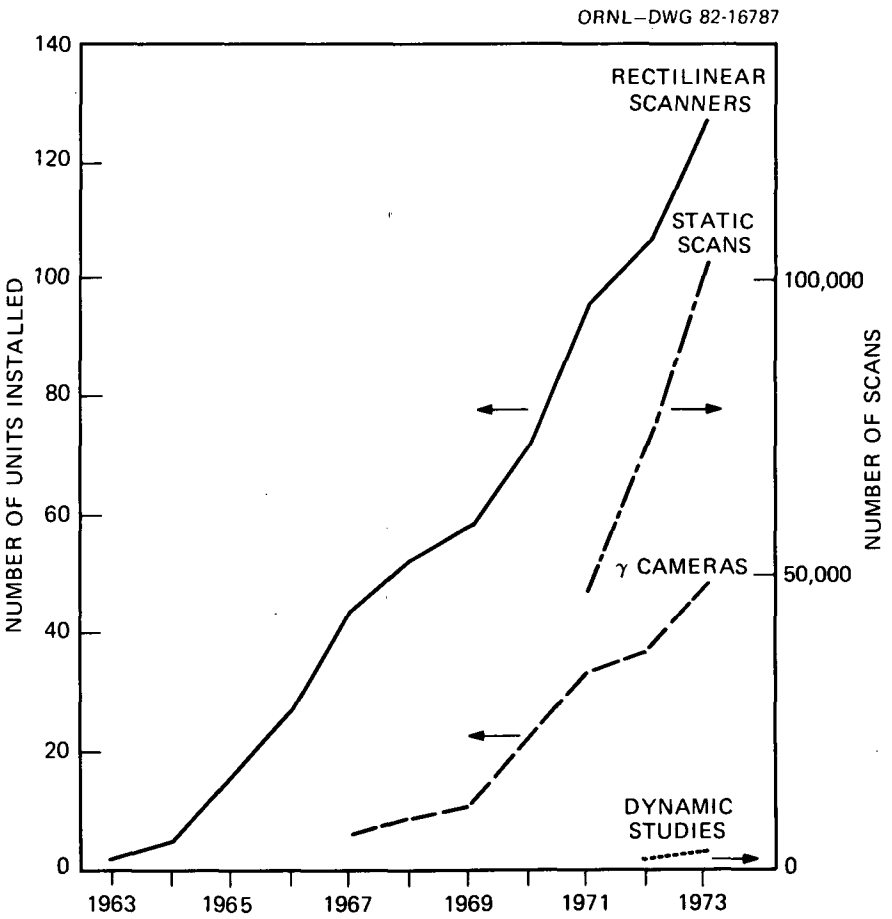

Figure 1.5. Number of scanners and γ cameras installed in the United Kingdom 1963–1973, and total number of static scans and dynamic studies carried out, 1971–1973.

directed attention to methods of sewage treatment at the hospital prior to dilution in municipal wastes. Analysis at these tracer levels is difficult. Table 1.4, from Krieger et al. (1980), lists some of the procedures required; most of these procedures were found to be capable of detecting the elements listed at the 1-pCi/L or 1-pCi/g (0.04-Bq/L or 0.04-Bq/g) level at the 2σ confidence level.

The report of the United Nations Scientific Committee on the Effects of Atomic Radiation (UNSCEAR 1977) refers to the curie-level discharge of activities, mainly of ^{131}I and ^{32}P, administered for therapeutic uses. Population dose figures quoted there relate only to the patient dose, though some German work by Stieve and Kaul has attempted to estimate effluent doses. Since

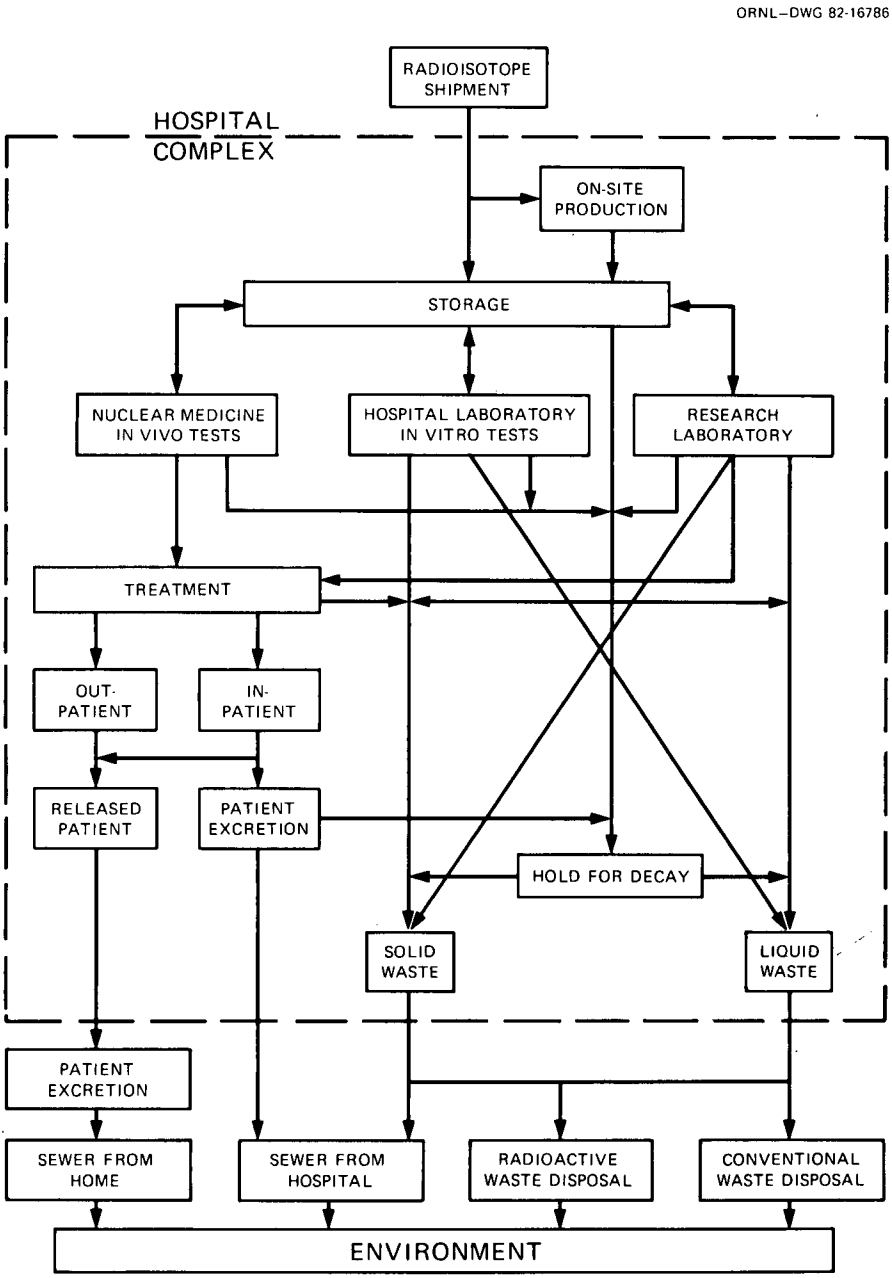

Figure 1.6. Hospital radioisotope flow diagram. Source: Leventhal, L., et al. 1980. "Assessment of Radiopharmaceutical Usage Release Practices by Eleven Western Hospitals," in *Effluent and Environmental Radiation Surveillance,* ed. J. J. Kelly, STP698, American Society for Testing and Materials, Philadelphia. Reprinted with permission.

Table 1.2. Cumulative procedures by compound for Hospital 9

Type of procedure	Total number of procedures			1972 studies			
	1969	1970	1971	Isotope	Form	Total procedures	Average dose per procedure
Angiogram				^{99m}Tc	Pertechnetate		
Bone marrow scan				^{99m}Tc	Sulfur colloid		
Bone scan				^{99m}Tc	Polyphosphate	68	10 mCi
Brain scan or cerebral blood flow or both	335	493	444	^{99m}Tc	Pertechnetate	410	10 mCi
Heart scan or flow or both				^{99m}Tc	Pertechnetate		
Liver scan or spleen scan or both	181	335	343	^{99m}Tc	Sulfur colloid	330	2 mCi
Lung scan		235	204	^{99m}Tc	MAA	216	2 mCi
Lung ventilation/perfusion scan				^{99m}Tc	MAA		
Parotid gland scan				^{99m}Tc	Pertechnetate		
Pericardial scan		4	5	^{99m}Tc	Pertechnetate	6	5 mCi
Placental localization		10	10	^{99m}Tc	Pertechnetate	13	800 μCi
Renal scan or renal blood flow or both		25	28	^{99m}Tc	DTPA	36	2 mCi
Thyroid scan				^{99m}Tc	Pertechnetate		
Blood volume	25	28	20	^{131}I	RISA		5 μCi
Cisternogram		5	5	^{131}I	RISA H	2	100 μCi
Liver scan	10			^{131}I	Rose Bengal		500 μCi
Placental localization	5			^{131}I	RISA		5 mCi
Renal scan	15			^{203}Hg	Chlormerodrin		100 μCi
Renogram	10	15	15	^{131}I	Hippuran	20	100 μCi
Thyroid uptake	300	250	260	^{131}I	Sodium iodide	244	10 μCi
Thyroid scan	199	249	240	^{131}I	Sodium iodide	191	25—50 μCi
Thyroid cancer				^{131}I	Sodium iodide		20 mCi
Thyroid therapy	10	15	12	^{131}I	Sodium iodide	15	5—10 mCi

Table 1.2 (continued)

Type of procedure	Total number of procedures			1972 studies			
	1969	1970	1971	Isotope	Form	Total procedures	Average dose per procedure
Blood volume				^{125}I	RISA		
Blood volume			5	^{51}Cr	Sodium chromate	28	25 μCi
Gastrointestinal protein loss				^{51}Cr	Sodium chromate		
Red blood cell survival or sequestration or both	1	1	1	^{51}Cr	Sodium chromate	1	75 μCi
Cardiac scan				^{113m}In			
Bone scan			38	^{18}F	Sodium fluoride	32	2—3 mCi
Bone metastases	8	6	5	^{32}P	Sodium phosphate	2	2 mCi × 3
Effusions	2	1	1	^{32}P	Colloid chromic	2	10 mCi
Cisternogram				^{111}In	DTPA		
Iron kinetic study	1	1	1	^{59}Fe	Citrate	1	15 μCi
Pancreas scan	1	1	1	^{75}Se	Methionine	1	150 μCi
Effusions				^{198}Au	Colloid		
Schilling test	50	50	50	^{57}Co	Cyanocobaltamine	53	0.5 μCi
Lung perfusion and inhalation				^{113m}In			
Thyroid perchlorate				^{131}I	Iodide		
Liver-lung scan				^{99m}Tc	Sulfur colloid and MAA		
Bone scan	25	39	6	^{85}Sr	Nitrate		100 μCi
Lung scan	118			^{131}I	MAA		200 μCi

Source: Leventhal, L. et al. 1980. "Assessment of Radiopharmaceutical Usage Release Practices by Eleven Western Hospitals," in *Effluent and Environmental Radiation Surveillance,* ed. J. J. Kelly, STP 698, American Society for Testing and Materials, Philadelphia. Reprinted with permission.

Table 1.3. Hospital effluent bolus tests, Run 2

Nuclear medicine procedure:	Brain scan, ^{99m}Tc, pertechnetate
Dose administered:	10 mCi
Time of dose administration:	12:45
Time of excretion:	13:45
Predicted excretion activity:	0.33 mCi
Actual excretion activity:	0.37 mCi

	Volume (L)	Concentration (dpm/L)	Activity (dpm)	Flow rate (L/min)	Time (min)
Urine	0.180	4.38×10^9	7.88×10^8		
Toilet bowl	2.0	3.94×10^8	7.88×10^8		
Flush	5.0	1.58×10^8	7.88×10^8	60.0	0.33
Effluent	1161.	4.62×10^5	5.36×10^8	378.5	3.067
Sample	2.74	4.62×10^6	1.27×10^6	0.89	3.067

Loss factor= 0.68, percent loss = 32%
Dilution factor (avg) = 0.00172
Inverse dilution factor = 580.0
Peak/average = 2.36
Total peak duration = 3.6 min
Volume dilution = 6.3
Turbulence dilution = 92.0

Source: Leventhal, L. et al. 1980. "Assessment of Radiopharmaceutical Usage Release Practices by Eleven Western Hospitals," in *Effluent and Environmental Radiation Surveillance,* ed. J. J. Kelly, STP 698, American Society for Testing and Materials, Philadelphia. Reprinted with permission.

Table 1.4. Summary of procedures evaluated for analysis of radiopharmaceuticals in sewage

	Method principle	
	Treated sewage	Dried sewage sludge
Iodine	Scavenge interferences, reduce to iodide state, precipitate AgI, purify as PdI_2	Caustic fusion, dissolve, extract into CCl_4, purify as PdI_2
Cobalt	Concentrate as hydrous oxide, scavenge acid residue, precipitate basic sulfide, purify as potassium cobaltinitrite	Digest and leach with acid, scavenge acid residue, precipitate basic sulfide, purify as potassium cobaltinitrite
Chromium	Concentrate as hydroxide, extract reduced chromium into ether, back extract into NH_4OH, purify as $BaCrO_4$	Caustic fusion, water leach, hydroxide precipitation, cation exchange concentration, purify as $BaCrO_4$
Strontium	Concentrate as carbonate, precipitate as nitrate, scavenge interferences, purify as $SrCO_3$	Caustic fusion, water leach, carbonate precipitation, concentrate as nitrate, scavenge interferences, purify as $SrCO_3$
Selenium	Concentrate by evaporation, scavenge impurities, reduce with SO_2 to metal, dissolve, purify by reduction to selenium metal	Digest and leach with acid, reduce to +4 state, collect as metal, dissolve, purify by reducing to selenium metal with SO_2

Source: Krieger, H. et al. 1980. "Evaluation of Methodoloy for Quantifying Radiopharmaceuticals in Tertiary-Treated Sewage," in *Effluent and Environmental Radiation Surveillance,* ed. J. J. Kelly, STP 698, American Society for Testing and Materials, Philadelphia. Reprinted with permission.

treated sewage is not normally ingested directly, its use for irrigation purposes may have to be considered; however, most nuclear medicine departments are located in large cities where use of wastewater for irrigation is fairly improbable. The U.S. Environmental Protection Agency report quoted earlier (USEPA 1977) points out that in the United States there has been an average increase in nuclear medicine procedures in excess of 17% per year, and a high proportion (21%) of such procedures are performed on patients under the age of 30. This increase undoubtedly also affects both the occupational exposure and the production of wastes during the manufacture of radiopharmaceuticals (Keyes et al. 1976).

The widespread use of radioimmunoassay procedures, radioactive urine analyses, and other research methods employing labeled organic compounds

has greatly increased the use of liquid scintillation detection units. The organic phosphor solutions, usually based on toluene or xylene, constitute a rather large volume of liquid organic contaminated waste that must be disposed of. Disposal in liquid form is potentially hazardous and environmentally no longer acceptable. For that reason, incineration is preferred, but there are still a number of technical problems to be solved before incineration can be considered an acceptable alternative to present methods of disposal. Since most of the activity involved is long-lived ^{3}H or ^{14}C, both readily diluted in the environment, the impact is ethical and regulatory in nature rather than a major localized source of contamination. However, again, the cumulative activities involved may be substantial.

The final medical use of radionuclides to be covered here concerns the use of plutonium batteries to power cardiac pacemakers. Thousands of people are alive today because pacemakers help their hearts to function. Sealed sources of ^{238}Pu, typically 4 Ci (~150 GBq) in activity, are surgically implanted in the patients. Table 1.5 lists the radiation doses to critical groups associated with such patients (USEPA 1977). (The general population dose value to the U.S. population is probably an invalid extrapolation.) As an environmental source term, concern has been expressed about removal of sources by embalmers, accidental removal, and similar contingencies, but none of these scenarios have much credibility as significant source terms. The encapsulation itself will withstand considerable abuse, even stomach acids (Rundo et al. 1977), so that remobilization into groundwater is highly improbable.

1.5. THE NUCLEAR FUEL CYCLE

One of the primary areas of interest is the environmental impact of nuclear power generation. As public concern and adversary action have spread, the nuclear industry has had to account for the impact not only from power generation itself, but also from all other associated operations. A flowchart for these operations, presented in Fig. 1.7, shows the principal material flow for the nuclear fuel cycle. Because resource conservation and economic considerations have, by and large, favored the recycling of unused uranium fuel and of any plutonium produced, the overall operation listed is usually referred to as the nuclear fuel cycle. Those steps preceding power generation constitute the "front end" and those following it, the "back end" of the fuel cycle. Political considerations, concerned with weapons proliferation and potential diversion of plutonium, have discouraged a closed cycle (i.e., the recycling of uranium and plutonium) in the United States, resulting in an open-ended fuel cycle for commercial power plants, but not for military activities. Other countries, which are poorer in natural resources and therefore unwilling to waste a valuable energy resource, are proceeding with closed-cycle operations. In addition to material flow, energy balance (i.e., fuel cycle total energy input compared to useful

Table 1.5. Radiation doses to critical groups from cardiac pacemakers (assuming 10,000 implanted cardiac pacemakers with plutonium batteries)

Relationship to pacemaker patients	Group population	Individual dose [mrem/(person-year)]			Total dose to group [(person-rem)/year]	
		Dose from pacemaker[a]	Average dose			
			Medical X rays	Natural background radiation	Dose from pacemaker[b]	Natural background radiation
Spouses	6,430	5—7.5	73	102	42	646
Household members	8,950	1—1.5	73	102	12	912
Work associates[c]	72,000	0.1—0.2	73	102	10.5	7,344
Nonwork associates[c]	218,000	0.05—0.1	73	102	14.5	22,378
Total in U.S. populace not included above		<< 0.01	73	102	49	21,400,000
Total dose to U.S. population excluding dose to patients[d]					128	

[a]Dose will vary depending upon the plutonium content, fuel characteristics, and shielding effects of a particular pacemaker model.

[b]Integrated dose using 4 Ci of plutonium, which is the average amount of plutonium used in any battery.

[c]A patient is predicted to associate with about 30 persons during his daily activities.

[d]U.S. population of 210,000,000.

Source: U.S. Environmental Protection Agency 1977. *Radiological Quality of the Environment in the United States*, EPA 520/1-77-009, Washington, D.C.

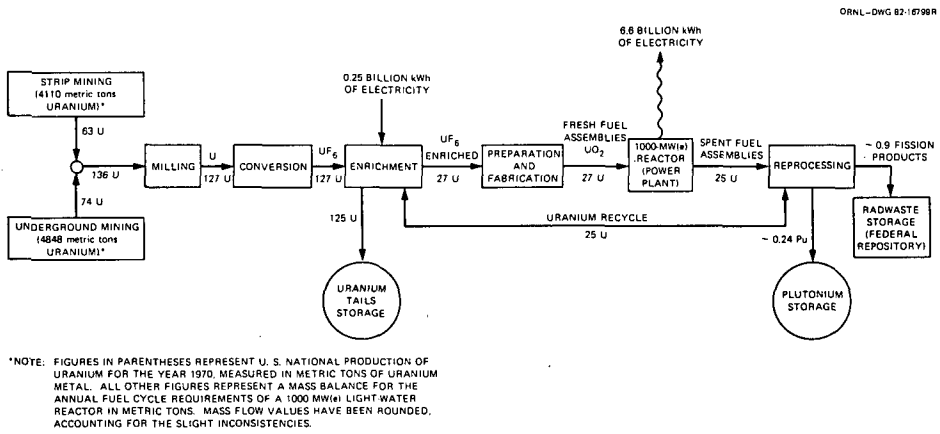

*NOTE: FIGURES IN PARENTHESES REPRESENT U. S. NATIONAL PRODUCTION OF URANIUM FOR THE YEAR 1970, MEASURED IN METRIC TONS OF URANIUM METAL. ALL OTHER FIGURES REPRESENT A MASS BALANCE FOR THE ANNUAL FUEL CYCLE REQUIREMENTS OF A 1000 MW(e) LIGHT-WATER REACTOR IN METRIC TONS. MASS FLOW VALUES HAVE BEEN ROUNDED, ACCOUNTING FOR THE SLIGHT INCONSISTENCIES.

Figure 1.7. The light-water-reactor fuel cycle.

energy output) is an important criterion for power generation flow sheets; for light-water reactors, that energy balance looks very favorable.

Among the various stages of the nuclear fuel cycle, the following have a major potential for injecting radioactive materials into the environment, that is, generating radioactive source terms: (1) mining and milling of uranium ores, leading to liberation of radon and radon daughters, (2) nuclear reactor operations, both from routine effluents and from effluents released following an accident, (3) transportation of spent fuel and high-level wastes, (4) reprocessing of spent fuel and waste treatment, and (5) radioactive waste disposal.

Other stages of the fuel cycle may result in other types of environmental impact, for example, stages involving the consumption of substantial amounts of power (such as fuel enrichment), but these will not be considered here. The operation of central interest is, of course, the generation of power, and this will be considered first.

1.5.1 Nuclear Power Plants

A nuclear power plant generates electricity by converting the energy produced by atomic fission of ^{235}U into high-pressure steam, which in turn drives a turbine generator. Several different types of plants have been devised for this purpose; among them are the gas-cooled reactors [advanced gas-cooled reactor (AGR) and high-temperature gas-cooled reactor (HTGR)], the light-water-cooled reactors [boiling-water reactor (BWR) and pressurized-water reactor (PWR)], and the heavy-water-moderated reactors [heavy-water reactor (HWR) and Canadian deuterium-uranium (CANDU) reactor]. Figure 1.8 illustrates schematically some of these types of steam-generating plants. They differ mainly in the method of steam generation, the neutron moderator, and the ^{235}U content of the fuel (natural or enriched).

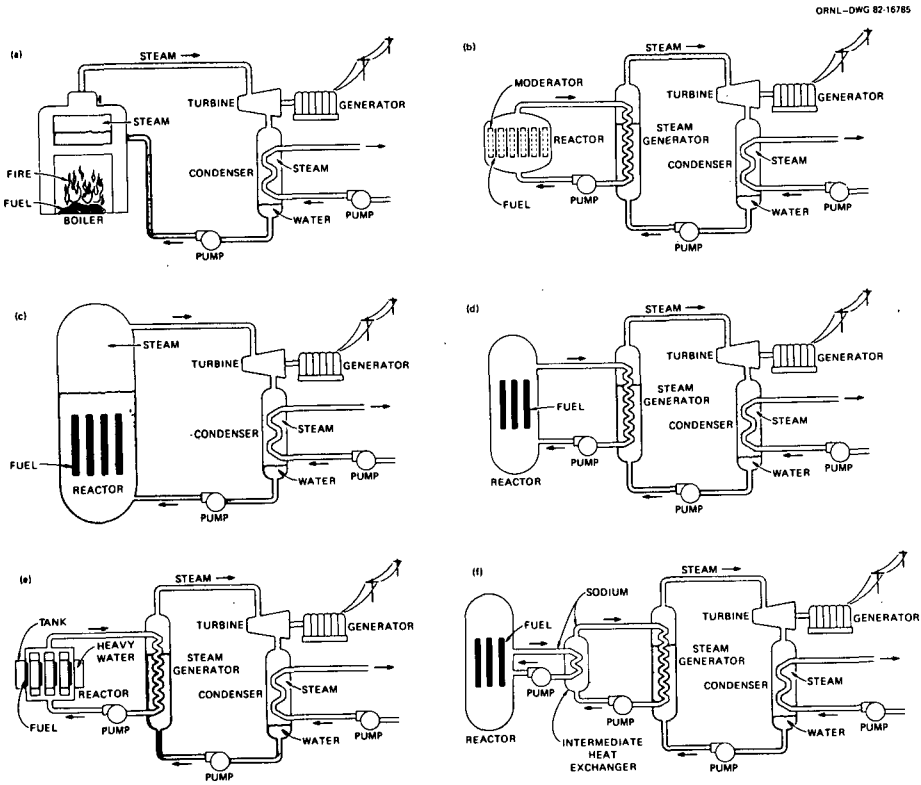

Figure 1.8. Schematic diagrams of the principal types of steam-generating plants: (a) fossil fuel plant, (b) gas-cooled reactor, (c) boiling-water reactor, (d) pressurized-water reactor, (e) heavy-water reactor, (f) liquid-metal-cooled fast breeder reactor (LMFBR).

In assessing the environmental impact of a nuclear power plant, one is mainly concerned with the heat rejected (typically about 66% of the energy produced initially), the protection of plant personnel against radiation, any radioactive waste and spent fuel shipped from the plant, and any radioactive materials released to the environment in the airborne and liquid effluent streams. It is mainly the last of these that is of interest here. Because most of the operating reactors in the United States are light-water reactors of the boiling-water or pressurized-water types, attention is focused on these two types.

By reference to Fig. 1.8(d), it is seen that PWRs operate with two coolant loops, the primary one filled with water at pressure, though below the critical point, which circulates through the hot reactor core, cooling it and conducting the heat away, and the secondary one, in which steam is generated in the

steam generator, passed to the turbine, and condensed back to water in the externally cooled condenser. In the BWR [Fig. 1.8(c)], steam is produced inside the reactor vessel, passed directly to the turbine, and then condensed to water, all in a single loop. This difference has the consequence that any active contaminants in the core coolant remain confined to the reactor building in the PWR, whereas they travel through the turbine in the BWR and may be present in any steam release. On the other hand, in the PWR some efficiency may be lost in the heat exchanger, and metallurgical difficulties have arisen with some steam generator designs. Careful control must be kept on coolant water chemistry, pH, trace impurities, corrosion products, and chemical products of the radiolytic decomposition of the water. The hot analytical samples withdrawn from the primary coolant at intervals constitute one component of contaminated liquid that must be treated as radioactive waste. Table 1.6 lists some representative operating parameters and conditions used in calculating releases of radioactive material in liquid and gaseous effluents from a PWR (USNRC 1978).

As the ^{235}U in the fuel undergoes fission, two new atoms (or fission products) appear in the fuel for each uranium atom destroyed. Since the fuel elements are encased in Zircaloy cladding, these fission products normally have no option but to stay in the fuel, although they may diffuse through the fuel to the fuel-cladding interface or may coalesce to form gas bubbles, both of which may cause swelling or distortion of the fuel. The fission-product inventory in the fuel will build up as fuel burnup proceeds; the shorter-lived fission products will reach equilibrium concentrations between production rate by fission and decay rate, while the longer-lived ones will keep increasing their concentration. This fission-product inventory is Source Term I for any migration model (see Fig. 1.9).

The precise distribution and mobility of the various fission products within the fuel pellets depends on the operational history, the temperature distribution within the fuel, and the chemical state of each fission product within the UO_2 environment. As burnup proceeds, the UO_2 pellet degrades mechanically due to swelling, which accompanies the appearance of the fission products as interstitial impurities, fast-neutron-induced radiation damage, hydrogen and helium embrittlement, variations in the radial temperature gradient as the conductivity is affected by structural changes and impurity buildup, and lattice changes resulting from stoichiometry changes due to a changing U/O ratio in the fuel matrix. Some elements, such as the noble gases, hydrogen (both ^{1}H and ^{3}H), and the more volatile elements, may migrate by diffusion, recoil effects, or along fracture cracks to the pellet-cladding interface. Other elements remain chemically bound in the UO_2 or are less mobile under prevailing temperatures. Some of them may, in fact, migrate toward the hotter region at the pellet center. It is the mobile nuclides at the fuel-pellet interface that are of prime interest, since they are the ones most likely to escape from the fuel elements.

Table 1.6. Principal parameters and conditions used in calculating releases of radioactive material in liquid and gaseous effluents from San Onofre Nuclear Generating Station, Units 2 and 3

Reactor power level [MW(t)]	3600
Plant capacity factor	0.80
Failed fuel (%)	0.12[a]
Primary system:	
Mass of coolant (lb)	5.6×10^5
Letdown rate (gal/min)	40
Shim bleed rate (gal/d)	1×10^3
Leakage to secondary system (lb/d)	100
Leakage to containment building	*b*
Leakage to auxiliary building (lb/d)	160
Frequency of degassing for cold shutdowns (per year)	2
Secondary system:	
Steam flow rate (lb/h)	1.5×10^7
Mass of liquid in steam generator (lb)	1.7×10^5
Mass of steam in steam generator (lb)	1.2×10^4
Secondary coolant mass (lb)	2.2×10^6
Rate of steam leakage to turbine building (lb/h)	1.7×10^3
Containment building volume (ft^3)	2×10^6
Annual frequency of containment purges, during shutdown	4
Annual frequency of containment purges, at power	20
Iodine partition factors, gas/liquid:	
Leakage to auxiliary building	0.0075
Leakage to turbine building	1.0
Main condenser/air ejector, volatile species	0.15

Liquid radwaste system decontamination factors

	Coolant radwaste system	Miscellaneous liquid-waste system	Chemical-waste system
I	1×10^5	1×10^3	1×10^4
Cs, Rb	2×10^5	2×10^1	1×10^5
Others	1×10^6	1×10^3	1×10^5

Table 1.6 (continued)

Liquid radwaste system decontamination factors

	All nuclides except iodine	Iodine
Radwaste evaporator DF	10^4	10^3
Coolant radwaste system evaporator DF	10^3	10^2

	Anions	Cs, Rb	Other nuclides
Boron recycle feed demineralizer DF, H_3BO_3	10	2	10
Primary coolant letdown demineralizer DF, Li_3BO_3	10	2	10
Evaporator condensate polishing demineralizer, H^+OH^-	10	10	10
Mixed-bed radwaste demineralizer	10^2	2	10^2
Steam generator blowdown demineralizer	10^2	10	10^2
Containment building internal recirculation system charcoal filter DF, iodine removal			10
Main condenser air-removal system charcoal bed DF, iodine removal			10

[a]This value is constant and corresponds to 0.12% of the operating power fission product source term, as given in NUREG-0017 (April 1976).

[b]One percent per day of the primary coolant noble gas inventory and 0.001% per day of the primary coolant iodine inventory.

Source: U.S. Nuclear Regulatory Commission 1978. *Draft Environmental Statement Relating to Operation of San Onofre Nuclear Generating Stations, Units 2 and 3*, NUREG-0490, Washington, D.C.

Various computer codes, such as CINDER, ORIGN, RIBD and others, have been developed to predict the escape probability from the fuel to the gap below the cladding as a function of fuel history, thermal cycling, and operating conditions. Similarly, attempts have been made, with varying success, to predict burnup damage to fuel materials.

The integrity of the Zircaloy cladding presents the major barrier in containing the fission products within the fuel elements. The cladding thickness typically is only of the order of 0.024–0.034 in. (0.61–0.86 mm), so it is subject to appreciable stress as the fuel swells and fission gas builds up beneath it.

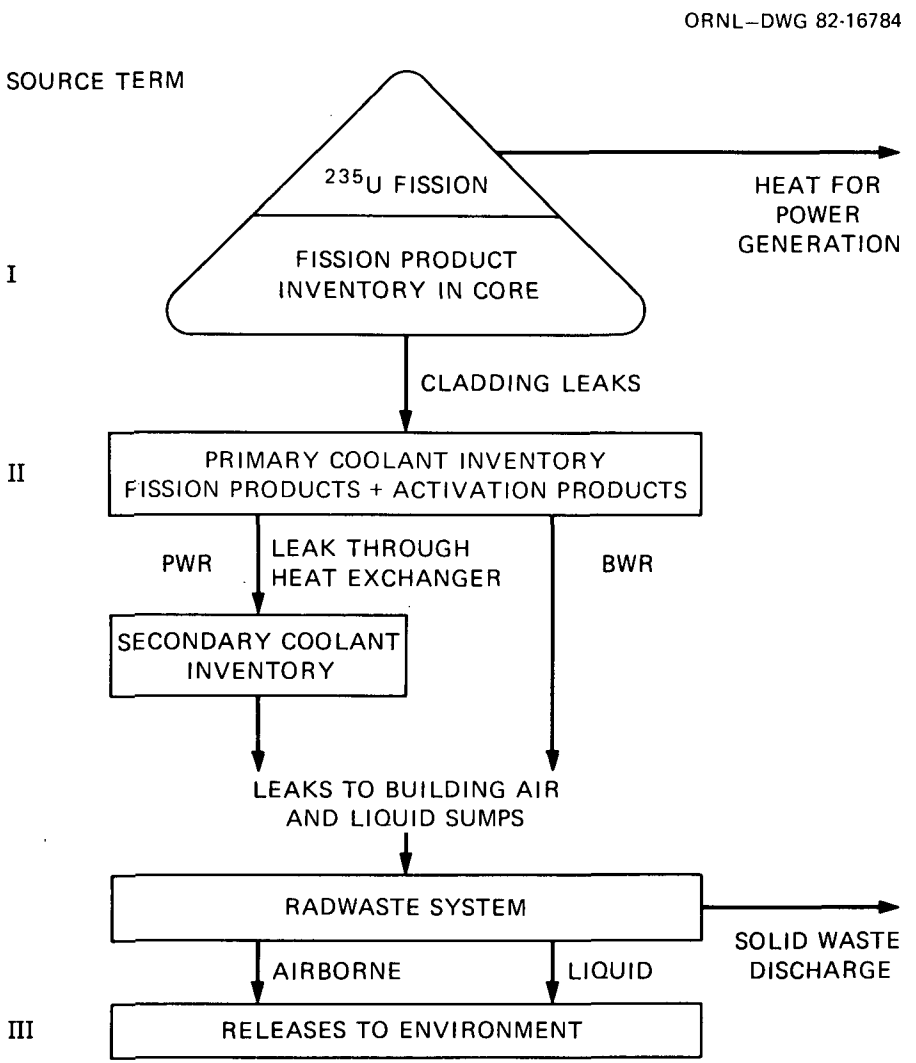

Figure 1.9. Source generation sequence.

As burnup proceeds, or because of some minor flaws in manufacture, small cracks may develop in the cladding, permitting some of the gaseous fission products and some of the less tightly bound nuclides that are "released" from the fuel to leak into the primary coolant. This leak rate again depends on a variety of factors: the operating temperature of the fuel, the extent of radiation damage in the cladding, stress corrosion effects, fatigue-induced growth of microcracks as the fuel undergoes thermal cycling, and gas embrittlement from

hydrogen and helium diffusing into or through the cladding. Stainless steel is more susceptible to hydrogen, and therefore tritium, diffusion than the Zircaloys, and this was one of the major factors favoring the choice of the latter as cladding materials in thermal-neutron reactors. Other conditions that may lead to cladding failure result from uneven positioning of the fuel pellets, fuel densification, nonuniform cooling effects around supporting grids, blister formation, and creasing or grooving resulting from imperfections in rolling or extrusion processes.

To some extent, such faults must be expected, even with tight quality control during manufacture, and the release of a limited amount of fission products to the coolant has to be accepted. Depending on plant specifications, the reactor may be operated with up to 0.25 to 1% of the fuel elements having such minor cracks, as determined by monitoring the activity in the primary coolant. For purposes of estimating routine environmental impact, it is assumed that all fuel elements will have such a failure rate. Similarly, one has to expect finite but limited diffusion of tritium through the cladding.

In addition to radionuclides leaking into the coolant because of cladding imperfections, there are a number of radionuclides that originate in the coolant itself. These represent three groups of impurities: (1) activated corrosion products, which are produced by the corrosive and erosive action of the circulating coolant along the entire pipe run and activated during their passage through the neutron flux in the core; (2) activated impurities in the water itself due to miscellaneous dilute impurities normally present in water, such as calcium, magnesium, manganese, and iron; and (3) those arising from additives introduced for pH control and water quality control.

Activation products formed by neutron activation of corrosion products from all of the loop materials involve mainly the $^{54}Fe(n,\gamma)^{55}Fe$, $^{50}Cr(n,\gamma)^{51}Cr$, $^{58}Ni(n,p)^{58}Co$, $^{59}Co(n,\gamma)^{60}Co$, and $^{56}Fe(n,t)^{54}Mn$ reactions. The relative importance of the activation products depends, of course, on the composition of the pipe materials employed. The buildup of leaked fission products and activitation products is controlled by passing part of the coolant through a demineralizer bed, where soluble ions are removed by ion exchange. Noble gases are obviously not removed by ion exchange and tend to dominate the coolant inventory (see Table 1.7). The data in Table 1.7 are estimated maximum concentration values for a "representative" PWR and are listed primarily as an indication of the relative concentrations of some of the major radionuclides. The detailed numbers would depend on the reactor design, its mode of operation, capacity factor, flux conditions, and structural materials in the coolant loop. For the case listed, a primary coolant mass of 5.6×10^5 lb (2.54×10^5 L) would represent a total inventory of roughly $200 \times 2.534 \times 10^2 = 50{,}800$ Ci $= 1.88 \times 10^{15}$ Bq. This quantity represents Source Term II in Fig. 1.9 and is the usual departure point for many calculations. To some extent this term can be reduced by a suitable choice of pipe materials and efficient demineralizer operation.

Table 1.7. Predicted reactor coolant inventory of fission products and corrosion products [1000-MW(e) PWR at 578°F][a]

Noble gas fission products		Fission products	
Isotope	μCi/mL	Isotope	μCi/mL
^{85}Kr	1.11	^{84}Br	3.0×10^{-2}
^{85m}Kr	1.46	^{88}Rb	2.56
^{87}Kr	0.87	^{89}Rb	6.7×10^{-2}
^{88}Kr	2.58	^{89}Sr	2.52×10^{-3}
^{133}Xe	1.74×10^{2}	^{90}Sr	4.42×10^{-5}
^{133m}Xe	1.97	^{90}Y	5.37×10^{-5}
^{135m}Xe	0.14	^{91}Y	4.77×10^{-4}
^{138}Xe	0.36	^{92}Sr	5.63×10^{-4}
		^{92}Y	5.54×10^{-4}
Total noble gases	187.3[b]	^{95}Zr	5.04×10^{-4}
		^{95}Nb	4.70×10^{-4}
		^{99}Mo	2.11
		^{131}I	1.55
Corrosion Products		^{132}Te	0.17
		^{132}I	0.62
Isotope	μCi/mL	^{133}I	2.55
		^{134}Te	2.2×10^{-2}
^{54}Mn	4.2×10^{-3}	^{134}I	0.39
^{56}Mn	2.2×10^{-2}	^{134}Cs	7.0×10^{-2}
^{58}Co	8.1×10^{-3}	^{135}I	1.4
^{59}Fe	1.8×10^{-3}	^{136}Cs	0.33
^{60}Co	1.4×10^{-3}	^{137}Cs	0.43
		^{138}Cs	0.48
		^{144}Ce	2.3×10^{-4}
Total corrosion products	3.7×10^{-2}	^{144}Pr	2.3×10^{-4}
		Total fission products	12.8[b]

[a]Contamination concentration corresponding to 1% failed fuel near end of fuel life.

[b]187.3 μCi/mL = 6.9 GBq/L; 12.8 μCi/mL = 0.47 Bq/L.

Source: Eichholz, G. G. 1977. *Environmental Aspects of Nuclear Power*, Ann Arbor Science Publishers, Ann Arbor, Mich. Reprinted with permission.

Because gaseous elements can escape relatively more readily from the primary coolant in a BWR, the noble gas inventory in the primary coolant of a BWR tends to be lower (Table 1.8). This implies, in turn, that the routine release of noble gases to the environment from BWRs tends to be substantially higher than that from PWRs. As Table 1.8 shows, the noble gas inventory in the PWR primary coolant can also be affected by periodic control tank purges.

Table 1.8. Concentrations of gaseous fission products in PWR and BWR primary coolants

Nuclide	Half-life	PWR (μCi/mL)[a]	PWR (μCi/mL)[b]	BWR (μCi/mL)
^{83m}Kr	1.86 h	5.5×10^{-2}	5.3×10^{-2}	1.2×10^{-3}
^{85m}Kr	4.4 h	2.9×10^{-1}	2.7×10^{-1}	1.9×10^{-3}
^{85}Kr	10.74 y	2.0×10^{-1}	3.1×10^{-2}	9.7×10^{-6}
^{87}Kr	76 min	1.6×10^{-1}	1.6×10^{-1}	5.7×10^{-3}
^{88}Kr	2.79 h	5.1×10^{-1}	4.9×10^{-1}	6.1×10^{-3}
^{89}Kr	3.18 min	1.2×10^{-2}	1.2×10^{-2}	2.4×10^{-2}
^{131m}Xe	11.96 d	2.3×10^{-1}	6.6×10^{-2}	8.4×10^{-6}
^{133m}Xe	2.26 d	5.4×10^{-1}	3.1×10^{-1}	1.2×10^{-4}
^{133}Xe	5.27 d	4.1	1.6	3.3×10^{-3}
^{135m}Xe	15.7 min	3.4×10^{-2}	3.4×10^{-2}	1.0×10^{-2}
^{135}Xe	9.16 h	8.5×10^{-1}	7.5×10^{-1}	9.6×10^{-3}
^{137}Xe	382 min	2.5×10^{-2}	2.5×10^{-2}	4.1×10^{-2}
^{138}Xe	14.2 min	1.2×10^{-1}	1.2×10^{-1}	3.2×10^{-2}
Total noble gases		7.1	3.9	1.3×10^{-1}
^{131}I	8.04 d	7.1×10^{-1}	5.6×10^{-1}	5.4×10^{-3}
^{133}I	208.8 h	8.6×10^{-1}	7.4×10^{-1}	3.1×10^{-2}

[a] Without volume control tank purge.
[b] With volume control tank purge.

Source: U.S. Environmental Protection Agency 1973. *Environmental Analysis of the Uranium Fuel Cycle, Part II: Nuclear Power Reactors,* EPA-520/9-73-0003c, Washington, D.C.

Not included in Table 1.7 are two other activation products of importance. The first is ^{16}N, produced by the $^{16}O(n,p)^{16}N$ reaction in the coolant water. Nitrogen-16 has a 7-s half-life, emits a 7-MeV gamma ray, and is of importance principally for its direct radiation effects on plant personnel and plant equipment, especially in BWRs, where the coolant loop carries it right through the turbine system. It is too short-lived to be of importance in plant effluents.

The other major radioactive material in the coolant is tritium, especially in PWRs, where boric acid is added to the primary coolant as a soluble reactivity control ("chemical shim"). The boron undergoes, among others, a $^{10}B(n,2\alpha)^{3}H$ reaction, which leads to substantial concentrations of tritium in the coolant. In addition, ^{3}H is produced by ternary fission in the fuel and, in BWRs, by the use of LiOH for pH control via the $^{6}Li(n,\alpha)^{3}H$ reaction. As a consequence, substantial amounts of tritium must be included in Source Term II (NCRP 1979). Attempts are made in some plants to hold tritium concentrations below 2.5 μCi/mL (92.5 MBq/L). Table 1.9 shows estimated maximum concentra-

Table 1.9. Radioactivity concentrations in the steam generators (secondary system)[a]

Isotope	Concentrations (μCi/g)	Isotope	Concentrations (μCi/g)
^{54}Mn	0.26×10^{-6}	^{134}Te	0.98×10^{-7}
^{56}Mn	0.13×10^{-5}	^{131}I	0.20×10^{-3}
^{58}Co	0.85×10^{-5}	^{133}I	0.19×10^{-3}
^{60}Co	0.26×10^{-6}	^{134}I	0.25×10^{-5}
^{59}Fe	0.35×10^{-6}	^{135}I	0.53×10^{-4}
^{51}Cr	0.31×10^{-6}	^{133m}Xe	0.25×10^{-7}
^{84}Br	0.12×10^{-6}	^{133}Xe	0.22×10^{-5}
^{85m}Kr	0.17×10^{-7}	^{135m}Xe	0.94×10^{-7}
^{85}Kr	0.37×10^{-7}	^{135}Xe	0.56×10^{-7}
^{87}Kr	0.98×10^{-8}	^{138}Xe	0.54×10^{-8}
^{88}Kr	0.29×10^{-7}	^{134}Cs	0.18×10^{-4}
^{88}Rb	0.57×10^{-5}	^{136}Cs	0.12×10^{-4}
^{89}Rb	0.13×10^{-6}	^{137}Cs	0.90×10^{-4}
^{89}Sr	0.32×10^{-6}	^{138}Cs	0.25×10^{-5}
^{90}Sr	0.96×10^{-8}	^{137m}Ba	0.84×10^{-4}
^{91}Sr	0.60×10^{-7}	^{140}Ba	0.35×10^{-6}
^{90}Y	0.11×10^{-7}	^{140}La	0.19×10^{-6}
^{91m}Y	0.17×10^{-7}	^{144}Ce	0.24×10^{-7}
^{91}Y	0.47×10^{-6}	^{144}Pr	0.24×10^{-7}
^{99}Mo	0.37×10^{-3}	Tritium	0.29×10^{-3}
^{99m}Tc	0.24×10^{-3}		
^{99}Tc	0.26×10^{-11}		
^{132}Te	0.19×10^{-4}		

[a]Based on 0.25% failed fuel, 110 lb/h primary-to-secondary leak rate, 30 gal/min per unit blowdown rate, tritium concentration of 2.5 μCi/mL in primary system.

Source: Tennessee Valley Authority 1974. *Final Environmental Statement, Sequoyah Nuclear Plants Units 1 and 2,* Chattanooga, Tenn.

tions of activity in the secondary coolant loop of a PWR, assuming 0.25% failed fuel and a 110-lb/h (50-kg/h) leak rate across the heat exchanger (TVA 1974).

Some of the contained trace radionuclides may escape from the primary and/or secondary coolant loops with any water leak or steam release. Such release paths include pressurizers, air ejectors, steam valves, gland seals, turbine seals and any other dripping pipes. The gaseous and volatile components end up in the containment vessel atmosphere; the liquids go to various floor drains, sumps, and retention tanks. The "Radwaste" system is designed to extract and retain as much of this residual activity as possible so that the amount finally released from the plant to the environment can be described to be "as low as reasonably achievable" (ALARA). This criterion is a major objective in nuclear plant operations.

The transfer of radioactive materials from the coolant system to the containment building air and waste-water system will depend on the chemical forms, the existing or presumed leak rates, and the means of purging the air or water lines. These factors will vary from plant to plant with the specific layout and equipment employed and will also differ for routine operations, maintenance conditions, and a range of accident scenarios short of the design-basis accident.

The gaseous component will contain primarily noble gases (xenon, krypton, helium), hydrogen (HT), ^{16}N, with too short a lifetime to make a significant contribution beyond the coolant system itself, the halogens (I_2, CH_3I, and Br_2) and some semivolatiles, such as RuO_4, Cs, and fine particulates carrying fission products. Of these, the fate of airborne iodine has attracted the greatest attention, since it may give rise to the limiting environmental exposure under accident conditions. Much of the iodine would be expected to interact with exposed metal surfaces inside the containment or converted to soluble forms in the presence of steam or water vapor and thus end up in the liquid radwaste stream. Similarly, most of the HT should be converted to HTO by means of catalytic converters to minimize buildup of explosive mixtures of oxygen and hydrogen in the radwaste system. Table 1.6 (USNRC 1978) indicates some of the assumptions for leak rates and iodine partition factors made for the San Onofre plant. It is important to remember that the noble gas activity released anywhere is typically 10^6 to 10^7 times higher than the iodine activity.

The liquid component receives contaminated water from leaks in pumps, valves, gaskets, etc., as well as from the mopping or hosing down of floors and from laboratory drains. Table 1.10, for the Bellefonte Nuclear Plant (USAEC 1974), gives the quantities involved per year for two reactors.

1.5.2 Radwaste Treatment Systems

The function of the radwaste system is to reduce the residual activity in air streams and liquids to be released to the environment to as low a level as is

Table 1.10. Radioactive liquid waste quantities

Waste source	Quantity (dual plant) (ft^3/y)	Assumptions and comments
Tritiated waste		
Miscellaneous system leakage	5,800	5-gal/h leakage
Sluicing of ion exchange resins	2,800	14 transfers per year at 200 ft^3 each
Regeneration of deborating demineralizers	18,200	14 regenerations per year at 1,300 ft^3 each
Sampling and laboratory drains	4,700	20 samples per day at 5 gal per sample
Filter backwash	1,200	20 backwashes per year at 30 ft^3 each
Subtotal	32,700	All tritiated waste recycled
Nontritiated waste		
Miscellaneous system leakage	5,800	5-gal/h leakage
Spent fuel cask decontamination	50,000	30 decontaminations per year at 1,600 ft^3 each
Sample drains	1,100	4 samples per day at 5 gal per sample
Subtotal	56,900	
Chemical waste		
Laboratory drains	5,800	
Decontamination drains	1,000	500 items at 2 ft^3 each
Subtotal	6,800	
Detergent wastes		
Laundry drains	28,800	600 gal/d
Shower and sink drains	28,800	20 showers per day at 30 gal each
Subtotal	57,600	
Total liquid discharged	121,300	(Sum of nontritiated, chemical, and detergent wastes)

Source: U.S. Atomic Energy Commission 1974. *Draft Environmental Statement: Bellefonte Nuclear Plant,* Docket Nos. 50-438/439, Washington, D.C.

practical and can be justified by cost-benefit analysis (USNRC 1976b). The degree of effectiveness of such treatment will depend on the condition of the liquids, their impurity content, their hardness ("clean" or "dirty") and organic content, their pH and temperature, and the possible presence of complexing reagents. Typically, all contaminated liquid waste streams are stored and allowed to decay for some time to remove short-lived nuclides, filtered to remove suspended solids and flocculants, and purified in a demineralizer. Residual materials are then removed by evaporators or centrifuge, with the evaporator bottoms, filters, and spent demineralizer resins constituting a major part of the solid waste being shipped from the plant. Figure 1.10 shows a typical flow sheet for such a system. The decontamination factors (DFs) obtained for such a system depend on the above-listed parameters and must be known to be included in any modification of the source term prior to release of the remaining liquid as an "effluent" to any receiving stream. This release is usually done by adding it to the outgoing flow of condenser cooling water.

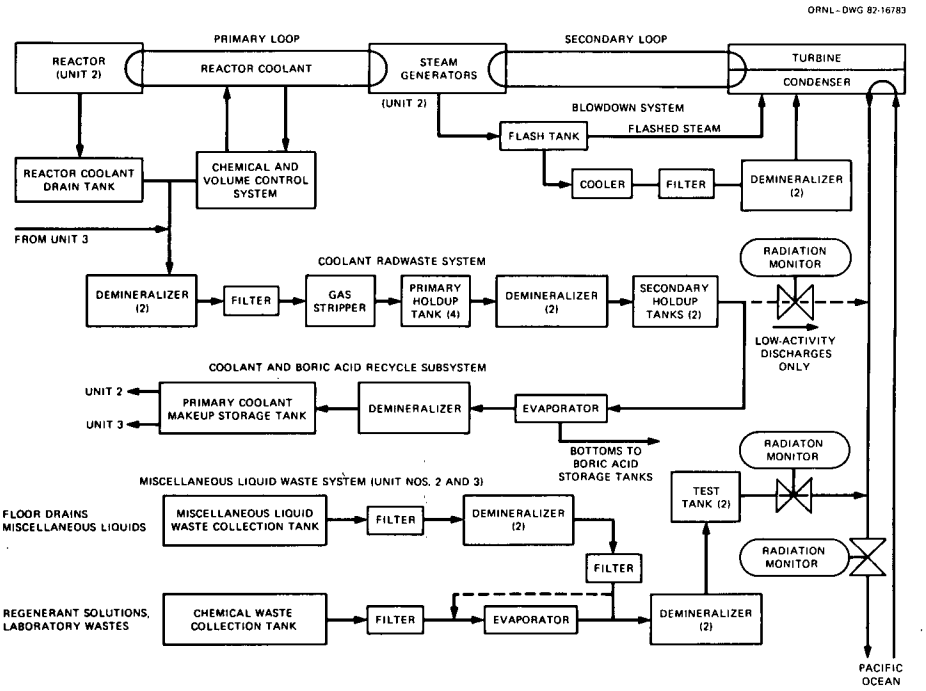

Figure 1.10. Radioactive liquid waste treatment systems at San Onofre Nuclear Generating Station, Units 2 and 3. Source: U.S. Nuclear Regulatory Commission 1978. *Draft Environmental Statement Related to Operation of San Onofre Nuclear Generating Stations, Units 2 and 3,* NUREG-0490, Washington, D.C.

The DFs obtainable with standard radwaste systems have been substantially improved, partly under the impetus of the decontamination problems resulting from the accident at Three Mile Island. Nevertheless, it is important to stress that there is a practical limit set to the complexity and elaboration of such systems by considerations of plant reliability, maintainability, and cost-effectiveness. This is particularly evident for ion-exchange demineralizers, where the DF depends greatly on temperature, "cleanness" of the water (i.e., the presence of interfering ions), and the use cycle, and for charcoal beds and delay line systems for the retention of noble gases. For most operational systems, the DF values quoted are found to be based on small-scale laboratory tests that are not necessarily representative of plant-scale operations.

Since tritium is not affected by any of the common radwaste treatment methods, a decision must be made as to whether to release it all under highly diluted conditions or to recycle it with purified water to use as makeup water for the primary coolant. Figure 1.11 shows a flow sheet for the latter option (TVA 1974). As a consequence of the Three Mile Island accident, free release of tritium-contaminated water has been severely restricted in some states, even for low concentrations.

The airborne component is less easily handled. For one thing, not all of it can be contained at any given moment the way liquids can be stored. All that

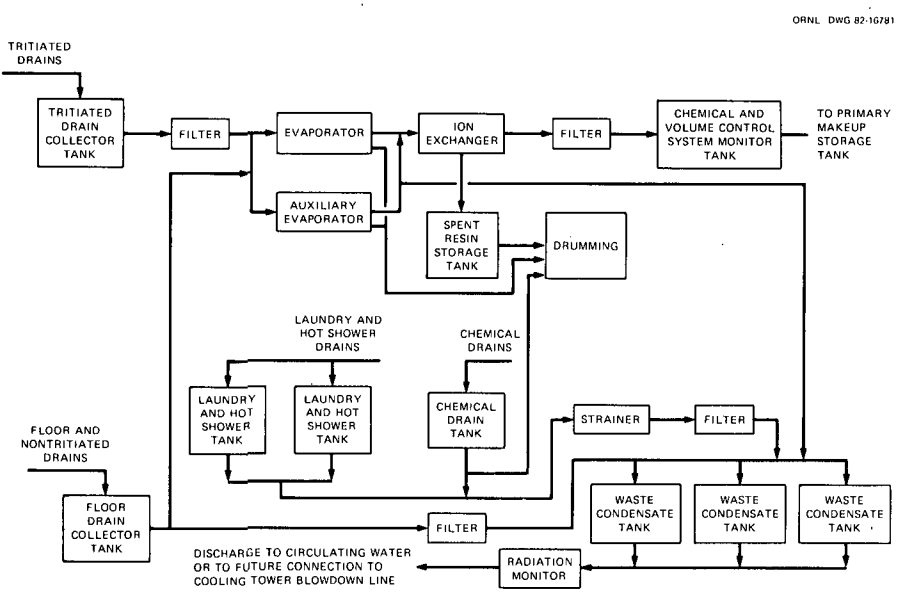

Figure 1.11. Liquid radwaste, tritium recycle system—Sequoyah Nuclear Plant. Source: Tennessee Valley Authority 1974. *Final Environmental Statement, Sequoyah Nuclear Plants, Units 1 and 2,* Chattanooga, Tenn.

can be done is to purify the containment building air routinely and bleed off a certain fraction for radwaste treatment and final release. To minimize the chance of hydrogen explosions, catalytic recombiners are commonly used to convert free H_2, and hence HT, into water, which is then added to the liquid waste stream. To reduce noble gas activity, the air is pumped slowly through delay tanks with residence times from 30 min to 1–3 d. This removes the bulk of the active xenon and krypton isotopes by decay, leaving mainly some of the 5-d ^{133}Xe and all of the 10-y ^{85}Kr. The air is then passed through a filter bed, consisting of a prefilter, a charcoal bed, and an absolute filter, to remove particulates and volatile elements; a refrigerated charcoal filter or freon absorber may be added to remove noble gases. Figures 1.12 and 1.13 show simplified flow sheets for typical BWR and PWR gaseous waste systems.

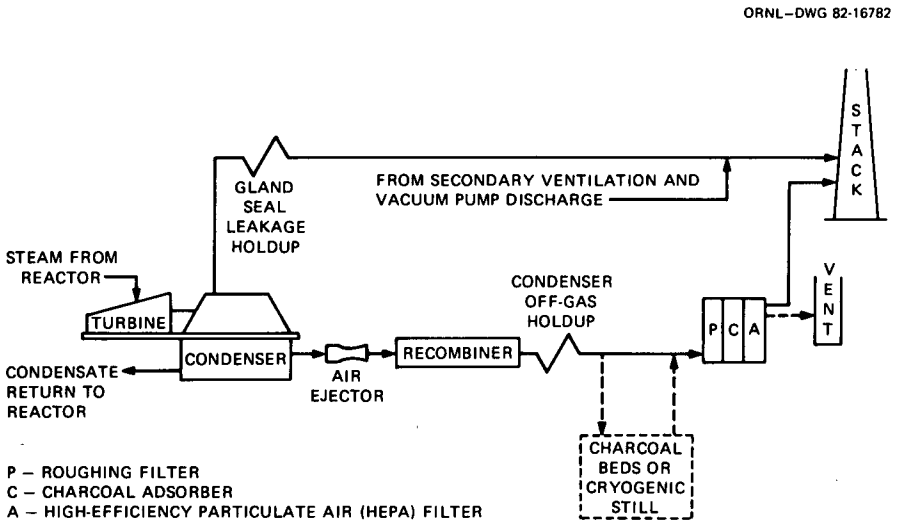

Figure 1.12. BWR gaseous waste system. Source: U.S. Atomic Energy Commission 1973. *The Safety of Nuclear Power Reactors (Light-Water-Cooled) and Related Facilities,* WASH-1250, Washington, D.C.

Additional difficulties arise for iodine because some of it, perhaps 10%, may be in organic form, such as CH_3I. As Table 1.6 indicates, this affects the partition coefficients between liquid and gaseous phases, and also affects the DF values for charcoal bed adsorption and ion exchange removal. It is also important in estimating accident consequences, since ^{131}I may represent the critical nuclide (Eichholz 1977; USNRC 1975), though there has been some reevaluation of this aspect following the Three Mile Island accident. Impregnated charcoal and silver zeolite are used to reduce iodine releases.

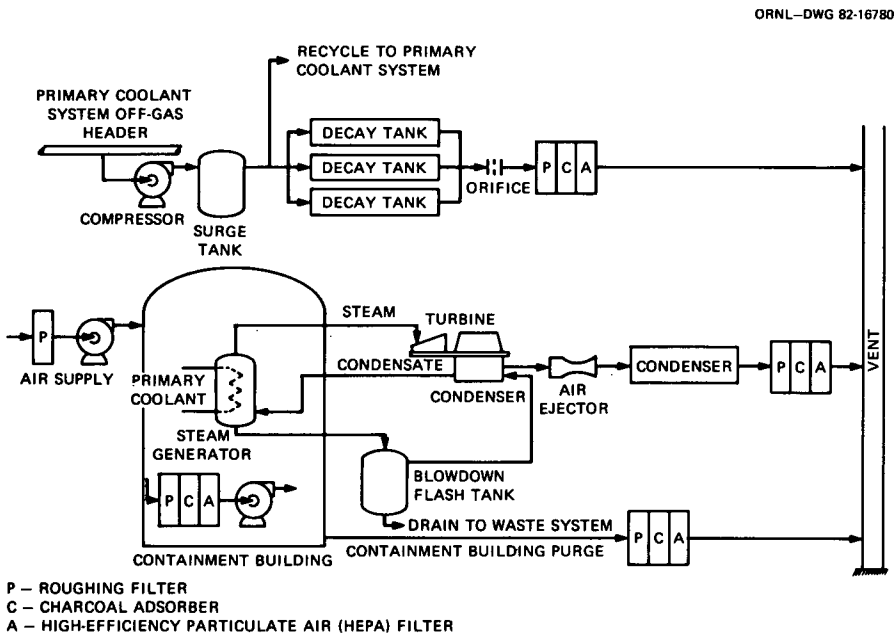

Figure 1.13. PWR gaseous waste system. Source: U.S. Atomic Energy Commission 1973. *The Safety of Nuclear Power Reactors (Light-Water-Cooled) and Related Facilities,* WASH-1250, Washington, D.C.

After radwaste treatment, the remaining streams should be pure enough to meet the ALARA criterion for release to the environment, either continuously or in batches. Table 1.11 indicates the order of magnitude of these releases, on an annual basis, as calculated for one plant with conservative assumptions (TVA 1974). This constitutes the final source term—Source Term III—for any environmental dispersion calculations. Note that the gaseous releases for that plant are dominated by xenon and krypton, on the order of kilocuries per year, and by tritium; tritium also far and away predominates in liquids, with only fractional curie quantities for all other radionuclides, amounts that are trivial in comparison to the releases of radiopharmaceuticals mentioned earlier. Actual releases vary enormously—even for the same plant, from year to year, and among nominally similar plant designs—depending on operating conditions, fuel conditions, and maintenance problems. Tables 1.12 and 1.14 from a 1977 UNSCEAR report and Table 1.13 from a more recent report (Tichler and Benkovitz 1981) show the kind of variations found and the degree to which the ALARA levels could be maintained for just two effluent components. More extensive tables will also be found in the UNSCEAR report and in Tichler and Benkovitz (1981).

Table 1.11. Annual liquid and gaseous release by isotopes[a] (Two units—0.25% failed fuel)

Isotope	Liquid release (Ci)	Gaseous release (Ci)
^{84}Br	0.329×10^{-4}	0.786×10^{-5}
^{85}Kr	0.0	$0.312 \times 10^{+4}$
^{85m}Kr	0.0	$0.425 \times 10^{+2}$
^{87}Kr	0.0	$0.200 \times 10^{+2}$
^{88}Kr	0.0	$0.608 \times 10^{+2}$
^{88}Rb	0.149×10^{-2}	0.839×10^{-4}
^{89}Rb	0.328×10^{-4}	0.509×10^{-4}
^{89}Sr	0.135×10^{-2}	0.410×10^{-6}
^{90}Sr	0.531×10^{-4}	0.146×10^{-7}
^{91}Sr	0.393×10^{-4}	0.208×10^{-7}
^{90}Y	0.397×10^{-4}	0.191×10^{-7}
^{91}Y	0.226×10^{-2}	0.683×10^{-6}
^{92}Y	0.583×10^{-5}	0.428×10^{-8}
^{95}Zr	0.308×10^{-3}	0.889×10^{-7}
^{95}Nb	0.333×10^{-3}	0.892×10^{-7}
^{99}Mo	$0.530 \times 10^{+0}$	0.216×10^{-3}
^{132}Te	0.307×10^{-1}	0.127×10^{-4}
^{134}Te	0.324×10^{-4}	0.635×10^{-7}
^{129}I	0.0	0.0
^{131}I	$0.510 \times 10^{+0}$	0.647×10^{-2}
^{132}I	0.539×10^{-1}	0.247×10^{-2}
^{133}I	$0.158 \times 10^{+0}$	0.293×10^{-2}
^{134}I	0.603×10^{-2}	0.955×10^{-3}
^{135}I	0.280×10^{-1}	0.755×10^{-3}
^{133m}Xe	0.0	$0.111 \times 10^{+3}$
^{133m}Xe	0.0	$0.613 \times 10^{+2}$
^{133}Xe	0.0	0.602×10^{-4}
^{135}Xe	0.0	$0.157 \times 10^{+3}$
^{135m}Xe	0.0	$0.143 \times 10^{+3}$
^{138}Xe	0.0	$0.669 \times 10^{+1}$
^{134}Cs	0.994×10^{-1}	0.279×10^{-4}
^{136}Cs	0.363×10^{-1}	0.115×10^{-4}
^{137}Cs	$0.502 \times 10^{+0}$	0.140×10^{-3}
^{138}Cs	0.670×10^{-3}	0.577×10^{-5}
^{140}Ba	0.108×10^{-2}	0.363×10^{-6}
^{140}La	0.618×10^{-3}	0.314×10^{-6}
^{144}Ce	0.720×10^{-4}	0.355×10^{-7}
^{144}Pr	0.672×10^{-4}	0.357×10^{-7}
^{51}Cr	0.114×10^{-2}	0.337×10^{-6}
^{54}Mn	0.116×10^{-2}	0.316×10^{-6}
^{56}Mn	0.944×10^{-3}	0.491×10^{-6}
^{59}Fe	0.136×10^{-2}	0.392×10^{-6}

Table 1.11 (continued)

Isotope	Liquid release (Ci)	Gaseous release (Ci)
^{58}Co	0.348×10^{-1}	0.972×10^{-5}
^{60}Co	0.122×10^{-2}	0.309×10^{-6}
^{3}H	0.350×10^{3}	$0.300 \times 10^{+3}$

[a]Above gaseous releases include 60-d holdup radwaste system.

Source: Tennessee Valley Authority 1974. *Final Environmental Statement, Sequoyah Nuclear Plant, Units 1 and 2,* Chattanooga, Tenn.

Subsequent movement in the environment to some extent is governed by the point of release of the decontaminated air and water and the rate of release. The liquid component of Source Term III is fairly easily characterized, since it is readily controlled and monitored. The release point, usually into the condenser coolant outlet stream, is well defined. As Figs. 1.10 and 1.11 indicate, the waste is typically held in holdup tanks and is released batchwise as needed. The airborne releases are less well defined. Most of the gaseous effluents would emerge from the plant stack after radwaste treatment, but, particularly at BWRs, there may be significant releases through roof vents of the turbine building, which are less readily monitored and assessed. These releases would be continuous but may vary with particular operations and maintenance procedures. Included in this might be occasional bursts of airborne activity resulting from malfunctions or leaks of filters, gaskets, or pumps. The source term does not include any solid material from the radwaste system, such as evaporator bottoms, filters, or ion exchange resins, which are stored as solids in drums or are shipped off to appropriate disposal sites. An outline for recommended procedure and computer codes for source term determination is given in Regulatory Guide 1.112, which also contains a listing of needed data (USNRC 1976a).

The above discussions have been confined to routine operations of power plants. An additional set of source terms must be developed for accident scenarios. Traditionally, this has involved analysis of a "design-basis accident," such as a loss-of-coolant accident in a light-water reactor (USNRC 1975), under a variety of conservative assumptions. Starting with the core inventory (Source Term I) and the coolant inventory (Source Term II), release situations

Table 1.12. Tritium discharged in airborne effluents from reactors in various countries, 1973—1974

Reactor	Release (Ci)		Normalized release [Ci/MW(e)y]	
	1973	1974	1973	1974
Pressurized-water reactors				
Germany, F. R.				
Obrigheim	20.2	11.5	0.067	0.039
Stade		11.1		0.018
United States				
Yankee Rowe	8.4	3.8	0.070	0.037
Indian Point 1	25.4	0.32		0.0024
San Onofre	268.9	91.4	1.02	0.26
Connecticut Yankee	50.6	0.012	0.18	0.000023
R. E. Ginna	1.1	0.37	0.0028	0.0015
Point Beach 1, 2	25.5	42.8	0.039	0.056
H. B. Robinson	2.5	51.5	0.0058	0.094
Palisades	0.18	0	0.00066	0
Maine Yankee	1.89	7.2	0.0049	0.017
Surry 1, 2	42.4	60.4	0.051	0.090
Turkey Point 2, 3	4.1	9.2	0.0076	0.010
Indian Point 2	2.0	19.9	0.050	0.053
Ft. Calhoun	0.33	0.75	0.0048	0.0027
Prairie Island		3.9		0.024
Oconee 1, 2	13.1	878	0.048	1.39
Zion 1, 2		180		0.34
Arkansas 1		0.030		0.00046
Kewaunee		109		0.60
Three Mile Island		12.7		0.053
Total	466	1494		
Electrical energy [MW(e)y]	5393	8014		
Overall normalized release [Ci/MW(e)y]	0.09	0.19		
Boiling-water reactors				
United States				
Big Rock Point	77.1	38.7	1.61	1.00
Humboldt Bay	1.9	1.7	0.040	0.040
LaCrosse	50.6	18.3	2.24	0.49
Oyster Creek	0.32	0.42	0.00078	0.00098
Nine Mile Point	26.8	15.8	0.067	0.042
Dresden 2, 3	10.0	114	0.010	0.15
Millstone Point	1.7	7.9	0.0079	0.019

Table 1.12 (continued)

Reactor	Release (Ci)		Normalized release [Ci/MW(e)y]	
	1973	1974	1973	1974
	Boiling-water reactors			
Monticello				
Quad Cities 1, 2	34.0	29.0	0.030	0.031
Pilgrim 1	14.0	8.0	0.030	0.035
Vermont Yankee	1.0	2.2	0.0049	0.0078
Peach Bottom 2, 3		5.6		0.0094
Browns Ferry		0.65		0.0015
Cooper Station		0.016		0.000077
Total	217	242		
Electrical energy [MW(e)y]	4340	5094		
Overall normalized release [Ci/MW(e)y]	0.050	0.048		

Source: United Nations Scientific Committee on the Effects of Atomic Radiation 1977. *Sources and Effects of Ionizing Radiation*, United Nations, New York.

can be postulated with or without core melt, involving venting of all the noble gas inventory, 50% of the halogens, and up to 10% of other fission products. As a consequence of the Three Mile Island accident, other, perhaps more probable, accident scenarios are being studied, each of them leading to a different source term at the release point. In addition, such predictions of accident consequences must include a realistic estimate of additional unforeseen pathways due to explosions, natural disasters, and hostile action. Once the release source term is established, existing environmental models can be used to predict dose effects, allowing for the short period of effluent injection.

1.5.3 Fuel Cycle Operations

It would take excessive space to address the various fuel cycle operations as sources of environmental radioactivity in detail; each of those listed contributes some characteristic source terms. Table 1.15 summarizes the overall environmental impact of the uranium fuel cycle as a whole; clearly, the radiological effluents constitute a relatively minor hazard component.

Of the front-end operations, mining of uranium ore is important from the health physics aspect because of the substantial hazard to miners from inhalation of radon daughters, mainly in underground mines, unless a high level of

Table 1.13. Tritium discharged in liquid effluents from U.S. reactors, 1970–1979

Facility	1970	1971	1972	1973	1974	1975	1976	1977	1978	1979
					Boiling-water reactors					
Big Rock Point	5.40E+01	1.03E+01	1.04E+01	1.97E+01	5.10E+00	5.73E+00	2.41E+00	8.83E+00	4.05E+00	5.45E+00
Browns Ferry					2.80E+00	1.04E+00	<4.02E+00	2.40E+01	3.08E+00	1.32E+00
Brunswick						3.20E+00	5.90E+00	8.93E+00	1.41E+01	3.09E+01
Cooper					1.70E+00	8.25E+00	8.43E+00	9.04E+00	7.51E+00	6.63E+00
Dresden 1	5.00E+00	8.70E+00	4.33E+01	1.85E+01	1.88E+01	2.70E+01	2.00E+02	8.90E−02	1.31E+01	1.50E+00
Dresden 2, 3	3.10E+01	3.85E+01	2.59E+01	2.58E+01	2.26E+01	5.40E+01	1.97E+01	5.00E+00	1.92E+01	1.93E+01
Duane Arnold						3.30E+01	3.40E+01	2.13E−01	1.19E+02	2.90E−01
Edwin I. Hatch						6.12E+00	8.98E+00	1.20E+01	9.00E+00	1.23E+01
Fort St. Vrain[a]										1.23E+02
Humboldt Bay	7.00E+00	7.50E+00	1.30E+01	5.13E+01	3.17E+01	2.01E+01	1.30E+01	5.26E−01	3.63E−02	3.91E−02
James A. Fitzpatrick						5.03E+00	4.20E+00	3.35E+00	1.90E+00	1.52E+00
LaCrosse	2.00E+01	9.14E+01	1.20E+02	1.03E+02	1.15E+02	1.27E+02	4.10E+01	4.86E+01	4.72E+01	3.54E+01
Millstone 1		1.27E+01	2.09E+01	3.70E+00	2.41E+01	8.03E+01	2.01E+01	4.41E+00	3.20E+00	7.92E+00
Monticello		5.92E−01	<1.00E−01	0.00E+00	0.00E+00	0.00E+00	0.00E+00	0.00E+00	0.00E+00	0.00E+00
Nine Mile Point	2.00E−01	1.24E+01	2.78E+01	4.65E+01	1.87E+01	2.81E+01	2.46E+00	2.49E+00	N/R[b]	6.78E+00
Oyster Creek	2.20E−01	2.15E+01	6.16E+01	3.59E+01	1.41E+01	1.79E+01	3.86E+01	1.88E+01	1.96E+01	1.40E+00
Peach Bottom				<1.00E+01	1.00E+01	3.08E+01	7.37E+01	7.09E+01	3.24E+01	4.28E+00
Pilgrim			4.20E+00	4.00E+01	1.05E+01	1.82E+01	4.67E+01	3.27E+01	2.98E+00	1.34E+01
Quad-Cities			4.70E+00	2.45E+01	3.40E+01	5.37E+01	4.98E+01	2.64E+01	1.72E+01	1.76E+00
Vermont Yankee				1.00E+01	0.00E+00	0.00E+00	1.60E+00	8.44E−01	N/R[b]	4.04E+00
					Pressurized-water reactors					
Arkansas One 1					2.56E+01	4.60E+02	2.12E+02	2.45E+02	2.94E+02	1.68E+02
Arkansas One 2										5.27E+01
Beaver Valley							8.60E+00	1.08E+02	3.49E+02	9.59E+01
Calvert Cliffs						2.63E+02	2.74E+02	5.75E+02	4.56E+02	5.14E+02
Crystal River								1.66E+02	1.54E+02	1.66E+02
Davis-Besse								9.01E+00	2.15E+02	2.45E+02
Donald C. Cook						5.64E+01	1.92E+02	2.86E+02	6.24E+02	1.22E+03
Fort Calhoun				1.58E+01	1.24E+02	1.11E+02	1.22E+02	1.57E+02	1.50E+02	2.58E+02
Haddam Neck	7.40E+03	5.83E+03	5.89E+03	3.90E+03	2.24E+03	5.67E+03	4.85E+03	6.67E+03	3.94E+03	3.55E+03
H.B. Robinson		1.18E+02	4.05E+02	4.32E+02	4.49E+02	6.24E+02	9.80E+02	6.85E+02	4.73E+02	4.29E+02
Indian Point 1, 2				2.75E+01	4.79E+01	7.94E+01	3.32E+02	3.71E+02	5.12E+02	3.75E+02
Indian Point 3							Shown with other unit		2.56E+02	1.15E+02

Table 1.13 (continued)

Facility	1970	1971	1972	1973	1974	1975	1976	1977	1978	1979
					Pressurized-water reactors					
Joseph M. Farley									5.91E+01	9.40E+01
Kewaunee					9.24E+01	2.77E+02	1.80E+02	2.95E+02	2.96E+02	2.49E+02
Maine Yankee			9.20E+00	1.54E+02	2.19E+02	1.77E+02	3.67E+02	1.53E+02	3.15E+02	2.02E+02
Millstone 2						7.60E+00	2.77E+02	2.11E+02	2.01E+02	2.54E+02
North Anna									2.82E+02	3.13E+02
Oconee				7.05E+01	3.50E+02	3.55E+03	2.19E+03	1.92E+03	1.17E+03	8.94E+02
Palisades			2.08E+02	1.85E+02	8.10E+00	4.16E+01	9.63E+00	5.58E+01	1.01E+02	1.26E+02
Point Beach		2.66E+02	5.63E+02	5.56E+02	8.33E+02	8.85E+02	6.94E+02	9.99E+02	1.29E+03	8.92E+02
Prairie Island				<1.00E−01	1.42E+02	4.54E−01	1.00E−01	1.35E+03	5.51E+02	6.25E+02
Rancho Seco						1.32E+02	0.00E+00	8.55E−02	N/R[b]	N/R[b]
R.E. Ginna	1.10E+02	1.54E+02	1.19E+02	2.86E+02	1.95E+02	2.60E+02	2.42E+02	1.19E+02	2.42E+02	2.40E+02
Salem							4.00E−02	2.96E+02	4.46E+02	7.26E+02
San Onofre	4.80E+03	4.57E+03	3.48E+03	4.07E+03	3.81E+03	4.00E+03	3.39E+03	1.79E+03	2.50E+03	2.32E+03
St. Lucie							1.33E+01	2.42E+02	1.28E+02	1.28E+02
Surry			5.00E+00	4.88E+02	2.45E+02	4.42E+02	7.82E+02	4.08E+02	7.47E+02	3.57E+02
Three Mile Island 1					1.30E+02	4.63E+02	1.89E+02	1.92E+02	1.55E+02	5.59E+01
Three Mile Island 2									3.83E+01	7.81E+01
Trojan							3.60E+01	3.11E+02	1.59E+02	6.80E+01
Turkey Point				3.29E+02	5.80E+02	7.97E+02	7.71E+02	8.24E+02	1.17E+03	9.40E+02
Yankee Rowe	1.50E+03	1.68E+03	8.03E+02	6.94E+02	3.14E+02	2.47E+02	1.56E+02	1.39E+02	1.96E+02	1.75E+02
Zion				1.00E+01	2.74E+02	1.03E+03	7.47E+02	7.24E+02	7.25E+02	5.01E+02

[a]High-temperature gas-cooled reactor.
[b]N/R = not reported.

Source: Tichler, J., and Benkovitz, C. 1981. *Radioactive Materials Released from Nuclear Power Plants: Annual Report 1979,* NUREG/CR-2227 (BNL-NUREG-51416), Brookhaven National Laboratory, Upton, N.Y.

Table 1.14. Noble gases discharged in airborne effluents from reactors in various countries, 1970–1974

Reactor	Startup year	Net electrical power [MW(e)]	Release (kCi)					Normalized release [Ci/MW(e)y]				
			1970	1971	1972	1973	1974	1970	1971	1972	1973	1974
Pressurized-water reactors												
Belgium												
BR-3, Mol	1962	10			0.25					190		
France												
SENA, Chooz	1967	270	0.003	4.5	31.3	19.9		0.02	20	130	82	
Germany, F. R.												
Obrigheim	1968	328	7.7	1.46	3.20	2.93	13.5	27	5.7	12		
Stade	1972	630			2.45	2.61	0.89		6.5			
Biblis	1974	1147					0.06					
Italy												
Trino, Vercellese	1964	247	0.019	0.59	1.03			0.13	3.8	4.5		
Japan												
Mihama 1	1970	340	0.9	1.4	0.62	0.51	0.07	11	5.6	4.9	5.4	2.8
Mihama 2	1972	500			0.26	0.34	0.34			1.1	1.2	1.1
Takahama 1	1974	826					0.07					0.27
Netherlands												
Borssele	1973	447				0.31	5.83				4.0	18
United States												
Yankee Rowe	1961	175	0.017	0.013	0.018	0.035	0.040	0.12	0.08	0.25	0.29	0.38
Indian Point 1	1962	265	1.7	0.36	0.54	0.12	0.61	39	4.1	3.8		4.5
San Onofre	1968	430	4.2	7.67	19.1	11.0	1.78	12	21	59	42	5.0
Connecticut Yankee	1968	575	0.7	3.25	0.65	0.032	0.0074	1.7	6.8	1.3	0.12	0.015
R. E. Ginna	1970	420	10.0	31.8	11.8	0.58	0.76	38	100	43	1.5	3.2
Point Beach 1, 2	1970/72	2 × 497		0.84	2.81	5.75	9.74		2.1	7.9	9.9	13
H. B. Robinson	1971	700		0.018	0.26	3.1	2.31		0.061	0.51	7.2	4.2
Palisades	1971	700			0.51	0.45	0.00003			2.3	1.7	0.0038
Maine Yankee	1972	790			0.002	0.16	6.36			0.04	0.41	16
Surry 1, 2	1972/73	2 × 788			0.00001	0.87	55.0			0.0003	1.0	82

Table 1.14 (continued)

Reactor	Startup year	Net electrical power [MW(e)]	Release (kCi)					Normalized release [Ci/MW(e)y]				
			1970	1971	1972	1973	1974	1970	1971	1972	1973	1974
Pressurized-water reactors												
Turkey Point 3, 4	1972/73	2 × 693				0.53	4.66				0.99	5.2
Indian Point 2	1973	873				0.015	5.58				0.38	15
Ft. Calhoun	1973	457				0.066	0.30				0.96	1.1
Prairie Island 1, 2	1973/74	2 × 530				0.008	0.36				3.6	2.2
Oconee 1, 2, 3	1973/74	3 × 886				9.3	19.4				35	31
Zion 1, 2	1973	2 × 1050				0.004	2.99				0.052	5.6
Arkansas One 1	1974	820					0.20					3.0
Kewaunee	1974	520					3.35					18
Three Mile Island	1974	810					0.92					3.8
Total			25.2	51.9	74.8	58.6	135.1					
Electrical energy generated [MW(e)y]			1906	3124	3960	6083	9045					
Overall normalized release [Ci/MW(e)y]			13.2	16.6	18.9	9.6	14.9					

Source: United Nations Scientific Committee on the Effects of Atomic Radiation, 1977. *Sources and Effects of Ionizing Radiation*, United Nations, New York.

Table 1.15. Summary of environmental considerations for uranium fuel cycle[a] [normalized to model light-water reactor (LWR) annual fuel requirement (WASH-1248) or reference year (NUREG-0116)]

Natural resource use	Total	Maximum effect per annual fuel requirement or reference reactor year of model 1000-MW(e) LWR
Land (acres)		
Temporarily committed[b]	100	
Undisturbed area	79	
Disturbed area	22	Equivalent to 110-MW(e) coal-fired power plant
Permanently committed	13	
Overburden moved (millions of metric tons)	2.8	Equivalent to 95-MW(e) coal-fired power plant
Water (millions of gallons)		
Discharged to air	160	Equals 2% of model 1000-MW(e) LWR with cooling tower
Discharged to water bodies	11,090	
Discharged to ground	127	
Total water	11,377	Less than 4% of model 1000-MW(e) LWR with once-through cooling
Fossil fuel		
Electrical energy (thousands of megawatt hours)	323	Less than 5% of model 1000-MW(e) LWR output
Equivalent coal (thousands of metric tons)	118	Equivalent to the consumption of a 45-MW(e) coal-fired power plant
Natural gas (millions of standard cubic feet)	135	Less than 0.3 of model 1000-MW(e) energy output
Effluents—chemical (metric tons)		
Gases (including entrainment)[c]		
SO_x	4,400	
NO_x[d]	1,190	Equivalent to emissions from 45-MW(e) coal-fired power plant for a year

Table 1.15 (continued)

Natural resource use	Total	Maximum effect per annual fuel requirement or reference reactor year of model 1000-MW(e) LWR
Hydrocarbons	14	
CO	29.6	
Particulates	1,154	
Other gases		
F^-	0.67	Principally from UF_6 production, enrichment, and reprocessing. Concentration within range of state standards—below level that has effects on human health
HCl	0.014	
Liquids		
SO_4^{2-}	9.9	From enrichment, fuel fabrication, and reprocessing steps. Components that constitute a potential for adverse environmental effect are present in dilute concentrations and receive additional dilution by receiving bodies of water to levels below permissible standards. The constituents that require dilution and the flow of dilution water are NH_3—600 cfs; NO_3—20 cfs; fluoride—70 cfs.
NO_3^-	25.8	
Fluoride	12.9	
Ca^{2+}	5.4	
Cl^-	8.5	
Na^+	12.1	
NH_3	10.0	
Fe	0.4	
Tailings solutions (thousands of metric tons)	240	From mills only—no significant effluents to environment
Solids	91,000	Principally from mills—no significant effluents to environment
Effluents—radiological (curies)		
Gases (including entrainment)		
^{222}Rn		Presently under reconsideration by the Nuclear Regulatory Commission

Table 1.15 (continued)

Natural resource use	Total	Maximum effect per annual fuel requirement or reference reactor year of model 1000-MW(e) LWR
^{226}Ra	0.02	
^{230}Th	0.02	
Uranium	0.034	
Tritium	18,100	
^{14}C	24	
^{85}Kr	400,000	
^{106}Ru	0.14	Principally from fuel reprocessing plants
^{129}I	1.3	
^{131}I	0.83	
^{99}Tc		Presently under consideration by NRC
Fission products and transuranics	0.203	
Liquids		
Uranium and daughters	2.1	Principally from milling—included in tailings liquor and returned to ground—no effluents and therefore no effect on environment
^{226}Ra	0.0034	From UF_6 production
^{230}Th	0.0015	
^{234}Th	0.01	From fuel fabrication plants—concentration 10% of 10 CFR Part 20 for total processing 26 annual fuel requirements for model LWR
Fission and activation products	5.9×10^{-6}	
Solids (buried on site)		
Other than high level (shallow)	11,300	9100 Ci comes from low-level reactor wastes and 1500 Ci comes from reactor decontamination and decommissioning—buried at land burial facilities; mills produce 600 Ci—included in tailings returned to ground; about 60 Ci comes from conversion and spent-fuel storage; no significant effluent to the environment.

Table 1.15 (continued)

Natural resource use	Total	Maximum effect per annual fuel requirement or reference reactor year of model 1000-MW(e) LWR
TRU[e] and HLW[e] (deep)	1.1×10^7	Buried at federal repository
Effluents—thermal (billions of British thermal units)	4,063	Less than 5% of model 1000-MW(e) LWR
Transportation (person-rem)		
Exposure of workers and general public	2.5	
Occupational exposure (person-rem)	22.6	From reprocessing and waste management

[a]In some cases where no entry appears, it is clear from the background documents that the matter was addressed and that, in effect, this table should be read as if a specific zero entry had been made. However, there are other areas that are not addressed at all in this table. Table S-3 of WASH-1248 does not include health effects from the effluents described in this table or estimates of releases of radon-222 from the uranium fuel cycle or estimates of ^{99}Tc — released from waste management or reprocessing activities. These issues which are not addressed at all by this table may be the subject of litigation in individual licensing proceedings. Data supporting this table are given in the *Environmental Survey of the Uranium Fuel Cycle, WASH-1248,* April 1974; the *Environmental Survey of the Reprocessing and Waste Management Portions of the LWR Fuel Cycle,* NUREG-0116 (Suppl. 1 to WASH-1248), and the *Public Comments and Task Force Responses Regarding the Environmental Survey of the Reprocessing and Waste Management Portions of the LWR Fuel Cycle,* NUREG-0216 (Suppl. 2 to WASH-1248) and the Record of the final rulemaking pertaining to Uranium Fuel Cycle Impacts from Spent Fuel Reprocessing and Radioactive Waste Management, Docket RM-50-3. The contribution from reprocessing, waste management, and transportation of wastes is maximized for either of the two fuel cycles (uranium only and no recycle). The contribution from transportation excludes transportation of cold fuel to a reactor and of irradiated fuel and radioactive wastes from a reactor which are considered in Table S-4 of Sect. 51.20(g). The contribution from the other steps of the fuel cycle is given in columns A to E of Table S-3A of WASH-1248.

[b]The contributions to temporarily committed land from reprocessing are not prorated over 30 y because the complete temporary impact accrues regardless of whether the plant services 1 reactor for 1 y or 57 reactors for 30 y.

[c]Estimated effluents based on combustion of equivalent coal for power generation.

[d]1.2% from natural gas use and process.

[e]TRU = transuranium; HLW = high-level waste.

ventilation and dust removal can be maintained. These effects are direct, somatic, and do not lead to any long-range effluents, except by enhancement of radon levels in the air in the vicinity of the mine.

Milling of uranium ores leads to a separation of the purified uranium, with its low specific activity, from the accompanying radium and its daughters. The mill tailings are retained in tailings storage areas as sludges or dried precipitates and are potential sources of high levels of radon emanation. The effects of this on surrounding populations through inhalation or contamination of the water supply have been studied widely (Travis et al. 1979). The source term involves radium and relatively short-lived radon daughters, and finally 22-y ^{210}Pb. The use of uranium mill tailings in landfills at Grand Junction, Colorado, and Elliott Lake, Ontario, has also been investigated in detail, but any effects are strictly local, confined to individual buildings.

Transportation of spent fuel is included in all environmental impact assessments. Tables 1.16 and 1.17 list representative contents of spent fuel after 33 GWd/metric ton of burnup and 150 d of cooling. Various accident conditions can be modeled; however, in general, only airborne releases are assumed to lead to any significant exposures.

The same material, of course, constitutes the input to any reprocessing plant. Although present U.S. policies rule out any immediate reprocessing of commercial fuel, military reprocessing is going on unabated, any breeder program is predicated on the availability of reprocessing facilities, and many industrialized countries are continuing development of reprocessing capabilities to conserve energy resources. Depending on the capacity of the plant, the total flow capacity will involve multiples of the nuclides listed in Tables 1.16 and 1.17. Similar, but more elaborate, radwaste treatment systems than are used at power plants must be employed and, subject to the ALARA criterion, an effluent source term can be developed for the plant. This may involve very large quantities of tritium and noble gases (i.e., ^{85}Kr) unless steps are taken to retain them. Volatilization of ruthenium, as RuO_4, is a special problem; the radwaste system must be designed to retain it as much as possible.

The final step in the fuel cycle consists of solidification, immobilization, and burial of all radioactive wastes. This has been discussed extensively in recent years (Eichholz 1977; Adams and Rogers 1978; USDOE 1979; NAS 1978; USDOE 1981), and the technology seems to be well established. Complications arise if one insists on disposal of unreprocessed fuel as spent fuel. Table 1.18 lists the predominant activities involved and the associated heat production. Separate environmental models are being developed for solidified, encapsulated waste products buried in various geological media. Only the liquid pathway is considered here in order to estimate population dose commitments over an infinite period due to various seepage and water incursion processes. Anticipated population doses are very low, the time scale goes well beyond the next ice age, and a certain air of unreality is associated with many of these calculations.

Table 1.16. Representative quantities of potentially significant fission products in spent reactor fuels[a]

Isotope	Half-life (y)	Curies per metric ton	Grams per metric ton	Release state	Notes
^{3}H	12.3	800	0.083	Gas	>95% released as HTO
^{85}Kr	10.7	10,500	27	Gas	
^{99}Tc	2.13×10^{5}	15	880	Semivolatile	Oxide, boiling point 200°C
^{103}Ru	0.11	180,000	5.7	Semivolatile	Tetroxide, boiling point 80°C
^{106}Ru	1.01	820,000	240	Semivolatile	^{103m}Rh + ^{106}Rh daughters
^{125m}Te	0.16	6,500	0.36	Semivolatile	Oxide, boiling point 750°C
^{127m}Te	0.30	25,000	2.7	Semivolatile	^{127}Te daughter
^{129m}Te	0.09	13,000	0.42	Semivolatile	^{129}Te daughter
^{129}I	17×10^{6}	0.04	250	Volatile	Boiling point 184°C
^{131}I	0.02	2.0	<0.01	Volatile	Boiling point 184°C
^{134}Cs	2.05	100,000	77	Semivolatile	Oxide, boiling point 750°C
^{135}Cs	3×10^{6}	1.2	1400	Semivolatile	
^{137}Cs	30.2	106,000	1200	Semivolatile	^{137m}Ba daughter
^{89}Sr	0.14	100,000	3.5	Solid	
^{90}Sr	28.9	60,000	430	Solid	^{90}Y daughter
^{91}Y	0.16	190,000	7.8	Solid	
^{93}Zr	0.95×10^{6}	2	490	Solid	
^{95}Zr	0.18	400,000	19	Solid	^{95m}Nb + ^{95}Nb daughters
^{95}Nb	0.10	800,000	21	Solid	
^{125}Sb	2.73	13,000	12	Solid	
^{141}Ce	0.09	80,000	2.8	Solid	
^{144}Ce	0.78	800,000	250	Solid	^{144}Pr + ^{144}Nd daughters
^{147}Pm	2.62	200,000	220	Solid	
^{155}Eu	5.0	40,000	87	Solid	

[a]Burnup = 33 GWd(t)/metric ton; cooling time = 150 d.

Source: U.S. Environmental Protection Agency 1974. *Environmental Protection Agency 1974. Environmental Radiation Dose Commitment: An Application to the Nuclear Power Industry,* EPA-520/4-73-002, Washington, D.C.

1.6 CONCLUSION

This chapter constitutes a condensed overview of the various sources of "technologically enhanced" radiation that may impact on the environment. Industrial and medical uses typically involve only a limited number of radionuclides, making it easier to predict environmental pathways. In contrast, nuclear power plants generate a wide spectrum of nuclides and hence an extensive series of source terms. This makes all models for the prediction of their subsequent movement rather difficult to work with and makes it attractive to concentrate on a smaller number of critical nuclides and critical population groups. Furthermore, a suitable choice must be made between "deterministic" and "probabilistic" models, a subject that is covered in later chapters.

Table 1.17a. Representative quantities of actinides present in spent reactor fuels[a]

Isotope	Half-life (y)	Uranium fuels		Plutonium-recycle fuels	
		Curies per metric ton	Grams per metric ton	Curies per metric ton	Grams per metric ton
^{235}U	710×10^6	<1	8,000	<1	3,000
^{236}U	24×10^6	<1	4,000	<1	1,500
^{238}U	4510×10^8	<1	950,000	<1	950,000
^{237}Np	2×10^6	<1	600	1	200
^{238}Pu	86	4,000	230	6,000	340
^{239}Pu	24,400	500	8,100	750	12,000
^{240}Pu	6,580	650	2,900	1,000	4,400
^{241}Pu	13	150,000	1,300	300,000	2,600
^{242}Pu	379,000	2	510	5	1,300
^{241}Am	458	750	230	2,000	620
^{243}Am	7,800	20	100	200	1,000
^{242}Cm	0.45	35,000	10	250,000	75
^{244}Cm	17.6	2,000	25	25,000	300
Total (excluding uranium)		193,000	14,000	585,000	23,000

[a]Burnup = 33 GWd(t)/metric ton; cooling time = 150 d.

Table 1.17b. Representative quantities of corrosion products present in spent reactor fuels[a]

Isotope	Half-life (y)	Curies per metric ton	Grams per metric ton	Release state
^{54}Mn	0.86	30,000	3.9	Solid
^{55}Fe	2.7	20,000	8.3	Solid
^{59}Fe	0.12	500	<0.01	Solid
^{58}Co	0.20	30,000	1.0	Solid
^{60}Co	5.26	2,000	1.8	Solid

[a]Burnup = 33 GWd(t)/metric ton; cooling time = 150 d.

Source: U.S. Environmental Protection Agency 1974. *Environmental Radiation Dose Commitment: An Application to the Nuclear Power Industry,* EPA-520/4-73-002, Washington D.C.

Table 1.18. Radioactivity of irradiated fuel[a] (curies per metric ton of uranium)[b]

	Cooling period (d)		
	90	150	365
Fission products	6.19×10^6	4.39×10^6	2.22×10^6
Actinides (Pu, Cm, Am, etc.)	1.42×10^5	1.36×10^5	1.24×10^5
Total	6.33×10^6	4.53×10^6	2.34×10^6
Predominant fission products in gaseous form included in radioactivity of irradiated fuel (curies per metric ton of uranium)			
^{85}Kr	1.13×10^4	1.12×10^4	1.08×10^4
^{131m}Xe	1.06×10^2	3.27×10^0	1.08×10^{-5}
^{131}I	3.81×10^2	2.17×10^0	1.98×10^{-8}
Thermal energy in irradiated fuel (watts per metric ton of uranium)			
Thermal energy	2.71×10^4	2.01×10^4	1.04×10^4

[a] Estimated burnup 33,000 MWd per metric ton of uranium.
[b] Approximately two assemblies per metric ton of uranium.
Source: Oak Ridge National Laboratory 1970. *Siting of Fuel Reprocessing Plants and Waste Management Facilities,* ORNL-4451, Oak Ridge, Tenn.

1.7 PROBLEMS

(Some of the problems given below assume access to a nuclide chart and making "reasonable" assumptions.)

1. Calculate the mass, carrier-free, of 5 mCi of (a) ^{90}Sr, (b) ^{131}I, and of 15 GBq of (c) ^{99}Mo, (d) ^{32}P, and (e) ^{241}Am.

2. Select the most convenient bombardment reaction for the commercial production of the following radionuclides: (a) ^{65}Zn, (b) ^{210}Po, (c) ^{3}H, (d) ^{42}K, (e) ^{18}F, (f) ^{123}I, (g) ^{67}Ga. Indicate the specific activity attainable, whether the material may be carrier-free, and what competing reactions one may have to consider in each case.

3. A hospital purchases an isotope generator containing initially 30 mCi of ^{99}Mo (half-life of 66 h). Calculate the maximum quantity of the 6-h ^{99m}Tc daughter that will grow in, and estimate how often and for how long it will be possible to milk off 5-mCi quantities of ^{99m}Tc.

4. Calculate the amount of krypton, xenon, and iodine produced in the complete fission of 100 g of ^{235}U. If this burnup occurs over a period of 1 y, calculate the fission rate, assuming steady power levels and the average equilibrium concentration of ^{131}I.

5. Estimate the ^{85}Kr content in a reactor core containing 100 tons of UO_2 after 2 y of operation at a burnup of 33,000 MWd/metric ton (assume 3% enrichment and no leakage).

6. In problem 5, assume that 1% of the fuel leaks, and estimate the annual and daily release of ^{85}Kr from the plant. What would be the effect of a 3-d holdup before release?

7. Define the working-level (WL) unit for radon daughters in air. The atmosphere in a certain mine contains radon daughters in equilibrium at a concentration of 0.3 WL. Calculate the concentrations of radon and the individual daughters this implies. If only 40% of ^{218}Pb was attached to particulates, how would this affect the apparent working levels measured? If ventilation reduces the later radon daughters to 70% of equilibrium, what concentration of each would 0.3 WL then imply?

8. A typical radon concentration in open air near the ground is 1.3×10^{-16} Ci/cm^3. What is the corresponding WL? Calculate the amount of ^{210}Pb collected on an air filter of 85% collection efficiency operating for 2 h at a sampling flow rate of 35 ft^3/min. How much ^{210}Pb would there be after 16-h storage of the filter?

9. Compare methods of control for noble-gas release from nuclear power plants. What are the respective arguments in favor of continuous release to the atmosphere or for complete retention?

10. Estimate the tritium inventory in a 1000-MW(e) PWR after 350 d of operation. Assume a coolant volume of 80,000 gal. Making reasonable assumptions regarding fuel leakages and other leak rates, calculate the effluent water flow needed to hold tritium concentrations below 1% of the maximum permissible concentration in water ($MPC_w = 0.03$ μCi/cm^3).

11. In the reactor described in problem 10, assume a dissolved air content of 50 ppm in the primary coolant and calculate the amount of ^{14}C produced. If this is released continuously as CO_2 with other stack gases, estimate the dilution needed to keep it below 1% of the maximum permissible concentration in air ($MPC_a = 10^{-5}$ μCi/cm^3).

12. Estimate the amount of activity accumulated on the primary coolant demineralizer resin of a 1000-MW(e) PWR after 6 months of operation at power. How much activity would be left after 30-d storage before shipping?

13. Calculate the amount of plutonium accumulated in 1 ton of UO_2 after 30,000 MWd/metric ton burnup, both neglecting plutonium burnup and including it.

14. Estimate the hazards involved and discuss procedures to handle the wastes and scintillation fluids at a major hospital using 200 mCi/week of ^{99m}Tc-labeled pharmaceuticals and 10 mCi/week of ^{14}C-labeled tracer compounds.

REFERENCES

Adams, J. A., and Rogers, V. L. 1978. *A Classification System for Radioactive Waste Disposal—What Waste Goes Where?* NUREG-0456, U.S. Nuclear Regulatory Commission, Washington, D.C.

Cameron, J. F., and Clayton, C. G. 1971. *Radioisotope Instruments,* Pergamon Press, Oxford.

Eichholz, G. G. 1977. *Environmental Aspects of Nuclear Power,* Ann Arbor Science Publishers, Ann Arbor, Mich.

Keyes, J. W., Beierwaltes, W. H., Moses, D. C., and Carey, J. E., eds, 1976. *CRC Manual of Nuclear Medicine Procedures,* 2d ed., CRC Press, Cleveland.

Krieger, H., Frishkorn, G., Martin, E., and Jacobs, B. 1980. "Evaluation of Methodology for Quantifying Radiopharmaceuticals in Tertiary-Treated Sewage," in *Effluent and Environmental Radiation Surveillance,* STP 698, ed. J. J. Kelly, American Society for Testing and Materials, Philadelphia.

Leventhal, L., Melgard, R., Claridge, D. E., and Kendricks, H. 1980. "Assessment of Radiopharmaceutical Usage Release Practices by Eleven Western Hospitals," in *Effluent and Environmental Radiation Surveillance,* STP 698, ed. J. J. Kelly, American Society for Testing and Materials, Philadelphia.

Moghissi, A. A., and Carter, M. W. 1975. *Public Health Implications of Radioluminous Materials,* FDA-76-8001, U.S. Bureau of Radiological Health, Rockville, Md.

Moghissi, A. A., Paras, P., Carter, M. W., and Barker, R. E., eds. 1978. *Radioactivity in Consumer Products,* NUREG/CP-0001, U.S. Nuclear Regulatory Commission, Washington, D.C.

National Academy of Sciences (NAS) 1978. *Radioactive Wastes at the Hanford Reservation,* Washington, D.C.

National Council on Radiation Protection and Measurement (NCRP) 1979. *Tritium in the Environment,* NCRP Report 62, Washington, D.C.

Rundo, J., Fairman, W. D. Essling, M., and Huff, D. R. 1977. "Ingestion of ^{241}Am Sources Intended for Domestic Smoke Detectors: Report of a Case," *Health Phys.* **33,** 561-66.

Tennessee Valley Authority (TVA) 1974. *Final Environmental Statement, Sequoyah Nuclear Plant Units 1 and 2,* Chattanooga, Tennessee.

Tichler, J., and Benkovitz, C. 1981. *Radioactive Materials Released from Nuclear Power Plants: Annual Report 1979,* NUREG/CR-2227 (BNL-NUREG-51416), Brookhaven National Laboratory, Upton, N.Y.

Travis, C. C., Cotter, S. J., Watson, A. P., Randolph, M. L., McDowell-Boyer, I. M., and Fields, D. E. 1979. *A Radiological Assessment of ^{222}Rn Released from Uranium Mills and Other Natural and Technologically*

Enhanced Sources, ORNL/NUREG-55, Oak Ridge National Laboratory, Oak Ridge, Tenn.

United Nations Scientific Committee on the Effects of Atomic Radiation (UNSCEAR) 1977. *Sources and Effects of Ionizing Radiation,* United Nations, New York.

U.S. Atomic Energy Commission (USAEC) 1974. *Draft Environmental Statement: Bellefonte Nuclear Plant,* Docket Nos. 50-438/439, Washington, D.C.

U.S. Department of Energy (USDOE) 1979. *Draft Environmental Impact Statement: Management of Commercially Generated Radioactive Waste,* DOE/EIS-0046-C, Washington, D.C.

U.S. Department of Energy (USDOE) 1981. *Draft Environmental Statement: Defense Waste Processing Facility—Savannah River Plant,* DOE/EIS-0082D, Washington, D.C.

U.S. Environmental Protection Agency (USEPA) 1977. *Radiological Quality of the Environment in the United States, 1977,* EPA 520/1-77-009, Washington, D.C.

U.S. Nuclear Regulatory Commission (USNRC) 1975. *Reactor Safety Study,* WASH-1400, Appendixes 7 and 8, Washington, D.C.

U.S. Nuclear Regulatory Commission (USNRC) 1976a. *Calculation of Releases of Radioactive Materials in Gaseous and Liquid Effluents from Light-Water-Cooled Power Reactors,* Regulatory Guide 1.112, Washington, D.C.

U.S. Nuclear Regulatory Commission (USNRC) 1976b. *Cost-Benefit Analysis for Radwaste Systems for Light-Water-Cooled Nuclear Power Reactors,* Regulatory Guide 1.110, Washington, D.C.

U.S. Nuclear Regulatory Commission (USNRC) 1978. *Draft Environmental Statement Related to Operation of San Onofre Nuclear Generating Stations, Units 2 and 3,* NUREG-0490, Washington, D.C.

2 Transport of Radionuclides in the Atmosphere

By H. D. BRENK,*
J. E. FAIROBENT,† *and* E. H. MARKEE, JR.†

2.1 INTRODUCTION

Radioactive releases from various nuclear facilities may contribute to radiation exposure through a number of pathways:

- *External exposures* by direct radiation from radioactive plumes or from radionuclides deposited on the ground, and
- *Internal exposure* due to inhalation and ingestion of radioactive material.

The magnitude of exposure is dependent on atmospheric dispersion and deposition processes.

Figure 2.1 is a schematic presentation of the atmospheric processes which affect airborne releases. Elements of an airborne plume are affected by turbulent eddies in the atmosphere which *diffuse* the effluent material as the entire plume is being *transported* downwind. Generally, the combined influences of diffusion and transport are called *dispersion.* As the plume disperses, certain removal mechanisms may affect the effluent. For example, under certain conditions, gaseous and particulate effluents may become involved in precipitation formation processes within a cloud and be subsequently removed with the precipitation. This removal process is referred to as *rainout.* The removal of gaseous or particulate material below cloud by contact with falling precipitation is

*Brenk Systemplanung, Heinrichsallee 38, D-5100 Aachen, Federal Republic of Germany.
†U.S. Nuclear Regulatory Commission, Washington, D.C. 20555.

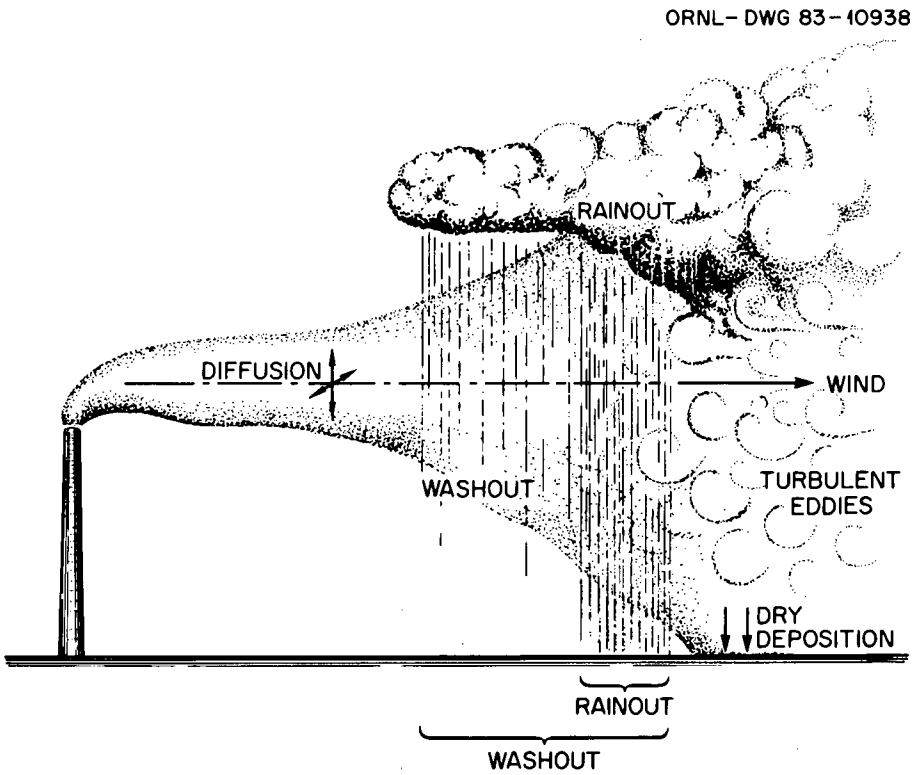

Figure 2.1. Atmospheric dispersion and removal processes.

referred to as *washout*. Effluent material may also be removed through gravitational settling, or through contact with the ground, vegetation, or other ground cover such as buildings. These removal mechanisms are referred to collectively as *dry deposition*. Radioactive material may decay during transport. Some effluents may also undergo chemical transformations during transport.

This chapter will provide a brief introduction to atmospheric dispersion processes and removal mechanisms which affect airborne releases of radioactive material. The principal focus of this chapter will be on the bases for and the use of the Gaussian plume model for atmospheric dispersion, and some basic understanding of the removal processes which affect airborne material. Although the Gaussian model is widely used because of the relative ease of calculation, the model is based on fundamental concepts of turbulent diffusion. The results produced by using this model are in reasonable agreement with experimental data.

References such as *Meteorology and Atomic Energy* (Slade 1968) (and its upcoming revision, "Atmospheric Sciences and Energy Production") and the *Handbook on Atmospheric Diffusion* (Hanna 1982) provide much more extensive discussions of atmospheric diffusion processes. The *Workbook of Atmospheric Dispersion Estimates* (Turner 1967) provides additional information concerning applications of the Gaussian model.

2.2 ATMOSPHERIC TURBULENCE AND DISPERSION

2.2.1 Characterization of the Planetary Boundary Layer

Radioactive materials from sources such as nuclear power plants, medical facilities, and research reactors are typically released to the atmosphere between the ground surface and an elevation of 100 m into a region of the atmosphere called the "planetary boundar layer" (PBL). The height of the PBL generally ranges from about 200 to about 2000 m. Within this layer, ground surface effects are important. Diurnal variations in air temperature due to heating and cooling of the earth's surface are discernable through the PBL. Within this layer, wind speed tends to increase with height and wind direction tends to vary with height as a result of reduced friction between the air and earth's surface.

The stability of the atmosphere within the PBL largely determines the intensity of turbulence and, subsequently, the diffusion processes which affect effluents released into this layer. The stability of the PBL can be illustrated by examining the behavior of a displaced parcel of air which is not subject to other motions in the atmosphere and which does not mix with its environment. In simple terms, if the displaced parcel of air is subject to no net force as a result of its new surroundings, the atmosphere can be considered to be neutral; if the displaced parcel is subject to forces which act to move the parcel further away, the atmosphere can be considered to be unstable; and if the displaced parcel is subject to forces which act to restore the parcel to its original position, the atmosphere can be considered stable. The stability of the PBL can be related to temperature lapse rate. The temperature of dry air in the atmosphere tends to decrease with height at a rate of $-0.98°C/100$ m, called the dry adiabatic lapse rate. If a parcel of air is displaced adiabatically at this lapse rate, the parcel will have the same temperature and density as its surroundings and is, therefore, subject to no net force. This atmospheric condition is neutral. If the parcel of air is displaced adiabatically into an environment which has a lapse rate greater than the dry adiabatic lapse rate, the parcel displaced upward will be warmer and less dense than its environment and will be accelerated upward. Similarly, if an air parcel is displaced downward in this situation, it will be cooler and more dense than its environment and will be accelerated downward. This atmospheric condition is called unstable. If the parcel is displaced adiabatically into an environment which has a lapse rate

less than the dry adiabatic lapse rate, the parcel displaced upward will be cooler and more dense than its environment and will be decelerated to return to its original level. Similarly, if a parcel is displaced downward in this situation, it will be warmer and less dense than its environment and will be accelerated upward to return to its original level. This atmospheric condition is called stable. Figure 2.2 presents an illustration of these stability conditions in the PBL. Typically, unstable conditions tend to occur near the surface on a sunny day; neutral conditions tend to occur during windy and cloudy conditions; and stable conditions tend to occur on clear nights with low wind speeds.

These thermal factors (buoyancy) are one source of atmospheric turbulence. The other source is generated by airflow over rough surfaces and obstacles and is considered to be mechanical in nature. The description of the effect of turbulence on effluent diffusion is complicated by the variety of forces acting in the atmosphere.

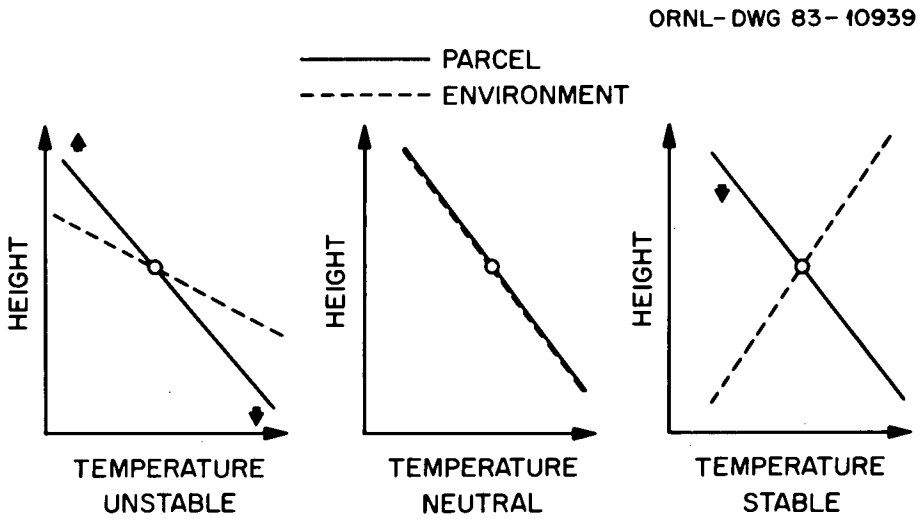

Figure 2.2. Illustration of PBL stability conditions (Hanna 1982).

2.2.2 Characterization of Turbulent Diffusion

The two approaches most commonly used to describe turbulent diffusion are gradient transport theory and statistical theory. The *gradient transport theory* (commonly called *K*-theory) deals with atmospheric transport at a fixed point, similar to the theory of molecular diffusion originally presented by Fisk in the mid-nineteenth century, proportional to the local concentration gradient.

Thus, the vector flux $\vec{S}$ through an area element dA at a certain point is equal to

$$\vec{S} = -K\nabla\Psi \ , \tag{2.1}$$

where K is the turbulent diffusion coefficient and Ψ is the pollutant concentration within the infinitely small volume element dV. (Note: In the United States, χ is commonly used rather than Ψ to represent concentration.)

Assuming no sources or sinks in dV, the change of the pollutant concentration with respect to time is

$$\frac{\partial\Psi}{\partial t} = -div\ \vec{S} \ , \tag{2.2}$$

$$\frac{\partial\Psi}{\partial t} = \nabla K\nabla\Psi + K\nabla^2\Psi \ . \tag{2.3}$$

The assumption of spatial homogeneity, which means that

$$\nabla K = 0 \ ,$$

results in the so-called *Fickian diffusion equation*:

$$\frac{\partial\Psi}{\partial t} = K\nabla^2\Psi \ . \tag{2.4}$$

Because this diffusion theory concentrates on the atmospheric transport at a fixed point in space, it may be said to be Eulerian in nature. This means that it considers properties of the fluid motion relative to a spatially fixed coordinate system.

The *statistical theory* differs considerably from the gradient transport theory. Instead of studying the material flux at a fixed space point, one studies the history of motion of individual fluid particles and tries to determine from these the statistical properties necessary to represent diffusion. This approach is Lagrangian in nature.

For *large diffusion times*, i.e., nearly uncorrelated particle motion, both the gradient transport theory and the statistical theory supply the well-known normal Gaussian distribution of the pollutant material in the atmosphere as a fundamental solution (Slade 1968; Pasquill 1974).

In terms of the gradient transport theory, the pollutant concentration (here: activity concentration) may be written as

$$\Psi = \frac{Q}{[(4\pi t)^3 K_x K_y K_z]^{1/2}} \times \exp - \left[\frac{(x-x_0)^2}{4K_x t} + \frac{(y-y_0)^2}{4K_y t} + \frac{(z-z_0)^2}{4K_z t} \right], \tag{2.5}$$

where *x, y, and z* are axes as presented in Figure 2.3,

Q = activity released,
K = diffusion coefficients,
t = time.

In terms of the statistical theory, the pollutant concentration may be expressed as

$$\Psi = \frac{Q}{(2\pi)^{3/2}\sigma_x \sigma_y \sigma_z} \times \exp \left\{ - \frac{1}{2} \left[\frac{(x - x_0)^2}{\sigma_x^2} + \frac{(y - y_0)^2}{\sigma_y^2} + \frac{(z - z_0)^2}{\sigma_z^2} \right] \right\}, \tag{2.6}$$

where σ^2 ($= 2Kt$) represents the variance of the well-known Gaussian distribution (Walpole 1978).

2.3 GAUSSIAN PLUME MODEL

Equation (2.6) describes the extent and concentration distribution of an effluent cloud due to a single point-type release, where $P(x_0,y_0,z_0)$ is the center of the cloud. This equation forms the basis for the Gaussian "puff" models. In these models the transport of each puff is determined from a wind field which can vary with time and space (Start et al. 1974).

Assuming not a single but a series of distinctly separate point-type releases, which move away from the point of release $P(0,0,z_0)$ (Fig. 2.3), in

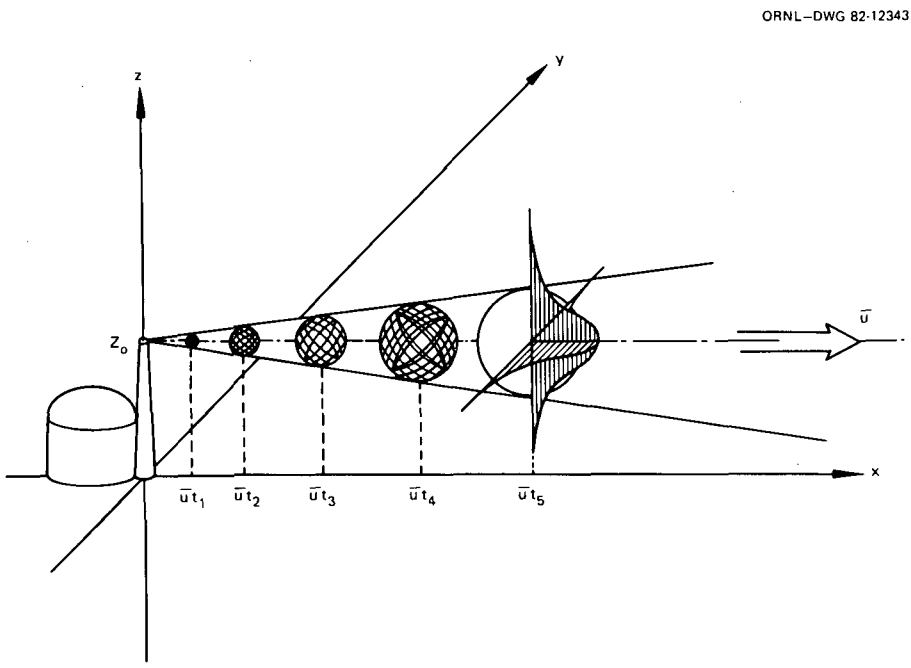

Figure 2.3. Gaussian diffusion of single puffs.

the form of growing clouds at mean velocity $\bar{u}$ and along the abscissa (x axis), the concentration distribution of each individual cloud may be specified as

$$\Psi = \frac{Q}{(2\pi)^{3/2}\sigma_x\sigma_y\sigma_z} \times$$

$$\exp\left\{-\frac{1}{2}\left[\left(\frac{x - \bar{u}t}{\sigma_x}\right)^2 + \left(\frac{y}{\sigma_y}\right)^2 + \left(\frac{z - z_0}{\sigma_z}\right)^2\right]\right\}, \qquad (2.7)$$

where Q denotes the total pollutant amount in each specific case, and t denotes the traveling time of a cloud. Equation (2.7) describes a situation like the one illustrated graphically in Fig. 2.3. In the immediate vicinity of the source, the cloud is still negligibly small. It then grows due to the dilution effect of the atmospheric diffusion in all directions, producing a pollutant concentration of normal distribution. In general, the concentration distributions along all coordinate axes are different. For the specific case of equal diffusion

in all directions (Fig. 2.3), spherical clouds will form, featuring a spherosymmetric normal distribution of the pollutant.

The individual clouds are transported at mean velocity $\bar{u}$, so that after a certain time t they have covered the distance x.

For a continuous series of releases, a plume consisting of an infinite number of overlapping individual clouds tranported along the x axis at velocity $\bar{u}$, and integrated over the time interval of release can be assumed.

Assuming diffusion along the x axis is small compared to transport and can be neglected and assuming total reflection on the ground, it is possible to calculate the concentration distribution inside the plume by means of Eq. (2.8).

$$\Psi = \frac{\dot{Q}}{2\pi\bar{u}\sigma_y\sigma_z} \times$$

$$\exp\left[-\frac{y^2}{2\sigma_y^2}\right]\left[\exp\left[-\frac{(z-H)^2}{2\sigma_z^2}\right] + \exp\left[\frac{(z+H)^2}{2\sigma_z^2}\right]\right], \qquad (2.8)$$

where

$\dot{Q}$ = release rate (activity/time), and
H = effective stack height.

Equation (2.8) may be illustrated using the schematic representations of the plume in Figs. 2.4 and 2.5. Neglecting diffusion along the x axis implies that the individual spherical clouds in Figure 2.3 form infinitely thin slices instead. A continuous release provides for the fact that an infinitely large number of these thin slices with the pollutant amount $\dot{Q}$ will line up in a row, thus forming a continuous series of slices; i.e., a plume. In this case, a Gaussian distribution (Fig. 2.4) will likewise occur along the two axes in transverse direction to the basic flow. The concentration in the plume will double after having reached the ground, where it is entirely reflected (according to convention). This is achieved mathematically by assuming a virtual source at $z = -H$ and superposing the plumes of both sources for $z > 0$. The term

$$\exp\left[\frac{-(z+H)^2}{2\sigma_z^2}\right]$$

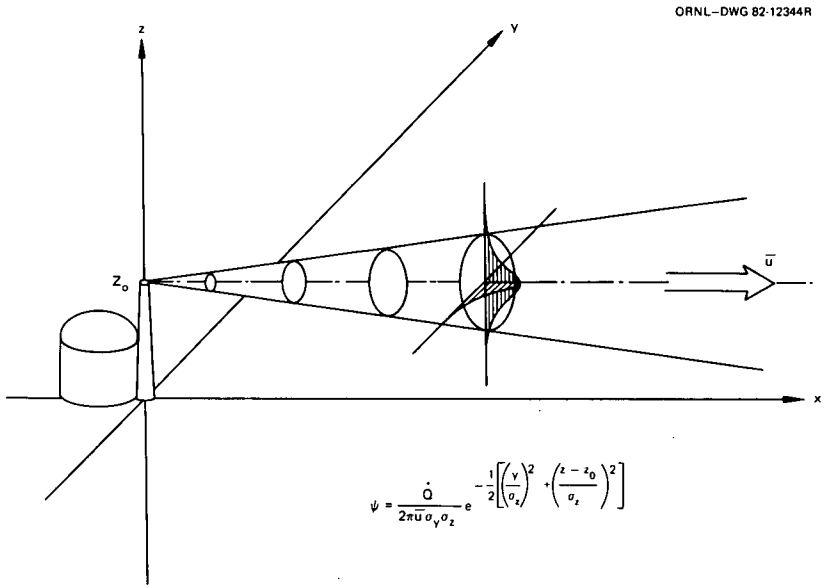

Figure 2.4. Gaussian plume diffusion.

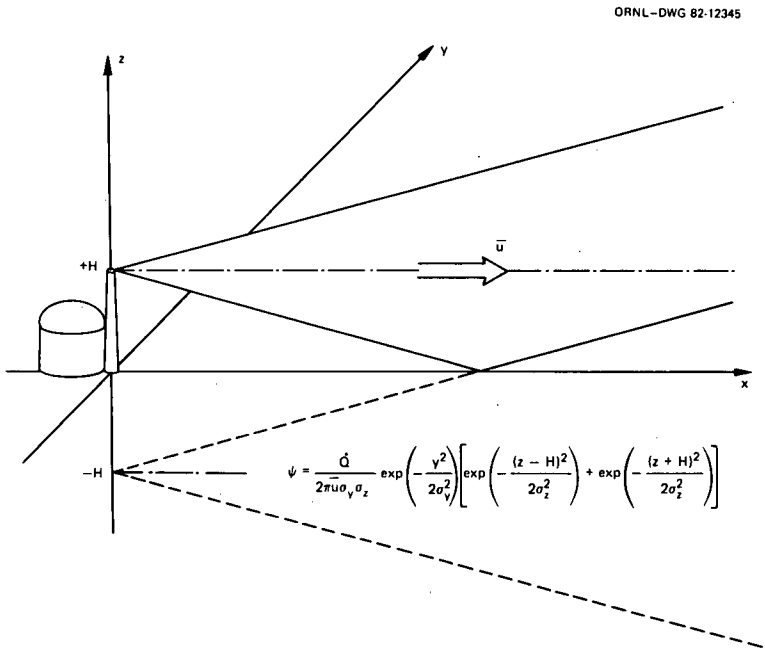

Figure 2.5. Scheme for the total reflection at the underlying surface (i.e., no ground absorption).

in Eq. (2.8) originates from this virtual source. The procedure ensures that there is no diffusion normal to the ground. In other words, the diffusion flux in z direction, S_z, is

$$S_z \propto \frac{\partial \Psi}{\partial z} = 0, \quad \text{for } z = 0 .$$

2.3.1 Prerequisites and Assumptions

Equation (2.8) is the basic equation of the *Gaussian plume model*, from which all the other computational equations used within this chapter are derived. It would go beyond the scope of this chapter to derive this equation from the statistical theory step by step, taking into account all the theoretical prerequisites, assumptions, and boundary conditions required. In this respect, reference is again made to the original literature (see, for example, Slade 1968; Hanna 1982).

To enable an adequate evaluation and a sufficient understanding of the practical possibilities and limits of application of the Gaussian plume model, the most important prerequisites and assumptions need to be discussed. Theoretically, the model is valid under the following essential conditions:

- homogeneity of turbulence,
- stationary turbulence conditions and steady-state pollutant concentration,
- sufficiently long diffusion times,
- spatially constant basic flow,
- nonzero wind speed,
- the continuity condition must hold true,
- total reflection of the plume on the ground.

These conditions will be illustrated in the following subsections.

2.3.1.1 Homogeneity of Turbulence

Homogeneity of turbulence means that the equalization of the concentration due to turbulent diffusion is equal at every point in space. In mathematical terms, this means that

$$\nabla K = 0 . \tag{2.9}$$

Hence,

$$K(x,y,z) = const. \tag{2.10}$$

In the real atmosphere, however, this state practically never occurs. Horizontal homogeneity is reached approximately when the local topography exhibits only minor differences, such as in the case of flat plains with minor surface roughness.

Vertical homogeneity occurs even less often, because of the buoyancy and gravity forces always present. Wind velocity increasing with height is a typical example of the vertical inhomogeneity of the atmosphere (Sect. 2.3.1.4).

2.3.1.2 Stationary Turbulence Conditions and Steady-State Pollutant Concentration

To derive the Gaussian plume model, we assumed mass transport in the direction of the x axis. In this case Eq. (2.4) would read

$$\frac{\partial \Psi}{\partial t} + \bar{u}\frac{\partial \Psi}{\partial x} = K_x\frac{\partial^2 \Psi}{\partial x^2} + K_y\frac{\partial^2 \Psi}{\partial y^2} + K_z\frac{\partial^2 \Psi}{\partial z^2} . \tag{2.11}$$

The assumption of steady-state pollutant concentration means

$$\frac{\partial \Psi}{\partial t} = 0 .$$

When simultaneously neglecting the diffusion in the x direction (Sect. 2.3.1.5), Eq. (2.11) will give

$$\bar{u}\frac{\partial \Psi}{\partial x} = K_y\frac{\partial^2 \Psi}{\partial y^2} + K_z\frac{\partial^2 \Psi}{\partial z^2} . \tag{2.12}$$

Imagining an area transverse to the flow inside the plume (Fig. 2.6), Eq. (2.12) implies that the amount of material transported from a specific location at mean velocity $\bar{u}$ into the area is just equal to that amount which can be transported away by diffusion in the $y-z$ plane. This is the case when atmospheric turbulence and release source strength are constant in terms of time.

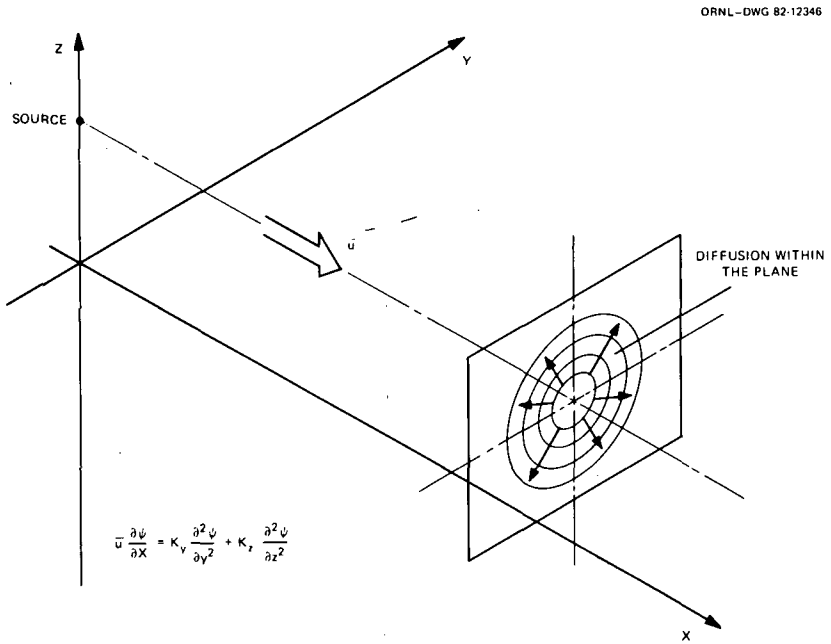

Figure 2.6. Explanation of stationary Gaussian plume diffusion.

In reality, however, neither the turbulence nor the release source strength is constant over longer periods of time. The turbulence of the atmosphere varies with the diurnal cycle of insolation and changes in the general weather situation. The release of radioactive substances from nuclear installations also varies with time.

As a rule, approximately stationary conditions occur only within a range of hours. For example, when examining the probability for a constant wind direction within a 5° sector at Karlsruhe, the following probabilities* are obtained for the durations listed:

15 min	80%
30 min	65%
1 h	35%
2 h	15%
5 h	5%
10 h	0%

*The data are applicable to Karlsruhe, Federal Republic of Germany, and to all states of turbulence (Thomas 1975).

Similar observations apply to other parameters of turbulence, such as wind velocity or the stability of atmospheric stratification. This implies that the pollutant concentration can be calculated according to Eq. (2.8) for relatively short durations only. If a calculation of pollutant concentration is required for longer periods of time, e.g., 12 months, the pollutant concentrations must be superposed in each specific case for constant turbulence conditions (Sect. 2.4.1).

2.3.1.3. The Effect of Diffusion Times

Because of the theoretical derivation of the Gaussian plume model, the pollutant concentration calculated according to Eq. (2.8) represents a mean value over a certain diffusion time (Slade 1968). The implications of this statement may be illustrated by means of Fig. 2.7.

If the time-averaged diagrams of the plume were extended to distances quite far from the source, the boundaries of the time-smoothed plume would meander, because the longer length of the plume would come under the influence of eddies that are quite large in area. The averaging time used originally, therefore, would be too short to show a time-averaged picture of these larger fluctuations. A longer time average appropriate to this greater distance would, again, be too short for distances greater yet.

It is important to recognize that eddies larger than the plume dimension cause the plume to meander, whereas those that are smaller tend to tear it

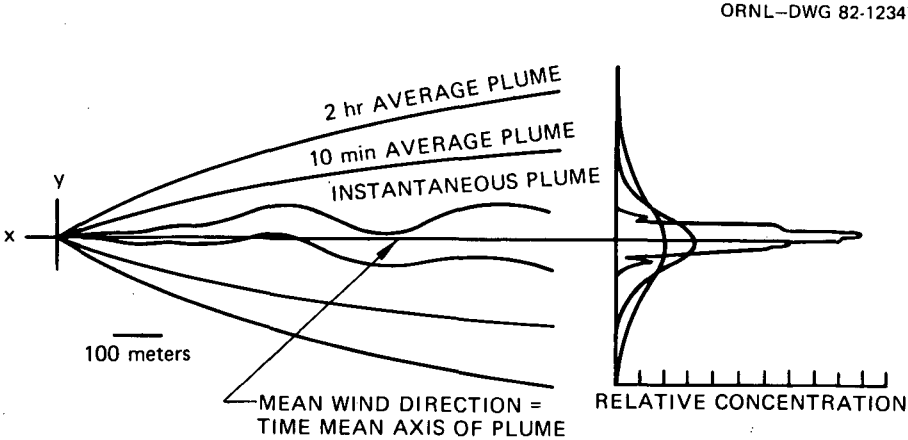

Figure 2.7. The diagram on the left represents the approximate outlines of a smoke plume observed instantaneously and of plumes averaged over 10 min and 2 h. The diagram on the right shows the corresponding cross-plume distribution patterns (Slade 1968).

apart (Fig. 2.8). Thus, as the diffusion time increases and the plume reaches greater and greater distances and grows in size, larger and larger turbulent eddy sizes become effective in diffusing the cloud, and smaller eddies become increasingly ineffective.

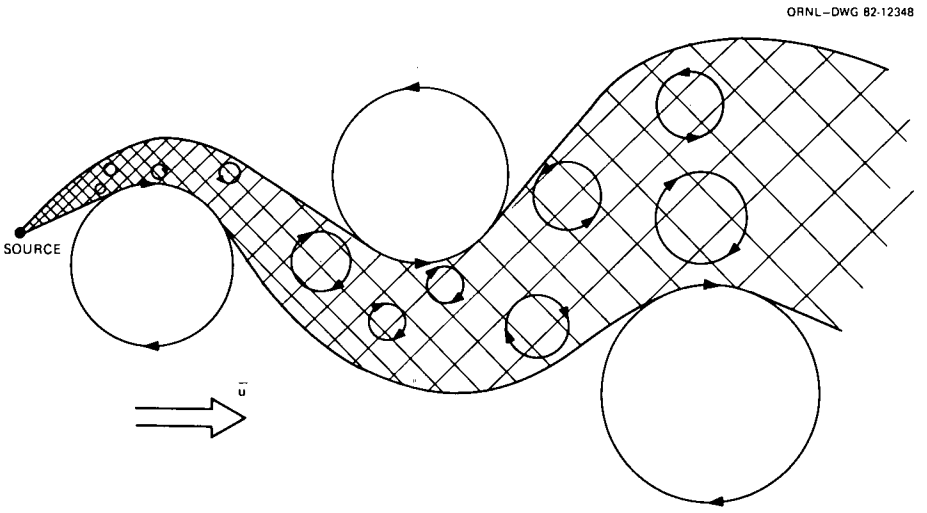

Figure 2.8. Eddies that are larger than the plume tend to cause the plume to meander, whereas those that are smaller tend to tear it apart.

With respect to the averaging time, this shows clearly that for increasing source distances the averaging time must also be increased in order to get a sufficiently smoothed pollutant distribution. Otherwise, the concentrations observed do not generally correspond with the concentrations calculated according to Eq. (2.8).

This becomes important with respect to the experimental determination of the diffusion parameters σ, which we are going to deal with in Sect. 2.3.3.2.

Another effect is that Eq. (2.8) is not able to predict short-period fluctuations, i.e., to predict single instantaneous values of the pollutant concentration in the air. Due to the very long averaging time for the assessment of routine releases, this is of little importance. However, in the case of accidental releases, this may lead to difficulties, since it becomes impossible to make an adequate prediction of the short-term pollutant concentration resulting from an accidental release.

2.3.1.4 Significance of the Spatially Constant Basic Flow

In principle, the spatial constancy of the basic flow,

$$\frac{\partial \bar{u}}{\partial x} = \frac{\partial \bar{u}}{\partial y} = \frac{\partial \bar{u}}{\partial z} = 0 \,, \tag{2.13}$$

is a property that is already covered by the requirement of homogeneity. However, this property can limit the practical application of the Gaussian plume model.

For horizontal changes, Eq. (2.13) is essentially fulfilled. In the vertical direction, however, there is a pronounced wind profile (Fig. 2.9), which changes depending on surface roughness, geographical latitude, and stability of the atmosphere. Accordingly, the wind velocity increases in proportion to the height with the wind direction initially remaining constant, while changing to the geostrophic wind at greater heights. Apart from the air density, the geostrophic wind depends on the Coriolis force and pressure gradient.

The wind velocity increasing with height and the change in wind direction corresponding to the Ekman spiral is graphically represented in Fig. 2.9, based on theoretical considerations (Lettau 1962), for a mean latitude and roughness in the northern hemisphere.

Accordingly, a relatively quick change of the wind velocity in proportion to height takes place in the lower boundary layer which is important to pollutant diffusion near ground level. Up to a height of about 150 m, the wind

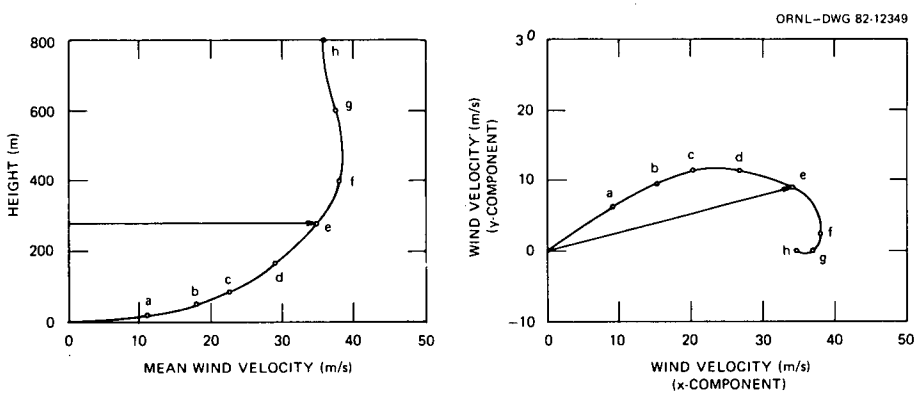

Figure 2.9. Horizontal wind velocity u as a function of height and direction. The values have been calculated for median latitude and roughness length (Lettau 1962).

direction remains almost constant, while turning into the geostrophic wind direction at heights between 150 and 800 m.

Some experimental investigations have shown that the change in wind direction during stable weather situations starts at a height of only 40 m and reaches 26° on the average at a height of 200 m. During unstable weather situations, the turn of the wind direction begins at a height of about 80 m and reaches a mean value of 2° at 100 m and a mean value of 11° at 200 m (Hübschmann 1981).

For describing the height dependence of the scalar wind, an exponential formulation is generally selected within the scope of applications to environmental assessments. This results in

$$\frac{u(z)}{u(z_0)} = \left[\frac{z}{z_0}\right]^m , \tag{2.14}$$

where

m = exponent of vertical velocity wind profile,

in which z_0 is located by definition 10 m above undisturbed terrain (e.g., 10 m above the highest buildings). The exponent m is highly dependent on the surface roughness (see Table E in the appendix of this chapter).

An alternative to the exponential formulation in meteorology is the logarithmic formulation,

$$u(z) = \frac{u^*}{\kappa} \ln \frac{z}{\ell}, \quad \ell \leqslant z < z_{max} . \tag{2.15}$$

where

ℓ = the roughness length,
u^* = the friction velocity (L/T), and
k = von Karmann's constant.

Newberry et al. (1974) divided natural surface into four roughness categories:

- *Category 1*: $0.1 \leqslant m \leqslant 0.15$, or $0.005\ m \leqslant \ell \leqslant 0.05\ m$; sea, plain, or open country without major obstacles.
- *Category 2*: $0.15 \leqslant m \leqslant 0.25$, or $0.05\ m \leqslant \ell \leqslant 0.5\ m$; open country with a few trees or bushes.

- *Category 3*: $0.25 \leqslant m \leqslant 0.35$, or $0.5 \leqslant \ell \leqslant 1.5$ m; dense forestry, small towns, or suburbs.
- *Category 4*: $0.35 \leqslant m \leqslant 0.45$, or $1.5 \text{ m} \leqslant \ell \leqslant 3$ m; metropolitan areas.

2.3.1.5 Meaning of a Nonzero Wind Speed

A further important prerequisite for the application of the Gaussian plume model consists in neglecting the diffusion along the abscissa versus the transport of material with the wind velocity in Eq. (2.11) (Pasquill 1974):

$$K_x \frac{\partial^2 \Psi}{\partial x^2} \ll \bar{u} \frac{\partial \Psi}{\partial x} \quad . \tag{2.16}$$

This applies to wind velocities above approximately 0.5 m/s. In the real atmosphere, this prerequisite is generally fulfilled, in particular for heights above 100 m. For lower heights (e.g., for ground releases) and higher fractions of calms, the Gaussian plume model is not strictly applicable. For such cases, it may be necessary to introduce the diffusion term in the x direction into the solution again and thus to base the calculations either on the Gaussian puff model (Start et al. 1974; Doury 1980; Vogt et al. 1979) or on other more sophisticated numerical models (Hoffman et al. 1978).

2.3.1.6 Condition for Continuity and Total Reflection on the Ground

The continuity condition for the Gaussian plume model reads as follows:

$$\int_0^\infty \iint_{-\infty}^{+\infty} \Psi(x,y,z) \cdot \bar{u} \, dy \, dz \, dt = Q \quad . \tag{2.17}$$

This means that the free atmosphere must not have any sources or sinks. The basic flow of activity $\bar{u} \cdot \Psi$ through a random element of area transverse to the direction of flow in the $y-z$ plane, in $\text{Bq}/(\text{m}^2 \cdot \text{s})$ for instance, must be equal to the total amount of activity released, Q, when integrated over the time of release and the entire $y-z$ plane; i.e., in the final analysis, the total amount of activity must pass through any $y-z$ plane at the point x.

In the real atmosphere, however, the condition for continuity defined according to Eq. (2.17) is not fulfilled. Here, both sources (resuspension of radionuclides) and sinks (dry and wet deposition, radioactive decay, etc.) must be expected. These discontinuities in the atmosphere are not taken into account in actual fact in the derivation of the Gaussian plume model. However, it is

current practice to introduce the sinks into the calculation again via balancing the amount of activity transported:

$$\frac{\partial Q}{\partial t} = -\lambda Q - \Lambda Q - v_g \int_{-\infty}^{+\infty}\int \Psi(x,y,0)\, dx\, dy \,, \tag{2.18}$$

where $\Psi(x,y,0)$ is given by Eq. (2.8).

The assumption of a total reflection on the ground is not fulfilled either, since, in reality, there is a deposition on the ground. However, this assumption tends to lead to an overestimation of the pollutant concentration in air and, thus, to more conservative values.

2.3.1.7 Practical Consequences

The theoretical prerequisites, assumptions, and boundary conditions for the Gaussian plume model are rarely completely fulfilled in the atmosphere. However, through development of the diffusion parameters (σ's) from the results of field studies, the Gaussian model can produce results which are in reasonable agreement with data.

This applies essentially to the homogeneity condition (including the spatially constant wind velocity), to the condition of continuity, and to the total reflection on the ground, as well as to any possible limitations of the diffusion with height due to temperature inversions.

In view of the requirement of stationary turbulence conditions, it will be necessary to categorize the different states of turbulence in the atmosphere and organize the experiments in such a way that a relevant set of diffusion parameters is ascertained for all states of turbulence. This procedure offers the possibility of calculating pollutant concentrations over periods of time longer than those given by the duration of stationary turbulence. In the concrete case, this will be necessary for assessing, e.g., the annual radiation exposure.

2.3.2 Classification of Turbulence

The overall state of turbulence in the atmosphere is composed of a buoyant (convective) and a mechanical fraction. Depending on the weather situation and ground surface conditions, the convective turbulence predominates at one time and the mechanical turbulence at another.

The causal connections for their formation and effect are shown in Figure 2.10. It is obvious that the intensity of turbulent diffusion is subject to large variations in terms of time and location due to the complexity of its causes. The overall condition of the atmosphere may be subdivided into several individual "states" for which the theoretical assumption of a stationary, homogeneous atmosphere is fulfilled for a certain period of time at a fixed location.

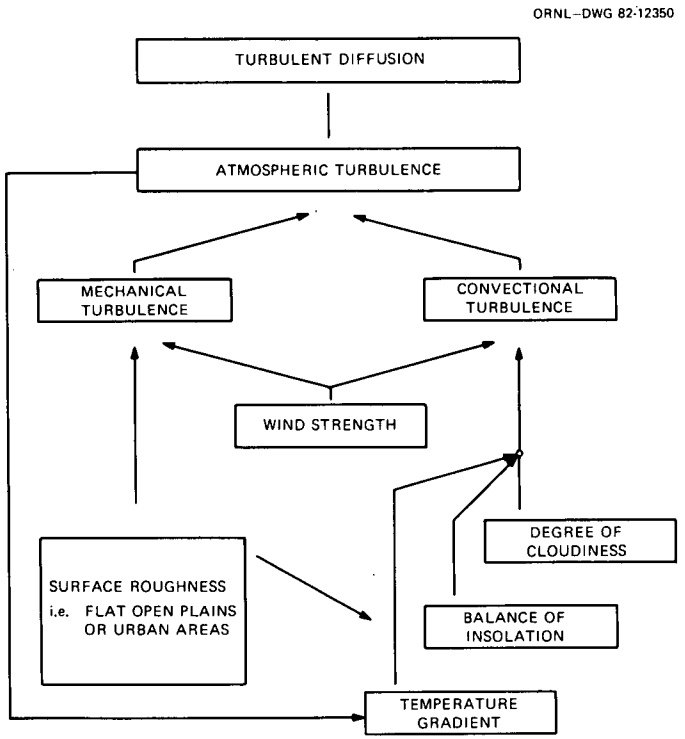

Figure 2.10. Influence scheme of the turbulent diffusion.

Although direct measurements of turbulence should be used to determine these states, such measurements are not practical due to difficulty and expense. Consequently, atmospheric turbulence is usually inferred from available meteorological information.

Using information from the diffusion experiments performed for Project Prairie Grass, Pasquill (1962) distinguished six stability classes from A (highly unstable stratification) to F (highly stable stratification). The criteria for Pasquill's original classification considered the relationship of wind speed, isolation (amount of incoming solar radiation), and cloudiness. Table 2.1 presents the meteorological conditions used to derive the Pasquill stability classes (see Hanna 1982 or Turner 1967). These types of meteorological measurements are available at National Weather Service (NWS) offices.

Turner subsequently developed criteria to determine Pasquill stability classes more objectively using cloud cover and height; solar angle (as a function of time, date, and location); and wind speed. A similar classification scheme has been developed by Klug (1969) with reference to Pasquill using

Table 2.1. Pasquill stability categories

A: Extremely Unstable Conditions
B: Moderately Unstable Conditions
C: Slightly Unstable Conditions
D: Neutral Conditions[a]
E: Slightly Stable Conditions
F: Moderately Stable Conditions

Surface Wind Speed at 10 m (m/s)	Daytime Insolation			Nighttime Conditions	
	Strong	Moderate	Slight	Thin Overcast or >3/8 Cloudiness[b]	≤3/8 Cloudiness
<2	A	A—B	B		
2—3	A—B	B	C	E	F
3—5	B	B—C	C	D	E
5—6	C	C—D	D	D	D
>6	C	D	D	D	D

[a]Applicable to heavy overcast day or night.
[b]The degree of cloudiness is defined as that fraction of the sky above the local apparent horizon that is covered by clouds.

exclusively synoptic data. It is based on the degree of cloudiness and the wind velocity at a height of 10 m over undisturbed ground.

Other authors do not confine themselves to purely synoptic data, but use either the radiation balance or the temperature gradient or both in conjunction with the wind velocity, instead of the degree of cloudiness, for evaluating the turbulent diffusion, since both the radiation balance and the temperature gradient reflect in a way the condition of the ground surface. The radiation balance is, among other things, a function of variations in the reflection capacity of the ground surface. The temperature gradient, although being governed primarily by convective turbulence, is also influenced through changes in mechanical turbulence.

Such a system, which also considers the effect of the ground surface, is used in a slightly modified form by, for example, McElroy et al. (1968, 1969). By means of the standard deviation of the horizontal fluctuation of the wind direction and using the Richardson number, which constitutes a measure for the vertical temperature stratification of the atmosphere, the authors define four stability classes, presented in Table 2.2.

Table 2.2. Definition of stability classes according to McElroy et al. (1968, 1969)

σ_ϑ	Richardson number (dimensionless)		
(deg)	<-0.01	± 0.01	>0.01
24 to 30	B_2' (B)[a]		
18 to 22	B_1' (C)		
15 to 20		C (D)	
8 to 13			D (E)

[a]The corresponding Pasquill stability classes are given in parentheses.

A procedure involving relatively high expense in terms of measuring techniques is used by Polster and Vogt in Jülich (Federal Republic of Germany), Table 2.3 (Vogt 1970). Basically, the system is similar to that of Pasquill. In order to keep the classification error as small as possible, however, they simultaneously determine the degree of cloudiness, the radiation balance, and the temperature gradient in addition to the wind velocity.

Although the three additional values are in part redundant, the radiation balance and temperature gradient take account of different characteristics of the ground surface, so that they also supplement each other to a certain extent. Among other things, this procedure is aimed at taking better account of the ground surface condition during the implementation of diffusion experiments.

Furthermore, there are several other systems of determination which are widely used to classify atmospheric turbulence. These systems use one parameter only—either

- the vertical temperature lapse rate (also referred to as either ΔT or vertical temperature gradient), or
- the horizontal fluctuation of the wind direction, *cf* (Slade 1968; Singer et al. 1966), or
- the Richardson number, or
- the Monin-Obukhov length, *cf* (Gifford 1976).

Table 2.3. Alternative definition of the stability classes according to Vogt (1970)

	Time of day	Sun height, α	Degree of cloudiness						
Synoptic Observations	Day	>50°	≤4/8	5/8 ... 7/8 ≤4/8	8/8 5/8 ... 7/8 ≤4/8	8/8 5/8 ... 7/8 ≤4/8	8/8 >4/8 (0) ... 8/8 Fog		
		31° ... 50°							
		16° ... 30°							
		8° ... 15°							
		≤7°							
	Night	--					8/8	5/8 ... 7/8 Fog	≤4/8
Insolation Index			4	3	2	1	0	−1	−2
Measurement of Insolation, cal/cm²·min			>0.60	0.60 ... 0.35	0.34 ... 0.16	0.15 ... 0.09	0.08 ... −0.01	−0.02 ... −0.04	≤−0.05
Measurement of Stability [temperature gradient ($\Delta T/\Delta z$), °C/100 m, measured at heights of 120 m and 20 m]			≤−1.5	−1.4 ... −1.2	−1.1 ...−0.9	−0.8 ... −0.7	−0.6 ... 0.0	0.1 ... 2.0	>2.0
Wind Velocity (u), m/s									
<1			A	A	B	C	D^+	G	G
1 ... 1.9			A	B	B	C	D^+	G	G
2 ... 2.9			A	B	C	D	D	E	F
3 ... 4.9			B	B	C	D	D	D	E
5 ... 6.9			C	C	D	D	D	D	E
≥7			D	D	D	D	D	D	D

Vertical temperature gradient, an attempt to relate the thermal characteristics of the atmosphere to turbulence intensity, is relatively simple to measure on a fixed tower and is one of the measurements made routinely at nuclear power plants. ΔT is a function of surface characteristics of height of measurement. Table 2.4 presents the ΔT classification scheme promulgated by the NRC. Note that the NRC has added an "extremely stable" class ("*G*")* because of their concern about accidental releases of radioactive material from nuclear power plants during low-wind-speed, stable atmospheric conditions. Such an extremely stable class has also been promulgated by Vogt (1970). The ΔT method is probably most appropriate when measured over relatively low height intervals, such as from 10 m to 60 m above the ground and for the consideration of releases near ground level. Measurements through deeper atmospheric layers do not properly reflect changes nearer the surface. ΔT is a poor indicator of unstable conditions and should not be considered the best stability indicator for evaluating diffusion from elevated release points (at heights above about 100 m). ΔT is probably most useful in estimating turbulent intensity during low-wind-speed, stable conditions because the measurement is unaffected by instrument response to wind speed. But ΔT is regarded primarily as an indicator of vertical diffusion.

*The NRC developed σ_y and σ_z curves for "*G*" stability using the following relationships to the σ_y and σ_z curves for "*F*" stability:

$$\sigma_y(G) = 2/3\ \sigma_y(F)$$
$$\sigma_z(G) = 3/5\ \sigma_z(F)$$

Table 2.4. Classification of atmospheric stability by vertical temperature difference

Stability classification	Pasquill categories	Temperature change with height (°C/100 m)
Extremely unstable	*A*	$\Delta T/\Delta z \leq -1.9$
Moderately unstable	*B*	$-1.9 < \Delta T/\Delta z \leq -1.7$
Slightly unstable	*C*	$-1.7 < \Delta T/\Delta z \leq -1.5$
Neutral	*D*	$-1.5 < \Delta T/\Delta z \leq -0.5$
Slightly stable	*E*	$-0.5 < \Delta T/\Delta z \leq 1.5$
Moderately stable	*F*	$1.5 < \Delta T/\Delta z \leq 4.0$
Extremely stable	*G*	$4.0 < \Delta T/\Delta z$

Wind direction fluctuations (Fig. 2.11) are the direct result of the intensity of turbulence, and, as such, are functions of surface characteristics and heights of measurement. The standard deviations of horizontal wind direction fluctuations (σ_θ) have been related to stability classes.* Table 2.5 presents the σ_θ classification scheme promulgated by the NRC, based on an analysis performed by Slade (1968). Again, note that the NRC has included a "*G*"

*Standard deviations of horizontal and vertical wind direction fluctuations can also be used to estimate σ_y and σ_z without interfering a stability class.

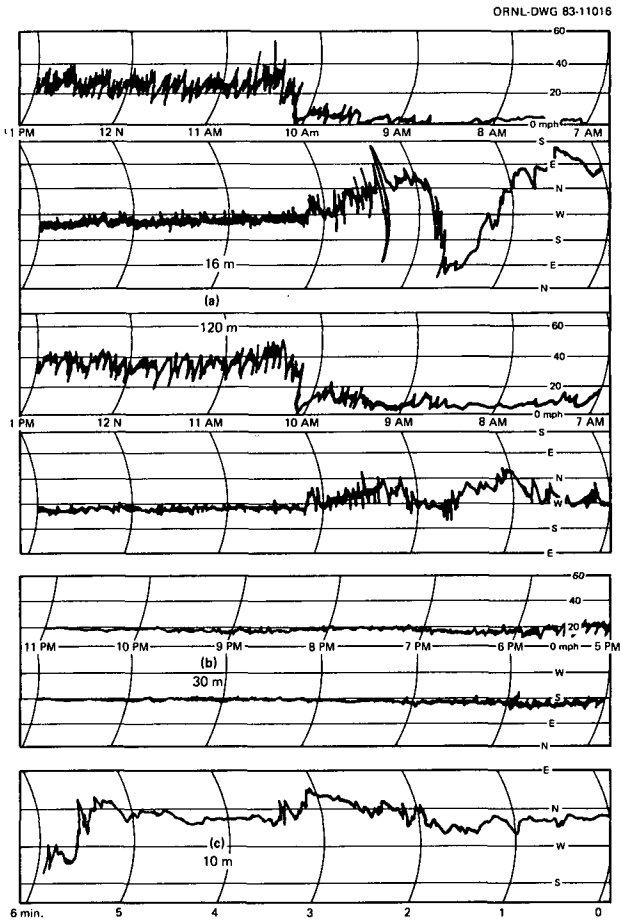

Figure 2.11. Typical horizontal wind-speed and -direction traces. (*a*) Differences in characteristics for simultaneous recordings at 16 and 120 m (chart speed, 3 in./h). (*b*) Example of a very steady wind trace (chart speed, 3 in./h). (*c*) High-speed trace (chart speed, 3 in./min). (Slade 1968)

Table 2.5. Classification of atmospheric stability[a] by standard deviation of horizontal wind direction (σ_θ)

Stability classification	Pasquill categories	σ_θ[b] (deg)
Extremely unstable	*A*	$\sigma_\theta \geq 22.5$
Moderately unstable	*B*	$22.5 > \sigma_\theta \geq 17.5$
Slightly unstable	*C*	$17.5 > \sigma_\theta \geq 12.5$
Neutral	*D*	$12.5 > \sigma_\theta \geq 7.5$
Slightly stable	*E*	$7.5 > \sigma_\theta \geq 3.8$
Moderately stable	*F*	$3.8 > \sigma_\theta \geq 2.1$
Extremely stable	*G*	$2.1 > \sigma_\theta$

[a]Use of σ_θ to represent atmospheric stability when wind speeds are less than 1.5 m/s should be substantiated. If σ_θ is to be used as an indicator of vertical diffusion (atmospheric stability), adjustments to the sampling interval may be needed to eliminate wind fluctuations in the horizontal which do not occur in the vertical, especially during nighttime conditions.

[b]Determined for a 15-min to 1-h period for horizontal diffusion.

class for comparability for the ΔT classification scheme. The applicability of the standard deviation of horizontal wind direction is determined by the responsiveness of the wind vane used for measurements and the methodology used to calculate the standard deviation of the fluctuations. Many wind vanes are not sufficiently responsive at low wind speeds to allow a meaningful determination of wind direction fluctuations. The NRC, for example, suggests use of σ_θ only for wind speeds greater than 1.5 m/s. In addition, the NRC recommends that σ_θ be determined from no less than 180 instantaneous values of wind direction to achieve a meaningful representation of the standard deviation. But σ_θ is regarded primarily as an indicator of horizontal diffusion.

To accommodate their relative strengths, the ΔT and σ_θ are sometimes used in conjunction in what is called a "split sigma" approach. The "split sigma" aproach usually takes the form of deriving horizontal stability class

according to σ_θ and vertical stability class according to ΔT, and σ_y and σ_z values are determined accordingly. In this approach, the ΔT method is generally used to represent a single stability class for diurnal wind speed conditions (e.g., less than 1.5 m/s).

Indicators of turbulence such as the Richardson number, bulk Richardson number, and Monin-Obukhov length, provide relationships which reflect both thermal and mechanical turbulence in the vertical. These indicators are shown for comparison.

$$\text{Richardson number} = \frac{g}{T} \cdot \frac{\left(\frac{\partial T}{\partial z} + \Gamma\right)}{\left(\frac{\partial \bar{u}}{\partial z}\right)^2}, \tag{2.19}$$

where

g = acceleration due to gravity,
T = temperature,
Γ = adiabatic lapse rate,
$\bar{u}$ = mean wind speed, and
z = height above ground.

The quantity $\partial u/\partial Z$ represents wind shear.

$$\text{Bulk Richardson number} = \frac{g}{T} \cdot \frac{\left(\frac{\partial t}{\partial z} + \Gamma\right) Z^2}{u_Z{}^2}, \tag{2.20}$$

where

u_z = wind speed at the geometrical mean of the heights used to determine the temperature gradient.

$$\text{Monin-Obukhov Length, L} = \frac{u_*^3 C_p \rho T}{kgH}, \tag{2.21}$$

where

u_* = friction velocity as determined from the surface shear stress $u_* = (\tau/\rho)^{1/2}$,

C_p = specific heat at constant pressure,
ρ = density,
τ = shear stress,
k = von Karman's constant,
g = acceleration due to gravity, and
H = vertical heat flux.

Table 2.6 presents a relationship between the Pasquill stability classes, Richardson number, and Monon-Obukhov length.

Table 2.6. Relations between Pasquill type and turbulence criteria R_i and L for flow over short grass (Gifford 1976)

Pasquill type	R_i (at 2 m)	L (m)
A	−1.0 to −0.7	−2 to −3
B	−0.5 to −0.4	−4 to −5
C	−0.17 to −0.13	−12 to −15
D	0	∞
E	0.03 to 0.05	35 to 75
F	0.05 to 0.11	8 to 35

2.3.3 Diffusion Parameters

The Gaussian model has been expressed in terms of diffusion parameters, σ_y and σ_z. Probably the most subjective and controversial aspect of using the model is selection of appropriate horizontal or vertical coefficients. Table 2.7 summarizes a number of field experiments used in deriving these parameters.

2.3.3.1 Major Test Series

Table 2.7 compiles what are generally thought to be the most important test series for determining the diffusion parameters. This compilation covers tracer experiments exclusively. Besides the test site and name of the project,

Table 2.7. Some important diffusion test series (Vogt 1977)

Test site (project)	Tracer	Release height (m)	Duration (min)	Range (km)	Sampling height (m)	Roughness length (m)	Number of tests
Harwell, U.K. (BEPO Series) (Stewart et al. 1958)	^{41}Ar	61	15–60	10	0–300		88
ONeill, Nebraska, U.S. (Prairie Grass) (Barad et al. 1958)	SO_2	0.5	10	0.8	1.5	0.01	70
Massachusetts, U.S. (Round Hill) (Cramer et al. 1959)	SO_2	0.3	10	0.2	1–5	0.1	
Hanford, Wash., U.S. (Green Glow) (Barad et al. 1962)	ZnS	0.35–1	30–60	25	1.5–70		80
NRTS, Idaho, U.S. (Islitzer, 1961)	Uranine	46	30	3.2	1		16
Brookhaven, N.Y., U.S. (Singer et al. 1966)	^{41}Ar	108	30-90	60	Surface	1	
St. Louis, Mo., U.S. (McElroy et al. 1968)	Zn-Cd-sulfide	Near ground	60	16	Surface (to 300)	1–2	32
Cadarache, France (Le Quinio 1962)	Uranine	5–50	30–60	10	1		100
Karlsruhe, F.R.Germany (König et al. 1973)	HTO $CFCl_3$, CF_2 BR_2	60 100	3 x 20 3 x 20	3.5 3.5	1 1	1–2 1–2	25
Jülich, F.R. Germany (Vogt et al. 1974)	^{64}Cu ^{166}Ho	50 100	30–60 30–60	11 11	1–250 1–250	1–2 1–2	65

Table 2.7 contains the most relevant data on the experimental conditions: type of tracer, release height and duration, sampling range and height, roughness length, and number of tracer experiments. These data are important but not sufficient for evaluating the reliability, comparability, and application range of the test results. It must be said that the measurements or at least the documentation of the meteorological data required for interpretation of the results (such as vertical profile of wind velocity and wind direction, temperature gradient, and wind fluctuations) still leave much to be desired. In certain studies (e.g., Prairie Grass Project, St. Louis Diffusion Studies), the emission heights were near ground level; in other test series, they corresponded to medium stack heights (50 to 100 m). As to the emission or sampling periods (varying between 10 and 90 min), the test series are not always comparable. In the Prairie Grass and Round Hill tests, the sampling grid extended only over relatively small source distance ranges, so that the values extrapolated from the measured diffusion parameters for larger source distances are very speculative. Sampling was essentially effected near ground level.

The number, range, and informative value of additional vertical distribution measurements carried out for some of the tests are restricted. The data on roughness lengths, which are available only to a minor extent, show that the surface roughness at the individual sites differs very much. These differences are all important to consider when comparing the measurement results.

2.3.3.2 Various Parameter Systems

Not all of the test series described have led to a set of source-distance–dependent diffusion parameters covering all diffusion categories, that is, all relevant types of diffusion for effluent plumes. The following discussion describes some of the most important systems of diffusion parameters, based chiefly on the test series listed in Table 2.7.

2.3.3.2.1. ***The Pasquill-Gifford system.*** The most common compilation of σ_y and σ_z values are those presented by Gifford (1961). Gifford developed σ_y and σ_z values representative of each stability class (sect. 2.3.2) as functions of downwind distance (Figs. 2.12 and 2.13), often called the Pasquill-Gifford (PG) curves. These curves can be approximated by the equations

$$\sigma_y(x) = (a_1 \ln x + a_2)x \tag{2.22}$$

and

$$\sigma_z(x) = \frac{1}{2.15} \exp(b_1 + b_2 \ln x + b_3 \ln^2 x), \tag{2.23}$$

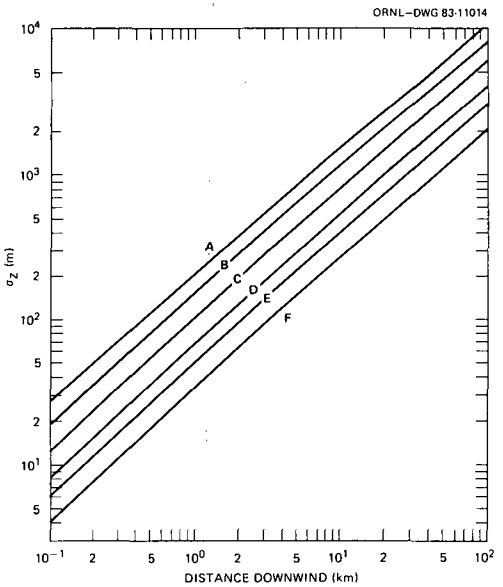

Figure 2.12. Horizontal dispersion coefficient as a function of downwind distance from the source (Turner 1967).

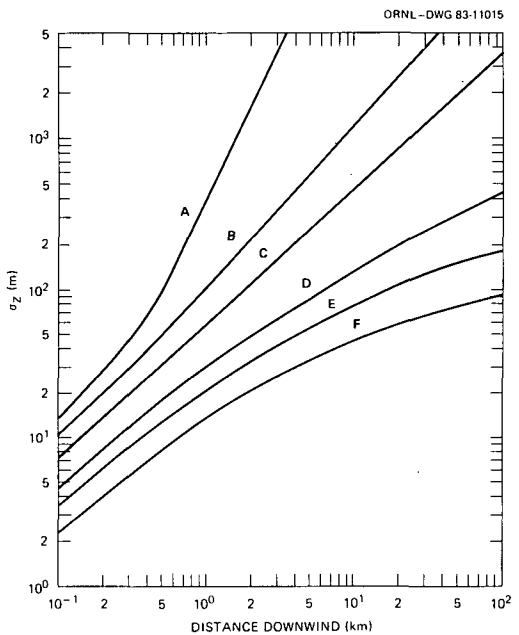

Figure 2.13. Vertical dispersion coefficient as a function of downwind distance from the source (Turner 1967).

the coefficients of which are specified in Table 2.8. Because of the origin of the diffusion measurements used for their derivation, these functions are strictly applicable for short-term (6–10 min) releases near ground level in uniform terrain (low roughness length) out to distances less than 1 km. Extrapolations of σ_y and σ_z values out to distances on the order of 100 km have little basis in observation.

Generally, the Pasquill-Gifford curves of σ_y and σ_z provide reasonable estimates of the magnitude of long-term concentrations from releases at or near ground level. The PG curves are least appropriate for elevated releases or releases in complex terrain. The slope of the σ_z curve for extremely unstable conditions is questionable. Some modifications to the PG curves for specific situations are discussed later.

2.3.3.2.2. ***The Klug system.*** In 1964, Klug reevaluated the available data from major U.S. tracer test series and compared the results of the combined test series Prairie Grass and Round Hill and the experiments of Hanford and Idaho Falls with the Pasquill data (Klug 1964). Based on the evaluations of the Prairie Grass experiments, Klug specified in a later study a system of diffusion parameters (Klug 1969) that is suited for application to short-term ground-level releases over terrain with a low surface roughness, in the same way as the Pasquill system. In his comparison with the data of Pasquill and Brookhaven National Laboratory, Klug does not exceed source distances of 2 or 3 km. In this range, the diffusion parameters can be described by power functions, such as

$$\sigma_y(x) = p_y x^{q_y} \tag{2.24}$$

and

$$\sigma_z(x) = p_z x^{q_z} , \tag{2.25}$$

where x is the source distance and the coefficients p and q are specified in Table 2.8.

2.3.3.2.3. ***The Brookhaven system.*** The tracer experiments carried out at Brookhaven have been evaluated by Singer and Smith (Singer et al. 1966). At medium distances, the results are based on oil mist measurements; at longer distances of up to 60 km, they are based on measurements of the ^{41}Ar concentration distribution. Four types of diffusion are defined by the authors.

Classification is according to gustiness based on wind direction traces, recorded by a Bendix Friez aerovane located 107 m above ground level. No diffusion parameters are specified for the class of maximum gustiness, type A (fluctuations of the wind exceeding 90 deg). The approximate assignment of the diffusion parameters recommended for the remaining four classes that, in the light of power functions according to Eqs. (2.24) and (2.25), are dependent on the source distance x, is specified in Table 2.8. This table also shows the

Table 2.8. Diffusion coefficients of the different systems of diffusion parameters for all stability classes (Vogt 1977)

	Diffusion category	A	B	C	D	E	F	Roughness category
	a_1	−0.0234	−0.0147	−0.0117	−0.0059	−0.0059	−0.0029	
	a_2	0.3500	0.2480	0.1750	0.1080	0.0880	0.0540	
Pasquill-	b_1	0.8800	−0.9850	−1.1860	−1.3500	−2.8800	−3.8000	I
Gifford	b_2	0.1520	0.8200	0.8500	0.7930	1.2550	1.4190	
	b_3	0.1475	0.0168	0.0045	0.0022	−0.0420	−0.0550	
		V	IV	III_2	III_1	II	I	
	p_y	0.4690	0.3060	0.2300	0.2190	0.2370	0.2730	
	q_y	0.9030	0.8850	0.8550	0.7640	0.6910	0.5940	
Klug	p_z	0.0170	0.0720	0.0760	0.1400	0.2170	0.2620	I
	q_z	1.3800	1.0210	0.8790	0.7270	0.6100	0.5000	
			B_2	B_1	C		D	
	p_y		0.4000	0.3600	0.3200		0.3100	
	q_y		0.9100	0.8600	0.7800		0.7100	
Brookhaven	p_z		0.4110	0.3260	0.2230		0.0620	3
	q_z		0.9070	0.8590	0.7760		0.7090	
			(B)	(C)	(D)	(E)		
	p_y		1.7000	1.4400	0.9100	1.0200		
	q_y		0.7170	0.7100	0.7290	0.6480		
St. Louis	p_z		0.0790	0.1310	0.9100	0.9300		3–4
	q_z		1.2000	1.0460	0.7020	0.4650		
		A	B	C	D	E	F	
	p_y	(0.8685)	0.8685	0.7184	0.6248	1.6910	5.3820	
Jülich[a]	q_y	(0.8097)	0.8097	0.7837	0.7672	0.6211	0.5778	
(50 m)	p_z	(0.2222)	0.2222	0.2149	0.2048	0.1616	0.3960	3–4
	q_z	(0.9680)	0.9680	0.9438	0.9358	0.8094	0.6183	
		A	B	C	D	E	F	
	p_y	0.2294	0.2270	0.2236	0.2217	(1.6910)	(5.3820)	
Jülich[a]	q_y	1.0032	0.9704	0.9380	0.9048	(0.6211)	(0.5778)	
(100 m)	p_z	0.0965	0.1551	0.2474	0.3980	(0.1616)	(0.3960)	3–4
	q_z	1.1581	1.0236	0.8900	0.7552	(0.8094)	(0.6183)	

[a] A more recent set of diffusion parameters for effective release heights of 50, 100, and 180 m is given in the appendix of this chapter.

association between gustiness classes and diffusion categories determined by Pasquill. Since the experiments at Brookhaven were carried out under conditions typical for the release of pollutants from industrial plants (the tracer was released, as a rule, at a height of 108 m, with emission periods of ~1 h, and its dispersion was measured over terrain of medium roughness), the results should be applicable in many practical instances.

2.3.3.2.4. ***St. Louis system.*** In evaluating the tracer test series carried out at St. Louis, McElroy and Pooler used the common Gaussian model for the 26 experiments carried out during daytime. A simpler box model was used in view of the limited data material for the more stable meteorological conditions during the 12 experiments carried out in the evening. In doing so, it was assumed that the vertical profiles of wind velocity and tracer concentration were significantly interrelated (McElroy et al. 1968). When summing up the results, trial classifications were carried out according to the Pasquill-Turner diffusion categories, to modified Brookhaven gustiness classes, and to a combination of horizontal wind direction fluctuations as a criterion of the horizontal turbulence component and the Richardson number as a criterion of the vertical stability (see Table 2.2). The St. Louis experiments likewise revealed source distance dependence of the diffusion parameters representable as power functions within the entire measuring range of up to 16 km. The coefficients specified in Table 2.8 reflect the last-mentioned classification (horizontal wind fluctuations and Richardson number), which, according to the authors, is the best way of summarizing the test results obtained. The four diffusion categories have not been designated by McElroy and Pooler. The classification made in Table 2.8 can be substantiated by the meteorological conditions specified in McElroy et al. (1968). In this connection, account had to be taken of both the metropolitan site and the statement that neither low wind conditions nor extremely high wind velocities occurred during the experiments. Since the experiments were carried out over the relatively flat area of metropolitan St. Louis, with emission taking place near ground level and the emission duration being 1 h, it is to be expected that the resulting diffusion parameters are applicable to diffusion calculations for metropolitan sites and, possibly, other sites of extreme surface roughness.*

2.3.3.2.5. ***The Jülich system.*** The tracer experiments carried out in the vicinity of the Jülich Nuclear Research Center at emission heights of 50 and 100 m and during emission periods of 1 h have been evaluated separately according to the above emission levels. The diffusion categories during experimentation were determined by three alternative systems (Table 2.3). To classify the stability classes, the most probable diffusion category resulting from the three alternative methods was taken.

*See also Briggs (1973).

The experiments are carried out up to a source distance of 11 km. The source distance dependence of the diffusion parameters, again, is described by power functions, the coefficients of which are listed separately in Table 2.8 for emission levels of 50 and 100 m.

For these two emission levels, substantial differences have been found: the diffusion parameters are smaller at the 100-m level than at the 50-m level for all diffusion categories, chiefly governed by mechanical turbulence, because the impact of the turbulence caused by obstacles on the ground is reduced with increase in height. Only in the case of highly unstable strata are the diffusion parameters, as anticipated, higher at the 100-m level, since the turbulence component resulting from thermal convection is more developed at longer distances from the ground boundary layer. Since the mechanical turbulence caused by surface roughness reaches its maximum at high wind velocities, there is a maximum increase in diffusion parameters for diffusion categories D and C as compared with those of low roughness (Pasquill 1974; Klug 1969), causing the σ_z values for diffusion categories C and D at an emission height of 50 m to approach the values of category B. Although parts of the experiments were carried out chiefly over arable land (medium surface roughness) and others chiefly over woodland (higher surface roughness), these differences in roughness did not result in significant differences with regard to the diffusion parameters. This may be attributed to the fact that the dispersion is not decisively governed by the local roughness conditions, but by the mean roughness lengths over extended entrance regions and diffusion distances. Considering the experimental conditions, *the diffusion parameters measured in Jülich should be applicable to sites with medium to higher surface roughness, which is due to settlements, vegetation, and other ground obstacles (Table 2.8).*

2.4 PRACTICAL APPLICATION OF THE GAUSSIAN PLUME MODEL IN THE CASE OF ROUTINE RELEASES

2.4.1 Normalized Time-Integrated Air Concentration

An important quantity in practical dose evaluations is the dose equivalent H. Apart from a few exceptions, the dose equivalent is directly proportional to the time-integral of the activity concentration, being calculated over the entire period of exposure:

$$H \alpha \int_0^t \Psi(x,y,0)\, dt \ . \tag{2.26}$$

In the case of routine releases, the exposure periods of interest are days, weeks, months, or years.

Basically, the calculation of the time-integrated activity concentration χ is quite simple. However, it poses initial problems insofar as the prerequisite of stationary turbulence required for the computation of Ψ does not apply to the entire duration of release or exposure, respectively. For this reason, the release duration is broken into individual duration intervals Δt, in which the stationary condition is fulfilled. Then the contributions of the individual duration intervals are superimposed to obtain the total contribution.

By additional identification of each state of turbulence in the duration interval Δt_ν by means of the wind direction ϕ, (note: usual U.S. convention for horizontal wind direction is θ) wind velocity of the velocity level k, and diffusion category j, which is sufficiently accurate for practical calculations, the time-integrated activity concentration in the wind direction ϕ may be calculated as follows:

$$\chi_\phi = \int_0^t \Psi \, dt \cong \sum_{jk} \Psi_{\phi jk} \cdot \sum_{\nu} \Delta t_{\phi jk\nu} \tag{2.27}$$

$$\cong \frac{\sum_{jk} \Psi_{\phi jk} \cdot \sum_{\nu} \Delta t_{\phi jk\nu} \cdot \Delta t}{\sum_{\phi jk\nu} \Delta t_{\phi jk\nu}}$$

$$\cong \sum_{jk} p_{\phi jk} \cdot \Psi_{\phi jk} \cdot \Delta t$$

$$\cong \bar{\Psi}_\phi \cdot \Delta t \ ,$$

in which ${}^p\phi_{jk}$ is the frequency of the joint occurrence of a certain combination jk in the direction ϕ related to all of the combinations ϕjk. For easier application, the wind rose is divided into n sectors of equal size. If the wind direction ϕ denotes the direction of the angle-bisecting line of a sector i, as shown in Fig. 2.14,

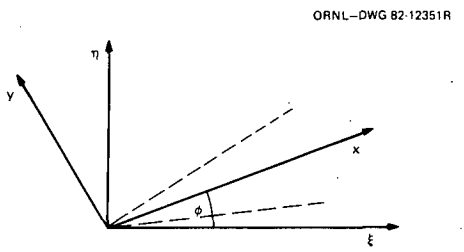

Fig. 2.14. Sector I of the wind rose (dispersal sectors).

and if it is assumed that all effluent plumes falling into this sector coincide with the direction of the bisector, the following equation is valid:

$$\chi_i = \bar{\Psi}_i \Delta t \ , \tag{2.28}$$

where

$$\bar{\Psi}_i = \sum_{jk} p_{ijk} \frac{n}{2\pi x} \int_{-\infty}^{+\infty} \Psi_{\phi jk}(x,y,0)\, dy \ . \tag{2.29}$$

In connection with the relative frequency p and based on the assumptions made before, the direction ϕ has been replaced by the index of the dispersion sector i.*

Taking into account the basic equation (2.8), the following is now obtained for the time-integrated activity concentration:

$$\chi_i(x,0) = \dot{Q}\Delta t \sum_{jk} p_{ijk} \frac{n}{(2\pi^3)^{1/2}\bar{u}_{jk}x} \cdot \frac{\exp[-H^2/(2\sigma_{zj}^2(x))]}{\sigma_{zj}(x)} \ . \tag{2.30}$$

For convenience, we divide both sides of Eq. (2.30) by $Q = \dot{Q}\Delta t$. This leads to the so-called χ/Q-value,

$$\frac{\chi_i}{Q} = \sum_{jk} p_{ijk} \frac{n}{(2\pi^3)^{1/2} x \bar{u}_{jk}} \cdot \frac{\exp[-H^2/(2\sigma_{zj}^2(x))]}{\sigma_{zj}(x)} \ , \tag{2.31}$$

which we will refer to in the following as *long-term dispersion factor.* This factor is usually applied to evaluate the radiation exposure in the case of submersion in an electron-emitting cloud and inhalaton due to routine releases. The parameter p_{ijk} represents three-dimensional dispersion meteorological statistics for the joint occurrence of wind in direction of sector i, atmospheric stability in class j, and wind speed in class k. It is known for most applications.

For $n = 16$, and a particular sector i, where $p_{ijk} \equiv n_{jk}/N$, and $\bar{u}_k$ being the representative wind speed in class k, Eq. (2.31) can be expressed in the form used by the NRC in Regulatory Guide 1.111:

$$\frac{\chi}{Q} = 2.032 \sum_{jk} \frac{n_{jk}}{N} \left[x\, \bar{u}_k\, \sigma_{zj}\right]^{-1} \exp\left[-\frac{H^2}{2\sigma_{zj}^2}\right] \ , \tag{2.32}$$

*Note that $\sum_{ijk} p_{ijk} = 1$.

In this equation, n_{jk} is the length of time (in hours) of the joint occurrence of a particular wind direction, wind speed class k, and atmospheric stability class j, and N is equal to the total hours of data.

Figure 2.15 shows the source distance dependence of the long-term dispersion factor χ/Q integrated over all wind directions for various diffusion parameter systems. It demonstrates that the height and source proximity of the maxima corresponds to the influence of surface roughness, which decreases from the metropolitan site of St. Louis to Jülich (where at a height of 50 m the surface roughness has a stronger effect than at a height of 100 m) and Brookhaven, and to the conditions of the Prairie Grass experiments, which are reflected specifically in the Klug system.

The systems of Brookhaven, Pasquill-Gifford, and Klug involve very flat maxima with partly pronounced secondary maxima. The Jülich measurements show that the environmental exposure is overestimated by a factor of 1.7 if it is calculated for a release height of 100 m with the diffusion parameters measured at a 50-m release height instead of using the values ascertained at the 100-m level.

This comparison shows that it is very important to use a diffusion parameter system measured under boundary conditions comparable to those prevailing

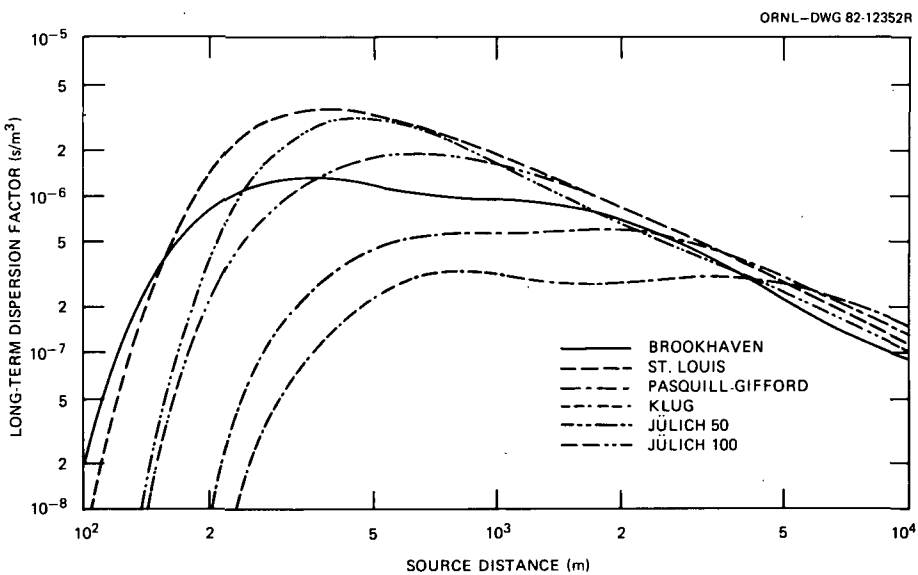

Figure 2.15. Long-term-dispersion factor according to Eq. (2.30), but integrated over all wind directions for a release height of 100 m as a function of source distance for different diffusion parameter systems (calculated with the meteorological statistics of Jülich, Germany).

at the site under consideration. This applies not only to the surface roughness, but also to the release heights.

It was mentioned in Sect. 2.3.1.6 that the radioactive decay and deposition of nuclides on the ground during transport can be taken into account via the solution of Eq. (2.18). Considering the dispersion of the waste air plume up to a source distance of approximately 10 km, the plume depletion due to ground deposits can usually be neglected. In the case of short-lived radionuclides only, Eqs. (2.31) or (2.32) have to be multiplied by the following depletion factor

$$f_{jk}(x) = \exp\left(-\lambda_r \frac{x}{\bar{u}_{jk}}\right) , \tag{2.33a}$$

or

$$f_k(x) = \exp\left(-\lambda_r \frac{x}{\bar{u}_k}\right) , \tag{2.33b}$$

respectively.

Illustrative Example

Evaluate the χ/Q value according to Eq. (2.31) for a source distance of 1000 m in sector $i = 3$, diffusion category $j = 3$ (D), and wind velocity class $k = 9$. For this purpose there are several tables in the appendix of this chapter.

In Table A we find the coefficients for the diffusion parameter $\sigma_z(x)$.If we assume an effective release height of 100 m, we get

$$\sigma_{z,3}(x) = p_{z,3}\, x^{q_{z,3}} = 0.265 \cdot 1000^{0.818} = 75.4 \text{ m} .$$

In order to calculate the representative wind velocity $\bar{u}_{jk}$, we make use of Eq. (2.14);

$$\bar{u}_{3,9} = \bar{u}_k(z_0) \cdot \left(\frac{H}{z_0}\right)^{m_3} \approx 9 \text{ knots} \cdot 0.5 \frac{\text{m/s}}{\text{knot}} \cdot \left(\frac{100}{10}\right)^{0.28}$$

$$= 8.57 \text{ m/s} ,$$

where

z_0 is the height of the anemometer (here 10 m), and

m_j is the exponent of the vertical wind profile, taken from Table E in the appendix of this chapter.

Now, assuming no radioactive depletion, χ/Q becomes

$$\frac{\chi_{339}}{Q} = (1.06 \cdot 10^{-2}) \frac{16}{\sqrt{2\pi^3} \cdot 1000 \cdot 8.57 \cdot 75.4} \cdot \exp\left[\frac{1}{2}\left(\frac{100}{75.4}\right)^2\right] \cdot 1$$

$$= 8.03 \times 10^{-8} \text{ s/m}^3 \ (p_{339} = 1.06 \times 10^{-2} \text{ from Appendix Table B}) .$$

If we evaluate the χ/Q values in the way shown in the example for 16 dispersion sectors of 22.5° and the corresponding combinations jk, based on the meteorological data listed in Table B of the appendix of this chapter, a matrix of long-term dispersion factors can be obtained. Such a matrix is shown in Tables 2.9 and 2.10. It can also be illustrated by a couple of isopleths in the vicinity of the source, as depicted in Fig. 2.16.

2.4.1.1 Modifications of the Diffusion Parameters

For specific dispersion situations not covered by the common diffusion parameter systems, a number of modifications have been developed on the basis of the original *PG* curves.

Where diffusion is enhanced in areas of increased surface roughness and complexity, diffusion is likewise generally inhibited by flow over smooth surfaces such as water. Dispersion experiments over cold water (Michael 1974) indicated that σ_y over water could be about a factor of two less than the σ_y predicted using the standard PG curve for "*F*" stability at a distance of 6 km. An approach for estimating reduced atmospheric diffusion for long over-water fetches is to assume that the rate of diffusion over water is similar to that obtained by a reduction of one or two PG stability classes for similar meteorological conditions over land. However, estimates of diffusion over water are dependent on the temperature difference between the air and water surface, and the distance of over-water fetch. Diffusion may be enhanced by air flow over a relatively warm body of water because of the destabilizing effect of heating the air from below. The transition from over-land characteristics to over-water characteristics is not immediate, and significant travel over water may be required for such a transition to occur.

Table 2.9. Matrix of the long-term-dispersion factor[a,b] (χ/Q) in s/m^3 as a function of source distance and wind direction (direction of impact) for a 16-sector wind rose and meteorological data of the site of the Jülich Nuclear Research Center (Federal Republic of Germany), release height: 100 m

Source distance (m)	Sectors							
	East							South
	1	2	3	4	5	6	7	8
1.00E+01	0.0	0.0	0.0	0.0	0.0	0.0	0.0	0.0
2.51E+01	0.0	0.0	0.0	0.0	0.0	0.0	0.0	0.0
6.31E+01	3.71E−22	5.98E−22	9.74E−22	1.80E−21	1.00E−21	9.90E−22	1.32E−21	1.46E−21
1.00E+02	5.64E−12	9.10E−12	1.48F−11	2.75E−11	1.52E−11	1.51E−11	2.01E−11	2.23E−11
1.58E+02	2.88E−09	4.63E−09	7.58E−09	1.40E−08	7.79E−09	7.70E−09	1.02E−08	1.13E−08
3.98E+02	3.19E−08	6.84E−08	1.10E−07	1.40E−07	8.60E−08	7.32E−08	6.53E−08	5.49E−08
1.00E+03	5.21E−08	1.38E−07	1.74E−07	1.55E−07	9.40E−08	6.49E−08	5.10E−08	3.63E−08
2.51E+03	2.47E−08	5.67E−08	6.72E−08	5.98E−08	3.57E−08	2.44E−08	1.98E−08	1.43E−08
6.31E+03	9.02E−09	1.61E−08	1.83E−08	1.73E−08	1.01E−08	7.23E−09	6.13E−09	4.92E−09
1.58E+04	3.46E−09	4.74E−09	5.12E−09	5.24E−09	2.93E−09	2.24E−09	1.96E−09	1.81E−09
3.98E+04	1.12E−09	1.33E−09	1.39E−09	1.50E−09	8.15E−10	6.49E−10	5.76E−10	5.77E−10
1.00E+05	3.15E−10	3.46E−10	3.56E−10	3.94E−10	2.11E−10	1.72E−10	1.54E−10	1.61E−10

[a]The χ/Q values have been calculated with σ values, valid for 100-m release height, according to Table A in the appendix of this chapter.

[b]The χ/Q values represent long-term averages over about 8 years (69,774 single values).

Table 2.10. Matrix of the long-term-dispersion factor[a,b] (*χ/Q) in s/m³ as a function of source distance and wind direction (direction of impact) for a 16-sector wind rose and meteorological data of the site of the Jülich Nuclear Research Center (Federal Republic of Germany), release height: 100 m

Source distance (m)	Sectors							
	West							North
	9	10	11	12	13	14	15	16
1.00E+01	0.0	0.0	0.0	0.0	0.0	0.0	0.0	0.0
2.51E+01	0.0	0.0	0.0	0.0	0.0	0.0	0.0	0.0
6.31E+01	1.49E−21	9.23E−22	5.67E−22	9.14E−22	6.93E−22	4.80E−22	4.32E−22	3.24E−22
1.00E+02	2.27E−11	1.40E−11	8.62E−12	1.39E−11	1.05E−11	7.31E−12	6.58E−12	4.93E−12
1.58E+02	1.15E−08	7.13E−09	4.40E−09	7.09E−09	5.37E−09	3.71E−09	3.33E−09	2.51E−09
3.98E+02	6.85E−08	4.47E−08	3.73E−08	6.45E−08	5.52E−08	2.87E−08	2.13E−08	2.62E−08
1.00E+03	4.85E−08	4.14E−08	3.30E−08	7.44E−08	7.86E−08	3.74E−08	3.09E−08	3.85E−08
2.51E+03	1.88E−08	1.82E−08	1.47E−08	3.23E−08	3.71E−08	1.97E−08	1.59E−08	1.88E−08
6.31E+03	5.90E−09	5.98E−09	5.08E−09	1.07E−08	1.37E−08	9.48E−09	7.30E−09	7.67E−09
1.58E+04	1.90E−09	1.95E−09	1.72E−09	3.66E−09	5.29E−09	4.54E−09	3.41E−09	3.25E−09
3.98E+04	5.61E−10	5.77E−10	5.22E−10	1.12E−09	1.72E−09	1.61E−09	1.20E−09	1.10E−09
1.00E+05	1.50E−10	1.55E−10	1.42E−10	8.05E−10	4.82E−10	4.71E−10	3.50E−10	3.16E−10

[a]The χ/Q values have been calculated with σ values, valid for 100-m release height, according to Table A in the appendix of this chapter.

[b]The χ/Q values represent long-term averages over about 8 years (69,774 single values).

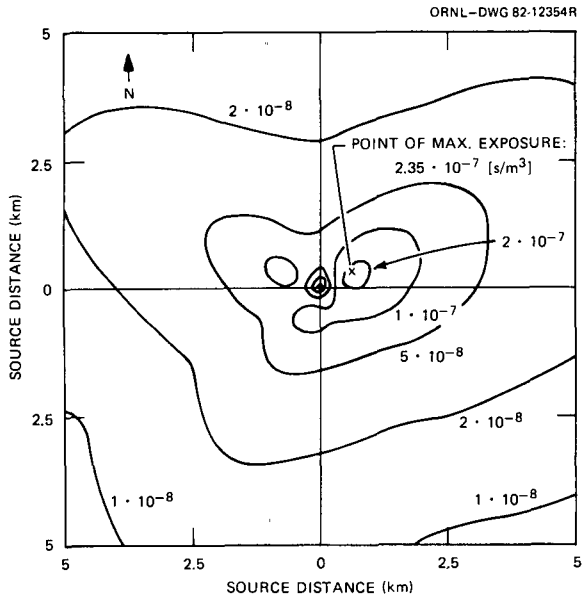

Figure 2.16. Isopleths of the long-term-dispersion factor, calculated for a release height of 100 m and σ-values determined for Jülich according to Table 2.8. Radioactive depletion was not taken into account (Brenk 1978).

Another terrain feature where the σ_y and σ_z values are likely significantly different than the standard values is a desert. Because of the relatively smooth surface and pronounced surface effects on temperature lapse rate (e.g., more radiational cooling at night resulting in strong temperature inversions), σ_z values are generally lower over deserts. However, plume meandering tends to increase σ_y values over deserts.

Irregular terrain also affects diffusion and the applicability of standard diffusion parameter sets, e.g., as compiled in Table 2.8. Each complex terrain situation is different, although diffusion overall is most probably enhanced. However, flow over and around obstructions should be examined for decreases in plume height relative to the ground surface or for physical restrictions to plume spread (e.g., valley or canyon walls).

Other adjustments to σ_y and σ_z to consider the effects of nearby buildings or to consider enhanced diffusion during low-wind-speed conditions have ben incorporated into the basic Gaussian diffusion formula. One of the earliest additions to the Gaussian diffusion model was an adjustment to estimate increased diffusion around buildings. A turbulent "wake" is formed downwind of a structure (see Figs. 2.17 and 2.18). Material released at or nearby the

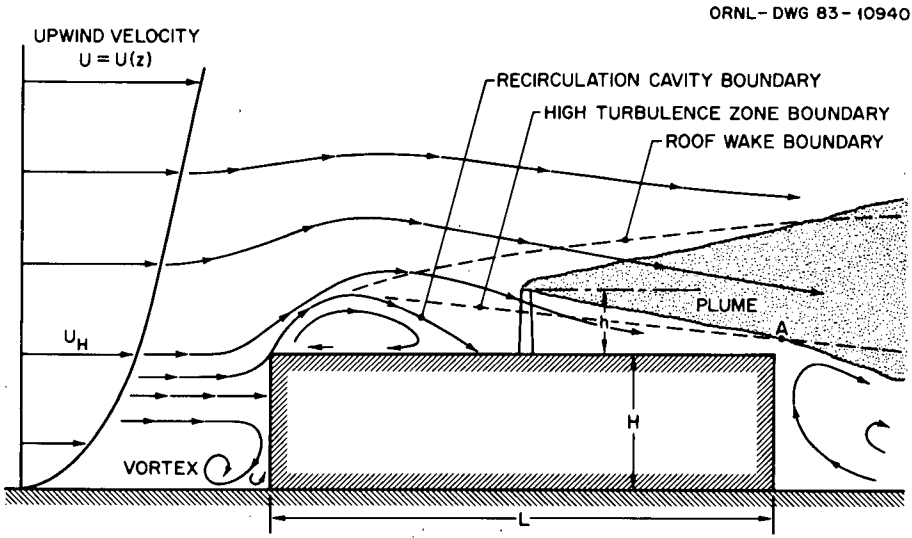

Figure 2.17. Flow over center of a long, flat building roof for wind perpendicular to the upwind face. (Wilson 1979).

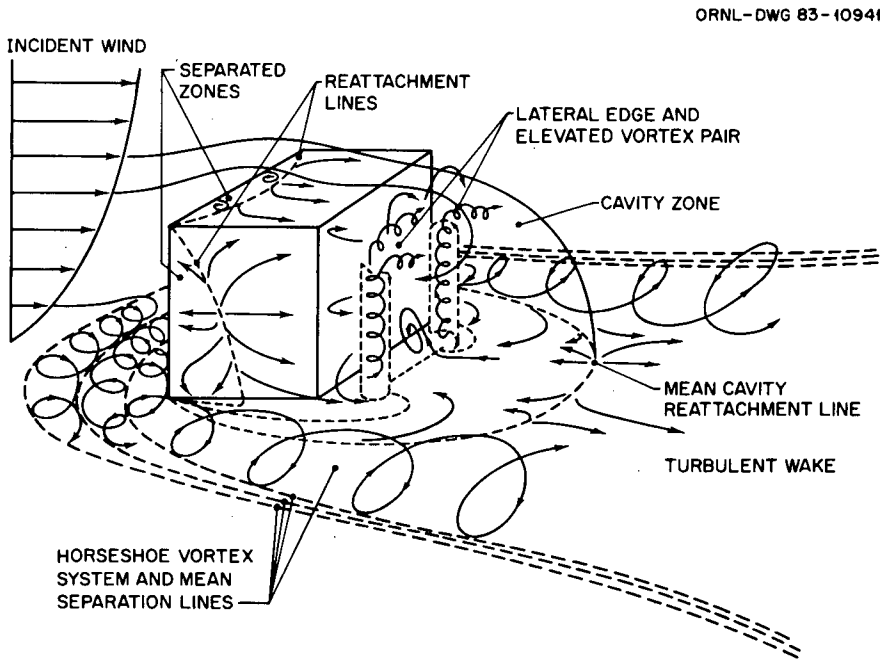

Figure 2.18. Model of flow near a sharp-edged building in a deep boundary layer (Hosker 1979).

building will most likely be entrained into the wake, thereby enhancing diffusion. The most common form of the Gaussian model to consider the effect of building wakes for short-term plume centerline calculations is

$$\bar{\chi}/Q = [(\pi\sigma_y\sigma_z + cA)\bar{u}]^{-1} , \tag{2.34}$$

where

A = cross-sectional area of the building normal to the flow, and
c = "shape factor" to represent the fraction of A over which the plume is dispersed; $c = 0.5$ is a conservative value which is commonly used.

Using this equation to represent conditions at short distances from the buildings leads to unrealistically large diffusion because of the magnitude of cross-sectional area completely overwhelms small values of σ_y and σ_z. Therefore, the NRC has limited the effect of buildings of no more than one-third of the diffusion expected without the building for short-term centerline calculations. For calculations of the building wake effect for long sampling times, the adjustment is made only to σ_z (because diffusion is assumed to be uniform in the horizontal over the sector of interest) in the form

$$\Sigma_Z = \left[\sigma_z^2 + \frac{\pi D^2}{2}\right]^{-\frac{1}{2}} , \tag{2.35}$$

where

Σ_Z = the adjusted vertical diffusion parameter, and
D = building height.

Again, the NRC limits the building effect such that Eq. (2.35) is no more than $\sqrt{3}\sigma_z$.

Diffusion during low-wind-speed, stable conditions has been observed to exceed that predicted using the standard values of σ_y and σ_z. Using diffusion experiments which were designed to estimate the enhanced horizontal diffusion for ground-level releases, the NRC has formulated adjustments to σ_y as functions of stability class and wind speed. This enhancement of σ_y is limited to hourly average calculations. NRC Regulatory Guide 1.145 contains the methodology for this adjustment (Snell, 1981) and supplies supporting information about the approach.

2.4.1.2 Release Height Modifications

The distinction between releases considered as ground-level and those considered as elevated is somewhat ill-defined. A common approach is to assume an elevated release when the release point is 2.5 times the height of nearby structures. Another common approach is to assume a ground-level release when the release point is below the height of the building. Releases from points at the tops of buildings tend to escape the building wake under certain conditions; become completely entrained into the building wake under certain conditions; or behave as mixtures of these two types for the remaining conditions. A critical determination in calculating ground-level concentrations from elevated or partially elevated releases is the plume rise of the effluent being ejected. The amount of plume rise determines the "effective stack height" for use in calculating ground-level concentrations. In all of the equations presented herein for calculating concentrations, the parameter H is the effective height of the plume. Plume rise may increase the effective stack height by appreciable factors (2 to 10) which may reduce ground-level concentrations by factors up to 100. Plume rise may be due either to momentum, bouyancy, or a combination. Briggs (1975) has summarized available plume rise models. For most plumes, early rise is probably dominated by momentum. Most nuclear facilities do not generate enough heat to make bouyancy a significant factor in plume rise. Generally, the determination of effective stack height is affected by the physical height of the stack, plume rise, downwash during relatively high wind speeds, and consideration of terrain features. Plume rise due to momentum is a complex function of the exit velocity, atmospheric stability, and wind speed. The determination of the effective height of release is generally presented in the form

$$H = h_s + h_{pr} - h_t - c \ ,$$

where

H = effective stack height,
h_s = physical stack height,
h_{dpr} = plume rise,
h_t = height of terrain, and
c = downwash correction (due to high wind speeds relative to effluent exit velocity).

2.4.1.3 Treatment of Calms

As mentioned already in Sect. 2.3.1.5, the Gaussian plume model is not strictly applicable when the wind speed $\bar{u}$ approaches zero, e.g., in

Eq. (2.31). Obviously the equations with $\bar{u}$ in the denominator are not valid when $\bar{u} = 0$. Seldom is the atmosphere truly motionless; however, wind speed often cannot be measured because it is below that required to initiate instrument response. This condition, when wind speed is below the starting or threshold speed of the anemometer, is called "calm." An approach for estimating a mean wind speed for calm conditions is to assume that $\bar{u}$ is equal to one-half the starting threshold of the anemometer. This approach is most appropriate when a relatively sensitive anemometer (i.e., starting threshold of about 0.5 m/s) is in use. Another approach is to assign the arbitrarily low wind speed, such as 0.1 m/s, to calm conditions. When less sensitive anemometers (i.e., starting thresholds on the order of 1–2 m/s) are used, both the starting threshold and frequency of calm conditions should be examined to determine a representative wind speed for calm conditions.

Another difficulty is the assignment of wind direction during calm conditions. An approach to distribute calms by wind direction using an annual joint frequency is to distribute calms in proportion to the directional distribution in the lowest non-calm wind speed class for a particular atmospheric stability class. This approach assumes that no pronounced directional bias exists for all low wind speed conditions in a particular stability class. Assigning wind direction for short-term calm conditions may be accomplished by assuming the last available non-calm wind direction measurement is valid during the period of calm. If the calm condition persists for a number of hours, then wind direction could be assumed to vary from the last non-calm direction to the next non-calm direction. However, this approach is completely subjective and requires some understanding of local meteorological and topographical conditions.

2.4.1.4 Treatment of Non-Straight-Line Airflows

The simple model described in this chapter assumes straight-line airflow between the source and the receptor. This assumption is most valid near the source, although this validity may vary considerably among sites. Thus, the applicability of the straight-line airflow assumption must be considered for each site. For example, an effluent released in a well-defined river valley will most likely follow the confines of the valley rather than remain in a straight-line trajectory. A number of variable-trajectory models are available to consider spatial and temporal variations in airflow. These models track individual puffs of plume segments over appropriate time intervals (e.g., a puff of plume segment released every 30 minutes). Individual elements are followed until they are transported beyond the area of interest or until their concentration is too low to be a significant contributor to the concentration at a particular receptor. Sometimes the results of a variable-trajectory model are compared to the results of the straight-line model to determine adjustments to the straight-line model to approximate the effects of spatial and temporal variations in airflow. USNRC Regulatory Guide 1.111 provides additional information for

consideration of spatial and temporal variations in airflow in the vicinity of nuclear power plants.

2.4.1.5 Mixing Height

For assessments of atmospheric diffusion out to large distances from the sources, the depth of the mixing layer is an important concern. The mixing layer is the atmospheric layer (based at the ground surface) in which effluents can continue to diffuse in the vertical direction. Often, a temperature inversion aloft will act as a "boundary" to continued vertical diffusion. The rate of diffusion across the "boundary" is small compared to the rate of diffusion within the mixing layer. The height of the mixing layer is called the mixing height. After an effluent plume diffuses to the mixing height, the concentration distribution in the vertical will become more uniform. Mixing heights change diurnally and seasonally, generally being largest on summer afternoons and least on autumn mornings. Mixing heights also vary considerably by geographic location. Holzworth (1972) has published extensive summaries of mixing height information for the United States.

2.4.2 Normalized Time- and Volume-Integrated Air Concentration

Photon radiation is not attenuated appreciably by air. For example, the intensity of typical photon rays (~0.7 MeV) is reduced to one-half its initial value at distances on the order of 100 m. A point of interest may experience significant photon radiation from an effluent plume although the point may be well outside of the plume. For dose estimations it is necessary, therefore, to consider the radiation contribution of the total plume. Thus, the exposure caused by photon radiation is directly proportional to the time- and volume-integrated photon flux in the plume (Chapter 8). For the geometry given in Fig. 2.19, this results in

$$H \propto \int_0^t \int_{(V)} \Psi\,(x,y,z) \cdot \frac{e^{-\mu r}}{r^2} \cdot B(\mu r)\, dV\, dt \;, \tag{2.36}$$

with Ψ taken from Eq. (2.8) and

$$r = \sqrt{(x-\xi)^2 + (y-\eta)^2 + (z-\zeta)^2}\,.$$

It has often been critically noted in the literature (see Hoffman et al. 1978) that the dose contributions to sectors adjacent to the downwind sector are not included in the calculations, especially near the point of release.

In this case, however, we do take into account the dose contributions of the adjacent sectors. Following a procedure analogous to that in Sect. 2.4.1 and

ORNL–DWG 82-12353R

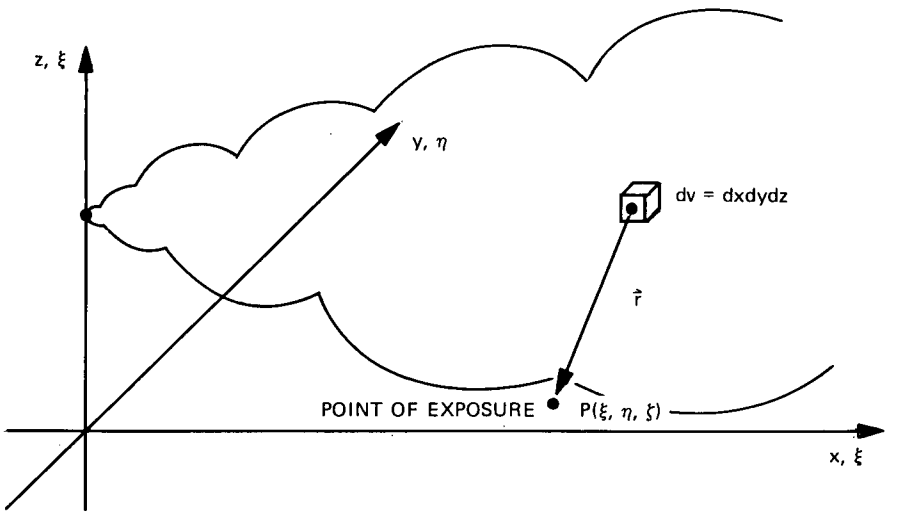

Figure 2.19. Geometry for photon exposure from the plume.

dividing the result by the source strength, Q, we get the term $\chi_{\gamma i}$ which will be referred to in the following as the gamma-submersion factor.

$$\frac{\chi_{\gamma i}}{Q} = \sum_{jk} \frac{f_{jk}}{\bar{u}_{jk}} \cdot \tag{2.37}$$

$$\left[p_{ijk} \cdot R_{1j} + p_{\rho jk} \cdot R_7 + \sum_{\kappa=2}^{6} (p_{\nu jk} + p_{\mu jk}) R_\kappa \right]$$

with

$$\rho = \begin{cases} i + 6, i \leq 6 \\ i - 6, i > 6 \end{cases}$$

$$\nu = \begin{cases} i + \kappa - 1, i + \kappa \leq 13 \\ i + \kappa - 13, i + \kappa > 13 \end{cases}$$

$$\mu = \begin{cases} i - (\kappa - 1), \kappa - i < 1 \\ i - \kappa + 13, \kappa - i \geq 1 \end{cases}$$

and

$$R_{1j} = \int_{-\infty}^{+\infty} \int \int \frac{e^{-\mu r}}{r^2} \cdot B(\mu r) \frac{n \cdot \exp[-(z-H)^2/(2\sigma_{zj}^2(x))]}{(2\pi)^{3/2} \cdot x \cdot \sigma_{zj}(x)} \, dx \, dy \, dz \tag{2.38}$$

$$R_\kappa = \int_{F_\kappa} \frac{n}{2\pi\rho} \cdot \frac{1}{r^2} \cdot B(\mu r) \cdot e^{-\mu r} \, dF_\kappa \, . \tag{2.39}$$

The derivation of Eq. (2.37) is explained in more detail in (Brenk 1978; or Rohloff et al. 1979). In the latter reference the reader will also find a discussion of the energy-dependence of R_{1j} and R_κ, as well as the manner of the numerical evaluation of these terms. More recent, improved numerical evaluations of R_{1j} and R_κ are explained (Rohloff 1981).

For the meteorological data of Jülich, the gamma submersion factor is depicted in Fig. 2.20 as a function of downwind distance and release height. In Fig. 2.21, it is given in the form of isopleths within an area of 100 km^2. Moreover, in Tables 2.11 and 2.12, the gamma submersion factor is listed for all 16 sectors of the wind rose up to a source distance of 100 km.

When the plume spread is large compared to the mean free path of photons in air, the plume can be treated like a semi-infinite cloud (excluding ground shine). For these cases the dose is directly proportional to the long-term dispersion factor, χ/Q (see Chapter 8).

But if the receptor or the point of interest is not submersed in a semi-infinite cloud, volume integrations as shown above are always needed. A simplification of the integration procedure based on Pasquill-Gifford diffusion parameters is presented by Healy in Slade (1968).

2.4.3 Normalized Ground Contamination

The radiation exposure caused by photon and electron irradiation from the ground as well as ingestion of contaminated food is strongly governed by dry and wet deposition of radioactive aerosols, gases, and vapors. These two processes may be essentially attributed to two meteorological effects known as fallout and in-cloud (rainout) and below-cloud (washout) scavenging (Slade 1968). Because it is not always possible to distinguish between washout and rainout (e.g., for convective storms) we simply refer to both processes in the following as washout.

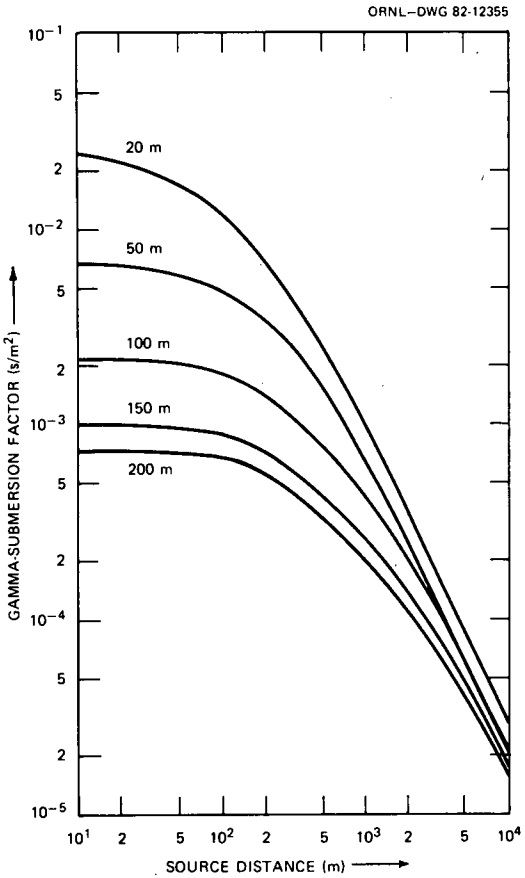

Figure 2.20. Gamma submersion factor for the main wind direction as a function of source distance and effective release height. The curves are valid for the side of the Jülich Nuclear Research Center, Germany (Brenk 1978). They have been calculated for σ-values (Jülich, 100 m) according to Table 2.8.

2.4.3.1 Dry Deposition

According to Chamberlain (1953), the ground contamination due to dry deposition (fallout processes) is nearly proportional to the activity concentration in air near ground, where the proportionality constant is the so-called deposition velocity, v_g. Thus, the normalized ground contamination (referred to in the following as *long-term fallout factor*) can be estimated by

$$\frac{F_i}{Q} = v_g \frac{\chi_i}{Q} \tag{2.40}$$

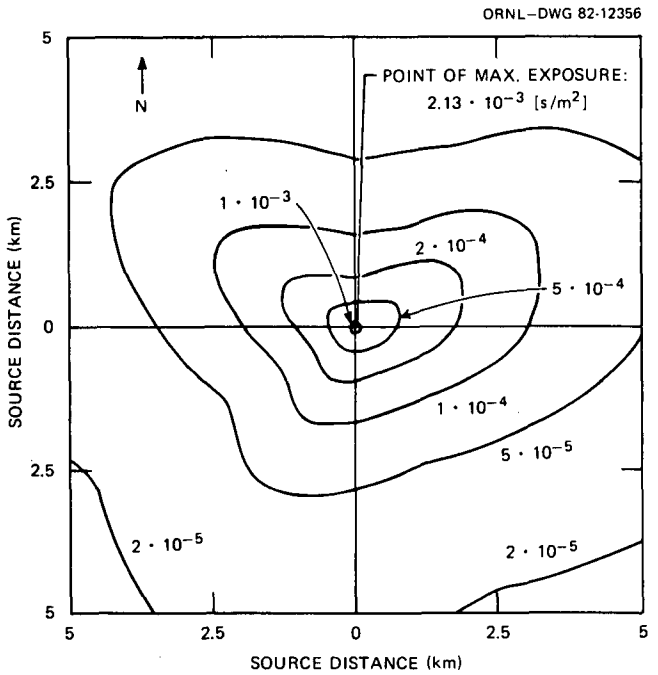

Figure 2.21. Isopleths of the gamma submersion factor calculated for the Jülich meteorological data without radioactive plume depletion. The effective release height is 100 m. The isopleths have been calculated for σ-values (Jülich, 100 m), according to Table 2.8 (Brenk 1978).

The deposition velocity is usually determined experimentally by measuring χ at a standard height, usually 1 m, and F for each isotope over various ground covers. Experimentally determined deposition velocities are also a function of wind velocity because the vertical profile of concentration changes with wind velocity. Thus, the deposition velocity is not constant even for specific effluents. The variations in boundary conditions, such as sorption characteristics and roughness of the underlying surface, and variations in the wind velocity for a given chemical composition of effluent, can cause the deposition velocity to vary by more than one order of magnitude in different experiments (see Chapter 11). It should be realized, however, that these deposition velocities are derived from relatively short-term (in the order of one hour) experiments and thus vary more than their long-term averages which are expected to be the proper values to estimate long-term deposition.

For effluents from nuclear facilities the following best estimates of the deposition velocity, based on experimental data may be adequate: 10^{-2} m/s for elemental iodine, 10^{-4} m/s for organic iodine, and 10^{-3} m/s for aerosols ($\approx$ 1 μ in diameter).

Table 2.11. Matrix of gamma-submersion factors[a,b] for 16 sectors of the wind rose (sectors of impact) as a function of source distance

Values are valid for the site of the Jülich Nuclear Research Center, (Federal Republic of Germany)

Source distance (m)	Sectors							
	East							South
	1	2	3	4	5	6	7	8
1.00E+01	1.65E−03	1.65E−03	1.65E−03	1.65E−03	1.64E−03	1.63E−03	1.62E−03	1.61E−03
2.51E+01	1.65E−03	1.66E−03	1.67E−03	1.66E−03	1.64E−03	1.61E−03	1.58E−03	1.55E−03
6.31E+01	1.53E−03	1.59E−03	1.61E−03	1.59E−03	1.53E−03	1.46E−03	1.39E−03	1.33E−03
1.00E+02	1.35E−03	1.44E−03	1.49E−03	1.46E−03	1.37E−03	1.26E−03	1.16E−03	1.10E−03
1.59E+02	1.07E−03	1.20E−03	1.27E−03	1.24E−03	1.11E−03	9.79E−04	8.68E−04	8.03E−04
3.98E+02	4.69E−04	6.39E−04	7.30E−04	6.89E−04	5.50E−04	4.29E−04	3.51E−04	3.08E−04
1.00E+03	1.63E−04	2.84E−04	3.36E−04	2.99E−04	2.09E−04	1.48E−04	1.17E−04	9.68E−05
2.51E+03	5.57E−05	1.04E−04	1.21E−04	1.06E−04	6.87E−05	4.74E−05	3.86E−05	3.07E−05
6.31E+03	1.86E−05	3.21E−05	3.61E−05	3.20E−05	2.06E−05	1.44E−05	1.20E−05	9.68E−06
1.59E+04	5.91E−06	8.95E−06	9.78E−06	8.85E−06	5.80E−06	4.14E−06	3.56E−06	2.96E−06
3.98E+04	1.76E−06	2.38E−06	2.54E−06	2.33E−06	1.57E−06	1.14E−06	1.00E−06	8.61E−07
1.00E+05	4.84E−07	6.05E−07	6.38E−07	5.91E−07	4.07E−07	2.94E−07	2.66E−07	2.34E−07

[a]The χ_γ/Q values have been evaluated with σ values, valid for 100 m release height, according to Table A in the appendix of this chapter.

[b]The χ_γ/Q values represent long-term averages over about 8 years (69,744 single values).

Table 2.12. Matrix of gamma-submersion factors[a,b] for 16 sectors of the wind rose (sectors of impact) as a function of source distance.

The values are valid for the site of the Jülich Nuclear Research Center, (Federal Republic of Germany)

Source distance (m)	Sectors							
	West							North
	9	10	11	12	13	14	15	16
1.00E+01	1.60E−03	1.60E−03	1.60E−03	1.60E−03	1.61E−03	1.62E−03	1.63E−03	1.64E−03
2.51E+01	1.54E−03	1.53E−03	1.53E−03	1.54E−03	1.56E−03	1.58E−03	1.60E−03	1.62E−03
6.31E+01	1.30E−03	1.30E−03	1.32E−03	1.34E−03	1.37E−03	1.40E−03	1.43E−03	1.48E−03
1.00E+02	1.07E−03	1.07E−03	1.10E−03	1.14E−03	1.18E−03	1.20E−03	1.22E−03	1.27E−03
1.59E+02	7.76E−04	7.83E−04	8.23E−04	8.86E−04	9.23E−04	9.22E−04	9.20E−04	9.67E−04
3.98E+02	3.04E−04	3.07E−04	3.34E−04	4.20E−04	4.56E−04	4.05E−04	3.68E−04	3.85E−04
1.00E+03	1.05E−04	1.05E−04	1.07E−04	1.74E−04	2.00E−04	1.48E−04	1.24E−04	1.29E−04
2.51E+03	3.56E−05	3.59E−05	3.40E−05	6.41E−05	7.68E−05	5.37E−05	4.50E−05	4.64E−05
6.31E+03	1.13E−05	1.16E−05	1.12E−05	2.12E−05	2.64E−05	1.95E−05	1.66E−05	1.65E−05
1.59E+04	3.38E−06	3.49E−06	3.57E−06	6.53E−06	8.32E−06	6.73E−06	5.81E−06	5.57E−06
3.98E+04	9.56E−07	9.84E−07	1.06E−06	1.88E−06	2.46E−06	2.14E−06	1.86E−06	1.73E−06
1.00E+05	2.55E−07	2.58E−07	2.88E−07	5.07E−07	6.83E−07	6.23E−07	5.40E−07	4.89E−07

[a]The χ_γ/Q-values have been evaluated with σ-values, valid for 100 m release height, according to Table A in the appendix of this chapter.

[b]The χ_γ/Q-values represent long-term averages over about 8 years (69,744 single values).

Illustrative Example

Evaluate the contamination C of the ground in sector 4 (east) 1000 m downwind of the source, due to dry deposition, if elemental ^{131}I and ^{137}Cs are released from a 100-m stack. Q may be 10^9 Bq (2.7×10^{-2} Ci) for each radionuclide.

$$C_i = v_g \left(\frac{\chi}{Q}\right)_i \cdot Q \ .$$

For a downwind distance of 1000 m, we find the χ/Q value in Table 2.9.

$$\left(\frac{\chi}{Q}\right)_4 = 1.55 \cdot 10^{-7} \text{ s/m}^3 \ .$$

In the case of elemental ^{131}I, the contamination results in

$$C_4 = 10^{-2}\text{m/s} \cdot 1.55 \cdot 10^{-7} \text{ s/m}^3 \cdot 10^9 \text{ Bq}$$

$$= 1.55 \text{ Bq/m}^2 \ (41.9 \text{ pCi/m}^2) \ .$$

Cesium-137 is assumed to form aerosols. Thus, in the case of cesium release, we get

$$C_4 = 10^{-3}\text{m/s} \cdot 1.55 \cdot 10^{-7} \text{ s/m}^3 \cdot 10^9 \text{ Bq}$$

$$= 0.155 \text{ Bq/m}^2 \ (0.419 \text{ pCi/m}^2) \ .$$

[End of Example]

2.4.3.2 Wet Deposition

According to Englemann (1970), the washout contamination of the ground from a radioactively contaminated plume with an average activity concentration

$$\bar{\Psi} = \frac{1}{L} \int_0^\infty \Psi(x,y,z) \ dz \qquad (2.41)$$

is given by*

$$\dot{W} = \omega I \bar{\Psi} \ , \tag{2.42}$$

where ω is the washout ratio and I is the precipitation intensity. With respect to the experimental determination of ω (most of them have been derived from measurement periods in the order of months, seasons, or even one year) [see Gatz (1972, 1974, 1975) or Brenk (1981)], it has a time integral character, and thus may be preferably used for the estimation of the consequences of long-term releases.

Thus, starting from the time integral of the activity concentration in air and evaluating the long-term sector mean value (see derivation of the long-term dispersion factor), we get the normalized wet ground deposition W/Q which we will refer to in the following as *long-term washout factor.*

$$\frac{W_i}{Q} = \sum_{jkl} q_{ijkl} \frac{\mathrm{n}}{2\pi \mathrm{x}} \int_o^\infty \int_{-\infty}^\infty \frac{\omega I_\ell}{L_j} \frac{\chi_{jk}(x,y,z)}{\mathrm{Q}} \, dy \, dz \ . \tag{2.43}$$

With

$$\frac{\chi_{jk}(x,y,z)}{Q} = \frac{1}{2\pi \bar{u}_{jk} \sigma_{yj} \sigma_{zj}} \exp\left[-\frac{y^2}{2\sigma_{yj}^2}\right] \times \left[\exp\left[-\frac{(z-H)^2}{2\sigma_{zj}^2}\right] + \exp\left[-\frac{(z+H)^2}{2\sigma_{zj}^2}\right]\right] , \tag{2.44}$$

we obtain

$$\frac{W_i}{Q} = \frac{n}{2\pi x} \sum_{jkl} q_{ijkl} \frac{\omega \ I_\ell}{u_{jk} L_j} \ . \tag{2.45}$$

For the evaluation of this formula, a four-dimensional joint frequency distribution of wind direction i, diffusion category j, wind velocity class k, and precipitation intensity class, ℓ, is required, which is not known for the majority of sites.

For this reason, a simplified practical approximation of Eq. (2.45), for which only a precipitation wind rose N_i is required, may be used. This precipitation wind rose supplies a frequency distribution of the annual precipitation

*The product $\omega \cdot I$ is also known as wet deposition velocity.

contribution in mm/yr connected with the wind direction i during the rainfall periods. Such precipitation wind roses may be more easily supplied by the National Weather Service than the four-dimensional frequency distributions.

In order to formulate such a practical approximation, we make use of the simplifications in Eqs. (2.46), (2.47), and (2.48).

$$q_{ijkl} \approx q_{il} \cdot p_{jk} \ . \tag{2.46}$$

Equation (2.46) means that the statistical correlation between wind direction and precipitation, on the one hand, and diffusion category and wind velocity, on the other hand, is negligible. Moreover, Eq. (2.46) implies that the combination diffusion category and wind velocity is the same for both rainfall and all meteorological situations including rainfall periods.

Further simplifications are:

$$\bar{u} = \sum_{jk} p_{jk} \cdot u_{jk}, \quad p_{jk} = \sum_{i} p_{ijk} \ ; \tag{2.47}$$

i.e., the actual representative wind velocity u_{jk} (Sect. 2.3.1.4) in Eq. (2.42) can be replaced by the long-term average value $\bar{u}$.

$$\bar{L} = \frac{1}{\sum_{j} q_j(1/L_j)} \ ; \tag{2.48}$$

i.e., the vertical mixing layer L_j, depending on the diffusion category j, can be replaced by a mean value $\bar{L}$. In Eq. (2.48), q_j is the frequency distribution of the diffusion categories j correlated with rain.

Making use of these simplifications, Eq. (2.45) results in the following *long-term washout factor*:

$$\frac{W_i}{Q} = \frac{\alpha n}{2\pi x} \cdot \frac{\omega N_i}{\bar{u}\bar{L}} \ , \quad x \geqslant 200 \text{ m} \ , \tag{2.49}$$

where α is a conversion constant,

$$\alpha = 3.17 \cdot 10^{-11} = \frac{\text{m} \cdot \text{yr}}{10^3 \text{ mm} \cdot 365 \cdot 24 \cdot 3600 \text{ s}}$$

and N_i is defined by

$$N_i = \sum_{\ell} q_{i\ell} \cdot I_\ell \cdot 8760 \text{ h/yr} . \tag{2.50}$$

In accordance with Brenk (1981), the following parameter values may be used:

$$\bar{L} \approx 500 \text{ m} ,$$

$$\omega = \begin{cases} 2 \cdot 10^5, & \text{for elemental iodine,} \\ 3 \cdot 10^5, & \text{for aerosols.*} \end{cases}$$

Illustrative Example

Evaluate the contamination C on the ground in sector 4 (east) 1000 m downwind of the source, due to wet deposition. We assume that 10^9 Bq (27 mCi) of elemental ^{131}I was released during one year. The ground contamination in sector 4 is given by the following relation:

$$C_4 = \left[\frac{W}{Q}\right]_4 \cdot Q ,$$

where $(W/Q)_4$ is the long-term washout factor according to Eq. (2.49). First, we want to evaluate the total amount of rain in sector 4 during one year. This can be calculated by making use of Eq. (2.50). The $q_{i\ell}$ values and the mean values of each precipitation class I_ℓ may be taken from Tables C and D in the appendix of this chapter.

*This value is based on extensive statistical evaluation of field experimental data.

$q_{4\ell}$	I_ℓ (mm/h)	$q_{4\ell} \cdot I_\ell$
4.96E−3	9.44E−2	4.68E−4
0		
4.06E−3	1.88E−1	7.63E−4
1.20E−3	2.66E−1	3.19E−4
2.15E−3	3.76E−1	8.08E−4
1.95E−3	5.31E−1	1.04E−3
1.03E−3	7.50E−1	7.73E−4
1.45E−3	1.06	1.54 E−3
7.17E−4	1.50	1.08 E−3
1.02E−3	2.11	2.15 E−3
5.59E−4	2.99	1.67 E−3
2.58E−4	4.22	1.09 E−3
1.00E−4	5.96	5.96 E−4
5.73E−4	8.41	4.82 E−3
		1.71E−2

$$N_4 = \sum_l q_{4\ell} I_\ell \cdot 8760 \text{ h/yr} = 150 \text{ mm/yr} .$$

If we further assume that

n = 16, because we have a 16-sector wind rose,
$\bar{u}$ = 3.5 m/s,
$\bar{L}$ = 500 m,

the ground contamination results in

$$C_4 = 3.17 \cdot 10^{-11} \frac{\text{m·yr}}{\text{mm·s}} \cdot \frac{16 \cdot 2 \cdot 10^5 \cdot 150\text{mm·s} \cdot 10^9 \text{ Bq}}{2\pi \cdot 1000\text{m} \cdot 500\text{m} \cdot 3.5 \text{ m·yr}}$$

$$= 1.38 \text{ Bq/m}^2 \quad (37.4 \text{ pCi/m}^2) .$$

Another common approach to the evaluation of wet deposition processes is based on the following relationship which uses a washout rate, Λ, instead of the washout ratio, ω.

$$\dot{W} = \int_0^\infty \Lambda \Psi \, dz \ , \tag{2.51}$$

where Λ is defined by

$$\Psi(t) = \Psi(t=0) \cdot e^{-\Lambda t} \ . \tag{2.52}$$

It can be derived by field experiments measuring the depletion of the air concentration, Ψ, as a function of time, e.g., Burtsev (1969), Graedel (1974), and Radke (1974). The time, t, is the duration of rainfall.

The washout rate is a function of rain drop size, rain drop–size distribution, and the physico-chemical attributes of the plume. These parameters, themselves functions of the space coordinates (x,y,z), cause the washout rate to be a space-dependent parameter, too. For practical application, however, the washout rate is assumed to be constant with respect to space, because there is little chance of its space-dependent empirical determination. In other words: Λ in Eq. (2.52) represents a space-averaged value.

Thus, introduction of Eq. (2.8) into Eq. (2.51) results in

$$\dot{W} = \frac{\Lambda \dot{Q}}{(2\pi)^{1/2} \bar{u} \sigma_y(x)} \exp\left[- \frac{y^2}{2\sigma_y^2 (x)} \right] . \tag{2.53}$$

Because of its definition in Eq. (2.52) and its usual field experimental derivation (the washout rate is usually determined from relatively short measurement intervals and single individual precipitation situations), the Λ values are of instantaneous, transient character and apply preferably to individual scavenging situations. For this reason, Eq. (2.53) may be used in the case of short-term releases, e.g., on the order of one hour.

For higher precipitation rates, Eq. (2.53) should be modified to account for plume depletion via wet deposition. Using the exponential removal rate of Eq. (2.52), the relationship can be written

$$\dot{W} = \frac{\Lambda \dot{Q}}{(2\pi)^{1/2} \bar{u} \sigma_y(x)} \exp\left[- \left(\frac{y^2}{2\sigma_y^2 (x)} + \frac{\Lambda x}{\bar{u}} \right) \right] , \tag{2.54}$$

Adequate values of Λ are given, e.g., in Slade (1968). In Brenk (1981), we find the following estimates for nuclear power plant releases:

$$\Lambda = \begin{cases} 8.0 \cdot 10^{-5} \cdot I^{0.6}, & \text{for elemental iodine;} \\ 1.2 \cdot 10^{-4} \cdot I^{0.4}, & \text{for aerosols,} \end{cases}$$

where I is the actual precipitation intensity in mm/h.

2.5 PROBLEMS

1. Explain why it is impossible to predict the activity concentration in air for longer time periods (one month or one year) using Eq. (2.8), the basic equation of the Gaussian plume model.

   What can be done if you want to evaluate the mean activity concentration for one year?

   Hint: See Sect. 2.3.1 and Sect. 2.4.1.

2. Compare the effects of eddies larger and smaller than the dimensions of a Gaussian plume.

3. Are you able to predict short-period fluctuations of the activity concentration in air using Eq. (2.8)?

   What are the consequences of this answer with respect to short-term accidental releases?

4. Given are two nuclear power plant sites for which environmental dose assessments are to be done. Site 1 is surrounded by flat, open country without major obstacles. In the vicinity of Site 2, we find dense forest with some small, scattered towns.

   Which of the σ-parameter-systems, listed in Table 2.6, will result in the most reliable χ/Q-value for Site 1 and Site 2, respectively? The release height of both power plants is 100 m.

   What are the principal reasons for your choice?

5. Evaluate the distance x_{max} (the point of maximum exposure), i.e., where the χ/Q-value (Eq. 2.31) reaches its maximum. Notice that the σ-values are also functions of x.

   Evaluate the maximum of the term

$$\frac{\chi \cdot \bar{u}}{Q}$$

on the basis of Eq. (2.31), if

$$\begin{aligned} p_{ijk} &= 1, \\ n &= 16, \\ \sigma_{zj}(x) &= p_{zj}x^{q}zj, \text{ for } j = 3, \text{ and} \\ H &= 50 \text{ m}. \end{aligned}$$

Compare the values $\chi \cdot \bar{u}/Q$ for the σ-parameter-systems of KLUG(III_1) and JÜLICH (50m,D) listed in Table 2.8.

What is the main reason for the fact that $\chi \cdot \bar{u}/Q$ of the Jülich system is higher than that of the Klug system up to a range of about 2000-m source distance?

6. Evaluate the χ/Q-value for Xe-138 as a function of the source distance x up to $x = 100$ km. The radioactive decay of Xe-138 has to be taken into account using Eqs. (2.31) and (2.33a).

   The χ/Q-value without radioactive decay may be taken from Table 2.9 for Sector 3. The radioactive half-life $T_{0.5}$ of Xe 138 is equal to 14.13 minutes.

$$\lambda = \frac{\ln 2}{T_{0.5}} \quad .$$

   The depletion factor $f_{jk}(x)$ may be approximated by

$$f(x) = \exp(-\lambda \cdot x/\bar{u})$$

   with

$$\bar{u} = 5 \text{ m/s} \quad .$$

   Make a log-log-plot of χ/Q versus x.

   1. χ/Q without depletion.
   2. χ/Q with depletion due to radioactive decay.

7. Fig. 2.20 shows the isopleths of the gamma submersion factor as an example. For greater source distances the shapes of the isopleths are similar to those of the χ/Q-values in Fig. 2.15. In comparison to the χ/Q-isopleths, those of the gamma submersion factor become smoother for

smaller source distances. Finally they approach circles around the source for source distances under 250 m.

Please explain this phenomenon.

8. A nuclear power plant with a stack height of 100 m (no plume rise) continuously releases a total iodine-131 activity, Q, of 0.03 Ci in one year.

   Evaluate the average ground contamination for this year for Sector 2 of the wind rose, 1000 m downwind of the source. Assume that all iodine was released in elemental form. As the ground contamination is caused by dry and wet deposition as well, we have

$$C_2 = \left(\frac{F_2}{Q} + \frac{W_2}{Q}\right) Q \quad ,$$

   The long-term dispersion factor, χ/Q, may be taken from Table 2.9. The total amount of rain in Sector 2, N_2, can be evaluated as shown in Sect. 2.4.3.2, making use of Tables C and D in the appendix of this chapter.

   Further assumptions are

$$\begin{aligned} n &= 16, \\ \bar{u} &= 5 \text{ m/s, and} \\ \bar{L} &= 500 \text{ m.} \end{aligned}$$

9. The probability, p, that we will find any weather combination ijk is equal to

$$p = \sum_{ijk} p_{ijk} = 1 \quad .$$

   The probability, q, that we will meet a combination ijk correlated with rain of the intensity level l is given by

$$q = \sum_{ijkl} q_{ijkl} = 0.111$$

for Table D in the appendix of this chapter (i.e., it rains 11.1% of the time).

Evaluate the probability, q_i/q, that the wind blows in the direction of Sector i while it is raining. Do this for the sectors 2, 4, 6, 8, 10, 12, 14, and 16 and use Table D. Compare the results with the probability that the wind blows in the direction of sectors 2, 4, 6, 8, 10, 12, 14 and 16 for all weather situations (rain *and* no rain).

What are the consequences of this comparison with respect to the evaluation of the ground contamination due to dry and wet deposition?

Hint: Remember that $F_i \propto p_i$ and $W_i \propto q_i$.

10. Attached is an example of an annual joint frequency distribution of wind speed and direction by atmospheric stability class as it might be prepared by the National Weather Service. Wind speed classes are identified by the *maximum* value for each class. Sixteen wind direction sectors are represented, as are 7 (A-G) atmospheric stability classes. The values presented in the tables are percent occurrences. For example, wind from the north during "D" stability with speeds between 0.75 m/s and 1.0 m/s occurred 0.365% of the time for an annual period of record.

    Calculate an annual average χ/Q value from a ground-level release for a receptor located at a distance of 5000 m in the south-southwest direction. Use the following σ_{zj} value for "G" stability at a distance of 5000 m: 22 m. The depth of vertical mixing is 1000 m. The depth of vertical mixing is 1000 m. The other σ_{zj}-values may be taken from Fig. 2.13.

    Hint: Use Eq. (2.32). Note that the wind direction in this frequency distribution is not the direction of impact but the direction from which the wind blows.

    Solution: The release is at ground level, so $H = 0$. At a distance of 5000 m, the effects of building wake are negligible. Because the receptor is located in the south-southwest sector, the wind direction of interest is north-northeast.

    A simple method for performing this calculation is to set up two matrices: one of frequency versus stability and average wind speed, and one of χ/Q versus stability and average wind speed. Once the χ/Q values for each wind speed/stability pattern are calculated, the values are multiplied by the corresponding frequency of occurrence. The annual average χ/Q is the sum of the product of frequency times χ/Q.

Data set for problem 10: joint frequency distribution of wind speed and direction[a]

Max (m/s)	N	NNE	NE	ENE	E	ESE	SE	SSE	S	SSW	SW	WSW	W	WNW	NW	NNW	Total
STABILITY CLASS A																	
0.27																	
0.50																	
0.75																	
1.00																	
1.50															0.011	0.011	0.02
2.00	0.034		0.011							0.011							0.05
3.00		0.011	0.046		0.011		0.023	0.080	0.034	0.011		0.011					0.22
5.00		*0.011*	*0.011*	*0.011*			*0.023*	*0.091*	*0.171*	*0.080*	*0.046*	*0.034*	*0.034*	*0.034*	*0.046*	*0.023*	*0.61*
10.00									0.011				0.011	0.046			0.06
15.00																	
Total	0.03	0.02	0.07	0.01	0.01		0.05	0.17	0.22	0.10	0.05	0.05	0.05	0.08	0.06	0.03	0.99
STABILITY CLASS B																	
0.27																	
0.50																	
0.75																	
1.00			0.011	0.011											0.011		0.03
1.50	0.023			0.011			0.011										0.04
2.00		0.011	0.011	0.011	0.011	0.011	0.023		0.011							0.023	0.11
3.00	0.034	0.057	0.057	0.023	0.023	0.011		0.080	0.068	0.011	0.023	0.034				0.046	0.46
5.00	0.034	0.023	0.046	0.011	0.011		0.046	0.034	0.160	0.068	0.046	0.068	0.103	0.068	0.091	0.023	0.83
10.00	0.011					0.011			0.011	0.046	0.057	0.068	0.080	0.068	0.046	0.057	0.45
15.00																	
Total	0.10	0.09	0.13	0.07	0.05	0.03	0.08	0.11	0.25	0.13	0.13	0.17	0.18	0.14	0.15	0.15	1.95
STABILITY CLASS C																	
0.27																	
0.50																	
0.75																	
1.00		0.011	0.023									0.011		0.011	0.011	0.011	0.08
1.50	0.023	0.011	0.046	0.023				0.011				0.011			0.011	0.023	0.16
2.00	0.034	0.091	0.034	0.034	0.011	0.023	0.011	0.034	0.011	0.046	0.034		0.046	0.011	0.057	0.068	0.54
3.00	0.160	0.091	0.148	0.057	0.011	0.023	0.103	0.114	0.183	0.080	0.080	0.057	0.046		0.068	0.205	1.42
5.00	0.160	0.091	0.114	0.023		0.011	0.057	0.103	0.297	0.126	0.354	0.217	0.103	0.114	0.148	0.274	2.19
10.00	0.023	0.011					0.011		0.068	0.068	0.057	0.091	0.011	0.091	0.046	0.046	0.52
15.00																0.011	0.01
Total	0.40	0.31	0.37	0.14	0.02	0.06	0.18	0.26	0.56	0.32	0.53	0.39	0.21	0.23	0.34	0.64	4.94

Data set for problem 10: (continued)

Max (m/s)	N	NNE	NE	ENE	E	ESE	SE	SSE	S	SSW	SW	WSW	W	WNW	NW	NNW	Total
STABILITY CLASS D																	
0.27	0.002	0.001					0.001	0.001							0.001	0.002	0.01
0.50	0.046	0.034	0.011	0.011		0.011	0.023	0.034	0.011	0.011			0.011		0.023	0.057	0.28
0.75	0.126	0.091	0.114	0.034	0.011	0.023	0.011		0.011	0.011	0.046	0.023	0.023	0.023	0.080	0.057	0.68
1.00	0.365	0.388	0.251	0.217	0.057	0.011	0.080	0.057	0.126	0.068	0.126	0.057	0.080	0.103	0.263	0.377	2.62
1.50	0.753	1.199	0.925	0.559	0.194	0.080	0.285	0.228	0.388	0.251	0.285	0.377	0.228	0.205	0.491	0.571	7.02
2.00	0.731	1.450	1.256	0.457	0.103	0.137	0.183	0.274	0.514	0.434	0.411	0.365	0.205	0.183	0.205	0.308	7.21
3.00	1.404	2.420	1.621	0.411	0.137	0.160	0.468	0.514	1.644	0.970	1.142	0.525	0.171	0.251	0.285	0.696	12.82
5.00	1.986	1.678	1.073	0.171	0.023	0.034	0.354	0.365	1.370	1.632	1.381	0.571	0.331	0.422	0.365	1.233	12.99
10.00	0.434	0.091	0.114	0.011	0.023	0.011	0.126	0.046	0.502	0.445	0.148	0.126	0.160	0.148	0.137	0.605	3.12
15.00							0.057										0.05
Total	5.85	7.35	5.37	1.87	0.55	0.47	1.59	1.52	4.57	3.82	3.54	2.04	1.21	1.34	1.85	3.91	46.84
STABILITY CLASS E																	
0.27	0.019	0.042	0.046	0.021	0.015	0.007	0.009	0.011	0.024	0.016	0.021	0.010	0.003	0.008	0.011	0.011	0.27
0.50	0.228	0.514	0.559	0.263	0.183	0.080	0.114	0.137	0.297	0.194	0.263	0.126	0.034	0.103	0.137	0.137	3.36
0.75	0.217	0.445	0.445	0.274	0.091	0.023	0.057	0.137	0.194	0.285	0.205	0.148	0.080	0.034	0.046	0.103	2.78
1.00	0.342	0.936	1.062	0.342	0.171	0.057	0.114	0.148	0.297	0.365	0.285	0.342	0.171	0.103	0.068	0.171	4.97
1.50	0.434	1.461	1.495	0.411	0.068	0.034	0.183	0.148	0.479	0.502	0.594	0.297	0.194	0.046	0.137	0.137	6.62
2.00	0.228	0.765	0.902	0.114	0.011	0.023	0.057	0.137	0.445	0.514	0.320	0.171	0.034	0.080	0.080	0.137	4.01
3.00	0.263	0.879	0.845	0.126	0.023	0.023	0.057	0.023	0.594	1.347	0.468	0.171		0.114	0.205	0.194	5.33
5.00	0.160	0.160	0.205	0.034		0.011	0.103	0.046	0.263	1.176	0.217	0.080	0.080	0.046	0.046	0.126	2.75
10.00	0.011	0.011	0.011				0.023	0.103	0.103	0.217	0.011		0.011			0.44	
15.00							0.023										0.02
Total	1.90	5.21	5.57	1.59	0.56	0.26	0.75	0.81	2.70	4.62	2.38	1.36	0.60	0.54	0.73	1.02	30.59
STABILITY CLASS F																	
0.27	0.015	0.033	0.044	0.040	0.024	0.009	0.025	0.017	0.014	0.034	0.030	0.019	0.007	0.004	0.007	0.021	0.34
0.50	0.148	0.320	0.422	0.388	0.228	0.091	0.240	0.160	0.137	0.331	0.285	0.183	0.068	0.034	0.068	0.205	3.31
0.75	0.080	0.160	0.411	0.114	0.103	0.057	0.160	0.057	0.114	0.217	0.274	0.103	0.046		0.068	0.171	2.13
1.00	0.103	0.240	0.285	0.285	0.023	0.023	0.103	0.103	0.205	0.126	0.183	0.046	0.023	0.057	0.057	0.046	1.90
1.50	0.057	0.080	0.205	0.114			0.057	0.034	0.126	0.251	0.217	0.034		0.023		0.046	1.24
2.00		0.068	0.023	0.023			0.011	0.011	0.034	0.103	0.080	0.023	0.011	0.023		0.011	0.42
3.00		0.023	0.011						0.011	0.057	0.023		0.046				0.17
5.00	0.011								0.011		0.011						0.03
10.00													0.011				0.01
15.00																	
Total	0.41	0.92	1.40	0.96	0.38	0.18	0.60	0.38	0.65	1.12	1.10	0.41	0.21	0.14	0.20	0.50	9.58
STABILITY CLASS G																	
0.27	0.013	0.018	0.021	0.017	0.011	0.005	0.009	0.011	0.014	0.018	0.015	0.016	0.003	0.008	0.010	0.019	0.20
0.50	0.148	0.205	0.240	0.194	0.126	0.057	0.103	0.126	0.160	0.205	0.171	0.183	0.034	0.091	0.114	0.217	2.37
0.75	0.091	0.057	0.160	0.114	0.023	0.034	0.034	0.023	0.046	0.091	0.160	0.114	0.011	0.011	0.034	0.057	1.06
1.00	0.023	0.034	0.114	0.034			0.057	0.011	0.046	0.126	0.217	0.103	0.091	0.011	0.046	0.068	0.98
1.50			0.023	0.011		0.011		0.023	0.011	0.068	0.103	0.091	0.023	0.011			0.37
2.00			0.011	0.011				0.011	0.011		0.011	0.011	0.011	0.023			0.10
3.00																	
5.00																	
10.00																	
15.00																	
Total	0.28	0.031	0.57	0.38	0.16	0.11	0.20	0.20	0.29	0.51	0.68	0.52	0.17	0.16	0.20	0.36	5.10

*Total hours considered are 8760; wind measured at 10.2 m.

$\bar{u}$	Frequency (%)						
	A	B	C	D	E	F	G
0.135	0	0	0	0.001	0.042	0.033	0.018
0.385	0	0	0	0.034	0.514	0.320	0.205
0.625	0	0	0	0.091	0.445	0.160	0.057
0.875	0	0	0.011	0.388	0.936	0.240	0.034
1.25	0	0	0.011	1.199	1.461	0.080	0
1.75	0	0.011	0.091	1.450	0.765	0.068	0
2.50	0.011	0.057	0.091	2.420	0.879	0.023	0
4.00	0.011	0.023	0.091	1.678	0.160	0	0
7.50	0	0	0.011	0.091	0.011	0	0
12.50	0	0	0	0	0	0	0

σ_z	$\chi/Q = \frac{2.032}{\bar{u}_k x \sigma_{z_j}}$						
	A	B	C	D	E	F	G
	1000	650	270	89	56	34	22

$\bar{u}$	$\chi/Q = \frac{2.032}{\bar{u}_k x \sigma_{z_j}}$						
	A	B	C	D	E	F	G
0.135	-	-	-	3.38-5	5.38-5	8.85-5	1.37-4
0.385	-	-	-	1.19-5	1.88-5	3.10-5	4.80-5
0.625	-	-	-	7.31-6	1.16-5	1.91-5	2.96-5
0.875	-	-	1.72-6	5.22-6	8.29-6	1.37-5	2.11-5
1.25	-	-	1.20-6	3.65-6	5.81-6	9.56-6	-
1.75	-	3.57-7	8.60-7	2.61-6	4.15-6	6.83-6	-
2.50	1.63-7	2.50-7	6.02-7	1.83-6	2.90-6	4.78-6	-
4.00	1.02-7	1.56-7	3.76-7	1.14-6	1.81-6	-	-
7.50	-	-	2.01-7	6.09-7	9.68-7	-	-
12.50	-	-	-	-	-	-	-

$\bar{u}$	$\chi/Q \cdot \frac{u_{jk}}{N}$						
	A	B	C	D	E	F	G
0.135	-	-	-	3.38-10	2.26-8	2.92-8	2.47-8
0.385	-	-	-	4.05-9	9.66-8	9.92-8	9.84-8
0.625	-	-	-	6.65-9	5.16-8	3.06-8	1.69-8
0.875	-	-	1.89-10	2.03-8	7.76-8	3.29-8	7.17-9
1.25	-	-	1.32-10	4.38-8	8.49-8	7.65-9	-
1.75	-	3.93-11	7.83-10	3.78-8	3.17-8	4.64-9	-
2.50	1.79-11	1.43-10	5.48-10	4.43-8	2.55-8	1.10-9	-
4.00	1.12-11	3.59-11	3.42-10	1.91-8	2.90-9	-	-
7.50	-	-	2.21-11	5.54-10	1.06-10	-	-
12.50	-	-	-	-	-	-	-

Therefore,

$$\sum_{jk} \chi/Q \cdot \frac{u_{jk}}{N} = 9.2 \cdot 10^{-7} \text{ s/m}^3 \quad .$$

REFERENCES

Barad, M. L., and Haugen, D. A. 1958. *Project Prairie Grass,* Geophysical Research Paper No. 59, Vols. I, II, and III, Air Force Cambridge Research Center, Bedford, Mass.

Barad, M. L., and Fuquay, J. J. 1962. *The Green Glow Diffusion Program,* HW-71400, Vol. II, Hanford Engineering Development Laboratory.

Bundesminister des Innern. 1981. Verwaltungsvorschrift zur Änderung der ersten Allgemeinen Verwaltungsvorschrift zum Bundesimmissionsschutzgesetz (Technische Anleitung zur Reinhaltung der Luft - TA Luft) Stand: Bonn, September 1981.

Brenk, H. D. 1978. "Ein anwendungsbezogenes Konzept zur Berechnung der Umweltbelastung durch Abluftemissionen kerntechnischer Anlagen für Standorte in der Bundesrepublik Deutschland, JüL-*Rep.* No. 1485.

Brenk, H.D., and Vogt, K. J. 1981. "The Calculation of Wet Deposition from Radioactive Plumes," *Nucl. Saf.*, **22** (3).

Briggs, G. A. 1973. *Diffusion Estimation for Small Emissions,* ATDL Contribution File No. 79, Atmospheric Turbulence and Diffusion Laboratory.

Briggs, G. A. 1975. "Plume Rise Predictions," in *Lectures on Air Pollution and Environmental Impact Analyses,* Workshop Proceedings, American Meteorological Society, Boston, pp. 59–111.

Burtsev, I. I., Burtseva, L. N., and Malakhov, S. G. 1969. *Characteristics of a Washout of a ^{32}P Aerosol Injected into a Cloud,* USAEC Report UCRL-Trans-10404, University of California, Lawrence Livermore Laboratory, NTIS.

Cawse, P. A. 1978. Cited as personal communication by W.G.N. Slinn et al., in W.G.N. Slinn et al., "Some Aspects of the Transfer of Atmospheric Trace Constituents Past the Air-Sea Interface," *Atmos. Environ.* **12:** 2055–2067.

Chamberlain, A. C. 1953. *Aspects of Travel and Deposition of Aerosol and Vapor Clouds,* British Report AERE-HP/R-1261.

Cramer, H. E., Record, F. A., and Vaughn, H.C. 1959. *The Study of the Diffusion of Gases or Aerosols in the Lower Atmosphere,* AFCRC-TR-59-207, Massachusetts Institute Technol.

Doury, A. 1980. "Practiques Francaises en Matiere D'Evaluation Quantitative de la Pollution Atmospherique Potentielle Liee aux Activities Nucleaires," Commissariat a l'Energie Atomique Rapport DSN No. 397, 92260 Fontenay aux Roses, France.

Engelmann, R. J. 1970. *Scavenging Prediction Using Ratios of Concentration in Air and Precipitation in Precipitation Scavenging,* CONF-700601.

Gatz, D. F. 1972. "Washout Ratios in Urban and Non-Urban Areas," paper presented at the Meeting of the American Meteorological Society.

Gatz, D. F. 1974. "Scavenging Ratio Measurements in METROMEX," in *Precipitation Scavenging,* AEC Symposium Series, R. G. Semonin, and R. W. Beadle, coordinators. CONF-741003, NTIS, pp. 71–87.

Gatz, D. F. 1975. "Estimates of Wet and Dry Deposition of Chicago and Northwestern Indiana Aerosols in Southern Lake Michigan," paper presented to Second Interagency Committee on Marine Sciences and Engineering Conference on the Great Lakes, Argonne, Ill.

Geiss, H., Nester, K., Thomas, P., and Vogt, K. J. 1981. "In der Bundesrepublik Deutschland Exerimentell Ermittelte Ausbreitungsparameter für 100 m Emissionshöhe," Gemeinsamer Bericht der Kernforschungsanlage Jülich und des Kernforschungszentrums Karlsruhe, Jül-1707, KfK-3095.

Geiss, H. 1982. Kernforschungsanlage *Jülich,* Abt.: ASS. Personal Communication.

Gifford, F. A., Jr. 1961. "Use of Routine Meteorological Observations for Estimating Atmospheric Dispersion," *Nucl. Saf.* **2**(4): 44–57.

Gifford, F. A., Jr. 1976. "Turbulent Diffusion Typing Schemes—A Review," *Nucl. Saf.* **17**: 68–86.

Golder, D. 1972. "Relation Among Stability Parameters in the Surface Layer," *Boundary Layer Meteorol.***3,** 47–58.

Graedel, T. E., et al. 1974. "Field Measurements of Submicron Aerosol Washout by Rain," in *Precipitation Scavenging,* AEC Symposium Series, R. G. Semonin, and R. W. Beadle, coordinators, CONF-741003, NTIS, 503–523.

Hanna, S. R., Briggs, G. A., and Hosker, R. P., Jr. 1982. *Handbook on Atmospheric Diffusion,* Technical Information Center, U.S. Department of Energy.

Hoffman, F. O., Schaeffer, D. L., Miller, C. W., Garten, Ch. T. 1978. "The Evaluation of Models Used in the Environmental Assessment of Radionuclide Releases," CONF-770901, Gatlinburg, Tenn.

Holzworth, G. C. 1972. *Mixing Heights, Wind Speeds—Potential for Urban Air Pollution Throughout the Continental United States,* AP-101, U.S. Environmental Protection Agency, Office of Air Programs, Research Triangle Park, N.C.

Hosker, R. P., Jr. 1979. "Empirical Estimation of Wake Cavity Size Behind Block-Type Structures," in preprints, *4th Symposium on Turbulence, Diffusion, and Air Pollution,* American Meteorological Society, Boston, pp. 603–609.

Hübschmann, W. 1981. Karlsruhe Nuclear Research Center, F. R. of Germany. Personal Communication. AEA80 International Atomic Energy Agency, 1980. *Atmospheric Dispersion in Nuclear Power Plant Siting,* Safety Series No. 50-SG-S3.

ICRP 16. 1977. "Recommendations of the International Commission on Radiological Protection," Vol. 1, No. 3, (Pergamon Press).

Islitzer, N. F. 1961. "Short Range Atmospheric Dispersion Measurements From an Elevated Source," *J. Meteorl.* **18,** 443.

Kiefer, H., et al. 1979. Jahresbericht der Hauptabteilung Sicherheit, Kernforschungszentrum Karlsruhe, KfK 2939.

Klug, W. 1964. "Meteorologische Einflussgrössen in der Ausbreitungsrechnung," *Staub.* **24,** 396.

Klug, W. 1969. "Ein Verfahren zur Bestimmung der Ausbreitungsbedingungen aus synoptischen Beobachtungen," *Staub.* **29,** 143.

König, L. A., Nester, K., Schütelkopf, H., and Winter, M. 1973. "Experimente am Kernforschungsentrum Karlsruhe zur Bestimmung der atmosphärischen Ausbreitung mit Hilfe verschiedener Leitsubstanzen," KFK-1918, Kernforschungszentrum Karlsruhe.

Lettau, H. H. 1962. "Theoretical Wind Spirals in the Boundary Layer of a Barotropic Atmosphere," *Beiträge zur Physik der Atmosphäre* **35,** S. 195–212.

LeQuinio, R. L. 1962. "Operation Bourdon 1962," Commissariat a l'Energie Atmomique, CEN Saclay, France.

McElroy, J. L. 1969. "A Comparative Study of Urban and Rural Dispersion," *J. Appl. Meteorl.* **8.**

McElroy, J. L., and Pooler, F. 1968. *St. Louis Dispersion Study Vol. II—Analysis,* U.S. Department of Health, Education and Welfare, Arlington, Va.

Michael, P., Raynor, G. S., and Brown, R. M. 1974. "Atmospheric Diffusion from an Offshore Site," in *Proceedings of Symposium on Physical Behavior of Radioactive Contaminants in the Atmosphere,* IAEA, Vienna, Austria.

Newberry, C. W., and Eaton, K. J. 1974. *Wind Loading Handbook,* Build. Res. Establishment Rep., Building Res. Station, Department of the Environment, London.

U.S. Nuclear Regulatory Commission. 1972. "On-Site Meteorological Programs," *Reg. Guide 1.23 (Safety Guide 23).*

Nuclear Regulatory Commission. 1977. "Methods for Estimating Atmospheric Transport and Dispersion of Gaseous Effluents in Routine Releases from Light-Water-Cooled Reactors," *Reg. Guide 1.111.*

Nuclear Regulatory Commission. 1977. "Atmospheric Dispersion Models for Potential Accident Consequence Assessments at Nuclear Power Plants," *Reg. Guide 1.145.*

Pasquill, F. 1961. "The Estimation of the Dispersion of Wind-Borne-Material," *Met. Mag.* **90,** 33.

Pasquill, F. 1962. *Atmospheric Diffusion,* van Nostrand, London.

Pasquill, F. 1974. *Atmospheric Diffusion,* 2d Edition, Ellis Horwood Limited, New York.

Radke, L. F., et al. 1974. "A Case Study of Plume Scavenging by a Rain Shower," in *Precipitation Scavenging,* AEC Symposium Series, R. G.

Semonin, and R. W. Beadle, coordinators, CONF-741003, NTIS, pp. 425–436.

Rohloff, F., Brunen, E., Brenk, H. D., Geiss, H., and Vogt, K. J. 1979. LIGA—Ein Programm zur Berechnung der *l*okalen *i*ndividuellen *G*ammasubmersionsdosis durch *A*bluftfahnen, Jül-Rep. No. 1577.

Rohloff, F., and Brunen, E. 1981. LIGA 2–Ein verbessertes Rechenprogramm zur Berechnung der *l*okalen *i*ndividuellen *G*ammasubmersionsdosis durch *A*bluftfahnen aus kerntechnischen Anlagen, Report der Kernforschungsanlage Jülich, Jül-1736.

Singer, I. A., and Smith, M. E. 1966. "Atmospheric Dispersion at Brookhaven National Laboratory," *Air and Water Poll. Int. J.* **10,** 125–135.

Slade, D. H. (ed.). 1968. *Meteorology and Atomic Energy,* TID-24190.

Snell, W. G., and Jubach, R. W. 1981. *Technical Basis for Regulatory Guide 1.145,* "Atmospheric Dispersion Models for Potential Accident Assessments at Nuclear Power Plants," NUREG/CR-2260, prepared for the Division of Health, Siting, and Waste Management, Office of Nuclear Regulatory Research, USNRC, Washington, D.C.

Start, G. E., and Wendell, L. L. 1974. "Regional Effluent Dispersion Calculations Considering Spacial and Temporal Meteorological Variations," NOAA Tech. Memo ERL-ARL-44.

Stewart, N. G., Gale, H. J., and Crooks, R. N. 1958. "The Atmospheric Diffusion of Gases Discharged from the Chimney of the Harwell Reactor BEPO," *Int. J. Air Pollut.* **1,** 87.

Thomas, P. 1975. "Beständigkeit der atmosphärischen Ausbreitungsbedingungen in Abhängigkeit der Tageszeit," KFK-Report 2214.

Turner, D. B. 1967. *Workbook of Atmospheric Dispersion Estimates,* Public Health Service, Publication 999-AP-26, Robert A. Taft Sanitary Engineering Center, Cincinnati, Ohio.

Vogt, K. J. 1970. "Umweltkontamination und Strahlenbelastung durch radioaktive Abluft aus kerntechnischen Anlagen," Jül-Rep. 637-ST.

Vogt, K. J. 1977. "Empirical investigations of the Diffusion of Waste Air Plumes in the Atmosphere," *Nucl. Technol.* **34.**

Vogt, K. J., and Geiss, H. 1974. "Tracer Experiments on the Dispersion of Plume over Terrain of Major Surface Roughness," Jül-1131-ST.

Vogt, K. J., Straka, J., and Geiss, H. 1979. "An Extension of the Gaussian Plume Model for the Case of Changing Weather Conditions," paper presented at the *10th International Technical Meeting on Air Pollution Modeling and its Application of the NATO/CCMS Air Pollution Pilot Study,* Rome.

Walpole, R. E., and Myers, R. H. 1978. "Probability and Statistics for Engineers and Scientists," 2d Edition, Macmillan, New York.

Wilson, D. J., 1979. "Flow Patterns over Flat-Roofed Buildings and Applications to Exhaust Stack Design," *ASHRAE Trans.,* **85**(2): 284–295.

APPENDIX TO CHAPTER 2

Table A Set of Diffusion Parameters for Three Effective Release Heights and Six Diffusion Categories. (Parameters Evaluated Above Relatively Rough Terrain.)

Table B Three-Dimensional Meteorological Statistics (p_{ijk}) for 10 of 16 Sectors i of the Wind Rose (Sectors of Impact), 6 Diffusion Categories j and 30 Wind Velocities k.

Table C Classification of the Precipitation Intensity (I).

Table D Two-Dimensional Statistics (q_{il}) of the Precipitation Intensity for 8 of 16 Sectors of the Wind Rose (Sector of Impact) and 31 Classes of Precipitation Intensity.

Table E Exponent of the Vertical Wind Profile.

Table A. Set of diffusion parameters for three effective release heights and six stability classes

Diffusion category	Roughness[a] category of the site	Diffusion coefficients[b] (BMI 1981; Geiss 1982) p_y	q_y	p_z	q_z
Effective release height: 50 m					
A ($j = 6$)		1.503	0.833	0.151	1.219
B ($j = 5$)		0.876	0.823	0.127	1.108
C ($j = 4$)	3–4	0.659	0.807	0.165	0.996
D ($j = 3$)		0.640	0.784	0.215	0.885
E ($j = 2$)		0.801	0.754	0.264	0.774
F ($j = 1$)		1.294	0.718	0.241	0.662
Effective release height: 100 m					
A ($j = 6$)		0.170	1.296	0.051	1.317
B ($j = 5$)		0.324	1.025	0.070	1.151
C ($j = 4$)	3–4	0.466	0.866	0.137	0.985
D ($j = 3$)		0.504	0.818	0.265	0.818
E ($j = 2$)		0.411	0.882	0.487	0.652
F ($j = 1$)		0.253	1.057	0.717	0.486
Effective release height: 180 m					
A ($j = 6$)		0.671	0.903	0.0245	1.500
B ($j = 5$)		0.415	0.903	0.0330	1.320
C ($j = 4$)	3–4	0.232	0.903	0.104	0.997
D ($j = 3$)		0.208	0.903	0.307	0.734
E ($j = 2$)		0.345	0.903	0.546	0.557
F ($j = 1$)		0.671	0.903	0.484	0.500

[a] Roughness length: about 0.5 to 3 m.

[b] $\sigma_y = p_y x^{q_y}$, $\sigma_z = p_z x^{q_z}$.

Table B. Three-dimensional meteorological statistics (p_{ijk})[a] of dispersal conditions: 10 of 16 sectors i of the wind rose (sectors of impact), 6 Diffusion Categories j, and 30 Wind Velocities k

The statistics are valid for the site of the Jülich Nuclear Research Center (Federal Republic of Germany) and are based on meteorological data of about 8 years (69,774 values).

	(Sector i = 1)						
k[b]	$j \rightarrow$ 1	2	3	4	5	6	
	F[c]	E	D	C	B	A	
1	3.15E−04	1.00E−04	0.0	0.0	0.0	0.0	4.15E−04
2	1.82E−03	9.31E−04	2.14E−04	8.59E−05	7.16E−05	0.0	3.12E−03
3	3.25E−03	1.67E−03	3.86E−04	8.59E−05	2.14E−04	8.59E−05	5.70E−03
4	4.72E−03	2.06E−03	3.72E−04	2.86E−04	4.01E−04	2.72E−04	8.12E−03
5	7.02E−04	1.80E−03	1.83E−03	1.57E−04	3.00E−04	8.59E−05	4.88E−03
6	1.00E−04	1.36E−03	2.43E−03	2.14E−04	3.15E−04	4.29E−05	4.47E−03
7	2.86E−05	7.73E−04	2.56E−03	2.86E−04	1.00E−04	1.43E−05	3.76E−03
8	0.0	2.72E−04	2.63E−03	1.71E−04	1.14E−04	0.0	3.19E−03
9	0.0	1.43E−04	2.14E−03	2.57E−04	1.14E−04	0.0	2.66E−03
10	0.0	1.14E−04	1.92E−03	3.15E−04	2.86E−05	0.0	2.37E−03
11	0.0	1.28E−04	2.36E−03	3.00E−04	1.43E−05	0.0	2.80E−03
12	0.0	2.86E−05	1.66E−03	2.00E−04	0.0	0.0	1.89E−03
13	0.0	0.0	1.77E−03	4.29E−05	0.0	0.0	1.82E−03
14	0.0	0.0	1.51E−03	5.73E−05	0.0	0.0	1.57E−03
15	0.0	0.0	9.17E−04	0.0	0.0	0.0	9.17E−04
16	0.0	0.0	8.88E−04	0.0	0.0	0.0	8.88E−04
17	0.0	0.0	5.87E−04	0.0	0.0	0.0	5.87E−04
18	0.0	0.0	4.87E−04	0.0	0.0	0.0	4.87E−04
19	0.0	0.0	2.43E−04	0.0	0.0	0.0	2.43E−04
20	0.0	0.0	3.15E−04	0.0	0.0	0.0	3.15E−04
21	0.0	0.0	1.86E−04	0.0	0.0	0.0	1.86E−04
22	0.0	0.0	8.59E−05	0.0	0.0	0.0	8.59E−05
23	0.0	0.0	7.16E−05	0.0	0.0	0.0	7.16E−05
24	0.0	0.0	1.43E−05	0.0	0.0	0.0	1.43E−05
25	0.0	0.0	5.73E−05	0.0	0.0	0.0	5.73E−05
26	0.0	0.0	2.86E−05	0.0	0.0	0.0	2.86E−05
27	0.0	0.0	1.43E−05	0.0	0.0	0.0	1.43E−05
28	0.0	0.0	1.43E−05	0.0	0.0	0.0	1.43E−05
29	0.0	0.0	0.0	0.0	0.0	0.0	0.0
30	0.0	0.0	2.86E−05	0.0	0.0	0.0	2.86E−05
	1.09E−02	9.40E−03	2.57E−02	2.46E−03	1.67E−03	5.01E−04	5.07E−02[d]

Table B. (continued)

	(Sector i = 2)						
k^b	$j \rightarrow$ 1	2	3	4	5	6	
	F[c]	E	D	C	B	A	
1	2.00E−04	1.43E−04	4.29E−05	0.0	1.43E−05	0.0	4.01E−04
2	1.64E−03	7.02E−04	1.86E−04	2.86E−05	4.29E−05	2.86E−05	2.63E−03
3	2.89E−03	1.21E−03	3.00E−04	1.14E−04	2.86E−04	1.14E−04	4.93E−03
4	4.29E−03	2.68E−03	5.01E−04	2.72E−04	2.72E−04	3.72E−04	8.39E−03
5	7.59E−04	2.75E−03	3.39E−03	2.72E−04	4.01E−04	1.71E−04	7.75E−03
6	2.14E−04	2.66E−03	5.40E−03	4.58E−04	4.29E−04	8.59E−05	9.25E−03
7	1.00E−04	2.26E−03	8.06E−03	6.59E−04	4.01E−04	2.86E−05	1.15E−02
8	7.16E−05	1.46E−03	9.50E−03	7.02E−04	3.86E−04	0.0	1.21E−02
9	0.0	8.59E−04	9.55E−03	1.31E−03	2.14E−04	0.0	1.19E−02
10	0.0	3.58E−04	9.33E−03	1.34E−03	4.29E−04	0.0	1.14E−02
11	0.0	1.86E−04	9.71E−03	1.59E−03	7.16E−05	0.0	1.15E−02
12	0.0	2.86E−05	6.65E−03	1.11E−03	0.0	0.0	7.79E−03
13	0.0	0.0	5.60E−03	5.01E−04	0.0	0.0	6.10E−03
14	0.0	0.0	4.91E−03	3.43E−04	0.0	0.0	5.25E−03
15	0.0	0.0	3.45E−03	1.57E−04	0.0	0.0	3.61E−03
16	0.0	0.0	2.65E−03	5.73E−05	0.0	0.0	2.70E−03
17	0.0	0.0	2.20E−03	0.0	0.0	0.0	2.20E−03
18	0.0	0.0	2.00E−03	0.0	0.0	0.0	2.00E−03
19	0.0	0.0	1.33E−03	0.0	0.0	0.0	1.33E−03
20	0.0	0.0	1.04E−03	0.0	0.0	0.0	1.04E−03
21	0.0	0.0	6.30E−04	0.0	0.0	0.0	6.30E−04
22	0.0	0.0	6.73E−04	0.0	0.0	0.0	6.73E−04
23	0.0	0.0	3.00E−04	0.0	0.0	0.0	3.00E−04
24	0.0	0.0	3.00E−04	0.0	0.0	0.0	3.00E−04
25	0.0	0.0	1.57E−04	0.0	0.0	0.0	1.57E−04
26	0.0	0.0	2.86E−05	0.0	0.0	0.0	2.86E−05
27	0.0	0.0	5.73E−05	0.0	0.0	0.0	5.73E−05
28	0.0	0.0	1.43E−05	0.0	0.0	0.0	1.43E−05
29	0.0	0.0	1.43E−05	0.0	0.0	0.0	1.43E−05
30	0.0	0.0	5.73E−05	0.0	0.0	0.0	5.73E−05
	1.01E−02	1.53E−02	8.81E−02	8.94E−03	2.95E−03	8.02E−04	1.26E−01[d]

Table B. (continued)

	(Sector i = 3)						
k^b	$j \rightarrow$ 1	2	3	4	5	6	
	F[c]	E	D	C	B	A	
1	1.15E−04	1.14E−04	7.16E−05	0.0	1.43E−05	1.43E−05	3.29E−04
2	1.79E−03	9.17E−04	1.14E−04	8.59E−05	1.57E−04	4.29E−05	3.11E−03
3	2.77E−03	1.77E−03	4.58E−04	1.43E−04	3.86E−04	1.57E−04	5.68E−03
4	4.46E−03	3.86E−03	7.73E−04	3.43E−04	7.30E−04	6.87E−04	1.08E−02
5	6.74E−04	2.79E−03	5.05E−03	5.01E−04	5.15E−04	1.28E−04	9.67E−03
6	1.43E−04	1.93E−03	7.09E−03	7.73E−04	1.26E−03	1.86E−04	1.13E−02
7	4.30E−05	1.30E−03	9.91E−03	1.14E−03	1.14E−03	4.29E−05	1.36E−02
8	7.16E−05	5.15E−04	1.03E−02	1.37E−03	1.01E−03	0.0	1.33E−02
9	2.86E−05	2.72E−04	1.06E−02	2.20E−03	5.01E−04	0.0	1.36E−02
10	1.43E−05	2.86E−05	9.77E−03	2.59E−03	6.44E−04	0.0	1.30E−02
11	0.0	8.59E−05	1.00E−02	2.76E−03	1.28E−04	0.0	1.30E−02
12	0.0	7.16E−05	7.46E−03	1.76E−03	0.0	0.0	9.30E−03
13	0.0	0.0	7.23E−03	7.88E−04	0.0	0.0	8.02E−03
14	0.0	0.0	5.36E−03	4.29E−04	0.0	0.0	5.79E−03
15	0.0	0.0	4.22E−03	1.57E−04	0.0	0.0	4.36E−03
16	0.0	0.0	3.32E−03	1.28E−04	0.0	0.0	3.45E−03
17	0.0	0.0	2.53E−03	0.0	0.0	0.0	2.53E−03
18	0.0	0.0	2.35E−03	0.0	0.0	0.0	2.35E−03
19	0.0	0.0	1.37E−03	0.0	0.0	0.0	1.37E−03
20	0.0	0.0	9.02E−04	0.0	0.0	0.0	9.02E−04
21	0.0	0.0	7.88E−04	0.0	0.0	0.0	7.88E−04
22	0.0	0.0	4.15E−04	0.0	0.0	0.0	4.15E−04
23	0.0	0.0	2.86E−04	0.0	0.0	0.0	2.86E−04
24	0.0	0.0	2.14E−04	0.0	0.0	0.0	2.14E−04
25	0.0	0.0	1.57E−04	0.0	0.0	0.0	1.57E−04
26	0.0	0.0	1.43E−04	0.0	0.0	0.0	1.43E−04
27	0.0	0.0	2.86E−05	0.0	0.0	0.0	2.86E−05
28	0.0	0.0	0.0	0.0	0.0	0.0	0.0
29	0.0	0.0	2.86E−05	0.0	0.0	0.0	2.86E−05
30	0.0	0.0	1.43E−05	0.0	0.0	0.0	1.43E−05
	1.01E−02	1.36E−02	1.01E−01	1.52E−02	6.50E−03	1.26E−03	1.47E−01

Table B. (continued)

(Sector i = 4, East)

k[b]	$j \rightarrow$ 1	2	3	4	5	6	
	F[c]	E	D	C	B	A	
1	2.14E−04	2.29E−04	4.29E−05	4.29E−05	4.29E−05	0.0	5.73E−04
2	1.64E−03	1.16E−03	3.15E−04	8.59E−05	2.43E−04	5.73E−05	3.51E−03
3	2.98E−03	2.63E−03	8.45E−04	3.00E−04	6.87E−04	4.29E−04	7.88E−03
4	6.13E−03	4.71E−03	1.49E−03	4.44E−04	1.18E−03	9.31E−04	1.49E−02
5	1.07E−03	3.38E−03	5.21E−03	8.16E−04	1.71E−03	5.87E−04	1.27E−02
6	1.00E−04	1.86E−03	6.73E−03	9.88E−04	2.07E−03	3.86E−04	1.21E−02
7	8.59E−05	8.88E−04	7.66E−03	1.08E−03	1.67E−03	8.59E−05	1.14E−02
8	7.16E−05	3.00E−04	6.82E−03	1.47E−03	1.60E−03	0.0	1.02E−02
9	4.29E−05	2.29E−04	7.28E−03	1.76E−03	8.31E−04	0.0	1.01E−02
10	0.0	4.29E−05	6.11E−03	1.83E−03	7.30E−04	0.0	8.72E−03
11	0.0	2.86E−05	6.82E−03	1.70E−03	1.28E−04	0.0	8.68E−03
12	0.0	1.43E−05	4.44E−03	1.00E−03	0.0	0.0	5.46E−03
13	0.0	0.0	3.48E−03	4.01E−04	0.0	0.0	3.88E−03
14	0.0	0.0	2.10E−03	3.15E−04	0.0	0.0	2.42E−03
15	0.0	0.0	2.03E−03	5.73E−05	0.0	0.0	2.09E−03
16	0.0	0.0	1.43E−03	2.86E−05	0.0	0.0	1.46E−03
17	0.0	0.0	1.24E−03	0.0	0.0	0.0	1.24E−03
18	0.0	0.0	7.73E−04	0.0	0.0	0.0	7.73E−04
19	0.0	0.0	5.58E−04	0.0	0.0	0.0	5.58E−04
20	0.0	0.0	3.72E−04	0.0	0.0	0.0	3.72E−04
21	0.0	0.0	2.29E−04	0.0	0.0	0.0	2.29E−04
22	0.0	0.0	1.71E−04	0.0	0.0	0.0	1.71E−04
23	0.0	0.0	2.14E−04	0.0	0.0	0.0	2.14E−04
24	0.0	0.0	5.73E−05	0.0	0.0	0.0	5.73E−05
25	0.0	0.0	1.14E−04	0.0	0.0	0.0	1.14E−04
26	0.0	0.0	2.86E−05	0.0	0.0	0.0	2.86E−05
27	0.0	0.0	1.43E−05	0.0	0.0	0.0	1.43E−05
28	0.0	0.0	0.0	0.0	0.0	0.0	0.0
29	0.0	0.0	0.0	0.0	0.0	0.0	0.0
30	0.0	0.0	2.86E−05	0.0	0.0	0.0	2.86E−05
	1.23E−02	1.54E−02	6.66E−02	1.23E−02	1.09E−02	2.47E−03	1.20E−01[d]

Table B. (continued)

	(Sector i = 6)						
k^b	$j \rightarrow$ 1	2	3	4	5	6	
	F[c]	E	D	C	B	A	
1	2.14E−04	1.57E−04	4.29E−05	1.43E−05	5.73E−05	0.0	4.87E−04
2	9.45E−04	5.73E−04	3.86E−04	1.28E−04	2.29E−04	2.86E−05	2.29E−03
3	1.36E−03	1.47E−03	6.30E−04	1.57E−04	6.59E−04	8.59E−05	4.37E−03
4	1.93E−03	1.84E−03	9.60E−04	5.30E−04	7.73E−04	6.73E−04	6.72E−03
5	3.00E−04	1.31E−03	2.85E−03	6.01E−04	1.11E−03	4.01E−04	6.59E−03
6	7.16E−05	6.59E−04	2.47E−03	4.58E−04	1.11E−03	1.86E−04	4.97E−03
7	1.43E−05	4.44E−04	2.47E−03	5.87E−04	6.01E−04	4.29E−05	4.17E−03
8	0.0	2.86E−04	1.92E−03	6.01E−04	4.01E−04	0.0	3.21E−03
9	0.0	1.28E−04	1.80E−03	6.30E−04	2.14E−04	0.0	2.78E−03
10	0.0	1.43E−05	1.23E−03	4.87E−04	1.14E−04	0.0	1.84E−03
11	0.0	1.43E−05	1.17E−03	4.29E−04	4.29E−05	0.0	1.66E−03
12	0.0	0.0	8.45E−04	3.29E−04	0.0	0.0	1.17E−03
13	0.0	0.0	6.16E−04	1.14E−04	0.0	0.0	7.30E−04
14	0.0	0.0	3.29E−04	7.16E−05	0.0	0.0	4.01E−04
15	0.0	0.0	1.86E−04	0.0	0.0	0.0	1.86E−04
16	0.0	0.0	1.43E−04	0.0	0.0	0.0	1.43E−04
17	0.0	0.0	1.00E−04	0.0	0.0	0.0	1.00E−04
18	0.0	0.0	1.43E−04	0.0	0.0	0.0	1.43E−04
19	0.0	0.0	2.86E−05	0.0	0.0	0.0	2.86E−05
20	0.0	0.0	0.0	0.0	0.0	0.0	0.0
21	0.0	0.0	1.43E−05	0.0	0.0	0.0	1.43E−05
22–30	0.0	0.0	0.0	0.0	0.0	0.0	0.0
	4.84E−03	6.92E−03	1.83E−02	5.14E−03	5.33E−03	1.41E−03	4.20E−02[d]

Table B. (continued)

	(Sector i = 8, South)						
k^b	$j \rightarrow$ 1	2	3	4	5	6	
	F[c]	E	D	C	B	A	
1	5.30E−04	3.58E−04	4.29E−05	1.43E−05	1.43E−05	0.0	9.60E−04
2	1.26E−03	9.17E−04	4.44E−04	1.71E−04	1.00E−04	4.29E−05	2.93E−03
3	1.07E−03	7.59E−04	3.43E−04	2.14E−04	2.57E−04	2.57E−04	2.90E−03
4	1.04E−03	9.74E−04	5.87E−04	2.29E−04	5.58E−04	7.88E−04	4.18E−03
5	1.71E−04	5.01E−04	1.28E−03	3.00E−04	9.02E−04	4.44E−04	3.61E−03
6	1.43E−05	5.73E−05	1.11E−03	3.43E−04	7.88E−04	5.15E−04	2.83E−03
7	0.0	5.73E−05	1.17E−03	3.00E−04	4.01E−04	4.29E−05	1.97E−03
8	0.0	0.0	7.88E−04	1.28E−04	2.57E−04	0.0	1.17E−03
9	0.0	0.0	4.44E−04	1.28E−04	7.16E−05	0.0	6.44E−04
10	0.0	1.43E−05	1.86E−04	4.29E−05	2.86E−05	0.0	2.72E−04
11	0.0	0.0	1.28E−04	2.86E−05	0.0	0.0	1.57E−04
12	0.0	0.0	2.86E−05	0.0	0.0	0.0	2.86E−05
13	0.0	0.0	0.0	1.43E−05	0.0	0.0	1.43E−05
14	0.0	0.0	2.86E−05	1.43E−05	0.0	0.0	4.29E−05
15	0.0	0.0	0.0	1.43E−05	0.0	0.0	0.0
16–30	0.0	0.0	0.0	0.0	0.0	0.0	0.0
	4.09E−03	3.64E−03	6.60E−03	1.94E−03	3.38E−03	2.09E−03	2.17E−02[d]

Table B. (continued)

(Sector i = 10)

k^b	$j \rightarrow$ 1	2	3	4	5	6	
	F[c]	E	D	C	B	A	
1	2.72E−04	8.59E−05	1.43E−05	0.0	0.0	0.0	3.72E−04
2	7.59E−04	5.44E−04	2.14E−04	7.16E−05	7.16E−05	5.73E−05	1.71E−03
3	9.31E−04	8.02E−04	3.00E−04	1.57E−04	2.14E−04	2.14E−04	2.62E−03
4	1.63E−03	1.17E−03	4.29E−04	2.14E−04	4.58E−04	5.01E−04	4.41E−03
5	4.29E−04	1.28E−03	1.33E−03	2.43E−04	5.44E−04	2.29E−04	4.07E−03
6	2.72E−04	1.86E−03	1.57E−03	1.71E−04	5.58E−04	1.71E−04	4.61E−03
7	1.14E−04	1.59E−03	1.66E−03	1.57E−04	4.29E−04	4.29E−05	3.99E−03
8	4.29E−05	1.41E−03	1.50E−03	4.29E−04	4.29E−04	0.0	3.82E−03
9	0.0	7.30E−04	1.77E−03	3.86E−04	2.43E−04	0.0	3.13E−03
10	0.0	1.86E−04	1.43E−03	3.58E−04	1.71E−04	0.0	2.14E−03
11	0.0	7.16E−05	1.11E−03	3.86E−04	5.73E−05	0.0	1.63E−03
12	0.0	1.43E−05	6.44E−04	1.43E−04	0.0	0.0	8.02E−04
13	0.0	0.0	3.43E−04	8.59E−05	0.0	0.0	4.29E−04
14	0.0	0.0	2.14E−04	4.29E−05	0.0	0.0	2.57E−04
15	0.0	0.0	1.00E−04	1.43E−05	0.0	0.0	1.14E−04
16	0.0	0.0	1.43E−05	1.43E−05	0.0	0.0	2.86E−05
17	0.0	0.0	2.86E−05	0.0	0.0	0.0	2.86E−05
18	0.0	0.0	1.43E−05	0.0	0.0	0.0	1.43E−05
19–30	0.0	0.0	0.0	0.0	0.0	0.0	0.0
	4.45E−03	9.77E−03	1.27E−02	2.88E−03	3.18E−03	1.21E−03	3.42E−02[d]

Table B. (continued)

(Sector i = 12, West)

k^b	$j \rightarrow$ 1	2	3	4	5	6	
	F[c]	E	D	C	B	A	
1	3.43E−04	2.86E−05	1.43E−05	2.86E−05	1.43E−05	1.43E−05	4.44E−04
2	1.10E−03	4.87E−04	1.57E−04	4.29E−05	7.16E−05	4.29E−05	1.90E−03
3	2.23E−03	7.30E−04	4.15E−04	1.28E−04	3.29E−04	1.57E−04	3.99E−03
4	3.33E−03	1.41E−03	5.01E−04	3.86E−04	6.30E−04	5.30E−04	6.80E−03
5	1.66E−03	2.16E−03	2.19E−03	3.86E−04	8.31E−04	2.86E−04	7.52E−03
6	9.60E−04	3.26E−03	3.02E−03	4.01E−04	1.00E−03	1.14E−04	8.77E−03
7	1.03E−03	2.80E−03	3.52E−03	7.59E−04	5.73E−04	4.29E−05	8.74E−03
8	8.74E−04	2.57E−03	3.23E−03	7.16E−04	7.30E−04	0.0	8.14E−03
9	1.86E−04	1.87E−03	3.71E−03	6.73E−04	2.00E−04	0.0	6.65E−03
10	0.0	1.37E−03	2.82E−03	4.87E−04	1.71E−04	0.0	4.85E−03
11	0.0	1.17E−03	3.09E−03	6.01E−04	4.29E−05	0.0	4.91E−03
12	0.0	6.16E−04	2.12E−03	5.58E−04	0.0	0.0	3.29E−03
13	0.0	1.43E−05	1.60E−03	2.14E−04	0.0	0.0	1.83E−03
14	0.0	2.86E−05	1.49E−03	1.57E−04	0.0	0.0	1.67E−03
15	0.0	0.0	7.88E−04	1.28E−04	0.0	0.0	9.17E−04
16	0.0	0.0	5.15E−04	7.16E−05	0.0	0.0	5.87E−04
17	0.0	0.0	4.01E−04	0.0	0.0	0.0	4.01E−04
18	0.0	0.0	3.58E−04	0.0	0.0	0.0	3.58E−04
19	0.0	0.0	1.28E−04	0.0	0.0	0.0	1.28E−04
20	0.0	0.0	1.28E−04	0.0	0.0	0.0	1.28E−04
21	0.0	0.0	8.59E−05	0.0	0.0	0.0	8.59E−05
22	0.0	0.0	0.0	0.0	0.0	0.0	0.0
23	0.0	0.0	1.43E−05	0.0	0.0	0.0	1.43E−05
24–30	0.0	0.0	0.0	0.0	0.0	0.0	0.0
	1.17E−02	1.85E−02	3.03E−02	5.74E−03	4.60E−03	1.18E−03	7.21E−02[d]

Table B. (continued)

	(Sector i = 14)						
k^b	$j \rightarrow$ 1	2	3	4	5	6	
	F[c]	E	D	C	B	A	
1	3.58E−04	1.43E−05	5.73E−05	1.43E−05	0.0	0.0	4.44E−04
2	2.43E−03	5.30E−04	2.86E−05	1.00E−04	5.73E−05	5.73E−05	3.21E−03
3	5.38E−03	8.74E−04	1.43E−04	5.73E−05	2.43E−04	1.00E−04	6.80E−03
4	7.59E−03	1.04E−03	2.29E−04	2.29E−04	3.15E−04	3.43E−04	9.76E−03
5	2.42E−03	1.76E−03	1.06E−03	1.71E−04	2.86E−04	5.73E−05	5.76E−03
6	1.03E−03	2.13E−03	1.28E−03	1.57E−04	2.43E−04	0.0	4.85E−03
7	5.44E−04	2.13E−03	1.96E−03	2.86E−04	1.86E−04	0.0	5.11E−03
8	3.72E−04	1.70E−03	1.79E−03	2.43E−04	1.00E−04	0.0	4.21E−03
9	7.16E−05	1.61E−03	1.43E−03	3.00E−04	0.0	0.0	3.42E−03
10	0.0	1.08E−03	1.43E−03	3.15E−04	1.43E−05	0.0	2.85E−03
11	0.0	7.45E−04	1.44E−03	1.71E−04	0.0	0.0	2.36E−03
12	0.0	4.72E−04	9.17E−04	1.86E−04	0.0	0.0	1.57E−03
13	0.0	1.43E−05	8.31E−04	2.86E−05	0.0	0.0	8.74E−04
14	0.0	0.0	4.44E−04	1.14E−04	0.0	0.0	5.58E−04
15	0.0	0.0	4.15E−04	0.0	0.0	0.0	4.15E−04
16	0.0	0.0	2.14E−04	0.0	0.0	0.0	2.14E−04
17	0.0	0.0	1.28E−04	0.0	0.0	0.0	1.28E−04
18	0.0	0.0	1.86E−04	0.0	0.0	0.0	1.86E−04
19	0.0	0.0	4.29E−05	0.0	0.0	0.0	4.29E−05
20	0.0	0.0	2.86E−05	0.0	0.0	0.0	2.86E−05
21	0.0	0.0	1.43E−05	0.0	0.0	0.0	1.43E−05
22	0.0	0.0	2.86E−05	0.0	0.0	0.0	2.86E−05
23–30	0.0	0.0	0.0	0.0	0.0	0.0	0.0
	2.02E−02	1.41E−02	1.41E−02	2.37E−03	1.44E−03	5.58E−04	5.28E−02[d]

Table B. (continued)

	(Sector i = 16, North)						
k^b	$j \rightarrow$ 1	2	3	4	5	6	
	F[c]	E	D	C	B	A	
1	3.29E−04	7.16E−05	4.29E−05	1.43E−05	0.0	0.0	4.58E−04
2	1.92E−03	8.16E−04	2.00E−04	5.73E−05	1.14E−04	1.43E−05	3.12E−03
3	3.56E−03	1.31E−03	3.00E−04	1.86E−04	2.43E−04	1.00E−04	5.71E−03
4	4.72E−03	2.19E−03	3.58E−04	2.29E−04	2.72E−04	2.00E−04	7.98E−03
5	9.45E−04	1.53E−03	1.51E−03	1.28E−04	1.86E−04	7.16E−05	4.38E−03
6	8.59E−05	9.45E−04	1.89E−03	7.16E−05	2.29E−04	1.43E−05	3.23E−03
7	2.86E−05	4.15E−04	1.93E−03	2.14E−04	1.43E−04	0.0	2.73E−03
8	0.0	1.57E−04	1.74E−03	3.43E−04	1.28E−04	0.0	2.37E−03
9	0.0	5.73E−05	1.49E−03	2.43E−04	1.43E−05	0.0	1.80E−03
10	0.0	8.59E−05	1.40E−03	1.43E−04	1.43E−05	0.0	1.64E−03
11	0.0	7.16E−05	1.59E−03	1.00E−04	1.43E−05	0.0	1.77E−03
12	0.0	0.0	8.16E−04	0.0	0.0	0.0	8.16E−04
13	0.0	0.0	7.30E−04	0.0	0.0	0.0	7.30E−04
14	0.0	0.0	4.87E−04	0.0	0.0	0.0	4.87E−04
15	0.0	0.0	1.57E−04	0.0	0.0	0.0	1.57E−04
16	0.0	0.0	1.14E−04	0.0	0.0	0.0	1.14E−04
17	0.0	0.0	1.14E−04	0.0	0.0	0.0	1.14E−04
18	0.0	0.0	1.43E−05	0.0	0.0	0.0	1.43E−05
19—22	0.0	0.0	0.0	0.0	0.0	0.0	0.0
23	0.0	0.0	5.73E−05	0.0	0.0	0.0	5.73E−05
24—29	0.0	0.0	0.0	0.0	0.0	0.0	0.0
30	0.0	0.0	1.43E−05	0.0	0.0	0.0	1.43E−05
	1.16E−02	7.66E−03	1.49E−02	1.73E−03	1.36E−03	4.01E−04	3.77E−02[d]

[a] $\sum_{ijk} p_{ijk} = 1$.

[b] The symbol k is the index of the classes of the wind velocity. It also denotes the mean value of the corresponding wind velocity in knots (e.g., for $k = 3$, the wind velocity $\bar{u}_k(z_0) = 3$ knots ≈ 1.5 m/s).

[c] Pasquill classes A–F.

[d] This value is equal to $p_i = \sum_{jk} p_{ijk}$. It can be interpreted as the probability that the wind blows in the direction of sector i.

Table C. Classification of the precipitation intensity (I) used for evaluation of the two-dimensional precipitation statistics ($q_{i\ell}$), Index i of the windrose sector, index ℓ of the class of precipitation intensity

Class of precipitation intensity (index ℓ)	Class boundaries (mm/h)	Class mean values[a] (mm/h)
1	$0 < I \leqslant 1.00E-2$	5.00E−3
2	$1.00E-2 < I \leqslant 1.41E-2$	1.19E−2
3	$1.41E-2 < I \leqslant 2.00E-2$	1.68E−2
4	$2.00E-2 < I \leqslant 2.82E-2$	2.37E−2
5	$2.82E-2 < I \leqslant 3.98E-2$	3.35E−2
6	$3.98E-2 < I \leqslant 5.62E-2$	4.73E−2
7	$5.62E-2 < I \leqslant 7.94E-2$	6.68E−2
8	$7.94E-2 < I \leqslant 1.12E-1$	9.44E−2
9	$1.12E-1 < I \leqslant 1.58E-1$	1.33E−1
10	$1.58E-1 < I \leqslant 2.24E-1$	1.88E−1
11	$2.24E-1 < I \leqslant 3.16E-1$	2.66E−1
12	$3.16E-1 < I \leqslant 4.47E-1$	3.76E−1
13	$4.47E-1 < I \leqslant 6.31E-1$	5.31E−1
14	$6.31E-1 < I \leqslant 8.91E-1$	7.50E−1
15	$8.91E-1 < I \leqslant 1.26$	1.06
16	$1.26 < I \leqslant 1.78$	1.50
17	$1.78 < I \leqslant 2.51$	2.11
18	$2.51 < I \leqslant 3.55$	2.99
19	$3.55 < I \leqslant 5.01$	4.22
20	$5.01 < I \leqslant 7.08$	5.96
21	$7.08 < I \leqslant 1.00E+1$	8.41
22	$1.00 < I \leqslant 1.41E+1$	1.19E+1
23	$1.41 < I \leqslant 2.00E+1$	1.68E+1
24	$2.00E+1 < I \leqslant 2.82E+1$	2.37E+1
25	$2.82E+1 < I \leqslant 3.98E+1$	3.35E+1
26	$3.98E+1 < I \leqslant 5.62E+1$	4.73E+1
27	$5.62E+1 < I \leqslant 7.94E+1$	6.68E+1
28	$7.94E+1 < I \leqslant 1.12E+2$	9.44E+1
29	$1.12E+2 < I \leqslant 1.58E+2$	1.33E+2
30	$1.58E+2 < I \leqslant 2.24E+2$	1.88E+2
31	$I > 2.24E+2$	2.66E+2

[a]Geometric mean values (except for $\ell = 1$ and $\ell = 31$) because of the log-normal character of the frequency distribution of the precipitation intensity.

Table D. Two-dimensional statistics ($q_i\ell$) of the precipitation intensity for 8 of 16 sectors of the wind rose (sector of impact) and 31 classes of precipitation intensity

The statistics are valid for the site of the Jülich Nuclear Research Center (Federal Republic of Germany) and are based on 8 years of meteorological data (69,774 values)

Class of precipitation intensity ℓ	East Sector			South Sector
	2	4	6	8
1–7	0.0	0.0	0.0	0.0
8	5.47E−03	4.96E−03	1.15E−03	4.59E−04
9	0.0	0.0	0.0	0.0
10	3.50E−03	4.06E−03	9.89E−04	2.87E−04
11	1.09E−03	1.20E−03	2.72E−04	1.00E−04
12	1.71E−03	2.15E−03	3.44E−04	2.01E−04
13	1.91E−03	1.95E−03	3.15E−04	1.58E−04
14	1.13E−03	1.03E−03	3.01E−04	1.29E−04
15	1.19E−03	1.45E−03	4.44E−04	1.20E−04
16	6.16E−04	7.17E−04	1.86E−04	7.17E−05
17	7.31E−04	1.02E−03	2.15E−04	8.60E−05
18	3.30E−04	5.59E−04	1.86E−04	2.87E−05
19	4.30E−05	2.58E−04	8.60E−05	2.87E−05
20	5.73E−05	1.00E−04	2.87E−05	0.0
21	2.87E−05	5.73E−05	1.43E−05	0.0
22–31	0.0	0.0	0.0	0.0
$q_i = \sum_{\ell} q_i\ell$	1.78E−02	1.95E−02	4.53E−03	1.68E−03

Class of precipitation intensity ℓ	West Sector			North Sector
	10	12	14	16
1–7	0.0	0.0	0.0	0.0
8	3.58E−04	9.17E−04	9.89E−04	1.10E−03
9	0.0	0.0	0.0	0.0
10	3.58E−04	9.03E−04	8.17E−04	6.59E−04
11	4.30E−05	3.44E−04	2.01E−04	1.86E−04
12	2.29E−04	3.58E−04	4.30E−04	4.01E−04
13	2.44E−04	4.01E−04	4.73E−04	2.87E−04
14	1.43E−04	3.15E−04	2.29E−04	2.29E−04
15	2.29E−04	4.59E−04	4.01E−04	2.58E−04
16	1.29E−04	1.43E−04	2.29E−04	1.72E−04
17	1.43E−04	2.15E−04	2.29E−04	7.17E−05
18	2.87E−05	8.60E−05	1.15E−04	2.87E−05
19	4.30E−05	7.17E−05	7.17E−05	7.17E−05
20	0.0	1.43E−05	1.43E−05	1.43E−05
21	2.87E−05	1.43E−05	0.0	0.0
22–31	0.0	0.0	0.0	0.0
$q_i = \sum_{\ell} q_i\ell$	1.98E−03	4.24E−03	4.20E−03	3.48E−03

Table E. Exponents of the vertical wind profile, cf. Eq. (2.14) of this chapter

Diffusion category	Wind Profile Exponents, m_j	
A ($j = 6$)	0.09	0.10[a]
B ($j = 5$)	0.20	0.15
C ($j = 4$)	0.22	0.20
D ($j = 3$)	0.28	0.25
E ($j = 2$)	0.37	0.30
F ($j = 1$)	0.42	0.30

[a]These values have been recommended by the U.S. Environmental Protection Agency in EPA-450/2-77-018, 1977.

3 Transport of Radionuclides in Surface Waters

By G. H. JIRKA,* A. N. FINDIKAKIS,† Y. ONISHI,‡
and P. J. RYAN**

3.1 INTRODUCTION

The purpose of aquatic transport and diffusion calculations is to provide estimates of the radionuclide concentrations within a water body and the radionuclide deposition on the shoreline and bottom from both routine and accidental releases of liquid effluents. These calculations provide a link between the effluent releases and direct or indirect pathways to man for dose calculations.

The wide variety of mathematical models for assessing hydrologic transport of pollutants (radionuclides) ranges from simple algebraic models to sophisticated multidimensional models based on numerical solutions to the advection-diffusion equation and the associated hydrodynamic equations. However, the emphasis on model development has far outweighed the efforts on model verification, and caution and a considerable amount of judgment are required in both model selection and application.

The emphasis in this chapter is on the use of simple models. For example, in contrast to heat disposal calculations, where highly accurate knowledge of the distribution of excess temperature in space and time is required, most dose calculations are based on cumulative effects. Concentration variations in space and time are often not important, and a conservative approach is usually both cost effective and desirable. The limitations of the simple models will be discussed, and some examples will be given. More complex models, which may be

*Cornell University, Ithaca, N.Y.
†Bechtel Civil & Minerals, Inc., San Francisco, and Stanford University.
‡Pacific Northwest Laboratory operated by Battelle Memorial Institute, Richland, Wash.
**Bechtel Civil and Minerals, Inc., San Francisco.

required in some situations, will be briefly discussed; and relevant references will be listed.

The overall distribution of radionuclides in surface waters is controlled by four distinct transport and transformation processes subject to different source conditions, as summarized in Table 3.1. Thus, depending on water body characteristics, the surrounding terrestrial and atmospheric conditions, and the physicochemical aspects of a particular radionuclide, many processes may be considered. The present chapter, however, focuses on three particular dispersal phases: Section 3.2 deals with the rapid initial mixing phase that is controlled by the characteristics of the effluent and the discharge structure; Section 3.3 treats the far-field mixing by ambient advection and diffusion processes that occur over much larger distances; and Sect. 3.4 addresses the role of sediment effects in intermedia transfer, direct transport, and transient storage. Generally, it is found that these three phases are of vital importance in most radionuclide assessment scenarios. The inclusion of other transport and

Table 3.1. Major mechanisms affecting radionuclide migration and fate in surface waters

Transport and transformation processes
Transport
Water movement
Discharge-induced advection and diffusion
Ambient advection and diffusion
Sediment movement
Intermedia transfer
Adsorption and desorption
Precipitation and dissolution
Volatilization
Degradation and decay
Radionuclide decay
Transformation
Yield of daughter product
Point and nonpoint source/sink contributions
Direct discharge: routine or accidental
Dry and wet deposition from atmosphere
Runoff and soil erosion from land surfaces
Seepage from or to groundwater

transformation processes and source terms (see Table 3.1) is often relatively straightforward.

The major emphasis in this chapter is on the treatment of continuous, controlled radionuclide releases from engineered structures, with minor attention given in Sect. 3.3 to accidental releases.

3.2 INITIAL MIXING

When the quantity of effluent is small and the receiving water body is relatively large, rapid initial mixing by means of a properly designed discharge structure is an effective means of reducing the radionuclide concentrations. In some cases, it is the only feasible way to meet regulatory requirements.

The initial, or near-field, mixing process is based on a high level of turbulence produced by means of the discharge momentum (jet action) and/or the discharge buoyancy (plume action). The process is relatively rapid inasmuch as it occurs over a short distance, typically equal to 10 to 100 times the characteristic discharge dimension (e.g., the square root of the discharge cross-sectional area). Large dilutions on the order of 10 to 100 can be achieved.

In this context, dilution S is defined as the ratio

$$S = \frac{C_0}{C}, \tag{3.1}$$

where C_0 is the discharge concentration (or concentration excess) and C is the concentration at some point of interest (e.g., at the end of the near-field zone).

Frequently, the initial mixing process is dominant over the much more gradual and sluggish far-field mixing processes, which are driven by considerably lower turbulence levels in the ambient river, lake, or coastal environment.

Factors that affect initial dilution are the momentum and buoyancy of the effluent, the outfall configuration and location, and the receiving water characteristics (depth and current) in the vicinity of the outfall. Separate predictive models have been developed for surface and submerged discharges, single-point and multiport outfalls; deep and shallow, and stagnant and flowing water; and buoyant (positive and negative) and nonbuoyant effects. The more important combinations of the above parameters are discussed and some example calculations are shown. Three separate types of outfall are important in design practice: surface-point discharges, submerged-point discharges, and multiport diffusers. These configurations are discussed here, with buoyant and nonbuoyant discharges being treated as subclasses. The buoyant case is emphasized because it is standard practice to mix the routine release of radionuclides with the cooling-water discharge for once-through systems and with the blowdown for closed-cycle systems.

A basic assumption in all initial mixing calculations is that the effluent characteristics (total heat, total radionuclides, etc.) are conservative. This assumption is almost always realistic because of the small time scales involved.

3.2.1 Surface-Point Discharges

Surface discharges consist of an outfall at (e.g., an open channel) the free water surface or close to (e.g., slightly submerged pipe) it. Such discharges have received substantial attention over the past decade, in particular as buoyant surface jets for waste heat disposal. A concise summary of the properties of buoyant surface jets, comprising the results of mathematical models and data from field and laboratory experiments, has been given by Jirka, Adams, and Stolzenbach (1981).

The major parameter describing the dynamic characteristics of the buoyant surface jet is a discharge densimetric Froude number F_0:

$$F_0 = \frac{U_0}{\sqrt{(\Delta\rho/\rho_0)g\ell_0}}, \tag{3.2}$$

where U_0 is the (mean) discharge velocity (m/s), ρ_0 is the ambient density (kg/m^3), $\Delta\rho$ is the discharge density deficit (kg/m^3), g is the acceleration of gravity (m/s^2), and ℓ_0 is a characteristic length scale (m) of the discharge, which is related to its cross-sectional area A_0 by

$$\ell_0 = \sqrt{A_0/2}.$$

A rectangular discharge channel, for example, with depth h_0 and half-width b_0 has

$$\ell_0 = \sqrt{h_0 b_0}.$$

However, the actual channel cross-sectional shape (i.e., the separate values of h_0 and b_0) is of limited dynamic importance except for very small Froude numbers $F_0 \to 1$ (Jirka et al. 1981).

3.2.1.1 Stagnant and Weak Crosscurrents

Deep receiving water. A deep receiving water condition exists when the vertical extent of the buoyant jet is sufficiently less than the existing water depth H. Three models are in general use for this case, the models developed by Stolzenbach and Harleman (1971), Prych (1972), and Shirazi and Davis (1974). The three models are available in the form of computer codes, which are relatively inexpensive and simple to use and are well documented. The Shirazi and Davis model is also available in a workbook format. The application of these models yields spatially detailed predictions of the concentration (or temperature excess) field of the surface buoyant jet. Figure 3.1 shows typi-

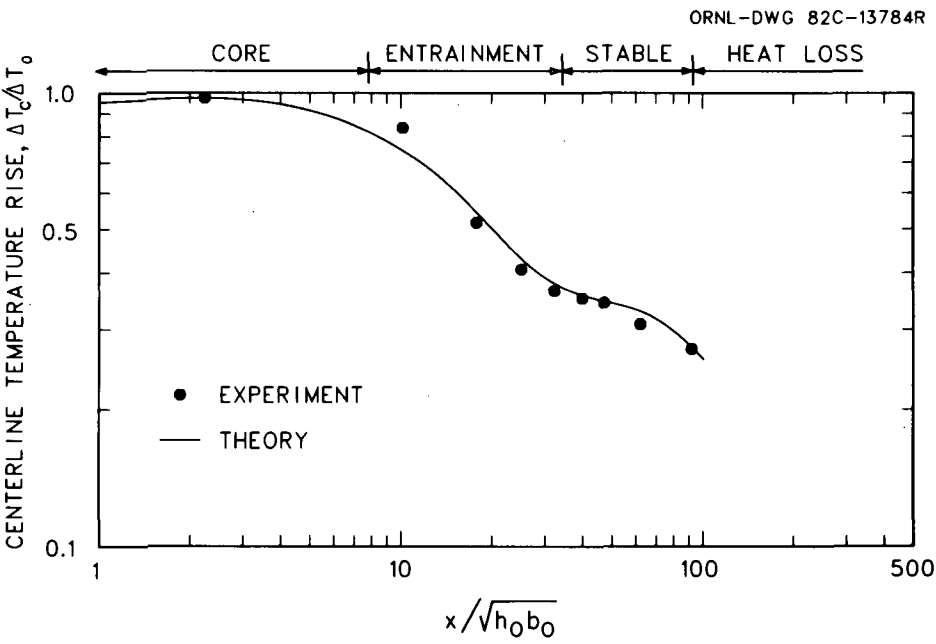

Figure 3.1. Theoretical calculations and experimental data for centerline dilution in surface plumes. Source: Stolzenbach, K. D., and Harleman, D. R. F. 1971. *An Analytical and Experimental Investigation of Surface Discharges of Heated Water,* Technical Report 135, Massachusetts Institute Technol., R. M. Parsons Lab. Water Resources and Hydrodynamics, Department Civil Engineering, Cambridge.

cal centerline dilution estimates for a thermal plume obtained with the Stolzenbach and Harleman (1971) model. Provided that certain simplifying conditions are met, the predictions with the above models are found to be reasonably reliable (for a complete assessment, see Dunn et al. 1975 or Jirka et al. 1975).

For radionuclide computations, however, it is usually sufficient to deal with a few bulk features of the near-field mixing process (e.g., the bulk dilution S_s and the transition distance x_t) while neglecting its internal detail. The bulk, or stable, dilution S_s is reached at the end of the near field when the jet has been stabilized and vertical entrainment has ceased.

The transition distance x_t is a useful measure for the extent of the near-field zone. The following expressions for S_s and x_t can be readily used as the starting conditions of a far-field calculation:

$$S_s = 1.4F_0, \tag{3.3}$$

$$x_t = 15\ell_0 F_0. \tag{3.4}$$

Another important parameter is the maximum vertical penetration of the surface jet:

$$h_{max} = 0.42 \ell_0 F_0 , \tag{3.5}$$

which occurs at an approximate distance $5.5\ \ell_0 F_0$ from the outfall.

Example 3.1. Consider an outfall with a flow of 0.5 m^3/s through a channel of rectangular cross section with width 1 m and flow depth 0.5 m with initial density difference $(\Delta\rho/\rho) = 0.002$ into a stagnant semi-infinite water body.

Find the extent of the near-field region and the bulk dilution in the near field:

$$U_0 = \frac{0.5}{1 \cdot 0.5} = 1\ \text{m/s},$$

$$\ell_0 = \left[1 \cdot \frac{0.5}{\sqrt{2}}\right]^{1/2} = 0.5\ \text{m},$$

$$F_0 = \frac{1}{\sqrt{0.002 \cdot 9.81 \cdot 0.5}} = 10.1,$$

$$x_s = 15 \cdot 0.5 \cdot 10.1 = 75.8\ \text{m},$$

$$S = 1.4 \cdot 10.1 = 14.1.$$

Thus, the initial concentration of any radionuclide released from this outfall will be reduced by a bulk factor of 14 after the near-field mixing. [End of example]

In case of truly stagnant conditions, the jet trajectory is, of course, a straight line. If a weak crossflow persists, the trajectory is curved in the direction of the crossflow. Also, the mixing mechanism is somewhat affected by the generally more vigorous mixing produced by the action of the crossflow (see Adams et al. 1975). Still, Eqs. 3.1, 3.2, and 3.5 can be used for conservative estimates of buoyant jets in weak crossflow. Alternatively, the workbook by Shirazi and Davis (1974) can be used.

Several limiting cases of buoyant jet behavior exist, for which the above equations (Eq. 3.3 in particular) do not hold. Three major limiting circumstances are addressed in the following: (1) too shallow receiving water, (2) strong cross currents, and (3) confining lateral boundary.

Shallow receiving water. When the jet behavior is significantly affected by the bottom, the receiving water can be said to be shallow. Virtually all major cooling-water outfalls are in this category. A criterion for shallow water conditions obtained from experimental and field data (Jirka et al. 1981) is

$$\frac{h_{max}}{H} > 0.75 , \tag{3.6}$$

where H is the water depth at the point of maximum plume depth, h_{max}. An empirical correction r_s can be applied to the deep water equations for dilution to account for the inhibiting effect of a shallow receiving water. Thus, bulk dilution under shallow conditions $\hat{S}_s$ can be estimated by

$$\hat{S}_s = r_s S_s . \tag{3.7}$$

The empirical factor r_s is given by

$$r_s = \left(\frac{0.75}{h_{max}/H} \right)^{0.75} . \tag{3.8}$$

3.2.1.2 Strong Crossflow (Shoreline-Attached Jets)

For strong crossflows, the effluent plume may be pinned to the downstream shoreline; and the entrainment of uncontaminated water into the plume is inhibited from one side. In shallow water, where the plume is in contact with the bottom, the ambient crossflow is prevented from passing under the jet; and a relatively lower crossflow can cause shoreline attachment. The main parameters in determining shoreline attachment are the relative crossflow velocity, $R = U_a/U_0$ (where U_a is the crossflow velocity) and the shallowness factor h_{max}/H. On the basis of limited field and laboratory data, Jirka et al. (1975, 1981) obtained a criterion for shoreline attachment for a perpendicular discharge and a straight shoreline as

$$R > 0.05 \left(\frac{h_{max}}{H} \right)^{-3/2} . \tag{3.9}$$

No simple model predictions are available in the literature to estimate the near-field mixing of strongly deflected shoreline-attached jets. In part, this problem is due to the fact that the mixing is often governed more by the ambient crossflow than by the discharge. Mixing in this case is more a far-field than an actual near-field process and could be controlled by engineering design. Thus, some empirical equations (e.g., Carter 1969) indicate a continued mixing process, which is better described by a far-field model.

Detailed experimental studies on strongly deflected jets (see the summary by Adams et al. 1975) indicate that the actual near-field mixing in attached jets is always considerably less than in the corresponding nonattached shallow jet that would be predicted by Eq. 3.7.

A recirculation zone between the lee side of the jet and the shoreline reentrains already mixed water. Depending on the amount of blocking (see Eq. 3.9), the degree of reentrainment may be up to 100% so that the surface jet entrains ambient undiluted water from only one side. Hence, for conservative estimation purposes, the initial dilution of an unattached shallow water surface jet may be taken as

$$\left[\hat{S}_s\right]_{\text{attached}} = \frac{1}{2}\hat{S}_s , \tag{3.10}$$

where $\hat{S}_s$ is given by Eq. 3.7. The extent of the near-field zone may be estimated by the crossflow deflection length scale x_c (Jirka et al. 1981),

$$x_c = 2\frac{\ell_0}{R} \tag{3.11}$$

or by x_t (Eq. 3.4), whichever is less.

3.2.1.3 Surface Discharges with Zero or Negative Buoyancy

All the models discussed previously are strictly valid only for buoyant discharges. Whenever the discharge has some buoyancy, albeit small, $\Delta\rho \to 0$, and F_0 is large, the results are still applicable and simply indicate large dilutions and considerable distance until the jet subsides. The fact that the ambient environment usually exhibits some variability in density should not be overlooked as a factor in the ultimate stabilization of practically all discharges. A truly nonbuoyant jet is simply predicted by the classical result (Albertson et al. 1951)

$$S(x) = 0.32\frac{x}{D} , \tag{3.12}$$

where D is the equivalent diameter of a round half-jet. Equation 3.12 indicates continuous dilution with increasing distance x. In practice, however, an ultimate transition is provided by an eventual stabilization or by the ambient turbulence level beginning to dominate over the weakening jet turbulence.

Finally, a negatively buoyant jet, discharged at the surface and sinking to the bottom, behaves in an inverse manner to a submerged buoyant jet riding to the surface and is amenable to the models of the following section.

3.2.2 Submerged-Point Discharges

Whenever the discharge is located well below the surface of the water body and usually close to the bottom, it is analyzed by means of a submerged discharge model. This section discusses single-port (point) discharges, and multiport diffusers are addressed in Sect. 3.2.3.

Numerous complications arise when one deals with submerged discharges. First and foremost among these is the depth of the receiving water relative to the dynamic characteristics of the discharge. As illustrated in Fig. 3.2, two fundamental conditions can exist: (1) a deep receiving water condition, in which a distinct buoyant jet rises to the surface and dilution occurs because of turbulent jet entrainment up to the surface level; if the receiving water is sufficiently stratified, the jet trajectory can, in fact, be shortened and the jet ceases when a terminal (equilibrium) level is reached; and (2) a shallow receiving water, in which the discharge momentum is sufficiently strong to cause a dynamic breakdown of the buoyant jet motion and create a local recirculation zone.

This dynamic distinction into deep and shallow water conditions is important, as entirely different techniques must be used for the analysis of each

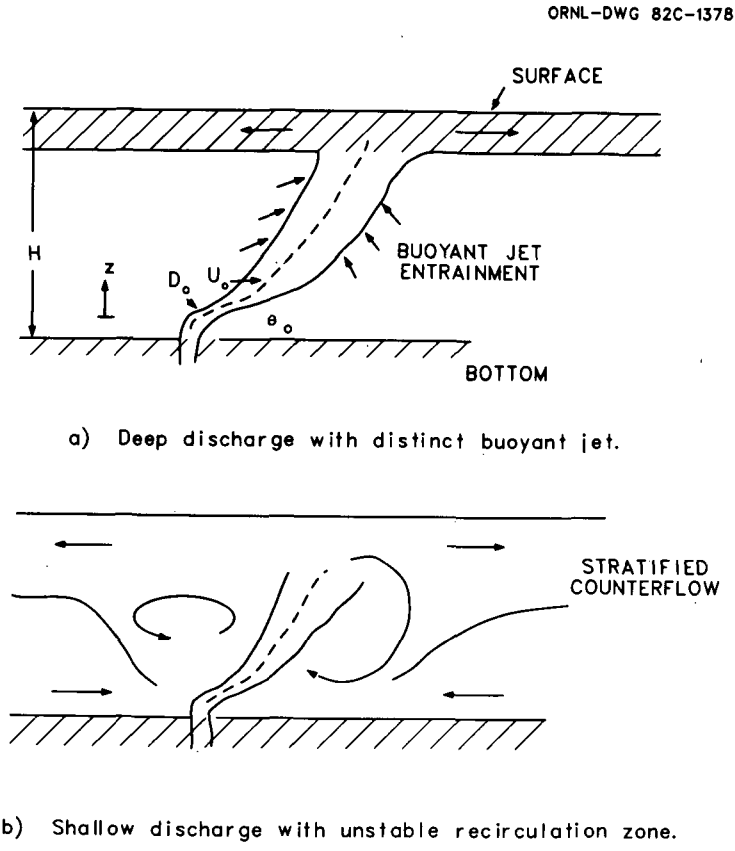

Figure 3.2. Possible interaction of receiving water and discharge characteristics.

case. The discharge condition is characterized by the relative water depth H/D and a densimetric Froude F_0 number

$$F_0 = \frac{U_0}{\sqrt{(\Delta\rho/\rho)gD}}, \tag{3.13}$$

where D = diameter of the outfall.

A stability analysis of Lee and Jirka (1974, 1981) yielded the following approximate condition for deep receiving water (stable flow field):

$$\frac{H}{D} > 0.22F_0, \tag{3.14}$$

with apparently little sensitivity to the discharge angle θ_0.

Simple buoyant jet models can be used for the deep condition. On the other hand, the mixing achieved in the local recirculation zone of a shallow discharge must be analyzed on the basis of stratified counterflow models (Fig. 3.2). In practice, most heated discharge situations fall into the shallow water range. Hence, any associated radionuclide release is similarly affected. Ambient stratification and crossflow are additional factors to be considered in the dilution analysis of submerged discharges.

3.2.2.1 Stagnant or Weak Crosscurrents

Deep receiving water. Several submerged buoyant jet models exist (e.g., Abraham 1963; Fan and Brooks 1963; Hirst 1972) and should be used whenever reasonably complex discharge conditions occur (arbitrary angle θ_0). However, two limiting conditions are of interest: the vertical and the horizontal discharges. The vertical buoyant plume, $\theta = 90°$, with reasonably small discharge Froude number F_0, gives a centerline dilution S_c (i.e., the minimum value in the plume) as a function of normalized vertical distance z/D (Rouse et al. 1952).

$$S_c = 0.11\left(\frac{z}{D}\right)^{5/3} F_0^{-2/3}, \tag{3.15}$$

where z is the distance above the nozzle, and D is the effective diameter of the nozzle (including the effect of contraction at a sharp-edged orifice).

The predictions of various jet models and experimental data for horizontal submerged discharges are summarized on a simple nondimensional graph (Fig. 3.3) presented by Roberts (1977). When Eq. 3.15 or Fig. 3.3 is used for predictive purposes, it is always necessary to ascertain that the deep water condition, Eq. 3.14, is satisfied as well. The maximum vertical distance (Fig. 3.2) to which jet mixing takes place is given only approximately by the total water

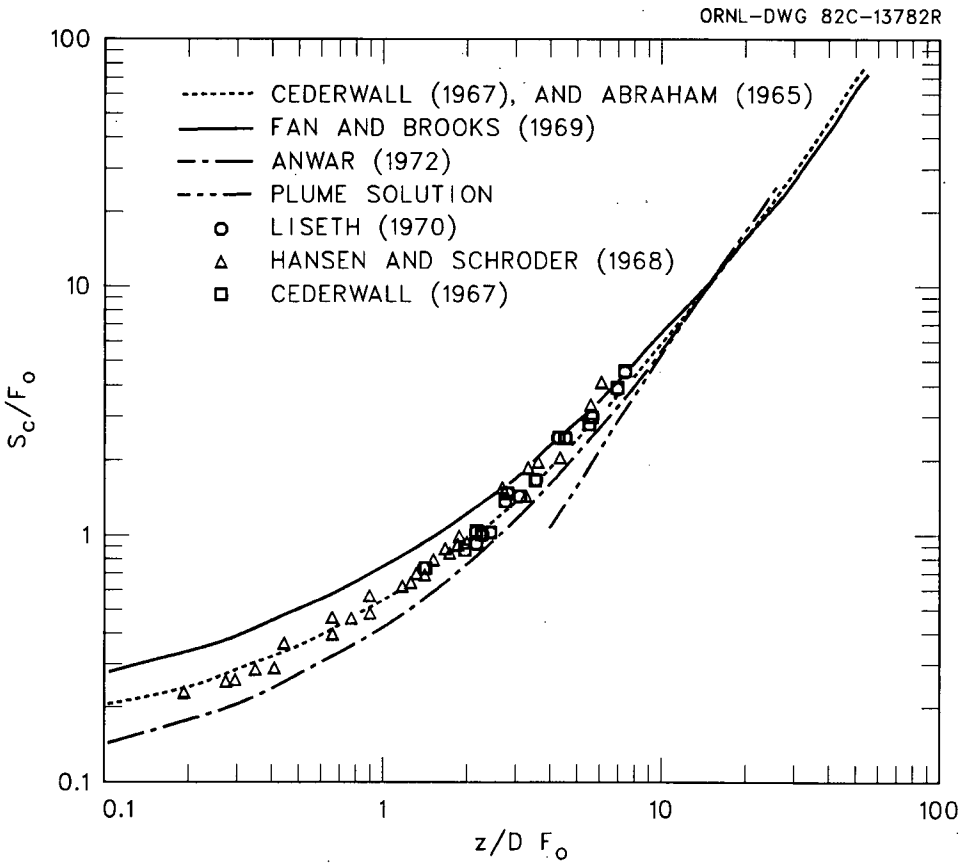

Figure 3.3. Centerline dilution of a submerged, horizontal, round, buoyant jet in a stagnant, uniform fluid. Source: Roberts, P. J. W. March 1977. *Dispersion of Buoyant Wastewater Discharged from Outfall Diffuses of Finite Length,* KH-R-35, W. M. Keck Lab., California Institute Technol., Pasadena.

depth H. Since a mixed layer forms at the surface, it is common to reduce this vertical distance to 80% of H. Also, it is often useful to set up a bulk dilution factor S for the entire near field that is related to the centerline dilution by

$$S \approx 1.4 S_c \ , \tag{3.16}$$

as has been done for the surface discharges.

Example 3.2. An outfall pipe, 0.6 m in diameter, is discharging a heated effluent to an unstratified lake. A horizontal discharge is used to maximize mixing. The water depth at the discharge point is 6 m, the discharge velocity is 3 m/s, and the normalized initial density difference is 0.003. What is the approximate centerline dilution when the buoyant discharge impinges on the water surface?

Compute discharge densimetric Froude number:

$$F_0 = \frac{3}{\sqrt{0.003 \cdot 9.81 \cdot 0.6}} = 22.6 \ .$$

Check if discharge is in the deep water range (Eq. 3.14): $H/D = 10 > 0.28 F_0 = 6.3$. Equation 3.14 is satisfied. Therefore, simple buoyant jet analysis is applicable. Take maximum vertical distance: $z = 0.8H = 4.8$ m. Using Fig. 3.3 with $z/DF_0 = 4.8/(0.6 \cdot 22.6) = 0.35$ gives $S_c/F_0 = 0.3$, or a centerline dilution $S_c = 6.8$. Thus, the near-field mixing for this discharge is characterized by a bulk dilution factor of $S = 1.4 \cdot 6.8 = 9.6$. [End of example]

The buoyant jet may become trapped below the free surface if the receiving water is stratified. For estimates of the maximum penetration height and the associated mixing, more detailed references should be consulted (e.g., Jirka et al. 1975; Fischer et al. 1979), or computer models may be used (e.g., Fan and Brooks 1969; Hirst 1972).

Shallow receiving water. The strong dynamic effect of the discharge within the shallow water column can create complicated flow patterns. Again, the two limiting cases of vertical and horizontal discharges can be used readily to bracket the expected behavior. For the vertical discharge, Lee and Jirka (1981) give a bulk dilution which characterizes the local recirculation cell:

$$S = 0.9\left(\frac{H}{D}\right)^{5/3} F_0^{-2/3} \ . \tag{3.17}$$

Equation 3.17 is applicable when the deep water condition, Eq. 3.14, is not satisfied. If the discharge is horizontal, however, it is often reasonable and conservative to treat it simply as a surface discharge in shallow water, since the jet quickly rises to the surface and then behaves like a surface jet. Thus, the dilution estimates of Eq. 3.7 may be used with proper transposition of variables $\ell_0 = \sqrt{(1/2)(\pi D^2/4)}$. For further discussion and some empirical data, see Jirka et al. (1975).

3.2.2.2 Moderate to Strong Crossflows

A crossflow tends to act as an additional dilution mechanism in conjunction with that achieved by discharge momentum and buoyancy. Thus, for conservative estimates of radionuclide accumulation, the formulas in the previous paragraphs that neglect the crossflow may suffice. This is especially applicable for shallow receiving water in which the crossflow influence is somewhat weaker because of the depth limitation.

If more comprehensive predictions for deep discharges are required, several analyses are available in computer form (e.g., Fan and Brooks 1969; Hirst 1971; Shirazi and Davis 1971; Schatzmann 1976) or as summary diagrams (e.g., Shirazi and Davis 1971; Jirka et al. 1975; Wright 1977). The similarity of these analyses to some of the atmospheric diffusion models in crosswind with or without ambient stratification, which are treated in Chapter 2, should be noted here.

3.2.3 Submerged Multiport Diffusers

A multiport diffuser is the most effective method for achieving a high degree of initial dilution. The diffuser is a linear structure consisting of many closely spaced ports, or nozzles, which inject high-velocity jets into the receiving water. The ports may be attached as risers to a buried pipe or may simply be openings in a pipe lying on the bottom of the receiving water.

As for the single port discharge, it is again most important to realize that the dynamics of the discharge may result in the form of a stable deep water or an unstable shallow water discharge. This is easily visualized by considering Fig. 3.2 and replacing the simple round opening of diameter D with a two-dimensional slot opening of width B. This is a convenient representation of the actual diffuser. The equivalent slot width B for a diffuser with nozzles of diameter D and lateral spacing ℓ, which ensures similar dynamic effects, is given by

$$B = \frac{\pi D^2}{4\ell} .$$

The dynamic parameters for discharge stability of a multiport diffuser, then, are its equivalent slot densimetric Froude number and relative water depth

$$F_s = \frac{U_0}{\sqrt{(\Delta\rho/\rho)gB}} \quad \text{and} \quad \frac{H}{B} . \tag{3.18}$$

A stability analysis by Jirka and Harleman (1973) (see also Jirka 1982) gives the following condition for the deep receiving water:

$$\frac{H}{B} > 1.84 F_s^{4/3}(1+\cos^2\theta_0)^2 , \tag{3.19}$$

thus indicating some dependence on the discharge angle with the horizontal θ_0. Ambient crossflow is often another destabilizing factor (i.e., it causes vertical mixing over the water column) and has been considered in a complete stability diagram by Jirka (1982).

Most diffuser problems of practical interest in energy-related discharges are of the shallow water variety. Deep water diffusers are typically encountered in sewage disposal applications and occasionally for blowdown diffusers from closed-cycle cooling operations.

3.2.3.1 Deep Receiving Water

Stagnant conditions. Satisfactory estimates of bulk dilution are usually obtained by simply considering the vertical buoyant plume $\theta_0 = 90°$ and F_s sufficiently small so that Eq. 3.19 holds. Further, as long as Eq. 3.19 is satisfied, all nonvertical discharges tend to the rising buoyant plume anyway. Also, a frequent design in deep water conditions is the alternating diffuser in which adjacent nozzles point to different sides. In this case, $\theta_0 = 90°$ is a convenient dynamic approximation. The centerline dilution S_c as a function of vertical instance z/B is (Rouse et al. 1952)

$$S_c = 0.39 \frac{z}{B} F_s^{-2/3}. \tag{3.20}$$

A bulk dilution S for a maximum vertical distance value of 0.8 H to account for the surface layer would be larger by $\sqrt{2}$:

$$S = 0.44 \frac{H}{B} F_s^{-2/3}. \tag{3.21}$$

The applicability of Eq. 3.20 to deep diffuser problems has been demonstrated (e.g., Jirka and Harleman 1973; Koh and Brooks 1975). If the ambient environment is stratified, the buoyant jet may become trapped at some terminal level.

Ambient crossflows. The direction of the crossflow relative to the diffuser alignment (i.e., the axis of the main pipe) is an additional and critical parameter. The perpendicular alignment is the preferred case because it intercepts the greatest crossflow and maximizes mixing. An experimental study of a deep water diffuser by Roberts (1977, 1979) yielded the following dilution estimates for near-field bulk dilutions. For weak crossflow, the dilution is still related to the buoyancy of the discharge (i.e., its Froude number):

$$S = 0.27 \frac{H}{B} F_s^{-2/3}. \tag{3.22}$$

In this case, the crossflow has, in fact, a nonconservative effect (compare to Eq. 3.21) because it causes some blocking of entrainment at the downstream side of the diffuser plume.

For strong crossflows, the dilution is given by a simple ratio between the total crossflow sweeping over the diffuser line, $U_a L_D H$, and the total discharge flow Q_0:

$$S = C_1 \frac{U_a L_D H}{Q_0}, \tag{3.23}$$

where U_a is the crossflow velocity and L_D is the length of the diffuser. Ideally, the constant C_1 should be unity, but Roberts found a smaller and hence conservative $C_1 = 0.58$, apparently due to some incomplete mixing and buoyant restabilization (see also Jirka 1973). Values of C_1 are given by Roberts (1977) as a function of the orientation and strength of crossflows and the buoyancy of effluent. Widths of the plume at the surface are also given so that the initial conditions for use in far-field models can be easily specified.

3.2.3.2 Shallow Receiving Water

Multiport diffusers in shallow conditions, frequently used for thermal discharges, can have a large number of possible flow configurations and mixing mechanisms. Also, highly site-specific designs (i.e., different types of nozzle orientation and current alignments) are possible. Three major diffuser types have been used in recent design practice. the unidirectional diffuser, the staged diffuser, and the alternating diffuser. The diffuser configuration and the resulting flow fields are shown in Fig. 3.4. A comprehensive account of diffuser dynamics and analysis techniques is given by Jirka (1982).

Stagnant receiving water. The unidirectional and staged diffuser designs produce vertically mixed (uniform) diffuser plumes that sweep in the direction of the discharge nozzles. Very high dilutions can be achieved if the initial discharge velocity (momentum input) is high. The bulk dilution for such diffusers is given by

$$S = C_2 \sqrt{H/B}. \tag{3.24}$$

The factor C_2 is equal to $1/\sqrt{2}$ for unidirectional diffusers and 0.67 for staged diffusers (Jirka 1982). Almquist and Stolzenbach (1980) give a lower value (0.45) for C_2 for staged diffusers. In essence, Eq. 3.24 indicates the total flow rate immediately downstream from a diffuser relative to the discharge flow Q_0. Considerable additional mixing can take place as the concentrated diffuser plume gradually diffuses further downstream. This procedure is still a near-field process and is represented in dilution analyses of Lee and Jirka (1980) and diagrams by Jirka (1982). Equation 3.24 can be taken again as a conservative lower limit.

The alternating diffuser with the unstable recirculation zone for shallow water is predicted by stratified flow theory to have a bulk dilution of

$$S = C_3 \frac{H}{B} F_s^{-2/3}, \tag{3.25}$$

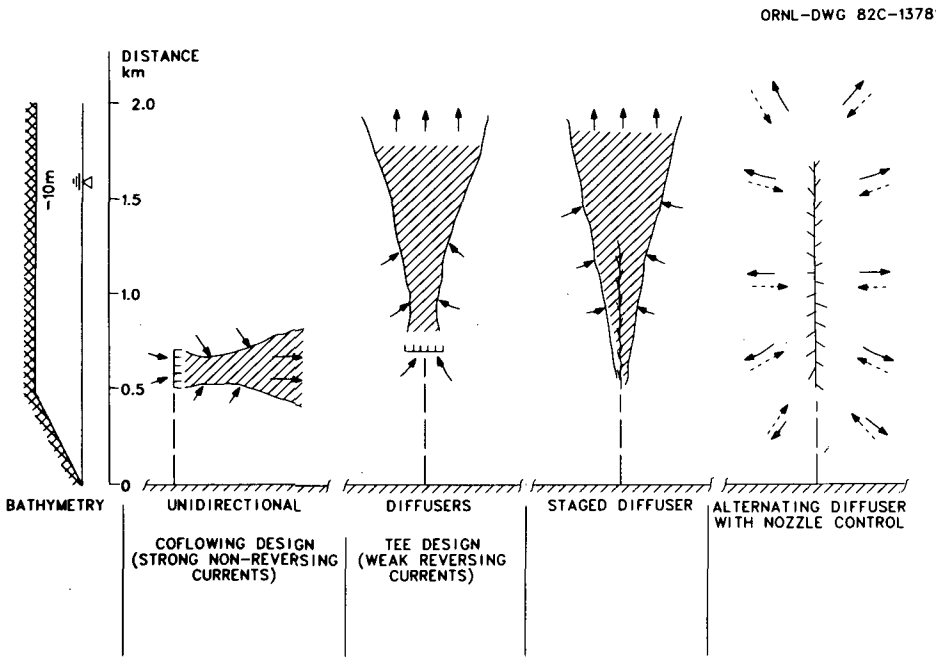

Figure 3.4. Diffuser configuration and flow fields in coastal environments.

with $C_3 = 0.45$ to 0.55, depending on the friction effects in the counterflow. Equation 3.25 appears to be qualitatively similar to Eq. 3.21; that is, it is also a buoyancy-driven flow. (Note that the deep water condition described by Eq. 3.19 is not satisfied in this case, whereas it holds for the case of Eq. 3.21.)

Ambient crossflows. A variety of interactions may exist in this case, depending upon diffuser type and alignment (Jirka 1982). A type frequently employed when the ambient current is steady and in only one direction is the coflowing diffuser (i.e., a unidirectional design with perpendicular alignment). The bulk dilution is given then by the combined effect of crossflow and diffuser mixing:

$$S = \frac{1}{2}\frac{U_a L_D H}{Q_0} + \frac{1}{2}\left[\left(\frac{U_a L_D H}{Q_0}\right)^2 + 2\frac{H}{B}\right]^{1/2} . \qquad (3.26)$$

Equation 3.26 is of particular interest for diffusers in river applications as long as the diffuser length is sufficiently shorter than the river width. If the diffuser covers the entire river, Eq. 3.26 would, of course, be superseded by the proportional mixing:

$$S = \frac{Q_R}{Q_0}, \tag{3.27}$$

as the diffuser-induced action cannot result in more mixing than is provided by the river flow Q_R.

Example 3.3. Consider an alternating diffuser with 120 nozzles 0.15 m in diameter spaced 0.4 m apart. The diffuser discharges 10 m^3/s into open coastal waters with a depth of 6 m. The relative density difference is $\Delta\rho/\rho = 0.002$. To estimate the dilution,

$$A_n = \frac{\pi 0.15^2}{4} = 0.0177\ m^2 ,$$

$$B = \frac{0.0177}{0.4} = 0.044\ m ,$$

$$U_0 = \frac{10}{120 \cdot 0.0177} = 4.71\ m/s ,$$

$$F_s = \frac{4.71}{\sqrt{0.003 \cdot 9.81 \cdot 0.044}} = 130.9 ,$$

$$\frac{H}{B} = \frac{6}{0.044} = 136.3 < 1.84\, F_s^{4/3} = 130.9 ;$$

that is, Eq. 3.19 is not satisfied.

Using Eq. 3.25, with $C_3 = 0.5$,

$$S = 0.5 \frac{6}{0.044} 130.9^{-2/3} = 2.6 . \quad \text{[End of example]}$$

Example 3.4. Consider a blowdown diffuser with 40 nozzles 5 cm in diameter discharging in the direction of ambient stream flow. The nozzle spacing is 0.3 m and the depth of the receiving water is 1.5 m, and the stream is much wider than the diffuser length. The total discharge flow rate is 0.3 m^3/s, and the ambient velocity is 0.6 m/s.

$$\text{Nozzle area } A_n = \frac{\pi(0.05)^2}{4} = 0.00196\ m^2 ,$$

$$\text{Equivalent slot width } B = \frac{0.00196}{0.3} = 0.065\ m ,$$

$$\text{Total nozzle area} = 40(0.00196) = 0.0784\ m^2 ,$$

$$U_0 = \frac{0.3}{0.0784} = 3.83\ m/s .$$

The bulk dilution in the absence of crossflow can be estimated from Eq. 3.24:

$$S = \frac{1}{\sqrt{2}} \sqrt{\frac{1.5}{\sqrt{0.0065}}} = 10.7 \ .$$

In the presence of a crossflow $U_a = 0.6$ m/s, the dilution can be estimated from Eq. 3.26:

$$S = \frac{1}{2}\left[\frac{0.6 \cdot 40 \cdot 0.3 \cdot 1.5}{0.3}\right] + \frac{1}{2}\left[\left[\frac{0.6 \cdot 40 \cdot 0.3 \cdot 1.5}{0.3}\right]^2 + 2\left[\frac{1.5}{0.0065}\right]\right]^{1/2} = 39 \ .$$ [End of example]

3.3 FAR-FIELD MIXING

After a radionuclide discharge has passed through the relatively rapid initial mixing process of the near field, its further fate is determined by transport and diffusion processes in the ambient far field. Because these processes are typically much slower, much longer distances and time frames must be considered. These concerns result in two important consequences: it may be important to include radioactive decay and other physical/chemical transformation processes; the total physical dimension of the receiving water body and its net advective transport character must be considered.

For example, the long-term radionuclide accumulation in a coastal bay or in an inland reservoir is often controlled simply by the average throughflow and flushing rate, and the internal distribution processes (e.g., diffusion and circulation) may be largely irrelevant. Thus, this section is organized on the basis of water bodies with highly variable geometric or advective transport characteristics: rivers with a well-defined net transport, estuaries with strongly oscillating tidal flow but often weak net transport, small lakes or reservoirs with strong boundary limitations and weak transport, and the ocean or large lakes with practically "unlimited" dimensions.

3.3.1 Rivers

Rivers are typically wide and shallow water bodies with strong advective and turbulent flow. After the initial mixing process, the effluent is usually mixed over the shallow depth, is advected downstream by the river flow, and is diffused laterally across the river. After sufficient distance, the effluent becomes fully mixed across the entire width. Hence, it becomes expedient to analyze this situation in stages: (1) transverse mixing and (2) longitudinal advection and dispersion.

3.3.1.1 Transverse Mixing

Useful examples of transverse mixing in a shallow river with uniform depth H and ambient velocity U are illustrated in Fig. 3.5, which shows the case of a steady-state, relatively concentrated ("point") discharge by means of

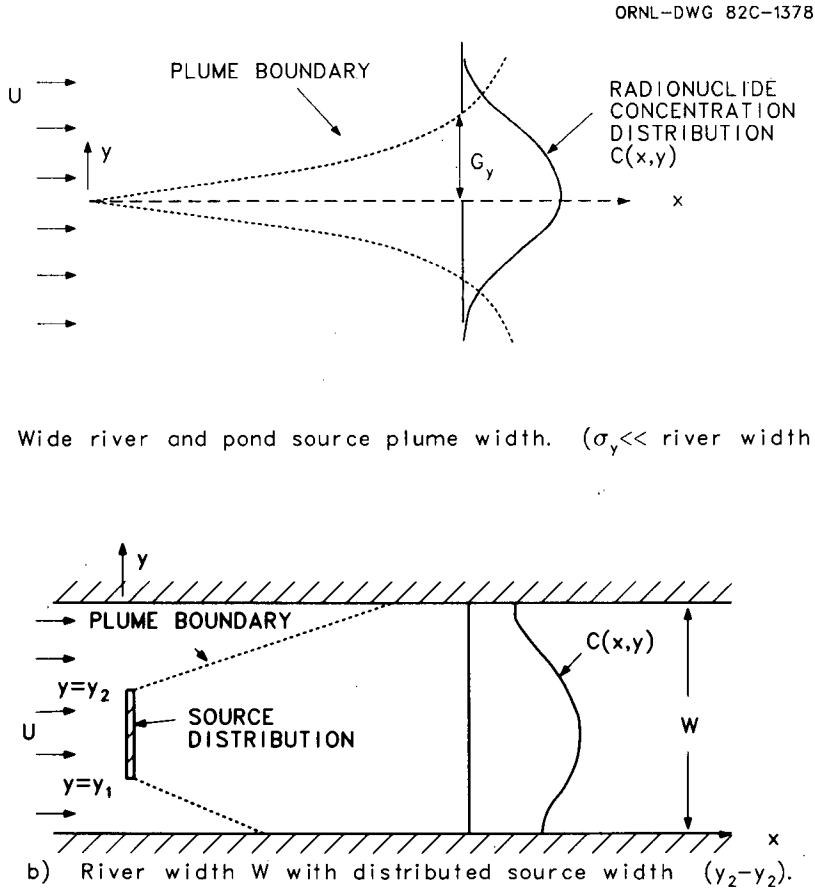

Figure 3.5. Two examples of transverse mixing in river with uniform depth H and velocity U.

a single submerged pipe which causes rapid vertical mixing. As long as the plume width is much less than the total river width, a simple prediction for the two-dimensional radionuclide concentration is

$$C(x,y) = \frac{Q_i C_i}{H\sqrt{4\pi K_y U x}} \exp\left[-\frac{y^2 U}{4K_y x} - \frac{\lambda x}{U}\right], \qquad (3.28)$$

where

C_i = initial concentration,

Q_i = initial effluent flow rate (m^3/s),

x = longitudinal distance (m),

y = lateral distance (m),

λ = radioactive decay (= ln 2/half-life),

K_y = transverse diffusion coefficient (m^2/s).

Note that C_i and Q_i may refer to the variables after the initial mixing process (as determined by any of the models of the previous section). The product C_iQ_i is related to the actual discharge variables C_0, Q_0 as $C_iQ_i = C_0Q_0$ by virtue of mass conservation. The coefficient K_y, which expresses the effect of transverse turbulent diffusion (often with superimposed secondary flow circulations), is generally related to the energy-dissipation characteristics of the channel as

$$K_y = \beta_y u_* H \,, \tag{3.29}$$

where u_* = shear velocity = $\sqrt{gHs}$ and s = channel slope. The coefficient β_y is typically of the order of 0.6 ± 0.3 in reasonably straight rivers (see Fischer et al. 1979). In meandering rivers, β_y can be considerably larger (see Yotsukura and Sayre 1976), and in that case the far-field plume is, of course, no longer straight as sketched in Fig. 3.5 but follows the general curvature of the river. The standard deviation of the lateral Gaussian concentration distribution given by Fig. 3.5a is

$$\sigma_y = \sqrt{2K_y x/U} \,, \tag{3.30}$$

and Eq. 3.28 is applicable only as long as no significant interaction with the river banks exists. Whenever the initial source dimension is significant and/or the plume interacts with the river banks (Fig. 3.5b), the concentration distribution is given by

$$\begin{aligned} C(x,y) = {} & \frac{Q_i C_i}{Q_r} \exp\left[-\frac{\lambda x}{U_a}\right] \\ & \times \left\{1 + 2\sum_{n=1}^{\infty} \exp\left[-\frac{n^2\pi^2 K_y x}{Q_r^2}\right] \frac{2W}{n\pi(y_2 - y_1)} \right. \\ & \left. \times \sin\left[n\pi\frac{(y_2-y_1)}{W}\right] \cos\left[n\pi\frac{(y_1+y_2)}{W}\right] \cos\left[n\pi\frac{y}{W}\right]\right\} . \end{aligned} \tag{3.31}$$

Note that $UHW = Q_r$ is the river flow rate. In practice, only two to three terms of the series given in Eq. 3.31 need to be included as the plume approaches rapidly full mixing across the entire width. The initial source width and location (y_1, y_2) may be given by the location of a diffuser or by the extent of the near field of a surface discharge ($y_1 = 0$ in that case). Similarly, the source variables C_i and Q_i are related to the discharge values by means of a near-field model.

Uniform conditions across the river width have been assumed in Eqs. 3.28 and 3.31. A more nearly accurate approach is to use a coordinate system with the cumulative discharge as the transverse variable in place of y (Yotsukura and Sayre 1976; Fischer et al. 1979). Also, if the radionuclide discharge is part of a cooling-water outfall, additional buoyancy-induced lateral mixing may take place (Paily and Sayre 1978; Schatzmann and Nauduscher 1980).

3.3.1.2 Longitudinal Advection and Dispersion

Once the effluent is laterally mixed, its further transport under steady-state conditions is effected mostly by simple advection by the river flows. If the effluent is rapidly decaying or in highly unsteady conditions (e.g., in the case of an accidental release), it becomes important to also include the mechanism of longitudinal dispersion, that is, a combination of differential shear flow (nonuniform river velocity distribution) and cross-sectional turbulent mixing. The complete concentration expression for a steady-state release is

$$C(x) = \frac{C_0 Q_0}{Q_R \sqrt{1+\alpha}} \exp\left[\frac{xU}{2K_L}(1-\sqrt{1+\alpha})\right], \tag{3.32}$$

where

α = $4\lambda K_L/U^2$,

x = downstream distance from the release point (m),

K_L = longitudinal dispersion coefficient (m^2/s).

Generally, the shear flow effect is so significant that the coefficient K_L is two to three orders of magnitude larger than the transverse coefficient K_y. A useful approximate equation for K_L has been given by Fischer et al. (1979):

$$K_L = 0.011 U^2 W^2/(Hu_*) \ . \tag{3.33}$$

In many practical cases, it is found that $\alpha << 1$ (i.e., advection indeed dominates), and Eq. 3.32 can therefore be approximated simply by the so-called "plug-flow" equation:

$$C(x) = \frac{C_0 Q_0}{Q_R} \exp\left[-\frac{\lambda x}{U}\right] . \tag{3.34}$$

For many radionuclides, the half-life $\tau = \ln 2/\lambda$ is much longer than the travel time x/U in a river stretch. Then, the following obvious expression holds:

$$C(x) = \frac{C_0 Q_0}{Q_R} \quad \text{if } \tau \gg \frac{x}{U} , \tag{3.35}$$

For an instantaneous accidental release of radionuclide mass M_0, the time- and space-dependent concentration distribution is

$$C(x,t) = \frac{M_0}{WH\sqrt{4\pi K_L t}} \exp\left[-\frac{(x-Ut)^2}{4K_L t} - \lambda t\right] . \tag{3.36}$$

Equation 3.36 expresses the downstream motion of a radionuclide pulse at velocity U and its simultaneous longitudinal spread as indicated in Fig. 3.5b. A useful measure of the longitudinal extent of the dispersing pulse is its standard deviation

$$\sigma_L = \sqrt{2K_L t} , \tag{3.37}$$

which grows with the square root of time. Equation 3.36 is a useful first-order model for estimating exposure levels downstream from accidental releases.

Example 3.5. Consider a wide, straight section of a river with $Q = 40$ m/s, $W = 40$ m, $H = 2$ m, and slope $s = 10^{-4}$. A blowdown diffuser 8 m long at the near shoreline discharges 0.2 m^3/s of effluent with a concentration of 1 mCi/m^3 of ^{134}Cs. To determine the concentrations at distances of 0.5, 1, and 5 km, respectively, downstream,

$$u^* = \sqrt{gHs} = \sqrt{9.81 \cdot 2 \cdot 10^{-4}} = 0.044 \text{ m/s} .$$

Assuming $\beta_y = 0.6$, we have

$$K_y = 0.6(0.044)(2) = 0.053 \text{ m}^2/\text{s} .$$

Since the half-life of ^{134}Cs is 2.06 y ($\lambda = 1.07 \times 10^{-8}$ s^{-1}), the effect of decay on the concentration will be negligible. Substituting in Eq. 3.31, we obtain the results shown in the following table.

Concentration (10^{-6} Ci/m^3) as a function of distance across channel

Fraction of distance across channel	Distance downstream (m)		
	500	1000	5000
0	1.82	1.41	0.68
0.1	1.65	1.32	0.67
0.2	1.21	1.10	0.65
0.3	0.72	0.81	0.61
0.4	0.34	0.52	0.56
0.5	0.12	0.30	0.50
0.6	0.03	0.15	0.44
0.7	0.01	0.06	0.39
0.8	0	0.02	0.35
0.9	0	0.01	0.33
1.0	0	0	0.32

Example 3.6. Consider the release of 1 Ci of ^{134}Cs in the river channel of the previous example. Assuming that the release is uniform over the width of the channel, to estimate the distribution of radioactivity 1 h, 6 h, and 1 d, respectively, after release,

$$W = 40 \text{ m and } H = 2 \text{ m}, U = \frac{40}{2 \cdot 40} = 0.5 \text{ m/s} .$$

The longitudinal dispersion coefficient can be estimated from Eq. 3.33:

$$K_L = 0.011 \frac{0.5 \cdot 40^2}{2 \cdot 0.044} = 50 \text{ m}^2/\text{s} .$$

Substituting in Eq. 3.36, we can estimate the radioactivity distribution along the channel. The concentration distribution is shown on Fig. 3.6.

3.3.2 Estuaries

Transport and dispersion processes in estuaries are considerably more complicated than those in nontidal rivers. The oscillatory tidal motion with cyclic variations in velocity and elevation causes complex hydrodynamic conditions, which in turn affect concentration distributions. The difference in density between fresh- and saltwater superimposes additional vertical ("baroclinic") circulations. Finally, wind-driven currents in wide, shallow (baylike) estuaries also play an important role. A detailed analysis of pollutant distributions in an estuary usually requires a thorough field investigation, including tracer studies,

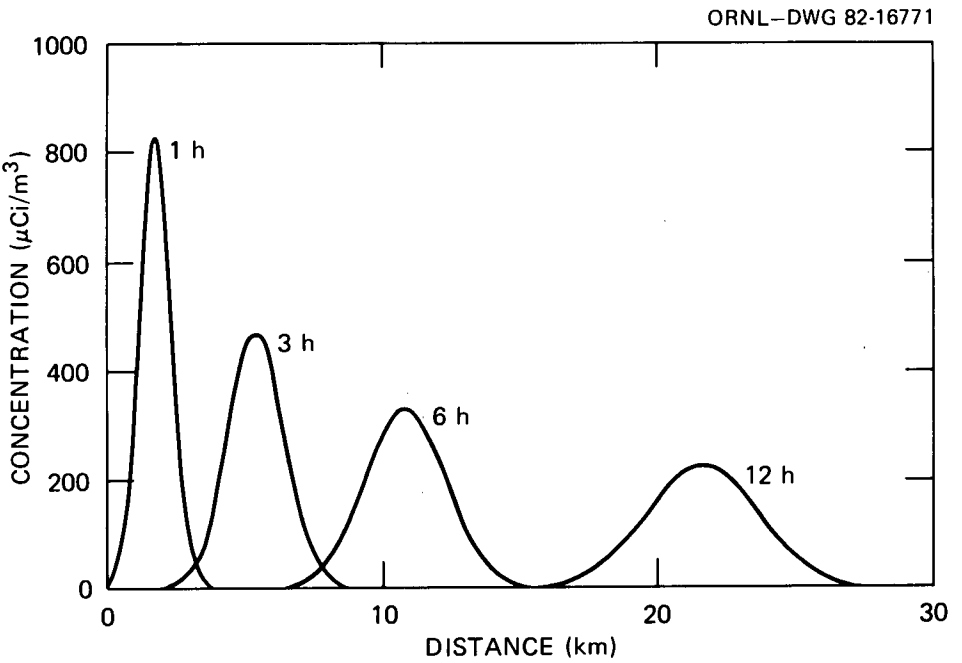

Figure 3.6. Dispersion of the dose release of Example 3.6.

to determine its hydrodynamic and mixing patterns. The information and data thus obtained can be used in the selection and application of reasonably detailed estuary or coastal transport models. Several such models with different degrees of complexity have been developed in recent years (e.g., one-dimensional: Thatcher and Harleman 1973; horizontally two-dimensional: Leendertsee and Liu 1972; Wang and Connor 1975). Still, the application of the models is by no means straightforward, and decisions must be made regarding the value of appropriate dispersion coefficients and specification of boundary conditions, notably at the ocean boundary. For further discussions on these aspects, see Cheng (1976), Jirka et al. (1975), and Fischer et al. (1979).

It must be stressed that, depending on pollutant characteristics, higher dimensional models or very fine temporal resolution may be quite redundant and useless. For example, for steady-state releases of relatively conservative substances (very small λ), the mean residence time, as dictated by the net freshwater flow through the estuary, determines the long-term average concentrations. Since concentration gradients tend to be small, the details of the internal distribution process are then relatively unimportant.

Perhaps the simplest approach to estuary analysis is that of Stommel (1953) for salt concentration. With salt used as a conservative substance that

is distributed along an estuary (distance x), a simple balance between advection and longitudinal dispersion gives

$$U_f S = K_T \frac{dS}{dx} , \tag{3.38}$$

where S is the salt concentration, U_f is the average freshwater velocity (determined by dividing the total freshwater inflow by the cross-sectional area), and K_T the tidal dispersion coefficient that accounts for the numerous possible internal distribution processes above. Equation 3.38 represents the mean balance over a typical tidal cycle. Thus, by measuring the typical average salt conditions in an estuary (limited, of course, to the length of salt intrusion), one can evaluate its mean tidal dispersion coefficient K_T. Typical estimates for K_T range from 50 to 300 m^2/s (see Fischer et al. 1979). Once K_T has been estimated, then the longitudinal distribution $C(x)$ of any other pollutant that is released in a steady-state fashion, at a distance L upstream of the estuary mouth, is given by (Stommel 1953):

$$C(x) = \frac{C_0 Q_0}{Q_R \sqrt{1+\alpha}} \times \frac{\exp\left[\frac{(x-L)U_f}{2K_T}(1-\sqrt{1+\alpha})\right] - \exp\left[\frac{(x-L)U_f}{2K_T}(1+\sqrt{1+\alpha})\right]}{\exp\left[\frac{LU_f}{2K_T}(1-\sqrt{1+\alpha})\right] - \exp\left[\frac{LU_f}{2K_T}(1+\sqrt{1+\alpha})\right]} , \tag{3.39}$$

where Q_R = freshwater (river) flow and $\alpha = 4\lambda K_T / U_f^2$, and the origin of the x-axis is located at the release point, with the x-positive direction downstream. In fact, Eq. 3.39 is a generalization of Eq. 3.32 (for which $L \to \infty$), with the added boundary condition of $C = 0$ at the estuary mouth. Another typical feature of Eq. 3.38 is that significant concentrations are predicted upstream from the discharge point (negative x). This phenomenon is a consequence of the large dispersion coefficient, which in part describes the effect of the oscillatory flow.

3.3.3 Small Lakes and Reservoirs

Small natural or man-made impoundments, cooling ponds in particular, represent an extreme situation of geometric constraints and limited advective transport. The definition of "small" is made here on the basis of the residence time (e.g., throughflow time) relative to the decay time of the radionuclide. The half-life of many radionuclides is considerably longer than impoundment

residence time (typically of the order of a few days to weeks). Hence, except for a small initial mixing region, usually in the form of a buoyant surface jet for cooling ponds, the radionuclide concentration is essentially uniform within the entire impoundment, and a simple bulk analysis suffices for predictive purposes.

Figure 3.7 shows such a system which consists of a water body volume V with a net throughflow q, either natural or in the form of an artificial

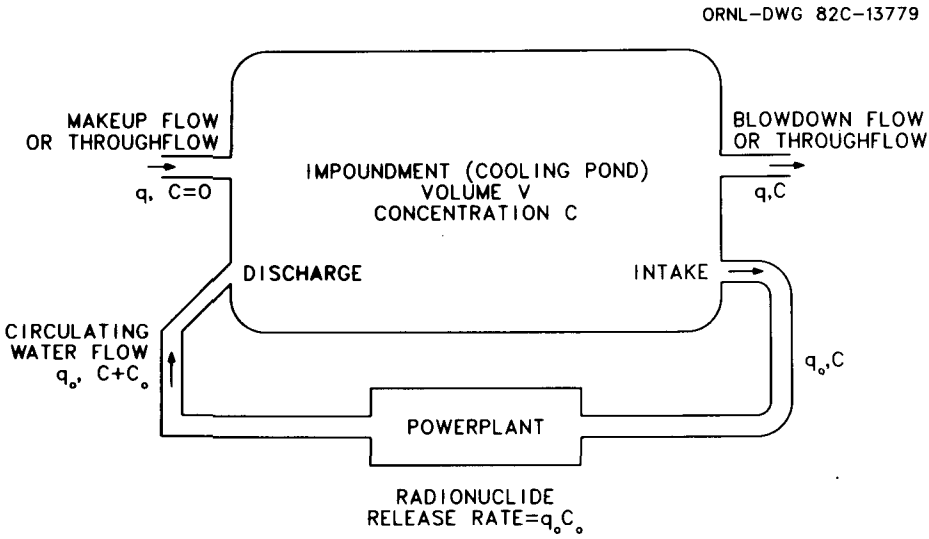

Figure 3.7. Schematics of small impoundment with continuous radionuclide release.

makeup/blowdown scheme, and circulating water flow rate q_0, such as the condenser flow, and a radionuclide release rate q_0C_0. Neglecting any concentration gradients within the impoundment and assuming a uniform concentration C, a radionuclide mass balance gives

$$\frac{dC}{dt} = -\frac{(q+\lambda V)C}{V} + \frac{q_0C_0}{V} . \tag{3.40}$$

Assuming that at time $t = 0$, $C = 0$, the solution of Eq. 3.40 is

$$C = \frac{C_0}{q/q_0+\lambda V/q_0}\left\{1-\exp[(-q/V+\lambda)t]\right\} . \tag{3.41}$$

In studies of releases of radionuclides with half-lives much longer than the impoundment replacement time V/q, it suffices to consider the steady-state solution:

$$C = \frac{C_0}{q/q_0 + \lambda V/q_0} \quad . \tag{3.42}$$

The two controlling parameters in Eq. 3.40 are the flow ratio q/q_0 and the time ratio $\lambda V/q_0$. If the throughflow is limited (i.e., $q/q_0 \rightarrow 0$, and for long decay times, that is, $\lambda V/q_0 \rightarrow 0$), the concentration builds up to large values, which is undesirable. Hence, this simple model stresses the role of strong advective effects in limited water bodies. The basic assumptions in the formulation of the above model are not satisfied if rapid decay takes place (i.e., $\lambda V/q_0 \rightarrow 1$) since significant concentration gradients exist then within the impoundment. In this case, the three-dimensional distribution of the concentration is closely related to the internal flow distribution and thermal structure (stratification) within the impoundment. Work by Ryan and Harleman (1973) and Jirka and Watanabe (1980) has suggested three major types of cooling pond circulation patterns: the deep stratified pond, the shallow dispersive pond, and the shallow recirculating pond. Simple analytical models for these types (Jirka and Watanabe 1980) are readily adapted for steady-state radionuclide circulation. More complex numerical models are needed for unsteady release and/or unsteady hydrologic conditions (Jirka et al. 1978; Octavio et al. 1980). Several simple reservoir models are discussed in Regulatory Guide 1.113 (USNRC 1977).

In the case of small and medium reservoirs which are horizontally homogeneous and where vertical thermal stratification is the primary factor that determines the inflow and outflow dynamics, one-dimensional models such as the MIT model (Octavio et al. 1980) or the model developed by Imberger and his co-workers (Fischer et al. 1980) can be adapted for determining radionuclide distribution.

In reservoirs where the assumption of horizontal homogeneity is not realistic, two- or three-dimensional numerical models can be used to simulate the reservoir hydrodynamics. Once the reservoir circulation has been determined, conservation equations can be solved to determine the distribution of radionuclide releases. A review of numerical hydrodynamic models for reservoirs has been presented by Johnson (1981).

3.3.4 Oceans and Great Lakes

The main feature of pollutant dispersal in oceans or large lakes is their unlimited extent, seemingly without constraints (except for a possible shoreline) on net advection or dispersion. The normal approach to pollution analysis

for such environments is to first determine the velocity field and then compute the dispersion of the release (instantaneous or continuous) which is carried by that velocity field. If small masses with negligible buoyancy are involved, the actual dynamic coupling between those two phases of the analysis can always be neglected. The estimation of the coastal or oceanic velocity field can, in the simplest case, proceed by analysis of existing hydrographic data or through additional field studies (drogue or dye releases, etc.). Alternatively, and involving considerably greater effort, hydrodynamic circulation models which consider the actual coastal geometry and forcing functions (wind, tide, etc.) can be employed to generate the detailed velocity field. It should not be overlooked that the adequacy and accuracy of any such model ultimately hinges on high-quality field data to define reliable boundary conditions (e.g., at the open ocean boundary) and some verification data. Reviews of circulation models for coastal environments or inland seas have been presented by Cheng (1976), Allender (1976), and Simons (1980). The use of multidimensional numerical models may be a quite costly and elaborate task. Some basic factors that must be considered in selecting and using such numerical hydrodynamic models are discussed in Sect. 3.3.5.

Once the advective field has been defined, the dispersion of a radionuclide release can be simply analyzed in a Lagrangian approach by following the moving center of mass of the release (or a series of different masses for continuous releases). The major problem lies, however, in the definition of the diffusive characteristics of the ocean environment. The analysis by means of constant diffusion (or dispersion) coefficients (i.e., the classical Fickian diffusion approach, which is quite applicable to rivers) does not hold for oceanic situations. The reason for this shortcoming is the fact that the diffusing mechanism in a river has a definite maximum length scale (e.g., the size of the largest eddies in the cross-stream direction) while an ocean does not. Oceanic turbulence is generated by a variety of sources (tide, wind, and large-scale eddy breakdown) which can have very large associated length scales. For a concise discussion of oceanic turbulence, see Csanady (1973). Thus, a diffusing mass is subject to larger and larger eddies, which results in an ever increasing diffusion coefficient. A typical approach is to assume that the eddy diffusivity increases as the four-thirds power of the eddy size, the well-known four-thirds law. The most convenient approach therefore is to completely abandon the gradient diffusion concept and use the empirical diffusion diagrams of Okubo (1971). Okubo's diagrams give the growth of the standard deviation of a diffusing patch as a function of time after release, as obtained from a number of experimental sources under different conditions. A best-fit for this data is

$$\sigma_r = 0.011 t^{2.34} , \tag{3.43}$$

where σ_r is the radial standard deviation (in centimeters) and t is the diffusion time (in seconds).

Equation 3.43 is readily applied to two particular radionuclide release situations. In both cases the vertical extent of the water column is given by a value H, which may represent the water depth in a shallow coastal zone or the depth of the mixed layer that is bounded at its lower end by a thermocline-limiting downward diffusion. The concentration distribution for an instantaneous release of a radionuclide mass M_0 is expressed as a function of the radial distance r:

$$C(r) = \frac{M_0}{H\pi\sigma_r^2} \exp\left[-\frac{r^2}{\sigma_r^2}\right] . \tag{3.44}$$

The distribution for a continuous release Q_0C_0 into a steady uniform crossflow (direction x) of magnitude U is:

$$C(x,y) = \frac{Q_0C_0}{2\pi H\sigma_y^2} \exp\left[-\frac{y^2}{2\sigma_y^2}\right] , \tag{3.45}$$

where

$$\sigma_y^2 = \frac{\sigma_r^2}{2} .$$

The longitudinal x position in Eq. 3.45 is implicit, since for each particular σ_y there is an associated time t (Eq. 3.43) and hence $x = Ut$. Generalizations of this Lagrangian approach for continuous releases to unsteady, variable-direction velocity fields have been made in the transient plume model of Adams et al. (1975).

The alternative to the above Lagrangian analysis is the Eulerian approach in the form of a solution of the advection-diffusion equation with a decay term. Analytic solutions to this equation exist for simple velocity fields. A useful simple solution in this category is the steady-state solution for a uniform source of finite extent in steady uniform flow presented by Brooks (1960). Brooks solved the advection-diffusion equation

$$U\frac{\partial C}{\partial x} = \frac{\partial}{\partial y}\left(K_y\frac{\partial C}{\partial y}\right) - \lambda C , \tag{3.46}$$

under different assumptions for the spatial variation of the eddy diffusivity K_y. These solutions are based on the assumption that at the interface of the near

field and far field, the effluent is uniformly distributed over a width b and depth h (Fig. 3.8) and that beyond that point one-dimensional advection and lateral diffusion are the primary transport mechanisms. The solution of Eq.

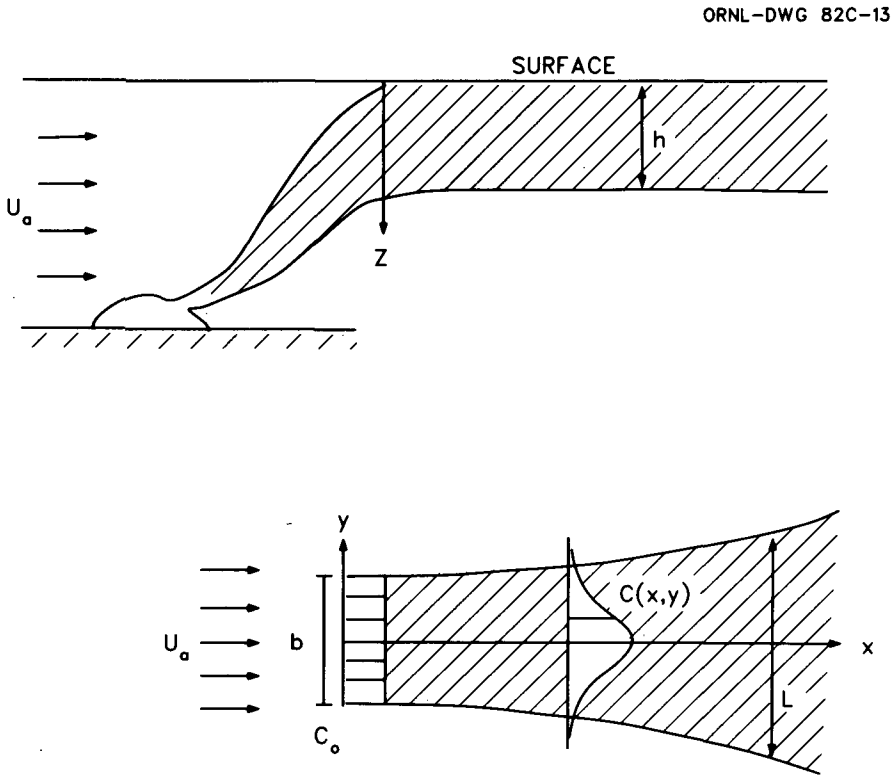

Figure 3.8. Definition sketch for Brooks model.

3.46 for the boundary conditions described in Fig. 3.8 and for constant eddy diffusivity is

$$C = \frac{C_0}{2}\exp\left[-\frac{\lambda x}{HU}\right]\left\{\operatorname{erf}\left[\frac{(y+b/2)}{2}\sqrt{\frac{U}{K_y x}}\right] - \operatorname{erf}\left[\frac{(y-b/2)}{2}\sqrt{\frac{U}{K_y x}}\right]\right\} . \quad (3.47)$$

The solution of Eq. 3.46 under the assumption that the eddy viscosity varies as $K_y = K_{y_0}(L/b)^{4/3}$, where K_{y_0} is the value of the eddy viscosity at $x = 0$, is

$$C = \frac{C_0}{2}\exp\left[-\frac{\lambda x}{HU}\left\{\operatorname{erf}\left[\frac{\left(y+\frac{b}{2}\right)}{2}\sqrt{\frac{1.5}{\left(1+\frac{8K_{y_0}x}{Ub^2}\right)^3-1}}\right]\right.\right.$$
$$\left.\left.-\operatorname{erf}\left[\frac{\left(y-\frac{b}{2}\right)}{2}\sqrt{\frac{1.5}{\left(1+\frac{8K_{y_0}x}{Ub^2}\right)^3-1}}\right]\right\}\right]. \tag{3.48}$$

Another useful simple analytic solution exists for the case of an instantaneous release of a dose M from a vertical line source located at $x = 0$, $y = y_s$ into a large water body of depth H, where the primary transport mechanisms are constant current U and turbulent transport. The solution of the governing equation

$$\frac{\partial C}{\partial t} + U\frac{\partial C}{\partial x} = K_x\frac{\partial^2 C}{\partial x^2} + K_y\frac{\partial^2 C}{\partial y^2} - \lambda C \tag{3.49}$$

is

$$C = \frac{M_0}{4\pi t H\sqrt{K_x K_y}}\exp\left[-\frac{(x-Ut)^2}{4K_x t} - \lambda t\right]$$
$$\times\left\{\exp\left[-\frac{(y-y_s)^2}{4K_y t}\right] + \exp\left[-\frac{(y+y_s)^2}{4K_y t}\right]\right\}, \tag{3.50}$$

where K_x, K_y are dispersion coefficients and t is the time after the release.

3.3.5 Basic Considerations in Numerical Modeling of Aquatic Transport

The development and the growing availability of large computers over the last two decades have created a continuously increasing interest in numerical modeling of pollutant transport and dispersion in natural water bodies. The numerical models developed for this purpose are, in the more general case, numerical solutions of the continuity, heat balance, and momentum equations for the flow and temperature fields and mass balance equations for any other constituents.

In most cases the equations for the flow and the temperature fields can be solved independently of the equations for the other constituents, since they are not practically coupled to them. The obtained velocity field is then used for the solution of the equations for different constituents. All numerical models of this type make use of the Boussinesq approximation; thus, the effect of density variations is significant only in the gravity term of the vertical momentum equation. In flows where vertical accelerations are small, the assumption of hydrostatic pressure distribution can be made, which reduces the number of governing equations, eliminating the vertical momentum equation. Another commonly used simplifying assumption is the rigid-lid approximation in which water surface oscillations are ignored. Explicit simulation of such oscillations imposes severe restrictions on the size of the step used to advance the numerical solution in time, thus increasing substantially the computation cost of the simulation.

Most of the difficulties encountered in the numerical prediction of the flow, temperature field, and pollutant dispersion in large water bodies lie in two general areas—turbulence modeling and the numerical scheme used for solving the equations.

Turbulence modeling is today an active field of research. Despite the intense research efforts in recent years, there are no universally applicable turbulence models yet. Therefore, any turbulence model should be used with special care, and considerable judgment should be applied to determine whether the explicit or implicit assumptions made for the derivation of the model are applicable in the case under consideration. A discussion of available turbulence models is beyond the scope of this chapter. The reader can find a concise but comprehensive review of turbulence models and their application to hydraulics in Rodi (1980). An excellent collection of state-of-the-art papers on turbulence modeling with emphasis on the comparison between computation and experiment can be found in the proceedings of the 1980–81 AFOSR-HTTM Stanford Conference on Complex Turbulence Flows.

Numerical models used for the solution of the hydrodynamic equations are usually classified as finite-difference (FD) or finite-element (FE) models, according to the method used for the spatial approximation of the field variables. FD models have a longer history, and there are more well-documented FD than FE codes available for hydrodynamic simulations. However, the FE method enjoys a growing popularity, because it offers the flexibility to perform simulations in flow regimes of any geometrical shape, makes the treatment of boundary conditions easy, and allows the modeler to focus the analysis on areas of interest by making the FE net denser in these areas. The major drawback of the FE method is that, in most formulations, it involves the solution of large sparse linear systems, which may impose substantial computer time and storage requirements. The development of more efficient algorithms for the solution of sparse linear systems and the advancement of collocation

methods will definitely enhance the potential of the FE method in multidimensional hydrodynamic simulations. The available literature on both methods is extensive. Reviews of several FD schemes can be found in Roache (1972), Policastro and Dunn (1976), and Noye (1976). Reviews of the available experience from the use of the FE method in hydrodynamic simulations can be found in Cheng (1978) and Zienkiewicz (1978).

The selection of the proper FD scheme or the proper order and type of elements in the FE approach must be the subject of careful consideration. Special care must also be given in the selection of the time-stepping scheme. It is important to know the effect of the numerical scheme on the amplitude and phase speed of the solution. Discussions on amplitude and phase errors in FD solutions can be found in Abbott (1981) and in FE solutions in Gray and Pinder (1978). Another important aspect of the selection of a numerical scheme for hydrodynamic and transport computations is its ability to handle cases where the convective terms in the governing equations play a dominant role. Several special FD schemes are available for convection-dominated flows. A critical discussion of some of these schemes, which usually are called "upwind" schemes, can be found in Leonard (1981). The search for a satisfactory treatment of convection-dominated flows with FE algorithms led to the development of the Petrov-Galerkin formulation (Brooks and Hughes 1982). A collection of papers on this subject can be found in the proceedings of the Conference on FE Solutions for Convection-Dominated Flows (Hughes 1979).

3.3.6 Effect of Radionuclide Volatilization

As noted in Chapter 1, some of the radionuclides in the liquid waste stream may be in the form of volatilizing liquids or in dissolved gas form. In any case, upon release the liquid wastes encounter pressure changes with essentially atmospheric pressure conditions in the environment. The gaseous phase of a radionuclide then tends to escape to the atmosphere via the air-water interface. If the radionuclide is uniformly mixed over the water column H, as has been assumed in all preceding models, this escape mechanism can be represented by a single term

$$\left[\frac{dC}{dt}\right]_e = K(C - C_s) \ , \tag{3.51}$$

where C is the vertically uniform radionuclide gas concentration and C_s its saturation value. C_s is governed by Henry's law in equilibrium with the partial pressure of that gas in the surrounding atmosphere (usually, $C_s = 0$ for radionuclides). K is a depth average loss coefficient that is related to the actual surface transfer coefficient K_L by $K = K_L/H$.

Useful estimates for K can be obtained from the related problem of oxygen exchange, although there is some uncertainty as to how molecular differences between different gases affect the transfer processes. The equation by Tsivogliu and Wallace (1972),

$$K = 1420Us \ (\mathrm{d}^{-1}) \ , \tag{3.52}$$

where U is the velocity in meters per second and s is the slope, has been found to give good predictions for riverine situations (Rathbun 1977). For oceanic conditions, experimental work by Peng et al. (1979) suggests K_L values between 1 and 4 m/d. The corresponding K would then depend on the water column depth H. The additional effect of the escape term $(dC/dt)_e$ given by Eq. 3.51 is readily included in the earlier predictive equations (Eqs. 3.28, 3.31, 3.32, 3.34, 3.36, 3.39, 3.42, 3.44, and 3.45) by substituting a modified decay rate $\lambda_K = \lambda + K$ in place of the usual λ. In particular cases, the rate of surface transfer K may overshadow that of direct decay. The qualitatively similar and usually much more important effect of transfer between the sediment-water interface is treated in the following section.

3.4 SEDIMENT EFFECTS

Radionuclide transport in surface water is controlled by various mechanisms, as indicated in Table 3.1. Some of these mechanisms are due to sediment-radionuclide interactions. The transport of radionuclides in surface waters may stop permanently or slow down temporarily if the radionuclides are adsorbed from solution onto sediments. Both suspended and bed sediments adsorb radionuclides, but suspended sediment usually adsorbs more radionuclides than does bed sediment per unit weight of sediment. When adsorption occurs, the water body's concentration of dissolved radionuclides is lowered, and the radionuclides may become less available to aquatic biota and man. This nonavailability may be reversed, however, as it is possible for radionuclides that have accumulated in the bed to be desorbed or become resuspended with sediment, thus forming a long-term source of pollution.

Models that do not include sediment-radionuclide interactions predict that radionuclides will be removed from surface waters at the same rate at which water is exchanged. In reality, sorption effects cause some radionuclides to be flushed out more slowly, usually at the approximate rate at which sediment is exchanged in the water system (USNRC 1978; USEPA 1978). The following examples illustrate the important role that sediments play in radionuclide migration.

1. Field measurements obtained from the Clinch River near Oak Ridge National Laboratory in Tennessee in the early 1960s indicated that approximately 90% of ^{137}Cs released was adsorbed by the river's

suspended sediment within a 10-mile reach downstream of the effluent discharge (Churchill et al. 1965).

2. Data from the Irish Sea near the Windscale Nuclear Fuel Reprocessing Plant show that 95% of the plutonium and 20% of the cesium discharged to the Irish Sea from the plant have been adsorbed onto marine sediment and have remained in the Irish Sea (Hetherington 1976). (The remaining percentages of plutonium and cesium are in the dissolved form and for all practical purposes are eliminated from the sea by dilution.) The presence of ^{239}Pu and ^{137}Cs in core samples taken from the Windscale vicinity caused Hetherington to conclude that migrating radionuclides attach themselves to suspended sediments and eventually settle to the ocean floor.

Clearly, neglecting the possibility of sediment-radionuclide interactions precludes an accurate prediction of radionuclide distributions in time and space for many cases.

Most transport models fail to account for radionuclide adsorption/desorption mechanisms; transport, deposition, and resuspension of radionuclides sorbed by sediments; and radionuclide accumulation in bed sediment. These models are best suited to cases where the radionuclides in question are not easily adsorbed by sediment (i.e., the radionuclides have small distribution coefficients) and sediment concentrations in a receiving water body are low. However, in cases where radionuclides have a high affinity to sediments (i.e., the radionuclides have large distribution coefficients) and sediment concentrations in a receiving water body are high, or the long-term migration and accumulation of radionuclides in bed sediment are probable, the sediment-radionuclide interactions must be included in the analysis.

3.4.1 Adsorption/Desorption Mechanisms

Radionuclide adsorption/desorption mechanisms include ion exchange, precipitation-mineral formation, complexation-hydrolysis, oxidation-reduction, and colloid and polymer formulation. The extent to which a radionuclide is adsorbed is commonly measured by its equilibrium distribution coefficient, or K_d. Confusion about the use of the K_d concept is common, because the term means different things to different people. Chemists use it only when certain rigorous assumptions are met. Engineers, on the other hand, use K_d in a broader sense, such that

$$K_d = \frac{\text{amount of radionuclide sorbed on sediment}}{\text{amount of radionuclide left in solution}}$$

The K_d value for each radionuclide depends on various parameters, including radionuclide state and concentration, sediment type and concentration, the flow characteristics and water quality of a receiving surface water

body, and contact time. A detailed description of radionuclide adsorption/desorption mechanisms is presented in Onishi et al. (1981).

Although it is impossible to generalize and establish one K_d value for each radionuclide, most radionuclide transport models require that this be done. To satisfy this need, Onishi et al. (1981) prepared a range of K_d values (Table 3.2) from documents they reviewed. Freshwater and marine environments were separated in this table to show the importance of cation competition for those nuclides which adsorb by ion exchange reactions. Also, marine environments have a very narrow pH range around the mean value of pH 8.1. For elements that are adsorbed by hydrolysis and colloidal polymer precipitation, K_d values in seawater are often larger than those in freshwater. The latter has a wider pH range and less tendency to promote coagulation.

Table 3.2 gives the reader some idea of the magnitude of K_d values. Median K_d values vary plus or minus an order of magnitude for those values greater than 10^2.

The simplest and crudest approach to obtain concentrations of radionuclides with some effects of radionuclide adsorption/desorption is to first use the methods discussed in Sects. 3.2 and 3.3 to estimate dissolved radionuclide concentrations. The corresponding concentrations of particulate radionuclides (those adsorbed by sediment) can then be obtained by multiplying the dissolved radionuclide concentrations by distribution coefficients. However, strictly speaking, the radioactivity of the total radionuclide (sum of dissolved and particulate radionuclides) will not be conserved in this approach. The next approach is to use the simple methods discussed in Sects. 3.4.2 through 3.4.5 below.

If the solutions obtained by these simple methods reveal that a radionuclide release may possibly lead to adverse impacts on environment and man, more sophisticated numerical models with more complete sediment-radionuclide interactions (e.g., adsorption/desorption; and transport, deposition, and resuspension of contaminated sediment) must be used. These numerical models include TODAM (Onishi et al. 1982a) and CHNSED (Field 1976) for one-dimensional models; SERATRA (Onishi et al. 1976, 1982c) and FETRA (Onishi et al. 1976; Onishi 1981) for two-dimensional models; and FLESCOT (Onishi and Trent 1982) for a three-dimensional model. Among these models, SERATRA has been most extensively applied, including the model testing application to Cattaraugus and Buttermilk Creeks in New York (Onishi et al. 1982d). Table 3.3 lists existing models developed mainly for the simulation of radionuclide transport in surface waters [adapted from Onishi et al. (1981)].

3.4.2 Rivers

With few exceptions, the models that account for sediment-radionuclide interactions were developed for rivers. Descriptions of two simple models follow.

Table 3.2. Gross average K_d (mL/g) for selected radionuclides with emphasis on oxidizing conditions (Onishi et al. 1981)

Elements	Freshwater		Saline water	
	Range	Median	Range	Median
Am	85–40,000	5×10^3	97–650,000	10^4
Ce	7,800–140,000	10^4	9,700–10^7	5×10^4
Cr[a]	0–10^3	Low	0–10^3	Low
Cs	50–8×10^4	10^3	17–10^4	3×10^2
Co	1,000–71,000	5×10^3	7,000–300,000	10^4
Cm	100–70,000	5×10^3		
Eu	200–800	5×10^2	5,000–130,000	10^4
Fe[a]	10^3–10^4	5×10^3	20,000–450,000	5×10^4
I	0–75	10	0–100	10
Mn[a]	10^2–10^4	10^3	10^2–10^4	10^3
Np[a]	0.2–127			
P[a]		High		High
Pu	10^2–10^7	10^5	10^2–10^5	5×10^4
Pm	10^3–10^4	5×10^3	10^3–10^5	10^4
Ra	10^2–10^3	5×10^2	10^1–10^3	10^2
Ru	Complicated chemistry (multiple species)	Variable	Complicated chemistry (multiple species)	Variable
Sr	8–4,000	1,000	6–400	50
Tc[a]	0–10^2	5	0	0
Th	10^3–10^6	10^4	10^4–10^5	5×10^4
^{3}H	0	0	0	0
U[a]	16			
Zn	10^2–10^3	5×10^2	10^3–10^4	5×10^3
Zr	10^3–10^4	10^3	10^3–10^5	10^4

[a]Highly dependent on oxidation-reduction conditions.

Fletcher and Dotson Model (1971). The model developed by Fletcher and Dotson (1971) is one of the first models to compute the radionuclide dose to man through liquid and gaseous pathways. The model uses an unsteady, one-dimensional, liquid-pathway submodel to calculate temporal and longitudinal distributions of dissolved radionuclide concentration as well as the concentration of radionuclides attached to suspended and bottom sediments of various sizes. The dissolved radionuclide concentration at a given location is found by applying the mass conservation equation with radioactive decay as follows:

$$C_{x,t} = \frac{1}{Q_{x,t}}\left[Q_{(x-\Delta x,t-\Delta t)}C_{(x-\Delta x,t-\Delta t)}e^{-\lambda\Delta t} + \sum_1^n Q_i C_i\right], \quad (3.53)$$

Table 3.3. Summary of radionuclide-transport models (adapted from Onishi et al. 1981)

Author and/or model	Transport modeled			Mechanisms				Hydrodynamics simulation	None or compartment	Dimensionality			Time dependence		Solution technique		Water body[c]	Field application
	Dissolved radionuclides	Particulate[a] radionuclides	Sediment	Advection	Diffusion/ dispersion	Adsorption	Radioactive decay			1D	2D	3D	Steady state	Dynamic	Analytical	Numerical[b]		
Fletcher and Dotson 1971	X	X	X	X			X			X				X		FD	R,L	
Bramati et al. 1973	X	S		X		X				X			X		X		R,L	X
Soldat et al. 1974	X	S		X		X	X			X			X			FD	C,E,R,L	X
Watts 1976	X	S		X		X				X			X		X		R	X
Martin et al. 1976	X			X		X				X				X		FD	R,L	X
Buckner and Hayes 1976	X	X		X	X	X	X			X				X		FD	R	X
Shih and Gloyna 1976	X	B		X	X	X				X				X	X		R	
Armstrong and Gloyna 1968	X	B		X	X	X				X				X		FD	R	
White and Gloyna 1969	X	B		X	X	X				X				X		FD	R	
Shull and Gloyna 1968	X	X		X		X				X			X		X		R	
Onishi et al. 1976, 1977, 1978, 1979, 1981, 1982																		
FETRA	X	X	X	X	X	X	X				X		X	X		FE	C,E,R	X
SERATRA	X	X	X	X	X	X	X				X			X		FE	R,L	X
TODAM	X	X	X	X	X	X	X			X				X		FE	R,E	X
FLESCOT	X	X	X	X	X	X	X	X				X		X		FD	R,E,C,L	X
Fields 1976 (CHNSED)	X	X	X	X		X				X				X		FD	R	
Chapman 1977		X		X	X	X	X			X				X		FD	R	
Smith et al. 1977	X	X		X	X	X	X		X				X			FD	RL	X
Vanderploeg et al. 1976	X	X				X	X		X					X	X		L	X
Booth 1976	X	X				X	X		X					X	X		L	
Falco, Onishi, and Arnold	X	X		X		X	X			X				X	X		R	
Churchill, 1976	X	X		X		X	X			X	X			X		FD	E	X
Eraslan et al. 1977																		
RADONE	X			X	X					X				X		I	E,R	
RADTWO	X			X	X						X			X		I	C,E,L	
HOTSED		X	X			X		X		X				X		I	E,R	
O'Connor and Farley, 1978	X	X		X		X	X	X			X		X			FD	E	X
Ditoro et al. 1981	X	X	X	X	X	X	X		X					X		FD	R,E,L	X
USNRC River Model, 1978	X	X		X		X	X			X			X		X		R	X
USNRC Lake Model, 1978	X	X		X		X	X		X				X		X		L	X
USNRC Estuarine Model, 1978	X	X		X	X	X	X			X				X	X		E	X

[a] S = for shore sediment only, B = for bed sediment only.
[b] *FD = finite difference, FE = finite element, I = integration.*
[c] C = coastal system and Great Lakes, E = estuarine systems, R = river systems, L = lakes and impoundments.

where

$C_{x,t}$ = dissolved radionuclide concentration at location x and time t,

C_i = dissolved radionuclide concentration in tributary,

$Q_{x,t}$ = flow rate at location x and time t,

Q_i = tributary flow rate,

λ = radionuclide decay.

The sediment transport rate S_T is found analytically from the following equation:

$$S_T = aQ^b \ , \tag{3.54}$$

where Q is the flow rate and a and b are constants that must be estimated for each sediment size range. The concentration of radionuclides attached to sediment (C_p) is calculated from the known dissolved radionuclide concentration and the distribution coefficient (K_d) by

$$C_{Px,t} = K_d C_{x,t} \ . \tag{3.55}$$

The Fletcher and Dotson model is one of the simplest models for calculating dissolved and sorbed radionuclide concentrations. However, because the amount of radionuclide adsorbed on the sediment is not subtracted from the dissolved concentration, strictly speaking, the mass conservation in a stream reach is not satisfied. Thus, the model should not be used when a significant amount of radionuclides is adsorbed by sediments.

Example 3.7. Let us assume that a nuclear facility is discharging at 10 m^3/s, a radioactive effluent containing 2 pCi/L of ^{137}Cs into a river whose rate of flow is 500 m^3/s. Assume that the river velocity is 0.5 m/s and that k_d = 500 mL/g. What are the dissolved and particulate radionuclide concentrations 100 km downstream from the nuclear facility? Assume that no tributary exists, that is, $Q_i = 0$. Since the half-life of ^{137}Cs is 30.2 y,

$$\lambda = \frac{\ln 2}{30.2 \cdot 60 \cdot 60 \cdot 24 \cdot 365} = 7.28 \cdot 10^{-10} \ .$$

The travel time Δt is

$$\Delta t = \frac{100 \cdot 1000}{0.5} = 200{,}000 \text{ s} \ .$$

Hence, the dissolved ^{137}Cs concentration 100 km downstream is calculated by Eq. 3.53 as

$$C = \frac{1}{500 + 10}\,(10 \cdot 2e^{-7.28 \cdot 10^{-10} \cdot 200{,}000} + 0)$$

$$= 0.03921 \text{ pCi/L} .$$

Since $K_d = 500$ mL/g, the particulate ^{137}Cs concentration is calculated by Eq. 3.55 as

$$C_p = (500/1000) \cdot 0.03921$$

$$= 0.01961 \text{ pCi/g} .$$

Assuming that $a = 0.0004$ and $b = 3$, the sediment transport rate S_T in Eq. 3.54 becomes

$$S_T = 0.0004 \cdot (500 + 10)^3 = 53{,}060 \text{ g/s} .$$

Hence, if we assume that all of the particulate ^{137}Cs is transported by sediment, the sediment carries

$$S_T \cdot C_p = 53{,}060 \cdot 0.01961 = 1041 \text{ pCi/s} ,$$

and the rate of dissolved ^{137}Cs is

$$C \cdot Q = 0.03921 \cdot 1000 \cdot (500 + 10) = 19{,}997 \text{ pCi/s} .$$

The total amount of ^{137}Cs being transported is the sum of dissolved and particulate ^{137}Cs:

$$19{,}997 + 1041 = 21{,}038 \text{ pCi/s} .$$

Since the release rate is

$$2 \cdot 1000 \cdot 10 = 20{,}000 \text{ pCi/s}$$

and the decay rate is over 200,000 s, the total ^{137}Cs should be

$$20{,}000 \cdot e^{-\lambda t} = 20{,}000 \cdot e^{-7.28 \cdot 10^{-10} \cdot 200{,}000}$$

$$= 19{,}997 \text{ pCi/s} .$$

Computed dissolved and particulate ^{137}Cs concentrations may be adjusted to maintain the mass balance. Hence, these concentrations are finally estimated as

$$C = 0.03921 \cdot \frac{19{,}997}{21{,}038} = 0.03727 \text{ pCi/L}$$

$$C_p = 0.01961 \cdot \frac{19{,}997}{21{,}038} = 0.01864 \text{ pCi/g} .$$

Onishi et al. (1981) Mixing-Tank Model with Sediment Transport. A mixing-tank transport model, similar to one used for simulating pesticide transport in streams (Onishi et al. 1980b), is described below (also see Fig. 3.9). The following assumptions are made:

1. River reaches are divided into segments and are represented by a series of tanks. Within each segment (or a tank) sediments and radionuclide concentrations are completely mixed.
2. Radionuclide and sediment contributions from point and nonpoint sources are treated as lateral influx that is uniformly distributed along the river reach for each segment.
3. Dissolved and particulate radionuclides are linearly related by a distribution coefficient.
4. Dissolved and particulate radionuclides reach their equilibrium conditions within one time step.
5. Particulate radionuclide deposition to the riverbed and resuspension from the bed do not occur.

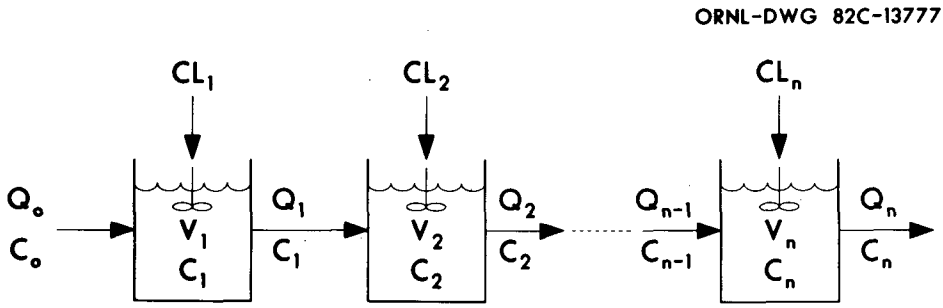

Figure 3.9. Mixing-tank model.

The mass conservation of sediment in the nth tank leads to the following sediment transport equation:

$$\frac{\partial S_n}{\partial t} = -S_n\left[\frac{1}{V}\left(\frac{\partial V}{\partial t}+Q\right)\right]_n + \frac{Q_{n-1}S_{n-1}+SL_n}{V_n}, \qquad (3.56)$$

where

Q_n = flow discharge from nth tank,

S_n = sediment concentration in the nth tank,

SL_n = lateral influx of sediment,

V_n = water volume of the nth tank,

t = time.

The mass balance of the dissolved and particulate radionuclides in the nth tank is

$$\frac{\partial C_n}{\partial t} = \frac{1}{V_n(1+S_nK_d)}\Big[(1+S_{n-1}K_d)Q_{n-1}C_{n-1}+(CL_n+C_pL_n) - (1+S_nK_d)Q_nC_n-\lambda V_nC_n(1+S_nK_d) - C_n\frac{\partial}{\partial t}\{V_n(1+S_nK_d)\}\Big], \tag{3.57}$$

$$C_{Pn} = K_dC_n, \tag{3.58}$$

where

C_n = dissolved radionuclide concentration in the nth tank,

C_{Pn} = particulate radionuclide concentration in the nth tank,

CL_n = lateral influx of dissolved radionuclide,

C_PL_n = lateral influx of particulate radionuclide,

K_d = distribution coefficient of radionuclide.

By substituting Eq. 3.58 for Eq. 3.57, Eqs. 3.56 and 3.57 are then solved to obtain the sediment and dissolved radionuclide concentrations, S_n, C_n, in the nth tank. In general, Eqs. 3.56 and 3.57 must be solved numerically, as was done in Onishi et al. (1980b). However, for the following simplified case, an analytical solution, which is similar to that obtained in USNRC (1978) for a dissolved-only radionuclide case, can be obtained:

$C_o = 0$

$CL_n = 0$ for all n

$S_n = S_{n-1} = \cdots = S_i =$ constant for time and all n .

Q_n, V_n are not functions of time for all n. The radionuclide release into the first segment during the duration of Δt is

$$M_1 = (CL_1 + C_pL_1)\,\Delta t \quad .$$

Hence, for an instantaneous release of M_1 (let's say in curies), the concentration of dissolved radionuclides in the nth river reach (or tank) is

$$C_n = \frac{\dfrac{M_1}{1+S_nK_d}\prod_{i=1}^{n-1} Q_i}{\prod_{i=1}^{n} V_i}\left[\sum_{j=1}^{n}\frac{(-R_j)\exp(-R_jt)}{\prod_{\substack{k=1\\k\neq j}}^{n+1}(R_k-R_j)}\right], \tag{3.59}$$

where

$$R_j = \frac{Q_j}{V_j} + \lambda\,,$$

$$R_{n+1} = 0\,.$$

A particulate radionuclide concentration is then obtained by Eq. 3.58. The total radionuclide concentration CT_n is then calculated by

$$CT_n = C_n + S_nC_{Pn}\,. \tag{3.60}$$

The models discussed above are some of the simple ones that take into account some of the sediment-radionuclide interactions. An estuarine model discussed in the following section (Sect. 3.4.3) may also be applied to river systems. If the sediment-radionuclide interactions must be included more completely, more sophisticated models such as CHNSED (Field 1976), SERATRA (Onishi et al. 1980a), or TODAM (Onishi et al. 1982a) must be used.

3.4.3 Estuaries

Two major characteristics of the estuarine environment are reversible tidal flow and salinity. Estuaries have substantially faster flowing water during part of the tidal cycle than their tidally averaged flow would indicate, yet their downstream net transport is relatively small. This type of flow behavior allows for resuspension and subsequent redeposition of some fine sediment during each tidal cycle. As such, sediment and water are in more intimate contact in an estuary than in a reservoir or lake. Salinity is also an important factor in any analysis, because salinity causes sediment flocculation at certain levels and also affects adsorption/desorption mechanisms. It is difficult to select a single K_d value for a study area because of these factors (Wrenn et al. 1972, Onishi and Trent 1982, Schell and Siblay 1982).

None of the simple radionuclide-transport models can simulate reversible tidal flow and salinity impact. However, if the tidal flow is averaged over several tidal cycles, most of the models discussed in Sect. 3.4.2 may be applicable to estuaries. The following model developed by Codell at the U.S. Nuclear Regulatory Commission is useful for understanding the migration and fate of radionuclides in estuaries and rivers. The model accounts for sediment-migration velocities and tidally averaged flow velocities.

NRC Estuaries Model with Sedimentation (USNRC 1978). As illustrated in Fig. 3.10, a water layer of thickness d_1 is in contact with a movable sedi-

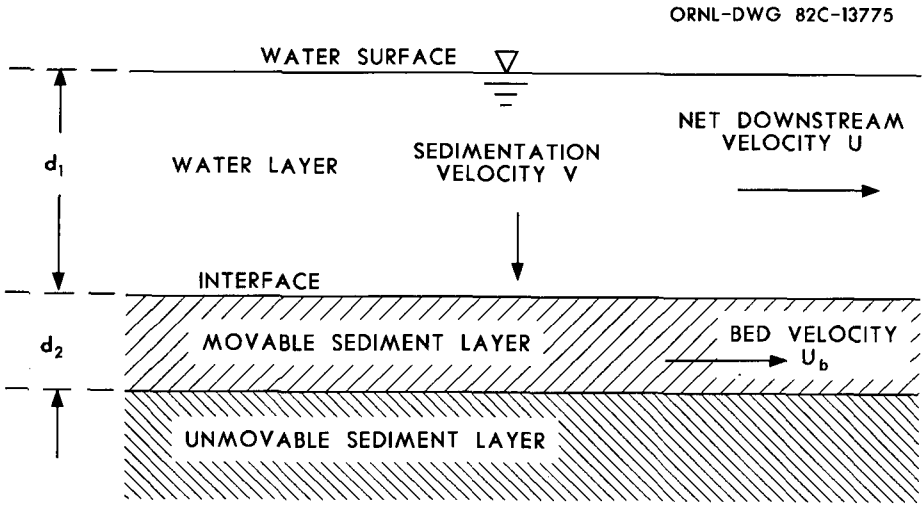

Figure 3.10. NRC estuarine model.

ment layer of thickness d_2. The water layer is moving with a net tidally averaged downstream velocity of U, and the erodible bed is moving with a net downstream velocity, U_b. Diffusive transport from tidal oscillations in the water and sediment layers is assumed to be constant with the longitudinal dispersion coefficients, D_{dx} and D_{xb}, respectively. Sedimentation and burial occur uniformly at vertical velocity v. As before, it is assumed that dissolved and particulate radionuclides are in equilibrium and are related by Eq. 3.58.

The differential equation describing the radionuclide concentration in the water phase becomes

$$\frac{\partial C}{\partial t} + U' \frac{\partial C}{\partial x} = E'_L \frac{\partial^2 C}{\partial x^2} - \lambda' C \ , \tag{3.61}$$

where

$$U' = \frac{fU + (1-f)U_b K_d}{f + (1-f)K_d} ,$$

$$E_L' = \frac{fD_{dx} + (1-f)D_{xb}K_d}{f + (1-f)K_d} ,$$

$$f = \frac{d_1}{d_1 + d_2} , \quad (1-f) = \frac{d_2}{d_1 + d_2} .$$

The solution to Eq. 3.61 for an instantaneous release of M_1 Ci at $x = 0$ is

$$C = \frac{M_1}{aA\sqrt{4\pi E_L' t}} \exp - \left[\frac{(x - U't)^2}{4E_L' t} + \lambda' t \right] \tag{3.62}$$

where

a = $f + (1-f)K_d$,
A = cross-sectional area of an estuary,

$$\lambda' = \lambda + \frac{K_d \frac{v}{d_2} (1-f)}{f + (1-f)k_d} .$$

If a more complete analysis of radionuclide migration and accumulation is required, a more detailed model such as FLESCOT (Onishi and Trent 1982) is needed. FLESCOT has been applied to the Hudson River estuary to predict three-dimensional distributions of a radionuclide as well as distributions of tidal flow, salinity, and sediments, given the effects of tidal flow and salinity on distribution coefficients. Other models such as the one-dimensional TODAM (Onishi et al. 1982a) and the two-dimensional FETRA (Onishi 1981) are also applicable to estuaries if more than simple analytical solutions are required.

3.4.4 Coastal Waters and Oceans

In general, sediment effects on radionuclide transport in coastal waters and oceans are less important than in other surface waters, because both sediment concentrations and the distribution coefficients tend to be smaller. In some cases (e.g., the Irish Sea), however, the sediment effects become extremely significant (Hetherington 1976).

Since models must be at least two-dimensional to predict radionuclide distributions in coastal waters and oceans, all of the one-dimensional models

described in Sects. 3.4.1 and 3.4.2 are not applicable. However, the two- and three-dimensional models and analytical solutions discussed in Sects. 3.2 and 3.3, together with Eq. 3.55, may be used to estimate dissolved and particulate radionuclides if all particulate radionuclides are being suspended (see Example 3.7 in Sect. 3.4.2).

Numerical models such as FLESCOT (Onishi and Trent 1982) and FETRA (Onishi 1981) are available for oceans and coastal waters, respectively. For example, FETRA (Onishi et al. 1982b, Onishi and Thompson 1982) has been applied to the Pacific Coast and Irish Sea to simulate radionuclide migrations affected by coastal currents and wave-suspended sediments.

3.4.5 Lakes

Unique processes are responsible for the distribution and movement of radonuclides in lakes. Basically, water flow is slower in lakes because they are relatively deep and confined. The major processes affecting radionuclide movement are (1) flow conditions, (2) stratification and seasonal turnover, (3) sediment interaction, and (4) biotic interaction.

Because lakes have small flow velocities, sediments introduced into them tend to fall directly to the lake bottom. During this process, the sediment may adsorb radionuclides and carry them to the lake bottom. In the absence of sediment movement, radionuclides are either adsorbed or desorbed from the bed sediment. The two lake models presented below are relatively simple.

NRC Lake Model (USNRC 1978). A two-layer lake model has been developed by Codell at the Nuclear Regulatory Commission (Fig. 3.11). As shown in Fig. 3.11, this unsteady model divides a lake into water and bed-sediment compartments through which radionuclides are exchanged by direct adsorption/desorption mechanisms and sediment deposition. The following assumptions were made for the model:

- Water inflow and outflow are constant.
- Sedimentation rate is constant.
- The thickness of the sediment layer remains constant. (If sedimentation occurs, it is assumed that the affected portion of the original bed layer becomes inactive, and it is eliminated from the analysis.)
- Dissolved and particulate radionuclides are in equilibrium.
- Both dissolved and particulate radionuclides undergo decay.

In this model, mass balance equations for dissolved and particulate radionuclides are

$$\frac{dC}{dt} = \frac{W(t)}{V} + C_p\lambda_1 - C\lambda_2 , \tag{3.63}$$

$$\frac{dC_p}{dt} = C\lambda_3 - C_p\lambda_4 , \tag{3.64}$$

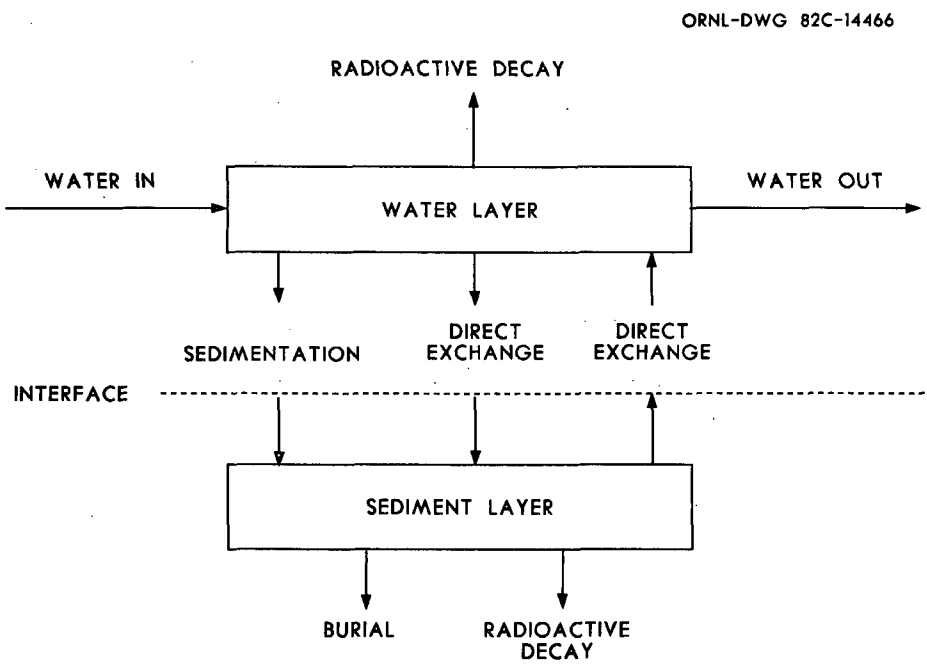

Figure 3.11. NRC two-layer lake model.

where

V = lake volume (m^3),

$W(t)$ = input rate of radioactive material (Ci/year).

$$\lambda_1 = \frac{K_f}{d_1 K_d}, \tag{3.65}$$

$$\lambda_2 = \frac{q}{V} + \lambda + \frac{vK_d}{d_1} + \frac{K_f}{d_1}, \tag{3.66}$$

$$\lambda_3 = \frac{vK_d}{d_2} + \frac{K_f}{d_2}, \tag{3.67}$$

$$\lambda_4 = \lambda + \frac{v}{d_2} + \frac{K_f}{d_2 K_d}, \tag{3.68}$$

where

d_1 = depth of water layer,

d_2 = depth of sediment layer,

K_f = coefficient of direct radionuclide transfer (m/year),

q = freshwater flow rate (m^3/year),

v = sedimentation velocity (m/year),

λ = radionuclide decay rate (1/year).

For an instantaneous release of M_1 Ci, the water-phase concentration can be solved from Eqs. 3.63 and 3.64:

$$C_i = \frac{M_1}{V(S_1-S_2)}\left[(\lambda_4+S_1)e^{S_1 t} - (\lambda_4+S_2)e^{S_2 t}\right]. \tag{3.69}$$

where

$$S_{1,2} = \frac{-(\lambda_2 + \lambda_4)\ (\pm\sqrt{(\lambda_2 + \lambda_4)^2 - 4(\lambda_2\lambda_4 - \lambda_3\lambda_1)}}{2}.$$

This instantaneous solution, as any other instantaneous solution, can be generalized for more general radionuclide releases using the following convolution integral:

$$C(t) = \int_0^t C_i(t-\tau)\,G(\tau)\,d\tau\,,$$

where

$C(t)$ = dissolved concentration at time t,

$C_i(t-\tau)$ = analytical solution for concentration at time $t-\tau$ for an instantaneous release which occurred at time $t = 0$,

$G(\tau)$ = a function defining a noninstantaneous release rate of radionuclide.

Booth (1975) has developed a numerical compartment-type lake model that includes complex interactions of radionuclides, sediments, and biota. Smith et al. (1977) also have reported the numerical steady-state, compartment-type model, EXAMS, applicable to lakes and rivers. EXAMS includes various chemical degradation processes. With these models, as with the NRC lake model, data on sediment behavior must be supplied to the

model; that is, the models themselves do not simulate sediment behavior. SERATRA (for river-run reservoirs) and FLESCOT, reported in Onishi et al. (1980a) and Onishi and Trent (1982), respectively, are also applicable to lakes.

3.5 CONCLUSIONS

The principal mechanisms and processes which affect the migration and fate of radionuclides entering surface waters are transport, mixing, intermedia transfer, degradation and decay, and transformation. The focus throughout this chapter has been on simple models for describing the aquatic dispersal of radionuclides through water and sediment movement.

Dispersal through water movement was treated by distinguishing between the initial mixing zone or near-field, where mixing is dominated by the characteristics of the effluent and the outfall structure, and the far-field, where ambient advection and diffusion processes determine the extent of mixing.

A substantial body of experimental and theoretical research over the last fifteen years has resulted in understanding the basic factors of near-field mixing. Simple models in the form of semi-empirical expressions are available for many different outfall configurations and designs.

In all cases the extent of the near-field and the dilution depend on the momentum and buoyancy of the effluent and the depth of the receiving water and ambient current conditions.

Far-field mixing and dispersal is characterized by much larger length and time scales than the near-field mixing. Since the geometry, size, and internal circulation of the receiving body are the dominant factors, the treatment of far-field mixing depends on the type of the water body. Simple analytic solutions are available for estimating radionuclide concentrations in rivers, estuaries, ponds, and small lakes. These solutions, however, must be used carefully because they are based on several assumptions regarding the uniformity of different flow and mixing parameters throughout the receiving water body. Prediction of dispersal in large lakes and the ocean is a more difficult task. In the general case preliminary estimates of dispersal can be obtained by using available hydrographic data or specially designed dye and drogue field studies. Analytic solutions are available only for some simple velocity fields. Numerical models can be used to estimate the velocity field and mixing of released substances in large water bodies for different possible combinations of forces driving the circulation. Successful use of numerical models requires an understanding of key aspects of their formulation and the assumptions upon which it is based. A "black box" approach must be avoided.

Radionuclide concentration in surface waters can be affected by volatilization or by absorption on suspended and bedload sediment. A simple approach for estimating volatilization effects has been included. Simple models that account for sediment-radionuclide interactions for rivers, estuaries, and lakes

have been discussed. The sediment-radionuclide interaction should be included in the assessment of the impact of radionuclides with long half-lifes if the radionuclides in question have high affinity to the sediment and if the concentration of suspended particles, especially fine particles, is high.

3.6 PROBLEMS

1. An outfall discharges 0.8 m^3/s containing 1 mCi/m^3 of ^{134}Cs. The cross section of the outfall channel is rectangular, 2 m wide and 0.5 m deep. The receiving water is 10 m deep and is assumed to be stagnant. The ambient water temperature is 10°C and the discharge temperature is 17°C. Estimate the size of the near-field zone and the ^{134}Cs concentration at the edge of the near field. Solve the problem for the case that the depth of the receiving water is 2.5 m. Also, what is the extent of the near-field and ^{134}Cs concentration at the transition distance when there is an ambient crossflow of 0.5 m/s?
2. A 700-MW nuclear power plant is discharging its condenser cooling water into a coastal area. Due to tidal variations the water depth in the discharge vicinity varies between 6 m at low water and 7.5 m at high water. The bottom topography can be assumed as reasonably flat. The cooling water flow rate is 25 m^3/s with a condenser temperature rise of 15°C and carries an isotope water concentration of 0.005 $\mu Ci/cm^3$. The ambient water temperature is 18°C. For the two extreme tidal conditions, determine the extent of the near-field mixing zone, the near-field dilution factors, and the final concentration of the isotope. The discharge canal has a width of 10 m and a depth of 1 m and 2.5 m, respectively, depending on tidal conditions.
3. A liquid radwaste effluent discharge from an industrial plant is by means of a single pipe located at the bottom of an ocean coastal region. The local water depth is 15 m. The effluent has a water density equal to fresh water and has a ^{60}Co concentration of 5 $\mu Ci/cm^3$. The flow rate is 0.5 m^3/s. Examine the final isotope concentration at the surface of the unstratified ocean for two different discharge strategies:
   - high-velocity discharge at 10 m/s, and
   - low-velocity discharge at 1 m/s.
4. A submerged outfall pipe, 0.7 m in diameter, discharges 1.1 m^3/s of heated water into a vertically mixed water body 4.5 m deep. The effluent contains 0.8 mCi/m^3 of ^{134}Cs. The ambient temperature is 9°C and the effluent temperature is 8°C higher than the ambient. Estimate the radionuclide concentration at the point where the discharge plume reaches the water surface for two alternative outfall designs: (a) a vertical pipe and (b) a horizontal pipe. Solve the problem for summer weather condi-

tions when the temperature of the receiving water is 23°C. Also, examine the case that the outfall is located at an alternative site where the depth of the lake is 3.5 m.

5. A submerged alternating diffuser outfall discharges 5 m^3/s into a large nonstratified lake. The diffuser has 100 nozzles 15 cm in diameter, spaced 2 m apart. The depth of the lake near the outfall is 3 m and the diffuser is located at the bottom. The effluent contains 1.2 mCi/m^3 of a radionuclide. The relative density difference of the buoyant discharge is $\Delta\rho/\rho = 0.003$. Estimate the radionuclide concentration at the surface. What would be the effect of an 0.6 m/s longshore current on the radionuclide surface contentration?
6. A blowdown diffuser carries the effluent from a wet cooling tower that serves as a heat dissipation system for a 2000-MW nuclear plant. The diffuser is located in a run-of-the-river reservoir in which the velocities may vary from zero (essentially stagnant) to 0.25 m/s depending on the dam operation that controls the reservoir. The reservoir is very wide (1 km). The diffuser is 50 m long, consisting of 50 nozzles of 10 cm diameter in a undirectional arrangement and is located in 2 m depth. The blow rate is 0.8 m^3/s and carries an isotope concentration of 0.08 $\mu Ci/cm^3$. Determine the concentration after the near-field mixing is completed for the two reservoir flow conditions.
7. A river outfall discharges 0.3 m^3/s containing 0.5 mCi/m^3 of ^{134}Cs. The outfall design provides for a pipe discharging at the middle of a 200-m-wide river. The channel slope is $s = 0.0002$ and the river flow is $Q_R = 6000$ m^3/s. Estimate the ^{134}Cs concentration profile at 100, 500, and 1000 m downstream of the outfall. (Compute the depth of flow h using the formula $h = (nQ_R/ws^{1/2})^{3/5}$, where w is the river width and n is Manning's n, which in this case can be taken equal to 0.03.) How would the above computed concentration profiles change during a dry year when the river flow is expected to be $Q_R = 100$ m^3/s? Also, solve the problem for the case that instead of a pipe the outfall is a 20-m-long diffuser, normal to the river axis with its one end located at 20 m and the other at 40 m from the river bank.
8. An accidental dump of radioactive wastewater occurred in a stream with a width of 50 m, an average depth of 1.2 m, a bottom slope of 0.0005, and a discharge of 20 m^3/s. A 4000-L water volume containing 1 Ci/L of ^{212}Pb with a half-life of 10.6 h was released instantaneously. Find the time and the magnitude of the maximum concentration that occurred at a water intake located 15 km downstream.
9. Assume that an accidental release of similar magnitude to that in problem 5 takes place during the summertime in one of the Great Lakes. Due to thermal stratification with an upper mixed layer depth of 12 m, the diffusion will take in a vertically uniform layer of that thickness. Determine the

maximum concentration and the horizontal size (radius) of the diffusing path for times of 1, 6 and 24 h after the accident.

10. One Ci of ^{134}Cs is instantaneously released to a river having a constant width of 50 m and a constant depth of 5 m. The river discharge and sediment concentration are 200 m^3/s and 100 mg/L, respectively. The half-life and distribution coefficient of ^{134}Cs are 2.06 y and 5000 mL/g, respectively. Dividing the river into 20-km segments, calculate peak concentrations of dissolved, particulate, and total ^{134}Cs at 50 and 90 km downstream from the release point by using Eqs. 3.58 through 3.60.
11. Assume the same conditions as in problem 10, except river discharge increases by 40 m^3/s for each 20 km downstream from the release point due to a series of tributaries which do not have ^{134}Cs. Calculate the peak concentrations of dissolved and particulate ^{134}Cs at 50 and 90 km downstream from the release point.
12. Two mCi of ^{65}Zn with a half-life of 244 d and a distribution coefficient of 5000 mL/g is instantaneously released to an estuary. Assume that the average water depth and the thickness of the active bed layer are 5 m and 5 cm, respectively. The estuarine width is 500 m. Further, tidally averaged flow velocity and sediment velocity are assumed to be 0.05 and 0.001 m/s, respectively. Longitudinal dispersion coefficients for the water and sediment layers are assumed to be 100 m^2/s and 0.1 m/s, respectively. The sediment concentration is 40 mg/L. By using Eqs. 3.58 and 3.62, estimate the time of peak concentration of ^{65}Zn at 50 km downstream from the release point and the levels of both dissolved and particulate ^{65}Zn at that time.
13. Five mCi of ^{90}Sr is released to a lake with a water volume of 1,000,000 m^3. The water discharges to and from the lake are the same (5 L/s). The water depth and the thickness of the active sediment layer are 20 and 0.05 m, respectively. The sedimentation velocity for this lake is assumed to be 1 cm/y. The coefficient of the direct radionuclide transfer between the water and sediment layers is assumed to be 0.01 m^2/s. The half-life and the distribution coefficient of ^{90}Sr are 29 y and 500 mL/g, respectively. With Eqs. 3.58 and 3.69, calculate dissolved and particulate concentrations of ^{90}Sr in the lake 3 y after the ^{90}Sr release to the lake.

REFERENCES AND BIBLIOGRAPHY

Abraham, G. 1963. *Jet Diffusion in Stagnant Ambient Fluid,* Publication 29, Delft Hydraulics Lab.

Abraham, G. 1967. "Jets with Negative Buoyancy in Homogeneous Fluid, *J. Hydraul. Res.* **5** (4).

Abbott, M. B. 1974. *Computational Hydraulics: Elements of Free-Surface Flows,* Pitman, Loudon.

Adams, E. E., Harleman, D. R. F., Jirka, G. H., and Stolzenbach, K. D. 1979. *Heat Disposal in the Water Environment,* Massachusetts Institute Technol.

Adams, E. E., Stolzenbach, K. D., and Harleman, D. R. F. 1975. *Near and Far Field Analysis of Buoyant Surface Discharges into Large Bodies of Water,* Technical Report 205, Massachusetts Institute Technol., R. M. Parsons Lab. Water Resour. and Hydrodynamics, Department Civil Engineering, Cambridge.

Albertson, M. L., Dai, Y. B., Jensen, R. A., and Rouse, H. 1950. "Diffusion of Submerged Jets," *Trans. Am. Soc. Civ. Eng.* **115.**

Almquist, C. W., and Stolzenbach, K. D. June 1976. *Staged Diffusers in Shallow Water,* Technical Report 213, Massachusetts Institute Technol., R. M. Parsons Lab. Water Resour. and Hydrodynamics, Department Civil Engineering, Cambridge.

Anwar, H. O. July 1972. "Appearance of Unstable Jet," *J. Hydr. Div., Am. Soc. Civ. Eng.* **98** (HY1), 1143–56.

Booth, R. S. 1975. *A System Analysis Model for Calculating Radionuclide Transport Between Receiving Waters and Bottom Sediment,* ORNL/TM-4751, Union Carbide Corp., Nuclear Div., Oak Ridge Natl. Lab.

Brooks, A. N., and Hughes, T. J. R. 1982. "Streamline Upwind/Petrov-Galerk Formulations for Convection Dominated Flows with Particular Emphasis on the Incompressible Navier-Stakes Equations," *Comp. Methods in Applied Mech. and Eng.*

Brooks, N. H. 1960. *Diffusion of Sewage Effluent in an Ocean Current,* proceedings of the 1st International Conference on Waste Disposal in the Marine Environment, Pergamon.

Carter, H. H. 1969. *A Preliminary Report on the Characteristics of a Heated Jet Discharged Horizontally into a Transverse Current, Part I, Constant Depth,* Technical Report 61, Chesapeake Bay Institute, Johns Hopkins Univ., Baltimore.

Carter, H. H., Schiemer, E. W., and Regier, R. 1973. *The Buoyant Surface Jet Discharging Normal to an Ambient Flow of Various Depths,* Technical Report 81, Chesapeake Bay Institute, Johns Hopkins Univ., Baltimore.

Cederwall, K. 1971. *Buoyant Slot Jets into Stagnant or Flowing Environments,* KH-R-25, W. M. Keck Lab. Water Resour. and Hydraulics, California Institute Technol., Pasadena.

Cheng, R. T. S. 1976. "Modeling of Hydraulic Systems," *Adv. Hydrosci.* **11**, 208–84.

Churchill, M. A., Cragwall, J. A., Andrews, R. W., and Jones, S. L. 1965. *Concentrations, Total Sediment Loads, and Mass Transport of Radionuclides in the Clinch and Tennessee Rivers*, ORNL-3721, suppl. 1, Union Carbide Corp., Nuclear Div., Oak Ridge Natl. Lab.

Csanady, G. T. 1973. *Turbulent Diffusion in the Environment*, Reidel Publishing, Hingham, Mass.

Ditoro, D. M., Fitzpatrick, J. J., and Thomann, R. V. 1981. *Documentation for Water Quality Analysis Simulation Program (WASP) and Model Verification Program (MVP).* Prepared for the Environmental Research Laboratory, U.S. Environmental Protection Agency in Duluth, Minnesota, by Hydroscience, Inc., Westwood, N.J.

Dunn, W. E., Policastro, A. J., and Paddock, P. A. 1975. *Surface Thermal Plumes: Evaluation of Mathematical Models for the Near- and Complete Field*, Argonne Natl. Lab., Cent. Environ. Stud.

Fan, L.-N., and Brooks, N. H. 1969. *Numerical Solution of Turbulent Buoyant Jet Problems*, KH-R-18, W. M. Keck Lab. Hydraulics and Water Resour., California Institute Technol., Pasadena.

Fields, D. E. 1976. *CHNSED: Simulation of Sediment and Trace Contaminant Transport with Sediment/Contaminant Interaction*, ORNL/NSF/EATC-19, Oak Ridge National Laboratory, Oak Ridge, TN.

Fischer, H. B., List, E. J., Koh, R. C. Y., Imberger, I., and Brooks, N. H. 1979. *Mixing in Inland and Coastal Waters*, Academic Press, New York.

Fletcher, J. F., and Dotson, W. L., eds. 1971. *Hermes—A Digital Computer Code for Estimating Regional Radiological Effects from the Nuclear Power Industry*, HEDL-TME-71-1968, U.S. AEC.

Hetherington, J. A. 1976. *Behavior of Plutonium Nuclides in the Irish Sea, Environmental Toxicity of Aquatic Radionuclides: Models and Mechanisms,* ed. Morton and Miller, Ann Arbor Science, Ann Arbor, Mich.

Hirst, E. 1971. "Buoyant Jets Discharged to Quiescent Stratified Ambients," *J. Geophys. Res.* **76** (30).

Hirst, E. A. 1972. "Buoyant Jets with Three-Dimensional Trajectories," *Proc. Am. Soc. Civ. Eng.* **98** (HY11).

Hughes, T. J. R., ed. 1979. *Finite Element Methods for Convection Luminated Flows,* American Society Mechanical Engineers, New York.

Jirka, G. H., Abraham, G., and Harleman, D. R. F. July 1975. *Assessment of Techniques for Hydrothermal Impact Prediction,* Report 203, Massachusetts Institute Technol., R. M. Parsons Lab. Water Resour. and Hydrodynamics, Department Civil Engineering, Cambridge.

Jirka, G. H., Adams, E. E., and Stolzenbach, K. D. 1981. "Properties of Buoyant Surface Jets," *J. Hydr. Div., Am. Soc. Civ. Eng.* **107**, 1467–88.

Jirka, G. H., and Harleman, D. R. F. 1978. *The Mechanics of Submerged Multiport Diffusers for Buoyant Discharges in Shallow Water*, Technical Report 169, R. M. Parsons Lab. Water Resour. and Hydrodynamics, Department Civil Engineering, Cambridge.

Jirka, G. H., and Watanabe, M. May 1980. "Thermal Structure of Cooling Ponds," *J. Hydr. Div., Am. Soc. Civ. Eng.* **106** (HY5), 701–15.

Jirka, G., Watanabe, M., Octavio, K. H., Cerco, C., and Harleman, D. R. F. 1978. *Mathematical Models for Cooling Ponds and Lakes, Part A: Model Development and Design Considerations*, Technical Report 238, Massachusetts Institute Technol., R. M. Parsons Lab. Water Resour. and Hydrodynamics, Department Civil Engineering, Cambridge.

Jirka, G. H. 1982. "Multiport Diffuser for Heat Disposal: A Summary," *J. Hydr. Div. Am. Soc. Civ. Eng.* **108,** 1025–1068.

Johnson, B. H. February 1980. *A Review of Numerical Reservoir Hydrodynamic Modeling*, U.S. Army Corps Engineers, Waterways Experiment Station, Vicksburg.

Klein, S. J., Caldwell, B. J., and Lilly, J. M., eds. 1981. *1980–81 AFOSR-HTTM Stanford Conference on Complex Turbulent Flows,* Thermosciences Div., Department Mech. Engineering, Stanford University, Stanford, Calif.

Koh, R. C. Y., Brooks, N. H., List, E. J., and Wolanski, E. J. 1974. *Hydraulic Modeling of Thermal Outfall Diffusers for the San Onofre Nuclear Power Plant,* KH-R-30, Calif. Inst. Tech., Kerckhoff Labs. Biology, Pasadena.

Lee, J. H. W., and Jirka, G. H. 1981. "Vertical Round Buoyant Jet in Shallow Water," *J. Hydr. Div., Am. Soc. Civ. Eng.* **107** (HY12), 1651–75.

Lee, J. H. W., Jirka, G. H., and Harleman, D. R. F. 1974. *Stability and Mixing of a Vertical Round Buoyant Jet in Shallow Water,* Technical Report 195, Massachusetts Institute Technol., R. M. Parsons Lab. Water Resour. and Hydrodynamics, Department Civil Engineering, Cambridge.

Leendertse, J. J., and Liu, S.-K. June 1975. *A Three-Dimensional Model for Estuaries and Coastal Seas: Volume II, Aspects of Computation,* R-1764-OWRT, RAND Corp., Santa Monica, Calif.

Leonard, B. P. 1979. "A Survey of Finite Differences of Opinion on Numerical Muddling of the Incomprehensible Defective Confusion Equation," in *Finite Element Methods for Convection Dominated Flows,* vol. 34, ed. T. J. R. Hughes, American Society Mechanical Engineers, New York.

Liseth, P. 1970. *Mixing of Merging Buoyant Jets from a Manifold in Stagnant Receiving Water of Uniform Density,* HEL 23-1, Hydraulic Engineering Lab., Univ. California, Berkeley.

Okubo, A. 1971. "Oceanic Diffusion Diagrams," *Deep-Sea Res.* **18.**

Onishi, Y. September 1981. "Sediment and Contaminant Transport Model." *J. Hydr. Div., Am. Soc. Civ. Eng.* **107** (HY9), 1089–1107.

Onishi, Y., Johanson, P. A., Baca, R. G., and Hilty, E. L. 1976. *Studies of Columbia River Water Quality—Development of Mathematical Models of Sediment and Radionuclide Transport Analysis,* BNWL-B-452, Pacific Northwest Laboratory, Richland, Wash.

Onishi, Y., Schreiber, D. L., and Codell, R. B. 1980a. "Mathematical Simulation of Sediment and Radionuclide Transport in the Clinch River, Tennessee," *Contaminants and Sediments,* R. A. Baker, ed., Vol. 1, Ch. 18, Ann Arbor Science Publishers, Inc., Ann Arbor, Mich., pp. 393–406.

Onishi, Y., Whelan, G., Parkhurst, M. A., Olsen, A. R., and Gutknecht, P. J. 1980b. *Preliminary Assessment of Toxaphene Migration and Risk in the Yazoo River Basin, Mississippi,* Battelle, Pacific Northwest Labs., Richland, Wash.

Onishi, Y., Serne, R. J., Arnold, E. M., Cowan, C. E., and Thompson, F. L. 1981. *Critical Review: Radionuclide Transport, Sediment Transport, and Water Quality Mathematical Modeling; and Radionuclide Adsorption/ Desorption Mechanisms,* NUREG/CR-1322, PNL-2901, Pacific Northwest Laboratory, Richland, Wash.

Onishi, Y., and Trent, D. S. 1982. *Mathematical Simulation of Sediment and Radionuclide Transport in Estuaries,* NUREG/CR-2423, PNL-4109, Pacific Northwest Laboratory, Richland, Wash.

Onishi, Y., and Thompson, F. L. 1982. *Evaluation of Long-Term Radionuclide Transport and Accumulation in the Pacific Coastal Water,* Battelle, Pacific Northwest Laboratories, Richland, Wash.

Onishi, Y., Whelan, G., and Skaggs, R. L. 1982a. *Development of a Multimedia Radionuclide Exposure Assessment Methodology for Low-Level Waste Management,* PNL-3370, Pacific Northwest Laboratory, Richland, Wash.

Onishi, Y., Myers, D. A., and Argo, R. S. 1982b. "Sediment and Toxic Contaminant Transport Modeling in Coastal Waters," Proceedings of the Fourth International Symposium of Finite Element Method of Flow Problems, *Finite Element Flow Analysis,* T. Kawai, ed., University of Tokyo Press, Tokyo, Japan, pp. 733–740.

Onishi, Y., Yabusaki, S. B., and Kincaid, C. T. 1982c. "Performance Testing of the Sediment-Contaminant Transport Model, SERATRA," *Proceedings of the Conference on Applying Research to Hydraulic Practical,* P. E. Smith, ed., ASCE, pp. 623–632.

Onishi, Y., Yabusaki, S. B., Kincaid, C. T., Skaggs, R. L., and Walters, W. H. 1982d. *Sediment and Radionuclide Transport in Rivers—Radionuclide Transport Modeling for Cattaraugus and Buttermilk Creeks, New York,* NUREG/CR-2425, PNL-4111, Pacific Northwest Laboratory, Richland, Wash.

Pinder, G. F., and Gray, W. G. 1977. *Finite Element Simulation in Surface and Subsurface Hydrology,* Academic Press, New York.

Policastro, A. J., and Dunn, W. E. 1976. "Numerical Modeling of Surface Thermal Plumes," presented in the International Advanced Summer Course on Heat Disposal from Power Generation, sponsored by the International Center for Heat and Mass Transfer, Dubzevnik, Yugoslavia, August 23–28; to be published in the proceedings.

Prych, E. A. 1972. "A Warm Water Effluent Analyzed as a Buoyant Surface Jet," *Svoriges Meteorologista Och Hydrologista Institut, Serie Hydrologi* **21,** Stockholm, Sweden.

Roache, P. J. 1972. *Computational Fluid Dynamics,* Hermosa, Albuquerque, N. Mex.

Roberts, P. J. W. March 1977. *Dispersion of Buoyant Wastewater Discharged from Outfall Diffuses of Finite Length,* KH-R-35, W. M. Keck Lab. Engineering Materials, California Institute Technol., Pasadena.

Roberts, P. J. W. 1979. "Line Plume and Ocean Outfall Dispersion," *Proc. Am. Soc. Civ. Eng., J. Hydr. Div.,* HY4.

Rodi, W. 1980. *Turbulence Models and Their Application in Hydraulics—A State of the Art Review,* IHAR Publication.

Rouse, H., Yih, C. S., and Humphreys, H. W. 1952. "Gravitational Convection from a Boundary Source," *Tellus,* **4.**

Ryan, P. J., and Harleman, D. R. F. February 1972. *Analytical and Experimental Study of Transient Cooling Pond Behavior,* Technical Report 161, Massachusetts Institute Technol., R. M. Parsons Lab. Water Resour. and Hydrodynamics, Cambridge.

Schell, W. R., and Sibley, T. H. 1982. *Distribution Coefficient for Radionuclides in Aquatic Environment—Final Summary Report,* NUREG/CR-1869, prepared for the U.S. Nuclear Regulatory Commission by Laboratory of Radiation Ecology, College of Fisheries, University of Washington, Seattle, Wash.

Shirazi, M. A., and Davis, L. R. 1974. *Workbook of Thermal Plume Prediction—Vol. 2—Surface Discharges,* EPA-R2-72-0056, Environmental Protection Technology Series, U.S. Environmental Protection Agency, Corvallis, Oreg.

Simons, T. J., and Lam, D. C. L. 1980. "Some Limitations of Water Quality Models for Large Lakes: A Case Study of Lake Ontario," *Water Resour. Res.* **16** (1), 105–16.

Smith, J. H., Mabey, W. R., Bohonos, N., Holt, B. R., Lee, S. S., Chou, T. W., Bomberger, D. C., and Mill, T. 1977. *Environmental Pathways of Selected Chemicals in Freshwater Systems, Part I: Background and Experimental Procedures,* EPA-600/7-77-113, SRI Int., Menlo Park, Calif.

Stolzenbach, K. D., and Harleman, D. R. F. 1971. *An Analytical and Experimental Investigation of Surface Discharges of Heated Water,* Technical Report 135, Massachusetts Institute Technol., R. M. Parsons Lab. Water Resources and Hydrodynamics, Department Civil Engineering, Cambridge.

Stommel, H. 1949. "Horizontal Diffusion Due to Oceanic Turbulence," *J. Mar. Res.* **8** (3).

Thatcher, M. L., and Harleman, D. R. F. 1972. *A Mathematical Model for the Prediction of Unsteady Salinity Intrusion in Estuaries*, Technical Report 144, Massachusetts Institute Technol., R. M. Parsons Lab. Water Resour. and Hydrodynamics, Department Civil Engineering, Cambridge.

U.S. Environmental Protection Agency, Division of Standards and Criteria, Office of Water and Hazardous Materials (USEPA) 1978. *Kepone Mitigating Project Report.*

U.S. Nuclear Regulatory Commission (USNRC) 1978. *Liquid Pathway Generic Study. Impacts of Accidental Radioactivity Releases to the Hydrosphere from Floating and Land-Based Nuclear Power Plant,* NUREG-0040.

Wang, J., and Connor, J. J. April 1975. *Mathematical Modeling of Near Coastal Circulation,* Technical Report 200, Massachusetts Institute Technol., R. M. Parsons Lab. Water Resour. and Hydrodynamics, Cambridge.

Wrenn, M. E., Lauer, G. J., Jinks, S., Hairr, L., Mauro, J., Friedman, B., Wohlgemuth, D., Hernandez, J., and R'e, G. 1972. *Radioecological Studies of the Hudson River,* Progress Report to Con. Edison Company of New York.

Wright, S. J. May 1977. "Mean Behavior of Buoyant Jets in a Crossflow," *J. Hydr. Div., Am. Soc. Civ. Eng.* **103** (HY5), 499–513.

Yotsukura, N., and Sayre, W. W. 1976. "Transverse Mixing in Natural Channels," *Water Resour. Res.* **12** (4).

Zienkiewicz, O. C. 1977. *The Finite Element Method,* 3d ed., McGraw, London.

4 Transport of Radionuclides in Groundwater

By R. B. CODELL* *and* J. D. DUGUID†

4.1 INTRODUCTION

Groundwater flow is one of the likely pathways for radionuclides released from waste disposal areas. Groundwater transport is also a major pathway for certain classes of accidental and normal releases from nuclear facilities such as power plants, fuel reprocessing plants, and mining or milling operations. The primary emphasis of this chapter will be groundwater transport of radionuclides using waste disposal as an application. Concentrations of radionuclides that could reach the biosphere and the resulting consequences must be predicted using scenarios of events and processes that are possible but unlikely to occur at the disposal site. Estimations of groundwater flow and transport are important in assessing the performance of a disposal system because they are probable migration pathways between the nuclear waste and the biosphere.

The transport of radionuclides through the ground can be estimated by the use of tracers, groundwater dating, mathematical models, or by a combination of all of the above. Chemical or radioactive tracers may be deliberately introduced to the groundwater and monitored through wells for the direct determination of groundwater velocity and transport. Alternatively, pollutants not deliberately introduced to the groundwater may also be traced.

Groundwater dating is a technique by which the age of a region of groundwater may be estimated from the concentration of an atmospheric

*U.S. Nuclear Regulatory Commission, Hydrologic Engineering Section, Washington, D.C.

†Battelle Office of National Waste Terminal Storage Integration, Germantown, Md.

radionuclide it contains. Tritium released since the beginning of the nuclear era can be used to date water up to several decades. Water may be dated using ^{14}C over longer periods of hundreds to thousands of years. Direct measurements of the migration of radionuclides released from naturally occurring uranium and thorium ore bodies can be used as a close analog to man-made radioactive waste disposal situations.

Using groundwater flow and transport models provides a means to calculate the expected concentrations of radionuclides following release to the environment. Where groundwater contamination of wells or surface water bodies such as lakes, streams, or rivers occurs, the radionuclide concentrations are used in other pathway models to calculate the consequences of the release. Pathway models consist of surface water transport models and biological pathway models, which in turn provide the basis for dose calculations. Doses to humans arise through the contamination of drinking water and food and from contaminated surfaces such as flood plains and beaches.

This chapter discusses current practice in groundwater flow and transport modeling as well as data requirements and possible misuses of models. A set of analytical models is presented along with illustrations of their use.

4.1.1 Types of Groundwater Assessments

4.1.1.1 Geologic Isolation of High-Level Waste

Actual tests and demonstrations of the behavior of a high-level waste (HLW) repository system cannot be performed over the operational lifetime of the repository. Therefore, we must rely on mathematical models for performance assessments, using data collected over comparatively short periods of time, to predict the long-term performance of the system. This is the only means by which the cumulative effects of changes in the properties of the respository system, the effects of various design features of the repository, and the effects of the repository on the environment can be analyzed. Performance assessment not only provides this type of analysis but also provides information that is useful in guiding research and development activities in site selection, repository design, and waste package design. Performance assessment treats concepts that can be quantified, that is, failure analysis and consequence assessment (Klingsberg and Duguid 1980).

An assessment of the long-term performance of a repository analyzes the events and processes that could release radionuclides from the waste and the phenomena that might transport radionuclides to the biosphere. These phenomena may be roughly classified as those that occur in the near field (where waste and repository phenomena dominate) and those that occur in the far field (at a greater distance from the repository where natural phenomena dominate). Although these two regions are not separated by a precisely defined

boundary, the distinction is useful because the physical and chemical effects of heat and radiation from the waste are limited to the near field (Klingsberg and Duguid 1980). Different methods of analysis are therefore appropriate for the two regions. Near-field analysis studies the combined effects of heat, radiation, repository design and construction, and the waste package. Far-field analysis studies the effects of events that arise from natural phenomena, and from potential human actions after the repository has been sealed. These far-field phenomena usually appear in the geosphere and the biosphere outside of the repository. Both near-field and far-field performance must be considered in determining how well the natural and the man-made components of the disposal system meet the criteria for repository performance.

4.1.1.2 Shallow Land Burial

For near-surface disposal such as shallow land burial, the analysis of system performance is similar to that of isolation of high-level waste with two major exceptions: (1) groundwater flow and transport models must frequently consider the unsaturated zone and (2) the wastes are not heat producing. The analysis proceeds in much the same fashion as for high-level waste and includes the development of a source term through corrosion or breaching of waste containers, defining an appropriate leach rate for the waste form, developing a system release scenario, and calculating groundwater flow and radionuclide transport for use in the biosphere models and dose codes (Aikens et al. 1979).

4.1.1.3 Uranium Mining and Milling

There are several potential groundwater contamination problems associated with the mining, milling, and waste disposal operations necessary to produce uranium fuels (USNRC 1979; Shepard and Cherry 1980).

The greatest waterborne contamination hazard to groundwater is the seepage from tailings ponds resulting from conventional milling procedures. The waste stream contains about half solids and half water, which is usually disposed of in ponds (tailings ponds) formed behind earth or rubble dams. Tailings are sometimes reburied in the ore pits. Acid leach mills are the most prevalent type. Tailings ponds usually receive highly acidic (pH 0.5–2) water and tailings, but in some cases tailings are first neutralized.

The wastes from the tailings ponds differ most from other forms of nuclear waste because of their unique chemistry. In acidic tailings, most of the radioactive and other chemical wastes are in the dissolved state. Acidic wastes are sometimes neutralized to reduce the solubility of pollutants, but in some cases the wastes slowly become acidic because of oxidation of pyrite (iron sulfide). The behavior of the radioactive contaminants varies from very simple to very complex. Probably the most radiologically significant radioactive waste

component present is radium, which has a fairly simple chemistry since it exists only in +2 valence state. Uranium and several other radioactive waste compounds behave in a much more complicated fashion, since they may exist in several different valence states and form complex compounds (Landa 1980).

The solubility of all of the contaminants is high for low-pH conditions and decreases markedly at higher pH. Neutralization by carbonates, such as limestone, either added deliberately or encountered in the environment, however, can mobilize uranium in the form of soluble carbonate complexes. Uranium may also be mobilized in an oxidizing environment or by certain organic chemicals in groundwater (Shephard and Cherry 1980).

4.1.1.4 Nuclear Power Plant Accidents

Postulated accidental releases of radioactivity to the groundwater pathway have been evaluated for a wide range of nuclear facilities either for generic sites or in actual reactor licensing reviews. The accidental releases considered range from small leaks from contaminated water streams in nuclear plants to major releases caused by a core meltdown accident (USNRC 1975; USNRC 1978; Niemczyk 1981).

Consideration given to nuclear power plant accident releases to groundwater differs from those for high- and low-level waste disposal or other fuel cycle problems in several important respects: (1) The risk of contamination would exist only for the lifetime of the plant. Administrative controls would be in effect during this period, so mitigative measures could presumably be taken should an accidental release occur; (2) The isotopes of importance in nuclear power plant liquid pathway accidents are generally those with high dose factors and/or half-lives of years to tens of years, notably ^{3}H, ^{134}Cs, ^{137}Cs, ^{89}Sr, ^{90}Sr, and ^{106}Ru. Unlike nuclear waste, long-lived radionuclides, actinides, and transuranics have been shown to be of much lower importance (USNRC 1978); (3) For a given event, consequences of radioactive release to the groundwater pathway typically present much smaller risks than release to the airborne pathway. These consequences should not be neglected in citing studies for nuclear power plants, however.

4.2 TYPES OF GROUNDWATER MODELS

4.2.1 Groundwater Models for Low-Level Waste

The assessment of a low-level waste burial ground requires three types of models: (1) models to determine the portion of the radioactive source released if infiltrating water contacts the waste, (2) mathematical models in terms of measurable hydrologic parameters that predict the migration of radionuclides from the source to locations accessible to the public, and (3) models for

determining the potential radiation dose using the radionuclide concentrations that reach accessible locations. In this chapter only item 2 will be discussed. Dose assessments are covered in other sections of this document. Source term definitions defy simple explanation and cannot be adequately covered in this report.

Although difficult to analyze, the near field is as important and complex for shallow land disposal as for deep geological disposal. Most of the action is in the disposal trench and determines what is available for future groundwater transport. Determining the water balance and the amount of water infiltrating is difficult. Determining the leaching and release from chemically and physically heterogeneous wastes such as low-level wastes is even more difficult. To date, no model adequately addresses the problem of modeling the near-field environment for shallow land burial.

The calculation of transport of radionuclides from shallow land burial sites is complicated by the waste frequently being leached in the unsaturated zone, and the movement of waste to the water table must consider both flow and transport through this zone. Here, in the simplest case, flow and transport may be assumed to be downward in one dimension. Water flow rates from a water balance can be used to approximate the unsaturated flow used as input to the radionuclide transport model. Radionuclide transport in the unsaturated zone can also be assumed to be downward and one dimensional. These simplifying assumptions can be used to calculate the concentrations of radionuclides being released to the water table as a function of time. More rigorous calculations can also be done using two- and three-dimensional models of unsaturated flow and transport. However, considering the uncertainty in the magnitude of the source term, these sophisticated calculations are warranted only when a large amount of data is available and/or detailed results are required. Below the water table either numerical or analytical models of two- or three-dimensional groundwater flow and radionuclide transport can be used to calculate the concentration of radionuclides released at locations accessible to the public.

4.2.2 Groundwater Models for High-Level Waste Repositories

4.2.2.1 Far-Field Performance

Although there are significant differences in the state of development and verification of different far-field models, these models are sufficiently well advanced to be used in assessments of repository performance at either generic or specific sites. In general, the procedure for calculating the far-field effects of a repository breach is shown in Fig. 4.1.

After the scenarios that have to be modeled have been identified, the next step in a performance assessment is to predict their consequences. Whether the scenarios will actually occur cannot be predicted with complete certainty, but

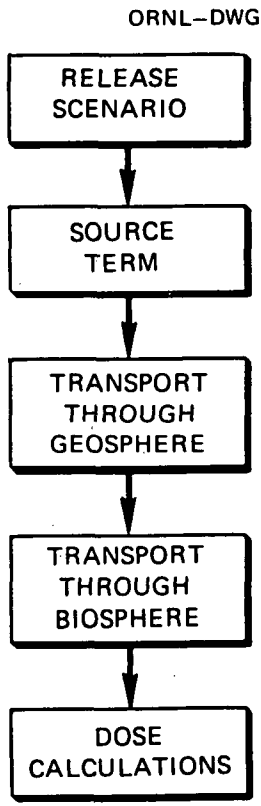

Figure 4.1. Elements of far-field risk assessment. Source: Klingsberg, C., and Duguid, J. 1980. *Status of Technology for Isolating High-Level Radioactive Waste in Geologic Repositories,* U.S. Department of Energy, Tech. Inf. Cent., Oak Ridge, Tenn.

where possible the probabilities of their occurrences are estimated. Probabilities are, however, highly uncertain for the events that have occurred in the region around a repository site only a few times in geologic history or that may not have occurred there at all. For this reason, the assessment of repository performance relies heavily on predictions of the consequences of scenarios rather than on predictions of their probabilities.

The source term describes the waste at all times; it specifies the radionuclides present and the physical and chemical conditions of the waste. The radionuclide concentrations at the time of the breach can be calculated from their original concentrations in the waste.

Source term evaluation is highly site-specific, depending on such factors as the chemistry of the waste, the host rock, and the groundwater. Also, interaction between natural and man-made components can play an important

role in defining release mechanisms. Further discussion of this important aspect of waste-migration modeling is beyond the scope of this book (Klingsberg and Duguid 1980).

Once the source term has been defined, transport through the geosphere is determined by modeling fluid flow into and away from a repository. The output from the geosphere transport codes is a prediction of the radionuclide concentrations reaching the biosphere as a function of time. As contaminants move with groundwater, they may be sorbed and thus retarded by the rocks through which they pass. The parts of the contaminant transport models that describe sorption generally assume equilibrium between the concentration of contaminants in the fluid and the concentration on the rock surfaces.

Because models of flow through fractures tend to be specific to particular types of fracture systems, they are less universally applicable than porous media models (Duguid and Lee 1977). There are two basic problems for the modeling of material transport in fractured media. One problem is to assemble sufficient data to be able to adequately describe the hydrology of the far-field region surrounding a repository site. The determination of effective permeabilities and fracture connections is difficult, and a considerable amount of research remains before reliable methods will be available. The second problem is to understand the sorption process in the fractured rocks; although sorption is effective in porous rocks, it might be much less effective in fractured rocks. Successful modeling of flow in fractured aquifers is extremely limited. Modeling of radionuclide transport in fractured aquifers is nonexistent at the present time. Current models for porous media are being used with equivalent formulations and conservative assumptions to establish bounds on the effects of flow through fractured media (Klingsberg and Duguid 1980).

4.2.2.2 Near-Field Performance

Models for assessing the performance of a high-level waste repository in the near field must take into account mechanical stresses, heat flow, chemical interactions, and radiation-induced physical-chemical processes. All of these phenomena, in addition to the properties of the host rock, affect the environment of the emplaced waste.

The following sections discuss three principal types of models required for near-field analysis: heat transfer models, thermomechanical models, and models of physical and chemical interactions among the emplaced waste, the components of the waste package, and the host rock.

Heat Transfer Models. Thermal models based on physical laws provide an accurate portrayal of heat flow and changes in temperature. The experimental results to date suggest that predictions of temperature within a few percent of measured values can be achieved. Consideration of heat transfer is important because temperature gradients can be a driving force in groundwater flow.

Over 40 such models are identified as useful in the studies of waste disposal (SAI 1979).

Thermomechanical Models. The models are based on relations derived from laws of physics and functional relationships between stress and strain that are obtained from laboratory tests. Because repository rocks are inhomogeneous and may be fractured, generic functional laws are more difficult to obtain for rocks than for most other construction materials.

Thermomechanical codes are currently being used to analyze the uplift and subsidence, room stability and rate of closure, hole stability and rate of closure, canister movement, pillar stability, thermomechanical effects on groundwater flow, stresses and strains at critical locations in the rock mass, and mechanical failure of the rock mass. These phenomena are most important to flow in fractured rocks. Current research emphasis is on the relationship between permeability and change in functional geometry due to stress (SAI 1979).

Chemical Models. To predict the near-field behavior of a repository requires analyses of the interactions between the emplaced package components and the host rock. These interactions fall into six general categories: (1) the movement of fluids in the vicinity of the waste package, (2) the corrosion of the canister and sleeve materials by these fluids, (3) the dissolution of the waste form by groundwater containing the added corrosion products, (4) the sorption of radionuclides by the rocks and the engineered components of the repository, (5) the absorption of radiation emitted by the waste, and (6) the alteration of chemical phases and properties in the vicinity of the canisters. A study of these interactions predicts the kinds, amounts, and chemical state of the radionuclides available for entry into the groundwater system (Jenne 1979).

4.2.3 Groundwater Models for Mill Tailings Waste Migration

The modeling of transport from mill tailings is similar in many ways to other types of groundwater waste migration problems such as low-level radioactive waste disposal. The unique aspects of the modeling of mill tailings wastes are the complex chemistry of the wastes and the process of neutralization, especially by rocks in the transport pathway. Concentrations of chemicals may be quite high in a mill tailings pond, which complicates the transport processes. Typical equilibrium concepts such as the retardation factor and K_d will not work well for complicated, nonlinear phenomena such as precipitation, which may be particularly severe at high concentrations. Unsaturated flow in some of the pond settings and the transient existence of the milling operations may present special modeling problems (Shepard and Cherry 1980; USNRC 1979).

4.3 EQUATIONS FOR GROUNDWATER FLOW AND RADIOACTIVITY TRANSPORT

The movement of radionuclides in groundwater can be described by two equations: one for the movement of the carrier fluid (water) and one for the mass transport of the dissolved constituents (radionuclides). In using these equations, the movement of the carrier in the region under consideration must be known before the transport equation can be solved.

The following discussion of the equations associated with the movement of groundwater and the transport of dissolved radioactive substances can be used only as a general guide. A person intending to use models to analyze a specific problem would usually need the aid of an experienced groundwater hydrologist and modeler. A set of highly simplified transport models is presented in Sect. 4.5.3, along with examples of their use.

4.3.1 Groundwater Flow

Radioactive releases may travel in the unsaturated region (e.g., region above the water table) before entering the zone of saturation (e.g. below water table). However, the release can also be directly into the zone of saturation. The predominant direction of the unsaturated flow is downward until the flow reaches the zone of saturation. Within the zone of saturation the flow is predominantly lateral.

The governing equations in the unsaturated zone consist of a set of coupled equations for the movement of gas and water. To date, only computer codes of limited applicability are available for the solution of these coupled gas-water equations (Lappala 1981). When the assumptions are made that the water moves as a single phase and that no trapped air pockets exist, a single governing equation for saturated-unsaturated flow is obtained (ANS 1980).

$$\left(\frac{\theta}{n'}\alpha' + \theta\beta' + \frac{d\theta}{dh}\right)\frac{\partial h}{\partial t} = \nabla\cdot\left(\bar{\bar{k}}(h)\cdot(\nabla h + \nabla z)\right), \qquad (4.1)$$

where

θ = the moisture content (dimensionless),
n' = total porosity (dimensionless),
α' = the modified coefficient of compressibility of the medium (1/cm),
β' = the modified coefficient of compressibility of water (1/cm),
h = the pressure head (cm),
t = the time (s),
$\bar{\bar{k}}$ = the hydraulic conductivity tensor (cm/s),
z = the elevation head (cm),
∇ = the del operator.

Equation 4.1 is nonlinear because, for unsaturated flow, both hydraulic conductivity and moisture content are functions of pressure head.

The solution of Eq. 4.1 in three dimensions is generally impractical. Simplifications must usually be found. Depending on the nature of the problem, analytical or numerical methods like the ones described in Reeves and Duguid (1975) and Reeves et al. (1977) can be used to analyze saturated-unsaturated flow.

The hydraulic conductivity is a tensor that accounts for directional properties (anisotropy) that arise in formations such as layered sediments (i.e., hydraulic conductivity is different in different directions). If the coordinate system is oriented parallel to the principal components of hydraulic conductivity, only the principal components of the tensor are required. If the medium is further assumed to be homogeneous and isotropic (i.e., properties of the medium are not direction dependent), hydraulic conductivity becomes a scalar and Eq. 4.1 becomes (ANS 1980)

$$\nabla^2 H = \frac{S_s}{K} \frac{\partial H}{\partial t}, \tag{4.2}$$

where

H = the total head = h + z (cm),
S_s = $\rho g (\alpha + n\beta)$ = Specific Storage Coefficient (1/cm),
ρ = the water density (g/cm^3),
g = the acceleration of gravity (cm/s^2),
α = the coefficient of compressibility of the medium (cm·s^2/g),
β = the coefficient of compressibility of water (cm·s^2/g).

This equation is valid for saturated flow in confined aquifers. For a confined aquifer of thickness b, the storage coefficient and transmissivity are respectively defined as

$$S = S_s b \quad \text{and} \quad T = Kb \tag{4.3}$$

and Eq. 4.2 becomes

$$\nabla^2 H = \frac{S}{T} \frac{\partial H}{\partial t}. \tag{4.4}$$

In simulations using Eq. 4.4, the boundary conditions of leakage should be used when appropriate. For problems involving leaky aquifers, methods like those described by Bredehoeft and Pinder (1970) can be used.

For unconfined aquifers where compressibility of the medium and the water is relatively unimportant compared to the vertical movement of the free surface (water table), the continuity equation can be written as follows (ANS 1980):

$$\nabla^2 H^2 = \frac{2S_y}{K}\frac{\partial H}{\partial t}, \tag{4.5}$$

where S_y is the specific yield of the aquifer (dimensionless).

For specific yield of steady flow in either confined or unconfined aquifers, Eqs. 4.4 and 4.5 reduce respectively to the following:

$$\nabla^2 H = 0 \tag{4.6}$$

$$\nabla^2 H^2 = 0. \tag{4.7}$$

For simplified cases, analytical solutions of Eqs. 4.4, 4.5, 4.6, and 4.7 such as those given in Carslaw and Jaeger (1959) can be used. For more complex situations, numerical solutions such as those described in Gray et al. (1977) should be used.

An approximation of the flux (volume of flow per unit cross-sectional area) in the major flow direction can be obtained using Darcy's law:

$$V_x = -K\frac{dH}{dx} \sim -K\frac{\Delta H}{\Delta x}, \tag{4.8}$$

where $\Delta H/\Delta x$ is the hydraulic gradient in the direction of flow.

This approximation is crude but in many cases it is acceptable because of the inability to accurately measure spatial variations in the hydraulic conductivity. Use of this equation assumes a homogeneous isotropic medium in which the gradient is constant over the increment. The actual velocity of a nonadsorbed tracer would be greater than the flux since water is moving only in the pore spaces. The pore velocity (or seepage velocity), U, may be approximated by dividing the flux by the effective porosity:

$$U = V_x/n_e. \tag{4.8a}$$

Example 4.1. For saturated groundwater flow, calculate the pore or seepage velocity in an "average" sandstone under a gradient of 0.01 cm/cm. Use arithmetic mean values in tables.

Equation 4.8a applies. The arithmetic mean hydraulic conductivity, K, is 3.31×10^{-4} cm/s from Table 4.5. The arithmetic mean effective porosity, n_e, is 0.21 from Table 4.4. Therefore,

$$U = V_x/n_e = -K\frac{\Delta H}{\Delta x}/n_e = 3.31\times10^{-4}\,\text{cm/s} \times 0.01/0.21$$
$$= 1.58\times10^{-5}\,\text{cm/s}.$$

[End of Example 4.1]

The difficulty associated with the solution of the flow and transport in the unsaturated zones leads naturally to approximation methods. The time of travel can be estimated by assuming that the mean downward velocity v is proportional to the rate of recharge of water at the surface, r, and inversely proportional to the mean volumetric water content, θ:

$$v = r/\theta . \tag{4.9}$$

The recharge rate, r, can be estimated by methods described in Sect. 4.3.4. The volumetric water content, θ, can be conservatively assumed to be equal to the field capacity, which is the maximum water content where moisture can no longer be held against gravity. Field capacity is equal to the specific retention S_r, which is defined as

$$S_r = n_e - n , \tag{4.10}$$

where n is the total porosity and n_e is the effective porosity. Representative values of n_e and n are tabulated in Sect. 4.4.2.

4.3.2 Mass Transport

The most general form of the mass transport equation is for transport in saturated-unsaturated media. If local equilibrium of mass transfer and first-order chemical reactions are assumed, sorption can be represented as a linear relationship, and the general mass transport equation can be written as (ANS 1980)

$$R_d\theta\frac{\partial c}{\partial t} - \nabla\cdot(\theta\overline{\overline{D}}\cdot\nabla c) + \nabla\cdot(\overline{V}c) + \left[R_d\frac{\partial\theta}{\partial t} + \lambda\theta R_d\right]c = 0 , \tag{4.11}$$

where

c = the concentration of dissolved constituent (g/cm^3),
$\overline{\overline{D}}$ = the dispersion tensor (cm^2/s),
$\overline{V}$ = the flux (cm/s),
λ = the radioactive decay constant:

$$\lambda = \ln 2/\text{half-life of isotope (1/s)} . \tag{4.12}$$

The term R_d is the retardation coefficient

$$R_d = \frac{n}{n_e} + \frac{\rho_b}{n_e}K_d , \tag{4.13}$$

where

n = the total porosity,
n_e = the effective porosity,
ρ_b = the bulk density (g/cm^3),
K_d = the distribution coefficient (mL/g).

More conservatively, by assuming $n = n_e$, R_d can be estimated as

$$R_d = 1 + \frac{\rho_b}{n_e} K_d . \tag{4.14}$$

An equivalent retardation factor may be defined for fracture flow where the exposed area of the fracture is used rather than the porosity (Freeze and Cherry 1978).

Example 4.2. Calculate the retardation coefficient, R_d, for strontium in an "average" fine sandstone with a bulk density, ρ_b, of 2.8 g/cm^3 and a distribution coefficient of 20 mL/g.

The arithmetic mean values of n, n_e are found from Tables 4.3 and 4.4 to be 0.34 and 0.21 respectively. The retardation coefficient, R_d, calculated from Eq. 4.13 is therefore

$$R_d = \frac{0.34}{0.21} + \frac{2.8}{0.21} \times 20 = 268.3 .$$

Equation 4.14 gives

$$R_d = 1 + \frac{2.8}{0.21} \times 20 = 267.7 .$$

[End of Example 4.2]

For the important case when the medium is assumed to be fully saturated, the mass transport equation becomes

$$R_d \frac{\partial c}{\partial t} - \nabla \cdot (\overline{\overline{D}} \cdot \nabla c) + \nabla \cdot \left(\frac{\overline{V} c}{n} \right) + \lambda R_d C = 0 . \tag{4.15}$$

If the dispersion tensor is assumed to be homogeneous and isotropic and the flux is assumed to be parallel to the x-axis, Eq. 4.15 can be written as

$$R_d \frac{\partial c}{\partial t} - \nabla \cdot (\overline{\overline{D}} \cdot \nabla c) + \frac{\overline{V}}{n} \cdot \nabla c + \lambda R_d c = 0 . \tag{4.16}$$

When the fluid flux is assumed to be uniform and steady, Eq. 4.16 becomes

$$\frac{\partial c}{\partial t} - \frac{D_x}{R_d} \frac{\partial^2 c}{\partial x^2} - \frac{D_y}{R_d} \frac{\partial^2 c}{\partial y^2} - \frac{D_z}{R_d} \frac{\partial^2 c}{\partial z^2} + \frac{U}{R_d} \frac{\partial c}{\partial x} + \lambda c = 0 , \tag{4.17}$$

where U is the pore velocity defined by Eq. 4.8a and D_x, D_y, and D_z are the dispersion coefficients in the x, y, and z directions respectively (cm^2/s), as described in Sect. 4.4.1.

The approximate rate of movement of the radionuclide is U/R_d, which may be used to estimate the travel time.

The above equations are strictly valid only for isotropic media (i.e., media whose hydraulic conductivity is uniform in all directions) but may be applied to slightly anisotropic formations when the dispersivities are obtained from field studies.

4.3.3 Chain Decay of Radionuclides

Radionuclides decay either to stable products or to another radioactive species called a daughter. In some species several daughter products may be produced before the parent species decays to a stable element. This process is particularly important for modeling actinides and transuranics. In considering this process over the transport path of radionuclides, one transport equation must be written for each original species and each daughter product to yield the concentration of each radionuclide (original species and daughter products) at points of interest along the flow path. In a constant one-dimensional velocity field, the general equations can be written as (Burkholder and Rosinger 1980)

$$\begin{aligned}
R_{d1}\frac{\partial c_1}{\partial t} + U\frac{\partial c_1}{\partial x} &= D_x\frac{\partial^2 c_1}{\partial x^2} - R_{d1}\lambda_1 c_1 \ , \\
R_{d2}\frac{\partial c_2}{\partial t} + U\frac{\partial c_2}{\partial x} &= D_x\frac{\partial^2 c_2}{\partial x^2} - R_{d2}\lambda_2 c_2 + R_{d1}\lambda_1 c_1 \ , \\
R_{di}\frac{\partial c_i}{\partial t} + U\frac{\partial c_i}{\partial x} &= D_x\frac{\partial^2 c_i}{\partial x^2} - R_{di}\lambda_i c_i + R_{d,i-1}\lambda_{i-1} c_{i-1} \ ,
\end{aligned} \tag{4.18}$$

where

R_{di} = the retardation factor for species i,
U = the pore velocity = V_x/n_e,
c_i = the concentration of species i,
D_x = the dispersion coefficient,
λ_i = the decay coefficient for species i.

Equation 4.18 describes the material balances of the ith member of a decay chain and all preceding chain members.

Analytical models incorporating chain decay with different sorption properties for each daughter are available for up to a three-component chain (Burkholder and Rossinger 1980). A simpler analytical formulation applies if all daughters are assumed to have equal sorption properties. The concentration c_i of the ith daughter in terms of the parent concentration is

$$c_i = \frac{\lambda_i c_1}{\lambda_1}\prod_{m=1}^{i-1}\lambda_m \sum_{j=1}^{i}\frac{e^{-\lambda_j t}}{\prod_{k\neq j}^{i}(\lambda_k - \lambda_j)} . \tag{4.19}$$

For long chain decays with sorption considerations, numerical solutions are practically mandatory (Burkholder and Rosinger 1980; Dillon et al. 1979).

4.3.4 Percolation of Water into the Ground

An important part of the analysis of the migration of contaminants in groundwater is the determination of the rate of release of the contaminant at the source (e.g., leaching of low-level waste) and determining the speed of transport of the groundwater. Both of these aspects of the migration problem frequently involve knowing the rate at which water infiltrates the ground either from a surface water body such as a river or pond or directly from rainfall (percolation). Infiltration is most important for shallow land burial but less important for a deep repository not affected by local recharge. For example, the source of radioactive contamination at a low-level waste site may be limited by the amount of rainfall that penetrates the land surface and comes in contact with the buried waste. The flow of groundwater in the water table aquifer is directly related to the rate at which surface water recharges it. This rate of infiltration of rainwater may be an important boundary condition for shallow land burial problems (Aikens et al. 1979).

Percolation of rainwater is frequently estimated by calculating the water budget for the root zone. Water enters the root zone through infiltration from rainfall and is removed by the evaporation directly from the surface, by transpiration from vegetation, and by seepage vertically to the water table. Both rigorous (Gupta et al. 1978) and empirical (Thornthwaite et al. 1957) methods of performing a water budget are in common use. These methods can be found in standard hydrology textbooks along with coefficients that apply to a variety of soil and vegetation types and climates (Chow 1964).

4.4 PARAMETERS FOR TRANSPORT AND FLOW EQUATIONS

4.4.1 Dispersion and Diffusion in Porous Media

4.4.1.1 Molecular Diffusion

Dispersion in Eq. 4.11 is actually a combination of molecular diffusion and mechanical dispersion, which are processes that irreversibly distribute dissolved constituents within porous media. Molecular diffusion results from the random movement of molecules at a very small scale. Diffusion within fluids depends on fluid properties such as temperature, concentration, and viscosity as well as temperature and concentration gradients. In a one-dimensional, nonflowing diffusion process, transport due to diffusion is usually related to Fick's law:

$$\frac{\partial c}{\partial t} = \frac{\partial}{\partial x} D' \frac{\partial c}{\partial x} , \tag{4.20}$$

where D' is the effective diffusion coefficient for porous media, which typically varies from about 10^{-5} to 10^{-8} cm^2/s. The effective diffusion coefficient D' will be lower than the molecular diffusion coefficient in a free liquid because diffusion will be inhibited by the pore structure (Evanson and Dettinger 1980).

4.4.1.2 Dispersion

Dispersion describes the mechanical mixing of dissolved constituents by the complex flow paths the fluid must take in the porous medium. Variability of path length and velocity from the mean results in longitudinal and lateral spreading of the dissolved constituents.

Laboratory investigations have shown that in porous media, longitudinal dispersion is related to the seepage velocity. For an isotropic medium, the dispersion coefficients D_{ij} can be described in terms of the longitudinal and transverse dispersivity (Scheidegger 1961):

$$\theta D_{ij} = \alpha_T V \delta_{ij} + (\alpha_L - \alpha_T) V_i V_j / V , \qquad (4.21)$$

where

δ_{ij} = 1 for $i = j$, $\delta_{ij} = 0$ for $i \neq j$ (Kronecker delta function),

θ = the volumetric water content,

α_T = the transverse dispersivity (cm),

α_L = the longitudinal dispersivity (cm),

V = the magnitude of the flux (cm/s),

V_i, V_j = the components of the flux (cm/s).

Even in small-scale laboratory experiments in uniform porous media, dispersion processes usually dominate the diffusion processes. Dispersion depends on flow, however. For very low flow rates, molecular diffusion, which is independent of flow, may dominate the diffusion.

4.4.1.3 Macrodispersion

Experiments with packed laboratory columns generally yield dispersivities having dimensions on the order of the median grain diameter, ranging from millimeters to centimeters. If the dispersivities measured in the laboratory were used in a transport model for a large aquifer, dispersion would be grossly underpredicted. At the aquifer scale, it appears that the heterogeneities in permeability, fracturing, stratification and other properties of the medium, sampling errors and model approximations are more important to producing dispersive behavior than mixing around individual grains and pores in the laboratory-scale experiments (Evenson and Dettinger 1980; Anderson 1979).

Field studies tend to support the hypothesis that macrodispersion is largely a result of heterogeneity in hydraulic conductivity. Dispersivity also apparently increases with the length scale of the experiment. There is a tendency for large dispersivities to coincide with experiments involving large distances.

The Fickian analogy for dispersion (Eq. 4.20) does not always behave satisfactorily, and the dispersion cannot be characterized with a parameter as simple as the dispersivity. The assumptions of homogeneity of the medium break down if the heterogeneities are not random or if they are large in comparison to the aquifer being modeled (Winograde and Pearson 1976).

The cases in which the simple dispersion models are likely to fail are

1. Media in which a few extensive conductivity variations dominate the transport process.
2. Media in which conductivity variations are abrupt, severe, and tend to follow well-defined paths.
3. Observations that are made on a scale that is small compared to the scale of the variation.
4. Media that show variations in conductivity that cannot be modeled as a random field with apparently random values, spatial extents, and orientation assumed by the aquifer properties (Evenson et al. 1980).

These phenomena have been described generically as "channeling." Evenson et al. (1980) suggest that media in which these phenomena are likely to occur (fracture systems, karst, etc.) should not be modeled according to Fick's law without extensive justification. Models capable of dealing with these problems are extremely complex and beyond the scope of this book (Evenson et al. 1980).

4.4.1.4 Determination of Dispersion

It is frequently the case that the only way the values of dispersion coefficients can be determined for a given site is by direct observation of either man-made or naturally occurring tracers. Tracers that have been deliberately introduced are used in groundwater studies in single- or double-well pumping experiments over relatively short distances and times. Direct tracer methods have several disadvantages in groundwater studies:

1. Because groundwater velocities are rarely large under natural conditions, undesirably long times are normally required for tracers to move significant distances through the flow system. For this reason, only small, nonrepresentative portions of the flow field can be measured.
2. Because geological materials are typically quite heterogeneous, numerous observations are usually required to adequately monitor the passage of the tracer through the portion of the flow field under investigation. The measurements themselves may actually disturb the flow field significantly.

Values of dispersivities obtained from a wide range of tracer experiments and also those based on numerical models of observed groundwater solute transport cases are presented in Tables 4.1 and 4.2, respectively. (Anderson 1979; Evenson and Dettinger 1980). These values represent site-specific cases and should be extrapolated to other cases only with extreme caution. Furthermore, the dispersivities reported in Table 4.2 probably reflect processes, such as numerical dispersion, that are inaccuracies of the mathematical model and are not measured in nature.

4.4.2 Porosity and Effective Porosity

The parameters *porosity* and *effective porosity* (or *specific yield*) are necessary for the solution of the flow and solute transport equations. The porosity of a soil or rock is a measure of the interstitial space relative to the space occupied by solid material and is expressed quantitatively as the percentage of the total volume occupied by the interstices.

The porosity of a sedimentary deposit depends chiefly on the shape and arrangement of its constituent particles, the degree of assortment of its particles, the cementation and compaction to which it has been subjected, the dissolution of mineral matter by water, and the fracturing resulting in open joints other than interstices. The porosity of many sedimentary deposits is increased by the irregular angular shapes of its grains. Porosity decreases with increases in the variety of size of grains because small grains fill interstices between larger grains. Table 4.3 gives representative values of porosity for a wide range of soils and rocks.

The effective porosity is the portion of the porosity that can be considered to be available for the flow of groundwater through a porous medium. Not all of the water in the interstices of saturated rock or soil is available for flow. Part of the water is retained in the interstices by the forces of molecular attraction or is trapped in dead-end pores. The amount of water trapped is greatest in media having small interstices. Table 4.4 gives representative values of effective porosity for a wide range of soils and rocks.

4.4.3 Hydraulic Conductivity for Saturated Flow

The hydraulic conductivity, K, for an isotropic, homogeneous saturated medium determines the rate at which water moves through the porous medium for a given hydraulic gradient. Hydraulic conductivity is a property that depends on the properties of both the fluid and the medium and has units of velocity (cm/s). A measure of the hydraulic conductivity, which is a property of the porous medium alone, is the intrinsic permeability k, that has units of length squared and is usually expressed in darcys (one darcy $= 9.87 \times 10^{-9}$ cm^2).

Table 4.1. Dispersivity values α_L and α_T obtained directly through measurements of tracer breakthrough curves in groundwater solute transport

Setting	α_L (m)	α_T (m)	Δx^a (m)	$\bar{U}^b$ (m/d)	Method
Chalk River, Ontario alluvial aquifer	0.034				Single-well tracer test
Chalk River, strata of high velocity	0.034–0.1				Single-well
Alluvial aquifer	0.5				Two-well
Alluvial, strata of high velocity	0.1				Two-well
Lyons, France alluvial aquifer	0.1–0.5				Single-well
Lyons (full aquifer)	5				Single-well
Lyons (full aquifer)	12.0	3.1–14		7.2	Single-well test with resistivity
Lyons (full aquifer)	8	0.015–1		9.6	Single-well test with resistivity
Lyons (full aquifer)	5	0.145–14.5		13	Single-well test with resistivity
Lyons (full aquifer)	7	0.009–1		9	Single-well test with resistivity
Alsace, France alluvial sediments	12	4			Environmental tracer
Carlsbad, N. Mex. fractured dolomite	38.1		38.1	0.15	Two-well tracer
Savannah River, S.C. fractured schistgneiss	134.1		538	0.4	Two-well
Barstow, Calif. alluvial sediments	15.2		6.4		Two-well
Dorset, England					
chalk (fractured)	3.1		8		Two-well
(intact)	1.0		8		Two-well
Berkeley, Calif. sand/gravel	2–3		8	311–1382	Multiwell trace test
Mississippi limestone	11.6				Single-well
NTS, carbonate aquifer	15				Two-well tracer
Pensacola, Fla. limestone	10		312	0.6	Two-well

[a] Δx = distance between wells in two-well test.

[b] $\bar{U}$ = groundwater seepage velocity.

Source: Evenson, D. E., and Dettinger, M. D. 1980. *Dispersive Processes in Models of Regional Radionuclide Migration,* University of California, Lawrence Livermore Laboratory, Livermore.

Table 4.2. Dispersivity values α_L and α_T obtained by calibration of numerical transport models against observed groundwater solute transport

Setting	α_L (m)	α_T (m)	Δx^a (m)	$\bar{U}^b$ (m/d)	Method[c]
Rocky Mtn. Arsenal alluvial sediments	30.5	30.5	305		Areal (moc)
Arkansas River Valley coalluvial sediments	30.5	9.1	660×1320		Areal (moc)
California alluvial sediments	30.5	9.1	305		Areal
Long Island glacial deposits	21.3	4.3	Variable (50–300)	0.4	Areal (fe)
Brunswick, Ga. limestone	61	20	Variable		Areal (moc)
Snake River, Idaho fractured basalt	91	136.5	640		Areal
Idaho, fractured basalt	91	91	640		Areal (fe)
Hanford site, Wash. fractured basalt	30.5	18			Areal (rw)
Barstow, Calif. alluvial deposits	61	18	305		Areal (fe)
Roswell Basin, N. Mex. limestone	21.3				Areal
Idaho Falls, lava flows and sediments	91	137	Variable		Areal
Barstow, Calif. alluvial sediments	61	0.18	3×152		Profile (fe)
Alsace, France alluvial sediments	15	1			Profile
Florida (SE) limestone	6.7	0.7	Variable		Profile
Sutter Basin, Calif. alluvial sediments	80–200	8–20	(2–20 km)		3-D (fe)

[a] Δx = grid size in program.

[b] $\bar{U}$ = groundwater seepage velocity.

[c] (fe) indicates use of a finite-element model; (moc) indicates method of characteristics; and (rw) indicates a random-walk model.

Source: Evenson, D. E., and Dettinger, M. D. 1980. *Dispersive Processes in Models of Regional Radionuclide Migration,* University of California, Lawrence Livermore Laboratory, Livermore.

Table 4.3. Typical values of porosity of aquifer materials

Aquifer material	Number of analyses	Range	Arithmetic mean
Igneous Rocks			
Weathered granite	8	0.34–0.57	0.45
Weathered gabbro	4	0.42–0.45	0.43
Basalt	94	0.03–0.35	0.17
Sedimentary Materials			
Sandstone	65	0.14–0.49	0.34
Siltstone	7	0.21–0.41	0.35
Sand (fine)	245	0.25–0.53	0.43
Sand (coarse)	26	0.31–0.46	0.39
Gravel (fine)	38	0.25–0.38	0.34
Gravel (coarse)	15	0.24–0.36	0.28
Silt	281	0.34–0.51	0.45
Clay	74	0.34–0.57	0.42
Limestone	74	0.07–0.56	0.30
Metamorphic Rocks			
Schist	18	0.04–0.49	0.38

Source: McWhorter, D. B., and Sunada, D. K. 1977. *Ground-Water Hydrology and Hydraulics,* Water Resources Publications, Fort Collins, Colo. Reprinted with permission.

Hydraulic conductivity, K, and intrinsic permeability, k, are generally related by the equation

$$K = \frac{kg\rho}{\mu}, \tag{4.22}$$

where g is the acceleration of gravity, ρ is the density of the fluid, and μ is the viscosity of the fluid. Table 4.5 gives representative values of hydraulic conductivity in centimeters per second for a sample of common porous materials (McWhorter and Sunada 1977).

Environmental factors may affect the hydraulic conductivity of a given porous medium. For example, ion exchange on clay and colloid surfaces will cause changes in mineral volume and pore size and shape. Changes in pressure may cause compaction of the material or may cause gases to come out of solution, which would reduce the hydraulic conductivity (Davis and De Wiest 1965).

4.4.4 Adsorption and Retardation Coefficients

An important mechanism in retarding the migration of radionuclides in groundwater is sorption, which is defined to include all rock-water interactions

Table 4.4. Typical values of effective porosity (or specific yield) of aquifer materials

Aquifer material	Number of analyses	Range	Arithmetic mean
Sedimentary Materials			
Sandstone (fine)	47	0.02–0.40	0.21
Sandstone (medium)	10	0.12–0.41	0.27
Siltstone	13	0.01–0.33	0.12
Sand (fine)	287	0.01–0.46	0.33
Sand (medium)	297	0.16–0.46	0.32
Sand (coarse)	143	0.18–0.43	0.30
Gravel (fine)	33	0.13–0.40	0.28
Gravel (medium)	13	0.17–0.44	0.24
Gravel (coarse)	9	0.13–0.25	0.21
Silt	299	0.01–0.39	0.20
Clay	27	0.01–0.18	0.06
Limestone	32	~0–0.36	0.14
Wind-Laid Materials			
Loess	5	0.14–0.22	0.18
Eolian Sand	14	0.32–0.47	0.38
Tuff	90	0.02–0.47	0.21
Metamorphic Rock			
Schist	11	0.22–0.33	0.26

Source: McWhorter, D. B., and Sunada, D. K. 1977. *Ground-Water Hydrology and Hydraulics,* Water Resources Publications, Fort Collins, Colo. Reprinted with permission.

that cause the radionuclides to migrate at a slower rate than the groundwater itself. The amount of sorption is dependent on both the chemistry of the water and of the rocks; and, because some of the chemical reactions are slow, it is a function of time as well.

Values of sorption coefficients are required to calculate the travel time of key radionuclides from the source to the biosphere. The sorption coefficients are usually obtained using a standard batch test where rocks are put in contact with groundwater in which small amounts of radionuclides have been mixed. The problem with this type of approach is that more detailed geochemical data are necessary to support the validity of the sorption measurement over the expected travel time of the radionuclides (which may be of the order of thousands of years). To provide the justification for using simple sorption coefficients, a detailed understanding of the geochemical mechanisms of rock-water interactions must be attained. Such mechanisms as dissolution/precipitation, complexing, adsorption/desorption, phase transformations, and solubility should be understood for radionuclides of interest in the geochemical

Table 4.5. Typical values of hydraulic conductivity of porous materials

Material	Number of analyses	Range (cm/s)	Arithmetic mean (cm/s)
Igneous rocks			
Weathered granite	7	$(3.3–52) \times 10^{-4}$	1.65×10^{-3}
Weathered gabbro	4	$(0.5–3.8) \times 10^{-4}$	1.89×10^{-4}
Basalt	93	$(0.2–4250) \times 10^{-8}$	9.45×10^{-6}
Sedimentary materials			
Sandstone (fine)	20	$(0.5–2270) \times 10^{-6}$	3.31×10^{-4}
Siltstone	8	$(0.1–142) \times 10^{-8}$	1.9×10^{-7}
Sand (fine)	159	$(0.2–189) \times 10^{-4}$	2.88×10^{-3}
Sand (medium)	255	$(0.9–567) \times 10^{-4}$	1.42×10^{-2}
Sand (coarse)	158	$(0.3–6610) \times 10^{-4}$	5.20×10^{-2}
Gravel	40	$(0.3–31.2) \times 10^{-1}$	4.03×10^{-1}
Silt	39	$(0.09–7090) \times 10^{-7}$	2.83×10^{-5}
Clay	19	$(0.1–47) \times 10^{-8}$	9×10^{-8}
Metamorphic rocks			
Schist	17	$(0.002–1130) \times 10^{-6}$	1.9×10^{-4}

Source: McWhorter, D. B., and Sunada, D. K. 1977. *Ground-Water Hydrology and Hydraulics,* Water Resources Publications, Fort Collins, Colo. Reprinted with permission.

environment. The effect of heat, radiation, or high concentrations of chemicals will be particularly important close to the source of release in some situations. Much of this understanding for shorter periods of time and close to the points of release can be obtained through a combination of laboratory and field experiments combined with data from natural systems that can be used as analogs. However, over longer time periods or far from the points of release, all of the data must be obtained from studies of the natural system.

Natural analogs of interest for application to radionuclide migration include hydrothermal ore deposits, intrusive magmas into generic host rocks, uranium ore bodies, rich thorium deposits, natural fission reactors, and underground nuclear explosions (Klingsberg and Duguid 1979). Also, the behavior of natural radionuclides and their decay products in host rock formations can provide the data necessary to choose conservative sorption coefficients for use in the transport models are conservative over the range of geochemical conditions and the transport travel times expected.

Tables 4.6 and 4.7 give typical ranges of distribution coefficients (K_d) for several significant randionuclides in an assortment of rocks and soils (Isherwood 1981). These tables illustrate some of the sensitivity of K_d to

Table 4.6. Distribution coefficients: strontium and cesium

	K_d (mL/g)	
	Sr	Cs
Basalt, 32–80 mesh	16–135	792–9520
Basalt, 0.5–4 mm, 300 ppm TDS	220–1220	39–280
Basalt—0.5–4 mm, sea water	1.1	6.5
Basalt-fractured in situ measurement	3	
Sand, quartz—pH 7.7	1.7–3.8	22–314
Sands	13–43	100
Carbonate, greater than 4 mm	0.19	13.5
Dolomite, 4000 ppm TDS	5–14	
Granite, greater than 4 mm	1.7	34.3
Granodiorite, 100–200 mesh	4–9	8–9
Granodiorite, 0.5–1 mm	11–23	1030–1810
Hanford sediments	50	300
Tuff	45–4000	800–17800
Soils	19–282	189–1053
Shaley siltstone greater than 4 mm	8	309
Shaley siltstone greater than 4 mm	1.4	102
Alluvium, 0.5–4 mm	48–2454	121–3165
Salt, greater than 4 mm saturated brine	0.19	0.027

Source: Isherwood, D. 1981. *Geoscience Data Base Handbook for Modeling a Nuclear Waste Repository*, NUREG/CR-0912, vols. 1 and 2, U.S. Nuclear Regulatory Commission.

factors such as particle size and chemistry of the water phase. Values of K_d should be extrapolated to situations other than those for which they were determined only with extreme caution.

4.5 METHODS OF SOLUTION FOR GROUNDWATER MOVEMENT

4.5.1 Introduction

Over the past several years, numerous mathematical models have been developed to simulate the flow of groundwater and the transport of radioactive and chemical substances, particularly in the field of waste management. Discussion of the virtually hundreds of groundwater models is beyond the scope of this chapter, but two excellent compilations of groundwater models are available (Bredehoeft 1978; SAI 1981).

Groundwater mathematical models can be broadly classified as either numerical or analytical. Numerical techniques are usually direct solutions of

Table 4.7. Distribution coefficients: thorium and uranium

K_d (mL/g)	Conditions
	Thorium
160,000	Silt loam, Ca-saturated clay, pH 6.5
400,000	Montmorillonite, Ca-saturated clay, pH 6.5
160,000	Clay soil, 5 m*M* $Ca(NO_3)_2$, pH 6.5
40–130	Medium sand, pH 8.15
310–470	Very fine sand, pH 8.15
270–10,000	Silt/clay, pH 8.15
8	Schist soil, 1 g/L Th, pH 3.2
60	Schist soil, 0.1 g/L Th, pH 3.2
120	Illite, 1 g/L Th, pH 3.2
1000	Illite, 0.1 g/L Th, pH 3.2
<100,000	Illite, 0.1 g/L Th, pH >6
	Uranium
62,000	Silt loam, U(VI), Ca-saturated, pH 6.5
4400	Clay soil, U(VI), 5 m*M* $Ca(NO_3)_2$, pH 6.5
300	Clay soil, 1 ppm UO^{+2}, pH 5.5
2000	Clay soil, 1 ppm UO^{+2}, pH 10
270	Clay soil, 1 ppm UO^{+2}, pH 12
4.5	Dolomite, 100–325 mesh, brine, pH 6.9
2.9	Limestone, 100–170 mesh, brine, pH 6.9

Source: Isherwood, D. 1981. *Geoscience Data Base Handbook for Modeling a Nuclear Waste Repository,* NUREG/CR-0912, vols. 1 and 2, U.S. Nuclear Regulatory Commission.

the differential equations describing water movement and solute transport, using methods such as finite differences or finite elements. These methods always require a digital computer, a large quantity of data, and an experienced modeler-hydrologist. The validity of the results from numerical models depends strongly on the quality and quantity of the input parameters. Analytical models are usually approximate or exact solutions to simplified forms of the differential equations for water movement and solute transport. Such models are simpler to use than numerical models and can generally be solved with the aid of a calculator, although computers are also used. Analytical models are much more severely limited to simplified representations of the physical situations. However, they are extremely useful for scoping the problem to determine data needs or the applicability of more detailed numerical models.

Several of the more important types of numerical and analytical models are discussed below.

4.5.2 Numerical Methods

4.5.2.1 Finite Difference

One approach that has been applied to the solution of groundwater equations involves finite-difference approximations. To apply these approximations, the region under consideration is usually divided into a rectangular grid. The intersections of the grid are called nodal points and represent the position at which the solution for unknown values such as hydraulic head are obtained. When difference equations are written for all nodes and boundary conditions are applied, a system of n algebraic equations in n variables can be solved for the variables at each node for each time increment (Faust and Mercer 1980).

4.5.2.2 Finite Element

The finite-element method is a numerical method where a region is divided into subregions, called elements, whose shapes are determined by a set of points called nodes (similar to the finite-difference grid). The first step is to derive an integral representation of the partial differential equations. This is commonly done by using the method of weighted residuals or the variational method. The next step is to approximate the dependent variables (head or concentration) in terms of interpolation functions called basis functions.

Once the basis functions are specified and the elements defined, the integral relationship must be expressed for each element as a function of the coordinates of all nodal points of the element. Then the values of the integrals are calculated for each element. The values for all elements are combined and boundary conditions applied to yield a system of first-order linear differential equations in time (Faust and Mercer 1980).

4.5.2.3 Method of Characteristics

The method of characteristics is used in convection-dominated transport problems where finite-difference and finite-element approaches suffer from "numerical dispersion" or solutions that oscillate. The approach is not to solve the transport equations directly but to solve an equivalent system of ordinary differential equations that are obtained by rewriting the transport equation using the fluid particles as a reference point. This is accomplished numerically by introducing a set of moving points (reference particles) that can be traced within the stationary coordinates of a finite-difference grid block and allowed to move a distance proportional to the velocity and elapsed time. The moving particles simulate the convective transport because concentration is a function of spreading or convecting of the particles. Once the convective effects are known, the remaining parts of the transport equation are solved using finite-difference approximations (Faust and Mercer 1980).

4.5.2.4 Random-Walk Method

A method similar in many ways to the method of characteristics is the random-walk method. In this approach, a particle-tracing advection model is used to simulate advection. At the end of each advection time step, the particles are dispersed by being displaced a random distance in a random direction. Concentrations are calculated by counting the resulting number of elements in each cell and comparing this to the initial conditions. This solution technique is based on the realization that a normal probability distribution is a solution to Fick's Law of diffusion. This method of transport modeling is easily implemented and provides simulations whose accuracy are limited only by the number of particles that can be traced. The main disadvantage of this method and the method of characteristics is the difficulty and expense of keeping track of large numbers of particles (Evenson and Dettinger 1980).

4.5.2.5 Flow Network Models

The numerical simulation by finite differences or finite elements of groundwater flow and solute transport problems in two and three dimensions can be costly in terms of computational resources. Flow network models such as the network flow and transport model (NWFT) (Campbell et al. 1980) are those that can be used to describe two- or three-dimensional fields in a much more efficient way by a network of interconnecting one-dimensional flow segments. Fluid discharge and velocity are determined by requiring conservation of mass at the segment junctions. Radionuclide migration from the points of release is calculated by assuming that transport occurs along a single one-dimensional path having a length equal to the total migration path length. The network model is particularly useful when it is used in conjunction with a more complicated two- or three-dimensional model to first define the flow and concentration field for a particular example. The network model is first matched or tuned to the results of the complicated model. The tuned network model may then be used for further computations with a much smaller commitment of computational resources then the original model for further runs and sensitivity experiments.

4.5.2.6 Advection Models

There are groundwater solute modeling situations where the phenomenon of dispersion, together with its many uncertainties, is only a minor factor in describing the transport of contaminants in groundwater. For example, the flux of contaminant entering a river that is recharged from a contaminated aquifer is much less sensitive to dispersion than the concentration in a particular well. In the former case, the contaminated groundwater would enter over a wide area, which would tend to smear out the effect of dispersion. For similar reasons, the transport from nonpoint sources of contamination such as large

low-level radioactive waste landfills would diminish the sensitivity of modeled results to dispersion. A flow model can be used to generate a velocity potential field and stream lines. The flow patterns from the sources to the sinks can then be used to formulate the arrival time distribution, which can be used to calculate the concentration of flux of a contaminant at the point of use. Either numerical or analytical solutions of the flow equations are used to estimate groundwater velocities, the length of the path of a contaminant, and the arrival time distribution (Nelson 1978).

4.5.3 Analytical Models

Analytical groundwater transport models can be used for certain types of analyses where available data do not warrant a more complicated study. Such models are useful for scoping the transport problem and may frequently be adequate for regulatory needs if model coefficients are chosen conservatively.

A series of simple analytical models that have been used at the U.S. Nuclear Regulatory Commission (NRC) is presented below. Many of these models have been computerized and are available from the NRC (Codell et al. 1982). In their simplest forms, however, they may be used with the aid of only a calculator.

The models are developed for the limiting case of undirectional saturated convective transport of a single dissolved substance with three-dimensional dispersion in an isotropic aquifer as discussed in Sect. 4.3.2:

$$\frac{\partial c}{\partial t} + \frac{U}{R_d}\frac{\partial c}{\partial x} = \frac{D_x}{R_d}\frac{\partial^2 c}{\partial x^2} + \frac{D_y}{R_d}\frac{\partial^2 c}{\partial y^2} + \frac{D_z}{R_d}\frac{\partial^2 c}{\partial z^2} - \lambda c \ , \qquad (4.23)$$

where

c is the concentration in the liquid phase (Ci/cm^3),
D_x, D_y, D_z are the dispersion coefficients in the x, y, and z directions respectively (cm^2/s),
λ is the decay coefficient = ln 2/half-life (1/s),
U is the x component groundwater pore velocity (cm/s),
R_d is the retardation coefficient (dimensionless).

The dispersion coefficient can be approximated from Eq. 4.21. In this case $V_2 = V_3 = 0$, $V_1 = V$, and θ can be approximated for saturated flow by the effective porosity, n_e. Also, since $U = V/n_e$,

$$D_x = \alpha_L U \qquad (4.23a)$$

$$D_y = \alpha_T U \qquad (4.23b)$$

$$D_z = \alpha_T U \ , \qquad (4.23c)$$

where α_L and α_T are the longitudinal and transverse dispersivities respectively.

4.5.3.1 Point Concentration Model

The first model developed is used for calculating the concentration in the aquifer at some point downgradient of a release (e.g., water supply well).

Equation 4.23 is solved in terms of Green's functions:

$$c_i = \frac{1}{n_e R_d} X(x,t) Y(y,t) Z(z,t) , \tag{4.24}$$

where c_i is the concentration at any point in space for an instantaneous one-curie release, n_e is the effective porosity of the medium, and X, Y, Z are the Green's functions in the x, y, z coordinate directions, respectively. Equation 4.24 has been developed for a variety of boundary and source configurations:

1. For the case of a point source at $(0, 0, z_s)$ in an aquifer of infinite lateral (x, y) extent and depth b, as illustrated in Fig. 4.2,

$$c_i = \frac{1}{n_e R_d} X_1 Y_1 Z_1 , \tag{4.25}$$

where

$$X_1 = \frac{1}{\sqrt{4\pi D_x t/R_d}} \exp\left[- \frac{(x - Ut/R_d)^2}{4D_x t/R_d} - \lambda t \right] , \tag{4.26}$$

$$Y_1 = \frac{1}{\sqrt{4\pi D_y t/R_d}} \exp\left(- \frac{y^2}{4D_y t/R_d} \right) , \tag{4.27}$$

$$Z_1 = \frac{1}{b}\left\{ 1 + 2 \sum_{m=1}^{\infty} \exp\left(- \frac{m^2 \pi^2 D_z t}{b^2 R_d} \right) \cos m\pi \frac{z_s}{b} \cos m\pi \frac{z}{b} \right\} ; \tag{4.28}$$

2. For the vertically averaged concentration in case 1 above (equivalent to a vertical line source of length b),

$$c_i = \frac{1}{n_e R_d} X_1 Y_1 Z_2 , \tag{4.29}$$

where

$$Z_2 = \frac{1}{b} ; \tag{4.30}$$

3. For a horizontal line source of length w centered at $(0, 0, z_s)$, as illustrated in Fig. 4.3,

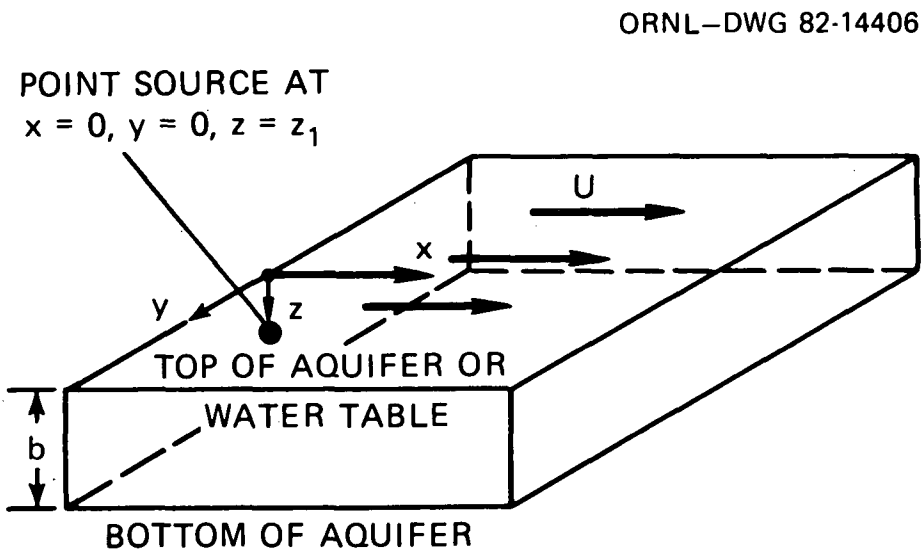

Figure 4.2. Idealized groundwater system for point concentration model, point source.

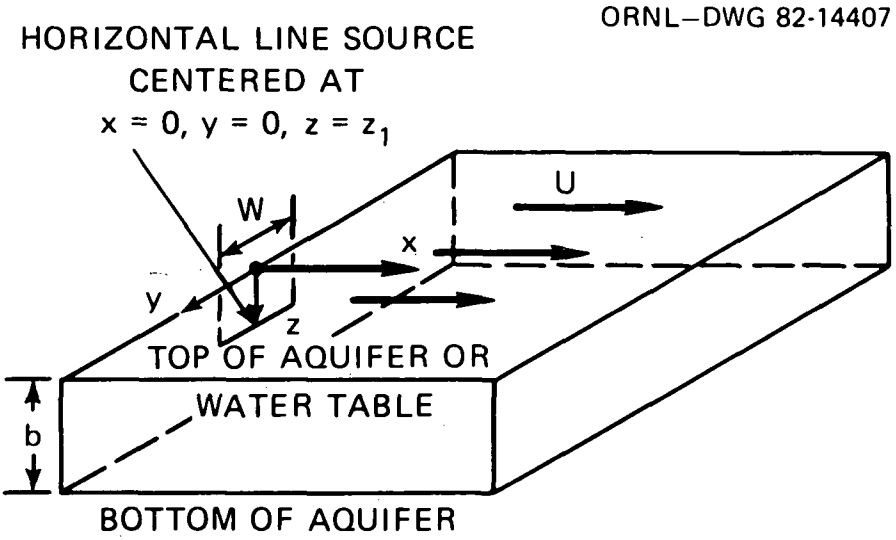

Figure 4.3. Idealized groundwater system for point concentration model, horizontal line source.

$$c_i = \frac{1}{n_e R_d} X_1 Y_2 Z_1 , \tag{4.31}$$

where

$$Y_2 = \frac{1}{2w}\left\{ \operatorname{erf}\frac{(w/2+y)}{\sqrt{4D_y t/R_d}} + \operatorname{erf}\frac{(w/2-y)}{\sqrt{4D_y t/R_d}} \right\} \tag{4.32}$$

and erf is the error function. Tables of the error function are available in standard mathematical texts (Abramowitz 1970);

4. For the vertically averaged concentration in case 3 above (equivalent to an area source of width w and depth b),

$$c_i = \frac{1}{n_e R_d} X_1 Y_2 Z_2 ; \tag{4.33}$$

5. For a point source at $(0, 0, z_s)$ in an aquifer of infinite lateral extent and depth,

$$c_i = \frac{1}{n_e R_d} X_1 Y_1 Z_3 , \tag{4.34}$$

where

$$Z_3 = \frac{1}{\sqrt{4\pi D_z t/R_d}}\left\{ \exp\left[-\frac{(z-z_s)^2}{4D_z t/R_d} \right] + \exp\left[-\frac{(z+z_s)^2}{4D_z t/R_d} \right] \right\}; \tag{4.35}$$

6. For a horizontal line source of width w centered at $(0, 0, z_s)$ in an aquifer of infinite lateral extent and depth,

$$c_i = \frac{1}{n_e R_d} X_1 Y_2 Z_3 ; \tag{4.36}$$

7. For a horizontal area source of length l and width w centered at $(0, 0, 0)$ in an aquifer of constant depth b, as illustrated in Fig. 4.4, Eq. 4.24 becomes

$$c_i = \frac{1}{n_e R_d} X_2 Y_2 Z_2 , \tag{4.37}$$

where

$$X_2 = \frac{1}{2l}\left\{ \operatorname{erf}\frac{\left[x+\frac{l}{2}\right]-\frac{ut}{R_d}}{\sqrt{4D_x t/R_d}} - \operatorname{erf}\frac{\left[x-\frac{l}{2}\right]-\frac{ut}{R_d}}{\sqrt{4D_x t/R_d}} \right\} \exp(-\lambda t) . \tag{4.38}$$

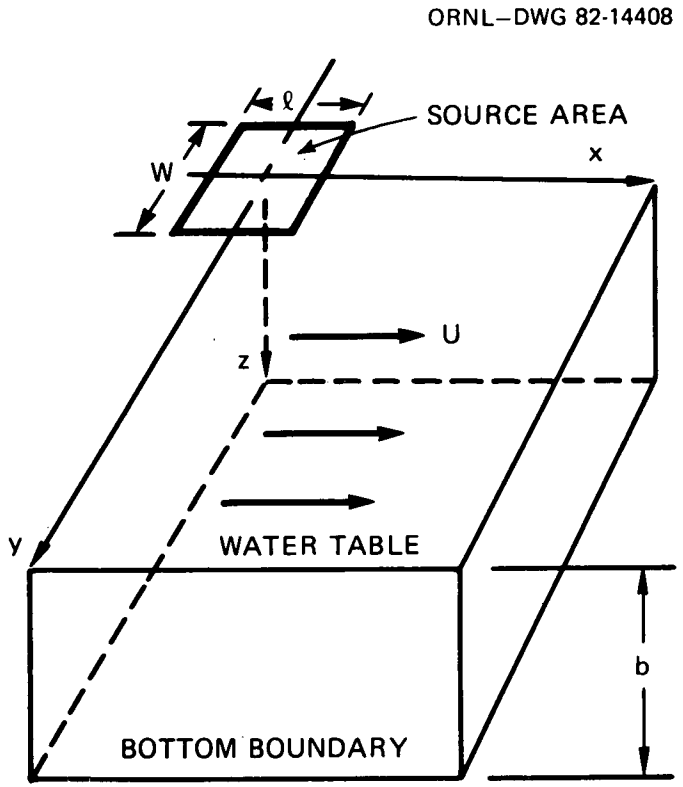

Figure 4.4. Vertically averaged groundwater dispersion model.

Example 4.3. Concentration in an aquifer of limited thickness.

One curie of a radioactive pollutant leaks quickly into a water table aquifer through a highly permeable ground cover over a square surface area 50 m on a side. The pollutant has a half-life of 30 y. A well tracer test indicates that the groundwater is moving in the direction of two wells at a speed, U, of 1.5 m/d and that the longitudinal and transverse dispersivities, α_L and α_T, are 20 to 10 m, respectively.

The saturated thickness of the water table aquifer, b, is 50 m and has an effective porosity, n_e, of 0.2. The pollutant has been determined to have a retardation coefficient, R_d, of 20 in the aquifer.

Calculate the concentration of the pollutant in wells whose downgradient coordinates with respect to the center of the source area are

(a) x = 200 m, y = 0 m
(b) x = 400 m, y = 50 m

The wells are screened over the entire depth of the aquifer.

Case 7 in Sect. 4.5.3.1 applies to this example, since the source is a horizontal area type and the wells are screened over the total depth, which would vertically average the concentration.

Equation 4.37 is therefore evaluated with Green's function:

X_2 determined by Eq. 4.38,
Y_2 determined by Eq. 4.32, and
Z_2 determined by Eq. 4.30,

The dispersion coefficients are calculated by Eqs. 4.23a and 4.23b.

$$D_x = \alpha_L U = 20 \times 1.5 = 30 \text{ m}^2$$
$$D_y = \alpha_T U = 10 \times 1.5 = 15 \text{ m}^2$$

Figure 4.5 shows the concentration as a function of time calculated for the two wells. [End of Example 4.3]

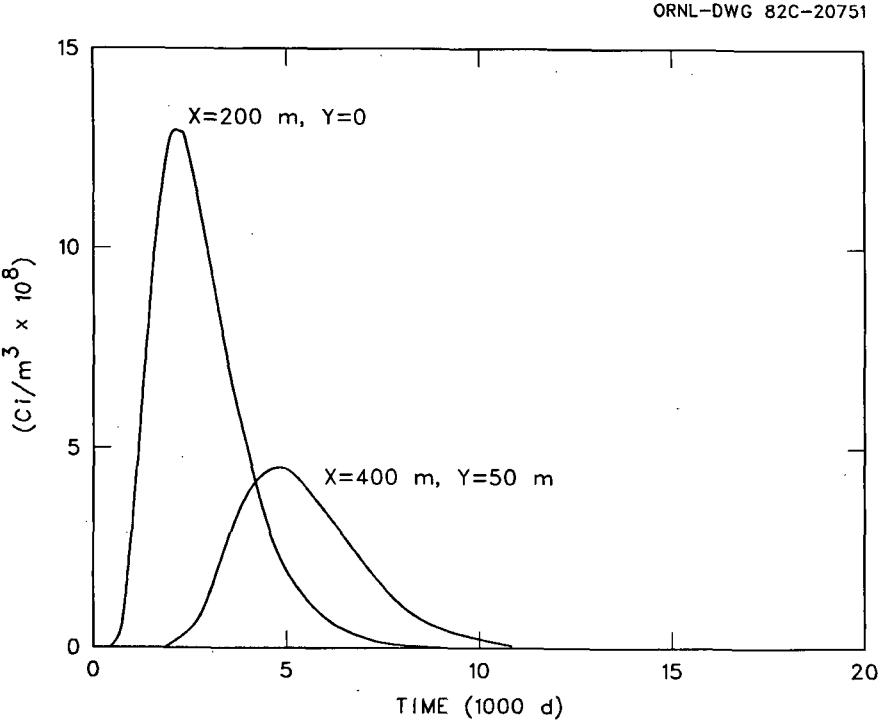

Figure 4.5. Concentration in downgradient wells for Example 4.3.

4.5.3.2 Flux Models

The flux model is used to calculate the discharge rate of a radionuclide entering a surface water body that has intercepted the aquifer containing the transported material as depicted in Fig. 4.6. It is assumed that all material

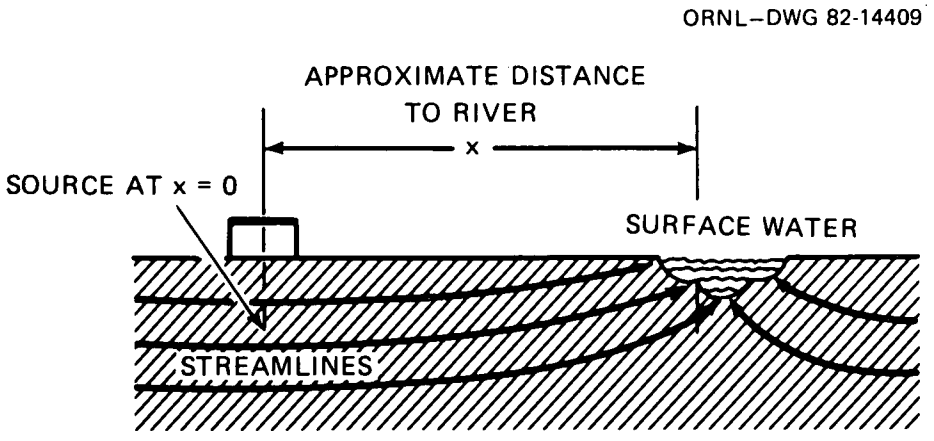

Figure 4.6. Groundwater–surface water interface, flux model.

entering the aquifer eventually enters the surface water except for that which has been lost through radioactive decay. The assumptions that apply to the point concentration model also apply to this model. The model provides only the rate of input to the surface water at an average distance x downgradient from the surface. Actually, the contamination would enter the surface water as a diffuse patch, but the model described here gives no information about the spatial distribution of this patch.

In the unidirectional flow field assumed, the flux F (Ci/s) of material crossing an area $dA = dy\ dz$ perpendicular to the x axis is described by the equation

$$\frac{dF}{dA} = \left[Uc - D_x \frac{\partial c}{\partial x}\right] n_e , \tag{4.39}$$

where c is the concentration in the dissolved phase. The total flux across the plane would be

$$F = n_e \int_0^b \int_{-\infty}^{\infty} \left(Uc - D_x \frac{\partial c}{\partial x} \right) dy\, dz \,. \tag{4.40}$$

4.5.3.3 Source Released from a Vertical Plane ($x = 0$)

If C_i is the concentration from an instantaneous release of 1 Ci at $x = 0$ and time $t = 0$, as described by Eq. 4.25, then the resulting flux at distance x downgradient would be

$$F_i = \frac{\left(x + \frac{Ut}{R_d} \right)}{4\sqrt{D_x \pi t^3 / R_d}} \exp\left[\frac{\left(x - \frac{Ut}{R_d} \right)^2}{4D_x t / R_d} - \lambda t \right]. \tag{4.41}$$

4.5.3.4 Horizontal Area Source

For conditions expressed by Eq. 4.37, the corresponding flux would be

$$F_i = \frac{1}{2\ell\sqrt{\pi D_x t / R_d}} \left[\frac{u}{R_d} \sqrt{\pi D_x t / R_d} \left[\operatorname{erf}(z_1) - \operatorname{erf}(z_2) \right] - \frac{D_x}{R_d} \left[\exp(-z_1^2) - \exp(-z_2^2) \right] \right] \cdot \exp(-\lambda t) \,, \tag{4.42}$$

where

$$z_1 = \frac{x - \frac{u}{R_d} t + \frac{\ell}{2}}{\sqrt{4D_x t / R_d}} \,, \text{ and } z_2 = \frac{x - \frac{u}{R_d} t - \frac{\ell}{2}}{\sqrt{4D_x t / R_d}} \,.$$

Example 4.4. For the same conditions in the previous example (Sect. 4.5.3.1), calculate the flux of the pollutant into a river intercepting the groundwater flow, which is a distance x of 2000 m downgradient from the center of the source.

Equation 4.42 applies in this case. Figure 4.7 shows the flux into the river as a function of time. [End of Example 4.4]

4.5.3.5 Generalization of Instantaneous Models

Equations 4.8 and 4.23 are formulated only in terms of instantaneous releases. They can be generalized for arbitrary releases by use of the convolution integral:

$$\theta = \int_0^t f(\tau) \theta_i (t - \tau) d\tau \,, \tag{4.43}$$

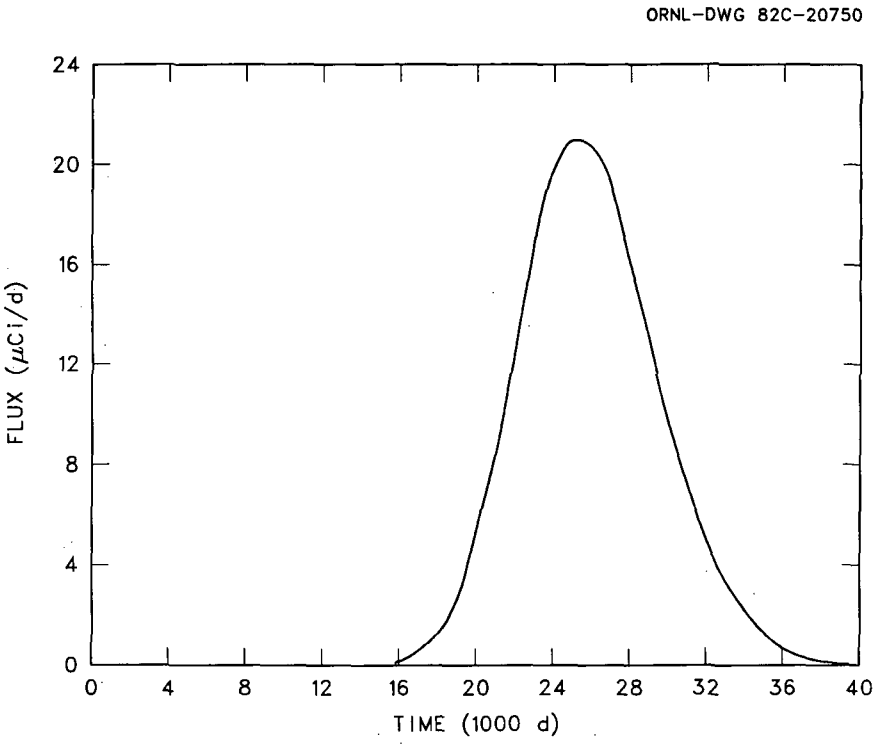

Figure 4.7. Flux of pollutant into river for Example 4.4.

where θ is the solution at time t for the arbitrary release, $\theta_i(t - \tau)$ is the solution at time $(t - \tau)$ for an instantaneous release at $(t - \tau) = 0$, and $f(\tau)$ is the source release rate at τ in curies/s.

Certain analytical solutions can be found to Eq. 4.43 for simple source release rate functions. For example, Wilson develops the solution to Eq. 4.43 for a continuous release in terms of the "well function" (Wilson and Miller 1978). Most useful solutions to Eq. 4.43 use numerical integration, generally involving a digital computer.

Several special precautions must be taken, however, to peserve computational accuracy, because the terms within the integral of Eq. 4.43 can be very nearly zero over part of the integration range. Computer programs for solving the equations in this section are described by Codell et al. (1982). Program listings in BASIC and FORTRAN are given in this reference. A computer tape of the programs is also available from NRC.

An alternate method that could be used to simulate a continuous source function is to present the continuous source as a series of instantaneous ones. The analytical solutions are then linearly summed. Complicated area source

terms can also be solved in an analogous fashion by representing the source area by a series of point sources and linearly summing the solutions.

4.5.4 Simplified Analytical Methods for Minimum Dilutions

Simplified forms of the equations of Sect. 4.5.3 have been developed for calculating the minimum dilutions (i.e., maximum concentration) of volume V_τ of a substance instantaneously released from a point source into an aquifer.

4.5.4.1 Dilution at Downgradient Wells in Confined Aquifiers for an Instantaneous Point Source at the Surface

At some distance downgradient from a release at the surface of a confined aquifer, the concentration can be considered to be mixed in the vertical direction. Close to the point of release, or in an unconfined aquifer, the vertical dispersion will not be influenced by the vertical boundaries of the aquifer. Between these regions there is a region where the concentration cannot be considered mixed, but the boundaries (top and bottom) affect the dispersion. The degree of vertical mixing can be characterized in a confined aquifer of constant thickness and uniform transport properties by the factor

$$\phi = \frac{b^2}{\alpha_T x} , \tag{4.44}$$

where

α_T = the vertical (transverse) dispersivity,

b = the thickness of the aquifer (ft),

x = the distance downgradient of the release.

The factor ϕ can be used to characterize the aquifer in three approximate regions:

(a) If $\phi < 3.3$, the release may be considered to be within 10% of being vertically mixed in the aquifer;

(b) If $\phi > 12$, the release may be considered to be within 10% of being unaffected by the vertical boundaries of the aquifer;

(c) If $3.3 < \phi < 12$, the release is neither completely mixed nor unaffected by the boundaries.

Different methods apply to each of the three regions.

Vertically Mixed Region ($\phi < 3.3$). For an instantaneous release at $x = 0$, the minimum dilution corrected for decay directly downgradient of a source would be

$$D_L = R_d 4\pi n_e \frac{\sqrt{\alpha_L \alpha_T} x b}{V_T} \exp(\lambda t) , \tag{4.45}$$

where

D_L = minimum dilution = c_0/c,
R_d = retardation coefficient,
n_e = effective porosity,
V_T = volume of liquid source term (cm^3),
α_L, α_T = dispersivities (cm) in the indicated direction,
x = distance downgradient (cm),
b = aquifer thickness (cm),
t = travel time (y),
λ = decay constant = $\ln 2/t_{1/2}$ (1 y).

The travel time, t, can be approximated as

$$t = \frac{x}{U} R_d , \tag{4.46}$$

where U is the pore velocity defined by Eq. 4.8a.

Unmixed Region ($\phi > 12$). For an instantaneous release at $x = 0$ on the surface of the aquifer, the minimum dilution of the surface of the aquifer directly downgradient from the source would be

$$D_L = \frac{n_e R_d (4\pi x)^{3/2} \sqrt{\alpha_L \alpha_T^2}}{2V_T} \exp(\lambda t) , \tag{4.47}$$

where α_L, α_T are dispersivities in the indicated direction and the other terms are as previously defined.

Intermediate Region ($3.3 < \phi < 12$). For an instantaneous release at $x = 0$ on the surface of an aquifer, the minimum dilution on the surface of the aquifer directly downgradient from the source would be

$$D_L = \frac{R_d 4\pi n_e \sqrt{\alpha_L \alpha_T} x b}{V_T F(\phi)} \exp(\lambda t) , \tag{4.48}$$

where

$$F(\phi) = 1 + 2\sum_{n=1}^{\infty} \exp\left(\frac{-n^2\pi^2}{\phi}\right) \tag{4.49}$$

and the other terms are as previously defined.

The function $F(\phi)$ is conveniently plotted in Fig. 4.8. It can be easily seen that for small values of ϕ, F approaches the value of 1.0, which yields the vertically mixed case. For large values of ϕ, the slope of F is 1/2, and the unmixed case prevails. This method may be used for any value of ϕ that can be read on Fig. 4.6.

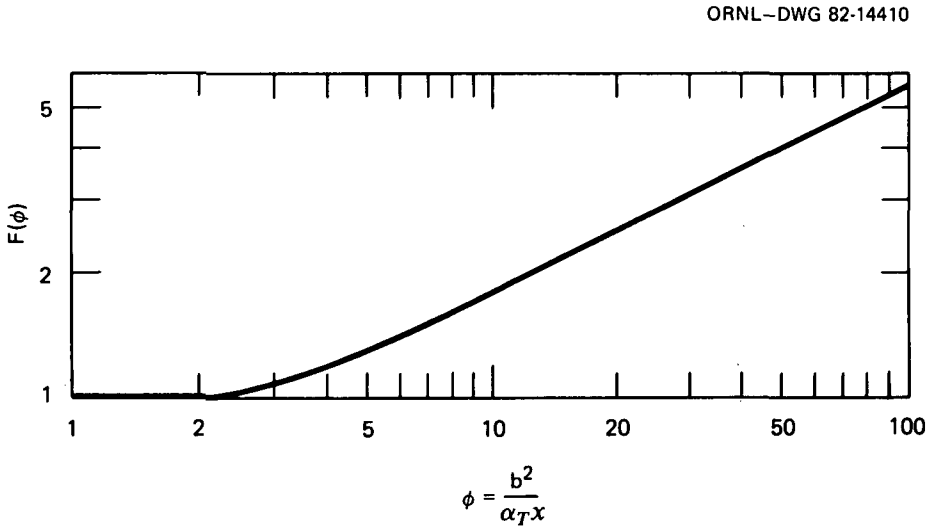

Figure 4.8. Mixing factor for confined aquifers.

4.5.4.2 Groundwater–Surface Water Interface—Instantaneous Source

For an instantaneous release to the groundwater at $x = 0$, the minimum dilution in an intercepting river, corrected for decay, can be found to be

$$D_L = \frac{2R_dQ\sqrt{\pi\alpha_L x}}{UV_T}\exp(\lambda t)\,, \tag{4.50}$$

where

Q = flow rate of river (cm^3/s),

α_L = the longitudinal dispersivity of the aquifer (cm),

V_T = the volume of release (e.g., tank volume) (cm^3),

U = pore velocity of groundwater (cm/s).

4.5.5 Models for Population Doses

If interdictive or mitigative methods to restrict water use are not taken into account, population dose from contaminated groundwater is proportional to the time-averaged concentration. Relatively simple equations can be used for estimating average concentration in ground water or in surface water supplies contaminated by groundwater. Two equations are presented below that are useful for population dose estimates.

4.5.5.1 Quantity of Released Radioactivity Crossing a Vertical Plane

In the case of groundwater flow to an intercepting river, the total quantity M (curies) of the dissolved substance entering the river would be

$$M = \int_0^\infty F\,dt\,, \tag{4.51}$$

where F is the flux defined for either an instantaneous point or vertical plane source by Eq. 4.40 or a horizontal area source by Eq. 4.42. Equation 4.51 can be integrated graphically or numerically and in some cases may have an analytical solution.

If dispersion is relatively small (e.g., $\alpha_x << \ell$), the following approximation may be used:

$$M = M_0 e^{-\lambda t} \text{ curies}\,, \tag{4.52}$$

where M_0 is the quantity of radioactivity released instantaneously from the source (curies), t is the travel time (y), and λ is the decay coefficient (1/y).

If the substance is being released from the source at a rate proportional to the quantity remaining (e.g., a leaching source term),

$$M = M_0 \frac{\lambda'}{\lambda' + \lambda} e^{-\lambda t}\,, \tag{4.53}$$

where λ' is the release rate from the source (1/y) and M_0 is the initial quantity of material in the source term (curies).

4.5.5.2 Direct Groundwater Usage

A model for calculating the quantity of a radionuclide ingested by a population using the contaminated groundwater was developed by the U.S. Nuclear Regulatory Commission (USNRC 1978). Groundwater usage was considered to be spatially continuous instead of being from discrete well points.

The total amount of the released radionuclide ingested by the population is

$$I = \int_0^\infty \int_{-\infty}^{\infty} \int_{-\infty}^{\infty} c Q_g \, dx \, dy \, dt \,, \tag{4.54}$$

where

I = the ultimate number of curies ingested from the release,
c = the groundwater concentration (Ci/L),
Q_g = the groundwater withdrawal rate for drinking water purposes ($m^3/d \cdot km^2$).

If all usage is restricted beyond downgradient distance ℓ from the release point, Eq. 4.54 may be integrated in closed form to give

$$I = \frac{\dfrac{M_0 Q_g}{2 n_e R_d b} \exp\left[\dfrac{U\ell}{2D_x} - \left[\dfrac{R_d \ell^2 (\lambda + \gamma)}{D_x}\right]^{1/2}\right]}{\sqrt{\lambda+\gamma}(\sqrt{\lambda+\gamma} - \sqrt{\gamma})} \,, \tag{4.55}$$

where

$$\gamma = \frac{U^2}{4 R_d D_x} \,.$$

M_0 is the total quantity of the radionuclide discharged to the point source, and the other terms are as previously defined.

If usage of the groundwater is restricted between two downgradient distances, ℓ_1 and ℓ_2, the curies ingested would be defined:

$$I = I(\ell_1) - I(\ell_2) \,, \tag{4.56}$$

where $I(\ell_1)$ and $I(\ell_2)$ are evaluations of Eq. 4.55 for ℓ_1 and ℓ_2 respectively.

Example 4.5. The use of several of the simpler analytical models in Sects. 4.5.4 and 4.5.5 will be demonstrated by way of a hypothetical example:

Leakage into the ground rapidly empties a 1000-ft^3 tank containing 4000 μCi/mL of ^3H, 2000 μCi/mL of ^{90}Sr, and 3000 μCi/mL of ^{137}Cs at a nuclear

site and remains undetected. The site is 50 ft above the mean level and 3000 ft upgradient from a river that has representative low flow of 5000 ft^3/s and is the sink for all surficial groundwater in the area. There are two shallow wells located 400 and 2500 ft directly downgradient from the site of the spill. Groundwater exists in a homogeneous alluvial sand layer 100 ft thick under water table conditions. Dispersivities for the sand have been determined in the near field from single-well tracer tests to be 0.5 ft for α_T and 1.0 ft for α_L. The bulk density ρ_b of the sand is 2.6 g/cm^3. Its total porosity n and effective porosity n_e are 0.4 and 0.25, respectively. The permeability K is 0.02 cm/s. Distribution coefficients K_d for the sand have been determined to be 0, 2.0, and 20.0 mL/g for dilute solutions of ^3H, ^{90}Sr, and ^{137}Cs, respectively. From the above information calculate the following:

(a) the maximum concentrations of the radioactive components in the river,

(b) the maximum concentrations of the components in the near well,

(c) the maximum concentrations of the components in the far well, and

(d) the total quantity of each radionuclide escaping to the river.

Solution. (a) If it is assumed that the source is released over a short period, Eq. 4.50 for instantaneous releases may be used to calculate the maximum river concentrations of ^3H, ^{90}Sr, and ^{137}Cs. First determine the pore velocity U from Eq. 4.8a and the effective porosity n_e:

$$U = \frac{V_x}{n_e} = -\frac{K\dfrac{\Delta H}{\Delta x}}{n_e} .$$

The gradient

$$\frac{\Delta H}{\Delta x} = \frac{-50 \text{ ft}}{3000 \text{ ft}} = -0.0167 ;$$

therefore,

$$U = \frac{-2 \times 10^{-2} \text{ cm/s} \times -0.0167}{0.25} \times \frac{86{,}400 \text{ s/d}}{30.48 \text{ cm/ft}} = 3.78 \text{ ft/d} .$$

The retardation coefficients for ^3H, ^{90}Sr, and 137Cs can be determined from Eq. 4.14:

$$^3H \qquad R_d = 1 + \frac{2.6}{0.4} \times 0.0 = 1 ,$$

$$^{90}Sr \qquad R_d = 1 + \frac{2.6}{0.4} \times 2.0 = 14 ,$$

$$^{137}Cs \qquad R_d = 1 + \frac{2.6}{0.4} \times 20 = 131 .$$

The travel times for the three components are calculated by Eq. 4.46:

$$^{3}\text{H} \qquad t = \frac{xR_d}{U} = \frac{3000\ \text{ft} \times 1}{3.78\ \text{ft/d}} \times \frac{\text{y}}{365\ \text{d}} = 2.17\ \text{y},$$

$$^{90}\text{Sr} \qquad t = \frac{3000\ \text{ft} \times 14}{3.78\ \text{ft/d}} \times \frac{\text{y}}{365\ \text{d}} = 30.4\ \text{y},$$

$$^{137}\text{Cs} \qquad t = \frac{3000\ \text{ft} \times 131}{3.78\ \text{ft/d}} \times \frac{\text{y}}{365\ \text{d}} = 284.8\ y.$$

The half-lives of ^{3}H, ^{90}Sr, and ^{137}Cs are 12.3 y, 29 y, and 30.1 y, respectively. The decay-corrected minimum dilutions in the river are found by applying Eq. 4.50:

$$^{3}\text{H} \qquad D_L = \frac{2 \times 1.0 \times \frac{5000\ \text{ft}^3}{\text{s}} \times \sqrt{\pi \times 1.0\ \text{ft} \times 3000\ \text{ft}}}{3.78\ \text{ft/d} \times 1000\ \text{ft} \times \frac{\text{d}}{86{,}400\ \text{s}}} \times \exp\left(\frac{\ln 2}{12.3\ \text{y}} \times 2.17\ \text{y}\right)$$

$$= 2.51 \times 10^{7},$$

$$^{90}\text{Sr} \qquad D_L = \frac{2 \times 14 \times \frac{5000\ \text{ft}^3}{\text{s}} \times \sqrt{\pi \times 1.0\ \text{ft} \times 3000\ \text{ft}}}{3.78\ \text{ft/d} \times 1000\ \text{ft} \times \frac{\text{d}}{86{,}400\ \text{s}}} \times \exp\left(\frac{\ln 2}{29\ \text{y}} \times 30.4\ \text{y}\right)$$

$$= 6.42 \times 10^{8},$$

$$^{137}\text{Cs} \qquad D_L = \frac{2 \times 131 \times \frac{5000\ \text{ft}^3}{\text{s}} \times \sqrt{\pi \times 1.0\ \text{ft} \times 3000\ \text{ft}}}{3.78\ \text{ft/d} \times 1000\ \text{ft} \times \frac{\text{d}}{86{,}400\ \text{s}}} \times \exp\left(\frac{\ln 2}{30.1\ \text{y}} \times 284.8\ \text{y}\right)$$

$$= 2.05 \times 10^{12}.$$

The peak concentrations in the river are determined by dividing the tank concentrations by the dilution factors:

$$c(^3\text{H}) = 4000\ \mu\text{Ci/mL}/2.51\times10^7 = 1.59\times10^{-4}\ \mu\text{Ci/mL}\,,$$

$$c(^{90}\text{Sr}) = 2000\ \mu\text{Ci/mL}/6.42\times10^8 = 3.12\times10^{-5}\ \mu\text{Ci/mL}\,,$$

$$c(^{137}\text{Cs}) = 3000\ \mu\text{Ci/mL}/2.05\times10^{12} = 1.46\times10^{-9}\ \mu\text{Ci/mL}\,.$$

(b) Minimum dilution in well (400 ft downgradient).

First determine whether or not thickness of the aquifer would affect the result by calculating the factor ϕ from Eq. 4.44:

$$\phi = \frac{b^2}{\alpha_T x} = \frac{(100\text{ ft})^2}{0.5\text{ ft}\times 400\text{ ft}} = 50\,.$$

Therefore, in this region the release will be relatively unaffected by the thickness of the aquifer, and Eq. 4.48 applies.

The travel times are estimated using the retardation factors and pore velocity calculated above:

$$^3\text{H} \qquad t = \frac{400\text{ ft}\times 1}{3.78\text{ ft/d}}\times\frac{\text{y}}{365\text{ d}} = 0.29\text{ y}\,,$$

$$^{90}\text{Sr} \qquad t = \frac{400\text{ ft}\times 14}{3.78\text{ ft/d}}\times\frac{\text{y}}{365\text{ d}} = 4.06\text{ y}\,,$$

$$^{137}\text{Cs} \qquad t = \frac{400\text{ ft}\times 131}{3.78\text{ d}}\times\frac{\text{y}}{365\text{ d}} = 38\text{ y}\,.$$

Applying equation 4.51:

$$^3\text{H} \qquad D_L = \frac{0.25\times 1\times(4\pi\times 400\text{ ft})^{3/2}\sqrt{1\text{ ft}\times 0.5\text{ ft}\times 0.5\text{ ft}}}{2\times 1000\text{ ft}^3} \times\exp\left(\frac{\ln 2}{12.3\text{ y}}\times 0.29\text{ y}\right)$$

$$= 22.6\,,$$

$$^{90}\text{Sr} \qquad D_L = \frac{0.25\times 14\times(4\pi\times 400\text{ ft})^{3/2}\sqrt{1\text{ ft}\times 0.5\text{ ft}\times 0.5\text{ ft}}}{2\times 1000\text{ ft}^3} \times\exp\left(\frac{\ln 2}{29\text{ y}}\times 4.06\text{ y}\right)$$

$$= 343.6\,,$$

$$^{137}\text{Cs} \qquad D_L = \frac{0.25\times 131\times(4\pi\times 400\text{ ft})^{3/2}\sqrt{1\text{ ft}\times 0.5\text{ ft}\times 0.5\text{ ft}}}{2\times 1000\text{ ft}^3} \times\exp\left(\frac{\ln 2}{30.1\text{ y}}\times 38\text{ y}\right)$$

$$= 6999.9\,.$$

The peak well concentrations are therefore 177 μCi/mL for ^{3}H, 5.8 μCi/mL for ^{90}Sr, and 0.43 μCi/mL for ^{137}Cs.

(c) Well 2500 ft downgradient. Calculate ϕ for this region from Eq. 4.44:

$$\phi = \frac{(100\text{ ft})^2}{0.5\text{ ft} \times 2000\text{ ft}} = 8.0 .$$

Therefore, this well is in the intermediate region, and Eq. 4.48 applies. The factor F (ϕ) can be read from Fig. 4.7 to be 1.6. Travel times for each component calculated from Eq. 4.46 are

$$^{3}\text{H} \qquad t = \frac{2500\text{ ft} \times 1}{3.78\text{ ft/d}} \times \frac{\text{y}}{365\text{ d}} = 1.81\text{ y} ,$$

$$^{90}\text{Sr} \qquad t = \frac{2500\text{ ft} \times 14}{3.78\text{ ft/d}} \times \frac{\text{y}}{365\text{ d}} = 25.4\text{ y} ,$$

$$^{137}\text{Cs} \qquad t = \frac{2500\text{ ft} \times 131}{3.78\text{ ft/d}} \times \frac{\text{y}}{365\text{ d}} = 237.4\text{ y} .$$

Applying Eq. 4.48:

$$^{3}\text{H} \qquad D_L = \frac{1 \times 4\pi \times 0.25\sqrt{0.5\text{ ft} \times 0.5\text{ ft}} \times 2500\text{ ft} \times 100\text{ ft}}{1000\text{ ft}^3 \times 1.6} \times \exp\left(\frac{\ln 2}{12.3\text{ y}} \times 1.81\text{ y}\right)$$

$$= 271.8 .$$

$$^{90}\text{Sr} \qquad D_L = \frac{14 \times 4\pi \times 0.25\sqrt{0.5\text{ ft} \times 0.5\text{ ft}} \times 2500\text{ ft} \times 100\text{ ft}}{1000\text{ ft}^3 \times 1.6} \times \exp\left(\frac{\ln 2}{29\text{ y}} \times 25.2\text{ y}\right)$$

$$= 6275 ,$$

$$^{137}\text{Cs} \qquad D_L = \frac{131 \times 4\pi \times 0.25\sqrt{0.5\text{ ft} \times 0.5\text{ ft}} \times 2500\text{ ft} \times 100\text{ ft}}{1000\text{ ft}^3 \times 1.6} \times \exp\left(\frac{\ln 2}{30.1\text{ y}} \times 237.4\text{ y}\right)$$

$$= 7.61 \times 10^{6} .$$

The peak well concentrations are therefore 14.7 μCi/mL for ^{3}H, 0.32 μCi/mL for ^{90}Sr, and 3.9×10^{-4} μCi/mL for ^{137}Cs.

(d) Quantity Q of each radionuclide eventually reaching river.

Equation 4.51 applies to this case because $\alpha_L << \ell$ (i.e., 1 ft vs 1000 ft). Travel times are estimated in part (a) above. The quantity of each radionuclide initially in the tank is the concentration multiplied by the volume. Therefore,

$$^{3}H \qquad Q = 4000\ \mu Ci/mL \times 1000\ ft^3 \times 28{,}300\ mL/ft^3 \times \exp\left(\frac{-\ln 2}{12.3\ y} \times 2.17\ y\right) \times 10^{-6}\ Ci/\mu Ci$$

$$= 1.002 \times 10^5\ Ci\ ,$$

$$^{90}Sr \qquad Q = 2000\ \mu Ci/mL \times 1000\ ft^3 \times 28{,}300\ mL/ft^3 \times \exp\left(\frac{-\ln 2}{29\ y} \times 30.4\ y\right) \times 10^{-6}\ Ci/\mu Ci$$

$$= 27{,}370\ Ci\ ,$$

$$^{137}Cs \qquad Q = 3000\ \mu Ci/mL \times 1000\ ft^3 \times 28{,}300\ mL/ft^3 \times \exp\left(\frac{-\ln 2}{30.1\ y} \times 284.7\ y\right) \times 10^{-6}\ Ci/\mu Ci$$

$$= 120.7\ Ci\ .$$

4.6 MODEL VALIDATION

Hydraulic flow and transport models can be validated (tested) only by comparison with field data and, in the case of numerical models, by comparison with the analytical solution of a simplified set of equations. In general, the model is a set of equations, and validation consists of comparison of the solution of these equations with field-measured data. Regardless of whether the solution is obtained by analytical or numerical techniques, true validation can be done only through comparison with field measurements. Agreement of a numerical solution with an analytical solution of the same equations shows only that the numerical techniques work and that no errors exist in the computer code.

4.6.1 Model Calibration

Models are calibrated for a specific problem by starting with an initial set of parameter estimates (field- or laboratory-measured), running the model for the problem, and comparing the results with observed values. If the comparison is poor, the parameter estimates are modified, the model is rerun, and results

are again compared with observed data. This process is continued until the desired level of agreement between observed data and the simulation is obtained (Mercer and Faust 1980). The modification of boundary conditions and parameters is subjective and requires a considerable amount of knowledge of the region being simulated and experience on the part of the modeler. The boundary conditions and parameters used in the final simulation must still be in agreement with the knowledge and understanding of the geology and hydrology of the site. Through this process the equations of groundwater flow in porous media have been well tested and verified. The equations of flow through fractured media have been tested to some extent, but the equations of transport through fractured media remain largely untested.

Where enough data on hydraulic heads and variation of head over long time periods are available, the inverse of the equations for head can be solved for the spatial distribution of permeability. The solution of the inverse problem (Newman 1973) is useful because it yields a spatial distribution of parameters that are consistent with the hydrology of the site under consideration. In this process, field-measured parameters are useful for comparison with computer-generated parameters to ensure that the generated values are realistic.

For the transport equations, the inverse problem has not been solved because the results are not unique.

4.6.2 Misuse of Models

The three most common misuses of models are overkill, inappropriate prediction, and misinterpretation.

Overkill is defined as using a more sophisticated model than is appropriate for the available data or the level of result desired. The temptation to apply the most sophisticated computational tool to a problem is difficult to resist. A question that often arises is: when should three-dimensional models be used as opposed to two-dimensional or one-dimensional models? Inclusion of flow in the third dimension, usually vertical, is recommended only in thick aquifers or if permeability changes drastically across the thickness of the aquifers. Inclusion of the third dimension requires substantially more data than one- and two-dimensonal models. For example, saturated-unsaturated flow through a shallow land burial site is truly a three-dimensional problem. However, the data are seldom available to consider more than one dimension above the water table.

In many cases, sophisticated models are used too early in analysis of a problem. One should begin with the simplest model appropriate to the problem and program toward the more sophisticated models until the desired level of results is achieved. In transport problems the flow modeling should be completed and checked against the understanding of site hydrology before a transport model is applied.

Misinterpretations usually arise because inappropriate boundary conditions were selected or the hydrologic history of a site has been misread. Under either

of these conditions the simulated data will not match the hydrologic history of the site.

Perhaps the worst misuse of a model is blind faith in model results. Simulated data that contradict hydrologic intuition almost always arise from a mistake in some data entry, an error in the computer code, or application of a model to a problem for which it was not designed. The latter case can occur in application of an analytical solution that was obtained using boundary conditions that are different from those to which the solution is being applied (Mercer and Faust 1980).

High-quality field data on contaminant or radionuclide transport in groundwater are scarce. The collection of data necessary for very detailed modeling efforts is extremely costly since the aquifer in which the transport is taking place can be measured only indirectly from wells. Several well-known validation efforts are discussed by Roberston (1974b), Codell (1978), Pinder (1973), Wilson (1978), Evenson and Dettinger (1980), Anderson (1979), and Isherwood (1981).

4.7 PROBLEMS

1. Saturated groundwater flow—Determine the seepage velocity for an average coarse gravel for a groundwater gradient of 0.002.
2. Unsaturated flow—A water balance shows that 10 cm/y of water infiltrate the ground and recharge the water table. Calculate the average downward velocity of the water in the unsaturated zone, which is a fine sand.
3. Retardation coefficient—Calculate the retardation coefficient for cesium in an average sand with a bulk density of 2.8 g/cm^3 and K_d of 50 mL/g.
4. Groundwater concentration—Calculate the concentration as a function of time 1500 m directly downgradient of a 1-Ci instantaneous point source in an infinitely deep aquifer. The seepage velocity is 1 m/d. The x, y, and z dispersivities are 50 m, 20 m, and 1 m, respectively. The effective porosity is 0.2. The retardation coefficient is 20. The half-life of the substance is 10 y.
5. Dilution in groundwater—For the same conditions in problem 4, consider that the 1 Ci was dissolved in 1000 L of water. Calculate the minimum dilution in the well using the equations of Sect. 4.5.4.1.
6. Dilution in river—For the same conditions as problem 4, calculate the minimum dilution in an intercepting river having an average flow rate of 10 m^3/s.
7. Population dose for average usage—Waste is being discharged to an aquifer ingested by downgradient users at a rate of 0.1 m^3/(d km^2). All

users are greater than 5000 m and less than 10,000 m downgradient. The properties of the radionuclide and the aquifer are $U = 1$ m/d, $\alpha_x = 100$ m, $n_e = 0.2$, $R_d = 3$, $b = 100$ m, $t_{1/2} = 30$ y. Calculate the curies ingested for each curie released.

8. Groundwater flux—Equation 4.51 is an approximation only. The true total quantity of flux passing a plane is more accurately determined by integrating the flux expressed by Eqs. 4.41 or 4.42 from $t = 0$ to $t = \infty$. Graphically integrate the flux from Eqs. 4.41 or 4.42 for a range of parameters and determine how well Eq. 4.54 agrees.

REFERENCES

Abramowitz, M., and Stegun, I., eds. November 1970. *Handbook of Mathematical Functions,* Applied Mathematics Series 55, Nat. Bur. Standards.

Aikens, A. E., Berlin, R. E., Clancy, J., and Oztunali, O. I. 1979. *Generic Methodology for Assessment of Radiation Doses from Groundwater Migration of Radionuclides in LWR Wastes in Shallow Land Burial Trenches,* Atomic Industrial Forum, Washington, D.C.

American Nuclear Society 1980. *Evaluation of Radionuclide Transport in Ground Water for Nuclear Power Sites,* Report 2.17 La Grange Park, Ill.

Anderson, M. P. November 1979. "Using Models to Simulate the Movement of Contaminants Through Groundwater Flow Systems," pp. 97–156 in *CRC Critical Reviews in Environmental Control.*

Barraclough, J. T., Teasdale, W. E., Robertson, J. B., and Jenson, R. G. 1967. *Hydrology of the National Reactor Testing Station Idaho 1966,* Open File Report TID-4500, U.S. Geol. Surv., Water Resour. Div., Idaho Falls, Idaho.

Bredehoeft, J., and Pinder, G. 1970. "Digital Analysis of Areal Flow in Multilayer Groundwater Systems: Aquatic Three Dimensional Model," *Water Resour. Res.* **G**(3), 883–88.

Bredehoeft, J. O. 1978. *Utilization of Numerical Groundwater Models for Water Resources Management,* EPA 60018-012, U.S. Environ. Protection Administration.

Burkholder, H. C., and Rosinger E. L. J. June 1980. "A Model for the Transport of Radionuclides and Their Decay Products Through Geologic Media," *Nucl. Technol.* **49,** 150–58.

Campbell, J. E., Kaestner, P. C., Langkopf, P. S., and Lantz, R. B. February 1980. *Risk Methodology for Geologic Disposal of Radioactive Waste: The Network Flow and Transport (NWFT) Model,* NUREG/CR-1190, U.S. Nuclear Regulatory Commission.

Carslaw, H., and Jaeger, J. 1959. *Conduction of Heat in Solids,* Oxford, Univ. Press, London.

Chow, V. T., ed. *Handbook of Applied Hydrology,* McGraw-Hill, New York, 1964.

Codell, R. B., and Schreiber, D. L. 1978. "NRC Models for Evaluating the Transport of Radionuclides in Groundwater," in *Management of Low-Level Radioactive Waste,* ed. M. W. Carter, A. A. Moghissi, and B. Kahn, Pergamon, New York.

Codell, R. B., Key, K. T., and Whalen, G. February 1982. *A Collection of Mathematical Models for Dispersion in Surface and Ground Water,* NUREG-0868, U.S. Nuclear Regulatory Commission.

Davis, S. M., and De Wiest, R. M. M. 1965. *Hydrogeology,* Wiley, New York.

Dillon, R. T., Lantz, R. B., and Pahwa, S. B. 1978. *Risk Methodology for Geologic Disposal of Radioactive Waste: The Sandia Waste Isolation Flow and Transport (SWIFT) Model,* SAND 78-1267, Sandia Natl. Lab., Albuquerque, N.Mex.

Duguid, J., and Lee, R. C. Y. 1977. "Flow in Fractured Porous Media," *Water Resour. Res.* **13**(3), 558–66.

Evenson, D. E., and Dettinger, M. D. May 1980. *Dispersive Processes in Models of Regional Radionuclide Migration,* Univ. Calif., Lawrence Livermore Lab., Livermore.

Faust, C. R., and Mercer, J. W. July–August 1980. "Ground Water Modeling: Numerical Models," *Ground Water,* **18**(4).

Freeze, R. A., and Cherry, J. 1979. *Groundwater,* Prentice-Hall, Englewood Cliffs, N.J.

Gray, W., Pinder, G., and Brebbia, C. 1977. *Finite Elements in Water Resources,* Penlach Press, London.

Gupta, S. K., Tanji, K., Nielsen, D., Biggar, J., Simmons, C., and MacIntyre, J. 1978. *Field Simulation of Soil-Water Movement with Crop Water Extraction,* Water Science and Engineering Paper 4013, Department Land, Air, and Water Resour. Univ. Calif., Davis.

Isherwood, D. January 1981. *Geoscience Data Base Handbook for Modeling a Nuclear Waste Respository,* NUREG/CR-0912, collective vols. 1 and 2, U.S. Nuclear Regulatory Commission.

Jenne, E. A., ed. 1979. *Chemical Modeling in Aqueous Systems,* ACS Symposium Ser. 93, American Chemical Society, Washington, D.C.

Klingsberg, C., and Duguid, J. October 1980. *Status of Technology for Isolating High-Level Radioactive Waste in Geologic Repositories,* U.S. DOE, Tech. Inf. Cent., Oak Ridge, Tenn.

Landa, E. 1980. "Isolation of Uranium Mill Tailings and the Component Radionuclides from the Biosphere—Some Earth Science Perspectives," *U.S. Geol. Surv. Cir.* **814.**

Lappala, E. G. June 1981. *Modeling of Water and Solute Transport Under Variably Saturated Conditions: State of the Art, Modeling and Low-Level Waste Management: An Interagency Workshop,* ed. C. A. Little and L. E. Stratton, Natl. Tech. Inf. Serv., Springfield, Va.

McWhorter, D. B., and Sunada, D. K. 1977. *Ground-Water Hydrology and Hydraulics,* Water Resour. Publications, Fort Collins, Colo.

Mercer, J. W., and Faust, C. R. "Ground-Water Modeling: An Overview," *Ground Water* **18**(2), 108–15.

Mercer, J. W., and Faust, C. R. "Ground-Water Modeling: Applications," *Ground Water* **18**(5), 486–97.

Nelson, R. W. June 1978. "Evaluating the Environment Consequences of Groundwater Contamination, Parts 1, 2, 3, and 4," *Water Resour. Res.* **14**(3), 409–50.

Neuman, S. P. 1973. "Calibration of Distributed Parameters in Groundwater Flow Models Viewed as a Multiple—Objective Decision Process Under Uncertainty," *Water Resour. Res.* **9**, 1006–21.

Niemczyk, S. J., Adams, K. G., Murfin, W. B., Ritchle, L. T., Eppel, E. W., and Johnson, J. D. June 1981. *The Consequences from Liquid Pathways After a Reactor Meltdown Accident,* NUREG/CR-1598, U.S. Nuclear Regulatory Commission.

Perlmutter, N. M., and Lieber, M. 1970. *Disposal of Plating Wastes and Sewage Contaminants in Groundwater and Surface Water, South Farmingdale–Massapequa Area, Nassau County, New York,* Water Supply Paper 1879-G, U.S. Geol. Survey.

Pinder, G. F. 1973. "A Galerkin Finite Element Simulation of Groundwater Contamination on Long Island, New York," *Water Resour. Res.* **9**(6), 1657–69.

Reeves, M., and Duguid, J. February 1975. *Water Movement Through Saturated-Unsaturated Porous Media: A Finite Element Galerkin Model,* ORNL-4927, Union Carbide Corp., Nuclear Div., Oak Ridge Natl. Lab.

Reeves, M., Francis, C., and Duguid, J. December 1977. *Quantitative Analysis of Soil Chromatography. I. Water and Radionuclide Transport,* ORNL-5337, Union Carbide Corp., Nuclear Div., Oak Ridge Natl. Lab.

Robertson, J. B. 1974. *Digital Modeling of Radioactive and Chemical Waste Transport in the Snake River Plain Aquifer at the National Reactor Testing Station, Idaho,* Open File Report IDO-22054, U.S. Geol. Surv., Water Resour. Div., Idaho Falls, Idaho.

Robertson, J. B., Schoen, R., and Barraclough, J. T. 1974. *The Influence of Liquid Waste Disposal on the Geochemistry of Water at the National Reactor Testing Station,* Open File Report IDO-22053, U.S. Geol. Surv., Water Resour. Div., Idaho Falls, Idaho.

Scheidigger, A. E. 1961. "General Theory of Dispersion in Porous Media," *J. Geophys. Res.* **66**(18), 3273–78.

Science Applications, Inc. (SAI) 1979. *Tabulation of Waste Isolation Computer Models, ONWI-78,* Office Nuclear Waste Isolation, Battelle Memorial Institute, Columbus, Ohio.

Shepard, T. A., and Cherry, J. A. "Contaminant Migration in Seepage from Uranium Mill Tailings Impoundments—An Overview," pp. 299–331 in *Uranium Mill Tailings Management,* proceedings of Third Symposium, Nov. 24–25, 1980, Civil Engineering Department, Colorado State Univ., Fort Collins, Colo.

Tabulation of Waste Isolation Computer Models, vols. 1.2, 1979. ONWI-78, Science Applications Inc.

Thornthwaite, C. W., and Mather, J. 1957. "Instructions and Tables for Computing Potential Evaportranspiration and the Water Balance," *Publications in Climatology,* Lab. Climatology, Centerton, N.J.

U.S. Nuclear Regulatory Commission (USNRC) April 1979. *Draft Generic Environmental Impact Statement on Uranium Milling,* NUREG-0511, collective vols. 1 and 2.

U.S. Nuclear Regulatory Commission (USNRC) February 1978. *Liquid Pathway Generic Study,* NUREG-0440.

U.S. Nuclear Regulatory Commission (USNRC) October 1975. *Reactor Safety Study, An Assessment of Accident Risks in U.S. Commercial Nuclear Power Plants,* WASH-1400.

Wilson, J. L. and Miller, P. J. April 1978. "Two Dimensional Plume in Uniform Ground-Water Flow." *J. Hydraulics Division, ASCE* **104**(HY4), 503–14.

Winograde, I. J., and Pearson, F. J. 1976. "Major Carbon 14 Anomaly in a Regional Carbonate Aquifer: Possible Evidence of Megascale Channelling, South Central Great Plains," *Water Resour. Res.* **12**(6), 1125.

5 Terrestrial and Aquatic Food Chain Pathways

Harold T. Peterson, Jr.*

5.1 INTRODUCTION

Radionuclides discharged into the environment can result in radiation exposure of man through a variety of mechanisms. Radioactive materials present in air, water, or food can be inhaled or ingested into the body. Some of these materials may become incorporated in tissues and organs, thereby resulting in internal irradiation of body organs. Radiation doses can also result from absorption in the body of radiation emitted from extracorporal radioactive materials. This external irradiation may be due to beta and gamma radiation† emitted from radioactive materials in air or water or deposited on the ground, or from direct radiation from nuclear facilities, waste storage facilities, or nuclear weapons.

A simplified diagram of the routes by which radioactive materials released from a nuclear facility can reach man is shown in Fig. 5.1. Each of these possible routes that can lead to radiation exposure of man is termed an exposure pathway. As can be seen, these routes are both numerous and varied. In some cases they are relatively simple, such as inhalation of airborne radioactive materials. In other cases, these routes may be complex multistep processes. For example, particulate radionuclides are deposited onto forage, which is then eaten by a cow; a portion of the material ingested by the cow may be secreted

*Senior Environmental Health Physicist, Office of Nuclear Regulatory Research, U.S. Nuclear Regulatory Commission, Washington, D.C. All views expressed in this Chapter are the personal views of the author and should not be taken as the official views of the Nuclear Regulatory Commission or of its staff.

†Alpha radiation will not penetrate the dead layer of skin and therefore is not a significant form of external irradiation.

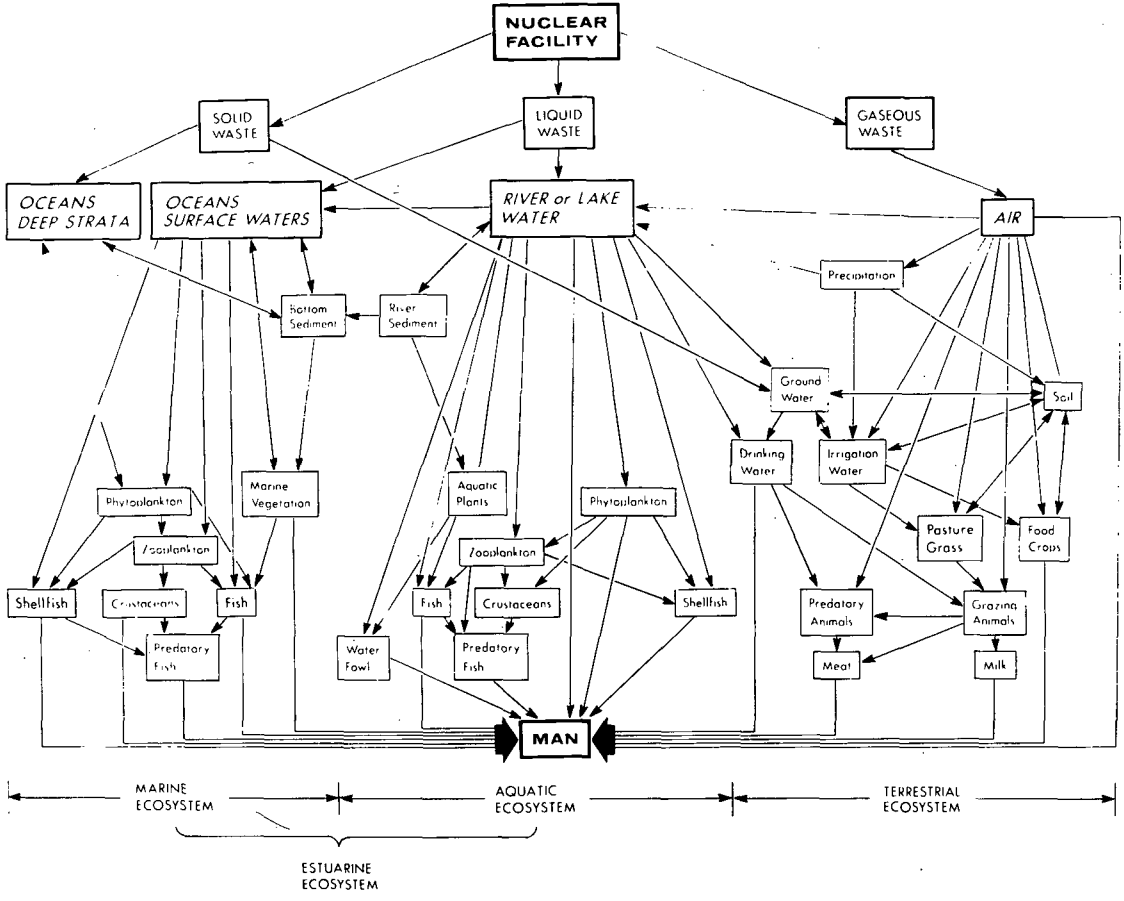

Figure 5.1. Potential Radiation Exposure Pathways Leading to Man

into milk, which is consumed by man. This is known as the air-grass-cow-milk pathway.

Unlike atmospheric and hydrospheric dispersion processes which invariably lead to a dilution or lessening of the concentration of a radionuclide in the environment, some of these environmental transport processes can lead to physical, chemical, or biological reconcentration so that the concentration of a radionuclide in an environmental medium may be considerably higher than the initial concentration of the radionuclide in air or water at the point of release. This will be termed bioaccumulation, although it should be recognized that sometimes the underlying mechanism may be due to physical or chemical processes rather than those involving living organisms. The purpose of this chapter is to discuss these environmental transport processes and the methods by which they may be evaluated.

5.1.1 Ecosystems

An ecosystem is the combination of the abiotic (nonliving) physiochemical environment and the assemblage of biotic (living) organisms that combine together to form an interrelated and interdependent system, an ecological system or ecosystem. This interdependence between the nonliving and living components is an important concept in understanding the effect of man's actions on his environment and in describing radionuclide transport processes.

As shown in Fig. 5.1, there are three primary* types of basic environments, or ecosystems, that can be used to provide a natural classification of radiation exposure pathways: the terrestrial (land), aquatic (freshwater), and marine (saltwater) ecosystems. There is also a fourth ecosystem, the estuarine ecosystem, which has characteristics that combine the qualities of both the aquatic and marine ecosystems.

The various radiation exposure pathways will be discussed separately by grouping them according to these ecosystems. It should be recognized, however, that such a distinct grouping is somewhat artificial since, as shown in Fig. 5.1, there are pathways that cross between the different types of ecosystems. For example, water from a river containing radioactive materials may be used for irrigation of crops, thereby entering the terrestrial ecosystem. Similarly, radioactive materials adsorbed onto soil may be washed off into a river, pass through an estuary, and eventually be deposited in the ocean, thereby involving all four ecosystems.

5.1.2 Types of Exposure Pathways

Exposure pathways can be classified according to the temporal relationship between the radionuclide concentration in the environment and the rate of

*Ecologists divide these still further into regional ecosystems or *biomes* such as forest, tundra, prairie, rain forest, etc., which differ in their characteristics.

release of that radionuclide from a nuclear facility. Three general classes of pathways can be defined based upon this relationship: (1) transitory exposure pathways, (2) integrating exposure pathways, and (3) cumulative-integrating exposure pathways.

A transitory exposure pathway is a pathway where the radionuclide concentration is directly proportional to the rate of release of the radionuclide into the environment:

$$C_i(t) = w_i(t,\tau)\,\dot{Q}_i(t-\tau) \quad , \tag{5.1}$$

where

$C_i(t)$ = concentration of radionuclide i in the environment at the time t,

$\dot{Q}_i(t-\tau)$ = activity release rate of radionuclide i at time $t-\tau$, and

$w_i(t,\tau)$ = dispersion function that describes the relationship between the concentration and release rate.

The environmental concentration will persist only as long as there is a continuing release of the radionuclide into the environment.

An example of a transitory exposure pathway would be external irradiation from a short-lived gaseous radionuclide. In this case the dispersion function would be an atmospheric dispersion model:

$$w_i(t,\tau) = \left[\frac{\chi}{\dot{Q}}(r,\theta,t)\right] e^{-\lambda_i \tau} \quad ,$$

where

$\chi(r,\theta,t)/\dot{Q}$ = value of the atmospheric dispersion function at location (r,θ) and time t, and

$e^{-\lambda_i \tau}$ = factor that accounts for radioactive decay during transit.

The airborne concentration would be

$$C_i(r,\theta,t) = \chi_i(r,\theta,t) = \left[\frac{\chi}{\dot{Q}}(r,\theta,t)\right] e^{-\lambda_i \tau}\,\dot{Q}_i(t-\tau) \quad .$$

The radionuclide concentration in an integrating exposure pathway increases with continuing release of radioactive materials into the environment and may persist beyond the cessation of these releases. The concentration of radionuclide i is given by the time integral of the release rate and functions representing the dispersion and buildup processes:

$$C(t) = \int_0^t a\, u(s,z)\, w(s,z)\, Q(s-z)\, ds \quad , \tag{5.2}$$

where

$u(s,z)$ = a transfer function that describes the accumulation process.

A simple example of an integrating exposure pathway would be the buildup of a radionuclide released into a small lake or pond. If initial mixing is neglected, the dispersion function is simply the inverse of the pond volume,

$$w(s,\tau) = 1/V \quad .$$

The rate of change of the concentration of radionuclide i would be described by:

$$\frac{dC_i(t)}{dt} = \frac{Q_i(t-\tau)}{V} - \left[\lambda_i + \frac{\dot{v}}{V}\right] C_i(t) \quad ,$$

where

V = volume

λ = radioactive decay constant for radionuclide i, and

$\dot{v}$ = outflow rate from the pond (volume per time).

The solution to this equation is

$$C_i(t) = C_i(O)e^{-(\lambda_i + \dot{v}/V)t} +$$

$$e^{-(\lambda_i + \dot{v}/V)t} \int_0^t e^{(\lambda_i + \dot{v}/V)s} \frac{Q_i(s-\tau)}{V}\, ds \quad .$$

The transfer function can be seen to be $\exp(\lambda_i + \dot{v}/V)s$. For a constant release rate of $\dot{Q}_i(s-\tau) = \dot{Q}$, the concentration is given by:

$$C_i(t) = C_i(O)e^{-(\lambda_i + \dot{v}/V)t} +$$

$$\frac{\dot{Q}}{V(\lambda + \dot{v}/V)}[1 - e^{-(\lambda_i + \dot{v}/V)t}] ,$$

which asymptotically approaches an equilibrium value of

$$C_i(\infty) = \frac{\overline{Q}}{\lambda V + \dot{v}} .$$

Figure 5.2 shows the buildup of two radionuclides in an integrating pathway, a short-lived radionuclide ($T_{1/2} = 10$) and a much longer lived radionuclide ($T_{1/2} \sim 10{,}000$) for a system where $\dot{v}/\dot{V} = 0.02$. As is evident, the longer-lived radionuclide takes a longer time to approach an equilibrium level, and that level is higher than for the shorter-lived radionuclide.

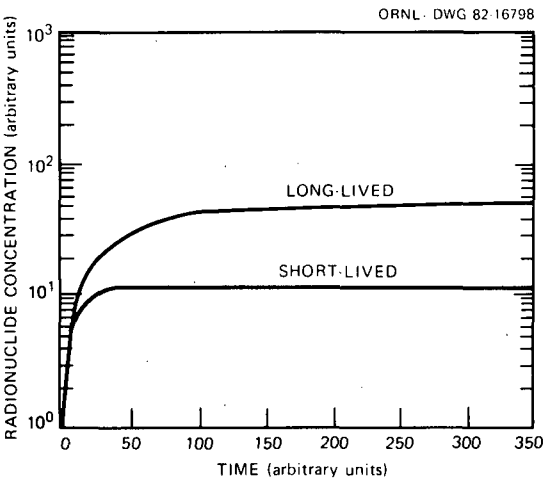

Figure 5.2. Accumulation of a short-lived and a long-lived radionuclide in an integrating exposure pathway.

The cumulative integrating exposure pathway involves a second integrating process. In this type of pathway the radionuclide concentration in the medium of interest is derived from a integrating exposure pathway. The concentration in this second medium is given by:

$$C_{i2}(T_2) = \int_{T_1}^{T_2} v(t) C_{i1}(t)\, dt =$$

$$\int_{T_1}^{T_2} v(t) \int_0^t au(s,\tau) w(s,\tau) Q(s-\tau) ds dt \quad , \tag{5.3}$$

where

$v(t)$ = a buildup function.

An example of a cumulative integrating pathway would be a fish that lives in the pond used in the preceding example of integrating pathway. Let the rate of accumulation of radionuclide i in the fish be described by

$$\frac{dC_{Fi}(t)}{dt} = I_i\, C_{wi}(t) - (\lambda_i + r)\, C_F(t) \quad , \tag{5.3a}$$

where

$C_{wi}(t)$ = radionuclide concentration in water,

$C_{Fi}(t)$ = radionuclide concentration (per unit mass) in the fish at time t,

I_i = rate of intake (uptake) (volume per unit mass),

λ_i = radioactive decay constant, and

r = rate constant for biological elimination of the stable element i.

The solution for the radionuclide concentration in the fish is

$$C_{Fi}(T_2) = C_{Fi}(T_1) e^{-(\lambda_i + r)(T_2 - T_1)}$$

$$+ e^{-(\lambda_i + r)T_2} \int_{T_1}^{T_2} C_{wi}(t)\, I_i e^{(\lambda_i + r)t}\, dt \quad . \tag{5.3b}$$

The accumulation function can be seen to be $w(t) = I\,e^{(\lambda_i + r)t}$. If Eq. (5.2a) is substituted for $C_{wi}(t)$ and the initial radionuclide concentrations in both fish and water are zero, the result is

$$C_{Fi}(T_2) = \frac{\dot{Q}_i I_i}{V\lambda_i + \dot{v}} \left[\frac{1 - e^{-(\lambda_i + r)(T_2 - T_1)}}{(\lambda_i + r)} - e^{-(\lambda_i + \dot{v}/V)T_2} \left\{ \frac{1 - e^{-(r - \dot{v}/V)(T_2 - T_1)}}{(r - \dot{v}/V)} \right\} \right] .$$

The concentration in the fish asymptotically approaches an equilibrium value of

$$C_{Fi}(\infty) = \frac{\dot{Q}_i I_i}{(V\lambda_i + \dot{v})(\lambda_i + r)} .$$

Figure 5.3 shows the uptake predicted by this equation, with r corresponding to a biological half-life of 300 and $I = 1$ for two radionuclides having radiological or physical half-lives of 10 (short-lived) and 10,000 (long-lived). As in Fig. 5.2, $\dot{v}/V = 0.02$.

In addition to providing insight into the development of models for dose assessment, the classification of an exposure pathway as transitory, integrating, or cumulative integrating has significance in determining the sampling or measurement frequencies for environmental monitoring programs. The environmental radionuclide concentration in a transitory exposure pathway will vary directly with the release rate and, therefore, can be highly variable with time. For this reason, accurate estimation of this concentration requires continuous or integrating monitoring such as continuous air particulate sampling or thermoluminescent dosimetry. The radionuclide concentration in an integrating pathway is less variable, as the integral of the release rate will be less variable than the release rate itself. For this reason, batch sampling rather than continuous monitoring may suffice if the effective mean life of the radionuclide in the environment is long compared to the interval between samples. The radionuclide concentration in a cumulative integrating pathway will vary even more slowly with fluctuations in the radionuclide release rate than in an integrating pathway. In such situations, annual sampling may be sufficient to determine the concentration of moderately long lived radionuclides.

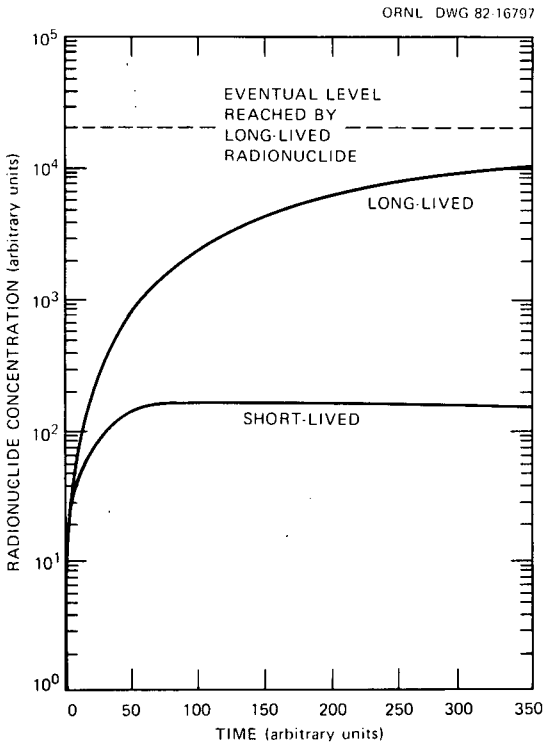

Figure 5.3. Uptake of a short-lived and a long-lived radionuclide in a cumulative integrating pathway.

5.1.3 Presentation of Material and Selection of Model Parameter Values

The organization of this chapter emphasizes environmental transport processes and an understanding of the basic assumptions and limitations involved in the measurement and use of environmental transport parameters. Particular emphasis is placed upon kinetic or time-dependent models of environmental transport processes. Although static or equilibrium models and parameters derived from equilibrium measurements are commonly employed for environmental radiation dose assessment, these models are generally applicable only to continuous release situations. In order to evaluate doses from single or intermittent releases (such as accident situations) or to compare predicted environmental concentrations with levels measured under transient

exposure situations, a basic understanding of the temporal variation of environmental processes is necessary. The time-dependent environmental transport model can usually be readily adapted for continuous release conditions, whereas it is generally difficult to adjust static or equilibrium models and parameters to handle transient release conditions. The static values can, however, be used to estimate the total intake from a transient situation.

The parameter values* presented in the tables or text should be viewed as examples of possible values rather than as recommended "best" values based upon an exhaustive search of the literature. There is no single parameter value that is applicable to all exposure situations. Where possible, several literature values are presented in order to give the reader an appreciation of the variability of the measured values.

Some efforts have been made to analyze the statistical distribution of reported parameter measurements [FUL-70, HOF-79, and later sections of this text]. These efforts are valuable in understanding the possible ranges of parameters and the degree to which a particular numerical value may result in underestimates or overestimates of actual doses. However, there are cautions to be observed in using such statistical tabulations. These evaluations generally assume that various parameters are statistically independent and unrelated. However, in many situations there may be interdependence between various parameters. A simple illustration of this is the relationship between the fraction of airborne deposition retained on vegetation and the amount consumed by a grazing animal. For sparse vegetation, less of the deposited material is retained on the vegetation, but the animal must browse over a much greater land area to consume its daily food requirements, thereby increasing its radionuclide intake. Failure to consider such interrelationships and treating factors separately may result in apparent statistical ranges of combined parameters that are much greater than actually possible in nature.

Another factor in using parameters from such statistical distribution is the choice of the appropriate percentile of the distribution for selection of the parameter value. Selection of an extremely high percentile will ensure that the resulting dose estimates are conservative (in the sense of limiting the possibility of underestimating actual doses), but the combined selection of all parameters in a model at an extreme range (say the 99th percentile) will seriously bias the estimated dose. In this author's opinion, the use of such conservatism was better suited to times when the individual dose limit was 500 millirem per year, than when used for numerical cost-benefit (optimization) analyses which underlie current environmental radiation standards (such as NRC's Appendix I to 10 CFR Part 50 or EPA's Uranium Fuel Cycle Standards in 40 CFR Part

*Parameters derived by this author from other published data are so indicated or are enclosed in parentheses.

190). Such analyses require "realistic"* dose estimates rather than conservative overestimates in order not to distort their underlying objectives. The use of realistic choices for parameters, together with knowledge of their possible ranges and an understanding of the environmental factors which affect them, should lead to better dose assessments than the arbitrary choice of extreme conservative assumptions.

5.2 THE TERRESTRIAL ECOSYSTEM

5.2.1 Introduction

The terrestrial ecosystem is the most important of the four general classifications of ecosystems. Not only does man reside within this ecosystem, a significant portion of human food also comes from terrestrial sources. Radioactive materials can enter the terrestrial ecosystem in a variety of ways: from the atmosphere through deposition, from water used for irrigation, or from soil contaminated by ground water or deposited radionuclides.

Some of the principal exposure pathways do not involve bioaccumulation mechanisms. These direct exposure pathways are generally transitory and include: inhalation (and transpiration), external irradiation from airborne materials, and external irradiation from radioactive materials contained within buildings or storage tanks. Radiation doses from these sources can be estimated directly from atmospheric diffusion calculations, shielding calculations, and knowledge of occupancy factors or inhalation rates. (See Chapter 6). Although these direct pathways may be major contributors to radiation doses from nuclear facilities, they do not involve bioaccumulation processes and will not be discussed here.

The principal terrestrial exposure pathways that do involve bioaccumulation processes are generally integrating or cumulative integrating exposure pathways. These include buildup of deposited radionuclides on soil and vegetation, transfer of radioactive materials from the soil to plants, and incorporation of radioactive materials in animal products such as meat, milk, and eggs.

*By "realistic," I mean a combination of a model and its parameters that results in calculated doses, dose rates, or environmental radionuclide concentrations which are close to values actually measured in the environment. Whether a model (and its parameters) is "realistic" can be determined only by field verification of the predicted values. The underlying model (or algorithm) may be a simplistic (or even incorrect) representation of actual environmental processes or bioaccumulation mechanisms. However, such a model, if it gives reasonably accurate predictions, may be preferable to a highly sophisticated, theoretically correct model that requires so many input parameters that it cannot be reasonably applied in practice.

5.2.2 Transfer of Radioactive Materials Between Air and the Ground Surface

5.2.2.1 Kinetics of Radionuclide Deposition

The buildup of radionuclides on vegetation or in soil as a result of deposition of airborne radioactive materials is an important process in several exposure pathways. It is a major source of radionuclide contamination of terrestrial food products such as vegetables, meat, and milk. Deposited beta- and gamma-emitting radionuclides contribute to exposure from external irradiation. Deposited radioactive materials also can become airborne due to wind action (resuspension) and serve as a source of radionuclide inhalation or additional ground contamination.

The rate of accumulation of deposited material at a particular location (x,y) is given by the product of the air concentration at specified height above that location, $\chi(x,y,z,t)$ and an empirical rate constant, v_g, which has units of velocity (distance/time, e.g., meters per second) and is termed the deposition velocity:

$$\frac{dC_A(x,y,t)}{dt} = v_g\chi(x,y,z,t) \ , \tag{5.4}$$

where $C_A(x,y,t)$ is the areal concentration (activity per unit area). Material deposited onto soil or vegetation can be removed by leaching or washoff from rain, by resuspension, or physical removal by harvesting or by ingestion by herbivores. These bio-physical removal processes will be depicted by a single removal rate constant, r. In addition, there are losses due to radioactive decay. The net rate of radionuclide buildup, allowing for these removal mechanisms is given by:

$$\frac{dC_A(x,y,t)}{dt} = v_g\chi(x,y,z,t) - (r+\lambda)C_A(x,y,t) \ . \tag{5.5}$$

The general solution to the above equation can be found by segregating the terms containing $C_A(x,y,t)$, multiplying both sides by an integrating factor of $e^{(\lambda+r)t}$, and integrating. The deposited activity at a time T_2 is:*

$$C_A(x,y,T_2) = C_A(x,t,T_1)e^{-(\lambda+r)(T_2-T_1)} +$$

$$e^{-(\lambda+r)T_2}\int_{T_1}^{T_2} v_g\chi(x,y,z,t)e^{(\lambda+r)t}dt \ . \tag{5.6}$$

*Note that deposition is an integrating process with an accumulation function of $e^{(r+\lambda)t}$.

For a constant airborne concentration, $\chi(x,y,z,t) = \bar{\chi}(x,y,z)$ the solution [for $T_1 = 0$, $C_A(x,y,o) = 0$ and $T_2 = T$] is:

$$C_A(x,y,T) = \frac{v_g \bar{\chi}(x,y,z)}{(r+\lambda)} [1 - e^{-(r+\lambda)T}] \quad . \tag{5.7}$$

This shows that the deposited radioactive material will buildup with time at a rate determined by the deposition velocity, v_g, the average airborne concentration, $\bar{\chi}(x,y,z)$, and the removal rate constants r and λ and will asymptotically approach an equilibrium value of

$$C_A(x,y,\infty) = \frac{v_g \bar{\chi}(x,y,z)}{(r+\lambda)} \quad . \tag{5.8}$$

For long-lived radionuclides, the equilibrium deposition will be limited by the biophysical removal rate constant, r, as λ will be small. For short-lived radionuclides, the equilibrium areal concentration will also be limited by the radioactive decay constant λ. As would be expected, with equivalent deposition velocities and air concentrations, the equilibrium amount of deposited material will be higher for longer-lived radionuclides than for shorter-lived radionuclides.

Example 5.1. Calculate the ratio of the equilibrium deposition on grass of radioiodine-131 ($T_{½}$ = 8.05 days) to the atmospheric concentration, assuming a v_g of 1 cm/sec and a removal half-time from biophysical processes (i.e., other than radioactive decay) of 14 days.

This ratio is given from Eq. (5.8):

$$\frac{C_A(x,y,\infty)}{\bar{\chi}(x,y,z)} = \frac{v_g}{r_\rho + \lambda} \quad .$$

$$r_\rho = \frac{\ln 2}{14} = 0.0495 \text{ d}^{-1}$$

$$\lambda = \frac{\ln 2}{8.05} = 0.0861 \text{ d}^{-1}$$

$$v_g = (0.01 m/sec)(8.64 \times 10^4 \text{s/d}) = 864 \, m/d, \; so$$

$$\frac{C_A}{\bar{\chi}} = \frac{8.64 \times 10^2 \text{m/d}}{0.1356\,\text{d}^{-1}} = 6.37 \times 10^3 \left[m = \frac{pCi/m^2}{pCi/m^3} \right] .$$

[End of Example]

For long-lived radionuclides, the equilibrium deposition will be limited by the bio-physical removal rate constant r as λ will be small. For short-lived radionuclides, the equilibrium areal concentration will also be limited by the radioactive decay constant λ. As would be expected, with equivalent deposition velocities and air concentrations, the equilibrium amount of deposited material will be higher for longer-lived radionuclides than for shorter-lived radionuclides.

5.2.2.2 Measurement and Use of Deposition Velocities

As noted previously, the deposition velocity is an empirical parameter which is measured in field experiments. These experiments are generally short-term so that removal processes and radioactive decay can be neglected. In this case, equation (5.5) can be integrated directly to give:

$$C_A(x,y,t) = v_g \int_0^T \chi(x,y,z,t)dt \text{ or } v_g = \frac{C_A(x,y,T)}{\int_0^T \chi(x,y,z,t)dt} . \quad (5.9)$$

Deposition velocity can also be expressed in terms of the flux of material (deposition rate) as

$$v_g = \frac{dC_A(x,y,t)/dt}{\chi(x,y,z,t)} . \quad (5.10)$$

The deposition velocity is determined by measuring the amount of material deposited per unit area during time T, and dividing this by the time-integrated air concentration at a reference height (z) above the test area. This height is usually 1 m. The air concentration is usually determined by placing an air sampler at 1 m above the test plot. The amount of activity deposited can be determined by survey meter readings taken at a known fixed height above the plot (or by field gamma spectrometry) together with a conversion factor to convert the counting rate or exposure rate into activity per unit area. A second method of measuring deposition is by carefully cutting the vegetation from a known area of the test plot and determining the amount of deposited material by radiochemical or gamma spectrometric analysis. *Deposition velocities measured by these two methods will not usually agree.*

If the survey instrument method is used, the measurement will indicate the *total amount of deposition,* including material deposited on vegetation and material deposited onto the soil. If only the vegetation is analyzed, the deposition velocity will reflect the deposition rate only onto vegetation. The ratio of the amount of material deposited onto vegetation to the amount of total deposition is termed the retention factor, f_R:

$$f_R = \frac{\text{amount of material deposited onto vegetation}}{\text{amount of total deposition onto soil + vegetation}} .$$

Table 5.1 contains representative measurements of f_R. The retention has also been reviewed by Miller et al. [MIL-78] and Miller [MIL-80a]. For deposition onto forage, Chamberlain [CHA-70] gives a functional dependence between f_R and the dry forage density Y_D(kg/m^2):

$$f_R = 1 - exp(-\gamma Y_D) \ , \tag{5.11}$$

where γ ranges between 2.3 and 3.3 m^2/kg for forage crops. Miller [MIL-67] found higher values of γ for dry deposition and values about 2.25 times higher for deposition under damp conditions (relative humidity greater than 90%), as

Table 5.1. Fraction of total initial deposition retained on vegetation

Material	Vegetation type	Dry density kg/m^2	Fraction of Initial deposition on		Ratio Total/ vegetation	Reference
			Vegetation f_R	Soil + Detritus		
Elemental Iodine	Wheat grass	0.050	(0.42)	(0.58)	(2.38)	HAW-66
			(0.72)	(0.28)	(1.39)	HAW-66
	Pasture grass	0.071	(0.74)	(0.26)	(1.35)	HAW-66
			(0.63)	(0.37)	(1.59)	BU-68
			(0.71)	(0.29)	(1.41)	BU-68
			(0.59)	(0.41)	(1.69)	BU-68
			(0.59)	(0.41)	(1.69)	BU-68
I_2 (Windscale)	grass	~0.20	0.82 ± 0.09	(0.18)	(1.22)	BOO-58
I_2	clover	0.042	(0.27)	(0.73)	(3.67)	CHA-60b
	dandelion	0.026	(0.72)	(0.28)	(1.38)	CHA-60b
	dandelion	0.042	(0.24)	(0.76)	(4.11)	CHA-60b
	dandelion	0.046	(0.29)	(0.71)	(3.4)	CHA-60b
Simulated fallout particles 44–88 μm	Fescue grass	0.44	0.69	(0.31)	(1.46)	PET-72
	Blue grass	0.57	0.79	(0.21)	(1.26)	PET-72
	Bermuda grass	0.52	0.82	(0.18)	(1.22)	PET-72
	Zoysia grass	0.75	0.76	(0.24)	(1.31)	PET-72

shown in Table 5.2. In using deposition velocities from the literature, it is necessary to ascertain which method of measurement was used, since as the results can differ by a factor of 4 or more. Selection of the appropriate deposition velocity will depend upon the pathway being analyzed. If external exposure from deposited material is of primary interest, then the deposition velocity which should be used is the total deposition velocity including both vegetation and soil components. If deposition onto vegetation is of primary interest as an input to determining the radionuclide concentration in a food product, then the vegetation deposition velocity (v_g) rather than the total deposition velocity (v_t) should be used, or the total deposition velocity should be multiplied by the retention factor f_R; $v_g = f_R v_t$. Although it is not often recognized, the deposition velocity used in plume depletion calculations should be the total deposition velocity v_t rather than the vegetation deposition velocity.

5.2.2.3 Factors Affecting Deposition

Theory. Sehmel and Hodgson [SEH 76a] give the deposition flux to a surface as

$$\dot{N} = -(\epsilon + D)\frac{dC}{dz} - v_{\text{term}}C \ ,$$

where

$\dot{N}$ = mass flux (mass/area time),

C = air concentration (mass/volume),

v_{term} = terminal settling velocity (distance/time),

dc/dz = the variation of the air concentration with height,

D = Brownian diffusion constant for the material (area/time), and

ϵ = eddy diffusion constant (eddy diffusivity) (area/time).

The eddy diffusivity describes transport by atmospheric turbulence, while the Brownian diffusivity describes molecular diffusion.

By definition, the deposition velocity is the flux per unit air concentration and, therefore, is given by:

$$v_g = -\frac{\dot{N}}{C} = (\epsilon + D)\frac{d \ln C}{dz} + v_{\text{term}} \ , \tag{5.12}$$

Table 5.2. Parameters for deposition interception on vegetation[a]

A. Silicate particles [MIL-67]

Plant	Damp Conditions $\gamma(ft^2/g)$	Damp Conditions (m^2/kg)	Dry Conditions $\gamma(ft^2/g)$	Dry Conditions (m^2/kg)	Damp / Dry
Bean	0.104	9.67	0.042	3.91	2.47
Beet	0.130	12.1	0.060	5.58	2.17
Cabbage	0.036	3.35	0.022	2.05	1.63
Carrot	0.049	4.56	0.024	2.23	2.04
Corn	0.032	2.98	0.046	4.28	0.70
Leek	0.035	3.26	0.014	1.30	2.51
Lettuce	0.150	14.0	0.051	5.30	2.64
Orange	0.070	6.51	0.024	2.23	2.92
Potato	0.149	13.8	0.074	6.88	2.00
Grass	0.132	12.3	0.072	6.70	1.84
(Grass from Table 5.1)				6.05	

B. Simulated Fallout (1–44 μm) [WIT-71]

Plant	Y_D (g/ft^2)	Y_D (kg/m^2)	$\gamma(ft^2/g)$	$\gamma(m^2/kg)$	f_R*
Soybean					
(leaves)	12.80	0.138	0.025	2.32	0.321
(stem)	9.28	0.100	0.008	0.774	0.074
(total)	22.08	0.238	0.033	3.094	0.395
Sorghum					
(leaves)	5.44	0.0585	0.017	1.58	0.091
(stem)	6.34	0.0682	0.001	0.093	0.004
(axil)	0.38	0.0041	0.758	70.51	0.288
(total)	12.16	0.130	0.776	72.18	0.383

C. Simulated Fallout (44–88 μm) [WIT-70]

Plant	Y_D (g/ft^2)	Y_D (kg/m^2)	$\gamma(ft^2/g)$	$\gamma(m^2/kg)$	f_R*	(f_R)
Squash	6.37	0.0685	0.196	18.23	1.249	0.713
Soybean	11.41	0.123	0.090	8.37	1.027	0.643
Sorghum	5.38	0.0578	0.091	8.46	0.489	0.537
Tespedeza	1.88	0.020	0.040	3.72	0.075	0.0724
Peanuts	4.45	0.0478	0.022	2.046	0.098	0.0932

D. Simulated Fallout (88–175 μm) [WIT-69 and WIT-70]

Plant	Y_D (g/ft^2)	Y_D (kg/m^2)	$\gamma(ft^2/g)$	$\gamma(m^2/kg)$	f_R*	(f_R)
Squash	6.37	0.0685	0.139	12.93	0.885	0.587
Soybean	1.41	0.123	0.101	9.40	1.152	0.684
Sorghum	5.38	0.0578	0.020	1.860	0.108	0.102
Tespedeza	1.88	0.020	0.010	0.93	0.019	0.0186
Peanuts	4.45	0.0478	0.013	1.209	0.058	0.0562
White Pine	44.64	9.480	0.0054	0.502	0.242	0.214
Red Oak	9.88	0.106	0.0354	3.29	0.349	0.295

[a]From [MIL-80]: $f_R = 1 - \exp(-\gamma Y_D)$, where Y_D is the dry vegetation density (kg/m^2) and γ has units of m^2/kg. For small values of Y_D, $1 - \exp(-\gamma Y_D) \simeq \gamma Y_D = f_R^*$ which is the form used by Miller [MIL-67] and other authors cited above.

where $d \ln C = dc/C$. The terminal settling velocity (or Stokes velocity), v_{term}, for a particle is (to a first approximation) given by:

$$v_{term} = \frac{g\,\delta^2(\rho - \rho')}{18\eta} \quad . \tag{5.13}$$

where g = gravitational acceleration constant,

δ = particle diameter,

ρ = particle density,

η = viscosity of air, and

ρ' = density of air.

The terminal settling velocity and, consequently, the deposition velocity is proportional to the product of the particle density and the square of its diameter.* The eddy diffusivity, ϵ, is a function of atmospheric stability and is given by:

$$\epsilon(z) = u_*^2\, z/(d\bar{u}/dz) \quad , \tag{5.14}$$

where

z = height above ground surface,

$d\bar{u}/dz$ = vertical wind speed gradient, and

u_* = *friction velocity,*

which is related to the wind speed variation with height:

$$\bar{u}(z) = \frac{u_*}{k} \ln\left(\frac{z}{z_0}\right) \quad , \tag{5.15}$$

where k is a constant (von Karman's constant, 0.41) and z_0 is the height at which the wind speed goes to zero and is termed the *surface roughness* or *roughness length.* Both u_* and z_0 can be determined from the variation in wind speed with height.

*The square root of this product, $(\rho\delta^2)^{1/2}$, is termed the *aerodynamic diameter* of the particle.

When these terms are inserted into Eq. 5.12, the result is

$$v_g = \left(\frac{u_*^2 z}{d\bar{u}/dz} + D \right) \frac{d \ln C}{dz} + \frac{g\delta^2(\rho - \rho')}{18\eta} \quad . \tag{5.16}$$

Although the actual expressions derived by Sehmel and Hodgson are considerably more complex than this equation, the above relationship does qualitatively indicate the principal parameters that influence the deposition velocity. The deposition velocity for larger particles increases with particle size (settling velocity term), but increases with decreasing particle size for small particles due to Brownian diffusion (see Figure 5.4). Sehmel and Hodgson also predict that the deposition velocity will be proportional to the friction velocity, u_*, and the surface roughness, z_0.

Experimental evidence. Field and small-scale experiments conducted in Idaho [HAW-66, ZIM-69, BU-66, BU-68] showed that, at least for unstable atmospheric conditions, the deposition velocity of radioiodine varied with the parameter $u_*^2/\bar{u}$ (the square of the friction velocity divided by the wind speed) and could be expressed as a function of either u_* or $\bar{u}$. Numerous experiments [HAW-66, ZIM-69, BU-66, BU-68, HEI-74, HEI-76] have shown that the

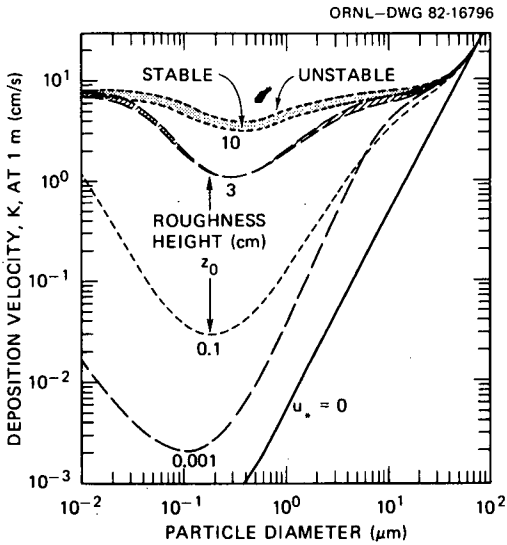

Figure 5.4. Effect of particle size and surface roughness on predicted deposition velocities. From [SEH-76a].

deposition velocity for radioiodine increases with increasing vegetation density, Y_D.

There is considerable evidence that the condition of the leaf surface has an important influence on the deposition velocity for gases. Whether the pores on the surface of the leaf (stomata) are open (daytime) or closed (nighttime) appears to be the most important factor, as higher leaf uptake, hence higher deposition velocities, of CO_2 [CHA-60a, CHA-70], O_3 [CHA-70], NO_2 [CHA-70], tritiated water vapor [BEL-79], and radioiodine [HCU-63] have been reported when the stomata are open than when they are closed.

Increased radioiodine deposition velocities have been attributed to high relative humidities [BAR-63, MIL-67, HEI-76]. Heinemann and Vogt [HEI-80a] found a twofold higher deposition velocity for iodine deposition onto moist grass over dry grass. There is some evidence from the Idaho CERT data that the radioiodine deposition velocity increases at low temperatures and low relative humidities; however, there does not appear to be a consistent relationship that applies to all experimental studies. Measured deposition parameters are summarized in Tables 5.3, 5.4, and 5.5.

5.2.2.4 Wet Deposition

In addition to dry deposition, radioactive materials may also be scavenged from the air by precipitation (rain, snow, and sleet) and deposited on the ground. The rate of total (wet plus dry) deposition can be expressed as (after Pierson and Keane [PEI-62]):

$$\frac{dC_A}{dt} = (v_g + b\dot{R}W_v)\,\chi(t) - (\lambda_e + k\dot{R})\,C_A \ , \tag{5.17}$$

where

v_g = dry deposition velocity (m/sec),

b = fraction of material retained on vegetation from wet deposition (analogous to f_R for dry deposition),

$\dot{R}$ = rainfall rate (m/sec) [$(\dot{R}(\text{m/sec}) = 2.8 \times 10^{-7}\,\dot{R}(\text{mm/hr})$],

λ_e = rate constant for loss from vegetation from processes other than washoff (including radioactive decay) (1/sec),

k = constant describing the loss of material from vegetation due to washoff (1/m) (see Section 5.6.7),

Table 5.3. Reported radioiodine deposition parameters from field experiments

Form[a]	Vegetation	Atmospheric conditions	D	Deposition velocity v_g(m/sec)	Normalized deposition velocity ($v_g/\bar{u}$)	Transfer factors: $v_D = v_g/D$ (m^3/kg-sec)	Transfer factors: $v_D(u^2/\bar{u})$ (m^2/kg)	$v_D/\bar{u}$ [m^2/kg (dry)]	References
I_2	wheat grass or pasture grass	unstable	8	(1.37±0.69)E−02	(2.25±1.0)E−03	0.12±0.04	1.92±0.55	(2.0±0.96)E−02	[HAW-66, BU-68]
	wheat grass or pasture grass	stable	5	(0.31±0.2)E−02	(3.3±2.6)E−03	(4.6±3.0)E−02	0.80±0.36	(4.4±3.5)E−02	[BU-68]
	dry grass		18	(1.03±0.75)E−02		(7.9±5.7)E−02			[HEI-80a]
	pasture grass	stable[b]	2	(2.6±1.3)E−02	(3.9±2.8)E−02	0.33±0.15	4.0±3.6	0.48±0.34	[BU-68]
	Pasture grass	night	2	(1.1±0.37)E−03	(7.0±2.5)E−04	(1.9±1.5)E−02	0.14±0.02	(9.6±2.0)E−03	[BU-68]
	moist grass		5	(2.7±2.2)E−02		0.144±0.071			[HEI-80a]
	pasture grass	neutral	1	8E−03	1.6E−03	0.115	1.41	0.023	[BU-68]
	rye grass		12	(8.6±6.8)E−03	(3.0±2.9)E−03	(5.7±3.2)E−02	1.79±1.51	(3.9±4.3)E−02	[HEI-74, HEI-76]
	grass		4	v_I = (2.0±0.4)E−04					[CHA-60b]
	clover		5	(2.0±1.3)E−02		0.164±0.045			[HEI-80a]
	clover		3	(1.2±0.2E−02		0.14±0.03			[HEI-74]
	clover	stable	1	3.0E−03	9.0E−04	0.071	3.52	0.021	[CHA-60b]
	dandelion	unstable	2	(1.1±0.3)E−02	2.9E−04	0.36±0.20	7.0±3.6	(9.0±3.2)E−02	[CHA-60b]
		stable	1	5E−03	3.6E−03	0.12	7.3	8.9E−02	[CHA-60b]
CH_3I	pasture grass	unstable[b]	1	~1E−04	~6E−05	~1E−03	~1E−02	~6E−04	[BU-68]
	pasture grass	unstable	1	1E−06	~2E−07	~1E−05	~2E−04	~2E−04	[BU-68]
		stable	1	~1E−06	~3E−07	~1E−05	~8E−05	~3E−06	[BU-68]
	pasture grass	stable		1E−05	4.2E−06				[ATK-67]
				(0.14-2.4)E−05	(0.58-10)E−06				

[a] Expected form.
[b] Very high surface roughness (z_o) ~0.4 m calculated from wind velocity profile.

Table 5.4. Results of small-scale radioiodine deposition experiments[a]

Form	Vegetation type	Deposition velocity		Transfer factors		Reference
		v_g (m/sec)	Normalized (v_g/u)	V_D (m^3/kg-sec)	V_D/u [m^2/kg (dry)]	
I_2[b]	pasture grass	(1.4±0.9)E−03	(1.2±0.79)E−03	(1.8±1.6)E−02	(1.6±1.4)E−02	[BU-68]
		1.8E−02	1.6E−02	0.25	0.23	[BU-68]
	rye grass			(2.2±1.9)E−02		[HEI-74]
	spinach leaves	1.6E−03	7.9E−03	1.2E−02	5.9E−02	[NAK-80b]
50% inorganic, 50% organic (HIO_4, HIO_3)	spinach leaves	(2.6±0.8)E−04	(1.3±0.4)E−04	(2.2±0.7)E−03	(1.1±0.35)E−03	[MIY-73]
	chinese cabbage	(1.4±0.6)E−04	(0.7±0.3)E−04	(5.2±2.2)E−04	(2.6±1.1)E−04	[MIY-73]
(85% CH_3I, 15% C_2H_5I)	beet leaves	(2.4±0.5)E−04	(1.2±0.25)E−04	(1.5±0.8)E−03	(7.4±4.3)E−03	[MIY-73]
CH_3I	grass	8.6E−05	8.6E−05			[ATK-67]
	clover	9.0E−05	9.0E−05			[ATK-67]
	rye grass			(1.6±0.3)E−04		[HEI-74]
	grass	1E−04				[HEI-80a]
	spinach leaves[c]	2.3E−05	1.1E−04	1.7E−04	8.4E−04	[NAK-80a]

[a]Some of these values appear lower than comparable field data and should be used with caution.
[b]Expected form.
[c]Assumed density 1.7 kg/m^2 wet, 92. l% water.

Table 5.5. Miscellaneous deposition velocities

Material	Deposited onto	Deposition velocity (m/sec)	Reference
CO_2	grass	2E−04[a]	[CHA-60a]
Kr-85	grass	2.3E−13	[VOI-70]
Ruthenium (from waste calciner)	grass	SE−05	[BUN-65]
Fallout Particulates	grass	2E−03	In [CHA-60a]
Iodine (I^2)	snow	3.43−03	[BU-68]
	sand	1.9E−03	[BU-68]
	soil	3.3E−03	
	water	(2.12E−03)$\bar{u}$−(1.2E−03)	[ALL-75]
Iodine (50% inorganic, 50% organic)	soil	2.7E−04	[MIY-73]
	sand	2.5E−05	[MIY-73]
	water	IE−05	[MIY-73]
Iodine particulate (on $CuSO_4$	grass	IE−03	[HEI-80a]
Plutonium-238	bean plant		[CAT-76]
Citrate (AMAD[b] = 1.6 μm)	bean plant	4.9E−05	[CAT-76]
Nitrate (AMAD[b] = 2.3 μm)	bean plant	8.4E−05	[CAT-76]
Oxide (fresh, (AMAD[b] = 1.3 μm)	bean plant	6.4E−05	[CAT-76]
Oxide (aged, (AMAD[b] = 0.73 μm)	bean plant	3.8E−05	[CAT-76]

[a]2E−04 = 2×10^{-4}.
[a]AMAD = Activity median aerodynamic diameter.

W_v = volumetric *washout factor,** which is defined as:

$$W_v = \frac{\text{activity per unit volume of rain}}{\text{activity per unit volume of air}} \quad . \tag{5.18}$$

Pierson and Keane [PEI-62] suggested that the retention factor has the form:

$$b = 1 - m\dot{R} \quad , \tag{5.19}$$

*This is more commonly expressed in mass concentration as

$$W_m = \frac{\text{activity per unit mass of rain}}{\text{activity per unit mass of air}} \quad ,$$

$W_v = W_m(\rho \text{ rain}/\rho \text{ air})$. Since water has a density of about 10^3 kg/m^3 and air (20°C, 760 mm Hg) is 1.2 kg/m^3, $W_v \sim 830\ W_m$.

where m is a retention parameter (in units of inverse rainfall rate). Data shown in Table 5.6 indicate the possibility that this retention parameter may be associated with the washout coefficient rather than with plant retention, so that $W_v(\dot{R}) = W_v[1 - m\dot{R}]$. A power function has also been used for this relationship: $W_v(\dot{R}) = W_v R^{0.5-0.6}$ [BRE-81].

Estimated values for some of the constants are shown in Table 5.6. Other washout factors are shown in Table 5.7. The form of the retention coefficient b, $1\text{-}m\dot{R}$ approximates the first two terms of the Maclaurin series expansion of $\exp(-m\dot{R})$ so that the exponential form may also be used for b. The exponential form offers the advantage that it does not become negative for high rainfall rates. Inserting this expression for b, the total deposition rate is given by:

$$[v_g + W_v\dot{R}(e^{-m\dot{R}})]\chi \ . \tag{5.20}$$

In general, retention from wet deposition is less than unity due to the combination of deposition and washoff processes. Milbourn and Taylor [MIL-65] report spray retention factors of 0.15−0.30, averaging 0.22. Bergström [BER-67] reports wet retention factors for iodine on grass of 0.3 in light rain and 0.1−0.2 in heavy rain. Weiss et al. [WEI-75] report reactor iodine retention factors of 0.09−0.52 for wet deposition, which predominated over dry deposition. Reanalyses of Miller's [MIL-67] data for wet deposition indicate initial wet retention factors of 0.16 for grasses and 0.45 for grains.

By comprison with the dry deposition case, it can be seen that the ground concentration that corresponds to a constant air concentration of χ for a constant rainfall rate $\dot{R}$ will be:

$$C_A(t) = \frac{(v_g + b\dot{R}W_v)\chi}{(\lambda_e + k\dot{R})}[1 - \exp - (\lambda_e + k\dot{R})t] \ , \tag{5.21}$$

which approaches an equilibrium value of

$$C_A(\infty) = \frac{(v_g + b\dot{R}W_v)\chi}{(\lambda_e + k\dot{R})} = \frac{[v_g + \dot{R}W_v e^{-m\dot{R}}]\chi}{(\lambda_e + k\dot{R})} \ . \tag{5.22}$$

The term $b\dot{R}W_v\chi$ has units of the rate of wet deposition per unit area of ground (activity/m^2-sec) and is analogous to the product $v_g\chi$ for dry deposition.

Example 5.2. Calculate the equilibrium deposition of radioiodine by rain out as a multiple of the average atmospheric concentration for the following parameters:

Table 5.6. Derived estimates of washout parameters[a]

Material	Y variate and units	R units	Fitted parameters for actual units[b]			For R in m/sec mass units	For R in m/sec volume units	Reference for data
			α_1	α_2	$m = -\alpha_2/\alpha_1$	W_M	W_v	
Gases								
$^{38}Cl_2$	Deposition rate per m^2-sec	mm/hr	(0.388)	(−0.0404)	(0.104)	(1680)	1.4×10^6	(SIN-77)
SO_2	A sec^{-1}	mm/hr	(4.15×10^{-5})	(-4.70×10^{-7})	(0.011)	(149)	(1.2×10^5)	
		mm	(0.244)	(-4.91×10^{-3})	(0.020)	(1060)	(8.8×10^5)	
I_2	A sec^{-1}	mm/hr	(2.77×10^{-6})	(6.97×10^{-7})	(0.030)	(700)	(8.3×10^4)	[ENG-66]
Soluble particles								
No aerosol	mg/L	mm	(0.274)	(-5.38×10^{-3})	(0.0198)	(1190)	(9.9×10^5)	
Rhodamine	A sec^{-1}	mm/hr	A. (2.26×10^{-4})	(-8.00×10^{-6})	(0.034)	(815)	(6.8×10^5)	Dana and Wolf
			B. (5.47×10^{-4})	(-3.24×10^{-5})	(0.059)	(1970)	(1.6×10^6)	in [SLI-77]
Fallout ^{131}I					0.015 ± 0.013	420	3.5×10^5	[PEI-62]
^{140}Ba					-0.010 ± 0.027	480	4.0×10^5	[PEI-62]

[a] $Y = \alpha R + \alpha_2 R^2$. R = rainfall rate or rainfall.

[b] Note that the units of the parameter m are the inverse units of R. The use of m values from this table in Eq. 5.19 requires R to be in mm/hr.

Table 5.7. Washout factors for various materials[a]

Material	Washout Factors: Mass, W_M (kg_{air}/kg_{rain})	Washout Factors: Volumetric, W_V (m^3_{air}/m^3_{rain})	Reference
Soluble gases			
Water vapor–10°C	500	(4×10^5)	[ENG-66]
Water vapor–0°C	240	(2×10^5)	[ENG-66]
Water vapor–10°C	110	(9×10^4)	[ENG-66]
Water vapor–20°C	60	(5×10^4)	[ENG-66]
CO_2	1.0	(~830)	[SLI-78]
$^{38}Cl_2$	(1680)	(1.4×10^6)	Table 5.6
SO_2	(150)	(1.2×10^5)	Table 5.6
	190	(1.6×10^5)	[SLI-78]
	60–180	$(0.5–1.5)\times10^5$	[SLI-78]
	(1060)	(8.8×10^5)	Table 5.6
Soluble particulates			
Generally	(~1200)	(1.01×10^6)	[ES-73]
Rhodamine dye	(815)	(6.8×10^5)	Table 5.6
Rhodamine dye	(1970)	(1.6×10^6)	Table 5.6
NaCl aerosol	(1190)	(9.9×10^5)	Table 5.6
NaCl aerosol	(1180)	9.8×10^5	[SLI-78]
Insoluble particulates			
Generally	(361)	3×10^5	[BRE-81]
Generally	(1050)	8.7×10^5	[ES-73]
^{238}Pu (fallout)	(300 ± 130)	$(2.5\pm1.0)\times10^5$	[MAG-67]
^{239}Pu (fallout)	(434 ± 132)	$(3.6\pm2.2)\times10^5$	[MAG-67]
^{239}Pu (fallout)	(8.55 ± 1240)	$(7.1\pm10.3)\times10^5$	[BOR-74]
^{210}Pb (natural)	430	(3.6×10^5)	[CHA-60a]
Lead	290	2.4×10^5	[SLI-78]
Fallout radionuclides	$(1.2\pm0.36)\times10^3$	$(1\pm0.3)\times10^6$	[SLI-78]
^{137}Cs	230	(1.9×10^5)	[CHA-60b]
^{137}Cs	560	(4.6×10^5)	[PEI-62]
^{137}Cs (old source)	600–800	$(5.0–6.6)\times10^5$	[ENG-66]
^{137}Cs	(920 ± 965)	$(7.6\pm8.0)\times10^5$	[BOR-74]
^{137}Cs (new source)	1050–1100	$(8.7–9.1)\times10^5$	[ENG-66]
^{140}Ba	480	(4.0×10^5)	[PEI-62]
^{90}Sr	(710 ± 370)	$(5.9\pm3.1)\times10^5$	[MAG-67]
	(870 ± 675)	$(7.2\pm5.6)\times10^5$	[BOR-74]
^{106}Ru	(675 ± 400)	$(0.56\pm0.33)\times10^5$	[BOR-74]
^{54}Mn	(900 ± 410)	$(7.5\pm3.4)\times10^5$	[BOR-74]
^{95}Zr	130	(1.1×10^5)	[CHA-60b]
	500	(4.2×10^5)	[PEI-62]
	(570 ± 380)	$(4.7\pm3.1)\times10^5$	[BOR-74]

Table 5.7. (continued)

Material	Washout Factors: Mass, W_M (kg_{air}/kg_{rain})	Washout Factors: Volumetric, W_V (m^3_{air}/m^3_{rain})	Reference
Iodine			
Fallout (particulate)	420	(3.5×10^5)	[PEI-62]
	300–1500	$(2.5\text{–}12.4)\times10^5$	[EAC-63]
Elemental iodine,	3000	(2.5×10^6)	[POS-70]
pH 5	3000	(8.3×10^5)	[POS-70]
	(241)	2.0×10^5	[BRE-81]
Methyl (alkyl) iodides,	1–50	$(8.3\text{–}41.5)\times10^3$	[EAC-63]
pH 5	4.2	(3.5×10^3)	[POS-70]
	5	(4.2×10^3)	[POS-70]

[a]Values in parentheses calculated by this author.

Rainfall rate, $\dot{R}$, = 2.5 mm/hr; washoff rate constant, k, = 0.025 mm^{-1}; m = 0.025 hr/mm; washout coefficient, W_v, = 8.3×10^4; removal rate constant = 0.1356 $days^{-1}$.

The appropriate formula is given by Eq. 5.22 with $v_g = 0$:

$$\frac{C_A(\infty)}{\chi} = \frac{\dot{R}W_v e^{-m\dot{R}}}{(\lambda_e + k\dot{R})} =$$

$$\dot{R}W_v = (2.5 \text{ mm/hr})\,(24 \text{ hr/day})\,(10^{-3} \text{ m/mm}).\,(8.3 \times 10^4 \text{ pCi/m}^3 \text{ rain per pCi/m}^3 \text{ air}) = 4.98 \times 10^3 \text{ pCi/m}^2 \text{ day per pCi/m}^3 \text{ air}$$

$$k\dot{R} = (2.5 \times 10^{-2} \text{ mm}^{-1})\,(2.5 \text{ mm/hr})\,(24 \text{ hr/day}) = 1.5 \text{ day}^{-1}$$

$$\exp\text{-}m\dot{R} = \exp\text{-}[(0.025 \text{ hr/mm})\,(2.5 \text{ mm/hr})] = \exp\text{-}0.0625 = 0.9394$$

$$\lambda_e = k\dot{R} = 1.6356 \text{ day}^{-1}$$

$$\frac{C_A}{\chi} = \frac{(0.9394)(4.98 \times 10^3 \text{ pCi/m}^2 \text{ day per pCi/m}^3)}{1.6356 \text{ day}^{-1}}$$

$$= 2.86 \times 10^3 \text{ pCi/m}^2 \text{ per pCi/m}^3 \ .$$

This is approximately half the dry deposition calculated in the example in Section 5.2.2.1 [End of Example]

Pelletier et al. [PEL-65] suggested an equation for total deposition of the form:

$$\frac{C_A \text{ (pCi/m}^2)}{\chi \text{(pCi/m}^3)} = H(a - e^{-p\dot{R}}) \ ,$$

where

H = characteristic height,
(H = (1.18 ± 0.53) × 10^5m, range (0.7−2.0) × 10^5m),

$\dot{R}$ = rainfall rate (inches/month),

p = constant (p = 0.11 month/inch), and

a-1 = to the fraction of dry deposition
(a = 1.05 ± 0.01, range 1.04 − 1.065).

Comparing this form to Eq. (5.22), it can be seen that if

$$H = \frac{\dot{R}W_v}{\lambda_e + k\dot{R}} = a - 1 = \frac{v_g}{\dot{R}W_v} \text{ and } m = p \ ,$$

then

$$\frac{v_g + \dot{R}W_v[1 - e^{-m\dot{R}}]}{\lambda_e + k\dot{R}}$$

results, which is a cumulative, long-term form of Eq. 5.22.

Considerable theoretical efforts have been devoted to modeling wet deposition processes. The reader is directed to several of the primary references on this topic [ENG-66, ENG-70, STY-70, SEM-77, SLI-78]. The principal characteristics that affect wet deposition are particle and raindrop size, rainfall rate, and the solubility of the radioactive material in water [POS-70].

Unlike dry deposition, which primarily involves depletion of the airborne material at the ground surface, wet deposition depletes the entire volume of the cloud. For the purpose of cloud depletion, the rate of wet deposition per unit air concentration integrated over the entire height of the air column affected

by washout is used for depletion. This quantity is termed the washout coefficient, Λ, and

$$\Lambda = \frac{dC_A/dt}{\int_0^h \chi(z)dz} = \frac{dC_A/dt}{h\bar{\chi}(\bar{z})} = \frac{b\dot{R}W_v}{h} \text{ or } \Lambda = \frac{\dot{R}W_v e^{-m\dot{R}}}{h} , \quad (5.23)$$

where h is the height of the air column affected by precipitation. Since both b and W_v are dimensionless, R has units of meters per second, and h has units of meters, then Λ has units of inverse time (sec^{-1}). Depletion of the cloud is time dependent rather than distance dependent:

$$\chi(t) = \chi_0 e^{-\Lambda t} \text{ or} \quad (5.24a)$$

$$\chi(t) = \chi_0 \exp - [b\dot{R}W_v t/h] . \quad (5.24b)$$

5.2.2.5 Conversion of Areal Concentrations into Mass Concentrations

In order to convert the amount deposited per unit area (areal concentration, C_A) into the mass concentration, C_M, (per unit mass) of soil or vegetation, it is necessary to divide the areal concentration by the soil density per unit area or by the mass of vegetation per unit area (termed the vegetation density or, in the case of farm products, the yield or weight per unit area). In the case of soil, it is necessary to specify the depth of interest.

The areal soil density is given by $\rho_A = \rho z$, where ρ is the soil density (typically 1.6−2.6 g/cm^3 or 1600−2600 kg/m^3) and z is the depth of interest (cm or m). For determining uptake by plants from soil, root depths of 0.15−0.2 m are common, so that areal soil densities of 240−520 kg/m^2 are reasonable for this use. This calculational process assumes a uniform distribution of the radionuclide with depth which would be more typical of tilled soil used for agriculture.

In the case of vegetation, the mass concentration C_M is obtained by dividing the areal concentration by the vegetation density Y_D (kg/m^2). As the amount of water in vegetation is highly variable and dependent upon collection and storage techniques, use of the dry-weight yield or dry vegetation density [kg(dry)/m^2] is preferable. Use of the quotient of a deposition velocity (v_g) divided by the dry-weight vegetation density Y_D gives a transfer rate between air and vegetation in units of m^3/kg-sec, which can be used directly to calculate radionuclide concentrations for vegetation. This quantity is given the symbol V_D and can be measured directly as well as being calculated from the two separate quantities. The use of this transfer factor is reported to give more

reproducible results than the use of deposition velocity [BU-68, HEI-74]. Values of V_D are given in Tables 5.3 and 5.4.

5.2.2.6 Resuspension of Deposited Material

Resuspension rate and resuspension factor. Material originally deposited on the ground surface may become airborne through wind action. This process is termed **resuspension**. There are three mechanisms that result in movement of particles deposited onto surfaces [TRA-76]: surface creep (essentially, particles rolling across the surface), saltation [akin to bouncing of particles whereby they become airborne for short distances (~10 m)], and true suspension (in which particles that were once deposited on the ground may become completely airborne and travel up to thousands of meters).

The rate of change of deposited material may be represented as:

$$\frac{dC_A}{dt} = v_g\chi(t) - SC_A \ , \tag{5.25}$$

where

C_A = areal concentration (per m^2) of material on the ground,

v_g = deposition velocity (m/sec),

$\chi(t)$ = airborne concentration (per m^3), and

S = **suspension rate** (1/sec), or the fraction of deposited material resuspended per unit time.

The loss of material from the surface due to migration downward in soil or loss by mechanisms other than resuspension has been neglected in this equation for simplicity. The equilibrium solution to this equation is

$$\frac{dC_A}{dt} = 0, \text{ so } v_g\chi(T) = SC_A \ . \tag{5.26}$$

The ratio of the airborne concentration to the areal concentration of deposited material is

$$\frac{\chi(T)}{C_A} = \frac{S}{v_g}\frac{(1/sec)}{(m/sec)} = K\,(1/m) . \tag{5.27}$$

The quantity K is known as the **resuspension factor** and has units of inverse length (1/m). True equilibrium conditions would apply to an infinite

plane of uniform surface concentration, as it should be evident that an air concentration at a given location results from resuspension of material from the ground surface at some distance upwind.

Measured suspension rates or resuspension factors show considerable variation, ranging over four orders of magnitude [SLI-78]. One factor that influences these measurements is the soil depth from which the areal concentration is evaluated. The areal concentration is usually measured by sampling soil to some depth z, and determining the radionuclide (volumetric) concentration in this soil sample, $C_v(z)$. The areal concentration is then computed as

$$C_A = z\, C_v(z) \ . \tag{5.28}$$

For example, Volchok calculated a plutonium resuspension factor of $10^{-9}m^{-1}$ based upon a 20-cm-depth soil sample and a value of $10^{-6}m^{-1}$ for the same deposit based upon measuring only the surface concentration by pressing a sticky film onto the soil (cited in [LIN-78]).

Slinn [SLI-78] has suggested the use of a "resuspension velocity" akin to the deposition velocity which is defined by

$$v_R = Sz \ . \tag{5.29}$$

where z is the depth of the soil layer. Substitution of Eq. (5.27) for S in Eq. (5.29) yields

$$v_R = v_g K z \ . \tag{5.30}$$

If applied to Volchok's results, this suggests an "effective surface depth" of about 2×10^{-4} m, or 200 μm. As noted by Linsley [LIN-78], use of resuspension factors without knowledge of the associated soil depth is of limited value. Calculations of the product of the resuspension factor and associated soil depth (Table 5.8) suggest that the product Kz (which I term the "resuspension constant") might be less variable than the resuspension factor.

Factors affecting resuspension. One of the principal factors affecting resuspension is the wind velocity (or friction velocity, u_*). The general relationship is that the resuspension rate and resuspension factor increase with wind speed. However, the precise relationship is unclear. Theoretical relationships indicate that the resuspension rate should increase as u_*^2 or u_*^3. The models of Healy [HEA-74] and Travis [TRA-76] suggest u_*^3. The results of Anspaugh et al. [ANS-76] suggest that the dependence is u_*^2 or u_*^3. Sehmel and Lloyd [SEH-76b] find exponents of $u_*^{6.5}$.

Table 5.8. Resuspension parameters

Material	Depth of deposit z m	Resuspension parameters: Resuspension factor, K m^{-1}	Resuspension parameters: "Resuspension constant" Kz	Reference
Plutonium (Rocky Flats soil)	0.2	10^{-9}	(2×10^{-10})	Volchok in [LIN-78]
	2×10^{-4}	10^{-6}	(2×10^{-10})	Volchok in [LIN-78]
Plutonium (NTS soil)	~0.03	10^{-11}	$(3\times10^{-11}$	Anspaugh et al. in [LIN-78]
Plutonium (mud flats)	0.001	4×10^{-8}	(4×10^{-11})	Anspaugh et al. in [LIN-78]
Plutonium (moist soil)	0.01	2×10^{-10}	(2×10^{-12})	[GAR-78]
Plutonium (SRP field)	0.05	10^{-9}	(5×10^{-11})	Milham et al. in [LIN-78]
Uranium in soil				
(Surrey)	0.01	5×10^{-9}	(5×10^{-11})	Bennett in [LIN-78]
(N.Y.)	0.01	1×10^{-8}	(1×10^{-10})	Bennett in [LIN-78]
Radioiodine (from vegetation)		2×10^{-6}		[HAW-66]

Particle size also affects resuspension. In general, true resuspension affects soil particles that are less than 50 μm [in TRA-76]. However, smaller particles can attach to larger soil particles and larger particles can be broken up so that long-term behavior cannot, in general, be predicted from the initial particle size of the deposited material.

Weathering and migration of surface deposits deeper into the soil also affect resuspension rates. Initial resuspension factors of 10^{-4} to 10^{-5} m^{-1} for fresh deposits tend to decrease with time even when migration is inhibited such as on asphalt. Sehmel [SEH-76c] found that material was resuspended from an asphalt road by vehicular traffic so that the fraction of initial resuspension per vehicle pass was 10^{-5} to 10^{-2}. However, this dropped by 2 to 3 orders of magnitude within 30 days. Linsley [LIN-78] recommends a resuspension factor of 10^{-5} m^{-1} if there is regular disturbance by pedestrian or vehicular traffic and a decreasing function of time thereafter:

$$K(t \text{ in days}) = [10^{-6}\exp(-0.01t) + 10^{-9}]\,m^{-1} \quad . \tag{5.31}$$

This is similar to the functions proposed by other studies, although an initial value of 10^{-5} is sometimes used rather than 10^{-6}. Linsley believes the smaller value is more appropriate to well-vegetated soils, whereas the 10^{-5} factor has generally been measured in desert environments. The *Reactor Safety Study* [NRC-75] used the following expression:

$$K(t \text{ in years}) = [10^{-9} + 10^{-5}\exp - 0.6769t]\,m^{-1} \quad . \tag{5.32}$$

Lassey [LAS-80] recommended the inclusion of a second exponential term:

$$K(t \text{ in years}) = [10^{-9} + 10^{-5}\exp - 0.6769t$$

$$+ 9 \times 10^{-5}\exp - 5.776t]\, m^{-1} . \qquad (5.33)$$

This term enhances the importance of the resuspension pathway, even for short-lived radionuclides such as iodine-131.

***Example* 5.3.** Using Eq. 5.32, calculate the plutonium concentration in air above a plot uniformly contaminated with plutonium at an initial level of 0.2 $\mu Ci/m^2$. Calculate the air concentration following the initial deposition at 1 year, 10 years, and 100 years following the initial contaminating event.

Initially ($t = 0$) and $K = 10^{-5}$, so the airborne concentration is (10^{-5} m^{-1}) (0.2 $\mu Ci/m^2$) = 2×10^{-6} $\mu Ci/m^3$.

At 1 year, $K = 5.08 \times 10^{-6}$, so the airborne concentration is 1.02×10^{-6} $\mu Ci/m^3$.

At 10 years, $K = 1.249 \times 10^{-8}$, and the resulting airborne concentration is 2.50×10^{-9} $\mu Ci/m^3$.

At 100 years, $K = 10^{-9}$, so the concentration would be 2×10^{-10} $\mu Ci/m^3$. [End of Example]

5.2.2.7 Retention of Deposited Material on Vegetation

Material deposited on vegetation may be lost through a variety of processes, which include removal by wind (including resuspension) or rain (washoff), consumption of the vegetation by herbivores, and volatilization* or evaporation, in addition to radioactive decay. If the radionuclide concentration on vegetation is expressed in terms of concentration per unit mass (pCi/kg) rather than on an area basis (pCi/m^2), then plant growth should be included as an apparent "removal" mechanism.

The results of the Idaho CERT tests suggest that the loss-rate constant of deposited material from vegetation is composed of the following terms [BU-66]:

$$\lambda_{\text{eff}} = \lambda + r_p = \lambda + \lambda_g + \lambda_w + \lambda_p , \qquad (5.34)$$

*Sublimation of iodine has been suggested [HOL-63] as a possible removal mechanism, but this has not been confirmed.

where

λ = radioactive-decay constant,

λ_g = plant-growth-rate constant

λ_w = loss-rate constant for weathering (both wind removal and washoff), and

λ_p = "plant factor" loss rate.

Initial growth can be represented as an exponential process $\exp(\lambda_g t)$ so that the mass concentration will decrease as $\exp\text{-}\lambda_g t$. For short time intervals, the growth exponential term can be approximated by $1 + \lambda_g t$, which is consistent with Miller's [MIL-67] expression for growth: $1 + gt$ (where $g = \lambda_g$). Milbourn and Taylor [MIL-65] showed that the biological removal half-time for strontium sprayed onto vegetation was approximately 17 (16.6) days when expressed on an area basis and 8.6 days when expressed on a mass basis. This difference corresponds to a growth rate constant (λ_g) of 0.026 days^{-1} or a growth doubling time of 27 days. Miller [MIL-67] estimated a growth constant of 0.024 days^{-1} from Windscale data. A value of 0.052 days^{-1} was estimated for spring grass growth from the CERT data [BU-66]. Kirchmann et al. [KIR-67] estimated growth-rate constants of 0.0239 days^{-1} (doubling time of 29 days) for ryegrass and 0.0328 days^{1} (T_B = 21 days) for clover. Aarkrog's [AAR-75] data for barley and wheat give growth-rate constants of 0.035 and 0.039 days^{-1}, respectively. All of these values give growth doubling times around 20 days (13-29 days).

Weathering losses consist of wind removal, washoff, and possibly volatilization. The CERT experiments [BU-66] indicate that the wind-removal-rate constant is approximately 0.03 days^{-1} ($T_{½B}$ = 23 days) and has the form:

$$\lambda_{w(\text{wind})} = a\,\bar{u}^2 \,. \tag{5.35a}$$

Their values indicate that a would be of the order of 7.1×10^{-9} sec/m^2 for $\bar{u}$ = 7 m/sec. This dependence on wind speed is similar to that of resuspension.

Miller [MIL-67] suggested that the wind-removal-rate is a constant:

$$\lambda_{w(\text{wind})} = k_w\,\bar{u} \,. \tag{5.35b}$$

His values for k_w ($1.2 - 5.9 \times 10^{-5}$ m^{-1}) suggest wind weathering half-times of the order of 0.14 – 0.65 days for a 1-m/sec wind speed. Similar short-term weathering rates were found by Witherspoon and Taylor [WIT-69]

for the loss of particles from pine and oak trees: 0.255 and 0.124 days, respectively. In both studies [MIL-67 and WIT-69], the particles were much larger than those in natural aerosols. Such a rapid removal process may affect the measurement of deposition parameters and might be a cause of the variability in measured deposition velocities. Beyond this effect, it would not be expected to greatly affect long-term retention, as longer removal half-times are measured beyond one day after deposition.

The weathering rate constant for removal by rainfall can be represented as:

$$\lambda_{w(\text{wet})} = k\dot{R} \; . \tag{5.36}$$

where $\dot{R}$ is the rainfall rate (in mm/hr = $L/m^2 \cdot hr$). Values of k calculated from both natural rainfall and artificial washing appear similar (Table 5.9).

Table 5.9. Washoff constants

Radionuclide	Material/conditions	k(mm^{-1})	Reference for data
^{90}Sr	Grass (washing)	(0.0238)	[KRI-69]
	Grass (long-term)	0.009 ± 0.018	[PEI-62]
$^{89}Sr^a$	Cabbage	(0.0236)	in [RUS-66]
$^{95}Zr^a$	Cabbage	(0.0218)	in [RUS-66]
$^{106}Ru^a$	Cabbage	(0.0256)	in [RUS-66]
Ruthenium chloride	Romaine lettuce	(0.0625)	[BIT-72]
Nitrosylruthenium chloride	Romaine lettuce	(0.0428)	[BIT-72]
Nitroslyruthenium tetranitrate	Romaine lettuce	(0.0914)	[BIT-72]
Nitrosylruthenium hydroxide	Romaine lettuce	(0.0529)	[BIT-72]
$^{131}I^a$	Cabbage	(0.0256)	in [RUS-66]
^{131}I	Grass	0.020 ± 0.028	[PEI-62]
$^{137}CS^a$	Cabbage	(0.0197)	in [RUS-66]
	Grass (washing)	(0.0343)	[KRI-69]
	160 delay before washing	(0.0197)	[KRI-69]
$^{144}Ce^a$	Cabbage	(0.0245)	in [RUS-66]
^{238}Pu dioxide	Bush beans (4 mm)	(5.25 ± 2.75)E−03	[CAT-80]
	Bush beans (17 mm)	(1.4 ± 0.5)E−03	[CAT-80]
	Sugar beets (17 mm)	(0.010 ± 0.0029)	[CAT-80]
^{238}Pu hydrated dioxide	Bush beans (4 mm)	(6.5 ± 3.5)E−03	[CAT-80]
	Bush beans (17 mm)	(2.6 ± 0.7)E−03	[CAT-80]
	Sugar beet (17 mm)	(2.5 ± 0.6)E−03	[CAT-80]
Silicate particles	Grass	(0.0626)	[MIL-67]
	Grain heads	(0.0685)	[MIL-67]

[a]Results of Middleton and Squire—assumes only loss after 28 days is from washoff.

Based upon a value of k of 0.025 mm^{-1}, typical average rainfall rates of 2.5 mm/day would yield a weathering half-time of 11 days. This is very similar to reported weathering half-times. Average annual rainfall rates in the United States vary from 7 in./year (0.49 mm/day) in Arizona to 67 in./year (4.7 mm/day) in Alabama. This would result in average weathering half-times between about 6 and 56 days (neglecting other processes). This suggests that the washoff rate parameter should not be used together with an effective weathering half-time.

The mechanism underlying the "plant factor" term is not well defined. Bunch *et al.* [BU-66] have suggested that it could represent volatilization or actual loss of plant surface material. Moorby and Squire [MOO-63] have suggested that the waxy cuticle of plants is shed during the growing season.The CERT experiments indicate values of λ_p of about 0.02 $days^{-1}$, which would correspond to a removal half-time of 35 days.

Long-term retention studies following the Windscale reactor accident and the results of Dahlman *et al.* [DAH-69] indicate the possibility of a two-component retention curve. Although the longer-lived component was observed only in the fall and winter months and could be due to temperature-induced changes in plant characteristics, a two-component retention curve can also be derived from the results of Krieger and Burmann [KRI-69], whose studies were performed in the summer months. Their studies involved duplicate plots, one exposed and one covered. The difference between the short-lived component rate constants of the covered and uncovered plots indicates weathering half-times of 5.4, 6.4, 10.0, and 8.2 days for the four experiments (Table 5.10), or an average (of inverse half-times) of 4.9 days. The suggested retention function of

$$f_R(t) = 0.70 \exp-(\lambda + 0.138)t + 0.30 \exp-(\lambda + 0.0144)t \qquad (5.37)$$

corresponds to a short-term (weathering) half-time of 5 days and a longer-term half-time of approximately 48 days, which might be related to the "plant factor" removal term. For radioiodine-131 ($\lambda = 0.086$ $days^{-1}$), the predictions of this equation for a one-month period, when fitted by a single exponential equation, yield an effective half-time of 5 days and a biological half-time of 13.6 days, in excellent agreement with reported values [THO-65] and Table 5.11.

5.2.3 Radionuclide Accumulation in Soil

The accumulation of radionuclides in soil is of primary importance in estimating the long-term contamination of food crops and animal feeds. For this purpose, the radionuclide concentration in the soil layer equivalent to the depth of plant root penetration is of principal interest. This depth is nominally

Table 5.10. Results of long-term retention studies

Radionuclide	Plant conditions	Fitted radionuclide retention function (L in days)	Initial retention	Weathering rate parameters			
				Short term component		Long-term component	
				λ (days^{-1})	$T_{½}$ (days)	λ (days^{-1})	$T_{½}$ (days)
Windscale accident data [BOO-58]							
Radioiodine-131	Dying-exposed	f_R = 0.64 exp-0.198t + 0.33 exp-0.100t	0.97	0.11	6.2	0.014	48.6
Ruthenium-103,106	Dying-exposed	f_R = 0.66 exp-0.090t + 0.08 exp-0.016t	0.74	0.073[a]	9.5[a]	0.014[a]	49.2
Cesium-137	Dying-exposed	f_R = 1.0 exp-0.141t + 0.19 exp-0.021t	1.19	0.141	4.9	0.021	32.8
Experimental spray application [KRI-67]							
Strontium-85	Tall-protected	f_R = 0.714 exp-0.072t + 0.35 exp-0.0134t	1.049	0.061[a]	11.3	0.00275[a]	252
	exposed	f_R = 0.516 exp-0.200t + 0.20 exp-0.0130t	0.716	0.187	3.7	0.0023[a]	300
	Short-protected	f_R = 0.621 exp-0.763t + 0.395 exp-0.0230t	1.016	0.065	10.6	0.0124	56
	exposed	f_R = 0.656 exp-0.151t + 0.309 exp-0.0245t	0.965	0.141	4.9	0.0139	50
Cesium-134	Tall-protected	f_R = 0.612 exp-0.0614t + 0.349 exp-0.0190t	0.961	0.053[a]	13.0	0.0182	38
	exposed	f_R = 0.680 exp-0.102t + 0.234 exp-0.0077t	0.914	0.102	6.8	0.0069	100
	Short-protected	f_R = 0.626 exp-0.0891t + 0.479 exp-0.0187t	1.105	0.0889[a]	7.8	0.0179	38.8
	exposed	f_R = 0.788 exp-0.148t + 0.335 exp-0.0118t	1.123	0.147	4.7	0.0110	63.0
Fescue grass [DAH-69]							
Cesium-137	Living (per kg)	f_R = 0.464 exp-0.0629t + 0.536 exp-0.0107t	1.0	0.0629	11.0	0.0107	64.6
	Living (per m^2)	f_R = 0.447 exp-0.0507t + 0.553 exp-0.0183t	1.0	0.0507	13.7	0.0183	37.8
Suggested function	(exposed)	f_R = 0.70 exp-(λ + 0.138)t + 0.30 exp-(λ + 0.0144)t	1.0	0.138	5.0	0.0144	48

[a]Not included in the estimation of the suggested retention function.

Table 5.11. Measured retention half times on soil and vegetation

Material/(Season)	Effective λ_E (days^{-1})	Effective T_E (days)	Biological r (days^{-1})	Biological T_B (days)	Reference
Iodine-131 (λ = 0.086 days^{-1})					
Range grass (s)	0.188	3.7	0.102[a]	6.8	[BU-66, #1]
Pasture (f)	0.136	5.7	0.05	13.9	[BU-66, #2]
Pasture (w)	0.106	6.5	0.02	34.6	[BU-66, #7]
Grass (f)	~0.12	5.8	~0.03	~24	[SOL-63]
Grass (unclipped)	0.169	4.1	0.083[a]	8.4	[CHW-65]
Grass	0.139	5.3	0.053	13.1	[MAR-65]
Grass	0.141	4.9	0.055	12.5	[BOO-58]
Grass	0.120	5.8	0.035	~20	[BER-67]
Hay	0.128	5.4	0.042	16.4	[BER-67]
Green chop	0.192	3.6	0.106[a]	6.5	[BER-67]
Grass (washoff)	0.257	2.7	0.171[a]	4.1	[WEI-65]
Grass (sp, s)	(0.178)	(3.9)	0.092	7.5±0.5	[HE-80]
Clover (s)	(0.236)	(2.9)	0.150	4.6±0.5	[HE-80]
Clover (f)	(0.138)	(5.0)	0.052	13.4±2.6	[HE-80]
Desert plant (s)	0.125	5.5	0.0385	18.1	[MAR-63a]
Sagebrush (s)	0.173	4.0	0.087[a]	8.0	[CHW-65]
Cheatgrass (s)	0.239	2.9	0.153[a]	4.5	[CHW-65]
Soil (dry)	0.124	5.6	0.038	18.2	[CHW-65]
Strontium-90 ($\lambda = 6.78 \times 10^{-5}$days^{-1})					
Ryegrass-clover[b]	0.0225	30.8	0.0225	30.8	[MID-60]
Strontium-89 (λ = 0.0136 days^{-1})					
Cabbage			0.0070(?)	98.7	[MOO-63]
Cabbage			0.0285	24	[MOO-63]
Grass (area)	0.054	12.8	0.040	17	[MIL-65]
Grass (weight)	0.080	8.7	0.066[a]	10.4	[MIL-65]
Growth rate constant			0.026	26.6	
Cesium-137 ($\lambda = 6.3 \times 10^{-5}$days^{-1})					
Pasture:					
Permanent (area)	0.0223	31	0.0223	31	[KIR-67]
Permanent (weight)	0.0462	15	0.0462[a]	15	[KIR-67]
Temporary (area)	0.0178	39	0.0178	39	[KIR-67]
Temporary (weight)	0.0506	13.7	0.0506[a]	13.7	[KIR-67]
Growth rate constant (temporary)			0.0328	21.1	
Growth rate constant (permanent)			0.0239	29.0	
Ryegrass-clover[b]	0.0268	25.9	0.0268	25.9	[KIR-72]
Ruthenium-103 (λ = 0.0173)					
Grass (area)	0.10	~10	~0.08	8.4	[KIR-72]
Grass (weight)	0.125	~8	~0.10	6.4	[KIR-72]
Growth rate constant			0.025	~28	[KIR-72]

[a] May include growth.
[b] Primarily growth.

around 1 m, but it is dependent on the plant species and the depth of the water table. In arid regions, where the water table lies deep beneath the surface, root depths may exceed several meters; if the water table is high, roots may be only a few feet in length.

Radionuclides will enter the soil from surface deposits and with irrigation water and will be lost from the rooting zone by infiltration into deeper soil strata and by radioactive decay (lateral movement will be assumed to be negligible). The net rate of radionuclide accumulation can be represented as the difference between the radionuclide input rate I_v per unit soil mass and the rates of removal by radioactive decay and infiltration:

$$\frac{dC_s}{dc} = I_V - \lambda C_S - L_I C_S , \tag{5.38}$$

where

I_v = radionuclide input rate from atmospheric deposition and irrigation,

λ = radioactive-decay-rate constant,

C_S = radionuclide concentration in the soil, and

L_I = rate constant for loss by infiltration.

If the input and infiltration rates are constant, the buildup of the radionuclide concentration in the soil will be given by:

$$C_S(t) = \frac{I_v}{\lambda + L_I} [1 - \exp - (\lambda + L_I)t] . \tag{5.39}$$

5.2.3.1 Radionuclide Input to the Soil

Atmospheric deposition processes have been discussed previously with reference to the deposition onto vegetation (Section 5.6). The general expression for the rate of wet and dry deposition, Eq. 5.20, can be adapted to represent the rate of radionuclide input to the soil. The deposition rate onto soil represents the difference between the total areal deposition rate and the deposition into vegetation given by Eq. 5.20. For dry deposition, this difference is simply the difference between the total deposition velocity and the deposition velocity onto vegetation: $v_T - v_g$. In general, the total deposition velocity is approximately twice the vegetation deposition velocity (see Table 5.1) so that this difference is $2v_g - v_g = v_g$.

In the case of wet deposition, the fraction deposited onto vegetation, f, ranges between 0.1 and 0.5 (see Section 5.6.4) so that the fraction available for entry into the soil is $1 - f$, or 0.5–0.9 times the wet deposition rate, or:*

$$(1 - f)\dot{R}W_v e^{-m\dot{R}} . \tag{5.40}$$

A portion of the total deposition may be lost as surface runoff, the fraction remaining is $1 - L_R$ where L_R is the fractional runoff loss. The sum of the wet and dry deposition rates per unit surface area is

$$\chi[(1 - L_R)v_g + (1 - L_R)(1 - f)\dot{R}W_v e^{-m\dot{R}}] .$$

The input rate per unit soil mass to the root depth L is:†

$$I_{v_{dep}} = \frac{\chi[(1 - L_R)v_g + (1 - L_R)(1 - f)\dot{R}W_v e^{-m\dot{R}}]}{\rho L} , \tag{5.41}$$

where ρ is the soil density.

The contribution from irrigation is similar. It is the irrigation rate (volume per unit area per time) $\dot{V}$, corrected for runoff losses, times the radionuclide concentration in the irrigation water, C_W, divided by the soil density and root zone depth:

$$I_{V_{irrig}} = \frac{1 - L_R)\dot{V}C_W}{\rho L} . \tag{5.42}$$

Since aerial deposition is associated with airborne effluents, and irrigation water is primarily associated with liquid effluents; these two contributions are usually evaluated separately.

5.2.3.2 Surface Runoff

The fraction of irrigation water or rainfall lost as surface runoff will depend primarily upon the permeability of the soil and the slope of the land.

*Recall that $W_v(\dot{R}) = W_v e^{-m\dot{R}}$ where the exponential term is believed to be associated with the precipitation scavenging efficiency.

†Readers might note that washoff of material previously deposited onto plants has been neglected. To a first approximation this contribution may be included by multiplying I_v by $[1 + k\dot{R}/(\lambda + k\dot{R})]$ where k is the washoff rate constant.

Compact, impermeable soils with steep slopes will lose a correspondingly larger fraction of water than level, highly permeable soils. The mass balance of the water on the soil (neglecting evaporation losses) can be represented as the sum of the rate of infiltration into the soil and the rate of volume loss as surface runoff:

$$\dot{V}_T = \dot{V}_I + \dot{V}_R \ . \tag{5.43}$$

The fraction lost as runoff is therefore:

$$L_R = \frac{\dot{V}_T - \dot{V}_I}{\dot{V}_T} = 1 - \frac{\dot{V}_I}{\dot{V}_T} \ . \tag{5.44}$$

The permeability of the soil, K, is defined as the water volume transmitted per unit surface area per unit time or

$$K = \frac{\dot{V}_I}{dA} \quad \text{so that}$$

$$\dot{V}_I = KdA \ . \tag{5.45}$$

The rate of water input is equal to the rainfall or irrigation rate per unit area times the area or

$$\dot{V}_T = \dot{R}dA \text{ or } \dot{V}dA \ .$$

The fractional runoff is therefore:

$$L_R = 1 - \frac{KdA}{\dot{R}dA} = 1 - \frac{K}{\dot{R}} \ . \tag{5.46}$$

On level land, even when the rainfall rate exceeds the soil permeability, there will be little runoff; and the water will puddle on the surface and slowly percolate into the soil. It seems reasonable for the runoff to be proportional to the slope ($s = \Delta h/\Delta x$) of the land so that there is correspondingly greater surface

runoff on steeper slopes. A rough approximation of this effect would be to multiply Eq. 5.46 by the slope, s:

$$L_R = s\,(1 - \frac{K}{\dot{R}})\,. \tag{5.47}$$

The fraction reaching the soil is then given by

$$1 - L_R = 1 - s(1 - \frac{K}{\dot{R}}) \quad \text{for } K < \dot{R} \text{ and} \tag{5.48}$$

$$1 - L_R = 1 \quad \text{for } K \geqslant \dot{R}\,.$$

In evaluating the runoff loss, the instantaneous rainfall or irrigation rate should be used rather than long-term averages. Values for typical soil permeabilities, K, are given in Table 5.12.

Table 5.12. Representative soil properties

Soil type	Void fraction, p	Apparent soil density (1-p)	Field moisture capacity[a] (%)	Typical infiltration rate[b] and permeability cm/hour
				(Multiply by 10 to get L/m^2-hr) (Multiply by 87.65 to get m/yr)
Sandy	0.38	1.65	9	5
	(0.32-0.42)	(1.55-1.80)	(6-12)	(2.5-25)
Sandy	0.43	1.50	14	2.5
Loam	(0.40-0.47)	(1.40-1.60)	(10-18)	(1.3-7.5)
Loam	0.47	1.40	22	1.3
	(0.43-0.49)	(1.35-1.50)	(18-26)	(0.75-2.0)
Clay	0.49	1.35	27	0.75
Loam	(0.47-0.51)	(1.30-1.40)	(23-31)	(0.25-1.5)
Silty	0.51	1.30	31	0.25
Clay	(0.49-0.53)	(1.25-1.35)	(27-35)	(0.025-0.50)
Clay	0.53	1.25	35	0.50
	(0.51-0.55)	(1.20-1.30)	(31-39)	(0.13-1.0)

[a] Field moisture capacity refers to the fraction of the saturation water capacity retained by capillary action and incorporated into water of hydration.

[b] Actual rates may differ considerably due to soil structure and mechanical disturbances compression, tilling, etc.

Source: after Table 7.4 in [IRS-50].

5.2.3.3 Infiltration Loss

Losses of radionuclides from the root zone by infiltration into deeper soil layers are generally neglected in estimating radionuclide accumulation in soils. This leads to conservative overestimates of long-term accumulation. Factors such as high soil permeability and low adsorption properties, which result in apprecible infiltration losses, also result in increased radionuclide uptake by plants. Failure to consider infiltration losses in soils having these properties might result in significant overestimates of long-term radionuclide accumulation in both soil and food crops.

For long-term migration, the net transport velocity can be approximated from a mass balance on the water input and loss from the soil:

$$v = \frac{\dot{V}_{infil}}{dA} = (\dot{R} + \dot{V})(1 - \bar{L}_R) - (\dot{E} + \dot{T}) , \tag{5.49}$$

where

$\dot{R}$ = rainfall rate,

$\dot{V}$ = irrigation rate (less the average surface runoff),

$\dot{E}$ = rate of loss per unit area from evaporation,

$\dot{T}$ = rate of loss per unit area from transportation plants, and

$\dot{E} + \dot{T}$ = the consumptive loss rate.

Table 5.13 provides typical values of $\dot{R}$ and $\dot{E} + \dot{T}$ for various regions. Some measured infiltration rates are given in Table 5.14.

5.2.4 Radionuclide Contamination of Forage and Food Crops

5.2.4.1 Mechanisms Resulting in Contamination of Vegetation by Radioactive Materials

Radionuclide contamination of forage and food crops is a principal component of several exposure pathways that lead to the intake of radioactive materials by man. There are several mechanisms that can result in the contamination of vegetation by radioactive materials as shown in the left-hand portion of Fig. 5.5. These mechanisms, in turn, are influenced by the biophysical processes shown in the right-hand portion of Fig. 5.5. External surface contamination occurs as a result of aerial deposition and surface adsorption of radioactive materials. External contamination results from absorption and biological uptake of radionuclides through roots, leaves, stems, flowers, and fruits.

Table 5.13. Regional water use factors[a]

Area	Approximate annual precipitation R region	m/year	Consumptive (E + T) Water use for reference crop (meters) length of growing season 300 d+	259–300 d	200–250 d	150–200 d
West Coast	Southern	0.4	0.9	0.8		
	North	1.0	0.9	0.8	0.7	0.5
	Alaska	1.4				
	Hawaii	0.6				
West	Interior Mountains & high plains	0.4		1.1	0.9	0.75
	Desert	0.2		1.3	1.1	0.95
Mid-West	Central Plains	0.8		1.0	0.9	0.75
	Great Lakes	0.8		1.0	0.9	0.75
	Interior Valleys	1.1	1.0	0.95	0.8	0.60
Southeast	Atlantic Gulf Coasts	1.3	0.9	0.75	0.8	0.7
	Interior Valleys	1.1	1.0	0.95	0.8	0.6
East Coast	North Atlantic	1.0				0.6
	Mid-Atlantic	1.0			0.7	0.6
	Interior Valleys	1.1		0.8	0.7	0.6
	Puerto Rico	1.6				

Crop water factors (CWF)

Alfalfa	1.00	Lettuce	0.30
Beans	0.42	Melons	0.40
Berries	0.40	Nuts	0.60
Carrots	0.40	Pasture	~0.90
Citrus	0.80	Peas	0.30
Clover	0.90	Potatoes	0.50
Corn	0.40	Sugar Beets	0.82
Grain	~0.40	Tomatoes	0.47

[a] $\dot{V} = \dot{R} - E + T$. If $\dot{R}$ - CWF (E + T) > 0, then $\dot{V} = 0$ and R − E + T = v. If $\dot{R}$ − CWF (E + T) < 0, then $\dot{V}$ = CWF (E + T) − $\dot{R}$.

Source: adapted from Tables 11.12 and 11.13 in [ISR-50)].

External contamination. External contamination of vegetation involves mainly physical processes such as wet and dry deposition of airborne effluents and resuspended material. These processes have been discussed previously. External contamination will be the primary mechanism for contamination of food and feed crops by short-lived radionuclides when there is a continuing source of effluent release. An illustration of the relative importance of external contamination is shown in Table 5.15.

External surface contamination may also result from ion exchange reactions on roots or other plant surfaces. These processes follow the general ion exchange selection rules and are responsible for the uptake of ions from the soil solution by dead plant matter or damaged roots [FRI-67, page 84]. This form of surface contamination is important primarily for root crops such as carrots and radishes.

Table 5.14. Infiltration loss rate constants

Radionuclide	Annual water input rate (mm/yr = L/m² yr)	Fractional loss from soil	Equivalent washout constant[a] k (mm^{-1})	Infiltration loss $\dot{V}_{net}$ = 900 mm per year (yr^{-1})
Sodium-22	230	0.21	(9.13E−04)[b]	
	400	0.83	(2.08E−03)	
	(least-squares regression constrained to 0 loss at 0 input)		(3.7E−03)	(3.33)
Manganese-54	230	0.05	(2.17E−04)	
	400	0.05	(1.25E−04)	
			(1.71E−04)	(0.154)
Cobalt-60	230	0.02	(8.70E−05)	
	400	0.02	(5.0E−05)	
			(6.85E−05)	(0.062)
Zinc-65	230	0.03	(1.30E−04)	
	400	0.03	(7.50E−05)	
			(1.0E−04)	(0.092)
Strontium-90	900			0.015
Cesium-137	230	0.005	(2.17E−05)	
	400	0.005	(1.25E−05)	
			(1.71E−05)	(0.015)

[a]k corresponds to the washoff loss rate constant in Section 5.6.4. Multiplication by the net water input in (L/m^2 yr or mm/yr) will give L_f.

[b]9.13E−04 = 9.13×10^{-4}.

Source: after [DEL-72] and [DEL-73].

Internal contamination. Internal contamination of plants occurs primarily from root uptake of radionuclides from the soil solution. However, absorption of soluble deposited materials through leaves, stems, flowers (inflorescence), or fruits may also result in internal contamination of food crops. Internal uptake involves biologically regulated mechanisms and does not follow the usual ion exchange selection rules.

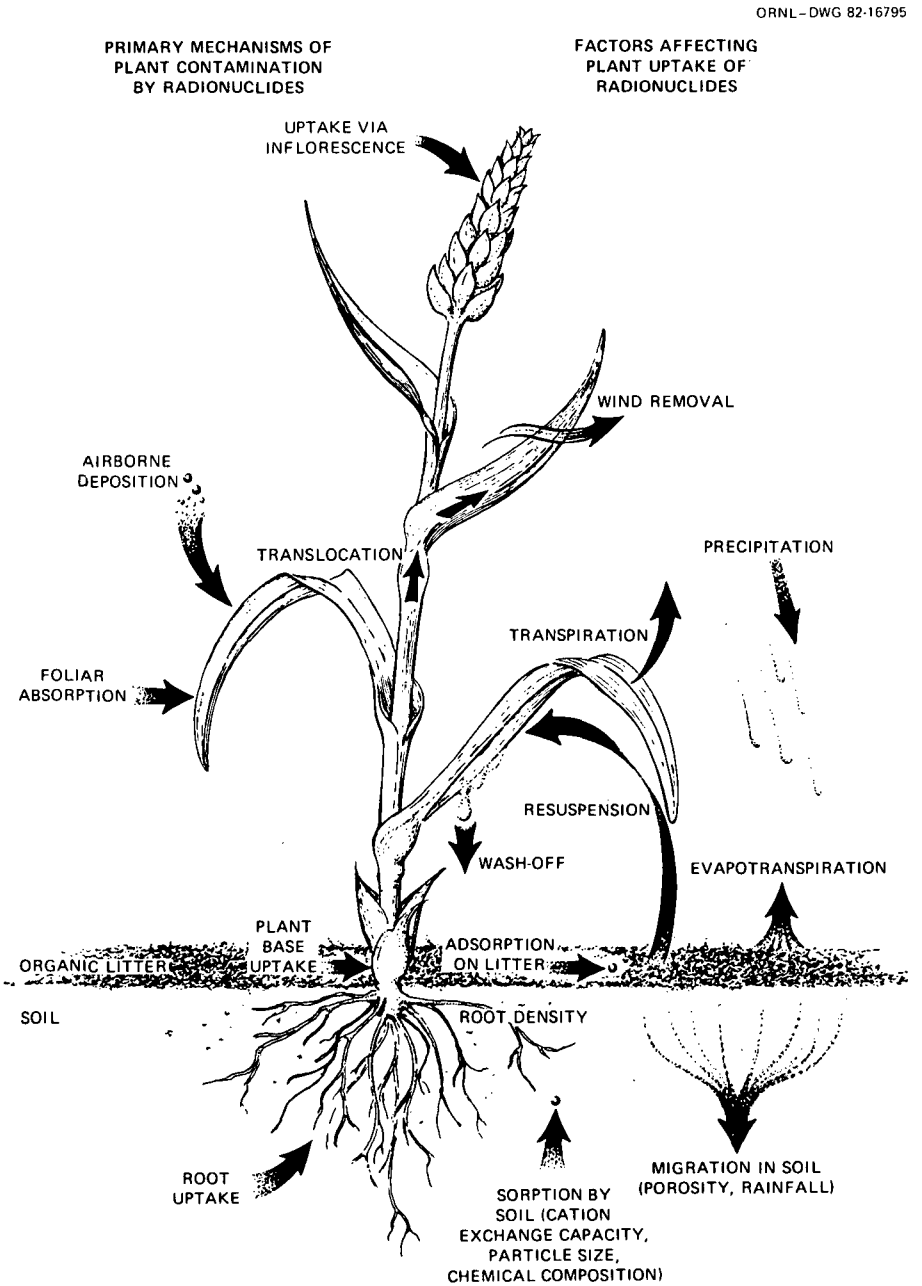

Figure 5.5. Potential pathways for contamination of vegetation.

Table 5.15. Relative contribution of foliar deposition to plutonium concentrations in crops grown in the same soils

Crop	Plutonium concentration fCi/g (dry)		External contamination %
	Field	Greenhouse	
Wheat straw	88.0	3.0	97
Soybean plants	52.2	5.6	89
Corn leaves	33.5	1.1	97

Source: after [ADR-80b].

5.2.4.2 The Plant-to-Soil Concentration Ratio*

Radionuclide uptake by plants from soil has generally been described by an empirical concentration ratio *CR*, which is defined as:

$$CR = \frac{\text{radionuclide activity per unit mass of plant}}{\text{radionuclide activity per unit mass of soil}} \quad (5.50)$$

The radionuclide soil concentrations are generally expressed in terms of oven-dried soil weight. However, the radionuclide concentrations in crops have been reported both in terms of fresh (or wet) weight and dry weight. The relationship between the fresh and dry concentration ratios is:

$$B_{iv} = CR\,(\text{fresh}) = \frac{CR\,(\text{dry})}{(FW/DW)} \quad (5.51)$$

The water content of crops may range up to 90–95% of the total weight for such crops as lettuce and tomatoes so that the fresh-to-dry-weight ratio may be as much as 20 (see Table 5.16). Therefore there can easily be an order-of-magnitude difference between the concentration ratios expressed on the basis of a wet or a dry vegetation weight. Caution should be used when taking *CR* values from the literature to ascertain which method of measurement was used. Representative fresh-to-dry-weight ratios are given in Table 5.16 to aid in converting between the two bases of measurement. However,

*The ratio of plant-to-soil radionuclide concentrations has been variously termed the "soil-to-plant transfer factor," "discrimination factor," "accumulation factor," and "discrimination ratio." A panel of researchers has recommended that the term "concentration ratio" be used and that this be expressed on a dry-weight basis [WOR-75].

Table 5.16. Fresh-to-dry-weight ratios for food crops and forage

Forage (fresh)		Forage (dry)		Grains	
Alfalfa	4.4	Alfalfa	1.1	Barley	1.08
Clover	5.0	Barley	1.1	Rice	1.14
Grass	*5.5*	*Oat*	*1.1*	*Wheat*	*1.15*
Silage	4.2	Soybean	1.1	Corn	3.8
Class[a]	4.5	Wheat	1.1	Class[a]	1.1
		Class[a]	1.1		

Root vegetables (+ tubers)						Leafy vegetables			
A		*B*		*C*		*A*		*B*	
Potato	4.5	Beets	7.9	Radishes	18	Asparagus	12.0	Broccoli	9.1
Sweet potato	3.4	Carrots	8.5	Turnips	11.8	Cabbage	13	Brussel sprouts	6.8
Yam	3.8	Onions	8.6	Class[a]	13	Cauliflower	12	Kale	8.0
Class[a]	4.0	Class[a]	8.2			Celery	16	Spinach	10.8
						Lettuce	20	Turnip greens	10
						Rhubarb	19	Class[a]	8.5
						Spinach	12		
						Class[a]	12.6		

Fruits						Legumes			
A		*B*		*C*		*A (dry)*		*B (fresh)*	
Apples	6.7	Cucumbers	20	Grapefruit	8.6	Lima beans	3.1	Green beans	10
Apricots	6.8	Eggplant	13	Oranges	7.1	Peas	5.9	Class[a]	10
Bananas	4.1	Peppers	15	Peaches	9.2	Class[a]	3.5		
Blackberries	6.4	Pumpkin	11.9	Strawberries	9.9				
Blueberries	6.0	Squash	16.7	Class[a]	8.3	Nuts			
Cherries	5.1	Tomatoes	15						
Figs	4.4					Chestnuts	2.1		
Pears	6.0					Peanuts	1.06		
Pineapple	6.8					Class[a]	1.0		
Plums	5.3								
Raspberries	5.7								
Class[a]	5.7								

[a]Class values represent the 84th percentile lower bound ($\bar{x} + s/\sqrt{n}$) on the average and are based on a range of values reported including multiple values for the same crop which are not shown here. Values are based primarily on the percentage water content reported in WAT-63, where dry weight = 1 − [0.01 × (percent water)], together with additional values from AD-75, STE-80a, and BRA-80.

these values may vary by more than 30% depending upon the crop, time between harvest and weighing, and climatic factors such as relative humidity. In order to avoid confusion, the term "concentration ratio" and the symbol "CR" will be limited to concentrations expressed on a dry-mass basis and the term "soil-to-plant transfer factor" and symbol B_{iv} will be used exclusively for the wet-weight basis.*

Concentration ratios for fission and activation products are shown in Table 5.17 and for natural radionuclides and the actinides in Table 5.18. These values are based upon measured radionuclide uptake in the edible portions of various crops and therefore should be more applicable to radiological dose assessments than values based on average stable element concentrations in plants generally and averages of the element levels generally found in soils. Separate values are given for aerial deposition and for other conditions where the literature indicates a significant effect on radionuclide uptake. These conditions are discussed in the following section.†

5.2.4.3 Factors Affecting Radionuclide Uptake by Plants from Soil

Plant uptake of radionuclides from soils is affected by numerous processes and factors. Because of the multiplicity of factors, plant-to-soil concentration ratios may exhibit considerable variability. Among the more important factors which affect plant uptake are:

a. the physicochemical form of the radionuclide,
b. plant species and internal translocation within the plant;
c. soil characteristics
d. stable element concentrations,
e. fertilizers and agricultural chemicals
f. chelating agents, and
g. the distribution of radionuclides within the soil.

Each of these factors is discussed in the following sections.*

Physicochemical form of the radionuclide. The physical and chemical form of a radionuclide can greatly modify its retention by soil and uptake by plants. Table 5.19 illustrates the relationship between the soil-to-solution distribution factor and the relative uptake of several transuranium elements. The forms most tightly bound to soil (highest K_D) are also those which exhibit the lowest relative uptake by plants.

*Readers should note that the soil-to-plant transfer factors in NRC Regulatory Guide 1.109 [NRC-77] are expressed on a wet-weight basis.

†Since this section was prepared, the author has noted the publication of a comprehensive review of soil-to-plant concentration ratios by [NG-82a].

Table 5.17. Some representative plant to soil concentration ratios for fission and activation products

$$CR = \frac{\text{pCi/kg dry edible part}^a}{\text{pCi/kg dry soil}}$$

Radionuclide/ conditions	Forage		Grains (kernels)		Leafy	Root		Legumes	Fruits	References for data
	Legumes: Alfalfa, Clover, Sorghum	Grasses	Wheat, Oat, Barley	Corn, Rice (dry)	Cabbage Lettuce, Spinach	Radish, Carrot Turnip, Beet	Potato, Sweet Potato	Bean, Pea, Soybean (bean)	Tomatoes, Cucumbers, Apples, etc.	
Sodium-22					72.5(6)					[DEL-73]
Chromium-51										[PER-60]
aerial[b]		0.18(1)			0.031(2)	0.026(1)			0.022(3)	
Manganese-54		0.53(2)	0.35(2)		0.72(1)	0.08(4)	0.14(1)	0.24(1)	0.046(4)	[DEL-72], [DEL-73],
pH < 5.5 (root pH > 7.0)		9.2(2)	3.4(2)		0.48(1)	0.20(1)				[STE-80a]
Cobalt-60		0.04(8)	0.029(3)	0.01(1)	0.08(6)	0.045(3)	0.046(3)			[MYT-69], [GRU-77],
aerial[b]		0.26(2)	0.20(1)							[DSO-79], [STE-80b]
pH < 5.5		0.06(4)	0.044(4)	8.0E-03(1)		0.21(4)	0.10(4)	0.62(4)	0.07(1)	
pH < 5.5, histosol		1.0(1)	0.38(1)			1.3(1)				
Zinc-65					0.68(6)					[PER-60], [DSO-79]
aerial[b]	1.5(1)	0.70(1)		0.38(1)					0.055(49)	
Strontium-90	3.1(15)	1.25(4)	0.22(25)	0.027(7)	2.2(12)	1.8(17)	0.47(5)	1.8(6)	0.24(7)	[ROM-54], [ROM-57], [ROM-60]
Low Ca < 1 g/kg	17.3(6)	3.2(10)	0.24(6)	0.042(2)	7.6(3)	3.5(5)	0.53(3)	4.8(2)	0.44(4)	[BAR-61], [EV-62], [SAR-66]
Low Ca + pH < 5.5	4.1(2)	1.5(8)				83.6(1)[c]	3.0(1)[c]	17.5(1)[c]		[SAR-68], [BOU-69], [DEL-71]
Florida soils	14.9(1)[c]	8.7(7)[c]			24(1)[c]	2.5(1)			1.3(1)	[GAR-71], [STE-80b]
Zirconium-Niobium-95	0.13(2)	0.058(2)			7.2E-03(2)	0.018(5)		1.4E-04(2)	5.4E-04(2)	[SAR-66]
Ruthenium-106	0.27(2)	0.26(11)	0.01(3)	9.8E-04(2)	0.056(4)	0.058(7)	0.015(2)	0.038(7)	0.012(4)	[ROM-54], [ROM-57],
pH < 5.5		0.45(2)	0.16(1)			0.11(2)		0.08(2)		[SAR-66], [SAR-68]
Iodine-129	1.84(1)	0.25(1)				0.03(4)	0.03(1)			[RIC-74], [CLI-76],
aerial[b]					0.07(2)	0.14(2)			0.08(2)	[KIE-76]
Cesium-137	0.093(9)	0.048(24)	0.019(11)	7.8E-03(3)	0.022(14)	0.037(11)	0.032(3)	0.061(7)	0.026(4)	[ROM-57], [FRE-58],
K < 80 mg/kg	0.39(7)	0.20(15)	0.054(4)	0.027(1)	0.32(2)	0.18(5)	0.12(2)	0.26(2)	0.11(2)	[BAR-61], [SAR-66],
Florida soils	42.6(1)[c]	29.1(8)[c]			17.5(1)	4.5(1)			1.5(1)	[SAR-68], [GAR-71], [DEL-73], [STE-80b], [HEI-80b]
Cerium-144 + (rare earths)	0.072(3)	0.023(13)	1.06E-3(5)	8.1E-04(3)	0.036(6)	0.044(7)	6.7E-03(3)	0.033(5)	2.8E-03(6)	[ROM-54], [ROM-57],
pH < 5.5		0.22(1)				0.16(1)		0.14(1)		[SAR-66], [SAR-68]

[a] Values generally represent the 84th percentile bound on the mean $(\bar{x} + s/\sqrt{n})$ when more than one observation was made. This means that the probability $\bar{x} \leq$ value $\simeq 0.84$. Numbers in parentheses indicate number of distinct crop-soil pairs used.

[b] Aerial values represent gross plant-to-soil concentrations ratios and include external contamination from deposited and resuspended material. These values should be used when deposition and resuspension are not assessed separately.

[c] *Small scale experiment results which may not be typical of field conditions.*

Table 5.18. Plant-to-soil concentration ratios for naturally-occurring radionuclides and actinides

$$CR = \frac{\text{pCi/kg dry edible part}}{\text{pCi/kg dry soil}^a}$$

Radionuclide conditions	Forage		Grains (kernels)		Leafy	Root		Legumes	Fruits	References for data
	Legumes: alfalfa, clover, sorghum	Grasses	Wheat oat, barley	Corn, rice (dry)	Cabbage, lettuce, spinach	Radish, carrot, turnip, bett	Potato, sweet potato	Bean, pea, soybean (bean)	Tomatoes, cucumbers, apples, etc.	
Lead-210										[MCD-79], [DED-70], [MIL80b]
aerial[b]		0.10(9)	0.012(2)	0.016(1)	0.046(5)	0.13(7)	0.021(1)	0.078(1)	0.038(1)	
Polonium-210		6.8E-03(7)	1.9E-04(2)	1.9E-05(1)	7.3E-03(3)	6.4E-03(5)	1.5E-04(1)	3.5E-05(1)	[FRA-68], [HAN-70],	
aerial[b]	0.21(1)	0.026(2)	0.049(1)	0.016(1)	0.22(1)	0.29(2)	0.044(1)	0.058(2)	0.06(2)	[MIL-80b]
Radium-226	0.10(24)	0.040(9)	0.058(4)		0.44(2)	0.17(2)			3.5E-03(1)	[KIR-68], [MCD-79], [MIL-80b]
aerial[b]	0.49(6)	0.30(24)	1.3(3)		0.75(1)	0.29(1)	0.024(1)			
Thorium-232	4.6E-03(1)	2E-03(1)	2E-03(1)			3.0E-04(1)	1.2E-04(1)	3E-04(2)	[BON-80]	
aerial-external[b]							2.0E-03(1)			
Uranium-238, U^{232}	3.9E-04(1)	5.0E-03(11)	1.6E-04(2)			3E-04(1)	9.0E-04(1)	1.0E-03(2)	1.7E-03(3)	[AD-75], [SCH-80a], [BON-80]
aerial-external[b]	0.017	0.017(1)	1.0E-03(1)				9.9E-03(1)			[MIL-80b]
Neptunium-237		0.026(14)	5.1E-04(11)					4.6E-03(11)		[WAL-80], [SCH-80b]
aerial[b]	0.19(2)	0.092(1)	0.015(1)					0.013(1)		
pH > 7		4.8E-03(5)	1.2E-04(4)					0.4E-04(4)		
Plutonium-239	2.3E-04(24)	9.2E-05(35)	1.5E-06(20)		1.75E-04(3)	3.7E-04(5)	1.4E-03(1)	8.1E-06(19)		[AD-75], [GAR-74], [AU-77],
aerial[b]	0.066(7)	0.014(9)	0.011(8)	0.011(4)	1E-03(1)	4.6E-03(1)	1E-03(5)	1.0E-03(5)	1.0E-04(2)	[BRO-78], [CAT-76], [BON-80],
microspheres		3.9E-09(2)			2.9E-08(1)					[ADR-80a], [WAL-80], [SCH-80b], [SMI-80], [SMI-81]
Americium-241	1.7E-03(13)	2.1E-03(33)	2.8E-05(21)					6.4E-05(17)		[AD-75], [SCH-76], [AU-77],
aerial[b]	0.019(3)	0.042(7)	7.4E-03(1)		0.05(1)	0.024(1)				[BRO-78], [ARD-80a], [WAL-80], [SCH-80b]
Curium-244	2.3E-03(10)	3.2E-04(10)	6.2E-06(10)					8.4E-05(12)		[SMI-80], [SCH-80b], [WAL-80],
aerial[b]	0.037(3)	0.016(4)	3.5E-03(1)	9.4E-03(4)				5.6E-03(1)		[SMI-81]
pH > 0.7	3.5E-04(2)	3.0E-05(2)	3.1E-06(2)					8.0E-06(4)		

Notes:

[a] Values represent the 84th percentile bound on the mean ($\bar{x} + s\sqrt{n}$). This means that the probability $\bar{x}$ < value is 0.84. Numbers in parentheses indicate number of distinct crop soil pairs used for this calculation.

[b] Aerial values represent gross plant-to-soil concentration ratios and include external contamination from deposited and resuspended materials. These values should be used when deposition onto vegetation and resuspension are not separately evaluated.

Table 5.19. Some examples of the relationship of plant uptake of actinide elements to the soil-to-solution distribution coefficients

Element (oxidation state)	$\log_{10} K_D$	Relative uptake by plants	Reference
Neptunium (V)	0	3×10^4	[WAT-80]
Plutonium (IV)	4.0	4	[WAT-80]
Americium (III)	1.8	35	[WAT-80]
Curium (III)	2	39	[WAT-80]
Plutonium (IV)	5.5		[DAH-76]
Thorium (IV)	5.2		[DAH-76]
Uranium (VI)	3.6		[DAH-76]
Neptunium (V)	2.5		[DAH-76]

Note: The experimental conditions differ between the two sets of data so the distribution coefficients are not comparable.

Different oxidation states of the same element exhibit different relative uptakes. For the actinide elements, the general order of uptake is:

$$Np\,(V, NpO_2^+) > Pu\,(VI, PuO_2^{+2}) > U\,(VI, UO_2^{+2}) \tilde{} = Cm\,(III, Cm^{+3}) =$$

$$Am\,(III, Am^{+3}) > Th\,(IV, Th^{+4}) > Pu\,(IV, Pu^{+4}) \ .$$

This order is the inverse of the affinity for forming complexes with inorganic and organic ligands [DAH-76].

The physical form of the radionuclide also can have an important influence on plant uptake. Simulated fallout that was heat treated up to 80−1000°C showed a marked reduction in solubility and decreased plant-to-soil concentration ratios by up to two orders of magnitude compared with untreated controls [SAR-68]. Similarly, sintered ceramic spheres containing plutonium show plant-to-soil concentration ratios orders of magnitude less than given by the same nuclide in a more available form [AD-75]. Special plant-to-soil concentration ratios are indicated in Table 5.18 for plutonium in the form of sintered ceramic spheres.

Plant species and translocation. Leguminous plants (peas, soybeans, snap beans, alfalfa, clover, etc.), which have a symbiotic relationship with nitrogen-fixing bacteria in their roots, often exhibit higher radionuclide uptake than non-legumes. The concentration ratios for actinide uptake by plants are sometimes an order of magnitude higher for legumes than for other species such as grasses [SCH-80b, WAL-80]. A difference is also apparent with most fission and activation product radionuclides, as shown in Table 5.17. Roots and grains

often exhibit higher concentration ratios than other crops or other parts of the plant. This may in part be due to external surface contamination.

The degree of radionuclide translocation within plants is an important factor governing the radionuclide content of food products such as fruits and grains. Highly soluble elements may be translocated from the deposition site. For example, Dahlman et al. [DAH-69] found that 20% of the ^{137}Cs deposited onto fescue grass was translocated to the roots in 8 days and 25% was translocated in 14 days. Elements which are not soluble in plant fluids will tend to remain at the site of deposition. Hungate et al. [HUN-63] found that only a few percent of the radioiodine (either as I_2 or $I-$) was translocated in bean or geranium plants.

The degree of translocation depends upon the nature of the plant and on the chemical properties and form of the radionuclide. The importance of translocation is shown in Table 5.20. The alkaline earth elements, strontium and radium, are more mobile than the radionuclides of lead, polonium, or thorium and, consequently, should reach higher relative concentrations in leaves, grains, and fruits from soil uptake than less mobile elements. A general guide to the relative mobility of various elements is presented in Table 5.21.

The concentrations of immobile or slightly mobile elements in fruits and grains will be generally lower than in leaves, stems, or roots. Because of these differences concentration ratios based upon the average stable element concentration in entire plants or in a variety of plant species should be considered only to be order-of-magnitude indicators of actual concentration ratios for the edible portions. More precise useful estimates of soil-to-plant transfer can be obtained using concentrations in the edible parts of specific food crops and

Table 5.20. Translocation of radionuclides in plants grown in nutrient solutions

$$\text{Concentration factor} = \frac{\text{pCi/kg fresh}}{\text{pCi/L water}}$$

Radionuclide	Plant	CF roots	CF shoots	% transported to shoots	Reference
^{89}Sr	Bean	142	83.14	75.82	DSO-70
^{226}Ra	Bean	1787	84.60	20.62	DSO-70
^{210}Pb	Bean	4246	2.69	0.32	DSO-70
^{210}Po	Bean	3324	0.58	0.09	DSO-70
^{230}Th	Bean	4185	0.91	0.12	DSO-70
^{59}Fe	Maize	482	5.49	4.43	DSO-79
^{58}Co	Maize	1930	2.68	0.53	DSO-79
^{54}Mn	Maize	1454	151.80	30.92	DSO-79
^{65}Zn	Maize	687	178.10	43.93	DSO-79

Table 5.21. Relative mobility of elements in plants

Mobile	Intermediate (species dependent)	Immobile[a]
Potassium	Lithium	Boron
Sodium	Barium	Lead
Rubidium	Iron	Polonium
Cesium	Manganese	Thorium
Magnesium	Zinc	Plutonium
Calcium	Cobalt	
Strontium	Copper	
Phosphorus	Molybdenum	
Sulfur	Radium	
Chlorine		

[a]In the absence of chelating agents.

Source: Adapted with modification from the results of Bukovac and Wittwer cited in Table 8.1 of [EPS-72].

associated soil concentrations. Such data are available only for the more significant radionuclides such as cesium, strontium, and the actinides. For other elements, the more approximate "whole plant average" concentration ratios have to be used.

Soil characteristics. The importance of soil characteristics in affecting radionuclide uptake by plants was shown by the relationship between the soil-to-solution distribution coefficient and the relative uptake of actinides by plants in Table 5.19. The type of soil can have a profound effect on soil retention characteristics. Sandy soils composed of large particles do not have the retention capacity of clay soils, which are composed of smaller particles having larger surface areas. The difference between sandy soil and clay soil (see Table 5.22) is particularly pronounced for cesium, which is highly sorbed onto clay.

The soil acidity (expressed as pH) can affect the availability of elements from soil. In high pH (alkaline) soils, insoluble precipitates may be formed with carbonate, hydroxyl, phosphate, or sulfide ions which will significantly reduce the availability to plants. In acid (low pH) soils, the hydrogen ions can displace other cations thereby making radionuclides more available to plants. In highly acid soil (pH < 5.5), plants may assimilate sufficient quantities of trace elements (particulary iron and manganese) to be toxic to plant growth [FOT-78], page 323). Special concentration ratios have been given in Tables 5.17 and 5.18 for highly acid soils where radionuclide uptake may be enhanced. The effect of soil pH on radionuclide uptake is illustrated in Fig. 5.6.

Table 5.22. Effect of soil type on radionuclide uptake by plants

Radionuclide	Soil	Plant-to-soil concentration ratio						
		Bean fruit	Clover tops	Carrots root	Radish root	Lettuce head	Tomatoes fruit	Wheat grain
Strontium-85	sandy	0.245	4.77	1.85	3.80	1.41	0.306	0.309
	loam	1.6E−02	1.43	0.522	1.35	0.490	3.8E−02	0.110
	clay	0.106	1.62	0.409	0.815	0.265	0.166	6.5E−02
Cesium-137	sandy	4.63E−02	9.28E−02	8.30E−02	3.12E−02	0.324	8.40E−02	6.17E−02
	loam	1.56E−03	4.52E−02	3.94E−03	4.46E−03	1.27E−02	4.59E−04	6.77E−04
	clay	1.37E−02	4.81E−02	1.83E−02		8.31E−02	1.67E−02	1.29E−02
Ruthenium-106	sandy	1.33E−03	0.273	4.68E−02		2.65E−02	5.92E−02	
	loam	8.62E−04	3.37E−02	1.07E−02		1.88E−02	7.35E−04	
	clay							
Zr-Nb-95	sandy	1.37E−04	0.117	2.89E−02	1.74E−02	7.17E−03	3.76E−04	
	loam	3.39E−05	4.41E−02	9.26E−02	6.59E−03	2.31E−03	5.42E−04	
	clay							
Cerium-144	sandy	6.55E−04	8.45E−02	2.36E−02		4.74E−02	3.86E−03	
	loam	3.15E−04	4.97E−02	6.84E−03	2.33E−03	1.89E−02	1.45E−03	
	clay	4.69E−05	4.74E−02	1.16E−02		8.27E−03	1.35E−03	1.38E−04

Source: data from [SAR-68].

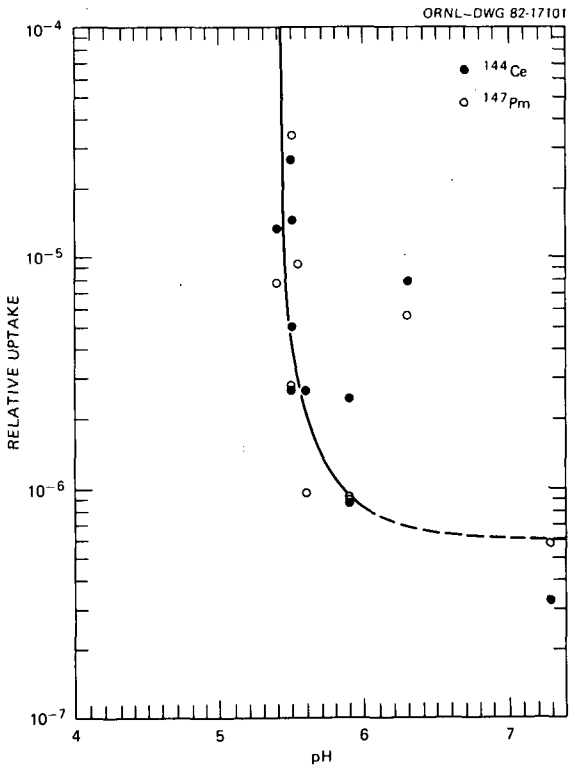

Figure 5.6. Effect of soil pH on radionuclide uptake [CUM-71].

Chemically similar stable elements—the "observed ratio". The presence of chemically similar stable elements can have a significant effect on radionuclide uptake by plants. Studies of radionuclide uptake from nutrient solution indicate that the active uptake of ions by plants appears to involve a "carrier" molecule which reacts with the ion, forming an intermediate product which is passed through the plant membrane. Once inside the plant, this intermediate product dissociates, releasing the ion.

The presence of chemically similar stable elements can affect radionuclide uptake by competing with the radionuclide for the available "carrier" molecules. This process is termed competitive inhibition [FRI-67, page 98] and is also similar to enzyme-catalyzed biochemical reactions. Models of radionuclide uptake from soil based upon the Michaelis-Menten competitive inhibition model can be used to predict the effect of stable elements on radionuclide uptake. These models show that in soils having low concentrations of analogous stable elements, radionuclide uptake by plants is enhanced, sometimes by orders of magnitude above the levels normally found. An example of this is shown

in Fig. 5.7 which depicts the effect of soil potassium on the uptake of ^{137}Cs by oat shoots as measured by Cummings et al. [CUM-69]. This effect is particularly prominent in certain Florida soils which have both a low potassium concentration and a low soil cation exchange capacity. It is a primary contributor to the high cesium concentrations found in Florida milk [GAR-71] and Florida residents [ROE-69].

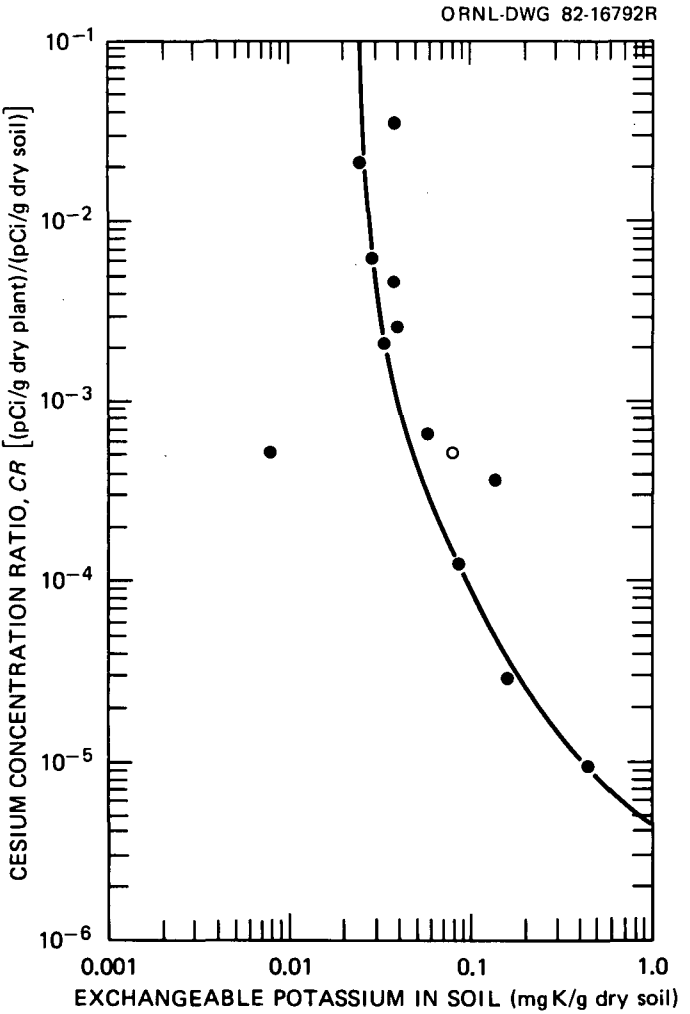

Figure 5.7. The effect of soil exchangeable potassium levels on the uptake of ^{137}Cs by oat shoots based upon the data of Cummings et al. [CUM-69]. The solid line represents the results of least-squares regression plot to a model proposed by the author.

The effect of stable elements on radionuclide uptake by plants has been reflected in the use of element ratios to predict the transport of radionuclides in the food chain. The ratio of the radionuclide concentration to the stable element concentration has widely been used for the strontium-calcium and cesium-potassium element pairs*. The ratio of the radionuclide: stable element concentrations in one medium to the radionuclide: stable element concentration in a precursor pathway is called the **observed ratio,** O. R. [COM-57]:

$$\text{Observed Ratio (O.R.)} = \frac{(C_{\text{radionuclide}}/C_{\text{stable element}})_{\text{medium}}}{(C_{\text{radionuclide}}/C_{\text{stable element}})_{\text{precursor}}} \quad (5.52)$$

The "observed ratio" has also been called the "discriminator factor". In the case of uptake from soil the observed ratio can be described as the product of two discrimination factors:

$$\text{O.R.}_{\text{plant/soil}} = \text{DF}_{\text{plant}} \cdot \text{DF}_{\text{soil}} \quad (5.53)$$

The observed ratio may be used together with measurements of the analogous stable element concentration in plants, $[A_p]$, and in soil, $[A_s]$, and the estimated radionuclide concentration in soil $[B_s^*]$ to estimate the radionuclide concentration in plants $[B_p^*]$:

$$[B_p^*] = \text{O.R.}^{B/A}_{\text{plant/soil}} \cdot \frac{[A_p]}{[A_s]} \cdot [B_s^*] \quad (5.54)$$

More commonly, however, the ratio of the radionuclide concentration to the stable element concentration in the plant is desired as this can be used together with other observed ratios (such as $\text{OR}_{\text{milk/plant}}$ and $\text{OR}_{\text{bone/milk}}$ to predict the radionuclide concentration is human organs for internal dose calculations:

$$[B^*_{\text{organ}}] = (\text{O.R.}^{B/A}_{\text{plant/soil}})(\text{O.R.}^{B/A}_{\text{milk/plant}})(\text{O.R.}^{B/A}_{\text{organ/milk}})[A_{\text{organ}}]\frac{B_s^*}{A_s} \quad (5.55)$$

*This ratio has been expressed in "strontium units" or "sunshine units" (S.U.) where

$$1\text{S.U.} = \frac{1\text{picocurie of strontium}-90}{\text{gram of calcium}}$$

A related expression for the cesium-potassium element pair is the "cesium unit".

where

$[B^*_{organ}]$ = radionuclide concentration in the human organ,

$[A_{organ}]$ = stable element concentration in the human organ, and

$[B_s^*]/[A_s]$ = ratio of the radionuclide concentration in soil to the stable element concentration in soil.

Some observed ratios for alkaline earth elements and calcium are given in Table 5.23. Note that strontium, which is more chemically analogous to calcium, is not discriminated against as effectively as the discrimination against the heavier elements. Also note the apparent decreased discrimination (higher O.R.) shown by the legumes and the one root crop (carrots).

Fertilizers and agricultural chemicals. Fertilizers and chemical additions to soils can effect both the stable element concentration in soils and soil acidity (pH). One of the most common soil treatments is the addition of lime to decrease soil acidity (raise soil pH). Figure 5.8 illustrates the effects of limestone ($CaCO_3$) additions on soil pH, exchangeable calcium concentration, and

Table 5.23. Plant-to-soil observed ratios for the alkaline earth elements

Nuclide	Plant		Observed ratio[a]	References
Strontium	Grains:	Corn	0.58	(a)
		Oat	0.58	(a)
		Barley	0.40-0.45	(b)
		Buckwheat	0.43-0.49	
	Grasses:	Sudan Grass	0.46	(a)
		Brome grass	0.50	(a)
	Legumes:	Clover	0.82	(a)
		Soybean	0.79	(a)
		Alfalfa	0.82	(a)
		Cowpea	0.79	(a)
			0.37-0.53	(b)
	Leafy:	Tobacco	0.78	(a)
		Cabbage	0.78	(a)
Barium	Grains:	Barley	0.02-0.022	(b)
		Buckwheat	0.023-0.028	(b)
	Legumes:	Cowpeas	0.053-0.057	(b)
Radium	Grains:	Barley (straw)	0.028	(c)
	Grass:	Rye grass	0.051	(c)
	Leafy:	Cabbage (leaf)	0.03	(c)
	Root:	Carrot (root)	0.12	(c)

[a]Observed Ratio = (pCi/gram calcium) plant/(pCi/gram calcium) soil

Sources: (a) data from Menzel and Heald in [FRI-60], p. 55, Table 5, (b) [MEN-54], (c) [KIR-68].

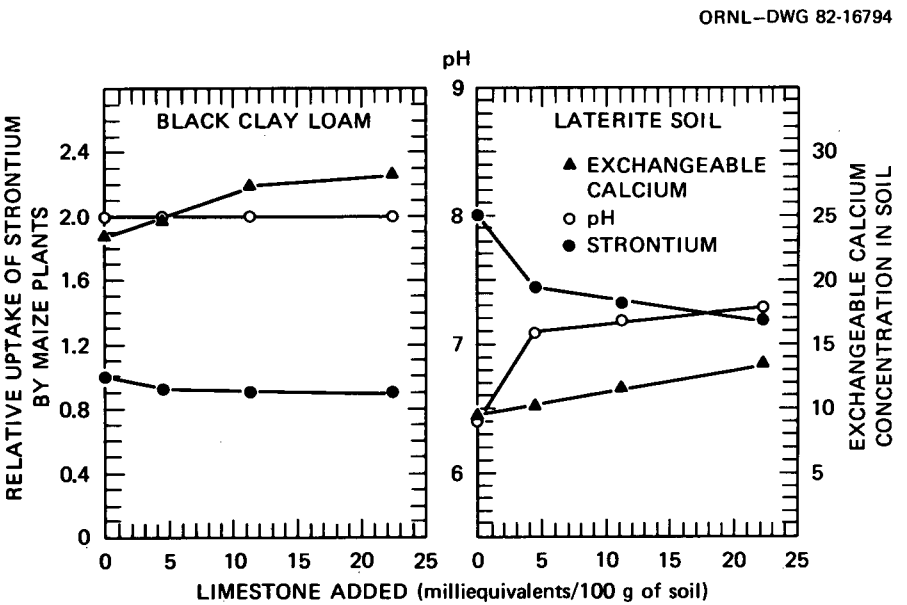

Figure 5.8. The effect of limestone ("lime") additions on strontium-89 uptake by maize plants, soil acidity (pH), and exchangeable calcium concentration in two soils. The strontium uptake is plotted relative to the uptake in the black clay loam without any limestone added. Data from Mistry et al. [MIS-73].

the uptake of strontium-89 from two types of soils. The effect of the lime is more pronounced on the laterite soil which initially had a lower pH, lower exchangeable calcium concentration, and resulted in a greater plant uptake of strontium. The decreased strontium uptake appears to be primarily associated with an increase in pH, possibly due to the decreased solubility of $SrCO_3$ in alkaline conditions.

Fertilizers added to supply nitrogen can also affect soil pH and radionuclide uptake. Fertilizers containing nitrogen in the form of ammonium compounds may give rise to acid soils, particularly when applied to sand and sandy loam [FOT-78], p. 347). The effect of ammonium sulfate* on the uptake of cesium by lettuce is shown in Table 5.24. Fertilizers with nitrogen in the nitrate form (potassium or calcium nitrates) may decrease soil acidity as may phosphate fertilizers such as rock phosphate and bone meal. The modern "superphosphate" fertilizers generally do not have a major effect on soil acidity. Except for the formation of insoluble phosphates, these fertilizers would not be expected to have a major effect on radionuclide uptake by plants.

*Care should be exercised in generalizing without considering the particular circumstances. For instance, ammonium sulfate has been found to *reduce* the uptake of strontium, possibly by the formation of the slightly soluble sulfate [KWA-67].

Table 5.24. Effect of chemical additions to soil on cesium-137 uptake by lettuce

	Approximate amount added to soil (kg/m^2)	Plant-to-Soil concentration ratio (pCi/kg dry plant) / (pCi/kg dry soil)	Change from control (%)
Control	0	0.020 ± 0.0006	0
Calcium chloride	0.011	0.018 ± 0.001	−10
$CaCl_2$	0.034	0.017 ± 0.0008	−15
Calcium nitrate	0.011	0.024 ± 0.001	+20
$Ca(NO_3)_2$	0.034	0.036 ± 0.004	+80
Potassium sulfate	0.011	0.027 ± 0.0008	+35
K_2SO_4	0.034	0.038 ± 0.002	+90
Ammonium sulfate	0.011	0.046 ± 0.005	+130
$(NH_4)_2SO_4$	0.034	0.127 ± 0.015	+535

Source: data from [SCH-65].

Organic materials such as peat moss, composted materials, and manure can affect radionuclide uptake by plants by changing the ion exchange capacity, pH, and stable element content of soils. The organic content of soil is particularly important in influencing the soil retention of technetium (as pertechnetate) [WIL-74, ROU-78] and methyl iodide [WIL-74].

Chelating agents. Certain organic compounds called chelating agents can form stable complexes with metallic ions, leading to a reduction in soil adsorption of these ions. This reduced soil adsorption can lead to greater mobility of these ions in soil and also may result in their ions being more readily available to plants. Common chelating agents are listed in Table 5.25.

The effectiveness of chelating agents in increasing plant uptake of radionuclides depends upon several factors, including the chemical nature of the radionuclide, soil properties (particularly soil acidity or pH), and the nature and concentration of the chelating agent. Certain chelating agents are effective only at very high pH values (as indicated in Table 5.25) and consequently influence plant uptake only in very alkaline soils. Other chelating agents, such as EDTA and DTPA, exhibit complexing ability at lower pH values (higher acidities) and would be effective over most soil pH ranges.

Table 5.26 shows the effect of chelating agents on the uptake of several radionuclides from an alkaline calcareous soil. There is very little influence on the uptake of ^{106}Ru, which may exist primarily as an anion and is not complexed, but the uptake of the lanthanides may be increased by several orders of magnitude. The chelated radionuclides also have increased mobility within the plant. This is particularly evident in Table 5.26 from the increased percentage of the total activity that was transported to the leaves.

Table 5.25. Common chelating agents

Symbol	Chemical name	Molecular weight	Effective pH range for calcium complexion
CDTA	Cyclohexane—1,2—diaminetetraacetic acid	346	>4.5
DTPA	Diethylenetriamine pentaacetic acid	393	>6.5
DHEEDDA	Dihydroxyethyl ethylenediamine diacetic acid	264	>7
EDDHA	Ethylenediamine di(o-hydroxyphenylacetic acid)	360	>9
EDTA	Ethylenediaminetetraacetic acid	380	>5
HEEDTA	Hydroxyethyl ethylenediamine triacetic acid	278	>5.5
NTA	Nitrilotriacetic acid	191	>6
Ra-156	Commercial analog of EDDHA	306	>9.5

Source: after [ESS-62].

Table 5.26. Effect of chelating agents on the uptake and distribution of several radionuclides in bean plants

		Percentage of total activity in				Relative uptake: chelate ÷ control				
Nuclide	Chelating agent	Leaf	Fruit	Stem	Root	Leaf	Fruit	Stem	Root	Total plant
Y-91	Control	9.0	0.45	0.91	89.6					
	DTPA[a]	94.2	0.50	3.0	2.3	249	260	776	6.1	238
	CDTA[b]	88.2	0.90	2.2	8.7	143	29	34	1.4	14.6
	EDDHA[c]	24.7	0.39	1.5	73.4	4.1	1.3	2.4	1.2	1.5
Ru-106	Control	51.1	1.0	9.8	38.1					
	DTPA[a]	50.5	2.8	6.3	40.4	1.0	2.8	0.7	1.1	1.0
	CDTA[b]	30.6	1.1	8.0	60.3	0.6	1.1	0.8	1.6	1.0
	EDDHA[c]	51.2	0.9	4.0	44.0	0.9	0.8	0.4	1.0	0.9
Ce-144	Control	14.2	1.8	8.0	76.0					
	DTPA[a]	90.9	0.6	3.6	4.9	197	10.4	13.7	2.0	30.8
	CDTA[b]	12.2	6.2	19.7	61.9	1.2	5.1	3.6	1.2	1.5
	EDDHA[c]	14.1	0.9	4.5	80.5	0.9	0.45	0.5	1.0	0.9
Pm-147	Control	25.4	3.0	7.5	64.2					
	DTPA[a]	94.7	0.37	1.9	3.0	2113	69.3	144	26.6	565
	CDTA[b]	54.2	0.5	2.8	42.5	10.7	0.8	1.9	3.3	5.0
	EDDHA[c]	33.5	1.7	4.1	60.7	2.7	1.2	1.1	2.0	2.0

Conditions: Sorrento loam pH 7.8, 1.8% organic matter in 1.6 kg pots.

[a]DTPA—diethylenetriamine pentaacetic acid, 100 mg/kg.

[b]CDTA—cyclohexane—1,2—diaminetetraacetic acid, 100 mg/kg.

[c]EDDHA—ethylenediamine di(o-hydroxphenylacetic acid), 100 mg/kg.

Source: after [ESS-63].

Like ruthenium in this respect, cesium does not form complexes with these compounds; consequently, they have little effect on cesium uptake [ESS-62]. Strontium does complex with EDTA and other chelates, but exhibited only a slight increase in plant uptake in the presence of chelates (maximum uptake about 25% higher with NTA than for the control). This lack of effect may have been due to competition between the radionuclides and the high level of calcium in this calcareous soil for the chelating agent [NOR-69]. It is possible that strontium uptake could be increased by chelation in soils with lower calcium content. The effect of chelating agents is particularly pronounced for certain transuranic elements, which are not generally absorbed by plants under normal soil conditions. The increased uptake in the presence of DTPA is evident in Table 5.27.

As indicated previously, increased radionuclide mobility in soils and increased plant uptake resulting from chelating agents may be important at low-level-waste sites where decontamination agents containing chelates may be buried [CHA-76, MEA-78, ESS-79]. The effects of chelating agents may also be important in certain situations where metal chelates are administered as agricultural supplements to remedy nutrient deficiencies [ESS-62, CAT-78]. Chelates of iron, zinc, and manganese are commonly used to remedy such deficiencies because their lower soil retention results in higher plant uptake per unit mass added to soil [WAL-56]. These agents can also result in chelation and increased plant uptake of radionuclides. However, this increased uptake may be partially compensated for by increased infiltration due to lower retention in the soil matrix.

Table 5.27. Effect of chelating agents on soil-to-plant transfer of transuranic elements (100 mg chelating agent per kg of soil)

Radionuclide	Plant	Chealting agent	Concentration ratio, CR	Ratio of uptake with chelate to control		Reference
				Range	Mean	
Pu-239	Alfalfa	Control	5.5E−05			[ROM-70]
		EDDHA[a]	3.1E−04		5.7	[ROM-70]
		DTPA[b]	1.2E−03		21.3	[ROM-70]
	Alfalfa	Control	4.8E−03			[ROM-70]
		EDDHA[a]	8.5E−03		1.77	[ROM-70]
		EDDHA[a]	2.5E−03		0.52	[ROM-70]
			3.3E−03		0.69	[ROM-70]
	Pea (leaf)	Control	6.8E−04			[LIP-76]
			(6.27-7.4)E−04			[LIP-76]
		DTPA$_b$	0.50	656-858	737 ± 107	[LIP-76]
Am-241	Bush bean	Control	(4.7 ± 1.2)E−03			[WAL-79]
		DTPA[b]	0.57	9.5-310	122	[WAL-79]

[a]Ethylenediamine di(o-hydroxyphenylacetic acid)
[b]Diethylenetriamine pentaacetic acid.

Distribution of radionuclides in soil. Plant root systems generally resemble an inverted tree with most of the root lying closer to the soil surface. Because of this distribution, plant uptake of water from the soil is greatest nearer the surface and declines with depth, as shown in Fig. 5.9 (a) and (b). Only when the water nearer the surface is depleted do plants draw appreciable water from deeper zones.

Radionuclides are generally drawn up by plant roots along with the water. As a consequence of the root distribution and distribution of water intake with depth, radionuclide uptake by plants generally decreases with the depth in soil, as shown in Fig. 5.9 (c) and (d). The relative uptake from various depths will depend upon the type of vegetation, the properties of the soil, and the height of the water table, all of which affect the root distribution pattern. The radionuclide mobility in the soil is also an important factor. The strontium uptake pattern shown in Fig. 5.9 (c) shows a lesser influence of depth than the uptake of cesium, presumably because the strontium is less tightly bound to the soil and more able to diffuse to the plant roots. The more tightly bound cesium exhibits

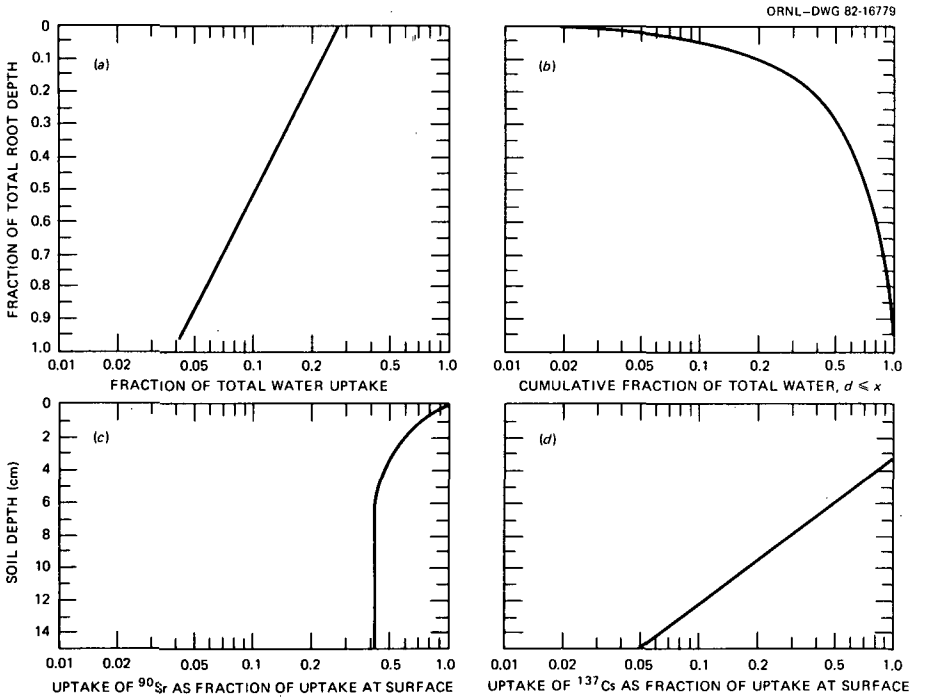

Figure 5.9. (a) Fractional water uptake by alfalfa with depth and cumulative water intake. (b) From Arizona Agricultural Experimental Station data in Foth [FOT-78], Figure 4.16, p. 81. (c) Fractional uptake of Strontium-90 and Cesium-137. (d) With depth of radionuclide in soil. Based on the data of Kirchmann et al. [KIR-67] for grass.

an uptake profile similar to that of the water intake. The effect of both plant type and soil type on the relative uptake at different soil depths is shown in Table 5.28. The relative uptake from a depth of 20 cm is higher for the more deeply rooted alfalfa than for the shallow rooted ryegrass in all soil types. The relative uptake from a depth of 20 cm is higher in sandy soil for both plants, again presumably due to the lower soil retention and greater mobility.

Table 5.28. Effect of radionuclide depth in soil on plant uptake

Crop	Soil type radionuclide	Relative uptake uptake (at 20 cm)/uptake (surface) Prairie humus	Podzol	Sand
Grass	Strontium-90	0.15	0.06	0.18
	Cesium-137	0.09	0.05	0.20
	Radium-226	0.26	0.14	0.16
Alfalfa	Strontium-90	0.36	0.05	0.37
	Cesium-137	0.26	0.38	0.56
	Radium-226	0.12	0.50	0.20

Source: data from [GRZ-72].

It should be noted that the uptake shown in Fig. 5.9 (c) and (d) and in Table 5.28 was determined by placing a contaminated soil layer at different depths. Consequently, the decreased uptake with depth is not due to the vertical profile of the radionuclide concentration but is primarily a result of the plant root and water intake distributions. In the natural environment, the combination of the vertical radionuclide distribution and root uptake pattern will lead to a more pronounced decrease of plant radionuclide uptake with increasing depth. This is shown for ^{89}Sr in Table 5.29; approximately 85% of the uptake comes from the first 25% of the root depth. Because of this effect, tilling contaminated soils can produce a reduction in plant uptake and becomes a possible protective measurement in case of accidental contamination.

The decrease in radionuclide uptake with depth in soil also may affect the validity of plant-to-soil concentration ratios (*CR*s) obtained from small pot experiments. In most small-scale experimental studies, the radionuclide concentration is uniform throughout the root zone. In nature, a uniform soil profile would generally be restricted only to the upper layer (approximately 0.2−0.3 m) of tilled soil, whereas crop roots may penetrate well below this zone. The decreased radionuclide uptake with root and soil depth generally results in lower *CR* values being measured in field studies than in small pot experiments.

Table 5.29. Fraction of strontium uptake derived from different soil depths

Depth		Percentage of total uptake				
	Fraction of total	Alfalfa (lucerne)		Ryegrass		
cm	depth		cumulative		cumulative	Reference
10	0.125	40	40	49	49	[MIL-62]
20	0.25	46	86	35	84	[MIL-62]
40	0.50	6	92	9	93	[MIL-62]
80	1.00	8	100	7	100	[MIL-62]
			Grass			
			cumulative			
0–5	0.25	50	50			[POE-72]
5–10	0.50	25	75			[POE-72]
10–20	1.00	25	100			[POE-72]

Comparison studies of crops grown in the same soils in containers of different sizes [STE-80a] confirm this effect. An illustration of the effect of experiment size on the ^{54}Mn concentration ratio is shown in Fig. 5.10.

5.2.4.4 Vegetation Contamination from Irrigation

Contamination of both soil and vegetation can occur if water containing radioactive materials is used for irrigation. The fraction of the radioactive

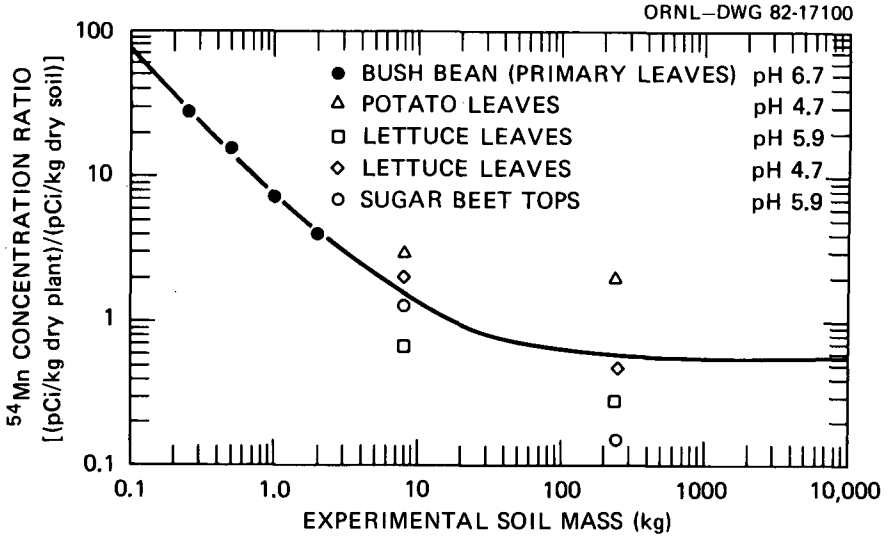

Figure 5.10. The effect of experiment size on the plant-to-soil concentration ratio for manganese-54 uptake by leafy plants [STE-80a].

material in the water that is taken up by the plant will depend upon several factors, especially the mode of irrigation. There are several methods of irrigating cultivated crops, including distribution of the water through surface furrows, through porous subterranean pipes, drip irrigation involving application of water to localized portions of the soil, and sprinklers [FOT-78, pp. 108−109]. Total flooding of fields is also used, primarily for rice cultivation.

The importance of the soil radionuclide retention properties will depend upon the degree of soil contact resulting from the different modes of irrigation. This degree of soil contact is smallest for sprinkler or spray irrigation and flooding and greatest for irrigation by surface furrows.

Direct contamination from spray irrigation. Radionuclide uptake by plants from irrigation can occur by direct contamination from contact with the water or by indirect contamination from contact with soil that has been contaminated by the water. Direct contamination from spray irrigation would be expected to resemble wet deposition (Section 5.2.2.4). Equation (5.21) can be modified to describe this process:

$$C_M(t) = \frac{C_A}{Y_v} = \frac{C_w I e^{-mi}}{Y_v(\lambda_e + kI)}[1 - \exp - (\lambda_e + kI)t] \ , \tag{5.56}$$

where

C_M = the mass concentration (activity/mass) of the radionuclide on the plant,

$C_A = C_w I e^{-mi}$ = the areal concentration (activity/m^2) deposited per unit area of plant

Y_v = the vegetation density (kg/m^2),

C_w = the radionuclide concentration in the irrigation water (activity/L) and

I = the irrigation rate* (liters per hour per m^2, L/m^2 · hr).

The remaining parameters are as defined in Eq. (5.21).

This expression describes the interception of irrigation spray by the entire aboveground portion of the plant. In order to determine the radionuclide concentration in a specific food product (grain, leaves, fruit, etc.), it is necessary to multiply this expression by a factor, f, which is the fraction of the total plant activity that reaches the edible part of the plant. The factor includes both the fraction of the material deposited on the edible portion and

*Recall that a rainfall rate of 1 mm/hr = 10^{-3}m^3/m^{2}hr = 1L/m^{2}hr.

translocation to the edible portion of material deposited elsewhere on the plant.

For short time periods, Eq. (5.56) can be approximated* by:

$$C_M = \frac{C_w \dot{I} t f e^{-m\dot{I}}}{Y_v} = \frac{C_w V f e^{-m\dot{I}}}{Y_v} , \tag{5.57}$$

where V is the total volume of water applied per unit area ($V = \dot{I}t$). The ratio C_M/C_W has been measured and provides a water-to-plant transfer factor, F:

$$F = \frac{C_M\,(\text{activity/kg plant})}{C_W\,(\text{activity/L of water})} = \frac{f e^{-m\dot{I}} V}{Y_v} . \tag{5.58}$$

Another transfer factor may be obtained by dividing both sides of this equation by V:

$$c_{sp} = \frac{F}{V} = \frac{C_M(\text{activity/kg plant})}{C_W(\text{activity/L})\,V(\text{L/m}^2)} = \frac{f e^{-m\dot{I}} V}{Y_v V} , \tag{5.59}$$

This represents the radionuclide concentration in the plant per unit activity per surface area. The radionuclide concentration in the plant may be calculated from:

$$C_M\,(\text{activity/kg}) = F C_W\,(\text{activity/L}) = c_{sp} C_W\,(\text{activity/L}) V(\text{L/m}^2) . \tag{5.60}$$

Tabulated values of F and c_{sp} are given in Table 5.30.

Indirect contamination from irrigation water. Radionuclides present in irrigation water distributed by surface furrows or subterranean conduits will interact with the soil prior to entering crops. Barbier et al. [BAR-61] have proposed a model to describe this process, which is similar to the model developed in Section 5.2.3 for radionuclide accumulation in soil. Their model relates the radionuclide concentration in the vegetation to the radionuclide concentration in the irrigation water:

$$r\left(\frac{\text{pCi/kg plant}}{\text{pCi/L}}\right) = \frac{c_{irr}\left(\frac{\text{pCi/kg plant}}{\text{pCi/m}^2}\right) \dot{V}(\text{L/m}^2 \cdot \text{yr})}{\lambda(\text{yr}^{-1}) + \Psi(\text{yr}^{-1})} , \tag{5.61}$$

*For small values of x [$x = (\lambda_e + k\dot{I})t$], e^{-x} can be approximated by $1 - x$, so that $1 - e^{-x}$ is approximately equal to x.

Table 5.30. Water-to-plant transfer factors for direct contamination by spray irrigation

Radionuclide reference	Plant part	FW[a]/DW	Irrigation volume (L/m^2)	Transfer factors: Fresh weight basis c_{sp} ($\frac{m^2}{kg\ fresh}$)	Fresh weight basis F ($\frac{L}{kg\ fresh}$)	Dry weight basis c_{sp} ($\frac{m^2}{kg\ dry}$)	Dry weight basis F ($\frac{L}{kg\ dry}$)
Sodium-22	Green beans pod	(5)	150	(4.7E−04)	0.07	(2.4E−03)	(0.35)
[DEL-73]	Lettuce leaf	(10)	150	(6.0E−03)	0.9	(0.06)	(9.0)
	Carrot root	(8.5)	150	(1.3E−02)	1.7	(0.11)	(14.4)
	Apple fruit	(6.7)	400	(1.75E−04)	0.07	(1.17E−03)	(0.47)
Chromium-51 (Cr^{+3})	Lettuce leaf	(10)			2−5		(20−50)
[BIT-72] (CrO_4^{-2})	Lettuce leaf	(10)			0.5–1.0		(5−10)
Manganese-54	Green beans pod	(5)	150	(2.7E−04)	0.04	(1.35E−03)	(0.20)
[DEL-73]	Lettuce leaf	(10)	150	(5.0E−03)	0.75	(0.05)	(7.5)
	Carrot root	(8.5)	150	(~0)	~0	~0	~0
	Apple fruit	(6.7)	400	(1.25E−04)	0.05	(8.4E−04)	(0.34)
Cobalt-60	Green beans pod	(5)	150	(4.8E−03)	0.72	(0.024)	(3.6)
[DEL-73]	Lettuce leaf	(10)	150	(1.05E−02)	1.57	(0.105)	(15.7)
	Carrot root	(8.5)	150	(2.7E−03)	0.4	(0.023)	(3.4)
	Apple fruit	(6.7)	400	(2.0E−04)	0.08	(1.3E−03)	(0.54)
Zinc-65	Green beans pod	(5)	150	(8.0E−04)	0.12	(4.0E−03)	(0.6)
[DEL-73]	Lettuce leaf	(10)	150	(1.07E−02)	1.6	(0.107)	(16)
	Carrot root	(8.5)	150	(3.3E−03)	0.5	(0.028)	(4.25)
	Apple fruit	(6.7)	400	(3.75E−04)	0.15	(2.5E−03)	(1.0)
Strontium-90	Young vegetation		15	(1.3−4.6)E−02	0.2−0.7		
	Old vegetation		15	(2.3−6.0)E−02	0.34−0.9		
Sodium-22	Green beans pod	(5)	150	(4.7E−04)	0.07	(2.4E−03)	(0.35)
Ruthenium-106	Lettuce (leaf)	(10)			0.15[a]		(1.5)
[BIT-72]	Lettuce				0.5[b]		(5.0)
	Tomato fruit	(15)			0.05[a]		(0.75)
Cesium-137	Green beans pod	(5)	150	(4.9E−03)	0.73	(0.0245)	(3.65)
	Lettuce leaf	(10)	150	(0.01)	1.5	(0.1)	(15)
	Carrot root	(8.5)	150	(2.7E−03)	0.4	(0.023)	(3.4)
	Apple fruit	(6.7)	400	(3.75E−04)	0.15	(2.5E−03)	(1.0)

[a]Assumed fresh/dry weight conversion factor.
[b]All ruthemium compounds except nitrosyl ruthenium hydroxide.

where

r = the ratio of the radionuclide concentration in vegetation* to the radionuclide concentration in the irrigation water,

c_{irr} = the ratio of the radionuclide concentration in vegetation* to the radionuclide activity deposited by the water per unit surface area of soil,

$\dot{V}$ = the annual irrigation rate ($L/m^2/yr$),

λ = the radionuclide decay constant, and

Ψ = the fraction f of radionuclide lost per year through infiltration.

The equilibrium values for radionuclide accumulation in soil from irrigation water are given by

$$C_{soil} = \frac{C_W (1 - L_R) \dot{V}}{\rho L (\lambda + \Psi)} . \tag{5.62}$$

The radionuclide concentration in the plant can be obtained by multiplying both sides of this expression by the plant-to-soil concentration ratio, CR, so that

$$C_{plant} = CR \cdot C_{soil} = \frac{C_W \cdot CR \cdot (1 - L_R) \dot{V}}{\rho L (\lambda + \Psi)} . \tag{5.63}$$

The parameter r in Eq. 5.61 is the ratio of C_{plant} to C_W; therefore,

$$r = \frac{r'}{(\lambda + \Psi)} = \frac{CR \cdot (1 - L_R) \dot{V}}{\rho L (\lambda + \Psi)} . \tag{5.64}$$

Comparison of this expression to Eq. 5.61 shows that the parameter c_{irr} is

$$c_{irr} = \frac{CR \cdot (1 - L_R)}{\rho L} , \tag{5.65}$$

*Note that the parameters c and r, like the concentration ratio, can be expressed in terms of fresh (wet) weight or dry vegetation weight.

where

CR = plant-to-soil concentration ratio,

L_R = fraction lost by surface runoff,

ρ = bulk density of the soil, and

L = effective root depth of the plant.

Values of the transfer parameters c_{irr}, r', and r, together with the experimental conditions under which they were obtained, are shown in Table 5.31. These parameters are dependent upon the type of crop and soil, as might be expected from the relationship shown in Eq. 5.65 between these parameters and the plant-to-soil concentration ratio. The importance of soil type may be seen from the ^{90}Sr and ^{137}Cs values for a low-potassium and low-calcium soil (denoted by *a*), which are generally an order-of-magnitude larger than the transfer factors for more typical agricultural soils.

The mode of irrigation may also have a significant effect on the radionuclide content of food crops, as shown in Table 5.32. Irrigation of crops using surface irrigation furrows appears to transfer only about half as much ^{90}Sr or ^{137}Cs to the plant as either subterranean irrigation or spray. Losses along the furrow may account for this difference. The transfer of cesium from subterranean irrigation conduits appears to be slightly higher (by about 20%) than from sprinkler spray. This may be due to soil retention of the spray material in soil layers above the roots.

Flooding. Irrigation by complete flooding of fields is used for rice cultivation. Radionuclides in the irrigation water may enter the plant via the stem base as well as via the roots. As in the case of sprinkler irrigation, uptake from the water is generally higher than from soil due to the absence of soil sorption processes. The uptake by the grain from water is about two orders of magnitude greater than from soil and can be extremely high for cesium, which otherwise is tightly bound to soil [MYT-69, BIT-72]. The magnitude of increased uptake from flooded soil is considerably lower than that from water, typically being around a factor of 3, depending upon the radionuclide and the soil type. Less retentive soil (such as laterite soil) permits greater soil-to-plant transfer from flooded as well as unflooded fields [OSO-79, MIS-73].

5.2.5 Radionuclide Transfer to Animal Food Products

5.2.5.1 Uptake and Retention of Radionuclides by Animals

The transfer of a radionuclide from animal feed to a food product depends upon the metabolism of the animal. The simplest model of this process is shown in Fig. 5.11. This model has two compartments: the first compartment typically represents the blood and the second compartment the organ or food

Table 5.31. Water-to-plant radionuclide transfer factors for indirect contamination of crops by irrigation of soil with contaminated water

Radionuclide	Crop (Edible portion)	FW/DW	Test irrigation volume, V (L/m^2)	Area-to-plant: Transfer factor, c_{irr} m^2 kg (fresh)	Area-to-plant: Transfer factor, c_{irr} m^2 kg (dry)	Transfer rate factor: Water-to-plant $r' = c_{irr} \times V$ L kg (fresh)/yr	Transfer rate factor: Water-to-plant $r' = c_{irr} \times V$ L kg (dry)/yr
Sodium-22 ($\lambda = 0.266\ yr^{-1}$)	Lettuce	(10)	230	0.17	(1.7)	(39.1)	(390)
			400			(68)	(680)
	Green beans	(5)	400	3E−04	1.5E−03	(0.069)	(0.345)
						(0.12)	(0.6)
	Carrots	(8.5)	230	0.13	(1.10)	(29.9)	(254)
			400			(52)	(442)
	Apples	(6.7)	230	1E−04	(6.7E−04)	(0.023)	(0.154)
			400			(0.04)	(0.27)
Manganese-54 ($\lambda = 0.817\ yr^{-1}$)	Lettuce	(10)	250	(0.5-2)E−04[a]	(0.5-2)E−03[a]	(0.012-0.05)[a]	(0.125-0.5)[a]
	Apples	(6.7)	1430	(0.5-2)E−04	(0.34-1.34)E−04	(0.7-2.8)E−02	(0.05-0.19)
Cobalt-60 ($\lambda = 0.132\ yr^{-1}$)	Lettuce	(10)	250	(2-4)E−04	(2-4)E−03	(0.05-0.1)	(0.5-1.0)
	Lettuce	(10)	230	1.2E−03	(0.012)	(0.28)	(2.8)
	Green beans	(5)	230	9E−04	(4.5E−03)	(0.21)	(1.04)
	Carrots	(8.5)	230	1.6E−03	(0.014)	(0.37)	(3.1)
	Apples	(6.7)	230	2.0E−05	(1.34E−04)	(4.6E−03)	(0.031)
	Apples	(6.7)	1430	(0.5-2)E−05	(0.34-1.34)E−04	(0.7-2.8)E−02	(0.048-0.19)
Zinc-65 ($\lambda = 1.03\ yr^{-1}$)	Lettuce	(10)	230	0.014	(0.14)	(3.22)	(32.2)
	Green beans	(5)	230	8.9E−03	(4.4E−02)	(2.05)	(10.2)
	Carrots	(8.5)	230	2E−03	(0.017)	(0.46)	(3.9)
Strontium-90 ($\lambda = 0.0248\ yr^{-1}$)	Lettuce	(10)	515	1.3E−03	(0.013)	(0.67)	(6.7)
	Tomatoes	(16.7)	500	(0.5-1)E−04	(0.84–1.7)E−03	(0.025–0.05)	(0.42–0.84)
			500	3.3E−05	(5.5E−04)	(0.0165)	(0.28)
		16.7	500	3.2E−04[a]	(5.3E−03)[a]	(0.16)[a]	(2.65)
	Potatoes	4.22	500	2.7E−04	(1.14E−03)	(0.135)	(0.57)
		5.0	500	2.0E−03[a]	(0.01)[a]	(1.0)[a]	(5.0)[a]

Table 5.31 (continued)

Radionuclide	Crop (Edible portion)	FW/DW	Test irrigation volume, V (L/m^2)	Area-to-plant: Transfer factor, c_{irr} m^2 kg (fresh)	Area-to-plant: Transfer factor, c_{irr} m^2 kg (dry)	Transfer rate factor: Water-to-plant $r' = c_{irr} \times V$ L kg (fresh)/yr	Transfer rate factor: Water-to-plant $r' = c_{irr} \times V$ L kg (dry)/yr
	Green beans	5.0	500	5.5E−04	2.75E−03	(0.275)	(1.4)
	Apples	6.7	500	(1.4)E−04	(0.67-2.7)E−03	(0.05-0.20)	(0.34–1.34)
Niobium-95 ($\lambda = 7.23\ yr^{-1}$)	Lettuce	(10)	250	(1-7)E−04	(1-7)E−03	(0.025-0.175)	(0.25-1.75)
Ruthenium-106 ($\lambda = 0.693\ yr^{-1}$)	Lettuce	(10)	250	(1-2)E−04	(1-2)E−03	(0.025-0.05)	(0.25–0.5)
	Apples	(6.7)	1430	(1-2)E−04	(0.7-1.3)E−03	(0.14-0.28)	(0.96-1.9)
Cesium-134 ($\lambda = 0.30\ yr^{-1}$)	Lettuce	(10)	250	(1-2)E−04	(1-2)E−03	(0.25-0.5)	(0.25-0.5)
Cesium-137 ($\lambda = 0.023\ yr^{-1}$)	Lettuce	(1)	250	(1-5)E−04	(1-5)E−03	(0.025–0.125)	(0.25–1.25)
			500	1.4E−03	(1.4E−02)	(0.70)	(7.0)
			500	7.0E−03[a]	(0.07)[a]	(3.5)[a]	(35)[a]
	Green beans	(5)	250	6E−05	(3E−04)	(0.015)	(0.075)
			745	6.6E−04	(3.3E−03)	(0.48)	(2.4)
	Potatoes	4.22	500	5.8E−05	(2.45E−04)	(0.029)	(0.12)
		5	500	3.6E−03[a]	(0.018)[a]	$(1.8)_a$	(9.0)[a]
	Tomatoes	16.7	500	1.8E−05	(3.0E−04)	(9E−03)	(0.15)
			500	(0.1-1)E−05	(0.17_1.7)E−04	(0.5-5)E−03	(0.8-8.3)E−02
			500	3.6E−04[a]	(6.0E−03)[a]	(0.18)[a]	(3.0)[a]
	Carrots	(8.5)	500	2E−05	(1.7E−04)	(0.01)	(0.085)
	Apples	(6.7)	500	1E−05	(6.7E−05)	(0.005)	(0.033)
Cerium-141 ($\lambda = 7.91\ yr^{-1}$)	Lettuce	(10)	500	(3-7)E−04	(3-7)E−03	(0.15-0.35)	(1.5-3.5)
Cerium-144 ($\lambda = 0.888\ yr^{-1}$)	Lettuce	(10)	500	(3-7)E−04	(3-7)E−03	(0.15-0.35)	(1.5-3.5)

Table 5.31 (continued)

Radionuclide	Crop (Edible portion)	Long-term equilibrium transfer parameters: Annual irrigation rate ($L/m^2 \cdot yr$)	Infiltration rate ψ yr^{-1}	Buildup factor = $(1/\lambda + \psi)$	Water-to-plant, r: L kg (fresh)	Water-to-plant, r: L kg (dry)	Reference
Sodium-22	Lettuce	230	0.21	(2.1)	(82) 80	(820)	[DEL-73]
(λ = 0.266 yr^{-1})		400	0.83	(0.91)	(62)	(620)	[DEL-73]
	Green beans	230	0.21	(2.1)	(0.145) 0.2	(0.72)	[DEL-73]
		400	0.83	(0.91)	(0.11)	(0.55)	[DEL-73]
	Carrots	230	0.21	(2.1)	(62.8) 61	(534)	[DEL-73]
		400	0.83	(0.91)	(47)	(400)	[DEL-73]
	Apples	230	0.21	(2.1)	(0.048)	(0.324)	[DEL-73]
		400	0.83	(0.91)	(0.036)	(0.244)	[DEL-73]
Manganese-54	Lettuce	(500)	0	(1.22)[a]	(0.03–0.12)[a]	(0.30–1.2)[a]	[DEL-71]
(λ = 0.817 yr^{-1})	Apples	(500)	0	(1.22)	(0.03–0.12)	(0.12–0.82)	[DEL-71]
Cobalt-60	Lettuce	500	0	(7.60)	(0.38–9.7)	(3.8–90)	[DEL-71]
(λ = 0.132 yr^{-1})	Lettuce	500	0.02	(6.60)	(4.0) 4.3	(39.6)	[DEL-73]
	Green beans	500	0.02	(6.60)	(3.0) 3.2	(29.7)	[DEL-73]
	Carrots	500	0.02	(6.60)	(5.3) 5.7	(4.8)	[DEL-73]
	Apples	500	0.02	(6.60)	(0.066)	(0.44)	[DEL-73]
	Apples	500	0	7.6	(0.019–0.076)	(0.13–0.51)	[DEL-71]
Zinc-65	Lettuce	800	0.03	0.941	(10.5) 10.5	(105)	[DEL-73]
(λ = 1.03 yr^{-1})	Green beans	800	0.03	0.941	(6.7) 6.2	(34)	[DEL-73]
	Carrots	800	0.03	0.941	(1.50) 1.51	(12.8)	[DEL-73]
Strontium-90	Lettuce	500	0.02	22.3	(15.0)	(150)	[BAR-61, DEL-71]
(λ = 0.0248 yr^{-1})	Tomatoes	500	0.015	25.1	0.6–1.25	(10–21)	[DEL-71]
		500	0.01	28.8	0.5	(7.9)	[BAR-61]
		500	0.04	15.4	2.5[a]	(41)[a]	[BAR-61]
	Potatoes	500	0.02	22.3	(3.0) 2.5	(12.7)	[BAR-61]
		500	0.04	15.4	15[a]	(77)[a]	[BAR-61]
	Green beans	500	0.02	22.3	(6.1)	(30)	[BAR-61]
	Apples	500	0.015	25.1	(1.25–5.0)	(8.6–34)	[DEL-71]

Table 5.31 (continued)

Radionuclide	Crop (Edible portion)	Long-term equilibrium transfer parameters: Annual irrigation rate ($L/m^2 \cdot yr$)	Infiltration rate ψ yr^{-1}	Buildup factor = $(1/\lambda + \psi)$	Water-to-plant, r: L kg (fresh)	Water-to-plant, r: L kg (dry)	Reference
Niobium-95 ($\lambda = 7.23\ yr^{-1}$)	Lettuce	250	0	0.138	(3.4–24)E−03	(0.034–0.24)	[DEL-71] [DEL-71]
Ruthenium-106 ($\lambda = 0.30\ yr^{-1}$)	Lettuce	250	0	1.44	(3.6–7.2)E−02	(0.36–0.72)	[DEL-71]
	Apples	1430	0	1.44	(0.21–0.41)	(1.4–2.8)	[DEL-71]
Cesium-134 ($\lambda = 0.30\ yr^{-1}$)	Lettuce	250	0	3.32	(0.08–0.17)	(0.8–1.7)	[DEL-71]
Cesium-137 ($\lambda = 0.023\ yr^{-1}$)	Lettuce	500	0	43.3	(2.0–10)	(22–110)	[DEL-71]
		500	0	43.3	(30)	(300)	[BAR-61]
		500	0.01	30.2	(105)[a]	(1050)[a]	[BAR-61]
	Green beans	500	0.005	35.6	1.1	(5.3)	[DEL-73]
		500	0	43.3	(20)	(100)	[BAR-61]
	Potatoes	500	0	43.3	1.3	5.3	[BAR-61]
		500	0.01	30.2	(54)[a] 50[a]	(270)[a]	[BAR-61]
	Tomatoes	500	0	43.3	0.4	(6.5)	[BAR-61]
		500	0	43.3	(0.022–0.22)	(0.36–3.6)	[DEL-71]
		500	0.01	30.2	5.0[a]	(90)[a]	[BAR-61]
	Carrots	500	0.005	35.6	(0.36)	(3.0)	[DEL-73]
	Apples	500	0.005	35.6	(0.18)	(1.2)	[DEL-71]
Cerium-141 ($\lambda = 7.91^{-1}$)	Lettuce	500	0	0.1265	(0.079–0.044)	(0.19–0.4)	[DEL-71]
Cerium-144 ($\lambda = 0.888\ yr^{-1}$)	Lettuce	500	0	1.126	(0.17–0.39)	(1.7–3.9)	[DEL-71]

[a]This soil has a low cation exchange capacity and low exchangeable potassium and calcium levels.

Note: Values in parentheses [except (3-7)E−03] were not presented in the cited literature.

Table 5.32. Effect of irrigation method on water-to-plant indirect transfer factors

Radionuclide crop	Space furrow				Subterranean conduit				Surface spray			
	Volume, V L/m^2-yr	c_{irr} m^2/kg(fresh)	$r' = cV$ L/kg(fr)-yr	r^a L/kg(fresh)	Volume, V L/m^2-yr	c_{irr} m^2/kg(fresh)	$r' = cV$ L/kg(fr)-yr	r^a L/kg(fresh)	Volume, V L/m^2-yr	c_{irr} m^2/kg fresh	$r' = cV$ L/kg(fr)-yr	r^a L/kg(fresh)
Strontium-90[b]												
lettuce	680	5.4E−04	0.37	(6.7)	334	1.43E−03	0.47	(17.4)	540	1.4E−03	0.75	(17.4)
	1000	8.1E−04	0.81	(10.0)	514	1.3E−03	0.65	(16.1)	690	1.4E−03	0.96	(17.4)
green beans	1260	3.1E−04	0.39	(3.5)	650	5.4E−04	0.35	(6.0)	840	5.5E−04	0.44	(6.1)
Cesium-137[c]												
lettuce	680	2.75E−04	0.19	(6.0)	334	9.1E−04	0.31	(19.7)	540	1.22E−03	0.65	(26.4)
	1000	1.5E−03	1.5	(32.5)	514	2.7E−03	1.39	(58.4)	690	2.1E−03	1.5	(45.9)
green beans	1260	1.22E−04	0.15	(2.64)	650	8.8E−04	0.58	(24.8)	840	4.4E−04	0.36	(16.0)

[a] r is calculated for an assumed annual irrigation rate of 500 L/m^2 for the purpose of comparison.
[b] Parameters: $x = 0.02\ yr^{-1}$, $\lambda = 0.0248\ yr^{-1}$, $1/(\lambda + p) = 22.3$ for strontium-90
[c] Parameters: $x = 0\ yr^{-1}$, $\lambda = 0.023\ yr^{-1}$, $1/\lambda = 43.3$ for cesium-137.
Source: data from [BAR-61].

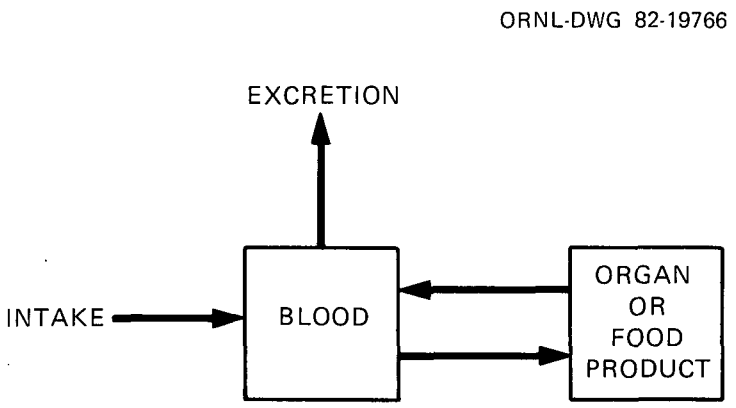

Figure 5.11. Two-compartment transfer model.

product of interest. Radionuclides enter through the blood and pass in and out of the second compartment but may leave the system only through the blood compartment. Losses due to radioactive decay occur in both compartments. The difference in the input and excretion rates from the compartment representing the food product will determine the radionuclide content in the food product.

The simple two-compartment model described above has been successfully used for some applications. However, three- or four-compartment models (or more) are more typically used to describe radionuclide metabolism. These models are discussed in Sheppard's book [SHE-62]. A general *n*-compartment model will be used to develop the feed-to-food-product transfer factor. A similar model (with different numerical parameters) would be used for the radionuclide concentration in either animal organs such as beef liver or animal products such as eggs or milk.

These models were derived from measurements of the radionuclide secretion or buildup in the animal or animal product following intake of the radionuclide. In some cases the radionuclide was injected into the bloodstream. The results of this approach have to be modified to account for the fact that the GI tract acts as a barrier to the radionuclide reaching the bloodstream during natural exposure situations. Nevertheless, this approach may be useful for determining the metabolism of very insoluble materials or materials that do not readily pass through the intestinal wall (such as plutonium). In most laboratory studies, a single oral administration of the radionuclide is used. However, in field studies the animal is often exposed to multiple intakes. Care should be taken when using literature parameters to ascertain whether "one-shot" or continuous intake was used.

The general form of the retention equation for a peripheral compartment in the general mammalian model* is

$$a_j(t) = a_0(0) \sum_{i=0}^{n} \left(\frac{\beta_j \cdot x_i}{\beta_j - \lambda_{ie}} \right) e^{-\lambda_{ie} t} \quad , \tag{5.66}$$

where β_j represents the fractional exchange rate (exchange rate divided by the fraction of the total material in the body which is contained in compartment j), λ_{ie} represents the effective loss rate constant for loss from compartment i, and

$$x_i = \frac{\prod_{k=1}^{n} (\lambda_{ie} - \beta_k)}{\prod_{\substack{k=o \\ k \neq i}}^{n} (\lambda_{ie} - \lambda_{ke})} \quad . \tag{5.67}$$

Equation 5.66 can be simplified to:

$$a_j(t) = a_0(0) \sum_{i=0}^{n} K_i e^{-(\lambda + r_i)t} \quad , \tag{5.68}$$

where K_i represents the terms in parentheses† in Eq. 5.66, and the effective removal rate constant for compartment i, λ_{ie}, has been replaced by its components, the radioactive decay constant for the particular radionuclide λ and the biological removal rate for the element from compartment i, r_i. Except in the case of tritium, ^3H, the difference in atomic mass between isotopes generally has a negligible effect provided that both the radionuclide and the stable element are in the same physicochemical form. Equation 5.66 represents the time variation of the radionuclide concentration in compartment j following a single short-term (essentially instantaneous) intake or injection into the central compartment, which, in the general mammalian model, is the blood. Single-intake retention functions for milk for several radionuclides are given in Table 5.33.

The radionuclide concentration in the compartment following an intake or input that varies with time according to a specified function, $I_{in}(t)$, is represented by

$$C_j(t) = \int_0^t I_{in}(t-\tau) \sum_{i=1}^{n} K_i e^{-(\lambda + r_i)\tau} d\tau = \sum_{i=0}^{n} K_i \int_0^t I_{in}(t-\tau) e^{-(\lambda + r_i)\tau} d\tau \quad . \tag{5.69}$$

*For the development of this equation, see Chapter 4 in [SHE-62].

† Note that K_i is also dependent on the radionuclide because of the presence of λ_{ie} in the coefficients of the terms in Eq. 5.66.

Table 5.33. Retention functions for stable elements in milk following a single intake

$$[C(t) = a_1 e^{-b_1 t} + a_2 e^{-b_2 t} + a_3 e^{-b_3 t} + a_4 e^{-b_4 t} (+ a_5 e^{-b_5 t})]$$

Element	Parameter values[a] (for t in days)
Barium (Ba-140)	$a_1 = 6.3 \times 10^{-4}$, $b_1 = 0.76$; $a_2 = 2.7 \times 10^{-5}$, $b_2 = 0.083$; $a_3 = -6.6 \times 10^{-4}$, $b_3 = 1.04$.
Cesium and rubidium	$a_1 = 3.6 \times 10^{-3}$, $b_1 = 0.69$; $a_2 = 1.5 \times 10^{-3}$, $b_2 = 0.17$; $a_3 = 4.0 \times 10^{-5}$, $b_3 = 0.023$; $a_4 = -5.1 \times 10^{-3}$, $b_4 = 1.84$.
Iodine (British values)	$a_1 = 5.6 \times 10^{-3}$, $b_1 = 0.94$; $a_2 = 7.5 \times 10^{-5}$, $b_2 = 0.032$; $a_3 = -5.7 \times 10^{-3}$, $b_3 = 6.93$
(CERT Idaho) [BU-66]	$a_1 = 9 \times 10^{-3}$; $b_1 = 0.88$; $a_2 = 0.98$, $b_2 = 1.15$; $a_3 = 9 \times 10^{-3}$, $b_3 = 0.102$
Strontium (British)	$a_1 = 5.5 \times 10^{-4}$, $b_1 = 0.48$; $a_2 = 1.0 \times 10^{-6}$, $b_2 = 0.017$; $a_3 = -5.5 \times 10^{-4}$, $b_3 = 1.58$
Tellurium	$a_1 = 5.5 \times 10^{-4}$, $b_1 = 1.09$; $a_2 = 5.2 \times 10^{-5}$, $b_2 = 0.14$; $a_3 = -6.1 \times 10^{-4}$, $b_3 = 2.34$
Polonium-210 [WAT-69]	$a_1 = 3.0 \times 10^{-5}$, $b_1 = 0.19$; $a_2 = 2.8 \times 10^{-6}$, $b_2 = 0.021$

[a] Values derived principally from [GAR-67].

When the radionuclide intake by the animal is constant [I_{in} (t $-$ τ) = IC_0], Eq. 5.69 becomes

$$C_j(t) = \sum_{i=0}^{n} \frac{K_i I_{in}}{\lambda + r_i} [1 - e^{-(\lambda + r_i)t}] \ . \tag{5.70}$$

This equation describes the concentration in compartment j at time t from a continuous intake of a radionuclide at a constant intake rate I_{in} per unit time. The equilibrium concentration that is approached following long-term continuous intake is given by

$$C_j(\text{equilibrium}) = \lim_{t \to \infty} C_j(t) = \sum_{i=0}^{n} \frac{K_i I_{in}}{\lambda + r_i} \ . \tag{5.71}$$

When this expression is normalized to a unit intake rate, it represents the intake-to-food-product transfer factor,

$$f_m^* = \frac{C_j(\text{equilibrium})}{I_{in}} = \sum_{i=1}^{n} \frac{K_i}{\lambda + r_i} \ . \tag{5.72}$$

These factors are tabulated as the intake-to-meat, intake-to-milk, and intake-to-egg transfer factors and are generally expressed as the percentage of the

daily intake transferred per unit mass (or volume for milk) to the food product (e.g., percent-day per liter or percent-day per kilogram). The values in this chapter are expressed as days per liter for milk and days per kilogram for meat in order to avoid numerical errors associated with failure to convert percentages.

5.2.5.2 Application to Grazing Animals

The general mammalian model must be modified to apply it to grazing animals in order to account for the time dependence of the radionuclide intake by the animal. This, in turn, is dependent upon the time variation of the radionuclide concentration on the forage. There are two contamination situations that are of importance for radiation dose assessment purposes: short-term and long-term.

Short-term contamination (accident situations). For accident situations, the event that causes the contamination of the forage is considered to be of short duration compared to the effective half-life on the forage. In such cases, the initial contamination can be represented by the product of a deposition rate (given by Eq. 5.20) and the duration of the contaminating event, T:

$$C_A(0) = \Sigma\left[v_g + W_r \dot{R} e^{-m\dot{R}}\right]\chi T \quad . \tag{5.73}$$

The areal concentration at time t following the contaminating event is given by*

$$C_A(t) = C_A(0)e^{-\lambda_e t} \quad , \tag{5.74}$$

where $C_A(0)$ is given above and λ_e is the effective removal rate constant for loss from the vegetation (including washoff, resuspension, and, for small plots, loss due to consumption of the vegetation by the grazing animal).

The unit of $C_A(t)$ is activity per unit area (e.g., becquerels per square meter). In order to convert this into the daily intake by a grazing animal, it is necessary to either convert the concentration per unit area to the concentration per unit mass or to express the daily forage consumption by the grazing animal in terms of the equivalent area of forage consumed per day; the latter quantity is termed the Utilized Area Factor *(UAF)* by Koranda [KOR-65]:

$$UAF = \frac{\text{kilogram (dry) forage ingested/cow-day}}{\text{kilogram forage produced/square meter}} \quad . \tag{5.75}$$

*The function describing retention has historically been described by a single exponential decay term rather than the two-term expression given in Sect. 5.6.7.

If the areal radionuclide concentration C_A is converted to the vegetation mass concentration, the daily radionuclide intake by the herbivore is

$$I_{in}(t) = \frac{I C_A(0) e^{-\lambda_e t}}{Y_D} \quad , \tag{5.76}$$

where I is the rate of forage consumption by the herbivore (kg/d)* and Y_D is the forage density (kg/m^2).* If the *UAF* (area) approach is used, the daily radionuclide intake by the animal is

$$I_{in}(t) = (UAF) C_A(0) e^{-\lambda_e t} \quad . \tag{5.77}$$

Both of these terms will be represented by the general expression,

$$I_{in}(t) = C_0 e^{-\lambda_e t} \quad , \tag{5.78}$$

where C_0 is either $I\ C_A(0)/Y_D$ or $(UAF)\ C_A(0)$ depending on the approach used. Values for the forage intake rates and utilized area factors for various feeding practices are given in Tables 5.34 and 5.35, respectively.

Substituting Eq. 5.78 into Eq. 5.69 gives:

$$\begin{aligned} C_j(t) &= \int_0^t C(0) \exp[-\lambda_e \tau] \sum_{i=1}^{n} K_i \exp[-(\lambda + r_i)(t-\tau)]\, d\tau \\ &= C(0) \sum_{i=1}^{n} K_i \exp[-(\lambda + r_i)t] \int_0^t \exp\left\{-[\lambda_e - (\lambda + r_i)]\tau\right\} d\tau \\ &= C(0) \sum_{i=1}^{n} K_i \left[\frac{\exp[-(\lambda + r_i)t] - \exp(-\lambda_e t)}{\lambda_e - (\lambda + r_i)}\right] \quad . \end{aligned} \tag{5.79}$$

As the effective loss rate from the pasture $\lambda_e = \lambda + r_p$, the last equation reduces to a form that is essentially independent of the isotope:

$$\frac{C_j(t)}{C(0)} = e^{-\lambda t} \sum_{i=1}^{n} \frac{K_i}{r_p - r_i} [\exp(-r_i t) - \exp(-r_p t)] \quad . \tag{5.80}$$

*Note: I and Y_D can be expressed on the basis of either dry or fresh (wet) weight, but both quantities must be expressed using a common basis.

Table 5.34. Major forage crop yields [kg (dry)/m^2] in various geographic regions of the United States

Crop	Western States	South Central States	East North Central States	North Atlantic States	South Atlantic States	West North Central States	U.S. average	Kilogram per dry intake
Wild hay	0.24 0.17-0.31	0.22 0.18−0.24	0.33 0.33[a]			0.18 0.16−0.28	0.20 0.16−0.33	9.1
Lespedeza		0.28 0.24−0.35	0.27 0.24−0.29		0.24 0.14−0.28	0.24 0.22−0.24	0.26 0.14−0.35	11.8
Clovers, clover-grass mixtures	0.35 0.24−0.44	0.30 0.17−0.32	0.37 0.31−0.47	0.34 0.29−0.42	0.23 0.17−0.31	0.33 0.26−0.39	0.34 0.17−0.47	11.8
Grain hay	0.35 0.22−0.50	0.24 0.17−0.29	0.30 0.30[a]	0.38 0.35−0.42	0.22 0.20−0.30	0.25 0.21−0.31	0.28 0.17−0.50	11.8
Other hay	0.31 0.20−0.47	0.28 0.24−0.35	0.29 0.26−0.35	0.20 0.17−0.20	0.32 0.17−0.44	0.28 0.23−0.35	0.29 0.17−0.47	11.8
Sorghum forage	0.27 0.22−0.89	0.33 0.31−0.62			0.36 0.22−0.38	0.58 0.35−0.89	0.40 0.22−0.89	13.6
Alfalfa, alfalfa-grass mixtures	0.70 0.43−1.13	0.52 0.42−0.62	0.51 0.44−0.55	0.45 0.39−0.55	0.36 0.29−0.47	0.49 0.32−0.59	0.53 0.29−1.13	13.6

[a]One state reporting.
Source: [KOR-65].

Table 5.35. *UAF* values (m^2/d) for major forage crops by geographic region and management practices

	Western States	South Central States	East North Central States	North Atlantic States	South Atlantic States	West North Central States	U.S. average
			Countinuous grazing				
Wild hay	37.5	41.3	27.6[a]			50.5	45.5
	29–53	37–50	27.6			32–57	28–57
			Rotation and strip grazing				
Clover, clover-grass mixes	33.7	39.3	31.9	34.7	51.3	35.8	34.7
	27–45	37–69	25–38	28–38	39–69	30–45	25–69
Lespedeza		42.1	43.7		49.2	49.2	45.4
		34–49	41–49		42–84	49–54	34–84
Grain hay	33.7	49.2	39.3[a]	31.3	53.6	47.2	42.1
	24–54	41–69	39.3	28–34	39–59	38–56	24–69
Other hay	38.1	42.1	40.7	59.0	36.9	42.1	40.7
	25–59	34–49	34–45	37–69	27–69	34–51	25–69
Wild hay	49.2	53.6	35.7[a]			65.5	59.0
	38–69	49–65	35.7			42–74	36–74
			Green chop or silage				
Alfalfa, alfalfa mixes	19.4	26.1	26.7	30.2	37.8	27.7	25.7
	12–32	22–32	25–31	25–35	29–47	23–42	12–47
Sorghum forage	50.4	41.2			37.8	23.4	34.0
	15–62	22–44			36–62	15–39	15–62

[a]One state reporting (Wisconsin).
Source: [KOR-65].

Integration of Eq. 5.79 provides a measure of the total quantity of the radionuclide present in the food product during this time period. This quantity, when multiplied by the daily intake rate by man of the food product, represents the total radionuclide intake, which is needed to calculate the internal radiation dose. This integral is

$$\int_0^\infty C_j(t)\,dt = \frac{C_0}{\lambda_e} \sum_{i=1}^{n} \frac{K_i}{(\lambda + r_i)} \quad , \tag{5.81}$$

The summation term is the forage-to-food transfer function, f_m^*, given by Eq. 5.72, so the total radionuclide concentration in the food product over all time can be expressed as

$$\int_0^\infty C_j(t)\,dt = \frac{C_0}{\lambda_e} f_m^* \ . \tag{5.82}$$

Long-term situations. For long periods of time removal mechanisms will affect the radionuclide concentrations on forage, and the concentration will be given by Eq. 5.21 multiplied by f_R, the retention factor:

$$C_A(t) = \frac{f_R(v_g + b\dot{R}W_v)\chi}{(\lambda_e + k\dot{R})}\left\{1 - \exp[-(\lambda_e + k\dot{R})t]\right\} \ . \tag{5.83}$$

When this term and the vegetation intake rate I are substituted into Eq. 5.69, the result is

$$C_j(t) = \frac{f_R(v_g + b\dot{R}W_v)\chi}{\lambda_e + k\dot{R}} \sum_{i=1}^{n} IK_i \left\{ \frac{1 - \exp[-(\lambda + r_i)t]}{\lambda + r_i} - \left[\frac{\exp[-(\lambda + r_i)t] - \exp[-(\lambda_e + k\dot{R})t]}{r_p - r_i + k\dot{R}} \right] \right\} \ . \tag{5.84}$$

The terms in parentheses represent the initial transient condition. Exposure to a constant radionuclide concentration in air will result in a radionuclide concentration in the food product which increases as

$$C_j(t) = \frac{f_R(v_g + b\dot{R}W_v)\chi}{\lambda_e + k\dot{R}} \sum_{i=1}^{n} K_i I \left[\frac{1 - \exp[-(\lambda + r_i)t]}{\lambda + r_i} \right] \ . \tag{5.85}$$

This expression will eventually approach an equilibrium concentration in the food product of

$$C_j(\text{equilibrium}) = \lim_{t \to \infty} C_j(t) = \frac{f_R(v_g + b\dot{R}W_v)\chi}{\lambda_e + k\dot{R}} \sum_{i=1}^{n} \frac{K_i I}{\lambda + r_i} \ . \tag{5.86}$$

The term preceding the summation represents the equilibrium radionuclide concentration on the forage (see Eq. 5.22). The ratio of the equilibrium

concentration in the food product to the intake concentration represents the forage-to-food transfer factor, which is the same as the factor described in Eq. 5.72. The equilibrium radionuclide concentration in the food product is therefore

$$C_j(\text{equilibrium}) = \frac{(v_g + b\dot{R}W_v)\chi}{\lambda_e + k\dot{R}} f_m^* \quad . \tag{5.87}$$

The transfer factor f_m^* in the long-term radionuclide intake situation represents the ratio of the equilibrium concentration of the radionuclide in the food product per unit concentration of the radionuclide in the forage. In the short-term exposure (or accident) condition, f_m^* will be equal to the total activity of the radionuclide that appears in the food for each unit of activity ingested by the animal. Based on these models, the transfer factors are numerically identical. Values of f_m^* are shown in Tables 5.36 for milk, 5.37 for meat, and 5.38 for eggs. With the exception of the egg values, which are for specific radionuclides, the values are for the stable element f_m, not f_m^*. To use these values for a specific radionuclide, an approximate correction factor for radioactive decay is $f_m^* = f_m/(1 + \lambda/r)$, where r is the effective biological excretion rate in milk and λ is the radioactive decay constant.

5.2.5.3 Factors Affecting Radionuclide Concentration in Animal Food Products

Vegetation density. Burman et al. [BUR-66] noted that there is more uptake from open grazing than from green chop and more uptake from sparser pastures than from lusher vegetation. A possible explanation is the ingestion of the grass mat, which may be more highly contaminated (over the long term) than the upper portions of the vegetation. Another factor that contributes to higher intakes from sparse pastures is the greater area that must be covered by the animal to get the same intake. For example, in order to consume 15 kg of vegetation, a cow would have to cover 30 m^2/d when the vegetation density is 0.5 kg/m^2 and 150 m^2/d when the forage density is 0.1 kg/m^2. Thus, the use of larger browsing areas with sparse vegetation could result in greater intake of contaminated dirt and closer cropping of the vegetation.

Season. The season affects vegetation density, its nutritional value, and the relative metabolic rate of the cow. The Controlled Environmental Radioiodine Tests (CERT) conducted in the 1960s found the following relationship for the total ^{131}I secretion into milk [BU-66]:

Season	[μCi-d/L] ÷ [μCi/g(dry)]
Spring	64
Summer	620
Fall	580
Winter	18

Table 5.36. Radionuclide transfer factors from intake to cows' milk[a]

Element	Transfer factor from intake to cows' milk f_m (d/L)	Element	Transfer factor from intake to cows' milk f_m (d/L)
H (tritium)	1.4E−02	Sb ($SbCl_3$)	2.0E−05
C	1.5E−02	Te	2.0E−04
Na	3.5E−02	I	9.9E−03
P	1.6E−02	Cs	7.1E−03
K	7.2E−03	Rare earths ($CeCl_3$)	2.0E−05
Ca	1.1E−02	Ta (oxalate)	2.8E−06
Cr	2.0E−03	W (sodium tungstate)	2.9E−04
Mn	8.4E−05	Re (sodium perrhenate)	1.3E−03
Fe	5.9E−05	Rare metals (Os, Pt, Ir, Au)	(5.0E−06)[b]
Co	2.0E−03	Hg, $HgCl_2$	9.7E−06
Ni	1.0E−02	Tl, $Tl(NO_3)_2$	1.3E−03
Cu	1.7E−03	Pb	2.6E−04
Zn	1.0E−02	Bi	5.0E−04
Br	2.0E−02	Po	1.4E−02
Kr	2.0E−02	Rn	3.0E−02
Rb	1.2E−02	Ra	4.5E−04
Sr	1.4E−03	Ac	(2.0E−05)[c]
Y	2.0E−05	Th	5.0E−06
Zr	8.0E−02	Pa	5.0E−06
Nb	2.0E−02	U	6.1E−04
Mo	1.4E−03	Np	5.0E−06
Tc	9.9E−03	Pu (PuO_2)	(2.7E−09)[d]
Ru ($RuCl_2$ or RuNO)	6.1E−07	Transuranics	(2.0E−05)[c]

[a] Data primarily from the compilation by [NG-77].

[b] Based upon iridium and gold experimental values rather than derived default values given in [NG-77].

[c] Based on value for rare earths (lanthanides).

[d] This chemical form of plutonium is more likely to be released from nuclear facilities than most other forms of plutonium. However, the f_m value of some complexed forms of plutonium can be higher; for example, a value of 1.0E−07 is given by [NG-77] for plutonium citrate.

Temperature is an important component of these seasonal effects: the secretion of radioiodine into milk is 6.5 times higher at 33°C than at 5°C [LEN-79].

Type of animal. The metabolism and size of the animal can make a significant change in the dose received by man. An extreme example of this is the relative concentration of radioiodine in milk from cows and milk from goats having the same radioiodine intake. The f_m^* (percentage of daily intake per liter) for the goat for ^{131}I is 46.7%, and for the cow it is 0.42%. These values reflect the relative volume of milk produced: 7.5–14 kg/d for the cow and 1.2 kg/d for the goat [LEN-69]. Note that in practice these differences would be less because the goat would consume proportionally less contaminated herbage.

The age of the animal also affects its metabolism and consequently the secretion of radionuclides. The biological half-life of ^{137}Cs in cows and calves following oral dosing was about 10 d (7–14 d) in the cows but only 4 d (3.5–4.5 d) in the calves [TWA-69].

Farming practices and stable element intake. Farming practices, such as the use of fertilizer and tilling, and the type of feed can have a significant

Table 5.37. Transfer factors for transfer to meat and eggs[a]

Element	f_m (d/kg)				
	Beef	Pork	Lamb	Chicken	Eggs
Na	8.3E−03				
P	4.9E−02				
K	1.8E−02				1.1
Ca	1.6E−03			4.4E−02	0.44
Cr	9.2E−03				
Mn	5.0E−04	3.6E−03	5.9E−03	6.1E−02	0.065
Fe	2.1E−02	2.6E−02	7.3E−02	1.5	1.3
Co	1.2E−02				
Ni	(2.0E−03)				
Cu	(1.3E−02)				
Rb	1.1E−02				
Sr	8.1E−04	3.9E−02	2.2E−03	3.5E−02	0.3
Y	1.0E−03			1.0E−02	2E−03
Zr	(2.1E−02)				
Nb	2.0E−03[b]			2E−03	3E−03
Mo	6.8E−03			5E−03	0.5
Tc	(8.7E−03)				
Ru	2.0E−03			7E−03	6E−03
Sb	(1.2E−03)				
Te	(1.5E−02)				
I	(7.2E−03)				
Cs	2.0E−03			1E−02	5E−03
Rare earths	(2.9E−04)				
W	3.7E−02				
Hg				2.7E−02	
Pb	4E−04				
Po	4.5E−03				
Ra	5.1E−04[c]				
Th	2.0E−04[c]				
U	3.4E−04[c]				
Pu	(1.0E−06)				
Transuranics	(3.6E−06 Am)				

[a]Beef values in parentheses are from [Ng-79]; the remaining values in the table are from [NG-82].

[b]A value of 0.25 is given in [Ng-79]. This appears to be out of line with the chicken values.

[c]Low [NG-82b].

influence upon the secretion of radionuclides into food products. One affect of fertilization is to increase the vegetation density. Straub and Fooks [STR-63] fertilized a pasture and, by so doing, doubled the grass yield; this, in turn, led to a 50% reduction in the level of radioiodine in the milk produced by cows feeding in that pasture.

Table 5.38. Transfer factors for radionuclide incorporation into hens' eggs following oral administration

Radionuclide	Transfer factor (fraction of intake)			
	Days per gram[a]		Days per whole egg[b]	Days per kilogram
	Albumen	Yolk		
^{89}Sr	1.3E−04	1.7E−04	6.6E−03	0.13
^{91}Y	~ 0	9E−07	1.4E−05	2.7E−04
^{95}Nb	1.0E−07	1.1E−06	2.1E−05	4.0E−04
^{99}Mo	5.9E−05	3.4E−04	7.2E−03	0.14
^{103}Ru	1.0E−07	4.0E−06	6.7E−05	1.3E−03
^{131}I	1.6E−04	1.7E−03	3.2E−02	0.62
^{132}Te	3.6E−05	3.9E−04	7.3E−03	0.14
^{134}Cs	5.4E−04	6.8E−05	1.7E−02	0.33
^{140}Ba	7.2E−06	3.6E−04	6.0E−03	0.12
^{140}La	6.0E−07	1.3E−06	3.9E−05	7.6E−04
^{142}Pr	1.4E−06	1.2E−06	6.1E−05	1.2E−03
^{144}Ce	1.6E−06	4.0E−07	5.4E−05	1.0E−03
^{147}Nd	~ 0	2.0E−07	3.6E−06	7.0E−05
^{147}Pm	1.4E−06	4.4E−06	1.1E−04	2.1E−03.

[a]Data from [MRA-64].

[b]Average weight: albumen (egg white), 30 g; yolk, 16 g per 51.6-g egg [MRA-64].

Stable elements in fertilizers and in feeds or feed supplements also tend to suppress radionuclide transfer into animal food products. An intake of 2 g/d of stable iodine reduces the level of radioiodine in cow's milk by 50% [BUS-63]. Good farming practices such as fertilization can reduce the ^{90}Sr level in milk by as much as a factor of 5 [UND-67]: there is a threefold reduction in the levels of Ca and Sr isotopes in milk produced by cows when their stable calcium intake is increased from 0.25%/d to 1.7%/d [COM-61].

Other sources of radionuclide intake. Although consumption of forage is generally the principal means of radionuclide entry into grazing animals, there are other sources of potential radionuclide contamination. Airborne radionuclides can be inhaled by grazing animals. A cow's inhalation rate is roughly 100 L/min [ALT-74], or 144 m^3/d.

Soil on the plant base may also be consumed by grazing animals. Soil can contribute 4% of the dry matter consumed by cows and up to 20% of the intake by sheep [in SIM-79].

Drinking water can also be an important source of radionuclide intake in the absence of forage contamination. For example, cows drinking water from deep wells had 40 nCi/L of ^{222}Rn in their milk, with an f_m^* of 0.023 and 0.038. Cows consume approximately 60 L/d [ALT-74].

Transfer into secondary products. Fresh milk is used to make a variety of dairy products such as butter, cheese, ice cream, and evaporated or condensed milk. Relatively large quantities of milk may be used in the production of these products; for example, it takes approximately 21 kg of milk to produce 1 kg of butter. Depending upon the product and the process used, the radionuclide concentration in the dairy product may differ considerably from that in the milk. For example, plutonium is almost totally (0.975 ± 0.022) transferred to cheese with co-precipated milk solids, resulting in an effective reconcentration of a factor of 5, since the solids comprise about 20% of the milk [MIL-72]. The relative concentrations of cesium, strontium, and iodine in milk products is shown in Table 5.39.

***Example* 5.4:** The concentration of radioiodine in milk following a single contaminating event can be approximated by [PET-70]:

$$C(t) = ID_o\, 1.86 \times 10^{-2}\, [\exp(-0.114t) - \exp(-0.90t)]$$

Table 5.39. Transfer of radionuclides from milk to milk products[a]

Product	Radionuclide concentration in milk products ÷ radionuclide concentration in milk		
	^{134}Cs	^{85}Sr	^{131}I
Fresh cheese			
(Whole) rennet	1.3	3.9	3.0
Acid fermented	0.75	0.66	2.2
(Skin) rennet	1.5	3.8	2.8
Acid fermented	1.4	0.97	2.7
Fermented cheese			
Cottage cheese	0.86	4.7	2.3
Hard cheese	0.57	6.6	2.3
Pressed cheese	0.90	6.3	1.7
Buttermilk	1.0	0.92	0.99
Cream (24%)	0.87	0.60	0.73
Butter	0.11	0.09	0.36
Casein			
Rennet	2.6	20.	4.0
Acid	1.2	10.0	3.6

[a]Based upon French agricultural practice.
Source: [KIR-66].

where

$C(t)$ = concentration in milk at time t (days) after the event,

I = daily forage consumption by the cow (kg/day or m^2/day),

D_o = initial activity present on the forage (pCi/kg or Bq/m^2).

1. Determine the total activity of radioiodine secreted into milk. Express this as a fraction of the first day's radioiodine intake by the cow.
2. Determine the fraction of the total dose which would be delivered and the fraction which would be prevented if cows were removed from pasture and fed uncontaminated feed 1 day, 2 days, and 1 week after the initial contamination.

Solution (1). The first day's radioiodine intake by the cow is ID_o so that the normalized equation is:

$$1.86 \times 10^{-2} \left[\exp(-0.114t) - \exp(-0.90t)\right] .$$

The total secretion into milk is:

$$C_t = \int_o^\infty C(t)dt$$

$$= \lim_{t\to\infty} 1.86 \times 10^{-2} \left\{\frac{1-\exp(-0.114t)}{0.114} - \frac{1-\exp(-0.9t)}{0.9}\right\}$$

$$= 1.86 \times 10^{-2} \left[1/0.114 - 1/0.90\right]$$

Answer: 0.14.

Solution (2). The amounts that would be delivered if the cows were removed from pasture after various time intervals are obtained by inserting specific times into the above integral instead of the infinite upper limit. These evaluations give:

Time cows removed from pasture after contaminating event	Value of time-dependent term (in braces above)	Fraction of first day's intake by cow delivered per liter	Percentage of total quantity (dose) delivered	Percentage of dose prevented by removal from contaminated feed
1 day	0.286	5.31 E-03	3.7%	96.3%
2 days	0.861	1.60 E-02	11.2%	88.8%
7 days	3.71	6.91 E-02	48.5%	51.5%

[End of Example]

5.3 Aquatic, Marine, and Estuarine Ecosystems

5.3.1 Introduction

These three systems refer to freshwater (aquatic), saltwater (marine) and brackish water (estuarine) environments. The estuarine ecosystem usually acts as a bridge between the other two environments. This interface happens most frequently when rivers and streams flow into bays and other arms of the sea. Although different species may occupy the same niche in different systems, the components of the systems are similar and can be modeled and discussed together.

The behavior of radioactive materials in the various waters is not necessarily the same. The physicochemical form of the radionuclide is generally more important in determining bioaccumulation in these ecosystems than in the terrestrial ecosystem.

The terrestrial food chain leading to man generally consists of 2 or 3 *trophic levels* (separate steps in the food chain). These chains usually are the vegetation → herbivore chain for consumption of fruits and vegetables by man and the vegetation → herbivore → consumer (predator) chain for man's intake of meat, poultry, eggs, and milk. Most of the terrestrial food products are grown or produced in situations where most of the factors which can affect productivity (and radionuclide transfer) are or can be controlled or modified. Moreover, these activities take place in a fairly well-defined geographical area.

In the aquatic and marine environment the regularity described above seldom exists. The food chains such as: algae → zooplankton → crustacean → sunfish → bass. This type of food chain is made more complex by the factor that the predator may consume several different types of prey often from several different trophic levels (Fig. 5.12). The nature of this *food web* can change considerably with location in the same water body as different niches in the food web may be filled by different organisms.

Another factor which complicates modeling of the aquatic ecosystem is that there are numerous species in the aquatic food chain which are mobile and can move over considerable distances. An extreme example is the salmon which is born in freshwater, grows to maturity in the ocean and then returns to the system of its birth to spawn. In many cases this mobility, requires the use of radionuclide concentrations averaged over long distances and several types of environments in order to predict radionuclide uptake by this type of organism.

5.3.2 Physicochemical Processes

The physicochemical form of a radionuclide can be more variable in aquatic and marine ecosystems than in the terrestrial ecosystem and may also have greater effect upon radionuclide transfer. Three important mechanisms

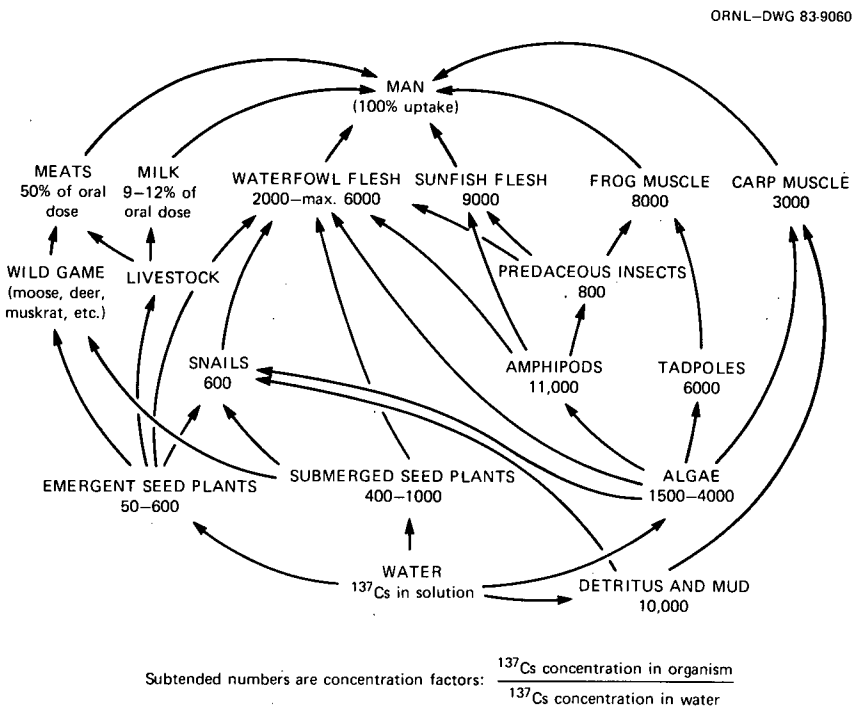

Figure 5.12. A freshwater food web illustrating the pathways to man for cesium-137 in the aquatic environment. From [PEN-58].

which affect radionuclide concentrations in these ecosystems are colloid formations, co-precipitation and sorption-desorption on sediments and suspended solids. These mechanisms provide a means for reconcentration of dissolved and particulate radionuclides [ANC-73].

5.3.2.1 Colloid Formation

Colloids are suspensions of very fine particulates usually of insoluble compounds. Their small size (usually 0.005 to 0.2 μm) acts to hinder precipitation as does the usual presence of an electric charge. Colloid formation is typical for a variety of the heavier elements including the rare earths (La, Ce, etc.) or some of the transition elements (such as Co and Fe), thorium and uranium. These colloidial particles may pass through conventional paper filters but do not pass through membranes. Colloid formation is an important source of reconcentration from the dissolved phase for those radionuclides which form colloids. The particles formed are also within the size range consumed by many aquatic organisms and this may provide entry into the food chain. Studies in an estuary in the United Kingdom showed that ^{65}Zn, ^{59}Fe and ^{60}Co were

adsorbed on fine particulates which appeared to be the mechanism for uptake by oysters [PRE-69]. Freshwater studies showed that zirconium hydrolyzed to a colloidal form [BEN-66]. Zirconium and especially niobium also form hydrated oxides with strong colloid forming tendencies in sea water [HAM-67].

5.3.2.2 Co-Precipitation

A radionuclide present in water in low (tracer) concentrations can be precipitated along with another element present at a higher concentration by a process called *co-precipitation.* This process is favored if the radionuclide reacts with the precipitant to form a crystalline lattice similar to that of the major element or if the radionuclide forms an insoluble precipitate with the precipitant (*Paneth-Fajans rule*). This co-precipitation of radium with barium sulfate is an example which satisfies both conditions. Ferric hydroxide $Fe(OH)_3$ may be precipitated under a variety of natural conditions and is an important "carrier" of radionuclides which may be co-precipitated with it. Releases from the U.K. Windscale reprocessing plant show that ^{90}Sr, ^{134}Cs and ^{137}Cs were principally in soluble form while ^{106}Ru, ^{144}Ce, ^{95}Zr-^{95}Nb were either complexed, co-precipitated or absorbed on materials [PEN-72]. As these surfaces included fishing tackle, nets, and the edible seaweed *Porphyra,* this deposition constitutes a pathway for human exposure [PRE-69].

5.3.2.3 Sorption-Desorption on Suspended Solids and Sediments

Suspended material including suspended sediments can play an important role for the transport of radionuclides in rivers, and in interactions with the biota. Friend *et al.* [FRI-63] found that about 92% of the ^{60}Co, 96% of the ^{65}Zn, and 95% of the ^{137}Cs were lost from water within 4 days. There was appreciable transfer to suspended solids. In the Clinch River (Tennessee) about 90% of the cesium-137 was on suspended material whereas 80-90% of the ^{90}Sr, ^{106}Ru, and ^{60}Co remained in solution. Only about 3% of the released activity was accumulated in the streambed [PAR-65].

Suspended solids can be transported considerable distances. Some deposition of sediments occurs in areas of low current but far greater deposition takes place in the tidal intrusion zone where there is contact with salt water. In the Savannah River this mixing occurs 200 km below the release point. Both sediments and other suspended material accumulate at dams and other impoundments.

River waters are depleted in the alkaline earth elements, calcium, strontium, and magnesium, compared to seawater. When the freshwater and saltwater mix in the estuary, the concentrations of these elements are lowered by virtue of the dilution by the river water [LOW-66]. This is in contrast to the behavior of the transition elements, iron, manganese, copper, cobalt, zinc and nickel which are depleted in the seawater. Mixing of river water with seawater

in an estuary results in the raising of both the electrolyte concentration and the pH. Under these conditions collodial clay particles coalesce and precipitate and collodial iron, manganese, scandium, aluminum and silica form gelatinous hydroxides.

Precipitation of ferric hydroxide can result in co-precipitation of ^{95}Zr-^{95}Nb, ^{106}Ru-^{106}Rh, ^{144}Ce-^{144}Pr and the transition elements [LOW-67]. This scavenging and precipitation helps maintain the depleted concentrations of the transition elements in seawater and may, in turn, account for the affinity and high concentrations shown by marine organisms for these elements.

Phosphorus is rapidly adsorbed by sediments in the estuarine environment. In addition it is effectively co-precipitated with ferric hydroxide so that most phosphorus-32 in the estuary is on the bottom [LOW-69].

In the oceans, strontium, cesium, zinc, and copper exist primarily as ionic species, cesium for example is almost totally in solution. Other elements exist mainly in particulate form. These include Fe, Mn, Co, the rare earths, Ru, Ze, Nb, Y and Th. About 90 percent of the iron in the top 100m of the ocean is particulate; cobalt and ruthenium have smaller fractions in the particulate form [JEN-69].

The distribution of a radionuclide among water, suspended solids, and sediment is affected by the concentration of ions which can compete with the radionuclide for sorption sites. This distribution will therefore depend upon the ionic concentration or salinity of the water and differ among freshwater, estuarine, and marine ecosystems. The difference between estuarine and marine *distribution coefficients,* K_d's,* for various sediment compositions are shown in Table 5.40. Distribution coefficients for cesium-137 adsorbed onto freshwater

*See Chapter 3 for a discussion of K_d.

Table 5.40. Effect of seawater on radionuclide retention by sediments in estuarine and marine systems[a]

System	Distribution coefficient (K^d)		
	Medium sand	fine sand	Clay
	Estuarine		
(Cl^- 14 g/L)			
^{144}Ce	700	1,000	10,000
^{91}Y	250	700	1,500
	Marine		
(Cl^- 19 g/L)			
^{144}Ce	450	500	5,000
^{91}Y	140	0	350

[a]Data from [MUR-73].

sediments have been found to range between 3,400 to 18,000 [GUS-69b]. However, in seawater, the high ionic concentration of sodium (0.5 Molar [GOL-71]) and potassium limit the sediment K_d values to around 1,300 [DUU-71].

The lower distribution coefficients in waters of higher ionic content can result in a change in the distribution of radionuclides among water, suspended solids, and sediment as the material moves toward the ocean. Radionuclides deposited onto sediments and suspended solids in freshwater portions of the rivers may be leached out or desorbed by the high ionic content of seawater when these materials reach the estuarine environment. Such leaching also can occur in the estuary during tidal reverses [MUR-73].

5.3.3 RADIONUCLIDE UPTAKE—THE CONCENTRATION FACTOR APPROACH

5.3.3.1 The Concentration Factor

The intake of an element by a simple* aquatic organism may be represented by:

$$\frac{dC}{dt} = \frac{I_w}{m} C_w - rC \ . \tag{5.88}$$

where C is the concentration in the organism, C_w is concentration in water, I_w is the intake rate by the organism, m is the mass of the organism and r is the biological elimination rate of the element by the organism. This equation has the solution:

$$C(t) = \frac{I_w C_w}{mr}[1 - \exp(-rt)] \ . \tag{5.89}$$

Thus the concentration of the element in the organism will build up with time asymptotically approaching an equilibrium value of:

$$C_{equil} = \lim_{t \to \infty} C(t) = \frac{I_w C_w}{mr} \ . \tag{5.90}$$

The ratio of the concentration in the organism to that in water is:

$$\frac{C_{equil}}{C_w} = \frac{I_w}{mr} \ . \tag{5.91}$$

*Real organisms tend to be represented by two- to four-compartment models rather than this one-compartment model.

This ratio is termed the **concentration factor,*** *CF**, and is defined as:

$$\text{concentration factor} = \frac{\text{equilibrium concentration in organism}}{\text{concentration in water}} \tag{5.92}$$

The requirement for equilibrium to have been reached between the organism and its environment is important for obtaining consistent measurements of the concentration factor as is evident from comparing Eqs. (5.89) and (5.90).

The preceding derivation also applies to radionuclides except that, in addition to biological elimination, losses by radioactive decay must be accounted for by replacing r by $r + \lambda$. Equation (5.89) then becomes:

$$C_f^*(t) = \frac{I_w C_w^*}{m(r+\lambda)}[1 - \exp - (r+\lambda)t] \tag{5.93}$$

and Eq. (5.91) becomes:

$$CF^* = \frac{I_w}{m(r+\lambda)} \quad . \tag{5.94}$$

The concentration of the radionuclide in the organism can be expressed as:

$$C_f^*(t) = CF^* C_w^* \tag{5.95}$$

where CF^* indicates consideration of radioactive decay.

This expression follows from substituting Eq.(5.94) into Eq. (5.93). Note that it is possible to define the ratio of the radionuclide concentration in the organism to that in the water for any time period. This ratio of concentrations is not the true concentration factor but approaches it asymptotically with increasing time. The time required for equilibrium to be nearly attained depends on the radionuclide half-life and the biological half-life of the element in the organism. The effective half-life is:

$$T_e = \frac{T_{bio} \times T_{½}}{T_{bio} + T_{½}} \text{ or } T_e = \frac{\ln 2}{\lambda + r} \quad . \tag{5.96}$$

Equilibrium is generally approached close enough for practical purposes within 10 effective half-lives.

*The concentration factor has also been termed the accumulation factor, accumulation coefficient, bioaccumulation factor or discrimination factor.

For the true equilibrium situation, the concentration factor for the radionuclide [given by Eq. (5.94)] is slightly less than the concentration factor for the stable element [as given by Eq.(5.91)], providing that both elements are in the same physiochemical form. This can be seen by taking the ratio of the two concentration factors:

$$\frac{CF^*}{CF} = \frac{r}{r+\lambda} = \frac{1}{1+\lambda/r} \text{ and } CF^* = \frac{CF}{1+\lambda/r} = \frac{CF}{1+T_{bio}/T_{½}} \quad . \quad (5.97)$$

Because of this, concentration factors determined from measurements of the stable element concentrations in the organism and in water should provide a quantitative indication of the behavior of isotopic radionuclides. Equation (5.97) shows that the concentration factor for radionuclide with a very short half-life (compared to the biological half-life of the element) could be appreciably lower than that of the analogous stable element. A long-lived radionuclide on the other hand, should behave similarly to the stable isotope.

Concentration factors for freshwater systems are given in Table 5.41. Those applicable to saltwater systems are given in Table 5.42.

Example 5.5: Fish consumption in East Tennessee is estimated to be 24 pounds per year [COW-66]. The following radionuclides were noted in river water:

	Water concentration (pCi/L) [PAR-66]	Concentration factor fish flesh (L/kg)
Cobalt-60	18	60
Strontium-90	4.5	20
Ruthenium-106	345	70
Cesium-137	21	600

What is the annual intake of each of these radionuclides from fish consumption?

Solution: The average radionuclide concentration in fish flesh is given by the product of the water concentration and the concentration factor. The annual intake is the product of the concentration in the fish and the annual intake of fish (10.9 kg/yr).

Nuclide	Water (pCi/L)	Fish (pCi/kg)	Annual Intake (pCi/yr)
Cobalt-60	18	1080	1.18E + 04
Strontium-90	4.5	90	9.80E + 02
Ruthenium-106	345	24,150	2.63E + 05
Cesium-137	21	12,600	1.37E + 05

[End of Example]

Table 5.41 Radionuclide concentration factors for freshwater organisms

Element/ nuclide	Freshwater concentration factor (L/kg fresh mass)[a]								
	Aquatic plants		Crustaceans		Molluscs		Fish		References
Sodium-24	Green algae[a]	6.6E+01	Crayfish[a]	2.3E+03	Snail[a]	2.0E+02	Minnow[a]	1.3E+02	[a]DAV-58b
Phosphorus-32	Green algae[b]	2.8E+05	Crayfish[b]	1.3E+04	Snail[b]	6.0E+04	Small fish[a]	1.65E+05	[a]DAV-58a; [b]DAV-58b
	Algae[d]	(0.05-1.13)E+05					Minnow[b]	1E+05	[c]PRE-69; [d]CUS-66
							Fish[c]	1.6E+03	
		4.6E+05						3.8E+05	
Sulfur-35					Clam	2.4E+02			HAR-69
Chromium-51	Benthic algae[b]	1.6E+03	Crayfish[c]	2.4E+02	Clam[a]	4.4E+02	Minnow[c]	1.9E+02	[a]HAR-69, [b]LOW-71
	Phytoplankton[b]	2.4E+03	Crustacean[b]	1.0E+02	Molluscs[b]	4.4E+02	Fish[b]	7E+01	[c]DAV-58b
	Green algae[c]	4.0E+03			Snail[c]	2.5E+03			
		3.9E+03		2.9E+02		4.4E+02		1.15E+02	
Manganese-54	Plankton[c]	4.2E+02	Crayfish	1.0E+3	Bivalues	6.3E+02	Fish[b]	8.0E+01	[a]HAR-69;[b]LOW-71;
	Phytoplankton[b]	4.0E+03	Bluecrab[c]	1.4E+03	Clam[a]	4.0E+02	Fish[d]	2.3E+02	[c]LEN-71; [d]HER-75;
	Benthic algae[b]	2.3E+03	Crustacean	1.9E+03	Mollusc[b]	1.2E+04	Catfish[c]	5.0E+1	[e]DAV-58b; [f]VAN-75
	Potamogeton[e]	2.8E+03					Alewife[c]	1.3E+02	
	Plants[d]	2.4E+02					White perch[c]	6.0E+01	
		7.0E+03		1.9E+03		9.2E+03		1.6E+02	
Manganese-56	Green algae[c]	1.1E+04					Minnow[c] or $CF^c = 0.32/[Mn]$ where [Mn] is ppm or mg/L.	2.5E+01	
Iron-59	*Benthic algae*[a]	4.8E+03	*a*	2.4E+03	*a*	9.6E+03	Fish[a]	1.6E+03	[a]LOW-71; [b]HER-75
	Phytoplankton[a]	4.5E+04					Fish[b]	5.4E+02	
								2.0E+03	

Table 5.41 (continued)

Element/ nuclide	Freshwater concentration factor (L/kg fresh mass)*								
	Aquatic plants		Crustaceans		Molluscs		Fish		References
Cobalt-60	Benthic algae[c]	8.0E+02	Crustacean[c]	5.0E+02	Clam[b]	7.9E+02	Salmon[e]	8.2E+03	[a]JEN-69; [b]HAR-69;
	Phytoplankton	1.5E+03	Decapod[d]	8.0E+02	*c*	6.0E+02	Fish[c]	1.0E+01	[c]LOW-71; [d]FUK-73;
	Algae[b,d]	2.0E+03			*d*	2.0E+03	Fish[d]	6.0E+01	[e]FRI-65; [f]HER-75
	Plants[f]	2.2E+02			Snail[d]	2.0E+03	Gizzard shad[e]	1.8E+01	
							White bass[e]	5.0E−01	
							Fish[f]	1.30E+02	
Cobalt-58	Plants[f]	5.3E+02							
		2.3E+03		8.8E+02		1.85E+03		1.25E+02	
Nickel-63	Phytoplankton	5.0E+03							LOW-71
	Benthic algae	1.0E+03							
Copper-64	Green algae	6.6E+03	Crayfish	3.0E+01	Snail	5.6E+02	Minnow	9.2E+00	DAV-58b
Zinc-65	Algae[a]	6.E+03	Crayfish[e]	4.1E+03	Clam[b]	4.1E+03	Bluegill[c]	1.6E+03	[a]HAR-65; [b]HAR-69
	Green algae[e]	1.4E+05			Snail[e]	1.7E+04	Bass[c]	6E+02	[c]HAR-64; [d]PRE-69
	Algae[f]	(0.3–19)E+03					Catfish[c]	8.0E+02	[e]DAV-58b; [f]CUS-66;
	Plants[f]	1.5E+02					Fish[d]	1.8E+02	[g]HER-75
							Minnow[e]	9.1E+01	
							Fish[f]	5.1E+02	
		1.6E+04						8.3E+02	
Strontium-89,90	Algae[a]	6.0E+02			Mollusc[f]	3.2E+02	Carp[e]	8.2E+00	[a]HAR-65; [b]HAR-64
	Plants[d]	1.3E+02					Bass[e]	1.15E+00	[c]BRY-66; [d]HER-75
	Plants[d]	2.0E+01					Catfish[e]	1.1E+01	[e]FRI-65; [f]VAN-75
							Trout[e]	2.1E+01	
							Trout[d]	2.0E+01	
							Bone[d]	2.4E+03	
							Flesh	2.8E+01	
							or fresh[f] = 178/[Ca]$^{1.21}$ and bone = 1.5E+04/[Ca]$^{1.15}$ for calcium in ppm or mg/L.		
		6.4E+02							

Table 5.41 (continued)

Element/ nuclide	Freshwater concentration factor (L/kg fresh mass)*									
	Aquatic plants		Crustaceans		Molluscs		Fish		References	
Zirconium-95	Plants[a]	(3.6–80)E+03	*b*	1.6E+03	Snail[b]	1.6E+02	*b*	2.6E+00	[a]BRY-66; [b]BEN-66;	
	Algae[b]	6.4E+02			Clam[b]	2.6E+00			[c]HER-75	
	Plants[c]	1.5E+02								
		3.4E+04								
Technetium-95m	Algae	2.7E+02					Carp	6E+01	BLA-81	
							Gambusia	7.8E+01		
Molybdenum-99	Algae	8		1E+02		6.0E+01		1.0E+01	LOW-71	
Ruthenium-106	Phytoplankton[a]	2.0E+05	*d*	1.0E+02	*a*	3.0E+00	*a*	5E–02	[a]LOW-71; [b]BRY-66;	
	Algae	3.9E+02	*c*	2.0E+02	Clam[c]	1.2E+00	*c*	1.8E+00	[c]BEN-66; [d]FRI-65;	
	Algae[c]	1.3E+03			Snail[c]	2.3E+02	Gizzard shad[d]	8.6E+00(w)	[e]HER-75	
	Plants[b]	(2.5–25)E+02					White bass[d]	4.5E-01(w)		
	Plants[c]	3.0E+01					Saugers[d]	4.5E-01(w)		
Ruthenium-103	Plants[e]	1.0E+02					*e*	7.0E+01		
		1.6E+03		2.3E+02		3.6E+00		1.9E+01		
Antimony-124,-125	Plants	3.0E+01						9.0E+01	HER-75	
		1.4E+02						1.0E+02		
Iodine-131	Algae[a]	4E+02	*b*	3.0E+01	Clam[a]	2.2E+02	Carp[a]	3.5E+01	[a]KOL-69a; [b]LOW-71;	
	Algae[c]	1.6E+02	*c*	7E+00	Clam[c]	1.1E+01	*b*	1.2E+01	[c]BEN-66; [d]HER-75	
	Benthic algae[b]	1.6E+02			*b*	5.0E+01	*c*	6E−01		
	Water lily[a]	1.2E+02			Snails[c]	8.0E+01		5.28E+02 (whole fish)		
				4.0E+01		2.2E+02		4.4E+01		

Table 5.41 (continued)

Element/ nuclide	Freshwater concentration factor (L/kg fresh mass)*								
	Aquatic plants		Crustaceans		Molluscs		Fish		References
Cesium-133	Plants[a]	3.2E+02	Amphipod[a]	7.0E+02			Trout[a]	5.6E+03	[a]HAK-75; [b]HER-75
Cesium-134							Fish[b]	2.0E+02	
Cesium-137	Algae[b]	1.2E+03	Shrimp[b]	1.1E+04	Clam[c]	2.2E+02	Coho salmon	4.1E+03	[a]JEN-69a; [b]HAR-65;
	Green algae[f]	(1.5-4)E+03	*Mysis*[c]	3.8E+02	Snail[f]	6E+02	Chinook salmon	4.75E+03	[c]HAR-69; [d]HAR-64;
	Elodea[f]	1E+03					Salmon[e]	1.0E+02	[e]GUS-69b; [f]PEN-58;
	Duckweed[g]	5E+02					Bluegill[k]	4.1E+02	[g]BRY-66; [h]FRI-65;
	Potomageton[g]	1E+03					Bluegil[b]	9.0E+02	[i]WAH-75; [j]KOL-69b
	Cladophora[i]	1E+03					Bass[e]	1.2E+03	[k]NEL-69a; [l]HER-75;
	Plants	1.3E+02					Catfish[d]	1.2E+03	[m]VAN-75
							Perch[e]	7.5E+02	
							Pike[e]	3.6E+03	
							Sunfish[f]	9.5E+03	
							Trout[f]	(2.5-3.7)E+03	
							Lake trout[f]	6.8E+03	
							Gizzard shad[k]	5.1E+02	
							Gizzard shad[h]	4.0E+01	
							Alewife[e]	2.7E+03	
							Smelt[e]	3.7E+03	
							Whitefish[f]	4.1E+03	
							Blk bullhead[h]	2.7E+02	
								1.7E+02	
		2.0E+03		2.2E+04		2.2E+02		5.6E+03	or for piscivorous fish:[m] CF = 1.5E+04/[K] and for nonpiscivorous fish:[m] CF = 5E+03/[K] *where* K = *potassium concentration* in ppm or mg/L. Divide by 5 for waters of turbidities greater than 50 ppm suspended soilds.[m]
							Other:		
							Bullfrog[f]	8.0E+03	
							Coot[f]	1.8E+03	
							Mallard duck[f]	1.0E+03	
							Ruddy duck[f]	2.2E+03	

Table 5.41 (continued)

Element/ nuclide	Freshwater concentration factor (L/kg fresh mass)[a]									
	Aquatic plants		Crustaceans		Molluscs		Fish			References
Cerium-141	Plants	2.7E+02							1.5E+02	HER-75
Cerium-144	Algae[c]	1.7E+04	*c*	9.8E+02	Clam[a]	9.0E+02	*c*		1.7E+00	[a]HAM-67; [b]BRY-66;
	Algae[d]	9.8E+03			Clam[c]	4.0E+00	(whole)[d]		6.4E+02	[c]BEN-66; [d]FON-63;
	Plants[b]	(2-20)E+02			Snail[c]	8.7E+02	*e*		1.6E+02	[e]HER-75
	Plants[d]	8.3E+02			Mollusc[d]	6.4E+03				
	Plants[e]	3.1E+02								
		9.8E+03				9.0E+03			1.25E+02	
Radium-226	Reed[a]	2.7E+04	*Gammarus*[b]	3.2E+03	Mussels[c]	(0.1-10)E+03	Trout[b]		8.4E+01	[a]VER-67; [b]STE-81
	Pondweed[b]	3.4E+03					Perch[c]		3.8E+03/[Ca]	[c]BOR-72; [d]JEN-69;
	Plants[d]	1.9E+02					Salmon[d]		2.2E+02	[e]DAV-73; [f]HER-75
							Salmon[e]		7.5E+02	
							f		7.9E+01	
		6.2E+03							3.8E+03/[CA]	
									(in ppm or mg/L or 5.2E+02	
Thorium	Plants	1.2E+03							8.0E+01	HER-75
Uraniun			*Gammarus*[a]	1.6E+01	Mussels[b] (U μg/L)	1E+03@0.1 μg/L 3E+02@1.0 μg/L 1E+01@10 μg/L 144/[U]	Trout[a]		7.5E+00	[a]STE-81; [b]DAV-73

Table 5.41 (continued)

Element/ nuclide	Freshwater concentration factor (L/kg fresh mass)*							
	Aquatic plants		Crustaceans		Molluscs	Fish		References
Plutonium-239,-240	Algae[b]	1.0E+04	Crayfish[b]	1.0E+03		Largemouth bass[b]	4.E-01	[a]DAH-76; [b]THO-75
	Plankton[c]	5.6E+03	*Mysis*[c]	7.5E+02		Bluegill[a]	3E+00	[c]WAH-75
						Shad[a]	4E+00	
						Minnow[b]	(0.9–7.5)E+00	
						Sculpin[c]	2.4E+02	
						Alewife[c]	2.5E+01	
						Smelt[c]	2.0E+01	
						Chinook salmon	3E+00	
						Lake trout	4E+00	
		1.1E+04		1.0E+03			8.0E+00	

*Underscored numerical values represent the antilog of the sum of the geometric mean, $\overline{\ln x}$, and the geometric standard deviation $\ln\sigma g$ of the values listed. This represents the 84th percentile of an assumed lognormal distribution of the values and should be a moderately conservative value. Based upon the values listed, the probability of exceeding the underscored value is approximately one-fifth (16%). The calculation is such that greater variability among the reported values will lead to a larger 84th percentile value due to a larger $\ln\sigma g$ being used. Thus, less precision in the estimates is reflected in a greater numerical concentration factor.

Table 5.42. Radionuclide concentration factors for estuarine and salt-water organisms (1-6)

Element/ nuclide	Marine concentration factor (L/kg fresh mass)*								
	Marine plants		Crustaceans		Molluscs		Fish		Reference
Sodium-24	*Stigeoclonium*[b]*	1.0E+02	–[a]	3.0E−01	–[a]	2.0E−01	–[a]	1.3E−01	[a]LOW-71; [b]FOS-59
							Lancetfish[b]*	(1-10)E+02	
Phosphorous-32	Benthic algae[a]	1E+04	–[a]	2.4E+04	–[a]	6E+03	–[a]	3.3E+04	[a]LOW-71; [b]FOS-59
	Phytoplankton[a]	3.4E+04					Lancetfish[b]*	1.0E+05	
	Stigeoclonium[b]	(1-10)E+05							
Scandium-46	*Stigeoclonium**	1.0E+05					Lancetfish[b]*	1.0E+05	F0S-59
Chromium-51	*Ulva*[b]	6.8E+03	Lobster[b]	1.9E+03	Mussel[b]	2.1E+03	Yellowtail[b]	2.85E+04	[a]YAM-65; [b]VAN-73
	Porphyra[a]	6.0E+03			Mussel[b]	2.9E+03	Pilchard[b]	6.0E+03	[c]FOS-59
	Kelp[a]	3.4E+03			Abalone[b]	6.9E+03	Sole[b]	3.7E+04	
	Stigeoclonium[c]*	(1-10)E+02					Mackerel[b]	7.8E+03	
							–[a]	9.0E+03	
							Lancetfish[c]*	1.0E+01	
		7.5E+03				6.4E+03		3.0E+04	
Manganese-54	*Ulva*[a]	8.0E+03	Lobster[d]	3.7E+02	Mussels[d]	2.8E+03	Yellowtail[a]	3.2E+02	[a]YAM-65; [b]PEN-72;
	Porphyra[a]	1.1E+04	Lobster[c]	8E+02	Mussels[d]	1.4E+03	Pilchard[a]	1.8E+03	[c]BRY-66; [d]VAN-73;
	Kelp[d]	4.5E+02	Lobster		Abalone[d]	4.5E+02	Sole[a]	9.7E+02	[e]COS-66
	Seaweed[c]	(5-25)E+03	whole	(6.3E+04)	Scallop[c]	5E+02	Mackerel[a]	6.2E+02	
	Chara[e]*	4E+04					–	4.0E+03	
							Plaice[b]	1.1E+02	
							Fish muscle[d]	(1.0-4.0)E+02	
							–[e]*	1.2E+01	
		2.5E+04		9.4E+02		2.3E+03		1.9E+03	
Iron-55,-59	*Ulva*[c]	1.8E+04	Lobster[c]	1.8E+03	Mussel[c]	1.1E+04	Yellowtail[c]	1.1E+04	[a]YAM-65; [b]FRA-75;
	Porphyra[c]	1.8E+04			Mussel[c]	3.0E+03	Sole[c]	1.1E+04	[c]VAN-73
	Kelp[c]	2.3E+03			Mussel[b]	(0.17-1.1)E+02	Pilchard[a]	1.4E+04	
					Abalone[c]	1.7E+04	Mackerel[a]	7.5E+03	
							Blennie[b]	(1.8-5.9)E+00	
		1.8E+04				2.1E+04		1.4E+04	

Table 5.42 (continued)

Element/ nuclide	Marine Concentration factor (L/kg fresh mass)*								
	Marine plants		Crustaceans		Molluscs		Fish		References
Cobalt-60	Ulva[e]	6.0E+02	Lobster[e]	1.4E+04	Mussels[e]	1.15E+03	Yellowtail[e]	4.0E+02	[a]YAM-65; [b]BHA-80;
	Porphyra[e]	1.6E+03	Prawns[b]	1.1E+01	Mussels[e]	1.25E+03	Sole[e]	1.0E+02	[c]ATE-61a; [d]BRY-66;
	Kelp[e]	2.2E+02	Crabs[b]	1.15(0.47-1.86)E+02	Abalone[e]	8.0E+02	–[a]	6E+01	[e]VAN-73; [f]COS-66
	Sargassium[b]	5.7E+02			Oysters[b]	4E+01	Bombay duck[b]*	1.5E+01	
	Seaweed[a]	1E+03					–[c]	1.6E+02	
	Chara[f]*	4.E+03					Whole[f]*	2.0E+01	
		1.4E+03		2.2E+02		2.4E+03		3.1E+02	
Copper-64	Plankton[a]	3E+04			–[a]	5E+03	–	1E+03	[a]LOW-71; [b]FOS-59
	Algae[a]	1E+02					Lancetfish*	1.0E+02	
	Stigeoclonium[b]*	1.E+04							
		3.8E+04							
Zinc-65	*Ulva*[f]	4.5E+03	Lobster[f]	1.3E+04	Mussel[f]	1.2E+04	Yellowtail[f]	4.2E+03	[a]YAM-65; [b]BHA-80;
	Porphyra[f]	8.5E+03	–[e]	2.0E+03	Abalone[f]	1.7E+04	Sole[f]	4.2E+03	[c]ATE-61a; [d]PRE-69;
	Kelp[f]	1.3E+03			Oysters[d]	1.1E+04	Pilchard[f]	1.5E+04	[e]LOW-71; [f]VAN-73;
	Plankton[e]	1.5E+04			–[e]	1.1E+04	Mackerel[f]	6.9E+03	[g]FOS-59
	Stigeoclonium[g]*	1.0E+05					–[a]	9E+03	
							–[e]	5E+02	
							Lancetfish[g]*	(1-10)E+03	
		9.6E+03				1.5E+04		1.35E+04	
Arsenic-76	*Stigeoclonium**	1.0E+04	–	–	–	–	Lancetfish*	1.0E+02	FOS-59
Strontium-89, -90	Many sp[a]	(2-6)E−01	Lobster[f]	1	*Mytilus* sp[b]	6.0E−01	*Micropogon*[b]	8.7E+00	[a]CAN-73; [b]ATE-61a;
	Calcareous sp[a]	(2.8,3.6)E+01	*Artemesia*[b]	0.5	*Mytilus*[c]	8.0E+00	*Scomber*[b]	2.8E+00	[c]PRE-69; [d]LOW-71;
	Fucus[c]	6.0E+00	*Hymenopenaeus*	1.4	*Mytilus*[f]	1.0E+01	*Raia*	3.0E−01	[e]VIL-78; [f]BRY-66
	Fucus[f]	2.0E+01	–[d]	3	*Mytilus* shell	1.0E+02	*Pleuronectes*	3.0E−01	[g]FOS-59
	Benthic algae[d]	9.6E+00	–[b]	25			Many sp[b]	2.0E+00	
	Porphyra[e]	1.0E+00			*Mesodesma* sp[b]	5.0E−01	–[d]	1.0E−01	
	Stigeoclonium[g]*	1.0E+04			–[e]	2.5E+01	–[e]		
					Littornia[f] (Winres)	3.0E+00		1.0E+00	
							Lancetfish[g]	1.0E+03	
		1.3E+01		1.5		9.6E+00		3.9E+00	

Table 5.42 (continued)

Element/ nuclide	Marine concentration factor (L/kg fresh mass)[a]												References
	Marine plants			Crustaceans			Molluscs			Fish			
Zirconium-95 Niobium-95	*Porphyra*[a]	4.2E+02		Lobster[b]	1.0E+01		Mussels[a]	9.5E+02		Muscle	(1.3)E+00		[a]HAM-67; [b]PRE-69;
	Fucus[b]	1.7E+03		Lobster[e]	1.0E+02		–[c]	2.0E+00	(Zr)	–[c]	1E+00	(Zr)	[c]LOW-71; [d]ANC-66;
	Benthic algae[c]	2.2E+03		Shrimp (whole)[b]	2.0E+02		–[c]	7.0E+00	(Nb)	–[c]	1E+02	(Nb)	[e]BRY-66
	Phytoplankton[c]	6.0E+04	(Zr)				Flesh[d]	1.7E+01	(Zr)				
	Phytoplankton[c]	1.0E+03	(Nb)	Shrimp[c]	2.0E+00	(Zr)	Whole[d]	1E+03	(Zr)				
	Algae[a]	1.0E+03		Shrimp[c]	3.E+00	(Nb)							
	Seaweed[e]	(0.35-1)E+03	(Zr)										
	Seaweed	(0.45-1)E+03	(Nb)										
		1.6E+03			2.8E+02			8.3E+02			3.7 E+01		
Ruthenium-103,-106	*Fucus*[c]	3.3E+02		Lobster[c]	2.5E+01		Mussel[b]	(5-9)E+00		Plaice[a]	1.2E+02		[a]PEN-72; [b]FRA-75;
	Porphyra[c]	1.8E+03		Lobster[e]	2.0E+03		Mussel[c]	2E+03		Plaice[b]	(0.4-1.6)E−01		[c]PRE-69; [d]VIL-78;
	Algae[e]	1.0E+02		Lobster[f]	(1-10)E+00		Flesh[e]	2.2E+01		Blennie[c]	1.0E+01		[e]ANC-66; [f]BRY-66
	Seaweed[f]	(0.15-20)E+02		Shrimp[b]	(0.6-4.8)E+00		Whole[e]	3.0E+01		Blennie[d]	3.0E+01		[g]COS-66
	Chara[g,a]	1.0E+03		Shrimp[c]	6E+02		(Whole)			Whole[e]	3.0E+01		
		2.2E+03			4.0E+02			3.8E+02			5.1E+01		
Silver-110m	Plankton[a]	2.3E+04		Shrimp (tail)[a]	9.5E+02		–[a]	7.1E+03		Albacore[b]	(0.33-1.1)E+03		[a]LOW-71; [b]ROB-71
							Squid[b]	5.9E+03		–[b]	(0.65–11)E+02		
Antimony-125	*Ulva*	1.1E+02		Lobster	1.7E+02		Mussels	2.9E+02		Yellowtail	6.1E+01		VAN-73
	Porphyra	2.3E+02					Mussels	3.9E+02		Sole	5.0E+01		
	Kelp	3.0E+01					Abalone	1.2E+02					
		2.5E+02						4.4E+02			6.4E+01		
Iodine-131	*Sargassium*[b]	1.1E+03		Prawns[b]	40(11-68)		Oysters[b]	3.0E+01		–[a]	3.3E+00		[a]HIY-64; [b]BHA-80;
	Ulva[b]	1.5E+03		Crabs[b]	60(31-93)					Bombay duck[b]	1.1E+01		[c]ATE-61a
										–[c]	7.0E+00		

Table 5.42 (continued)

Element/ nuclide	Marine concentration factor (L/kg fresh mass)*†									
	Marine plants		Crustaceans		Molluscs		Fish		References
Cesium-137	*Ulva*[d]	3.5E+01	Lobster[k]	3.2E+01	*Mytilus*[j]	2.4E+01	Tuna[a]	1.0E+02	[a]FOL-69; [b]YAM-65;
	Ulva[d]	2.0E+01	Lobster[g]	2.5E+01	*Mytilus*	9.0E+00	–[b]	5.0E+01	[c]PEN-72; [d]BHA-80;
	Porphyra[d]	8.0E+01	Crabs[a]	3.(0.8-5.1)E+01	*Mytilus*	(1-2)E+01	Plaice[c]	2.4E+01	[e]GIL-75; [f]ATE-61a;
	Kelp[d]	3.0E+01	Crabs[i]	2.5E+01	Mussels[g]	1.5E+01	Plaice[g]	4.5E+01	[g]PRE-69; [h]LOW-71;
	Sargassium	1.2E+02	Crabs[j]	3.0E+01	Oysters[a]	3.0E+01	–[c]	5.4E+01	[i]CHI-66; [j]BRY-66;
	Ulva[d]	2.0E+01	Shrimp (whole)[g]	1.0E+02	Squid[e]	5.0E+01	Bombay duck[d]	8.5E+00	[k]VAN-73; [l]COS-66;
	Fucus[j]	1.0E+02	Shrimp[h]	2.3E+01			Sardine[f]	(5-10)E+01	[m]FOS-59
	Fucus[j]	7(0.01-10)E+01					Mixed[f]	2.0E+01	
	Unspec[f]	(5.3-13.8)E+01					*Raia*[l]	8.4E+01	
	Chara[l]*	1.E+02					*Clupea* herring[j]	5.0E+01	
	*Stigeoclonium**	(1-5)E+03					*Pleuronectes*[j] flounder	5.0E+01	
							Whole	3.0E+01	
							Lancetfish[m]*	(5-10)E+03	
		2.0E+02		5.7E+01		3.5E+01		8.5E+01	
Cerium-141,-144 (rare earths)	*Ulva*[a]	3(1.8-5.2)E+02	–[c]	2.0E+00	Clam[a]	5(3-8.6)E+02	Flounder[a]	2.0(0.5-3.9)E+01	[a]SUZ-75; [b]ATE-61a;
	Sargassium[d]	2.5(1.4-3.5)E+02	–[d]	1.0E+03	–[c]	3.6E+02	–[b]	1.2E+01	[c]LOW-71; [d]VIL-78;
	Algae[c]	6.7E+02	Lobster[f]	1.0E+02	–[d]	1.0E+03	Yellowtail[a]	3.0(1.3-5.8)E+01	[e]ANC-66; [f]BRY-66;
	Plankton[c]	9.0E+04			Mussel[e]	1.0E+03	–[e]	3.0E−01	[g]COS-66
	Algae[e]	1.0E+04			Mussel		–[d]	2.0E+01	
	Seaweed[f]	(3-9)E+02			Flesh[e]	1.2E+03	Blennie[e]	3.0E+01	
	Chara[g]	1.5E+03					–[f]	1.2E+01	
							Whole[g]	6.5E+01	
		7.2E+02		1.4E+03		8.6E+02		6.4E+01	

Table 5.42 (continued)

Element/ nuclide	Marine concentration factor (L/kg fresh mass)*†									
	Marine plants		Crustaceans		Molluscs		Fish			Reference
Polonium-210	Benthic algae	1.0E+03	–	–	–	–	–	–	–	LOW-71
Lead-210	Benthic algae	7.0E+02	–	–	–	4.0E+01	–	–	–	LOW-71
	Phytoplankton	4.0E+04								
Radium-226	Benthic algae[b]	1.4E+03	–[b]	1.4E+02	–[b]	1.3E+03	–[a]	1.5E+01		[a]ATE-61a; [b]LOW-71
	Phytoplankton[b]	1.2E+04					–[b]	1.3E+02		[c]COS-66
	Chara[c]	6.7E+02					Whole[c]	2.0E+01		
		1.0E+04						1.1E+02		
Thorium-232	*Fucus*	1.3E+03	–	–	–	–				HOL-80
Thorium-228	*Fucus*	1.1E+04	–	–	–	–				
Uranium-238	*Fucus*	7.0E+02	–	–	–	–	–[a]	1.5E+01		[a]ATE-61a; [b]ATE-61b
							–[b]	2.0E+01		
								2.1E+01		
Plutonium-239, 240	*Porphyra*[a]	3.0E+03	Shrimp[a]	1.0E+01	*Mytilis*[a]	2.0E+03	Plaice[a]	1.0E+00		[a]MUR-79; [b]HOL-80
	Fucus[b]	1.4E+04	–[d]	3.0E+00	–[d]	2.6E+02	Salmon[b]	1.0E+00		[c]HET-75; [d]LOW-71;
	Fucus[f]	5.2E+02	–[e]	2.5E+02	–[e]	2.5E+02	–[d]	3.0E+00		[e]VIL-78; [f]GUA-77
	Benthic algae[d]	1.3E+03			*Littornia*[f]	2.0E+02	–[c]	5.0E+01		
	Phytoplakton[d]	2.6E+03			Snail					
					Dogwinkel[f]	7.0E+01				
		7.9E+03		1.9E+02		2.55E+02		2.7E+00		
Americium	*Porphyra*	1.0E+03	Shrimp[a]	2.0E+02	–	–	Plaice[d]	5.0E+00		[a]MUR-79; [b]HOL-80
	Fucus	1.8E+04								

*Indicates a value based on an estuarine locale which may not be typical of marine values. Except when they are of comparable magnitude to the marine values, these asterisk-marked values are not included in the averages.

†Underscored numerical values represent the antilog of the sum of the geometric mean, $\overline{\ln x}$, and the geometric standard deviation, $\ln \alpha q$, of the values listed. This represents the 84th percentile of an assumed lognormal distribution of the values and should be a moderately conservative value. Based upon the values listed, the probability of exceeding the underscored value is approximately one-fifth (16%). The calculation is such that greater variability among the repoted values will lead to a larger 84th percentile value due to a larger $\ln \sigma q$ being used. Thus less precision in the estimates is reflected in a greater numerical concentration factor.

5.3.3.2 Variables Affecting Radionuclide Uptake by Aquatic Biota and the Magnitude of the Concentration Factor

Method of measurement. The definition of the concentration factor does not make it clear whether the radionuclide concentration in water which should be used in the calculation of the CF is the initial or the final radionuclide concentration in water. This consideration is important principally in laboratory uptake studies and where uptake by the aquatic organism, sediments, or container can deplete the radionuclide level in water. In natural systems the volume of water is generally considerably greater than that "seen" by the organisms so the radionuclide concentration is not rapidly depleted. The importance of this effect depends upon the radionuclide and conditions. For example, the concentration factor computed for iodine in freshwater fish or the basis of the concurrent concentration in water was approximately twice that based upon the initial concentration in water [KOL-69b].

Whether the initial or concurrent radionuclide concentration in water is used depends in part on the application intended for the CF value. For determining the radionuclide content following a one-time release, the concentration factor based upon the initial radionuclide concentration in water would be acceptable. However, for most applications it is the concurrent radionuclide concentration which should be used.

Portion of organism analyzed. The appropriate concentration factor for use in radiation dose assessments is the one which best describes the radionuclide concentration in the portion of the organism which is consumed by man. As with terrestrial organisms, certain radionuclides preferentially concentrate in given organs of aquatic organisms. Strontium and radium are bone-seekers and concentrate in those tissues. Iron (^{59}Fe and ^{55}Fe) are primarily retained in the spleen and kidneys, ^{60}Co in the kidneys, ^{65}Zn in the spleen and liver. The liver of cod is used to make oil and also has higher levels of most radionuclides, such as ^{65}Zn, ^{140}Ba, ^{110m}Ag, ^{54}Mn and ^{60}Co, than muscle. Both croakers *(Micropogon undulatus)* and bluefish *(Pomatomus saltatrix)* showed high uptake of ^{89}Sr in scales and bone [CHI-66].

Concern for the appropriate concentration factor is particularly important for molluscs as many radionuclides may concentrate in the visceral organs or in the shell rather than in the edible body tissue. In most cases, the adductor muscle is the only part of the mollusc consumed. In decapod crustaceans, such as the crab and the lobster, only the muscle is consumed by man, except, perhaps, for the hepatopancreas of the crab [BRY-66].

In such cases, the use of concentration factors based upon the whole organism may considerably overestimate the concentration in the edible portions and consequently overestimate the radionuclide intake and radiation dose to man. Strontium-90, cesium-137, and manganese-54 are examples of radionuclides which concentrate in the shell of freshwater clams [HAR-69].

Schelske [SCH-72] found that the bay scallop had a concentration factor for stable manganese of 32,000 based upon the whole organism. However, only 7.5% of the manganese was present in the edible adductor muscle which had a concentration factor of only 2,500. Most of the manganese was in the kidney. Similar concerns apply to fish where radionuclides like $^{90,91}Y$, ^{95}Zr-^{95}Nb, ^{106}Ru, ^{144}Ce, and Pu are primarily associated with the GI tract and ^{90}Sr is primarily concentrated in the bone. Examples of this are shown in Table 5.43.

There are circumstances where concentration factors derived for the muscle of fish, crustaceans or molluscs can lead to underestimates of human intake. This occurs most commonly in circumstances when the whole organism is consumed. Consumption of raw clams, oysters, and mussels on the "half-shell" is common and generally includes the GI tract, kidney, and other organs not otherwise eaten. Small fish such as anchovies, sardine, smelt, and canned salmon may include the bones and, except for the salmon, the GI tract in the edible portion [BAP-70]. The potential importance of the inclusion of the GI tract to doses from ingesting these organisms can be seen from the relative plutonium concentration in a larger fish, the plaice. The concentration of $^{239+240}Pu$ (fCi/g wet) in various organs was [PEN-79]: gut 68, gut contents 3710, gill 9.3, skin 59, liver 255, kidney 703, bone 174, and muscle 8 fCi/g wet weight. The gut contents had a plutonium concentration over 400 times that in the muscle.

Local dietary habits are important in assessing the magnitude of such contributions to radiation doses. In some cases, the method of food preparation can alter the radionuclide concentration in edible portions. Crustaceans and molluscs are often prepared by cooking the entire animal. If food is cooked

Table 5.43. Examples of radionuclide localization in certain organs of freshwater fish

Species	Ratio of Strontium-90 concentration in bone to the concentration in flesh [FRI-65]	Species	Ratio of Plutonium concentration in GI tract to concentration in total fish less GI tract [DAH-76]
White bass	2.2	Large mouth bass	30
Sangers	2.2, 4.2	Bluegill sunfish	40
Gizzard shad	0.6	Goldfish	80
Carp	2.8, 5.0	Shad	200
Small mouth bass	0.7		
Carpsuckers	1.6		
Catfish	13.4		

for an appreciable period of time, there is a possibility of cross-contaminating muscle by radionuclides leached from the exoskeleton of the crustacean or the shell of the mollusc [TIN-69].

Stable element concentrations in water. The concentration factor approach presumes that the concentration of an element in an aquatic organism is directly proportional to the concentration of that element in water. Although this relationship may hold for microconstituents and trace elements (such as radioisotopes), it cannot be expected to hold over all concentration ranges or for all elements. A fish placed in water having a high calcium content does not acquire excess calcium without limit. On the other hand, a fish placed in water having a low calcium concentration still acquires sufficient calcium to maintain its bone composition. Aquatic organisms regulate the composition of their bodies, so that this composition is relatively constant despite variations in the environment. They do this by controlling the rate of uptake and the biological excretion rate [PET-71]. Uptake of trace stable elements and radionuclides primarily involves an exchange with existing stable element pools within the organism.

The regulated constant composition can be depicted as [PET-71]:

$$(x/m)_{equil} = \frac{IC_w}{mr} = \xi \ , \tag{5.98}$$

where

x = the amount of the stable element in an organ of m grams,

I = the intake rate,

C_W = the concentration of the element in water,

r = the biological elimination rate constant, and

ξ = the size of the stable element pool.

From the definition of the concentration factor given in Eq. (5.92), it can be seen that the concentration factor should be given by:

$$CF = \frac{(x/m)}{C_w} = \frac{\xi}{C_w} \ . \tag{5.99}$$

On logarithmic scales this expression would give a straight line of unit slope:

$$\ln CF = \ln \xi - \ln C_w \ . \tag{5.100}$$

Table 5.44 shows the results of fitting this equation to several sets of data on the concentration factor for calcium in fish bone and muscle. As predicted,

Table 5.44. Relationship of the concentration factors for calcium in freshwater fish to environmental calcium concentrations

Species	Tissue	Regression parameters in ln (CF) versus ln (C)[a]			
		Correlation coefficient	Slope ± S.E.	Antilog of intercept (mg/kg)	Average stable Ca content (mg/kg)
Perch[b]	Bone	−0.987	−0.940 ± 0.0051	28,850	35,700
	Muscle	−1.000	−1.057 ± 0.024	520	430
Pike[b]	Bone	−0.980	−0.989 ± 0.064	41,770	44,800
	Muscle	−1.000	−1.239 ± 0.020	1,170	560
Roach[b]	Bone	−0.968	−0.986 ± 0.091	34,200	34,900
	Muscle	−0.989	−1.067 ± 0.079	920	760
Brown trout[c]	Bone	−0.980	−1.00	59,000	60,800
	Muscle	−0.964	−1.01	138	141

[a]Analysis from [PET-71].
[b]Data from [AGN-67].
[c]Data from [TEM-64a].

the slopes of the regression equation are close to or equal to minus one and the logs of the intercepts correspond to the magnitude of the calcium content.

When two chemically analogous elements are present they compete for uptake and retention [PET-71]:

$$\xi = \frac{X_a}{m} + \frac{X_b}{m} = \frac{I_{wa}C_a}{mr_a} + \frac{I_{wb}C_b}{mr_b} \tag{5.101}$$

$$= \frac{I_{wb}}{mr_b}[C_b + (OR)_w C_a] \ ,$$

where (OR) is the *observed ratio*, which is equivalent to $(OR)_w = I_{wa}/I_{wb} \div r_a/r_b$. The term outside of the brackets in Eq. (5.101) can be seen to be the concentration factor for element B [see Eq. (5.91)]; therefore:

$$CF_b = \frac{\xi}{C_b + (OR)_w C_a} \ . \tag{5.102}$$

An equivalent expression for element A can be derived from Eq. (5.101) and the observed ratio as defined above:

$$CF_a = \frac{(OR)_w \xi}{C_b + (OR)_w C_a} \tag{5.103}$$

This expression states that a nonessential element (element A) will parallel the uptake of a chemically similar element but that the concentration factor of the nonessential element will differ from that of essential element. As nonessential elements are usually discriminated against by the organism, the concentration factor for the non-essential element will usually be lower than the CF of the essential element. Figure 5.13 shows this effect for ^{90}Sr and ^{45}Ca uptake by a saltwater fish, *Tilapia.* The ^{90}Sr is discriminated against, the

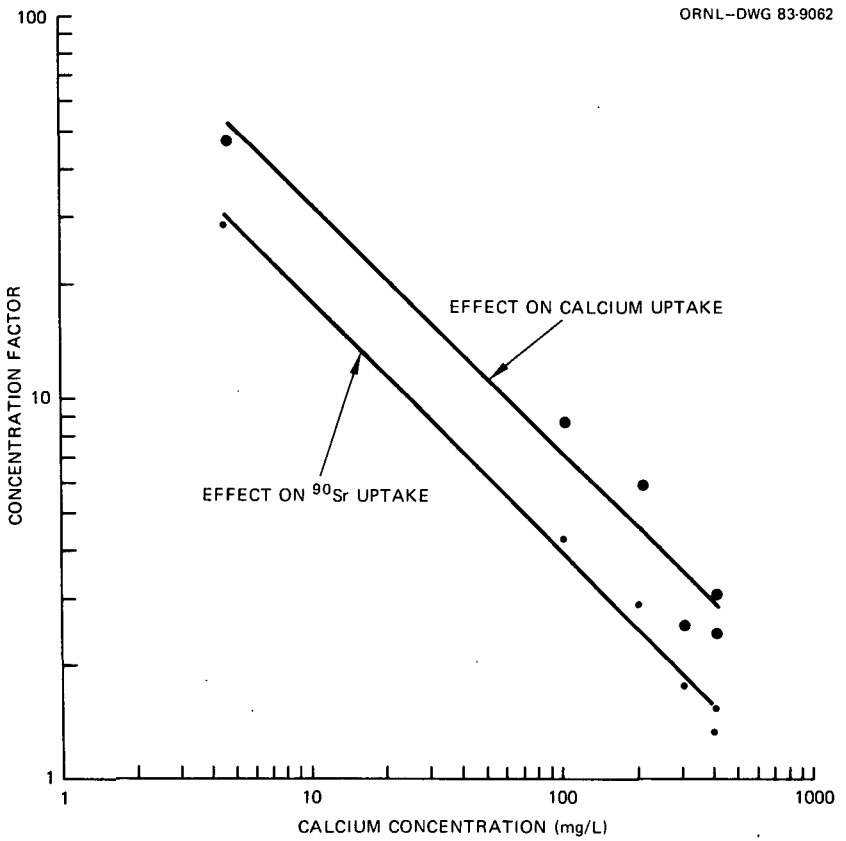

Figure 5.13. The effect of the stable calcium concentration on the concentration factors for uptake of ^{45}Ca and ^{90}Sr from seawater, by the euryhaline fish, *Tilapia mossambica.* Data from [TOW-63].

observed ratio averages about 0.52 [TOW-63]. The uptake of both radioelements decreases inversely with the stable calcium concentration in water.

The inverse dependence of radionuclide uptake on the ambient concentrations of analogous stable elements means that the radionuclide concentration factors for certain elements may vary appreciably from one location to another. Aside from the obvious differences between marine and freshwater systems, the variability of stable element concentrations in freshwater and estuarine ecosystems can be appreciable and can lead to appreciable differences in radionuclide uptake. Kolehmainen et al. [KOL-67b] found 10- to 100-fold differences in the ^{137}Cs content of the same species of fish in 12 Finnish lakes and 3 rivers.

Example 5.6: The concentration factor for ^{137}Cs in fish was found to vary inversely with the potassium concentration in water according to:

$$CF^{*}_{Cs} = 1470\ [K]^{-0.64},\ r = -0.96$$

(from [JIN-76]) for the potassium concentration expressed in mg K/L. Using this expression, estimate the cesium concentration factor for seawater (K = 380 mg/L); an estuary, the Hudson River (K = 17 mg/L) and an inland lake (K = 0.5 mg/L).

Solution:

	Potassium concentration mg/L	Concentration factor L/kg
Marine	380	33
Estuarine	17	240
Lake	0.5	2300

[End of Example]

Species. Radionuclide uptake and retention can vary among different species based upon feeding habits, habitat and position in the food web. Less variation would be expected for similar species. Table 5.45 presents concentration factors measured for three species of trout, king, chum, and silver trout for ^{60}Co, ^{137}Cs, and ^{226}Ra. The silver trout appears to have somewhat lower concentration factors. However, these values are sufficiently close (within a factor of 3) so that the values derived for one of these species could be used to predict radionuclide uptake by the other two species if more pertinent data were not available.

This consistency does not extend to the behavior of ^{137}Cs in freshwater systems where the differences in dietary patterns result in a factor of 3 differ-

Table 5.45. Interspecies differences in radionuclide uptake by trout

Nuclide	Trout species organ	Concentration factors, CF, L/kg[a]		
		King	Chum	Silver
^{60}Co	Muscle	9,400	9,280	5,950
	Liver	50,000	32,000	40,000
	Roe	42,000	60,000	25,550
^{137}Cs	Muscle	74	44	104
	Liver	62	31	24
	Roe	37	30	101
^{226}Ra	Muscle		750	220

[a]Data from [JEN-69].

ence in cesium concentrations and a factor of 2 difference in concentration factors [KOL-69a, NEL-67]. Differences between species due to dietary habits are exemplified by the uptake of plutonium by freshwater fish shown in Fig. 5.14. The bottom-feeding sculpin has a much higher concentration factor than species which do not feed exclusively on bottom organisms and thereby ingest contaminated sediment. The piscivorous fish have the lowest concentration factors.

The "trophic-level effect." Organisms which obtain food by the same number of steps between themselves and the primary producers (plants) are said to be at the same *"trophic level"*. Generally, because of inefficiency in the assimilation of radionuclides entering with food, the concentration of radionuclides decreases at higher trophic levels. This effect is illustrated in Fig. 5.14 by the plutonium and to a lesser extent by strontium.

Measurements of the concentration of cesium-137 in freshwater fish show that, in addition to the bottom-feeding species which ingest sediment, the larger predacious fishes tended to have a markedly higher cesium concentration than the smaller fish [PEN-65]. Moreover, the ratio of the cesium-137 to stable potassium in the fish was also found to increase with the trophic or feeding level. This reconcentration mechanism was of concern since the ultimate predator at the highest level is man. The "trophic level" effect is illustrated in Table 5.46.

Temperature. The effects of small increases in temperature on higher biota appear to increase biological activity and the uptake and excretion of radionuclides [OPH-65]. The biological elimination half-life decreases with increased temperature leading to increased turnover as shown in Table 5.47. The corresponding increase in the biological elimination rate should act to decrease the radionuclide accumulation.

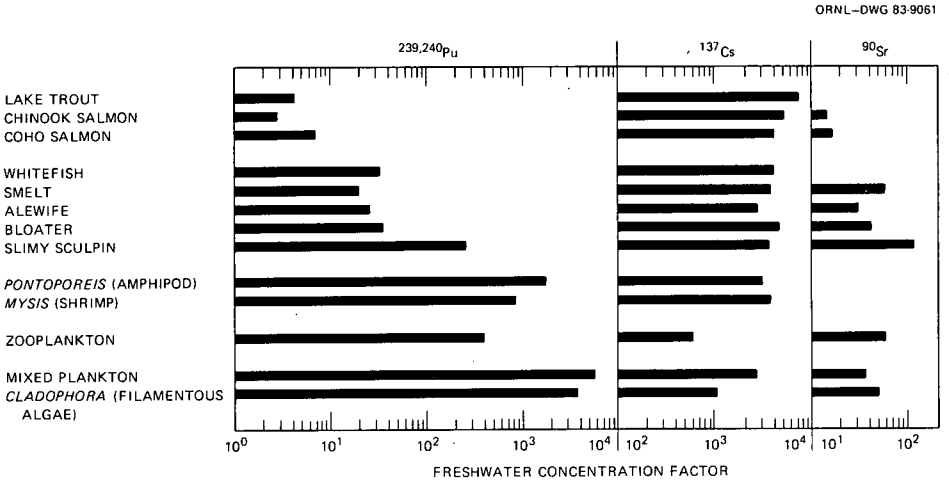

Figure 5.14. The concentration factors for $^{239-240}Pu$, ^{137}Cs, and ^{90}Sr in a freshwater ecosystem. Note the decreasing plutonium concentration factor and the increasing concentration factor for ^{137}Cs for more complex organisms (from [WAH-75]),

Table 5.46. Example of the "trophic level effect" for cesium in freshwater fish

Trophic level		Concentration factor[a]			Concentration[b]
		$CF^{137}Cs$	CF K	Ratio $CF_{Cs}:CF_K$	pCi ^{137}Cs/g K
II–III	Mixed small fish	410	285	1.4	1.6
IV	Perch	750	345	2.2	3.5
V	Northern pike	3620	475	7.6	5.4

[a]Data from [GUS-69b].
[b]Data from [GUS-67].

Acidity (pH). The acidity of the water can also affect radionuclide uptake with less uptake generally occurring in more acid (lower pH) waters. Values for the uptake of cesium by the water hyacinth show that the maximum uptake appears to be at a neutral pH [JAY-81].

Summary of the effects of environmental conditions. The number of factors which affects radionuclide uptake by aquatic animals and plants accounts in part for the variability of concentration factor values found in the literature. Kolehmainen et al. [KOL-67b] made a comprehensive study of Finnish lakes

Table 5.47. Effect of water temperature on the biological half-time in fish

Fish	Age (years)	Temperature (°C)	Biological half-life for ^{22}Na (days)
Perch	1-2	20±0.2	7
		8±3	15
Roach	1-2	20±0.2	7
		8±3	11
Rainbow trout	0.5-1	20±0.2	2.2
		14±1	2.5
		7±1	7
Crusian carp		20±0.2	10
		8±3	25

Source: data from [HAN-67].

in order to determine the source of the wide variation in the cesium-137 content of fish. They found that the main factors contributing to these differences were:

1. The potassium content of water affected 10- to 100-fold differences between lakes and resulted in very high ^{137}Cs levels in the entire biota in the most oligotrophic lakes.
2. The biological half-time for cesium in the fish (the "trophic level effect") was a major factor. The biological half-life varied from 20 to 200 days at (15°C) and caused up to a 10-fold difference in cesium levels.
3. The ^{137}Cs concentration in water was a minor factor - observed concentrations varied only by factors of 2 or 3 between lakes.
4. The type of food eaten by the fish was also a minor factor resulting in only 2- to 3-fold differences.

Duke and his associates [DUK-69] studied the effect of environmental conditions upon zinc-65 uptake in shellfish. Among the conditions they varied were salinity, stable zinc concentration, acidity (pH), and temperature. The smallest effects were noted upon changing the pH from 7.5 to 8.5 and changing the stable zinc concentration (Table 5.48). Changing the pH did produce a significant increase in the concentration factor for zinc in the crab. The principal factors affecting the concentration factor were the salinity and the temperature. A rise in salinity of 10 parts per thousand (from 25 to 35 p.p.t) produced decreases in the magnitudes of the concentration factors of 14 to 24%, except for the clam. A 10°C rise in temperature from 20°C to 25°C produced increases from 6 to 53% in the value of the zinc-65 concentration factor.

Table 5.48. Effect of changes in environmental conditions upon the concentration factor for Zinc-65 in shellfish[a]

Variable	Change	Effect upon the Zinc-65 concentration factor in			
		Oyster	Clam	Scallop	Crab
Salinity	from 25 ppt	193	18	350	216
	to 35 ppt	154[c]	17[d]	300[b]	164[c]
	Δ +40%	−20%	–	−14%	−24%
Zinc (Zn^{+2})	from 15 μg/L	146	22	282	216
	to 30 μg/L	125[b]	18[c]	231[c]	199[d]
	Δ +100%	−14%	−18%	−18%	−7.9%
pH	from 7.5	130	19	243	177
	to 8.5	144[d]	20[d]	269[d]	243[c]
	Δ factor of 10	+11%	–	+11%	+37%
Temperature	from 20°C	139	16	317	166
	to 25°C	213[c]	18[b]	338[d]	213
	Δ +25%	+53%	+12.5%	–	28%

[a]Data from [DUK-69].
[b]Statistically significant difference at the five percent confidence level.
[c]Statistically significant difference at the one percent confidence level.
[d]Not significantly different.

5.3.3.3 Problems Associated with the Use of Concentration Factors

The application of the pathway approach using a water-to-organism concentration factor is limited by the pertinency of the concentration factors taken from the literature to the actual site conditions. Concentration factors may represent measurements taken at only one point in time and of only a limited population [HAR-67]. One of the most difficult areas associated with measurements of concentration factors either in the laboratory or in the environment is to ensure that the organism is in equilibrium with the radionuclide concentration in water.

Laboratory measurements in aquaria generally involve initially labelling only the water. This will be adequate only for organisms which get their food directly from water, the primary producers [HAR-67]. Organisms higher in the food chain may be consuming food in which the radionuclide concentration is not in equilibrium with the water [HAR-67]. An example of such a case would be bottom-feeding fish which fed on organisms for which the principal source of radioactive materials is the sediment rather than water. Environmental measurements may avoid problems with non-uniform labelling but the conditions cannot be controlled nor can equilibrium be ensured since samples and concentration measurements may be made only at certain times and locations.

One approach to avoid some of these drawbacks is to rely upon measurements of stable element concentration in water and in the organism of interest. Although this does not ensure that equilibrium conditions exist, the organism is more likely to be in equilibrium with stable elements, if their concentration does not fluctuate greatly with time, than with radionuclides newly introduced into the system. Concentration factors based upon measuring analoguous stable elements in the environment offer another advantage in that site-specific concentration factors may be obtained from such measurements prior to plant construction. The use of stable element concentrations is also involved in an alternative approach to the use of concentration factors, the specific activity approach, which is discussed in the following section.

5.3.4 The Specific Activity Approach

The **specific activity** is the activity of a radionuclide per unit mass of the element.* The specific activity has units of activity per mass (e.g., pCi $^{90}Sr/g$ Sr or Bq $^{55}Fe/kg$ Fe). With few exceptions, the mass of the radioisotope is usually negligible compared to the mass of the stable isotope and can be neglected. If the annual limit on intake is known for a particular radionuclide, ALI,† and the annual intake of the analogous stable element I_i is also known, then the **limiting specific activity,** LSA, is given by:

$$LSA = \frac{(ALI)}{I_i} . \tag{5.104}$$

This represents the highest specific activity of the element in food, water or air. The use of the specific activity approach was proposed by the National Academy of Sciences [NAS-62] for dealing with the disposal of radioactive waste in marine waters. The specific activity approach was used for hazard assessments of the potential use of nuclear explosives to dig a trans-Panamanian Canal [LOW-69].

*The term specific activity has been used as activity per mass or volume in the same way as concentration (e.g. pCi/ml). This is confusing and the term concentration is preferred by this author for this purpose. The term for the limiting activity of a pure carrier-free radionuclide is the *intrinsic specific activity,* ISA, which is given by ISA = $\lambda N_a/A$ where N_a is Avogadro's number, 6.023×10^{23}, and A is the gram atomic mass.

†See ICRP Publication 30 for tables of annual limits on intake for Occupational Exposure, limits for other populations may be derived from these. International Commission of Radiological Protection, "Limits for Intakes of Radionuclides by Workers," *Annals of the ICRP* (3/4) (1978).

If X^* is the activity of the radioactive isotope and X_s is the mass of the stable isotope, then the specific activity can be written as:

$$SA = \frac{X^*}{X_m^* + X_s} \simeq \frac{X^*}{X_s} \tag{5.105}$$

where X_m^* the mass of the radioisotope is assumed to be negligible. In the specific activity approach for calculating doses, it is assumed that the specific activity in the organism is the same as its environment:

$$(SA)_{org.} = (SA)_{water} \tag{5.106}$$

so that

$$\frac{X^*_{org}}{X_{s\ org}} = \frac{X^*_{water}}{X_{s\ water}} \quad \text{or} \quad \frac{X^*_{org}}{X^*_{water}} = \frac{X_{s\ org}}{X_{s\ water}} . \tag{5.107}$$

This last expression is equivalent to assuming that the radionuclide concentration factor is equal to the stable element concentration factor since X_{org}/X_{water} is by definition, the concentration factor (Equation 5.92).

Example 5.7: The specific activity of ^{65}Zn in edible mussels near the mouth of a river was measured over a two-year period. The observed specific activities were [SEY-73]:

Date of measurement	Days elapsed	Specific activity μCi ^{65}Zn/g Zn
14 June	0	0.071
14 July	30	0.068
18 Sept	96	0.050
30 Nov	169	0.029
30 Dec	199	0.030
18 Feb	249	0.026
14 April	304	0.011
30 May	350	0.010

Assuming that the daily intake of zinc by man is 13 milligrams* and the whole body dose factor for ^{65}Zn is 6.96E-06 mrem/pCi ^{65}Zn [NRC-77], calculate the total radiation dose commitment from eating the mussels.

Solution: Assume that the zinc-65 specific activity of the mussels can be depicted by a single exponential function:

$$SP(t) = (SP_o) \exp[-\lambda_e t]$$

where λ_e is an effective removal constant combining biological elimination rate constant and the radioactive decay disintegration constant.

This equation can be converted to a linear form by taking logarithms of both sides:

$$\ln[SP(t)] = \ln[SP_o] - \lambda_e t$$

$$= b + mx \ .$$

This expression can then be fitted to the data by the least squares technique.† The results of this operation are:

$$\begin{aligned} \text{correlation coefficient } r &= 0.974 \\ \text{y-intercept} &= -2.510 = \ln [SP_o] \text{ so} \\ SP_o &= \text{antilog } [-2.510] = 0.0813 \ \mu\text{Ci/g Zn} \\ \text{slope} &= -0.00577 = \lambda_e \ . \end{aligned}$$

Therefore the zinc specific activity in the mussels can be depicted by:

$$SP(t) = (0.0813 \ \mu\text{Ci/gZn}) e^{-0.00577t} \ .$$

*This assumption implies that all dietary zinc comes from shellfish consumption which is clearly conservative. The average stable zinc content of mussel flesh is 310 micrograms so that a 13 mg intake requires about 42 grams (dry mass) or 215 grams (fresh mass) per day of mussel be consumed. The annual intake would be 78.5 kilograms.

†See any text on statistical regression analysis.

The integral of this equation gives the total amount of zinc-65 in the mussels. The total dose commitment is therefore:

$$\int_o^\infty \mathrm{SP(t)dt} = \frac{\mathrm{SP_o}}{\lambda_e} = \frac{0.0813\,\mu Ci^{65}Zn/gZn}{0.00577\,\mathrm{day}^{-1}}$$

$$= 14\ \mu\mathrm{Ci-days\ per\ gram\ of\ zinc}\ .$$

The total dose commitment is then given by the total zinc-65 content per gram of zinc multiplied by the daily zinc intake and the dose factor:

$$(14\ \mu\mathrm{Ci\text{-}days})/(\mathrm{gZn}) \times (13 \times 10^{-3}\mathrm{g/Zn\ day}) \times$$
$$(6.96 \times 10^{-6}\,\mathrm{mrem/pCi}\ ^{65}\mathrm{Zn}) \times (10^6\mathrm{pCi}/\mu\mathrm{Ci}).$$
$$= 1.3\ \mathrm{mrem}\ (1.27).$$

A more realistic assumption for the shellfish intake would give correspondingly lower doses. For example, an annual intake of 2.5 kilograms per year (6.8 grams per day fresh mass) would give a dose commitment of only 0.04 mrem. [End of example]

Kaye and Nelson [KAY-68] have set forth some conditions for the use of the specific activity model. These conditions are that:

(1) Stable and radioactive atoms of the element are completely mixed and behave similarly,
(2) The biological half-time is known,
(3) The organisms are in equilibrium with their environment,
(4) The concentrations of the stable element are known,
(5) The rates of growth of the organism are known, and
(6) The rates of input of radioactive atoms are constant.

In comparison with the concentration factor method it should be noted that assumptions (1), (3), and (6) are common to both methods. Assumption (4), while required for the specific activity approach, is not always needed in the concentration factor approach. Assumptions (2) and (5) are not needed explicitly for the concentration factor method but are implicitly considered because of the inverse relationship between the concentration factor and the effective elimination rate constants.

The first of these conditions is the one which is most unlikely to be satisfied except in the very long term. There may be a considerable difference between the physio-chemical form of a radioisotope and the chemical species

present in existing stable element pools. Many of these stable elements exist in the sediments and have only a slow turnover. Differences in physio-chemical form can result in the radionuclide being more biologically available if the stable element is complexed or adsorped on particulates. In this case the specific activity of the element in the organism will be considerably higher than the specific activity in water. An example of this effect is shown in Table 5.49.

The third condition of Kaye and Nelson, that the organism be in equilibrium with its environment, is capable of being confirmed by the measurements of specific activity themselves. This is illustrated by the data in Tables 5.50 and 5.51. Table 5.50 reflects data from a longstanding contaminated lake. As evidenced by the specific activity of the strontium in the components of the system equilibrium appears to be attained. This is not the case by the data in Table 5.51 for zinc in an estuary. The low ratio of the specific activities of the organisms compared to water indicates that equilibrium has not reached in this system. This is also indicated by the low specific activity of the zinc-65 in the fish. A possible reason for this disequilibrium is that ^{65}Zn accumulation from seawater by biota is much slower than from fresh water [CRO-69].

The specific activity in water and in the organism will reflect the degree of equilibrium attained. The rate of accumulation in the fish will be related to the metabolic turnover (biological half-life) of the fish. The concentration in the fish organs will be related to the availability and exchangability of the isotopic stable element in the fish. If the specific activities in the fish and the water are the same then it can be assumed that a reasonable degree of equilibrium has been obtained. It is only after the specific activity of the stable ele-

Table 5.49. Ratio of the specific activity in the organism (SA_o) to the specific activity in water (SA_w) showing the effect of differences in biological availability on specific activity ratios

Organism	Nuclide		
	$^{137}Cs(O)^a$	$^{65}Zn(-20)^a$	$^{60}Co(-40)^a$
Silver salmon (liver)	0.67	>4400	80
	1.33	(3800–5000)	(0–120)
Cololabis saira (saury)	~1.5	>100	~100
Diaphus theta	~1.	>340	40
Lampanyctus ritteri	0.5	>60	~40
Sergestes sirpilis		>300	100
Tactostoma macropus		>20	~70

[a]Number in parentheses is the percentage particulate in seawater.

[b]Source: From [PET-71] based upon data from [ROB-68], [RAN-68], and [PER-68] (chemical form).

Table 5.50. The specific activity of strontium-90 in a freshwater lake

Organism	Specific activity ($dpm^{90}SR/\mu g$ SR)	Ratio of specific activity in organism to specific activity in water
Water	38–47 (42.5)	1.0
Plants		
Brasenia schreberi	29	0.68
Pontederia cordata	31	0.73
Typha angustifolia	48	1.13
Nuphar variegatum	40	0.94
Fish (bone) $O.R._{bone/food}$		
Perch 0.44, 0.62	52	1.22
Bullhead 0.56	48	1.13
Carp 0.44		
Average		0.97

[a]Source: data from [OPH-69].

Table 5.51. The specific activity of zinc in an estuarine ecosystem

Component	Stable Zinc content (g Zn/g)	Radiozinc content $\mu Ci\ ^{65}Zn/g$	Specific activity (SA_o) $\mu Ci\ ^{65}Zn/gZn$	Ratio of SA_o/SA_w
Sediments	1.1E–05	2.1E–03	190	0.21
Water	2.2E–08	2.0E–05	910 (SA_w)	1.0
Clams	6.6E–06	2.1E–03	360	0.40
Oysters	5.8E–05	2.0E–02	340	0.37
Crabs	2.7E–05	6.7E–03	240	0.26
Fish	4.8E–03	8.2E–04	19	0.02
Average (biota)				0.26

Source: data from [BAP-63].

ment in the water has remained essentially constant that such an equilibrium can be reached [OPH-65].

A further example of disequilibrium, involving a long-lived radionuclide, is shown in Table 5.52. These measurements indicate a specific activity in the fish which is almost 700 times that of the water and 200 times that of the sediment. Unlike the example shown in Table 5.49, there is no reason to assume that a difference in chemical species exists. The apparent "enrichment" of the radionuclide with higher trophic levels becomes less surprising if one considers

that in the preceding year the specific activity in water was 0.26 μCi ^{129}I/g ^{127}I and four years previously it was 0.53 μCi/g ^{127}I [MAG-72]. It can be seen that the higher specific activities of the higher organisms reflect slower turn over rates (longer biological half-times) and the higher specific activities at prior times. The slow biological turnover has kept the organisms from reaching equilibrium with the lower specific activity shown for water in Table 5.52.

Table 5.52. The specific activity of iodine in the components of a small creek[a]

Media	Specific activity (μCi ^{128}I/g ^{127}I)	Ratio of specific activity to specific activity of	
		Water	Sediment
Water	2.6×10^{-4}	1.0	
Sediment	8.5×10^{-4}	3.3	1.0
Filamentous green algae	5.3×10^{-4}	2.0	0.62
Watercress	1.2×10^{-3}	4.6	1.4
Crayfish	6.2×10^{-2}	238	72.9
Fish	1.8×10^{-1}	692	212

[a]Buttermilk Creek on the site of the NFS Spent Fuel Reprocessing Plant in West Valley, New York.
Source: data from [RIC-74].

5.4 FACTORS MODIFYING DIETARY INTAKE OF RADIONUCLIDES

5.4.1 Accumulation and Delay Times

The previous sections have presented time-dependent models of radionuclide accumulation but have not specified the period of accumulation. In most cases, periods such as the length of the growing season are site-dependent. Nevertheless, it is useful to know the approximate magnitude of such time periods. Table 5.53 provides a set of assumed and measured values for the length of the accumulation period. The times for radionuclide accumulation in soil and sediments were taken to be the midpoint* of an assumed 30-year operating lifetime for a reactor. The end point of the operating lifetime could also be used as a period for evaluation.

*This is *not* equivalent to the radionuclide buildup reaching 50% of its equilibrium value. The accumulation of cobalt-60 ($T_{1/2}$ = 5.3 yrs), for example, would be 86.1% of the equilibrium level at 15 years while cesium-137 ($T_{1/2}$ = 30 years) would be only 29%.

Table 5.53. Assumed time intervals for the assimilation of radionuclides in food chain pathways

Pathway	Time period over which buildup is assumed to occur	Reference
Accumulation in soil	15 years[a]	[NRC-77]
Accumulation in sediment	15 years[a]	
Growing period of forage	30 days	[NRC-77]
Growing period of food crops	60 days	[NRC-77]
Typical periods from planting to harvest		
Barley	120 days	[ROM-57]
Beans, green	60 days	[ROM-57]
Carrots	75 days	[ROM-57]
Radishes	45 days	[ROM-57]
Lettuce	80 days	[ROM-57]
	35 days	[DEL-71]
Tomatoes	85 days	[DEL-71]
Apples (from beginning of season on a mature tree)	85 days	[DEL-71]

[a]This is assumed to be the midpoint of a 30–year nuclear power reactor operating lifetime.

The length of the growing season is used for evaluating the direct (wet and dry) deposition on to vegetation. It can also be used to determine to evaluate uptake from the soil *providing that a kinetic model of soil-plant transfer is used.* In most cases, the soil-to-plant concentration ratio, CR, is evaluated for the edible portion of the crop at the time of harvest. Hence, this parameter already includes the effect of plant accumulation. Only radionuclide buildup (usually multi-year) in the soil need be considered.

The models given previously in this chapter do not take into account any decay between food production and food consumption. Except for the hypothetical maximum receptor who consumes all his/her food from a garden plot with an associated family cow, actual situations include several periods of delay in the movement of food from producer to a more distant consumer. Some of these delays are specific to a given site and food distribution system. Some of these delay periods which are assumed by the Nuclear Regulatory Commission staff for licensing evaluations are given in Table 5.54. These times can then be used to calculate appropriate decay factors (DF = exp-λt) for short-lived radionuclides.

5.4.2 Losses During Food Preparation

In addition to losses from radioactive decay, the radionuclide content of food will usually be lower than the food crop due to losses during food preparation and cooking. These processes include rinsing and washing, peeling,

Table 5.54. Assumed distribution times between food production and consumption

Pathway	Distribution transport time between food production and consumption (days)	
	Maximally exposed individual	Member of the general population
Leafy vegetables	1	14
Other produce	6	14
Forage (ingestion by milch animal)		
fresh forage	0	0
stored feed	90	90
Milk	2	4
Meat (slaughter to consumption)	20	20
Drinking water (extraction from water source tap)	0.5	1
Fish and shellfish	1.0	10 commercial 7 sport

Source: [NRC-77].

cleaning, trimming, boiling, baking, roasting, broiling, and frying. The loss of activity is specific to the process and individual techniques so that it is difficult to generalize. Table 5.55 presents some data on the loss of iodine-131 from various crops as a result of rinsing and boiling. The efficiency of rinsing as a removal mechanism decreases with the time elapsed between the surface application of the radionuclide and rinsing. The percentage removal of this surface contamination is high. Lower results were found by Nakamura and Ohmond [NAK-80b], who found that the loss of iodine from spinach due to cooking was 33% when elemental iodine (I_2) was used and 58% when methyl iodide was used.

Thompson [THO-65] noted that underground crops (carrots, onion, potatoes) had higher contamination levels (1.02–1.87 pCi ^{90}Sr/g Ca) than aboveground crops (tomato, cabbage, green bean) (~ 0.43 pCi ^{90}Sr/g Ca). The fraction removed in food preparation ranged between 19 and 55%. Cereals have a high ^{90}Sr/Ca ratio. However, milled flour is lower than unmilled grain. The strontium concentrates in the husks [MID-65]. Table 5.56 presents estimates of losses due to peeling and hulling during food preparation.

Losses of radionuclides from meat, poultry, and fish due to preparation would be expected to be small sine the radionuclide concentration is evaluated separately for the edible portion (muscle) and usually omits organs or tissues like the GI tract which are removed in preparation. Neither cesium-137 nor potassium were lost from cooked tuna, for example [YOU-79]. There are obvious weight reductions due to trimming and boning. However, these mea-

Table 5.55. Removal of Iodine-131 from the surface of vegetables by rinsing and boiling

Vegetable	Percentage of activity removed by		
	Rinsing (15 minute delay)[a]	Rinsing (20 hour delay)[a]	Boiling (15 minute delay)[a]
Green beans	67 (46–90)	33 (32–36)	77 (65–96)
Tomatoes	77 (54–95)	51 (47–56)	85 (51–92)
Leaf lettuce	81 (65–93)	34 (26–49)	
Celery	47 (43–55)	34 (32–37)	77 (72–86)
Cauliflower	70 (48–87)	64 (60–69)	88 (85–90)
Peppers	56 (53–59)		66 (66–68)

[a]Time interval between spraying with the radioactive tracer and the application of the removal treatment method. Numbers in parens represent range of values observed.

Source: data from [THO-73].

sures do not affect the radionuclide concentration. Reductions due to trimming of meat, etc., are not usually factored into dietary intake reductions because the annual intakes are based upon prepared weights and include these reductions.

5.5 PROBLEMS

1. Classify the following exposure pathways as: transitory, integrating, or cumulative integrating pathways: by marking them with a T, I, or CI.
   a. Radionuclide uptake by crops from soil.
   b. External dose rate from deposited particulates.
   c. External dose rate from argon-41 (half-life 1.8 hours).
   d. Global airborne concentration of Krypton-85.
   e. Radionuclide concentration in a fish in a rapidly flowing stream.
   f. Radionuclide concentration in a fish in a small cooling pond.
   g. Radionuclide concentration in a public water supply.
   h. Radionuclide concentration in soil from irrigation with contaminated water.

Table 5.56. Reduction of radionuclide contamination of food crops by peeling and shelling

Radionuclide	Crop	Percentage reduction of activity	Retention modifying factor[a]	Reference
^{54}Mn	Potato	(11.6)[b]	(0.88)[b]	[STE-80b]
^{60}Co	Potato	(30.0)	(0.70)	[STE-80b]
^{90}Sr	Carrot	14.8	(0.85)	[SAR-66]
	Tomato	14.7	(0.85)	[SAR-66]
^{90}Sr	Potato	(5.9 ± 2.7)	(0.94 ± 0.3)	[ROM-60]
		(41.8)	(0.58)	[STE-80b]
^{95}Zr,	Carrot	88.2	(0.12)	[SAR-66]
^{95}Nb	Tomato	42.9	(0.57)	[SAR-66]
^{106}Ru	Carrot	84.7	(0.15)	[SAR-66]
	Tomato	23.8	(0.76)	[SAR-66]
^{137}Cs	Carrot	46.0	(0.54)	[SAR-66]
	Tomato	3.6	(0.96)	[SAR-66]
	Potato	(6)	(0.94)	[STE-80b]
^{144}Ce	Carrot	84.1	(0.16)	[SAR-66]
	Tomato	38.8	(0.61)	[SAR-66]
^{239}Pu,^{240}Pu	Beet	(98.7)	(0.013)	[ADR-80b]
	Potato	(92.5)	(0.075	[ADR-80b]
	Bushbean (shelled)	(54.7)	(0.45)	[ADR-80b]
	Soybean (shelled)	(30.0)	(0.70)	[ADR-80b]

[a]Includes the percentage lost in food preparation (i.e., the conversion of kilograms fresh to kilograms processed). These conversions are [WAT-63]: beans (0.40), beets (0.70), carrots (0.82), potatoes (0.81), soybeans (0.53), and tomatoes (0.88).

[b]Values in parentheses were calculated by this author from data in the reference.

Answer: a. CI, b. I, c. T, d. I, e. I, f. CI, g. T or I, h. I.

2. List at least four examples of exposure pathways that involve more than one type of ecosystem.

Answer:

1. Use of river water to irrigate crops.
2. Transport of contaminated soils into rivers, estuaries, and deposition in the ocean.
3. Use of sea shells as a source of calcium for agriculture.
4. Use of fish to make dietary supplements for livestock.
5. Use of river water for drinking water by livestock.
6. Use of manure to provide nutrients for aquaculture.
7. Use of sea water to produce table salt.

3. (a) Calculate the ratio of wet deposition to dry deposition *rates* for the following conditions:

$$\begin{aligned} v_g &= 0.01 \text{ m/sec} \\ R &= 10 \text{ mm/hr} = 2.78 \times 10^{-6} \text{m/sec} \\ W_v &= 5 \times 10^{-5} \\ m &= 0.030 \text{ hr/mm} \end{aligned}$$

Answer: 97.3

(b) Calculate the equilibrium deposition per unit air concentration for continuous deposition under the above conditions with $\lambda = 0.086$ days^{-1}, $k = 0.025$ mm^{-1} and r (dry removal only) $= 0.05$ days^{-1}. *Warning*: Use dimensional analysis to ensure that units are consistent.

Answer: 0.160.

4. (a) The ^{90}Sr-to-Ca ratio in the total diet follows the relationship:

$$P_{23}\left[\frac{^{90}\text{Sr(pCi·yr)}}{\text{g Ca}}\right] = 0.90\ d_i + 0.54\ d_{i-1} + 0.36 \sum_{m=1}^{\infty} d_{i-m} \exp[-0.10m] ,$$

where d_i is the deposition (mCi/km^2) in the current year i, d_{i-1} is the deposition in the preceding year, and d_{i-m} is the deposition m years prior to the year of interest. Given a continuous average annual release of 0.3 millicuries per year of ^{90}Sr from a BWR for 30 years, calculate the expected average ^{90}Sr-to-Ca ratio in the diet in the 30th year, assuming that 50% of the strontium is deposited within an 80 km radius of the facility. *Note*: The sum term can be reduced to geometric series:

$$\sum_{m=1}^{n} r^m = \sum_{m=o}^{n} (r^m) - 1 = \frac{(1-r^n)}{1-r} - 1 ,$$

with $r = e^{-0.10}$.

Answer: 3.46×10^{-5} pCi ^{90}Sr/g Ca.

(b) If the observed ratio of bone to diet is 0.15 and the dose rate to the bone marrow is 1.4 mrem/yr per pCi/g Ca, in bone, what is the average dose rate to bone marrow in the 30th year?

Answer: 7.26 μrem/year.

5. The annual average air concentration of plutonium-239 ($T_{½}$ = 24,400 years) near a spent fuel reprocessing plant is 100 aCi/m^3 (10^{-16}Ci/m^3).

   a. Given a mean total (soil + plant) deposition velocity of 5.6×10^{-3} m/sec, and an effective half-time on vegetation of 14 days, calculate

the areal/concentration on soil and on vegetation after 1 year, assuming that the vegetation retains 50% of the deposited material. (Assume no loss from the soil and no contribution from vegetation losses to the soil concentration.) There are 3.156×10^7 sec/year.
Solution: Dry deposition onto soil = 8.84×10^{-12} Ci/m^2 (8.84×10^6 aCi/m^2); dry deposition onto vegetation = 4.89×10^{-13} Ci/m^2 (4.89×10^5 aCi/m^2).

b. The annual rainfall is 900 mm (900 L/m^2 year) and the volumetric washout coefficient is 5×10^5 (m^3_{air}/m^3_{rain}). The fraction retained on vegetation [$e^{-mt}/(kt+\lambda) = 0.2$] is also lost with an effective half-time of 14 days. (Treat the material deposited on vegetation as dry deposition after computing the deposition rate.) Calculate the plutonium deposited on soil and vegetation from wet deposition.
Solution: Wet deposition onto soil = 3.6×10^{-11} Ci/m^2 (3.6×10^7 aCi/m^2); wet deposition onto vegetation = 4.98×10^{-13} Ci/m^2 (4.98×10^5 aCi/m^2).

c. Given that the vegetation density is 2 kg/m^2 and that the areal soil density is 240 kg/m^2, calculate separately the plutonium concentration on soil and vegetation from wet and dry deposition. (Assume uniform mixing in top 20 cm, due to tilling.)
Solution: The plutonium concentrations (Ci/kg) on vegetation and soil are as listed below.

	Soil	Plant
Dry deposition	3.682×10^{-14}	2.443×10^{-13}
Wet deposition	15.000×10^{-14}	2.488×10^{-13}
Total	18.682×10^{-14}	4.932×10^{-13}

d. The plutonium concentration ratio, CR, is 2.5×10^{-5}. Calculate the plutonium concentration in the vegetation from soil uptake. (Include the plutonium soil contributions from both wet and dry deposition.)
Solution: The uptake from the soil is 2.5×10^{-5} Ci/kg plant per Ci/kg soil times the total soil concentration of 18.68×10^{-14} or

$$(2.5 \times 10^{-5})(18.68 \times 10^{-14}) = 4.67 \times 10^{-18} \text{ Ci/kg}$$

This is about 1/100,000th of the direct deposition on the plant:

$$\frac{4.67 \times 10^{-18} Ci/kg}{4.93 \times 10^{-13} Ci/kg(direct)} = 9.5 \times 10^{-6} .$$

6. Radioiodine-131 concentration in milk resulting from continuing forage intake following a single contaminating event is given by: $c(t) = 0.0186\ I\ D_0$ (exp-0.141t - exp-0.90t) for t in days, where I is the daily forage intake (kg/day) and D_0 is the initial contamination level (activity/kilogram of vegetation).

a. Calculate the time and level (as % of initial intake) of the maximum concentration in milk.
Answer: $t_{max} = 2.42$ days; $C_{max} = 1.09$ %/L.
b. Calculate the fraction of the total dose commitment that would be delivered by stopping milk ingestion at 1 day, 2 days, 3 days, and 1 week following the initial contamination.
Answer: Total secretion (to infinity) is 11.1 %/L. The integrated secretion to 1 day is 0.51%/L or 0.046 (4.6%) of the total. The integrated secretion to 2 days is 1.52%/L or 0.136 (13.6%) of the total. The integrated secretion to 3 days is 2.62%/L or 0.236 (23.6%) of the total. The integrated secretion to 7 days is 6.2%/L or 55.8% of the total.

7. A farm with a 4-year-old child is located 1 kilometer from a nuclear power reactor. The child consumes 330 liters of fresh milk and 26 kilograms of fresh leafy vegetables per year from the family cow and family garden. Calculate the annual release limit for radioiodine-131 ($T_{½} = 8.05$ days) to conform to a design objective of 15 millirem per year thyroid dose given that:

a. The annual-average atmosphere dispersion factor is 4×10^{-6} sec/m^3.
b. The deposition velocity for radioiodine is 0.01 m/sec and the biological half-life on both forage and vegetables is 14 days.
c. The fraction of the daily iodine intake transferred to milk is 6×10^{-3} days/liter. The cow consumes 50 kg/day of grass from a field whose yield is 0.75 kg/m^2. The vegetable yield is 2 kg/m^2. The retention factor for both is 1.0.
d. The child's breathing rate may be assumed to be 2700 m^3/year and the occupancy factor is 0.5.
e. The radioiodine-131 committed dose equivalent factor for ingestion is 5.43×10^{-3} mrem/pCi; the committed dose equivalent factor for inhalation is 4.16×10^{-3} mrem/pCi (both to the thyroid gland) and the whole body dose equivalent rate from radioiodine deposited onto the ground is 2.80×10^{-9} mrem/hr per pCi/m^2.

Evaluate the doses from external radiation from deposited material, inhalation, and the ingestion of milk and leafy vegetables in arriving at the release limit.
Answers (including subcomponent calculations): The effective removal rate constant for vegetation is 5.73×10^{-7} sec^{-1}. The equilibrium deposi-

tion is 6.98×10^{-2} Ci/m^2 per Ci/sec. The doses per unit activity released are as follows:

Pathway	Dose factor (mrem/year)/ (Ci/sec)	Percentage of total
External dose rate (50% occ.)	97.7	$<10^{-6}$
Inhalation dose rate	2.25E+07	0.04
Vegetable ingestion dose	4.93E+09	9.0
Milk ingestion dose	5.0 E+10	90.9
	5.50E+10	

The limiting ^{131}I release rate is therefore: 15 millirem/year ÷ 5.50E+10 $= 2.73 \times 10^{-10}$ Ci/sec or 8.6 millicuries of iodine-131 per year.

8. (a) Assuming a one-compartment model of the secretion of radionuclides into meat, milk or eggs of the form

$$\frac{dC}{dt} = \frac{IF}{V_m} - (r + \lambda)\ C\ ,$$

where

C = radionuclide concentration,
r = biological excretion rate,
I = radionuclide intake rate,
V_m = milk volume, and
F = fraction of the stable element transferred to milk,

show that the equilibrium radionuclide concentration in these products is:

$$C\ (\text{equil}) = IF/(r + \lambda)\ V_m$$

and that the transfer factor f_m^* can be represented as:

$$f_m^* = \frac{F}{(r + \lambda)V_m}\ .$$

(b) Is the factor for the stable element (f_m) the same? If not, derive a modifying factor to apply to the stable element f_m to permit it to be used for an isotopic radionuclide.

Answer: $f_m^* = f_m/(1 + \lambda/r) = f_m \dfrac{T_{1/2}}{T_{1/2} + T_{bio}}$.

(c) What condition must be satisfied before this correction introduces a 25% change from the tabulated value?
Answer: $\lambda/r \geq 1/3$ or $T_{bio}/T_{½} \geq 1/3$.

9. (a) Assuming that the transfer factor from inhalation by a cow to milk is the same as from ingestion (f_m^*), show that the ratio of the concentration in milk from ingestion to the concentration from inhalation is:

$$\frac{v_g(UAF)}{(\lambda+r)\dot{I}_B} ,$$

where

v_g = deposition velocity,
UAF = utilized area factor,
g = radionuclide decay constant,
r = "weathering" loss rate, and
$\dot{I}_B$ = cow breathing rate (m^3/day).

(b) For $\dot{I}_B = 144$ m^3/day, $T_{½} = 8.05$ days, $T_B = 14$ days, $UAF = 45$ m^2/day, calculate the ingestion to inhalation ratio for methyl iodide (^{131}I) $v_g = 5 \times 10^{-6}$ m/sec and elemental iodine, $v_g = 0.01$ m/sec.

Answer: Ratio $\frac{C_{ingestion}}{C_{inhalation}}$ for $CH_3I = 0.995$; $I_2 = 1.99E+03$.

(c) What implications can be drawn from this calculation for accident situations? Note that over 80% of the iodine released in the Three Mile Island Accident was in the organic (methyl iodide) form.

10. The current MPC for cesium-137 corresponds to a dose of 500 millirem to the whole body and is 2×10^{-5} μCi/ml. This value is based upon a daily water intake of 2 liters. What is the whole body dose to a person consuming 50 kilograms per year of trout from a lake whose cesium concentration is at 1 percent of the maximum permissible concentration for water, if the concentration factor for cesium by trout in this lake is 1,000?
Answer: 340 mrem.

11. A radioactive spill has occurred in a bay. The radionuclide has a half-life of 280 days and a biological half-life in a fish of 350 days. The concentration factor (equilibrium conditions) is 150. However, the radionuclide was rapidly flushed out of the bay and measurable concentrations only persisted for 7 days. If the average concentration in water was 10 pCi/L, what is the concentration in the fish?
Answer: ~50 pCi/kg (46).

12. The radionuclide concentration factor for ^{106}Ru in a marine invertebrate species was 30. A fish which consumes these invertebrates as its sole food

source had a concentration factor of 1. What is the ratio of the radionuclide concentration in the fish to the radionuclide concentration in the invertebrates?

Answer: 1/30 or 0.033.

13. An exotic freshwater species of shrimp has been found at the site of your proposed reactor. The concentration factor for this species is unknown but the cesium-137 CF for a related marine species is 8. Given that the potassium concentration in the lake that receives your effluent is 3 ppm and that of seawater is 380 ppm (mg/l), estimate the concentration factor for the freshwater species.

Answer: About 1000 (1013).

14. A scallop has a manganese content of 7100 μg stable Mn/g in the kidney and 14 μg Mn/g in the muscle. The specific activity of manganese in the water is 0.014 pCi ^{54}Mn per μg of stable manganese. What is the ^{54}Mn concentration in the organs which would be reached if complete equilibrium were reached with the constant concentration in the seawater?

Answer: Kidney 99.4 pCi ^{54}Mn/g; muscle 0.2 pCi ^{54}Mn/g.

REFERENCES

AAR-75 Aarkog, A., "Radionuclide Levels in Mature Grain Related to Radiostrontium Content and Time of Direct Contamination," *Health Physics* **28**(5):557–562 (May 1975).

ABE-67 Åberg, B., and Hungate, F. P. (eds.), *Radioecological Concentration Processes* (Proc. of an International Symposium held in Stockholm, Sweden, 25–29 April 1966), Pergamon Press, Oxford (1967).

AD-75 Adams, W. H., Buchholz, J. R., Christenson, C. W., Johnson, G. L., and Fowler, E. B., *Studies of Plutonium, Americium, and Uranium in Environmental Matrices,* U.S.A.E.C. Rpt. LA-5661, Los Alamos, Scientific Laboratory (January 1975).

ADR-80a Adriano, D. C., Wallace, A., and Romney, E. M., "Uptake of Transuranic Nuclides from Soil by Plants Grown under Controlled Environmental Conditions," in [HAN-80], pp. 336–360.

ADR-80b Adriano, D. C., Corey, J. C., and Dahlman, R. C., "Plutonium Contents of Field Crops in the Southeastern United States," in [HAN-80], pp. 381–402.

AGN-67 Agnedal, P. O., "Calcium and Strontium in Swedish Waters and Fish and Accumulation of ^{90}Sr," in *Radioecological Concentration Processes* (B. Åberg and F. P. Hungate, eds.), Oxford: Pergamon Press (1967), pp. 879–895.

ALL-75 Allen, M. D., and Neff, R. D., "Measurements of Deposition Velocity of Gaseous Elemental Iodine on Water," *Health Physics* **28**(6):707–715 (June 1975).

ALT-74 Altman, P. L. and Dittmer, D. S., *Biology Data Book*, 2nd edition, Federation of American Societies for Experimental Biology, Bethesda, MD (1974), vol. III.

ANC-66 Ancellin, J., Vilquin, A., "Contaminations Experimentals d'Especes Marines par le Cerium-144, le Ruthenium-106, et le Zirconium-95," pp. 583–604 in [DIS-66].

ANC-73 Ancellin, J. Avargues, M., Bovard, P., Guegueniat, P., and Vilquin, A. "Aspects biologiques et physio-chimiques de la contamination radioactive déspeces et de sediments marins," pp. 225–241 in [MAR-73].

ANS-76 Anspaugh, L. R., Phelps, D. L., Kennedy, N. C., Shinn, J. H., and Reichman, J. M., "Experimental Studies on the Resuspension of Plutonium from Aged Sources at the Nevada Test Site," in [ES-76], pp. 727–742.

AQU-75 *Impacts of Nuclear Releases into the Aquatic Environment* (Proc. IAEA Symposium, Otaniemi, Finland, 30 June–4 July 1975), IAEA, Vienna (1975).

ATE-61a Aten, A. H. W., Jr., "Permissible Concentrations of Radionuclides in Sea Water," *Health Physics* **6**:114–125 (1961).

ATE-61b Aten, A. H. W., Jr., Dalenberg, J. W., and Bakkum, W.C.M., "Concentrations of Uranium in Fish," *Health Physics* **5**(314):225–226 (June 1961).

ATK-67 Atkins, D. H. F., Chadwick, R. C., Chamberlain, A. C., "Deposition of Radioactive Methyl Iodide to Vegetation," *Health Physics* **13**(1):91–92 (Jan. 1967).

AU-77 Au, F. H. F., Leavitt, V. D., Beckert, W. F., McFarlane, J. C., "Incorporation of Transuranics into Vegetable and Field Crops Grown at the Nevada Test Site," in *Transuranics in Desert Ecosystems*, Nevada Applied Ecology Group Report NVO-181 (November 1977), pp. 1–15.

BAP-63 Baptist, J. P., and Hoss, D. E., "Accumulation and Retention of Radionuclides by Marine Fish," pp. 14–19 in *Radiobiological Laboratory Annual Report 1963,* Bureau of Commercial Fisheries Circular 204 (1963).

BAP-70 Baptist, J. P., Hoss, D. E., and Lewis, C. W., "Retention of ^{51}Cr, ^{59}Fe, ^{60}Co, ^{65}Zn, ^{85}Sr, ^{95}Nb, ^{141m}In and ^{131}I by the Atlantic Croaker (*Micropagon undulatus*)," *Health Physics* **18**(2):141–148 (Feb. 1970).

BAR-61 Barbier, G., *Absorption de Radioelements du Sol Par Divers Legumes Cultives dans les Conditions de la Pratique,* French Atomic Energy Commission Rpt. CEA-1860 (1961).

BAR-63 Barry, P. J., and Chamberlain, A. C., "Deposition of Iodine onto Plant Leaves from Air," *Health Physics* **9**(12):1149–1154 (December 1963).

BEL-79 Belot, Y., Gauther, D., Camus, H., and Caput, C., "Prediction of the Flux of Tritiated Water from Air to Plant Leaves," *Health Physics* **37**(4):575–583 (October 1979).

BEN-66 Beninson, D., Van Der Elst, E., and Cancio, D., "Biological Aspects in the Disposal of Fission Products in Surface Waters," in [DIS-66], pp. 337–354.

BER-67 Bergström, S. O. W., "Transport of Fallout ^{131}I into Milk," in [ABE-67], pp. 159–173.

BHA-80 Bhat, I. S., Verma, P. C., Iyer, R. S., and Chandramouli, S. P., "Fate of Major Radionuclides in the Liquid Waste Released to Coastal Water," pp. 299–302 in vol. 3 [IRP-80].

BIO-79 *Biological Implications of Radionuclides Released from Nuclear Industries* (Proceedings IAEA Symposium, Vienna, Austria, 26–30 March 1979), IAEA, Vienna (1979), vol. II.

BIT-72 Bittel, R., Merlini, M., Beque, H., Berg, A., Myttenaere, C., Ravera, O., Verot, J. L., and Van Der Borght, O., "Etude du Transfer a L'homme par ses Aliments, des Radio-isotopes du Ruthenium, du Cobalt et du Zinc Rejects dan les Eaux Continentales," in [RAD-72], vol. II, pp. 869–890.

BLA-81 Blaylock, B. G., and Frank, M. L., "Bioaccumulation and Distribution of ^{95m}Tc in an Experimental Freshwater Pond," pp. 451–464 in [ENV-81].

BON-80 Bondietti, E. A., and Tamura, T., "Physiochemical Associations of Plutonium and Other Actinides in Soils," in [HAN-80], pp. 145–164.

BOO-58 Booker, D. V., "Physical Measurements of Activity in Samples from Windscale," United Kingdom Atomic Energy Research Establishment Rpt. AERE HP/R 2607 (1958).

BOR-72 DeBortoli, M., and Gaglione, P., "Radium-226 in Environmental Materials and Food," *Health Physics* **22**(1):43–48 (Jan. 1972).

BOR-74 DeBortoli, M., and Gaglione, P., "Variability of the Washout Ratio for Some Fallout Radionuclides," in *Physical Behavior of Radioactive Contaminants in the Atmosphere* (Proc. IAEA-WMO Symposium, Vienna, Austria, 12–16 November 1973), IAEA, Vienna (1974), pp. 167–179.

BOU-69 Bovard et al. 1969. "Estimation de la contamination de la ration alimentaire. Etude du transfert du césium et du strontium à travers la plante jusqúau produit consommable données experimentales," in [ENV-69], pp. 113–124.

BRA-80 Branagan et al. 1980. *Staff Review of Radioecological Assessment of the Wyhl Nuclear Power Plant,* U. S. NRC Report NUREG-0668 (June 1980).

BRE-81 Brenk, H. D., and Vogt, K. J., "The Calculation of Wet Deposition from Radioactive Plumes," *Nuclear Safety* **22**(3):362–371 (May–June 1981).

BRO-78 Brown, K. W., and McFarlane, J. C., "Plutonium Uptake by Plants Grown in Soil Containing Plutonium-238 Dioxide Particles," *Health Physics* **35**(3):481–485 (September 1978).

BRY-66 Bryan, G. W., Preston, A., and Templeton, W. L., "Accumulation of Radionuclides by Aquatic Organisms of Economic Importance in the United Kingdom," pp. 623–635 in [DIS-66].

BU-66 Bunch, D. F., *Controlled Environmental Radioiodine Tests—Progress Report Number Two,* U.S.A.E.C. Rpt. IDO-12053 (August 1966).

BU-68 Bunch, D. F., *Controlled Environmental Radioiodine Tests: Progress Report No. 3,* U.S.A.E.C, Rpt. IDO-12063 (January 1968).

BUN-65 Bunch, D. F., Markee, E. H., Jr., and Jessen, D. K., "Investigation of the Ruthenium Released to the Atmosphere from Operation of the Idaho Chemical Processing Plant Waste Calcination Facilities" (abstract), *Health Physics* **11**(8):823 (August 1965).

BUR-66 Burman, F. J., Fries, G. F., Anderson, M. J., and Stoddart, G. E. 1966. *J. Dairy Sci.* **49**:1219.

BUS-63 Bustard, L. K., Wood, D. H., Elefson, E. E., Ragan, H. A., and McClellan, R. O. 1963. "I^{131} in Milk and Thyroid of Dairy Cattle Following a Single Contamination Event and Prolonged Daily Administration," *Health Physics* **9**(12):1231–1234 (December 1963).

CAL-60 Caldecott, R. S., and Snyder, L. A. (eds.), *Radioisotopes in the Biosphere* (Proc. Symposium Univ. of Minnesota, 10–23 October 1959), University of Minnesota, Minneapolis, Minn. (1960).

CAN-73 Cancio, D., Llavro, J. A., Ciallella, N. R., and Beninson, D. J., "Incorporation of Radiostrontium by Marine Organisms," pp. 347–356 in [MAR-73].

CAT-76 Cataldo, D. A., Klepper, E. L., and Craig, D. K., "Fate of Plutonium Intercepted by Leaf Surfaces: Leachability and Translocation to Seed and Root Tissues," in [TRU-76], pp. 291–299.

CAT-78 Cataldo, D. A., Wildung, R. E., "Soil and Plant Factors Influencing the Accumulation of Heavy Metals by Plants," *Env. Health Perspectives* **27**:149–159 (December 1978).

CAT-80 Cataldo, D. A., and Vaughan, R. E., "Interaction of Airborne Plutonium with Plant Foliage," in [HAN-80], pp. 288–299.

CHA-60a Chamberlain, A. C., "Aspects of the Deposition of Radioactive and Other Gases and Particles," *Int. J. Air Pollution* **3**:63–88 (1960).

CHA-60b Chamberlain, A. C., Eggleton, A. E. J., Megan, W. J., and Morris, J. B., "Behavior of Iodine Vapor in Air," *Disc. Faraday Soc.* **30**:162–169 (1960).

CHA-70 Chamberlain, A. C., "Interception and Retention of Radioactive Aerosols by Vegetation," *Atmospheric Environment* **4**:57–63 (1970).

CHA-76 Champlin, J. B. F., and Eichholz, G. G., "Fixation and Remobilization of Trace Contaminants in Simulated Subsurface Aquifers," *Health Physics* **30**(2):215–219 (Feb. 1976).

CHI-66a Chipman, W. A., "Uptake and Accumulation of Chromium-51 by the Clam *Tapes decussatus*, in Relation to Physical and Chemical Form," in [DIS-66], pp. 571–582.

CHI-66 Chipman, W. A., "Food Chains in the Sea," Chapter 19 (pp. 421–453) in *Radioactivity in Human Diet* (R. S. Russell, ed.), Pergamon Press, Oxford (1966).

CLI-76 Cline, J. F., and Klepper, B., "Uptake of ^{129}I by Forage Crops," in [VAU-76], p. 178.

COM-57 Comar, C. L., Russell, R. S., and Wasserman, R. H., "Strontium-Calcium Movement from Soil to Man," *Science* **126**:485–492 (1957).

COS-66 Cosolito, F., Bath, D. W., Peterson, H. T., and Cohen, N. 1966. "Radiological Studies," Chapter 4 in *Ecological Survey of the Hudson River*, Report on PHS Contract PH-86-65 Neg. 141 (M. Eisenbud Project Director), December 20, 1966.

COW-66 Cowser, R. E., Snyder, W. S., McCammon, C. P., Straub, C. P., Kochtitzky, O. W., Hervin, R. L., Struxness, E. G., and Morton, R. J., "Evaluation of Radiation Dose to Man from Radionuclides Released to the Clinch River," pp. 639–669 in [DIS-66].

CRO-69 Cross, F. A., Dean, J. M., and Osterberg, C. L., "The Effect of Temperature Sediment, and Feeding on the Behavior of Four Radionuclides in a Marine Benthic Amphipod," pp. 450–460 in [NEL-69b].

CUM-69 Cummings, S. L., Bankert, L., Garrett, Jr., A. R., and Regnier, J. E., "^{137}Cs Uptake by Oat Plants as Related to the Soil Fixing Capacity," *Health Physics* **17**(1):145–148 (July 1969).

CUM-71 Cummings, S. L., and Bankert, L., "The Uptake of Cerium-144, Promethium-147 and Plutonium-238 by Oat Plants from Soils," *Radiological Health Data and Reports* **12**(2):83–85 (February 1971).

CUS-66 Cushing, C. E., and Watson, D. G., "Accumulation and Transport of Radionuclides by Columbia River Biota," pp. 551–570 in [DIS-66].

DAH-69 Dahlman, R. C., Auerbach, S. I., and Dunaway, P. B., "Behavior of ^{137}Cs-Tagged Particles in a Fescue Meadow," in [ENV-69], pp. 153–165.

DAH-76 Dahlman, R. C., Bondietti, E. A., and Eyman, L. D., "Biological Pathways and Chemical Behavior of Plutonium and Other Actinides in the Environment," in [FRI-76], pp. 47–80.

DAV-58a Davis, J. J., and Foster, R. F., "Bioaccumulation of Radioisotopes Through Aquatic Food Chains," *Ecology* **39**(3):530–535 (1958).

DAV-58b Davis, J. J., Perkins, R. W., Palmer, R. F., Hanson, W. C., and Cline, J. F. 1958. "Radioactive Materials in Aquatic and Terrestrial Organisms Exposed to Reactor Effluent Water," pp. 423–428 in Vol. 18, *Waste Treatment and Environmental Aspects of Atomic Energy,* of *Proceedings of the Second United Nations International Conference on the Peaceful Uses of Atomic Energy*, Geneva, the United Nations.

DAV-73 Davy, D. R., Giles, M. S., and Conway, N., "Pre-operational Assessment of the Discharge Limits and Relative Importance of Radioactive and Other Wastes from Uranium Production in Australia's Northern Territory," in [ENV-73], pp. 37–54.

DED-70 Dedolph, R., Ter Harr, G., Holtzman, R., and Lucas, H., Jr., "Sources of Lead in Perennial Rye Grass and Radishes," *Env. Sci. Technol.* **4**(3):217–225 (March 1979).

DEL-71 Delmas, J., Bouvard, P., Granby, A., Disdier, R., "Radio-contamination expérimentale de quelques espèces cultivées à l'aide d'effluents d'origines diverses," pp. 1103–1119 in *Radioecology Applied to the Protection of Man and His Environment* (Proc. CEC Symposium Rome 1971, Commission of the European Communities, Luxembourg) (1972).

DEL-73 Delmas, J., Granby, A., and Disdier, R., "Etudes Experimentales sur le Transfer dans les Cultures de Quelques Radionucleides Presents dans les Effluent des Centrales Electro-nucleaires," in [ENV-73], pp. 321–331.

DIS-66 *Disposal of Radioactive Wastes into Seas, Oceans and Surface Waters* (Proc. IAEA Seminar, Vienna, 16–20 May 1966), IAEA, Vienna (1966).

DNE-69 Nelson, D. J., and Evans, F. C., *Symposium on Radioecology* (Proc. 2nd National Sympos., Ann Arbor, Michigan, 15–17 May 1967) USAEC Rpt. Conf-670503 (1969).

DSO-70 D'Souza, T. J., and Mistry, K. B., "Comparative Uptake of Thorium-230, Radium-226, Lead-210, and Polonium-210 by Plants," *Radiation Botany* **10**:293–295 (1970).

DSO-79 D'Souza, T. J., and Mistry, K. B., "Uptake Distribution and Metabolic Fate of ^{59}Fe, ^{58}Co, ^{54}Mn, and ^{65}Zn in Plants and Their Mobility and Availability to Crops in Typical Black and Laterite Soils," in [ISO-79], pp. 407–425.

DUK-69 Duke, T., Willis, J., Price, T., and Fischler, K., "Influence of Environmental Factors on the Concentrations of ^{65}Zn by an Experimental Community," pp. 355–362 in [NEL-69b].

DUU-71 Duursma, E. K., and Gross, M. G., "Marine Sediments and Radioactivity," Chapter 6 in [NAS-71], pp. 147–160.

EAC-63 See [EGG-63].

EGG-63 Eggleton, R. E. J., Atkins, D. H., and Cousins, L. B., "Chemical and Physical Nature of Fallout I^{131} and Carrier-Free I^{131} Released in Air" (Abstract), *Health Physics* **9**(12):1111 (December 1963).

ENG-66 Englemann, R. J., "Calculation of Precipitation Scavenging of Particulates and Gases from the Atmosphere," *Nuclear Safety* **3**(3):354–364 (Spring 1966).

ENG-70 Engelmann, R. J., and Slinn, W. G. (coordinators), *Precipitation Scavenging (1970)*, U.S.A.E.C. Rpt. Conf-700601 (December 1970).

ENV-69 *Environmental Contamination by Radioactive Materials* (Proc. FAO-IAEA-WHO Seminar, Vienna, Austria, 24–28 March 1969), IAEA, Vienna (1969).

ENV-73 *Environmental Behavior of Radionuclides Released in the Nuclear Industry* (Proc. IAEA, OECD/NEA, WHO Symp., Aix-en-Provence, France, 14–18 May 1973), International Atomic Energy Agency, Vienna (1973).

ENV-81 *Environmental Migration of Long-lived Radionuclides*, Proc. IAEA, CEC, NEA (OECD) Symposium held in Knoxville, Tennessee, 27–31 July 1981.

EPS-72 Epstein, E., *Mineral Nutrition of Plants: Principles and Perspectives*, John Wiley and Sons, New York (1972).

ES-73 Esmen, N. A., "Atmospheric Scavenging of Soluble and Insoluble Matter," *The Science of the Total Environment* **2**:181–189 (1973).

ES-76 Engelmann, R. J., and Sehmel, G. A. (coordinators), *Atmosphere-Surface Exchange of Gaseous Pollutants*, (Proc. Sympos., Richland, Wash., 4–6 Sept. 1974), U.S. ERDA Rpt. Conf-740921 (1976).

ESS-62 Essington, E., Nishita, H., and Wallace, A., "Influence of Chelates on Availability of Fission Products to Plants Grown in Contaminated Soil," *Soil Science* **94**(2):96–105 (1962).

ESS-63 Essington, E., Nishita, H., and Wallace, A., "Effect of Chelating Agents on the Uptake of Y 91, Ru 106, Ce 144, and Pm 147 by Beans Grown in a Calcareous Soil," *Soil Science* **95**(5):331–337 (1963).

ESS-79 Essington, E. H., Fowler, E. B., and Polzer, W. L., "Retention of Low-Level Radioactive Waste Material by Soil," in *Low-Level Radioactive Waste Management* (J. E. Watson, Jr., ed.) (Proc. of Health Physics Society Twelfth Mid-Year Topical Symposium, Williamsburg, Virginia, 11–15 February 1979), EPA Report EPA-520/3-79-002 (May 1979), pp. 457–470.

EV-62 Evans, E. J., and Dekker, A. J., "Comparative Sr-90 Content of Agricultural Crops Grown in a Contaminated Soil," *Canadian Journal of Plant Science* **42**:252–258 (April 1962).

FOL-69 Folsom, T. R., Young, D. R., and Sreekumaran, C., "An Estimate of the Response Rule of Albacore to Cesium," in [DNE-69], pp. 337–345.

FON-63 Fontaine, Y. A. and Aeberhardt, A., "Etude Expermental de la Contamination Radioactive par le Cerium-144 d'une Communaute Complex d'eau douce Relisée en Laboratoire," *Health Physics* **9**(11):1047–1056 (Nov. 1963).

FOS-59 Foster, R. F., "The Need for Biological Monitoring of Radioactive Waste Streams," *Sewage and Industrial Wastes* **31**:1409–1415 (1959).

FOT-78 Foth, H. D., *Fundamentals of Soil Science*, Sixth Edition, John Wiley, N.Y. (1978).

FRA-75 Fraizier, A., and Ancellin, J. C., "Etude de la contamination de constituants du milieu marin par des formes solubles et insolubles de radionucleides," pp. 49–61 in [AQU-75].

FRE-58 Fredrickson, L., Erickson, B., Rasmuson, B., Gahne, B., Edvarson, K., and Low, K., "Studies on Soil-Plant-Animal Interrelationships with Respect to Fission Products," *Proceedings of the Second United Nations International Conference on the Peaceful Uses of Atomic Energy*, U.N., Geneva (1958), Vol. 18, pp. 449–470.

FRI-60 Fried, M., and Heald, W. R., "Radioisotopes in Soils: Soil-Plant Relationship," Chapter 4 in [CAL-60] pp. 47–59.

FRI-63 Friend, A. G., "Research Studies on the Clinch River and Mohawk River," in J. J. Sabo and P. H. Bedrosin, eds., *Studies of the Fate of Certain Radionuclides in Estuarine and Other Aquatic Environments,* U.S. Public Health Service Publication 999-R-3, May 1963.

FRI-65 Friend, A. G., Story, A. H., Henderson, C. R., and Busch, K. A., *Behavior of Certain Radionuclides Released into Fresh-Water Environments,* U.S. Public Health Service Publication 999-RH-13, June 1965.

FRI-67 Fried, M., and Broeshart, H., *The Soil-Plant System in Relation to Inorganic Nutrition*, Academic Press, N.Y. (1967).

FRI-76 Friedman, A. M. (ed.), *Actinides in the Environment* (Proc. Symposium, New York, N.Y., April 9, 1976), American Chemical Society, Washington, D.C. (1976).

FUK-73 Fukai, R., and Murry, C. N., "Environmental Behavior of Radiocobalt and Radiosilver Released from Nuclear Power Stations into Aquatic Systems," pp. 217–242 in [ENV-73].

FUL-70 Fultyn, R. V. "A Probabilistic Scheme for Predicting and Evaluating Hazards Resulting from Radioactive Emissions to the Atmosphere," Chapter 39 in [REI-70b], pp. 359–367.

GAR-67 Garner, R. J. "A Mathematical Analysis of the Transfer of Fission Products to Cow's Milk," *Health Physics* **13**(2):203–212 (Feb. 1967).

GAR-71 Garrett, A. R., Jr., Cummings, S. L., and Regnier, J. E., "Accumulation of ^{137}Cs and ^{90}Sr by Florida Forages in a Uniform Environment," *Health Physics* **21**(1):67–70 (July 1971).

GAR-74 Garland, T. R., Wildung, R. E., Neel, J. W., and Cataldo, D. A., "Factors Affecting Uptake and Distribution of Plutonium in Barley and Soybean Plants," in [VAU-74], pp. 30–36.

GIL-75 Gilat, E., Laichter, Y., and Shafrir, N. H., "Behaviour Cesium-137 in the Marine Environment," pp. 63–75 in [AQU-75].

GOL-71 Goldberg, E. D., Broecker, W. S., Gross, M. G., and Turekian, K. K., "Marine Chemistry," Chapter 5 in [NAS-71], pp. 137–146.

GRU-77 Grummit, W. E., "Transfer of Cobalt-60 to Plants from Soils Treated with Sewage Sludge," in *Radioecology and Energy Resources*, Proceedings of the Fourth National Symposium on Radioecology, May 12–14, 1975, Corvallis, Oregon (R. E. Cushing, ed.), Ecological Society of America Special Publication No. 1 (1979), pp. 331–335.

GRZ-72 Grzybowska, D., and Wlodek, S., "Contribution a L'etude du Transfert de ^{90}Sr, ^{137}Cs et ^{226}Ra de Sol Vers les Plantes," in [RAD-72], vol. II, pp. 1069–1077.

GUA-77 Guary, J. C. and Fraizier, A., "Influence of Trophic Level and Calcification on the Uptake of Plutonium Observed *in situ* in Marine Organisms," *Health Physics* **32**(12):21–28 (January 1977).

GUS-67 Gustafson, P. F., "Comments on Radionuclides in Aquatic Ecosystems," in [ABE-67], pp. 853–858.

GUS-69b Gustafson, P. F., "Cesium-137 in Freshwater Fish During 1954–1965," in [DNE-69], pp. 249–257.

HAK-75 Hakonson, T. E., and Whicker, F. W., "Cesium Kinetics in a Montane Lake Ecosystem," *Health Physics* **28**(6):699–706 (June 1975).

HAM-67 Hampson, B. L., "Restricted Dispersion of Zirconium-95 and of Niobium-95 after Release to the Sea in Nuclear Fuel Reprocessing Plant Effluent," *Health Physics* **13**(10):1093–1103 (October 1967).

HAN-67 Hanson, W. C., "Radioecological Concentration Processes Characterizing Arctic Ecosystems," in [ABE-67], pp. 183–190.

HAN-70 Hansen, W. R., and Watters, R. L., "Plant Uptake of ^{210}Po from Soil," *Radiation Botany* **10**:371–375 (1970).

HAN-80 Hanson, W. C. (ed.), "Transuranic Elements in the Environment," U.S. DOE Rpt. DOE/TIC-22800 (1980) (NTIS).

HAR-67 Harrison, F. L., "Concentration Factors—Their Use and Abuse," Lawrence Livermore Laboratory Report UCRL-50347 (November 7, 1967).

HAR-64 Harvey, R. S., "Uptake of Radionuclides by Freshwater Algae and Fish," *Health Physics* **10**(4):243–247 (Apr. 1964).

HAR-65 Harvey, R. S., "Savannah River Plant Biological Monitoring Program," *Health Physics* **11**(3): (Mar. 1965).

HAR-69 Harvey, R. S., "Uptake and Loss of Radionuclides by the Freshwater Clam *Lampsilis radiata* (Gmel.)," *Health Physics* **17**(1):149–154 (July 1969).

HAW-66 Hawley, C. A., Jr., (ed.), "Controlled Environmental Radioiodine Tests at the National Reactor Testing Station—1965 Progress Report," U.S.A.E.C. Rpt. IDO-12047 (February 1966).

HCU-63 Hungate, F. P., Cline, J. F., Uhler, R., and Selders, A. A., "Foliar Sorption of ^{131}I by Plants," *Health Physics* **9**:1159–1166 (1963).

HEA-74 Healy, J. W., *A Proposed Interim Standard for Plutonium in Soils,* U.S.A.E.C. Rpt. La-5483-MS, Los Alamos Scientific Laboratory (1974).

HEI-74 Heinemann, K., Vogt, K. J., and Angeletti, L., "Depot et Retention sur L'herbe de L'iode Elementaire et de L'iodure de Methyle," in *Physical Behavior of Radioactive Contaminants in the Atmosphere* (Proc. IAEA-WMO Symp., Vienna, 12–16 November 1973), IAEA, Vienna (1974), pp. 245–259.

HEI-76 Heinemann, K., Vogt, K. J., and L. Angeletti, "Deposition and Biological Half-life of Elemental Iodine on Grass and Clover," in [ES-76], pp. 146–151.

HEI-80a Heinemann, K., and Vogt, K. J., "Measurements of the Deposition of Iodine onto Vegetation and of the Biological Half-life of Iodine on Vegetation," *Health Physics* **39**(4):463–474 (September 1980).

HEI-80b Heine, K., and Wiechen, A., "Studies of the Transfer Factors of Sr-90 and Cs-137 in the Food Chain Soil-Plant-Milk," in [IRP-80], vol. III, pp. 397–400.

HER-75 Herrmann, H., Ruf, H., Hubel, K., and Lunsmann, W., "Radiological Effects of a Nuclear Power Plant on a River System, as Demonstrated by the Gundremmingen BWR on the Danube," pp. 461–472 in [AOU-75].

HET-75 Hetherington, J. A., Jefferies, D. F., and Lovett, M. B., "Some Investigations into the Behavior of Plutonium in the Marine Environment," in [AQU-75], pp. 193–210.

HIY-64 Hiyama, Y., and Khan, J. M., "On the Concentration Factors of Radioactive I, Co, Fe, and Ru in Marine Organisms," *Rec. Oceanogr. Works Japan* **7**:79–106 (1964).

HOF-79 Hoffman, F. O., and Baes III, C. F. (eds.), *A Statistical Analysis of Selected Parameters for Predicting Food Chain Transport and Internal Dose of Radionuclides,* U.S. NRC Report NUREG/CR-1004 (ORNL/NUREG/TM–282) (July 1979).

HOL-80 Holm, E., Persson, B. R., and Mattsson, S., "Studies of Concentration and Transfer Factors of Natural and Artificial Actinide Elements in a Marine Environment," in [IRP-80], vol. III, pp. 311–314.

HUN-63 Hungate, F. P., Cline, J. F., Uhler, R. L., and Selders, A. A., "Foliar Sorption of ^{131}I by Plants," *Health Physics* **9**(12):1159–1166 (December 1963).

IRP-80 *Proceedings of the 5th International Congress of the International Radiation Protection Association,* Jerusalem, Israel, 9–14 March 1980.

ISO-79 *Isotopes and Radiation in Research on Soil-Plant Relationships* (Proc. IAEA-FAO Symposium, Colombo, Sri Lanka, 11–15 December 1978), IAEA, Vienna (1979).

ISR-50 Israelsen, O. W., and Hansen, V. E., *Irrigation Principles and Practices*, 3d edition, J. Wiley & Sons, New York, N.Y. (1950).

JAY-81 Jayaraman, A. P., and Prabhakar, S., "The Water Hyacinth's Uptake of ^{137}Cs and ^{90}Sr and its Decontamination Potential as an Approach to the Zero-release Concept," pp. 557–569 in [ENV-81].

JEN-69 Jenkins, C. E., Langford, J. C., and Forster, W. O., "Iron-55 Concentrations in Columbia River Estuarine and Pacific Ocean Marine Organisms," in *Pacific Northwest Laboratory Annual Report for 1968, vol. II, Physical Sciences, Part 2, Radiological Sciences* (J. M. Nielsen, Manager), USAEC Report BNWL-1051, pp. 69–72.

JEN-73 Jenkins, C. E., and Langford, J. C., "^{55}Fe Concentrations and Specific Activities in North Pacific Marine Organisms," pp. 47–48 in *Pacific Northwest Laboratory Annual Report for 1972*, vol. II, part 2, USAEC Rpt. BNWL-1751, Part 2 (April 1973).

JIN-76 Jinks, S. M., and Wrenn, M. E., "Radiocesium Transport in the Hudson River Estuary," Chapter 11 in [MIL-76], pp. 207–223.

KAY-68 Kaye, S. V., and Nelson, D. J., "Analysis of Specific-Activity Concept as Related to Environmental Concentration of Radionuclides," *Nuclear Safety* **9**(1):53–58 (January–February 1968).

KIR-66 Kirchmann, R., Adam, V., and van Puymbraeck, S., "Radiocontamination des denies du lait de vache," in *Radioisotopes and Radiation in Dairy Science and Technology* (Proc. FAO-IAEA Seminar, Vienna, 12–15 July 1966), IAEA, Vienna, 1966, pp. 189–198, CONF-660711.

KIR-67 Kirchmann, R., Fagniart, E., and van Puymbroech, S., "Studies on Foliar Contamination by Radiocesium and Radiostrontium," in [ABE-67], pp. 475–483.

KIR-68 Kirchmann, R., Boulenger, R., and LaFontaine, A., "Absorption du ^{226}Ra par les Plantes Cultivees," in *Proceedings of the First International Congress on Radiation Protection* (W. A. Snyder et. al., eds.), Pergamon Press, Oxford (1968), vol. 2, pp. 1045–1051.

KIR-72 Kirchmann, R., and D'Souza, T. J., "Behavior of Ruthenium in an Established Pasture Soil and its Uptake by Grasses," in [ISO-72], pp. 587–593.

KLE-65 Klement, A. W., Jr., *Radioactive Fallout from Nuclear Weapons Test* (Proc. of Second AEC Conference, Germantown, MD, 3–6 November 1964), U.S.A.E.C. Rpt. Conf-765 (1965).

KLE-76 Klepper, B., Watson, D. G., and Cline, J. F., "Iodine-129 Concentration Factors for Food Products," in [VAU-76], p. 179.

KOL-67b Kolehmainen, S., Häsänen, E., and Miettinen, J. K., "^{137}Cs in the Plants, Plankton and Fish of the Finnish Lakes and Factors Affecting its Accumulation," pp. 407–415 in *Proc. First Intl. Conf. on Radiation Protection* (W. S. Snyder et al., eds.), Oxford, Pergamon Press (1967), vol. I.

KOL-69a Kolehmainen, S. E., "White Oak Lake Studies," pp. 128–136 in *Health Physics Division Annual Progress Report for Period Ending July 31, 1969*, Oak Ridge National Laboratory, U.S.A.E.C. Rpt. ORNL-446 (October 1969).

KOL-69b Kolehmainen, S., Takatalo, S., and Miettinen, J. K., "A Tracer Experiment with I-131 in an Oligatrophic Lake," in [DNE-69], pp. 278–284.

KOR-63 Kornegay, B. H., Vaughan, W. A., Jamison, D. K., and Morgan, J. M., Jr. (eds.), *Transport of Radionuclides in Fresh Water Systems*, (Proc. Conference, Austin, Texas, 30 January–1 February 1963) (July 1963).

KOR-65 Koranda, J. J., "Agricultural Factors Affecting the Daily Intake of Fresh Fallout by Dairy Cows," USAEC Rpt. UCRL-12479, University of California, Lawrence Livermore Laboratory (1965).

KRI-69 Krieger, H. L., and Burmann, F. J., "Effective Half-times of ^{85}Sr and ^{134}Cs for a Contaminated Pasture," *Health Physics* **17**(6):811–824 (December 1969).

KWA-67 Kwarat Skhelia, N. T., Glowry, G. G., Arnautor, T. N., and Gama Zova, E. K., "The Influence of Some Natural Factors on the Behavior of Radioactive Strontium in Soils," in [BER-67], pp. 19–37.

LAS-80 Lassey, K. R., "The Possible Importance of Short Term Exposure to Resuspended Radionuclides," *Health Physics* **38**(5):749–761 (May 1980).

LEN-69 Lengemann, F. W., "Radioiodine in the milk of cows and goats after oral administration of radioiodate and radioiodine," *Health Physics* **17**(4):565–569 (October 1969).

LEN-71 Lentsch, J. W., Kneip, T. J., Wrenn, M. E., Howells, G. P., and Eisenbud, M., "Stable Manganese and Manganese-54 Distributions in the Physical and Biological Components of the Hudson River Estuary," in [NEL-71], vol. II, pp. 752–768.

LEN-79 Lengemann, F. W., and Wentworth, R. A., "Extremes of Environmental Temperature and the Transfer of Radioiodine into Milk," *Health Physics* **36**(3):267–271 (March 1979).

LIN-78 Linsley, G. S., *Resuspension of the Transuranium Elements—A Review of Existing Data*, United Kingdom National Radiological Protection Board Report NRPB-R75 (August 1978).

LIP-76 Lipton, W. V., and Goldin, A. S., "Some Factors Influencing the Uptake of Plutonium-239 by Pea Plants," *Health Physics* **31**(5):425–430 (November 1976).

LOW-66 Lowman, F. G., Phelps, D. K., McClin, R., Raman de Vega, V., Oliver de Proovani, I., and Garcia, R. J., "Interactions of the Environmental and Biological Factors on the Distribution of Trace Elements in the Marine Environment," in [DIS-66], pp. 249–266.

LOW-67 Lowman, F. G., Stevenson, R. A., McClin, R., Scalera, E., and Ufret, S. L., "The Effects of River Out-flows upon the Distribution Patterns of Fallout Radioisotopes in Marine Organisms," in [ABE-67], pp. 735–752.

LOW-69 Lowman, F. G., "Radionuclides of Interest in the Specific Activity Approach," *Bio-Science* **19**(11):993–999 (November 1969).

LOW-71 Lowman, F. G., Rice, T. R., and Richards, F. A., "Accumulation and Redistribution of Radionuclides in Marine Organisms," Chapter 7 in [NAS-71].

MAG-67 Magno, P. J., Kauffman, P. E., and Shleien, B., "Plutonium in Environmental and Biological Media," *Health Physics* **13**(12):1325–1330 (December 1967).

MAG-72 Magno, P. J., Reavey, T. C., and Apidianakis, J. C., *Iodine-129 in the Environment Around a Nuclear Fuel Reprocessing Plant,* U.S. Environmental Protection Agency Report (October 1972).

MAR-73 *Radioactive Contamination of the Marine Environment* (Proc. IAEA Symp., Seattle, Wash., 10–14 July 1972), IAEA, Vienna (1973).

MCD-79 McDowell-Boyer, L. M., Watson, A. P., and Travis, C. C., "Review and Recommendations of Dose Conversion Factors and Environmental Transport Parameters for ^{210}Pb and ^{226}Ra," U.S. NRC Rpt. NUREG/CR-0574 (March 1979) (NTIS PB-294242).

MEA-78 Means, J. L., Crerar, D. A., and Duguid, J. O., "Migration of Radioactive Wastes: Radionuclide Mobilization by Complexing Agents," *Science* **200**(4349):1477–1480 (June 30, 1978).

MEN-54 Menzel, R. G., "Competitive Uptake by Plants of Potassium, Rubidium, Cesium, and Calcium, Strontium and Barium from Soils," *Soil Science* **77**(6):419–425 (June 1954).

MID-65 Middleton, L. J., "Influence of Dietary Composition on Radionuclide Intake," pp. 124–133 in *Agricultural and Public Health Aspects of Radioactive Contamination in Normal and Emergency Situations* (Proc. Seminar held at Scheveningen, The Netherlands, 11–15 December 1961), Food and Agriculture Organizations of the United Nations, Rome, FOA Atomic Energy Series No. 5 (1964).

MIL-62 Milbourn, G. M., and Taylor, R., "Absorption of Nutrients from Soil by Established Crops," in *Agricultural Research Council Radiobiological Laboratory Annual Report 1961–1962*, ARCRL-8 (Sept. 1962), pp. 71–73.

MIL-65 Milbourn, G. M., and Taylor, R., "The Contamination of Grassland with Radioactive Strontium. 1. Initial Retention and Loss," *Radiation Botany* **5**:337–347 (1965).

MIL-67 Miller, C. W., "The Retention by Foliage of Silicate Particles Ejected from the Volcano Irazu in Costa Rica," in [ABE-67], pp. 501–525.

MIL-72 Miller, C. L., Payne, J. G., Jr., Brettenhauer, E. W., and Moghissi, A. A., "Transfer of Plutonium from Milk to Cheese," *Health Physics* **22**(6): 563–565 (June 1972).

MIL-78 Miller, C. W., Hoffman, F. O., and Shaeffer, D. L., "The Importance of Variations in the Deposition Velocity Assumed for the Assessment of Airborne Radionuclide Releases," *Health Physics* **34**(6):730–734 (1978).

MIL-80a Miller, C. W., "An Analysis of Measured Values for the Fraction of a Radioactive Aerosol Intercepted by Vegetation," *Health Physics* **38**(4):705–712 (April 1980).

MIL-80b Milošević, Z., Moršić, E., Klajić, R., and Bauman, A., "Distribution of Uranium, ^{226}Ra, ^{210}Pb, and ^{210}Po in the Ecological Cycle in Mountain Regions of Central Yugoslavia," in [IRP-80], vol. III, pp. 331–334.

MIS-73 Mistry, K. B., Bhujbal, B. M., and D'Souza, T. J., "Influence of Agronomic Practices on Uptake of Fission Products by Crops from Soils of Regions Adjoining Nuclear Installations in India," in [ENV-73], pp. 303–319.

MIY-73 Miyanaga, I., Kasai, A., and Imai, K., "A Preliminary Experiment on the Deposition of Gaseous Radioiodine onto Environmental Materials," in [ENV-73], pp. 157-164.

MOO-63 Moorby, J., and Squire, H. M., "The Loss of Radioactive Isotopes from the Leaves of Plants in Dry Conditions," *Radiation Botany* **3**:163–167 (July 1963).

MRA-64 Mraz, F. R., Wright, P. L., Ferguson, T. M., and Anderson, D. L., "Fission Product Metabolism in Hens and Transference to Eggs," *Health Physics* **10**(11):777–782 (November 1964).

MUR-73 Murray, C. N., and Murray, L., "Adsorption-Desorption Equilibria of Some Radionuclides in Sediment-Fresh-water and Sediment-Seawater Systems," in [MAR-73], pp. 105–122.

MUR-79 Murray, C. N., and Avogadro, A., "Effect of a Long-Term Release of Plutonium and Americium into an Estuarine—Coastal Sea Ecosystem," *Health Physics* **36**(5):573–585 (May 1979).

MYT-69 Myttenaere, C., Bourdeau, P., and Bittel, R., "Importance Relative de L'eau et du Sol dans la Contamination Indireete en Radiocesium et Radiocobalt des Rizieres Irriquees," in [ENV-69], pp. 175–182.

NAK-80a Nakamura, Y., and Ohmomo, Y., "Factors Used for the Estimation of Gaseous Radioactive Iodine Intake Through Vegetation—I. Uptake of Methyl Iodide by Spinach Leaves," *Health Physics* **38**(3):307–314 (March 1980).

NAK-80b Nakamura, Y., and Ohmomo, Y., "Factors Used for the Estimation of Gaseous Radioactive Iodine Intake Through Vegetation—II. Uptake of Elemental Iodine by Spinach Leaves," *Health Physics* **38**(3):315–320 (March 1980).

NAS-62 National Academy of Sciences–National Research Council. *Disposal of Low-Level Radioactive Waste into Pacific Coastal Water,* NAS/NRC Publ. 985, NAS-NRC, Washington, D.C. (1962).

NAS-71 National Academy of Sciences – National Research Council, *Radioactivity in the Marine Environment,* NAS-NRC, Washington, D.C. (1971).

NEL-67 Nelson, D. J., Kevern, N. R., and Griffith, N. A., "Cesium and Potassium in Aquatic Food Chains," pp. 97–98 in *Oak Ridge National Laboratory Annual Progress Report for Period Ending July 31, 1967,* USAEC Rpt. ORNL-4168 (October 1967).

NEL-69a Nelson, D. J., "Cesium, Cesium-137, and Potassium Concentrations in White Crappie and Other Clinch River Fish," pp. 240–248 in [NEL-69].

NEL-69b Nelson, D. J., and Evans, F. C. (eds.), *Symposium on Radioecology* (Proc. Second National Symposium, Ann Arbor, Michigan, 15–17 May 1967), USAEC Rpt. CONF-670503 (March 1969).

NEL-71 Nelson, D. J. (ed.), *Radionuclides in Ecosystems* (Proc. of the Third National Symposium on Radioecology, Oak Ridge, Tenn., 10–12 May 1971), USAEC Rpt. CONF-710501 (1971).

NG-77 Ng, Y. C., Colsher, C. S., Quinn, D. J., and Thompson, S. E., *Transfer Coefficients for the Prediction of the Dose to Man Via the Forage-Cow-Milk Pathway from Radionuclides Released to the Biosphere,* University of California Lawrence Livermore Laboratory Report UCRL-51939 (July 1977).

NG-79 Ng, Y. C., Colsher, C. S., and Thompson, S. E., "Transfer Factors for Assessing the Dose from Radionuclides in Agricultural Products," in *Biological Implications of Radionuclides Released from Nuclear Industries,* Proc. Symp. Vienna 26–30 March 1979, vol. 2, pp. 295–318.

NG-82a Ng, Y. C., Colsher, C. S., and Thompson, S. E., *Soil-to-Plant Concentration Factors for Radiological Assessments.* NRC Report NUREG/CR-2975 (UCID-19463) (November 1982).

NG-82b Ng, Y. C., Colsher, C. S., and Thompson, S. E., *Transfer Coefficients for Assessing the Dose from Radionuclides in Meat and Eggs,* U.S. NRC Report NUREG/CR-2976, Lawrence Livermore National Laboratory Report UCID-19464 (December 1982).

NOR-69 Norvell, W. A., and Lindsay, W. L., "Reactions of EDTA Complexes of Fe, Zn, Mn, and Cu with Soils," *Soil Science Society of America Proceedings* 33:86–91 (1969).

NRC-75 U.S. Nuclear Regulatory Commission, *Reactor Safety Study—An Assessment of Accident Risks in Commercial Nuclear Power Plants,* WASH-1400 (NUREG-75/014) Appendix VI (1975).

NRC-77 Nuclear Regulatory Commission, "Calculation of Annual Doses to Man from Routine Release of Reactor Effluents for the Purpose of Evaluating Compliance with 10 CFR Part 50, Appendix I." Regulatory Guide 1.109 (Rev. 1) (October 1977).

NRC-82 Nuclear Regulatory Commission, *Calculational Models for Estimating Radiation Doses to Man from Airborne Radioactive Materials Resulting from Uranium Milling Operations,* NRC Regulatory Guide 3.51 (March 1982).

OPH-65 Ophel, I. L., "Remarks," in *Proceedings of the Second International Water Pollution Research Conference 1964,* Oxford, Pergamon Press (1965), pp. 275–286.

OPH-69 Ophel, I. L., and Judd, J. M., "Strontium-Calcium Relationships in Aquatic Food Chains," pp. 221–239 in [NEL-69b].

PAR-65 Parker, H. M., Foster, R. F., Ophel, I. L., Parker, F. L., and Reinig, W. C., "North American Experience in the Release of Low-Level Waste to Rivers and Lakes," pp. 62–71 in *Proceedings of the Third International Conference on the Peaceful Uses of Atomic Energy* (Proc. Conf., Geneva, 31 August–9 September 1964), vol. 14, United Nations, New York (1965).

PAR-66 Parker, F. L., Churchill, M. A., Andrew, R. W., Fredrick, S. J., Carrigan, P. H., Jr., Cragwall, J. S., Jr., Jones, S. L., Struxness, E. G., and Morton, R. J., "Dilution, Dispersal and Mass Transport of Radionuclides in the Clinch and Tennessee Rivers," pp. 33–54 in [DIS-66].

PEI-62 Peirson, D. H., and Keane, J. R., "Characteristics of Early Fall-Out from the Russian Nuclear Explosions of 1961," *Nature* **196**(4857):801–807 (December 1962).

PEL-65 Pelletier, C. A., Whipple, G. H., and Wedlick, H. L., "Use of Surface-Air Concentration and Rainfall Measurements to Predict Deposition of Fallout Radionuclides," in [KLE-65], pp. 723–736.

PEN-58 Pendleton, R. C., and Hanson, W. C., "Absorption of Cesium-137 by Components of an Aquatic Community," *Proceedings of the Second United Nations International Symposium on the Peaceful Uses of Atomic Energy,* vol. 18, pp. 419–422 (1958).

PEN-65 Pendleton, R. C., Mays, C. W., Lloyd, R. D., and Church, B. W. 1965. "A Trophic Level Effect on ^{137}Cs Concentration," *Health Physics* **11**:1503–10 (1965).

PEN-72 Pentreath, R. J., "The Roles of Food and Water in the Accumulation of Radionuclides by Marine Teleost and Elasmobranch Fish," in *Radioactive Contamination of the Marine Environment* (Proc. IAEA Symp., Seattle, Washington, 10–14 July 1972), IAEA, Vienna, pp. 421–435.

PEN-79 Pentreath, R. J., Lovett, M. B., Harvey, B. R., and Ibbett, R. D., "Alpha-Emitting Nuclides in Commercial Fish Species Caught in the Vicinity of Windscale, United Kingdom, and Their Radiological Significance," pp. 227–245 in [BIO-79].

PER-60 Perkins, R. W., Nielsen, J. M., Roesch, W. C., and McCall, R. C., "Zinc-65 and Chromium-51 in Foods and People," *Science* **132**:1895–1897 (December 23, 1960).

PER-68 Perkins, R. W., Robertson, D. E., and Rieck, H. G., "Ultra-sensitive Measurement of Radionuclides and Trace Element Constituents in the Ocean by Multi-dimensional Gamma-ray Spectrometry." *Pacific Northwest Laboratory Annual Report for 1967*, vol. II, Part 2, USAEC Rpt. BNWL-715 (1968), pp. 108–115.

PET-70 Peterson, H. T., Jr., and Smith J. M., "Guides for Predicting Thyroid Dose from Environmental Measurements Following Radioiodine Releases," in [REI-70b], Chapter 23, pp. 172–188.

PET-71 Peterson, H. T., Jr., "Stable Element and Radionuclide Reconcentration in Aquatic Ecosystems," in [VOI-71], vol. II, pp. 289–328.

PET-72 Peters, L. N., and Witherspoon, J. P., "Retention of 44–88 μ or μm Simulated Fallout Particles by Grasses," *Health Physics* **22**(3):257–260 (March 1972).

POE-72 Peolstra, P., and Frissel, M. J., "The Sr-90 Contamination of Grass; Based Upon Some Ecological Parameters," in [RAD-72], vol. II, pp. 1039–1056.

POS-70 Postma, A. K., "Effect of Solubilities of Gases on Their Scavenging by Raindrops," in [ENG-70], pp. 247–258.

PRE-69 Preston, A., and Jeffries, D. G., "Aquatic Aspects in Chronic and Acute Contamination Situations," pp. 183–211 in [ENV-69].

RAD-72 *Radioecology Applied to the Protection of Man and His Environment* (Proc. CEC Int. Symp., Rome, Italy, 7–10 Sept. 1971), Commission of the European Communities, Luxembourg (May 1972).

RAN-68 Rancitelli, L. A., Jenkins, C. E., and Haller, W. A., "Trace Element Content and the Specific Activity of Several Radionuclides in Silver Salmon Liver," *Pacific Northwest Laboratory Annual Report for 1967, vol. II, Physical Sciences, Part 2, Radiological Sciences,* USAEC Rpt. BNWL-715, Part 2 (1968), pp. 47–52.

REI-70b Reinig, W. C. (ed.), *Environmental Surveillance in the Vicinity of Nuclear Facilities* (Proc. HPS Mid-year Topical Symposium, 24–26 January 1968, Augusta, Ga.), Charles C. Thomas, Springfield, IL, 1971.

RIC-74 Rickard, W. H., et al., "Radionuclides in the Environment," in [VAU-74], pp. 192–204.

ROB-68 Robertson, D. E., Forster, W. O., Rieck, H. G., and Langford, J. C., "A Study of Trace Element and Radionuclide Behavior in a Northwest Pacific Ocean Ecosystem 350 Miles off Newport, Oregon," in *Pacific Northwest Laboratory Annual Report for 1967*, vol. II, Part 2, USAEC Rpt. BNWL-715, Part 2 (1968), pp. 92–108.

ROB-71 Robertson, D. E., "Silver Concenrations in Marine Organisms and Seawater," pp. 12–14 in *Pacific Northwest Laboratory Annual Report for 1970, vol. II, Physical Sciences, Part 2, Radiological Sciences,* (J. M. Nielsen (ed.), USAEC Rpt. BNWL-1551, Part 2 (March 1971).

ROE-69 Roessler, G. S., Dunavant, B. G., and Roessler, C. E., "Cesium-137 Body Burdens in Florida Residents," *Health Physics* **16**:673–679 (1969).

ROM-54 Romney, E. M., Rhoads, W. A., and Larson, K., *Plant Uptake of Sr-90, Ru-106, Cs-137 and Ce-144 from Three Different Types of Soils*, USAEC Rep. UCLA-294 (1954).

ROM-57 Romney, E. M., Neel, J. W., Nishita, H., Olafson, J. H., and Larson, K. H., "Plant Uptake of Sr-90, Y-91, Ru-106, Cs-137, and Ce-144 from Soils," *Soil Science* **83**(5):369–376 (May 1957).

ROM-60 Romney, E. M., Ehrler, W. L., Lange, A. H., and Larson, K. H., "Some Experimental Factors Influencing Radiostrontium Uptake by Plants," *Plant and Soil* **XII**(1):41–48 (January 1960).

ROM-70 Romney, E. M., Mork, H. M., and Larson, K. H., "Persistence of Plutonium in Soil, Plants, and Small Mammals," *Health Physics* **19**(4):487–491 (October 1970).

ROU-78 Routson, R. C., and Cataldo, D. A., "Accumulation of ^{99}Tc by Tumbleweed and Cheatgrass Grown on Arid Soils," *Health Physics* **34**(6):685–690 (June 1978).

RUS-66 Russell, R. S., *Radioactivity and Human Diet*, Pergamon Press, Oxford, U. K. (1966).

SAR-66 Sartor, J. D., Lane, W. B., and Allen, J. J., "Uptake of Radionuclides by Plants," Stanford Research Institute Report (NTIS No. AD-649009) (December 1966).

SAR-68 Sartor, J. D., Kruzic, P. G., Lane, W. B., and Mackin, J. L., "Experimental Investigation of Plant Uptake Contamination Factors," Stanford Research Institute Report TRC-6857 (NTIS No. AD-694531) (September 1968).

SCH-65 Schelske, C. L., Smith, W. D. C., and Lewis, J., "Radioactivity in Estuarine Environment," pp. 8–13 in *Radiobiological Laboratory, Beaufort, N.C., Annual Report 1964*, U.S. Department of the Interior, Fish and Wildlife Service, Bureau of Commercial Fisheries, Circular 217 (June 1965).

SCH-72 Schelske, C. L., "Fallout ^{54}Mn Accumulated by Bay Scallop *Argopecten irrodians* (Lamarck) Near Beaufort, North Carolina," in *Radioactive Contamination of the Marine Environment* (Proc. IAEA Symp., Seattle, Washington, 10–14 July 1972), IAEA, Vienna (1973), pp. 331–345.

SCH-76 Schulz, R. K., Tompkins, G. A., and Babcock, K. L., "Uptake of Plutonium and Americium by Plants from Soils," in [TRU-76], pp. 303–310.

SCH-80a Schreckhise, R. G., and Cline, J. F., "Uptake and Retention of ^{232}U in Peas and Barley," *Health Physics* **38**(3):341–343 (March 1980).

SCH-80b Schreckhise, R. G., and Cline, J. F., "Comparative Uptake and Distribution of Plutonium, Americium, Curium, and Neptunium in Four Plant Species," *Health Physics* **38**(5):817–824 (May 1980).

SEH-76a Sehmel, G. A., and Hodgson, W. H., "Predicted Dry Deposition Velocities," in [ES-76], pp. 399–419.

SEH-76b Sehmel, G. A., and Lloyd, F. D., "Particle Resuspension Rates," in [ES-76], pp. 846–855.

SEH-76c Sehmel, G. A., "Particle Resuspension from an Asphalt Road Caused by Car and Truck Traffic," in [ES-76], pp. 859–882.

SEM-77 Semonin, R. G., and Beadle, R. W. (coordinators), *Precipitation Scavenging (1974)*, (Proc. Symposium, Champaign, Illinois, 14–18 October 1974), U.S. ERDA Rpt. Conf-741003 (1977).

SEY-73 Seymour, A. H., and Nelson, V. A., "Decline of ^{65}Zn in Marine Mussels Following the Shutdown of Hanford Reactors," pp. 277–286 in [MAR-73].

SHE-62 Sheppard, C. W., *Basic Principles of the Tracer Method*, John Wiley and Sons, New York (1962).

SIM-79 Simmons, J. R., Linsley, G. S., and Jones, J. A., "A General Model for the Transfer of Radioactive Materials in Terrestrial Food Chains," U. K. National Radiological Protection Board Rep. NRPB-R89 (September 1979).

SIN-77 Singh, H. B., Salas, L. J., and Cavanagh, L. A., "Distribution, Sources, and Sinks of Atmospheric Halogenated Compounds," *J. Air Pollution Control Assoc.* **27**:332–336 (1977).

SLI-77 Slinn, W. G. N. 1977. "Precipitation Scavenging: Some Problems, Approximate Solutions and Suggestions for Future Research," pp. 1–60 in *Precipitation Scavenging (1974)* (Proc. Symposium, Champaign, Illinois, 1974), U.S. ERDA Rpt., CONF-741003 (1977).

SLI-78 Slinn, W. G. N., "Parameterizations for Resuspension and for Wet and Dry Deposition of Particles and Gases for Use in Radiation Dose Calculations," *Nuclear Safety* **19**(2):205–219 (March–April 1978) [Note errata in **19**(3):365 (May–June 1978)].

SMI-80 Smith, M. H., Alberts, J. J., Adriano, D. C., and McLeod, K. W., *Critical Pathways of Radionuclides to Man from Agro-Ecosystems,* U.S. Nuclear Regulatory Commission Contract Report NUREG/CR-1206 (Jan. 1980).

SMI-81 Smith, M. H., Alberts, J. J., Adriano, D. C., McLeod, K. W., and Pinder III, J. E., *Critical Pathways of Radionuclides to Man from Agro-Ecosystems,* U.S. NRC Report NUREG/CR-1990 (May 1981).

STE-80a Steffens, W., Führ, F., and Mittelstaedt, W., "Evaluation of Small Scale Laboratory and Pot Experiments to Determine Realistic Transfer Factors for the Radionuclides ^{90}Sr, ^{137}Cs, ^{60}Co, and ^{54}Mn," in [IRP-80], vol. III, pp. 343–346.

STE-80b Steffens, W., Mittelstaedt, W., and Führ, F., "The Transfer of Sr-90, Cs-137, Co-60, and Mn-54 from Soils to Plants—Results from Lysimeter Experiments," in [IRP-80], vol. III, pp. 347–350.

STE-81 Stegnar, P., and Kobal, I., "Uptake and Distribution of Radium and Uranium in the Aquatic Food Chain," in [ENV-81], pp. 364–373.

STR-63 Straub, C. P., and Fooks, J. H., "Cooperative Field Studies on Environmental Factors Influencing ^{131}I Levels in Milk," *Health Physics* **9**(12):1157–1195 (December 1963).

STY-70 Styra, B., et al. (eds.), *Atmospheric Scavenging of Radioisotopes* (Rep. Conf. Palanga, Lithuania S.S.R.), English Translation Conf-660673, TT69-55099 (NTIS)(1970).

SUZ-75 Suzuki, H., Koyanagi, T. and Saiki, M., "Studies on Rare Earth Elements in Seawater and Uptake by Marine Organisms," pp. 77–90 in [AQU-75].

TEM-64a Templeton, W. L., and Brown, V. M., "The Relationship between the Concentrations of Calcium, Strontium, and Strontium-90 in the Wild Brown Trout, *Salmo trutta,* L., and in some waters of the United Kingdoms. *Int. J. Air Water Poll.* **8**:49–75 (1964).

THO-65 Thompson, S. E., "Effective Half-Life of Fallout Radionuclides on Plants with Special Emphasis on Iodine-131," USAEC Rpt. UCRL-12388 (January 1965).

THO-67 Thompson, J. C., Jr., "Reconsideration of the ^{131}I Contribution from Fruits and Vegetables," *Health Physics* **13**(8):883–887 (August 1967).

THO-72 Thompson, S. E., Burton, C. A., Quinn, D. J., and Ng, Y. C., *Concentration Factors of Chemical Elements in Edible Aquatic Organisms*, University of California, Lawrence Livermore Laboratory Report UCRL-50564, (Rev. 1.) (October 1972).

THO-73 Thompson, J. C., Jr., and Howe, M., "Retention and Removal of I-131 from Contaminated Vegetables," *Health Physics* **24**(3):345–351 (March 1973).

THO-75 Thompson, M. A., "Plutonium in the Aquatic Environment Around the Rocky Flats Facility," pp. 213–216 in [AQU-75].

TIN-69 Ting, R. Y., "Use of Stable Element Distribution Patterns for Predicting Distribution of Radionuclides in Marine Organisms," *Bio Science* **19**(12):1082–1085 (December 1969).

TOW-63 Townsley, S. J., "The Effect of Environmental Ions on the Concentration of Radiocalcium and Radiostrontium by Eurhaline Teleosts," pp. 193–198 in *Radioecology*, V. Schulte and A. W. Klement, Jr. (eds.), Reinhold, New York (1973).

TRA-76 Travis, J. R., "A Model for Predicting the Redistribution of Particulate Contaminants from Soil Surfaces," in [ES-76], pp. 906–944.

TRU-76 *Transuranium Nuclides in the Environment* (Proc. IAEA-ERDA Symposium, San Francisco, Calif., 17–21 November 1975), IAEA, Vienna (1976).

TWA-69 Twardock, A. R., and Crackel, W. C., "Cesium-137 Retention by Cattle, Sheep, and Swine," *Health Physics* **16**(3):315–323 (March 1969).

UND-67 Underdahl, B., "The Influence of the Soil and the Way of Farming on the ^{90}Sr Concentration in Milk," in [ABE-67], pp. 73–76.

VAN-73 Van As, D., Fourie, H. O., Vleggaar, C. M., "Accumulation of Certain Trace Elements in Marine Organisms from the Sea Around the Cape of Good Hope," pp. 615–623 in [RAD-72].

VAN-75 Vanderploeg, H. A., Parzyck, D. C., Wilcox, W. H., Kercher, J. R., and Kaye, S. V., *Bioaccumulation Factors for Radionuclides in Freshwater Biology*, Oak Ridge National Laboratory Rpt. ORNL-5002 (November 1975).

VAU-74 Vaughan, B. E., *Pacific Northwest Laboratory Annual Report for 1974 to the USAEC Division of Biomedical and Environmental Research—Part 2, Ecological Sciences,* USAEC Rpt. BNWL-1500, Part 2 (December 1974).

VAU-76 Vaughan, B. E., *Pacific Northwest Laboratory Annual Report for 1975 to the USERDA Division of Biomedical and Environmental Research—Part 2. Ecological Sciences,* USERDA Rpt. BNWL-2000, Part 2 (February 1976).

VER-67 Verkhovskaja, I. N., Vavilov, P. P., and Maslov, V. I. "The Migration of Natural Elements Under Natural Conditions and Their Distribution According to Biotic and Abiotic Environmental Components," pp. 313–328 in [ABE-67].

VIL-78 Viliquin, A., Coulon, R., LeGrand, J., "Methode d'Evaluation des Consequences des Regects Radioactifs du Centre de la Hauge," pp. 363–383 in *Seminar on Radioactive Effluents from Nuclear Fuel Reprocessing Plants* (Karlsruhe, FRG 22–25 November 1977), Commission of the European Communities: Luxembourg, February 1978.

VOI-70 Voillequé, P. G., Adams, D. R., and Echo, J. B., "Transfer of Krypton-85 from Air to Grass," *Health Physics* **19**(6):835 (December 1970).

VOI-71 Voillequé, P. G., and Baldwin, B. R. (eds.), *Health Physics Aspects of Nuclear Facility Siting* (Proc. 5th Annual Health Physics Society Mid-year Topical Symposium, Idaho Falls, Idaho, 3–6 November 1970) (February 1971).

VOI-74 Voillequé, P. G., and Pelletier, C. A., "Comparison of External Irradiation and Consumption of Cow's Milk as Critical Pathways for ^{137}Cs, ^{54}Mn, and ^{144}Ce-^{144}Pr Released to the Atmosphere," *Health Physics* **27**(2):189–199 (August 1974).

WAH-75 Wahlgren, M. A., and Marshall, J. S., "The Behavior of Plutonium and Other Long-lived Radionuclides in Lake Michigan," pp. 227–243 in *Impacts of Nuclear Releases into the Aquatic Environment* (Proc. IAEA Symposium, Otaniemi, Finland, 30 June–4 July 1975), IAEA, Vienna (1975).

WAL-56 Wallace, A. (ed.), *Symposium on the Use of Metal Chelates in Plant Nutrition*, National Press, Palo Alto, California (1956).

WAL-79 Wallace, A., Schulz, R. K., Romney, E. M., and Nishita, H., *Biological Transport of Radionuclides at Low-Level Waste Storage Sites,* U.S. NRC Report NUREG/CR-0701 (March 1979).

WAL-80 Wallace, A., Romney, E. M., Schulz, R. K., Nishita, H., and Herman, D. J., *Vegetation Cover in Monitoring and Stabilization of Shallow Land Burial Sites,* U.S. NRC Report NUREG/CR-1358 (August 1980) (NTIS).

WAT-63 Watt, B. K., and Merrill, A. L., *Composition of Foods: Raw, Processed, Prepared,* Agricultural Handbook No. 8, U.S. Department of Agriculture (December 1963) (GPO).

WAT-80 Watters, R. L., Edgington, D. N., Hakonson, T. E., Hanson, W. C., Smith, M. H., Whicker, F. W., and Wildung, R. E., "Synthesis of the Research Literature," pp. 1–44 in [HAN-80].

WEI-75 Weiss, B. H., Voillequé, P. G., Keller, J. H., Kahn, B., Kreiger, H. L., Martin, A., and Phillips, C. R., *Detailed Measurement of ^{131}I in Air, Vegetation and Milk Around Three Operating Reactor Sites,* U.S. NRC Rpt. NUREG/75/021 (March 1975).

WIL-74 Wildung, R. E., Routson, R. C., Serne, R. J., and Garland, T. R., "Pertechnate Iodide and Methyl Iodide Retention by Surface Soils," in [VAU-74], pp. 37–40.

WIT-69 Witherspoon, J. P., and Taylor, F. G., Jr., "Retention of a Fallout Simulant Containing ^{134}Cs by Pine and Oak Trees," *Health Physics* **17**(6):825–829 (December 1969).

WOR-75 "Workshop on Environmental Research for Transuranium Elements" (Proc. Workshop, Seattle, Washington, 12–14 November 1975), ERDA-76-134 (NTIS).

YAM-65 Yamagata, N., "Evaluation of Marine Contamination with Radioisotopes of Long Half-life," *Health Physics* **11**(10):1005–1008 (October 1965).

YOU-79 Young, D. R., and Folsom, T. R., "Cesium Accumulation in Muscle Tissue of Marine Fishes," *Health Physics* **37**(5):703–706 (November 1979).

6 Reference Man: A System for Internal Dose Calculations

By J. W. POSTON*

6.1 INTRODUCTION

The concept of a standard man for use in internal dose calculations originated more than 30 years ago. When early health physicists compared their dose estimates due to inhaled or ingested radioactive material (or their estimates of permissible levels in air and water), they found that agreement on basic standards for radiation protection was not good. This lack of agreement was due primarily to the use of different values of some of the biological data in their dose calculations. For this reason, a "Standard Man" was proposed. This standard man was a test individual to be used in checking on the effect of various assumptions regarding the exposure situation and in comparing dose estimates made by individual health physicists.

The first agreements on a standard man were formulated by the National Council on Radiation Protection and Measurements (NCRP) at a conference held at Chalk River in 1949 (NCRP 1950). At that time, the selected parameters were thought to be appropriate for a typical radiation worker. This first "Standard Man" consisted mainly of the specification of the masses of some important organs and tissues, specifications on intakes of air, water, and a few elements, and some data on excretion. It should be made clear that the Standard Man used by health physicists was never intended to represent man in all his aspects. The main purpose was to specify only those characteristics that were needed for purposes of dosimetry.

*School of Nuclear Engineering and Health Physics, Georgia Institute of Technology.

6.2 GENERAL CONCEPTS

The type of data needed for an internal dose calculation has been specified by Snyder (1966). These data are grouped according to the parameters needed to estimate dose from a radionuclide that has entered the body. The dose to a selected organ during the first 2 d following intake [$D(T)$] is

$$D(T) = I \cdot 51 \int_0^T [R(t)E(t)/M(t)]dt \,, \tag{6.1}$$

where

I = intake of the radionuclide by the body at time 0,
51 = constant in units of (disintegrations/d) × (g-rad/MeV),
$R(t)$ = fractional retention in the organ of interest at time t,
$E(t)$ = effective energy absorbed in the organ per disintegration,
$M(t)$ = mass of the organ of interest at time t.

To estimate I, data on intake of air and water, or of various foods (such as milk), may be needed. The intakes are required if the goal is to calculate a limiting concentration in these substances that would produce a prescribed dose. If the time t is not long, the organ mass may be considered constant. However, in cases where the radionuclides remain in the body for many years, it may be necessary to consider the variation of organ mass as a function of time. The effective energy absorbed per disintegration will depend on the size and shape of the organ of interest. These parameters may not be constant over long periods, especially during the early years when rapid growth occurs. However, in a number of cases $E(t)$ is considered to be constant.

One of the most difficult tasks is to estimate the fractional retention, $R(t)$, in the organ at time t. The initial uptake in the organ and the rate of elimination from the organ are directly related to $R(t)$. A large amount of data on the metabolic activity of the body can be applied to this problem. For example, the intake of stable elements and the concentrations of stable elements in relevant organs and tissues provide valuable information concerning the retention of radioisotopes over extended periods. For this reason, data on the intake of stable elements and data on the composition of tissues are important considerations in choosing $R(t)$ for a particular radionuclide.

The most complete specification of Standard Man, as it developed during the early period, was that included as part of the ICRP Publication 2 (ICRP 1959). These data included the distribution of elements in the total body and in selected body organs, and the masses and effective radii of organs in the adult human body (see Table 6.1). In addition, data on the intake and excretion of Standard Man were given as well as specifications of the gastrointestinal tract and some information on the respiratory tract. However,

Table 6.1. Organs of Standard Man—mass and effective radius of organs of the adult human body

	Mass, (g)	Percent of total body[a]	Effective radius, (cm)
Total body[a]	70,000	100	30
Muscle	30,000	43	30
Skin and Subcutaneous tissue[b]	6,100	8.7	0.1
Fat	10,000	14	20
Skeleton			
Without bone marrow	7,000	10	5
Red marrow	1,500	2.1	
Yellow marrow	1,500	2.1	
Blood	5,400	7.7	
Gastrointestinal tract[a]	2,000	2.9	30
Contents of GI tract			
Lower large intestine	150		5
Stomach	250		10
Small intestine	1,100		30
Upper large intestine	135		5
Liver	1,700	2.4	10
Brain	1,500	2.1	15
Lungs (2)	1,000	1.4	10
Lymphoid tissue	700	1.0	
Kidneys (2)	300	0.43	7
Heart	300	0.43	7
Spleen	150	0.21	7
Urinary bladder	150	0.21	
Pancreas	70	0.10	5
Salivary glands (6)	50	0.071	
Testes (2)	40	0.057	3
Spinal cord	30	0.043	1
Eyes (2)	30	0.043	0.25
Thyroid gland	20	0.029	3
Teeth	20	0.029	
Prostate gland	20	0.029	3
Adrenal glands or suprarenal (2)	20	0.029	3
Thymus	10	0.014	
Ovaries (2)	8	0.011	3
Hypophysis (pituitary)	0.6	8.6×10^{-6}	0.5
Pineal gland	0.2	2.9×10^{-6}	0.04
Parathyroids (4)	0.15	2.1×10^{-6}	0.06
Miscellaneous (blood vessels, cartilage, nerves, etc.)	390	0.56	

[a]Does not include contents of the gastrointestinal tract.

[b]The mass of the skin is taken to be 2000 g.

Source: International Commission on Radiological Protection 1959. *Recommendations of the International Commission on Radiological Protection, Report of Committee II on Permissible Dose for Internal Radiation,* ICRP Publication 2, Pergamon, Oxford.

these data represented only a standard adult and did not apply to dose estimation for fetuses, infants, children, or for nonstandard adults. The importance of this deficiency, coupled with the increased awareness of population exposures, led to further research on Standard Man. In December 1963, Committee II of the International Commission on Radiological Protection (ICRP) requested that the Commission establish a Task Group for the revision and extension of the Standard Man concept. The intent was to extend and revise the Standard Man concept to provide a more adequate basis for assessment of exposure of all groups of the population. Snyder (1966) stated the problem clearly:

> The real need of the health physicist is not merely one Standard Man; for, however carefully he may be defined, he will still be representative of only a small fraction of the population the health physicist must consider. Thus, the concept of Standard Man should not merely define an individual but should include ranges of variations about this norm and provide procedures for taking these individual differences into account when they significantly alter the dose estimate.

Later, at the suggestion of the ICRP, the name was changed from Standard Man to Reference Man.

6.3 THE ICRP REFERENCE MAN

The work of the ICRP Task Group on Reference Man took a number of years to complete. Their report was published in 1975 (ICRP 1975). Even with its publication, members of the Task Group recognized that Reference Man, as defined in the publication, could be improved extensively. At the same time, the health physics profession throughout the world recognized the tremendous stride forward that this massive work represented.

The definition of a Reference Man actually involved three separate pieces of research. Snyder's Task Group certainly carried a tremendous burden over the years in attempting to define Reference Man. However, their load was lightened somewhat when the ICRP formed a Task Group on Lung Dynamics (Morrow et al. 1966), and Eve and Dolphin undertook the preparation of a special report concerning estimation of dose to the gastrointestinal tract (Eve 1966; Dolphin and Eve 1966).

The goal of all this research was to define Reference Man, in the first instance, as a typical radiation worker. It was important to give some indication of variability of the occupationally exposed group about this norm. Secondly, differences due to age, sex, or habits would be given where possible, with emphasis on fetuses, infants, and children.

The Task Group agreed to select data primarily to represent what was believed to be a typical individual of the European or American populations. Reference Man was defined as being 20–30 years of age, 170 cm in height, weighing 70 kg, and living in a climate with an average temperature of from 10 to 20°C. He was a Caucasian and a Western European or North American in habitat and custom.

The Reference Man report (ICRP 1975) consists of three sections. There is a large section that specifies anatomical values for the Reference Man; it is broken down into general organ systems (e.g., cardiovascular system or digestive system) and then into a discussion of individual organs and glands that comprise the system. The second section of the report gives the gross and elemental content of Reference Man. The third section presents the physiological data, including a daily balance of elements in the body of Reference Man. Calculations of the specific absorbed fraction of photon energy are appended to the report. These data are for twelve monoenergetic photon sources (0.01–4.0 MeV) located uniformly in 16 different organs, including the total body.

It is extremely difficult to separate the development of Reference Man from the work of the Task Group on Lung Dynamics (Morrow et al. 1966) and the work of Eve and Dolphin on the gastrointestinal tract (Eve 1966; Dolphin and Eve 1966). It is even more difficult to discuss the relationship of these three efforts without bringing them into focus as they relate to internal dosimetry calculations.

6.3.1 Internal Dose Calculations and Reference Man

The primary use of the Reference Man formulation has been in the revision of ICRP Publication 2 (ICRP 1959). The ICRP has recently released estimates of limits for intakes for occupationally exposed workers (ICRP 1979). These reports have embodied all aspects of Reference Man, including models of the lung and gastrointestinal tract. Actually, the component parts have been assimilated in a single sophisticated computer code (Watson et al. 1976). However, the component parts are discussed in detail in the following sections for clarity.

6.3.2 General Considerations

The evaluation of potential exposures to radioactive materials presents rather complex problems, which must be considered for each radionuclide in various chemical forms and in various forms of particulate dispersion. Each chemical form of each element has different specific properties of solubility, transfer across membranes, distribution among the various tissues in the body, in some cases deposition in certain tissues, and finally excretion from the body.

The principal factors considered in an internal exposure evaluation include (1) the chemical form in which the various nuclides occur, (2) the relative abundance of the nuclide, (3) the characteristics of the aerosol or the fine powder in which the nuclide occurs, (4) the aerodynamic behavior of the aerosol particles as they are inhaled and deposited in various sections of the respiratory system, (5) the movement of particles within the respiratory tract and out of it into the lymphatic system and the gastrointestinal tract, (6) the absorption of the nuclide into the bloodstream, (7) the distribution of the radionuclide among organs and tissues, and (8) the retention of the nuclide by the body. In addition, each radionuclide emits different radiations. The half-life, type of radiations emitted, and the energy of these radiations must be considered. Furthermore, although an organ would be affected by any radiation from nuclides deposited in it, gamma rays also irradiate adjacent organs (called "cross fire"). This circumstance presents formidable geometric problems in internal exposure evaluations.

6.3.3 The Lung Model

The inhalation model used in Reference Man is that defined by the ICRP Task Group but with some modifications in the parameters to reflect newer data (Morrow et al. 1966; Lindenbaum et al. 1972). The lung model consists of a nasopharyngeal region (N-P), a tracheobronchial region (T-B), a pulmonary region (P), and the lymph nodes (L). Deposition is governed by the activity median aerodynamic diameter (AMAD) or the mass median aerodynamic diameter (MMAD) of the aerosol. The deposition model is shown in Fig. 6.1 and the retention model in Fig. 6.2.

The retention model in Fig. 6.2 presents a schematic representation of all dust deposition sites and clearance processes. In this figure, D_1 through D_4 are the amounts or concentrations of dust in various respiratory volumes or areas. For example, D_1 is the total dust inhaled (i.e., air concentration), D_2 is the amount of dust deposited in the nasopharyngeal region, D_3 is the dust deposited in the tracheobronchial region, and D_4 is the dust deposited in the pulmonary region. Ordinarily, D_2, D_3, and D_4 are expressed as percentages of D_1 and may be determined from the deposition model (see Fig. 6.1). The radioactive or mass fraction of an aerosol that is deposited in the nasopharyngeal, tracheobronchial, and pulmonary regions is given in relation to the AMAD or the MMAD of the aerosol distributions. The model is intended for use with aerosol distributions that have an AMAD or MMAD between 0.2 and 10 μm with geometric standard deviations of less than 4.5. Provisional deposition estimates further extending the size range are given by broken lines. For the unusual distribution having an AMAD or MMAD greater than 20 μm, complete nasopharyngeal deposition can be assumed. The model does not apply to aerosols with AMADs or MMADs below 0.1 μm.

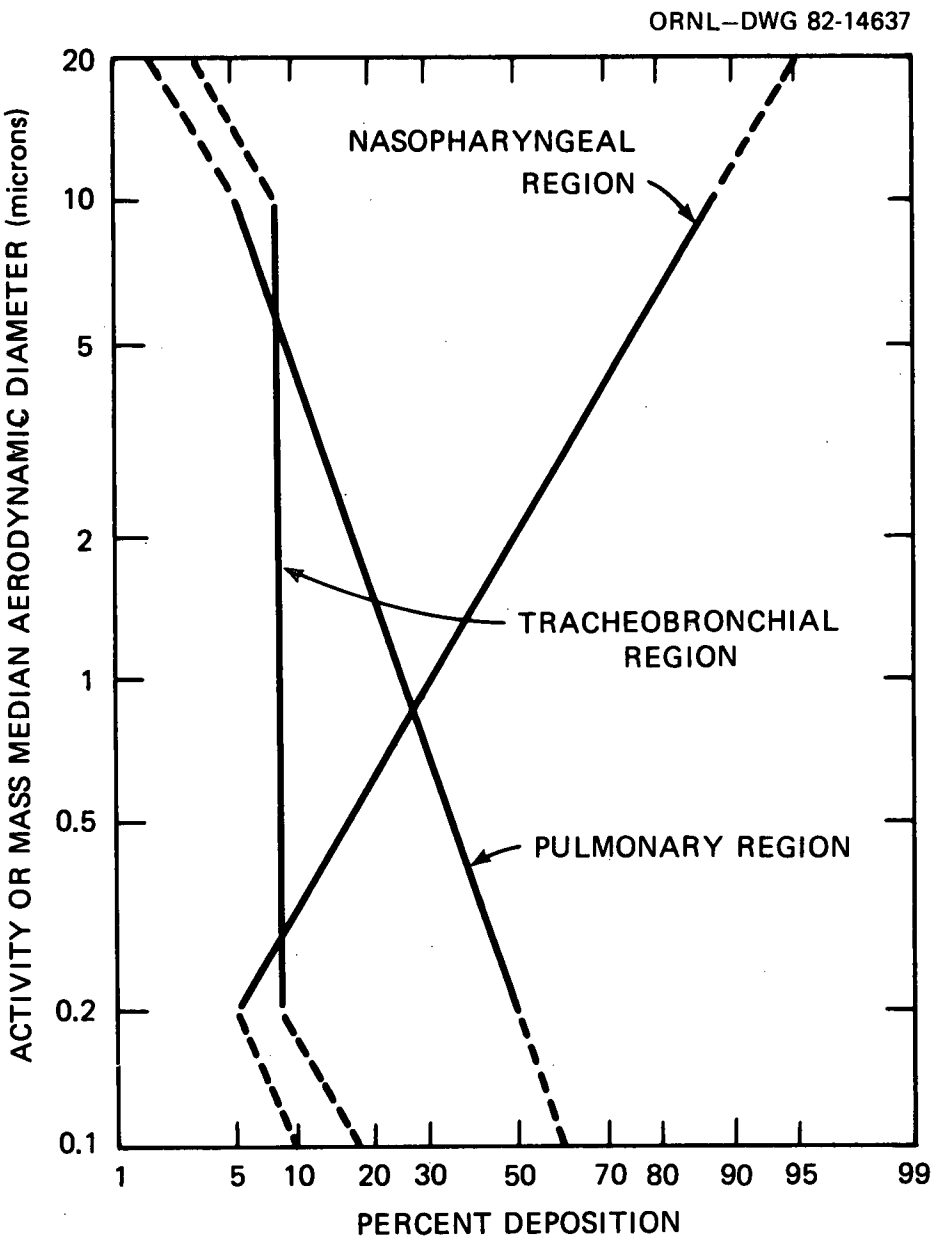

Figure 6.1. Deposition model. Source: Adapted from International Commission on Radiological Protection 1979. *Report of Committee 2, Limits for Intakes of Radionuclides by Workers,* ICRP Publication 30, *Ann. ICRP* 2(2–4).

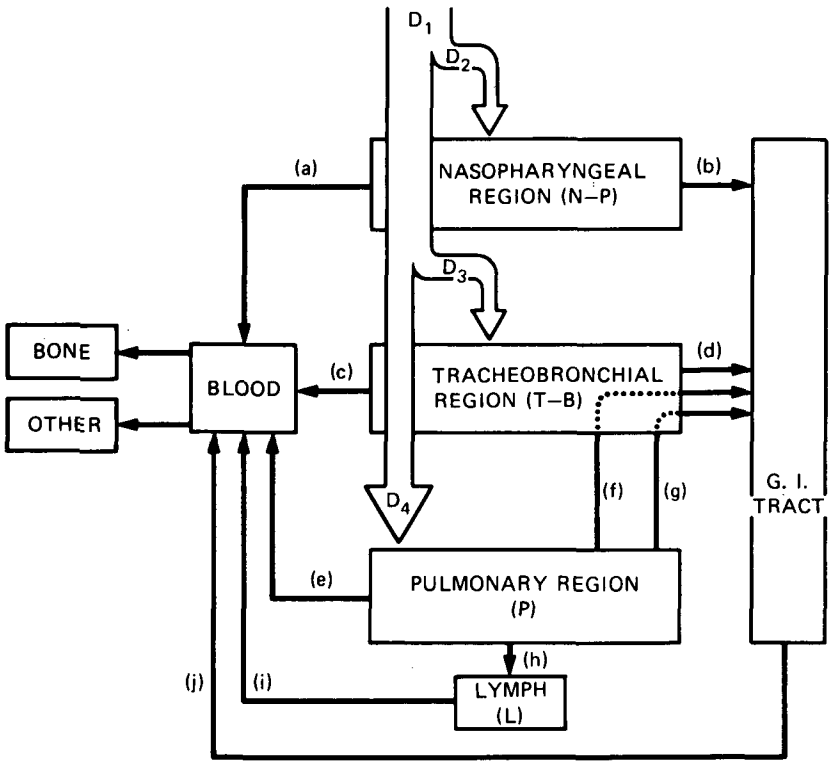

REGION	PATHWAY	COMPOUND CLASS (D)	(W)	(Y)
N–P	(a)	0.01 d/0.5	0.01 d/0.1	0.01 d/0.01
	(b)	0.01 d/0.5	0.4 d/0.9	0.4 d/0.99
T–B	(c)	0.01 d/0.95	0.01 d/0.5	0.01 d/0.01
	(d)	0.2 d/0.05	0.2 d/0.5	0.2 d/0.99
P	(e)	0.5 d/0.8	50 d/0.15	500 d/0.05
	(f)		1 d/0.4	1 d/0.4
	(g)		50 d/0.4	500 d/0.4
	(h)	0.5 d/0.2	50 d/0.05	500 d/0.15
L	(i)	0.5 d/1.0	50 d/1.0	1000 d/0.9

Figure 6.2. Retention model. Source: Adapted from International Commission on Radiological Protection 1979. *Report of Committee 2, Limits for Intakes of Radionuclides by Workers,* ICRP Publication 30, *Ann. ICRP* 2(3–4). See the text for description of pathways (a) through (j). In the table the first value is half-time for clearance (days), and the second value is the fraction leaving the region at the specified rate.

Calculations of the committed dose equivalent (H_{50}) due to internally deposited radionuclides assume an AMAD of 1 μm. Under this assumption, $D_2 = 0.30$, $D_3 = 0.08$, and D4 = 0.25. ICRP Publication 30 (ICRP 1979) also specifies a particle size correction method that allows the committed dose equivalent to be determined for aerosols with an AMAD different from the standard value.

The retention model has, in addition to the major respiratory regions, three other closely related organ systems: the gastrointestinal tract, systemic blood, and pulmonary lymph nodes. The letters "a" through "j" in Fig. 6.2 indicate the various absorption and translocation processes associated with the clearance of various compartments (Morrow et al. 1966):

Pathway	Description
(a)	Rapid uptake of material deposited in the nasopharynx region directly into the systemic blood.
(b)	Rapid clearance of all dusts from the nasopharynx region by ciliary-mucus transport.
(c)	Rapid absorption of dust deposited in the tracheobronchial compartment into the systemic circulation.
(d)	Analogous to (b) and represents the rapid ciliary clearance of the tracheobronchial region; the dust cleared by (d) goes quantitatively to the gastrointestinal tract.
(e)	Direct translocation of dust from the pulmonary region to the blood.
(f)	Relatively rapid clearance phase of the pulmonary region, which presumably depends on recruitable macrophages, and this in turn is coupled to the ciliary-mucus transport process; therefore, the dust cleared by (f) goes to the gastrointestinal tract via the tracheobronchial tree.

(g) Second pulmonary clearance process that is typically much slower than (f) but still depends on endocytosis and ciliary-mucus transport; the cleared dust goes via the tracheobronchial region to the gastrointestinal tract (the important distinction is that the clearance is apparently rate-limited in the pulmonary region by the nature of the deposited dust per se).

(h) Process describing the slow removal of dust from the pulmonary compartment via the lymphatic system; this process can be regarded as qualitatively similar to (g) with the exception that lymph transport replaces the ciliary-mucus transport.

(i) Secondary pathway in which dust cleared by the lymphatic system (h) is introduced into the systemic blood; this pathway obviously depends on the ability of the cleared material to penetrate the lymph tissue, especially the lymph nodes (this implies partial or complete dissolution of the dust particles, but the turnover of lymphocytes may contribute).

Note that this model specifies three compound classes in which material deposited in the pulmonary region of the lungs can be cleared. This classification applies to a range of half-times for D (less than 10 d), for W (from 10 to 100 d), and for Y (greater than 100 d).* The new classification is in sharp contrast to ICRP Publication 2 (ICRP 1959) in which materials were loosely classed as "soluble" and "insoluble."

The Reference Man report specifies a number of average respiratory values for use in dosimetric calculations. These data are summarized in Table 6.2. Note that adult activity is divided into three periods of equal length, whereas for the very young, much of the time is assumed to be spent resting. Alternate values for liters of air breathed per day which were about 40% higher than the values in Table 6.2 have been proposed. However, the Reference Man values are considered adequate for most situations.

*D = days; W = weeks; Y = years.

Table 6.2. Respiratory values for Reference Man

Activity	Adult man	Adult woman	Child (10 y)	Infant (1 y)	Newborn
			Liters of Air Breathed		
8 h working, "light activity"	9,600	9,100	6,240	2,500 (10 h)	90 (1 h)
8 h nonoccupational activity	9,600	9,100	6,240		
8 h resting	3,600	2,900	2,300	1,300 (14 h)	690 (23 h)
Total	2.3×10^4	2.1×10^4	1.5×10^4		
Percent breathed at work	42	43			
			Minute volume		
Resting (L/min)	7.5	6.0	4.8	1.5	0.5
Light activity (L/min)	20.0	19.0	13.0	4.2	1.5

Source: International Commission on Radiological Protection 1975. *International Commission on Radiological Protection, Task Group Report on Reference Man,* ICRP Publication 23, Pergamon, Oxford.

The minute volume (or respiratory volume) is the product of the tidal volume and frequency. Obviously, these latter parameters are dependent on the degree of activity, the altitude, and body temperature.

6.3.4 The Ingestion Model

Any exposure by ingestion, as well as any inhalation exposure, leads to radioactive materials entering the gastrointestinal tract. The dosimetric model for the gastrointestinal tract, shown in Fig. 6.3, is essentially that due to the work of Eve and Dolphin (Eve 1966; Dolphin and Eve 1966). In this work, subdivisions of the tract and transit times through these subdivisions were defined. Basically, the tract is divided into the stomach (S), the small intestine (SI), the upper large intestine (ULI), and the lower large intestine (LLI). Absorbed doses obtained by use of this model are considered to be averaged over the particular tract section. Table 6.3 presents pertinent facts on the average mass of food in each of the sections and the average length of time food stays in each section. This information is essentially that given by Eve (1966) or in the Reference Man report (ICRP 1975).

Each of the sections is considered a single compartment, and translocation from one compartment to the next is assumed to be governed by first-order kinetics. Thus, if $q(t)$ is the activity of ingested material in a compartment at time t, then the model is completely described by a set of differential equations. In addition, the model for a radioactive daughter produced in the gastrointestinal tract from its ingested parent radionuclide is completely described by a similar set of equations. Further, a system of similar equations can be devised that describes a chain of parent and daughter radionuclides. In this case, the activity of each daughter is determined by the activity of its predecessor in the chain. In all of these considerations, the metabolic behavior of the radioactive progeny is assumed to be the same as that of the ancestral radionuclide that was ingested.

Absorbed doses in the gastrointestinal tract for photon emitters are computed by use of the specific absorbed fraction technique reported by Snyder et al. (1974). For electrons, only a surface dose is computed. Alpha emitters are ineffective in reaching critical cells in the tract, and a factor is normally applied to calculated absorbed doses to express this fact.

The Reference Man report specifies many parameters that impact on the gastrointestinal tract model. These include data on the water balance for Reference Man as well as information on the dietary intake and excretion of certain major elements.

Table 6.4 presents a summary of the water balance data. The estimates for milk and tap water intakes are well documented, but the Task Group points out that the intake of other water-based fluids is probably underestimated. The total fluid intake of 1950 mL/d was selected as being representative of the actual values, which ranged from 1000 to 2400 mL/d at moderate temperatures.

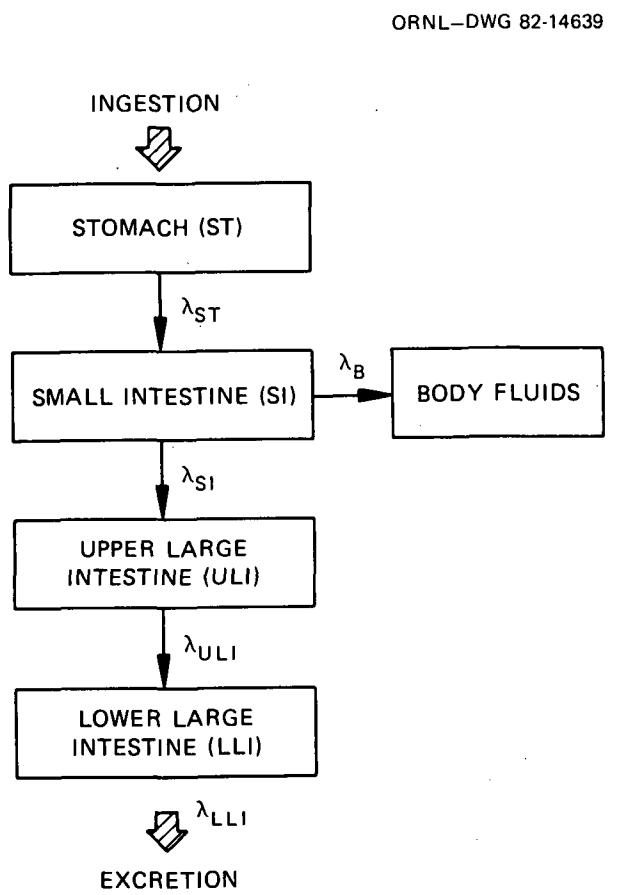

Figure 6.3. Mathematical model used to describe the kinetics of radionuclides in the gastrointestinal tract. Source: International Commission on Radiological Protection 1979. *Report of Committee 2, Limits for Intakes of Radionuclides by Workers,* ICRP Publication 30, *Ann. ICRP* **2**(3–4).

Insensible water loss is dependent on body surface area, body weight, body temperature, and metabolic rate. The daily loss through the skin is in the range of 350 to 1900 mL for adults. Of this amount, approximately one-quarter to one-third is lost through the lungs in expiration, with the remainder lost through the skin.

Table 6.5 summarizes the excretion parameters selected for Reference Man. The intake and loss of the major elements (i.e., carbon, hydrogen, oxygen, and nitrogen) are given in Table 6.6. The daily balance of other important elements selected for Reference Man is presented in Table 6.7. All of these

Table 6.3. Gastrointestinal Tract Model for Reference Man

Section of GI tract	Mass of walls[a] (g)	Mass of contents[a] (g)	Mean residence time (d)	λ (d^{-1})
Stomach	150	250	1/24	24
Small intestine	640	400	4/24	6
Upper large intestine	210	220	13/24	1.8
Lower large intestine	160	135	24/24	1

[a]Values from ICRP Publication 23 (ICRP 1975).

Source: International Commission on Radiological Protection 1979. *International Commission on Radiological Protection, Report of Committee 2, Limits for Intakes of Radionuclides by Workers,* ICRP Publication 30, *Ann. ICRP* **2**(3–4).

data are useful in the evaluation of exposure due to internally deposited radionuclides. However, it should be remembered that these values were selected as representative of an adult male and do not apply to a particular individual. For example, the total weight of feces lost each day by adults ranges from 60 to 500 g, with a mean value of 150 g (ICRP 1975). Yet, the Task Group selected 135 g for Reference Man (see Table 6.5). Similar statements also apply to the data on urinary excretion. The daily volume of urine for the adult ranges from 500 to 2900 mL, and a value of 1400 mL/d was selected for Reference Man.

Additional information contained in the Reference Man report is provided to assist in the evaluation of internal exposures in nonoccupational situations. Table 6.8 gives data on the dietary intake of populations in the United States, the United Kingdom, and Europe (i.e., European Economic Community). Note that these data represent per capita consumption and not the consumption of a Reference Man. In addition, the Task Group points out that these values (i.e., Table 6.8) are not intended for use in a dietary intake model.

Data on milk consumption are presented in Table 6.9. These data are calculated representative intakes for males and females as a function of age obtained from surveys in North America, Western Europe, and Australia. Milk consumption by adults varies widely according to personal habits. The Task Group selected 300 mL/d as the intake of milk for Reference Man. Data for an adult woman and a 10-year-old child were presented earlier in Table 6.4.

Table 6.4. Water balance for Reference Man

	Adult man		Adult woman		Child (10 y)	
	Gains (mL/d)	Losses (mL/d)	Gains (mL/d)	Losses (mL/d)	Gains (mL/d)	Losses (mL/d)
Milk	300	1400 in urine	200	1000 in urine	450	1000 in urine
Tap water	150	100 in feces	100	90 in feces	200	70 in feces
Other fluids	1500	850 insensible loss	1100	600 insensible loss	750	580 insensible loss
Total intake in fluids	1950		1400		1400	
In solid food	700	650 in sweat	450	420 in sweat	400	350 in sweat
By oxidation of food	350		250		200	
Totals	3000	3000	2100	2110	2000	2000

Source: International Commission on Radiological Protection 1975. *International Commission on Radiological Protection, Task Group Report on Reference Man,* ICRP Publication 23, Pergamon, Oxford.

Table 6.5. Excretion parameters for Reference Man

Parameter	Adult man	Adult woman	Child (10 y)	Infant (1 y)
		Urinary values		
Volume (mL/d)	1400	1000	1000	450
Specific gravity	1.02			1.01
pH	6.2			
Solids (g/d)	60	50	47	19
Urea (g/d)	22			
"Sugars" (g/d)	1			
Bicarbonates (g/d)	0.14	0.12		
		Fecal values (g/d)		
Weight	135	110	85	24
Water	105	90	70	19
Solids	30	20	19	5
Ash	17	15	6	1
Fats	5	4.5	4	3
Nitrogen	1.5	1.3	1	0.3
Other substances	6.5	5	8	0.7

Source: International Commission on Radiological Protection 1975. *International Commission on Radiological Protection, Task Report on Reference Man,* ICRP Publication 23, Pergamon, Oxford.

6.3.5 Computer Techniques

The models and data discussed above, as well as models for the retention and excretion of most elements, have been incorporated into a number of computer codes at various levels of sophistication. The code used for the latest ICRP calculations (ICRP 1979) is that described by Watson and Ford (1980). This large computer code is actually composed of three computer codes, two of which may be used as "stand alone" codes for specific calculational needs. These individual codes are called SEE, ICRP TIMED, and DOSE (Watson and Ford 1980).

The goal is to calculate the committed dose equivalent ($H_{50,T}$) and secondary and derived limits on occupational exposure. The committed dose equivalent in a particular organ or tissue T is simply the total dose equivalent

Table 6.6. Intake and loss of major elements in Reference Man

Element	Adult man	Adult woman	Child (10 y)	Infant (1 y)
		Dietary intake (g/d)		
Carbon	300	210	200	
Hydrogen	350	245	230	
Nitogen	16	13	10	
Oxygen	2600	1800	1700	
Sulfur	1	0.7	0.7	
		Urinary losses (g/d)		
Nitrogen	15	13	11	5
Hydrogen	160	130	110	50
Oxygen	1300	1100	970	420
Carbon	5	4	3	0.5
		Fecal losses[a] (g/d)		
Carbon	7	6	4.2	1.2
Hydrogen	13	11	8.6	2.5
Nitrogen	1.5	1.3	1.0	0.3
Oxygen	100	90	62	17

[a]Fats assumed to be $(C_{15}H_{31}C00)_3C_3H_5$, and "other substances" assumed to be $(C_6H_{10}0_5)_x$. See Table 6.5.

Source: International Commission on Radiological Protection 1975. *International Commission on Radiological Protection, Task Group Report on Reference Man,* ICRP Publication 23, Pergamon, Oxford.

(H) to which that organ or tissue would be committed for 50 y after intake of the radionuclide. Basically, the total dose equivalent is given by

$$H(\mathrm{T},t) = k\sum_i U_{\mathrm{Y}_i}(t)\cdot \mathrm{SEE}(\mathrm{T}\leftarrow \mathrm{Y}_i)\,, \qquad (6.2)$$

where $U_{y_i}(t)$ is the cumulated activity in various source organs Y_i at time t after deposition, and SEE(T$\leftarrow Y_i$) is the specific effective energy absorbed in the target organ T from each transformation in Y_i. The three program modules are designed to perform these calculations. The SEE code and the ICRP TIMED code supply the specific effective energies and the cumulated

Table 6.7. Daily balance of other important elements in reference man

Element	Intake (μg/d)		Losses (μg/d)		
	Food & fluids	Airborne	Urine	Feces	Others
Calcium	1.1×10^6		1.8×10^5	7.4×10^5	3.2×10^4–1.5×10^5 sweat; trace hair and other fluids
Cesium	10	0.025	9.0	<1.0	Sweat, saliva
Chromium	150	0.1	70	80	1 sweat, 0.6 hair, nails; trace other fluids
Cobalt	300	<0.1	200	90	4 sweat, 2.4 hair; trace other fluids
Copper	3.5×10^3	20	50	3.4×10^3	40–400 sweat; 3 hair, nails; 20 menstrual loss; trace other fluid
Iodine	200	0.5–35	170	20	6 sweat; 2.3 hair, other fluids
Iron	1.6×10^4	30	250	1.5×10^4	500 sweat; 13 hair, nails
Lead	440	10	45	300	65 sweat; 30 hair
Manganese	3.7×10^3	2	30	3.6×10^3	39 sweat; 2 hair, nails
Mercury	15	1	0–35	10	Trace sweat; 0.9 hair
Phosphorus	1.4×10^6		9×10^5	5×10^5	1×10^3 sweat; 1×10^2 hair; trace other fluids
Polonium[a]	3.2	<0.01	0.011	3.2	Trace, sweat, hair
Potassium	3.3×10^6		2.8×10^6	3.6×10^5	1.3×10^5 sweat; trace other fluids
Radium[b]	2.3		0.08	2.2	Not known
Sodium	4.4×10^6		3.3×10^6	1.0×10^5	8.7×10^5 sweat; 1.3×10^5 other fluids
Strontium	1.9×10^3		340	1.5×10^3	20 sweat
Sulfur	8.5×10^5	$1–4 \times 10^3$	8×10^5	1.4×10^5	2.6×10^3 sweat; 3.2×10^3 hair, nails
Thorium	3		0.1	2.9	
Uranium	1.9	7×10^{-3}	0.05–0.5	1.4–1.8	0.02 hair
Zinc	1.3×10^4	100	500	1.1×10^4	780 sweat; 30 hair, nails
Zirconium	4.2×10^4		150	4×10^3	

[a] Values are given in pCi/d of ^{210}Po (1 pCi $\simeq 2 \times 10^{-10}$ μg).
[b] Values are given in pCi/d of ^{226}Ra (1 pCi $= 1 \times 10^{-6}$ μg).

Source: International Commission on Radiological Protection 1975. *International Commission on Radiological Protection, Task Group Report on Reference Man,* ICRP Publication 23, Pergamon, Oxford.

Table 6.8. United States, British, and European Economic Community dietary intake

Food groups	Consumption per capita (g/d)		
	USA 1955[a]	UK 1962–65	EEC 1963–65
Milk[b] (as liquid)	508	382	287
Cheese	19	12	21
Meat and meat products	206	137	118
Fish and seafood	22	21	22
Eggs	47	34	21
Fats	49	44	63
Sugars and preserves	69	77	57
Potatoes	103	202	196
Other vegetables	202	118	180
Fruit	184	108	114
Cereals	207	246	346

[a]A more recent survey of household consumption in the U.S. for spring 1965 indicates a 10% decline in the consumption of milk products and fats, a 20% decline in flour and cereals (but 14% increase in bakery products), an increase of 10% in meats and poultry, a decline of less than 10% in sugar, and a decline of 15% in potato consumption as compared with the 1955 data.

[b]This includes milk and milk products with the exception of cheese, which is listed separately.

Source: International Commission on Radiological Protection 1975. *International Commission on Radiological Protection, Task Group Report on Reference Man,* ICRP Publication 23, Pergamon, Oxford.

Table 6.9. Model milk consumption

Age (y)	Male (mL/d)	Female (mL/d)
0.25	750	600
0.50	1000	800
0.75	850	650
1	580	500
2	500	440
3	490	440
4	490	430
5	490	430
6	490	440
8	490	440
10	480	420
12	470	390
15	440	330
17	410	280
20	330	200
40	270	140
60 and >60	250	130

Source: International Commission on Radiological Protection 1975. *International Commission on Radiological Protection, Task Group Report on Reference Man,* ICRP Publication 23, Pergamon, Oxford.

activity, respectively, for use in the DOSE code. These codes are discussed further below.

The SEE code incorporates much of the anatomical information given in Reference Man (ICRP 1975). A mathematical description of an adult human has been formulated and is used to provide estimates of photon absorbed fractions in the phantom. The phantom, developed originally by Fisher and Snyder (1967), has been reported widely, and over the years additional modifications have been made to it to make it more suitable for dose calculations (Snyder et al. 1974) and, at the same time, more realistic. The phantom is shown in Fig. 6.4 and 6.5, and Table 6.10 lists the source and target organ masses used in the ICRP calculations.

The total-body phantom consists of three principal sections: (1) an elliptical cylinder representing the arms, torso, and hips; (2) two truncated elliptical

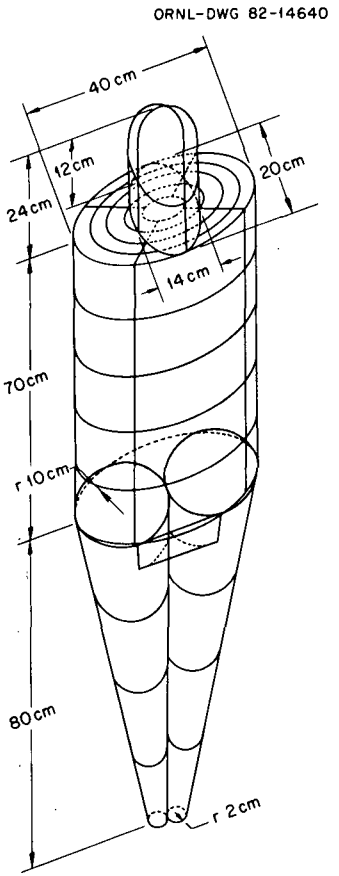

Figure 6.4. The adult human phantom.

cones representing the legs and feet, and attached to this is a small region with a plane front surface to contain an approximation of the testicles; and (3) an elliptical cylinder representing the neck region and the lower portion of the head, which is topped by half an ellipsoid. The exterior of the phantom is shown in Fig. 6.4. Note that the arms are not separated from the torso and that minor appendages such as fingers, feet, ears, chin, and nose are omitted. The dimensions of the phantom were chosen after consideration of the distribution of dimensions and weights of certain western populations (Altman and Dittmer 1962; Krogman 1941), of previous phantoms (Hayes and Brucer 1960), and Reference Man (ICRP 1975). The major deviation from the information given in Reference Man is that the adult phantom is 174 cm in height rather than the prescribed 170 cm.

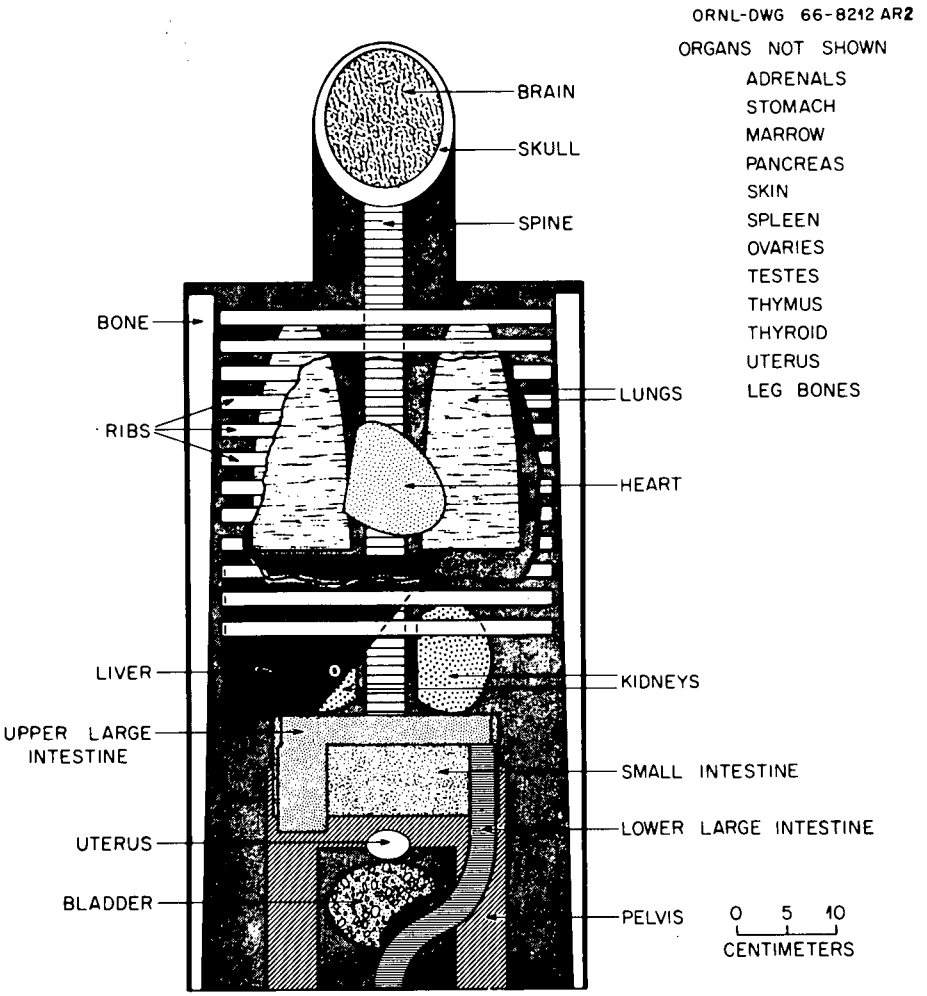

Figure 6.5. Anterior view of principal organs in the head and trunk of the phantom.

The phantom consists of three types of tissue: lung and skeletal tissue and other soft tissue. The composition and density of each type is shown in Table 6.11. The skeletal system represents the total content of the intact skeleton (see Fig. 6.6) and includes both bone and bone marrow. This material is considered to be distributed homogeneously throughout the skeleton. This is clearly a compromise due to the inability to represent more accurately the bone and marrow spaces. However, the distribution of yellow and red bone marrow is considered in the design (see Table 6.12, for example). Neverthe-

Table 6.10. Source and target organs and their masses

Source organ	Mass (g)	Target organ	Mass (g)
Adrenals	14	Adrenals	14
Bladder contents	200	Bone surfaces	120
Stomach contents	250	Bladder wall	45
Small intestine contents	400	Stomach wall	150
Upper large intestine contents	220	Small intestine wall	640
Lower large intestine contents	135	Upper large intestine wall	210
Kidneys	310	Lower large intestine wall	160
Liver	1,800	Kidneys	310
Lungs	1,000	Liver	1,800
Muscle	28,000	Lungs	1,000
Ovaries	11	Muscle	28,000
Pancreas	100	Ovaries	11
Cortical bone	4,000	Pancreas	100
Trabecular bone	1,000	Red marrow	1,500
Red marrow	1,500	Skin	2,600
Skin	2,600	Spleen	180
Spleen	180	Testes	35
Testes	35	Thymus	20
Thyroid	20	Thyroid	20
Total body	70,000	Uterus	80

Source: Watson, S. B., and Ford, M. R. 1980. *A User's Manual to the ICRP Code—A Series of Computer Programs to Perform Dosimetric Calculations for the ICRP Committee 2 Report,* ORNL/TM-6980, Oak Ridge National Laboratory, Oak Ridge, Tenn.

less, the tissue composition shown in Table 6.11 can be regarded only as an average. The composition is clearly not representative of different portions of the skeleton but only of the total.

The three tissue types used (i.e., lungs, skeleton, and other soft tissues) are composed principally of hydrogen, carbon, nitrogen, and oxygen. In the skeleton, additional elements amount to about 18% of the total mass, with calcium and phosphorus accounting for most of this. In the lungs, the composition is slightly different from that of other soft tissues in the remainder of the phantom because the lungs contain little fat and a larger fraction of blood than most organs. The densities of the skeletal region (bone plus marrow), lungs, and the remainder of the phantom are approximately 1.4862, 0.2958, and

Table 6.11. Elemental composition of different tissues of the phantom (% by weight)

Element	Skeletal tissue[a]d	Lung tissue[b]	Total body minus skeleton & lungs[c]
Hydrogen	7.04	10.21	10.47
Carbon	22.79	10.01	23.02
Nitrogen	3.87	2.80	2.34
Oxygen	48.56	75.96	63.21
Sodium	0.32	0.19	0.13
Magnesium	0.11	7.4×10^{-3}	0.015
Phosphorus	6.94	0.081	0.24
Sulfur	0.17	0.23	0.22
Chlorine	0.14	0.27	0.14
Potassium	0.15	0.20	0.21
Calcium	9.91	7.0×10^{-3}	0
Iron	8.0×10^{-3}	0.037	6.3×10^{-3}
Zinc	4.8×10^{-3}	1.1×10^{-3}	3.2×10^{-3}
Rubidium	0	3.7×10^{-4}	5.7×10^{-4}
Strontium	3.2×10^{-3}	5.9×10^{-6}	3.4×10^{-5}
Zirconium	0	0	8.0×10^{-4}
Lead	1.1×10^{-3}	4.1×10^{-5}	1.6×10^{-5}

[a]Density 1.4862 g/cm^3.
[b]Density 0.2958 g/cm^3.
[c]Density 0.9869 g/cm^3.

0.9869 g/cm^3, respectively. The values of the composition were obtained from the analysis of tissue specimens obtained from autopsies of 150 grossly normal U.S. adults (Tipton et al. 1966). These specimens were analyzed for a wide variety of trace elements. Values were selected from the literature for the major chemical elements to be consistent with physiological data on content of fat, water, and other constituents of these organs.

In addition to the mathematical description of the exterior surface of the phantom, the skeleton, and the lung region, a number of other organs were specified in the mathematical phantom. The description of the interior organs was generally correct as to size, shape, position, composition, and density. However, simplified equations were used to provide formulas that were readily calculated on a digital computer. This phantom serves as the basis for calculations of specific effective energies in the SEE code.

Basically, the formula for computing the specific effective energy (SEE) from source organ Y_i to target organ T is given by

$$\mathrm{SEE}(\mathrm{T} \leftarrow \mathrm{Y}_i) = \sum_j f_j E_j \Phi_j(\mathrm{T} \leftarrow \mathrm{Y}_i) Q_j N_j(\mathrm{T}) , \qquad (6.3)$$

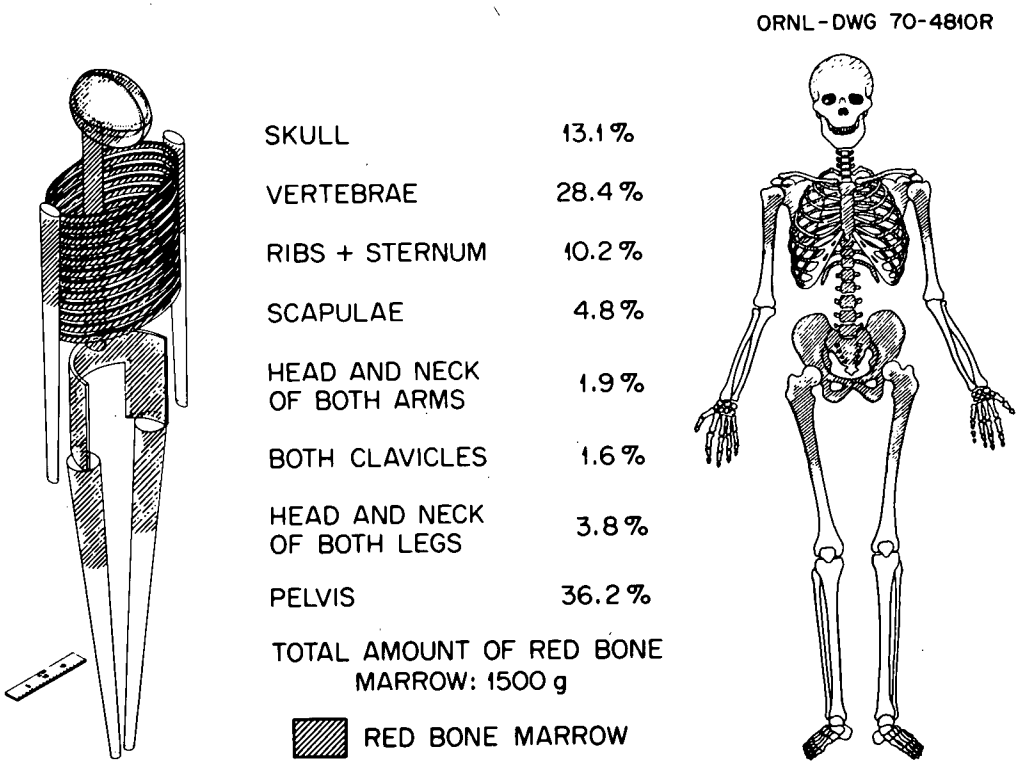

Figure 6.6. Idealized model of the skeleton for computer calculations with percentages of red bone marrow.

where

f_j = yield in particles per disintegration for radiation of type j,

E_j = average energy or unique energy of the jth type of radiation,

$\Phi_j(T \leftarrow Y_i)$ = specific absorbed fraction of energy (or fraction of energy absorbed per gram of target organ T) from the jth type radiation in source organ Y_i,

$Q_j, N_j(T)$ = appropriate quality factor and modifying factor for the j-type radiation in the target organ. $N_j(T)$ should be taken as one for all types of radiation.

The absorbed fraction, $\phi_j(T \leftarrow Y_i)$, where $\Phi_j(T \leftarrow Y_i) = \phi_j(T \leftarrow Y_i)$/mass of T, for photons used in calculating SEE was obtained principally by two methods. The primary method used Monte Carlo techniques, and all organ

Table 6.12. Masses of red and yellow marrow and bone in the phantom

Bone region	Red marrow (g)	Bone (g)	Yellow marrow (g)
Arms			
Upper	28.5	474	9.5
Lower	0	520	389
Clavicles	24	49	8
Legs			
Upper	57	2036	19
Lower	0	1588	461
Pelvis	543	177	181
Ribs	153	677	201
Scapulae	72	206	24
Skull			
Cranium	178.5	557	59.5
Mandible	18	439	6
Spine			
Upper	51	130	17
Middle	211.5	533	70.5
Lower	163.5	87	54.5
Total	1500	7473	1500

pairs for which the coefficient of variation* did not exceed 50% were accepted using this method. A secondary method made use of the buildup factor formulation of Berger (1968). This technique was used to calculate absorbed fractions for organ pairs failing to meet the coefficient of variation criterion. The table of photon-specific absorbed fractions used in the calculation of SEE values is given in a report by Snyder et al. (1974). The data are for 12 monoenergetic photons ranging in energy from 0.01 to 4 MeV and distributed uniformly in 22 source organs of a mathematical anthropomorphic phantom whose organs approximate those of their prototype in size, shape, composition, and density. The quality factor Q_j is assumed to be 1 for photon emitters.

*Coefficient of variation = $100\ \sigma_\phi/\phi$.

The absorbed fractions for electrons, positrons, and beta rays are assumed generally to be equal to zero if the source and target organs are separated, or equal to 1 if the organs coincide. Organs with walls are exceptions to this rule. In this case, the absorbed fractions are equal to one-half the ratio of the mass of the wall to the mass of the contents times a factor, v_j, representing the degree to which the particular radiation penetrates the gastrointestinal mucosa. For beta particles, etc. the factor is assumed to be 1.0.

For radionuclides in bone, additional modifications are required. The absorbed fractions for beta emitters in bone are a function of the source and target organs in question as well as the class of the radionuclide (i.e., surface or volume seeker). In addition, for surface-seeking radionuclides, the average energy must be considered. In all cases, the quality factor is assumed to be 1.0 for electrons, positrons, and beta rays.

For alpha particles and recoil nuclei, the energy is assumed to be absorbed in the source tissue. For organs with walls, the energy contribution is estimated from the surface dose. The absorbed fractions for recoil nuclei are assumed to be zero for the segments of the gastrointestinal tract. The absorbed fractions for dosimetry of radionuclides in bone have been recommended by the ICRP (1979). The quality factor Q_j is assumed to be 20 for alphas and alpha recoils.

The code also treats spontaneously fissioning radionuclides. SEE values for contributions arising in spontaneous fission from fission fragments, neutrons, gamma rays, and beta particles are also calculated in the SEE code package. The quality factor for fission fragments is 20, and v_j is 0.01.

The second module of the ICRP code is a modification of the TIMED program (Watson et al. 1976) renamed the ICRP TIMED code (Watson and Ford 1980). This code is used to compute the cumulated activity $U_{Y_i}(t)$ at some time t after a 1-μCi intake. The code was modified to meet the recommendations of ICRP Committee 2. The basic considerations used in the lung model, the gastrointestinal tract model, and the metabolic information available are embodied in this code.

The final module in this important calculation is the DOSE program. The purpose of this program is to combine the specific effective energy values computed by the SEE code and the cumulated activities calculated by the ICRP TIMED code to calculate dose equivalent. The dose equivalent is given by

$$H(\mathrm{T},t) = k \sum_i U_{\mathrm{Y}_i}(t) \cdot \mathrm{SEE}(\mathrm{T} \leftarrow \mathrm{Y}_i) , \qquad (6.4)$$

where $H(\mathrm{T},t)$ is the total dose equivalent. If $t = 50$ y, then the total dose equivalent is equal to the total committed dose equivalent ($H_{50,\mathrm{T}}$). In the ICRP calculations, the cumulated activity is in units of transformations per becquerel, and the specific effective energy is in units of million electron volts per gram per transformation. The factor k has the value 1.6×10^{-10} (J/MeV) · (g/kg). Using the calculated dose equivalent values, the annual limit on

intake (ALI) and the derived air concentrations (DAC) are calculated for a given chain of radionuclides.

6.4 SUMMARY

The concept of a Standard Man (later changed to Reference Man) for use in internal dose calculations originated more than 30 years ago. It was clear that the estimation of absorbed dose due to external or internal radiation sources required the specification of certain information regarding the exposed individual. For external radiation sources, the information required is little more than specification of the size and mass, dimensions, and elemental composition of certain organs. However, when the source is internal to the human body, the exposure situation is much more complex, requiring much more highly refined data.

This chapter has attempted to summarize the current state of Reference Man as it relates to internal exposure evaluations. The discussions have included not only the anatomical and physiological data given in the Reference Man report (ICRP 1975), but also the development of more detailed models of the gastrointestinal tract (Eve 1966) and the respiratory system (Morrow et al. 1966). Finally, these data and models are discussed in relation to available computer codes leading to the latest publications of the ICRP (1979).

This chapter has attempted to bring together pertinent information on a reference individual (Reference Man) for use in dose calculations. An understanding of the complexity of internal dose calculations makes it very clear that the Reference Man concept is the keystone to such calculations. Although many individuals have participated in these developments over the more than 20 years that have elapsed since the publication of the original Committee II report, the primary burden was borne by one individual, Walter S. Snyder. We shall always owe Walter a debt of gratitude for his work in this area and his firm resolve to complete the work. Many of us will remember the tough times when there seemed to be no end to the details to be considered. I, for one, shall always remember the twinkle in his eye when he came to me to share a problem or a story regarding the work. I am sure such memories guided those who carried the work forward after his death. Nevertheless, in my heart, this work shall always bear the indelible stamp of Walter S. Snyder.

6.5 PROBLEMS

1. Inhalation and ingestion parameters discussed in this chapter do not appear explicitly in the calculation of dose equivalent or committed dose equivalent. Explain the necessity for specifying these parameters and identify the role they play in setting limits for exposure to internally deposited radionuclides.

2. The absorbed fraction is defined as the ratio of the energy absorbed in an organ to energy emitted by the source. Assume that the radiation source is contained entirely in one organ. For a constant photon energy, how will the absorbed fraction vary as the organ size (mass) is increased?...decreased?

3. For an organ of constant mass, how will the absorbed fraction vary as the photon energy is increased?...decreased?

4. The text states that every exposure to radioactive materials via the inhalation pathway is also an exposure by the ingestion pathway. Explain.

5. Explain in your own words the meaning of the term "cross fire." Why is it an important consideration in internal dosimetry calculations?

6. Calculations of absorbed fractions for monoenergetic photon sources are included as an appendix to the Reference Man Report. These data are derived for idealized organ shapes, with the masses specified for Reference Man. Deduce the probable scaling laws that could be used to apply these Reference Man data to a nonstandard radiation worker.

7. The lung model and the gastrointestinal model discussed in this chapter differ significantly from earlier models. Investigate the early models; discuss the difference and the impact of these differences on internal dosimetry calculations.

8. In the latest formulations on internal dose published by the International Commission on Radiological Protection, alpha particles are assigned a quality factor (Q) of 20. Discuss the importance of this change in quality factor as it relates to the dosimetry of alpha-emitting radionuclides deposited in the skeleton.

REFERENCES

Altman, P. L., and Dittmer, D. S. 1962. "Growth Including Reproduction and Morphological Development," in *Biological Handbook,* Federation American Societies for Experimental Biology, Washington, D.C.

Berger, M. J. 1968. "Energy Deposition in Water by Photons from Point Isotropic Sources," *J. Nucl. Med.,* Suppl. No. 1, pp. 15–25.

Dolphin, G. W., and Eve, I. S. 1966. "Dosimetry of the Gastrointestinal Tract," *Health Phys.* **12**(2), 163.

Eve, I. S. 1966. "A Review of the Physiology of the Gastrointestinal Tract in Relation to Radiation Doses from Radioactive Materials," *Health Phys.* **12**(2), 131.

Fisher, H. L., Jr., and Snyder, W. S. 1968. *Distribution of Dose in the Body from a Source of Gamma Rays Distributed Uniformly in an Organ,* ORNL-4168, Union Carbide Corp., Nuclear Div., Oak Ridge Natl. Lab., p. 245.

Hayes, R. L., and Brucer, M. 1960. "Compartmentalized Phantoms for the Standard Man, Adolescent, and Child," *Int. J. Appl. Radiat. Isot.* **9,** 113.

International Commission on Radiological Protection (ICRP) 1959. *Recommendations of the International Commission on Radiological Protection, Report of Committee II on Permissible Dose for Internal Radiation,* ICRP Publication 2, Pergamon, Oxford.

International Commission on Radiological Protection (ICRP) 1975. *International Commission on Radiological Protection, Task Group Report on Reference Man,* ICRP Publication 23, Pergamon, Oxford.

International Commission on Radiological Protection (ICRP) 1979. *International Commission on Radiological Protection, Report of Committee II, Limits for Intakes of Radionuclides by Workers,* ICRP Publication 30. *Ann. ICRP* **2**(3–4) and **3**(1–4).

Krogman, W. M. 1941. "Growth of Man," *Tabulae Biol.* **20,** 712.

Lindenbaum, A., Lafuma, J., Rosenthal, M. W., Snyder, W. S., Taylor, D. M., Thompson, R. C., Izawa, M., Moskalev, Y. O., and Vaughn, M. 1972. *The Metabolism of Compounds of Plutonium and Other Actinides,* ICRP Publication 19, Pergamon, Oxford.

Morrow, P. E., Bates, D. V., Fish, B. R., Hatch, T. F., and Mercer T. T. 1966. "Deposition and Retention Models for Internal Dosimetry of the Human Respiratory Tract," *Health Phys.* **12,** 173.

National Council on Radiation Protection and Measurements (NCRP) 1950. *Chalk River Conference on Permissible Internal Dose, A Conference of Representatives from the United Kingdom, Canada, and the United States, Held in Chalk River, Canada, September 29–30, 1949,* RM-10.

Snyder, W. S. 1966. "The Standard Man in Relation to Internal Radiation Dose Concepts," *Am. Ind. Hyg. Assoc. J.* **27,** 539.

Snyder, W. S., Ford, M. R., Warner, G. G., and Watson, S. B. 1974. *A Tabulation of Dose Equivalent per Microcurie-Day for Source and Target Organs for an Adult for Various Radionuclides,* ORNL-5000, Union Carbide Corp., Nuclear Div., Oak Ridge Natl. Lab.

Tipton, I. H., Snyder, W. S., and Cook, M. J. 1966. "Elemental Composition of Standard Man," p. 241 in *Health Physics Division Annual Progress Report for Period Ending July 31, 1966,* ORNL-4007, Union Carbide Corp., Nuclear Div., Oak Ridge Natl. Lab.

Watson, S. B., and Ford, M. R. 1980. *A User's Manual to the ICRP Code—A Series of Computer Programs to Perform Dosimetric Calculations for the ICRP Committee 2 Report,* ORNL/TM-6980, Union Carbide Corp., Nuclear Div., Oak Ridge Natl. Lab.

Watson, S. B., Snyder, W. S., and Ford, M. R. 1976. *TIMED: A Computer Program for Calculating Cumulated Activity of a Radionuclide in the Organs of the Human Body at a Given Time, t, After Deposition,* ORNL/CSD/TM-17, Union Carbide Corp., Nuclear Div., Oak Ridge Natl. Lab.

7 Internal Dosimetry

By G. G. KILLOUGH* *and* K. F. ECKERMAN*

7.1 INTRODUCTION

Internal dosimetry, as it is presented in this chapter, seeks to estimate the radiation energy deposited in various organs and tissues of the body by alpha, beta, and photon emissions of radionuclides that are taken into the body by ingestion, inhalation, or direct injection. The deposited energy per unit mass, averaged over the organ or tissue of interest, is converted into one of several definitions of *dose* to the organ or tissue in ways that are described in Sect. 7.2.

Internal dose is not measured directly; it is inferred from estimates of intake by the application of radiation physics and mathematical models of translocation and metabolism of the material in the body. A principal aim of this chapter is to give the reader a first acquaintance with those methods and models that are currently being applied in internal dosimetry for purposes of radiation protection. While the models are simple in concept, making calculations with them can be tedious, and in some cases prohibitive, without the availability of a computer. We have selected examples for illustration, and most of the steps can be followed with paper and pencil (and pocket calculator). The purpose of these examples is to guide the reader to insights into the methods that underlie internal dose estimates. But we cannot offer sufficient information and instruction to assure the reader of independent expertise: tabulations of dosimetric information, such as Publication 30 of the International Commission on Radiological Protection (ICRP), rely on extensive libraries of data, considerable computing power, and the collective wisdom of many people who are expert in the relevant disciplines.

*Health and Safety Research Division, Oak Ridge National Laboratory, Oak Ridge, Tennessee 37830.

The general organization of the chapter is as follows:

Section 7.2. BASIC QUANTITIES. We define the concepts *absorbed dose, dose equivalent,* and *effective dose equivalent,* together with associated quantities and units. This material is concerned with the conversion of absorbed energy per unit mass of absorbing medium to dose.

Section 7.3. DOSE TO A TARGET ORGAN FROM RADIOACTIVITY IN SOURCE ORGANS. This section begins with consideration of the relationship between a distribution of activity in organs and tissues of the body and the resulting distribution of dose rate throughout the irradiated parts of the body. The specific absorbed fraction is defined and related to the concept of *S-factor* (average dose equivalent rate to a "target" organ per unit activity in a "source" organ), which is of particular utility in treating internal dose from penetrating radiations. The fundamental role of the specific absorbed fraction is emphasized by a discussion of interactions of alpha and beta particles and photons with matter. Finally, we address the practical problem of estimating specific absorbed fractions by an introductory look at Monte Carlo techniques.

Section 7.4. DYNAMIC MODELS OF RADIONUCLIDES IN THE BODY. From a single intake of a radionuclide, by inhalation, ingestion, or injection, the process of internal dose estimation must consider the distribution of radioactivity among the "source" organs and its variation over time. Such consideration entails mathematical models of translocation and metabolism of various physical and chemical forms of material. The models we discuss are essentially those used in the dosimetric calculations for ICRP Publication 30. In particular, we examine the systemic model consisting of the transfer compartment and its exchange of activity with other organs, whose metabolic dynamics are represented by multi-exponential retention functions. Special models for the respiratory and gastrointestinal tracts are explained; in the former case, the current ICRP model for deposition and retention of aerosols in the respiratory passages is included. A number of examples illustrate the application of the models to integration of the activity and its translocation over time.

Section 7.5. DOSE CONVERSION FACTORS FOR SELECTED RADIONUCLIDES. This section contains a tabulation of committed dose equivalent per unit intake by ingestion and inhalation for a selection of radionuclides that are important in environmental assessments of light-water reactor (LWR) fuel cycles. Results are given for several specific organs and for the effective dose equivalent.

7.2 BASIC QUANTITIES

In this section, we present definitions of the concepts *absorbed dose, dose equivalent,* and *effective dose equivalent* as they relate to internal dosimetry. Throughout the chapter, we shall give units in the paired format CM [SI], where the abbreviations stand for conventional metric and Système Internationale, respectively.

The *absorbed dose* at a point P of a mass distribution, due to a radiation event, is the limiting value of the quotient $\Delta\bar{\epsilon}/\Delta M$, where ΔM is the mass enclosed by a spherical volume element ΔV with center at P, $\Delta\bar{\epsilon}$ is the mean energy emitted by the event that is absorbed by ΔM, and the limit is taken as ΔV is shrunk to the point P:

$$D(P) = \lim_{\Delta V \to P}(\Delta\bar{\epsilon}/\Delta M) \ . \tag{7.1}$$

The special unit for absorbed dose is the rad [gray (Gy)]: 1 rad $= 10^{-2}$ J kg^{-1} [1 Gy = 1 J kg^{-1}].

The absorbed dose is an integral quantity, corresponding to the deposition of energy over time. The *absorbed dose rate* at P is defined as

$$\dot{D}(P) = \frac{d}{dt}D(P) \tag{7.2}$$

with units rad s^{-1} [Gy s^{-1}].

Absorbed dose is considered inadequate for prediction of health effects associated with irradiation of tissue, and a modified quantity has been introduced to carry additional information. The *dose equivalent* at the point P has been defined by the International Commission on Radiological Protection (ICRP, 1977) as

$$H(P) = D(P)Q(P)N \ , \tag{7.3}$$

where $Q(P)$, called the *quality factor*, weights the absorbed dose according to the biological effectiveness of the radiation types producing the dose. The factor N is the product of all other modifying factors; at present, $N = 1$ is the value assigned by the ICRP. The quality factor $Q(P)$ is defined as a function of the collision stopping power (L_∞) in water at the point P, by interpolation in Table 7.1. This definition seeks to take into account the range of relative biological effectiveness (RBE) while making $Q(P)$ independent of the specific organ or tissue or biological effect being considered. Direct computation of the value of $Q(P)$ from the foregoing information requires knowledge of the spectrum of each type of radiation at P to obtain the corresponding distribution of L_∞. For the limited purpose of comparing levels of exposure with limits

Table 7.1. Quality factor as a function of stopping power in water (ICRP Publication 26)

L_∞ in water (keV μm^{-1})	$\leqslant$3.5	7	23	53	$\geqslant$175
Q	1	2	5	10	20

expressed as dose equivalent, ICRP Publication 26 (1977) presents a simplification of the problem, which consists of effective estimates $\bar{Q}$ of the quality factor, depending only on primary radiation types (and not, for example, on specific organ geometries and distributions of the radiation source activity), as indicated in Table 7.2. The special unit of dose equivalent is the

Table 7.2. Effective estimates of quality factor for different radiation types (ICRP Publication 26)

Radiation type	$\bar{Q}$
X rays, γ rays, electrons	1
Neutrons, protons, singly-charged particles of rest mass greater than one atomic mass unit of unknown energy	10
α particles, multiply charged particles (and particles of unknown charge) of unknown energy	20

rem [Sievert (Sv)]: if the product of the quality factor and all other modifying factors is unity, 1 rem $= 10^{-2}$ J kg^{-1} [1 Sv = 1 J kg^{-1}].

The *dose equivalent rate* is defined as

$$\dot{H}(P) = \frac{d}{dt}H(P) \ . \tag{7.4}$$

In place of absorbed dose and dose equivalent evaluated at a point P of an organ or tissue, as defined above, we shall work with averages of these quantities over the mass of the organ or tissue whose irradiation is under discussion; we shall therefore drop the P notation and write D or H, sometimes with subscripts or superscripts, to indicate the result of this averaging (we choose to avoid the more suggestive but somewhat more cumbersome notations $\bar{D}$ and $\bar{H}$). Thus we shall interpret the (average) dose equivalent H as satisfying an equation of the form

$$H = \frac{1}{M}\int_{\boldsymbol{R}} H(P)\rho(P)dV(P) \ , \tag{7.5}$$

where M is the mass of the organ, and the integral is taken over all points P of the region $\boldsymbol{R}$ of space that the organ occupies; $\rho(P)$ is the local mass den-

sity, with volume element $dV(P)$. Dose rates will be assumed to have been averaged similarly, with an analogous notational convention.

In ICRP Publication 26 (1977), the Commission defined the *effective dose equivalent* as the sum of (average) dose equivalents to individual organs, H_T, with each term weighted by an organ weighting factor, W_T:

$$H_E = \sum_T W_T H_T \text{ rem [Sv]}, \tag{7.6}$$

where T ranges over the irradiated organs. The weighting factors W_T are based on organ-specific risk, per unit dose equivalent to the organ, of fatal health effects of *stochastic* type, i.e., those for which the probability of occurrence is a function of dose (malignant disease and genetic disorders), as opposed to *nonstochastic* effects, which are characterized by a deterministic causality relationship (such an effect will occur when the dose reaches or exceeds a threshold value; examples are the acute radiation syndrome and the formation of cataracts). Table 7.3 displays organ-specific risk factors adopted by the ICRP, together with the associated W_T; the total risk per unit uniform whole-body radiation is shown as 1.65×10^{-4} rem^{-1} [1.65×10^{-2} Sv^{-1}]. For uniform or nonuniform irradiation of the organs T, the product 1.65×10^{-4} rem^{-1} $\times$ H_E rem [1.65×10^{-2} Sv^{-1} $\times$ H_E Sv] may be interpreted as the total risk of fatal stochastic health effects, due to the particular radiation source, on the part of an individual receiving H_E rem [Sv] from that source.

The effective dose equivalent is of considerable value, in that it represents "dose" as a single quantity, in contrast to an array of individual organ doses or

Table 7.3. Stochastic risk per unit dose equivalent and corresponding organ-specific weighting factors (ICRP Publication 26)

Organ/tissue (T)	Risk (Sv^{-1})[a]	Weight (W_T)
Gonads	4.0×10^{-3}	0.25
Breast	2.5×10^{-3}	0.15
Red marrow	2.0×10^{-3}	0.12
Lung	2.0×10^{-3}	0.12
Thyroid	5.0×10^{-4}	0.03
Bone surfaces	5.0×10^{-4}	0.03
Remainder[b]	5.0×10^{-3}	0.30
Total	1.65×10^{-2}	

[a]For risk per rem, divide factors by 100.

[b]Remainder represents the risk of cancer in unspecified tissues of the body.

the "total body" dose, whose utility and applicability are open to question. The effective dose equivalent provides a measure of radiation insult which is consistent, in concept, with current understanding of the tissues at risk from radiation exposure.

We conclude this section by defining the *effective dose equivalent rate* as

$$\dot{H}_E = \sum_T W_T \dot{H}_T \text{ rem s}^{-1} [\text{Sv s}^{-1}] . \tag{7.7}$$

7.3 DOSE TO A TARGET ORGAN FROM RADIOACTIVITY IN SOURCE ORGANS

7.3.1 Introduction

The dose to a target organ of the body depends on the distribution of activity among source organs and the transport of the various radiations emitted in the nuclear transformation process. In general, the "target regions" as well as "source regions" will be identified as organs of the body, but this need not be the case when knowledge suggests otherwise. For example, the short-lived radon daughter radionuclides, when inhaled, are deposited on the tracheobronchial tree, from which they irradiate the basal cells of the bronchial epithelium as the target region of interest. Various computational procedures were employed in the past for estimating absorbed dose, given the necessary information on the distribution of activity within the body. Over the past decade, however, considerable effort has been devoted toward a unification of these procedures such that all types of radiations could be treated under a common scheme. The Medical Internal Radiation Dose (MIRD) Committee of the Society of Nuclear Medicine has spearheaded these efforts. The formalism set forth by the MIRD Committee (Loevinger and Berman, 1976) deals with the various radiations emitted in nuclear transformation of radionuclides in a simple yet consistent manner. This formalism also addresses absorbed dose and can be easily extended to the radiation-protection quantity of dose equivalent, as the ICRP (1979) has done in its development of secondary radiation protection limits.

7.3.2 Absorbed Fraction and Specific Absorbed Fraction

Development of a unified approach to estimation of absorbed dose for various radiations emitted in nuclear transformation of radionuclides was largely achieved through introduction of the absorbed fraction concept. Consider a source region $\boldsymbol{r}$ from which radiation of type i is being emitted. If a target region $\boldsymbol{v}$ has absorbed energy from the radiation emitted in the source region, then the absorbed fraction in $\boldsymbol{v}$ from $\boldsymbol{r}$, $\phi_i(\boldsymbol{v} \leftarrow \boldsymbol{r})$, is defined as the quotient of the energy imparted to the target region $\boldsymbol{v}$ and the energy, exclusive of rest

mass energy, emitted in the source region $\boldsymbol{r}$. That is, the absorbed fraction can be expressed as

$$\phi_i(\boldsymbol{v} \leftarrow \boldsymbol{r}) = \frac{\text{energy absorbed by target volume}}{\text{energy emitted by source region}} . \tag{7.8}$$

Note that the absorbed fraction is defined only for target regions which are volumes; however, no such constraint is placed on the source region, i.e., it can be a point, line, surface, or volume. The absorbed fraction quantity thus embodies not only the geometric variables of size, shape, and spatial relationship of the regions, but also the extent to which radiation is transported through the medium containing these regions.

The *specific absorbed fraction*, $\Phi_i(\boldsymbol{v} \leftarrow \boldsymbol{r})$, is defined as the absorbed fraction per unit mass of target; i.e.,

$$\Phi_i(\boldsymbol{v} \leftarrow \boldsymbol{r}) = \frac{\phi_i(\boldsymbol{v} \leftarrow \boldsymbol{r})}{m_{\boldsymbol{v}}} , \tag{7.9}$$

where $m_{\boldsymbol{v}}$ is the mass of the target volume. The specific absorbed fraction has the property that it can be defined for all target regions, including the important case of a point target. Recall from Sect. 7.2 that absorbed dose is a point function. One needs to note that there can be no points in common between the source and target regions unless at least one of the regions is a volume. An attempt to calculate the specific absorbed fraction for a point serving as both the source and target regions leads to a divergent mathematical expression.

If the source and target regions are in a homogeneous absorbing medium that is sufficiently large (relative to the range of the radiation) that edge effects are negligible, and if the activity is uniformly distributed in the source region, then the *uniform isotropic model* is said to apply. Under this model, the distribution of absorbed energy about the source region is a function only of distance from the source. The fraction of emitted energy absorbed per unit mass at a distance x can then be represented by the *point-isotropic specific absorbed fraction*, $\Phi_i(x)$. Since the emitted energy must be absorbed somewhere, the point-isotropic specific absorbed fraction must satisfy the constraint that

$$4\pi\rho \int_0^\infty x^2 \Phi_i(x)\,dx = 1 , \tag{7.10}$$

where ρ is the density of the homogeneous medium.

The point-isotropic specific absorbed fraction for the various radiations of interest provides the basic means of estimating specific absorbed fractions. Non-point source and target regions can be developed simply as the superposition of the point function. Thus the specific absorbed fraction between any

non-point target region $\boldsymbol{r}$ and a point source is the mean of the values of $\Phi_i(x)$ in the target region;

$$\Phi_i(\boldsymbol{r} \leftrightarrow P) = \overline{\Phi}_i(x) . \tag{7.11}$$

Furthermore, the specific absorbed fraction in any region $\boldsymbol{r}_1$ from a source in another region $\boldsymbol{r}_2$ is the mean of the values of the point-isotropic specific absorbed fraction for all pairs of points in the regions; i.e.,

$$\Phi_i(\boldsymbol{r}_1 \leftrightarrow \boldsymbol{r}_2) = \overline{\Phi_i(x)} , \tag{7.12}$$

where x is the distance between points randomly selected in $\boldsymbol{r}_1$ and $\boldsymbol{r}_2$. Equations 7.11 and 7.12 can be expressed in their integral representation, but for regions whose geometry is complex, i.e., other than spherical, recourse is often made to numerical evaluation of Eqs. 7.11 and 7.12 using Monte Carlo techniques.

As noted above, the point-isotropic specific absorbed fraction is a function only of distance. Thus in Eqs. 7.11 and 7.12, if the source and target regions are interchanged, the numerical value of the specific absorbed fraction would not be changed. The double-headed arrow in these equations indicates that either region may be the source or target region. This property of the uniform isotropic model is referred to as the *Reciprocity Theorem.* The conclusion of the theorem is that the specific absorbed fraction Φ_i is independent of which region is designated as the source and which is the target. In symbols,

$$\Phi_i(\boldsymbol{r}_2 \leftarrow \boldsymbol{r}_1) = \Phi_i(\boldsymbol{r}_1 \leftarrow \boldsymbol{r}_2) \equiv \Phi_i(\boldsymbol{r}_2 \leftrightarrow \boldsymbol{r}_1) \quad ; \tag{7.13}$$

$$\frac{\phi_i(\boldsymbol{v}_2 \leftarrow \boldsymbol{v}_1)}{m_2} = \frac{\phi_i(\boldsymbol{v}_1 \leftarrow \boldsymbol{v}_2)}{m_1} . \tag{7.14}$$

Note that these relationships apply to all radiations in the uniform isotropic model.

Example 7.1. The potential distribution of absorbed energy for a particular radiation type is often characterized in terms of the radius of the sphere about a point source in which 90% of the emitted energy would be absorbed. Assuming the uniform isotropic model, we derive the expression for the absorbed fraction in a sphere of radius R with a point source at the origin P of the sphere.

The point-isotropic specific absorbed fraction $\Phi(r)$ denotes the fraction of the emitted energy absorbed per unit mass at r. The absorbed fraction in a spherical shell of radius r and thickness dr (volume $4\pi r^2 dr$) about the point source is

$$\phi(\text{shell} \leftarrow P) = 4\pi r^2 dr \rho \Phi(r) ,$$

and thus

$$\phi(\text{sphere} \leftarrow P) = 4\pi\rho \int_0^R r^2 \Phi(r)\, dr \ ,$$

where ρ denotes the density of the absorbing medium. The specific absorbed fraction in the sphere would then be

$$\Phi(\text{sphere} \leftarrow P) = \frac{\phi(\text{sphere} \leftarrow P)}{\text{mass of sphere}} = \frac{3}{R^3} \int_0^R r^2 \Phi(r)\, dr \ .$$

From the reciprocity theorem, the specific absorbed fraction at the origin of the sphere containing a uniform distribution of activity would be

$$\Phi(P \leftarrow \text{sphere}) = \Phi(\text{sphere} \leftarrow P) = \frac{3}{R^3} \int_0^R r^2 \Phi(r)\, dr \ .$$

This expression has application to the practical problem of estimating the exposure rate in a radioactive cloud. The values of the limiting value of $\Phi(P \leftarrow \text{sphere})$ as $R \rightarrow \infty$ must await the development of the functional forms of $\Phi(r)$. [End of Example 7.1]

7.3.3 Absorbed Dose Rate per Unit Activity, *S*-factor

Consider an organ $\boldsymbol{T}$ of the body which is absorbing energy from activity in a source region $\boldsymbol{S}$ of the body. Let the activity, i.e., the nuclear transformation rate, in the source region be $A_{\boldsymbol{S}}$ and the mean energy emitted as radiation of type i per nuclear transformation be denoted as Δ_i. Then the rate of energy absorption in $\boldsymbol{T}$ per unit mass, which is by definition the mean absorbed dose rate, $\bar{D}_i(\boldsymbol{T} \leftarrow \boldsymbol{S})$, due to the activity in $\boldsymbol{S}$ is

$$\bar{D}_i(\boldsymbol{T} \leftarrow \boldsymbol{S}) = A_{\boldsymbol{S}} \Delta_i \Phi_i(\boldsymbol{T} \leftarrow \boldsymbol{S}) \ . \tag{7.15}$$

In general, more than one type of radiation will be associated with the nuclear transformation process of a particular radionuclide, and thus the mean absorbed dose rate is

$$\bar{D}(\boldsymbol{T} \leftarrow \boldsymbol{S}) = \sum_i \bar{D}_i(\boldsymbol{T} \leftarrow \boldsymbol{S}) = A_{\boldsymbol{S}} \sum_i \Delta_i \Phi_i(\boldsymbol{T} \leftarrow \boldsymbol{S}) \ . \tag{7.16}$$

If the activity is present in a number of source organs, then an additional summation must be considered to derive the mean absorbed dose rate in $\boldsymbol{T}$;

$$\bar{D}(\boldsymbol{T}) = \sum_{\boldsymbol{S}} A_{\boldsymbol{S}} \sum_i \Delta_i \Phi_i(\boldsymbol{T} \leftarrow \boldsymbol{S}) \ , \tag{7.17}$$

where the first summation is over all source regions $\boldsymbol{S}$.

Examination of the above equation reveals that the factors within the inner summation, i.e., Δ_i and $\Phi_i(\boldsymbol{T} \leftarrow \boldsymbol{S})$, reflect the physical data on the nuclear transformation process and the anatomical/radiation transport relationship between the source and target regions, respectively. Given an agreed-upon analog of the human body for estimation of the Φ_i (Chapter 6), then considerable effort can be saved through consideration of the additional quantity S. If we define $S(\boldsymbol{T} \leftarrow \boldsymbol{S})$ as

$$S(\boldsymbol{T} \leftarrow \boldsymbol{S}) = \sum_i \Delta_i \Phi_i(\boldsymbol{T} \leftarrow \boldsymbol{S}) , \tag{7.18}$$

then our expression for the mean absorbed dose rate reduces to

$$\bar{D}(\boldsymbol{T}) = \sum_{\boldsymbol{S}} A_{\boldsymbol{S}} S(\boldsymbol{T} \leftarrow \boldsymbol{S}) . \tag{7.19}$$

The quantity S represents the mean absorbed dose rate in $\boldsymbol{T}$ per unit radioactivity in $\boldsymbol{S}$. If S is considered to be invariant with time, that is, if the analog of the human body and its implied geometric relationships are independent of time, then integration of Eq. 7.19 yields

$$\bar{D}(\boldsymbol{T}) = \sum_{\boldsymbol{S}} \tilde{A}_{\boldsymbol{S}} S(\boldsymbol{T} \leftarrow \boldsymbol{S}) , \tag{7.20}$$

where $\tilde{A}_{\boldsymbol{S}}$ denotes the time integral of the activity in the source region (the *cumulated activity*). Thus S may also be defined as the mean absorbed dose per unit cumulated activity.

The S factor can be expressed in terms of dose equivalent by inclusion of the modifying factors in its defining equation; i.e,

$$S(\boldsymbol{T} \leftarrow \boldsymbol{S}) = \sum_i \Delta_i Q_i N \Phi_i(\boldsymbol{T} \leftarrow \boldsymbol{S}) , \tag{7.21}$$

where Q_i and N are the factors discussed in Sect. 7.2. In developing its recommendations on secondary limits, the ICRP (1979) introduced the *specific effective energy* quantity, $\mathrm{SEE}(\boldsymbol{T} \leftarrow \boldsymbol{S})$. This quantity is given by the right hand side of Eq. 7.21; however, units of MeV g^{-1} $(\mathrm{nt})^{-1}$ were retained, where nt denotes the number of nuclear transformations.

7.3.4 Specific Absorbed Fractions for Various Radiations

The three principal modes of nuclear transformation are beta decay, alpha decay, and isomeric transition. An additional process, spontaneous fission, is available for some of the nuclides of larger mass; however, this mode of decay will not be discussed here. The principal radiations involved in these modes of nuclear transformation are electrons (either negative or positive charge), alpha particles, and photons (electromagnetic radiation). These radiations differ

significantly in their energy deposition pattern, as a result of different mechanisms through which they interact with matter.

7.3.4.1 Interaction of Charged Particles with Matter

Charged particles passing through matter lose energy principally by Coulomb-force interactions with the atomic electrons of the absorbing medium. The energy loss in these interactions is sufficiently small that one can make use of the average rate at which the particle loses energy, i.e., the stopping power dE/dx, where dE is the average energy lost as the particle traverses the path element dx. Stopping power is a function of the type of charged particle, its energy, and the absorbing medium. It is usually expressed in units of MeV μm^{-1}, and in some instances mass stopping power ($= \rho^{-1} dE/dx$, where ρ is the density of the absorbing medium) is given. The units of mass stopping power are typically MeV/(g cm^{-2}).

The average path length that a charged particle of initial energy E_0 will travel before stopping can be written as

$$R_0 = \int_0^{E_0} \frac{dE}{(dE/dx)} .$$

The quantity R_0 is the *csda* range (*continuous-slowing-down-approximation*), which assumes that no catastrophic events, such as nuclear collisions, occur during the slowing-down process. The average distance that a charged particle penetrates in one direction, e.g., in a slab, would be less than the csda range. This is particularly true of electrons which experience considerable deflection in the collision events, and thus traverse a more tortuous path than do heavier charged particles.

The linear energy transfer (LET) of a charged particle in a medium is the quotient of the average energy dE_L locally imparted to the medium by a charged particle of a specified energy and the distance dl that the particle traverses:

$$L_\infty = \frac{dE_L}{dl} .$$

Note that the LET quantity directs attention to the energy deposited in the medium, while stopping power addresses the energy loss of the particle. Some of the lost energy may be imparted to the medium quite far from the track of the particle, e.g., bremsstrahlung photons. Thus LET can be viewed as a restricted stopping power, in that it is limited to energy losses which are locally imparted to the medium.

7.3.4.2 Electrons

A continuous energy spectrum of electrons is associated with beta decay. The spectrum ranges in energy from zero to the maximum energy permitted by the difference in the energy level of the parent and daughter nucleus. Electrons of discrete energy are also observed in nuclear transfer motions, as a result of processes involving orbital electrons.

Under the auspices of the MIRD Committee, Berger has tabulated point-isotropic specific absorbed fraction data for monoenergetic electron sources ranging in energy from 0.025 to 5 MeV (Berger, 1971). These data were later revised and extended downward to 0.0005 MeV and upward to 10 MeV in a National Bureau of Standards publication (Berger, 1973). To facilitate numerical use, Berger presents the data in terms of a scaled point kernel, $F(r/r_0)$, where r_0 is the csda range. The point-isotropic specific absorbed fraction $\Phi(r)$ in terms of Berger's scaled point kernel is

$$\Phi(r) = \frac{1}{4\pi\rho r^2 r_0} F(r/r_0) \ .$$

The tabulations were prepared for water as a surrogate medium for soft tissue. Table 7.4 presents the csda range (r_0) and the 90-percentile distance (x_{90}) in water as a function of electron energy. The 90-percentile distance is defined to be the radius of a sphere around a point source within which 90% of the emitted energy is absorbed. As can be seen from Table 7.4, electrons of energy up to about 2 MeV deposit their energy within a distance of less than 1 cm.

Organs of the body are of dimensions sufficiently large relative to the electron range that the electron absorbed fraction may be taken as unity if the source is uniformly distributed in the organ. Thus the specific absorbed fraction for electrons is

$$\Phi(\boldsymbol{T} \leftarrow \boldsymbol{S}) = \begin{cases} 1/M_{\boldsymbol{T}}, \text{ if } \boldsymbol{T} = \boldsymbol{S} \\ 0, \text{ if } \boldsymbol{T} \neq \boldsymbol{S} \ . \end{cases}$$

A notable exception to the above occurs for walled organs where the source resides in the contents, e.g., urinary bladder and the segments of the gastrointestinal tract.

For organs whose contents contain an electron emitter, the specific absorbed fraction in the wall of the organ from its contents is

$$\Phi(\text{wall} \leftarrow \text{contents}) = \frac{1}{2M_{\text{contents}}} \ ,$$

where M_{contents} is the mass of the contents. This relationship is derived from the fact that the dose rate at the surface of a half space containing a uniform

Table 7.4. Electron csda range (r_0) and 90-percentile distance in water

E_0 (MeV)	r_0 (g m^{-2})	x_{90} (g m^{-2})	E_0 (MeV)	r_0 (g m^{-2})	x_{90} (g m^{-2})
0.0005	2.272(−6)	1.510(−6)	0.08	9.562(−3)	7.732(−3)
0.0006	2.897(−6)	2.016(−6)	0.10	1.401(−2)	1.131(−2)
0.0008	4.325(−6)	3.120(−6)	0.15	2.760(−2)	2.219(−2)
0.0010	5.976(−6)	4.420(−6)	0.20	4.400(−2)	3.532(−2)
0.0015	1.092(−5)	8.358(−6)	0.30	8.263(−2)	6.614(−2)
0.0020	1.710(−6)	1.338(−5)	0.40	1.264(−1)	1.011(−1)
0.0030	3.279(−5)	2.620(−5)	0.50	1.735(−1)	1.388(−1)
0.0040	5.268(−5)	4.259(−5)	0.60	2.227(−1)	1.783(−1)
0.0050	7.652(−5)	6.215(−5)	0.80	3.248(−1)	2.603(−1)
0.0060	1.037(−4)	8.960(−5)	1.0	4.297(−1)	3.452(−1)
0.0080	1.689(−4)	1.386(−4)	1.5	6.956(−1)	5.616(−1)
0.010	2.482(−4)	2.043(−4)	2.0	9.613(−1)	7.819(−1)
0.015	5.042(−4)	4.163(−4)	3.0	1.485	1.230
0.020	8.374(−4)	6.907(−4)	4.0	1.997	1.682
0.030	1.715(−3)	1.407(−3)	5.0	2.499	2.138
0.040	2.851(−3)	2.327(−3)	6.0	2.991	2.586
0.050	4.222(−3)	3.434(−3)	8.0	3.950	3.510
0.060	5.807(−3)	4.712(−3)	10.0	4.880	4.447

distribution of activity is one-half the equilibrium dose rate at locations within the contaminated half space far from the interface. It should be noted that the approach for walled organs may be very conservative, in that the critical cells are typically considered to be the basal cells of the epithelial layer, which lie at some depth in the tissue; in the gastrointestinal tract, they are further shielded by a mucus layer. Thus the dose rate in the wall may decrease rapidly from the value at the surface, particularly for low-energy electrons. Consideration of these details in the dosimetric models must await further description of the location of the cells at risk.

Example 7.2. We show that $\Phi(\text{wall} \leftarrow \text{contents}) = 1/(2M_{\text{contents}})$.

The equilibrium dose rate within the contents of a walled organ which contains A activity-units is

$$\dot{D}_0 = \frac{A\Delta}{M_{\text{contents}}} .$$

The surface dose rate is taken to approximate the dose rate to the wall and is one-half the equilibrium dose rate; thus

$$\dot{D}(\text{wall} \leftarrow \text{contents}) = \tfrac{1}{2}\dot{D}_0$$

or

$$A\Delta\Phi(\text{wall}\leftarrow\text{contents}) = \tfrac{1}{2}\frac{A\Delta}{M_{\text{contents}}} ,$$

and thus

$$\Phi(\text{wall}\leftarrow\text{contents}) = \frac{1}{2M_{\text{contents}}} .$$

[End of Example 7.2]

7.3.4.3 Alpha Particles

An alpha particle, composed of two protons and two neutrons, is frequently emitted in the nuclear transformation process of heavy elements, i.e., of mass number greater than 200. A nucleus emitting an alpha particle loses four units of mass and two units of charge. Alpha particles exhibit a discrete energy which depends on the energy difference in the levels of the parent and daughter nuclei.

The theory of charged-particle interactions with matter is sufficiently well developed and supplemented by empirical data to permit calculation of stopping power. The expression for the energy loss experienced by a heavy charged particle was orginally developed by Bethe (1932) and Bloch (1933). Their expression, simplified for nonrelativistic alpha particles, is

$$\frac{dE}{dx} = 3.80\times10^{-25}\frac{NZ}{E_\alpha}\ln\left(548\frac{E_\alpha}{I}\right) , \tag{7.22}$$

where

dE/dx = linear stopping power (MeV μm^{-1}),

E_α = energy of the alpha particle (MeV),

I = average ionization potential of the absorbing atoms (eV), and

NZ = density of electrons in the absorbing medium (cm^{-3}).

For soft tissue, I and NZ are about 69 eV and 3.32×10^{23} cm^{-3}, respectively, and thus the stopping power is given by

$$\frac{dE}{dx} = \frac{0.1263}{E_\alpha}\ln(7.99E_\alpha) . \tag{7.23}$$

In air the stopping power expression is

$$\frac{dE}{dx} = \frac{1.37\times10^{-4}}{E_\alpha}\ln(6.52E_\alpha) . \tag{7.24}$$

For air, I and NZ are about 84 eV and $3.6\times10^{20}\,\mathrm{cm}^{-3}$, respectively.

Example 7.3. We compute the linear stopping power in air and tissue for a 6-MeV alpha particle. Note the significance of the logarithmic term involving I.

From Eqs. 7.23 and 7.24 for $E_\alpha = 6$ MeV, we have

$$(dE/dx)_{\text{air}} = 8.37\times10^{-5}\,\text{MeV}\,\mu m^{-1},$$

$$\text{and } (dE/dx)_{\text{tissue}} = 8.19\times10^{-2}\,\text{MeV}\,\mu m^{-1}.$$

Although the values of I for air and tissue are not identical (84 vs 69 eV), the logarithmic terms are comparable (3.67 vs 3.87). Stopping-power values are thus not highly sensitive to the ionization potential I. The ratio of the stopping powers is

$$(dE/dx)_{\text{tissue:air}} = 974,$$

which is approximately the ratio of the electron densities

$$(NZ)_{\text{tissue:air}} = 922.$$

[End of Example 7.3]

As the alpha particle slows down and reaches velocities comparable to orbital velocity of electrons in the absorber atoms ($E_\alpha \leq 2$ MeV), the particle will capture electrons from the absorbing medium and lose electrons to it. A correction must be introduced into the above stopping-power expressions to reflect the effective charge borne by the particle in this low energy region. The square of the charge on the slowing-down particle enters the coefficient of the stopping-power expression. The square of the effective charge $(z^*)^2$ of alpha particles below 1.6 MeV is taken from Whaling (1958) and is given in Table 7.5. Stopping-power values in this energy region are then computed as

$$dE/dx = \frac{(z^*)^2}{4}(dE/dx)_{\text{uncorrected}}, \tag{7.25}$$

where $(dE/dx)_{\text{uncorrected}}$ denotes the stopping power when the alpha particles are assumed to be doubly charged.

Table 7.5. Effective charge $(z^*)^2$ of low-energy alpha particles

E_α (MeV)	$(z^*)^2$	E_α (MeV)	$(z^*)^2$
0.2	1.8	0.8	3.3
0.3	2.0	0.9	3.4
0.4	2.4	1.0	3.5
0.5	2.8	1.2	3.7
0.6	3.0	1.4	3.9
0.7	3.2	1.6	4.0

Empirical stopping-power values and the range-energy relationship for alpha particles in tissue have been summarized by Walsh (1970). In Table 7.6, stopping-power values vs depth of penetration are presented for an 8-MeV alpha particle in tissue. These data can be utilized to address range-energy relationships and stopping-power values for alpha particles of any energy less than 8 MeV.

Table 7.6 Stopping power vs distance for alpha particles in tissue

x (μm)	E (MeV)	dE/dx (MeV μm^{-1})	x (μm)	E (MeV)	dE/dx (MeV μm^{-1})
0.0	8.00	0.0655	57.5	3.20	0.1250
2.5	7.84	0.0670	60.0	2.89	0.1320
5.0	7.68	0.0675	62.5	2.56	0.1450
7.5	7.51	0.0690	65.0	2.20	0.1590
10.0	7.34	0.0700	65.5	2.12	0.1620
12.5	7.16	0.0710	67.0	1.87	0.1770
15.0	6.94	0.0725	67.5	1.78	0.1810
17.5	6.81	0.0735	68.0	1.69	0.1890
20.0	6.63	0.0750	68.5	1.60	0.1910
22.5	6.44	0.0765	69.0	1.50	0.2000
25.0	6.25	0.0780	69.5	1.40	0.2050
27.5	6.06	0.0800	70.0	1.30	0.2160
30.0	5.86	0.0820	71.0	1.08	0.2400
32.5	5.65	0.0840	71.5	0.96	0.2500
35.0	5.44	0.0860	72.0	0.83	0.2620
37.5	5.23	0.0885	72.5	0.69	0.2790
40.0	5.01	0.0915	73.0	0.55	0.2890
42.5	4.78	0.0945	73.5	0.41	0.2790
45.0	4.53	0.0980	74.0	0.28	0.2480
47.5	4.30	0.1010	74.5	0.18	0.1920
50.0	4.05	0.1080	75.0	0.08	0.1200
52.5	3.78	0.1120	75.5	0.00	0.0000
55.0	3.50	0.1180			

Example 7.4. Using the data of Table 7.6, we estimate the range in tissue of alpha particles of energies of 4, 5, 6, 7, and 8 MeV.

From the table, we find that the range of an 8-MeV alpha particle in tissue is 75.5 μm. The range of alpha particles of energies less than 8 MeV can be estimated as the residual range of an 8-MeV alpha particle after it has slowed down to the desired energy.

4 MeV: The distance traveled by an 8-MeV alpha particle in losing 4 Mev of energy can be found by interpolation of the data in Table 7.6. After traveling 50 μm, the residual energy is 4.05 MeV; thus

$$50 + \left(\frac{52.5-50.0}{3.78-4.05}\right)(4-4.05) = 50.5 \ \mu m \quad .$$

The residual range is then 75.5 − 50.5 = 25 μm. Thus the range of a 4-MeV alpha is 25 μm in tissue.

5 MeV: We have

$$75.5 - \left[40.0 + \left(\frac{42.5-40.0}{4.78-5.01}\right)(5-5.01)\right] = 35.4 \ \mu m \quad .$$

Similar calculations for alpha particles at 6, 7, and 8 MeV yield 47.2, 61.2, and 75.5 μm, respectively. Tabulating the results, we have

E_α (MeV)	Range (μm)
4	25.0
5	35.4
6	47.2
7	61.2
8	75.5

[End of Example 7.4]

Example 7.5. At low energies, the charge carried by the alpha particle fluctuates because of continual captures and losses of electrons between the particle and the absorbing medium. From Table 7.5, we see that the squared effective charge $(z^*)^2$ of a 0.5-MeV alpha particle is 2.8. Using Eq. 7.22, we find that the uncorrected stopping power in tissue is

$$\frac{dE}{dx} = 0.350 \text{ MeV } \mu m^{-1} \quad .$$

Correcting for the effective charge of the particle, we have

$$\frac{dE}{dx} = \frac{2.8}{4} \times 0.350 = 0.245 \text{ MeV } \mu m^{-1} \ ;$$

this compares reasonably well with the estimate 0.285 MeV μm $^{-1}$ at 0.5 MeV from Table 7.6 [End of Example 7.5]

The point-isotropic specific absorbed fraction $\Phi(x)$ has not been tabulated in the literature for alpha particles. As noted above, the range of alpha particles in tissue is sufficiently small that for organs of the body, an absorbed frac-

tion of unity can be assumed. However, in some specific instances — such as alpha-emitting short-lived radon daughters deposited on the tracheobronchial tree — consideration must be given to the energy deposition pattern.

The point-isotropic specific absorbed fraction $\Phi(x)$ for any charged particle can be defined as

$$\Phi(x) = \frac{1}{4\pi x^2 \rho E_\alpha}(dE/dx)_x \ , \tag{7.26}$$

where $(dE/dx)_x$ is the stopping power of the particle at the energy it has after traveling a distance x, and E_α is the initial energy of the alpha emitter. In order to avoid the discontinuity at $x = 0$, the quantity $4\pi x^2 \rho \Phi(x)$ is often tabulated for the point-isotropic specific absorbed fraction. Table 7.7 presents the results of such a calculation, derived from the data of Table 7.6. The data have been normalized so that

$$4\pi\rho \int_0^\infty x^2 \Phi(x) dx = 1 \ . \tag{7.27}$$

The percent column denotes the percent of the energy of an 8-MeV alpha particle deposited in spheres of various radii. Note the units assigned to $\Phi(x)$, i.e., reciprocal picograms; a soft tissue density of 1 g cm^{-3} corresponds to 1 pg μm^{-3}.

Specific absorbed fractions for source-target pairs in the body are the same as employed for beta radiation. The exception is for the walls of the gastrointestinal tract, where only 1% of the alpha particles' energy is considered to penetrate the mucous lining of the tract.

7.3.4.4 Gamma Rays and X Rays

Gamma rays and x rays are electromagnetic radiations of short wavelength, orders of magnitude shorter than visible light. A nucleus in an excited state from which it is energetically impossible to de-excite through emission of particulate radiation (emission of alpha or beta particles) may de-excite through the emission of one or more photons of electromagnetic radiation. Many nuclides formed in beta or alpha decay may be in an excited state, and thus gamma-ray emission often accompanies these decays. Electromagnetic radiations associated with changes in nuclear state are referred to as gamma radiation.

The internal conversion process competes with gamma-ray emission as a de-excitation process. In this conversion process, an inner-shell orbital electron of the atom is ejected as a result of its interaction with the excited nucleus. The energy imparted to the electron, referred to as an internal conversion electron, corresponds to the energy difference of the nuclear levels involved, less the atomic binding energy of the electron. The fact that internal conversion

Table 7.7 Point isotropic specific absorbed fraction for 8-MeV alpha particles in tissue

x (μm)	$4\pi x^2\Phi(x)$ ($\mu m^2\,pg^{-1}$)	%	x (μm)	$4\pi x^2\Phi(x)$ ($\mu m^2\,pg^{-1}$)	%
0.0	8.079(−3)	0.00	57.5	1.542(−2)	60.40
2.5	8.264(−3)	2.04	60.0	1.628(−2)	64.36
5.0	8.325(−3)	4.12	62.5	1.788(−2)	68.63
7.5	8.511(−3)	6.22	65.0	1.961(−2)	73.32
10.0	8.634(−3)	8.36	65.5	1.998(−2)	74.31
12.5	8.757(−3)	10.54	67.0	2.183(−2)	77.44
15.0	8.942(−3)	12.75	67.5	2.232(−2)	78.55
17.5	9.066(−3)	15.00	68.0	2.331(−2)	79.69
20.0	9.251(−3)	17.29	68.5	2.356(−2)	80.86
22.5	9.436(−3)	19.63	69.0	2.467(−2)	82.07
25.0	9.621(−3)	22.01	69.5	2.528(−2)	83.32
27.5	9.867(−3)	24.44	70.0	2.664(−2)	84.61
30.0	1.011(−2)	26.94	71.0	2.960(−2)	87.43
32.5	1.036(−2)	29.50	71.5	3.084(−2)	88.94
35.0	1.061(−2)	32.12	72.0	3.232(−2)	90.52
37.5	1.092(−2)	34.81	72.5	3.441(−2)	92.18
40.0	1.129(−2)	37.59	73.0	3.565(−2)	93.93
42.5	1.166(−2)	40.46	73.5	3.441(−2)	95.69
45.0	1.209(−2)	43.42	74.0	3.059(−2)	97.31
47.5	1.246(−2)	46.49	74.5	2.368(−2)	98.67
50.0	1.332(−2)	49.71	75.0	1.480(−2)	99.63
52.5	1.381(−2)	53.11	75.5	0.000	100.00
55.0	1.455(−2)	56.65			

electrons have discrete energies provided the initial evidence that this process was distinct from beta-ray emission, where a spectrum of energies is observed. A deficiency in the orbital-electron structure occurs because of the ejection of an inner-shell electron. As the electronic configuration is established, x rays may be emitted as electrons from outer shells fill the inner-shell vacancy. The electromagnetic radiation emitted as a result of this rearrangement of orbital electrons is referred to as x ray.

Thus electromagnetic radiation is classified as gamma ray or x ray according to the origin of the radiation, not its energy. X rays are also emitted as charged particles, principally electrons, are stopped in a medium. A continuous spectrum of bremsstrahlung (*braking radiation*) x rays are emitted as electrons are stopped in the target element of a diagnostic x-ray tube. Since inner-shell orbital electrons may be ejected from atoms of the target, discrete x rays of energy characteristic of the target atoms may be superimposed on the bremsstrahlung spectra.

Electromagnetic radiation (photons) ionizes matter as a result of the photons' transferring energy to electrons of the medium through occurrence of discrete interaction events. Photons do not lose their energy in a reasonably continuous manner, but rather experience catastrophic interaction events. Thus one cannot associate a range, analogous to the csda range of electrons or alpha particles, with photon radiation. One characterizes the penetration power of photons by their probability of traversing a unit distance in the medium without interacting with the medium.

Photons transfer energy to electrons of the medium through three major interaction events: the *photoelectric effect, Compton scattering,* and *pair production.* The probability that a photon enters into one of these interaction events depends on its energy and the nature of the medium. Other photon interactions are possible, e.g., photonuclear reactions (γ,n); however, these interactions are of limited interest for dosimetry and are not discussed here.

In the photoelectric interaction, the entire energy of the photon is absorbed by an atom with an inner-shell electron (usually K- or L-shell) being ejected with a kinetic energy T:

$$T = h\nu_0 - \phi_e \ , \tag{7.28}$$

where $h\nu_0$ denotes the photon energy and ϕ_e the binding energy of the electron in the medium. The liberated electron is referred to as a *photoelectron.* It is necessary for the electron to be bound, because of conservation of momentum considerations; the residual atom in its recoil balances the momentum. If the photon is of sufficient energy that even the more tightly bound inner-shell electrons appear to be "free," then the probability of the photoelectric interaction is low. Similarly, as the photon energy approaches the binding energy of the inner-shell electrons, the probability of the event increases. Of course, if the binding energy of electrons in a given shell, e.g., the K-shell, is greater than the energy of the photon, these electrons cannot participate in the event; only electrons of L or higher shells contribute to the effect. Thus the probability (or *cross section*) for the photoelectric effect is highly energy dependent and, as indicated, will be strongly dependent on Z (the atomic number) of the absorber atoms. The probability or cross section per atom τ (m^2 $atom^{-1}$) varies approximately as the fourth power of the atomic nucleus and inversely with the cube of the photon energy;

$$\tau \propto \frac{Z^4}{(h\nu)^3} \ . \tag{7.29}$$

For low-energy photons and for high-Z absorbing media, the photoelectric effect will be the dominant interaction event.

In the Compton effect (or Compton scattering), a photon interacts with an atomic electron that is virtually free; i.e., its binding energy is much less than

the energy of the photon. The interaction results in a partial transfer of the photon's energy to the electron (called a *Compton electron*) with the photon proceeding with reduced energy and altered direction. It is the altering of the direction of photons (scattering into various angles), with the accompanying spectrum of energy associated with the scattered photon, that complicates the transport of photon energy.

If the incident energy of the photon ($h\nu_0$) is written in terms of the dimensionless quantity $\alpha \equiv h\nu_0/(m_0c^2)$, where m_0c^2 is the rest mass energy of an electron (0.511 MeV), then the energy of the Compton-scattered photon ($h\nu$) is

$$h\nu = \left[\frac{1}{1+\alpha(1-\cos\theta)}\right]h\nu_0 \ , \tag{7.30}$$

where θ is the angle of the Compton-scattered photon. The minimum energy of the Compton-scattered photon (maximum energy of the Compton electron) occurs with a complete backscatter of the photon, i.e., $\theta = 180°$. Electrons of the maximum energy define the so called *Compton edge* observed in gamma-ray spectroscopy.

Example 7.6. Let us compute the energy of the Compton edge for photons of 0.1, 0.3, 0.5, 0.8, 1.0, and 2.0 MeV. The Compton edge is the maximum energy which can be transferred to electrons in the Compton process. From Eq. 7.30, we see that if $\theta = 180°$, then the energy of the scattered photon is

$$h\nu_{\min} = \frac{1}{1+2\alpha}h\nu_0 \ . \tag{7.31}$$

The energy T imparted to the electron is then

$$T = h\nu_0 - h\nu = \left[\frac{2\alpha}{1+2\alpha}\right]h\nu_0 \ . \tag{7.32}$$

Thus one computes the following: $h\nu_0 = 0.1$ MeV; $\alpha = 0.1/0.511 = 0.196$; and $T = 0.028$ MeV, etc. The following tabulation is derived:

$h\nu_0$ (MeV)	T (MeV)
0.1	0.028
0.3	0.162
0.5	0.331
0.8	0.606
1.0	0.796
2.0	1.77

A rule of thumb in spectroscopy is that the Compton edge is taken to be one-fourth MeV below the photopeak (the full energy peak). We show next that this rule of thumb is a reasonable estimate. The energy difference between the photopeak and the Compton edge is $h\nu_0 - T$ or

$$h\nu_0 - T = h\nu_0\left(\frac{1}{1+2\alpha}\right) . \tag{7.33}$$

From the definition of α and by noting that $m_0c^2 \simeq$ ½ MeV, one has $\alpha = 2h\nu$; thus

$$h\nu_0 - T = h\nu_0\left(\frac{1}{1+4h\nu_0}\right) . \tag{7.34}$$

If $4h\nu_0 \gg 1$, then

$$h\nu_0 - T = \frac{1}{4} . \tag{7.35}$$

[End of Example 7.6]

The formulation by Klein and Nishina of an analytical expression for the Compton cross section was one of the early triumphs of quantum mechanics. The total cross section per electron for the process is given as

$$e^{\sigma} = 2\pi r_0^2\left\{\frac{1+\alpha}{\alpha^2}\left[\frac{2(1+\alpha)}{1+2\alpha} - \frac{\ln(1+2\alpha)}{\alpha}\right] + \frac{\ln(1+2\alpha)}{2\alpha} - \frac{1+3\alpha}{(1+2\alpha)^2}\right\} \text{ cm}^2/\text{electron} , \tag{7.36}$$

where r_0 is the classical radius of the electron ($r_0 = 2.818\times10^{-13}$ cm).

Example 7.7. We calculate the attenuation coefficient for the Compton process for 1-MeV photons in water. From Eq. 7.36, with $\alpha = 1.0/0.511$, one computes $e^{\sigma} = 2.11\times10^{-25}$ cm^2/electron. Water (H_2O) contains 10 electrons per molecule (2 from the H atoms + 8 from O) and there are 6.023×10^{23} (Avogadro's number) molecules per mole (1 mole is 18 g). Thus

$$10\ \frac{\text{electrons}}{\text{molecule}} \times 6.023\times10^{23}\ \frac{\text{molecules}}{\text{mole}} \times \frac{1\text{ mole}}{18\text{ g}} \times 2.11\times10^{-25}\ \text{cm}^2/\text{electron}$$

$$= 7.06\times10^{-2}\ \text{cm}^2/\text{g} .$$

As we shall see later, the total mass attenuation coefficient in water for a 1-MeV photon is exactly this value; i.e., the cross-section for the photoelectric effect at this energy is negligible, because the electrons are essentially free. [End of Example 7.7]

Interaction of a photon with the coulomb field of the nucleus can lead to the creation of a positively (positron) and a negatively charged electron with the disappearance of the photon. This process, referred to as pair production, can only occur if the photon is of energy greater than the rest mass energy of the formed pair [rest mass energy (m_0c^2) for an electron is 0.511 MeV]; thus the process has a threshold at 1.02 MeV. The energy of the photon in excess of the threshold is shared equally as kinetic energy of the pair. The kinetic energy of the created pair is dissipated as discussed for electrons: positrons lose their kinetic energy essentially as electrons do. As the positron slows down, it will capture an electron of the medium and be annihilated. This annihilation, essentially the reverse of pair production, results in conversion of the rest mass energy of the positron-electron pair into two photons of 0.511 MeV each. To satisfy conservation of momentum, the photons must be emitted in opposite directions, i.e., 180° apart. The probability per atom for pair production increases with increasing photon energy above the threshold and is proportional to the square of the atomic number (Z^2). Thus pair production is the dominant interaction even for high-energy photons and high-Z media.

A measure of the probability per unit distance (density distance) traveled by a photon that an interaction occurs is the mass attenuation coefficient. As the three interaction events discussed above are independent and mutually exclusive, the total mass attenuation coefficient (μ/ρ) is given as

$$\mu/\rho = \tau/\rho + \sigma/\rho + \kappa/\rho \ , \tag{7.37}$$

where τ/ρ, σ/ρ, and κ/ρ are the mass attenuation coefficients for the photoelectric, Compton, and pair production events. Tabulations of these coefficients for various elements and compounds of general interest are given by Evans (1968), Hubbell (1969), and Storm and Israel (1970). Values for other compounds or absorbing media can be computed as

$$\mu/\rho = \sum_i w_i(\mu/\rho)_i \ , \tag{7.38}$$

where $(\mu/\rho)_i$ is the tabulated value for the ith element, and w_i is the fraction by weight of the ith element in the medium of interest. The equation is valid because the chemical binding energies between atoms in a molecule are very small, thus not significantly altering the electronic binding energies.

As we have seen above, the transfer of energy from photons to matter is a two-step process involving first the conversion of the photon's energy to kinetic energy of secondary electrons, and then the electrons' dissipating the kinetic

energy through excitation and ionization of the absorbing medium. In principle, an evaluation of the energy dissipation in the medium would involve determination of the energy spectrum of the secondary electrons set in motion by the photon interactions, and determination of their energy deposition pattern through recourse to transport consideration (see above discussion of electrons). It is simpler, however, and in most instances adequate, to employ a procedure in which the energy transferred to secondary electrons is assumed to be deposited in the medium at the location of the photon interaction. Clearly, the transport of energy by the secondary electrons can be neglected if their range is small relative to the dimensions of the medium of interest and if the spatial details of the absorbed energy are not of interest.

The rate of energy transfer from photons to a medium is proportional to the number of photons passing through the volume element of interest (the photon flux) and the energy of these photons. The constant of proportionality is called the mass energy-transfer coefficient and is denoted by μ_{en}/ρ.

The mass energy-transfer coefficient is the weighted sum of the mass attenuation coefficients; i.e.,

$$\mu_{en}/\rho = f_\sigma(\sigma/\rho)+f_\tau(\tau/\rho)+f_\kappa(\kappa/\rho) \ . \tag{7.39}$$

The weights f_σ, f_τ, and f_κ indicate, for their respective interactions, the fraction of the photon energy which is converted into kinetic energy of secondary electrons and dissipated in the medium by collision losses. Note the restriction of the energy deposition to "collision losses"; radiative loss (bremsstrahlung) is excluded from the mass energy-transfer coefficient. It is beyond the scope of this chapter to develop the detailed prescription for estimation of the weights. But it is important that the reader note, for example, that the weights reflect only the energy transferred as kinetic energy of charged particles and thus energy emitted as x rays following photoelectric absorption; the rest mass energy of the positron-electron pair in the pair production process is excluded from the weight. It should be further noted that for the composition of body tissues and typical photon energies, the correction for bremsstrahlung energy loss by the secondary electrons is rather small.

7.3.4.5 Point-Isotropic Specific Absorbed Fraction

The fraction of the energy emitted by a point-isotropic source that is absorbed per gram at a distance x from the source [the point isotropic specific absorbed fraction $\Phi(x)$] can be expressed as

$$\Phi(x) = \frac{\mu_{en}}{\rho}\frac{e^{-\mu x}}{4\pi x^2}B_{en}(\mu x) \ , \tag{7.40}$$

where x is the distance from the point source, μ is the linear attenuation coefficient of the source energy, μ_{en}/ρ is the mass energy-transfer coefficient at

the source energy, and $B_{en}(\mu x)$ is the energy-absorption buildup factor. Examination of the above equation reveals that it includes a factor representing the attenuation of the photon flux $e^{-\mu x}$ and the geometric reduction $[1/(4\pi x^2)]$; the product of these factors with the mass energy-transfer coefficient yields the energy absorbed per gram due to the primary or uncollided photons (photons which have not experienced an interaction). However, because of the scattering of photons into the region of interest, it is necessary to modify the essentially uncollided calculation by the factor referred to as the energy absorption buildup factor. Such an approach is only possible within the uniform isotropic model.

Several tabulations of energy-absorption buildup data are available in the literature for application to body tissues. Berger presented such data in MIRD Pamphlet No. 5 (Berger, 1968) for a point source in water. More recently, Spencer and Simmons (1973) have published improved values applicable to 40 mean free paths ($\mu r = 40$), whereas Berger's data were applicable to 20 mean free paths. The Spencer and Simmons data are presented in terms of a ninth-degree polynomial; i.e.,

$$B_{en}(\mu r) = 1 + e^{-\alpha\mu r} \sum_{i=1}^{9} a_i(\mu r)^i \ . \tag{7.41}$$

For small values of μr, $B_{en}(\mu r)$ is approximately unity. The maximum buildup occurs for photons of about 100 MeV and is an increasing function of distance.

Example 7.8 We illustrate the use of Eq. 7.40 in estimating photon specific absorbed fraction data. Let us compute Φ(testicles←thyroid) for a 1-MeV photon. For volume source and target regions one would use Eq. 7.12 in conjunction with Eq. 7.40; however, both source and target regions are quite small (20 and 40 g, respectively) and separated by a distance that is large (~75 cm) relative to their spatial extent. Thus we may consider the source and target regions as point regions.

The mass attenuation coefficient (μ/ρ) and mass energy-transfer coefficient for a 1-MeV photon are 0.0706 and 0.0311 cm^2/g, respectively. From Spencer and Simmons (1973), the coefficients of the polynomial of Eq. 7.41 are:

i	a_i
1	7.1117356E−1
2	5.2335893E−1
3	−3.5185065E−2
4	1.2487894E−2
5	−1.0191981E−3
6	6.7697850E−5
7	−2.2691445E−6
8	4.3776058E−8
9	−2.7058007E−10
α	0.13636

If we assume a density of 1 g cm^{-3}, then the 75-cm separation corresponds to

$$\mu r = 0.0706 \text{ cm}^2 \text{ g}^{-1} \times 75 \text{ cm}$$
$$= 5.30 .$$

The energy-absorption buildup factor $B_{en}(\mu r)$ is

$$B_{en}(5.30) = 1 + e^{-0.13636 \times 5.30} \sum_{i=1}^{9} a_i (5.30)^i$$
$$= 1 + 20.09 e^{-0.7227}$$
$$= 10.75 .$$

From Eq. 7.40, then,

$$\Phi(75) = \frac{0.0311 \text{ cm}^2 \text{g}^{-1} \times e^{-5.30}}{4\pi (75 \text{ cm}^2)} B_{en}(5.30)$$
$$= 2.196 \times 10^{-9} \times 10.75$$
$$= 2.36 \times 10^{-8} \text{g}^{-1}.$$

Thus Φ(testicles←thyroid) = 2.36×10^{-8} g^{-1} at 1 MeV; the corresponding value tabulated in MIRD Pamphlet No. 5 Revised (Snyder et al., 1978) is 2.46×10^{-8} g^{-1}, based on the use of Eq. 7.12 in conjunction with Eq. 7.40. Note in this example the significance of the scattered photons; i.e., the specific absorbed fraction considering only the uncollided photon flux is only 2.20×10^{-9} g^{-1}. [End of Example 7.8]

7.3.4.6 Monte Carlo Transport Calculations

An obvious limitation of the point-isotropic specific absorbed fraction is that it is only strictly applicable to a uniform isotropic model. The human body is not a homogeneous absorbing medium, nor is it large relative to the "range" of photon radiation. The only computational method which can be applied to address radiation transport in a heterogeneous medium utilizes Monte Carlo techniques.

The Monte Carlo technique is distinguished from other numerical techniques in that random sampling of probability distribution functions is used to approximate the solution to the mathematical problem. Monte Carlo simulation of photon transport is, in principle, rather simple, straightforward, and requires only knowledge of elementary probability theory, the kinetics of photon interaction with matter, and the geometry of the system being simulated. However, to apply Monte Carlo methods to estimating photon specific

absorbed fractions, a considerable expenditure in code development must be done to (1) generate the origin and flight of photons from the source region, (2) determine the target regions in which interaction events lie, and (3) treat the kinetics of the interaction events. If we had to start afresh, the investment in code development and verification might well be prohibitive. However, aspects of the simulation, in particular the kinetics (item 3), have been developed into code packages, and we need only code the particular geometry (items 1 and 2) for the problem of interest. Several excellent references on Monte Carlo methods are available to aid the development effort (Carter and Cashwell, 1975; Cashwell and Everett, 1959; and Shreider, 1966).

The Monte Carlo approach to photon transport can probably be best understood in terms of the so-called complete analog approach. In that approach, a faithful simulation of the photon's flight and the radiation physics of the possible interactions is strictly maintained. The flight of a photon (a *history*) would be simulated and interaction events would be considered by sampling their probability distributions, the history being terminated when (1) the total energy of the photon has been deposited or (2) the photon escapes from the body.

As discussed above, the linear attenuation coefficients τ, σ, and κ represent the probability per unit distance of the photoelectric, Compton, and pair-production events. As these events are independent and mutually exclusive, the probability of a photon undergoing an interaction per unit distance is $\mu = \tau + \sigma + \kappa$.

Determination of the point at which an interaction occurs is basic to the simulation. The probability that an interaction occurs between x and $x + dx$, where x is a given distance from the origin of the photon, is the product of the probability that the photon reached x and the probability of an interaction in the differential element dx. Thus the probability of a photon interacting between x and $x + dx$, denoted by $p(x)dx$, is given as

$$p(x)dx = e^{-\mu x}\mu dx, \tag{7.42}$$

where the exponential factor represents the probability that the photon reaches x and μdx is the probability of interaction in the interval dx. The quantity $p(x)$ is a probability density function. The probability that an interaction occurs within distance ℓ is then

$$P(\ell) = \int_0^{\ell} p(x)dx = 1 - e^{-\mu\ell} . \tag{7.43}$$

The quantity $P(\ell)$ represents the cumulative distance-to-interaction distribution. Note that $P(\ell)$ satisfies the necessary conditions of a cumulative probability distribution function, in that its range lies between 0 and 1. In simulating the flight of the photon, we must randomly sample this distribution. To sample

the distribution, the random number, ξ, chosen uniformly from the region $0 < \xi < 1$, is equated to the distribution,

$$\xi = 1 - e^{-\mu \ell}, \tag{7.44}$$

and solving for ℓ we obtain

$$\ell = -\ln(1-\xi)/\mu. \tag{7.45}$$

However, as $1-\xi$ is itself a random number (complement of ξ), we can write

$$\ell = -\ln(\xi)/\mu. \tag{7.46}$$

This is the well-known expression for sampling the distance-to-interaction in Monte Carlo simulation of photon transport.

If the transport is in a heterogeneous medium, then various regions may have different linear attenuation coefficients. This is the case in the representation of the human body used in Monte Carlo calculations where three regions of different composition and density are considered, namely, soft tissue, lung, and skeleton. The above distance-to-interaction expression was developed for a single medium with linear attenuation μ. Two different approaches can be applied to determining the distance-to-interaction in a multi-medium problem. In one approach, one projects forward the photon flight to find what regions may be intersected, and one applies the above equation in each successive region until an interaction distance is determined or the photon escapes from the regions of interest. As one might expect, substantial geometric considerations would be involved, particularly if the regions are complex and numerous. An alternative approach which is computationally simpler, although its validity is not readily apparent, is often used. In this approach, the distance-to-interaction is determined from the same equation, but the maximum linear attenuation of the regions is used in the equation; that is,

$$\ell = -\ln(\xi)/\max(\mu_1, \mu_2, \cdots, \mu_n), \tag{7.47}$$

where $\max(\mu_1, \mu_2, \cdots, \mu_n)$ denotes the maximum value of the μ_i. The region in which this possible interaction site lies is then determined and a game of chance is played; that is, a random number ξ is obtained and if $\xi \leqslant \mu_i/\max(\mu_1, \mu_2, \cdots, \mu_n)$, the location is accepted as an interaction site. If the outcome of the game is not favorable, the photon is allowed to continue from the false position with an incremental distance-to-interaction picked as above. In general, it is computationally easier to determine in which region a potential interaction site lies and play the game of chance than to project the flight's intersection with geometric regions as required in the former approach.

Given that a photon interaction has occurred at location ℓ and that ℓ lies in region i of a heterogeneous medium, then the conditional probability that the

interaction was a photoelectric absorption event is τ_i/μ_i, a Compton scattering event σ_i/μ_i, or a pair-production event κ_i/μ_i. If a random number ξ, $0 < \xi < 1$, satisfies

$$\tau_i/\mu_i \leqslant \xi < (\tau_i+\sigma_i)/\mu_i \ , \tag{7.48}$$

then ξ determines that a Compton event occurred. If the random number ξ is such that

$$(\tau_i+\sigma_i)/\mu_i \leqslant \xi \leqslant (\tau_i+\sigma_i+\kappa_i)/\mu_i \ , \tag{7.49}$$

then the pair-production event is considered to occur. If ξ is less than or equal to τ_i/μ_i, then the photoelectric event is considered to occur. Note that if the photon energy is less than the pair-production threshold of 1.02 MeV, then $\kappa = 0$ and no ξ can satisfy the inequalities of Eq. 7.49.

The energy deposited, ΔE, in the region i as a result of the interactions can be summarized as

$$\Delta E = \begin{cases} E; \text{ photoelectric event} \\ E-E'; \text{ Compton event} \\ E-2m_0c^2; \text{ pair-production event,} \end{cases}$$

where E is the initial energy of the photon, E' is the energy of the Compton-scattered photon, and $2m_0c^2$ is the energy associated with creation of the positron-electron pair. The energy E' of the Compton-scattered photon is uniquely determined by the initial photon energy and the scatter angle (Eq. 7.30). The probability that the photon is scattered in a given angle is given by Monte Carlo sampling of the Klein-Nishina cross section. The Compton-scattered photon must then be simulated in the calculations such that its potential energy deposition is considered. In a similar fashion, the two photons associated with annihilation of the positron must also be simulated.

The complete analog Monte Carlo approach outlined above and flowcharted in Fig. 7.1 requires simulation of a very large number of histories, particularly for target regions far removed from the source. Thus, some type of weighting or biasing in the sampling of the probability distribution is often used. It is not our intent to discuss these details but rather to outline the general Monte Carlo approach, whose simplicity is evident in the complete analog approach.

Example 7.9. As a simple application of Monte Carlo techniques, we seek to calculate the number of photons experiencing their first interaction within a distance R from a point source. To carry out this exercise, we need only pick a random number ξ, $0 < \xi < 1$, and determine if the distance-to-interaction $\ell = -\ln(\xi)/\mu$ is less than R. If this condition is met, we count the event a success and pick a new random number for the next trial (history). We repeat this procedure for some finite number of histories and determine the fractional

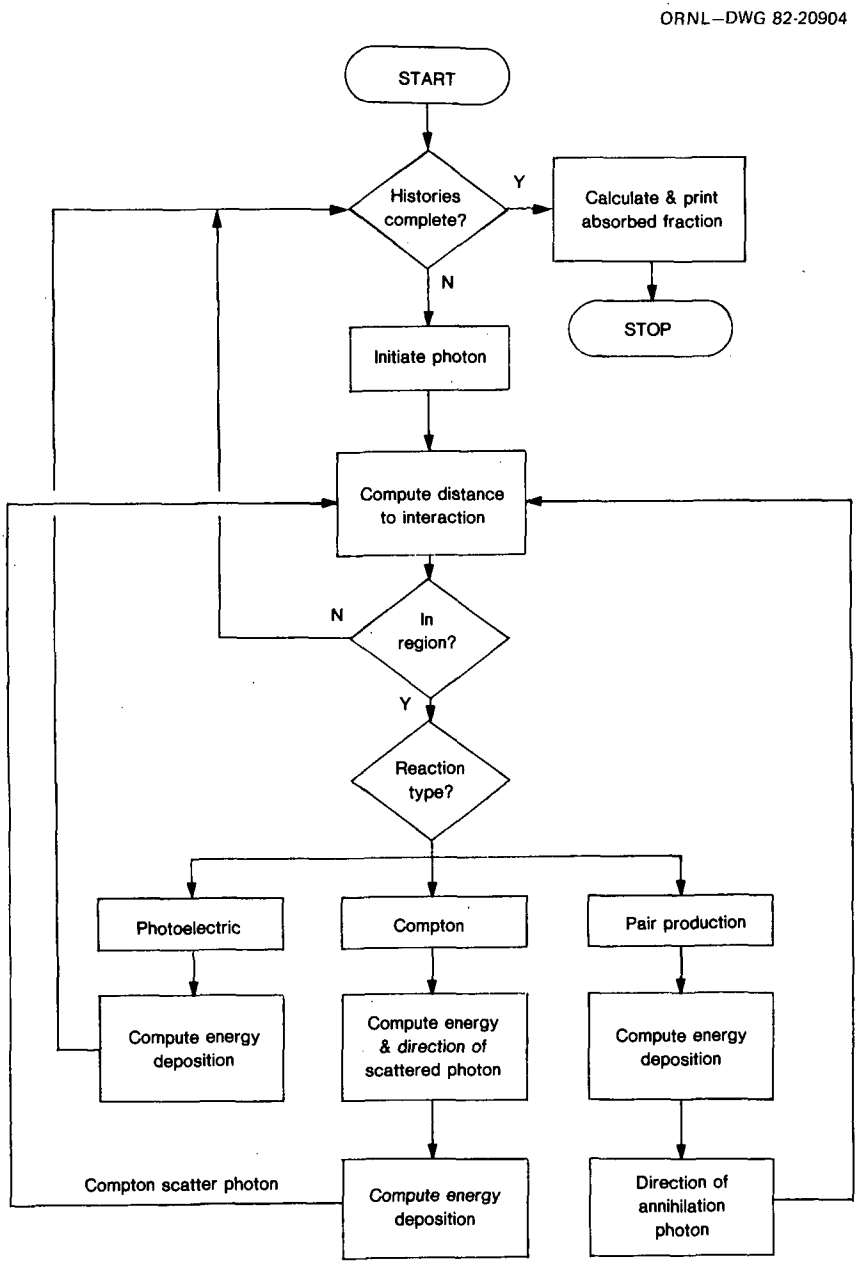

Figure 7.1. Flowchart for Monte Carlo simulation of photon histories.

successes. We would expect that after a large number of histories, the fraction of successful histories would be $1-e^{-\mu R}$. Tabulated below are results obtained for five simulations of various numbers of histories for $\mu = 1$, $R = 1$; i.e, $1-e^{-\mu r} = 0.632$.

Histories	Results	$\bar{x} \pm s$
100	0.67, 0.74, 0.70, 0.58, 0.66	0.670 ± 0.059
500	0.658, 0.650, 0.620, 0.652, 0.664	0.645 ± 0.015
1000	0.632, 0.614, 0.623, 0.624, 0.620	0.623 ± 0.007
5000	0.6444, 0.6262, 0.6370, 0.6268, 0.6310	0.633 ± 0.0077

This trivial example, which can be carried out on a programmable pocket calculator with a random-number generator, serves to indicate the statistical nature of the solution derived by using Monte Carlo methods. The statistical nature of the results makes testing of Monte Carlo codes difficult, as a slight change in code logic can result in a completely different series of random numbers and thus different decisions being made, leading to numerically different results. In the preliminary testing phase of a Monte Carlo code, it is often advantageous to carry out a problem similar to this example, that is, consider only first-interaction events. The expected numbers of first interactions in various regions can often be inferred from geometry considerations. [End of Example 7.9]

7.3.5 Special Topic: Energy Deposition in Skeleton

7.3.5.1 Tissues of the Skeleton

The skeleton is a complex structure composed of bone mineral (5 kg), yellow marrow (1.5 kg), red-hematopoietic active marrow (1.5 kg), and assorted connective tissues (2 kg) (ICRP, 1975). The numerical values given above are for the adult male. There is now general agreement that the radiosensitive tissues of the skeleton are the hematopoietic stem cells of the active marrow and the osteogenic cells, particularly those on the endosteal surfaces of bone (ICRP, 1968). Developing red blood cells are found in various stages of maturation within the active marrow. Thus the active marrow is of primary concern as a target tissue with respect to leukemia induction. The osteogenic cells are the precursors of cells involved in the formation of new bone (osteoblasts) and the resorption of bone (osteoclasts) and are of concern as a target tissue with respect to bone cancer induction. Note that bone mineral, the largest component of the skeleton, is not considered at risk; only soft tissue regions of the skeleton are of concern.

In the past, the dose equivalent estimated for bone was averaged over a mass of 7 kg (ICRP, 1959). The effective energy deposited in the skeleton was compared with that of radium for which human experience had indicated that

a skeletal burden of 0.1 μg ^{226}Ra might serve as a permissible level. In estimating the effective energy, a modifying factor of five (the N-factor of Eq. 7.3) was applied to all non-radium isotopes to account for lack of knowledge as to their deposition patterns to the radiosensitive tissues. Evaluation of the irradiation of the tissues now considered at risk necessitates that mineral bone, the source region, be further classified into two bone types: trabecular and cortical bone.

In the mature skeleton, the two bone types are reasonably distinct with regard to both appearance (see Fig. 7.2) and their retention of deposited radionuclides. Cortical bone is the hard compact bone found largely in the shafts of long bones. This bone type contains about four-fifths of the skeletal mineral, i.e. 4 kg (ICRP, 1975), and constitutes about one-half of the skeletal surface area. The surface area of the skeleton is about 12 m^2. If one assumes a mineral density of 2 g cm^{-3}, then the surface to volume ratio, S/V, of cortical bone is

$$\begin{aligned} S/V &= 6\times10^4\,\text{cm}^2 \times 2\,\text{g cm}^{-3} \div 4\times10^3\,\text{g} \\ &= 30\,\text{cm}^2/\text{cm}^3. \end{aligned} \tag{7.50}$$

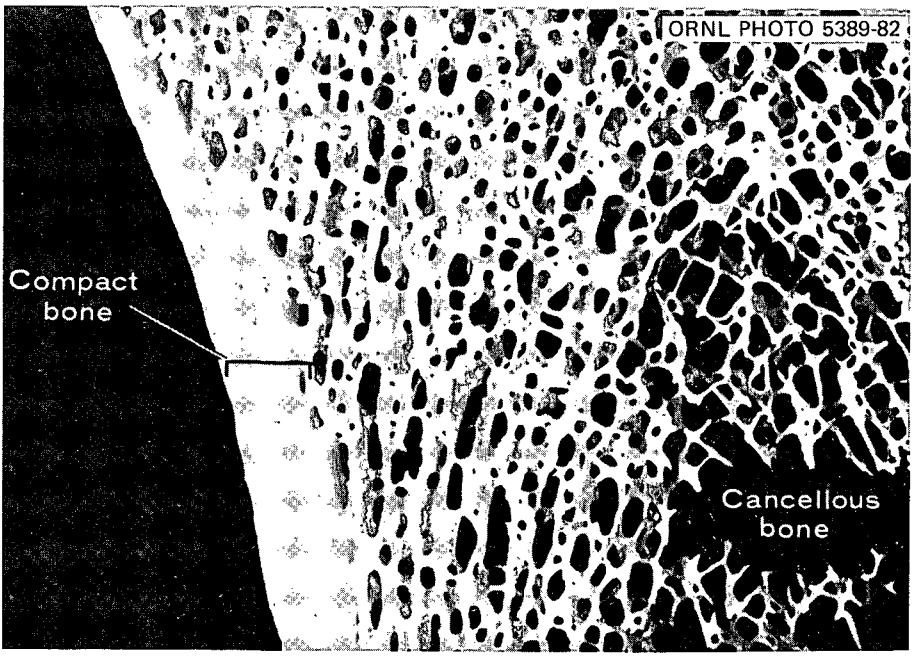

Figure 7.2. A section of the tibia, illustrating the compact (cortical) bone and the trabeculae of the cancellous (trabecular) bone. Source: Bloom, W., and Fawcett, D. W. 1975. *A Textbook of Histology,* Saunders, Philadelphia. Reprinted with permission.

The dominant microscopic structure of cortical bone is the Haversian system. Each Haversian system consists of a canal or space containing blood vessels, osteoblasts (bone-forming cells), and undifferentiated cells. The canals are typically 50 μm in diameter (ICRP, 1975) and with supporting channels serve to supply nutrient to the skeletal interior. The soft tissues lining the Haversian system are a component of the endosteal tissue, which is considered at risk for bone cancer (ICRP, 1968; ICRP, 1979).

Trabecular bone, sometimes referred to as cancellous bone, is the soft, spongy bone, composed of an apparently fragile lattice-work, which is interior to flat bones and the ends of long bones. Trabecular bone is characterized by a high surface to volume ratio; if one assumes that the mineral density of trabecular bone is 2 g cm^{-3} and that one-half of the skeletal surface area is associated with this bone type, then

$$S/V = 6 \times 10^4 \text{ cm}^2 \times 2 \text{ g cm}^{-3} \div 1 \times 10^3 \text{ g}$$
$$= 120 \text{ cm}^2/\text{cm}^3. \quad (7.51)$$

Thus the surface to volume ratio of trabecular bone is about four times that of cortical bone. The interlacing splinters of bone mineral (trabeculae) form cavities in which the active marrow is found. As trabecular bone totally contains the active marrow, this bone type is the major source region from which beta and alpha particles may originate to irradiate the active marrow.

7.3.5.2 Estimation of Energy Deposition

Estimation of energy deposition in the skeletal target regions is complicated by the geometric relationships between the source and target regions. The trabeculae and the marrow cavities they form in trabecular bone cannot be represented by simple solid geometric forms. To derive an estimate of the energy deposition in the marrow cavities, we need to consider the potential path taken by a charged particle (alpha or beta particle, or in the instance of photon irradiation, secondary electron) in its traversal of trabeculae and marrow cavities. If we assume that a particle originates in the mineral region, its energy upon entering a cavity will depend on its initial energy and that dissipated in traveling to the cavity, i.e., the residual energy as indicated by the range-energy relationships discussed in Sect. 7.3.4. The amount of energy deposited within a cavity is dependent on the path the particle takes through the cavity and the energy it had on entrance. If a particle has sufficient energy to traverse the cavity, it will encounter a trabecula on the far side, which (given sufficient energy) it may traverse and enter a second cavity. Calculations of the energy deposition thus require information on the lengths of possible paths particles may take through these two tissues. Such compilations are available for a limited number of bones (Beddoe et al., 1976). Using these data

and Monte Carlo sampling techniques, the flight of particles can be simulated as outlined in Sect. 7.3.4.

Example 7.10. The range of alpha particles is sufficiently limited that one can treat the mineral surface of trabecular bone as a flat plane; i.e., the radius of curvature of the marrow cavities is much greater than the particle range. Given this assumption, the mineral and marrow can be regarded as each occupying a half-space. We wish to estimate the fraction of the energy of alpha particles emitted in the volume of the mineral that is deposited in the marrow, that is,

$$\phi(\text{red marrow} \leftarrow \text{trabecular bone}) .$$

Consider a 6-MeV alpha particle whose range in soft tissue is 47.2 μm (see Example 7.4). The ratio of stopping powers in bone and soft tissue for alpha particles is about 1.95; thus the range in bone of 6-MeV alpha particles is 47.2/1.95 or 24.2 μm. Only alpha particles emitted within 24.2 μm of the interface can deposit energy in the marrow space. To carry out our estimate, we will employ Monte Carlo techniques in conjunction with the range-energy data of Table 7.6.

Assume a coordinate system with its origin at the interface, with bone mineral occupying the half-space $x < 0$ and marrow the region $x > 0$. We will simulate a volume source by random selection of points from which the particles are to be emitted; note that only the x coordinate need be established, because the half-spaces are infinite in the y and z directions. We further restrict our attention to the mineral region from which 6-MeV alpha particles can potentially reach the interface, namely, the region defined by $-24.2 < x_0 < 0$. The coordinates of the emission point are $(-24.2\xi,0,0)$, where the random number ξ is uniformly distributed in the interval 0 to 1. Given the origin of the particle, we now need to establish its direction (note that only particles traveling in the positive x direction can reach the interface). The direction can be simulated by random selection of direction cosines; recall that the parametric form of the equation of the line passing through (x_0,y_0,z_0) can be written as

$$x = x_0+\mu t , \quad y = y_0+\lambda t , \quad \text{and} \quad z = z_0+\nu t , \tag{7.52}$$

where μ, λ, and ν are direction cosines of the line. To generate direction cosines at random, consider a hemisphere of unit radius occupying the region $x > 0$. Points within the hemisphere can be selected at random as

$$x = \xi_1 , \quad y = 2\xi_2-1 , \quad \text{and} \quad z = 2\xi_3-1 , \tag{7.53}$$

where ξ_1, ξ_2, and ξ_3, are independent random numbers from the uniform distribution for the interval $0 \leqslant \xi \leqslant 1$. Note that the values of the y and z coordinates range from -1 to 1, while the x coordinate is between 0 and 1. If

$$x^2+y^2+z^2 > 1 , \tag{7.54}$$

we reject the point as it is outside the hemisphere. Rejection is a commonly employed technique in construction of random sampling schemes. What we are doing is selecting points in a box of dimension $1\times2\times2$ and rejecting any point that lies outside the enclosed hemisphere of volume $\frac{2}{3}\pi$. The efficiency of the scheme is the ratio of the two volumes; in this case, $\pi/6$ or about 52%. This is not a highly efficient scheme, but it is sufficient for our purpose here. If the point (x,y,z) is accepted, then direction cosines of the line passing through (0,0,0) and the point are

$$\mu = \frac{x}{(x^2+y^2+z^2)^{1/2}}, \qquad \lambda = \frac{y}{(x^2+y^2+z^2)^{1/2}}, \qquad \nu = \frac{z}{(x^2+y^2+z^2)^{1/2}}. \tag{7.55}$$

Having established the origin and direction of the alpha particle, we now must determine its path length in the mineral half-space. The parametric equations of the particle's flight are

$$x = x_0+\mu t\,, \quad y = \lambda t\,, \quad \text{and} \quad z = \nu t\,. \tag{7.56}$$

The particle will cross the interface at $x = 0$; solving the x-coordinate equation for t gives us $t = -x_0/\mu$. Thus the coordinate of the point of interception with the plane is

$$(0, -x_0\lambda/\mu, -x_0\nu/\mu)\,.$$

The path length ℓ of the particle is the distance between its origin $(x_0,0,0)$ and the intercept:

$$\ell = |x_0|\sqrt{1+(\lambda/\mu)^2+(\nu/\mu)^2}, \tag{7.57}$$

where $|x_0|$ denotes the absolute value of x_0.

Table 7.8 presents the results of a simulation of 5000 6-MeV alpha particles being emitted from the segment of the x axis given by $-24.2 < x < 0$ and in the positive x direction. All path lengths greater than the particle's range in bone were scored in a single bin labeled ">24.2"; some 50.8% of the simulations fell into this bin. Other path lengths were scored in 20 bins of equal width; the upper boundaries of the bins are indicated in the first column. The residual energy E_i is the energy of the particle after traveling a distance corresponding to the midpoint of the ith bin; these values were obtained from the data of Table 7.6 after the path in bone was multiplied by 1.95 to obtain an equivalent path in soft tissue. It is this energy which will be deposited in the marrow space.

Table 7.8. Calculation of ϕ(red marrow ← trabecular bone) for a volume-distributed alpha source of energy 6 MeV

ℓ (μm)	Number	Fraction×100	Deposited energy (MeV) per particle
1.21[a]	117	2.34	5.90
2.42	125	2.50	5.71
3.63	129	2.58	5.51
4.84	113	2.26	5.31
6.05	128	2.56	5.11
7.26	130	2.60	4.89
8.47	122	2.44	4.67
9.68	142	2.84	4.44
10.89	119	2.38	4.21
12.10	126	2.52	3.97
13.31	117	2.34	3.72
14.52	126	2.52	3.45
15.73	118	2.36	3.16
16.94	110	2.20	2.87
18.15	107	2.14	1.56
19.36	126	2.52	2.22
20.57	127	2.54	1.83
21.78	129	2.58	1.38
22.99	128	2.56	0.84
24.20	121	2.42	0.25
>24.20	2540	50.80	
Total	5000		$\sum_{i=1}^{20} F_i E_i = 1.77$

[a]For example, 117 alpha particles traversed a path length in bone between 0 and 1.21 μm (averaged path 0.60 μm) and entered the marrow half-space with 5.90 MeV of energy.

The absorbed fraction for the simulated emissions is the quotient of the deposited energy and the emitted energy, or

$$\phi = \frac{1}{6}\sum_{i=1}^{20} F_i E_i = \frac{1}{6} \times 1.77 = 0.3 . \tag{7.58}$$

Recall that we biased our simulation to consider only particles traveling in the positive x direction. If the emissions had been 4π- rather than 2π-isotropic, only one-half of the simulated particles would have traveled in the positive x direction. Thus for a 4π-isotropic source, the absorbed fraction would be 0.15.

We also need to translate the simulation to that of a volume-distributed source in trabecular bone (recall that we restricted the source region to a depth corresponding to a particle's range). An estimate of the fraction of trabecular

bone that lies within 24.2 μm of the surface is needed. The mass of trabecular bone is 1000 g, corresponding to a volume of 500 cm^3 (density of 2 g cm^{-3}), with a surface area of 6 m^2 (6 $\times$ 10^4 cm^2). The thickness t of a slab (rectangular solid) of surface area A and volume V is

$$t = 2V/A ;$$

we neglect the contribution of the edges to the surface area. Thus the average thickness of trabecular bone is about 170 μm. The fraction of trabecular bone within 24.2 μm of the surface is thus

$$2 \times 24.2 \div 170 \text{ or } 0.29 ,$$

where the factor of 2 enters because of the two slab surfaces. Only 29% of a volume-distributed alpha source would contribute an absorbed fraction of 0.15; thus,

$$\phi(\text{red marrow} \leftarrow \text{trabecular bone}) = 0.29 \times 0.15 = 0.044 .$$

In ICRP Publication 30, a nominal value of 0.05 was suggested for all alpha emitters. Our estimate, based on a small number of simulated emissions, is in excellent agreement with the recommended value. [End of Example 7.10]

The skeleton is continuously undergoing remodeling. In the case of the mature skeleton, resorptive and formative processes result in a turnover of the mineral with no change in the total quantity of mineral present. Radionuclides are incorporated into the mineral matrix by the formative process and removed by the resorptive process. Some radionuclides are capable of movement into the volume of the mineral matrix through a "diffusion-like process," while others tend to remain on the surface. For purposes of bone dosimetry, radionuclides are dichotomously classified as surface or volume seekers. The energy deposition in the sensitive tissues can be highly dependent on this classification, particularly for low-energy electron and alpha radiations.

Example 7.11. In an earlier example, the absorbed fraction in the red marrow for alpha particles uniformly distributed in the volume of trabecular bone was found to be 0.05. If the alpha emitter were distributed along the mineral surface, what would be the absorbed fraction? In Example 7.10, we indicated that the mineral and marrow regions can be represented by half-spaces when dealing with alpha radiation. For particles emitted in a 4π-isotropic manner at the interface of the half-spaces, geometric considerations indicate that one-half of the emissions would enter the marrow half-space at their initial energy. Thus for a surface deposit,

$$\phi(\text{red marrow} \leftarrow \text{trabecular bone}) = 0.5 .$$

Note that this value is an order of magnitude higher than the corresponding quantity for a volume distributed source. [End of Example 7.11]

Calculation of the energy deposition of alpha radiation in the skeletal tissues was considerably simplified by the assumption of half-space geometry. For electron radiation, e.g., beta particles, such a geometric simplification is not possible and recourse must be made to measurement of possible path lengths through the trabeculae and marrow cavities, refinements which we cannot enter into in this chapter. The nominal values for the absorbed fraction for skeletal tissues as suggested by Committee 2 of the ICRP are given in Table 7.9. Note the indicated energy dependence of the absorbed fraction for a surface-seeking beta emitter. For a high-energy beta emitter, the question of whether the emitter is on the surface or in the volume is relatively unimportant, because of the range of the particles. At lower energies, $E < 0.2$ MeV, the ranges of beta and alpha particles are similar, and thus the absorbed fraction for these radiations for surface deposits are the same.

Table 7.9. Absorbed fractions ϕ for bone dosimetry

Source organ	Target organ	α emitter		β emitter		
					On bone surface	
		Uniform in volume	On bone surface	Uniform in volume	$\bar{E}_\beta$>0.20 MeV	$\bar{E}_\beta$<0.20 MeV
Trabecular bone	Bone surface	0.025	0.25	0.025	0.025	0.25
Cortical bone	Bone surface	0.01	0.25	0.015	0.015	0.25
Trabecular bone	Red marrow	0.05	0.5	0.35	0.5	0.5
Cortical bone	Red marrow	0.0	0.0	0.0	0.0	0.0

Before closing our discussion on absorbed fractions in skeletal tissues, a few remarks are needed regarding photon radiation. The energy deposited in the skeleton by photon radiation is estimated using Monte Carlo methods as discussed in Sect. 7.3.4. In these simulations, the skeleton is represented as a uniform mixture of its components, since it is impossible to model the geometric details. The energy deposited in regions of the skeleton (total mass 10 kg) is partitioned among the various skeletal components according to their mass fractions. For example, if one assumes uniform irradiation of the skeleton, the energy deposition in the red marrow (mass 1.5 kg) is taken as 1.5/10 of that deposited in the homogeneous skeleton. This approximation is reasonable for photons of energy greater than about 0.2 MeV, where Compton interactions are the dominant interaction events. Recall that the Compton cross section is proportional to the electronic density, which has similar values for bone mineral and soft tissue; the result is that the skeleton appears as a uniform mixture. At lower photon energies, photoelectric interactions in the mineral region are the dominant events by which energy is deposited in the skeleton. Partitioning the deposited energy among the skeletal tissues by mass fraction

results in an overestimate of the energy deposition in the soft tissue regions. However, photoelectrons liberated by photon interactions in the mineral will irradiate the soft-tissue spaces of the skeleton, and thus one cannot neglect the presence of the bone mineral. The energy deposition in soft tissues of the skeleton is enhanced by their proximity to the mineral, and the magnitude of the enhancement is dependent on the photon energy. The transport of energy by secondary charged particles from their points of origin to the deposition of their energy needs to be considered to obtain realistic estimates of the energy deposition in the skeleton.

7.3.6 Illustrative Example: Calculation of S-factors

Given absorbed fraction data, S-factors can be computed from knowledge of the radiations emitted in nuclear transformations of the radionuclide of interest. Compilation of the radiations emitted in the nuclear transformations of the various radionuclides is not a trivial task; however, these data have been compiled by specialists for such application (Dillman, 1969; Kocher, 1981). In this section, we present several examples to illustrate the computation of the S-factor and its use.

Example 7.12. The principal region of residence of ^{90}Sr ($T_{1/2}$ = 29.12 y) in the body is the bone mineral region. Strontium-90 is a pure beta emitter (average energy 0.1957 MeV), which decays to ^{90}Y ($T_{1/2}$ = 64.0 h), also a pure beta emitter (average energy 0.9348 MeV). We wish to compute the appropriate S-factors for the skeletal tissues at risk.

The S-factor as defined by Eq. 7.18 can be written as follows:

$$S(\boldsymbol{T} \leftarrow \boldsymbol{S}) = \frac{1.6 \times 10^{-13}}{M_{\boldsymbol{T}}} \sum_i \Delta_i \phi_i(\boldsymbol{T} \leftarrow \boldsymbol{S}) ,$$

where Δ_i = product of the intensity of the ith radiation per nuclear transformation (nt) and its average or unique energy (MeV/nt); $\phi_i(\boldsymbol{T} \leftarrow \boldsymbol{S})$ = absorbed fraction of the ith radiation for the source-target pair; and $M_{\boldsymbol{T}}$ = mass of the target region (kg). The constant 1.6×10^{-13} represents the conversion from MeV to joules, and thus S has units of joule/kg-nt or Gy/nt. If a quality factor or other modifying factors are included, S should be expressed as Sv/nt. Note that 1 nt is equivalent to 1 Bq-s, and therefore S can be expressed as Sv/s per Bq.

As strontium is a member of the same chemical family as calcium (alkaline earth elements), we will assume that it is distributed in the volume of the mineral. We will also assume that ^{90}Y, as the daughter of ^{90}Sr, is volume distributed. Thus from Table 7.9, we have

$$\phi(\text{bone surface} \leftarrow \text{trabecular bone}) = 0.025 ,$$

$$\phi(\text{bone surface} \leftarrow \text{cortical bone}) = 0.015 ,$$

$$\phi(\text{red marrow} \leftarrow \text{trabecular bone}) = 0.35 .$$

We also have mass of bone surface = 0.12 kg, and mass of red marrow = 1.5 kg. For ^{90}Sr, Δ_i = 0.1957 Mev/nt; and

$$S(\text{bone surface} \leftarrow \text{trabecular bone})$$
$$= 1.6\times10^{-13} \times 0.025 \times 0.1957 \div 0.12$$
$$= 6.52 \times 10^{-15}\ \text{Gy/nt},$$
$$S(\text{bone surface} \leftarrow \text{cortical bone})$$
$$= 1.6\times10^{-13} \times 0.015 \times 0.1957 \div 0.12$$
$$= 3.91\times10^{-15}\ \text{Gy/nt},$$
$$S(\text{red marrow} \leftarrow \text{trabecular bone})$$
$$= 1.6\times10^{-13} \times 0.35 \times 0.1967 \div 1.5$$
$$= 7.31\times10^{-15}\ \text{Gy/nt}.$$

For ^{90}Y, Δ_i = 0.9348 MeV/nt, and the values are

$$S(\text{bone surface} \leftarrow \text{trabecular bone}) = 3.12\times10^{-14},$$
$$S(\text{bone surface} \leftarrow \text{cortical bone}) = 1.87\times10^{-14}, \text{ and}$$
$$S(\text{red marrow} \leftarrow \text{trabecular bone}) = 3.49\times10^{-14}\ \text{Gy/nt}.$$

In Example 7.19 (in Sect. 7.4.2), it is shown that the ingestion of 1 Bq of ^{90}Sr results in 0.3 Bq entering the blood. In addition, from Example 7.17 (in Sect. 7.4.1), the fifty-year residences (integrals of the retention in body tissues) for cortical and trabecular bone are shown to be 398 and 157 Bq-d per Bq uptake to blood, respectively. Let us use these data to estimate the committed dose equivalent to these tissues per unit ^{90}Sr ingested.

The number of nuclear transformations of ^{90}Sr occurring in the two types of bone mineral per unit activity ingested are

cortical:

0.3 Bq-blood/Bq-ingested × 398 Bq-d/Bq-blood

$\times\ 8.64\times10^4\ \text{s d}^{-1} \times 1$ nt/Bq-s

$= 1.03\times10^7$ nt in cortical bone per Bq ingested ;

trabecular:

0.3 Bq-blood/Bq-ingested × 157 Bq-d/Bq-blood

$\times\ 8.64\times10^4\ \text{s d}^{-1} \times 1$ nt/Bq-s

$= 4.07\times10^6$ nt in trabecular bone per Bq ingested.

Since the half-life of ^{90}Y is short relative to that of the parent nuclide, we can assume that each nuclear transformation of ^{90}Sr yields one nuclear transformation of ^{90}Y. Thus the committed dose equivalents per unit activity ingested (assuming 1 Sv = 1 Gy) are

$$H_{50}(\text{red marrow}) = 4.07\times10^{6}\ \text{nt/Bq-ingested} \times (7.31\times10^{-15} + 3.49\times10^{-14})\ \text{Sv/nt} = 1.72\times10^{-7}\ \text{Sv/Bq-ingested},$$

$$H_{50}(\text{bone surface}) = 4.07\times10^{6}\ \text{nt/Bq-ingested} \times (6.52\times10^{-15} + 3.12\times10^{-14})\ \text{Sv/nt} + 1.03\times10^{7}\ \text{nt/Bq-ingested} \times (3.91\times10^{-15} + 1.87\times10^{-14}) = 3.86\times10^{-7}\ \text{Sv/Bq-ingested.}$$

Note that the above values, in conjunction with an estimate of the intake of ^{90}Sr, can be used to compute the dose which the individual is committed to receive as a result of an intake. [End of Example 7.12]

The complexity of the calculation of the S-factor is dependent on the details of the radiations emitted in the nuclear transformations of the radionuclide.

Example 7.13. In Table 7.10 are shown the radiations emitted in nuclear transformations of ^{131}I. Note the multiple beta emissions and the presence of conversion electrons in the tabulation. X rays associated with vacancies in the K-shell created by the internal conversion of gamma radiations are also listed. As indicated at the bottom of the tabulation, some radiations have not been included in the listing (radiations representing less than 0.1% of the total energy for the radiation type).

$$^{131}I\ (8.040\ d) \xrightarrow[1.086\%]{\beta^-} {}^{131m}Xe\ (11.84\ d)$$

Specific absorbed fractions for photon radiation can be obtained from MIRD Pamphlet #5 Revised (Snyder et al., 1978). Values obtained from this source are tabulated below for the thyroid as the source organ and the thyroid and testes as target organs. Only data relevant to this example are shown.

Energy range (MeV)	Φ(thy.←thy.) kg^{-1}	Φ(testes←thy.) kg^{-1}
0.02 – 0.03	18.1 – 7.41	4.96×10^{-25} – 7.32×10^{-13}
0.05 – 0.10	2.42 – 1.44	1.67×10^{-8} – 7.87×10^{-7}
0.10 – 0.20	1.44 – 1.55	7.87×10^{-7} – 3.52×10^{-6}
0.20 – 0.50	1.55 – 1.66	3.52×10^{-6} – 1.17×10^{-5}
0.50 – 1.00	1.66 – 1.54	1.17×10^{-5} – 2.46×10^{-5}

Table 7.10. Radiation emissions of ^{131}I

Radiation	y_i (Bq-s)$^{-1}$	E_i (MeV)	$y_i \times E_i$
β^- 1	2.13(−2)	6.935(−2)[a]	1.48(−3)
β^- 2	6.20(−3)	8.693(−2)[a]	5.39(−4)
β^- 3	7.36(−2)	9.660(−2)[a]	7.11(−3)
β^- 4	8.94(−1)	1.915(−2)[a]	1.71(−1)
β^- 6	4.20(−3)	2.832(−2)[a]	1.19(−3)
γ 1	2.62(−2)	8.018(−2)	2.10(−3)
ce-K, γ 1	3.63(−2)	4.562(−2)	1.66(−3)
ce-L_1, γ 1	4.30(−3)	7.473(−2)	3.21(−4)
γ 4	2.65(−3)	1.772(−1)	4.70(−4)
γ 7	6.06(−2)	2.483(−1)	1.72(−2)
ce-K, γ 7	2.48(−3)	2.497(−1)	6.20(−4)
γ 12	2.51(−3)	3.258(−1)	8.18(−4)
γ 13	8.12(−1)	3.645(−1)	2.96(−1)
ce-K, γ 14	1.55(−2)	3.299(−1)	5.10(−3)
ce-L_1, γ 14	1.71(−3)	3.590(−1)	6.13(−4)
γ 16	3.61(−3)	5.030(−1)	1.82(−3)
γ 17	7.27(−2)	6.370(−1)	4.63(−2)
γ 18	2.20(−3)	6.427(−1)	1.41(−3)
γ 19	1.80(−2)	7.229(−1)	1.30(−2)
Kα_1 X ray	2.59(−2)	2.978(−2)	7.72(−4)
Kα_2 X ray	1.40(−2)	2.946(−2)	4.12(−4)
Listed X, γ, and $\gamma \pm$ radiations			3.80(−1)
Omitted X, γ, and $\gamma \pm$ radiations[b]			1.09(−3)
Listed β, ce, and Auger radiations			1.90(−1)
Omitted β, ce, and Auger radiations[b]			1.86(−3)
Listed radiations			5.70(−1)
Omitted radiations[b]			2.95(−3)

[a]Average energy (Mev).

[b]Each omitted transition contributes <0.100% to $\Sigma y_i E_i$ in its category.

Xenon-131m daughter, yield 1.11×10^{-2}, is radioactive. Xenon-131 daughter, yield 9.889×10^{-1}, is stable.

Tabulated below is a calculation of the photon radiation contribution to the S-factor for the thyroid and testes on the assumption that the thyroid is the source organ. In computing the specific absorbed fraction for the various photon radiations, log-log interpolation has been used.

Photon	E (MeV)	Δ (MeV/nt)	Φ(thy.←thy.)	Φ(testes←thy.)
γ 1	0.08	2.10×10^{-3}	1.70	2.28×10^{-7}
γ 4	0.1772	4.70×10^{-4}	1.53	2.71×10^{-6}
γ 7	0.2843	1.72×10^{-2}	1.59	5.58×10^{-6}
γ 12	0.3258	8.18×10^{-4}	1.61	6.67×10^{-6}
γ 14	0.3645	2.96×10^{-1}	1.62	7.73×10^{-6}
γ 16	0.5030	1.82×10^{-3}	1.66	1.17×10^{-5}
γ 17	0.6370	4.63×10^{-2}	1.62	1.52×10^{-5}
γ 18	0.6427	1.41×10^{-3}	1.62	1.53×10^{-5}
γ 19	0.7229	1.30×10^{-2}	1.60	1.74×10^{-5}
Kα_1 x ray	0.0298	7.72×10^{-4}	7.53	4.40×10^{-13}
Kα_2 x ray	0.0295	4.12×10^{-4}	7.71	2.09×10^{-13}
		$\Sigma \Delta_i \Phi_i =$	0.623	3.36×10^{-6}

The S-factor for the testes as a target need only consider the photon radiations. Thus

$$S(\text{testes} \leftarrow \text{thyroid}) = 1.6\times10^{-13} \times 3.36\times10^{-6}$$
$$= 5.38\times10^{-19} \text{ Gy/nt} .$$

For the thyroid as the target, the electron and beta radiation (non-penetrating radiations) must be considered. From the decay data tabulation, 0.190 MeV/nt is associated with these radiations. Recall that an absorbed fraction of unity will be considered for the non-penetrating radiations. If the thyroid mass is taken as 0.020 kg, then

$$S(\text{thyroid} \leftarrow \text{thyroid}) = 1.6\times10^{-13} \times (0.19/0.02 + 0.623)$$
$$= 1.62\times10^{-12} \text{ Gy/nt} .$$

Note the significance of the non-penetrating radiation in determining the S-factor for the thyroid as the target organ. In Table 7.11 (in Sect. 7.4.1), an S-factor value of 1.42×10^{-7} Sv/Bq-d or 1.64×10^{-12} Sv/nt is shown as obtained from Snyder et al. (1975). This value is based on a thyroid mass of 19.63 g as used in the mathematical phantom for Monte Carlo calculation of the radiation transport rather than the 20 g value recommended in the Reference Man report (ICRP, 1975). [End of Example 7.13]

7.4 DYNAMIC MODELS OF RADIONUCLIDES IN THE BODY

Following intake into the body by inhalation or ingestion, a radionuclide may be absorbed from the respiratory and gastrointestinal (GI) tracts into the blood, from which it may be taken up by other organs and subsequently removed at rates that depend on the organs' metabolic processes and the chemical properties of the particular material. For some radionuclides, the formation and decay of radioactive daughters are superimposed on the dynamics of uptake and removal. We shall index the members (species) of a decay chain with the symbol i, where $i = 1$ corresponds to the nuclide taken into the body (parent). If $q^i_{\boldsymbol{Y}}$ denotes the level of radioactivity of species i in organ $\boldsymbol{Y}$, then the *dose-equivalent rate* to target organ $\boldsymbol{T}$ due to this radioactivity is

$$\dot{H}^i_{\boldsymbol{T}\leftarrow\boldsymbol{Y}} = S^i_{\boldsymbol{T}\leftarrow\boldsymbol{Y}} q^i_{\boldsymbol{Y}} \quad \text{rem s}^{-1} \ [\text{Sv s}^{-1}] . \tag{7.59}$$

When radioactive daughters are absent, the superscript i will usually be omitted.

One of the fundamental problems of internal dosimetry is to characterize $q^i_{\mathbf{Y}}$ as a function of time for those source organs of interest for a particular radionuclide. Given this information (which depends on the history of intake of the parent radionuclide), the dose equivalent to target organ $\mathbf{T}$ may be expressed as

$$H_{\mathbf{T}} = \sum_{i=1}^{N} \sum_{\mathbf{Y}} \int_{t_1}^{t_2} S^i_{\mathbf{T}\leftarrow\mathbf{Y}}\, q^i_{\mathbf{Y}}(t)\, dt \quad \text{rem [Sv]}\,, \tag{7.60}$$

where the summations are taken over all radioactive species in the decay chain and all source organs $\mathbf{Y}$. The lower limit of integration, t_1, corresponds to the time of first contamination, and in many applications, t_2 is the life expectancy of the reference individual. For purposes of occupational radiation protection, it is common practice to assume $t_2 - t_1 = 50$ y, whereas in the area of environmental dosimetry, in which one is concerned with members of the general public, ranges of 70 and 100 y are sometimes used. When the range of integration corresponds to a terminal segment of the reference individual's lifetime, we speak of *committed dose equivalent* corresponding to the assumed intake of the parent radionuclide. In this discussion, we assume that the total intake occurs abruptly at time t_1 (an *acute* intake). The resulting dose is delivered incrementally, at a rate that varies with time, until the radioactivity is removed from the body.

Figure 7.3 is a schematic representation of the general compartment model of radionuclide movement within the body that will be discussed in this chapter. This arrangement is quite similar to that adopted by ICRP Committee 2 for ICRP Publication 30. Intake is by inhalation or ingestion, and in either case there is absorption of the radionuclide into blood and body fluids (corresponding roughly to the compartment labeled "transfer compartment" in Fig. 7.3) and thence to systemic organs. For certain of our discussions, it will be convenient to assume direct injection into the transfer compartment. In the following subsections, we discuss the components of this system and their mathematical formulations.

7.4.1 Transfer Compartment and Systemic Organs

In the model suggested by Fig. 7.3, material introduced into the transfer compartment is assumed to be removed by first-order kinetic processes with biological half-time T_{TC} usually equal to 0.25 d (but different for certain radionuclides). The systemic organs compete for the material with direct excretion from the transfer compartment. The allocation among these pathways is parameterized by the fractions $\theta_1, \cdots, \theta_M, \theta_{exc}$,

where

$$\theta_1 + \cdots + \theta_M + \theta_{exc} = 1\,. \tag{7.61}$$

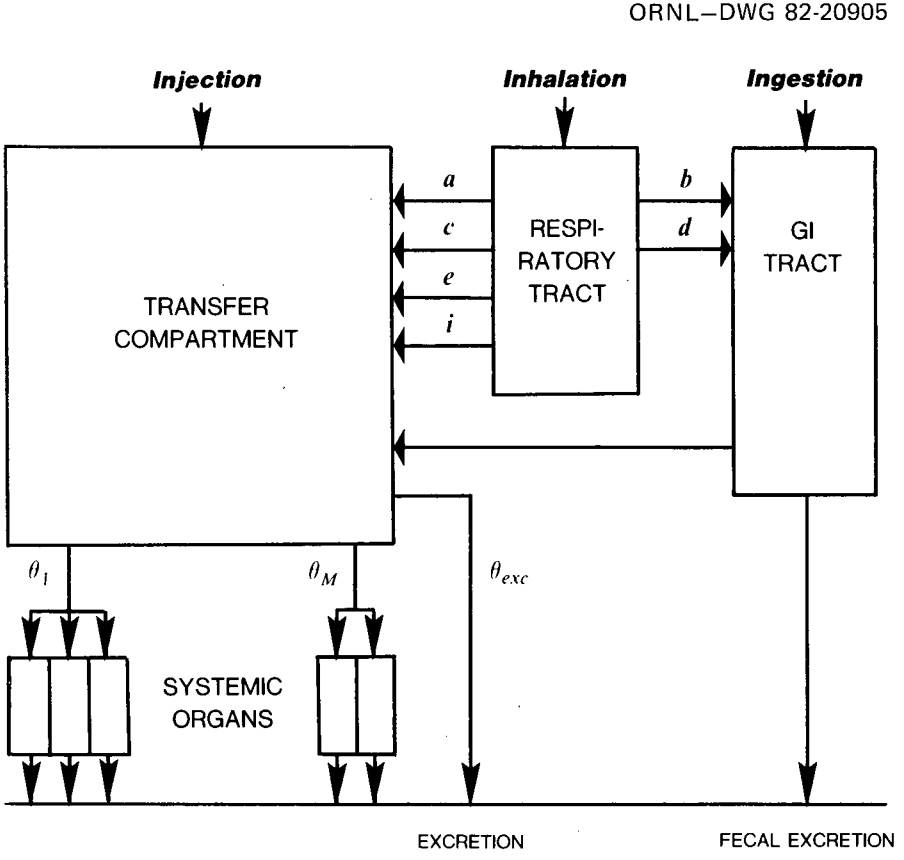

Figure 7.3. Schematic representation of models of uptake and retention of radionuclides in the body.

The loss from the transfer compartment by radiological decay is also computed. Thus, for q_0 μCi [Bq] initially present in the transfer compartment, the subsequent level $q_{TC}(t)$ is governed by the differential equation

$$\frac{d}{dt}q_{TC} = -(\lambda_R + \lambda_{TC})q_{TC}, \quad q_{TC}(0) = q_0 \quad , \tag{7.62}$$

[where $\lambda_{TC} = (\ln 2)/T_{TC}$], with solution

$$q_{TC}(t) = q_0 \exp[-(\lambda_R + \lambda_{TC})t] \, . \tag{7.63}$$

The rates of translocation of the contents of the transfer compartment to systemic organ $\mathbf{Y}_j$ and to the direct excretion pathway, respectively, are $\theta_j \lambda_{TC} q_{TC}$ and $\theta_{exc} \lambda_{TC} q_{TC}$ μCi s^{-1} [Bq s^{-1}].

Each systemic organ is represented by one or more compartments arranged in parallel, among which the translocated radioactivity is allocated. The material is usually treated as if it were excreted directly from these compartments by first-order kinetics, without feedback to the transfer compartment (an exception is the model for radioiodines, which we discuss in detail in Example 7.15). We denote the removal rate coefficient for compartment k of organ $\boldsymbol{Y}_j$ by $\lambda_{j,k}$, and the fractional allocation of radioactivity among the P_j compartments of organ $\boldsymbol{Y}_j$ by $a_{j,k}$, $k = 1, \cdots, P_j$ ($\Sigma_k a_{j,k} = 1$). The level of radioactivity, $q_{j,k}$, in compartment k satisfies the differential equation

$$\frac{d}{dt}q_{j,k} = \theta_j a_{j,k}\lambda_{TC}q_{TC} - (\lambda_R + \lambda_{j,k})q_{j,k}, \quad q_{j,k}(0) = 0 , \tag{7.64}$$

which has as its solution

$$q_{j,k}(t) = \frac{q_0\theta_j\lambda_{TC}a_{j,k}}{\lambda_{TC} - \lambda_{j,k}}\left(e^{-\lambda_{j,k}t} - e^{-\lambda_{TC}t}\right)e^{-\lambda_R t}, \tag{7.65}$$

when q_{TC} is given by Eq. 7.63. The total activity in organ $\boldsymbol{Y}_j$ is

$$q_j(t) = \sum_{k=1}^{P_j} q_{j,k}(t) . \tag{7.66}$$

It is usual to summarize the dynamics of the radionuclide in organ $\boldsymbol{Y}_j$ by means of a normalized retention function

$$r_j(t) = e^{-\lambda_R t}\sum_{k=1}^{P_j} a_{j,k}e^{-\lambda_{j,k}t} = e^{-\lambda_R t}R_j(t) , \tag{7.67}$$

where $R_j(t)$ represents retention without radiological decay. The function $r_j(t)$ can be interpreted as the surviving fraction, at time t, of an initial distribution of $a_{j,k}$ units of radionuclide in compartment k for $k = 1, \cdots, P_j$; $R_j(t)$ has a similar interpretation for a stable isotope when one exists. The response of the organ to a particular history of radioactivity, $q_{TC}(t)$, in the transfer compartment can then be generated by the convolution

$$q_j(t) = \int_0^t \theta_j q_{TC}(t-s)r_j(s)ds . \tag{7.68}$$

It may be verified that Eq. 7.68 gives the $q_j(t)$ of Eqs. 7.65 and 7.66 when q_{TC} is substituted from Eq. 7.63.

Example 7.14. As a first example to illustrate the formulas just presented, we consider the uptake of $q_0 = 1$ μCi [Bq] of ^{60}Co to the transfer compartment. Cobalt-60 has a radiological half-life of 1.92×10^3 d, so that $\lambda_R = 3.60\times10^{-4}$ d^{-1}. ICRP Publication 30 Part 1 (ICRP, 1979) assumes that 50%

of the cobalt entering the transfer compartment is excreted with biological half-time 0.5 d; of the remaining 50%, 5% is translocated to the liver and 45% is uniformly distributed among other organs and tissues. Of the translocated portion, fractions 0.6, 0.2, and 0.2 are assigned to parallel compartments with biological half-times 6, 60, and 800 d, respectively. Translation of these assumptions into parameters described previously for the model of Fig. 7.3 is as follows:

$$\theta_1 = 0.05 \quad \theta_2 = 0.45 \quad \theta_{exc} = 0.5 \quad (1 = \text{liver}, 2 = \text{other organs})$$

$$\left.\begin{array}{ll} a_{j,1} = 0.6 & \lambda_{j,1} = 0.693/(6\text{ d}) = 0.116\text{ d}^{-1} \\ a_{j,2} = 0.2 & \lambda_{j,2} = 0.693/(60\text{ d}) = 1.16\times10^{-2}\text{ d}^{-1} \\ a_{j,3} = 0.2 & \lambda_{j,3} = 0.693/(800\text{ d}) = 8.66\times10^{-4}\text{ d}^{-1} \end{array}\right\} \quad j = 1,2$$

$$\lambda_{TC} = 0.693/(0.5\text{ d}) = 2.77\text{ d}^{-1}$$

Substituting these values into Eqs. 7.65 and 7.66 gives

$$\begin{aligned} q_j(t) = \theta_j\big[&0.626\exp(-0.116t) + 0.201\exp(-1.16\times10^{-2}t) \\ &+ 0.200\exp(-8.66\times10^{-4}t) \\ &- (0.626+0.201+0.200)\exp(-1.39t)\big] \\ &\times\exp(-3.60\times10^{-4}t)\,. \end{aligned} \tag{7.69}$$

By making a table of values and plotting the curve, one sees that $q_j(t)$, initially zero as required, increases rapidly as radioactivity is translocated from the transfer compartment until a maximum value of $0.832\theta_j$ units occurs at approximately 2.3 d after deposition of 1 unit in the transfer compartment. The integral of Eq. 7.69 from 0 to 50 y (= 18,250 d) equals $185\theta_j$ activity-unit d and is the same as the integral to infinite time for the precision shown in our calculations.

The retention function for systemic organs, $r_j(t)$, is given by

$$\begin{aligned} r_j(t) = [&0.6\exp(-0.116t) + 0.2\exp(-1.16\times10^{-2}t) \\ &+ 0.2\exp(-8.66\times10^{-4}t)]\exp(-3.60\times10^{-4}t)\,; \end{aligned} \tag{7.70}$$

this function is normalized so that $r_j(0) = 1$. Because of the long radiological half-life of ^{60}Co, the holdup of radioactivity in the transfer compartment makes little difference in the activity integral for the systemic organs. If θ_j units of ^{60}Co were deposited directly in organ j, the activity integral would be

$$\tilde{q}_j = \int_0^{50\text{ y}} \theta_j r_j(t)\,dt = 185\theta_j \text{ activity-unit d},$$

the same result as before, to the precision shown. But for short-lived radionuclides, the material lost to radiological decay during its stay in the transfer

compartment can make a substantial difference in the dose computed for systemic organs. This point will be made in the next example, which deals with radioiodines. [End of Example 7.14]

Example 7.15. As a second example, we examine the metabolic model for iodine proposed by Riggs (1952) as adapted for ICRP Publication 30 Part 1 (ICRP, 1979). This three-compartment model represents iodine in the transfer compartment, thyroid, and all remaining organs and tissues (Fig. 7.4). Iodine deposited in the transfer compartment is removed with biological half-time 0.25 d, with 30% going to the thyroid and 70% to excretion. Removal from the thyroid occurs with biological half-time 120 d, and the iodine, in organic form, is deposited in a compartment representing other organs and tissues. From the latter compartment, 10% goes to fecal excretion and 90% is returned to the transfer compartment, with biological half-time 12 d for both pathways.

Note that this model violates the general scheme summarized in Fig. 7.3 in two ways: (1) The compartments for thyroid and "other organs" are not in parallel; the first clears into the second. (2) There is feedback from "other organs" to the transfer compartment. The differential equations and initial conditions are

$$\frac{d}{dt}q_{TC} = -(\lambda_{TC}+\lambda_R)q_{TC}+0.9\lambda_1 q_1, \qquad q_{TC}(0)=1;$$

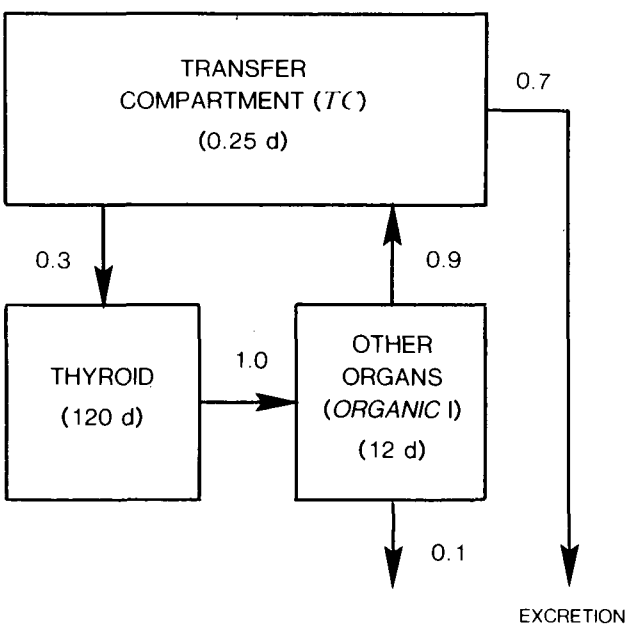

Figure 7.4. The Riggs/ICRP iodine model.

$$\frac{d}{dt}q_1 = 0.3\lambda_{TC}q_{TC} - (\lambda_1 + \lambda_R)q_1, \qquad q_1(0) = 0; \tag{7.71}$$

$$\frac{d}{dt}q_2 = \lambda_1 q_1 - (\lambda_2 + \lambda_R)q_2, \qquad q_2(0) = 0,$$

where subscripts 1 and 2 refer to the thyroid and "other tissues," respectively.

From the above description, we have $\lambda_{TC} = 0.693/(0.25\ \text{d}) = 2.77\ \text{d}^{-1}$, $\lambda_1 = 0.693/(120\ \text{d}) = 5.78\times10^{-3}\ \text{d}^{-1}$, and $\lambda_2 = 0.693/(12\ \text{d}) = 5.78\times10^{-2}\ \text{d}^{-1}$. One may solve Eq. 7.71 with $\lambda_R = 0$ to obtain the response for the stable element. Solutions for a specific radioiodine may then be obtained from these by multiplying each stable-element response by $\exp(-\lambda_R t)$. Performed by hand, the calculations can be tedious. We have carried them out with the aid of a computer program, and the results, for the given data, are

$$\begin{aligned} q_{TC}(t) &= [\exp(-2.77t) - 6.13\times10^{-4}\exp(-5.95\times10^{-2}t) \\ &\quad + 5.88\times10^{-4}\exp(-4.10\times10^{-3}t)]\exp(-\lambda_R t); \\ q_1(t) &= [-0.301\exp(-2.77t) + 9.49\times10^{-3}\exp(-5.95\times10^{-2}t) \\ &\quad + 0.291\exp(-4.10\times10^{-3}t)]\exp(-\lambda_R t); \\ q_2(t) &= [6.40\times10^{-4}\exp(-2.77t) - 3.20\times10^{-2}\exp(-5.95\times10^{-2}t) \\ &\quad + 3.13\times10^{-2}\exp(-4.10\times10^{-3}t)]\exp(-\lambda_R t). \end{aligned} \tag{7.72}$$

To illustrate the effect of holdup in the transfer compartment for short-lived radioiodines, we have prepared Table 7.11 for three isotopes with radiological half-lives that span a wide range: ^{129}I (5.73×10^9 d), ^{131}I (8.04 d), and ^{134}I (3.65×10^{-2} d). For each isotope, Table 7.11 gives the time-integrated response of each compartment of the model to an initial deposition of 1 activity unit in the transfer compartment; the total integrated response for the three compartments is also shown, and the percent of this total is given in parentheses for each compartment. Note the shift in the percent for the thyroid in going from the long-lived ^{129}I to the intermediate ^{131}I to the ephemeral ^{134}I. For each isotope, Table 7.11 also gives us the S-factor, S(thyroid←thyroid) and the 50-y committed dose equivalent.

Suppose the transfer compartment is not *dynamically* included in the model for the purpose of estimating the committed dose equivalent to the thyroid, and instead, 30% of the initial uptake is abruptly translocated to the thyroid where it is removed as before, with biological half-time 120 d. If the feedback pathway is neglected, the time integral of the thyroid's response, $\tilde{q}_1(t)$, is given by

$$\tilde{q}_1(t) = \frac{0.3}{\lambda_1 + \lambda_R}\left[1 - e^{-(\lambda_1+\lambda_R)t}\right]. \tag{7.73}$$

Table 7.11. The Riggs/ICRP model of iodine metabolism for 1 activity-unit initially deposited in the transfer compartment: results for three radioiodines

Isotope	^{129}I		^{131}I		^{134}I	
Half-life	5.73×10^{9} d		8.04 d		3.65×10^{-2} d	
Fifty-year time-integrated radioactivity (activity-unit d). Parenthesized numbers are percentages:						
Transfer compartment	0.5	(0.6)	0.4	(9.6)	0.046	(95.8)
Thyroid	71.0	(90.3)	3.2	(86.9)	0.002	(4.2)
Other organs and tissues	7.1	(9.0)	0.1	(3.5)	~0	~0
Total	78.6	(~100)	3.7	(100)	0.048	(100)
S-factor for thyroid[a]:						
rem $(\mu Ci\ d)^{-1}$	0.172		0.524		1.92	
[Sv $(Bq\ d)^{-1}$]	$[4.64\times10^{-8}]$		$[1.42\times10^{-7}]$		$[5.18\times10^{-7}]$	
Committed dose equivalent to thyroid:						
rem $(\mu Ci)^{-1}$	12		1.7		3.8×10^{-3}	
[Sv Bq^{-1}]	$[3.2\times10^{-6}]$		$[4.6\times10^{-7}]$		$[1.0\times10^{-9}]$	

[a]Snyder et al. (1975).

Table 7.12 shows the estimates of committed dose equivalent to the thyroid obtained from Eq. 7.73 in comparison with their counterparts from Table 7.11. Long-lived ^{129}I recycled by the Riggs/ICRP model delivers a dose to the thyroid that is greater by 35% than the estimate based on instantaneous translocation to the thyroid. For ^{131}I, the two estimates are nearly the same. But for the rapidly decaying ^{134}I, holdup in the transfer compartment of the Riggs/ICRP model results in an estimate of dose to the thyroid that is less by a factor of eight than that for immediate translocation. For nuclides with radiological half-lives that are short in comparison with the 0.25-day biological half-time of the transfer compartment, this example shows the potential importance of the preliminary holdup in the estimate of dose to a systemic organ; this importance diminishes as the radiological half-life significantly exceeds the biological half-time of the transfer compartment. [End of Example 7.15]

Example 7.16. We now illustrate the interplay of metabolism with the dynamics of production and decay of radioactive daughters in a decay chain. The chain to be considered is

$$^{210}Bi\ (5.013\ d) \xrightarrow{\beta^-} {}^{210}Po\ (138.4\ d) \xrightarrow{\alpha} {}^{206}Pb\ (\text{stable})\,.$$

Table 7.12. Comparison of committed dose equivalent to the thyroid due to uptake of radioiodine as estimated by (A) the Riggs/ICRP model and (B) instantaneous translocation

Isotope	^{129}I	^{131}I	^{134}I
Half-life	5.73×10^{9} d	8.04 d	3.65×10^{-2} d
(A) Riggs/ICRP model[a]:			
rem $(\mu Ci)^{-1}$	12	1.7	3.8×10^{-3}
[Sv Bq^{-1}]	[3.2×10^{-6}]	[4.6×10^{-7}]	[1.0×10^{-9}]
(B) Instantaneous translocation to thyroid of 30% of transfer compartment's contents[b]:			
rem $(\mu Ci)^{-1}$	8.9	1.7	3.0×10^{-2}
[Sv Bq^{-1}]	[2.4×10^{-6}]	[4.6×10^{-7}]	[8.1×10^{-9}]

[a]Table 7.11.

[b]Equation 7.73 with S-factors from Table 7.11.

Our calculations are drawn from the following metabolic assumptions, which were adapted from ICRP Publication 30 (ICRP, 1979):

BISMUTH. Of an initial deposition of bismuth in the transfer compartment, 30% goes to excretion, 40% goes to the kidneys, and the remaining 30% is distributed uniformly throughout the rest of the body's organs and tissues. Clearance of bismuth from the transfer compartment is rapid, occurring with biological half-time 0.01 d — not the 0.25 d taken as the usual default value. The retention function for bismuth in any systemic organ is assumed to be

$$R^1(t) = 0.6e^{-0.693t/0.6} + 0.4e^{-0.693t/5}, \tag{7.74}$$

where the superscript 1 indicates the first (parent) species in the decay chain.

POLONIUM. We assume that 10, 10, 10, and 70% of polonium deposited in the transfer compartment are translocated to the liver, kidneys, spleen, and all other tissues, respectively. In each of these compartments, the retention function is taken to be

$$R^2(t) = e^{-0.693t/50}. \tag{7.75}$$

The differential equations for the transfer compartment (TC) are

$$^{210}\text{Bi:} \quad \frac{d}{dt}q^1_{TC} = -(\lambda^1_{TC}+\lambda^1_R)q^1_{TC}, \quad q^1_{TC}(0)=1, \tag{7.76}$$

$$^{210}\text{Po:} \quad \frac{d}{dt}q^2_{TC} = -(\lambda^2_{TC}+\lambda^2_R)q^2_{TC}+\lambda^2_R q^1_{TC}, \quad q^2_{TC}(0)=0, \tag{7.77}$$

where $\lambda_{TC}^1 = 0.693/(0.01\ \text{d})$, $\lambda_{TC}^2 = 0.693/(0.25\ \text{d})$, $\lambda_R^1 = 0.693/(5.013\ \text{d})$, and $\lambda_R^2 = 0.693/(138.4\ \text{d})$. This system is easily solved by elementary methods; the solution is

$$^{210}\text{Bi:} \qquad q_{TC}^1(t) = e^{-\mu_{TC}^1 t}\ , \tag{7.78}$$

$$^{210}\text{Po:} \qquad q_{TC}^2(t) = \frac{\lambda_R^2}{\mu_{TC}^2 - \mu_{TC}^1}\left(e^{-\mu_{TC}^1 t} - e^{-\mu_{TC}^2 t}\right)\ , \tag{7.79}$$

where we define $\mu_{TC}^i = \lambda_{TC}^i + \lambda_R^i$, $i = 1, 2$. We consider translocation to kidneys only, for purposes of illustration. It is convenient to express the organ response for each nuclide species at time t as a convolution of total input with retention. For the parent species, ^{210}Bi, the expression is

$$q_K^1(t) = \int_0^t \theta_K^1 \lambda_{TC}^1 e^{-\mu_{TC}^1 (t-s)} r_k^1(s)\,ds\ , \tag{7.80}$$

where K denotes the kidneys, and accordingly, $\theta_K^1 = 0.4$. The retention function is of the form $r_K^1(t) = \exp(-\lambda_R^1 t) R_K^1(t)$, where $R_K^1(t)$ is given by Eq. 7.74. For the polonium daughter, we have

$$q_K^2(t) = \int_0^t [\theta_K^2 \lambda_{TC}^2 q_{TC}^2(t-s) + \lambda_R^2 q_K^1(t-s)] r_K^2(s)\,ds\ , \tag{7.81}$$

where $\theta_K^2 = 0.1$ and other notations are identical or analogous to those previously explained. The first term in the brackets is the rate of translocation of polonium formed in the transfer compartment to the kidneys; the second term gives the rate of formation of polonium from decay of bismuth *in the kidneys.* These convolution integrals may be evaluated by direct integration or Laplace transformation techniques to give closed-form solutions for the bismuth and polonium content in the kidneys. These solutions are

$$q_K^1(t) = \theta_K^1 \lambda_{TC}^1 \sum_{m=1}^{2} \frac{a_{Km}}{\mu_{TC}^1 - \mu_{Km}^1}\left(e^{-\mu_{Km}^1 t} - e^{-\mu_{TC}^1 t}\right)\ , \tag{7.82}$$

$$q_K^2(t) = \frac{\theta_K^2 \lambda_{TC}^2 \lambda_R^2}{\mu_{TC}^2 - \mu_{TC}^1}\left[\frac{1}{\mu_{K1}^2 - \mu_{TC}^1}\left(e^{-\mu_{TC}^1 t} - e^{-\mu_{K1}^2 t}\right) - \frac{1}{\mu_{K1}^2 - \mu_{TC}^2}\left(e^{-\mu_{TC}^2 t} - e^{-\mu_{K1}^2 t}\right)\right]$$

$$+ \lambda_R^2 \theta_K^1 \lambda_{TC}^1 \sum_{m=1}^{2} \frac{a_{Km}}{\mu_{TC}^1 - \mu_{Km}^1}\left[\frac{1}{\mu_{K1}^2 - \mu_{Km}^1}\left(e^{-\mu_{Km}^1 t} - e^{-\mu_{K1}^2 t}\right)\right. \tag{7.83}$$

$$- \frac{1}{\mu_{K1}^2 - \mu_{TC}^1} \left(e^{-\mu_{TC}^1 t} - e^{-\mu_{K1}^2 t} \right) \Bigg] .$$

The time integrals from $t = 0$ to $t = T$ (e.g., 18,250 d = 50 y) may be obtained from Eqs. 7.82 and 7.83 by replacing each exponential of the form e^{-bt} by $(1-e^{-bT})/b$.

An equivalent formulation of the convolution integrals (Eqs. 7.80 and 7.81) consists of the three differential equations

$$\frac{d}{dt} q_{K1}^1 = \theta_K^1 \lambda_{TC}^1 a_{k1}^1 q_{TC}^1 - \mu_{K1}^1 q_{K1}^1 , \tag{7.84}$$

$$\frac{d}{dt} q_{K2}^1 = \theta_K^1 \lambda_{TC}^1 a_{K2}^1 q_{TC}^1 - \mu_{K2}^1 q_{K2}^1 , \tag{7.85}$$

$$\frac{d}{dt} q_{K1}^2 = \theta_K^2 \lambda_{TC}^2 a_{K1}^2 q_{TC}^2 + \lambda_R^2 q_{K1}^1 + \lambda_R^2 q_{K2}^1 - \mu_{K1}^2 q_{K1}^2 , \tag{7.86}$$

where q_K^1 of our previous equations equals $q_{K1}^1 + q_{K2}^1$; these latter terms correspond to terms of the retention function for bismuth in the kidneys (Eq. 7.74).

When numeric values are substituted for parameters in the solutions given by Eqs. 7.82 and 7.83, the results are

$$q_{TC}^1(t) = \exp(-1.887 \times 10^{-2} t), \tag{7.87}$$

$$q_{TC}^2(t) = 7.511 \times 10^{-5} \exp(-2.778t) - 7.511 \times 10^{-5} \exp(-69.45t) , \tag{7.88}$$

$$q_K^1(t) = 0.2441 \exp(-1.294t) + 0.1603 \exp(-0.2769t) - (0.2441 + 0.1603) \exp(-69.45t) , \tag{7.89}$$

$$\begin{aligned} q_K^2(t) = {} & 4.049 \times 10^{-3} \exp(-1.887 \times 10^{-2} t) \\ & - 7.549 \times 10^{-6} \exp(-2.778t) \\ & - 9.590 \times 10^{-4} \exp(-1.294t) \\ & - 3.112 \times 10^{-3} \exp(-0.2769t) \\ & + 2.947 \times 10^{-5} \exp(-69.45t) . \end{aligned} \tag{7.90}$$

Integration of Eqs. 7.89 and 7.90 gives $\tilde{q}_K^1 = 0.762$ and $\tilde{q}_K^2 = 0.203$ activity-unit days for ^{210}Bi and ^{210}Po, respectively, in the kidneys. [End of Example 7.16]

The models discussed so far have assumed retention functions that can be expressed as normalized linear combinations of decaying exponential functions of time after uptake:

$$R(t) = \sum_{k=1}^{P} a_k e^{-\lambda_k t} , \qquad \sum_{k=1}^{P} a_k = 1 . \tag{7.91}$$

When such functions are fitted to experimental data, however, it is frequently the case that three or more terms are necessary to give a good representation, and consequently five or more parameters (a_k, λ_k) must be determined (the normalization condition in Eq. 7.91 reduces the number of a_k by one). Use of this functional form to fit data poses two disadvantages: (1) determination of a large number of parameters is inefficient and scientifically unpalatable when a smaller number can be made to suffice; (2) obtaining fits of Eq. 7.91 that are optimum in the sense of least squares can present serious numerical difficulties. In view of these considerations, alternative forms are sometimes introduced.

A decaying exponential function can be interpreted to represent removal of material from a compartment at a rate proportional to the amount present, where the coefficient of proportionality is constant; i.e., $dR/dt = -\lambda R$, where λ is a positive constant. Suppose a second removal process is present whose rate coefficient diminishes with increasing time asymptotically as $1/t$. We write the differential equation for R with the competing processes as follows:

$$\frac{dR}{dt} = -\lambda R - \frac{b}{t+\epsilon} R . \tag{7.92}$$

The parameter $\epsilon > 0$ is inserted to avoid singularity at $t = 0$; its value is small in comparison with the total time interval over which the equation is to be integrated. With the initial condition $R(0) = 1$, the differential equation (Eq. 7.92) has as its solution

$$R(t) = \epsilon^b (t+\epsilon)^{-b} e^{-\lambda t} . \tag{7.93}$$

With values of b $(0 < b < 1)$ and λ determined by regression procedures, functions of the form 7.93 have been highly successful in modeling the retention of bone-seeking radionuclides in the body. The factor $\epsilon^b (t+\epsilon)^{-b}$ is commonly referred to as a *power function.* In some work, functions $R = at^{-b}$ have been employed to represent retention data, where a denotes the fraction of the material administered that remains at the end of unit time, usually one day; the term *power function* is also applied to this form.

Without the exponential factor, the power function of Eq. 7.93 does not possess a convergent time integral to infinite time if $b \leqslant 1$. Thus, a metabolic process represented by such a function would not achieve steady state in any

finite time under the conditions of continuous administration of material at a constant rate (i.e., removal would never balance uptake).

Power-function models with exponential factors have found prominent use by a task group of ICRP Committee 2 for representing retention of the alkaline earth elements—calcium, strontium, barium, and radium. The task group's report, issued as ICRP Publication 20 (ICRP, 1973), proposes a model that involves products of exponential and power functions, with parameters that have been estimated by a process of fitting the model to various sets of retention data (Table 7.13). For whole-body retention, the form of the model is

$$R(t) = (1-p)e^{-mt} + p\epsilon^{b}(t+\epsilon)^{-b}[\beta e^{-r\lambda t} + (1-\beta)e^{-\sigma r\lambda t}], \quad (7.94)$$

where

$R(t)$ = the fraction of an initial injection, into the blood, that remains in the body at time t;

ϵ = a small time (0.3–3 d), related to initial turnover rate of the material;

Table 7.13. Values of the parameters for the alkaline earth metabolic model[a]

Parameter	Units	Calcium	Strontium	Barium	Radium
Independent					
b	dimensionless	0.10	0.18	0.237	0.415
ϵ	d	0.76	0.20	0.007	0.12
λ	y^{-1}	0.025	0.025	0.04	0.015
k	g Ca d^{-1}	0.275	0.275	0.275	0.275
η	dimensionless	1	3.80	37.1	36.5
σ	dimensionless	4	4	4	4
p	dimensionless	0.79	0.60	0.62	0.821
m	d^{-1}	0.10	0.25	0.75	0.4
ω	dimensionless	1	1	1.52	0.131
c	g Ca	1,000	1,000	1,100	1,000
$c_{SURFACE}$	g Ca	4	2	4	12
λ_{SUR}	d^{-1}	0.3	0.3	0.3	0.3
f_C	dimensionless	2.29	2.22	2.0	3.0
f_1	dimensionless	—	0.19–0.21	—	0.15–0.21
Dependent					
$10\eta k$	liter d^{-1}	2.75	10.4	102	100
β	dimensionless	0.532	0.555	0.564	0.608
r	dimensionless	0.826	0.949	0.991	0.997
f_T	dimensionless	2.01	1.78	1.54	1.94

[a]From ICRP Publication 20 (1973).

b = power function slope, determined by removal of material from bone to blood and subsequent excretion from the body;

λ = the rate of apposition and resorption in cortical bone (taken as 2.5% y^{-1} by the task group);

σ = the ratio of the turnover rates of trabecular and cortical bone (taken as 4);

β = the fraction of material taken up by bone that is deposited in cortical bone (assumed to be approximately 0.5 by the task group);

r = a factor which adjusts for redeposition of material as new bone at sites of resorption long after injection (estimated as 0.826, 0.949, 0.991, and 0.997 for calcium, strontium, barium, and radium, respectively);

m = the rate constant for early removal of material from whole body (d^{-1});

p = the fraction of the initial injection excluded from the early-removal component of the material;

t = time after the initial injection (d).

As the parameters suggest, this retention model is strongly related to the metabolism of alkaline earth elements by bone. The task group partitioned whole-body retention into bone surface, cortical bone volume, trabecular bone volume, blood, and soft tissue; and each type of bone was also divided into "old" and "new." It is not possible to go into detail here about the evolution and calibration of the model, but the report of the task group (ICRP, 1973) contains full and extended discussions. We content ourselves with the barest outline, arranged algorithmically, followed by numeric tables that provide time integrals of concentration per unit activity taken up by blood.

The task group assumed that the rate of excretion of an alkaline earth radionuclide from the body is proportional to its concentration in serum or plasma and quantified this assumption as follows:

$$\frac{dR}{dt} = -\eta k S \,, \tag{7.95}$$

where R is the whole-body retention function of Eq. 7.94; k is the excretion rate coefficient (urinary plus fecal; time^{-1}); η is the ratio of excretory plasma clearance of the radionuclide to that of calcium; and S is the activity per gram of calcium in blood serum or plasma. Since R has been prescribed and estimates of the parameters η and k exist (Table 7.13), Eq. 7.95 is a means of

computing S as a function of t. Given S, the retention for bone surface, R_{SURFACE}, is computed by solving the differential equation

$$\begin{aligned} \frac{d}{dt}R_{\text{SURFACE}} &= \lambda_{\text{SUR}}(c_{\text{SURFACE}}S - R_{\text{SURFACE}}) , \\ R_{\text{SURFACE}} &= 0 \text{ for } t=0 . \end{aligned} \tag{7.96}$$

The parameters λ_{SUR} and c_{SURFACE} denote the turnover rate coefficient (time^{-1}) and calcium content of the bone surface compartment, respectively. Retention in blood is expressed as

$$R_{\text{BLOOD}} = (3\times10^{-4})cS , \tag{7.97}$$

where 3×10^{-4} is the fraction of the body's calcium in blood plasma and c is grams of calcium in the body.

The retention function for cortical bone volume, R_{CORVOL}, is

$$R_{\text{CORVOL}} = \begin{cases} p\beta\epsilon^b(t+\theta)^{-b}e^{-r\lambda t} & \text{if } t>0 , \\ 0 \text{ if } t=0. \end{cases} \tag{7.98}$$

The quantity θ is time dependent, through whole-body retention R:

$$\theta = [f_C 0.8 c\lambda\omega(1-R)/(p\epsilon^b\beta\eta k)]^{-1/b} ; \tag{7.99}$$

this expression for θ was chosen to give the retention function R_{CORVOL} suitable asymptotic properties. The constant 0.8 is related to the fact that 80% of body calcium in cortical bone, $1/f_C$ is the fraction of activity deposited in cortical bone that is in new bone, and ω expresses isotopic discrimination between blood and bone. The other parameters in θ have been defined previously.

In trabecular bone, the retention function, R_{TRAVOL}, is given by

$$R_{\text{TRAVOL}} = f_T[0.2c\sigma\lambda\omega(1-R)/(\eta k)] , \tag{7.100}$$

where $f_T = 4f_C(1-\beta)/(\beta\sigma)$, and 0.2 is the remaining fraction of body calcium (body calcium not in bone is a fraction of one percent and is neglected in the bone model).

Retention in total cortical bone, total trabecular bone, and soft tissue is obtained from the functions already defined:

$$R_{\text{COR}} = R_{\text{CORVOL}} + \tfrac{1}{2}R_{\text{SURFACE}} , \tag{7.101}$$

$$R_{\text{TRA}} = R_{\text{TRAVOL}} + \tfrac{1}{2}R_{\text{SURFACE}} , \tag{7.102}$$

$$R_{\text{SOFT}} = R - R_{\text{COR}} - R_{\text{TRA}} - R_{\text{BLOOD}} . \tag{7.103}$$

The equations given above describe biological retention and do not account for radiological decay. If λ_R denotes the radiological decay rate coefficient for the alkaline earth radionuclide under study, the adjusted equations are

$$r = Re^{-\lambda_R t}, \tag{7.104}$$

$$r_{\text{CORVOL}} = R_{\text{CORVOL}} e^{-\lambda_R t}, \tag{7.105}$$

$$r_{\text{TRAVOL}} = R_{\text{TRAVOL}} e^{-\lambda_R t}, \tag{7.106}$$

$$S_R = Se^{-\lambda_R t}, \tag{7.107}$$

$$r_{\text{BLOOD}} = R_{\text{BLOOD}} e^{-\lambda_R t}, \tag{7.108}$$

$$\frac{d}{dt} r_{\text{SURFACE}} = \lambda_{\text{SUR}}(c_{\text{SURFACE}} S_R) - (\lambda_{\text{SUR}} + \lambda_R) r_{\text{SURFACE}}, \tag{7.109}$$

$$r_{\text{COR}} = r_{\text{CORVOL}} + \tfrac{1}{2} r_{\text{SURFACE}}, \tag{7.110}$$

$$r_{\text{TRA}} = r_{\text{TRAVOL}} + \tfrac{1}{2} r_{\text{SURFACE}}, \tag{7.111}$$

$$r_{\text{SOFT}} = r - r_{\text{COR}} - r_{\text{TRA}} - r_{\text{BLOOD}}. \tag{7.112}$$

Practical evaluation of these equations and their time integrals requires, for most purposes, the use of programmable computing equipment. But tabulations of integrated activities in the compartments of interest can be helpful with solving some problems of internal dose estimation. Tables 7.14 through 7.17 provide such tabulations of integrated activities for some of the alkaline earth radioisotopes. We will illustrate their use in the following example. Table 7.13 displays the parameter values used in computing Tables 7.14 through 7.17.

Example 7.17. For $^{90}\text{Sr}-^{90}\text{Y}$, we are concerned with the following decay chain:

$$^{90}\text{Sr (28.6 yr)} \xrightarrow[195.8\text{ keV}]{\beta^-} {}^{90}\text{Y (6.41 h)} \xrightarrow[934.8\text{ keV}]{\beta^-} {}^{90}\text{Zr (stable)}.$$

The very short half-life of ^{90}Y relative to ^{90}Sr makes it reasonable to assume that time-integrated concentrations of ^{90}Y activity in bone and soft tissue compartments are approximately equal to those of ^{90}Sr. Therefore, from Table 7.15, following uptake of 1 Bq of ^{90}Sr by blood, we have the 50-yr integrals 398, 157, and 18.4 Bq d in cortical bone, trabecular bone, and soft tissue, respectively, for each of ^{90}Sr and ^{90}Y. [End of Example 7.17]

Table 7.14. CALCIUM: Time integrals of retention functions (d) vs time after injection[a]

Isotope (half-life)	Time (y)	Blood	Bone surface	Soft tissue	Cortical bone	Trabecular bone	Whole body
Stable Ca	1	0.652	8.76	14.0	89.6	76.9	176.5
	50	1.03	14.3	14.3	2055.5	724.2	2761.6
	∞	1.09	15.2	14.3	2903.6	731.6	3642.8
^{41}Ca	1	0.652	8.76	14.0	89.6	76.9	176.5
(8×10^4 y)	50	1.03	14.3	14.3	2055.1	724.1	2761.2
	∞	1.09	15.2	14.3	2902.4	731.5	3641.6
^{45}Ca	1	0.573	7.57	10.6	44.4	38.6	92.9
(162.7 d)	50	0.579	7.66	10.6	53.7	45.9	110.4
	∞	0.579	7.66	10.6	53.7	45.9	110.4
^{47}Ca							
(4.538 d)	1[b]	0.237	2.10	1.59	1.70	1.62	5.12
^{49}Ca							
(8.7 min)	1[b]	8.3×10^{-4}	2.7×10^{-5}	0.0053	1.8×10^{-5}	1.7×10^{-5}	0.00615

[a]From ICRP Publication 20 (1973).

[b]Integral is the same for 1 y, 50 y, and infinite time.

Table 7.15. STRONTIUM: Time integrals of retention functions (d) vs time after injection[a]

Isotope (half-life)	Time (y)	Blood	Bone surface	Soft tissue	Trabecular bone	Cortical bone	Whole body
Stable Sr	1	0.245	1.64	13.4	25.8	33.2	71.1
	50	0.283	1.92	19.2	190.6	595.6	799.0
	∞	0.287	1.95	19.2	191.4	762.8	973.0
^{90}Sr	1	0.245	1.64	13.3	25.4	32.7	70.3
(28.1 y)	50	0.275	1.86	18.4	157.2	398.4	572.0
	∞	0.275	1.86	18.4	157.3	421.1	597.0
^{85}Sr	1	0.218	1.40	6.97	6.65	8.26	22.0
(64 d)	50[b]	0.218	1.40	6.98	6.72	8.36	22.2
^{89}Sr	1	0.214	1.37	6.39	5.54	6.84	18.9
(52 d)	50[b]	0.214	1.37	6.40	5.57	6.88	19.0
^{83}Sr							
(1.35 d)	1[b]	0.0870	0.215	0.920	0.163	0.177	1.35
^{91}Sr							
(9.67 h)	1[b]	0.0450	0.0439	0.377	0.0305	0.0327	0.486
^{87m}Sr							
(2.83 h)	1[b]	0.0196	0.00617	0.127	0.00420	0.00447	0.155
^{92}Sr							
(2.60 h)	1[b]	0.0184	0.00534	0.117	0.00363	0.00387	0.143
^{85m}Sr							
(70 min)	1[b]	0.0096	0.00127	0.0533	8.67×10^{-4}	9.25×10^{-4}	0.0647

[a]From ICRP Publication 20 (1973).

[b]Integral is the same for 1 y, 50 y, and infinite time.

Table 7.16. BARIUM: Time integrals of retention functions (d) vs time after injection[a]

Isotope (half-life)	Time (y)	Blood	Bone surface	Soft tissue	Cortical bone	Trabecular bone	Whole body
Stable Ba	1	0.0293	0.356	6.82	9.48	6.93	22.9
	50	0.0306	0.374	11.1	120.4	32.8	163.5
	∞	0.0307	0.375	11.1	130.6	32.8	174.4
^{133}Ba	1	0.0293	0.355	6.70	9.18	6.71	22.2
(10.7 y)	50	0.0301	0.367	9.85	60.0	24.7	94.5
	∞	0.0301	0.367	9.85	60.2	24.7	94.7
^{140}Ba							
(12.8 d)	1[b]	0.0261	0.270	1.52	0.585	0.481	2.60
^{131}Ba							
(11.7 d)	1[b]	0.0260	0.264	1.45	0.542	0.447	2.45
^{133m}Ba							
(38.9 h)	1[b]	0.0202	0.101	0.557	0.0959	0.0855	0.757
^{135m}Ba							
(28.7 h)	1[b]	0.0188	0.0781	0.477	0.0705	0.0633	0.629
^{139}Ba							
(83.2 min)	1[b]	0.00680	0.00198	0.0488	0.00161	0.00147	0.0587
^{137m}Ba							
(2.60 min)	1[b]	0.000285	2.5×10^{-6}	0.000456	3.1×10^{-6}	2.7×10^{-6}	0.000748

[a]From ICRP Publication 20 (1973).

[b]Integral is the same for 1 y, 50 y, and infinite time.

Table 7.17. RADIUM: Time integrals of retention functions (d) vs time after injection[a]

Isotope (half-life)	Time (y)	Blood	Bone surface	Soft tissue	Cortical bone	Trabecular bone	Whole body
^{226}Ra	1	0.0288	1.16	10.8	4.96	3.35	18.8
(1602 y)	50	0.0296	1.19	21.2	73.3	25.4	119.0
	∞	0.0297	1.19	21.5	100.4	25.9	147.7
^{228}Ra	1	0.0288	1.15	10.4	4.69	3.18	18.0
(5.75 y)	50	0.0292	1.17	16.2	22.0	11.7	49.8
	∞	0.0292	1.17	16.2	22.0	11.7	49.8
^{225}Ra							
(14.8 d)	1[b]	0.0250	0.868	2.14	0.665	0.582	3.36
^{223}Ra							
(11.4 d)	1[b]	0.0244	0.815	1.83	0.582	0.520	2.91
^{224}Ra							
(3.64 d)	1[b]	0.0209	0.516	0.933	0.306	0.289	1.53
^{227}Ra							
(41.2 min)	1[b]	0.00234	0.00111	0.0312	0.000601	0.000585	0.0348

[a]From ICRP Publication 20 (1973).

[b]Integral is the same for 1 y, 50 y, and infinite time.

7.4.2 Gastrointestinal (GI) Tract

The gastrointestinal (GI) tract is modeled as four discrete segments: stomach (*S*), small intestine (*SI*), upper large intestine (*ULI*), and lower large intestine (*LLI*). Table 7.18 summarizes some basic data about the segments and their contents. The conceptual model is that of Eve (1966) and has been adopted by ICRP Committee 2 as the basis for dosimetric computations for radiation protection. Mathematically, each segment is viewed as a compartment that clears into its successor by first-order kinetics, without feedback. It is assumed that essentially all absorption of radioactivity from the GI tract into body fluids occurs in the small intestine, at a rate $\lambda_{ab} q_{SI}$, where λ_{ab} is the rate coefficient (d^{-1}) and q_{SI} is the radioactivity in the contents of the small intestine. Figure 7.5 is a schematic diagram of the model, for which the differential equations are

$$\frac{d}{dt} q_S = -(\lambda_S + \lambda_R) q_S , \quad q_S(0) = 1 ; \tag{7.113}$$

$$\frac{d}{dt} q_{SI} = -(\lambda_{SI} + \lambda_{ab} + \lambda_R) q_{SI} + \lambda_S q_S , \quad q_{SI}(0) = 0 ; \tag{7.114}$$

$$\frac{d}{dt} q_{ULI} = -(\lambda_{ULI} + \lambda_R) q_{ULI} + \lambda_{SI} q_{SI} , \quad q_{ULI}(0) = 0 ; \tag{7.115}$$

$$\frac{d}{dt} q_{LLI} = -(\lambda_{LLI} + \lambda_R) q_{LLI} + \lambda_{ULI} q_{ULI} , \quad q_{LLI}(0) = 0 , \tag{7.116}$$

in which it is assumed that 1 activity unit (μCi [Bq]) is ingested into the stomach at time 0. The rate coefficients λ_S, λ_{SI}, λ_{ULI}, and λ_{LLI} govern clearance from the segment indicated by the subscript into the successor, or in case of the lower large intestine, out of the tract. These coefficients are based on

Table 7.18. Parameters for the model gastrointestinal tract

Segment	Mass of walls[a] (g)	Mass of contents[a] (g)	Mean residence time[b] (d)
Stomach (*S*)	150	250	1/24
Small intestine (*SI*)	640	400	4/24
Upper large intestine (*ULI*)	210	220	13/24
Lower large intestine (*LLI*)	160	135	24/24

[a] ICRP Publication 23 (1975).
[b] Eve (1966).

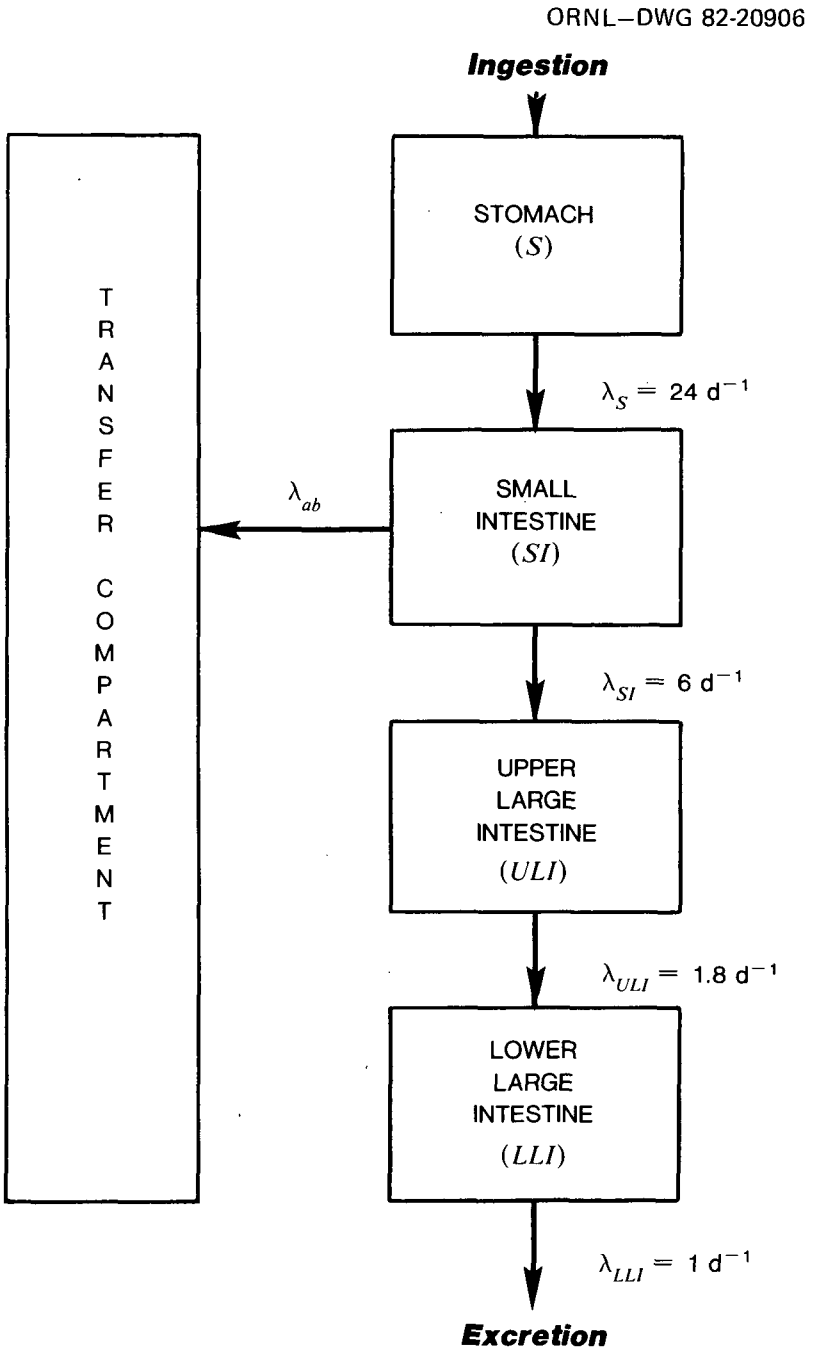

Figure 7.5. Schematic diagram of the model of radionuclide movement through the gastrointestinal tract.

mean residence times of material in the respective segments as estimated by Eve (1966): $\lambda_S = 24$, $\lambda_{SI} = 6$, $\lambda_{ULI} = 1.8$, and $\lambda_{LLI} = 1\ d^{-1}$; these values are reciprocals of the mean residence times in Table 7.18.

Absorption of a particular nuclide from the GI tract is characterized by a fraction, f_1, which means that fraction of a unit amount ingested that is absorbed into body fluids if no radiological decay occurs. Thus for a stable element, if one exists, f_1 is the fraction of the total amount cleared per unit time from the small intestine that is absorbed:

$$f_1 = \frac{\lambda_{ab} q_{SI}}{(\lambda_{SI}+\lambda_{ab}) q_{SI}},$$

from which we derive an expression for λ_{ab} in terms of f^1:

$$\lambda_{ab} = \frac{f_1 \lambda_{SI}}{1-f_1}. \tag{7.117}$$

The kinetic model, as formulated above, does not permit total absorption of a nuclide ($f_1 = 1$). ICRP Committee 2 substitutes a model in which material passes directly from the stomach into body fluids, without passing further down the GI tract, when the material is considered to be completely absorbed.

Note that the biological mean residence times for the segments, $1/\lambda_{seg}$ (where *seg* = *S*, *SI*, *ULI*, or *LLI*), are small relative to the integration of times of 50–100 yr that are typical of calculations for routine or chronic exposure. Consequently, the activity integrals

$$\tilde{q}_{seg} = \int_0^{+\infty} q_{seg}(t)\,dt \tag{7.118}$$

may be used in computing committed dose equivalent to the walls of the segments of the GI tract, rather than the corresponding integrals with the finite upper limit. Similarly, for an acute intake of radioactivity by ingestion, the cumulative transfer of activity from the small intestine to body fluids is essentially complete within eight times the biological half-time for removal of material from the small intestine, and therefore, within about one day. This cumulative transfer is $\lambda_{ab}\tilde{q}_{SI}$, where $\tilde{q}_{SI}$ is computed as in Eq. 7.118. By solving Eqs. 7.113 and 7.114 and integrating to obtain $\tilde{q}_{SI}$, we may show that the cumulative uptake from the GI tract, which we denote by A_g, is

$$A_g = \lambda_{ab}\tilde{q}_{SI} = \frac{\lambda_S \lambda_{ab}}{(\lambda_{ab}+\lambda_{SI}+\lambda_R)(\lambda_S+\lambda_R)}; \tag{7.119}$$

A_g is dimensionless and represents the fraction of ingested activity units that is absorbed from the GI tract. For a stable isotope (i.e., $\lambda_R = 0$), one may use

Eq. 7.117 to show that A_g reduces to f_1. For short-lived radionuclides, however, A_g diminishes asymptotically as $1/(\lambda_R)^2$.

Solving the differential equations 7.113 through 7.116 and integrating the solutions to infinite time, as in Eq. 7.118, we obtain the following results:

$$\tilde{q}_S = \frac{1}{\lambda_S+\lambda_R}; \tag{7.120}$$

$$\tilde{q}_{SI} = \frac{\lambda_S\tilde{q}_S}{\lambda_{ab}+\lambda_{SI}+\lambda_R}; \tag{7.121}$$

$$\tilde{q}_{ULI} = \frac{\lambda_{SI}\tilde{q}_{SI}}{\lambda_{ULI}+\lambda_R}; \tag{7.122}$$

$$\tilde{q}_{LLI} = \frac{\lambda_{ULI}\tilde{q}_{ULI}}{\lambda_{LLI}+\lambda_R}. \tag{7.123}$$

We remind the reader that the quantities $\tilde{q}_{seg}$ in Eqs. 7.120 through 7.123 are normalized to one ingested activity unit and therefore may be regarded as having units of time.

Example 7.18. Phosphorous-32 decays with radiological half-life 14.3 d. Phosphorous is readily absorbed from the small intestine, and ICRP Publication 30 gives $f_1 = 0.8$. If 1 activity unit of ^{32}P is ingested, the activity integrals for the segments of the GI tract may be computed directly from Eqs. 7.120 through 7.123:

$$\lambda_R = 0.693/(14.3\text{ d}) = 4.85\times10^{-2}\,\text{d}^{-1};$$

$$\lambda_{ab} = (0.8)(6)/(1-0.8) = 24\,\text{d}^{-1};$$

$$\tilde{q}_S = (1\text{ activity unit})/(24+4.85\times10^{-2})$$
$$= 4.16\times10^{-2}\text{ activity-unit d;}$$

$$\tilde{q}_{SI} = (24)(4.16\times10^{-2})/(24+6+4.85\times10^{-2})$$
$$= 3.32\times10^{-2}\text{ activity-unit d:}$$

$$\tilde{q}_{ULI} = (6)(3.32\times10^{-2})/(1.8+4.85\times10^{-2})$$
$$= 0.108\text{ activity-unit d;}$$

$$\tilde{q}_{LLI} = (1.8)(0.108)/(1+4.85\times10^{-2})$$
$$= 0.185\text{ activity-unit d.}$$

Fractional absorption of the radioactive phosphorous is

$$A_g = \lambda_{ab}\tilde{q}_{SI} = (24)(3.32\times10^{-2}) = 0.797,$$

i.e., nearly that of nonradioactive phosphorous, as one would expect from the fact that the radiological half-life is long relative to the biological half-time of phosphorous in the small intestine. [End of Example 7.18]

Equations 7.120 through 7.123 require generalization when radioactive daughter products are formed from the parent nuclide that is taken into the GI tract. We give the formulas for $\tilde{q}^i_{seg}$ (seg = S, SI, ULI, LLI) for radionuclide i in the decay chain, where, as in Eq. 7.118, the tilde indicates integration from 0 to infinite time. The results are

$$\tilde{q}^i_S = \begin{cases} \dfrac{\lambda^i_R}{\lambda_S+\lambda^i_R}\sum_{j=1}^{i-1}\beta_{ij}\tilde{q}^j_S, & i>1\,, \\ \dfrac{1}{\lambda_S+\lambda^1_R}, & i=1\,; \end{cases} \tag{7.124}$$

$$\tilde{q}^i_{SI} = \frac{1}{\lambda_{SI}+\lambda^i_{ab}+\lambda^i_R}\left(\lambda_S\tilde{q}^i_S+\lambda^i_R\sum_{j=1}^{i-1}\beta_{ij}\tilde{q}^j_{SI}\right)\,; \tag{7.125}$$

$$\tilde{q}^i_{ULI} = \frac{1}{\lambda_{ULI}+\lambda^i_R}\left(\lambda_{SI}\tilde{q}^i_{SI}+\lambda^i_R\sum_{j=1}^{i-1}\beta_{ij}\tilde{q}^j_{ULI}\right)\,; \tag{7.126}$$

$$\tilde{q}^i_{LLI} = \frac{1}{\lambda_{LLI}+\lambda^i_R}\left(\lambda_{ULI}\tilde{q}^i_{ULI}+\lambda^i_R\sum_{j=1}^{i-1}\beta_{ij}\tilde{q}^i_{LLI}\right)\,. \tag{7.127}$$

The summations in Eqs. 7.125 through 7.127 are understood to be zero when i = 1. These equations correspond to an acute intake at t = 0 of one activity unit into the stomach. The symbols β_{ij} denote branching ratios **from** nuclide species j **to** species i, where $j<i$.

Example 7.19. We illustrate the use of Eqs. 7.124 through 7.127 to calculate $\tilde{q}^i_{seg}$ for ^{90}Sr (i = 1) and ^{90}Y (i = 2) for the four segments of the GI tract. We assume that 1 Bq of ^{90}Sr is ingested. For soluble forms of strontium, ICRP Publication 30 gives f_1 = 0.30. Yttrium is poorly absorbed, and $f_1 = 10^{-4}$ is assumed. With these data, we calculate, using Eq. 7.117,

$$\lambda^1_{ab} = (0.30)(6)/(1-0.30) = 2.57\ \mathrm{d}^{-1}\,,$$

$$\lambda^2_{ab} = (10^{-4})(6)/(1-10^{-4}) = 6\times10^{-4}\,\mathrm{d}^{-1}\,.$$

Radiological decay-rate constants are $\lambda^1_R = 6.64\times10^{-5}\ \mathrm{d}^{-1}$ and $\lambda^2_R = 0.260\ \mathrm{d}^{-1}$, and for this chain, β_{21} = 1. Therefore

$$\tilde{q}^1_S = \frac{1}{24+6.64\times10^{-5}} = 4.17\times10^{-2}\,\mathrm{Bq\ d}\,,$$

$$\tilde{q}_S^2 = \frac{0.260}{24 + 0.260} \times 4.17 \times 10^{-2} = 4.46 \times 10^{-4} \text{ Bq d},$$

$$\tilde{q}_{SI}^1 = \frac{(24)(4.17 \times 10^{-2})}{6 + 2.57 + 6.64 \times 10^{-5}} = 0.117 \text{ Bq d},$$

$$\tilde{q}_{SI}^2 = \frac{[(24)(4.46 \times 10^{-4}) + (0.260)(0.117)]}{6 + 6 \times 10^{-4} + 0.260}$$

$$= 6.56 \times 10^{-3} \text{ Bq d},$$

$$\tilde{q}_{ULI}^1 = \frac{(6)(0.117)}{1.8 + 6.64 \times 10^{-5}} = 0.390 \text{ Bq d},$$

$$\tilde{q}_{ULI}^2 = \frac{[(6)(6.56 \times 10^{-3}) + (0.260)(0.390)]}{1.8 + 0.260}$$

$$= 6.83 \times 10^{-2} \text{ Bq d},$$

$$\tilde{q}_{LLI}^1 = \frac{(1.8)(0.390)}{1 + 6.64 \times 10^{-5}} = 0.702 \text{ Bq d},$$

$$\tilde{q}_{LLI}^2 = \frac{[(1.8)(6.83 \times 10^{-2}) + (0.260)(0.702)]}{1 + 0.260}$$

$$= 0.242 \text{ Bq d}.$$

The amounts of ^{90}Sr and ^{90}Y absorbed from the small intestine into the blood are, respectively,

$$A_g^1 = (2.57)(0.117) = 0.30 \text{ Bq},$$

$$A_g^2 = (6 \times 10^{-4})(6.56 \times 10^{-3}) = 3.9 \times 10^{-6} \text{ Bq}.$$

We see from this example that the assumption of integrated activities of ^{90}Y that approximate those for ^{90}Sr would substantially overestimate the contribution of the daughter nuclide to the dose to segments of the GI tract. The reason is the presence of biological half-times that are significantly shorter than the radiological half-life of ^{90}Y. [End of Example 7.19]

7.4.3 Respiratory Tract

The model respiratory tract which we shall discuss was developed for purposes of internal dosimetry by a task group of the ICRP and described in a published report (ICRP, 1966). Subsequent modifications have been incor-

porated, and the structure and parameterization given here are essentially those found in ICRP Publication 19 (1972) and in ICRP Publication 30 (1979). Sometimes it is referred to as the Task Group Lung Model (TGLM) to distinguish it from the earlier model that formed the basis of recommendations set forth in ICRP Publication 2 (1959). But at present, it probably is more appropriate to call it the ICRP lung model, and we shall use this designation.

The ICRP lung model is intended to apply to radioactivity-bearing aerosols introduced into the breathing passages by inhalation. The model is presented schematically in Fig. 7.6. Inhaled materials are assumed to belong to one of three discrete clearance classes, according to how rapidly they are removed from the respiratory passages. These clearance classes are designated as D (removal accomplished in days), W (weeks), and Y (years), and to each corresponds a set of parameter values for the dynamics of removal. The model identifies four major respiratory regions: nasal-pharynx (NP), tracheobronchial tree (TB), pulmonary region (P), and lymphatic tissue (L). Fractional depositions of inhaled particulates in the first three of these regions are given by the fractions D_{NP}, D_{TB}, and D_P, respectively (the sum of these is less than one, with the shortfall accounting for prompt exhalation). These fractions are functions of the activity median aerodynamic diameter (AMAD) of the inspired particles; a functional relationship between the fractions D_{NP}, D_{TB}, and D_P and AMAD is given by Fig. 7.7. The values of the fractions shown in Fig. 7.6 correspond to AMAD = 1 μm.

Each major region is subdivided into compartments, and we label the latter with boldface italic letters $\boldsymbol{a}$, $\boldsymbol{b}$, $\cdots$, $\boldsymbol{j}$. In the NP region, material deposited in compartment $\boldsymbol{a}$ is available for absorption into body fluids, while that deposited in compartment $\boldsymbol{b}$ is eventually swallowed and thus enters the GI tract. Similarly, material deposited in compartment $\boldsymbol{c}$ of the TB region is absorbed into body fluids, while compartment $\boldsymbol{d}$ represents material that is being moved upward by ciliary action, out of the lungs and into the GI tract. Material from compartments $\boldsymbol{f}$ and $\boldsymbol{g}$ of the pulmonary region (P) also enters compartment $\boldsymbol{d}$ and is moved upward and into the GI tract, with material from $\boldsymbol{f}$ being cleared rapidly from the lungs and that from $\boldsymbol{g}$ progressing very slowly. Compartment $\boldsymbol{e}$ in the pulmonary region represents absorption into body fluids, and material is removed from compartment $\boldsymbol{h}$ by lymphatic drainage. Lymphatic tissue is divided into two compartments ($\boldsymbol{i}$ and $\boldsymbol{j}$), with material that leaves compartment $\boldsymbol{i}$ entering body fluids. Compartment $\boldsymbol{j}$ represents material that is tenaciously retained in lymph and is applied only in the case of Class Y material to ten percent of the lymphatic burden, with the assumption that removal occurs only by radiological decay. Figure 7.6 tabulates, for each clearance class, the partition fraction F_ν and the biological half-time of removal, T_ν, for each compartment $\nu = \boldsymbol{a}, \boldsymbol{b}, \cdots, \boldsymbol{j}$. The partition fractions sum to one over all compartments of each major region; for example, $F_a + F_b = 1$.

ORNL–DWG 82-20907

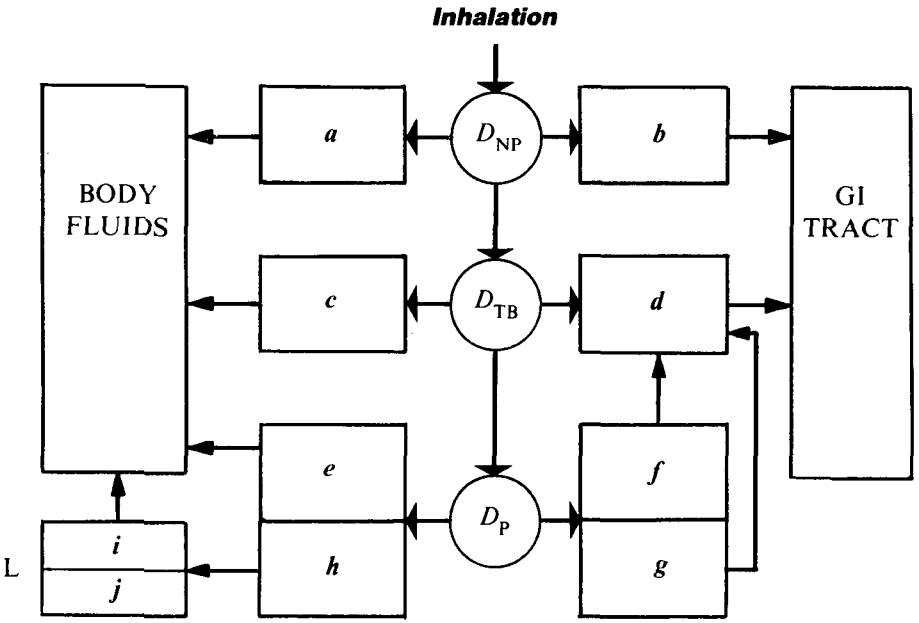

Region	Compartment	Clearance class					
		D		W		Y	
		T (d)	F	T (d)	F	T (d)	F
NP	*a*	0.01	0.5	0.01	0.1	0.01	0.01
(D_{NP}=0.30)	*b*	0.01	0.5	0.4	0.9	0.4	0.99
TB	*c*	0.01	0.95	0.01	0.5	0.01	0.01
(D_{TB}=0.08)	*d*	0.2	0.05	0.2	0.5	0.2	0.99
	e	0.5	0.8	50	0.15	500	0.05
P	*f*	n.a.	n.a.	1.0	0.4	1.0	0.4
(D_P=0.25)	*g*	n.a.	n.a.	50	0.4	500	0.4
	h	0.5	0.2	50	0.05	500	0.15
L	*i*	0.5	1.0	50	1.0	1000	0.9
	j	n.a.	n.a.	n.a.	n.a.	∞	0.1

n.a. means not applicable

Figure 7.6. The ICRP lung model.

The following system of differential equations, with initial conditions, provides a precise characterization of the model's dynamics. We assume that initially one acitivity-unit (μCi [Bq]) of the parent species is inhaled (i = 1), with no daughter activity. The differential equations describe the translocation

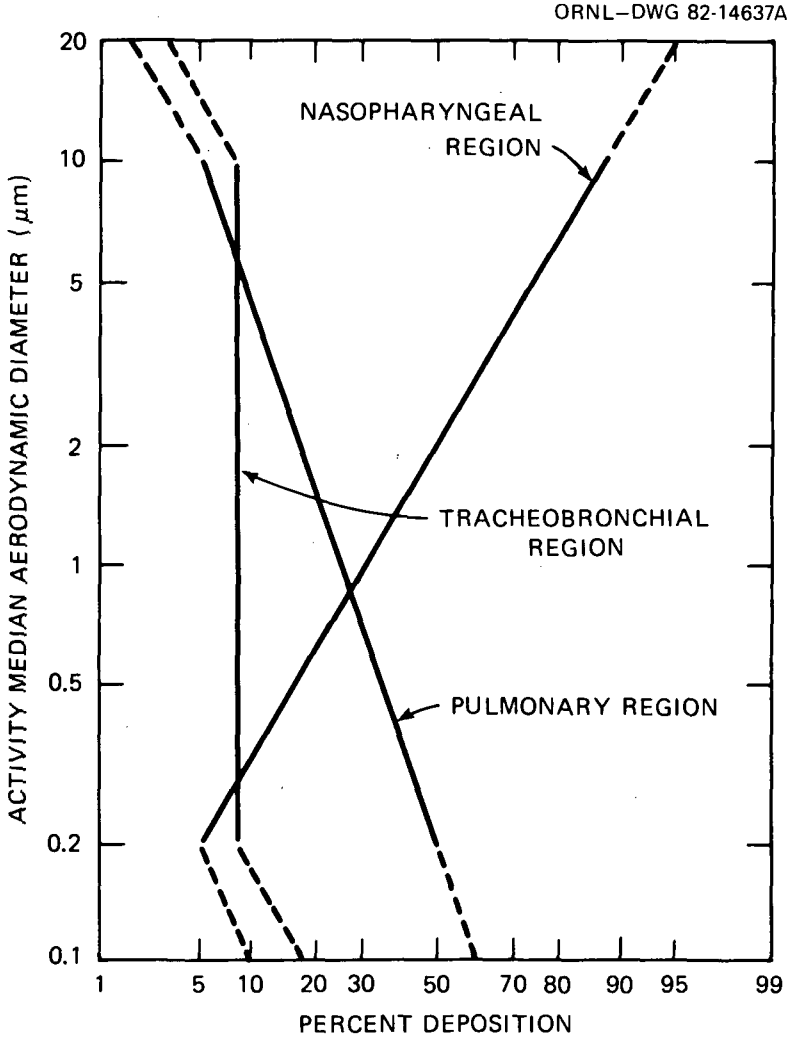

Figure 7.7. Respiratory deposition model for particulate material. The radioactivity or mass percentage of an aerosol that is deposited in the nasopharyngeal, tracheobronchial, and pulmonary regions (D_{NP}, D_{TB}, and D_P, respectively) is shown relative to the activity median aerodynamic diameter (AMAD) of the aerosol distribution. The model is intended for use within the AMAD range indicated by the solid lines, whereas the broken lines represent provisional estimates. For a distribution with AMAD > 20 μm, complete deposition in the NP region is to be assumed; the model should not be applied to aerosols with AMAD <0.1 μm. Source: Adapted from International Commission on Radiological Protection 1979. *Report of Committee 2, Limits for Inakes of Radionuclides by Workers,* ICRP Publication 30, *Ann. ICRP* 2(2–4).

and decay of the parent species and the formation and translocation of the daughter species ($i = 2, \cdots, N$), all as functions of time subsequent to the initial deposition of the parent. The notations q_a^i, q_b^i, $\cdots$, q_j^i stand for the activity of species i in the chain that is present in compartment a, b, $\cdots$, j at time t. In the equations, we denote the total inhaled activity of species i by I_0^i, and by our previous statement, this is one activity-unit if $i = 1$ (parent) and zero otherwise. Here are the equations:

$$\frac{d}{dt}q_a^i = -(\lambda_a+\lambda_R^i)q_a^i + F_a\lambda_R^i\sum_{j=1}^{i-1}\beta_{ij}q_a^j \ , \quad q_a^i(0) = F_aD_{\mathrm{NP}}I_0^i ; \tag{7.128}$$

$$\frac{d}{dt}q_b^i = -(\lambda_b+\lambda_R^i)q_b^i + F_b\lambda_R^i\sum_{j=1}^{i-1}\beta_{ij}q_b^j \ , \quad q_b^i(0) = F_bD_{\mathrm{NP}}I_0^i ; \tag{7.129}$$

$$\frac{d}{dt}q_c^i = -(\lambda_c+\lambda_R^i)q_c^i + F_c\lambda_R^i\sum_{j=1}^{i-1}\beta_{ij}q_c^j \ , \quad q_c^i(0) = F_cD_{\mathrm{TB}}I_0^i ; \tag{7.130}$$

$$\frac{d}{dt}q_d^i = -(\lambda_d+\lambda_R^i)q_d^i + \lambda_f q_f^i + \lambda_g q_g^i + F_d\lambda_R^i\sum_{j=1}^{i-1}\beta_{ij}q_d^j \ , \quad q_d^i(0) = F_dD_{\mathrm{TB}}I_0^i ; \tag{7.131}$$

$$\frac{d}{dt}q_e^i = -(\lambda_e+\lambda_R^i)q_e^i + F_e\lambda_R^i\sum_{j=1}^{i-1}\beta_{ij}q_e^j \ , \quad q_e^i(0) = F_eD_{\mathrm{P}}I_0^i ; \tag{7.132}$$

$$\frac{d}{dt}q_f^i = -(\lambda_f+\lambda_R^i)q_f^i + F_f\lambda_R^i\sum_{j=1}^{i-1}\beta_{ij}q_f^j \ , \quad q_f^i(0) = F_fD_{\mathrm{P}}I_0^i ; \tag{7.133}$$

$$\frac{d}{dt}q_g^i = -(\lambda_g+\lambda_R^i)q_g^i + F_g\lambda_R^i\sum_{j=1}^{i-1}\beta_{ij}q_g^j \ , \quad q_g^i(0) = F_gD_{\mathrm{P}}I_0^i ; \tag{7.134}$$

$$\frac{d}{dt}q_h^i = -(\lambda_h+\lambda_R^i)q_h^i + F_h\lambda_R^i\sum_{j=1}^{i-1}\beta_{ij}q_h^j \ , \quad q_h(0) = F_hD_{\mathrm{P}}I_0^i ; \tag{7.135}$$

$$\frac{d}{dt}q_i^i = -(\lambda_i+\lambda_R^i)q_i^i + F_i\Big(\lambda_R^i\sum_{j=1}^{i-1}\beta_{ij}q_i^j + \lambda_h q_h^i\Big) \ , \quad q_i^i(0) = 0 ; \tag{7.136}$$

$$\frac{d}{dt}q_j^i = -\lambda_R^i q_j^i + (1-F_i)\Big(\lambda_R^i\sum_{j=1}^{i-1}\beta_{ij}q_j^i + \lambda_h q_h^i\Big) \ , \quad q_j^i(0) = 0. \tag{7.137}$$

In Eqs. 7.128 through 7.137, note that the regional partition fractions F_v and the corresponding removal rate constants λ_v, $v = a, b, \cdots, j$, are not indexed by the superscript i and therefore are the same for all species in the decay chain. The effect of this choice is that the biological dynamics of all species that form within the respiratory passages will be the same as those of the parent species that was originally inhaled and deposited. The explanation is that the aerosol carrier to which minute particles of radioactivity are attached is assumed to determine the dynamic behavior of clearance to a greater degree than the attached radionuclides. In practice, however, there exists some ambiguity in this regard, because in the original task group report (ICRP, 1966), a considerable number of chemical compounds were classified as to overall biological half-time in the respiratory tract, without explicit reference to properties of the underlying aerosol carrier; the list of compounds was supplemented in the Reactor Safety Study (Nuclear Regulatory Commission, 1975, Appendix D of Appendix VI), with each compound being classified D, W, or Y. Even the particle size distribution of the aerosol is sometimes unknown when the model is applied. The solution of these and related problems must await further development of the basic research that supports the modeling and the characterization of the chemical and physical properties of the airborne radioactivity.

For a single radioactive species, Eqs. 7.128 through 7.137 may be solved by elementary methods. The solutions follow:

$$q_v(t) = F_v D_{\mathrm{NP}} e^{-(\lambda_v+\lambda_R)t}, \quad v = a, b; \tag{7.138}$$

$$\tilde{q}_v(t) = \frac{F_v D_{\mathrm{NP}}}{\lambda_v+\lambda_R}\left[1 - e^{-(\lambda_v+\lambda_R)t}\right], \quad v = a, b; \tag{7.139}$$

$$q_c(t) = F_c D_{\mathrm{TB}} e^{-(\lambda_c+\lambda_R)t}; \tag{7.140}$$

$$\tilde{q}_c(t) = \frac{F_c D_{\mathrm{TB}}}{\lambda_c+\lambda_R}\left[1 - e^{-(\lambda_c+\lambda_R)t}\right]; \tag{7.141}$$

$$\begin{aligned} q_d(t) = {} & F_d D_{\mathrm{TB}} e^{-(\lambda_d+\lambda_R)t} + \frac{\lambda_f F_f D_{\mathrm{P}}}{\lambda_f-\lambda_d}\left[e^{-(\lambda_d+\lambda_R)t} - e^{-(\lambda_f+\lambda_R)t}\right] \\ & + \frac{\lambda_g F_g D_{\mathrm{P}}}{\lambda_g-\lambda_d}\left[e^{-(\lambda_d+\lambda_R)t} - e^{-(\lambda_g+\lambda_R)t}\right]; \end{aligned} \tag{7.142}$$

$$\begin{aligned} \tilde{q}_d(t) = {} & \frac{F_d D_{\mathrm{TB}}}{\lambda_d+\lambda_R}\left[1 - e^{-(\lambda_d+\lambda_R)t}\right] \\ & + \frac{\lambda_f F_f D_{\mathrm{P}}}{\lambda_f-\lambda_d}\left[\frac{1-e^{-(\lambda_d+\lambda_R)t}}{\lambda_d+\lambda_R} - \frac{1-e^{-(\lambda_f+\lambda_R)t}}{\lambda_f+\lambda_R}\right] \end{aligned} \tag{7.143}$$

$$+\frac{\lambda_g F_g D_P}{\lambda_g-\lambda_d}\left[\frac{1-e^{-(\lambda_d+\lambda_R)t}}{\lambda_d+\lambda_R}-\frac{1-e^{-(\lambda_g+\lambda_R)t}}{\lambda_g+\lambda_R}\right];$$

$$q_v(t) = F_v D_P e^{-(\lambda_v+\lambda_R)t}, \quad v = e, f, g, h; \tag{7.144}$$

$$\tilde{q}_v(t) = \frac{F_v D_P}{\lambda_v+\lambda_R}\left[1-e^{-(\lambda_v+\lambda_R)t}\right], \quad v = e, f, g, h; \tag{7.145}$$

$$q_i(t) = \begin{cases} \dfrac{F_h F_i \lambda_h D_P}{\lambda_h-\lambda_i}\left[e^{-(\lambda_i+\lambda_R)t}-e^{-(\lambda_h+\lambda_R)t}\right], & \lambda_h \neq \lambda_i \\ F_h F_i \lambda_* D_P t e^{-(\lambda_*+\lambda_R)t}, & \lambda_h=\lambda_i=\lambda_* \end{cases} \tag{7.146}$$

$$\tilde{q}_i(t) = \begin{cases} \dfrac{F_h F_i \lambda_h D_P}{\lambda_h-\lambda_i}\left[\dfrac{1-e^{-(\lambda_i+\lambda_R)t}}{\lambda_i+\lambda_R}-\dfrac{1-e^{-(\lambda_h+\lambda_R)t}}{\lambda_h+\lambda_R}\right], & \lambda_h \neq \lambda_i \\ \text{fP} \\ F_h F_i \lambda_* D_P\left\{\dfrac{1-[1+(\lambda_*+\lambda_R)t]e^{-(\lambda_*+\lambda_R)t}}{(\lambda_*+\lambda_R)^2}\right\}, & \lambda_h=\lambda_i=\lambda_* \end{cases} \tag{7.147}$$

$$q_j(t) = (1-F_i)F_h D_P\left[e^{-\lambda_R t}-e^{-(\lambda_h+\lambda_R)t}\right]; \tag{7.148}$$

$$\tilde{q}_j(t) = (1-F_i)F_h D_P\left[\frac{1-e^{-\lambda_R t}}{\lambda_R}-\frac{1-e^{-(\lambda_h+\lambda_R)t}}{\lambda_h+\lambda_R}\right]. \tag{7.149}$$

We shall denote estimates of cumulative translocation from the respiratory tract into the body fluids (i.e., transfer compartment) and GI tract by A_l^i and B_l^i, respectively. These quantities may be expressed as

$$A_l^i = \lambda_a \tilde{q}_a^i + \lambda_c \tilde{q}_c^i + \lambda_e \tilde{q}_e^i + \lambda_i \tilde{q}_i^i, \tag{7.150}$$

$$B_l^i = \lambda_b \tilde{q}_b^i + \lambda_d \tilde{q}_d^i. \tag{7.151}$$

The fate of material entering the GI tract from compartments *b* and *d* and its residence time in the segments of the GI tract are estimated by the methods of Sect. 7.2 and Examples 7.18 and 7.19. The following example illustrates calculations for the respiratory and GI tracts following the acute intake by inhalation of 1 activity-unit (μCi [Bq]) of ^{32}P.

Example 7.20. We consider inhalation of 1 activity-unit of ^{32}P (T_R = 14.3 d, $\lambda_R = 4.85\times10^{-2}$ d^{-1}). Phosphorus compounds are assigned to Class D by ICRP Publication 30 Part 1 (ICRP, 1979), except for certain phosphates, which are considered to belong to Class W. We assume Class D for this calculation, that the carrier aerosol has AMAD = 1 μm, and we further assume

that the material brought up and swallowed behaves in the GI tract in accordance with Example 7.18. The following table indicates, for each respiratory compartment, the parameter values, the integrated activity ($\tilde{q}_\nu$), and the equation used in the calculation:

Compartment (ν)	F_ν	D	λ_ν (d^{-1})	$\lambda_\nu+\lambda_R$ (d^{-1})	Equation	$\tilde{q}_\nu$ (activity-unit d)
a	0.5	0.30	69.3	69.4	(7.139)	2.16×10^{-3}
b	0.5	0.30	69.3	69.4	(7.139)	2.16×10^{-3}
c	0.95	0.08	69.3	69.4	(7.141)	1.10×10^{-3}
d	0.05	0.08	3.47	3.51	(7.143)	1.14×10^{-3}
e	0.8	0.25	1.39	1.43	(7.145)	0.140
h	0.2	0.25	1.39	1.43	(7.145)	3.50×10^{-2}
i	1.0	—	1.39	1.43	(7.147)	3.37×10^{-2}

Note that compartments *f*, *g*, and *j* are not applicable to Class D. Substituting appropriate values from this table into Eqs. 7.150 and 7.151, we calculate

$$A_l = 0.467 \text{ activity-units to body fluids ,}$$

$$B_l = \underline{0.154} \text{ activity-units to GI tract}$$

$$0.621 \text{ activity-units cleared from respiratory tract.}$$

For 1 activity-unit inhaled, the deposition model gives $D_{NP}+D_{TB}+D_P = 0.630$ activity-units deposited in the respiratory passages. The difference $0.630-0.621 = 0.009$ is the fraction of the inspired activity-unit of ^{32}P that undergoes radiological decay in the respiratory passages and lymphatic tissue.

By referring to Example 7.18, we can compute the residence times of the ^{32}P that is transferred from the lungs to the GI tract. We have

$$\tilde{q}_S = (0.154)(4.16\times10^{-2}) = 6.41\times10^{-3} \text{ activity-unit d ,}$$

$$\tilde{q}_{SI} = (0.154)(3.32\times10^{-2}) = 5.11\times10^{-3} \text{ activity-unit d ,}$$

and similarly for the other segments. Finally, translocation to body fluids from the small intestine is

$$A_g = \lambda_{ab}\tilde{q}_{SI} = (24)(5.11\times10^{-3}) = 0.123 \text{ activity-units.}$$

The total translocation to body fluids, therefore, is

$$A_l + A_g = 0.467 + 0.123 = 0.590 \text{ activity-units.}$$

[End of Example 7.20]

We give an example involving a plutonium isotope to illustrate the model's treatment of Class Y materials.

Example 7.21. Plutonium-239 decays by alpha emission with half-life 8.81×10^{6} d ($\lambda_R = 7.87\times10^{-8}$ d^{-1}). ICRP Publication 30 Part 1 (ICRP, 1979) suggests that PuO_2 be assigned to Class Y for respiratory clearance, with GI-tract absorption parameter $f_1 = 10^{-5}$. For this example, we assume AMAD = 1 μm. Because of the extremely low activity of the ^{235}U daughter that is formed per transformation of ^{239}Pu, the rest of the decay chain can be neglected in the present context. The following table summarizes the calculation of cumulated activity in each respiratory compartment.

Compartment (ν)	F_ν	D	λ_ν (d^{-1})	$\lambda_\nu+\lambda_R$ (d^{-1})	Equation	$\tilde{q}_\nu$ (activity-unit d)
a	0.01	0.30	69.3	69.3	(7.139)	4.33×10^{-5}
b	0.99	0.30	1.73	1.73	(7.139)	0.172
c	0.01	0.08	69.3	69.3	(7.141)	1.15×10^{-5}
d	0.99	0.08	3.47	3.47	(7.143)	8.05×10^{-2}
e	0.05	0.25	1.39×10^{-3}	1.39×10^{-3}	(7.145)	8.99
f	0.4	0.25	0.693	0.693	(7.145)	0.144
g	0.4	0.25	1.39×10^{-3}	1.39×10^{-3}	(7.145)	71.9
h	0.15	0.25	1.39×10^{-3}	1.39×10^{-3}	(7.145)	27.0
i	0.9	—	6.93×10^{-4}	6.93×10^{-4}	(7.147)	48.7
j	0.1	—	0	7.87×10^{-8}	(7.149)	65.7

In these calculations, the exponential terms are all negligible, except $e^{-\lambda_R t}$, which occurs in Eq. 7.149, in connection with compartment *j*; this compartment represents trapping of Class Y material in the lymphatic tissue. We used t = 18,250 d (50 yr).

Notice the relatively large values of $\tilde{q}_\nu$ for the pulmonary and lymphatic regions, particularly compartments *g*, *h*, *i*, and *j*. In these last two compartments, the high exposure and the small mass of the respiratory lymph nodes (15 g) conspire to give a large dose to the lymphatic region, relative to the dose averaged over the NP, TB, and P regions. [End of Example 7.21]

7.5 DOSE CONVERSION FACTORS FOR SELECTED RADIONUCLIDES

Applications of the computational procedures outlined above have been implemented in various computer codes for the purpose of tabulating the committed dose equivalent in an array of organs of the body per unit activity inhaled or ingested. The utility of such tabulations is of course self evident, as well as the inherent limitations with regard to their application to a particular individual. In the tabulations presented here we have restricted consideration to the organs of Table 7.3, that is, the organs explicitly considered by the

ICRP to be at risk. We have included the "remainder" as the average committed dose equivalent among the five highest irradiated tissues which are not explicitly named in the table. The effective committed dose equivalent was computed in Eq. 7.6 as

$$H_{50,E} = \sum_{T} W_T H_{50,T}$$

where $H_{50,T}$ is the committed dose equivalent in target tissue T per unit intake, and the weighting factors w_T represent the fractional contribution of T to the total risk under uniform whole-body irradiation. The committed dose equivalent received by an organ was introduced in the context of occupational radiation protection, 50 years being generally inclusive of a working lifetime. The committed dose equivalent represents the total dose equivalent which an organ or tissue of the body is expected to receive over the 50-year period following exposure. For radionuclides whose retention times in the body are relatively short (~1 year), the committed dose equivalent for a single intake of one unit of radioactivity is numerically comparable to to the annual dose equivalent for a continuous intake of one unit of radioactivity per year. But for radionuclides with longer retention times in the body, the committed dose equivalent will underestimate the annual dose equivalent.

In a single dosimetric quantity, the effective committed dose equivalent represents the risk from irradiation of the body under uniform or nonuniform irradiation, the risk being the induction of fatal malignant disease and genetic disorders. A risk of $1.65 \times 10^{-2}\ \mathrm{Sv}^{-1}$ has been assigned (see Table 7.3).

As noted above, the weighting factors are based on fatal health effects. For some body tissue, the probability of inducing a cancer in that tissue and the probability of death are quite different, e.g., thyroid. Furthermore, the genetic weighting factor was based on consideration of disorders only in the first two generations, the parents and immediate offspring. To permit further consideration of health effects for these tissues, we have tabulated their committed dose equivalent per unit intake.

The data presented have been adopted from information compiled during the course of development of ICRP Publication 30. In ICRP Publication 30 (ICRP, 1979), the Commission published those dosimetric data needed to reproduce the secondary limits of intake. The values presented here in some cases may not be applicable to environmental situations. For example, in characterizing the influence of chemical form on the clearance of inhaled material from the respiratory passages, as well as fractional absorption from the gastrointestinal tract, primary attention was given to those compounds which might be expected to be present in the work place. In some instances, environmental factors might lead to higher uptake from the gastrointestinal tract (e.g., for uranium and plutonium), while in other cases, the values might be lower.

In most environmental applications, a more rigorous evaluation would require information on the time variation in the dose equivalent rates for the various tissues at risk. Given such detailed information, the time dependence of environmental concentrations, and therefore that of the intake (rather than simply the total intake), could be assessed with consideration of the years of remaining life, as derived from the age distribution of the exposed population. At this time, however, such information is not available for a large number of radionuclides. We wish to caution the reader that overestimates by factors of two to three in the risk may result from failure to consider the time-dependent nature of the organ dose equivalent rates and the years of life remaining.

7.5.1 Inhalation Exposure

Committed dose equivalent values per unit intake are given in Table 7.19 for a limited selection of radionuclides. The values presented are for an aerosol of AMAD $= 1$ μm with the indicated respiratory clearance class. Suggested assignment of chemical forms to clearance classification are presented in Table 7.20; but the reader is strongly urged to consult the discussion of metabolism of the element in ICRP Publication 30 (ICRP, 1979) for further details.

7.5.2 Ingestion Exposure

Committed dose equivalent values per unit intake are given in Table 7.21 for a limited selection of radionuclides. Suggested assignments of chemical forms to the f_1 parameter, the fractional absorption from the small intestine, are presented in Table 7.22; but we strongly urge the user to consult the discussion of the element's metabolism in ICRP Publication 30 (ICRP, 1979) for further details.

Table 7.19. Committed dose equivalent per unit intake via inhalation (Sv/Bq)

Nuclide		Clearance class	f_1	Gonads	Breast	R. Marrow	Lungs	Thyroid	Endosteal	Remainder	Effective
H	3		1.0E 00	1.70E-11	1.70E-11	1.70E-11	1.70E-11	1.70E-11	1.70E-11	1.70E-11	1.70E-11
BE	10	W	5.0E-03	5.94E-10	5.94E-10	1.77E-08	4.22E-08	5.94E-10	5.26E-08	2.44E-09	9.75E-09
		Y	5.0E-03	2.56E-10	2.56E-10	7.65E-09	7.78E-07	2.56E-10	2.27E-08	2.35E-09	9.58E-08
C	14[a]		0.0	6.36E-12	6.36E-12	6.36E-12	6.36E-12	6.36E-12	6.36E-12	6.36E-12	6.36E-12
C	14[b]		0.0	5.64E-10	5.64E-10	5.64E-10	5.64E-10	5.64E-10	5.64E-10	5.64E-10	5.64E-10
C	14[c]		0.0	7.83E-13	7.83E-13	7.83E-13	7.83E-13	7.83E-13	7.83E-13	7.83E-13	7.83E-13
NA	22	D	1.0E 00	1.77E-09	1.65E-09	2.73E-09	2.47E-09	1.60E-09	3.51E-09	2.00E-09	2.07E-09
NA	24	D	1.0E 00	1.78E-10	1.61E-10	2.13E-10	1.25E-09	1.53E-10	2.58E-10	2.35E-10	3.27E-10
P	32	D	8.0E-01	4.83E-10	4.83E-10	5.97E-09	2.50E-09	4.83E-10	5.81E-09	7.94E-10	1.64E-09
		W	8.0E-01	3.37E-10	3.37E-10	4.17E-09	2.56E-08	3.37E-10	4.05E-09	1.13E-09	4.19E-09
CA	41	W	3.0E-01	2.43E-12	2.98E-12	1.62E-09	4.53E-10	2.57E-12	3.65E-09	1.52E-11	3.64E-10
SC	46	Y	1.0E-04	1.30E-09	2.15E-09	2.21E-09	4.62E-08	2.02E-09	1.68E-09	4.79E-09	9.01E-09
CR	51	D	1.0E-01	2.71E-11	1.94E-11	2.68E-11	3.81E-11	1.82E-11	2.74E-11	3.55E-11	2.95E-11
		W	1.0E-01	2.21E-11	1.50E-11	1.87E-11	3.77E-10	1.10E-11	1.50E-11	4.93E-11	7.08E-11
		Y	1.0E-01	2.03E-11	1.58E-11	1.87E-11	5.34E-10	1.08E-11	1.39E-11	5.26E-11	9.03E-11
MN	54	D	1.0E-01	8.85E-10	9.13E-10	1.66E-09	1.18E-09	6.52E-10	2.56E-09	2.09E-09	1.42E-09
		W	1.0E-01	7.09E-10	8.59E-10	1.10E-09	6.66E-09	7.40E-10	1.25E-09	1.72E-09	1.81E-09
MN	56	D	1.0E-01	2.19E-11	1.47E-11	2.36E-11	4.40E-10	1.20E-11	2.05E-11	1.25E-10	1.02E-10
		W	1.0E-01	9.46E-12	7.79E-12	1.02E-11	5.37E-10	6.18E-12	8.23E-12	6.50E-11	8.91E-11
FE	55	D	1.0E-01	5.23E-10	5.09E-10	5.17E-10	5.19E-10	5.42E-10	5.14E-10	1.21E-09	7.26E-10
		W	1.0E-01	1.79E-10	1.74E-10	1.76E-10	1.06E-09	1.85E-10	1.75E-10	4.37E-10	3.61E-10
FE	59	D	1.0E-01	3.32E-09	3.01E-09	3.18E-09	3.50E-09	2.95E-09	2.91E-09	5.81E-09	4.00E-09
		W	1.0E-01	1.39E-09	1.26E-09	1.31E-09	1.38E-08	1.17E-09	1.11E-09	2.96E-09	3.30E-09
CO	57	W	5.0E-02	1.63E-10	1.56E-10	2.54E-10	4.05E-09	1.13E-10	1.97E-10	4.05E-10	7.12E-10
		Y	5.0E-02	1.24E-10	1.75E-10	5.98E-10	1.69E-08	2.71E-10	4.52E-10	8.22E-10	2.45E-09
CO	60	W	5.0E-02	4.05E-09	4.16E-09	4.25E-09	3.57E-08	3.72E-09	3.54E-09	7.65E-09	8.94E-09
		Y	5.0E-02	4.76E-09	1.84E-08	1.72E-08	3.45E-07	1.62E-08	1.35E-08	3.60E-08	5.91E-08
NI	59	D	5.0E-02	3.59E-10	3.46E-10	3.54E-10	3.59E-10	3.77E-10	3.51E-10	3.63E-10	3.58E-10
		W[d]	5.0E-02	1.09E-10	1.05E-10	1.06E-10	1.20E-09	1.14E-10	1.05E-10	1.40E-10	2.48E-10
NI	59		0.0	7.43E-10	7.15E-10	7.31E-10	7.14E-10	7.80E-10	7.25E-10	7.33E-10	7.31E-10
NI	63	D	5.0E-02	8.22E-10	8.22E-10	8.22E-10	8.74E-10	8.22E-10	8.22E-10	8.59E-10	8.39E-10
		W[d]	5.0E-02	2.47E-10	2.47E-10	2.47E-10	3.07E-09	2.47E-10	2.47E-10	3.67E-10	6.22E-10
NI	63		0.0	1.70E-09	1.70E-09	1.70E-09	1.73E-09	1.70E-09	1.70E-09	1.70E-09	1.70E-09

Table 7.19 (continued)

Nuclide		Clearance class	f_1	Gonads	Breast	R. Marrow	Lungs	Thyroid	Endosteal	Remainder	Effective
NI	65	D	5.0E-02	8.46E-12	6.48E-12	6.70E-12	3.11E-10	5.54E-12	5.79E-12	7.98E-11	6.55E-11
		W	5.0E-02	3.27E-12	2.95E-12	2.99E-12	3.81E-10	2.30E-12	2.38E-12	4.15E-11	5.99E-11
NI	65[d]		0.0	1.08E-11	1.21E-11	1.21E-11	6.80E-10	1.16E-11	1.14E-11	1.66E-11	9.32E-11
CU	64	D	5.0E-01	1.64E-11	1.23E-11	1.34E-11	2.03E-10	1.16E-11	1.20E-11	6.74E-11	5.29E-11
		W	5.0E-01	1.21E-11	7.26E-12	7.09E-12	3.35E-10	6.10E-12	6.34E-12	7.89E-11	6.93E-11
		Y	5.0E-01	1.24E-11	6.38E-12	7.12E-12	3.50E-10	4.98E-12	5.29E-12	9.20E-11	7.48E-11
ZN	65	Y	5.0E-01	3.03E-09	3.08E-09	3.62E-09	2.10E-08	3.02E-09	3.36E-09	4.66E-09	5.51E-09
ZN	69	Y	5.0E-01	2.77E-14	2.77E-14	3.56E-14	8.00E-11	2.77E-14	3.43E-14	3.21E-12	1.06E-11
SE	79	D	8.0E-01	5.79E-10	6.79E-10	6.79E-10	8.47E-10	6.79E-10	6.79E-10	4.24E-09	1.77E-09
		W	8.0E-01	5.98E-10	5.98E-10	5.98E-10	9.81E-09	5.98E-10	5.98E-10	3.77E-09	2.66E-09
RB	82	D	1.0E 00	2.52E-10	2.37E-10	2.54E-10	7.82E-10	2.38E-10	2.31E-10	3.15E-10	3.31E-10
		W	1.0E 00	1.69E-10	2.10E-10	2.18E-10	1.68E-09	2.06E-10	1.92E-10	3.31E-10	4.13E-10
RB	83	D	1.0E 00	3.28E-12	3.29E-12	3.30E-12	1.50E-10	3.29E-12	3.29E-12	1.13E-11	2.33E-11
		W	1.0E 00	1.13E-12	1.14E-12	1.14E-12	1.82E-10	1.14E-12	1.14E-12	5.31E-12	2.41E-11
RB	84	D	1.0E 00	2.84E-12	3.31E-12	3.27E-12	1.56E-10	3.12E-12	2.99E-12	1.97E-11	2.61E-11
		W	1.0E 00	8.51E-13	1.55E-12	1.51E-12	1.71E-10	1.43E-12	1.31E-12	4.98E-12	2.27E-11
RB	86	D	1.0E 00	1.34E-09	1.33E-09	2.32E-09	3.30E-09	1.33E-09	4.27E-09	1.38E-09	1.79E-09
RB	87	D	1.0E 00	7.16E-10	7.16E-10	1.27E-09	1.05E-09	7.16E-10	2.40E-09	7.20E-10	8.74E-10
RB	88	D	1.0E 00	1.31E-12	1.43E-12	1.45E-12	1.47E-10	1.37E-12	1.47E-12	1.38E-11	2.26E-11
RB	89	D	1.0E 00	1.34E-12	1.73E-12	2.02E-12	6.80E-11	1.61E-12	2.54E-12	8.14E-12	1.16E-11
SR	89	D	3.0E-01	4.16E-10	4.16E-10	5.63E-09	2.16E-09	4.16E-10	8.37E-09	1.32E-09	1.76E-09
		Y	1.0E-02	7.95E-12	7.96E-12	1.07E-10	8.35E-08	7.96E-12	1.59E-10	3.97E-09	1.12E-08
SR	90	D	3.0E-01	2.64E-09	2.64E-09	3.36E-07	3.73E-09	2.64E-09	7.27E-07	3.36E-09	6.47E-08
		Y	1.0E-02	2.69E-10	2.69E-10	3.28E-08	2.86E-06	2.69E-10	7.09E-08	5.73E-09	3.51E-07
SR	91	D	3.0E-01	6.41E-11	4.45E-11	1.23E-10	9.21E-10	4.08E-11	1.14E-10	3.33E-10	2.52E-10
		Y	1.0E-02	5.65E-11	1.74E-11	2.23E-11	2.13E-09	9.64E-12	1.27E-11	5.78E-10	4.49E-10
SR	92	D	3.0E-01	3.03E-11	2.44E-11	3.68E-11	7.12E-10	2.19E-11	2.56E-11	2.25E-10	1.70E-10
		Y	1.0E-02	1.02E-11	6.49E-12	6.98E-12	1.05E-09	3.92E-12	4.36E-12	2.90E-10	2.18E-10
Y	90	W	1.0E-04	9.52E-12	9.52E-12	2.79E-10	8.89E-09	9.52E-12	2.78E-10	3.40E-09	2.13E-09
		Y	1.0E-04	5.17E-13	5.17E-13	1.52E-11	9.31E-09	5.17E-13	1.51E-11	3.87E-09	2.28E-09
Y	91	W	1.0E-04	1.11E-10	1.11E-10	5.55E-09	5.25E-08	1.10E-10	5.54E-09	5.12E-09	8.72E-09
		Y	1.0E-04	8.20E-12	8.92E-12	3.19E-10	9.87E-08	8.50E-12	3.18E-10	4.20E-09	1.32E-08
Y	91M	W	1.0E-04	4.33E-13	7.13E-13	3.94E-12	4.19E-11	6.23E-13	3.79E-12	4.15E-12	7.09E-12

Table 7.19 (continued)

Nuclide	Clearance class	f_1	Gonads	Breast	R. Marrow	Lungs	Thyroid	Endosteal	Remainder	Effective
	Y	1.0E-04	3.21E-13	6.08E-13	7.74E-13	7.00E-11	5.02E-13	6.21E-13	3.74E-12	9.82E-12
Y 92	W	1.0E-04	4.86E-12	4.07E-12	1.28E-11	1.16E-09	3.69E-12	1.23E-11	1.67E-10	1.93E-10
	Y	1.0E-04	2.61E-12	1.50E-12	2.07E-12	1.24E-09	1.05E-12	1.51E-12	2.03E-10	2.11E-10
Y 93	W	1.0E-04	8.65E-12	5.79E-12	4.14E-11	2.40E-09	5.06E-12	4.04E-11	7.74E-10	5.29E-10
	Y	1.0E-04	5.31E-12	1.74E-12	4.04E-12	2.52E-09	9.26E-13	3.14E-12	9.25E-10	5.82E-10
ZR 93	D	2.0E-03	2.18E-11	4.68E-11	1.77E-07	8.68E-11	1.74E-11	2.18E-06	8.94E-11	8.67E-08
	W	2.0E-03	5.58E-12	1.20E-11	4.49E-08	3.30E-09	4.45E-12	5.54E-07	1.54E-10	2.25E-08
	Y	2.0E-03	2.82E-12	1.90E-11	1.93E-08	8.72E-08	2.28E-12	2.38E-07	1.73E-10	2.00E-08
ZR 95	D	2.0E-03	1.88E-09	1.91E-09	1.30E-08	2.17E-09	1.44E-09	1.03E-07	2.28E-09	6.39E-09
	W	2.0E-03	8.40E-10	9.32E-10	3.24E-09	1.86E-08	7.82E-10	2.17E-08	2.13E-09	4.29E-09
	Y	2.0E-03	5.73E-10	1.23E-09	1.35E-09	4.07E-08	1.16E-09	2.33E-09	2.77E-09	6.31E-09
ZR 97	D	2.0E-03	1.83E-10	1.09E-10	4.99E-10	2.09E-09	9.56E-11	5.09E-10	1.15E-09	7.37E-10
	W	2.0E-03	1.70E-10	5.79E-11	1.43E-10	3.95E-09	3.75E-11	1.23E-10	1.72E-09	1.06E-09
	Y	2.0E-03	1.84E-10	4.70E-11	6.37E-11	4.10E-09	2.31E-11	3.50E-11	2.04E-09	1.17E-09
NB 93M	W	1.0E-02	4.16E-10	3.32E-11	2.85E-10	4.86E-09	3.04E-11	7.43E-10	3.95E-10	8.68E-10
	Y	1.0E-02	1.55E-10	4.36E-11	1.14E-10	6.45E-08	1.14E-11	2.84E-10	3.04E-10	7.90E-09
NB 95	W	1.0E-02	4.84E-10	3.77E-10	6.72E-10	5.49E-09	3.14E-10	2.42E-09	9.86E-10	1.29E-09
	Y	1.0E-02	4.32E-10	4.07E-10	4.42E-10	8.32E-09	3.58E-10	5.13E-10	1.07E-09	1.57E-09
NP 97	W	1.0E-02	1.21E-12	1.50E-12	2.07E-12	1.44E-10	1.34E-12	1.79E-12	8.89E-12	2.08E-11
	Y	1.0E-02	8.65E-13	1.12E-12	1.14E-12	1.56E-10	9.20E-13	8.26E-13	1.05E-11	2.24E-11
MO 93	D	8.0E-01	9.27E-11	7.48E-11	2.11E-10	1.15E-10	7.06E-11	8.59E-10	5.70E-10	2.72E-10
	Y	5.0E-02	2.45E-11	2.82E-10	1.06E-10	6.29E-08	1.17E-11	2.35E-10	2.10E-10	7.68E-09
MO 99	D	8.0E-01	1.32E-10	1.29E-10	3.71E-10	1.17E-09	1.17E-10	5.40E-10	9.49E-10	5.42E-10
	Y	5.0E-02	9.51E-11	2.75E-11	5.24E-11	4.29E-09	1.52E-11	4.13E-11	1.74E-09	1.07E-09
TC 99	D	8.0E-01	4.52E-11	4.52E-11	4.52E-11	3.51E-10	1.21E-09	4.52E-11	5.78E-10	2.77E-10
	W	8.0E-01	3.99E-11	3.99E-11	3.99E-11	1.67E-08	1.07E-09	3.99E-11	6.26E-10	2.25E-09
TC 99M	D	8.0E-01	2.77E-12	2.15E-12	3.36E-12	2.28E-11	5.01E-11	2.62E-12	1.02E-11	8.80E-12
	W	8.0E-01	1.70E-12	1.52E-12	2.39E-12	3.07E-11	2.09E-11	1.78E-12	6.34E-12	7.21E-12
TC 101	D	8.0E-01	2.50E-13	3.03E-13	3.19E-13	2.83E-11	7.72E-12	2.80E-13	3.52E-12	4.84E-12
	W	8.0E-01	7.31E-14	1.52E-13	1.60E-13	3.01E-11	2.31E-12	1.36E-13	6.60E-13	3.94E-12
RU 103	D	5.0E-02	7.31E-10	6.07E-10	6.66E-10	1.02E-09	5.97E-10	6.18E-10	1.04E-09	8.24E-10
	W	5.0E-02	3.94E-10	3.18E-10	3.39E-10	9.86E-09	2.75E-10	2.71E-10	1.20E-09	1.75E-09
	Y	5.0E-02	3.07E-10	3.11E-10	3.19E-10	1.56E-08	2.57E-10	2.37E-10	1.25E-09	2.42E-09

Table 7.19 (continued)

Nuclide	Clearance class	f_1	Gonads	Breast	R. Marrow	Lungs	Thyroid	Endosteal	Remainder	Effective
RU 105	D	5.0E-02	2.70E-11	1.72E-11	1.88E-11	3.66E-10	1.50E-11	1.57E-11	1.40E-10	9.84E-11
	W	5.0E-02	1.57E-11	8.48E-12	9.50E-12	5.42E-10	6.46E-12	6.79E-12	1.36E-10	1.13E-10
	Y	5.0E-02	1.59E-11	6.61E-12	7.70E-12	5.73E-10	4.15E-12	4.62E-12	1.61E-10	1.23E-10
RU 106	D	5.0E-02	1.38E-08	1.37E-08	1.37E-08	1.80E-08	1.37E-08	1.37E-08	1.69E-08	1.52E-08
	W	5.0E-02	4.03E-09	4.03E-09	4.06E-09	2.11E-07	4.01E-09	4.00E-09	1.39E-08	3.18E-08
	Y	5.0E-02	1.30E-09	1.78E-09	1.76E-09	1.04E-06	1.72E-09	1.61E-09	1.20E-08	1.29E-07
RH 105	D	5.0E-02	3.49E-11	2.70E-11	2.90E-11	3.67E-10	2.57E-11	2.71E-11	2.20E-10	1.28E-10
	W	5.0E-02	2.23E-11	9.19E-12	1.12E-11	9.26E-10	6.77E-12	8.25E-12	3.89E-10	2.37E-10
	Y	5.0E-02	2.11E-11	5.61E-12	7.77E-12	9.58E-10	2.88E-12	4.46E-12	4.53E-10	2.58E-10
PD 107	D	5.0E-03	9.45E-13	9.45E-13	5.11E-12	2.89E-11	9.45E-13	1.36E-11	2.15E-10	6.94E-11
	W	5.0E-03	2.43E-13	2.43E-13	1.31E-12	1.53E-09	2.43E-13	3.50E-12	1.17E-10	2.19E-10
	Y	5.0E-03	1.05E-13	1.05E-13	5.68E-13	2.85E-08	1.05E-13	1.51E-12	9.71E-11	3.45E-09
PD 109	D	5.0E-03	9.26E-12	8.36E-12	2.16E-11	6.62E-10	8.09E-12	4.64E-11	4.51E-10	2.23E-10
	W	5.0E-03	3.33E-12	2.03E-12	4.94E-12	1.15E-09	1.69E-12	9.75E-12	4.41E-10	2.72E-10
	Y	5.0E-03	2.13E-12	5.11E-13	9.82E-13	1.20E-09	1.55E-13	9.58E-13	5.04E-10	2.96E-10
AG 110M	D	5.0E-02	3.26E-09	4.14E-09	4.03E-09	8.11E-09	1.70E-09	3.05E-09	2.55E-08	1.07E-08
	W	5.0E-02	2.33E-09	2.93E-09	2.88E-09	3.15E-08	2.01E-09	2.13E-09	1.02E-08	8.34E-09
	Y	5.0E-02	2.43E-09	7.10E-09	6.74E-09	1.20E-07	6.39E-09	5.19E-09	1.51E-08	2.17E-08
AG 111	D	5.0E-02	7.60E-11	7.48E-11	7.62E-11	1.08E-09	7.06E-11	7.37E-11	2.46E-09	9.12E-10
	W	5.0E-02	2.59E-11	1.89E-11	2.03E-11	7.81E-09	1.63E-11	1.78E-11	2.07E-09	1.57E-09
	Y	5.0E-02	1.69E-11	8.47E-12	9.92E-12	8.70E-09	6.19E-12	7.41E-12	2.03E-09	1.66E-09
CD 113M	D	5.0E-02	3.32E-08	3.32E-08	3.32E-08	3.38E-08	3.32E-08	3.32E-08	1.30E-06	4.13E-07
	W	5.0E-02	9.95E-09	9.95E-09	9.95E-09	4.02E-08	9.95E-09	9.95E-09	3.89E-07	1.27E-07
	Y	5.0E-02	4.72E-09	4.72E-09	4.72E-09	4.09E-07	4.72E-09	4.72E-09	1.86E-07	1.08E-07
CD 115M	D	5.0E-02	1.57E-09	1.57E-09	1.58E-09	3.39E-09	1.55E-09	1.57E-09	6.06E-08	1.95E-08
	W	5.0E-02	3.80E-10	3.78E-10	3.81E-10	4.66E-08	3.73E-10	3.74E-10	1.76E-08	1.11E-08
	Y	5.0E-02	1.06E-10	1.08E-10	1.08E-10	7.78E-08	1.05E-10	1.03E-10	7.41E-09	1.16E-08
SN 123	D	2.0E-02	7.52E-10	7.52E-10	5.73E-09	2.32E-09	7.49E-10	1.58E-08	1.88E-09	2.33E-09
	W	2.0E-02	1.81E-10	1.82E-10	1.36E-09	6.11E-08	1.81E-10	3.75E-09	3.70E-09	8.79E-09
SN 125	D	2.0E-02	2.60E-10	2.28E-10	3.62E-09	2.57E-09	2.10E-10	5.19E-09	1.87E-09	1.56E-09
	W	2.0E-02	1.59E-10	9.37E-11	7.26E-10	2.24E-08	7.62E-11	1.07E-09	4.38E-09	4.18E-09
SN 126	D	2.0E-02	1.43E-08	1.41E-08	5.62E-08	1.61E-08	1.31E-08	1.18E-07	1.70E-08	2.34E-08
	W	2.0E-02	4.95E-09	5.39E-09	1.69E-08	1.51E-07	4.90E-09	3.33E-08	1.20E-08	2.69E-08

Table 7.19 (continued)

Nuclide	Clearance class	f_1	Gonads	Breast	R. Marrow	Lungs	Thyroid	Endosteal	Remainder	Effective
SB 124	D	1.0E-01	9.15E-10	6.51E-10	1.53E-09	2.03E-09	5.68E-10	3.41E-09	2.10E-09	1.50E-09
	W	1.0E-02	1.04E-09	8.94E-10	1.09E-09	4.14E-08	6.74E-10	1.24E-09	4.18E-09	6.80E-09
SB 125	D	1.0E-01	3.19E-10	2.51E-10	6.49E-10	6.38E-10	2.28E-10	2.73E-09	7.16E-10	5.75E-10
	W	1.0E-02	3.60E-10	4.16E-10	5.35E-10	2.17E-08	3.24E-10	9.78E-10	1.45E-09	3.30E-09
SB 126	D	1.0E-01	9.11E-10	5.89E-10	1.09E-09	1.77E-09	5.08E-10	1.71E-09	1.81E-09	1.27E-09
	W	1.0E-02	1.32E-09	6.44E-10	7.97E-10	1.38E-08	4.80E-10	6.75E-10	3.19E-09	3.17E-09
SB 127	D	1.0E-01	2.34E-10	1.65E-10	4.94E-10	1.36E-09	1.50E-10	5.45E-10	1.09E-09	6.55E-10
	W	1.0E-02	2.52E-10	9.12E-11	1.61E-10	6.94E-09	6.15E-11	1.34E-10	2.33E-09	1.63E-09
TE 125M	D	2.0E-01	1.24E-10	1.07E-10	3.01E-09	4.66E-10	9.93E-11	3.21E-08	3.14E-10	1.52E-09
	W	2.0E-01	7.93E-11	7.08E-11	1.15E-09	1.04E-08	3.87E-11	1.18E-08	6.75E-10	1.97E-09
TE 127	D	2.0E-01	5.63E-12	6.49E-12	1.43E-11	2.77E-10	6.46E-12	1.44E-11	9.74E-11	6.74E-11
	W	2.0E-01	2.02E-12	1.88E-12	4.09E-12	4.27E-10	1.84E-12	4.09E-12	1.11E-10	8.60E-11
TE 127M	D	2.0E-01	2.49E-10	2.43E-10	1.37E-08	8.91E-10	2.39E-10	5.24E-08	6.90E-10	3.64E-09
	W	2.0E-01	1.10E-10	1.10E-10	5.36E-09	3.34E-08	9.66E-11	2.04E-08	1.66E-09	5.81E-09
TE 129	D	2.0E-01	1.75E-12	1.68E-12	1.97E-12	1.33E-10	1.63E-12	2.03E-12	2.40E-11	2.42E-11
	W	2.0E-01	5.05E-13	5.39E-13	6.19E-13	1.53E-10	5.09E-13	6.22E-13	7.28E-12	2.09E-11
TE 129M	D	2.0E-01	4.12E-10	4.00E-10	8.77E-09	2.16E-09	3.95E-10	2.01E-08	1.47E-09	2.53E-09
	W	2.0E-01	1.78E-10	1.69E-10	3.10E-09	4.03E-08	1.56E-10	7.05E-09	3.27E-09	6.47E-09
TE 131	D	2.0E-01	6.14E-12	5.53E-12	6.54E-12	2.54E-10	2.63E-09	6.21E-12	5.42E-11	1.29E-10
	W	2.0E-01	2.17E-12	2.67E-12	2.94E-12	2.99E-10	2.66E-09	2.61E-12	2.21E-11	1.24E-10
TE 131M	D	2.0E-01	1.93E-10	1.15E-10	2.39E-10	9.43E-10	3.28E-08	6.37E-10	5.63E-10	1.38E-09
	W	2.0E-01	2.34E-10	9.25E-11	1.41E-10	2.23E-09	3.61E-08	2.27E-10	9.46E-10	1.73E-09
TE 132	D	2.0E-01	3.77E-10	3.52E-10	4.95E-10	6.50E-10	5.87E-08	1.53E-09	5.65E-10	2.26E-09
	W	2.0E-01	4.15E-10	3.63E-10	4.27E-10	1.67E-09	6.28E-08	7.12E-10	7.89E-10	2.55E-09
TE 133M	D	2.0E-01	8.97E-12	7.82E-12	8.32E-12	1.82E-10	2.61E-09	6.94E-12	4.14E-11	1.17E-10
	W	2.0E-01	3.39E-12	4.91E-12	4.89E-12	2.06E-10	2.63E-09	4.13E-12	1.43E-11	1.10E-10
TE 134	D	2.0E-01	9.00E-12	8.72E-12	9.30E-12	6.02E-11	5.54E-10	8.58E-12	1.89E-11	3.44E-11
	W	2.0E-01	7.90E-12	7.96E-12	8.38E-12	6.60E-11	5.56E-10	7.78E-12	1.09E-11	3.23E-11
I 129	D	1.0E 00	8.69E-11	2.09E-10	1.40E-10	3.14E-10	1.56E-06	1.38E-10	1.26E-10	4.69E-08
I 130	D	1.0E 00	2.81E-11	4.87E-11	4.55E-11	6.03E-10	1.99E-08	4.03E-11	8.02E-11	7.14E-10
I 131	D	1.0E 00	2.53E-11	7.88E-11	6.26E-11	6.57E-10	2.92E-07	5.73E-11	8.31E-11	8.89E-09
I 132	D	1.0E 00	9.95E-12	1.41E-11	1.40E-11	2.71E-10	1.74E-09	1.24E-11	3.78E-11	1.03E-10
I 133	D	1.0E 00	1.95E-11	2.94E-11	2.72E-11	8.20E-10	4.86E-08	2.52E-11	5.00E-11	1.58E-09

Table 7.19 (continued)

Nuclide	Clearance class	f_1	Gonads	Breast	R. Marrow	Lungs	Thyroid	Endosteal	Remainder	Effective
I 134	D	1.0E 00	4.25E-12	6.17E-12	6.08E-12	1.43E-10	2.88E-10	5.31E-12	2.27E-11	3.55E-11
I 135	D	1.0E 00	1.70E-11	2.34E-11	2.24E-11	4.41E-10	8.46E-09	2.01E-11	4.70E-11	3.32E-10
CS 134	D	1.0E 00	1.30E-08	1.09E-08	1.18E-08	1.18E-08	1.11E-08	1.10E-08	1.39E-08	1.25E-08
CS 134M	D	1.0E 00	3.61E-12	3.39E-12	3.76E-12	6.40E-11	3.34E-12	3.55E-12	6.90E-12	1.18E-11
CS 135	D	1.0E 00	1.20E-09	1.20E-09	1.20E-09	1.41E-09	1.20E-09	1.20E-09	1.20E-09	1.23E-09
CS 136	D	1.0E 00	1.88E-09	1.67E-09	1.86E-09	2.32E-09	1.73E-09	1.70E-09	2.19E-09	1.98E-09
CS 137	D	1.0E 00	8.76E-09	7.84E-09	8.30E-09	8.82E-09	7.93E-09	7.94E-09	9.12E-09	8.63E-09
CS 138	D	1.0E 00	3.28E-12	4.02E-12	3.95E-12	1.59E-10	3.57E-12	3.55E-12	2.06E-11	2.74E-11
BA 139	D	1.0E-01	2.56E-12	2.46E-12	3.41E-12	2.53E-10	2.40E-12	2.49E-12	4.82E-11	4.64E-11
BA 140	D	1.0E-01	4.30E-10	2.87E-10	1.29E-09	1.66E-09	2.56E-10	2.41E-09	1.41E-09	1.01E-09
BA 141	D	1.0E-01	1.41E-12	1.47E-12	2.49E-12	1.16E-10	1.33E-12	4.73E-12	2.27E-11	2.18E-11
BA 142	D	1.0E-01	2.16E-12	1.60E-12	1.93E-12	5.48E-11	1.27E-12	1.42E-12	1.14E-11	1.11E-11
LA 140	D	1.0E-03	3.62E-10	2.05E-10	4.56E-10	1.66E-09	1.22E-10	4.03E-10	1.81E-09	9.33E-10
	W	1.0E-03	4.54E-10	1.45E-10	2.14E-10	4.21E-09	6.87E-11	1.41E-10	2.12E-09	1.31E-09
LA 141	D	1.0E-03	1.01E-11	9.84E-12	2.93E-11	6.46E-10	9.40E-12	1.20E-10	2.28E-10	1.57E-10
	W	1.0E-03	2.89E-12	2.68E-12	7.06E-12	8.88E-10	2.45E-12	2.36E-11	1.43E-10	1.52E-10
LA 142	D	1.0E-03	1.66E-11	1.13E-11	1.36E-11	3.01E-10	8.74E-12	1.11E-11	8.07E-11	6.84E-11
	W	1.0E-03	5.91E-12	6.28E-12	6.83E-12	3.50E-10	4.91E-12	5.39E-12	3.14E-11	5.50E-11
CE 141	W	3.0E-04	8.44E-11	7.12E-11	4.19E-10	1.12E-08	4.61E-11	3.79E-09	2.36E-09	2.25E-09
	Y	3.0E-04	5.54E-11	4.46E-11	8.96E-11	1.67E-08	2.55E-11	2.54E-10	1.26E-09	2.42E-09
CE 143	W	3.0E-04	7.06E-11	2.22E-11	7.77E-11	3.54E-09	1.21E-11	7.90E-11	1.35E-09	8.66E-10
	Y	3.0E-04	7.53E-11	1.66E-11	2.96E-11	3.88E-09	6.23E-12	1.64E-11	1.42E-09	9.16E-10
CE 144	W	3.0E-04	1.93E-09	1.97E-09	2.67E-08	1.83E-07	1.88E-09	4.54E-08	1.03E-07	5.84E-08
	Y	3.0E-04	2.79E-10	3.48E-10	2.88E-09	7.91E-07	2.92E-10	4.72E-09	1.91E-08	1.01E-07
PR 143	W	3.0E-04	4.25E-18	2.45E-18	2.73E-10	1.10E-08	1.58E-18	2.74E-10	2.25E-09	2.04E-09
	Y	3.0E-04	4.37E-18	2.22E-18	1.48E-11	1.33E-08	1.68E-18	1.49E-11	1.97E-09	2.19E-09
ND 147	W	3.0E-04	7.94E-11	3.76E-11	4.98E-10	8.42E-09	1.94E-11	2.33E-09	1.86E-09	1.72E-09
	Y	3.0E-04	8.41E-11	3.45E-11	9.19E-11	1.06E-08	1.82E-11	3.26E-10	1.76E-09	1.85E-09
PM 147	W	3.0E-04	1.88E-14	3.15E-14	8.16E-09	9.69E-09	1.32E-14	1.02E-07	5.89E-09	6.97E-09
	Y	3.0E-04	8.25E-15	3.60E-14	1.61E-09	7.74E-08	1.98E-14	2.01E-08	1.56E-09	1.06E-08
PM 148	W	3.0E-04	1.96E-10	7.85E-11	5.11E-10	1.26E-08	4.27E-11	4.80E-10	3.88E-09	2.81E-09
	Y	3.0E-04	2.12E-10	7.19E-11	1.07E-10	1.37E-08	3.82E-11	7.08E-11	4.10E-09	2.95E-09
PM 148M	W	3.0E-04	1.38E-09	1.28E-09	2.88E-09	2.25E-08	8.79E-10	9.05E-09	5.27E-09	5.46E-09

Table 7.19 (continued)

Nuclide	Clearance class	f_1	Gonads	Breast	R. Marrow	Lungs	Thyroid	Endosteal	Remainder	Effective
	Y	3.0E-04	1.19E-09	1.24E-09	1.36E-09	3.59E-08	1.05E-09	1.36E-09	3.58E-09	6.10E-09
PM 149	W	3.0E-04	3.16E-12	8.44E-13	7.94E-11	2.99E-09	3.69E-13	8.04E-11	1.24E-09	7.44E-10
	Y	3.0E-04	3.61E-12	8.20E-13	5.53E-12	3.12E-09	3.31E-13	5.01E-12	1.39E-09	7.93E-10
PM 151	W	3.0E-04	6.16E-11	1.59E-11	5.79E-11	1.58E-09	6.69E-12	9.73E-11	7.36E-10	4.38E-10
	Y	3.0E-04	7.17E-11	1.59E-11	2.72E-11	1.64E-09	6.18E-12	1.86E-11	8.39E-10	4.73E-10
SM 151	W	3.0E-04	4.03E-14	1.49E-13	1.10E-08	3.26E-09	1.32E-14	1.38E-07	7.51E-09	8.10E-09
SM 153	W	3.0E-04	2.36E-11	5.67E-12	6.66E-11	2.05E-09	1.51E-12	1.57E-10	8.84E-10	5.31E-10
EU 152	W	1.0E-03	1.31E-08	1.74E-08	7.91E-08	5.76E-08	8.25E-09	2.40E-07	9.99E-08	5.97E-08
EU 154	W	1.0E-03	1.17E-08	1.55E-08	1.06E-07	7.92E-08	7.14E-09	5.23E-07	1.13E-07	7.73E-08
EU 155	W	1.0E-03	3.56E-10	6.14E-10	1.43E-08	1.19E-08	2.40E-10	1.52E-07	1.11E-08	1.12E-08
EU 156	W	1.0E-03	6.12E-10	3.64E-10	1.14E-09	1.84E-08	2.16E-10	2.76E-09	3.91E-09	3.82E-09
TB 160	W	3.0E-04	9.36E-10	9.63E-10	4.43E-09	3.02E-08	6.54E-10	2.47E-08	4.84E-09	6.75E-09
HO 166M	W	3.0E-04	3.05E-08	4.84E-08	1.61E-07	1.08E-07	2.14E-08	8.87E-07	4.50E-07	2.09E-07
W 181	D	3.0E-01	1.11E-11	5.93E-12	5.04E-11	5.25E-11	2.71E-12	7.08E-11	7.56E-11	4.09E-11
W 185	D	3.0E-01	1.24E-14	6.15E-15	8.39E-11	3.80E-10	2.85E-15	2.55E-10	4.65E-10	2.03E-10
W 187	D	3.0E-01	2.99E-11	8.79E-12	2.32E-11	6.05E-10	4.37E-12	9.85E-11	2.66E-10	1.67E-10
PB 210	D	2.0E-01	3.18E-07	3.18E-07	3.75E-06	3.18E-07	3.18E-07	5.47E-05	4.69E-06	3.67E-06
BI 210	D	5.0E-02	1.96E-10	1.96E-10	1.96E-10	2.47E-09	1.96E-10	1.96E-10	1.26E-08	4.18E-09
	W	5.0E-02	6.47E-11	6.47E-11	6.47E-11	4.26E-07	6.47E-11	6.47E-11	5.66E-09	5.29E-08
PO 210	D	1.0E-01	4.04E-07	4.04E-07	4.04E-07	7.29E-07	4.04E-07	4.04E-07	7.40E-06	2.54E-06
	W	1.0E-01	1.26E-07	1.26E-07	1.26E-07	1.30E-05	1.26E-07	1.26E-07	2.30E-06	2.32E-06
PA 223	W	2.0E-01	3.38E-08	3.38E-08	2.24E-07	1.66E-05	3.38E-08	2.34E-06	6.14E-08	2.12E-06
PA 224	W	2.0E-01	1.56E-08	1.54E-08	1.13E-07	6.56E-06	1.53E-08	1.17E-06	3.55E-08	8.53E-07
RA 225	W	2.0E-01	3.07E-08	3.07E-08	1.58E-07	1.67E-05	3.07E-08	1.68E-06	3.63E-08	2.10E-06
RA 226	W	2.0E-01	1.02E-07	1.02E-07	6.64E-07	1.61E-05	1.02E-07	7.59E-06	1.07E-07	2.32E-06
RA 228	W	2.0E-01	1.83E-07	1.84E-07	7.38E-07	7.22E-06	1.83E-07	6.51E-06	1.87E-07	1.29E-06
AC 225	D	1.0E-03	5.22E-07	7.63E-11	3.72E-06	1.57E-06	4.03E-11	4.65E-05	2.53E-06	2.92E-06
	W	1.0E-03	8.70E-08	5.16E-11	6.19E-07	1.55E-05	2.89E-11	7.75E-06	4.53E-07	2.32E-06
	Y	1.0E-03	5.20E-09	4.66E-11	3.63E-08	1.79E-05	2.64E-11	4.53E-07	6.14E-08	2.19E-06
AC 227	D	1.0E-03	3.96E-04	6.66E-08	2.57E-03	1.23E-07	3.59E-08	3.21E-02	1.47E-03	1.81E-03
	W	1.0E-03	9.98E-05	1.70E-08	6.49E-04	6.80E-05	9.22E-09	8.10E-03	3.70E-04	4.65E-04
	Y	1.0E-03	3.56E-05	1.06E-08	2.33E-04	1.54E-03	6.47E-09	2.91E-03	1.34E-04	3.49E-04
TH 227	W	2.0E-04	5.36E-08	5.36E-08	2.43E-06	2.40E-05	5.35E-08	2.94E-05	1.47E-07	4.12E-06

Table 7.19 (continued)

Nuclide	Clearance class	f_1	Gonads	Breast	R. Marrow	Lungs	Thyroid	Endosteal	Remainder	Effective
	Y	2.0E-04	2.96E-09	2.98E-09	1.30E-07	3.58E-05	2.94E-09	1.58E-06	2.06E-08	4.37E-06
TH 228	W	2.0E-04	1.35E-06	1.35E-06	1.12E-04	9.48E-05	1.34E-06	1.37E-03	3.44E-06	6.75E-05
	Y	2.0E-04	2.26E-07	2.32E-07	1.87E-05	6.91E-04	2.30E-07	2.29E-04	6.05E-07	9.23E-05
TH 229	W	2.0E-04	2.76E-06	2.76E-06	1.15E-03	7.95E-05	2.76E-06	1.43E-02	7.05E-06	5.80E-04
	Y	2.0E-04	1.18E-05	1.18E-06	4.60E-04	1.99E-03	1.18E-06	5.73E-03	3.02E-06	4.67E-04
TH 230	W	2.0E-04	4.08E-07	4.08E-07	1.73E-04	1.61E-05	4.08E-07	2.16E-03	1.05E-06	8.80E-05
	Y	2.0E-04	1.72E-07	1.72E-07	6.99E-05	3.00E-04	1.72E-07	8.71E-04	4.48E-07	7.07E-05
TH 232	W	2.0E-04	7.62E-07	7.72E-07	8.93E-04	1.44E-05	7.44E-07	1.11E-02	1.87E-06	4.43E-04
	Y	2.0E-04	5.58E-07	6.14E-07	4.01E-04	9.40E-04	5.99E-07	4.99E-03	1.51E-06	3.11E-04
TH 234	W	2.0E-04	1.13E-10	1.08E-10	4.18E-09	4.66E-08	1.03E-10	7.83E-09	5.54E-09	8.04E-09
	Y	2.0E-04	2.11E-11	1.66E-11	2.56E-10	6.39E-08	1.27E-11	6.29E-10	5.80E-09	9.47E-09
PA 231	W	1.0E-03	6.90E-09	8.79E-09	6.97E-04	1.72E-05	7.64E-09	8.70E-03	2.86E-07	3.47E-04
	Y	1.0E-03	3.06E-09	5.65E-09	2.88E-04	7.47E-04	4.45E-09	3.60E-03	2.12E-07	2.32E-04
PA 233	W	1.0E-03	1.29E-10	8.32E-11	8.21E-10	1.19E-08	5.17E-11	7.37E-09	1.47E-09	2.24E-09
	Y	1.0E-03	1.29E-10	9.20E-11	1.96E-10	1.70E-08	5.62E-11	8.28E-10	1.48E-09	2.58E-09
U 232	D	5.0E-02	8.00E-08	8.06E-08	4.06E-06	4.07E-07	7.85E-08	6.42E-05	3.11E-06	3.43E-06
	W	5.0E-02	2.51E-08	2.53E-08	1.23E-06	2.49E-05	2.47E-08	1.94E-05	9.76E-07	4.02E-06
	Y	2.0E-03	1.69E-08	2.66E-08	4.68E-07	1.48E-03	2.43E-08	7.14E-06	5.86E-07	1.78E-04
U 233	D	5.0E-02	2.54E-08	2.54E-08	7.12E-07	3.22E-07	2.54E-08	1.12E-05	9.40E-07	7.53E-07
	W	5.0E-02	7.63E-09	7.63E-09	2.14E-07	1.62E-05	7.63E-09	3.36E-06	2.89E-07	2.16E-06
	Y	2.0E-03	2.69E-09	2.73E-09	7.39E-08	3.04E-04	2.70E-09	1.16E-06	1.09E-07	3.66E-05
U 234	D	5.0E-02	2.50E-08	2.50E-08	6.98E-07	3.18E-07	2.50E-08	1.09E-05	9.26E-07	7.37E-07
	W	5.0E-02	7.52E-09	7.52E-09	2.10E-07	1.60E-05	7.52E-09	3.29E-06	2.85E-07	2.13E-06
	Y	2.0E-03	2.65E-09	2.68E-09	7.22E-08	2.98E-04	2.65E-09	1.13E-06	1.06E-07	3.58E-05
U 235	D	5.0E-02	2.37E-08	2.38E-08	6.58E-07	2.95E-07	2.37E-08	1.01E-05	8.59E-07	6.85E-07
	W	5.0E-02	7.24E-09	7.33E-09	1.98E-07	1.48E-05	7.22E-09	3.05E-06	2.65E-07	1.97E-06
	Y	2.0E-03	2.84E-09	5.37E-09	7.15E-08	2.76E-04	4.11E-09	1.05E-06	1.02E-07	3.32E-05
U 236	D	5.0E-02	2.37E-08	2.37E-08	6.60E-07	3.01E-07	2.37E-08	1.04E-05	8.77E-07	7.01E-07
	W	5.0E-02	7.12E-09	7.12E-09	1.99E-07	1.51E-05	7.12E-09	3.12E-06	2.70E-07	2.01E-06
	Y	2.0E-03	2.51E-09	2.54E-09	6.83E-08	2.82E-04	2.51E-09	1.07E-06	1.00E-07	3.39E-05
U 237	D	5.0E-02	5.55E-11	3.39E-11	4.12E-10	6.13E-10	2.62E-11	4.02E-09	8.94E-10	5.32E-10
	W	5.0E-02	7.39E-11	2.78E-11	1.23E-10	4.26E-09	1.39E-11	8.35E-10	1.10E-09	9.03E-10
	Y	2.0E-03	8.15E-11	2.51E-11	5.23E-11	4.70E-09	1.00E-11	6.82E-11	1.19E-09	9.54E-10

Table 7.19 (continued)

Nuclide	Clearance class	f_1	Gonads	Breast	R. Marrow	Lungs	Thyroid	Endosteal	Remainder	Effective
U 238	D	5.0E-02	2.23E-08	2.23E-08	6.58E-07	2.80E-07	2.22E-08	9.78E-06	8.22E-07	6.62E-07
	W	5.0E-02	6.71E-09	6.74E-09	1.98E-07	1.42E-05	6.71E-09	2.94E-06	2.54E-07	1.90E-06
	Y	2.0E-03	2.42E-09	2.91E-09	6.88E-08	2.66E-04	2.73E-09	1.01E-06	9.61E-08	3.20E-05
NP 237	W	1.0E-02	3.07E-05	1.90E-08	1.91E-04	1.61E-05	1.03E-08	2.39E-03	1.03E-04	1.35E-04
NP 238	W	1.0E-02	2.06E-09	3.98E-11	1.32E-08	3.47E-09	2.19E-11	1.52E-07	7.63E-09	9.25E-09
NP 239	W	1.0E-02	7.42E-11	1.49E-11	1.47E-10	2.36E-09	5.84E-12	1.38E-09	1.00E-09	6.65E-10
PU 238	W	1.0E-04	2.79E-05	5.77E-11	1.76E-04	1.84E-05	4.60E-12	2.20E-03	9.60E-05	1.25E-04
	Y	1.0E-05	1.04E-05	6.04E-11	6.65E-05	3.20E-04	1.99E-12	8.31E-04	3.68E-05	8.50E-05
PU 239	W	1.0E-04	3.17E-05	2.98E-11	1.97E-04	1.73E-05	4.36E-12	2.47E-03	1.06E-04	1.40E-04
	Y	1.0E-05	1.20E-05	2.79E-11	7.60E-05	3.23E-04	2.34E-12	9.50E-04	4.16E-05	9.19E-05
PU 240	W	1.0E-04	3.16E-05	6.55E-11	1.97E-04	1.73E-05	5.56E-12	2.47E-03	1.06E-04	1.40E-04
	Y	1.0E-05	1.20E-05	6.51E-11	7.60E-05	3.23E-04	2.47E-12	9.50E-04	4.16E-05	9.19E-05
PU 241	W	1.0E-04	6.80E-07	4.16E-11	4.08E-06	7.45E-09	1.49E-11	5.10E-05	2.06E-06	2.81E-06
	Y	1.0E-05	2.76E-07	2.34E-11	1.70E-06	3.18E-06	7.80E-12	2.12E-05	8.90E-07	1.56E-06
PU 242	W	1.0E-04	3.01E-05	1.15E-10	1.88E-04	1.64E-05	2.96E-11	2.35E-03	1.01E-04	1.33E-04
	Y	1.0E-05	1.14E-05	8.90E-11	7.23E-05	3.07E-04	1.80E-11	9.04E-04	3.94E-05	8.73E-05
PU 244	W	1.0E-04	2.98E-05	4.06E-08	1.86E-04	1.63E-05	2.06E-08	2.31E-03	9.99E-05	1.31E-04
	Y	1.0E-05	1.13E-05	2.33E-08	7.17E-05	3.03E-04	1.35E-08	8.90E-04	3.92E-05	8.63E-05
AM 241	W	5.0E-04	3.25E-05	2.18E-09	2.03E-04	1.84E-05	7.50E-10	2.53E-03	1.09E-04	1.43E-04
AM 242	W	5.0E-04	1.94E-09	5.88E-13	1.37E-08	5.20E-08	1.65E-13	1.71E-07	9.06E-09	1.62E-08
AM 242M	W	5.0E-04	3.20E-05	1.61E-09	1.99E-04	4.20E-06	5.38E-10	2.48E-03	1.06E-04	1.39E-04
AM 243	W	5.0E-04	3.25E-05	1.81E-08	2.03E-04	1.78E-05	8.76E-09	2.53E-03	1.09E-04	1.43E-04
CM 242	W	5.0E-04	5.69E-07	3.29E-12	4.02E-06	1.55E-05	1.28E-13	5.03E-05	2.61E-06	4.78E-06
CM 243	W	5.0E-04	2.07E-05	6.35E-09	1.33E-04	1.94E-05	3.24E-09	1.67E-03	7.50E-05	9.61E-05
CM 244	W	5.0E-04	1.59E-05	4.40E-11	1.04E-04	1.93E-05	6.23E-12	1.31E-03	6.02E-05	7.61E-05
CM 245	W	5.0E-04	3.36E-05	7.28E-09	2.09E-04	1.80E-05	3.26E-09	2.62E-03	1.12E-04	1.48E-04
CM 246	W	5.0E-04	3.33E-05	3.82E-09	2.08E-04	1.82E-05	1.56E-09	2.60E-03	1.11E-04	1.47E-04

Table 7.19 (continued)

Nuclide	Clearance class	f_1	Gonads	Breast	R. Marrow	Lungs	Thyroid	Endosteal	Remainder	Effective
CM 247	W	5.0E-04	3.06E-05	2.70E-08	1.91E-04	1.67E-05	1.63E-08	2.39E-03	1.02E-04	1.35E-04
CM 248	W	5.0E-04	1.21E-04	1.34E-06	7.62E-04	6.67E-05	5.53E-07	9.49E-03	4.08E-04	5.37E-04
CF 252	W	5.0E-04	5.40E-06	6.26E-08	3.90E-05	3.74E-05	2.49E-08	4.86E-04	2.53E-05	3.27E-05
	Y	5.0E-04	1.07E-06	6.04E-08	7.75E-06	2.99E-04	3.02E-08	9.62E-05	5.10E-06	4.15E-05

[a]Carbon dioxide.

[b]Labeled organic compound.

[c]Carbon monoxide.

[d]Nickel carbonyl vapor.

Table 7.20. Assignment of clearance class and f_1 values for inhaled compounds

Element	Clearance class	f_1	Chemical compounds
Be	Y	5×10^{-3}	Oxides, halides, and nitrates
	W	5×10^{-3}	All other compounds
P	W	0.8	Phosphates of some particular elements
	D	0.8	All other compounds
Cr	Y	0.1	Oxides and hydroxides
	W	0.1	Halides and nitrates
	D	0.1	All other compounds
Mn	W	0.1	Oxides, hydroxides, halides, and nitrates
	D	0.1	All other compounds
Fe	W	0.1	Oxides, hydroxides, and halides
	D	0.1	All other compounds
Co	Y	5×10^{-2}	Oxides, hydroxides, halides, and nitrates
	W	5×10^{-2}	All other compounds
Ni	W	5×10^{-2}	Oxides, hydroxides, and carbides
	vapor	1.0	Nickel carbonyl
	D	5×10^{-2}	All other compounds
Cu	Y	0.5	Oxides and hydroxides
	W	0.5	Sulfides, halides, and nitrates
	D	0.5	All other compounds
Se	W		Oxides, hydroxides, and carbides
	D	0.8	All other compounds
Br	W	1.0	Bromides of all compounds
	D	1.0	Bromides of all compounds
Sr	Y	1×10^{-2}	Titanates
	D	0.3	Soluble compounds
Y	Y	1×10^{-4}	Oxides and hydroxides
	W	1×10^{-4}	All other compounds
Zr	Y	2×10^{-3}	Carbides
	W	2×10^{-3}	Oxides, hydroxides, halides, and nitrates
	D	2×10^{-3}	All other compounds
Nb	Y	1×10^{-2}	Oxides and hydroxides
	W	1×10^{-2}	All other compounds
Mo	Y	5×10^{-2}	Oxides, hydroxides, and disulfides
	D	0.8	All other compounds

Table 7.20 (continued)

Element	Clearance class	f_1	Chemical compounds
Tc	W	0.8	Oxides, hydroxides, halides, and nitrates
	D	0.8	All other compounds
Ru	Y	5×10^{-2}	Oxides and hydroxides
	W	5×10^{-2}	Halides
	D	5×10^{-2}	All other compounds
Rh	Y	5×10^{-2}	Oxides and hydroxides
	W	5×10^{-2}	Halides
	D	5×10^{-2}	All other compounds
Pd	Y	5×10^{-3}	Oxides and hydroxides
	W	5×10^{-3}	Nitrates
	D	5×10^{-3}	All other compounds
Ag	Y	5×10^{-2}	Oxides and hydroxides
	W	5×10^{-2}	Nitrates and sulfides
	D	5×10^{-2}	All other compounds
Cd	Y	5×10^{-2}	Oxides and hydroxides
	W	5×10^{-2}	Sulfides, halides, and nitrates
	D	5×10^{-2}	All other compounds
Sn	W	2×10^{-2}	Sulfides, oxides, hydroxides, halides, and nitrates
	D	2×10^{-2}	All other compounds
Sb	W	1×10^{-2}	Halides, hydroxides, sulfates, nitrates, sulfides, and oxides
	D	0.1	All other compounds
Te	W	2×10^{-1}	Oxides, hydroxides, and nitrates
	D	2×10^{-1}	All other compounds
La	W	1×10^{-3}	Oxides and hydroxides
	D	1×10^{-3}	All other compounds
Ce	Y	3×10^{-4}	Oxides, hydroxides, and fluorides
	W	3×10^{-4}	All other compounds
Pr	W	3×10^{-4}	Oxides, hydroxides, carbides, and fluorides
	W	3×10^{-4}	All other compounds
Nd	Y	3×10^{-4}	Oxides, hydroxides, carbides, and fluorides
	W	3×10^{-4}	All other compounds
Pm	Y	3×10^{-4}	Oxides, hydroxides, carbides, and fluorides
	W	3×10^{-4}	All other compounds

Table 7.20 (continued)

Element	Clearance class	f_1	Chemical compounds
Bi	D	5×10^{-2}	Bismuth nitrate
	W	5×10^{-2}	All other compounds
Po	W	0.1	Oxides, hydroxides, and nitrates
	D	0.1	All other compounds
Ac	Y	1×10^{-3}	Oxides and hydroxides
	W	1×10^{-3}	Halides and nitrates
	D	1×10^{-3}	All other compounds
Th	Y	2×10^{-4}	Oxides and hydroxides
	W	2×10^{-4}	All other compounds
Pa	Y	1×10^{-3}	Oxides and hydroxides
	W	1×10^{-3}	All other compounds
U	Y	2×10^{-3}	Highly insoluble oxides
	W	5×10^{-2}	Less soluble compounds
	D	5×10^{-2}	Soluble compounds
Pu	Y	1×10^{-4}	Dioxides
	W	1×10^{-4}	All other compounds

Table 7.21. Committed dose equivalent per unit intake via ingestion (Sv/Bq)

Nuclide		f_1	Gonads	Breast	R. Marrow	Lungs	Thyroid	Endosteal	Remainder	Effective
H	3	1.0E 00	1.70E-11	1.70E-11	1.70E-11	1.70E-11	1.70E-11	1.70E-11	1.70E-11	1.70E-11
BE	10	5.0E-03	2.42E-11	2.42E-11	7.23E-10	2.42E-11	2.42E-11	2.15E-09	3.66E-09	1.26E-09
NA	22	1.0E 00	2.81E-09	2.58E-09	4.29E-09	2.51E-09	2.50E-09	5.54E-09	3.18E-09	3.10E-09
NA	24	1.0E 00	3.43E-10	2.71E-10	3.74E-10	2.60E-10	2.60E-10	4.59E-10	5.31E-10	3.84E-10
P	32	8.0E-01	6.55E-10	6.55E-10	8.09E-09	6.55E-10	6.55E-10	7.87E-09	2.67E-09	2.37E-09
CA	41	3.0E-01	2.71E-12	3.19E-12	1.78E-09	2.84E-12	2.84E-12	4.01E-09	2.74E-11	3.44E-10
SC	46	1.0E-04	2.01E-09	2.51E-10	4.03E-10	4.86E-11	7.69E-12	1.39E-10	3.78E-09	1.73E-09
CR	51	1.0E-01	4.00E-11	7.51E-12	1.25E-11	4.38E-12	3.71E-12	7.86E-12	8.75E-11	3.98E-11
		1.0E-02	3.96E-11	4.49E-12	8.52E-12	9.47E-13	4.26E-13	3.19E-12	9.17E-11	3.93E-11
MN	54	1.0E-01	9.48E-10	2.77E-10	4.89E-10	2.29E-10	1.33E-10	5.71E-10	1.21E-09	7.48E-10
MN	56	1.0E-01	8.53E-11	1.76E-11	2.43E-11	8.80E-12	2.40E-12	1.06E-11	7.94E-10	2.64E-10
FE	55	1.0E-01	1.07E-10	1.04E-10	1.05E-10	1.02E-10	1.10E-10	1.05E-10	3.00E-10	1.54E-10
FE	59	1.0E-01	1.66E-09	7.37E-10	8.45E-10	6.35E-10	6.03E-10	6.51E-10	3.56E-09	1.81E-09
CO	57	5.0E-02	1.83E-10	4.10E-11	8.84E-11	2.89E-11	1.93E-11	4.92E-11	4.42E-10	2.01E-10
		3.0E-01	2.94E-10	1.58E-10	2.67E-10	1.63E-10	1.15E-10	2.12E-10	5.39E-10	3.20E-10
CO	60	5.0E-02	3.19E-09	1.10E-09	1.32E-09	8.77E-10	7.89E-10	9.39E-10	4.97E-09	2.77E-09
		3.0E-01	7.23E-09	5.08E-09	5.49E-09	4.96E-09	4.58E-09	4.81E-09	1.06E-08	7.28E-09
NI	59	5.0E-02	3.83E-11	3.58E-11	3.66E-11	3.50E-11	3.90E-11	3.62E-11	1.03E-10	5.67E-11
NI	63	5.0E-02	8.50E-11	8.50E-11	8.50E-11	8.50E-11	8.50E-11	8.50E-11	3.20E-10	1.56E-10
NI	65	5.0E-02	2.43E-11	5.63E-12	7.26E-12	2.75E-12	6.79E-13	2.89E-12	5.32E-10	1.68E-10
CU	64	5.0E-01	4.78E-11	1.59E-11	1.94E-11	1.28E-11	1.13E-11	1.39E-11	3.57E-10	1.26E-10
ZN	65	5.0E-01	3.56E-09	3.28E-09	4.50E-09	3.09E-09	3.21E-09	4.50E-09	4.59E-09	3.90E-09
ZN	69	5.0E-01	4.17E-13	4.17E-13	5.36E-13	4.17E-13	4.17E-13	5.18E-13	7.91E-11	2.40E-11
SE	79	8.0E-01	9.06E-10	9.06E-10	9.06E-10	9.06E-10	9.06E-10	9.06E-10	5.73E-09	2.35E-09
		5.0E-02	5.66E-11	5.66E-11	5.66E-11	5.66E-11	5.66E-11	5.66E-11	1.04E-09	3.51E-10
BR	82	1.0E 00	4.48E-10	3.81E-10	4.14E-10	3.84E-10	3.83E-10	3.80E-10	5.80E-10	4.52E-10
BR	83	1.0E 00	7.35E-12	7.34E-12	7.35E-12	7.35E-12	7.33E-12	7.33E-12	6.53E-11	2.47E-11
BR	84	1.0E 00	6.75E-12	6.62E-12	6.21E-12	6.99E-12	5.20E-12	5.56E-12	1.48E-10	4.91E-11
RB	86	1.0E 00	2.15E-09	2.14E-09	3.72E-09	2.14E-09	2.14E-09	6.86E-09	2.33E-09	2.53E-09
RB	87	1.0E 00	1.14E-09	1.14E-09	2.02E-09	1.14E-09	1.14E-09	3.80E-09	1.17E-09	1.33E-09
RB	88	1.0E 00	2.78E-12	2.82E-12	2.76E-12	2.91E-12	2.43E-12	2.75E-12	1.50E-10	4.71E-11
RB	89	1.0E 00	3.32E-12	3.38E-12	3.53E-12	3.68E-12	2.21E-12	4.19E-12	8.04E-11	2.65E-11
SR	89	3.0E-01	2.40E-10	2.40E-10	3.23E-09	2.40E-10	2.40E-10	4.81E-09	6.11E-09	2.50E-09

Table 7.21 (continued)

Nuclide	f_1	Gonads	Breast	R. Marrow	Lungs	Thyroid	Endosteal	Remainder	Effective
	1.0E-02	8.05E-12	7.98E-12	1.08E-10	7.97E-12	7.97E-12	1.61E-10	8.25E-09	2.50E-09
SR 90	3.0E-01	1.51E-09	1.51E-09	1.94E-07	1.51E-09	1.51E-09	4.19E-07	6.14E-09	3.85E-08
	1.0E-02	5.04E-11	5.04E-11	6.45E-09	5.04E-11	5.04E-11	1.39E-08	6.70E-09	3.23E-09
SR 91	3.0E-01	2.10E-10	4.98E-11	1.08E-10	3.05E-11	2.41E-11	7.90E-11	1.98E-09	6.74E-10
	1.0E-02	2.48E-10	3.57E-11	5.53E-11	9.81E-12	1.90E-12	2.02E-11	2.54E-09	8.39E-10
SR 92	3.0E-01	8.01E-11	2.69E-11	3.87E-11	1.89E-11	1.35E-11	2.13E-11	1.37E-09	4.43E-10
	1.0E-02	8.18E-11	1.70E-11	2.29E-11	7.22E-12	1.30E-12	8.49E-12	1.72E-09	5.43E-10
Y 90	1.0E-04	1.43E-14	1.27E-14	3.70E-13	1.26E-14	1.26E-14	3.67E-13	9.68E-09	2.91E-09
Y 91	1.0E-04	3.54E-12	5.54E-13	6.59E-12	2.02E-13	1.29E-13	6.13E-12	8.57E-09	2.57E-09
Y 91M	1.0E-04	6.94E-12	1.84E-12	2.24E-12	1.28E-12	1.17E-13	9.71E-13	2.92E-11	1.12E-11
Y 92	1.0E-04	1.96E-11	3.55E-12	4.91E-12	1.39E-12	1.77E-13	1.75E-12	1.70E-09	5.15E-10
Y 93	1.0E-04	2.20E-11	3.13E-12	4.93E-12	8.67E-13	1.26E-13	1.73E-12	4.09E-09	1.23E-09
ZR 93	2.0E-03	9.23E-14	1.97E-13	7.42E-10	1.15E-13	7.31E-14	9.14E-09	2.83E-10	4.48E-10
ZR 95	2.0E-03	8.16E-10	1.05E-10	2.14E-10	2.34E-11	8.27E-12	4.85E-10	2.53E-09	1.02E-09
ZR 97	2.0E-03	6.22E-10	8.12E-11	1.30E-10	1.75E-11	2.66E-12	4.55E-11	6.98E-09	2.28E-09
NB 93M	1.0E-02	3.34E-11	2.57E-12	2.32E-11	2.45E-12	2.44E-12	5.98E-11	4.25E-10	1.41E-10
NB 95	1.0E-02	8.05E-10	1.07E-10	1.99E-10	2.74E-11	1.18E-11	2.94E-10	1.47E-09	6.95E-10
NB 97	1.0E-02	1.45E-11	3.30E-12	4.20E-12	1.99E-12	2.11E-13	1.50E-12	1.94E-10	6.30E-11
MO 93	8.0E-01	1.27E-10	9.96E-11	2.82E-10	1.05E-10	9.42E-11	1.15E-09	7.79E-10	3.54E-10
	5.0E-02	2.54E-11	6.78E-12	1.97E-11	6.63E-12	5.89E-12	7.22E-11	1.74E-10	6.52E-11
MO 99	8.0E-01	2.21E-10	1.83E-10	5.33E-10	1.93E-10	1.64E-10	7.69E-10	2.08E-09	8.22E-10
	5.0E-02	2.18E-10	3.43E-11	8.32E-11	1.51E-11	1.03E-11	6.32E-11	4.28E-09	1.36E-09
TC 99	8.0E-01	6.04E-11	6.04E-11	6.04E-11	6.04E-11	1.62E-09	6.04E-11	1.02E-09	3.95E-10
TC 99M	8.0E-01	9.75E-12	3.57E-12	6.29E-12	3.14E-12	8.46E-11	4.05E-12	3.34E-11	1.58E-11
TC 101	8.0E-01	6.29E-13	4.06E-13	4.36E-13	4.13E-13	3.89E-12	2.55E-13	3.66E-11	1.14E-11
RU 103	5.0E-02	5.72E-10	1.20E-10	1.66E-10	7.31E-11	6.25E-11	9.53E-11	2.10E-09	8.24E-10
RU 105	5.0E-02	9.67E-11	1.59E-11	2.35E-11	6.21E-12	1.82E-12	8.89E-12	8.54E-10	2.87E-10
RU 106	5.0E-02	1.64E-09	1.44E-09	1.46E-09	1.42E-09	1.41E-09	1.43E-09	2.11E-08	7.40E-09
RH 105	5.0E-02	5.80E-11	8.97E-12	1.47E-11	3.85E-12	2.91E-12	6.75E-12	1.27E-09	3.99E-10
PD 107	5.0E-03	9.91E-15	9.91E-15	5.36E-14	9.91E-15	9.91E-15	1.43E-13	1.35E-10	4.04E-11
PD 109	5.0E-03	7.90E-12	6.27E-13	2.04E-12	1.49E-13	9.48E-14	1.02E-12	1.95E-09	5.87E-10
AG 110M	5.0E-02	2.99E-09	7.51E-10	9.42E-10	8.30E-10	1.81E-10	4.93E-10	6.08E-09	2.92E-09
AG 111	5.0E-02	3.58E-11	1.09E-11	1.38E-11	8.84E-12	7.48E-12	9.67E-12	4.51E-09	1.37E-09

Table 7.21 (continued)

Nuclide	f_1	Gonads	Breast	R. Marrow	Lungs	Thyroid	Endosteal	Remainder	Effective
CD 113M	5.0E-02	3.44E-09	3.44E-09	3.44E-09	3.44E-09	3.44E-09	3.44E-09	1.37E-07	4.35E-08
CD 115M	5.0E-02	1.84E-10	1.56E-10	1.68E-10	1.64E-10	1.61E-10	1.54E-10	1.42E-08	4.37E-09
SN 123	2.0E-02	3.80E-11	3.22E-11	2.41E-10	3.15E-11	3.13E-11	6.52E-10	7.35E-09	2.27E-09
SN 125	2.0E-02	2.88E-10	4.41E-11	2.08E-10	1.60E-11	9.78E-12	2.38E-10	1.07E-08	3.33E-09
SN 126	2.0E-02	2.41E-09	7.96E-10	2.72E-09	5.99E-10	5.51E-10	5.05E-09	1.33E-08	5.27E-09
SB 124	1.0E-01	1.74E-09	3.21E-10	6.16E-10	1.65E-10	1.18E-10	7.99E-10	6.81E-09	2.55E-09
	1.0E-02	1.78E-09	2.30E-10	3.81E-10	5.40E-11	1.76E-11	1.89E-10	7.34E-09	2.74E-09
SB 125	1.0E-01	5.24E-10	1.00E-10	2.26E-10	6.03E-11	4.62E-11	5.96E-10	1.96E-09	7.59E-10
	1.0E-02	5.27E-10	6.22E-11	1.21E-10	1.36E-11	5.58E-12	9.05E-11	1.99E-09	7.57E-10
SB 126	1.0E-01	2.73E-09	4.17E-10	7.23E-10	1.66E-10	1.05E-10	5.17E-10	6.29E-09	2.76E-09
	1.0E-02	2.89E-09	3.53E-10	5.93E-10	6.85E-11	1.74E-11	2.27E-10	6.77E-09	2.89E-09
SB 127	1.0E-01	5.88E-10	9.76E-11	2.11E-10	4.33E-11	3.16E-11	1.50E-10	5.39E-09	1.81E-09
	1.0E-02	6.14E-10	7.60E-11	1.33E-10	1.57E-11	4.54E-12	5.24E-11	5.87E-09	1.95E-09
TE 125M	2.0E-01	1.27E-10	4.64E-11	1.21E-09	4.35E-11	3.93E-11	1.27E-08	1.40E-09	9.92E-10
TE 127	2.0E-01	4.02E-12	3.00E-12	6.57E-12	2.89E-12	2.86E-12	6.45E-12	6.13E-10	1.97E-10
TE 127M	2.0E-01	1.25E-10	9.74E-11	5.43E-09	9.62E-11	9.43E-11	2.37E-08	2.98E-09	2.23E-09
TE 129	2.0E-01	1.59E-12	6.05E-13	7.64E-13	4.91E-13	3.36E-13	5.40E-13	1.79E-10	5.45E-11
TE 129M	2.0E-01	2.41E-10	1.66E-10	3.50E-09	1.59E-10	1.57E-10	7.99E-09	7.08E-09	2.89E-09
TE 131	2.0E-01	1.57E-11	4.96E-12	6.60E-12	3.39E-12	4.21E-09	3.59E-12	3.73E-10	2.44E-10
TE 131M	2.0E-01	7.38E-10	1.35E-10	2.42E-10	6.26E-11	4.29E-08	3.24E-10	3.07E-09	2.46E-09
TE 132	2.0E-01	5.41E-10	3.50E-10	4.44E-10	3.30E-10	5.95E-08	8.30E-10	1.49E-09	2.54E-09
TE 133M	2.0E-01	3.68E-11	1.14E-11	1.31E-11	8.33E-12	4.17E-09	6.51E-12	2.89E-10	2.26E-10
TE 134	2.0E-01	2.03E-11	1.37E-11	1.49E-11	1.29E-11	8.82E-10	1.23E-11	9.65E-11	6.63E-11
I 129	1.0E 00	1.38E-10	3.31E-10	2.21E-10	1.55E-10	2.48E-06	2.17E-10	2.13E-10	7.46E-08
I 130	1.0E 00	5.52E-11	7.32E-11	6.74E-11	7.18E-11	3.94E-08	6.12E-11	1.97E-10	1.28E-09
I 131	1.0E 00	4.07E-11	1.21E-10	9.44E-11	1.02E-10	4.76E-07	8.72E-11	1.63E-10	1.44E-08
I 132	1.0E 00	2.33E-11	2.52E-11	2.46E-11	2.64E-11	3.87E-09	2.19E-11	1.65E-10	1.92E-10
I 133	1.0E 00	3.63E-11	4.68E-11	4.30E-11	4.53E-11	9.10E-08	4.07E-11	1.55E-10	2.80E-09
I 134	1.0E 00	1.10E-11	1.17E-11	1.09E-11	1.25E-11	6.21E-10	9.32E-12	1.34E-10	6.56E-11
I 135	1.0E 00	3.61E-11	3.85E-11	3.65E-11	3.75E-11	1.79E-08	3.36E-11	1.54E-10	6.08E-10
CS 134	1.0E 00	2.06E-08	1.72E-08	1.87E-08	1.76E-08	1.76E-08	1.74E-08	2.21E-08	1.98E-08
CS 134M	1.0E 00	6.72E-12	6.28E-12	6.91E-12	6.42E-12	6.22E-12	6.57E-12	2.89E-11	1.33E-11
CS 135	1.0E 00	1.91E-09	1.91E-09	1.91E-09	1.91E-09	1.91E-09	1.91E-09	1.93E-09	1.91E-09

Table 7.21 (continued)

Nuclide	f_1	Gonads	Breast	R. Marrow	Lungs	Thyroid	Endosteal	Remainder	Effective
CS 136	1.0E 00	3.04E-09	2.65E-09	2.95E-09	2.62E-09	2.74E-09	2.71E-09	3.52E-09	3.04E-09
CS 137	1.0E 00	1.39E-08	1.24E-08	1.32E-08	1.27E-08	1.26E-08	1.26E-08	1.45E-08	1.35E-08
CS 138	1.0E 00	8.00E-12	8.00E-12	7.37E-12	8.53E-12	5.73E-12	6.47E-12	1.57E-10	5.25E-11
BA 139	1.0E-01	1.56E-12	5.17E-13	8.59E-13	3.89E-13	2.66E-13	4.38E-13	3.57E-10	1.08E-10
BA 140	1.0E-01	9.96E-10	1.59E-10	4.39E-10	6.63E-11	5.25E-11	5.53E-10	7.37E-09	2.56E-09
BA 141	1.0E-01	2.86E-12	1.22E-12	1.47E-12	1.10E-12	2.25E-13	1.27E-12	1.84E-10	5.65E-11
BA 142	1.0E-01	9.88E-12	2.52E-12	3.00E-12	1.57E-12	2.71E-13	1.24E-12	8.89E-11	3.01E-11
LA 140	1.0E-03	1.34E-09	1.80E-10	2.81E-10	4.01E-11	6.40E-12	9.77E-11	6.26E-09	2.28E-09
LA 141	1.0E-03	3.77E-12	7.07E-13	1.07E-12	2.72E-13	5.29E-14	6.06E-13	1.24E-09	3.74E-10
LA 142	1.0E-03	6.99E-11	1.54E-11	1.93E-11	8.40E-12	1.16E-12	7.40E-12	5.20E-10	1.79E-10
CE 141	3.0E-04	1.08E-10	1.11E-11	3.39E-11	1.43E-12	1.80E-13	2.30E-11	2.50E-09	7.83E-10
CE 143	3.0E-04	2.12E-10	2.32E-11	5.07E-11	3.82E-12	4.35E-13	1.61E-11	3.89E-09	1.23E-09
CE 144	3.0E-04	6.98E-11	1.22E-11	8.92E-11	6.52E-12	5.15E-12	1.28E-10	1.88E-08	5.68E-09
PR 143	3.0E-04	8.99E-18	1.09E-18	1.03E-12	1.91E-19	2.66E-20	1.03E-12	4.22E-09	1.27E-09
ND 147	3.0E-04	1.79E-10	1.87E-11	5.05E-11	2.44E-12	2.54E-13	2.22E-11	3.76E-09	1.18E-09
PM 147	3.0E-04	6.86E-15	7.45E-16	2.09E-11	1.96E-16	3.12E-17	2.61E-10	9.08E-10	2.83E-10
PM 148	3.0E-04	4.72E-10	6.11E-11	9.85E-11	1.19E-11	1.85E-12	3.49E-11	9.32E-09	2.94E-09
PM 148M	3.0E-04	2.18E-09	2.59E-10	4.41E-10	4.44E-11	6.47E-12	1.74E-10	4.75E-09	2.07E-09
PM 149	3.0E-04	9.19E-12	1.02E-12	2.27E-12	1.62E-13	1.78E-14	9.59E-13	3.56E-09	1.07E-09
PM 151	3.0E-04	2.11E-10	2.42E-11	4.94E-11	4.23E-12	4.55E-13	1.62E-11	2.49E-09	8.09E-10
SM 151	3.0E-04	2.12E-14	1.03E-15	2.76E-11	6.52E-16	3.27E-17	3.45E-10	3.04E-10	1.05E-10
SM 153	3.0E-04	7.17E-11	6.91E-12	2.72E-11	7.13E-13	2.35E-14	8.39E-12	2.62E-09	8.07E-10
EU 152	1.0E-03	1.33E-09	2.85E-10	9.19E-10	2.40E-10	6.55E-11	2.09E-09	3.92E-09	1.75E-09
EU 154	1.0E-03	1.37E-09	2.79E-10	1.15E-09	2.16E-10	5.71E-11	4.46E-09	6.32E-09	2.58E-09
EU 155	1.0E-03	9.83E-11	1.44E-11	1.56E-10	9.64E-12	1.78E-12	1.29E-09	1.09E-09	4.13E-10
EU 156	1.0E-03	1.22E-09	1.52E-10	2.56E-10	3.24E-11	5.23E-12	1.15E-10	7.04E-09	2.48E-09
TB 160	3.0E-04	1.17E-09	1.43E-10	2.54E-10	2.72E-11	4.29E-12	1.57E-10	4.90E-09	1.92E-09
HO 166M	3.0E-04	2.05E-09	3.48E-10	8.12E-10	2.15E-10	5.53E-11	2.35E-09	4.74E-09	2.18E-09
W 181	1.0E-02	7.33E-11	7.01E-12	3.26E-11	6.23E-13	5.41E-14	1.03E-11	2.31E-10	9.31E-11
	3.0E-01	5.36E-11	7.46E-12	4.85E-11	3.52E-12	1.39E-12	4.58E-11	1.84E-10	7.74E-11
W 185	1.0E-02	8.74E-14	8.98E-15	1.64E-12	9.45E-16	7.64E-17	4.90E-12	1.79E-09	5.38E-10
	3.0E-01	6.35E-14	8.78E-15	4.83E-11	3.54E-15	1.36E-15	1.47E-10	1.39E-09	4.28E-10
W 187	1.0E-02	2.59E-10	3.22E-11	5.89E-11	6.39E-12	7.70E-13	2.12E-11	2.22E-09	7.46E-10

Table 7.21 (continued)

Nuclide	f_1	Gonads	Breast	R. Marrow	Lungs	Thyroid	Endosteal	Remainder	Effective
	3.0E-01	1.90E-10	2.44E-11	5.09E-11	5.80E-12	9.00E-13	7.38E-11	1.64E-09	5.53E-10
PB 210	2.0E-01	1.25E-07	1.25E-07	1.48E-06	1.25E-07	1.25E-07	2.16E-05	1.85E-06	1.45E-06
BI 210	5.0E-02	1.97E-11	1.97E-11	1.97E-11	1.97E-11	1.97E-11	1.97E-11	5.71E-09	1.73E-09
PO 210	1.0E-01	8.23E-08	8.23E-08	8.23E-08	8.23E-08	8.23E-08	8.23E-08	1.52E-06	5.14E-07
RA 223	2.0E-01	4.26E-08	4.23E-08	2.80E-07	4.23E-08	4.23E-08	2.93E-06	1.10E-07	1.78E-07
RA 224	2.0E-01	2.12E-08	2.06E-08	1.52E-07	2.05E-08	2.05E-08	1.59E-06	7.15E-08	9.89E-08
RA 225	2.0E-01	3.37E-08	3.37E-08	1.68E-07	3.37E-08	3.37E-08	1.78E-06	4.09E-08	1.04E-07
RA 226	2.0E-01	9.16E-08	9.17E-08	5.98E-07	9.15E-08	9.15E-08	6.83E-06	1.03E-07	3.58E-07
RA 228	2.0E-01	1.58E-07	1.57E-07	6.53E-07	1.57E-07	1.57E-07	5.82E-06	1.63E-07	3.88E-07
AC 225	1.0E-03	1.36E-09	2.73E-11	7.99E-09	3.98E-12	5.49E-13	9.94E-08	8.57E-08	3.00E-08
AC 227	1.0E-03	8.31E-07	1.41E-10	5.40E-06	2.20E-10	7.55E-11	6.73E-05	3.08E-06	3.80E-06
TH 227	2.0E-04	2.95E-10	1.40E-10	5.69E-09	1.25E-10	1.23E-10	6.84E-08	2.47E-08	1.03E-08
TH 228	2.0E-04	2.53E-09	2.33E-09	1.93E-07	2.31E-09	2.30E-09	2.37E-06	3.86E-08	1.07E-07
TH 229	2.0E-04	4.69E-09	4.57E-09	1.91E-06	4.56E-09	4.55E-09	2.38E-05	2.80E-08	9.54E-07
TH 230	2.0E-04	6.82E-10	6.80E-10	2.89E-07	6.80E-10	6.80E-10	3.50E-06	1.54E-08	1.48E-07
TH 232	2.0E-04	1.25E-09	1.26E-09	1.48E-05	1.25E-09	1.21E-09	1.85E-05	1.47E-08	7.38E-07
TH 234	2.0E-04	3.12E-11	3.57E-12	1.84E-11	7.05E-13	2.88E-13	2.08E-11	1.23E-08	3.59E-09
PA 231	1.0E-03	1.21E-10	7.81E-11	5.78E-06	6.80E-11	6.33E-11	7.22E-05	1.71E-08	2.86E-06
PA 233	1.0E-03	2.58E-10	2.71E-11	6.89E-11	3.70E-12	4.81E-13	1.02E-10	3.00E-09	9.81E-10
U 232	5.0E-02	8.27E-09	8.33E-09	4.19E-07	8.29E-09	8.11E-09	6.53E-06	3.35E-07	3.54E-07
	2.0E-03	3.34E-10	3.33E-10	1.68E-08	3.32E-10	3.25E-10	2.65E-07	2.83E-08	1.87E-08
U 233	5.0E-02	2.62E-09	2.62E-09	7.36E-08	2.62E-09	2.62E-09	1.16E-06	1.10E-07	7.81E-08
	2.0E-03	1.07E-10	1.05E-10	2.95E-09	1.05E-10	1.05E-10	4.62E-08	1.78E-08	7.15E-09
U 234	5.0E-02	2.59E-09	2.58E-09	7.21E-08	2.58E-09	2.58E-09	1.13E-06	1.09E-07	7.66E-08
	2.0E-03	1.06E-10	1.03E-10	2.88E-09	1.03E-10	1.03E-10	4.52E-08	1.77E-08	7.06E-09
U 235	5.0E-02	2.67E-09	2.49E-09	6.81E-08	2.46E-09	2.45E-09	1.05E-06	1.03E-07	7.19E-08
	2.0E-03	3.34E-10	1.21E-10	2.78E-09	1.01E-10	9.82E-11	4.20E-08	1.84E-08	7.22E-09
U 236	5.0E-02	2.45E-09	2.45E-09	6.83E-08	2.45E-09	2.45E-09	1.07E-06	1.03E-07	7.26E-08
	2.0E-03	1.00E-10	9.79E-11	2.73E-09	9.79E-11	9.79E-11	4.28E-08	1.67E-08	6.68E-09
U 237	5.0E-02	1.75E-10	2.02E-11	9.50E-11	4.98E-12	2.77E-12	4.41E-10	2.59E-09	8.48E-10
	2.0E-03	1.81E-10	1.81E-11	5.69E-11	2.17E-12	2.31E-13	3.39E-11	2.67E-09	8.57E-10
U 238	5.0E-02	2.31E-09	2.31E-09	6.80E-08	2.30E-09	2.30E-09	1.01E-06	9.69E-08	6.88E-08
	2.0E-03	1.02E-10	9.33E-11	2.72E-09	9.22E-11	9.20E-11	4.04E-08	1.61E-08	6.42E-09

Table 7.21 (continued)

Nuclide	f_1	Gonads	Breast	R. Marrow	Lungs	Thyroid	Endosteal	Remainder	Effective
NP 237	1.0E-02	2.46E-06	1.52E-09	1.53E-05	2.37E-09	8.16E-10	1.91E-04	8.24E-06	1.07E-05
NP 238	1.0E-02	5.25E-10	4.83E-11	1.05E-09	1.10E-11	1.65E-12	1.22E-08	3.46E-09	1.67E-09
NP 239	1.0E-02	1.62E-10	1.72E-11	5.72E-11	2.73E-12	2.83E-13	1.55E-10	2.75E-09	8.80E-10
PU 238	1.0E-04	2.33E-08	1.43E-13	1.47E-07	7.31E-14	3.84E-15	1.93E-06	9.60E-08	1.07E-07
	1.0E-05	2.33E-09	1.02E-13	1.47E-08	9.69E-15	3.93E-16	1.83E-07	2.40E-08	1.50E-08
PU 239	1.0E-04	2.64E-08	6.85E-14	1.65E-07	3.90E-14	3.68E-15	2.06E-06	1.03E-07	1.19E-07
	1.0E-05	2.64E-09	4.68E-14	1.65E-08	5.25E-15	4.40E-16	2.06E-07	2.38E-08	1.59E-08
PU 240	1.0E-04	2.64E-08	1.47E-13	1.65E-07	8.29E-14	4.64E-15	2.06E-06	1.03E-07	1.19E-07
	1.0E-05	2.64E-09	9.95E-14	1.65E-08	9.72E-15	4.79E-16	2.06E-07	2.38E-08	1.60E-08
PU 241	1.0E-04	5.66E-10	3.49E-14	3.40E-09	6.48E-14	1.24E-14	4.24E-08	1.79E-09	2.36E-09
	1.0E-05	5.66E-11	3.73E-15	3.40E-10	6.50E-15	1.24E-15	4.24E-09	2.47E-10	2.56E-10
PU 242	1.0E-04	2.51E-08	2.69E-13	1.57E-07	1.17E-13	2.53E-14	1.96E-06	9.82E-08	1.13E-07
	1.0E-05	2.51E-09	1.85E-13	1.57E-08	2.36E-14	3.35E-15	1.96E-07	2.26E-08	1.52E-08
PU 244	1.0E-04	2.53E-08	8.42E-11	1.55E-07	4.64E-11	1.77E-11	1.93E-06	1.06E-07	1.15E-07
	1.0E-05	2.94E-09	5.41E-11	1.55E-08	1.01E-11	2.42E-12	1.93E-07	3.07E-08	1.76E-08
AM 241	5.0E-04	1.35E-07	1.33E-11	8.44E-07	1.72E-11	3.09E-12	1.06E-05	4.70E-07	5.94E-07
AM 242	5.0E-04	1.86E-11	9.18E-13	6.54E-11	1.38E-13	5.96E-15	7.84E-10	1.01E-09	3.40E-10
AM 242M	5.0E-04	1.33E-07	8.38E-12	8.26E-07	1.09E-11	2.20E-12	1.03E-05	4.42E-07	5.74E-07
AM 243	5.0E-04	1.35E-07	9.03E-11	8.44E-07	1.24E-10	3.60E-11	1.05E-05	4.69E-07	5.91E-07
CM 242	5.0E-04	2.60E-09	1.20E-13	1.84E-08	1.29E-14	5.33E-16	2.30E-07	2.95E-08	1.85E-08
CM 243	5.0E-04	8.64E-08	4.42E-11	5.56E-07	4.38E-11	1.34E-11	6.94E-06	3.31E-07	3.96E-07
CM 244	5.0E-04	6.64E-09	3.07E-13	4.36E-07	2.58E-13	2.58E-14	5.45E-06	2.69E-07	3.13E-07
CM 245	5.0E-04	1.40E-07	4.31E-11	8.72E-07	5.06E-11	1.34E-11	1.09E-05	4.83E-07	6.11E-07
CM 246	5.0E-04	1.39E-07	2.19E-11	8.65E-07	1.22E-11	6.45E-12	1.08E-05	4.80E-07	6.06E-07
CM 247	5.0E-04	1.28E-07	1.57E-10	7.95E-07	1.73E-10	6.75E-11	9.93E-06	4.43E-07	5.59E-07
CM 248	5.0E-04	5.21E-07	7.66E-09	3.17E-06	4.19E-09	2.29E-09	3.95E-05	1.78E-06	2.23E-06
CF 252	5.0E-04	3.09E-08	1.22E-09	1.68E-07	2.84E-10	1.00E-10	2.07E-06	1.53E-07	1.36E-07

Table 7.22. Assignment of f_1 values for ingested compounds

Element	f_1	Chemical compounds
Cr	0.1	Hexavalent compounds
	1×10^{-2}	Trivalent compounds
Co	5×10^{-2}	Oxides, hydroxides, and all other inorganic compounds
	0.3	All other inorganic and organic compounds
Se	5×10^{-2}	Elemental selenium and selenides
	0.8	All other compounds
Sr	0.3	Soluble compounds
	1×10^{-2}	Titanates
Mo	5×10^{-2}	Disulfides
	0.8	All other compounds
Sb	0.1	Tartar emetic
	1×10^{-2}	All other compounds
W	1×10^{-2}	Tungstic acid
	0.3	All other compounds
U	5×10^{-2}	Water soluble inorganic compounds
	2×10^{-3}	Insoluble compounds
Pu	1×10^{-5}	Oxides and hydroxides
	1×10^{-4}	All other compounds

REFERENCES

Beddoe, A.H., Darley, P.J., and Spiers, F.W. 1976. "Measurements of Trabecular Bone Structure in Man," *Phys. Med. Biol.* **21**, 589.

Berger, M.J. 1968. "Energy Deposition in Water by Photons from Point Isotropic Sources," *J. Nucl. Med.* Suppl. 1, 15.

Berger, M.J. 1971. "Distribution of Absorbed Dose around Point Sources of Electrons and Beta Particles in Water and Other Media," Pamphlet 7 of the Medical Internal Radiation Dose Committee, Society of Nuclear Medicine.

Berger, M.J. 1973. *Improved Point Kernels for Electron and Beta-Ray Dosimetry,* NBSIR 73-107, National Bureau of Standards.

Bethe, H.A. 1932. "Bremsformel für Elektronen relativistischer Geschwindigkeit," *Z. Physik* **76**, 293.

Bloch, F. 1933. "Bremsvermögen von Atomen mit mehreren Elektronen," *Z. Physik* **81**, 363.

Carter, L.L., and Cashwell, E.D. 1975. *Particle-Transport Simulation with the Monte Carlo Method,* ERDA Critical Review Series, TID-26607.

Cashwell, E.D., and Everett, C.J. 1959. *A Practical Manual on the Monte Carlo Method for Random Walk Problems,* Pergamon, Oxford.

Dillman, L.T. 1969. "Radionuclide Decay Schemes and Nuclear Parameters for Use in Radiation-Dose Estimation," Pamphlet 4 of the Medical Internal Radiation Dose Committee, Society of Nuclear Medicine.

Evans, R.D. 1968. "X-Ray and Gamma-Ray Interactions," pp. 93–155 in *Radiation Dosimetry* (F.H. Attix, W.C. Roesch, and E. Tochlin, eds.), Vol. 1, Academic Press, New York.

Hubbell, J.H. 1969. *Photon Cross Sections, Attenuation Coefficients, and Energy Absorption Coefficients from 10 keV to 100 GeV,* NSRDS-NBS 29, National Bureau of Standards.

International Commission on Radiological Protection (ICRP) 1959. ICRP Publication 2, Pergamon, Oxford.

International Commission on Radiological Protection (ICRP) 1968. *A Review of the Radiosensitivity of the Tissues in Bone,* ICRP Publication 11, Pergamon, Oxford.

International Commission on Radiological Protection (ICRP) 1972. *Alkaline Earth Metabolism in Adult Man,* ICRP Publication 20, Pergamon, Oxford.

International Commission on Radiological Protection (ICRP) 1975. *Report of the Task Group on Reference Man,* ICRP Publication 23, Pergamon, Oxford.

International Commission on Radiological Protection (ICRP) 1977. ICRP Publication 26, Pergamon, Oxford.

International Commission on Radiological Protection (ICRP) 1979. ICRP Publication 30, Supplement to Part 1, *Annals of the ICRP* **3**(1–4), Pergamon, Oxford.

Kocher, D.C. 1981. *Radioactive Decay Data Tables,* DOE/TIC-11026, U.S. Department of Energy.

Loevinger, R., and Berman, M. 1976. *A Revised Schema for Calculating the Absorbed Dose from Biologically Distributed Radionuclides,* Pamphlet 7 (revised) of the Medical Internal Radiation Dose Committee, Society of Nuclear Medicine.

Riggs, D.S. 1952. "Quantitative Aspects of Iodine Metabolism in Man," *Pharmacol. Rev.* **4**, 284–370.

Shreider, Y.A. ed. 1966. *The Monte Carlo Method,* Pergamon, Oxford.

Snyder, W.S., Ford, M.R., and Warner, G.G. 1978. *Estimates of Absorbed Fractions for Photon Sources Uniformly Distributed in Various Organs of a Heterogeneous Phantom,* Pamphlet 5 (revised) of the Medical Internal Radiation Dose Committee, Society of Nuclear Medicine.

Spencer, L.U., and Simmons, G.L. 1973. "Improved Moment Method Calculations of Gamma Ray Transport: Application to Point Isotropic Sources in Water," *Nucl. Sci. and Eng.* **50**, 20–31.

Storm, E., and Israel, H.I. 1970. "Photon Cross Sections from 1 keV to 100 MeV for Elements $Z = 1$ to $Z = 100$," *Nuclear Data Tables* **A7**, 565.

U.S. Nuclear Regulatory Commission, 1975. *Reactor Safety Study: An Assessment of Accident Risks in U.S. Commercial Nuclear Power Plants.* Appendix VI, *Calculation of Reactor Accident Consequences,* WASH-1400.

Walsh, P.J. 1970. "Stopping Power and Range of Alpha Particles," *Health Phys.* **19**, 312–316.

Whaling, W. 1958. "The Energy Loss of Charged Particles in Matter," pp. 193–217 in *Handbuch der Physik* (S. Flügge, ed.), Vol. 34, Springer, Berlin.

8 External Dosimetry

By D. C. KOCHER*

8.1 INTRODUCTION

From the point of view of environmental radiological assessments, the central problem in external dosimetry is to determine the dose to an individual or population due to the radiations emitted by radionuclides dispersed in the environment. The radiation dose from external exposure depends, in general, on the following:

1. the concentrations of the radionuclides in the environment as a function of time and distance from the location of the exposed individual or population;
2. the energies and intensities of the radiations of interest emitted by each radionuclide;
3. transmission of the emitted radiations through the different media between the source and receptor positions; and
4. transmission through body tissues of the radiations incident upon the exposed individuals, resulting in doses to particular body organs.

Calculation of the transmission of radiations through body tissues to obtain the dose to body organs is a complex problem that is beyond the scope of this chapter. Such calculations are usually based on Monte Carlo simulations of the scattering and absorption of the radiations in a mathematical phantom describing the so-called Reference Man, with the assumption that the phantom is irradiated isotropically (Berger 1974; Poston and Snyder 1974; O'Brien and Sanna 1976; O'Brien 1980). A primary concern of this chapter is the interpretation and implementation of the available Monte Carlo calculations of organ doses for radiological assessment purposes.

*Health and Safety Research Division, Oak Ridge National Laboratory.

In any calculation of external dose, the determination of the radionuclide concentrations in the environment is separate from all other factors involved because the dose rate at any time from a particular radionuclide is always proportional to the concentration at that time. In this chapter, therefore, we regard the concentrations as known quantities determined by either direct measurement or theories of environmental transport (e.g., see Chapters 2, 3, and 14). In general, the determination of the concentrations requires detailed consideration of both the rate and manner of radionuclide release, their movement in the environment, and radioactive decay, including production and decay of any radioactive daughter products.

Given the radionuclide concentrations in the environment as a function of time and location, the estimation of external dose may, but not necessarily, proceed according to the following logic:

1. specification of the particular mode of exposure (e.g., immersion in a radioactive cloud or irradiation from a contaminated ground surface);
2. specification of the particular radiation type (i.e., photons or electrons);
3. calculation of the absorbed dose in the medium (i.e., air or water) surrounding the exposed individual at the specified location;
4. modification of the absorbed dose in the medium to calculate the dose in a small piece of tissue at the same location;
5. modification of the dose in tissue to obtain the dose at the body surface by accounting for the perturbation of the radiation field due to the presence of the exposed individual; and
6. modification of the dose at the body surface to determine the dose to the body organs of interest.

The desired end result of any procedure, such as the one outlined above, is the estimation of dose to body organs for the particular mode of exposure and radiation type. As mentioned above, calculations of organ dose obtained using Monte Carlo techniques are available in the literature. Therefore, it might seem unnecessary to use the intermediate steps 3 through 6 above when the desired results appear to be already in hand. We emphasize, however, that the available organ dose calculations apply only to the special case of exposure via immersion in an infinite and uniformly contaminated source medium. Therefore, these results are not directly applicable to any other exposure conditions, such as irradiation from an infinite, uniformly contaminated ground surface or exposure to finite or nonuniformly contaminated source regions. For external exposure to photons, for example, most of the methods in current use for estimating organ doses for exposure conditions other than immersion in an infinite, uniformly contaminated medium are based on the assumption that the ratio of organ dose to the dose at the body surface (or, alternatively, organ dose to dose in the surrounding medium) for a given emitted energy is independent of the conditions of the exposure. This assumption allows a calculation of organ doses for photons

for arbitrary modes of exposure, provided the dose at the body surface (or dose in the surrounding medium) is calculated for the exposure mode of interest and the exposure mode for which organ doses are already available in the literature. An important purpose of this chapter is to show how steps 3 through 6 are carried out for any mode of exposure for the different radiations of importance in external dosimetry.

In this chapter, we restrict our attention to the two exposure modes that are usually the most important in environmental dose assessments—namely, exposure to a radioactive cloud in the atmosphere and exposure to a contaminated ground surface (e.g., from fallout). Other potentially important modes of exposure, such as immersion in contaminated water, can be treated in essentially the same manner as the cases studied here (Berger 1974; Kocher 1979; Kocher 1980a; Kocher 1981b).

In general, the only radiations emitted in significant quantities by radionuclides dispersed in the environment that can penetrate the body surface and give a dose to radiosensitive tissues are photons and electrons. Neutrons can be an important radiation for external dose in special cases, such as direct exposure in the proximity of a nuclear weapon detonation. However, neutrons emitted by radionuclides that decay via delayed neutron emission or spontaneous fission are relatively unimportant for routine or accidental releases from nuclear fuel cycle facilities and are not considered in this chapter. We are not concerned in external dosimetry with nonpenetrating radiations such as alpha particles and spontaneous fission fragments. (These radiations, of course, are very important in internal dosimetry.) The photon radiations of interest in radioactive decay include gamma rays from nuclear deexcitation, 511-keV annihilation gamma rays following positron emission, and X rays from atomic deexcitation. The electron radiations include continuous negative electrons and positrons from beta decay and discrete Auger and internal conversion electrons from atomic deexcitation. Concise reviews of these radiation processes are available in the literature (National Council on Radiation Protection and Measurements 1978; Dillman 1980; Kocher 1981a). Several compilations are available which give the energies and intensities for the photons and electrons emitted by a large number of radionuclides which might be encountered in radiological assessments (Dillman and Von der Lage 1975; Martin 1976; Kocher 1977; National Council on Radiation Protection and Measurements 1978; Kocher 1981a). Contributions to the photon spectrum from bremsstrahlung produced by scattering of emitted electrons are usually not considered in external dosimetry. In some cases, however, bremsstrahlung can be important, particularly for radionuclides that are pure beta emitters. Methods for calculating the photon spectrum from bremsstrahlung in a variety of scattering media are described by Dillman (1980).

Section 8.2 includes a general formula for the calculation of external dose based on the concept of the point-isotropic specific absorbed fraction. In Sect.

8.3, we apply the general formulation to simplified and idealized situations often assumed in environmental radiological assessments; namely, the assumptions that the distribution of sources is effectively infinite in extent and the radionuclide concentration is uniform throughout the source region. For these idealized situations, we develop the concept of the external dose-rate conversion factor and show how it is calculated for the two important cases of immersion in a semi-infinite, uniformly contaminated atmospheric cloud and exposure to an infinite, uniformly contaminated ground surface. In Sect. 8.4, we briefly discuss estimation of external dose for more realistic exposure situations involving finite sources with nonuniform radionuclide concentrations, and we consider corrections to calculated external doses to account for effects such as building shielding during indoor residence, terrain roughness, and penetration of radionuclides into the ground.

8.2 FUNDAMENTAL EQUATIONS OF EXTERNAL DOSIMETRY

In this section, we consider a general formulation for the calculation of external dose rates and dose for irradiation by photons and electrons emitted by arbitrary distributions of radionuclides in the environment.

The formulation is based on the concept of the point-isotropic specific absorbed fraction (Loevinger and Berman 1968; Berger 1968), which was originally introduced to calculate dose from internally deposited radionuclides. The specific absorbed fraction, which we denote by Φ, depends on the radiation type and the medium in which the emitted energy is being absorbed and is defined as follows:

$\Phi(r,E)$ = fraction of the emitted energy E absorbed per gram of material at a distance r from an isotropic point source. (8.1)

The utility of the specific absorbed fraction is illustrated by writing the equation for the absorbed dose rate from a monoenergetic point source of energy E. At a distance r from such a source having activity A at time t, the absorbed dose rate $\dot{D}$ is simply (Berger 1968)

$$\dot{D}(r,E,t) = k \times A(t) \times E \times \Phi(r,E) , \tag{8.2}$$

where

$\dot{D}$ = absorbed dose rate in Gy/s,

k = 1.6×10^{-10} g-Gy/MeV,

A = source activity in Bq,

E = energy of emitted radiation in MeV,

Φ = specific absorbed fraction in g^{-1}.

The value of the constant k is determined by the definition of the gray as one joule of absorbed energy per kilogram of material and the conversion factor from MeV to joules. The product of the factors k, A, and E gives the total energy emitted per unit time in g-Gy/s; and multiplication by the specific absorbed fraction Φ gives the amount of the total emitted energy that is absorbed per unit mass at the distance r.

For a point source embedded in an infinite absorbing medium, all of the emitted energy must be absorbed somewhere within the medium. Therefore, the specific absorbed fraction obeys the important normalization condition

$$4\pi \int_0^\infty \Phi(r,E) r^2 dr = 1/\rho , \tag{8.3}$$

where ρ is the density of the absorbing medium. This equation holds for any energy E and any functional form for the specific absorbed fraction and is strictly a consequence of conservation of energy.

The general equations for the absorbed dose rates from arbitrary distributions of radionuclides emitting photons and electrons of arbitrary energies follows from the dose rate for a point source in Eq. 8.2. As shown in Fig. 8.1, we let σ denote the volume or surface over which the radionuclides are distributed. For simplicity, we let the point P at which the absorbed dose rate is to be

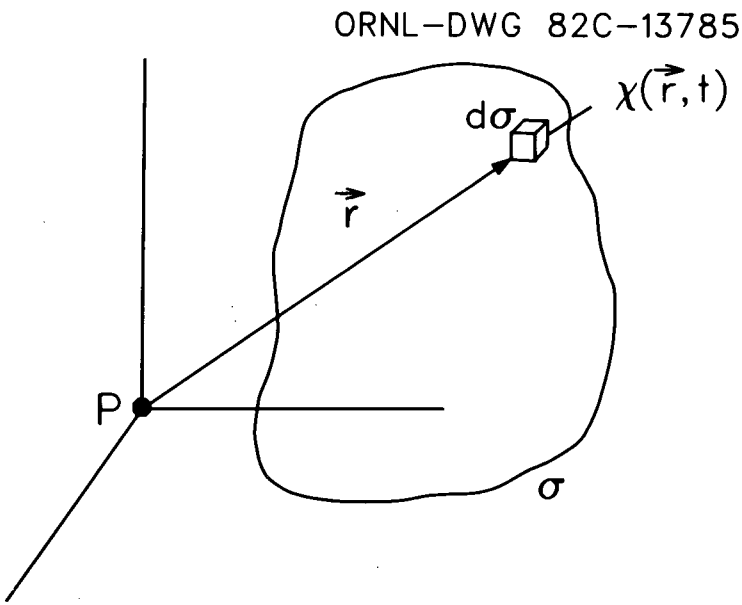

Figure 8.1. Coordinate system for calculation of external dose rate from arbitrary distribution of radioactive sources.

determined be located at the origin of the coordinate system. Then $\vec{r}$ denotes the vector distance from the point P to the volume or surface element $d\sigma$ in the source distribution. The quantity $\chi(\vec{r},t)$ denotes the radionuclide concentration at location $\vec{r}$ and time t in Bq per unit volume or area.

We consider first the absorbed dose rate at the point P for photons. We assume that the photon spectrum from radioactive decay consists of one or more discrete (i.e., monoenergetic) radiations, and we define

$f_{i\gamma}$ = intensity of ith photon γ in number per decay, and

$E_{i\gamma}$ = energy of ith photon in MeV.

From Eq. 8.2, the photon dose rate at point P and time t can then be written as

$$\dot{D}_\gamma(t) = k\sum_i f_{i\gamma}E_{i\gamma}\int_\sigma \chi(\vec{r},t)\Phi_\gamma(r,E_{i\gamma})d\sigma\,. \tag{8.4}$$

For electrons, the spectrum from radioactive decay may consist of discrete Auger and internal conversion electrons and continuous electrons from beta decay. The energy distribution of electrons from a given beta transition ranges from zero energy to a maximum value called the endpoint energy. Thus, we define

f_{ie} = intensity of ith discrete electron e in number per decay,

E_{ie} = energy of ith discrete electron in MeV,

$f_{j\beta}$ = intensity of electrons from jth continuous beta transition β in number per decay,

$E_{j\beta}^{\max}$ = endpoint energy in MeV for electrons from jth continuous beta transition, and

$N_{j\beta}(E)$ = probability density function for electrons from jth continuous beta transition.

The probability density function (i.e., the energy spectrum) $N_{j\beta}(E)$ for electrons emitted in beta decay gives the probability that a β^- or β^+ particle has energy between E and $E + dE$. This function is assumed to be properly normalized so that

$$\int_0^{E_{j\beta}^{\max}} N_{j\beta}(E)dE = 1\,. \tag{8.5}$$

This equation expresses the requirement that the emitted electron energy for each beta transition lie between zero energy and the endpoint energy. With the definitions given above, the electron ϵ* dose rate at point P can be written in

*In this chapter, we use ϵ to denote electrons in general and e to denote discrete electrons in particular. The symbol β is reserved for continuous electrons from beta decay.

terms of the separate contributions from the discrete and continuous radiations as

$$\dot{D}_\epsilon(t) = k\left[\sum_i f_{ie}E_{ie}\int_\sigma \chi(\vec{r},t)\Phi_\epsilon(r,E_{ie})\,d\sigma + \sum_j f_{j\beta}\int_0^{E_{j\beta}^{\max}} N_{j\beta}(E)E\int_\sigma \chi(\vec{r},t)\Phi_\epsilon(r,E)\,dE\,d\sigma\right]. \tag{8.6}$$

Equations 8.4 and 8.6 are the fundamental equations of external dosimetry and are obtained by integrating the point-source absorbed dose rate in Eq. 8.2 over the source distribution for each emitted energy and summing over all discrete or continuous radiations in the spectrum. The concentration χ depends in general on the vector $\vec{r}$, while the specific absorbed fraction Φ depends only on the scalar distance r.

From the dose rate $\dot{D}$ as a function of time, the dose for any time t of exposure is given by

$$D(t) = \int_0^t \dot{D}(\tau)\,d\tau\,. \tag{8.7}$$

8.3 IDEALISTIC (EASY) CALCULATIONS

In many environmental radiological assessments, the simplifying assumption is made that the distribution of sources at any location is effectively infinite or semi-infinite in extent and that the radionuclide concentration χ can be represented as uniform throughout the source region. With these assumptions, we are led to the concept of a dose-rate conversion factor, which we will usually call the dose-rate factor. For infinite or semi-infinite source regions with uniform radionuclide concentrations, Eqs. 8.4 and 8.6 can be expressed in the general form (Kocher 1979; Kocher 1980a; Kocher 1981b)

$$\dot{D}(t) = \chi(t)\times \mathrm{DRF}\,, \tag{8.8}$$

where *DRF* denotes the dose-rate factor defined by this equation as the dose rate per unit radionuclide concentration. The dose-rate factor thus embodies all aspects of the calculation except for the radionuclide concentration, which is assumed to be known.

In this section, we develop the equations for calculating the dose-rate factors for photons and electrons for immersion in a semi-infinite, uniformly contaminated atmospheric cloud and for exposure to an infinite, uniformly contaminated ground surface. As outlined in Sect. 8.1, we first calculate the absorbed dose rate in air at the specified location, then the absorbed dose rate in tissue, the dose rate at the body surface of an exposed individual, and finally the dose rate for the body organs of interest. These steps are not necessary for

the case of exposure via immersion in contaminated air because organ dose-rate factors are already available in the literature (see Sect. 8.3.1.4). It is also the case that calculation of the dose rate in tissue and dose rate at the body surface as intermediate steps is not necessary for any exposure mode involving air as the medium surrounding the exposed individual, which is the case for air immersion and ground-surface exposure considered here. However, these steps in the calculation are needed, for example, if submersion in contaminated water is an exposure mode of interest (Berger 1974; Kocher 1979; Kocher 1980a; Kocher 1981b). For the purpose of this presentation, performing a calculation through all possible intermediate steps illustrates some important concepts involved in estimating external dose for arbitrary exposure modes.

The equations for the dose-rate factors for immersion in contaminated air and exposure to a contaminated ground surface are derived in Sects. 8.3.1 and 8.3.2 respectively. Compilations of external dose-rate factors available in the literature are discussed in Sect. 8.3.3. In Sect. 8.3.4, we discuss the adequacy of the approximations inherent in the dose-rate factors—namely, that the contaminated atmospheric cloud or ground surface is effectively semi-infinite or infinite in extent with a uniform radionuclide concentration throughout the source region.

8.3.1 Immersion in Contaminated Air

The determination of dose-rate factors for immersion in a contaminated atmospheric cloud that is assumed to be infinite in extent with uniform radionuclide concentration is particularly simple because of the normalization condition for the specific absorbed fraction given in Eq. 8.3.

8.3.1.1 Dose-Rate Factors in Air

We begin by integrating Eqs. 8.4 and 8.6 over a source region that is assumed to be an infinite sphere with uniform radionuclide concentration. We use Eqs. 8.3 and 8.8 to give the dose-rate factors in air a for photons γ and electrons ϵ as

$$\mathrm{DRF}_{\gamma}^{a} = k\frac{1}{\rho_a}\sum_i f_{i\gamma}E_{i\gamma}, \tag{8.9}$$

$$\mathrm{DRF}_{\epsilon}^{a} = k\frac{1}{\rho_a}\left[\sum_i f_{ie}E_{ie} + \sum_j f_{j\beta}\int_0^{E_{j\beta}^{\max}} N_{j\beta}(E)E\,dE\right], \tag{8.10}$$

where

DRF = dose-rate factor in Gy/s per Bq per unit volume,

ρ_a = density of air in g per unit volume,

and the other quantities were defined in Sect. 8.2. If the unit of length is cm, the dose-rate factor is then given in units of Gy/s per Bq/cm^3, and the density of air is in units of g/cm^3. These equations give the so-called air kerma in air for photons and electrons.

We note that the dose-rate factors in air for this exposure mode have been determined without explicit knowledge of the specific absorbed fractions for photons or electrons. Rather, the equations follow directly from conservation of energy; that is, for an infinite medium with uniform radionuclide concentration, the energy absorbed per unit volume must be equal to the energy emitted per unit volume. We also note that the summation over the energies and intensities of the radiations in the photon and electron spectra is equal to the average energy per decay for each radiation type. Thus, if $\bar{E}$ denotes the average energy in MeV per decay, we may write

$$\mathrm{DRF}_\gamma^a = k\frac{1}{\rho_a}\bar{E}_\gamma, \tag{8.11}$$

$$\mathrm{DRF}_\epsilon^a = k\frac{1}{\rho_a}\bar{E}_\epsilon. \tag{8.12}$$

In practice, however, this is not a particularly useful result for external dosimetry because the desired organ dose-rate factors depend on the energy spectrum, not the average energy. But the equations nonetheless display the simple principle involved in determining the dose-rate factor in air.

Example 8.1. Krypton-85 emits a single photon of energy 514 keV with intensity 0.434% (Kocher 1981a). If we assume a density for air of 0.0012 g/cm^3 appropriate for dry air at 20°C and 750 mm pressure, the dose-rate factor in air for a unit source concentration of 1 Bq/cm^3 is

$$\begin{aligned}\mathrm{DRF}_\gamma^a &= (1.6\times10^{-10}\,\text{g-Gy/MeV})(3.15\times10^7\,\text{s/y}) \\ &\quad\times(0.00434)(0.514\ \text{MeV})/(0.0012\ \text{g/cm}^3) \\ &= 0.0094\ \text{Gy/y per Bq/cm}^3.\end{aligned}$$

[End of example]

8.3.1.2 Dose-Rate Factors for Tissue Embedded in Air

Given the dose-rate factors in air in Eqs. 8.9 and 8.10, we then imagine that a small piece of tissue is placed in the medium so that the radiation field is not perturbed by the presence of the tissue. The dose-rate factors in tissue are obtained from those in air by accounting for energy absorption in tissue relative to energy absorption in air.

For photons, the relative energy absorption in the two media is determined by the ratio of the mass energy-absorption coefficients in tissue and air. For electrons, the relative energy absorption is determined by the ratio of the mass stopping powers. The proper determination of these ratios for use with Eqs. 8.9

and 8.10, however, is not a trivial matter. The energies given in Eqs. 8.9 and 8.10 are the emitted energies, not the resulting energies incident upon the tissue. The emission of monoenergetic photons or electrons in an infinite, uniformly contaminated medium results in a continuous energy distribution at any point in the medium between zero energy and the emitted energy, due to the scattering and absorption of the emitted radiations. Therefore, in a proper calculation, one must perform a weighted average of the ratio of mass energy-absorption coefficients or mass stopping powers in tissue and air for each emitted energy over the energy distribution incident upon the tissue.

Dillman (1974) has calculated the energy spectra of scattered photons for monoenergetic photons between 10 keV and 10 MeV emitted in an infinite, uniformly contaminated atmospheric cloud. For example, the spectrum of scattered photons for 0.5-MeV emitted photons and 1 μCi/g source strength is shown in Fig. 8.2. If we define the ratio of energy absorption in tissue t to that in air a for the ith emitted photon as

$$R_{i\gamma} = \left[\frac{(\mu_{en}/\rho)_t}{(\mu_{en}/\rho)_a}\right]_i, \tag{8.13}$$

where

μ_{en}/ρ = photon mass energy-absorption coefficient in cm^2/g,

then Dillman has shown that this ratio, when properly averaged over the energy distribution of scattered photons, increases from a value of 0.95 at 10 keV emitted energy to a value of about 1.10 for emitted energies above 1 MeV. These results are given by the solid symbols in Fig. 8.3. Thus, the correction factor for energy absorption in tissue relative to that in air is 10% or less for all emitted photon energies. As an alternative to the correct calculations of Dillman, the ratio $R_{i\gamma}$ can be approximated by the ratio of the mass energy-absorption coefficients in tissue and air evaluated at the ith emitted photon energy (Kocher 1979; Kocher 1980a). These ratios are given by the open symbols in Fig. 8.3. This approximation, which does not account for scattering and absorption of the emitted photons in air, overestimates the correct ratio by about 10% at 10 keV but is accurate within 1% above 1 MeV. This is a useful approximation because it can easily be applied to any other exposure mode, such as irradiation from a contaminated ground surface, for which the scattered spectra are not the same as those for air immersion. Even more crudely, the energy-absorption ratio for tissue to air can be assumed to be a constant (1.14) independent of energy (Trubey and Kaye 1973). The error in this approximation is about 20% at 10 keV, decreasing to 7% or less above 0.2 MeV.

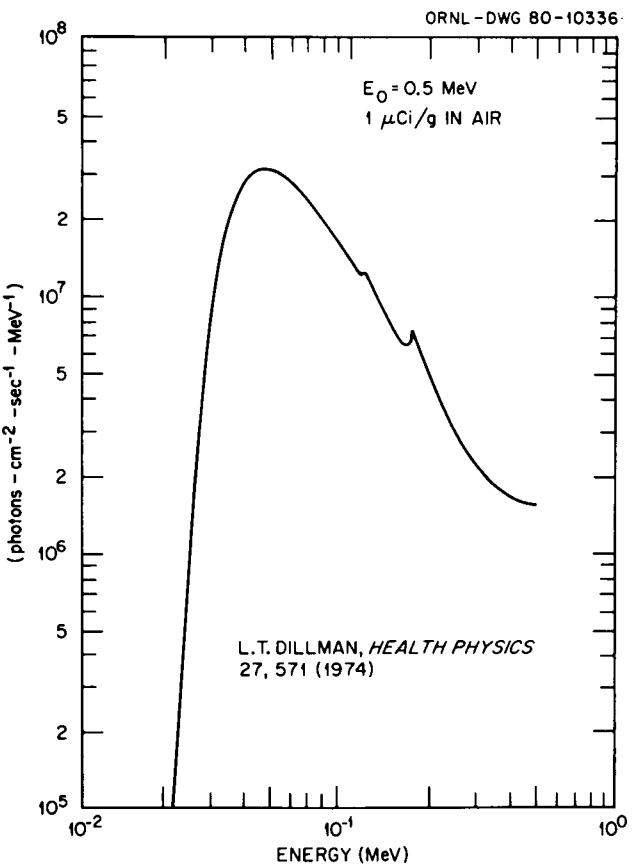

Figure 8.2. Spectrum of photons in air resulting from emission of monoenergetic photons of energy 0.5 MeV in an infinite, uniformly contaminated atmospheric cloud with source concentration of 1 μCi/g.

Example 8.2. In Sect. 8.3.1.1, the dose-rate factor in air for ^{85}Kr was calculated as 0.0094 Gy/y per Bq/cm^3. From Fig. 8.3, the tissue-to-air dose ratio for the scattered spectrum from a 514-keV photon is approximately 1.09. Therefore, if we assume a quality factor of 1 for converting absorbed dose to dose equivalent, the dose-rate factor in tissue is

$$\begin{aligned} \mathrm{DRF}_{\gamma}^{t} &= (0.0094 \text{ Gy/y per Bq/cm}^3)(1 \text{ Sv/Gy})(1.09) \\ &= 0.0102 \text{ Sv/y per Bq/cm}^3 . \text{ [End of example]} \end{aligned}$$

Berger (1974) has calculated the energy spectra of electrons resulting from the emission of monoenergetic electrons in an infinite, uniformly contam-

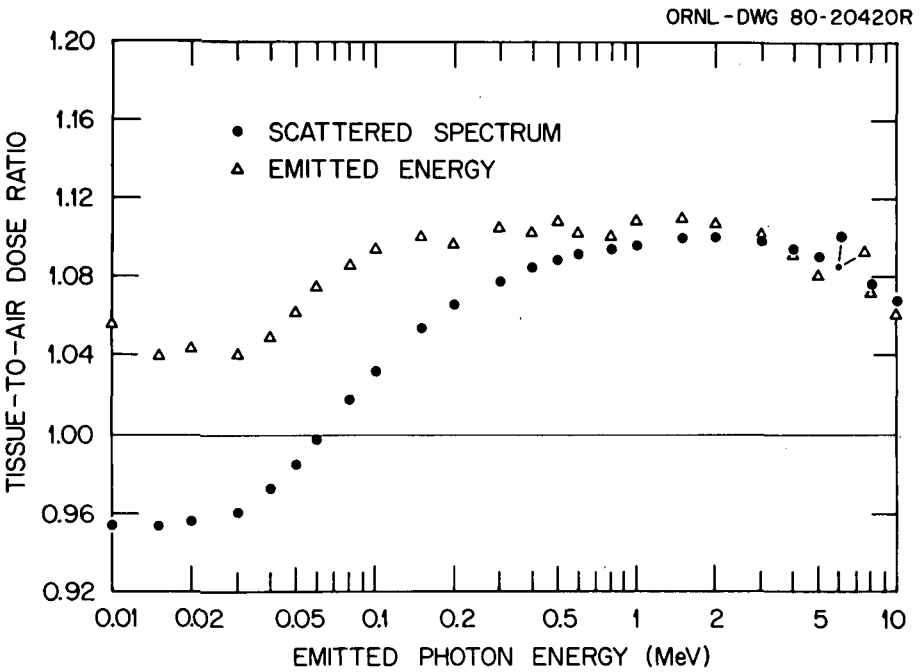

Figure 8.3. Ratio of dose in tissue to dose in air for tissue immersed in an infinite, uniformly contaminated atmospheric cloud vs emitted photon energy. The solid symbols give the dose ratio calculated as a weighted average over the scattered photon spectrum in air, and the triangles give the ratio evaluated at the emitted energy.

inated atmospheric cloud. The scattered spectrum for 0.5-MeV emitted electrons is compared with the spectrum for 0.5-MeV photons in Fig. 8.4. If the ratio of energy absorption in tissue to that in air for the ith electron is defined as

$$R_{i\epsilon} = \left[\frac{(dE/\rho dx)_t}{(dE/\rho dx)_a}\right]_i, \tag{8.14}$$

where

$dE/\rho dx$ = electron mass stopping power in MeV-cm^2/g,

then Berger has shown that this ratio decreases from a value of 1.15 at 10 keV to a value of 1.11 at 2 MeV. These results are shown by the solid symbols in Fig. 8.5. Thus, the variation of $R_{i\epsilon}$ with energy is considerably less than the variation of $R_{i\gamma}$ shown in Fig. 8.3. Approximating $R_{i\epsilon}$ either by the ratio of

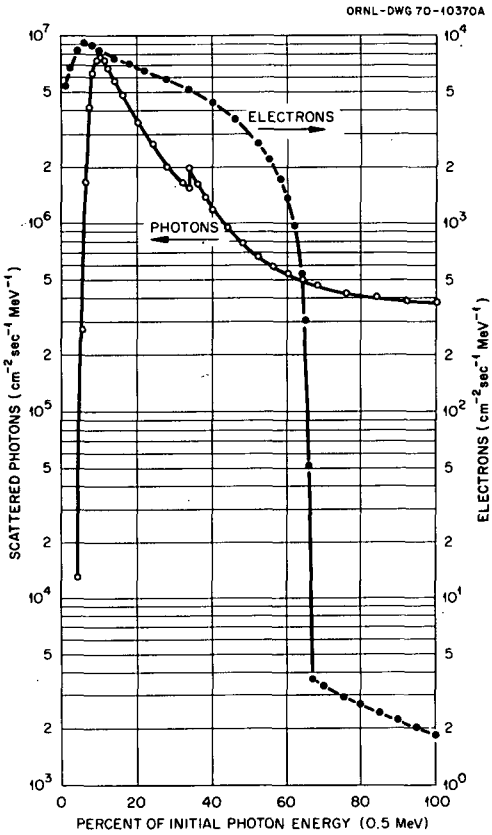

Figure 8.4. Comparison of spectra of scattered electrons and photons resulting from emission of monoenergetic electrons and photons of energy 0.5 MeV in an infinite, uniformly contaminated atmospheric cloud with source concentration of 1 μCi/g.

mass stopping powers at the ith emitted energy (Kocher 1979; Kocher 1980a), as shown by the open symbols in Fig. 8.5, or by the constant factor 1.14 (Trubey and Kaye 1973) results in errors of only 3% or less.

Regardless of the method chosen to evaluate the ratio of energy absorption in tissue to that in air, the dose-rate factors for tissue embedded in an infinite atmospheric cloud source are obtained from Eqs. 8.9, 8.10, 8.13, and 8.14 as

$$\mathrm{DRF}_{\gamma}^{t} = k\frac{1}{\rho_a}\sum_i f_{i\gamma}E_{i\gamma}R_{i\gamma}\,, \tag{8.15}$$

$$\mathrm{DRF}_{\epsilon}^{t} = k\frac{1}{\rho_a}\left[\sum_i f_{ie}E_{ie}R_{i\epsilon} + \sum_j f_{j\beta}\int_0^{E_{j\beta}^{\max}} N_{j\beta}(E)E\,R_{\epsilon}(E)dE\right]. \tag{8.16}$$

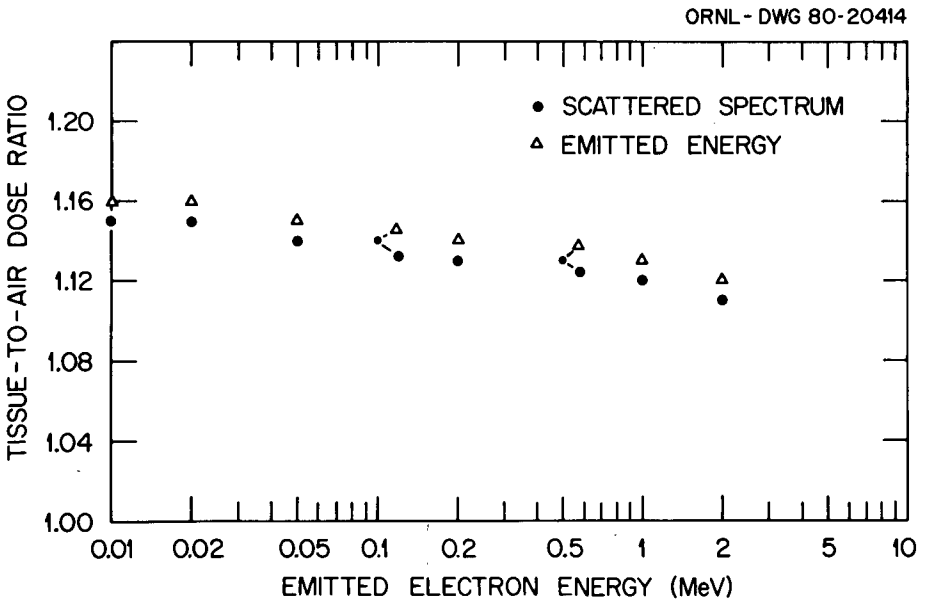

Figure 8.5. Ratios of dose in tissue to dose in air for tissue immersed in an infinite, uniformly contaminated atmospheric cloud vs emitted electron energy. The solid symbols give the dose ratio calculated as a weighted average over the scattered electron spectrum in air, and the triangles give the ratio evaluated at the emitted energy.

These equations give the so-called tissue kerma in air for photons and electrons. In the second term in Eq. 8.16 for electrons for beta decay, we have retained the tissue-to-air dose ratio $R_\epsilon(E)$ as an energy-dependent quantity inside the integral over the continuous electron energy spectrum, even though from Fig. 8.5 it is an excellent approximation to take this quantity as a constant equal to its value at the average energy $\bar{E}_{j\beta}$. The term for continuous electrons could then be written as the summation of the simple product $f_{j\beta}\bar{E}_{j\beta}R_{j\beta}$. As with Eq. 8.12, however, this latter simplication is not useful in obtaining organ dose-rate factors for continuous electrons because organ doses depend on the electron spectrum not the average energy.

8.3.1.3 Dose-Rate Factors for the Body Surface of an Exposed Individual

So far, we have calculated the dose-rate factors for a small piece of tissue embedded in an infinite, uniformly contaminated atmospheric cloud. We now account for the effective geometry of the exposure medium as it differs from an infinite sphere and the modification of the radiation field at the body surface due to self-shielding by the body tissues of an exposed individual.

Effective geometry of the atmospheric cloud. The dose-rate factor for immersion in contaminated air is commonly based on the assumption that an exposed individual is standing at the air-ground interface so that, in effect, the receptor position is located near the boundary of an infinite hemispherical source medium.

For photons, the dose rate at the air-ground interface of an infinite hemispherical cloud is usually assumed to be one-half of the dose rate at any point inside an infinite cloud (Dillman 1974). This is an intuitively reasonable result because one-half of the hypothetical source region contributing to the dose at the interface has been removed. Furthermore, if the photon mean-free-path in air (defined as $1/\mu_a$, where μ_a is the linear attenuation coefficient in air) is large compared with the height of an individual standing on the ground, it is reasonable to assume that the dose rate in air at any point up to that height is equal to the dose rate at the air-ground interface—namely, one-half of the infinite cloud value. Recent calculations (Ryman et al. 1981) have shown that at a height of 1 m above ground, which is the average height of body organs for an individual standing on the ground, it is a good approximation to assume that the photon dose-rate factor in air is reduced by a factor of 1/2 due to the air-ground interface effect for all but the lowest photon energies. For energies above 20 keV, the maximum error is less than 20% near 50 keV emitted energy and is less than 10% above 0.2 MeV. For energies below 20 keV, this approximation underestimates the dose-rate factor at 1 m height by as much as a factor of two due to the short photon mean-free-path in air (U.S. Department of Health, Education, and Welfare 1970), but this energy region is unimportant for external dosimetry.

For electrons, the dose rate at the air-ground interface is also assumed to be one-half of the dose rate in an infinite cloud (Berger 1974). However, it is customary to assume that the electron range in air is less than the average height of the body surface above ground (1 m). Therefore, the dose rate in air above ground from an infinite hemisphere is usually assumed to be the same as that from an infinite sphere. In principle, we should calculate the electron dose rate in air averaged over the height of the body surface above ground. Since the dose rate at the air-ground interface is reduced by about one-half for any electron energy, the presence of the air-ground interface reduces the electron dose rate averaged over the height of the body above ground by a factor between one-half for very high energies and one for very low energies. In practice, however, this averaging procedure has not been considered in the literature. Thus, our assumption of no reduction in dose rate due to the hemispherical source medium may provide a conservative overestimate of the dose-rate factor for electrons, depending on the body organ of interest and the height above ground of the organ compared with the electron range in air.

Self-shielding of radiations by body tissues. The radiation field at any point on the body surface is influenced by self-shielding by body tissues; that

is, the body shields the surface from one-half of the source region, and the dose rate depends on whether or not the radiations must penetrate body tissues to reach the body surface.

For photons, it is customary to make the conservative assumption that the body provides no shielding so that the dose rate at the body surface is not reduced compared with the dose rate in a small piece of tissue. Obviously, this is a poor assumption at the lowest energies where shielding by the body is almost complete (Dillman 1974). In actuality, the dose rate at the body surface is reduced by a factor between one-half and one, depending on the photon energy. We note, however, that any error in the assumption of no body shielding for photons is of no consequence for obtaining organ dose-rate factors for immersion in contaminated air because the organ dose-rate factors discussed in the next section for this exposure mode properly account for shielding by body tissues.

For electrons, it is clearly a good approximation to regard the body tissues as essentially impenetrable (National Academy of Sciences 1964). Therefore, self-shielding by the body reduces the electron dose-rate factor at the body surface by a factor of one-half for all electron energies of interest in radioactive decay.

Dose-rate factors for body surface. With the approximations described above for the effects of the air-ground interface and self-shielding by body tissues, the dose-rate factors for the body surface s of an exposed individual are given in terms of the dose-rate factors in tissue in Eqs. 8.15 and 8.16 by

$$\mathrm{DRF}_\gamma^s = \frac{1}{2}\mathrm{DRF}_\gamma^t, \tag{8.17}$$

$$\mathrm{DRF}_\epsilon^s = \frac{1}{2}\mathrm{DRF}_\epsilon^t. \tag{8.18}$$

8.3.1.4 Dose-Rate Factors for Body Organs

We come to the desired point of estimating the photon and electron dose-rate factors for the body organs of an exposed individual standing at the air-ground interface in an infinite, uniformly contaminated hemispherical cloud.

We define

$$G^m(E_i) = \text{ratio of absorbed dose rate in body organ } m \text{ to absorbed dose rate at the body surface for emitted energy } E_i. \tag{8.19}$$

The numerator in this equation is the dose rate that is obtained from Monte Carlo calculations given in the literature. Given this definition, the organ dose-rate factors for photons can be expressed from Eqs. 8.15 and 8.17 as

$$\mathrm{DRF}_\gamma^m = \frac{1}{2}k\frac{1}{\rho_a}\sum_i f_{i\gamma}E_{i\gamma}R_{i\gamma}G_\gamma^m(E_{i\gamma}). \tag{8.20}$$

The organ dose-rate factors for electrons are expressed similarly as

$$\mathrm{DRF}_{\epsilon}^{m} = \frac{1}{2} k \frac{1}{\rho_a} \left[\sum_i f_{ie} E_{ie} R_{i\epsilon} G_{\epsilon}^{m}(E_{ie}) + \sum_j f_{j\beta} \int_0^{E_{j\beta}^{\max}} N_{j\beta}(E) E R_{\epsilon}(E) G_{\epsilon}^{m}(E) dE \right]. \tag{8.21}$$

We note that it is not proper to simplify the second term in Eq. 8.21 for electrons from beta decay by evaluating the ratio G_{ϵ}^{m} at the average energy $\bar{E}_{j\beta}$, because electrons have a finite range in matter. Thus, if a given continuous spectrum of electrons between zero energy and the endpoint energy is incident upon the body surface, only a portion of that spectrum will penetrate the body tissues and reach the organs of interest. It could occur, for example, that the average energy is too low to penetrate to the desired organs, but higher energies between the average and the endpoint have a sufficient range. Therefore, the ratio in Eq. 8.19 must be applied to all energies in the continuous electron spectrum. It is still a reasonable approximation to evaluate the tissue-to-air scattering ratio $R_{\epsilon}(E)$ at the average energy $\bar{E}_{j\beta}$ and take the value outside the integral in Eq. 8.21 if so desired.

We mentioned at the beginning of this section that the photon dose-rate factors for air immersion can be calculated without explicit consideration of the intermediate steps of obtaining the dose-rate factors in tissue and at the body surface. If we were to define $G^{m}(E_i)$ as the ratio of organ dose to dose in air, instead of using the definition in Eq. 8.19, then the dose-rate factor for body organs could be obtained from the air kerma in Eq. 8.9 by multiplying each term by the redefined $G^{m}(E_i)$ and the factor of 1/2 in Eq. 8.17. This approach has been used in recent work (Kocher 1981b).

Organ dose-rate factors for photons. Organ doses for photons for immersion in a semi-infinite atmospheric cloud with uniform concentration are available in the literature. Therefore, we could just as well use these results to obtain organ dose-rate factors directly and not go through the calculations in Sects. 8.3.1.1 through 8.3.1.3. All that is necessary is to interpolate tabulated values for a particular organ with energy using the known spectrum of photons for the given radionuclide and to normalize the results to the desired unit source concentration in air. As discussed in Sect. 8.1, however, calculation of the ratios G_{γ}^{m} for photons as defined in Eq. 8.19 is useful if organ dose-rate factors for other modes of exposure are desired because the published organ doses are directly applicable only to exposure via immersion in contaminated air.

We caution, however, that it may not be a straightforward matter to take photon organ doses from the literature and apply them correctly to the given photon spectrum. Consider, for example, two sets of organ doses that have

been obtained by Monte Carlo techniques by Poston and Snyder (1974) and by O'Brien and Sanna (1976) and O'Brien (1980). For any given organ, it is evident (Kerr 1980) that the doses given by these two papers do not agree for energies above about 0.1 MeV, even when expressed in the same units. The primary reason for this discrepancy is that the organ doses calculated by Poston and Snyder are given for assumed energies emitted in the atmospheric cloud, whereas the energies for which O'Brien and Sanna give their results are those assumed to be incident upon the body surface. As we discussed in Sect. 8.3.1.3, these two energies are not the same because of scattering and absorption in air. The average energy incident upon the body surface is always less than the emitted energy. The definition of the energies used by Poston and Snyder is clearly the one which is appropriate for application to Eq. 8.20. On the other hand, O'Brien and Sanna's organ dose calculations are potentially more useful because they generally have a greater statistical accuracy than those of Poston and Snyder and extend to higher energies.

A rigorous procedure for using the calculations of O'Brien and Sanna (1976) and O'Brien (1980) to obtain organ dose-rate factors for immersion in contaminated air has been discussed by Kerr (1980) and recently implemented by Eckerman et al. (1980). In this procedure, dose-rate factors in units of dose rate per unit concentration of activity in air are obtained by integrating the dose per photon per unit area incident upon the body surface calculated by O'Brien and Sanna over the energy spectra of scattered photons in air (e.g., see Fig. 8.1) calculated by Dillman (1974). In this way, the calculations of O'Brien and Sanna can be expressed in terms of the emitted photon energy and, thus, are directly comparable with those of Poston and Snyder (1974). Examples of this comparison, in which the calculations are expressed as the ratio of organ dose to dose in air, are shown in Figs. 8.6 through 8.8. The results for total body in Fig. 8.6 illustrate that for most body organs the results of Eckerman et al. are systematically less than those of Poston and Snyder for the same emitted energy. The reason for this systematic discrepancy is not known. The results for the ovaries in Fig. 8.7 indicate the effect of the improved statistical accuracy in the O'Brien and Sanna data on obtaining a smooth energy dependence of the dose-rate factors, particularly for small, deep-lying organs. For red marrow, an important organ for external dosimetry, the newer calculations of Eckerman et al. shown in Fig. 8.8 are also systematically less than those of Poston and Snyder, and the discrepancy is as much as an order of magnitude for emitted energies below 0.2 MeV. This large difference results primarily from differences in the models used to describe energy absorption in red marrow in Reference Man. These differences have been discussed by Kerr (1980).

Given the photon organ dose-rate factors for immersion in contaminated air, obtained from the literature as described above, and the body-surface dose-rate factor for photons obtained from Eqs. 8.15 and 8.17, the ratio G_γ^m as a function of energy can then be calculated from the definition in Eq. 8.19.

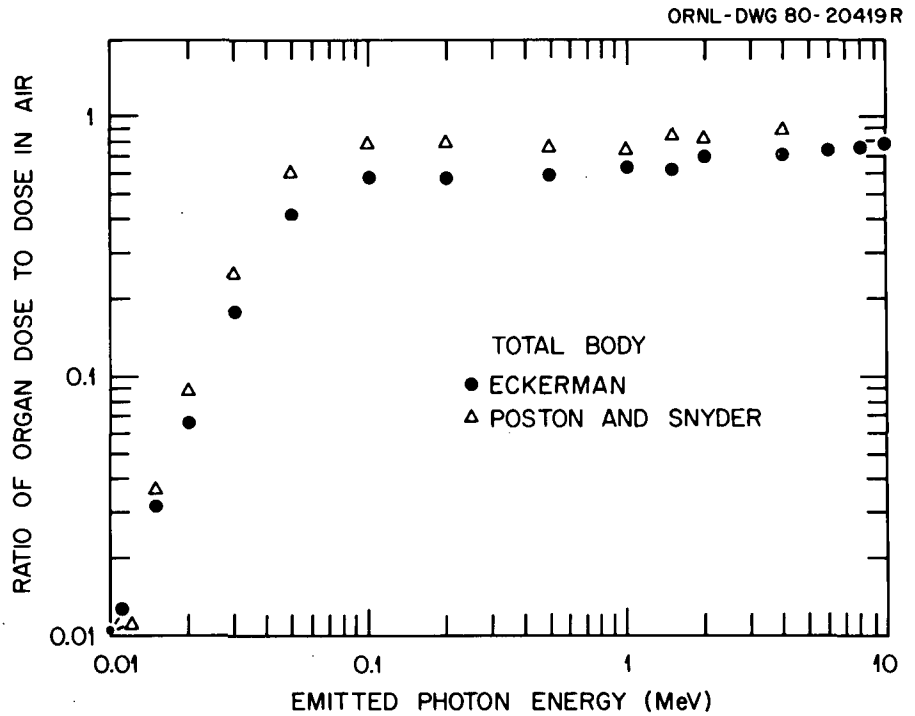

Figure 8.6. Ratios of dose to total body to dose in air for an infinite, uniformly contaminated atmospheric cloud vs emitted photon energy. The results of Poston and Snyder (1974) are compared with calculations of Eckerman et al. (1980).

For example, these ratios for total body, ovaries, and red marrow can be obtained from the results in Figs. 8.6 through 8.8 by dividing by the tissue-to-air scattering ratio shown in Fig. 8.3. Again, the ratios G_γ^m are useful for calculating organ doses for exposure modes other than immersion in contaminated air.

Example 8.3. In Sect. 8.3.1.1, the dose-rate factor in air for ^{85}Kr, which emits a single photon of energy 514 keV, was calculated as 0.0094 Gy/y per Bq/cm^3. We can then use the correction factor for air-ground interface effects given in Sect. 8.3.1.3 and the ratios of organ dose to dose in air given in Fig. 8.7, for example, to estimate the dose-rate factor for ovaries for an individual standing at the boundary of a semi-infinite atmospheric cloud. The organ-dose to air-dose ratio from the calculations of Eckerman et al. is seen to be about 0.5 for ovaries at the energy of interest; hence, the dose-rate factor is

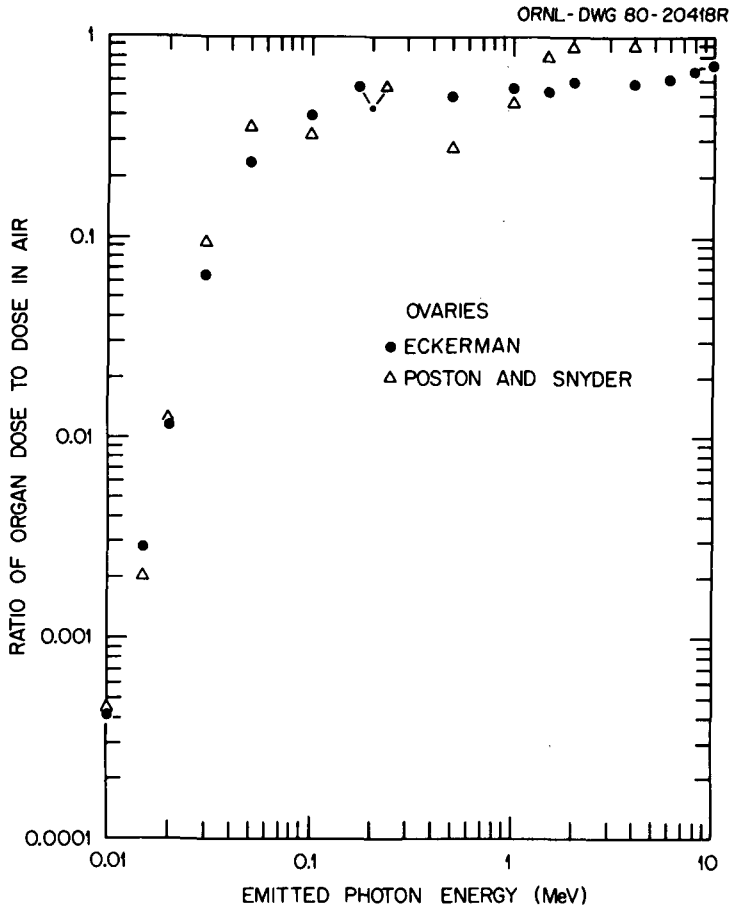

Figure 8.7. Ratios of dose to ovaries to dose in air for an infinite, uniformly contaminated atmospheric cloud vs emitted photon energy. The results of Poston and Snyder (1974) are compared with calculations of Eckerman et al. (1980).

$$\begin{aligned} \mathrm{DRF}_{\gamma}(\text{ovaries}) &= 1/2\ (0.0094\ \text{Gy/y per Bq/cm}^3)(1\ \text{Sv/Gy})(0.5) \\ &= 0.0024\ \text{Sv/y per Bq/cm}^3\ . \end{aligned}$$

This is the value given in Table 8.1 (see Sect. 8.3.3). [End of example]

Organ dose-rate factors for electrons. Because of the relative impenetrability of body tissues to electrons, only organs near the body surface need to be considered. The potentially important organs include the skin, the lens of the

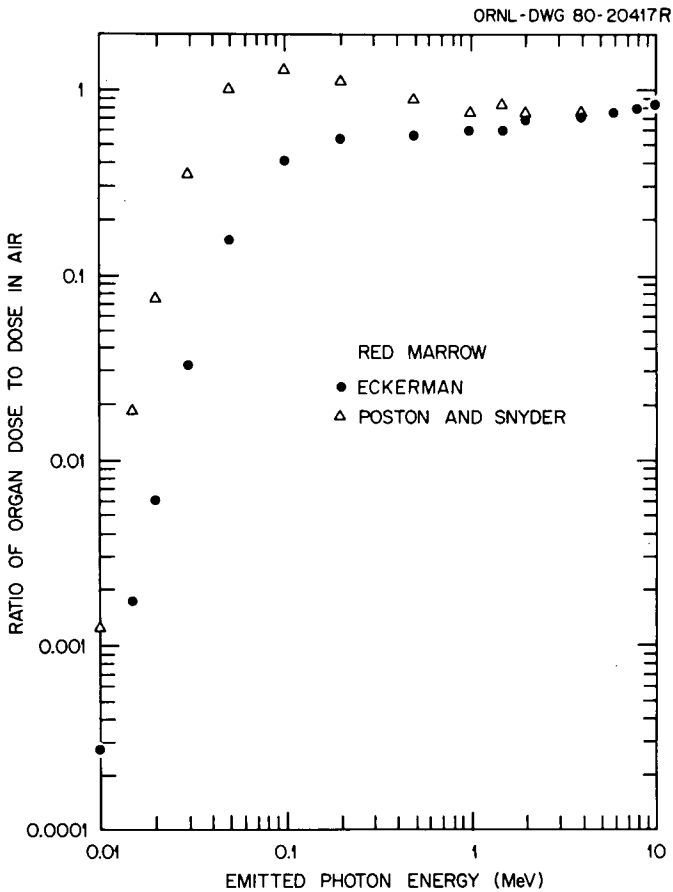

Figure 8.8. Ratios of dose to red marrow to dose in air for an infinite, uniformly contaminated atmospheric cloud vs emitted photon energy. The results of Poston and Snyder (1974) are compared with calculations of Eckerman et al. (1980).

eye, and the testes. In this chapter, we discuss only electron dose-rate factors for radiosensitive tissues of the skin, but the methods discussed are directly applicable to other organs of interest by taking into account the different depths of the organs below the body surface. Historically, the calculation of dose as a function of depth in tissue to estimate the dose to skin (or to other organs near the body surface) has been based on the empirical Loevinger equation (Fitzgerald et al. 1967), and the use of this equation remains widespread today (Healy and Baker 1968; Healy 1982), even though the equation does not

Table 8.1. Dose-rate factors for immersion in contaminated air

(Values are in Sv/y per Bq/cm^3)

Nuclide	Skin (electrons)	Breast (photons)	Lungs (photons)	Red marrow (photons)	Ovaries (photons)	Skeleton (photons)	Testes (photons)	Total body (photons)
^{3}H	0.0	0.0	0.0	0.0	0.0	0.0	0.0	0.0
^{14}C	5.9E-3	0.0	0.0	0.0	0.0	0.0	0.0	0.0
^{85}Kr	4.1E-1	3.3E-3	2.6E-3	2.7E-3	2.4E-3	3.1E-3	3.5E-3	2.8E-3
^{85m}Kr	4.2E-1	2.7E-1	1.8E-1	1.8E-1	1.5E-1	2.7E-1	2.5E-1	2.0E-1
^{88}Kr	6.6E-1	3.3E0	2.7E0	2.8E0	2.4E0	2.9E0	3.6E0	2.9E0
^{88}Rb	4.6E0	1.0E0	8.6E-1	8.8E-1	7.6E-1	9.1E-1	1.1E0	9.1E-1
^{90}Sr	2.9E-1	0.0	0.0	0.0	0.0	0.0	0.0	0.0
^{90}Y	2.0E0	0.0	0.0	0.0	0.0	0.0	0.0	0.0
^{95}Zr	1.1E-1	1.1E0	9.1E-1	9.2E-1	8.3E-1	1.0E0	1.2E0	9.7E-1
^{95}Nb	6.9E-3	1.1E0	9.5E-1	9.6E-1	8.6E-1	1.1E0	1.3E0	1.0E0
^{99}Tc	5.4E-2	9.8E-7	5.7E-7	4.1E-7	4.3E-7	9.9E-7	8.3E-7	6.3E-7
^{106}Ru	0.0	0.0	0.0	0.0	0.0	0.0	0.0	0.0
^{106}Rh	3.1E0	3.1E-1	2.5E-1	2.5E-1	2.2E-1	2.9E-1	3.3E-1	2.7E-1
^{129}I	3.5E-3	2.4E-2	5.6E-3	2.1E-3	4.0E-3	9.8E-3	1.6E-2	1.0E-2
^{131}I	2.6E-1	5.8E-1	4.4E-1	4.6E-1	3.9E-1	5.5E-1	6.0E-1	4.8E-1
^{133}I	7.6E-1	8.9E-1	7.3E-1	7.4E-1	6.5E-1	8.3E-1	9.7E-1	7.8E-1
^{131m}Xe	1.1E-1	2.1E-2	7.1E-3	4.8E-3	5.4E-3	1.1E-2	1.5E-2	1.1E-2
^{133}Xe	8.2E-2	7.1E-2	3.5E-2	2.3E-2	2.6E-2	6.2E-2	5.7E-2	4.2E-2
^{133m}Xe	2.5E-1	5.5E-2	3.1E-2	2.9E-2	2.5E-2	4.4E-2	4.8E-2	3.7E-2
^{135}Xe	5.4E-1	4.0E-1	2.8E-1	2.9E-1	2.4E-1	3.8E-1	3.9E-1	3.1E-1
^{134}Cs	2.3E-1	2.3E0	1.9E0	1.9E0	1.7E0	2.1E0	2.5E0	2.0E0
^{137}Cs	2.3E-1	0.0	0.0	0.0	0.0	0.0	0.0	0.0
^{137m}Ba	1.3E-1	8.8E-1	7.3E-1	7.4E-1	6.6E-1	8.2E-1	9.7E-1	7.8E-1
^{154}Eu	3.7E-1	1.9E0	1.6E0	1.6E0	1.4E0	1.7E0	2.1E0	1.7E0

Table 8.1 (continued)

(Values are in Sv/y per Bq/cm^3)

Nuclide	Skin (electrons)	Breast (photons)	Lungs (photons)	Red marrow (photons)	Ovaries (photons)	Skeleton (photons)	Testes (photons)	Total body (photons)
^{210}Pb	0.0	3.3E-3	1.1E-3	5.2E-4	8.3E-4	2.1E-3	2.3E-3	1.6E-3
^{214}Pb	4.2E-1	3.9E-1	2.9E-1	2.9E-1	2.4E-1	3.7E-1	3.9E-1	3.1E-1
^{210}Bi	7.1E-1	0.0	0.0	0.0	0.0	0.0	0.0	0.0
^{214}Bi	1.3E0	2.3E0	2.0E0	2.0E0	1.7E0	2.1E0	2.6E0	2.1E0
^{210}Po	0.0	1.3E-5	1.1E-5	1.1E-5	9.6E-6	1.2E-6	1.4E-5	1.1E-5
^{222}Rn	0.0	5.7E-4	4.6E-4	4.7E-4	4.1E-4	5.4E-4	6.2E-4	4.9E-4
^{226}Ra	3.2E-7	1.2E-2	7.6E-3	7.3E-3	6.1E-3	1.1E-2	1.1E-2	8.3E-3
^{230}Th	0.0	9.1E-4	3.8E-4	2.8E-4	2.9E-4	6.5E-4	6.0E-4	4.7E-4
^{231}Th	4.6E-2	2.5E-2	1.2E-2	8.3E-3	8.8E-3	2.0E-2	1.8E-2	1.4E-2
^{234}Th	7.9E-3	1.5E-2	8.1E-3	5.7E-3	6.1E-2	1.4E-2	1.2E-2	9.3E-3
^{234m}Pa	1.7E0	1.7E-2	1.4E-2	1.4E-2	1.3E-2	1.6E-2	1.9E-2	1.5E-2
^{234}U	3.4E-5	5.5E-4	1.1E-4	7.5E-5	8.2E-5	1.9E-4	2.2E-4	1.8E-4
^{235}U	5.0E-3	2.6E-1	1.7E-1	1.6E-1	1.4E-1	2.5E-1	2.4E-1	1.9E-1
^{236}U	1.9E-5	4.8E-4	8.1E-5	4.7E-5	5.8E-5	1.5E-4	1.7E-4	1.4E-4
^{238}U	1.3E-5	4.2E-4	6.8E-5	3.8E-5	4.9E-5	1.2E-4	1.5E-4	1.2E-4
^{238}Pu	0.0	4.9E-4	3.2E-5	1.4E-5	2.1E-5	5.7E-5	1.1E-4	1.1E-4
^{240}Pu	0.0	4.7E-4	3.3E-5	1.5E-5	2.2E-5	5.8E-5	1.1E-4	1.1E-4
^{241}Pu	0.0	0.0	0.0	0.0	0.0	0.0	0.0	0.0
^{241}Am	1.5E-5	4.0E-2	1.9E-2	1.0E-2	1.4E-2	3.4E-2	3.1E-2	2.3E-2

apply to discrete Auger and internal conversion electrons and, in some cases, is only a crude approximation for the continuous spectra of electrons from beta decay.

Much more appropriate to the calculation of electron dose-rate factors for skin are the depth-dose distributions calculated by Berger (1974) for tissue immersed in a semi-infinite radioactive cloud; these are based on specific absorbed fractions for electrons in tissue-equivalent material (Berger 1973). Table 1 of Berger (1974) and Table 7 of Berger (1973) directly give values of $G_\epsilon(E)$ as a function of depth in tissue for immersion in contaminated water so that the results for use in Eq. 8.21 can be obtained for the desired depth by interpolation with energy and depth and by applying correction factors discussed by Berger (1974) to give values appropriate for immersion in contaminated air. The user should note that Berger's values of G already include the factor of 1/2 in our equation, which accounts for self-shielding by body tissues, and that the values of G are given as a function of the ratio of depth in tissue to the electron range in water for emitted energy E_ϵ rather than as a function of depth in tissue alone. Berger (1974) also presents calculated depth-dose distributions for air immersion for selected radionuclides of importance in radiological assessments, and more extensive calculations for three different exposure modes based on these methods have been given by Kocher (1981b) and Kocher and Eckerman (1981). Traditionally, the dose-rate factor for skin is taken to be the value at the single depth of 7 mg/cm^2 in tissue. Dose-rate factors in tissue averaged over the depth of the radiosensitive portion of the skin have also been calculated by Kocher (1981b) and Kocher and Eckerman (1981).

For electrons, the ratio of skin dose to the dose at the body surface obtained for immersion in an infinite and uniformly contaminated source region is not useful in estimating dose-rate factors for skin for other exposure modes, such as ground-surface exposure or exposure to arbitrary distributions of sources, primarily because of the finite range of electrons in matter. A method for estimating skin dose-rate factors for other exposure modes is described in Sect. 8.3.2.4.

8.3.2 Exposure to a Contaminated Ground Surface

We now consider the determination of photon and electron dose-rate factors for exposure to an infinite, smooth, and uniformly contaminated ground surface. Contrary to the calculations for immersion in contaminated air presented in Sect. 8.3.1, explicit use of the specific absorbed fractions for photons and electrons is required for this exposure mode.

8.3.2.1 Dose-Rate Factors in Air

As indicated in Fig. 8.9, the dose-rate factors in air are to be calculated at the point P located at a height z above the contaminated ground surface σ.

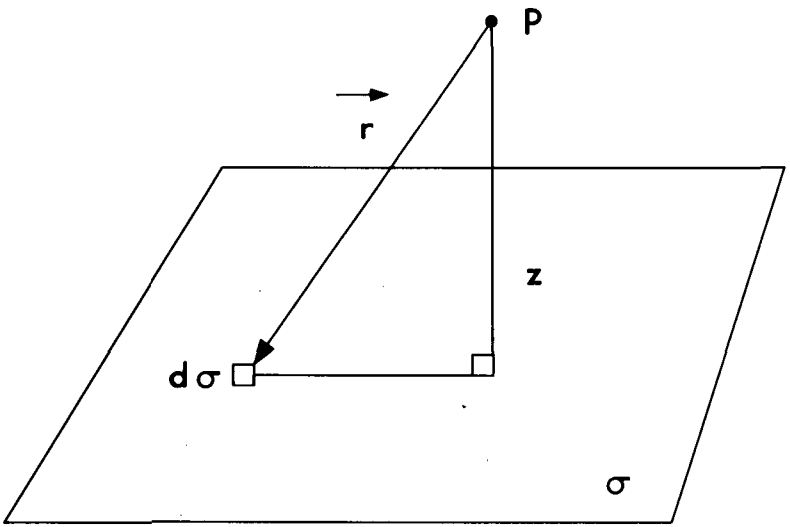

Figure 8.9. Coordinate system for calculation of external dose rate from contaminated ground surface.

From Eqs. 8.4, 8.6, and 8.8, the dose-rate factors in air for photons and electrons are given by

$$\mathrm{DRF}_{\gamma}^{a}(z) = k \sum_{i} f_{i\gamma} E_{i\gamma} \int_{\sigma} \Phi_{\gamma}^{a}(r, E_{i\gamma}) d\sigma , \tag{8.22}$$

$$\mathrm{DRF}_{\epsilon}^{a}(z) = k \Bigg[\sum_{i} f_{ie} E_{ie} \int_{\sigma} \Phi_{\epsilon}^{a}(r, E_{ie}) d\sigma + \sum_{j} f_{j\beta} \int_{0}^{E_{j\beta}^{\max}} N_{j\beta}(E) E \int_{\sigma} \Phi_{\epsilon}^{a}(r, E) dE \, d\sigma \Bigg] . \tag{8.23}$$

The dose-rate factors are in units of Gy/s per Bq/cm^2 if r and z are in cm. The dependence of the dose-rate factors on the height z occurs implicitly in the integral of the specific absorbed fraction over the ground surface.

Dose-rate factor for photons. For photons, the specific absorbed fraction in air is given by (Berger 1968)

$$\Phi_{\gamma}^{a}(r, E_{\gamma}) = (\mu_{\mathrm{en}}/\rho)_{a} \frac{1}{4\pi r^{2}} B_{\mathrm{en}}^{a}(\mu_{a} r) \exp(-\mu_{a} r) , \tag{8.24}$$

where

$(\mu_{en}/\rho)_a$ = mass energy-absorption coefficient in air in cm^2/g,

B^a_{en} = energy-absorption buildup factor in air,

μ_a = linear attenuation coefficient in air in cm^{-1}.

The term $1/4\pi r^2$ gives the radial dispersion of dose due only to the distance from a point source, $\exp(-\mu_a r)$ describes the reduction in the number of photons as a function of distance from the source due to scattering in air, $(\mu_{en}/\rho)_a$ describes energy absorption at the receptor position, and the buildup factor, which has a value greater than unity, accounts for the scattered photons which rescatter back to the receptor position.

From Eqs. 8.22 and 8.24, the dose-rate factor in air becomes

$$\mathrm{DRF}^a_\gamma(z) = \frac{1}{2} k \sum_i f_{i\gamma} E_{i\gamma} [(\mu_{en}/\rho)_a]_i \times \int_z^\infty \frac{1}{r} B^a_{en}(\mu_{a,i} r) \exp(-\mu_{a,i} r) dr \,. \tag{8.25}$$

Various analytical approximations are available for the buildup factor (Trubey 1966). An approximation that often leads to an easily integrable equation for the general form of the photon dose rate in Eq. 8.4 is the Berger form of the buildup factor (Trubey 1966) given by

$$B^a_{en}(\mu_a r) = 1 + C_a \mu_a r \exp(D_a \mu_a r) \,, \tag{8.26}$$

where the coefficients C_a and D_a are functions of the photon energy, and D_a must be less than one. These coefficients are obtained from linear least-squares fits of Eq. 8.26 to published buildup factors in air. The photon dose-rate factor in air is then given by

$$\mathrm{DRF}^a_\gamma(z) = \frac{1}{2} k \sum_i f_{i\gamma} E_{i\gamma} [(\mu_{en}/\rho)_a]_i \times \left[\widetilde{E}_1(\mu_{a,i} z) - \frac{C_{a,i}}{(D_{a,i} - 1)} \exp[(D_{a,i} - 1)\mu_{a,i} z] \right] , \tag{8.27}$$

where $\widetilde{E}_1(\mu_{a,i} z)$ is the well known first-order exponential integral

$$\widetilde{E}_1(\mu_{a,i} z) = \int_z^\infty \frac{1}{r} \exp(-\mu_{a,i} r) dr \,. \tag{8.28}$$

The dose-rate factor is normally evaluated at the single height $z = 1$ m, which is assumed to be the average height above ground of body organs for an

individual standing on the ground. At this height, the second term in Eq. 8.27, accounting for photon buildup in air, is a correction of only about 5% or less to the term given by the exponential integral.

Dose-rate factor for electrons. For electrons, an analytical equation for the specific absorbed fraction, analogous to Eq. 8.24 for photons, has not been developed. However, Berger (1973; 1974) has used Monte Carlo methods to calculate specific absorbed fractions in water for particular values of distance and energy. These values can be modified to give the specific absorbed fractions in air (Berger 1974), and the results can then be used to evaluate the dose-rate factor in Eq. 8.23 by numerical methods (Kocher 1979; Kocher 1980a; Kocher 1981b).

As we discussed in connection with Eq. 8.21 for the electron dose-rate factor for skin for immersion in contaminated air, we must remember that electrons have a finite range in air so that not all electrons emitted from the ground surface will reach the height z above ground. Thus, we cannot replace the integral over energy for electrons from beta decay in the second term in Eq. 8.23 by the average energy.

In order to minimize the dependence of the specific absorbed fraction on electron energy and, thus, to facilitate interpolation of tabulated values, Berger (1973; 1974) has introduced the dimensionless scaled point kernel, denoted by $F_\epsilon(r/r_0,E_\epsilon)$, which is defined by the equation

$$F_\epsilon(r/r_0,E_\epsilon)d(r/r_0) = 4\pi\rho\Phi_\epsilon(r,E_\epsilon)r^2dr \ , \tag{8.29}$$

where r_0 is the mean electron range at energy E_ϵ in the medium of density ρ. The scaling is accomplished by expressing distances in units of the electron range.

Using Eq. 8.29 for the scaled point kernel, the dose-rate factor in air for electrons can be written in the form (Kocher 1979; Kocher 1980a; Kocher 1981b)

$$\begin{aligned} \mathrm{DRF}_\epsilon^a(z) = \frac{1}{2}k\frac{1}{\rho_a}\Bigg[& \sum_i f_{ie}E_{ie}\frac{1}{r_0(E_{ie})}\Omega(z,E_{ie}) \\ & + \sum_j f_{j\beta}\int_0^{E_{j\beta}^{\max}} N_{j\beta}(E)E\frac{1}{r_0(E)}\Omega(z,E)dE\Bigg] , \end{aligned} \tag{8.30}$$

where $\Omega(z,E)$ is the integral over the ground surface of the scaled point kernel for energy E given by

$$\Omega(z,E) = \int_{z/r_0(E)}^{\infty}\frac{1}{x}F_\epsilon^a(x,E)dx \ , \tag{8.31}$$

and the dimensionless scaled distance x is defined as

$$x = r/r_0(E) . \tag{8.32}$$

Given the electron scaled point kernel F_ϵ^a in air as a function of energy and scaled distance x, obtained as described by Berger (1973; 1974), and the energy distribution $N_\beta(E)$ for continuous electrons given by the Fermi theory of beta decay (Evans 1955; Wu and Moskowski 1966), the dose-rate factor in air in Eq. 8.30 can be evaluated by numerical integration over energy and scaled distance (Kocher 1979; Kocher 1980a; Kocher 1981b; Kocher and Eckerman 1981). In practice, since electrons have a finite range in air, the upper limit of integration over the scaled distance in Eq. 8.31 is approximately 1.25.

We note again that the empirical Loevinger equation, which has often been used to calculate electron dose-rate factors from a contaminated ground surface (Trubey and Kaye 1973; Healy and Baker 1968; Healy 1982), does not apply to discrete electrons and is a reasonably accurate approximation for continuous electrons from beta decay only if the endpoint energy has a range in air considerably greater than the height z. Therefore, although the Loevinger equation is attractive because of its relatively simple form compared with the equations developed here, it should be used with considerable caution.

8.3.2.2 Dose-Rate Factors for Tissue Embedded in Air

Exactly as with immersion in contaminated air in Sect. 8.3.1.2, the dose-rate factors for a small piece of tissue at the height z can be obtained from the dose-rate factors in air by application of the factors $R_{i\gamma}$ and $R_{i\epsilon}$ in Eqs. 8.13 and 8.14, which give the ratios of mass energy-absorption coefficients and mass stopping powers in tissue and air respectively. Thus, for photons and electrons,

$$\begin{aligned} \mathrm{DRF}_\gamma^t(z) &= \frac{1}{2} k \sum_i f_{i\gamma} E_{i\gamma} [(\mu_{\mathrm{en}}/\rho)_t]_i \\ &\quad \times \left[\widetilde{E}_1(\mu_{a,i} z) - \frac{C_{a,i}}{(D_{a,i}-1)} \exp[(D_{a,i}-1)\mu_{a,i} z] \right] , \end{aligned} \tag{8.33}$$

$$\begin{aligned} \mathrm{DRF}_\epsilon^t(z) &= \frac{1}{2} k \frac{1}{\rho_a} \left[\sum_i f_{ie} E_{ie} R_{i\epsilon} \frac{1}{r_0(E_{ie})} \Omega(z, E_{ie}) \right. \\ &\quad \left. + \sum_j f_{j\beta} \int_0^{E_{j\beta}^{\max}} N_{j\beta}(E) E R_\epsilon(E) \frac{1}{r_0(E)} \Omega(z, E) dE \right] . \end{aligned} \tag{8.34}$$

A reasonable approximation of $R_{i\gamma}$ and $R_{i\epsilon}$ for ground-surface exposure is obtained by evaluating the ratios at the emitted energy (see Figs. 8.3 and 8.5) because the values calculated by Dillman (1974) and Berger (1968) to account

for scattering and absorption in air for immersion in contaminated air do not strictly apply to any other exposure mode.

8.3.2.3 Dose-Rate Factors for the Body Surface of an Exposed Individual

The dose-rate factors for the body surface of an individual standing on the ground can be obtained from the values for a small piece of tissue by accounting for the self-shielding by body tissues. As in Sect. 8.3.1.3, we assume no self-shielding for photons but a reduction in dose rate by a factor of two for electrons. Thus, the dose-rate factors for the body surface are taken to be

$$\mathrm{DRF}_{\gamma}^{s}(z) = \mathrm{DRF}_{\gamma}^{i}(z)\,, \tag{8.35}$$

$$\mathrm{DRF}_{\epsilon}^{s}(z) = \frac{1}{2}\mathrm{DRF}_{\epsilon}^{i}(z)\,. \tag{8.36}$$

8.3.2.4 Dose-Rate Factors for Body Organs

Calculations of organ doses for exposure to an infinite, uniformly contaminated ground surface using Monte Carlo techniques are not available in the literature. Therefore, approximations must be used to obtain organ dose-rate factors for this exposure mode.

Organ dose-rate factors for photons. For photons, we assume that the ratio of absorbed dose rate for organ m to the absorbed dose rate at the body surface for energy $E_{i\gamma}$, defined in Eq. 8.19 as $G_{\gamma}^{m}(E_{i\gamma})$, is the same for irradiation from a contaminated ground surface as it is for immersion in contaminated air. Because air is the medium between the source and receptor for both exposure modes, this is the same as assuming that the ratio of organ dose to dose in air is the same for ground-surface exposure and air immersion. Thus, the organ dose-rate factors for air immersion obtained from the calculations of Poston and Snyder (1974) or O'Brien and Sanna (1976) and O'Brien (1980), as described in Sect. 8.3.1.4, can be used for ground-surface exposure. The photon dose-rate factor for organ m is then assumed to be

$$\mathrm{DRF}_{\gamma}^{m}(z) = \frac{1}{2}k\sum_{i} f_{i\gamma}E_{i\gamma}[(\mu_{\mathrm{en}}/\rho)_t]_i \times\left[\widetilde{E}_1(\mu_{a,i}z) - \frac{C_{a,i}}{(D_{a,i}-1)}\exp[(D_{a,i}-1)\mu_{a,i}z]\right]G_{\gamma}^{m}(E_{i\gamma})\,. \tag{8.37}$$

The accuracy of the organ dose-rate factors obtained from Eq. 8.37 is not known. While the angular distribution of photons at the body surface is reasonably isotropic for immersion in contaminated air, the angular distribution at

a height of 1 m above a contaminated ground surface is quite anisotropic, with most of the photons coming from angles just below the direction of the horizontal (Beck and de Planque 1968). This result is illustrated in Fig. 8.10. Further-

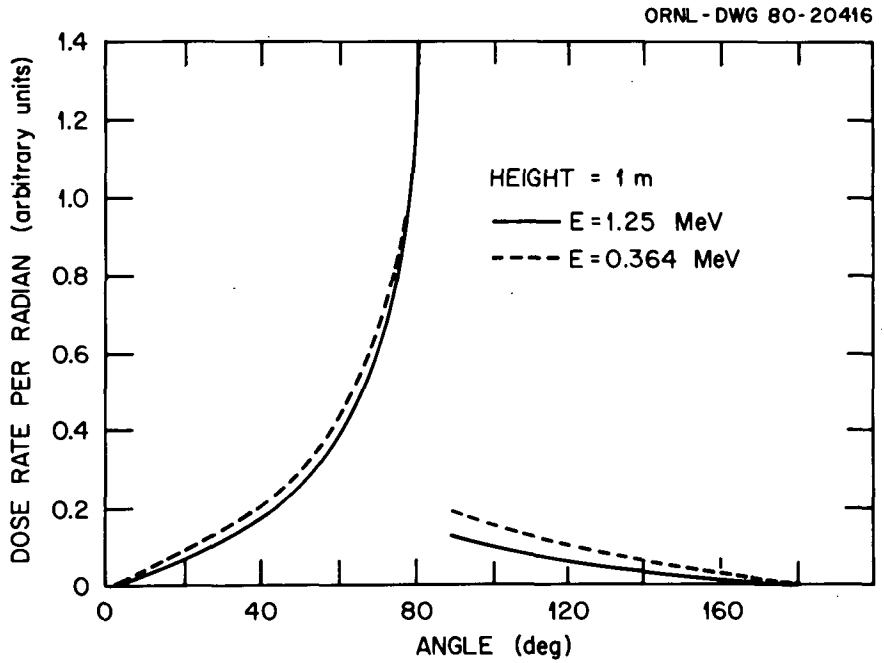

Figure 8.10. Angular distribution of the radiation field at a height of 1 m due to photons emitted from a smooth, infinite, uniformly contaminated ground surface for two different photon energies. An angle of 0° corresponds to the vertically downward direction. The portion of the angular distribution between 80° and 90° has been omitted.

more, the energy distribution at a height of 1 m for monoenergetic photons emitted from the ground surface (Beck and de Planque 1968) is somewhat different than the energy distribution for monoenergetic photons from an atmospheric cloud (Dillman 1974). Therefore, the ratio of organ dose to dose at the body surface is not likely to be the same for air immersion and ground-surface exposure. However, the possible errors in this assumption are not likely to be more than a few tens of percent for photon energies above about 0.1 MeV (Kocher 1981b).

Organ dose-rate factors for electrons. As with immersion in contaminated air, we consider only electron dose-rate factors for skin, but the methods are also applicable to other organs near the body surface. In Sect. 8.3.1.4, the values of the ratio of dose rate in skin to dose rate at the body surface for immersion in contaminated air were obtained directly from the G-factors as a function of energy and depth in tissue calculated by Berger (1973; 1974). However, these results are not directly applicable to the calculation of dose rates to skin from a contaminated ground surface because they do not properly account for the energy loss of electrons due to scattering in air between the ground and the body surface.

Electron dose-rate factors for skin are normally calculated for the single height $z = 1$ m above ground rather than averaging over the height of the body surface above ground. Conceptually, we should calculate the electron dose-rate factor for skin by accounting for transport of the radiations in air between the ground surface and the body surface at a height of 1 m followed by transport through the thickness of tissue between the body surface and the radiosensitive tissues of the skin. However, the problem of calculating specific absorbed fractions for propagation of electrons through two different media has not, to our knowledge, been treated in the literature. Therefore, we assume instead that it is a reasonable approximation to replace the desired thickness of tissue with an equivalent thickness in air, add this thickness to the assumed 1-m height of the body surface above ground, and calculate the dose-rate factor in tissue from Eqs. 8.34 and 8.36. Thus, in effect, we reduce the problem of transmission through two media to a problem involving only one medium for which the specific absorbed fraction is known. If z is the height of the body surface above ground, then we calculate the dose-rate factor for skin by assuming a height z' above ground given by

$$z' = z + 1.14(\rho_t/\rho_a)x \,, \tag{8.38}$$

where x is the distance from the body surface to the skin (equivalent to a depth of 7 mg/cm^2 in tissue), ρ_t and ρ_a are the densities of tissue and air respectively, and the factor 1.14 approximates the ratio of energy absorption in tissue to air (see Sect. 8.3.1.2). This method has recently been implemented by Kocher (1981b) and Kocher and Eckerman (1981). As described in Sect. 8.3.1.4, this method can also be used to obtain the dose-rate factor for skin by averaging calculated values over the thickness of the radiosensitive portions of the skin (Kocher 1981b; Kocher and Eckerman 1981).

Because the energy loss for electrons between the ground and the body surface depends on the height of the body surface above ground, it is obviously a crude approximation to calculate the electron dose-rate factor for skin for the single value $z = 1$ m. More properly, the dose-rate factor should be obtained by averaging over the height of the exposed individual; but this has not yet been attempted. The dose-rate factor for skin at a height of 1 m gives a rea-

sonable approximation to the average of values over the height above ground of the body surface only for electron energies of about 1 MeV and above. At lower energies, the dose-rate factor at 1 m underestimates the value averaged over height, particularly for energies below about 0.4 MeV where the calculated dose-rate factor is zero (Kocher and Eckerman 1981).

We note that the method embodied in Eq. 8.38 for replacing the distance from the body surface to the skin by an equivalent distance in air is appropriate for calculating skin doses for arbitrary distributions of sources and for calculating doses to other body organs.

8.3.3 Compilations of External Dose-Rate Factors

Compilations of external dose-rate factors for photons and electrons are available in the literature for those who are interested only in applying the results to the calculation of radiological impacts without being concerned with the details of how they are obtained.

For photons, external dose-rate factors have been published for 22 body organs for immersion in contaminated air, immersion in contaminated water, and exposure to a contaminated ground surface for each of 240 radionuclides of potential importance in routine releases from the nuclear fuel cycle (Kocher 1979; Kocher 1980a). In this compilation, only the dose-rate factors for the body surface are given for electrons. A more recent compilation of dose-rate factors has become available (Kocher 1981b) that considers approximately 500 radionuclides and includes electron dose-rate factors for skin for each of the three exposure modes. Electron dose-rate factors for skin for immersion in contaminated air can also be obtained for a few radionuclides from the depth-dose distributions given by Berger (1974).

An abbreviated tabulation of dose-rate factors for air immersion and ground-surface exposure is given in Tables 8.1 and 8.2 (Kocher 1981b). The photon results are based on the calculations of Eckerman et al. (1980) described in Sect. 8.3.1.4. The radionuclides selected are those of primary importance in routine releases from the nuclear fuel cycle. The values for skin are for a single depth in tissue of 7 mg/cm^2, and the values for ground-surface exposure assume a single height of 1 m. The values for air immersion assume a density of air of 1.189×10^{-3} g/cm^3 at 20°C and 750 mm pressure. In using these results, it is important to bear in mind that the values for a given radionuclide do not include any possible contributions from radioactive daughter products. Rather, the tabulations give separate entries for all such daughters. Thus, for example, the dose-rate factors for ^{137}Cs and the short-lived daughter ^{137m}Ba are given separately. In this particular case, it is almost always reasonable to assume that ^{137m}Ba will be in equilibrium with ^{137}Cs so that the dose-rate factors for the daughter can be multiplied by the known decay branching fraction of 0.946 (Kocher 1981a) and added to the values for

Table 8.2. Dose-rate factors for ground-surface exposure

(Values are in Sv/y per Bq/cm^2)

Nuclide	Skin (electrons)	Breast (photons)	Lungs (photons)	Red marrow (photons)	Ovaries (photons)	Skeleton (photons)	Testes (photons)	Total body (photons)
^{3}H	0.0	0.0	0.0	0.0	0.0	0.0	0.0	0.0
^{14}C	0.0	0.0	0.0	0.0	0.0	0.0	0.0	0.0
^{85}Kr	2.6E-4	6.7E-7	5.4E-7	5.6E-7	4.9E-7	6.3E-7	7.3E-7	5.8E-7
^{85m}Kr	3.6E-4	6.0E-5	4.0E-5	3.8E-5	3.2E-5	5.9E-5	5.5E-5	4.4E-5
^{88}Kr	7.7E-4	5.1E-4	4.3E-4	4.3E-4	3.7E-4	4.5E-4	5.5E-4	4.5E-4
^{88}Rb	5.1E-3	1.6E-4	1.4E-4	1.4E-4	1.2E-4	1.5E-4	1.8E-4	1.5E-4
^{90}Sr	4.4E-5	0.0	0.0	0.0	0.0	0.0	0.0	0.0
^{90}Y	3.4E-3	0.0	0.0	0.0	0.0	0.0	0.0	0.0
^{95}Zr	6.9E-6	2.1E-4	1.8E-4	1.8E-4	1.6E-4	2.0E-4	2.4E-4	1.9E-4
^{95}Nb	4.7E-6	2.2E-4	1.9E-4	1.9E-4	1.7E-4	2.1E-4	2.5E-4	2.0E-4
^{99}Tc	0.0	2.3E-10	1.3E-10	9.8E-11	1.0E-10	2.3E-10	2.0E-10	1.5E-10
^{106}Ru	0.0	0.0	0.0	0.0	0.0	0.0	0.0	0.0
^{106}Rh	4.4E-3	6.1E-5	5.0E-5	5.1E-5	4.5E-5	5.7E-5	6.6E-5	5.3E-5
^{129}I	0.0	1.3E-5	2.9E-6	1.1E-6	2.1E-6	5.1E-6	8.4E-6	5.5E-6
^{131}I	5.8E-5	1.2E-4	9.4E-5	9.6E-5	8.2E-5	1.2E-4	1.3E-4	1.0E-4
^{133}I	1.2E-3	1.8E-4	1.5E-4	1.5E-4	1.3E-4	1.7E-4	2.0E-4	1.6E-4
^{131m}Xe	0.0	1.0E-5	2.7E-6	1.5E-6	2.0E-6	4.5E-6	6.7E-6	4.5E-6
^{133}Xe	0.0	2.2E-5	9.6E-6	6.0E-6	7.2E-6	1.7E-5	1.7E-5	1.2E-5
^{133m}Xe	0.0	1.8E-5	7.9E-6	6.8E-6	6.3E-6	1.2E-5	1.4E-5	1.0E-5
^{135}Xe	5.6E-4	8.6E-5	6.1E-5	6.3E-5	5.1E-5	8.2E-5	8.4E-5	6.6E-5
^{134}Cs	1.0E-4	4.5E-4	3.8E-4	3.8E-4	3.4E-4	4.2E-4	5.0E-4	4.0E-4
^{137}Cs	7.4E-5	0.0	0.0	0.0	0.0	0.0	0.0	0.0
^{137m}Ba	2.9E-4	1.8E-4	1.5E-4	1.5E-4	1.3E-4	1.6E-4	1.9E-4	1.6E-4
^{154}Eu	4.0E-4	3.5E-4	2.9E-4	2.9E-4	2.6E-4	3.2E-4	3.8E-4	3.1E-4

Table 8.2 (continued)

(Values are in Sv/y per Bq/cm^2)

Nuclide	Skin (electrons)	Breast (photons)	Lungs (photons)	Red marrow (photons)	Ovaries (photons)	Skeleton (photons)	Testes (photons)	Total body (photons)
^{210}Pb	0.0	2.3E-6	3.9E-7	1.7E-7	2.8E-7	7.1E-7	8.6E-7	6.9E-7
^{214}Pb	1.9E-4	8.4E-5	6.1E-5	6.2E-5	5.2E-5	8.0E-5	8.4E-5	6.6E-5
^{210}Bi	1.1E-3	0.0	0.0	0.0	0.0	0.0	0.0	0.0
^{214}Bi	2.1E-3	4.0E-4	3.4E-4	3.4E-4	3.0E-4	3.6E-4	4.4E-4	3.6E-4
^{210}Po	0.0	2.5E-9	2.1E-9	2.1E-9	1.9E-9	2.3E-9	2.7E-9	2.2E-9
^{222}Rn	0.0	1.2E-7	9.5E-8	9.7E-8	8.5E-8	1.1E-7	1.3E-7	1.0E-7
^{226}Ra	0.0	2.6E-6	1.7E-6	1.6E-6	1.3E-6	2.5E-6	2.3E-6	1.8E-6
^{230}Th	0.0	8.2E-7	1.0E-7	7.0E-8	7.6E-8	1.8E-7	2.3E-7	2.1E-7
^{231}Th	0.0	1.2E-5	3.0E-6	2.1E-6	2.2E-6	5.2E-6	5.7E-6	4.6E-6
^{234}Th	0.0	4.4E-6	2.0E-6	1.4E-6	1.5E-6	3.5E-6	3.1E-6	2.4E-6
^{234m}Pa	3.0E-3	3.3E-6	2.7E-6	2.7E-6	2.4E-6	3.0E-6	3.6E-6	2.9E-6
^{234}U	0.0	9.7E-7	4.7E-8	2.5E-8	3.1E-8	8.0E-8	1.9E-7	1.9E-7
^{235}U	0.0	5.9E-5	3.8E-5	3.6E-5	3.0E-5	5.6E-5	5.2E-5	4.1E-5
^{236}U	0.0	9.1E-7	3.8E-8	1.8E-8	2.4E-8	6.5E-8	1.7E-7	1.7E-7
^{238}U	0.0	8.0E-7	3.3E-8	1.5E-8	2.1E-8	5.7E-8	1.5E-7	1.5E-7
^{238}Pu	0.0	1.1E-6	3.3E-8	1.2E-8	1.9E-8	5.5E-8	2.0E-7	2.1E-7
^{240}Pu	0.0	1.1E-6	3.2E-8	1.2E-8	1.9E-8	5.4E-8	2.0E-7	2.0E-7
^{241}Pu	0.0	0.0	0.0	0.0	0.0	0.0	0.0	0.0
^{241}Am	0.0	1.5E-5	5.4E-6	2.9E-6	4.0E-6	1.0E-5	9.6E-6	7.2E-6

the parent. A similar situation applies to the ^{106}Ru-^{106}Rh decay chain. For many radioactive decay chains, however, it is not reasonable to assume equilibrium between a parent radionuclide and its radioactive daughters. In these cases (e.g., ^{88}Kr-^{88}Rb, ^{95}Zr-^{95}Nb, and the complex actinide decay chains), the dose-rate factors can be combined only after due consideration of the laws describing production and decay of radioactive daughters with time (Evans 1955) and differences in environmental behavior between the parent and its daughters.

We emphasize again the usefulness of external dose-rate factors. For a particular exposure mode, the value gives the dose rate to a particular body organ per unit concentration of a radionuclide in the environment.

8.3.4 Adequacy of Idealized Dose-Rate Factors

Any user of published external dose-rate factors based on the calculations described in Sects. 8.3.1 and 8.3.2 should bear in mind that the results are strictly applicable only to idealized exposure conditions. In particular, the contaminated atmospheric cloud or ground surface is assumed to be infinite in extent; and the radionuclide concentration is assumed to be uniform throughout the source region. The question naturally arises as to the extent to which these conditions are ever realized for actual releases of radionuclides to the environment and subsequent exposures of the population.

Since electrons have a finite range in air, the infinite-source, uniform-concentration approximation is a good one, provided the actual concentration in an atmospheric cloud or on the ground surface does not vary significantly over a distance from the receptor position equal to the electron range. The maximum electron energy emitted by any radionuclide of potential importance in radiological assessments is about 10 MeV (Kocher 1981a), and, as shown in Fig. 8.11, the corresponding range in air is less than 40 m (National Academy of Sciences 1964). For most radionuclides, in fact, the maximum electron energy is less than 4 MeV, and the corresponding range in air is less than 20 m. Thus, the idealized dose-rate factors for electrons are appropriate for actual exposures of the population if the radionuclide concentration is approximately uniform over distances of only a few tens of meters from the receptor position. It seems likely that such conditions are reasonably achieved for sources that are widely dispersed in the environment. Only for unusual exposure conditions, such as the receptor position being located close to a point release near ground level, for example, would the idealized dose-rate factors not appear to be appropriate for electrons.

As opposed to electrons, photons do not have a finite range in air, as can be seen from the specific absorbed fraction in Eq. 8.24. However, the specific absorbed fraction decreases rapidly with distance from the source. Thus, as

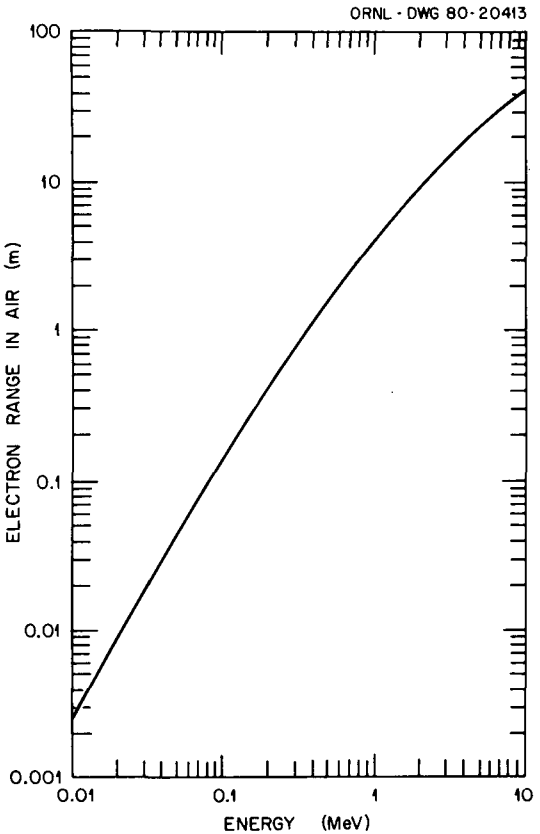

Figure 8.11. Electron range in air vs energy.

shown in Fig. 8.12, for an infinite, uniformly contaminated atmospheric cloud, about 85% of the dose at the receptor position is due to photons emitted within a distance of three mean-free-paths. The photon mean-free-path in air shown in Fig. 8.13 is less than 40 m for energies less than 50 keV but increases to about 250 m at 4 MeV and nearly 400 m at 10 MeV. Therefore, if the radionuclides emit significant numbers of high-energy photons, then the sources would have to be widely dispersed and the concentration would have to be approximately uniform over distances approaching 1 km from the receptor position in order for the infinite-source, uniform-concentration assumption to be appropriate. It is clear from this result that the use of photon dose-rate factors may result in considerable error in the estimated dose for many realistic exposure situations such as exposure to acute releases to the atmosphere or at locations close to the point of release. Unfortunately, however, more realistic calculations are considerably more difficult, as we shall discuss in Sect. 8.4.1.

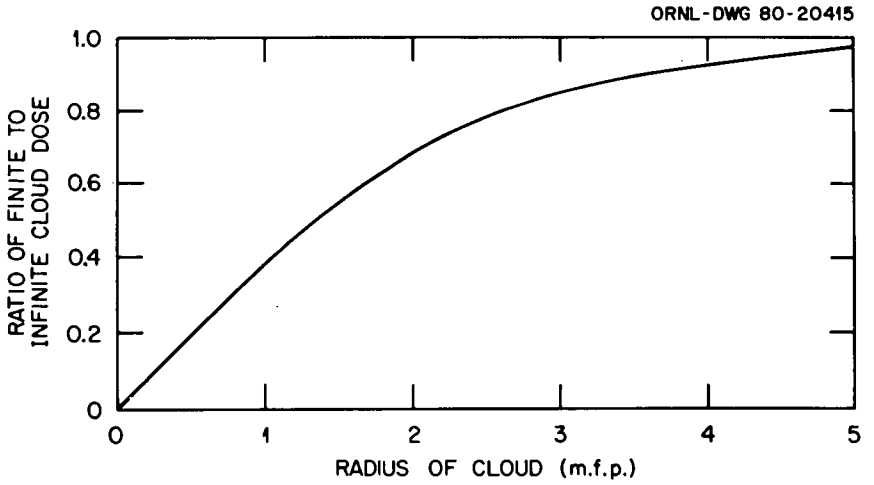

Figure 8.12. Ratio of photon dose at the center of a finite spherical atmospheric cloud with uniform source concentration to the dose in an infinite atmospheric cloud vs radius of the finite cloud in photon mean-free-paths.

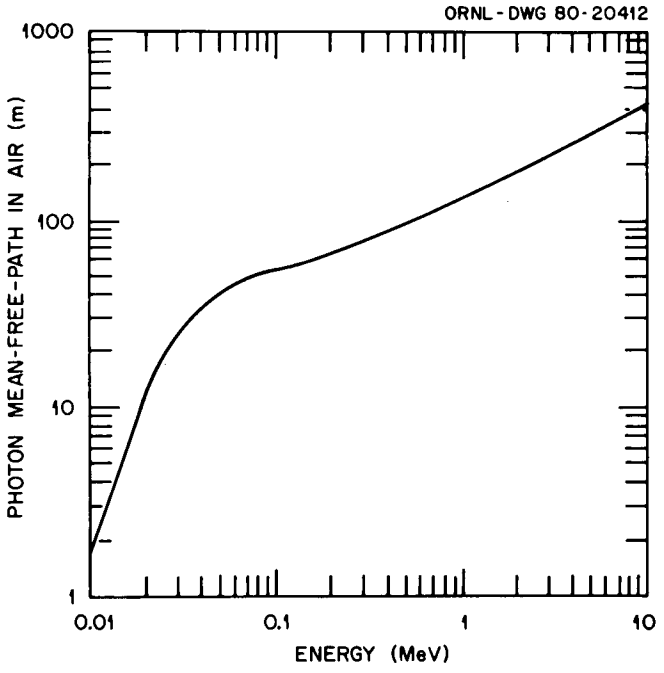

Figure 8.13. Photon mean-free-path in air vs energy.

Therefore, the idealized dose-rate factors are used quite extensively even for exposure situations for which they are not strictly applicable, particularly if the dose-rate factors are expected to provide conservative overestimates of the actual dose. The greatest care must be exercised in those cases where the dose-rate factors may seriously underestimate actual dose rates. An important example is discussed at the beginning of Sect. 8.4.

We also note that the dose-rate factors described here assume that all exposed individuals are standing outdoors on a smooth ground surface. Corrections to the dose-rate factors to account for effects such as building shielding during indoor residence, ground roughness and terrain irregularities, and penetration of radionuclides into the ground are considered in Sect. 8.4.2.

8.4 REALISTIC (DIFFICULT) CALCULATIONS

The use of dose-rate conversion factors to calculate the external dose to an exposed individual or population is idealistic because the calculations assume that the source region is effectively infinite in extent with uniform radionuclide concentration. It is obvious that such conditions are not necessarily approximated in actual exposure situations. In addition, the dose-rate factors for air immersion and ground-surface exposure assume that the exposed population spends 100% of the time outdoors on a smooth infinite ground surface. Thus, these dose-rate factors do not account for effects such as ground roughness and shielding by building walls during indoor residence.

In many exposure situations, the use of external dose-rate factors results in conservative overestimates of actual radiological impacts on the population. An example is provided by the case of exposure at locations along the centerline of a finite plume in the atmosphere following a release at ground level. There are, however, important cases for which dose-rate factors do not result in overestimates of dose. Consider, for example, exposure to an elevated cloud of photon-emitting radionuclides. Since the dose rate at ground level from the cloud is obtained by multiplying the dose-rate factor for immersion in contaminated air by the concentration in air at the receptor position, the predicted dose would be zero. This could be a severe underestimate of the actual dose from the elevated cloud.

In this section, we first give a brief discussion of the calculation of external dose for sources of finite extent with nonuniform radionuclide concentrations and then discuss the correction factors that account for the fact that man does not spend all of his time standing outdoors on a smooth ground surface.

8.4.1 Finite Sources and Nonuniform Radionuclide Concentrations

Because electrons have relatively short ranges in air, it seems reasonable in most cases to assume that the electron dose rate from immersion in contaminated air or exposure to a contaminated ground surface is adequately approxi-

mated by the external dose-rate factor multiplied by the radionuclide concentration in the air or on the ground at the location of the exposed individual. Therefore, we consider the calculation of external dose from finite sources with nonuniform concentrations for photons only.

8.4.1.1 Photon Dose Rate in Air

We first consider the calculation of absorbed dose rate in air at the location of the exposed individual since that is the initial step in obtaining estimates of organ dose rates. In general, such a calculation for a source of arbitrary spatial distribution requires recourse to the fundamental equation developed in Sect. 8.2, namely,

$$\dot{D}_\gamma^a(t) = k \sum_i f_{i\gamma} E_{i\gamma} \int_\sigma \chi(\vec{r},t) \Phi_\gamma^a(r, E_{i\gamma}) d\sigma , \tag{8.39}$$

where $\chi(\vec{r},t)$ is the radionuclide concentration, Φ_γ^a is the specific absorbed fraction in air given in Eq. 8.24 as

$$\Phi_\gamma^a(r, E_{i\gamma}) = \frac{1}{4\pi r^2} [(\mu_{en}/\rho)_a]_i B_{en}^a(\mu_{a,i} r) \exp(-\mu_{a,i} r) , \tag{8.40}$$

and the integral extends over the source region σ. As in Sect. 8.3.1.2, the dose rate at the body surface for photons can be estimated by multiplying each term in the summation in Eq. 8.39 by the ratio of the mass energy-absorption coefficient in tissue to air evaluated at the ith emitted energy.

Since the specific absorbed fraction is a function possessing spherical symmetry, it is evident that Eq. 8.39 is integrable in closed form or expressible in terms of the first-order exponential integral in Eq. 8.28 only if the radionuclide concentration χ possesses spherical or cylindrical symmetry about the receptor position or if χ can be expressed in terms of sums or differences of distributions possessing such symmetries. Otherwise, numerical integration is required to evaluate the dose rate.

For either acute or chronic releases of radionuclides to the atmosphere, the concentrations in the atmosphere and on the ground as a function of location and time are commonly estimated by use of the Gaussian plume model (Gifford 1968), which has been described in Chapter 2. It is not our purpose to discuss in detail the calculation of external dose from a Gaussian plume but rather to point out that the distributions of radionuclides in the air and on the ground obtained from this model are not amenable to closed-form solutions of Eq. 8.39. However, since the Gaussian plume model is so widely used, numerical and graphical solutions of Eq. 8.39 for such distributions have received considerable attention.

For exposure to a radioactive cloud, a considerable number of computer codes have been developed that predict the absorbed dose rate in air by numerical integration over a source region described by the Gaussian plume model (Strenge et al. 1976; Hoffman et al. 1977). Of particular interest to calculations for constant, chronic releases to the atmosphere is a vertically finite, sector-averaged Gaussian plume model recommended by the U.S. Nuclear Regulatory Commission (1977) for release heights above 80 m. The estimation of the dose rate in air for this model is described by Healy and Baker (1968) and Healy (1982).

Tabulations of dose rates from Gaussian plume atmospheric clouds as a function of release height, downwind distance, and stability class have recently become available (Brenk 1978; Rohloff et al. 1979; Lahti et al. 1981). The work of Brenk (1978) and Rohloff et al. (1979) has been described in Chapter 2. The available calculations are strictly applicable only to atmospheric radionuclides that do not deposit on the ground surface (i.e., noble gases). The calculations of Brenk are useful in that they estimate dose rates in all sectors, not just the sector in which plume travel occurs (Brenk 1978; Rohloff et al. 1979). The calculations of Lahti et al. (1981) consider dose rates only along the centerline of the plume, but the calculations are useful in radiological assessments because tabulated results are given for specific noble gas radionuclides.

Briggs (1974) has proposed a simplification of the Gaussian plume model in which the cross section of the plume perpendicular to the direction of motion is assumed to be rectangular and the radionuclide concentration in a given cross section is assumed to be uniform. This approximation is potentially useful in estimating dose rates from the plume because the dose rate from rectangular sources with uniform concentration can be evaluated (Hubbell et al. 1960; Dickson and Kerr 1975).

Calculation of the dose rate from a ground surface contaminated via the deposition of a finite Gaussian plume has received less attention than calculations for a finite atmospheric cloud. The usual procedure (U.S. Nuclear Regulatory Commission 1977) has been to incorporate plume depletion into the Gaussian plume model for atmospheric transport to estimate the concentration of activity on the ground at any location, but the dose rate at a given location is then obtained by multiplying the concentration at that position by the dose-rate factor for an infinite, uniformly contaminated ground surface developed in Sect. 8.3.2.1 and given by Eq. 8.27. Only the RSAC codes (Hoffman et al. 1977) calculate the dose rate above ground by performing a numerical integration over the Gaussian distribution of activity deposited on the ground. A graphical technique for estimating dose rates from a ground surface contaminated by a depositing Gaussian plume has been given by Healy and Baker (1968) and Healy (1982).

It is evident that there are a variety of methods available for estimating dose rates from distributions of radionuclides described by the Gaussian plume model. A user of any of the available computer codes, graphical techniques, or

tabulated results must be certain that the methods and assumptions employed therein are appropriate for the specific conditions to which they are being applied.

In general, it is obvious that Eq. 8.39 can more easily be evaluated if the source region can be divided into subregions in which the radionuclide concentration χ can be regarded as uniform. The source geometries for which Eq. 8.39 has been evaluated in a usable form if the radionuclide concentration is uniform include a line, disk, rectangle, cylindrical surface, semi-infinite volume, infinite slab, cylindrical volume, truncated right-circular cone, and spherical volume (Blizzard et al. 1968). In particular, division of the source region into a series of infinite slabs with uniform concentration parallel to the ground surface is a useful approximation for estimating the dose rate from an elevated Gaussian plume or a plume with low lid height during a chronic release to the atmosphere. The dose rate in air from an infinite slab with uniform concentration is easily obtained by integrating Eq. 8.27 for an infinite plane surface over the thickness of the slab. This method may also be useful in estimating the dose rate above ground from radionuclides uniformly dispersed into soil.

The discussion in this section is intended primarily to emphasize that the calculation of external dose rates for photons from finite sources with nonuniform concentrations is, in general, quite a difficult problem. Only in a few special cases can a result be obtained without recourse to numerical integrations involving extensive computer calculations. Such efforts are probably worthwhile only if the radionuclide concentration varies significantly over a distance of about three photon mean-free-paths from the receptor position compared with the concentration at the receptor position itself and if the use of idealized dose-rate factors would seriously underestimate expected dose rates. Otherwise, the use of the dose-rate conversion factors as developed in Sect. 8.3 is entirely reasonable.

8.4.1.2 Photon Dose Rates for Body Organs

As we have discussed in Sects. 8.3.1.4 and 8.3.2.4, organ dose rates for photons calculated by Monte Carlo techniques are available in the literature only for exposure via immersion in an infinite, uniformly contaminated source region. Therefore, approximations must be used to estimate organ doses for arbitrary exposure conditions involving finite sources and nonuniform radionuclide concentrations. The most commonly used approximations are based on the calculated dose at the body surface.

In Sect. 8.3.2.4, we calculated organ dose-rate factors for exposure to an infinite, uniformly contaminated ground surface by assuming that the ratio of organ dose to dose at the body surface for a given photon energy is equal to the ratio obtained for immersion in an infinite, uniform radioactive cloud. This approximation is used even though the energy and angular distributions of photons incident on the body surface are not the same for the two exposure modes. This is also a useful method for estimating organ doses for arbitrary exposure

conditions. While the organ doses obtained in this way are undoubtedly subject to error, depending on the photon energy and the size and location of the organ, it is expected that errors will be no more than a few tens of percent for most body organs for energies above 0.1 MeV.

Traditionally, the dose rate to total body has been the most commonly used measure of radiological impact on an individual or population from external exposure to radionuclides dispersed in the environment. The U.S. Nuclear Regulatory Commission (1977) has recommended that the dose to total body *tb* be calculated from the dose at the body surface *s* by applying a correction factor which accounts for the penetration of the photons through 5 cm of tissue. The ratio of dose rate to total body to the dose rate at the body surface for the ith photon is assumed to be given by

$$\dot{D}^{tb}_{\gamma,i}/\dot{D}^{s}_{\gamma,i} = (1+5\mu_{t,i})\exp(-5\mu_{t,i}) , \tag{8.41}$$

where

$\mu_{t,i}$ = linear attenuation coefficient for ith photon in tissue t in cm^{-1}.

That is, the penetration of photons through 5 cm of tissue is estimated by means of a simplified linear buildup factor multiplied by an exponential attenuation factor. The result in Eq. 8.41 is approximately correct for the dose rate to total body for immersion in contaminated air given in Table 8.1 [e.g., see Strenge et al. (1980)] and is assumed by the NRC to be applicable to any exposure condition. It has also been noted (Strenge et al. 1975) that except for low-energy photons, Eq. 8.41 gives the approximate dose rate for other organs of primary interest for immersion in contaminated air because many of the calculated organ dose rates do not vary by more than about 30% (e.g., see Table 8.1). By using an appropriate value for the thickness of tissue, Eq. 8.41 has also been used to estimate dose rates in organs which lie close to the body surface, such as the skin, eyes, and testes (Strenge et al. 1975). We again caution that the estimation of organ dose embodied in Eq. 8.41 is only approximate and, for a given exposure condition, may be particularly inappropriate for small, deep-lying body organs.

8.4.2 Corrections to Dose-Rate Factors

The dose-rate factors for immersion in contaminated air and exposure to a contaminated ground surface developed in Sect. 8.3 assume that man spends 100% of the time outdoors standing on a smooth infinite plane. In this section, we briefly consider corrections to these idealized dose-rate factors to account for effects such as shielding by buildings during indoor residence, ground roughness and terrain irregularities, and penetration of radionuclides into the ground. We again consider these effects for photons only.

The corrections for the various effects described above are applied as multiplicative factors to the idealized dose-rate factors calculated in Sect. 8.3 or to

the more sophisticated calculations described in Sect. 8.4.1. The dose correction factors are usually less than one. Therefore, if they are excluded from external dose calculations, the resulting dose estimates should provide conservative overestimates of actual doses.

8.4.2.1 Building Shielding Effects

Man's residence time inside buildings will normally result in a reduction in the external dose rate compared with no shielding in an outdoor environment. Analyses of building shielding effects for environmental dose assessments have been presented by several authors (Healy and Baker 1968; Healy 1982; Burson and Profio 1977; Kocher 1980b). Building shielding is specified by a quantity called the dose reduction factor, which is defined as the ratio of the dose rate inside a building to the corresponding dose rate outdoors. The dose reduction factor is thus usually less than one.

Immersion in contaminated air. In general, the dose reduction factor for immersion in contaminated air depends primarily on the photon energy and the wall thickness of the building structure. For typical family dwellings, the predicted dose reduction factors are usually within a factor of two of the value 0.5 recommended by the U.S. Nuclear Regulatory Commission (1977) for generic population dose assessments, provided that significant numbers of photons are emitted with energies above a few hundred keV (Kocher 1980b). Thus, the NRC default value is probably an adequate approximation for many releases of radioactivity to the atmosphere. We note one example to the contrary, however, which is of current interest. The primary radionuclide released during the Three Mile Island accident is believed to be ^{133}Xe (Battist et al. 1979), for which the emitted photon energies are 81 keV or less (Kocher 1981a). In this case, the estimated dose reduction factor for a typical family dwelling may be as low as 0.06, which is an order of magnitude less than the value recommended by the NRC (Kocher 1980b).

Example 8.4. In Sect. 8.3.1, we performed the various steps in a calculation of an organ dose-rate factor for exposure to an atmospheric cloud of ^{85}Kr. For ovaries, the result was 0.0024 Sv/y per Bq/cm^3. For a receptor position indoors, application of the generic dose reduction factor of 0.5 recommended by the U.S. Nuclear Regulatory Commission (1977) gives a dose-rate factor of $(0.0024 \times 0.5) = 0.0012$ Sv/y per Bq/cm^3. If we assume, for example, that an exposed individual spends 90% of the time indoors, the appropriate dose-rate factor is $(0.0024 \times 0.1) + (0.0012 \times 0.9) = 0.0013$ Sv/y per Bq/cm^3. [End of example]

Burson and Profio (1977) have given representative dose reduction factors for a cloud source for different types of structures. Values range from 1.0 for transportation vehicles to less than 0.2 for large office or industrial buildings at locations away from doors and windows. A user of these results should be

aware, however, that they were obtained for a particular photon spectrum—namely, the spectrum which would result from a hypothetical nuclear reactor accident involving core meltdown and containment rupture. Therefore, as we noted above, these dose reduction factors may not be applicable to cloud sources which primarily emit photons at energies less than a few hundred keV. Methods for calculating dose reduction factors for arbitrary source spectra, based on specific absorbed fractions, are discussed by Kocher (1980b).

Exposure to a contaminated ground surface. The study of building shielding effects for radionuclides deposited on the ground has been of interest for many years because of its civil defense applications. A detailed computational methodology called the engineering manual method has been developed to predict building shielding provided by any type of structure against surface-deposited fallout from a nuclear weapon detonation (Spencer 1962; U.S. Office of Civil Defense 1964). Burson and Profio (1977) have recently applied the engineering manual method to the calculation of shielding effects for transportation vehicles and a variety of building structures for fallout from a nuclear reactor accident. Representative dose reduction factors range from about 0.7 for automobiles to as low as 0.005 for the basement of large, multistory structures at locations away from doors and windows.

The engineering manual method can be difficult to apply routinely to radiological assessments involving arbitrary sources of radionuclides deposited on the ground and on inside and outside building surfaces. As an alternative, methods for estimating building shielding effects for deposited sources based on the photon specific absorbed fraction have recently been developed (Kocher 1980b). The calculations account for the shielding from activity deposited on the ground outside and on outside surfaces of the building and activity deposited on inside building surfaces. The resulting dose reduction factors for ground sources are usually comparable in magnitude to values for a radioactive cloud for the same photon spectrum. We note again that calculations based on the concept of the specific absorbed fraction have the advantage that results for any given photon spectrum are relatively easily obtained (Kocher 1980b).

Other considerations. Dose reduction factors from building shielding usually assume that the exposed individual indoors is standing at the center of the building on the ground floor. According to Burson and Profio (1977), the dose reduction factor for ground surface exposure is reduced further by approximately a factor of two-thirds for a location in the corner of a building. For exposure to a cloud source, Healy and Baker (1968) and Healy (1982) report that the dose reduction factor at the wall of a hemispherical building of a given radius is one-half of the value at the center of a building of twice the radius. For many single-story buildings, the roof provides very little shielding compared with the walls. Thus, for immersion in contaminated air, the overall dose reduc-

tion factor can be estimated as a weighted average by considering the fraction of the solid angle from the center of the building subtended by the roof and walls and applying the appropriate dose reduction factor to each part (Healy and Baker 1968; Healy 1982).

For populations in urban environments, a potentially important reduction in external dose is provided by the mutual shielding of buildings in close proximity to one another. Mutual shielding of buildings has not been considered in detail in the literature. In a recent calculation (Auxier et al. 1979), the simple assumption is made that neighboring buildings provide complete shielding from an atmospheric cloud and that the field of view inside a building is reduced by about one-half by the neighboring buildings. Thus, the presence of nearby buildings is assumed to further reduce the external dose rate by a factor of two.

8.4.2.2 Terrain Roughness and Ground Penetration Effects

The calculation of dose-rate factors from a contaminated ground surface given in Sect. 8.3.2 assumes that the ground is a smooth impenetrable surface. Realistic dose-rate estimates should account for ground roughness and terrain irregularities and for the penetration of deposited radionuclides into the ground.

Ground roughness and terrain irregularities provide a kind of natural shielding against external exposure from a contaminated ground surface. Estimated dose reduction factors for a variety of surfaces are given by Burson and Profio (1977). The values range from 1.0 for paved areas to as low as 0.5 for a deeply plowed field.

Example 8.5. Suppose a ground surface is uniformly contaminated with ^{131}I with a concentration of 1 pCi/cm^2. From Table 8.2, the photon dose rate to total body, assuming a smooth ground surface, is $(1.0 \times 10^{-4}$ Sv/y per Bq/cm$^2)(0.037$ Bq/pCi$) = 3.7$ μSv/y. If the ground surface is a deeply plowed field, then the dose reduction factor is about 0.5 and the dose rate to total body is $(3.7 \times 0.5) = 1.9$ μSv/y. If we also assume that the exposed individual is indoors and that the dose reduction factor is 0.5 from building shielding, the dose rate to total body is $(3.7 \times 0.5 \times 0.5) = 0.9$ μSv/y. [End of example]

Penetration of radionuclides into the ground reduces the external dose rate above ground because of the additional shielding provided by the soil. A proper treatment of these effects is quite difficult because the penetration of radionuclides into the ground depends on many factors, such as the element and its chemical form, the amount of rainfall, and the properties of the soil. In addition, the amount of shielding provided by a given depth of soil depends on the photon energy. Based on available data for a few radionuclides, the Reactor Safety Study (U.S. Nuclear Regulatory Commission 1975) recommends that

the dose rate above ground is reduced with time compared with the dose rate from an impenetrable surface according to the weathering function

$$f_w(t) = 0.63\exp(-1.13t) + 0.37\exp(-0.0075t), \qquad (8.42)$$

where the time t is given in years. This correction factor is applied to the dose-rate factor for ground surface exposure given in Eq. 8.27. If the radionuclides can be regarded as uniformly mixed into the soil to a certain depth (defined, for example, by the depth of a plowed field), then the source can be treated as an infinite, uniformly contaminated slab and the known dose-rate factor for this configuration can be applied (Blizzard et al. 1968).

8.5 SUMMARY

The major emphasis of this presentation has been directed toward the concept of a dose-rate conversion factor for external exposure to photons and electrons and its application to the estimation of individual or population dose following routine or accidental releases of radionuclides to the atmosphere. Dose-rate conversion factors are very useful for exposure situations in which the radionuclide concentration can be regarded as uniform within a certain distance of the exposed individuals. This distance is approximately equal to the electron range or to three photon mean-free-paths for the medium through which the radiations are transmitted, which is usually air. If this approximation is valid, the external dose rate is simply obtained by multiplying the known radionuclide concentration in the environment (e.g., in the atmosphere or on the ground) by the dose-rate factors for the organs of interest for the particular radionuclides. These dose-rate factors are available in published compilations.

A brief discussion has been given of calculations of external dose for photons for exposure situations in which the radionuclide concentration cannot be regarded as uniform and infinite in extent. Such calculations are based on the concept of the point-isotropic specific absorbed fraction. As a general rule, calculations for particular exposure situations of interest require large computers and sophisticated techniques of numerical integration. Although computer codes are generally available for this purpose, these situations may require special treatment on a case-by-case basis.

Finally, we have briefly discussed correction factors to calculated external dose rates to account for building shielding during indoor residence, ground roughness and terrain irregularities, and penetration of radionuclides into the ground. These effects may result in significant reductions in external dose for realistic population dose assessments.

In considering the need for relatively sophisticated external dose calculations (e.g., using the Gaussian plume model), rather than the easily used dose-rate factors described here, it is often worth bearing in mind that for many

exposure situations the uncertainty in estimated doses may be dominated by the uncertainty in the assumed radionuclide concentrations in the environment, rather than by the potential uncertainties resulting from application of the dose-rate factors themselves.

8.6 PROBLEMS

1. Derive Eqs. 8.9 and 8.10.
2. The dose-rate factors in air in Eqs. 8.9 and 8.10 are inversely proportional to the density of air. What happens as the density approaches zero? Using the definition of absorbed dose, convince yourself that this is a reasonable result for an infinite, uniformly contaminated source region.
3. Derive Eqs. 8.25 and 8.27.
4. Using data available in the *Radiological Health Handbook* (U.S. Department of Health, Education, and Welfare 1970), plot the photon specific absorbed fraction in Eq. 8.24 as a function of distance from a point source in an infinite water medium for a few photon energies between 10 keV and 10 MeV. (Be careful with units.) What is the approximate functional dependence of the specific absorbed fraction with distance? Try to verify the normalization condition in Eq. 8.3, either by crude numerical integration of your plots or by using Eq. 8.26 for the buildup factor and values of C_a and D_a obtained from least-squares fits to the data.
5. Derive Eqs. 8.30 and 8.31.
6. Using data available in the literature [e.g., National Academy of Sciences (1964)], what is the minimum electron energy emitted in an atmospheric cloud that can deliver a dose to radiosensitive tissues of the skin? What is the minimum electron energy which can reach a height of 1 m above a contaminated ground surface? What is the minimum electron energy which can irradiate the radiosensitive tissues of the skin at a height of 1 m above a contaminated ground surface? You may assume that the radiosensitive tissues of the skin lie at a depth of 7 mg/cm^2 below the body surface and that tissue has the same mass stopping power as water. Assume a density of air of 1.2×10^{-3} g/cm^3 and a density of tissue of 1.12 g/cm^3. (Answers: 0.067 MeV, 0.35 MeV, 0.37 MeV.)
7. (a). Beginning at time zero, a nuclear facility releases ^{131}I and ^{133}Xe such that a constant air concentration of 0.01 pCi/cm^3 for each radionuclide is maintained. Using data in Table 8.1, estimate the photon dose rate for total body and electron dose rate for skin from each nuclide received by an individual standing on the ground surface in the cloud. (Answers: 0.18 mSv/y and 0.10 mSv/y for ^{131}I; 0.016 mSv/y and 0.030 mSv/y for ^{133}Xe.) (b). If the deposition velocity of ^{131}I is 1 cm/s, plot the photon dose rate for total body from the contaminated ground surface as a function of time for a period of one year using data in Table 8.2 and calculate the total dose received over that time. [Solution to part (b): Let χ_a and χ_s denote

air and surface concentrations of ^{131}I, respectively. The activity on the ground surface increases with time due to deposition, but decreases with time due to radioactive decay. Thus χ_s obeys the differential equation $d\chi_s/dt = \chi_a v_d - \lambda^r \chi_s$, where v_d is the deposition velocity, $\chi_a v_d$ is the deposition rate, λ^r is the radioactive decay constant ($\ln 2/T_{1/2}$, where $T_{1/2}$ is the half-life), and $\lambda^r \chi_s$ is the removal rate of activity from the surface due to radioactive decay. For the given initial surface concentration [$\chi_s(t = 0) = 0$], solve this equation and show that χ_s as a function of time is given by $\chi_s(t) = (\chi_a v_d/\lambda^r)[1 - \exp(-\lambda^r t)]$. The dose received over a given time interval is proportional to the time-integral of χ_s over that period, which is called the exposure. Using the ^{131}I half-life of 8.04 d, show that the exposure over the first year is 9.7×10^3 pCi-y/cm^2. Application of the dose-rate factor in Table 8.2 then gives a dose for one year's exposure of 36 mSv.]

8. Try to derive the equation for the photon dose-rate factor in air at the ground surface for an infinite, uniformly contaminated slab of air of thickness x and height z above ground for the lower boundary of the slab. For simplicity, assume that only a single photon of energy E_γ is emitted. [Hint: Derivatives of exponential integrals obey the equation $d\tilde{E}_n(u)/du = -\tilde{E}_{n-1}(u)$ for $n > 1$.] By ignoring the terms depending on the photon buildup factor in air, check your equation against the result given by Blizzard et al. (1968).
9. Consider a unit activity of ^{131}I ($T_{1/2} = 8.04$ d) on the ground surface at time zero. Construct a plot showing the decrease in activity with time, assuming first that radioactive decay is the only loss mechanism, then assuming no radioactive decay but assuming the weathering function given by Eq. 8.42, and finally assuming both decay and weathering. Which of the two processes is more effective in reducing the surface activity with time? Why? Repeat the analysis for a unit concentration of ^{137}Cs ($T_{1/2} = 30.17$ y).
10. In problem 7 above, we derived an equation for the ground surface concentration of a radionuclide as a function of time, given a constant air concentration and deposition velocity and assuming that radioactive decay was the only mechanism for removal of activity. Try to derive a similar equation assuming removal of activity according to the weathering function in Eq. 8.42 as well as radioactive decay. (This is not an easy problem. The correct answer is not the equation for the surface concentration assuming radioactive decay only multiplied by the weathering function. Also, because the weathering function is a two-component exponential function, the surface concentration χ_s is not described by a single differential equation. Rather, χ_s has two components that are additive, and each component obeys a differential equation containing a single rate constant for one term in the weathering function.) [Answer: $\chi_s(t) = \chi_a v_d \{[0.63/(1.13 + \lambda^r)][1 -$

$\exp(-1.13 - \lambda^r)t] + [0.37/(0.0075 + \lambda^r)][1 - \exp(-0.0075 - \lambda^r)t]\}$.]

11. Try to derive the surface concentrations in problems 7 and 10 above by means of an integral equation. (Hint: At any time t after the beginning of the release, the surface concentration due to the activity deposited at a previous time t' is the amount of activity deposited over an incremental time interval $\Delta t'$ at that time modified by the function describing loss due to radioactive decay only or to decay and weathering over the time interval $t - t'$. The surface concentration at time t is then the sum of the contributions over all previous times t'.)

REFERENCES

Auxier, J. A., Berger, C. D., Eisenhauer, C. M., Gesell, T. F., Jones, A. R., and Masterson, M. E. 1979. *Report of the Task Group on Health Physics and Dosimetry*, President's Commission on the Accident at Three Mile Island.

Battist, L., Buchanan, J., Congel, F., Nelson, C., Nelson, M., Peterson, H., and Rosenstein, M. 1979. *Population Dose and Health Impact of the Accident at the Three Mile Island Nuclear Station (A Preliminary Assessment for the Period March 28 Through April 7, 1979)*, U.S. Government Printing Office.

Beck, H., and de Planque, G. 1968. *The Radiation Field in Air Due to Distributed Gamma-Ray Sources in the Ground*, HASL-195, Health and Safety Lab., U.S. Atomic Energy Commission.

Berger, M. J. 1968. *J. Nucl. Med. Suppl.* No. 1, 15.

Berger, M. J. 1973. *Improved Point Kernels for Electron and Beta-Ray Dosimetry*, NBSIR 73-107, Natl. Bur. Standards, U.S. Department of Commerce.

Berger, M. J. 1974. *Health Phys.* **26**, 1.

Blizzard, E. P., Foderaro, A., Goussev, N. G., and Kovalev, E. E. 1968. "Extended Radiation Sources (Point Kernel Integrations)," p. 363 in *Engineering Compendium on Radiation Shielding*, vol. 1, ed. by R. G. Jaeger, Springer-Verlag, New York.

Brenk, H. D. 1978. *Ein anwendungsbezogenes Konzept zur Berechnung der Umweltbelastung durch Abluftemissionen kerntechnischer Anlagen für Standorte in der Bundesrepublik Deutschland*, Jül–1485, Kernforschungsanlage Jülich GmbH, Jülich, Federal Republic of Germany.

Briggs, G. A. 1974. "Diffusion Estimation for Small Emissions," p. 83 in *Environmental Research Laboratories 1973 Annual Report*, ATDL-106, Atmospheric Turbulence and Diffusion Lab., U.S. Department of Commerce, Oak Ridge, Tenn.

Burson, Z. G., and Profio, A. E. 1977. *Health Phys.* **33**, 287.

Dickson, H. W., and Kerr, G. D. 1975. *Health Phys.* **29**, 131.

Dillman, L. T. 1974. *Health Phys.* **27**, 571.

Dillman, L. T. 1980. *EDISTR—A Computer Program to Obtain a Nuclear Decay Data Base for Radiation Dosimetry*, ORNL/TM-6689, Oak Ridge Natl. Lab.

Dillman, L. T., and Von der Lage, F. C. 1975. *Radionuclide Decay Schemes and Nuclear Parameters for Use in Radiation Dose Estimation*, MIRD Committee Pamphlet 10, Society of Nuclear Medicine, New York.

Eckerman, K. F., Kerr, G. D., and Raridon, R. 1980. *Health Phys.* **39**, 1054.

Evans, R. D. 1955. *The Atomic Nucleus*, Addison-Wesley, Reading, Mass.

Fitzgerald, J. J., Brownell, G. L., and Mahoney, F. J. 1967. *Mathematical Theory of Radiation Dosimetry*, Gordon and Breach, New York.

Gifford, F. A., Jr. 1968. "An Outline of Theories of Diffusion in the Lower Layers of the Atmosphere," p. 65 in *Meteorology and Atomic Energy 1968*, ed. by D. H. Slade, U.S. Atomic Energy Commission.

Healy, J. W. 1982. "Radioactive Cloud-Dose Calculations," in *Atmospheric Sciences and Power Production 1982*, U.S. Department of Energy, in press.

Healy, J. W., and Baker, R. E. 1968. "Radioactive Cloud-Dose Caculations," p. 301 in *Meteorology and Atomic Energy 1968*, ed. by D. H. Slade, U.S. Atomic Energy Commission.

Hoffman, F. O., Miller, C. W., Schaeffer, D. L., and Garten, C. T., Jr. 1977. *Nucl. Saf.* **18**, 343.

Hubbell, J. H., Bach, R. J., and Lamkin, J. C. 1960. *J. Res. Natl. Bur. Stand.* **64C**, 131.

Kerr, G. D. 1980. *Health Phys.* **39**, 3.

Kocher, D. C. 1977. *Nuclear Decay Data for Radionuclides Occurring in Routine Releases from Nuclear Fuel Cycle Facilities*, ORNL/NUREG/TM-102, Oak Ridge Natl. Lab.

Kocher, D. C. 1979. *Dose-Rate Conversion Factors for External Exposure to Photon and Electron Radiation from Radionuclides Occurring in Routine Releases from Nuclear Fuel Cycle Facilities*, NUREG/CR-0494, ORNL/NUREG/TM-283, Oak Ridge Natl. Lab.

Kocher, D. C. 1980a. *Health Phys.* **38**, 543.

Kocher, D. C. 1980b. *Nucl. Technol.* **48**, 171.

Kocher, D. C. 1981a. *Radioactive Decay Data Tables*, DOE/TIC-11026, U.S. Department of Energy.

Kocher, D. C. 1981b. *Dose-Rate Conversion Factors for External Exposure to Photons and Electrons*, NUREG/CR-1918, ORNL/NUREG-79, Oak Ridge Natl. Lab.

Kocher, D. C., and Eckerman, K. F. 1981. *Health Phys.* **40**, 467.

Lahti, G. P., Hubner, R. S., and Golden, J. C. 1981. *Health Phys.* **41**, 319.

Loevinger, R., and Berman, M. 1968. *J. Nucl. Med. Suppl.* No. 1, 7.

Martin, M. J. 1976. *Nuclear Decay Data for Selected Radionuclides*, ORNL-5114, Oak Ridge Natl. Lab.

National Academy of Sciences–National Research Council. 1964. *Studies in Penetration of Charged Particles in Matter*, Publication 1133.

National Council on Radiation Protection and Measurements. 1978. *A Handbook of Radioactivity Measurements Procedures*, Report 58.

O'Brien, K. 1980. "Human Dose from Radiation of Terrestrial Origin," p. 1163 in *Natural Radiation Environment III*, vol. 2, CONF-780422, U.S. Department of Energy.

O'Brien, K., and Sanna, R. 1976. *Health Phys.* **30**, 71.

Poston, J. W., and Snyder, W. S. 1974. *Health Phys.* **26**, 287.

Rohloff, F., Brunen, E., Brenk, H. D., Geiss, H., and Vogt, K. J. 1979. *LIGA-Ein Program zur Berechnung der lokalen individuallen Gammasubmersionsdosis durch Abluftfahnen*, Jül–1577, Kernforschungsanlage Jülich GmbH, Jülich, Federal Republic of Germany.

Ryman, J. C., Faw, R. E., and Shultis, J. K. 1981. *Health Phys.* **41**, 759.

Spencer, L. V. 1962. *Structure Shielding Against Fallout Radiation from Nuclear Weapons*, National Bureau of Standards Monograph 42, Natl. Bur. Standards, U.S. Department of Commerce.

Strenge, D. L., Watson, E. C., and Houston, J. R. 1975. *SUBDOSA—A Computer Program for Calculating External Doses from Accidental Atmospheric Releases of Radionuclides*, BNWL-B-351, Battelle-Northwest Lab., Richland, Wash.

Strenge, D. L., Watson, E. C., and Droppo, J. G. 1976. *Review of Calculational Models and Computer Codes for Environmental Dose Assessment of Radioactive Releases*, BNWL-B-454, Battelle-Northwest Lab., Richland, Wash..

Strenge, D. L., Acharya, S., Baker, D. A., Droppo, J. G., McPherson, R. B., Napier, B. A., Nieves, L. A., Soldat, J. K., and Watson, E. C. 1980. *Models Selected for Calculation of Doses, Health Effects, and Economic Costs Due to Accidental Radionuclide Releases from Nuclear Power Plants*, NUREG/CR-1021, PNL-3108, Battelle Pacific Northwest Lab., Richland, Wash.

Trubey, D. K. 1966. *A Survey of Empirical Functions Used to Fit Gamma-Ray Buildup Factors*, ORNL/RSIC-10, Oak Ridge Natl. Lab.

Trubey, D. K., and Kaye, S. V. 1973. *The EXREM III Computer Code for Estimating External Radiation Doses to Populations from Environmental Releases*, ORNL/TM-4322, Oak Ridge Natl. Lab.

U.S. Department of Health, Education, and Welfare. 1970. *Radiological Health Handbook.*

U.S. Nuclear Regulatory Commission. 1975. *Reactor Safety Study: An Assessment of Accident Risks in U.S. Commercial Nuclear Power Plants, Appendix VI. Calculation of Reactor Accident Consequences*, WASH-1400.

U.S. Nuclear Regulatory Commission. 1977. *Calculation of Annual Doses to Man from Routine Releases of Reactor Effluents for the Purpose of Evaluating Compliance with 10 CFR Part 50, Appendix I*, Regulatory Guide 1.109.

U.S. Office of Civil Defense. 1964. *Shelter Design and Analysis*, vol. 1, OCD-TR-20-(Vol. 1).

Wu, C. S., and Moskowski, S. A. 1966. *Beta Decay*, Interscience Publishers, New York.

9 Models for Special-Case Radionuclides

By J. E. TILL*

9.1 INTRODUCTION

Certain radionuclides, because of their ubiquitous nature and persistence in the environment, are given special consideration in radiological assessment. These radionuclides are ^{3}H, ^{14}C, ^{85}Kr, and ^{129}I. Each of these isotopes is transported beyond the region normally considered in the assessment of individual or population dose; however, their environmental half-lives are long, thus presenting the potential for very low exposures to large regional or global populations. Special models called global cycling models are used to evaluate this exposure.

For routine assessments of individual and population dose near the point of release, ^{85}Kr and ^{129}I are evaluated using the models described in earlier chapters; however, environmental radiological assessment of ^{3}H and ^{14}C is performed using methods different from those described in earlier chapters. This chapter discusses the special methods used to estimate the dose from ^{3}H and ^{14}C and the global cycling models used to evaluate the long-term impact of ^{3}H, ^{14}C, ^{85}Kr, and ^{129}I.

9.2 SPECIFIC ACTIVITY MODELS

Because of their ubiquitous character after being released to the environment, ^{3}H and ^{14}C are evaluated using specific activity methodology once their concentration in the atmosphere is known. Both undergo rapid and nearly uniform mixing among their stable element counterparts in nature.

*Radiological Assessments Corporation, Neeses, South Carolina.

Tritium is assumed to be transferred in environmental media and incorporated into the body through its association with water as ^3HOH (tritiated water). Carbon-14 follows the conversion of CO_2, becoming fixed in vegetation and reaching man primarily through the ingestion pathway.

The specific activity methodology for calculating dose from ^3H and ^{14}C assumes that an equilibrium state exists between their concentrations in the atmosphere (or water), food products, and body tissues, for a specified location. Because of the minimum number of parameters used in this approach (since transfer coefficients are eliminated), there is less uncertainty introduced into the dose calculations. If it is assumed that the individual permanently resides at the point where the atmospheric concentration is highest, an upper estimate of dose is established. However, if no account is taken of possible dilution of ^3H and ^{14}C in tissue due to ingestion of food products grown in areas where the atmospheric concentration is less, an unrealistically high prediction of dose may result. Thus, specific activity models need sufficient flexibility to permit insertion of site-specific data. Both ^3H and ^{14}C are important contributors to the total dose equivalent resulting from routine releases from certain types of reactors and fuel reprocessing facilities. Therefore, they are given individual consideration in this chapter.

9.3 TRITIUM

9.3.1 Evans' Specific Activity Model

Numerous methodologies have been proposed to calculate the dose from tritium released to the environment. Most of these methodologies are variations of an original specific activity approach first proposed by Evans (1969) following analyses for tritium in deer. Long-term exposure to tritium results in significant incorporation of tritium in organic molecules in body tissues, in addition to mixing of ^3HOH in body water. Based upon his experimental data, Evans calculated an upper limit of the dose that individuals could receive from chronic exposure to tritium assuming body hydrogen is uniformly labeled. A reference man of 70 kg contains 7 kg of hydrogen, approximately 4.8 kg of which is in body water and 2.2 kg in organic molecules (ICRP 1975). If the concentration in body water is known and it is assumed that organic molecules in the body are labeled to the same extent as body water, a body burden can be calculated.

Example 9.1. Calculate the dose rate to a reference (70-kg) man from tritium, assuming uniform labeling of body water and organic molecules and assuming a body water concentration of 1 μCi/L:

$$\frac{1\ \mu\text{Ci}}{\text{L } H_2O} \times \frac{1\ \text{L } H_2O}{\text{kg } H_2O} \times \frac{18\ \text{kg } H_2O}{2\ \text{kg } {}^1H} \times \frac{7.0\ \text{kg } {}^1H}{\text{reference man}} = 63\ \mu\text{Ci}\,. \quad (9.1)$$

Assuming a quality factor of 1.0 for beta particles from tritium, this body burden results in an annual dose rate of

$$\frac{63\ \mu Ci}{7\times10^4\ g}\times\frac{3.7\times10^4\ dis}{s\cdot\mu Ci}\times\frac{3.2\times10^7\ s}{y}\times\frac{0.006\ MeV}{dis}$$
$$\times\ \frac{1.6\times10^{-6}\ ergs}{MeV}\times\frac{10^3\ mrem}{100\ ergs/g}\ =\ 102\ mrem/y. \qquad (9.2)$$

[End of Example 9.1]

Evans reported further that his data indicated a labeling fraction in organic molecules to be between 0.62 and 1.0 in deer tissue, depending upon the specific organ to be considered, with a weighted average fraction of 0.85 to 1.0 extrapolated to reference man. (A labeling fraction of 1.0 indicates that the ^3H to ^1H ratios are equal when comparing body water and organic components.) Assuming that tritium in body water is uniformly distributed and assuming a labeling fraction of 0.85 for organically bound hydrogen in the body, one calculates a body burden of

$$\frac{[4.8\ kg\ +\ (0.85)(2.2\ kg)]}{7.0\ kg}\times 63\ \mu Ci\ =\ 60\ \mu Ci\ , \qquad (9.3)$$

which results in an annual dose of

$$\frac{60\ \mu Ci}{63\ \mu Ci}\times 102\ mrem\ =\ 97\ mrem\ . \qquad (9.4)$$

This annual dose of 97 mrem resulting from chronic exposure to a tritium concentration of 1 μCi/L in body water can be used to estimate the dose resulting from long-term exposures in the environment. Assuming an atmospheric concentration of tritium of 1 pCi/m^3, a moisture content of 6 g H_2O/m^3 of air, and a concentration of tritium in an individual equal to that in the atmosphere, the following annual dose is calculated:

$$\frac{1\ pCi}{m^3}\times\frac{m^3}{6\ g\ H_2O}\times\frac{97\ mrem}{\mu Ci/L}\times\frac{10^3\ g\ H_2O/L}{10^6\ pCi/\mu Ci}\ =\ 1.6\times10^{-2}\ mrem\ . \qquad (9.5)$$

If it is assumed that the concentrations of tritium in the atmosphere, water, all biota, and humans are equal at the site being evaluated, then this method of calculating dose is called the specific activity approach.

Unfortunately, it is not realistic to assume that the concentrations of tritium in body tissue and environmental media are equal for a given location because of contributions to the total water content of the body from sites where the specific activity of tritium may be lower (or higher) than the point of interest. Therefore, the specific activity approach described above must be modified to account for this important influence.

9.3.2 NCRP Model

The National Council on Radiation Protection and Measurements (NCRP 1979) proposed a model for calculating dose from tritium when the concentration of tritium is known in the water, food products, and air to which the individual is exposed. This technique for estimating dose applies to an equilibrium situation only and is not recommended for evaluating exposures resulting from pulse releases of tritium. The NCRP methodology assumes that the dose from tritium via the various pathways of exposure depends upon the relative contributions to the total water intake of a reference individual (Table 9.1).

Table 9.1. Contributions to total water intake of a reference individual

Source	Intake[a] (L/d)	Fraction
Drinking water	1.22	0.41
Food products[b]	1.27	0.42
Oxidation of food[c,d]	0.29	0.10
Inhalation[e]	0.13	0.04
Skin absorption	0.09	0.03
Total	3.00	1.00

[a]Values taken from National Council on Radiation Protection and Measurements 1979. *Tritium in the Environment,* NCRP Report No. 62, Washington, D.C.

[b]In food 0.72 L/d; in milk 0.53 L/d; in juice 0.02 L/d. Values taken from NCRP Report No. 62.

[c]Oxidation of food 0.25 L/d; oxidation of milk 0.04 L/d; oxidation of juice 0.002 L/d. Values taken from NCRP Report No. 62.

[d]This represents tritium entering the body as organically bound hydrogen which is oxidized to ^3HOH during metabolism.

[e]Assuming an absolute humidity of 6 g H_2O/m^3 in air.

The annual dose per unit concentration for 3.0-L/d water intake is described by the following expression:

$$D = (1.22C_w + 1.27C_{f1} + 0.29C_{f2} + 0.22C_a)\frac{1}{3.0} \times \mathrm{DRF}\,, \qquad (9.6)$$

where

D = annual dose (mrem),

C_w = concentration of tritium in drinking water (pCi/L),

C_{f1} = concentration of tritium in water in food (pCi/L),

C_{f2} = concentration of tritium oxidized to water upon metabolism of food (pCi/L),

C_a = concentration of tritium in atmospheric water (pCi/L),

DRF = dose rate factor (mrem/y per pCi/L).

The dose rate factor (DRF) used by the NCRP is 95×10^{-6} (mrem·L)/(pCi·y). The dose rate factor reported here is defined as the committed dose per integrated intake, or the equilibrium dose rate in millirems per year per constant intake concentration (pCi/L).

In order to calculate the dose from a chronic exposure to 1 pCi/m^3 of tritium in the atmosphere using the methodology proposed by the NCRP, several assumptions are needed. First, it is assumed that the atmospheric humidity is 6 g H_2O/m^3. The second assumption is that the concentrations of tritium in drinking water, food, and air are equal and as given by

$$\frac{1\ \text{pCi}}{\text{m}^3} \times \frac{\text{m}^3}{6\ \text{g}\ H_2O} = 1.7\times10^{-1}\ \text{pCi/g}\ H_2O$$

$$= 1.7\times10^{-1}\ \text{pCi/mL}\ H_2O\ . \qquad (9.7)$$

Then, from Eq. 9.6, the dose is given by

$$\left[(1.22+1.27+0.29+0.22)(1.7\times10^{-1}\ \text{pCi/mL}\ H_2O)\right] \times \frac{1}{3.0} \times$$

$$\times 10^3 \frac{\text{mL}}{\text{L}} \times 95\times10^{-6} \frac{\text{mrem/y}}{\text{pCi/L}} = 1.6\times10^{-2}\ \text{mrem/y}\ . \qquad (9.8)$$

This result is identical to the value calculated using the specific activity approach of Evans. The primary reason that the two results are equal is that in this example, it is assumed that the activity concentration of tritium in the water content of air is the same as that in drinking water and foodstuffs. This assumption is not always valid for chronic exposure conditions. One example occurs when the source of drinking water is relatively uncontaminated (for example, coming from a deep well), and thus the concentration of tritium in water, C_w, is significantly less than that in air, C_a. Another example is the case in which food products are grown away from the point being evaluated where the concentration of tritium in the air is lower.

Example 9.2. Calculate the annual dose rate to an individual who resides at a point where the atmospheric concentration of tritium is 1 pCi/m^3, the concentration in drinking water is 1% of that in air, and the average concentration of tritium in all food products is 50% of that in air. Assume a specific humidity of 6.0 g H_2O/m^3. Using Eq. 9.6 and adjusting the concentration factors to meet the prescribed conditions gives

$$\begin{aligned}&[1.22(1.7\times10^{-3})+1.27(8.5\times10^{-2})+0.29(8.5\times10^{-2})\\&\quad+0.22(1.7\times10^{-1})]\times10^{3}\times\frac{1}{3.0}\times95+10^{-6}\frac{\text{mrem/y}}{\text{pCi/L}}\\&\quad=5.5\times10^{-3}\,\text{mrem/y}\,.\end{aligned}\tag{9.9}$$

The effect of incorporating simulated site-specific data is to reduce the dose to approximately one-third in this example. This illustrates the need to have sufficient flexibility in a model for tritium assessment to allow for incorporation of site-specific data. [End of Example 9.2]

9.3.3 Modified NCRP Model

A primary advantage of the models proposed by Evans (1969) and the NCRP (1979) is simplicity. Other models for evaluating exposures from tritium that are more complex have been proposed (Moore et al. 1979; USNRC 1977); however, it has been demonstrated that the increased complexity does not necessarily improve the relative accuracy (Till et al. 1981).

Two minor modifications of the NCRP methodology would maintain its simplicity and would allow for incorporation of the dose from food products grown elsewhere. First, because current data concerning oxidized vs nonoxidized tritium components in food products are not well documented (Table 9.1), the two values (1.27 and 0.29) are combined to give 1.56. Second, the concentration of tritium in food products is broken into two parts: (1) that fraction grown at the point where the dose is being calculated and (2) that fraction grown at another location where the concentration of tritium in air is different than at the point of interest. The model is described by the following equation, a modification of Eq. 9.6:

$$D=\left[1.22C_w+1.56\left(\sum_{n=1,2,3,\ldots}C_{fn}\delta_n\right)+0.22C_a\right]\frac{1}{3.0}\times\text{DRF}\,,\tag{9.10}$$

which simplifies to

$$D=\left[0.41C_w+0.52\left(\sum_{n=1,2,3,\ldots}C_{fn}\delta_n\right)+0.07C_a\right]\text{DRF}\,,\tag{9.11}$$

where

D = annual dose (mrem),

C_w = concentration of tritium in drinking water (pCi/L),

C_{fn} = concentration of tritium in water of food products grown at location n (pCi/L),

δ_n = fraction of food products grown at location n,

C_a = concentration of tritium in air (pCi/L),

DRF = dose rate factor [(mrem·L)/(pCi·y)] (see Chapter 7).

9.3.4 Default Values for Tritium

9.3.4.1 Chemical Form

The two primary forms of tritium released to the environment from man-made sources are tritiated water vapor (^{3}HOH) and tritium-hydrogen gas (^{3}HH). Small amounts of tritium also exist as tritium gas (^{3}H^{3}H) and as tritiated methane (^{3}HCH). The chemical forms have different sources, distributions, and environmental sinks and proceed toward conversion to tritiated water vapor. Milham and Boni (1976) estimate that 16% of releases to the atmosphere from a major nuclear production complex are in the form of hydrogen gas and essentially all of the remaining in the form of tritiated water vapor. Little data are available regarding the rate of conversion of the gas to tritiated water vapor. For the purposes of radiological assessments, it is recommended that the chemical form of tritium released to the atmosphere be assumed to be ^3H_2O. One should recognize, however, that the effect of including chemical forms other than ^3H_2O would be to reduce the dose to individuals near the point of release.

9.3.4.2 Absolute Humidity

In the example problems given previously, a value of 6.0 g H_2O/m^3 has been used for the absolute humidity. Since the amount of tritium in air is inversely proportional to the absolute humidity, under- or overestimation of this parameter will significantly affect the results of the assessment. Because of the wide variability in atmospheric humidity from one location to another within the United States, it is advisable to select a value for absolute humidity based upon geographic location. Etnier (1980) estimated absolute humidity for 218 points within the 48 conterminous states of the United States and developed a cross-sectional map to use in dose calculations (Fig. 9.1). It is recommended that data from this map be used to evaluate exposures to the public from tritium unless site-specific values are available.

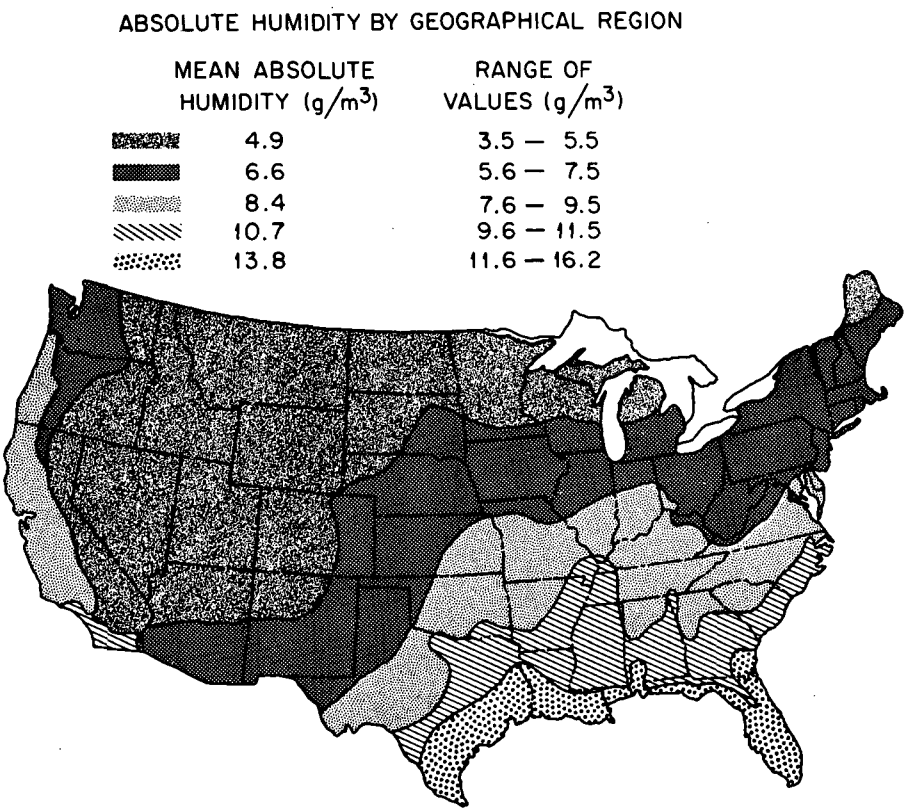

Figure 9.1. Absolute humidity by geographical region. Source: Etnier, E. L. 1980. "Regional and Site-Specific Absolute Humidity Data for Use in Tritium Dose Calculations," *Health Phys.* **39**(2), 318–20. Reprinted with permission of the Health Physics Society.

9.3.4.3 C_{fn} and C_w

If the concentrations of tritium in food products at location n (C_{fn}) and in drinking water (C_w) are not known, it is recommended that the concentration in food be assumed to be equal to that in air at location n and the concentration in drinking water be assumed to be 1% of that in air at location n. The assumption that tritium in food products is equal to that in air for location n may provide a conservative (high) estimate of dose. The U.S. Nuclear Regulatory Commission (USNRC 1977) suggests a value of 50% for food products based upon a model published by Anspaugh et al. (1972); however, more recent data by Murphy and Pendergast (1979) and Murphy et al. (1982) indicate that tritium concentration in vegetation rapidly approaches

that in air once a source term has been injected. The value for C_{fn} is one important area where additional research could be significantly beneficial. The assumption that the tritium concentration in drinking water, C_w, is 1% of that in air is strictly an "educated guess" to account for tritium that migrates from the atmosphere into drinking water supplies. Although there is no scientific basis for this number, it has been accepted as a default value in radiological assessments. If a drinking water supply is known to be contaminated by releases of tritium to the aquatic environment, then this assumption is no longer valid, and a separate calculation must be made to determine the concentration of tritium in the water.

9.4 CARBON-14

9.4.1 Killough's Specific Activity Model

The model for calculating the dose from environmental releases of ^{14}C assumes a steady-state relationship between carbon isotopes from the point of photosynthetic fixation through the food chain to man. Details of such a model were proposed by Killough and Rohwer (1978).

Carbon-14 is released in various chemical forms by nuclear facilities, the particular form depending on the type of facility; however, only the CO_2-bound component enters man's food chain. It is assumed that the radioactive CO_2 in the effluent plume mixes with the nonradioactive CO_2 that is present in the atmosphere in its ambient concentration. The ambient concentration of CO_2 varies considerably in diurnal and seasonal cycles and is locally influenced by industrial CO_2 sources. In fact, the specific activity of ^{14}C in the atmosphere can be reduced by the injection of nonradioactive carbon. This phenomenon is known as the Suess effect (Suess 1955).

If it is assumed that ambient air contains 330 ppm CO_2/m^3 (Baes et al. 1976), then the mass of carbon would be 0.18 g/m^3. The ground-level concentration of ^{14}C in air at location n, χ_n, is calculated using an atmospheric transport model as described in Chapter 2 for a given release rate Q (Ci/s). Then the specific activity for location n is expressed as

$$A_n^{\text{air}} = \chi_n/(0.18) \quad \frac{\text{pCi/m}^3}{\text{gC/m}^3}. \tag{9.12}$$

Carbon-14 reaches man via direct consumption of plant matter or meat or dairy products from animals that have fed on such plant matter. The fractionation effect in the assimilation of carbon by man and higher animals is insignificant in comparison with photosynthetic fractionation. Moreover, nearly all of the carbon in the body (all but about 0.01%) is sustained by dietary intake of carbon as opposed to inhalation (Fowler et al. 1976). Therefore, if animals feed on plant matter of specific activity A_n^{plant}, we assume for the steady-state model that the carbon in food products derived from these animals

has the same specific activity, which in turn equals A_n^{air}. It is emphasized that the applicability of such a model is limited to the case of release at a constant rate, where the exchange of ^{14}C between plants and animals and their exposure environment exists in a state of equilibrium.

To calculate the dose rate to man due to ingestion of ^{14}C under the above conditions, the following equation is used:

$$\dot{D}_{ig} = (\mathrm{DRF})_{ig} \sum_{n=1}^{N} (G_n/G) A_n^{air}, \tag{9.13}$$

where

$\dot{D}_{ig}$ = annual dose rate to organ i (mrem/y) due to ingestion of ^{14}C,

$(\mathrm{DRF})_{ig}$ = dose rate factor for organ i (mrem/y per pCi/g C) (see Chapter 7),

G_n = annual average intake of dietary carbon (g C/y) derived from the nth location,

G = total annual average intake of dietary carbon (g C/y),

A_n^{air} = estimated average daytime specific activity of ambient airborne carbon during the growing season at location n.

The report on Reference Man by the International Commission on Radiological Protection (ICRP 1975) recommends a value of $G = 300$ g C/d (1.1×10^5 g C/y) for a male adult. Estimation of the dose rate to an individual due to ingestion of ^{14}C requires an assumption about the distribution of sources of the individual's food throughout the area near the point of release. Table 9.2 is provided to assist in computing G_n once these assumptions are made. Inhalation is ordinarily a minor exposure pathway for ^{14}C, with dose rate factors that are about 1% of those for ingestion. For completeness, however, the equation for the inhalation dose rate is given below:

$$\dot{D}_{ih} = (\mathrm{DRF})_{ih} \bar{A}_n^{air}, \tag{9.14}$$

where

D_{ih} = annual dose rate to organ i (mrem/y) due to inhalation of ^{14}C,

$(\mathrm{DRF})_{ih}$ = dose rate factor for organ i (mrem/y per pCi/g C) (see Chapter 7),

Table 9.2. Contributions to total carbon intake of Reference Man[a]

Source	Intake rate of food group (g/d)	Intake rate of carbon (g/d)
Meat, fish, poultry	270	67
Vegetables, fruits, grain	534	56
Milk	261	18
Dairy products	347	114
Fats, oils, sugars	72	40
Total daily intake	1484	300

[a]These data assume that carbon intake through inhalation and drinking fluids other than milk is negligible. Actually, the carbon intake via this pathway can be estimated using a concentration of carbon in air of 0.18 g/m^3, an inhalation rate of 2.2×10^7 cm^3/d (ICRP 1975), and assuming that 75% of inhaled air is retained in the body to give an intake rate of 3.96 g C/d.

Source: National Council on Radiation Protection and Measurements 1983. *Radiological Assessment: Predicting the Transport, Bioaccumulation, and Intake by Man of Radionuclides Released to the Environment*, Report of Task Groups 2 and 3 of Committee 64, to be published in 1983. Used with permission.

A_n^{air} = annual average specific activity of airborne carbon (pCi/g C) where the exposed individual lives and works.

Since this exposure pathway is not limited by the operation of photosynthesis, A_n^{air} should be estimated on the basis of meteorological data sampled day and night through all seasons.

9.4.2 Default Values for Carbon-14

9.4.2.1 Chemical Form

For the purposes of routine radiological assessments, it is recommended that the chemical form of release of ^{14}C be assumed to be CO_2. Other chemical species, such as methane, ethane, and other hydrocarbons, are known to appear; in these forms, ^{14}C is unavailable for photosynthetic uptake in man's food chain until oxidation to CO_2 occurs. For methane, Ehalt (1973) gives estimates of atmospheric mean residence times that range from 0.7 to 6 y.

9.4.2.2 Meteorological Data

Although it is recommended that annual averaged meteorological data be used for routine assessments, it is noted that calculations have determined that replacing annual averaged meteorological data with an average taken during daylight hours for the growing season may increase the maximum individual dose by a factor of 2 for certain locations (Killough et al. 1976). This increase occurs because of the higher frequency of daytime Class A (unstable) conditions at that time. This characteristic should be borne in mind, particularly when ^{14}C is a major contributor to total dose.

9.5 GLOBAL CYCLING MODELS FOR ^{3}H, ^{14}C, ^{85}Kr, and ^{129}I

As indicated earlier, ^{3}H, ^{14}C, ^{85}Kr, and ^{129}I are transported beyond the range normally considered for radiological assessments and become mixed in the biosphere. Thus, they are potential sources of low-level exposure to large populations over long periods of time. Evaluation of the global impact of these radionuclides is not normally considered in the routine assessment for nuclear facility operation; however, it is important to have an understanding of their long-term behavior in the environment in order to predict their buildup and potential impact on future generations and to develop meaningful cost-benefit analyses of effluent treatment techniques. This section gives examples of global cycling models that have been proposed for each of these radionuclides. It concludes with an important precautionary note on the utility of such models.

9.5.1 Tritium Global Cycling Model

Because of the ubiquitous nature of tritium as ^{3}HOH, estimates of global population doses due to specific tritium sources have received considerable attention. Estimates of annual global dose commitments arising from a 1-Ci/y release to the atmosphere are found to range from $4. \times 10^{-4}$ man-rem/y (USEPA 1973) to 2.2×10^{-2} man-rem/y (Soldat and Baker 1979).

The basic assumption of global tritium models is that tritium follows the hydrologic cycle without discrimination. The standard approach to describing tritium distribution is to consider the primary water pools as compartments and to describe equilibrium concentrations in each compartment. The simplest model is a one-compartment model in which tritium is instantly and completely mixed with the circulating waters of the world. The volume of surface ocean water provides the primary contribution to compartment size. Activity is diminished only by radioactive decay. Two- and three-compartment models have also been proposed (USEPA 1973; NCRP 1979).

The difficulty with these simple models is that the compartments are very large and tritium concentrations are assumed to be uniform within each

compartment. In nature, tritium concentrations vary considerably, even in the equilibrium state, between numerous aqueous pools and geographical locations.

The most reasonable model, in terms of accounting for distinct accumulation pools, is of the type proposed by Easterly and Jacobs (1975) with seven compartments. This model is shown in Fig. 9.2. For this more refined

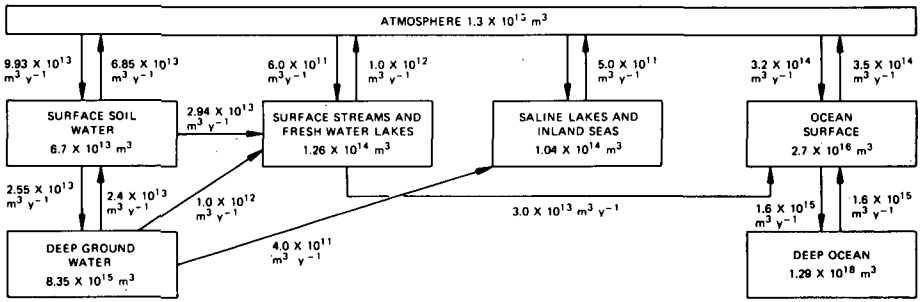

Figure 9.2. Seven-compartment model for global tritium cycling. Source: Easterly, C. E., and Jacobs, D. G. 1975. "Tritium Release Strategy for a Global System," in *Proceedings of an International Conference on Radiation Effects and Tritium Technology for Fusion Reactors,* Vol. III, ed. J. S. Watson and F. W. Wiffen, CONF-750989, U.S. Energy Research and Development Administration, Washington, D.C.

model, equilibrium assumptions are inappropriate; instead, transfer coefficients between compartments are estimated and the system is simulated until it reaches a pseudo-equilibrium state. This permits comparison of projections with different initial conditions and transfer coefficients. The mean residence times of water in the various compartments are 11 d in the atmosphere, 200 d in surface soil, 4.1 y in freshwater lakes, 13.8 y in the surface ocean, 210 y in saline lakes, 330 y in the deep ground, and 810 y in the deep ocean.

Figure 9.3 illustrates the concentrations resulting from a 1-MCi release of tritium to the 30–50°N latitude band as a function of time using the seven-compartment model. In order to estimate the collective dose commitment from ^3H to the world population due to a globally dispersed release of tritium, one must use the equation

$$H_\infty = \int_{t_0}^{+\infty} N(t) \cdot \dot{D}(t) \cdot dt \text{ man-rem}, \tag{9.15}$$

where

$N(t)$ = world population at time t,

$\dot{D}(t)$ = dose rate to an average individual at time t (rem/y),

t_0 = the year of the beginning of the release.

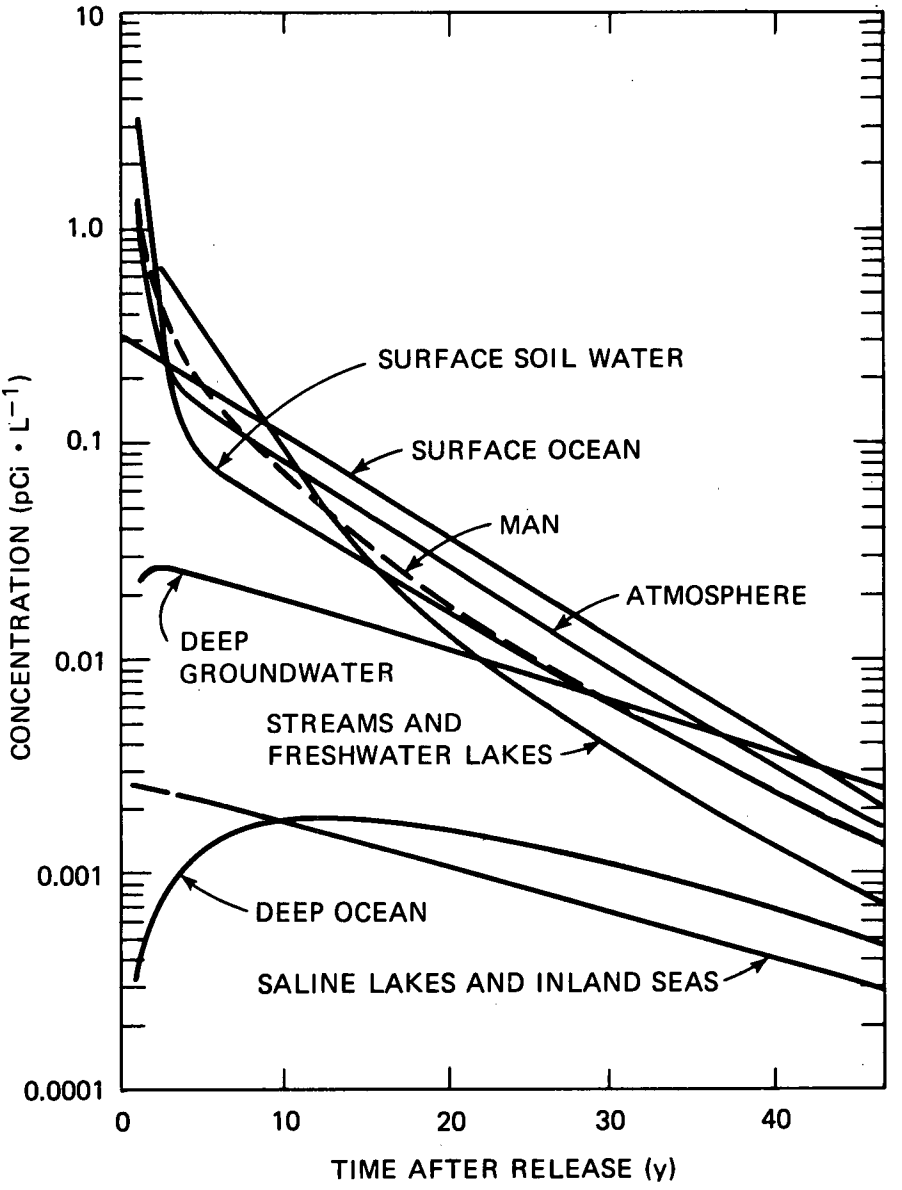

Figure 9.3. Concentrations resulting from a single atmospheric release of tritium (1 MCi) to the 30–50°N latitude band. Source: Adapted from National Council on Radiation Protection and Measurements 1979. *Tritium in the Environment,* NCRP Report 62, Washington, D.C. Reprinted with permission.

Estimation of the individual dose rate $\dot{D}(t)$ is made as follows:

$$\dot{D}(t) = (\mathrm{DRF}) \cdot F_w \cdot C_m(t) \text{ rem/y}, \tag{9.16}$$

where

DRF = dose equivalent rate factor described earlier (rem/y per g $^3H/m^3$) (see Chapter 7),

F_w = average fraction of body tissue that is water [0.75 (ICRP 1975)],

$C_m(t)$ = an estimate of the concentration of tritium in the body water of an average member of the population at time t (g $^3H/m^3$).

The factor $C_m(t)$ is estimated from a dynamic simulation of concentrations of released tritium in the water of several reservoirs of the global hydrologic cycle in proportion as the water from these sources is taken in by humans. Using assumptions suggested by the NCRP (1979), the partition of C_m may be written as follows:

$$C_m = \frac{0.99}{3.0} C_{\text{air}} + \frac{1.99}{3.0} C_{\text{water}} + \frac{0.02}{3.0} C_{\text{ocean}}, \tag{9.17}$$

where the variables on the right indicate the concentrations of tritium (g/m^3) in the media denoted by the subscripts. The first term is assumed to contribute to the concentration in body water by inhalation (0.13 L/d), absorption through the skin (0.09 L/d), and one-half of the concentration in water taken in food (0.77 L/d). The second term expresses the assumed contribution of the land waters through the remaining half of the water content in food and through drinking water (0.77 and 1.22 L/d). In the third term, a small contribution due to eating fish is taken into account. The total water intake is 3.0 L/d, as stated earlier.

Solutions to the seven-compartment model are carried out with a computer once the source terms have been established. The development of these source terms may include an estimate of tritium from all potential sources of release, such as nuclear facilities, consumer products, weapons testing, and natural production. Such an assessment has been carried out by Till et al. (1980), and the results are shown in Table 9.3. This table displays collective dose commitments from a hypothetical nuclear power scenario between the years 1975 to 2020 plus another 100 y to allow for tritium decay after 2020. The release of tritium from weapons testing occurred between 1940 and 1975, but the integration was also carried an additional 100 y. Natural background tritium was integrated over the same period as the nuclear power scenario.

Table 9.3. Global components of collective dose commitment to the world population from man-made and natural sources of ^3H

Exposure medium	Global collective dose commitment (man-rem) from ^3H released by		
	Nuclear power industry and consumer products released between 1975 and 2020	Nuclear weapons testing	Natural ^3H produced between 1975 and 2020
Atmosphere	6.3×10^4	4.8×10^5	9.1×10^4
Deep groundwater[a]	1.3×10^3	1.1×10^4	1.9×10^3
Freshwater lakes and streams[b]	1.6×10^6	5.2×10^5	9.9×10^4
Ocean surface	3.9×10^2	1.1×10^3	2.1×10^2
Total	1.7×10^6	1.0×10^6	1.9×10^5

[a]Contributes 20% of drinking water.
[b]Contributes 80% of drinking water.

Source: Till, J. E., et al. 1980. *Tritium—An Analysis of Key Environmental and Dosimetric Questions*, ORNL/TM-6990, Oak Ridge National Laboratory, Oak Ridge, Tenn.

Such comparisons of collective dose commitments must be made with caution, since satisfactory estimates of the first-pass and regional dose could account for a significant fraction of total collective dose commitment. This area of tritium global modeling needs considerable attention in the future.

9.5.2 Carbon-14 Global Cycling Model

The dose rate from ^{14}C to an average member of the world population can be estimated using a simple specific activity approach as follows:

$$\dot{D} = (\text{DRF})(\text{SpA}) \text{ rem/y}, \tag{9.18}$$

where

$\dot{D}$ = annual dose,

DRF = dose rate factor for a given body organ (rem/y per pCi/g C) (see Chapter 7),

SpA = specific activity in the exposure environment (pCi/g C).

The term *SpA* is defined as

$$\text{SpA} = 4.46[X/(X+Y)] \text{ Ci/gC}, \tag{9.19}$$

where X and Y are grams of released ^{14}C and total nonradioactive carbon, respectively, in the atmosphere and 4.46 Ci/g is the specific activity of pure ^{14}C. The atmospheric levels of X and Y are dynamic variables whose time histories are obtained from computer simulations of the dynamic nonlinear compartment described below.

The dynamic model used as an example for global carbon cycling was described by Killough and Till (1978) and is shown in Fig. 9.4. Its principal reservoirs are the atmosphere, the ocean, and the terrestrial biota, among which exchanges of nonradioactive and radioactive carbon are simulated. The ocean is subdivided into three layers. The terrestrial biota are represented by a slow- and rapid-turnover component with mean residence times of 41 and 2.2 y, respectively.

Exogenous inputs to the model are (1) the production rate of carbon dioxide from the combustion of fossil fuels, (2) the source term for ^{14}C entry into the system, and (3) a function that represents world population levels in the past and future. The reader should consult the article by Killough and Till (1978) for a complete description of the model and the precautions that must be taken when making the integration of its equations.

Table 9.4, taken from Fowler and Nelson (1979), lists 100-y dose commitment factors to the total body for 1 Ci of ^{14}C released to the atmosphere as calculated using this model. Environmental dose commitment

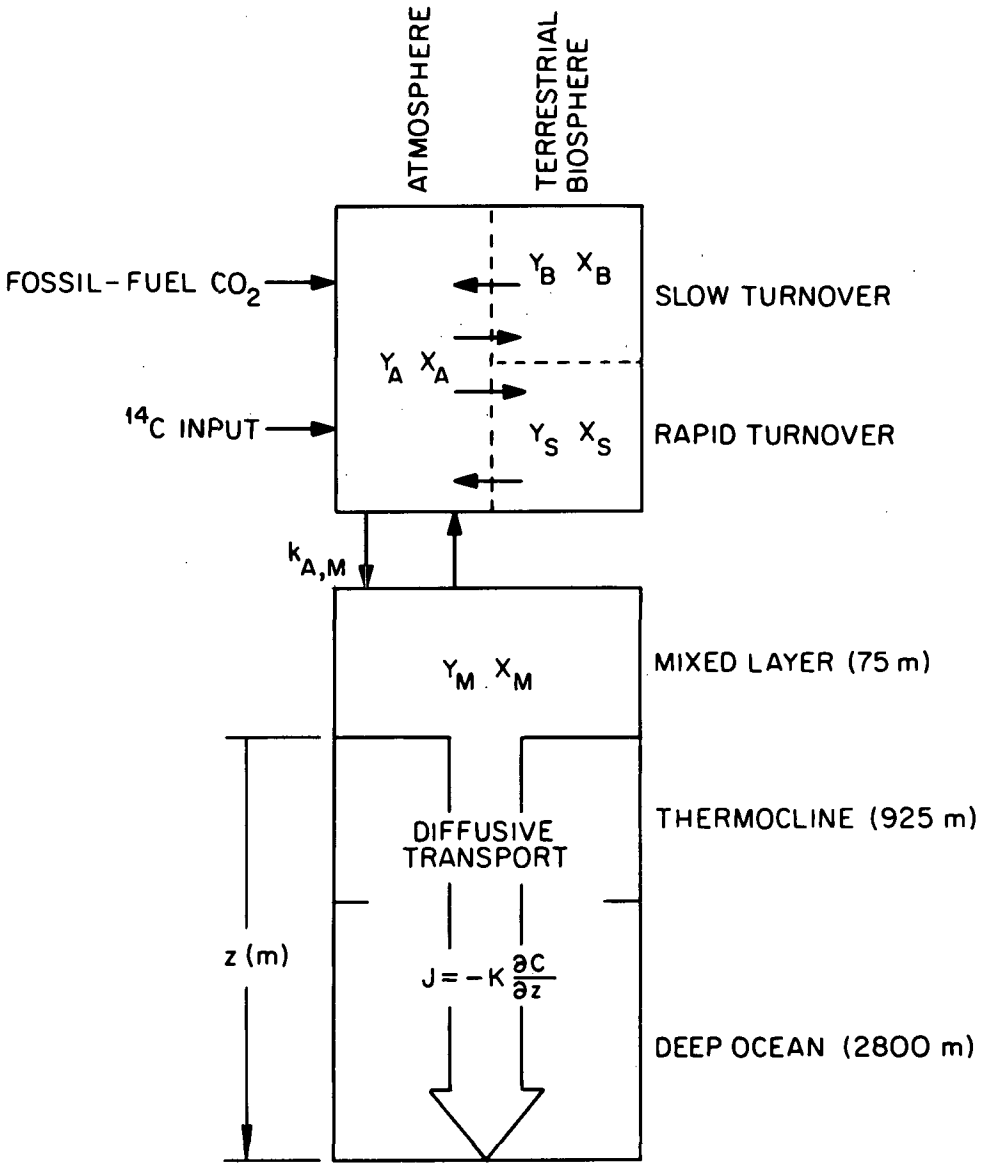

Figure 9.4. A schematic presentation of the box diffusion model of the global carbon cycle used for the environmental transport calculations for ^{14}C. Notation: Y = nonradioactive carbon: ^{12}C and ^{13}C (g); $X = {}^{14}C$ (g); $C = C(z, t)$ = concentration of carbon (g/m^3) at depth z and time t; K = diffusion coefficient (m^3/y). Source: Killough, G. G., and Till, J. E. 1978. "Scenarios of ^{14}C Releases from the World Nuclear Power Industry from 1975 to 2020 and Estimated Radiological Impact," *Nucl. Saf.* **19**(5), 602–17.

Table 9.4. Carbon-14 100-y environmental dose commitment factors

Year of release	100-y environmental dose commitment factors (man-rem/Ci)	
	Total body	Gonads
1976	25.5	9.71
1977	25.7	9.79
1978	25.9	9.87
1979	26.2	9.98
1980	26.4	10.1
1981	26.6	10.1
1982	26.8	10.2
1983	27.1	10.3
1984	27.3	10.4
1985	27.6	10.5
1986	27.8	10.6
1987	28.0	10.7
1988	28.2	10.7
1989	28.4	10.8
1990	28.6	10.9
1991	28.8	11.0
1992	29.0	11.0
1993	29.2	11.1
1994	29.4	11.2
1995	29.5	11.2
1996	29.7	11.3
1997	29.8	11.4
1998	30.0	11.4
1999	30.1	11.5
2000	30.3	11.6

Source: Fowler, T. W., and Nelson, C. B. 1979. *Health Impact Assessment of Carbon-14 Emissions from Normal Operations of Uranium Fuel Cycle Facilities*, EPA-520/5-80-004, U.S. Environmental Protection Agency, Washington, D.C.

factors for other organs are proportional to the ratios of the total body values shown in the table (see Chapter 7). Tabulations such as this allow one to use the results of the Killough model to project global impacts of ^{14}C releases without installing and running the computer code.

As in the case of ^{3}H, it is useful to make a comparison of population dose from ^{14}C produced from the nuclear power industry, natural sources, and nuclear weapons testing. The results of such a comparison are shown in Table 9.5.

Table 9.5. Global components of collective dose commitment to the world population from man-made and natural sources of ^{14}C

Date	Global collective dose commitment (man-rem) produced from ^{14}C released by		
	Nuclear power industry	Nuclear weapons testing	Natural ^{14}C produced between 1975 and 2020
1975		3.4×10^7	
1990	1.8×10^6	5.3×10^7	2.8×10^6
2005	1.1×10^6	6.9×10^7	9.1×10^6
2025	4.3×10^6	9.2×10^7	2.2×10^7
2075	8.9×10^6	1.5×10^8	4.1×10^7
Infinite time	1.9×10^8	3.2×10^9	8.8×10^8

Source: Killough, G. G., and Till, J. E. 1978. "Scenarios of ^{14}C Releases from the World Nuclear Power Industry from 1975 to 2020 and Estimated Radiological Impact," *Nucl. Saf.* **19**(5), 602–17.

9.5.3 Krypton-85 Global Cycling Model

A global cycling model for ^{85}Kr is shown in Fig. 9.5. This model is a simplified version of one first proposed by Kelly et al. and modified in a report of the Commission of the European Communities (1979). For this two-compartment model, instant and uniform mixing is assumed once the ^{85}Kr is released to the atmosphere in either the northern or southern hemisphere.

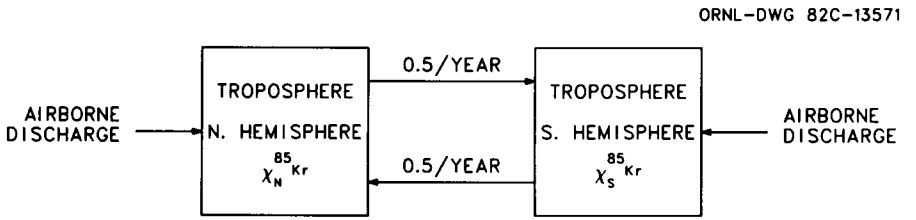

Figure 9.5. Two-compartment global cycling model for ^{85}Kr. Source: Commission of the European Communities 1979. *Methodology for Evaluating the Radiological Consequences of Radioactive Effluents Released in Normal Operations,* V/3865/79-EN, FR, Brussels. Reprinted with permission.

Exchange takes place between the tropospheres at a rate of every 2 y. The only removal of ^{85}Kr once it has been released to the atmosphere is by radioactive decay.

Exposure from ^{85}Kr is by external irradiation of the body. The dose to humans is estimated by integrating the concentration of ^{85}Kr in the atmosphere and multiplying by the dose rate factor and assumed population scenario as follows:

$$\dot{D}_i = (\mathrm{DRF})_i(\chi^{^{85}Kr}_{N \text{ or } S}) , \tag{9.20}$$

where

$\dot{D}_i$ = dose rate to organ i (rem/y),

$(\mathrm{DRF})_i$ = dose rate factor for organ i (rem/y per pCi/m^3),

$\chi^{^{85}Kr}_{N \text{ or } S}$ = atmospheric concentration of ^{85}Kr in the northern or southern hemisphere (pCi/m^3).

The value of $\chi^{^{85}Kr}$ is estimated using the model in Fig. 9.5 once a source term scenario has been established. The population dose commitment is then calculated using the equation

$$H_{(t_0,t_1)} = \int_{t_0}^{t_1} N(t)\cdot\dot{D}(t)\cdot dt \text{ man-rem} , \tag{9.21}$$

where

$N(t)$ = population scenario for the northern or southern hemisphere,

$\dot{D}(t)$ = dose rate at time t to an average individual (rem/y).

The model shown in Fig. 9.5 as an example is very likely an oversimplified approach to evaluating global exposure from ^{85}Kr. The NCRP (1975) states that there may be considerable variation in concentration of ^{85}Kr with latitude, especially since most of it will be released to the atmosphere in the northern hemisphere, between 35 and 45°N. This variation should be borne in mind when calculating population dose for the purposes of cost-benefit analyses.

9.5.4 Iodine-129 Global Cycling Model

Kocher (1981) proposed a nine-compartment model for assessing the dose of ^{129}I to the world population (Fig. 9.6). The mean residence time of ^{129}I in

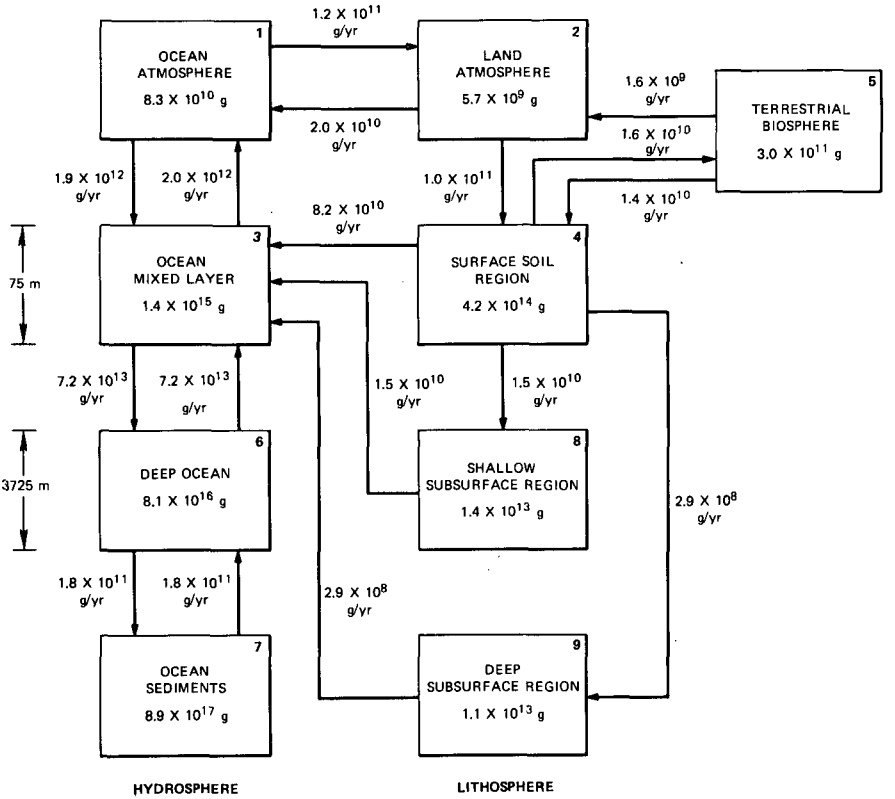

Figure 9.6. Nine-compartment model, global inventories, and fluxes for predicting ^{129}I transport and accumulation. Source: Kocher, D. C. 1981. "A Dynamic Model of the Global Iodine Cycle and Estimation of Dose to the World Population from Releases of Iodine-129 to the Environment," *Environ. Int.* **5**, 15–31. Reprinted with permission.

the atmosphere is only approximately 15 d, so that a release to the atmosphere from a point source is likely to be transported to land or the oceans before mixing throughout the global atmosphere has occurred. Thousands of years may then be required for the resulting localized distribution of ^{129}I on the earth's surface to enter into global circulation. Therefore, it is highly speculative to attempt to model ^{129}I global cycling, and consideration should first be given to its assessment on a regional or local scale for cost-benefit analyses.

Kocher used his model to estimate dose to the world population from release of 1 Ci of ^{129}I to the land atmosphere in 1980. The results of his study are shown in Table 9.6 for integration to various times. The value at infinite time (2.8×10^5 man-rem) is the complete global population dose commitment.

Table 9.6. World population doses to the thyroid from release of 1 Ci of ^{129}I to the land atmosphere using the model shown in Fig. 9.6

Time (years after release)	Dose (man-rem)
10^1	2.2×10^3
10^2	3.1×10^3
10^3	1.4×10^4
10^4	5.5×10^4
10^5	6.8×10^4
10^6	1.0×10^5
10^7	1.6×10^5
Infinity	2.8×10^5

Source: Adapted from Kocher, D. C. 1981. "A Dynamic Model of the Global Iodine Cycle and Estimation of Dose to the World Population from Releases of Iodine-129 to the Environment," *Environ. Int.* **5**, 15–31. Reprinted with permission.

Among the global cycling radionuclides, ^{129}I is likely to be the most difficult to model with any reasonable confidence because of its very long physical half-life (1.6×10^7 y). On the other hand, because of its very low specific activity, the source terms for its release to the environment are extremely small, and iodine is relatively easy to contain through efficient effluent treatment.

9.5.5 Global Cycling Models: The Need for Caution

The selection of an appropriate length of integration for global cycling radionuclides is an important and controversial issue that lacks firm guidance. If one accounts for the population dose during the release period only, then a reasonable scenario can be depicted (ordinarily less than 100 y for the generation of electricity by nuclear energy). However, this procedure neglects the residual commitment that remains in the environment after the cessation of the source term. On the other hand, estimating the dose to future generations involves projections of population growth and source terms that clearly are subject to considerable uncertainty.

In the study by Till et al. (1980) on ^3H, an integration time of the release scenario (1975 to 2020) plus 100 y (approximately 8 half-lives of tritium) was assumed. For global assessment of ^{14}C, Killough and Till (1978) used the

release scenario (again 1975 to 2020) plus 46,000 y (8 half-lives of ^{14}C). Bonka et al. (1979) recommend an integration time of 10,000 y for ^{129}I.

The problem of integration time is compounded when one carries the assessment through to estimates of health effects. Table 9.7 shows the health effects from ^{14}C calculated using the world population doses shown in Table 9.5 and applying risk factors from ICRP Publication 26 (ICRP 1977). Note that when integrated to infinite time (i.e., until all of the ^{14}C has decayed), there are projected to be 22,000 cases of cancer and 15,000 genetic effects caused by the nuclear industry. Although these figures may appear to be large, these health effects occur over a period of approximately 46,000 y. In reality, this is an insignificant number of health effects for the world population during such a long period of time. Also note that the health effects from natural ^{14}C formed during the period of the release scenario and that from nuclear weapons testing are 168,000, making the health effects resulting from the production of nuclear energy appear to be relatively less important.

Table 9.7. Cumulative induction of fatal and nonfatal cancers and genetic health effects from ^{14}C produced by the nuclear power industry, nuclear weapons testing, and natural formation

Date	Nuclear power industry		Nuclear weapons testing		Natural ^{14}C produced between 1975 and 2020	
	Cancer	Genetic effects	Cancer	Genetic effects	Cancer	Genetic effects
1975			4,000	2,600		
1990	21	14	6,300	4,100	330	216
2005	130	85	8,100	5,300	1,100	700
2025	510	330	11,000	7,100	2,600	1,700
2075	1,100	690	18,000	12,000	4,800	3,200
Infinite time	22,000	15,000	380,000	250,000	100,000	68,000

Source: Adapted from Killough, G. G., and Till, J. E. 1978. "Scenarios of ^{14}C Releases from the World Nuclear Power Industry from 1975 to 2020 and Estimated Radiological Impact," *Nucl. Saf.* **19**(5), 602–17.

Therefore, it is imperative that the length of integration be clearly specified when evaluating dose from global cycling radionuclides in order that the calculated population dose may be put into perspective. Comparisons between naturally produced ^{3}H, ^{14}C, ^{85}Kr, and ^{129}I are often helpful and may

eventually provide a basis for international standards to limit the buildup of these radionuclides in the environment.

As a final note, estimating the population dose from global cycling radionuclides may not be the best means of assessing their impact. Instead, comparing dose rates from releases of ^{3}H, ^{14}C, ^{85}Kr, and ^{129}I may be the best method for assessing their long-term impact, at least until better guidance can be provided by international organizations.

9.6 PROBLEMS

1. Use the modified NCRP technique to calculate the dose rate (mrem/y) from ingestion and inhalation to an individual residing 7241 m from a stack discharging 100,000 Ci/y of ^{3}H as ^{3}HOH. Assume that χ/Q is 3.1×10^{-8} s/m^3, that the individual receives drinking water from an uncontaminated source, and that all food products ingested are grown near the point of residence. The location of the release is in the extreme southeastern United States.

2. Using the assumptions in problem 1, estimate an upper limit of dose to an individual exposed to an accidential pulse release to the atmosphere of 10^7 Ci of ^{3}H as ^{3}HOH in a 24-h period. Explain why this would be an upper limit. What precautions would you take to reduce exposure to the public in this case?

3. Discuss the effect of chemical form of release of ^{3}H to the atmosphere on local and global dose. Would conversion of tritium to a chemical form other than ^{3}HOH be feasible as an effluent control technique to reduce the dose to the public from tritium?

4. What is the dose rate (mrem/y) to an individual chronically exposed to an atmospheric concentration of 1.6×10^{2} pCi/m^3 of ^{3}HOH? Assume that 25% of the food ingested is grown at this location, 25% is grown where the atmospheric concentration is 2.3 pCi/m^3, and 50% is grown where the atmospheric concentration is 5.2×10^{2} pCi/m^3. All drinking water consumed by the individual comes from a well having an activity concentration of 35 pCi/mL. Perform the calculation assuming a specific humidity of 3, 6, and 12 g H_2O/m^3.

5. Calculate the dose rate (mrem/y) to an individual exposed to a continuous release of $^{14}CO_2$ of 2.4 Ci/y. Assume that χ/Q is 5.3×10^{-7} s/m^3 and that 50% of the food ingested by the individual is grown near his place of residence and 50% is grown in an area having a χ/Q of 1.1×10^{-8} s/m^3. Use a total body dose rate factor for ingestion of 2.1×10^{2} rem/y per μCi/g C.

6. Discuss the importance of photosynthetic fixation on dose from $^{14}CO_2$. How might this process be used to control the exposure to individuals residing near the point of release?

7. Would you expect to find a significant variation between the dose to an infant and that to an adult from chronic exposure to ^{3}H and ^{14}C?

8. Describe the advantages and disadvantages of specific activity models over the various transport models described in earlier chapters. Could specific activity models be used for assessments of radionuclides other than ^{3}H and ^{14}C?

9. Explain the Suess effect in terms of global doses from ^{14}C emissions.

10. You are given the task of establishing a set of acceptable international standards for global cycling radionuclides. On what criteria would you base the standards? Should international standards be set to control the buildup of ^{3}H, ^{14}C, ^{85}Kr, and ^{129}I? Why?

11. Explain why caution must be used in calculating dose commitment from global cycling radionuclides. What would you propose as a reasonable and defensible length of integration for evaluating the four global cycling radionuclides?

REFERENCES

Anspaugh, L. R., Korando, J. J., Robertson, W. L., and Martin, J. R. 1972. *Dose to Man Via the Food-Chain Transfer Resulting from Exposure to Tritiated Water Vapor*, UCRL-73195, Rev. 1, Lawrence Livermore Laboratory, Livermore, Calif.

Baes, C. F., Jr., Goeller, H. E., Olson, J. S., and Rotty, R. M. 1976. *The Global Carbon Dioxide Problem*, ORNL-5194, Oak Ridge National Laboratory, Oak Ridge, Tenn.

Bonka, H., Gründler, D., and Horn, H.-G. 1979. "Problems Occurring While Carrying Out Cost-Benefit Analysis for ^{3}H, ^{14}C, ^{85}Kr, Iodine and Aerosols in Nuclear Facilities," in *Topical Seminar on the Practical Implications of the ICRP Recommendations (1977) and the Revised IAEA Basic Standards for Radiation Protection,* International Atomic Energy Agency, Vienna.

Commission of the European Communities 1979. *Methodology for Evaluating the Radiological Consequences of Radioactive Effluents Released in Normal Operations* Document No. V/3865/79-EN, FR, Brussels.

Easterly, C. E. and Jacobs, D. G. 1975. "Tritium Release Strategy for a Global System," in *Proceedings of International Conference on Radiation Effects and Tritium Technology for Fusion Reactors,* Vol. III, ed. J. S. Watson and F. W. Wiffen, CONF-750989, U.S. Energy Research and Development Administration, Washington, D.C.

Ehalt, D. H. 1973. "Methane in the Atmosphere," in *Carbon and the Biosphere*, Proceedings of the 24th Brookhaven Symposium in Biology, Upton, N. Y., May 16–18, 1972, ed. G. M. Woodwell and E. V. Pecan, AEC Symposium Series, CONF-720510, U.S. Atomic Energy Commission, Washington, D.C.

Etnier, E. L. 1980. "Regional and Site-Specific Absolute Humidity Data for Use in Tritium Dose Calculations," *Health Phys.* **39**(2), 318–20.

Evans, A. G. 1969. "New Dose Estimates from Chronic Tritium Exposures," *Health Phys.* **16,** 57–63.

Fowler, T. W., Clark, R. L., Grunhlke, J. M., and Russell, J. L. 1976. *Public Health Considerations of Carbon-14 Discharges from the Light-Water-Cooled Nuclear Power Reactor Industry*, ORP/TAD-76-3, U.S. Environmental Protection Agency, Washington, D.C.

Fowler, T. W., and Nelson, C. B. 1979. *Health Impact Assessments of Carbon-14 Emissions from Normal Operations of Uranium Fuel Cycle Facilities*, EPA 520/5-80-004, U.S. Environmental Protection Agency, Washington, D.C.

International Commission on Radiological Protection (ICRP) 1975. *Report of the Task Group on Reference Man*, ICRP Publication 23, Pergamon Press, Oxford.

International Commission on Radiological Protection (ICRP) 1977. *Recommendations of the International Commission on Radiological Protection (adopted January 17, 1977)*, ICRP Publication 26, Pergamon Press, Oxford.

Killough, G. G., Dixon, K. R., Edwards, N. T., Murphy, B. D., Rohwer, P. S., Harris, W. F., and Kaye, S. V. 1976. *Progress Report on Evaluation of Potential Impact of ^{14}C Releases from an HTGR Reprocessing Facility*, ORNL/TM-5284, Oak Ridge National Laboratory, Oak Ridge, Tenn.

Killough, G. G. and Rohwer, P. S. 1978. "A New Look at the Dosimetry of ^{14}C Released to the Atmosphere as Carbon Dioxide," *Health Phys.* **34**(2), 141–59.

Killough, G. G. and Till, J. E. 1978. "Scenarios of ^{14}C Releases from the World Nuclear Power Industry from 1975 to 2020 and Estimated Radiological Impact," *Nucl. Saf.* **19**(5), 602–17.

Kocher, D. C. 1981. "A Dynamic Model of the Global Iodine Cycle and Estimation of Dose to the World Population from Releases of Iodine-129 to the Environment," *Environ. Int.* **5**, 15–31.

Milham, R. C. and Boni, A. L. 1976. "Detection and Measurement of Tritium Forms Released from a Nuclear Production Complex," pp. 58–61 in *Proceedings of the 24th Conference on Remote Systems Technology*, American Nuclear Society, LaGrange Park, Ill.

Moore, R. E., Baes, C. F., III, McDowell-Boyer, L. M., Watson, A. P., Hoffman, F. O., Pleasant, J. C., and Miller, C. W. 1979. *AIRDOS-EPA: A Computerized Methodology for Estimating Environmental Concentrations and Dose to Man from Airborne Releases of Radionuclides*, ORNL-5532, Oak Ridge National Laboratory, Oak Ridge, Tenn.

Murphy, C. E., Jr., and Pendergast, M. M. 1979. "Environmental Transport and Cycling of Tritium in the Vicinity of Atmospheric Releases," in *Symposium on the Behavior of Tritium in the Environment*, ed. S. Freeman, International Atomic Energy Agency, Vienna.

Murphy, C. E., Jr., Sweet, C. W., and Fallon, R. D. 1982. "Tritium Transport Around Nuclear Facilities," *Nucl. Saf.* **23**(6), 677–85.

National Council on Radiation Protection and Measurements (NCRP) 1975. *Krypton-85 in the Atmosphere—Accumulation, Biological Significance, and Control Technology*, NCRP Report No. 44, Washington, D. C.

National Council on Radiation Protection and Measurements (NCRP) 1979. *Tritium in the Environment*, NCRP Report No. 62, Washington, D. C.

National Council on Radiation Protection and Measurements (NCRP) 1983. *Radiological Assessment: Predicting the Transport, Bioaccumulation, and Intake by Man of Radionuclides Released to the Environment*, Report of Task Groups 2 and 3 of Committee 64, to be published in 1983.

Soldat, J. K., and Baker, D. A. 1979. "Worldwide Population Doses from Tritium Released from Nuclear Facilities," pp. 575–81 in *Symposium on the Behavior of Tritium in the Environment,* ed. S. Freeman, International Atomic Energy Agency, Vienna.

Suess, H. E. 1955. "Radiation Concentration in Modern Wood," *Science* **122**(3166), 414–17.

Till, J. E., Meyer, H. R., Etnier, E. L., Bomar, E. S., Gentry, R. D., Killough, G. G., Rohwer, P. S., Tennery, V. J., and Travis, C. C. 1980. *Tritium—An Analysis of Key Environmental and Dosimetric Questions,* ORNL/TM-6990, Oak Ridge National Laboratory, Oak Ridge, Tenn.

Till, J. E., Etnier, E. L., and Meyer, H. R. 1981. "Methodologies for Calculating the Radiation Dose to Man from Environmental Releases of Tritium," *Nucl. Saf.* **22**(2), 205–13.

U.S. Environmental Protection Agency (USEPA) 1973. *Environmental Analysis of the Uranium Fuel Cycle.* Part III, *Nuclear Fuel Reprocessing,* EPA-520/9-73-003-D, Washington, D.C.

U.S. Nuclear Regulatory Commission (USNRC) 1977. *Calculation of Annual Doses to Man from Routine Releases of Reactor Effluents for the Purpose of Evaluating Compliance with 10 CFR Part 50, Appendix I,* Regulatory Guide 1.109, Washington, D.C.

10 Calculation of Health Effects in Irradiated Populations

By R. H. CLARKE*

10.1 INTRODUCTION

When ionizing radiations were first used early in this century, the most pressing need was to prevent exposure that could result in early harm to the health of an individual. These early effects on health occur after relatively high exposures to radiation. There is a "threshold" below which they are not observed; above this the severity of an effect increases with increasing exposure. These effects, known as nonstochastic effects, can be avoided in all normal circumstances by restricting exposures to levels below the threshold.

It was recognized considerably later that exposure to radiation might lead to delayed health effects, either in the exposed individual (somatic) or in his descendants (genetic). These effects are statistical in nature, occurring with a certain frequency in any irradiated population rather than predictably in any irradiated individual. These effects are known as the *stochastic* effects of radiation; and the severity of late stochastic effects, the most important of which are cancer and hereditary defects, is not related to the level of exposure (Fig. 10.1).

It is now assumed in radiological protection that the probability of occurrence of late stochastic effects is proportional to radiation exposure received and that there is no threshold. Using this assumption, commonly known as the linear no-threshold hypothesis, it is impossible in principle to eliminate late effects other than by eliminating exposure to radiation. The aim has therefore been to permit controllable exposure only when it is justified

*National Radiological Protection Board, United Kingdom.

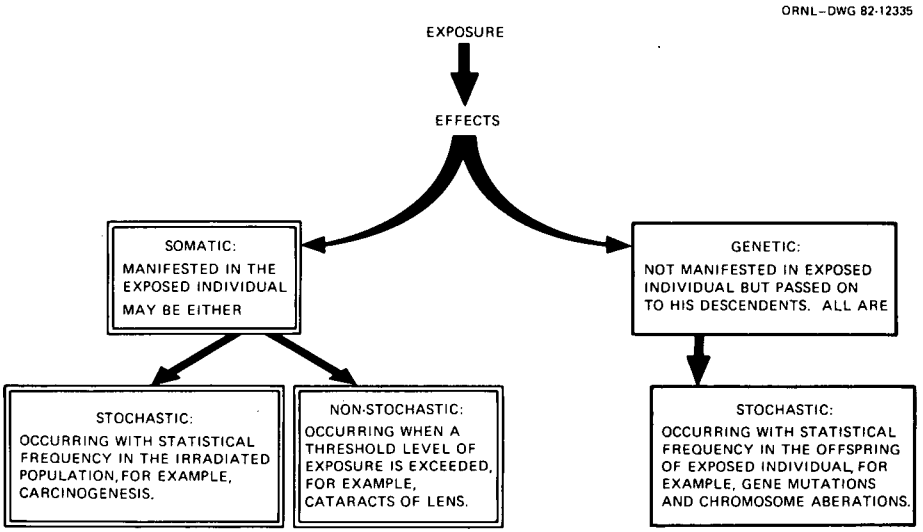

Figure 10.1. Effects of ionizing radiation.

after account is taken of all the benefits of the practice giving rise to the exposure and then to keep exposures acceptably low.

Thus the early history of radiological protection was mainly concerned with limits of "permissible doses" to individuals, which would prevent the occurrence of nonstochastic effects. However, the first publication of the International Commission on Radiological Protection (ICRP 1959) presented recommendations that

> all doses be kept as low as practicable, and that any unnecessary exposures be avoided.

By the time of Publication 9 (ICRP 1966) in 1966, this had evolved to the now famous recommendation that

> all doses be kept as low as is readily achievable, economic and social considerations being taken into account.

Further clarification of this recommendation was still required; it appeared in a later publication (ICRP 1973) in which the dose limits were still placed first, but in addition there was a recommendation to interpret "as low as is readily achievable" in terms of the techniques of differential cost-benefit analysis.

The system of dose limitation recommended by ICRP has been restated in Publication 26 (ICRP 1977a) with the requirements implying cost-benefit analysis elevated before the requirement for compliance with dose limits:

> (a) No practice shall be adopted unless its introduction produces a positive net benefit; (b) All exposures be kept as low as reasonably achievable, economic and social factors being taken into account; (c) The dose equivalent limits to individuals shall not exceed the limits recommended for the appropriate circumstances by the Commission.

This chapter refers to these in abbreviated form as (a) justification, (b) optimization, and (c) compliance with dose limits.

Justification requires the assessment of all the costs associated with the given practice and comparison with all the benefits from the practice. This procedure involves assessing the value of intangibles on both sides and, in any case, provides only one input to major decisions that usually also have strong political, economic, and other constraints. It is not clear that radiological protection considerations are a major input into the justification stage, and this chapter is restricted to the problem of carrying out the second and third objectives within a practice that is assumed to exist whether or not it has been justified overall. The inputs to optimization studies are estimates of the costs of health development and the costs of further reductions in health detriment. The main subject of this chapter is the assessment of health detriment. It addresses the biological bases on which the risks of the stochastic effects of irradiation are set and the dosimetric quantities that have been proposed by ICRP. The chapter later considers methods required for calculating more realistically the numbers of health effects in irradiated populations and discusses the implications for environmental modeling. The costs of health detriment and the application of cost-benefit analysis to optimization are beyond the scope of this chapter.

10.2 THE BIOLOGICAL BASES OF RADIATION PROTECTION

Evidence as to the types and total frequencies of the somatic radiation effects produced in human beings, that is, those produced in the exposed individuals themselves (e.g., cancer) rather than their descendants, by relatively high radiation doses has been forthcoming from a number of studies in which population groups have been studied over prolonged periods as long as 20 or 30 y. Reviews of these data were published in the latest report of the United Nations Scientific Committee on the Effects of Atomic Radiation (UNSCEAR 1977) and by the Committee on the Biological Effects of Ionizing Radiation (BEIR 1980). A very readable account of risk estimates is given in the Lauriston S. Taylor Lecture Series No. 2 published by the National Committee on Radiological Protection (NCRP 1978). A summary of the population groups from which the data are available follows.

a. Studies of the survivors of the atomic bombings of Hiroshima and Nagasaki in 1945. These results include not only the immediate or early effects of the exposures, but also in great detail late effects, particularly the induction of malignant disease. In a special group of 80,000 survivors, the frequencies of different types of fatal cancer and leukemia have been related to the estimated radiation doses received and compared with normal rates. Surveys of these data and the radiation assessments that result from them are published about every two years. A new review of the dosimetry from neutron and gamma radiation at Hiroshima and Nagasaki is being undertaken currently;

b. A registry of all tumors occurring in addition to those causing deaths as in (a) above in all Hiroshima and Nagasaki survivors. The data from the tumor registry have been used to investigate the incidence of a number of different types of cancer;

c. An "adult health study" of the frequency of the different types of illness in survivors of Hiroshima and Nagasaki and in their immediate offspring;

d. Records of frequency with which malignant tumors occur, or cause death, in groups of patients followed for prolonged periods after receiving radiotherapy for different conditions, for example, for ankylosing spondylitis surveyed in the United Kingdom, for ringworm of scalp in the United States and Israel, for mastitis in the United States, for benign uterine conditions in several countries, for supposed thymic enlargements in infants in the United States, or following frequent fluoroscopic examinations for pneumothorax in Canada. These sources are characterized by information on frequency of induction of different types of cancer in excess of that in control series, after known times following irradiation at known doses;

e. Detailed studies of the frequency of bone cancer in people who have incorporated radium into the body, in directly measured amounts, in the United States following occupational contamination or supposedly therapeutic administration;

f. Records of the frequency of bone cancer in the patients to whom a short half-life isotope of radium had been administered in the treatment of ankylosing spondylitis studied in German clinics;

g. Surveys of the frequency of liver and other malignant tumors in patients to whom a thorium preparation known as Thorotrast was administered at known dose levels as a radio-opaque medium for diagnostic purposes, particularly in Portugal, Denmark, and Germany; and

h. Records of the frequency of lung cancer in workers in uranium mines and other mines involving radioactive (radon) exposures. These studies, conducted over prolonged periods and at relatively accurately estimated levels of exposure, are from Czechoslovakia, the United States, Canada, and Sweden.

10.3 CALCULATION OF THE INCIDENCE OF STOCHASTIC HEALTH EFFECTS IN IRRADIATED POPULATIONS

When considering doses from routine releases of radioactivity, we may assume that the doses are sufficiently low that the only health effects requiring consideration are the stochastic effects, that is, delayed somatic and hereditary effects. The most important somatic effect is the induction of cancer some time after the radiation exposure. This cancer may or may not have a fatal outcome. The total health effects may be thought of as being comprised of three broad categories:

a. Cancers for which the cure rate is low and for which the period between diagnosis and death is usually short; these may be classified as fatal cancers;

b. Cancers for which the fatality rates may be low but for which there can be either physical or psychological reasons for reduced quality of life, particularly cancer of the breast or certain cancers of the thyroid. These may be classified as nonfatal cancers, and the importance to be assigned to these malignancies will be different from that to be associated with fatal cancers. A proportion of these cancers that prove fatal is taken into account with the fatal cancers; and

c. Serious transmissible disability in the descendants of irradiated parents that may be expressed over many generations. Again it is clear that there is no a priori reason why the weighting factor to be assigned to the serious hereditary defects is similar to that used for fatal or nonfatal cancers.

In calculating the consequences to the population of planned or unplanned releases of nuclides, it will be necessary to make the estimates as realistic as possible. The extent to which the already defined dosimetric quantities as set out by ICRP can be used in the above estimation of total health detriment will now be considered.

10.4 DOSIMETRIC QUANTITIES AVAILABLE FOR ESTIMATING HEALTH EFFECTS

10.4.1 Dose Equivalent

The absorbed dose from radiation (J/kg) is insufficient to predict the probability of harm to health. In radiation protection this problem has been

solved by introducing the concept of dose equivalent, H, which is related to absorbed dose, D, by modifying factors:

$$H = DQN \quad , \tag{10.1}$$

where Q is the Quality Factor of the radiation and N is the product of any other modifying factors, such as absorbed dose rate of fractionation. ICRP (1977a) has at present recommended a value of N equal to unity. The unit of dose equivalent is the Sievert (rem):

$$1Sv = 1J/kg = 100 \text{ rem} .$$

The Quality Factors currently recommended by the Commission are

X-rays, γ rays, and electrons—1

Neutrons, protons, and singly charged particles of rest mass greater than one atomic mass of unknown energy—10

α particles and multiply charged particles (and particles of unknown charge) of unknown energy—20

These Q values are to be used for internal and external radiation, are intended for use in radiological protection, and may not be representative of relative biological effectiveness for other than stochastic effects at relatively low doses. They may not apply, for example, to accidental high exposures.

10.4.2 Effective Dose Equivalent

The concept of a weighted mean whole-body exposure was introduced by ICRP (1977a) and subsequently designated *Effective Dose Equivalent,* H_E, defined as

$$H_E = \sum_T W_T H_T , \tag{10.2}$$

where H_T is the dose equivalent in tissue T and W_T is a weighting factor (for each tissue) that represents the ratio of the stochastic risk from irradiation of tissue T to that for the whole body when irradiated uniformly.

The calculations of H_E and values for W_T are discussed in Chap. 7. The principle involved is that for a given level of protection, the total risk should be the same, whether the whole body is irradiated uniformly or whether there is nonuniform or selective irradiation of particular organs.

In setting values of W_T, ICRP considered the protection of a working population by including the risk of fatal cancer in the exposed individual, together with the incidence of serious hereditary effects in the first two

generations of descendants of the irradiated parents. The inclusion of hereditary effects in only the children and grandchildren of the exposed worker was justified on the basis that the person would be primarily concerned with those effects he would observe in his lifetime, that is, in the first two generations (ICRP 1977b). There is no a priori reason for adding only this or any other proportion of the total number of expressible hereditary effects to those from fatal cancers. In fact, ICRP 26 (ICRP 1977a) recommends that in the estimation of total health effects, the hereditary effects be included for all future generations; these effects are estimated to be twice those in the first two generations.

Further, for uniform whole-body irradiation the incidence of nonfatal cancers, allowance for which is not included in the weighting factors derived for Effective Dose Equivalent, is likely to be comparable to that for fatal cancers (ICRP 1977b). The latest BEIR report (BEIR 1980) gives the incidence of malignancies as about three times the fatal rate, the majority being cancers of the skin, thyroid, or female breast.

Total incidence of malignancies may be more important in circumstances where nonuniform exposure of the body occurs. There will be practical situations in which Effective Dose Equivalent would be inappropriate for estimating health effects—for example, in the release to the atmosphere of a nuclide in such a way that the irradiation is predominantly of the skin, leading to a higher incidence of nonfatal skin cancers compared with that of fatal cancers from any whole-body dose.

Thus circumstances occur in which the Effective Dose Equivalent has limitations if used as a single quantity to express total health detriment in an irradiated population since it does not include nonfatal cancers or about half of the hereditary effects.

10.4.3 Committed Effective Dose Equivalent

The quantity *Committed Effective Dose Equivalent*, $H_{50,E}$, is defined as the integral over 50 y, following an intake of radioactivity, of the effective dose equivalent rate, $\dot{H}_E$,

$$H_{50,E} = \int_{t_0}^{t_0+50} \dot{H}_E(t)\, dt \quad , \tag{10.3}$$

where t_0 is the time at which intake occurs. The quantity $H_{50,E}$ has been introduced by ICRP for the purpose of controlling the intake of radionuclides with long physical and biological half-lives. The use of the quantity is meant to ensure compliance with dose limits for occupationally exposed individuals who may be receiving intakes of radioactivity in the course of a 50-y working lifetime.

The committed dose concept may be understood with the aid of Fig. 10.2. Suppose there are intakes in the first year of a nuclide having a long physical and biological half-life. The nuclide delivers dose *a* in the first year but remains in the body and without further intake leads to dose *b* in year 2 and doses *c* and *d* in years 3 and 4, respectively. If exposure continues at the same rate, then in the second year the dose is *a* from intakes in the second year plus *b*, already committed from the first year. After a number of years of exposure, the annual dose builds up to $(a + b + c + d)$, which is also the integrated dose from exposures in the first year. This is the committed dose concept that ensures that when a worker is exposed at the same committed dose from intakes each year throughout a working lifetime, his annual dose in his last year will be within the dose limits.

The Committed Effective Dose Equivalent may not be the most appropriate quantity to use when attempting to make realistic estimates of the

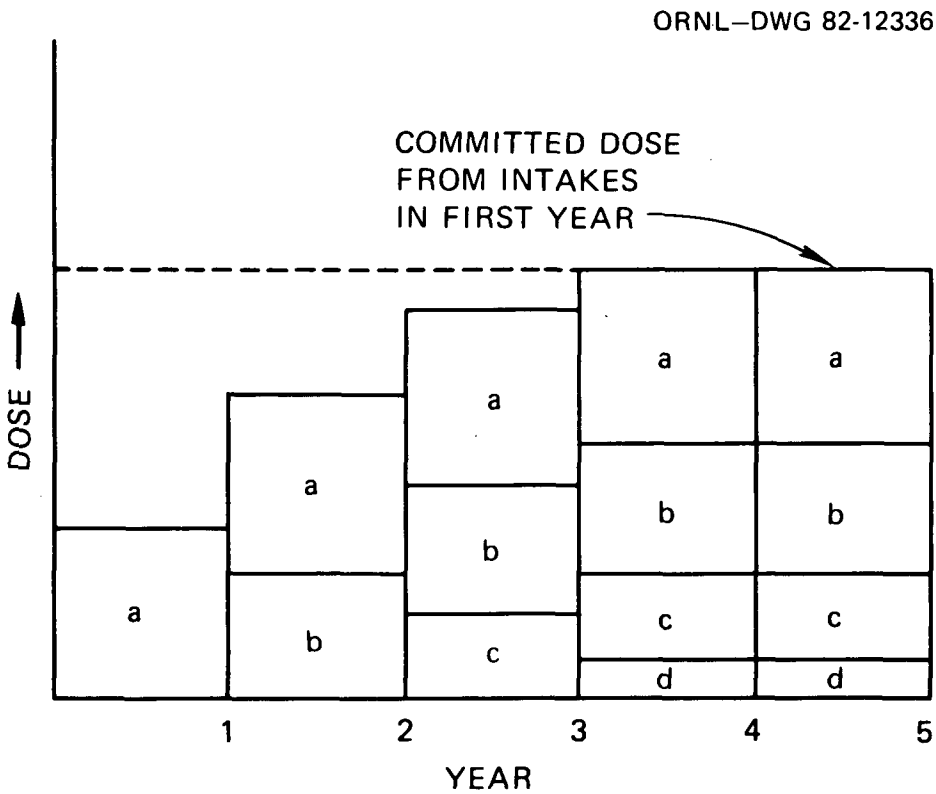

Figure 10.2. Illustration of committed dose concept.

total numbers of health effects on an irradiated population. The time over which the dose will be received following an intake of a radioactive material of long physical half-life will be a function of the age at intake, and the mean dose equivalent to be received by a population of a given age distribution could clearly be found. This is illustrated in Fig. 10.3, which shows the ratio of the

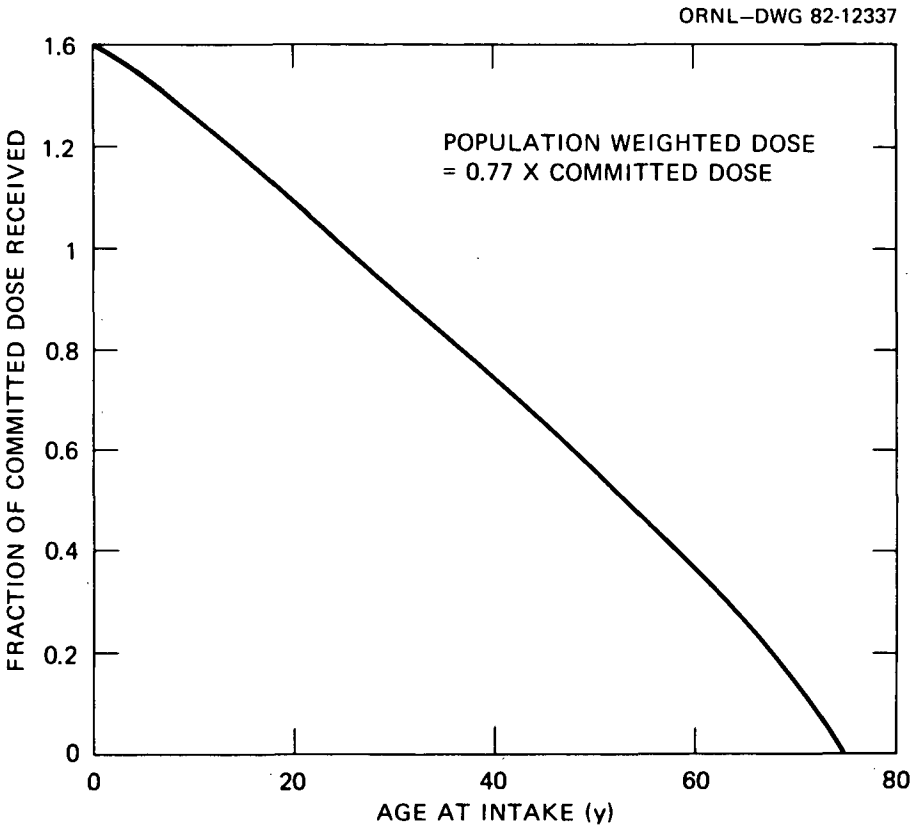

Figure 10.3. Ratio of committed dose to dose received for different ages at intake for ingestion of americium-241.

dose actually received as a function of age at intake to the committed dose for a nuclide of long physical half-life. The resulting Mean Effective Dose Equivalent in the population would still be subject to the same criticisms as those for the use of Effective Dose when assessing the total number of health effects.

A further problem is over the so-called latent period between the delivery of a dose of radiation and the development of an overt tumor. The use of the

ICRP system of dose limitation for calculating numbers of health effects assumes that the appearance of the effect is concomitant with the intake. Thus the committed dose is estimated and multiplied by the risk per unit dose equivalent to obtain the individual risk or, using collective doses (Sect. 4.3), to obtain the numbers of health effects. ICRP Publication 27 (ICRP 1977b) indicates that the ICRP Publication 26 fatal cancer coefficients are set on the basis that the individual lives long enough for the risk to be expressed following irradiation. This procedure neglects the significant delay between delivery of the dose and the recognition of the cancer. It is now widely accepted that there can be a considerable time delay before the manifestation of many cancers following exposure to ionizing radiation. In fact there is no single latent period, but there is a probability distribution function representing the time of appearance of tumors in an irradiated group of individuals.

The situation is most complex in the case of internally deposited emitters of long physical and biological half-life in the human body because, after incorporation into body tissues, irradiation of some tissues may continue over a prolonged period. The estimation of the number of health effects in a population irradiated by such nuclides requires consideration both of the time distribution of dose following intake at any given age and of the probability of cancer appearance following each increment of dose.

10.4.4 Collective Dose Equivalent

The relationship between health detriment and the distribution of dose equivalent in an exposed population is not simple, and no single quality can adequately represent the distribution. However, for many purposes ICRP (1977a) has recommended collective dose equivalent, S, in a population:

$$S = \sum_i H_i P_i \,, \tag{10.4}$$

where H_i is the per capita dose equivalent either in the whole body or in particular organs in a population P_i of subgroup i.

The collective dose equivalent associated with a given source of radiation exposure, S_K, is given by

$$S_K = \int_o^\infty HP(H)dH \,, \tag{10.5}$$

where P(H) is the number of individuals receiving dose equivalents between H and H + dH. The relationship between collective dose equivalent and health detriment depends on the validity of the linear dose-response relationship. ICRP has stressed that this is a cautious assumption, the reality of which has not been established.

Example 4.1. Suppose a routine release of a radioactive effluent into the atmosphere gives doses of 0.01 rem at 1 km to a population of 10^3, 0.001 rem at 10 km to a population of 10^5, 0.00001 rem at 100 km to a population of 10^6, and 0.0000001 rem at 1000 km to a population of 10^8.

Then the collective dose would be $0.01 \times 10^3 + 0.001 \times 10^5 + 0.00001 \times 10^6 + 0.0000001 \times 10^8 = 10 + 10 + 100 + 10 = 130$ man-rem. If the releases occurred in one year and the doses were received in the same year, the annual collective dose would be 130 man-rem. [End of Example 4.1.]

10.4.5 Collective Dose Equivalent Commitment

One of the purposes of an assessment of total health detriment is to use this in an optimization of the radiological protection of a practice giving rise to the detriment. The calculations and parameters used in the assessment of detriment should be as realistic as possible. Because optimization involves financial decisions, it is not correct to use conservative values of parameters that lead to wrong decision making and the spending of too much money, thereby defeating the objectives. Recognition of this principle should lead to a change in the selection of models and the choice of values for parameters in those models. According to ICRP Publication 26, the total health detriment is proportional to the collective dose commitment. This concept will now be discussed in more detail.

The Collective Dose Equivalent Commitment, S_c, is defined as the integral over all time of the collective dose equivalent rate S for that source:

$$S_c = \int_o^\infty \dot{S}(t)\,dt\,. \tag{10.6}$$

To perform this integration, postulations must be made about the existence of future generations, their spatial distribution, and their dietary habits. Apart from these difficulties, knowledge is also required as to the dose equivalent rates in all human body organs and tissues of interest as a function of time after intake. These data are not generally available, and a suggested alternative procedure involves separating external exposures (where in principle a simple integration over space and time can be performed) from internal exposure, in connection with which we know the committed dose equivalent per unit intake. The following practical definition of collective dose equivalent commitment is suggested:

$$S_c = H_{50} \int_o^\infty \dot{I}(t)\,dt\,, \tag{10.7}$$

where $\dot{I}$ is the collective intake rate. The integrated intake of radioactivity into a population is a quantity that may conveniently be calculated by environmental models. H_{50} is the committed dose per unit intake. It has been noted that the use of committed dose equivalent has some defects in the representation of total population dose.

Areas in which collective dose calculations utilizing effective dose may be efficient in assessing the total health detriment have been discussed. However, there are other problems in using these quantities, for example, in the implication that the risk per unit dose is treated in exactly the same way whether the doses are of the order of a few microrems or hundreds of millirems in a year or whether they are delivered now or in a million years. It is not clear that the same collective dose equivalent commitment, made up either from extremely small dose equivalents to members of a very large population or of much larger doses to members of a small population, should have the same weight in the optimizing process. There is no formal way of expressing this differentiation at the present time because of the assumption of a linear relationship between dose and risk. However, there is much evidence for the existence of nonlinear dose-response relationships and apparent thresholds in response (Clarke and Mayneord 1980). In addition, the idea was recently proposed that the cost associated with the collective effective dose equivalent may be a highly nonlinear function of individual dose (Clark and Fleishman 1980).

There might be advantages if the collective dose equivalent commitments were presented not only as single numbers but, where possible, broken down as functions of dose equivalent rate, time, space, or population group, which may aid the development of the philosophy of limiting environmental releases. This area, however, is subject to further research.

10.5 CALCULATIONS OF THE NUMBERS OF HEALTH EFFECTS

In addition to the distribution of the probability of risk in time following an increment of dose, realistic calculations of the numbers of somatic health effects must take into account the risk per unit dose equivalent in the various human body organs or tissues for the three categories of health detriment that have been identified: fatal cancers, nonfatal cancers, and serious hereditary defects. These points will now be considered in turn.

10.5.1 The Incidence of Late Somatic Effects

ICRP in Publication 26 recommends the adoption of certain risk coefficients for fatal cancer in particular human organs and tissues that are consistent with data taken from the reviews mentioned above and represent a scientific consensus of current evidence.

Numerical estimates of risk may be made using either an Absolute Risk Model or a Relative Risk Model. An Absolute Risk Model for cancer expresses the number of additional cases of cancer that arise per unit time per unit dose in a population of exposed individuals, or the total number of expected cancers in the group. The Absolute Risk Model neglects any possible correlation between the incidence of the radiation-induced effects and those due to other carcinogens to which the population is exposed. The Relative Risk Model, on the other hand, defines the ratio of the risk in the irradiated population to the risk in a comparable nonirradiated population. Thus the risk of radiation may be expressed as a percentage of the natural cancer incidence per unit dose and per unit time. These points are illustrated in Figs. 10.4a and 10.4b, which demonstrate the variation in the time of appearance of tumors for the two models. There appear to be two main criticisms of the Relative Risk Model. First, it necessarily predicts a very nonlinear response as a function of age at irradiation and there is no biological evidence in support of this effect for radiation damage. Figures 10.4c and 10.4d schematically represent the

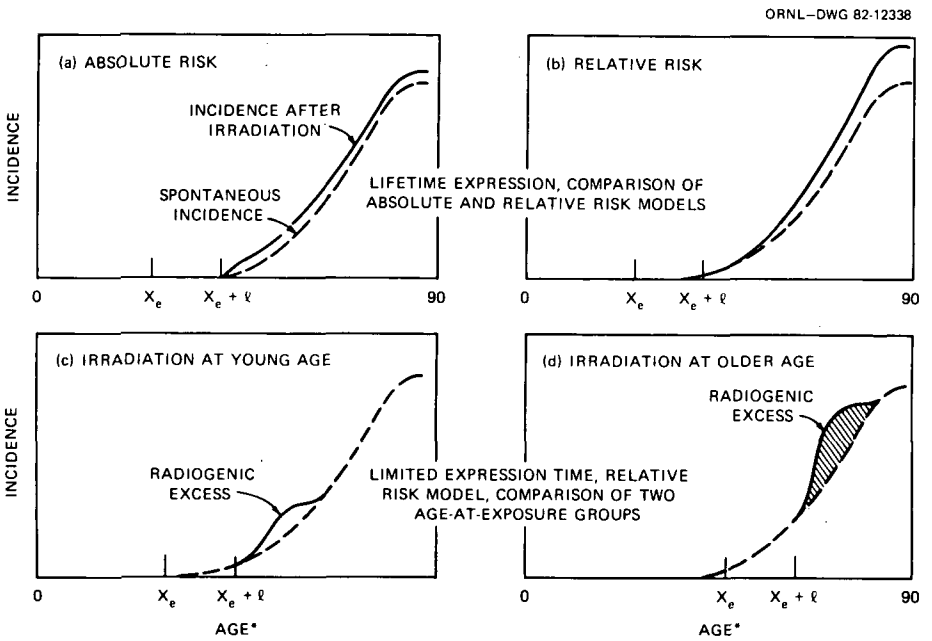

Figure 10.4. Radiation-induced cancer effect superimposed on spontaneous cancer incidence by age. Illustrations of various possibilities. Source: Committee on the Biological Effects of Ionizing Radiation (BEIR) 1980. National Academy of Sciences. Reprinted with permission.

increased incidence predicted by the Relative Risk Model for older ages at irradiation. Second, the Relative Risk Model predicts a higher total incidence than the Absolute Model for the same initial incidence rate, and there is little epidemiological evidence to support this difference. Nevertheless, the latest BEIR report (BEIR 1980) presents results in terms of both models, although ICRP has continued to use the Absolute Risk Model, and it is this model that is used here in the calculation of the number of health effects to be expected in the irradiated population.

10.5.2 Incidence of Cancer in Organs and Tissues

It is emphasized that risk estimates for individual organs cannot be determined accurately. As previously discussed, they are based on incomplete data and involve a large degree of uncertainty, particularly when applied to interpretation of health effects at low doses. With these limitations in mind, the risk estimates for cancer incidence and fatality given in Table 10.1 are applicable to an individual who will live long enough for the risk to be expressed, although they are derived from average cancer incidence and mortality for all ages. They represent a balanced judgement of the data expressed by UNSCEAR (1977) and BEIR (1980), together with other more specific data (Mays and Spiers 1978; Mays 1980; Dolphin 1979; Beebe et al. 1978; Smith and Stather 1976) and have recently been published in an NRPB report (Clarke and Smith 1980). The fatal cancer incidence and tissue classification are identical to those given by ICRP in Publication 26 since that document represents a consensus among scientists as to incidence of radiation-induced fatal malignancy.

The data in Table 10.1 apply to a population composed equally of young adult males and females. The "other organs" in the table are, for example, the liver, the individual segments of the gastrointestinal tract, salivary glands, and bladder. The individual organ risk for these remainder tissues is low, but the estimate of the total risk for irradiation is obtained by a comparison of the total malignancies produced relative to the risk of leukemia under the same conditions of irradiation (ICRP 1977a). Following ICRP in Publication 26, it would seem likely that no single one of the "other organs" had a fatal cancer risk greater than one-fifth of the total risk to these "other organs." This risk coefficient, ten mortalities per 10^6 rad, can reasonably be used for each of up to five organs or tissues receiving the highest doses from the irradiation and remaining after the specified organs in Table 10.1 have been considered.

The total number of fatal cancers for whole-body irradiation of young adults, summing from Table 10.1, is 126 per 10^6 rad; most of the medical evidence on which this number is based arose following absorbed doses of about 100 rad or more, and the ratio between the deaths due to leukemia and the sum of deaths from all other cancers is about 1:6. On the basis that lower doses, such as 10 rad, of low-LET radiation could be less carcinogenic than

Table 10.1. Incidence and mortality data associated with cancer in human organs and tissues (per 10^6 rad, low LET[a])

	Incidence	Mortality	Assumed 10+ year survival
Breast	50	25	25
Thyroid	100	5	95
Lung	20	20	0
Red bone marrow (leukemia)	20	20	0
Bone surface	5	5	0
Skin	100	1	99
Other organs	50	50	0
Total	345	126	

[a]LET = linear energy transfer.

higher doses (greater than 100 rad) and that the ratio between leukemia and the other cancers remains the same, UNSCEAR (1977) suggests a tentative value for the incidence of all cancers averaged over all ages of about 100 per 10^6 rad for these lower doses. The BEIR study (BEIR 1980) considered both acute and continuous exposure to radiation at low doses, and their conclusions are similar to those of UNSCEAR under both conditions.

The total incidence of nonfatal cancers (total incidence minus total fatal) can be seen from Table 10.1 to be in the region of 200 per 10^6 rad, mainly due to thyroid, skin, and surviving breast cancer. These data derive mainly from UNSCEAR (1977) and BEIR (1980) and are consistent also with statements made in ICRP Publication 27 (ICRP 1977b). Significant numbers of nonfatal cancers do not appear to arise in any of the other human body organs or tissues.

Example 4.2. Assume that a collective dose calculation on a population led to estimates of 2×10^6 man-rem to the thyroid, 10^5 man-rem to the whole body, and 10^6 man-rem to the lung. The resulting numbers of fatalities expected would be $5 \times 10^{-6} \times 2 \times 10^6 = 10$ for thyroid cancers, $126 \times 10^{-6} \times 10^5 = 12.6$ for malignancies in the whole body, and $20 \times 10^{-6} \times 10^6 = 20$ for lung cancers. These cancers would appear over a period of 30 years or so following the irradiation, and the cancers in the whole body would be statistically distributed over the organs and tissues in the proportions shown

by the risk figures in Table 10.1. In addition, there would be a total of 235 nonfatal cancers—200 from the thyroid collective dose and 35 from the whole-body irradiation. [End of Example 4.2]

10.5.3 Irradiation in Utero

There is strong evidence to suggest that cancers can develop in excess of the expected incidence in the first 10 y of life following irradiation of the embryo, although this excess was not observed in the children exposed in utero at Hiroshima and Nagasaki. However, the dose may have been so high that selective killing of many embryos in utero may have occurred. However, within the range (used for diagnosis) 0.2 to 2.2 rad of low-LET X rays, the risk estimate for fatal malignancies might be as high as 200 per 10^6 rad in exposed embryos according to UNSCEAR (1977), with about half of these possibly due to leukemia, and about one-quarter to tumors of the nervous system. Because of the large uncertainties, this estimate is not included in the summary table, but it should be borne in mind.

10.5.4 Hereditary Effects

It must again be emphasized that risk estimates of hereditary effects are based entirely upon animal studies, mainly mice, extrapolated to man. UNSCEAR (1977) calculates that if a population is exposed to low-LET radiation at the rate of 1 rem per generation, there will be 63 cases of serious hereditary disease per million live-born children in the first generation. The total genetic damage expressed over all generations is estimated to be 185 per million live-born per rem of parental exposure. The latest BEIR report (BEIR 1980) quotes a range of values, emphasizing the uncertainties in the data; it is estimated that 1 rem of parental exposure throughout the general population would result in an increase of between 5 and 75 additional serious genetic disorders per million live-born descendants. Such an exposure of 1 rem received in each generation is estimated to result, at genetic equilibrium, in an increase of between 60 and 1100 serious genetic disorders per million live-born descendants.

However, these latter estimates include the polygenic disorders. These are complex mutations involving several genes and are associated with major classes of disease including the phychoses and degenerative heart disease, which constitute the largest group of hereditary disease in Western populations. Mutation is thought to play a minor role in their etiology—they are irregularly inherited and are believed to be maintained largely by selection mechanisms. Because of this fact, some geneticists do not take polygenic disorders into account when estimating radiation-induced disease. If these disorders are excluded, then the UNSCEAR and BEIR values are in general agreement.

For a population continuously exposed to low levels of different qualities of radiation, a value of 10^{-4} per rem is recommended for the risk of serious hereditary disease expressed within the first two generations and 2×10^{-4} per rem is recommended for the risk expressed over all generations (ICRP Publication 26, para. 43). Taking the mean age of childbearing to be about 30 y, the incidence of hereditary disease following a single irradiation will be 80 per 10^6 rem in all generations and half this number in the first two generations.

10.6. TIME DISTRIBUTION OF RISK FOR CANCER AND HEREDITARY EFFECTS

The risk coefficients for the various tissues given by ICRP in Publication 26 assume that the irradiated individuals live long enough for the risk to be expressed. In ICRP Publication 27, it is stated that the mean latency for leukemia is in the region of 10 to 13 y and that for this form of blood cancer the distribution of intervals from exposure to death can now be approximately estimated (ICRP 1977b). The mean latency for other (solid) cancers is likely to be about twice as long, and the distribution of latencies for these cancers is assumed in ICRP Publication 27 to be twice as extended in time as for leukemia. Here the term *latency* is used to describe the period from receipt of a given dose of radiation to the death of the individual. On the basis of observations on a number of individuals, the spread in latencies can be interpreted to give a probability distribution of the emergence of an overt tumor following a given dose of radiation.

The form of the probability distribution function for the time of appearance of cancers in an irradiated population cannot be uniquely defined. It will depend on the particular type of cancer, the organ or tissue irradiated, the quality of the radiation, and very probably on the dose or the dose rate. Clarke and Mayneord suggested that a wide range of experimental data can be fitted by assuming a log-normal distribution of time of appearance following an increment of radiation (Clarke and Mayneord 1980). The assumption made in ICRP Publication 27 for the time distribution of risk following a given dose of radiation is that for leukemia the data for the Japanese survivors is used (Pochin 1979), and it has been shown that this distribution can be represented by a log-normal distribution (Clarke and Mayneord 1980). For solid cancers, it is assumed, in ICRP 27, that the probability distribution function for the time of appearance is the same as for leukemia, except that it is twice as extended in time; that is, the time scale is doubled and the shape retained (Pochin 1979). For calculating realistic expectations of health effects in irradiated populations, it would be reasonable to adopt a log-normal distribution of incidence with time to allow for the delay between dose and effect. Two examples of such a distribution are summarized in the following sections.

10.6.1 Assumed Time Incidence of Leukemia in Irradiated Populations

The time distribution of the incidence of leukemia can be described by a log-normal distribution with a median time of appearance (i.e., 50% incidence) of 12.5 y, and a standard deviation of $\sigma = 0.8$. These values are not meant to apply to any one set of observed data but are representative of the evidence for the time incidence of leukemia. The median and standard deviation are consistent with those used in ICRP Publication 27, and it may be shown that the time incidence of leukemia tends to have a fairly large standard deviation and the median time is established as short (Clarke and Mayneord 1980). The mode (the maximum rate of appearance of cancers) for these conditions occurs at about 7 y. The distribution is shown in Fig. 10.5. The mean time of cancer appearance is 17 y, and the large standard deviation means that the incidence would slowly fall away from about 25 y to approach zero at about 50 y after the dose of radiation.

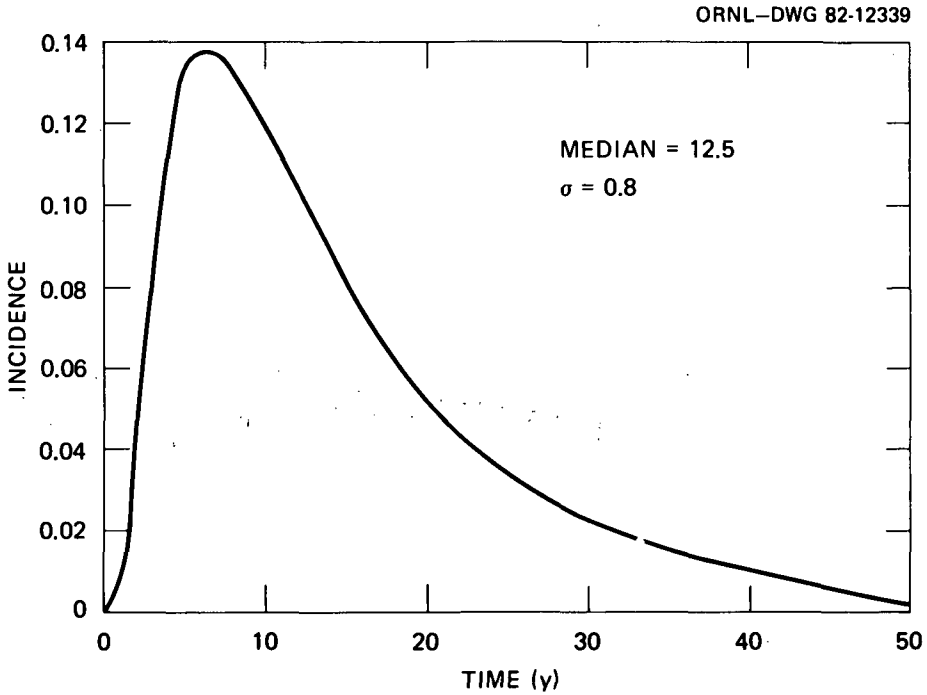

Figure 10.5. Proposed time incidence of leukemia following a single increment of radiation.

10.6.2 Assumed Time Incidence for Solid Tumors in Irradiated Populations

The assumption in ICRP Publication 27 is that solid cancers have twice the median time of appearance as that of leukemia, that their appearance is twice as extended in time, and that they thus have the same large standard deviation as is found for leukemias. This large standard deviation leads to early appearance of some solid cancers and to a mode that occurs sooner rather than later after the irradiation, at about 14 y for $\sigma = 0.8$. The cumulative incidence of each of most of the solid tumors is lower than that for leukemia so that the peak rate of incidence may be difficult to observe, and data only on the total incidence may be seen later, particularly for those organs or tissues where the natural incidence is high. Although the evidence for human solid cancers is not sufficient to be unequivocal, it seems that the mode is likely to occur later than the 13 y found using the standard deviation for leukemia. Clarke and Mayneord (1980), in presenting evidence on the time of tumor appearance for human and animal population groups, concluded that the standard deviation for solid tumors was perhaps half or less than half of that for leukemia. This would lead to a later appearance of the mode in the probability distribution function. These results are illustrated in Fig. 10.6, where the time incidences are compared for the same median but for standard deviations of $\sigma = 0.8$ (as assumed for leukemia) and for $\sigma = 0.4$. The smaller standard

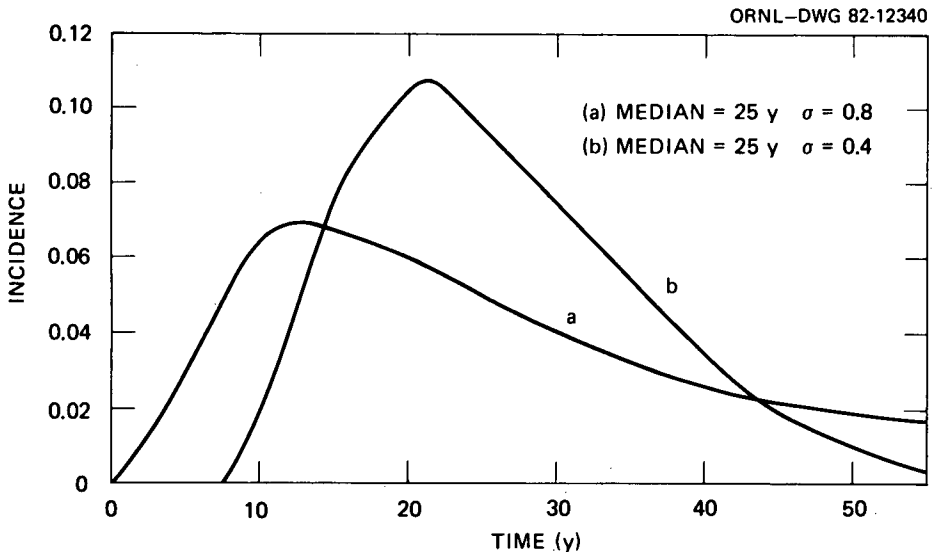

Figure 10.6. Time incidence of solid tumors following an increment of irradiation, demonstrating the effect of varying the standard deviation.

deviation gives a form that, it is felt, better reflects the features of the observed data in that there is a fairly long period with essentially zero risk followed by a gradual rise to a peak at about 20 y and a long "tail" continuing out to beyond 50 y after the irradiation. The larger value of standard deviation ($\sigma = 0.8$) leads to an indicated increase in probability of tumor appearance within a year or two of the irradiation, and to a great increase in incidence in the first 10 y, which is not apparent in observations.

For these reasons, it is likely that for solid tumors the median is 25 y and that these tumors appear log-normally distributed with a standard deviation equal to 0.4 (half the assumed value for leukemia).

Using these results, the variation in risk as a function of age and sex is similar to that shown in Fig. 10.7, which has been taken from ICRP Publication 27 (ICRP 1977b). This shows that, using the risk coefficient derived above and the time distribution of that risk, the age-averaged risk for males is 0.61 of the ICRP Publication 26 (ICRP 1977a) risk figure for somatic plus genetic risks, while that for females is 0.85 of the complete expression of risk. These figures make an allowance for the dose received up to the mean age of childbearing for estimating genetic risks.

The risk figures for males fall from about 1.2 times to 0.15 times the ICRP Publication 26 averaged values between the ages of 18 and 65, while the corresponding fall for females is from 1.5 to 0.35 of the ICRP 26 figures. Generally, the differences in risk between the sexes are not considered sufficient to establish different dose limits, and protection of the individual is sufficiently ensured by the application of a single dose limit regardless of age.

10.7 CONCLUSIONS

This chapter has explained how the assessment of total health detriment from effluents from nuclear installations may be undertaken as an input to optimization studies or for the assessment of the numbers of health effects following an unplanned release of radioactivity. The biological bases on which the numerical estimates for risks following irradiation of various human body organs and tissues are established have also been reviewed. In estimating this total health detriment, three separate categories of health effect have been identified; these may be described as fatal cancers, nonfatal cancers, and hereditary effects. It is proposed that the numbers of health effects are calculated in each category in turn; however, no attempts have been made to assign relative weighting factors to the three categories of health detriment that have been identified, although this is clearly an important consideration in applying the results of the calculations, either in optimization studies or in the analysis of hypothetical accident situations. The relative weighting may well depend upon the absolute numbers of health effects in each category in any

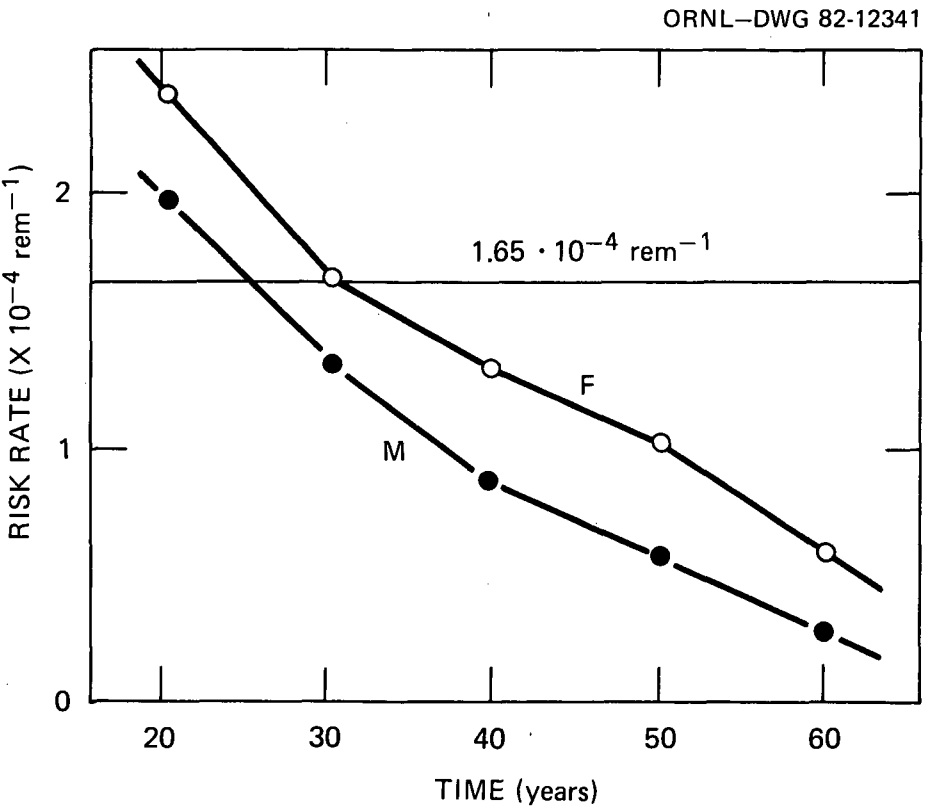

Figure 10.7. Variation with age and sex of risk (somatic + genetic) relative to nominal value of $1.65 \cdot 10^{-4}$ rem^{-1} adopted for radiation protection purposes by ICRP, this value being made up of $0.4 \cdot 10^{-4}$ rem^{-1} genetic and $1.25 \cdot 10^{-4}$ rem^{-1} as the mean value between that for males ($1.0 \cdot 10^{-4}$ rem^{-1}) and females ($1.5 \cdot 10^{-4}$ rem^{-1}) for a complete expression of carcinogenic risk. Source: International Commission on Radiological Protection (ICRP) 1977b. "Problems Involved in Developing an Index of Harm," ICRP Publication 27, *Annals of the ICRP* 1(4). Reprinted with permission.

practical assessment. Throughout this chapter a linear no-threshold, dose-response relationship has been assumed.

Despite the uncertainties in many of the data and processes used, it is generally agreed that we are now in a position to begin to assess, comprehensively, environmental discharges of radioactivity, both for the purpose of estimating their total health impact and for beginning the task of using optimization techniques for setting release limits.

REFERENCES

Beebe, G. W., Kato, H., and Land, C. E. 1978. "Studies of the Mortality of Atom-Bomb Survivors," *Radiat. Res.* **75,** 138–201.

Clark, M., and Fleishman, A. B. 1980. "The Cost of Collective Dose Equivalent," in f2iAEA Symposium on Application of the Dose Limitation System of Radiation Protection, March 1979, IAEA-SR-36/4.

Clarke, R. H. and Mayneord, W. V., 1980. "The Time of Appearance of Radiation Induced Carcinogensis and the Implications for Dose-Response Relationships," in *IAEA March 1979,* IAEA-SM-237/2.

Clarke, R. H., and Smith, H. 1980. *A Procedure for Calculating the Number of Stochastic Health Effects in Irradiated Populations,* NRPB-R102.

Committee on the Biological Effects of Ionizing Radiation (BEIR) 1980. National Academy of Sciences.

Dolphin, G. W. 1979. "Estimation of Risks to Humans Following Intake of Plutonium," in *6th International Congress of Radiation Research,* Tokyo, Japan.

International Commission on Radiological Protection (ICRP) 1959. *Recommendations of the International Commission on Radiological Protection,* ICRP Publication 1.

International Commission on Radiological Protection (ICRP) 1966. *Recommendation of the International Commission on Radiological Protection,* ICRP Publication 9.

International Commission on Radiological Protection (ICRP) 1973. *Implications of the Commission Recommendations that Doses Be Kept as Low as Ready Achievable,* ICRP Publication 22.

International Commission on Radiological Protection (ICRP) 1977a. "Recommendations of the International Commission on Radiological Protection," ICRP Publication 26, *Annals of the ICRP* **1**(3).

International Commission on Radiological Protection (ICRP) 1977b. "Problems Involved in Developing an Index of Harm," ICRP Publication 27, *Annals of the ICRP* **1**(4).

Mays, C. W. 1980. "Liver Cancer Risk," in *Symposium on Biological Implications of Radionuclides Released from Nuclear Industries, March 1979,* IAEA-Sm-237/42, Int. Atomic Energy Agency, Vienna.

Mays, C. W., and Spiers, H., 1978, "Bone Sarcoma to Man from ^{224}Ra, ^{226}Ra and ^{239}Pu," pp. 168–81 in *Biological Effects of* ^{226}Ra, EVR 5867e, ed. W. A. Muller and H. G. Ebert.

National Committee on Radiological Protection 1978. "Why be Quantitative about Radiation Risk Estimates?" by Edward Pochin, Second Lauriston S. Taylor Lecture, NCRP, Washington, D.C.

Pochin, E. E., 1979. Private communication.

Smith, H., and Stather, J. W. 1976. *Human Exposure to Radiation Following the Release of Radioactivity from Reactor Accident: A Quantitative Assessment of the Biological Consequences,* NRPB-R52, National Radiological Protection Board, Harwell, England.

United Nations Scientific Committee on the Effects of Atomic Radiation (UNSCEAR) 1977. *Sources and Effects of Ionizing Radiation,* UN E.7.7IX.1, United Nations, New York.

11 Evaluation of Uncertainties in Radiological Assessment Models

By F. O. HOFFMAN* *and* R. H. GARDNER†

11.1 INTRODUCTION

Assessment of radionuclide releases to the environment requires the use of mathematical models that can describe the transport of radionuclides from a source through the calculation of dose to humans. In these models, the values that quantify the relationships between numerous media, such as the transfer of radionuclides between air, water, land, food, and human tissues, are referred to as model parameters. The results of radiological assessments are used to assist in decisions about the acceptability of releases of radionuclides. Such decisions affect the licensing and design of a facility as well as the protective or emergency actions required to mitigate predicted consequences.

When using these models, a key question that should come to mind is: What is the accuracy of the model prediction? In the past, the use of conservative assumptions has led to model calculations that were expected to overestimate the actual dose received by members of the public. These assumptions included the postulation of hypothetical individuals who resided at the locations of maximum concentrations in air, water, or food and whose behavioral and dietary habits were such that their predicted dose would be higher than the expected average. Even so, most doses calculated for releases from nuclear facilities were only small fractions of the regulatory standards. Thus, efforts to determine uncertainties associated with model predictions were motivated more by scientific curiosity than by regulatory needs.

*Health and Safety Research Division, Oak Ridge National Laboratory.
†Environmental Sciences Division, Oak Ridge National Laboratory.

This situation has changed. Numerical guides and regulatory limits have been lowered substantially during the past few years (see Chapter 12). Previously, the maximum permissible dose to the whole body of a member of the general public was 500 mrem (FRC 1960). The current uranium fuel cycle standards of the U.S. Environmental Protection Agency (EPA) require reasonable assurance that the dose to the total body of any individual does not exceed 25 mrem (USEPA 1977). With the increasing restrictiveness of radiological protection standards, the calculation of dose to a conservatively postulated maximally exposed individual no longer produces estimates that can be considered well within dose limits (Hoffman and Kaye 1976).

Emphasis is now being placed on removing conservative assumptions and increasing the "realism" of model predictions. Dose calculations are being tailored to the actual locations of residences and to site-specific aspects of food production and consumption by individuals living near nuclear installations. Unfortunately, most environmental transfer coefficients and dose conversion factors are not determined on a site-specific basis. Yet, these are the parameters which are the most variable and which exhibit the most uncertainty in their estimation (Hoffman and Baes, eds. 1979). For many radionuclides, appropriate data for parameter estimation are unavailable, and parameter values must be derived using scientific judgment (Hoffman et al. 1978a, 1978b; Ng et al. 1978). Attempts to improve the realism of model predictions by removing conservative assumptions without accounting for remaining uncertainties will increase the probability of underestimation.

Therefore, when models using "realistic" rather than "conservative" assumptions result in dose predictions which approach a regulatory standard by even an order of magnitude, the question arises: Is there a possibility that actual doses might exceed the standard? This question now provides increased incentive for evaluating the uncertainties associated with current radiological assessment models.

11.2 SOURCES OF UNCERTAINTY

All environmental assessment models are inherently uncertain. At best, they can only approximate real-world phenomena. Detailed models are usually limited by the lack of data for model parameters; while simpler models, requiring much less information, reduce physically complex systems to a few equations. Errors in model predictions will therefore arise from a number of different sources.* Basically, these sources can be categorized as improper parameter estimation (parameter bias), improper model formulation (model bias), and stochastic effects due to random measurement and sampling errors or natural variation (parameter variability).

Model and parameter biases are particularly suspect when predictions are made for conditions distinctly different from those for which the models and their data bases were initially developed. Such situations are not uncommon.

*See Chapter 13 for additional discussion of sources of errors for models implemented with the use of computers.

For example, models composed of data bases derived from short-term observations are often used to predict impacts in the distant future (Kocher 1982). Models developed from experiments involving flat terrain and short distances have been used to predict air concentrations of radionuclides over large regions of complex topography (Miller et al. 1981). Models that predict the uptake of radionuclides from soil by vegetation under a variety of field conditions are sometimes based on data obtained from a limited number of greenhouse experiments on a few plant species grown in potted soil (Ng et al. 1982).

Parameter variability as a source of uncertainty is related to the use of deterministic models. Deterministic models use a single value for each parameter to produce a single prediction. These models ignore the effect of imprecise parameter estimation and system variability. For any assessment situation, model parameters are best represented by a range (or distribution) of values. This range translates into a range (or distribution) of model predictions. Failure to account for this range means that the predictions of deterministic models will be difficult to interpret when conservative assumptions have been removed from the calculation. To account explicitly for the imprecision in parameter estimation requires modeling approaches which are stochastic (i.e., probabilistic) rather than deterministic.

11.3 LIMITING THE SCOPE

The first step in an uncertainty analysis is to limit the scope. This requires an explicit statement of the objectives of the assessment and a determination of relevant radionuclides, exposure pathways, and model parameters. Limiting the scope of an uncertainty analysis avoids exhausting financial, physical, and human resources on aspects of assessment models that are not significant. The importance of specific radionuclides, exposure pathways, and parameters may be determined by a simple screening process or through a more rigorous mathematical sensitivity analysis.

11.3.1 Screening Procedures

The simplest approach in screening for unimportant radionuclides and exposure pathways is to compare model predictions against an arbitrary limit or established regulatory standard. In this approach, all radionuclides and exposure pathways failing to contribute more than some specified fraction of a dose limit (*DL*) are omitted from further analysis. The designation of this fraction is subjective and requires some advanced knowledge about the potential bias and variability associated with model predictions.

For screening purposes, large fractions of the *DL* can be specified for models known to be conservatively biased. Conversely, smaller fractions should be applied when models do not have a conservative bias and predictions are expected to be afflicted with a high degree of uncertainty.

The use of dose limits for screening implies that uncertainties in those portions of the model are of little interest if they do not exceed some fraction of established standards. In many situations, the combined dose prediction for

all exposure pathways and radionuclides will be of such a low magnitude that no uncertainty analysis will be required. On the other hand, using a fraction of the total predicted dose (effective or organ-specific) as a criterion for screening ensures that some radionuclides and exposure pathways will always be selected for further analysis.

Example 11.1. The current Environmental Protection Agency (EPA) limit for the uranium fuel cycle is 25 mrem to the total body and any organ, with the exception that the limiting dose for the thyroid is 75 mrem (USEPA 1977). A complete assessment for individuals residing near a nuclear installation that routinely releases small amounts of radionuclides to the atmosphere and the aquatic environment results in dose predictions for 9 pathways of exposure and 35 radionuclides (Table 11.1).

An uncertainty analysis for each possible exposure pathway and for the entire spectrum of 35 radionuclides is not practical. However, using 5% of the 25-mrem EPA limit for the total body and any organ (1.25 mrem) and 5% of

Table 11.1. Results of a hypothetical radiological assessment of routine releases of 35 radionuclides to the terrestrial and aquatic environment in the vicinity of a nuclear power facility

Exposure pathway	Principal radionuclides	Predicted dose (mrem)	Target tissue or organ
Aquatic			
Swimming	All 35	0.01	Total body
Exposure to sediments	All 35	0.03	Total body
Ingestion of fish	^{60}Co	0.008	Total body
	^{90}Sr	0.02	Bone
	^{137}Cs	0.8	Total body
Terrestrial			
Submersion in air	All 35	0.5	Skin
Exposure to ground surface	All 35	0.02	Total body
Ingestion of vegetables	^{131}I	0.5	Thyroid
Ingestion of milk	^{131}I	4.4	Thyroid
Ingestion of meat	^{137}Cs	0.1	Total body
Inhalation	^{131}I	0.03	Thyroid
	All others	0.03	Total body
Totals, all pathways and all radionuclides		1.0	Total body
		4.9	Thyroid
		0.02	Bone
		0.5	Skin

the 75-mrem EPA limit for the thyroid (3.75 mrem) as screening criteria reduces the scope of the uncertainty analysis to only those models and parameters that influence the exposure to ^{131}I (the ^{131}I dose to the thyroid exceeds the screening criterion by 30%). On the other hand, using 10% of the 1.0-mrem dose predicted for the total body (0.1 mrem) and 10% of the 4.9-mrem dose predicted for the thyroid (0.49 mrem) as screening criteria increases the scope of the analysis to the models and parameters influencing exposure to ^{137}Cs in fish and meat, and exposure to ^{131}I in milk and vegetables.

In these cases, it is assumed that either set of screening criteria—5% of the EPA limits or 10% of the total predicted doses—would be small enough to preclude exclusion of a potentially important radionuclide or exposure pathway. [End of Example 11.1]

11.3.2 Sensitivity Analysis

Sensitivity analysis usually involves perturbing each parameter of a model by a small amount while leaving all other parameters at preselected nominal values, and quantifying the relative effect on the model prediction. The parameters having the greatest influence on the model predictions are then designated as the most sensitive parameters in the model.* However, in environmental models, large parameter uncertainty or variability may produce results quite different from those obtained by small parameter perturbations (Gardner et al. 1982). For this reason, we recommend that sensitivity analyses be performed by varying each parameter over its entire expected range.

Example 11.2. The simplest kind of model employed in radiological assessments is the multiplicative chain, where the structure of the model is

$$\text{Dose} = Q \cdot A \cdot B \cdot C \cdot D_f \tag{11.1}$$

where

Q = constant release rate,

A = physical dispersion in the atmospheric or aquatic system,

B = transfer through food chains,

C = rate of food consumption,

D_f = dose conversion factor.

A sensitivity analysis, performed by increasing or decreasing each parameter by a fixed percent of the nominal value, would indicate that each parameter is equally important. However, a different conclusion will be reached by varying

*This procedure is often referred to as "Tomovic" sensitivity, because Tomovic first defined this quantity mathematically (Tomovic 1963).

each parameter over its expected range. For example, if Q were to vary by two orders of magnitude, A by a factor of 2, B by a factor of 10, C by a factor of 3, and D_f by a factor of 4, the ranking of parameter importance would be $Q > B > D_f > C > A$, a result quite different from traditional sensitivity analysis. [End of Example 11.2]

Example 11.3. Most assessment models currently in use employ formulations similar to Eq. 11.2 for predicting the transport of radionuclides from a given deposition rate to a concentration in edible vegetation (see Chapter 5):

$$C_{iv} = d\left[\frac{r[1-\exp(-(\lambda_{ir}+\lambda_w)t_e)]}{Y_v(\lambda_{ir}+\lambda_w)} + \frac{B_{iv}[1-\exp(-(\lambda_{ir}+\lambda_{is})t_b)]}{p(\lambda_{ir}+\lambda_{is})}\right]\exp(-\lambda_{ir}t_h)\,, \tag{11.2}$$

where

C_{iv} = concentration of radionuclide i in vegetation (Ci/kg),

d = average deposition rate [Ci/(m^2·d)],

r = fraction of the initial deposit intercepted by the edible portion of vegetation (unitless),

Y_v = standing biomass of edible vegetation (kg/m^2),

λ_{ir} = radiological decay constant (d^{-1}),

λ_w = environmental loss constant for removal of radionuclides from surface of vegetation (d^{-1}),

t_e = length of time vegetation is exposed to contaminated air (d),

B_{iv} = ratio of concentration in soil to concentration in vegetation (plant/soil concentration ratio) (unitless),

p = effective surface density of soil within a specified rooting depth (kg/m^2),

λ_{is} = environmental loss constant for radionuclides in soil (d^{-1}),

t_b = the time soil is exposed to contaminated air (d),

t_h = the time between harvest and consumption (d).

For this example, preselected nominal values and ranges for nuclide-independent and nuclide-dependent parameters (assuming the deposition rate d to be a constant) are listed in Table 11.2.

Table 11.2. Preselected nominal values and ranges for nuclide-independent and nuclide-dependent (for ^{131}I) parameters

Parameter	Minimum value	Nominal value	Maximum value
	Nuclide-independent parameters		
r (unitless)	0.05	0.2	0.5
Y_v (kg/m^2)	0.5	1.0	2
λ_w (d^{-1})	0.035	0.05	0.07
t_e (d)	30	45	60
p (kg/m^2)	200	220	250
t_b (d)	5,500	11,000	18,000
t_h (d)	2	5	7
	Nuclide-dependent parameters (for ^{131}I)		
B_{iv} (unitless)	0.01	0.06	0.5
λ_{is} (d^{-1})	1×10^{-5}	1.0×10^{-3}	8.22×10^{-3}
λ_{ir} (d^{-1})		8.66×10^{-2}	

Note that under any specific set of conditions, the choice of nominal and extreme values could be substantially different from those given in this example. *Sound judgment should always be used to evaluate the relevancy of nominal values and parameter ranges prior to conducting sensitivity analyses.*

The results of a sensitivity analysis performed on the above nominal values and ranges are given in Table 11.3 and are presented for the radionuclide ^{131}I. Results for ^{133}I and ^{129}I are also included in Table 11.3 to compare the effect of radioisotopes of similar biochemical behavior but exhibiting different decay constants. The decay constant λ_{ir} for ^{133}I is 0.797 d^{-1}. For ^{129}I, it is 1.12×10^{-10} d^{-1}. In Table 11.3, sensitivity indexes are calculated by substituting the minimum and maximum (from Table 11.2) for the nominal value of a parameter, while holding all other parameters at their nominal values, to produce a maximum and a minimum value of the vegetation concentration (C_{iv}^{max}, C_{iv}^{min}). Each index in Table 11.3 can be derived using

$$\text{Sensitivity index} = 1 - (C_{iv}^{min}/C_{iv}^{max}) . \tag{11.3}$$

For example, raising the nominal value of r from 0.2 to its maximum of 0.5 produces

$$C_{iv}^{max} = 2.37 \text{ pCi/kg vegetation}$$

for a constant ^{131}I deposition rate (d) of 1 pCi/(m^2·d). Lowering the value of r to 0.05 produces

Table 11.3. Sensitivity of a dose transfer model to the range of parameter values

Parameter	Sensitivity index[a]		
	^{131}I	^{133}I	^{129}I
r	0.90	0.90	0.72
Y_v	0.75	0.75	0.57
λ_w	0.22	0.038	0.27
t_e	0.02	<0.01	0.12
p	<0.01	<0.01	0.083
t_b	<0.01	<0.01	<0.01
t_h	0.35	0.98	<0.01
B_{iv}	0.02	<0.01	0.38
λ_{is}	<0.01	<0.01	0.44

[a]A sensitivity index of 1.0 indicates complete sensitivity; a sensitivity index less than 0.01 indicates that the model is insensitive to changes in the parameter.

$$C_{iv}^{\min} = 0.239 \text{ pCi/kg} .$$

The ^{131}I sensitivity index for parameter r is therefore

$$\text{Sensitivity index} = 1 - (0.239/2.37) = 0.90.$$

A sensitivity index of less than 0.01 indicates numerical insensitivity to changes in values of a parameter. The results of the analysis show the most important parameters for ^{131}I to be r and Y_v. The insensitivity of parameters t_e, p, t_b, B_{iv}, and λ_{is} for ^{131}I permits Eq. 11.2 to be simplified to

$$C_{iv}^{\text{I-131}} = d \cdot r \cdot [\, Y_v(\lambda_w + \lambda_{ir}) \,]^{-1} \exp(-\lambda_{ir} t_h). \tag{11.4}$$

It is evident in Table 11.3 that for ^{133}I, uncertainties in C_{iv} will be dominated by changes in parameter t_h. The high sensitivity of t_h is attributable to the relatively short half-life of ^{133}I (20.9 h). Because of the low sensitivity of parameter λ_w, Eq. 11.4 for ^{133}I can be simplified further to

$$C_{iv}^{\text{I-133}} = d \cdot r \cdot (Y_v \lambda_{ir})^{-1} \exp(-\lambda_{ir} t_h) . \tag{11.5}$$

For ^{129}I (as indicated in Table 11.3), only the parameters t_b and t_h in Eq. 11.2 are insensitive. Therefore, Eq. 11.2 for ^{129}I transforms to

$$C_{iv}^{I\text{-}129} = d\left[\frac{r[1-\exp(-\lambda_w t_e)]}{Y_v \lambda_w} + \frac{B_{iv}}{p\lambda_{is}}\right]. \tag{11.6}$$

Note that the expressions $(\lambda_w + \lambda_{ir})$ and $(\lambda_{is} + \lambda_{ir})$ in Eq. 11.2 essentially equal λ_w and λ_{is}, respectively, in Eq. 11.6 because of the extremely small value $(1.12 \times 10^{-10}\,d^{-1})$ of λ_{ir} for ^{129}I. [End of Example 11.3]

In the context of this chapter, sensitivity analysis is presented as a useful tool to reduce the number of parameters and exposure pathways that must be considered prior to the analysis of model uncertainties.

11.4 MODEL VALIDATION

The best method for analyzing the uncertainties associated with model predictions is a process that we refer to as model validation. Although there are many interpretations as to what constitutes a "valid" model (Mankin et al. 1977), for practical purposes a model may be considered "valid" when sufficient testing has been performed to ensure an acceptable level of model accuracy. The acceptability of model accuracy is a subjective determination and will vary on a case-by-case basis.

Because of the deterministic nature of present radiological assessment models, only one prediction of dose is made for a given radionuclide release, exposure pathway, and target organ. Releases of radionuclides, environmental concentrations, and the behavior and physiology of individuals within a population are variable quantities. Therefore, the validation of radiological assessment models begins with the comparison of a single predicted quantity against a distribution of measured observations (Fig. 11.1). This comparison should be made for measurements representing the range of conditions for which the model is intended (Fig. 11.2).

For each set of conditions selected for model testing, the procedure is expected to produce different predicted and measured quantities. These results can be compared by dividing each prediction by the corresponding distribution of measured values to produce a frequency distribution of predicted-to-observed ratios (P/O) for each set of conditions (Fig. 11.3). These P/O ratios may be pooled into one general distribution representing the overall uncertainty associated with generic applications of the model.

11.4.1 Application of P/O Ratios

A distribution of P/O ratios provides a measure of uncertainty due to predictive bias and system variability. For example, a log-symmetrical distribution of P/O ratios having a median value of 1.0 and a standard deviation of

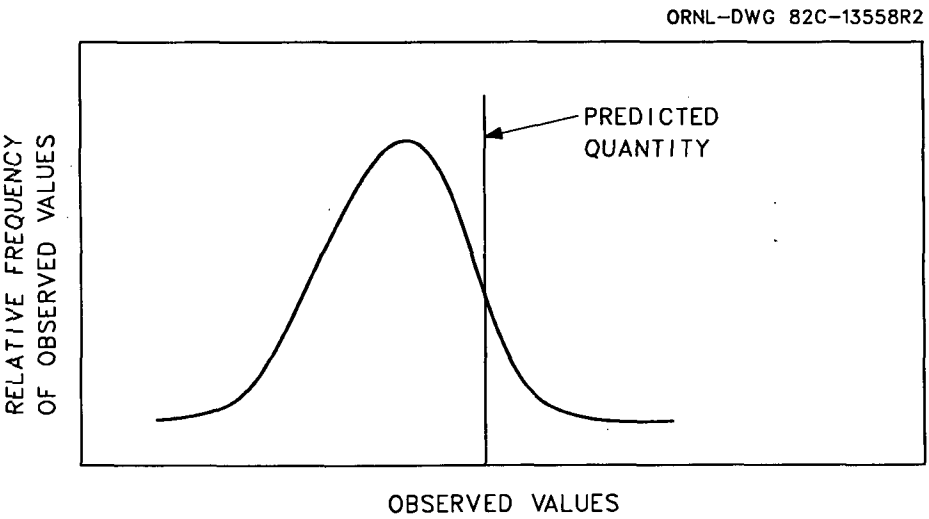

Figure 11.1. Model validation begins with the comparison of a single predicted quantity against a distribution of measured observations.

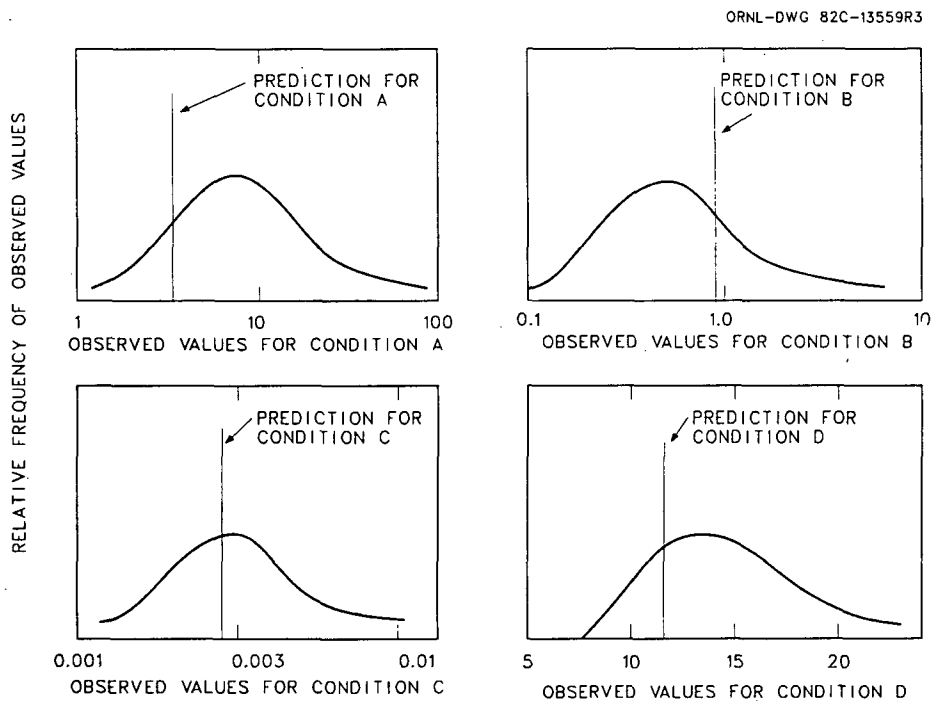

Figure 11.2. Model validation involves comparing predictions with observations over a range of conditions.

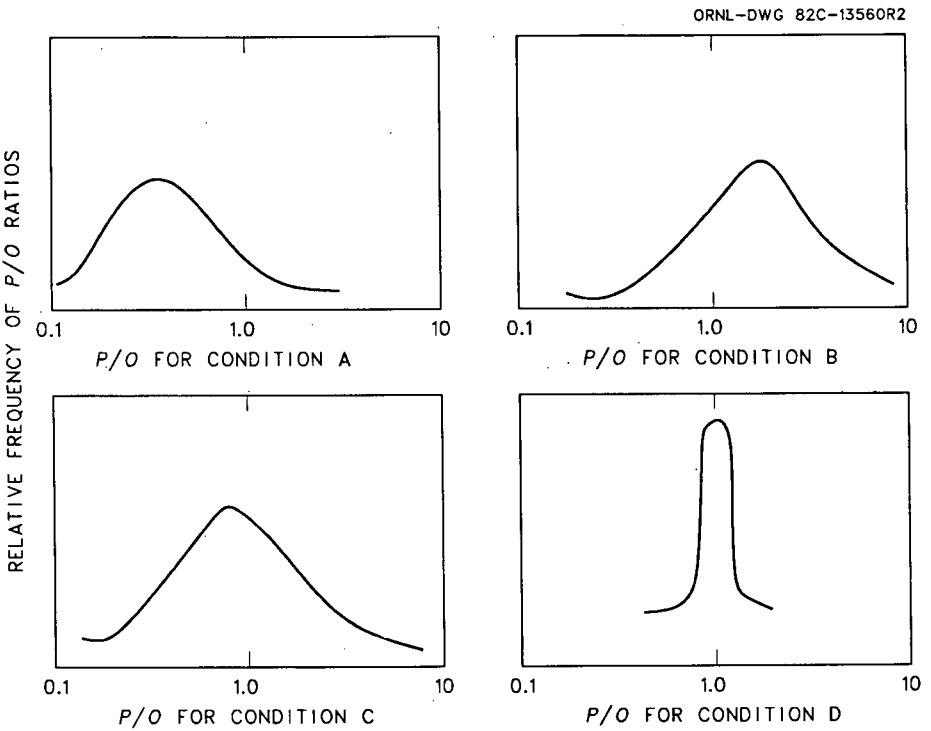

Figure 11.3. Dividing each prediction by the corresponding set of observations (P/O) for conditions A through D produces frequency distributions of predicted-to-observed ratios for each set of conditions.

0.2 indicates no systematic bias with a 20% relative error due to system variability. On the other hand, a log-symmetrical distribution of P/O ratios having a median value of 10 and a standard deviation of 0.2 indicates a strong bias with a tendency to overpredict by a factor of 10. In this case, only 2% relative error is due to system variability (Fig. 11.4).

If a model is being applied to an assessment situation having characteristics similar to conditions in which validation experiments have been performed, then P/O ratios can be used to calibrate model predictions to reduce systematic bias. The remaining uncertainty after calibration will be due to system variability (Fig. 11.5). Distributions of the reciprocals of P/O ratios can also be used in this situation, to estimate the probability that dose limits or environmental standards will not be exceeded because of the uncertainties in model predictions (Fig. 11.6).

Example 11.4. Assume that a nuclear facility is located in flat terrain characterized by relatively predictable weather patterns. A simple atmospheric dispersion model is used to predict an annual average air concentration for a

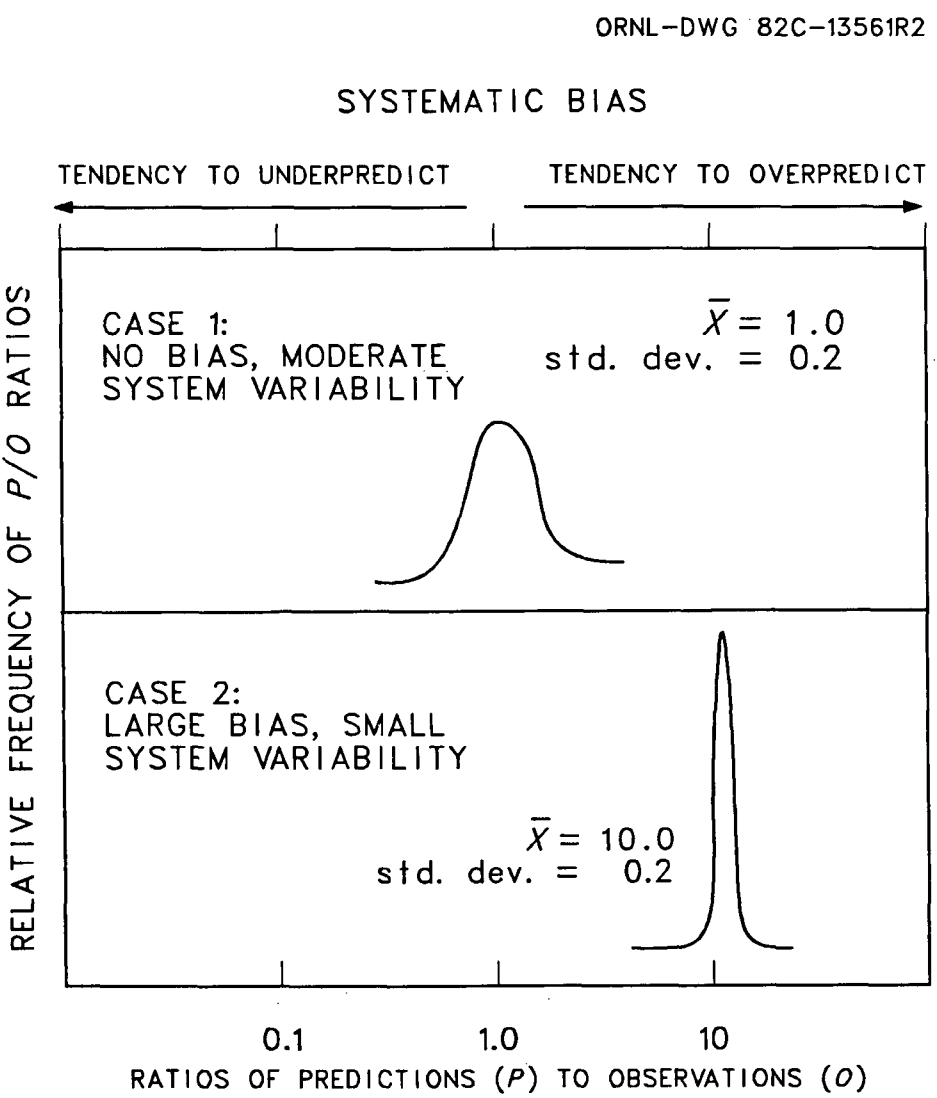

Figure 11.4. Distributions of *P/O* ratios are useful indicators of model bias and system variability.

location situated 70 km from the source of release. For a given release of ^{85}Kr, the model predicts an annual average concentration of 38 pCi/m^3. How uncertain is this prediction?

Suppose that a review of the literature shows that this model has been tested under meteorological and topographic conditions very similar to those

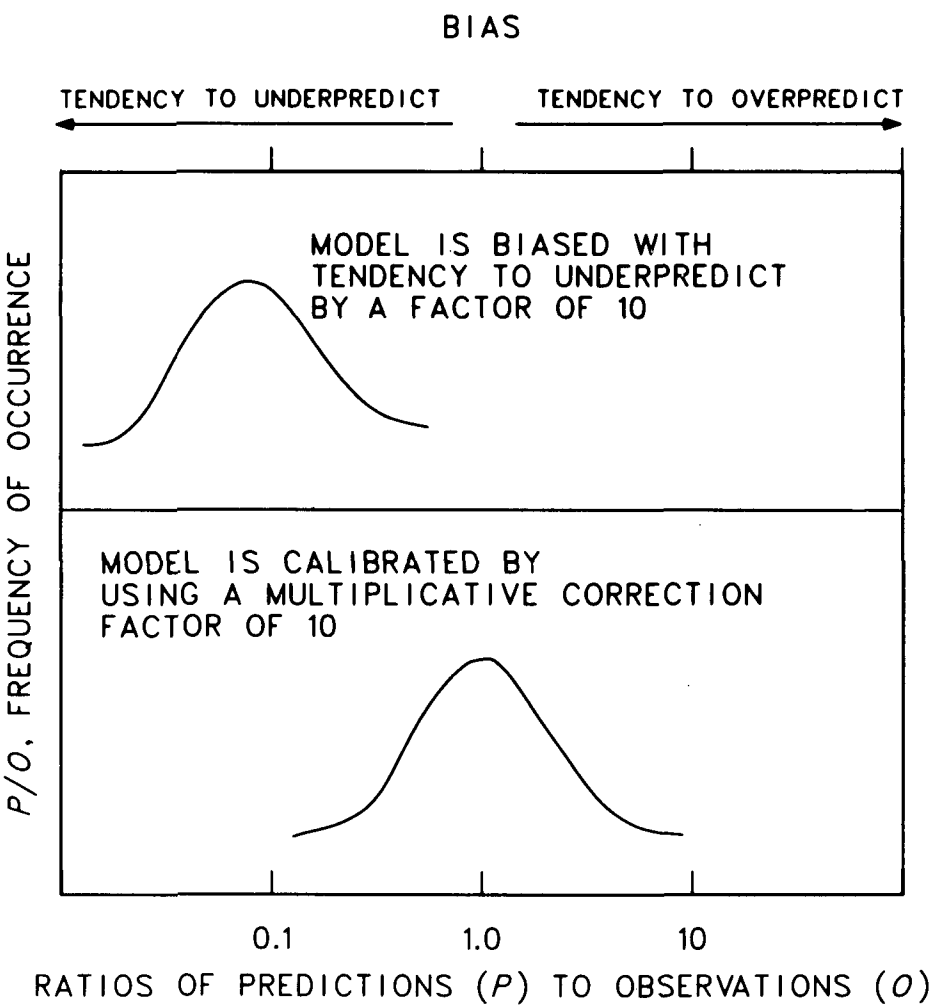

Figure 11.5. Distributions of P/O ratios can be calibrated to eliminate bias, but system variability remains constant.

prevalent in the area of the site being assessed. The results of these tests produce a lognormal distribution of P/O ratios, with a geometric mean (X_g) of 2.41 and a geometric standard deviation (s_g) of 1.45.*

An interval (defined by X_{min} and X_{max}) expected to include 95% of all P/O ratios is calculated as

*See Example 11.7 in Sect. 11.3.3 for further explanation of the geometric mean and the geometric standard deviation.

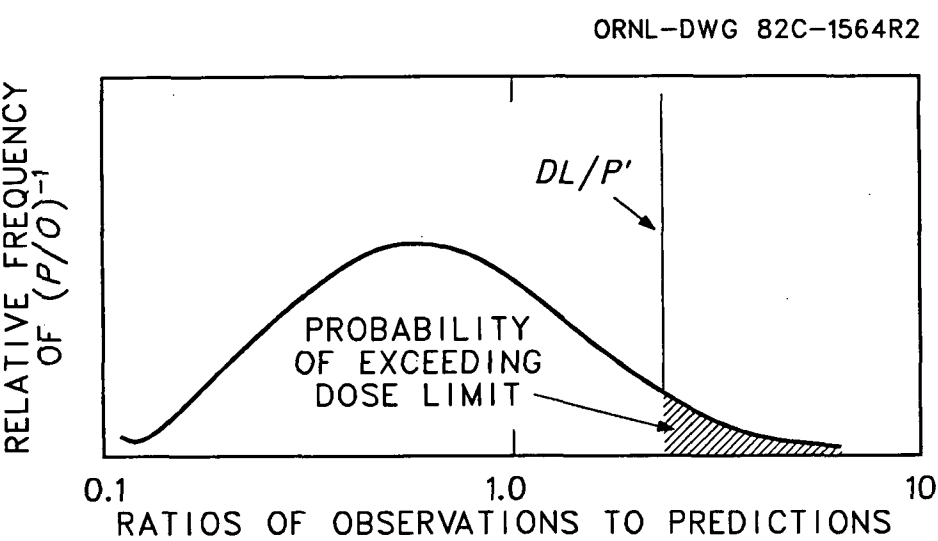

Figure 11.6. Distribution of $(P/O)^{-1}$ ratios is useful when comparing a prediction from a given assessment (P') with a standard (DL).

$$X_{\max} = X_g s_g^2 \tag{11.7}$$

and

$$X_{\min} = X_g / s_g^2 . \tag{11.8}$$

The geometric mean of P/O ratios indicates that the simple dispersion model will overpredict on the average by a factor of about 2.4. The results obtained by the use of the values of the geometric mean and geometric standard deviation in Eqs. 11.7 and 11.8 indicate that the range of overprediction should be between a factor of 1.1 and a factor of 5.1. Systematic bias is reduced through calibration by dividing the model prediction by the geometric mean of P/O ratios. Thus, an unbiased prediction of the air concentration is (38 pCi/m^3) ÷ (2.41) = 16 pCi/m^3, and the 95% interval for this calibrated prediction is 7.6 to 34 pCi/m^3. [End of Example 11.4]

Example 11.5. An arbitrary limit (L) of 40 pCi/m^3 is assumed. What is the probability of this limit not being exceeded if the uncalibrated model in Example 11.3 predicts an air concentration (P') of 38 pCi/m^3?

Using lognormal statistics, we find that

$$z = \frac{\ln(L) - \ln(P'/X_{g_{P/O}})}{\ln(s_{g_{P/O}})} , \tag{11.9}$$

where

$X_{g_{P/O}}$ = the geometric mean of P/O ratios, 2.41,

$s_{g_{P/O}}$ = the geometric standard deviation of P/O ratios, 1.45,

z = the number of standard deviations in a standard normal distribution corresponding to a specific level of cumulative probability (Table 11A.1 in Appendix 11A, at the end of this chapter).

Thus,

$$z = \frac{\ln(40.0) - \ln(38.0/2.41)}{\ln(1.45)} = 2.51 .$$

This z value of 2.51 corresponds to the 0.9940 cumulative probability in Table 11A.1. Thus, we would conclude that there is greater than a 99% chance that uncertainties in the predicted value P' would not result in actual air concentrations exceeding the limit L. Conversely, we conclude that there is less than a 1% chance that the limit L would be exceeded. Note that we draw these conclusions assuming that the distributions of P/O ratios are directly relevant to the conditions for which the predicted quantity P' has been produced, and that these distributions are obtained from a sufficiently large number of observations. This assumption will always be subject to question. [End of Example 11.5]

11.4.2 Application of Correlation Analyses

Another measure of model performance is obtained by comparing model predictions with observations over a range of environmental conditions and testing for correlations between predictions and observations.

Strong correlations indicate that differences among observations can be explained by the model. Weak correlations indicate that differences among observations are controlled by factors unaccounted for by the model. Weak correlations can be the consequence of a number of factors, including a poor model structure, poor parameterization of the model, or high system variability.

It is possible for a model to be a poor predictor, yet exhibit a strong correlation between predictions and observations (Fig. 11.7). In these cases, predictions tend to differ from observations by a proportional quantity. Because of the strong correlation, all that is required to improve the performance of the model is calibration of model predictions by a constant factor.

Example 11.6. In an attempt to test the atmospheric dispersion model contained within the AIRDOS-EPA computer code (Moore et al. 1979), a correlation analysis was made between predicted annual average air concentra-

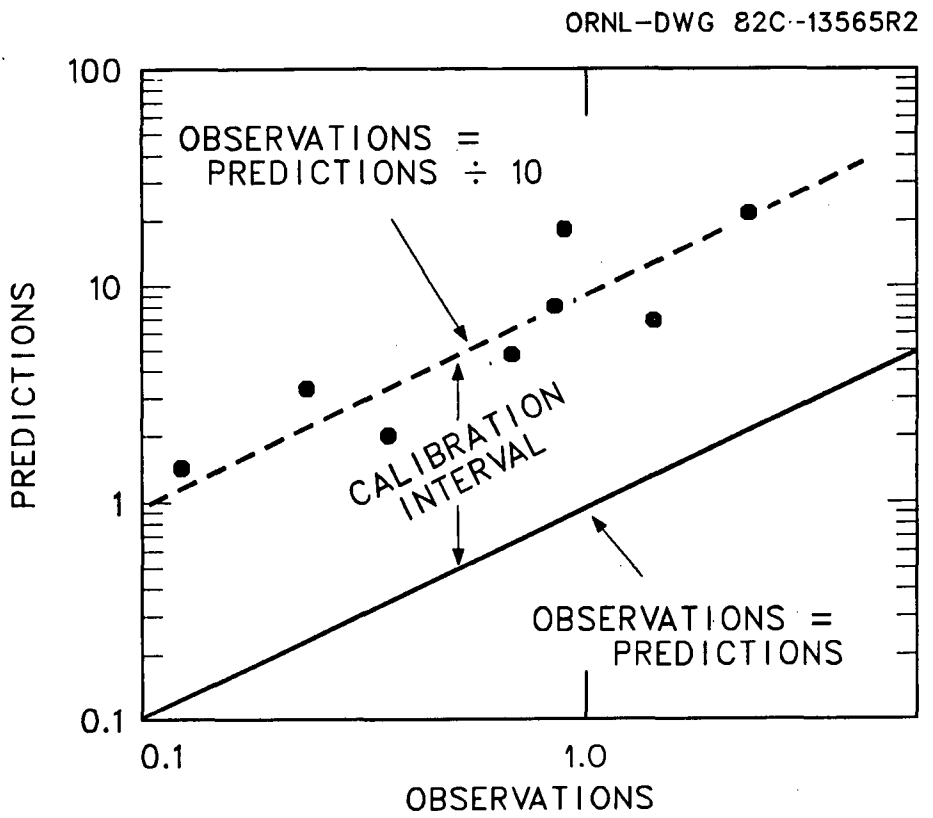

Figure 11.7. A regression of model predictions and observations reveals strong correlations but a consistent tendency for the model to overpredict. Calibrating by 10^{-1} improves model performance.

tions of ^{85}Kr released from a nuclear fuel reprocessing facility and measured air concentrations obtained from 13 sampling locations averaged for a period of one year (Fields et al. 1981). The results of this analysis are reproduced in Fig. 11.8.

The points plotted in Fig. 11.8 are the relationships between the predicted values and measured values of ^{85}Kr air concentrations for the 13 monitoring stations. The position of each point is determined by the location of the predicted value on the y axis of the figure and the location of observed values on the x axis. The solid line indicates the relationship where predictions are equal to observations.

Note that the solid line intercepts none of the plotted points. Upon initial inspection, it seems as if the atmospheric dispersion model is a relatively poor

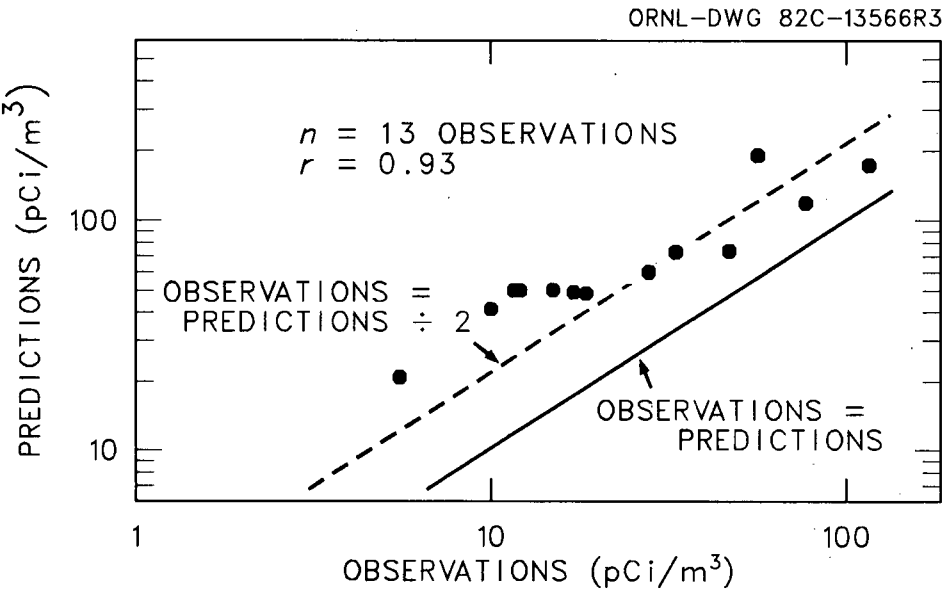

Figure 11.8. Comparison of predicted and observed annual average ^{85}Kr ground-level air concentrations (adapted from Fields et al. 1981).

predictor of the observed values. However, the linear correlation coefficient (r) is 0.93, indicating a strong correlation between predictions and observations. Thus, although the model provides a poor fit to the observed points, most of the differences among observations are explained by the model. The accuracy of the model is improved by calibrating model predictions using a correction factor to improve the fit to the plotted points. The result of model calibration is depicted by the dashed line in Fig. 11.8, whereby model predictions have been divided by a factor of 2.

The correlation analysis presented in Fig. 11.8 is typical of situations where model predictions are biased, but the amount of system variability unexplained by the model is small in comparison with the range of predictions and observations. In this case, model bias is conservative; i.e., predictions tend to overestimate observations. The cause of this bias has been attributed to underestimation of the average mixing height of the atmosphere (Fields et al. 1981; Buckner 1981). [End of Example 11.6]

11.4.3 Limitations of Model Validation

Model validation requires testing over the full range of conditions for which predictions are intended. This demands a substantial investment in time and financial resources. Most validation studies have been restricted to com-

ponents of assessment models and limited to relatively short time periods and few locations. Often, it is difficult to distinguish between so-called "validation" tests, in which model predictions have been prefitted to the observed data, and true comparisons between model predictions and independent sets of observations. In other cases, validation is nearly impossible due to the extremely low levels of predicted concentrations and doses or to the extensive time periods considered by the model (Lindackers and Bonnenberg 1980).

One source of information for model validation could be data acquired from current monitoring programs at nuclear installations. However, these programs are seldom adequate to permit a reliable comparison between model predictions and reported data (Eichholz 1978; USNRC 1982). Most monitoring programs are designed specifically to demonstrate compliance with established limits or technical specifications, and changes in the experimental or sampling design and improvements in detection limits must be made before data obtained from these programs are suitable for testing assessment models.

11.5 PARAMETER UNCERTAINTY ANALYSES

What can be done when validation information is not readily available or sufficiently complete to quantify model uncertainties? If the structure of a model is relatively unbiased (i.e., it adequately represents the actual situation being assessed), then we can make use of parameter uncertainty analyses* to estimate the uncertainty in model predictions. Parameter uncertainty analysis uses an estimated frequency distribution of values for each model parameter to produce a frequency distribution of model predictions (Fig. 11.9). The distribution of model predictions can be compared with the deterministic prediction of an assessment model or with established limits to estimate potential bias and the possibility of exceeding established limits (Fig. 11.10).

Parameter uncertainty analysis is also useful for determining the contribution of each parameter to the total uncertainty in the model prediction. This information provides guidance for further research to improve parameter estimation and reduce uncertainty.

*Numerous synonyms for parameter uncertainty analysis exist in the literature. In the past, we have used the terms imprecision analysis (Schwarz and Hoffman 1981), statistical sensitivity analysis (Shaeffer 1980), and error analysis (Gardner et al. 1980). Others refer to the process described by parameter uncertainty analysis as error propagation (Collee et al. 1980). In Chapter 13, it is classified as probabilistic modeling. In this chapter, we use the term parameter uncertainty analysis because we believe it to be more descriptive of the process.

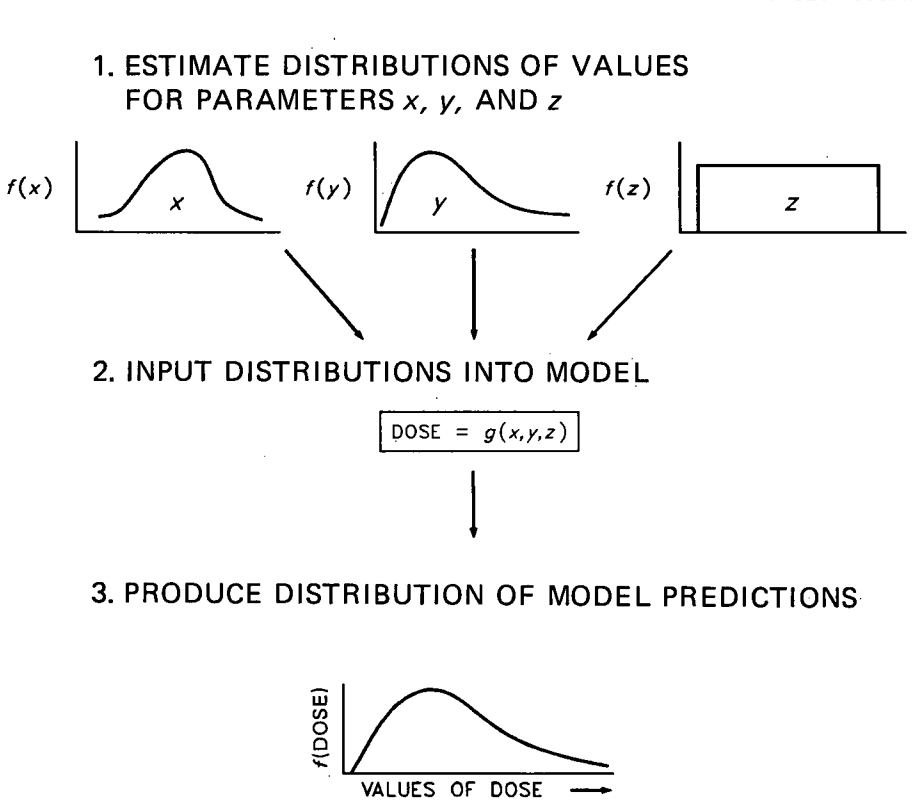

Figure 11.9. The concept of parameter uncertainty analysis: Distributions of parameter values are used as model input to produce output in the form of a distribution of predicted values.

11.5.1 Estimating Parameter Uncertainty

The first step in a parameter uncertainty analysis is to determine the potential spread of values associated with each input parameter. The general conditions normally encountered and procedures for estimating parameter uncertainty are outlined in Table 11.4. Ideally, parameter values should be derived from site-specific research. When adequate data exist, the appropriate statistical distribution and its moments, e.g., mean and variance (Hahn and Shapiro 1967; Johnson and Kotz 1970), can be determined for each parameter. In practice, adequate site-specific data are seldom available. Many parameters employed in radiological assessment models can only be estimated indirectly

ORNL-DWG 82C-13568R2

1. PRODUCE A DISTRIBUTION OF MODEL PREDICTIONS.

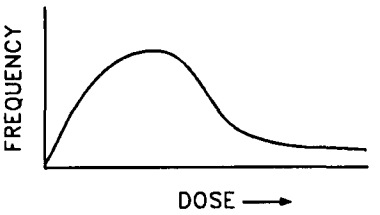

2. COMPARE WITH ASSESSMENT PREDICTION.

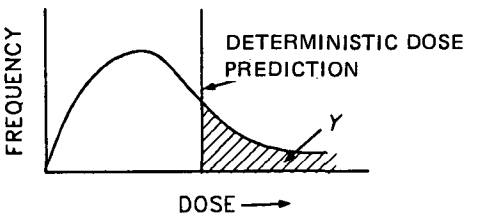

Y = PROBABILITY OF DETERMINISTIC DOSE PREDICTION BEING EXCEEDED

3. COMPARE WITH DOSE LIMITS.

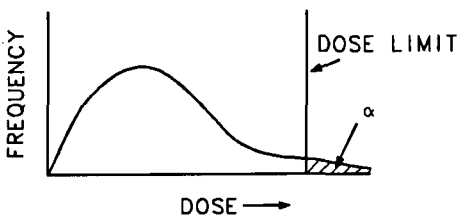

α = PROBABILITY OF DOSE LIMIT BEING EXCEEDED

4. PRIORITIZE IMPORTANT PATHWAYS AND PARAMETERS.

Figure 11.10. Objectives of parameter uncertainty analysis.

Table 11.4. Procedures for estimating parameter uncertainty

Condition	Procedure
Site-specific data available	Analyze data statistically
Site-specific data not available, but data available for other sites	Statistically analyze only those data relevant to conditions comparable to those prevailing at the specific site
Available data is limited to radionuclides of related chemical elements or differing environmental conditions	Use judgment to estimate expected range of parameter values based on environmental, chemical, and physical similarities

from similar values reported in the literature. Thus, a major effort must be invested in the search for relevant data. Often judgments must be exercised and manipulations performed on data obtained from the literature before estimates of parameter values can be made that are consistent with specific assessment conditions (Ng et al. 1978, 1982; Shaeffer 1981; Bennett 1981; Hoffman et al. 1982).

When estimating parameter uncertainty through a review of literature, large ranges of values are expected. Table 11.5 lists the results of a team effort at Oak Ridge National Laboratory that estimated parameter variability from values reported in the literature. These values were considered relevant to parameters defined in the Nuclear Regulatory Commission's (NRC) Regulatory Guide 1.109 (USNRC 1977). All parameter values in Table 11.5 conformed to a lognormal distribution and are listed according to their first percentile, mode, median, mean, and 99th percentile.

Large variability is expected for parameters that have been derived from individual observations taken over relatively short time periods and/or a range of environmental conditions. Much less variability is expected in parameters estimated from site-specific data averaged over long time periods, large areas, and large populations. More parameter variability is expected for assessments of doses to individual members of critical population groups than is expected for collective dose assessments for large populations.

Example 11.7. The milk transfer coefficient (F_m) relates the steady-state concentration of a radionuclide per liter of milk to a daily intake of the radionuclide by a dairy cow. For radiological assessments of ^{137}Cs, a generic default value for F_m of 0.012 d/L is given in Regulatory Guide 1.109 (USNRC 1977). What is the uncertainty associated with this generic default value? Assume that site-specific data on the F_m for ^{137}Cs are not available. To

Table 11.5. Distribution of values[a] for selected food chain parameters used in NRC Regulatory Guide 1.109

Parameter	X_{01}[b]	Mode	Median	Mean	X_{99}[b]	NRC[c]
Ratio of vegetation interception fraction to forage density, r/Y_v [m^2/kg (dry wt)]	0.64 (0.01)	1.5 (0.33)	1.8 (0.50)	2.0 (0.59)	5.1 (0.99)	1.1 (0.12)
Environmental half-time of materials deposited on vegetation, T_w (d)						
Particulates	8.2 (0.01)	13.9 (0.40)	14.9 (0.50)	15.4 (0.55)	27.2 (0.99)	14.0 (0.41)
Iodines	4.8 (0.01)	9.06 (0.38)	9.97 (0.50)	10.5 (0.56)	20.5 (0.99)	14.0 (0.86)
Milk transfer coefficient for dairy cows, F_m (d/L)						
Iodine	2.8E-3 (0.01)	7.4E-3 (0.29)	1.0E-2 (0.50)	1.2E-2 (0.61)	3.6E-2 (0.99)	6.0E-3 (0.17)
Stontium	3.4E-4 (0.01)	9.3E-4 (0.30)	1.2E-3 (0.50)	1.4E-3 (0.60)	4.2E-3 (0.99)	8.0E-4 (0.21)
Cesium	1.7E-3 (0.01)	4.8E-3 (0.28)	6.7E-3 (0.50)	8.0E-3 (0.61)	2.6E-2 (0.99)	1.2E-2 (0.84)
Beef transfer factor, F_f (d/kg)						
Cesium	1.7E-3 (0.01)	5.8E-3 (0.21)	1.1E-2 (0.50)	1.5E-2 (0.66)	7.3E-2 (0.99)	4.0E-3 (0.10)
Freshwater finfish bioaccumulation factor, B_{ip} (L/kg)						
Iodine	7.8 (0.01)	23 (0.27)	33 (0.50)	40 (0.62)	140 (0.99)	15 (0.10)
Strontium	0.17 (0.01)	0.43 (0.04)	11 (0.50)	56 (0.82)	730 (0.99)	30 (0.71)
Cesium	170 (0.01)	640 (0.19)	1300 (0.50)	1900 (0.67)	9900 (0.99)	2000 (0.68)
Annual consumption of milk by infants, U_{ap}^{M} (L/y)	190 (0.01)	287 (0.42)	299 (0.50)	305 (0.54)	476 (0.99)	330 (0.69)

[a]Values in parentheses are the estimated percentiles associated with the location of each parameter value within the distribution of parameter values.

[b]X_{99} represents the estimated 99th percentile of the distribution; X_{01} represents the first percentile.

[c]NRC generic default values recommended in NRC Regulatory Guide 1.109 for use in lieu of site-specific information.

Source: Hoffman, F. O., and Baes, C. F., III, eds. 1979. *A Statistical Analysis of Selected Parameters for Predicting Food Chain Transport and Internal Dose of Radionuclides,* U.S. Nuclear Regulatory Commission Report ORNL/NUREG/TM-282, Oak Ridge National Laboratory, Oak Ridge, Tenn.

answer this question, we analyze data reported in the literature, including only those data that are relevant to the site for which the assessment is intended. Upon a careful evaluation of the literature, the following values are considered relevant.

Values of F_m for ^{137}Cs obtained from the literature (d/L)

6.4×10^{-3}	4.9×10^{-3}	4.5×10^{-3}
1.3×10^{-2}	9.8×10^{-3}	3.5×10^{-3}
1.5×10^{-2}	8.9×10^{-3}	4.1×10^{-3}
1.5×10^{-2}	4.1×10^{-3}	2.5×10^{-3}
1.6×10^{-2}	2.5×10^{-3}	4.6×10^{-3}
9.2×10^{-3}	7.5×10^{-3}	4.8×10^{-3}
1.4×10^{-2}	3.6×10^{-3}	1.2×10^{-2}
9.6×10^{-3}	8.7×10^{-3}	9.9×10^{-3}
7.1×10^{-3}	4.8×10^{-3}	1.5×10^{-2}

There are 27 observations, with a mean value ($\bar{X}$) of 8.2×10^{-3} d/L and a standard deviation of 4.3×10^{-3} d/L (coefficient of variation = 52%). Graphing the data on lognormal probability paper demonstrates that the data can be approximated by a straight line (Fig. 11.11) and thus can be assumed to conform to a lognormal distribution. The data plotted in Fig. 11.11 are arranged according to the expression $[(i - 0.375)/(n + 0.25)]$, where i is the rank order of observations and n is the total number of observations.

The logarithmic transformation of the values of F_m, i.e.,

$$\ln(6.4 \times 10^{-3}) = -5.05,$$
$$\ln(1.3 \times 10^{-2}) = -4.34,$$
$$\ln(1.5 \times 10^{-2}) = -4.20,$$
$$\ln(9.2 \times 10^{-3}) = -4.69,$$
etc.,

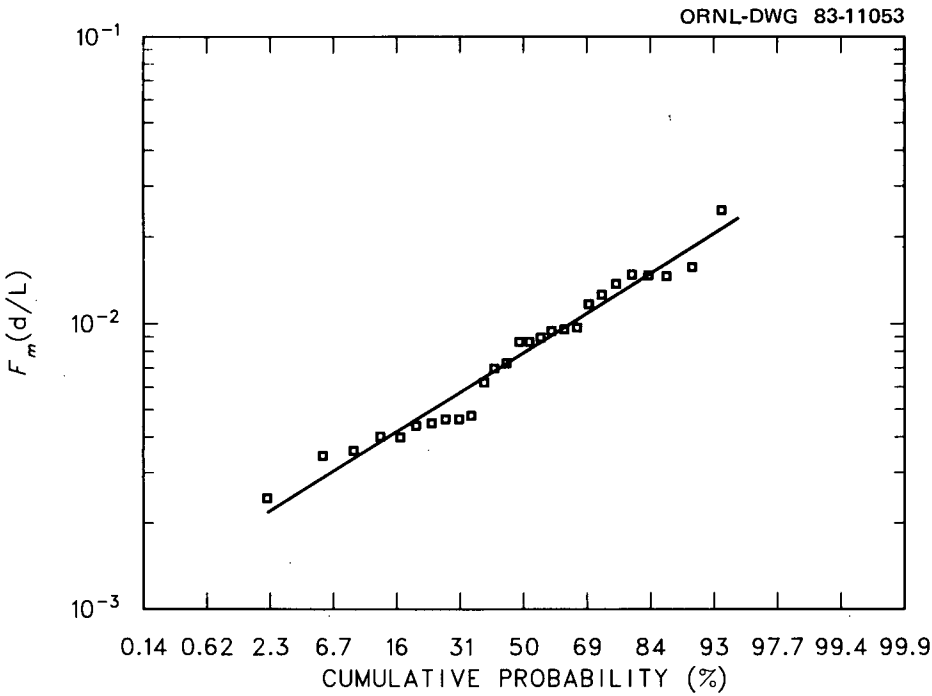

Figure 11.11. Lognormal probability plot of the milk transfer coefficient F_m for cesium in dairy cows.

produces a mean (μ) and a standard deviation (σ) of the log-transformed values of -4.95 and 0.572, respectively.*

The geometric mean (X_g) and geometric standard deviation (s_g) are anti-logs of μ and σ and are estimated as

$$X_g = e^{\mu} \tag{11.10}$$

and

$$s_g = e^{\sigma}. \tag{11.11}$$

The geometric mean is equivalent to the median, or 50th percentile, of a lognormal distribution. The geometric standard deviation is a multiplicative error estimator, where $X_g s_g$ and X_g/s_g describe an interval about X_g encompassing 68% of the log-normal distribution.

For the example of F_m using the above values of μ and σ,

$$X_g = e^{\mu} = e^{-4.95} = 7.1\times10^{-3}\,\mathrm{d/L},$$

and

$$s_g = e^{\sigma} = e^{0.572} = 1.77.$$

The percentile associated with the NRC generic value (a) of the F_m for ^{137}Cs is obtained from

$$\begin{aligned} z &= \frac{\ln(a)-\ln(X_g)}{\ln(s_g)} \\ &= \frac{\ln(1.2\times10^{-2}\,\mathrm{d/L})-\ln(7.1\times10^{-3}\,\mathrm{d/L})}{\ln(1.77)} \\ &= 0.92\ . \end{aligned} \tag{11.12}$$

In Table 11A.1 in Appendix 11A (at the end of this chapter), the cumulative probability is 0.82 (or the 82nd percentile) for $z = 0.92$.

Thus, if the estimates of parameter variability are relevant, the generic value employed by the NRC is conservatively biased. However, there is still a 18% chance of the NRC default value being exceeded by values within our estimated distribution of F_m, even though the NRC value is greater than the

*Throughout this chapter the symbols μ and σ will be used to denote the mean and standard deviation, respectively, of log-transformed values.

geometric mean by almost a factor of 2. Ultimately, our estimated distribution of F_m should be combined with distributions of other model parameters before evaluating the final effect in the dose prediction. [End of Example 11.7]

11.5.2 Combining Parameter Uncertainty

11.5.2.1 Simple Analytical Approaches

Simple analytical approaches have been used on a variety of radiological assessment models (Schubert et al. 1967; Shaeffer and Hoffman 1979; Hoffman and Baes 1979; Garten 1980). The approaches discussed in the following sections relate to models that can be reduced or modified into additive or multiplicative chains.

Additive models. The simplest approach to estimate the uncertainty in model predictions from the combined uncertainty of the parameters is to reduce model structure to an expression of additive terms of the form

$$y = a + b + c + \cdots + n , \tag{11.13}$$

In an additive model, y will be normally distributed if the parameters a, b, c, ... n are also normally distributed and statistically independent. The distribution of y may therefore be estimated by determining the value of $\bar{X}_y$ and s_y^2.

For an additive model, $\bar{X}_y$ and s_y^2 are simply obtained by the sums of means and variances of all parameters:

$$\bar{X}_y = \bar{X}_a + \bar{X}_b + \bar{X}_c + \cdots + \bar{X}_n \tag{11.14}$$

and

$$s_y^2 = s_a^2 + s_b^2 + s_c^2 + \cdots + s_n^2 . \tag{11.15}$$

If the variances of the parameters are comparable or if the number of parameters is sufficiently large, the distribution of y will tend to approximate a normal distribution with a mean value $\bar{X}_y$ and a variance s_y^2, even when parameter distributions are not normal (Bendat and Piersol 1966; Feller 1971). This is in accordance with the central limit theorem in statistics.

This approach is limited to those assessment models which can be reduced to an additive equation. Two cases that come to mind are:

1. The collective dose equivalent (S) for a given population (ICRP 1977),

$$S = \sum_{i=1}^{n} H_i P_i , \tag{11.16}$$

where S is the sum of the per capita dose equivalent (H_i) in the whole body or any specified organ or tissue for the number of persons (P_i) in a given population subgroup (i), and the summation is performed over all population subgroups in the exposed population. For S to be normally distributed, the product H_iP_i must be a random variable and the number of population subgroups (i) must be large and exposed from independent sources.

2. Cost-benefit analyses (ICRP 1977), which can be expressed additively as

$$B = V-(P+X+Y), \tag{11.17}$$

where the net benefit (B) of a product involving radiation is equal to the difference between its gross benefit (V) and the sum of the basic cost of production (P), the cost of achieving a certain level of radiation protection (X), and the cost of total societal and environmental detriment (Y) involved in production, operation, use, and disposal of the product.

Multiplicative models. Many assessment models are composed of, or can be expressed as, simple multiplicative chains of parameters of the form

$$y = a \cdot b \cdot c \cdot \cdots \cdot n . \tag{11.18}$$

Multiplicative chains can be readily converted to additive chains through log-transformation. Thus, Eq. 11.18 becomes

$$\ln(y) = \ln(a)+\ln(b)+\ln(c)+\cdots+\ln(n) . \tag{11.19}$$

Since Eq. 11.19 is an additive model, $\ln(y)$ will tend to be normally distributed. Thus, the distribution of y will approximate a lognormal distribution. If the parameters a through n are lognormally distributed, the distribution of y will be lognormal. If the parameters are statistically independent, the mean and variance of $\ln(y)$ will be the sums of the mean and variances of log-transformed values of all model parameters.

Often, y is lognormally distributed even when there are relatively few parameters in the model. This is due to the multiplicative nature of the model and to the fact that parameters with large relative error are often the product of multiplicative processes and thus are themselves lognormally distributed (May 1976; Aitchison and Brown 1969).

Examples of multiplicative models are numerous:

1. The water-fish-man exposure pathway (USNRC 1977),

$$R_{ij} = C_i \cdot B_i \cdot U_f \cdot D_{ij} , \tag{11.20}$$

where the dose (R) to organ or tissue j from ingestion of a radionuclide i is the product of the concentration in water (C_i), the water-to-fish steady-state bioac-

cumulation factor (B_i), the annual rate of consumption of fish (U_f) and the ingestion dose conversion factor (D_{ij}).

2. The ^{14}C specific activity model (Killough and Rohwer 1978),

$$\dot{R}_{\text{total body}} = A \cdot (1 - f) \cdot D_r , \tag{11.21}$$

where the total body dose rate ($\dot{R}$) is a product of the specific activity of ^{14}C in air (A), the fraction of total carbon in the body derived from relatively uncontaminated sources (f), and the steady-state dose rate factor (D_r).

3. The dose equivalent (ICRP 1977),

$$H = D \cdot Q \cdot N , \tag{11.22}$$

where the dose equivalent (H) is a product of the absorbed dose (D), the quality factor (Q), and the product of all other modifying factors (N).

4. The radiological health detriment to a population (ICRP 1977),

$$G_i = P \cdot \overline{H} \cdot \bar{r}_i , \tag{11.23}$$

where the number of health effects (G_i) is a product of the estimated number of persons in the population (P), the estimated average per capita dose equivalent ($\overline{H}$), and the estimated average per capita risk ($\bar{r}_i$) of suffering a health effect (i).

Parameter importance. If the importance of a parameter is indicated by its contribution to the total model uncertainty, then in additive models, parameter importance will be a direct function of s^2. Thus,

$$I_i = s_i^2 / s_y^2 , \tag{11.24}$$

where I_i is the importance index, s_i^2 is the variance of parameter i, and s_y^2 is the variance of the values predicted by the model. For a multiplicative model, the variances are of the log-transformed values.

Example 11.8. Suppose that land previously contaminated with radionuclides is being considered for conversion to pasture, and that the feasibility of this action is best determined by an assessment model. Further suppose that, although much general information exists, site-specific parameter values are not available.

Screening approaches and sensitivity analyses indicate that the primary radionuclide of concern is ^{137}Cs and the model structure can be simplified to a multiplicative chain of the form

$$R_{\text{total body}} = C_s \cdot B_v \cdot Q_m \cdot F_m \cdot U_m \cdot D_f , \tag{11.25}$$

where $R_{(\text{total body})}$ is the committed dose for a one-year intake of ^{137}Cs, C_s is the soil concentration, B_v is the plant/soil concentration ratio, Q_m is the daily amount of pasture vegetation consumed by a grazing dairy animal, F_m is the milk transfer coefficient, U_m is the annual consumption of milk by a human receptor, and D_f is the dose equivalent conversion factor for the total body resulting from an annual intake of ^{137}Cs.

For a given soil concentration, the assessment model is deterministic and employs the following single values for each parameter:

Parameter	Generic value
B_v [pCi/kg (dry wt) vegetation per pCi/kg (dry wt) soil]	1.5×10^{-2}
Q_m [kg (dry wt)/d]	12.5
F_m (d/L)	1.2×10^{-2}
U_m (L/y)	310
D_f (mrem/pCi)	7.97×10^{-5}

Multiplication of these values results in a predicted dose of 5.56×10^{-5} mrem/y per $\text{pCi}\cdot\text{kg}^{-1}$ soil, or approximately 0.056 mrem/y per $\text{pCi}\cdot\text{g}^{-1}$ soil. Assuming a mean soil concentration of 33 $\text{pCi}\cdot\text{g}^{-1}$, the predicted dose is approximately 1.9 mrem from one year's consumption of milk produced by cows grazing on this pasture.

Let us suppose that an evaluation of relevant literature data results in the following estimates of the geometric mean (X_g) and the geometric standard deviation (s_g), which are derived from the mean of log-transformed data (μ) and the variance of log-transformed data (σ^2) for the above parameters:

Parameter	X_g	s_g	μ	σ^2
B_v	5.5×10^3	1.4	−5.20	0.113
Q_m	11.0 kg/d	1.26	2.4	0.0534
F_m	6.7×10^{-3} d/L	1.77	−5.01	0.326
U_m	95 L/y	2.23	4.55	0.643
D_f	3.7×10^{-5} mrem/pCi	1.32	−10.2	0.077

The effect of parameter uncertainty is analyzed by substituting μ for $\bar{X}$ and σ^2 for s^2 in Eqs. 11.14 and 11.15. Thus,

$$\mu_{\text{dose}} = \ln(3.3\times10^4\ \text{pCi/kg}) + (-5.2) + 2.4 + (-5.01) + 4.55 + (-10.2)$$
$$= -3.06$$

and

$$\sigma^2_{\text{dose}} = 0.113 + 0.0534 + 0.326 + 0.643 + 0.077$$
$$= 1.21\ .$$

The geometric mean (X_g) and geometric standard deviation (s_g) of the dose prediction are

$$X_g = e^{\mu} = \exp(-3.06) = 0.047 \text{ mrem}$$

(see Eq. 11.10) and

$$s_g = \exp(\sqrt{\sigma^2}) = \exp(\sqrt{1.21}) = 3.0$$

(see Eq. 11.11).

The deterministic prediction of Eq. 11.25 (e.g., the prediction with all parameters set at their nominal values) is 1.9 mrem, which is approximately a factor of 40 higher than the estimated geometric mean value of 4.7×10^{-2} mrem.

The probability of parameter uncertainty resulting in a prediction underestimating the actual dose is determined according to Eq. 11.12:

$$\begin{aligned} z &= [\ln(1.9 \text{ mrem}) - \ln(0.047 \text{ mrem})]/\ln(3.0) \\ &= 3.37 . \end{aligned}$$

The z value of 3.37 is associated with a cumulative probability of 0.9996 (Table 11A.1 in Appendix 11A, at the end of this chapter). Thus, there is less than a 0.1% probability of the deterministic assessment prediction of 1.9 mrem resulting in an underestimate, and greater than a 99.9% chance of an overestimate. We would conclude that the assessment prediction is conservatively biased. [End of Example 11.8]

Example 11.9. What is the order of importance of the parameters in Eq. 11.25? What is the relative contribution of their uncertainty to the total predictive uncertainty of the model?

Parameter importance for simple multiplicative chains can be determined by substituting σ_i^2 and σ_y^2 for s_i^2 and s_y^2 in Eq. 11.24; σ_i^2 is the variance of the logarithms for each parameter, and σ_y^2 is the variance of the logarithms of the predicted dose. The parameter importance rank and relative contribution of parameter uncertainty are as follows:

Parameter	Importance rank	σ_i^2/σ_y^2 = uncertainty contribution
U_m	1	(0.643/1.21) = 0.531
F_m	2	(0.326/1.21) = 0.269
B_v	3	(0.113/1.21) = 0.093
D_f	4	(0.077/1.21) = 0.064
Q_m	5	(0.053/1.21) = 0.044

The most important parameter is the annual milk consumption (U_m), which contributes more than 50% to the total uncertainty in the dose prediction.

Improved estimates of U_m will greatly reduce the uncertainty in the dose prediction, but little will be gained by efforts to improve values of σ_i^2 for Q_m or D_f. [End of Example 11.9]

Example 11.10. After screening out negligible pathways of exposure and associated radionuclides, we find that the most pronounced radiological impact from future low-probability accidental releases from light-water reactors is the inhalation of airborne ^{131}I. Again, the model can be reduced to a simple multiplicative chain:

$$R = Q \cdot (\bar{\chi}/Q) \cdot U_I \cdot D_f , \tag{11.26}$$

where Q is the total release of ^{131}I in μCi, $(\bar{\chi}/Q)$ is the short-term atmospheric dispersion factor in s/m^3, which relates a short-term release (Q) in μCi to a time-integrated air concentration $(\bar{\chi})$ in μCi·s/m^3, U_I is the inhalation rate in m^3/s, and D_f is the inhalation dose equivalent conversion factor for the thyroid of members of the general public in rem/μCi inhaled.

Assume that an in-depth analysis of the variability of each parameter either has not been, or cannot be, performed. In this case, only approximate judgments of minimum and maximum values can be made. Estimates of minimum and maximum values are as follows:

Parameter	Minimum estimate	Maximum estimate
Q (μCi)	1×10^7	1×10^9
$\bar{\chi}/Q$ (s/m^3)	3×10^{-6}	8×10^{-5}
U_I (m^3/s)	3×10^{-5}	6×10^{-4}
D_f (rem/μCi)	0.5	30

Combining minimum values with each other produces a lower-limit dose prediction of 0.45 mrem. Combining maximum values produces an upper-limit estimate of 1.4×10^3 rem. This is a range that spans almost six orders of magnitude! At the lower end, the predicted dose is insignificant. At the upper end, serious thyroid damage would be expected. Unless there are strong positive correlations between the parameters, extreme limits are associated with very low probabilities. Thus, simple combination of ranges in this manner produces results that are meaningless.

Our objective in this example should be to correctly assess the uncertainties by combining means (μ) and variances (σ^2) of the logarithms for each parameter. In this example, we approximate μ and σ^2 by applying judgment and assuming a log-uniform distribution for each parameter:

$$\mu = [\ln(\text{min}) + \ln(\text{max})]/2 , \tag{11.27}$$

and

$$\sigma^2 = [\ln(\text{max}/\text{min})]^2/12 . \tag{11.28}$$

These equations are derived from those given for the mean and variance of a continuous uniform distribution (Neter et al. 1978). A log-uniform distribution is simply a uniform distribution of logarithms.

Using Eqs. 11.27 and 11.28, the following values of μ_i and σ_i^2 are calculated:

Parameter	μ_i	σ_i^2
Q	18.4	1.77
$\bar{\chi}/Q$	−11.1	0.90
U_i	−8.92	0.75
D_f	1.35	1.40

Using Eqs. 11.14 and 11.15, and substituting μ and σ^2 for $\bar{X}$ and s^2, respectively, permits an estimation of μ_R and σ_R^2:

$$\mu_R = \sum_i \mu_i = -0.27$$

and

$$\sigma_R^2 = \sum_i \sigma_i^2 = 4.82 .$$

The geometric mean (X_g) of the predicted dose is

$$X_g = \exp(\mu_R) = 0.76 \text{ rem} .$$

The geometric standard deviation (s_g) of the predicted dose is

$$s_g = \exp(\sqrt{\sigma_R^2}) = 9.0 .$$

In this example, model predictions will approximate a lognormal distribution because of the multiplicative combination of parameters whose values of σ^2 are of the same order of magnitude. A dose prediction having a 95% chance of not being exceeded can therefore be roughly approximated using lognormal statistics:

$$X_{95} = \exp(\mu + 1.65\sigma) = X_g s_g^{1.65} = 0.76(9.0)^{1.65}$$
$$= 29 \text{ rem} . \qquad (11.29)$$

At this level of exposure there would be no immediate thyroid damage, but evacuation or the distribution of potassium iodide tablets might be considered for critical population groups. Note that the 95th percentile dose estimate is almost a factor of 50 less than the extreme maximum value calculated by combining upper-limit parameter values. The cumulative probability associated

with the extreme estimate of 1.4×10^3 rem is calculated using Eq. 11.12 and Table A11.1 (in the appendix of this chapter):

$$z = [\ln(X_{\max}) - \ln(X_g)]/\ln(s_g)$$
$$= [\ln(1.4 \times 10^3) - \ln(0.76)]/\ln(9.0) = 3.42\ ;$$

in Table A.11.1, a z value of 3.42 equals a cumulative probability of 0.9997. Thus we can conclude that the extreme estimate of 1.4×10^3 rem exceeds the 0.9995 cumulative probability of a lognormal distribution. [End of Example 11.10]

Example 11.11. A thyroid dose estimate on the order of 30 rem is sufficiently large to warrant reevaluation of the estimates of parameter uncertainty presented in Example 11.10.

Let us assume that reinspection of the model represented by Eq. 11.29 reveals a possible negative correlation between the inhalation rate (U_I) and the inhalation dose equivalent conversion factor (D_f). This possibility exists because U_I is partially related to the size of an individual, D_f is inversely related to individual size, and retention of particulates by the respiratory tract is inversely proportional to U_I at high rates of respiration.

So far, we have discussed only the combination of parameter uncertainties for statistically independent variables. For correlated parameters, additional terms are required. In the case where two additive parameters (a and b) are correlated, the term to be added to or subtracted from Eq. 11.15 is

$$\pm 2s_{ab} = 2rs_a s_b\ . \tag{11.30}$$

In Eq. 11.30, r is the linear correlation coefficient, s_{ab} is the covariance term, and s_a and s_b are the standard deviations of parameters a and b, respectively (Snedecor and Cochran 1967). For multiplicative models, the standard deviations, σ_a and σ_b, of the log-transformed values of the parameters can be substituted for s_a and s_b. Note that the sign of s_{ab} is determined by the sign of the correlation coefficient r.

Suppose, for the sake of our example, that parameters $\ln(U_I)$ and $\ln(D_f)$ exhibit a strong negative correlation, corresponding to an r of -0.80.

The values of σ for $\ln(U_I)$ and $\ln(D_f)$ are 0.87 and 1.18, respectively. Therefore, the additional term, expressed by Eq. 11.30, to account for parameter correlation is

$$2r\sigma_{U_I}\sigma_{D_f} = 2(-0.8)(0.87)(1.18) = -1.64\ .$$

In Example 11.10 the total variance of the log-transformed model prediction (σ_R^2) was 4.82. Accounting for the correlation between $\ln(U_I)$ and $\ln(D_f)$ reduces this total variance to

$$\sigma_R^2 = \left[\sum_i \sigma_i^2\right] \mp 2\sigma_{U_I D_f} = 4.82 - 1.64 = 3.18 .$$

The revised estimate of the geometric standard deviation is

$$s_g = \exp(\sqrt{\sigma_R^2}) = \exp\sqrt{3.18} = 5.9 .$$

Thus, the revised estimate of the 95th percentile dose prediction, using Eq. 11.29, is

$$X_{95} = X_g s_g^{1.65} = 0.76(5.9)^{1.65} = 14 \text{ rem} .$$

The negative correlation between U_I and D_f caused, in this example, a 50% reduction in the 95th percentile dose of 29 rem, calculated by assuming no correlations between model parameters. Of course, we would expect even further changes in the distribution of predicted doses with improved estimates of parameter uncertainty. [End of Example 11.11]

11.5.2.2 Complex Analytical Approaches

Some situations may arise where the model cannot be reduced to an additive or multiplicative structure and the distributions of input values and model output are complex. Analytical approaches to address these situations may be developed, but will be very complex. For a detailed discussion of analytical solutions to parameter uncertainty analyses of selected model formulations, see Ku (1966). Additional formulas for the propagation of parameter uncertainties as a function of structural differences in models are given in Table 11A.2 in Appendix 11A, at the end of this chapter. These formulas provide an approximate estimate of the variance of model predictions given relative errors for input variables. Generally, for complex situations, we find it more convenient to use a computer to numerically propagate parameter uncertainties.

11.5.2.3 Numerical Approaches

Development of computerized methods to numerically solve the combined effect of parameter uncertainty on model predictions has been an area of rapid growth, with many techniques undergoing revision even as published documentation becomes available. The most widely used methods are related to a Monte Carlo approach, which randomly samples values for model parameters from a preselected probability distribution (Rubenstein 1981; Gardner et al. 1982; Gardner et al. 1980; Matthies et al. 1981; O'Neill et al. 1981; Gardner and O'Neill 1982; Dunning and Schwarz 1981; Schwarz and Hoffman 1981; Henrion 1979; McKay et al. 1979; Iman et al. 1980; Carney et al. 1981).

Monte Carlo methods produce a single predicted value, or model solution, from a single set of randomly selected parameter values. The results of numerous (500 to 10,000) iterations of model solutions are then statistically summarized. The advantage of this procedure is that the uncertainty in model predictions can be based on any number of different theoretical or empirical distributions specified for model parameters. Statistical designs applied to the random sampling process, such as Latin hypercube sampling, provide an increase in efficiency and reduced costs (Cranwell and Helton 1982; Iman et al. 1980; McKay et al. 1979).

Parameter importance is determined by correlating randomly selected parameter values with the resultant model predictions. Thus, the relationship between parameter variability and model predictions can be measured with the simple correlation coefficient (r) (Snedecor and Cochran 1967). Values of r may range from -1.0 to 1.0. If $r = 0$, no relationship exists between the variability of a parameter and model predictions. If r is either 1 or -1, there is a perfect positive or negative relationship between parameter variability and model predictions. In this latter case, an r of 1 would indicate that all of the uncertainty in the model prediction is explained by the uncertainty of a single parameter. The percent of the variability in model predictions contributed by variability in a parameter is expressed by the squared value of the correlation coefficient (r^2), referred to as the coefficient of determination. Thus, a regression analysis between model predictions and a given parameter producing an r of -0.5 indicates that the parameter is negatively correlated with 25% of the uncertainty in the model output due to parameter variability, and with small values of the parameter producing large predicted values.

In a recent application of Monte Carlo computer techniques, regressions of rank-transformed values of parameters and predictions have produced more reliable results than regressions of the actual values (Helton et al. 1981). Rank transformation involves replacing the values selected for model parameters and the resulting predictions produced through Monte Carlo techniques by their corresponding ranks (i.e., the smallest value is given rank 1, the next smallest value is given rank 2, and so on up to the largest value, which is given a rank corresponding to the number of computer iterations used to produce a distribution of parameter values and model predictions). Rank transformations are useful for representing a variety of relationships between parameter values and model predictions and for minimizing the effects of extreme values (Iman and Conover 1979). Thus, correlation coefficients (r) calculated from ranks of parameter values and model predictions are a better indicator of parameter importance than are simple correlation coefficients produced from regression performed on actual values.

Example 11.12. A simple demonstration of a Monte Carlo parameter uncertainty analysis can be made with the following model, composed of additive, multiplicative, and exponential components:

$$R = D_f(b \cdot c + d \cdot e)\exp(-\lambda \cdot t), \tag{11.31}$$

where R is the estimated dose, D_f is the dose conversion factor, b and d are consumption rates for two kinds of contaminated foods, and c and e are the concentrations of radioisotopes in those two foods. The exponentiated terms λ and t represent, respectively, the decay constant for a specific isotope and the time delay before consumption of the contaminated food. This model is intended to predict the radiation dose (R) from consumption of contaminated foods from two independent pathways.

Now, suppose that the values of these parameters have not been directly measured for the site in question and, with the exception of the physical constant λ, are unknown. Because direct measurements have not been made, means, variances, and distributional characteristics of model parameters are unknown. The best we can do is establish upper and lower limits for each parameter and assume that the probability of observing values between these limits is equal. This defines a uniform distribution and establishes, for this analysis, a very conservative assumption. That is, improvement in the information base for each parameter will very likely result in an improvement in the uncertainties associated with predictions of R.

Therefore, assume that lower and upper limits are: D_f [1,5]; b [0.1, 0.3]; c [0.03, 0.06]; d [10, 30]; e [0.004, 0.009]; and t [4, 12]. The decay constant λ is fixed at 0.5. This provides the minimum information necessary for an initial uncertainty analysis. Monte Carlo iterations are performed by random selection of parameter values from each uniform distribution specified by the above limits. This process is repeated a large number of times (500 in the examples to follow), and the results are statistically summarized. The Monte Carlo iterations form a large data set from which the uncertainties in R and relationship to individual parameters can be obtained.

The frequency distribution of R (Fig. 11.12) is skewed, typical of models dominated by multiplicative interactions and exponential terms. Rank order correlations of the parameters with R indicates that t is the most important parameter, accounting for 81% of the variability in R. Of the remaining parameters, D_f is the most important (9.9%) and b is the least important (<0.1%). Together, the remaining parameters account for 19% of the uncertainty in R. Obviously, uncertainties associated with t will dominate uncertainties in R. That is, significant improvements in estimates of all parameters other than t will account for less than 19% improvement in model predictions.

Let us assume that the bounds for t (4 to 12 d) are realistic; i.e., the extremes have actually been observed. Have we then approached the limits of predictability for this model? Suppose some additional information becomes available concerning t, so that the expected value, or mode, of 8 d is known. This information, along with the upper and lower limits, describes a triangular frequency distribution in values of t. Repeating the Monte Carlo simulations

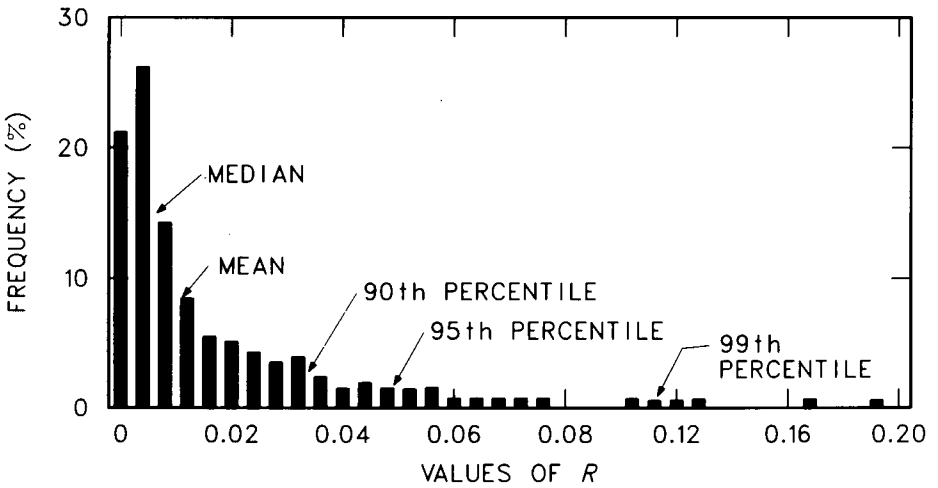

Figure 11.12. Frequency plot of R generated after 500 computer iterations using Monte Carlo techniques to randomly sample from uniform distributions prescribed for six parameters in a dose assessment model.

with this information results (Case II, Table 11.6) in a 24% decrease in the expected value of R and 36% and 27% decreases in the 95th and 99th percentiles, respectively.

Another form of information which can affect the uncertainties associated with model improvements is correlations between parameters. For instance, in this model D_f might be correlated with d, indicating that the dose conversion factor and the consumption rate of food from a particular pathway are related.

Table 11.6. Means, standard deviations, and 95th and 99th percentiles of predictions from 500 Monte Carlo iterations of the model (Eq. 11.31)

Case[a]	Mean dose	Standard deviation	95th percentile	99th percentile
I	1.4	1.8	5.1	9.7
II	1.1	1.2	3.2	7.0
III	1.0	1.0	3.0	6.1

[a]Case I simulations were performed with parameter values drawn from the uniform distribution; Case II, with values of t drawn from a triangular distribution; and Case III, with the addition (to the triangular distribution) of a correlation between D_f and d of -0.5.

Case III (Table 11.6) investigates the possible effect of such a relationship with a correlation between D_f and d equal to -0.5. Thus, without new experiments and with very little reanalysis of the data, information involving the frequency distribution of t and a relationship between D_f and d have been added to the simple limits of possible parameter values for the Monte Carlo simulations. Inspection of Table 11.6 indicates that these improvements result in a 28% decrease in the mean, a 43% decrease in the standard deviation, and 41 and 37% decreases in the 95th and 99th percentiles, respectively. [End of Example 11.12]

Example 11.13. Figure 11.13 is a frequency distribution of discrete intervals produced by Monte Carlo procedures. Five hundred computer iterations were used to sample parameter values from triangular, normal, and lognormal distributions estimated from literature data and investigator judgment (Hoffman et al. 1982). The model is similar in structure to the complex suite of algorithms in NRC Regulatory Guide 1.109 (USNRC 1977) describing terrestrial food chain transport and internal dosimetry. The following exposure pathways were considered for a given deposition rate of ^{90}Sr:

- Deposition-leafy vegetables-human receptor,
- Deposition-nonleafy vegetables-human receptor,
- Deposition-pasture-dairy cows-milk-human receptor, and
- Deposition-pasture-beef cattle-meat-human receptor.

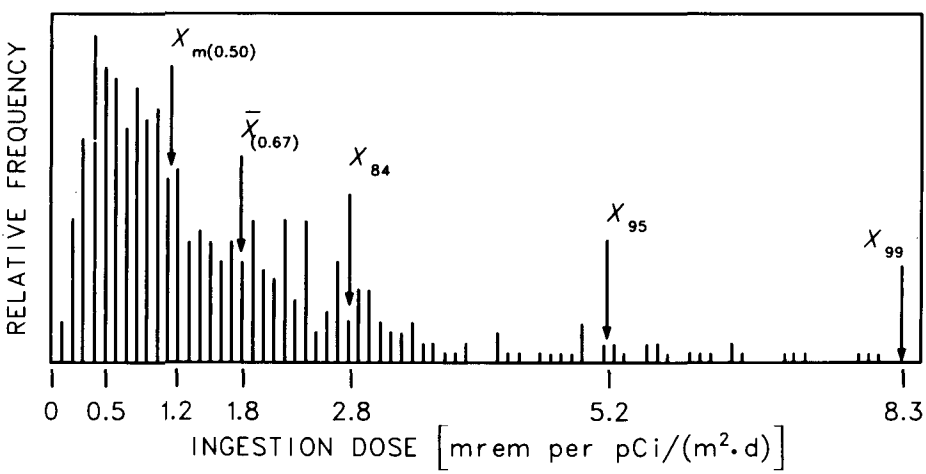

Figure 11.13. A frequency distribution of the predicted ^{90}Sr ingestion dose to bone surface via terrestrial food pathways subsequent to a continuous rate of deposition of 1 pCi/(m^2·d) for 15 years; X_m, X, X_{84}, X_{95}, and X_{99} are the median, mean, 84th, 95th, and 99th percentiles of the distribution, respectively (from Hoffman, Gardner, and Eckerman 1982).

The predicted values constitute a 50-y committed dose equivalent to the endosteal region of the bone. Rank correlation of parameter values and model predictions revealed that 50% of the total uncertainty could be attributed to the uncertainty associated with the deposition-nonleafy vegetables-human pathway. The most important single parameter was the rate constant for ^{90}Sr removal from the root zone of the soil, which contributed 18% to the total uncertainty. The ^{90}Sr dose conversion factor was the second most important parameter, contributing 10%, although its variability was low ($s_g = 1.4$). The importance of the dose factor was the result of this parameter being common to all four exposure pathways.

The analysis indicated greater variability for single exposure pathways ($s_g \geq 3.0$) than for combined exposure to all pathways ($s_g = 2.4$). This effect was the result of the additive nature of multiple exposure pathways. Nevertheless, multiplicative components of the model and lognormally distributed parameter values predominated, producing an approximately lognormal distribution of model predictions (Fig. 11.13).

Comparing the deterministic prediction of the NRC Regulatory Guide to the distribution of ^{90}Sr bone surface doses predicted with Monte Carlo procedures indicated a large degree of conservatism in the NRC prediction. The NRC-predicted dose was approximately a factor of 10 greater than the geometric mean of the distribution and exceeded the 99th percentile, due mainly to assumptions about human dietary habits and the dose conversion factor. In this case, the NRC Regulatory Guide model employed a dose conversion factor for the total bone rather than for the endosteal region of the bone (Hoffman et al. 1982). If Regulatory Guide 1.109 had employed a comparable dose factor for the endosteal region of the bone, the deterministic model prediction would have approximated the 80th percentile of Fig. 11.13. [End of Example 11.13]

11.5.3 Limitations of Parameter Uncertainty Analyses

Most deterministic models are not designed to estimate the effects of parameter variability or parameter uncertainty, and little attention has been placed on specifying possible correlations and interactions between model parameters. These correlations can have a pronounced influence on the results of parameter uncertainty analysis (Schwarz and Dunning 1982; Gardner et al. 1980; Lindackers and Bonnenberg, eds. 1980). Correlations between parameters may either increase or decrease the effects of parameter uncertainty from the case where parameters are statistically independent, depending on the structure of the model, the functional role of the parameter, and whether the correlations are positive or negative.

Perhaps the most important limitation of parameter uncertainty analysis is unforeseen bias in the model formulation and bias in the estimated range (or distribution) of model parameters. Model and parameter bias will cause the

results of the analysis to differ substantially from the actual range of events occurring under a specific set of conditions. However, if the extent of parameter uncertainty has been conservatively estimated to account for possible errors in model formulation, then estimation of the 95% or 99% range of model predictions should encompass the outcome of the real system (Fig. 11.14). This expectation must be based on judgment until confirmed by experimental field validation. Accounting for unforeseen bias is essential in order for the results of parameter uncertainty analysis to be useful in decision making.

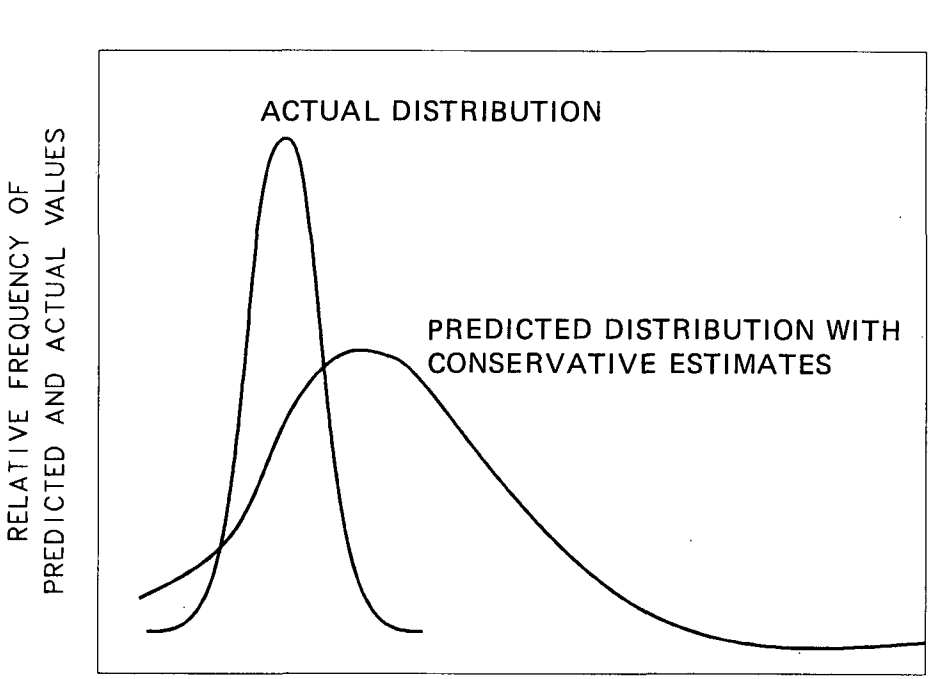

Figure 11.14. Model and parameter bias will cause the results of parameter uncertainty analysis to differ from the real system, but conservative estimation of parameter variability should produce results that encompass the actual range.

11.6 MODEL COMPARISON

In the past, the method most frequently used to indicate uncertainty was comparison of the results of different models or computer codes. Extreme caution must be used in analyzing the results of model comparisons, because many radiological assessment models have a similar derivation in mathematical form and sources of data. Thus, comparison among models will not usually involve

the evaluation of truly independent results. We believe that the greatest value of model comparison is identification of obvious discrepancies among models.

When models are compared, care must be taken to identify

- Differences in model structure,
- Differences in underlying assumptions, and
- Differences in sources of data for estimating parameters.

Ease of model implementation is also relevant, as the "best" model for a given assessment may often be the model that is easiest to use, yet produces results that are within an "acceptable" margin of error. In this case, the degree of error is determined by field validation tests or parameter uncertainty analyses. Again, the degree of "acceptable" error is a subjective judgment which should be made on a case-by-case basis.

Example 11.14. In an attempt to evaluate the uncertainty in a given model, an investigator decides to compare the predictions of the model against those of various other models. Here is the result of the comparison:

Model number	Predicted dose (mrem)
1 (initial model)	23
2	21
3	19
4	75
5	20
6	22

The prediction of Model 1 appears to be in agreement with all but Model 4. The tendency would be to discard Model 4 as an outlier and take an average of the predictions of the remaining five models. Assuming a limit of 25 mrem, we might conclude that our initial model demonstrates general compliance. This conclusion may be misleading. Examining the differences in model structure, underlying assumptions, and data bases among the various models could easily warrant different conclusions. For instance, if Models 1, 2, 3, 5, and 6 all have common parameter values derived from a limited survey of the literature, but Model 4 includes a reexamination of available data in which only relevant, site-specific conditions were included, then Model 4 may provide the most reliable prediction. Furthermore, parameter uncertainty analysis may show that the variability about the predictions of Models 1, 2, 3, 5, and 6 encompasses a full order of magnitude, whereas the variability about the predictions of Model 4 is only a factor of 3. In this case, parameter uncertainty analysis would indicate a high likelihood for exceeding the dose limit of 25 mrem, no matter which of the six models is employed. [End of Example 11.14]

Example 11.15. A variety of documented computer codes and regulatory models can be used to evaluate the terrestrial food chain transport of radionuclides and the subsequent dose to members of critical population groups. Table 11.7 presents a comparison of the results of three such models with the geometric mean and 95% range estimated using parameter uncertainty analyses. The predicted values are 50-year committed dose equivalents to the bone surface of a reference adult resulting from a 30-year deposition of ^{90}Sr onto agricultural land at a continuous rate of 1 pCi/(m^2·d).

The comparison of the result produced by the three models (IAEA 1982), AIRDOS/EPA (Moore et al. 1979), NRC 1.109 (USNRC 1977) indicates that the predicted quantities are relatively good agreement. However, the geometric mean (X_g) produced by parameter uncertainty analysis for the nonleafy vegetable pathway differs from these results by more than one order of magnitude, and the 95% range produced for the individual exposure pathways varies over two orders of magnitude. This range encompasses almost

Table 11.7. A comparison of predictions[a] of bone surface dose from the continuous deposition of ^{90}Sr on agricultural land using a variety of terrestrial food chain transport models

Pathway	Selected models			X_g[c]	95% range[c]
	IAEA[b]	AIRDOS/EPA	NRC 1.109[b]		
	mrem per pCi/(m^2·d) for 30-y deposition				
Leafy vegetables	1.05 (0.89)[c]	0.20 (0.39)	0.26 (0.51)	0.27 (0.50)	0.030–2.4
Nonleafy vegetables	5.29 (0.98)	2.62 (0.94)	2.09 (0.92)	0.34 (0.50)	0.025–4.7
Milk	0.20 (0.58)	0.28 (0.68)	0.102 (0.34)	0.15 (0.50)	0.011–2.1
Meat	0.045 (0.44)	0.029 (0.33)	0.031 (0.31)	0.055 (0.50)	0.003–0.97
Combined pathways	6.59 (0.97)	3.12 (0.86)	2.46 (0.79)	1.20 (0.50)	0.21–6.9

[a]Values in parentheses are cumulative percentiles produced by comparing the model predictions of IAEA, AIRDOS/EPA, and NRC 1.109 with a distribution of predicted doses generated by parameter uncertainty analyses. The values in parentheses indicate the probability that the dose prediction will be conservative (i.e., tend to overpredict).

[b]Models adapted for use with ICRP 30 bone surface dose factors (ICRP 1980).

[c]Geometric mean (X_g) and 95% range (from Hoffman et al. 1982) estimated from parameter uncertainty analyses on a model of similar structure to the IAEA, AIRDOS/EPA, and NRC 1.109 models.

all of the predictions of each of the three models. A careful analysis of these models reveals close similarities in both the mathematical formulation and the data bases from which parameter values were derived. Thus, the initial impression given by model comparison is misleading, as more agreement between deterministic predictions of these models is shown than is warranted by the large variability identified through uncertainty analysis. [End of Example 11.15]

Example 11.16. Model comparison is most useful when one of the models has been field tested (subjected to validation), or when one of the models is associated with a known level of accuracy. For example, complete-equilibrium specific-activity models for ^{3}H and ^{14}C generally give maximum upper-limit dose estimates for population groups residing near the source of release of these radionuclides (Hoffman et al. 1982). Therefore, comparison of complete-equilibrium specific-activity models with other "more realistic" types of models will show how far the estimates of these "realistic" models are from a maximum upper limit.

Such a comparison is illustrated in Table 11.8. The results indicate that the ^{3}H and ^{14}C pathway models used in NRC Regulatory Guide 1.109 (USNRC 1977) are about a factor of 3 less than the maximum upper-limit estimate provided by the complete-equilibrium model.

Table 11.8. A comparison between NRC Regulatory Guide 1.109 and specific-activity calculations of annual dose equivalent to a maximally exposed individual for given concentrations of ^{3}H and ^{14}C

Calculational approach	Pathway	Annual dose equivalent[a]	
		^{3}H	^{14}C
Reg. Guide 1.109	Air-vegetables-man	2.9×10^{-3}	2.3×10^{-1}
Reg. Guide 1.109	Air-vegetation-milk-man	7.7×10^{-4}	7.3×10^{-2}
Reg. Guide 1.109	Air-vegetation-meat-man	3.3×10^{-4}	6.7×10^{-2}
Reg. Guide 1.109	Air-all terrestrial pathways-man	4.0×10^{-3}	3.7×10^{-1}
Specific activity[b]	All pathways	1.2×10^{-2}	1.3

[a]Annual dose equivalent (mrem/y) resulting from 1 pCi/m^3 in aboveground air.

[b]Assuming complete equilibrium of specific activity between the atmosphere and the human body; dose equivalents therefore represent maximum upper-limit estimates.

Source: *Variability in Dose Estimates Associated with the Food Chain Transport and Ingestion of Selected Radionuclides,* NUREG/CR-2612, F. O. Hoffman, R. H. Gardner, and K. F. Eckerman, U.S. Nuclear Regulatory Commission, 1982.

For ^{14}C, subsequent investigation to explain these discrepancies revealed that the transfer factors in the Regulatory Guide model have been derived directly from the assumption of complete equilibrium of ^{14}C specific activity between the atmosphere and terrestrial food products. Therefore, no difference between the two models should be expected. Upon closer inspection, however, we found that the carbon fraction of vegetation is substantially underestimated in the Regulatory Guide. [End of Example 11.16]

11.7 IMPROVING CONFIDENCE IN MODEL PREDICTIONS

Confidence in model predictions will depend upon the degree to which validation studies have been successfully performed and the ability to reduce the variability associated with model parameters. With increased model validation, confidence in model predictions will improve as discrepancies between predictions and observations are defined and subsequently reduced. The reduction of parameter variability is best approached through quantification of correlations with readily measurable environmental variables usually not formally included in the model structure, such as climate, soil pH, suspended sediment content of water, and plant and animal taxa. Correlating parameters with measurable physical, chemical, or ecological variables should permit a better fit to conditions prevailing at a given site without the need for expensive site-specific experiments to empirically obtain relevant parameter values. At the present time, such correlations exist for only a few radionuclides and a few environmental media. Much remains to be done to address this important area of research.

11.8 PROBLEMS

1. After screening for critical exposure pathways and important radionuclides, a sensitivity analysis reveals that a given assessment situation can be evaluated using a simple multiplicative chain model of the form

$$\text{Dose} = Q \cdot A \cdot B \cdot C \cdot D \, .$$

Given that Q through D_f are statistically variable and lognormally distributed, what is the geometric mean (X_g) of the predicted dose and the geometric standard deviation (s_g) when X_g and s_g for each independent parameter are

Parameter	X_g	s_g
Q (μCi/y)	100	4.0
A (s/m^3)	1×10^{-6}	1.4
B (m^3/L)	3000	1.6
C (L/y)	100	1.6
D_f (rem/μCi)	11	1.5

(Be sure to make the units consistent.)

2. What is your estimate from the first problem above of a dose prediction that would have a 99% probability of not being exceeded?

3. How much of the total uncertainty in the predicted dose is contributed by parameter Q?

4. You are a regulator in charge of assigning default values to a generic assessment model. Would your choice of the default values be closer to the mode, median, mean, or 84th, 95th, or 99th percentile of the distribution of values for each parameter. Why?

5. As a consequence of your choice of a default value in the above problem, what percentile would be associated with your predicted dose (assuming that uncertainties about the predicted dose are approximated by a lognormal distribution)?

6. In a model that is basically multiplicative, will the percent error associated with its prediction tend to increase or decrease with additional parameters? (Assume that the new parameters have uncertainties that are no larger than the most uncertain parameter presently in the model.) What will happen with a model that is basically a summation of parameters?

7. Congress has just appropriated funds to validate assessment models. Design an experiment for validating the models used to assess the dose equivalent resulting from a release of ^{137}Cs to the aquatic environment. How would you propose to distinguish between error due to structural bias of the model and error due to parameter variability?

8. If a model has not been validated, what measures could you take to improve confidence in its use?

9. Under what situations will a simple model be more realistic than a more sophisticated, complex model?

10. Assume that it is required to assess the dose to a specific individual resulting from a future planned release of radioactivity. In this particular case, site-specific information for model parameters, including information on the physiological and metabolic parameters of the individual, are known. What are the remaining sources of uncertainty?

11. When evaluating uncertainties, how would you propose combining validation data and parameter uncertainty analyses? Assume that validation data exists only for atmospheric dispersion and that only estimates of parameter uncertainties are possible for the remaining components of the assessment model.

12. How would you use an evaluation of uncertainties to prioritize future research needs?

13. Which models described in this book are afflicted with the greatest uncertainty? Of these, which are amenable to validation under field conditions?

REFERENCES

Aitchison, J., and Brown, J. A. C. 1969. *The Lognormal Distribution*, Cambridge Univ. Press, New Rochelle, N.Y.

Bendat, J. S., and Piersol, A. G. 1966. *Measurement and Analysis of Random Data*, Wiley, New York.

Bennett, B. G. 1981. "The Exposure Commitment Method in Environmental Pollutant Assessment," *Environ. Monit. and Assess.* **1**, 21–36.

Buckner, M. R. (compiler) 1981. Proceedings of the First SRL Model Validation Workshop, Hilton Head, S.C., November 19–21, 1980, DP-1597, Savannah River Laboratory, Aiken, S.C.

Carney, J. H., Gardner, R. H., Mankin, J. B., and O'Neill, R. V. 1981. *SEAP: A Computer Program for the Error Analysis of a Stream Model,* ORNL/TM-7694, Union Carbide Corp., Nucl. Div., Oak Ridge Natl. Lab.

Collee, R., Abee, H. H., Cohen, L. K., Ed, D., Eisenhower, E. H., Jarvis, A. N., Fisenne, I. M., Jackson, M., Johnson, R. H., Jr., Olson, D., and Peel, J. 1980. "Reporting Environmental Radiation Measurement Data," pp. 6–1 through 6–34 in *Upgrading Environmental Radiation Data*, Health Physics Society Committee Report HPSR-1, EPA 520/1-80-012, U.S. Environ. Protection Agency.

Cranwell, R. M., and Helton, J. C. 1982. "Uncertainty Analysis for Geologic Disposal of Radioactive Waste," pp. 131–144 in *Proceedings of the Symposium on Uncertainties Associated with the Regulation of the Geologic Disposal of High-Level Radioactive Waste, Gatlinburg, Tennessee, March 9–13, 1981,* CONF-810372, ed. D. C. Kocher.

Dunning, D. E., Jr., and Schwarz, G. 1981. "Variability of Human Thyroid Characteristics and Estimates of Dose from Ingested ^{131}I," *Health Phys.* **40**, 661–75.

Eichholz, G. G. 1978. "Planning and Validation of Environmental Surveillance Programs at Operating Nuclear Power Plants," *Nucl. Saf.* **1**, 486–96.

Federal Radiation Council 1960. *Background Material for the Development of Radiation Protection Standards*, Staff Report 1.

Feller, W. 1971. *An Introduction to Probability Theory and its Applications,* 2d ed., vol. II, Wiley, New York.

Fields, D. E., Miller, C. W., and Cotter, S. J. 1981. "The AIRDOS-EPA Computer Code and Its Application to Intermediate Range Transport of ^{86}Kr from the Savannah River Plant," pp. 49–60 in *Proceedings of the Symposium on Intermediate Range Atmospheric Transport Process and Technology Assessment, Gatlinburg, Tennessee, October 1–3, 1980,* CONF-801064.

Gardner, R. H., and O'Neill, R. V. 1982. "Error Analysis," in *Symposium Proceedings, HDR Sciences Modeling Workshop,* Santa Barbara, California. February 5–6, 1981.

Gardner, R. H., O'Neill, R. V., and Hoffman, F. O. 1982. "Assessing Model Uncertainties," pp. 199–208 in *Proceedings of the Symposium on Uncertainties Associated with the Regulation of the Geologic Disposal of High-Level Radioactive Waste, Gatlinburg, Tennessee, March 9–13, 1981,* CONF-810372, ed. D. C. Kocher.

Gardner, R. H., O'Neill, R. V., Mankin, J. B., and Kumar, D. 1980. "Comparative Error Analysis of Six Predator-Prey Models," *Ecology* **61,** 323–32.

Garten, C. T., Jr. 1980. "Statistical Uncertainties in Predicting Plutonium Dose to Lung and Bone from Contaminated Soils," *Health Phys.* **39,** 99–103.

Hahn, G. J., and Shapiro, S. S. 1967. *Statistical Models in Engineering,* Wiley, New York.

Helton, J. C., Brown, J. B., and Iman, R. L. 1981. *Risk Methodology for Geologic Disposal of Radioactive Waste: Asymptotic Properties of the Environmental Transport Model,* SAND 79-1908, Sandia Natl. Lab., Albuquerque, N.Mex.

Henrion, M. 1979. "Designing a Computer Aid for Decision Analysis," *IEEE Trans. Syst. Man. Cybern.* (October 1979), pp. 187–193.

Hoffman, F. O., and Baes, C. F., III, eds. 1970. *A Statistical Analysis of Selected Parameters for Predicting Food Chain Transport and Internal Dose of Radionuclides,* ORNL/NUREG/TM-282, Union Carbide Corp., Nuclear Div., Oak Ridge Natl. Lab.

Hoffman, F. O., Gardner, R. H., and Eckerman, K. F. 1982. *Variability in Dose Estimates Associated with the Food Chain Transport and Ingestion of Selected Radionuclides,* NUREG/CR-2612, U.S. Nuclear Regulatory Commission.

Hoffman, F. O., and Kaye, S. V. 1976. "Terrestrial Exposure Pathways: Potential Exposure of Man from the Environmental Transport of Waste Nuclides," pp. 524–38 in *Proceedings of the International Symposium on Management of Wastes from LWR Fuel Cycle, Denver, Colorado. July 11–16, 1976,* CONF-76-0701, U.S. ERDA.

Hoffman, F. O., Shaeffler, D. L., Miller, C. W., and Garten, C. T., Jr., eds. 1978a. *The Evaluation of Models Used for the Environmental Assessment of Radionuclide Releases,* proceedings of a workshop held in Gatlinburg, Tenn., Sept. 6–9, 1977, CONF-770901.

Hoffman, F. O., Shaeffer, D. L., Baes, C. F., III, Little, C. A., Miller, C. W., Dunning, D. E., Jr., Rupp, E. M., and Shor, R. W. 1978b. "An Evaluation of Uncertainties in Radioecological Models," pp. 610–48 in *Radioaktivität und Umwelt,* vol. 2, ed. H. J. Kellerman, Fachverband für Strahlnschutz.

Iman, R. L., and Conover, W. J. 1979. "The Use of the Rank Transform in Regression," *Technometrics* **21,** 499–509.

Iman, R. L., Conover, W. J., and Campbell, J. E. 1980. *Risk Methodology for Geologic Disposal of Radioactive Waste: Small Sample Sensitivity Analysis Techniques for Computer Models, with an Application to Risk Assessment,* NUREG/CR-1397, U.S. Nuclear Regulatory Commission.

Iman, R. L., Davenport, J. M., and Ziegler, D. K. 1980. *Latin Hypercube Sampling (Program User's Guide),* SAND 79-1473, Sandia Natl. Lab., Albuquerque, N.Mex.

International Atomic Energy Agency (IAEA) 1982. *Generic Models and Parameters for Assessing the Environmental Transfer of Radionuclides from Routine Releases: Exposures of Critical Groups,* IAEA Safety Series No. 57, Int. Atomic Energy Agency, Vienna.

International Commission on Radiological Protection (ICRP) 1975. *Report of the Task Group on Reference Man,* ICRP Publication 23, Pergamon, New York.

International Commission on Radiological Protection (ICRP) 1977. *Recommendations of the International Commission on Radiological Protection,* ICRP Publication 26, Pergamon, New York.

International Commission on Radiological Protection (ICRP) 1979. *Radionuclide Release into the Environment: Assessment of Doses to Man,* ICRP Publication 29, Pergamon, New York.

International Commission on Radiological Protection (ICRP) 1980. *Limits of Intakes of Radionuclides by Workers,* ICRP Publication 30, supplement to Part 1. Pergamon, New York.

Johnson, N. L., and Kotz, S. 1970. *Distributions in Statistics: Continuous Univariate Distributions,* vol. 1, Houghton Mifflin Co., Boston.

Kaye, S. V., Hoffman, F. O., McDowell-Boyer, L. M., and Baes, C. F., III 1982. "Development and Application of Terrestrial Food Chain Models to Assess Health Risks to Man from Releases of Pollutants to the Environment," in *International Symposium on Health Impacts of Different Sources of Energy, Nashville, Tennessee, USA. June 22–26, 1981,* IAEA-SM/63, Int. Atomic Energy Agency, Vienna.

Killough, G. G., and Rohwer, P. S. 1978. "A New Look at the Dosimetry of ^{14}C Released to the Atmosphere as Carbon Dioxide," *Health Phys.* **34,** 141–159.

Kocher, D. C., ed. 1982. *Proceedings of the Symposium on Uncertainties Associated with the Regulation of the Geologic Disposal of High-Level Radioactive Waste, Gatlinburg, Tennessee, March 9–13, 1981,* NUREG/CP-0022, CONF-810372.

Ku, H. H. 1966. "Notes on the Use of Propagation of Error Formulas," *J. Res. Nat. Bur. Stand. Sect. C* **70**(4), 236–273.

Ku, H. H. ed. 1969. *Precision Measurement and Calibration: Statistical Concepts and Procedures,* Special Publication 300, vol. 1, Natl. Bur. Standards.

Lindackers, H. H., and Bonnenberg, H. 1980. *Proceedings of a Workshop on Accuracy In Dose Calculations for Radionuclides Released to the Environment. September 10–14, 1979*, Aachen, Federal Republic of Germany, GUW, Aldenhoven.

Mankin, J. B., O'Neill, R. V., Shugart, H. H., and Rust, B. W. 1977. "The Importance of Validation in Ecosystem Analysis," pp. 63–71 in *New Directions in the Analysis of Ecosystems*, Simulations Councils Proceedings Series, vol. 5, No. 1, ed. G. S. Innis.

Matthies, M., Eisfeld, K., Paretzke, H., and Wirth, E. 1981. "Stochastic Calculations for Radiation Risk Assessment: A Monte Carlo Approach to the Simulation of Radiocesium Transport in the Pasture-Cow-Milk Food Chain," *Health Phys.* **40**, 764–769.

May, R. M., ed. 1976. *Theoretical Ecology: Principles and Applications*, Saunders, Philadelphia.

McKay, M. D., Conover, W. J., and Beckman, R. J. 1979. "A Comparison of Three Methods for Selecting Values of Input Variables in the Analysis of Output from a Computer Code," *Technometrics* **21** (2) 239–45.

Miller, C. W., Cotter, S. J., and Hanna, S. R. eds. 1981. *Symposium on Intermediate Range Atmospheric Transport Processes and Technology Assessment, Gatlinburg, Tenn., October 1–3, 1980*, CONF-801064, U.S. DOE.

Moore, R. E., Baes, C. F. III, McDowell-Boyer, L. M., Watson, A. P., Hoffman, F. O., Pleasant, J. C., and Miller, C. W. 1979. *AIRDOS-EPA: A Computerized Methodology for Estimating Environmental Concentrations and Dose to Man from Atmospheric Releases of Radionuclides*, EPA 520/1-79-009.

Neter, J., Wasserman, W., and Whitmore, G. A. 1978. *Applied Statistics*, Allyn, Boston.

Ng, Y. C., Colsher, C. S., and Thompson, S. E. 1978. "Transfer Coefficients for Terrestrial Food Chains — Their Derivation and Limitations," pp. 455–81 in *Radioactivitat und Umwelt*, vol. 1, Fachverband für Strahlenschutz.

Ng, Y. C., Colsher, C. S., and Thompson, S. E. 1982. *Soil-to-Plant Concentration Factors for Use in Radiological Assessments*, NUREG/CR-2975 (UCID-19463).

O'Neill, R. V., Gardner, R. H., Hoffman, F. O., and Schwarz, G. 1981. "Effects of Parameter Uncertainty on Estimating Radiological Dose in Man: A Monte Carlo Approach," *Health Phys.* **40**, 760–64.

O'Neill, R. V., Gardner, R. H., and Mankin, J. B. 1980. "Analysis of Parameter Error in a Nonlinear Model," *Ecol. Modelling* **8**, 297–311.

Rao, R. C. 1965. *Linear Statistical Inference and its Applications*, 2d ed., Wiley, New York.

Rubenstein, R. Y. 1981. *Simulation and the Monte Carlo Method*, Wiley, New York.

Schubert, J., Brodsky, A., and Tyler, S. 1967. "The Log-Normal Function as a Stochastic Model of the Distribution of Strontium-90 and Other Fission Products in Humans," *Health Phys.* **13**, 1187–1204.

Schwarz, G., and Dunning, D. E, Jr. 1982. "Imprecision in Estimates of Dose from Ingested ^{137}Cs Due to Variability in Human Biological Characteristics," *Health Phys.* **43**, 631–645.

Schwarz, G., and Hoffman, F. O. 1981. "Imprecision of Dose Predictions for Radionuclides Released to the Environment: An Application of a Monte Carlo Simulation Technique," *Environment International* **4**, 289–97.

Shaeffer, D. L. 1980. "A Model Evaluation Methodology Applicable to Environmental Assessment Models," *Ecol. Modelling* **8**, 275–95.

Shaeffer, D. L. 1981. "A Two Compartment Model for the Transport of ^{131}I via the Pasture-Cow-Milk Pathway," *Health Phys.* **41**, 155–64.

Shaeffer, D. L., and Hoffman, F. O. 1979. "Uncertainties in Radiological Assessments — A Statistical Analysis of Radioiodine Transport via the Pasture-Cow-Milk Pathway," *Nuclear Technol.* **45**, 99–106.

Snedecor, G. W., and Cochran, W. G. 1967. *Statistical Methods,* Iowa State Univ. Press, Ames.

Tomovic, R. 1963. *Sensitivity Analysis of Dynamic Systems,* McGraw-Hill, New York.

U.S. Environmental Protection Agency (USEPA) 1977. 40 CFR Pt. 190, "Environmental Radiation Protections Standards for Nuclear power Operations," *Fed. Regist.* **42** (9) 2858–61.

U.S. Nuclear Regulatory Commission (USNRC) 1975. *Numerical Guides for Design Objectives and Limiting Conditions for Operation to Meet the Criterion "as Low as Practical" for Radioactive Material in Light-Water-Cooled Nuclear Power Reactor Effluents. Opinion of the Commission,* Docket RM-50-2.

U.S. Nuclear Regulatory Commission (USNRC) 1977. *Calculation of Annual Doses to Man from Routine Releases of Reactor Effluents for the Purpose of Evaluating Compliance with 10 CFR Part 50, Appendix I,* Regulatory Guide 1.109, rev. 1, October 1.

U.S. Nuclear Regulatory Commission (USNRC) 1982. *Proceedings of the Workshop on Environmental Assessment held at National Bureau of Standards, Gaithersburg, Maryland, December 15–18, 1981,* NUREG/CP-0025.

APPENDIX 11A

CUMULATIVE PROBABILITY DETERMINATION, ERROR PROPAGATION FORMULAS, AND RELATIONSHIP BETWEEN POPULATION STATISTICS AND SAMPLE STATISTICS

DETERMINATION OF CUMULATIVE PROBABILITIES

In a standard normal distribution,

z = the number of standard deviations by which a given value X departs from the mean $\bar{X}$ of the distribution.

The cumulative probabilities in Table 11A.1 correspond to the area $1 - \alpha$ under the standard normal curve from $-\infty$ to $z(1 - \alpha)$. Thus, these cumulative probabilities indicate the probability of a given value X not being exceeded by other values in the distribution. In an example where $X = 100$, the standard deviation of the distribution $s = 30$, and the mean value $\bar{X} = 90$,

$$z = \frac{X-\bar{X}}{s} = \frac{100-90}{30} = 0.33, \qquad \text{(A11.1)}$$

and the cumulative probability is 0.6293. Because of the approximate nature of assessment models, we interpret this cumulative probability as approximately the 63rd percentile.

For the normal distribution:

the 50th percentile = the mean $\bar{X}$,

the 84th percentile = the mean $\bar{X}$ + the standard deviation s ,

the 95th percentile = $\bar{X} + 1.65s$,

the 99th percentile = $\bar{X} + 2.33s$,

Table 11A.1. Cumulative probabilities of the standard normal distribution

Entry is area $1 - \alpha$ under the standard normal curve from $-\infty$ to $z(1 - \alpha)$

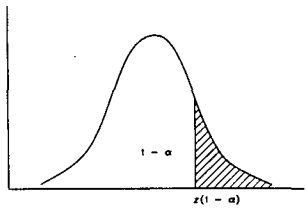

z	.00	.01	.02	.03	.04	.05	.06	.07	.08	.09
.0	.5000	.5040	.5080	.5120	.5160	.5199	.5239	.5279	.5319	.5359
.1	.5398	.5438	.5478	.5517	.5557	.5596	.5636	.5675	.5714	.5753
.2	.5793	.5832	.5871	.5910	.5948	.5987	.6026	.6064	.6103	.6141
.3	.6179	.6217	.6244	.6293	.6331	.6368	.6406	.6443	.6480	.6517
.4	.6554	.6591	.6628	.6664	.6700	.6736	.6772	.6808	.6844	.6879
.5	.6915	.6950	.6985	.7019	.7054	.7088	.7123	.7157	.7190	.7224
.6	.7257	.7291	.7324	.7357	.7389	.7422	.7454	.7486	.7517	.7549
.7	.7580	.7611	.7642	.7673	.7704	.7734	.7764	.7794	.7823	.7852
.8	.7881	.7910	.7939	.7967	.7995	.8023	.8051	.8078	.8106	.8133
.9	.8159	.8186	.8212	.8238	.8264	.8289	.8315	.8340	.8365	.8389
1.0	.8413	.8438	.8461	.8485	.8508	.8531	.8554	.8577	.8599	.8621
1.1	.8643	.8665	.8686	.8708	.8729	.8749	.8770	.8790	.8810	.8830
1.2	.8849	.8869	.8888	.8907	.8925	.8944	.8962	.8980	.8997	.9015
1.3	.9032	.9049	.9066	.9082	.9099	.9115	.9131	.9147	.9162	.9177
1.4	.9192	.9207	.9222	.9236	.9251	.9265	.9279	.9292	.9306	.9319
1.5	.9332	.9345	.9357	.9370	.9382	.9394	.9406	.9418	.9429	.9441
1.6	.9452	.9463	.9474	.9484	.9495	.9505	.9515	.9525	.9535	.9545
1.7	.9554	.9564	.9573	.9582	.9591	.9599	.9608	.9616	.9625	.9633
1.8	.9641	.9649	.9656	.9664	.9671	.9678	.9686	.9693	.9699	.9706
1.9	.9713	.9719	.9726	.9732	.9738	.9744	.9750	.9756	.9761	.9767
2.0	.9772	.9778	.9783	.9788	.9793	.9798	.9803	.9808	.9812	.9817
2.1	.9821	.9826	.9830	.9834	.9838	.9842	.9846	.9850	.9854	.9857
2.2	.9861	.9864	.9868	.9871	.9875	.9878	.9881	.9884	.9887	.9890
2.3	.9893	.9896	.9898	.9901	.9904	.9906	.9909	.9911	.9913	.9916
2.4	.9918	.9920	.9922	.9925	.9927	.9929	.9931	.9932	.9934	.9936
2.5	.9938	.9940	.9941	.9943	.9945	.9946	.9948	.9949	.9951	.9952
2.6	.9953	.9955	.9956	.9957	.9959	.9960	.9961	.9962	.9963	.9964
2.7	.9965	.9966	.9967	.9968	.9969	.9970	.9971	.9972	.9973	.9974
2.8	.9974	.9975	.9976	.9977	.9977	.9978	.9979	.9979	.9980	.9981
2.9	.9981	.9982	.9982	.9983	.9984	.9984	.9985	.9985	.9986	.9986
3.0	.9987	.9987	.9987	.9988	.9988	.9899	.9989	.9989	.9990	.9990
3.1	.9990	.9991	.9991	.9991	.9992	.9992	.9992	.9992	.9993	.9993
3.2	.9993	.9993	.9994	.9994	.9995	.9994	.9994	.9995	.9995	.9995
3.3	.9995	.9995	.9995	.9996	.9996	.9996	.9996	.9996	.9996	.9997
3.4	.9997	.9997	.9997	.9997	.9997	.9997	.9997	.9997	.9997	.9998

Selected percentiles

Cumulative probability $1 - \alpha$:	.90	.95	.975	.98	.99	.995	.999
$z(1 - \alpha)$:	1.282	1.645	1.960	2.054	2.326	2.576	3.090
Cumulative probalility $1 - \alpha$:	.10	.05	.025	.02	.01	.005	.001
$z(1 - \alpha)$:	−1.282	−1.645	−1.960	−2.054	−2.326	−2.576	−3.090

Example: $P(Z \leq 1.83) = .9664$, so $z(.9664) = 1.83$

Source: *Applied Statistics,* J. Neter, W. Wasserman, and G. A. Whitmore, Allyn and Bacon, Boston, 1978, Table B-1.

For the lognormal distribution:

the 50th percentile = $\exp(\mu)$,
where μ is the mean of the log-transformed data;

the mean = $\exp[\mu + (\sigma^2/2)]$,
where σ^2 is the variance of log-transformed data

the 84th percentile = $\exp(\mu + \sigma)$

the 95th percentile = $\exp(\mu + 1.65\sigma)$

the 99th percentile = $\exp(\mu + 2.33\sigma)$

NOTE: In these examples we assume the estimates of $\bar{X}$, s, μ, and σ to be derived from a sufficiently large number.

ERROR PROPAGATION FORMULAS

Table 11A.2 presents some additional error propagation formulas dependent on various functional forms of mathematical equations. Note that Eqs. 11.14 and 11.15 in the text have been derived from the first example given in Table 11A.2.

For lognormally distributed model solutions, estimates of the mean of the log-transformed solution μ and its variance σ^2 can be obtained from estimates of the untransformed mean $\bar{X}$ and variance s^2 by the following equations (Dunning and Schwarz, 1978):

$$\mu = \ln \frac{\bar{X}}{[1 + (s/\bar{X})^2]^{1/2}} \qquad \text{(A11.2)}$$

$$\sigma^2 = \ln[1 + (s/\bar{X})^2] \qquad \text{(A11.3)}$$

RELATIONSHIP BETWEEN POPULATION STATISTICS AND SAMPLE STATISTICS

The relationship between population statistics and sample statistics is given in Table 11A.3 (also taken from Collee et al., 1981). In this chapter, all estimates of parameter and model uncertainties are calculated using sample statistics.

Table 11A.2. Propagation of error formulas for some simple functions

Function form*	Approximate variance	Additional term if u and v are correlated
$x = au \pm bv$	$s_x^2 = a^2 s_u^2 + b^2 s_v^2$	$\pm 2ab s_{uv}$
$x = auv$	$\frac{s_x^2}{\bar{X}_x^2} = \frac{s_u^2}{\bar{X}_u^2} + \frac{s_v^2}{\bar{X}_v^2}$	$+2 \frac{s_{uv}}{\bar{X}_u \bar{X}_v}$
$x = \frac{au}{v}$	$\frac{s_x^2}{\bar{X}_x^2} = \frac{s_u^2}{\bar{X}_u^2} + \frac{s_v^2}{\bar{X}_v^2}$	$-2 \frac{s_{uv}}{\bar{X}_u \bar{X}_v}$
$x = u^2$	$s_x^2 = 4\bar{X}_u^2 s_u^2$	
$x = \sqrt{u}$	$s_x^2 = 1/4 \frac{s_u^2}{\bar{X}_u^2}$	
$x = au^{\pm b}$	$\frac{s_x^2}{\bar{X}_x^2} = b^2 \frac{s_u^2}{\bar{X}_u^2}$	
$x = ae^{\pm bu}$	$\frac{s_x^2}{\bar{X}_x^2} = b^2 s_u^2$	
$x = cu^{\pm a} v^{\pm b}$	$\frac{s_x^2}{\bar{X}_x^2} = a^2 \frac{s_u^2}{\bar{X}_u^2} + b^2 \frac{s_v^2}{\bar{X}_v^2}$	$2(\pm a)(\pm b) \frac{s_{uv}}{\bar{X}_u \bar{X}_v}$
$x = \ln u$	$s_x^2 = \frac{s_u^2}{\bar{X}_u^2}$	
$x = a \ln(\pm bu)$	$s_x^2 = a^2 \frac{s_u^2}{\bar{X}_u^2}$	

*Where a, b and c are constants; u and v are independent variables which are assumed to be statistically independent; and the value of x is finite and real [e.g., $v \neq 0$ for ratios with v as denominator, $u > 0$ for $\sqrt{u}$ and $\ln u$, and $(\pm bu) > 0$ for $\ln(\pm bu)$].

Table A.2 has been taken from Collee et al. (1981). In the equations for error propagation, s^2 is the variance and s_{uv} is the covariance term.

Table 11A.3. The relationship between population statistics and sample statistics

Population parameters[a]	Sample statistics[b] (Estimators of parameters)
M_x (mean - first moment) $= \frac{1}{N}\sum_{i=1}^{N} X_i$	$\bar{X} = \frac{1}{n}\sum_{i=1}^{n} X_i$
V_x (variance - second central moment) $= \frac{1}{N}\sum_{i=1}^{N}(X_i - \bar{X})^2$	$s_x^2 = \frac{1}{n-1}\sum_{i=1}^{n}(X_i - \bar{X})^2$
S_x (standard deviation of x about the population mean M_x)	$s_x = \sqrt{s_x^2}$
$S_{\bar{x}}$ (standard error of the mean, or standard deviation of the average)	$s_{\bar{x}} = \frac{1}{\sqrt{n}} s_x$
$S_{xy} = S_{yx}$ (covariance)	$s_{xy} = s_{yx} = \frac{1}{n-1}\sum_{i=1}^{n}(X_i - \bar{X})(Y_i - \bar{Y})$
$\frac{S}{M}(100)$ (coefficient of variation, or relative standard deviation, expressed in percent)	$cv_x = \frac{s_x}{\bar{X}}(100)$

[a] Where N is the total number within a population.
[b] Where n is the size of the sample.

12 Regulatory Standards for Environmental Releases of Radionuclides*

By J. W. N. HICKEY† *and* J. NEHEMIAS‡

12.1 INTRODUCTION

Regulation of the use of radioactive materials by the U.S. nuclear industry is determined by Federal laws as described below. Federal agencies implement the laws through development of regulations, guides, and other appropriate standards. Further standards are developed through the recommendations of national and international advisory bodies, such as the National Council on Radiation Protection and Measurements and the International Commission on Radiological Protection. This chapter discusses the general nature of laws, regulations, and other standards as they relate to control of environmental releases of radioactive materials. Parts of this chapter are based on a more comprehensive description of all aspects of regulation of the nuclear industry, prepared by Peterson and Mattson (1978).

---

*Although the authors are employed by the U.S. Nuclear Regulatory Commission, the opinions expressed in this chapter are those of the authors and do not necessarily represent views of the Commission. The material in this chapter should not be used for determining compliance with Federal regulations.

†Office of Nuclear Material Safety and Safeguards, U.S. Nuclear Regulatory Commission, Washington, D.C.

‡Office of Nuclear Reactor Regulation, U.S. Nuclear Regulatory Commission, Washington, D.C.

12.2 HISTORICAL PERSPECTIVE

Early uses of ionizing radiations were based principally upon two spectacular scientific observations at the turn of the century: in January of 1896, Roentgen first announced his discovery of X rays; in November of the same year, Becquerel announced his discovery of radiations emanating from uranium.

Widespread interest in these two new phenomena led to many studies of the properties of these newfound radiations and to early discovery of their potential for practical use in creating images of tissues and organs by differential absorption. Before the end of 1896, a number of medical researchers had reported successful uses of therapeutic radiation doses in the treatment of cancer patients. Unfortunately, also before the end of 1896, unexpected injuries to the hands and skin occurred as a result of high radiation exposures. Roentgen himself sustained severe, painful injury to the back of his left hand.

These early injuries resulted from short-term exposures at high radiation levels and provided ample evidence that such doses could cause serious, acute injuries. Over the next several decades, data began to accumulate indicating that long-term effects, principally leukemia and cancer, could also result from high radiation levels, but might not be manifested until 20 or more years after the original exposure. A dramatic example of this phenomenon was the case of the women who were hired to paint radium luminescent paint on wristwatch dials. It was common practice among these women to point their brushes with their tongues, and many of them subsequently developed cancer as a result of radium being deposited in their bones.

Concern about these matters in the scientific community led to the development of organizations interested in both the beneficial and hazardous aspects of radiation. By the early 1920s, the British Roentgen Society had been formed in England and the Roentgen Ray Society in the United States.

These societies, in conjunction with other national bodies, held the First International Congress of Radiology in London in 1925. The Second International Congress was held in Stockholm in 1928. At the second meeting, the International Committee on X-ray and Radium Protection was formed and soon thereafter began the process of developing radiation protection recommendations. After a number of organizational and name changes, this committee has come to be the present International Commission on Radiological Protection (ICRP).

In the United States, a similar development process took place. Beginning in 1929, discussions among the officers of the American Roentgen Ray Society, the Radiological Society of North America, and the Radium Society resulted in the consolidation of their radiation protection activities into a single committee, which was called Advisory Committee on X-ray and Radium

Protection. Following a number of organizational and name changes, this committee has come to be the present National Council on Radiation Protection and Measurements (NCRP).

Beginning in the 1920s, researchers began developing methods for the quantifying of radiation measurements. They also sought to define a "tolerance dose" (a dose that could be "tolerated" without serious harm) and the precursor of current dose limits for workers. In 1934, based on these studies, the NCRP adopted an occupational tolerance exposure rate of 0.1 R/d; the ICRP adopted the value of 0.2 R/d. At that time, most of the individuals involved believed that no harmful effects would occur at these levels.

Over a period of time, these advisory bodies moved away from the concept of a "tolerance dose." During the 1950s, they adopted the conservative position that there probably is no radiation dose threshold below which no harm could occur. They concluded that, for the purposes of establishing radiation protection standards, the assumption should be made that there is some radiation risk associated with any radiation dose, however small, and that the risk decreases with decreasing dose. Given the assumption that lower dose means lower risk at any dose level, they concluded that, as a matter of policy, exposures to individuals and to human populations should be kept "as low as practicable," a term subsequently changed to "as low as is reasonably achievable" (ALARA).

During this period, these advisory bodies developed the concept of a "maximum permissible dose" (MPD). In 1958 the ICRP defined the MPD as "that dose, accumulated over a long period of time or resulting from a single exposure, which, in the light of present knowledge, carries a negligible probability of severe somatic or genetic injuries; futhermore, it is such a dose that any effects that ensue more frequently are limited to those of a minor nature that would not be considered unacceptable by the exposed individual and by competent medical authorities" (ICRP 1959a).

In the late 1950s, the ICRP and the NCRP adopted amendments and additions to their recommendations on radiation protection, including recommendations on permissible doses to body organs from radioactive materials deposited in the body, and on control of exposures to members of the public residing near controlled areas.

In 1959, the U.S. Federal Radiation Council was formed to provide a Federal policy on human radiation exposure and to advise the President with respect to radiation matters. This body and its successor agency, the U.S. Environmental Protection Agency, have developed radiation protection guidance for all Federal agencies. Specific details as to the form and content of this guidance, and its application by Federal agencies, are presented and discussed in the following sections of this chapter.

12.3 LEGISLATIVE BACKGROUND

Current Federal regulation of environmental releases of radioactive materials is based primarily on the Atomic Energy Act of 1954, the Energy Reorganization Act of 1974, and the Clean Air Act Amendments of 1977.

Prior to 1954, the U.S. Government essentially controlled atomic energy facilities. The Atomic Energy Act of 1954 created a framework for Federal control of civilian industrial use of radioactive materials by private industry, to be regulated by the U.S. Atomic Energy Commission (AEC). The Presidential Reorganization Plan No. 3 of 1970 (not a law) transferred AEC functions related to establishment of generally applicable environmental standards to the U.S. Environmental Protection Agency (EPA). The AEC was thereby made responsible for limiting environmental releases in such a manner that EPA's generally applicable environmental standards would be met. The Atomic Energy Act also authorized the AEC to enter into agreements with any State or group of States to perform inspections or other functions on a cooperative basis, as the Commission deemed appropriate.

The Federal Radiation Council (FRC) was formed in 1959 (Public Law 86-373) to provide a Federal policy on human radiation exposure. A major function of the Council was to "advise the President with regard to radiation matters, directly or indirectly affecting health including guidance for all Federal agencies."

The Energy Reorganization Act of 1974 abolished the AEC. The principal regulatory elements of the AEC were reestablished as the U.S. Nuclear Regulatory Commission (NRC), and the remaining elements were established as the Energy Research and Development Administration (later incorporated into the U.S. Department of Energy). The Department of Energy retains regulatory authority over most of its own operations.

The Clean Air Act Amendments of 1977 give the EPA authority to establish air quality criteria and to define acceptable control techniques. This legislation extended the EPA's authority, previously limited (by Presidential Reorganization Plan No. 3 of 1970) to the setting of generally applicable environmental standards, to include the setting of limits on doses to nonworkers from the entire nuclear industry and on total released quantities of certain radionuclides.

12.4 ORGANIZATIONS WITH RADIATION PROTECTION RESPONSIBILITIES

12.4.1 Federal Radiation Council (FRC)

The FRC's principal function, as stated previously, was to provide guidance to all Federal agencies on radiation protection matters. In the course of implementing this authority, the FRC developed and published eight reports

addressing various general and specific aspects of radiation protection. Presidental Reorganization Plan No. 3 of 1970 abolished the FRC and transferred its functions to the EPA.

12.4.2 U.S. Environmental Protection Agency (EPA)

The EPA has three independent functions related to radioactive environmental releases:

1. Develop and promulgate radiation protection guidance to Federal agencies. This function was transferred from the abolished FRC.
2. Establish generally applicable environmental radiation standards pursuant to the Atomic Energy Act. This function was transferred from the AEC.
3. Establish air quality criteria and control techniques based on the Clean Air Act Amendments of 1977.

12.4.3 U.S. Nuclear Regulatory Commission (NRC)

The NRC regulates the nuclear industry pursuant to the Atomic Energy Act. The NRC regulations are included in Title 10 of the *Code of Federal Regulations* (1982) and have the force of law. In addition, the NRC publishes Regulatory Guides, which describe acceptable methods for compliance with specific regulations, and other documents that provide additional information relevant to these regulations and the Regulatory Guides. Regulatory Guides do not, of themselves, define all acceptable methods; compliance with the guides is not required if satisfactory alternative methods are developed to provide a comparable level of protection for radiation workers or for the public.

12.4.4 U.S. Department of Defense (DOD)

As provided by the Atomic Energy Act, the DOD regulates most of its own activities involving nuclear weapons and nuclear-powered vessels. However, most other DOD activities involving radioactive material are regulated by the NRC.

12.4.5 U.S. Department of Energy (DOE)

DOE facilities and contractor-operated national laboratories are not subject to NRC regulation, but follow the DOE manual (USDOE 1978), which is generally consistent with the NRC regulations and with FRC and EPA radiation protection guidance to Federal agencies.

12.4.6 AEC/NRC Agreement States

In accordance with the Atomic Energy Act as amended, the AEC/NRC has established agreements with 26 States. Within each of these Agreement States, the State is solely responsible for licensing and direct regulation of the use of by-product materials and small quantities of source or special nuclear materials. Agreement States, however, must develop and implement radiation protection regulations that are compatible with NRC regulations.

12.4.7 Radiation Protection Advisory Bodies

The National Council on Radiation Protection and Measurements (NCRP) and the International Commission on Radiological Protection (ICRP), respectively, are the national and international radiation protection advisory bodies, whose recommendations provide the scientific basis for U.S. standards. These bodies are made up of national and international experts in biology, medicine, genetics, health physics, and other related scientific disciplines. These agencies publish, from time to time, specific recommendations on radiation protection matters. Their recommendations have been widely adopted and form the basis for radiation protection standards throughout the world.

12.5 REGULATORY STANDARDS

12.5.1 Methodology

The application of a standard depends upon its qualitative and quantitative aspects. Some standards are merely advisory; others have the force of law. Some limit doses to the general public; others limit concentrations or quantities of radioactive materials released. Some apply to maximum or average doses, others to specific whole-body or organ doses or to individual or population doses. Relevant background information must be understood to ensure effective implementation of the standard.

12.5.2 EPA Standards

12.5.2.1 Federal Radiation Protection Guidance

The EPA is responsible for preparing radiation protection guidance for issuance by the President to Federal agencies. This function was formerly carried out by the Federal Radiation Council (FRC), which was abolished when the EPA was established. The guidance is advisory and does not have the force of law. However, Federal regulations have generally been consistent with FRC and EPA guidance.

Table 12.1 summarizes existing Federal radiation protection guidance applicable to members of the public affected by radioactive releases from normal operations involving peacetime applications of radiation or radioactive materials. Guidance is provided for doses to individuals in the environment, with a lower value given for a "suitable sample" of the most highly exposed sector of the population. In typical situations involving releases of radioactive materials to the environment, doses to individuals are not known. In such cases, guidance for the suitable population sample is the appropriate standard.

Table 12.1. Federal radiation protection guides for population exposures from normal operations

Type of exposure	Limit
Individual whole-body dose	0.5 rem/y
Average gonad dose	5 rem over 30 y
Individual thyroid dose	1.5 rem/y
Average thyroid dose	0.5 rem/y
Individual bone marrow dose	0.5 rem/y
Average bone marrow dose	0.17 rem/y
Individual bone dose	1.5 rem/y, or 0.003 μg ^{226}Ra body burden or biological equivalent
Average bone dose	0.5 rem/y, or 0.001 μg ^{226}Ra body burden or biological equivalent

Sources: (1) Federal Radiation Council, "Report 1, Background Material for the Development of Radiation Protection Standards," *Fed. Regist.*, May 18, 1960. (2) Federal Radiation Council, "Report 2, Background Material for the Development of Radiation Protection Standards," *Fed. Regist.*, Sept. 26, 1961.

Table 12.2 summarizes graded scales of action for regulatory officials appropriate for different levels of population exposure resulting from such normal operations. Generally, if doses to the population are projected to be less than 10% of those given in Table 12.1 (range I), only periodic confirmatory radiological surveillance is necessary. However, if projected doses are within ranges II or III, additional surveillance and control measures are appropriate. Table 12.2 also specifies transient daily rates of intake for radium, iodine, and strontium corresponding to each range.

Table 12.2. Federal radiation protection guides: graded scales of action for normal operations

A. Action levels

Range	Dose rate	Action
I	Less than 10% of limits	Periodic surveillance
II	10% to 100% of limits	Quantitative surveillance and routine control
III	Greater than limits	Control measures

B. Ranges of intake

Radionuclide	Transient daily intake (pCi)		
	Range I	Range II	Range III
^{226}Ra	0–2	2–20	20–200
^{131}I (children)	0–10	10–100	100–1,000
^{90}Sr	0–20	20–200	200–2,000
^{89}Sr	0–200	200–2,000	2,000–20,000

Sources: (1) Federal Radiation Council, "Report 1, Background Material for the Development of Radiation Protection Standards," *Fed. Regist.*, May 18, 1960. (2) Federal Radiation Council, "Report 2, Background Material for the Development of Radiation Protection Standards," *Fed. Regist.*, Sept. 26, 1961.

Table 12.3 summarizes guidance for accidental releases. The guidance allows an official to make a decision regarding appropriate protective action based on projected doses that could be eliminated by such action. For example, consider an accident that results in releases of ^{131}I. If projected, reducible doses would exceed 30 rad to the thyroid, protective action, such as withdrawing milk from the food supply, would be appropriate.

Revisions of existing radiation guidance have been proposed by the EPA (USEPA 1981). Any final revisions would be published in the *Federal Register.*

12.5.2.2 Generally Applicable Environmental Standards

In addition to the Federal radiation protection guidance provided by the EPA, the only generally applicable environmental radiation standard published

Table 12.3. Federal protective action guides for accidental releases

Exposure pathway	Projected dose	
	^{131}I	^{89}Sr, ^{90}Sr, and ^{137}Cs
1. Transmission through the pasture-cow-milk chain		
Individual	30 rad to the thyroid	10 rad in the first year to the bone marrow or whole body
Suitable sample of exposed population	10 rad to the thyroid of a one-year-old child	3 rad in the first year to the bone marrow or whole body of a one-year-old child
2. Transmission through feed crops to animals (including dairy cattle) and plant crops used directly for human food		
Individual	*a*	5 rad in the first year to the bone marrow or whole body
Suitable sample of exposed population	*a*	3 rad in the first year to the bone marrow or whole body of a one-year-old child
3. Long-term transmission through soil into plants		
Individual	*a*	0.5 rad in the first year to the bone marrow or whole body
Suitable sample of exposed population	*a*	0.2 rad in the first year to the bone marrow or whole body of a one-year-old child

[a]No guidance given for ^{131}I due to short half-life.

Sources: (1) Federal Radiation Council, "Report 5, Background Material for the Development of Radiation Protection Standards," *Fed. Regist.*, Aug. 22, 1964. (2) Federal Radiation Council, "Report 7, Background Material for the Development of Radiation Protection Standards," *Fed. Regist.*, May 22, 1965.

by the EPA to date is set forth in Title 40, *Code of Federal Regulations*, Part 190 (40 CFR Part 190), "Environmental Radiation Protection Standards for Nuclear Power Operations." This regulation has the force of law; NRC licensees and DOE facilities must comply with it. The NRC enforces the application of 40 CFR Part 190 by its fuel cycle licensees.

The provisions of 40 CFR Part 190 are summarized in Table 12.4. This regulation applies to all activities involved in the entire uranium fuel cycle,

Table 12.4. Summary of 40 CFR Part 190, Environmental Radiation Protection Standards for Nuclear Power Operations

1. 40 CFR 190 applies to: uranium mills, uranium hexafluoride production, uranium fuel fabrication, uranium-fueled light-water power reactors, uranium fuel reprocessing
2. 40 CFR 190 *excludes*: mining, waste disposal, transportation, radon and radon daughters.
3. 40 CFR 190 annual dose limits for members of the public:
   25 mrem — whole body
   75 mrem — thyroid
   25 mrem — any other organ
4. 40 CFR 190 release limits (per gigawatt-year of electrical energy produced):
   ^{85}Kr — 50,000 Ci
   ^{129}I — 5 mCi
   ^{239}Pu and other long-lived transuranics — 0.5 mCi
5. Effective dates:
   December 1, 1980, for uranium mills
   January 1, 1983, for ^{85}Kr and ^{129}I
   December 1, 1979, for all other cases

excluding mining, transportation, and waste disposal, and does not apply to radon and radon daughter products. Fuel cycle facilities must operate such that total annual whole-body and organ doses to individuals do not exceed 25 mrem (thyroid doses must not exceed 75 mrem). Potentially overlapping effects must be considered when more than one nuclear facility may affect a particular area. Release limits for ^{85}Kr, ^{129}I, and long-lived transuranic elements are included in 40 CFR Part 190.

12.5.2.3 Clean Air Act

The Clean Air Act Amendments of 1977 give the EPA authority to regulate airborne radioactive releases from all nuclear facilities. This regulatory process includes identifying radioactive materials as hazardous pollutants as well as establishing enforcement standards. In this unusual situation, the EPA has authority overlapping that of the NRC over its licensees. The Clean Air Act covers this overlap and specifies that EPA and NRC work together to minimize duplication of effort.

To date, the EPA has not published any Clean Air Act standards applicable to radioactive releases.

12.5.3 NRC Standards

12.5.3.1 General Radiation Protection Standards

Radiation protection standards applicable to NRC licensees are contained in Title 10, *Code of Federal Regulations*, Part 20 (10 CFR Part 20), "Standards for Protection Against Radiation." These regulations have the force of law; compliance with them is required. Tables 12.5 and 12.6 summarize the provisions of 10 CFR Part 20 that are applicable to releases to "unrestricted areas." Limits on annual average concentrations are specified for releases of individual radionuclides and mixtures of identified radionuclides. These limits are generally consistent with FRC, NCRP, and ICRP recommendations.

12.5.3.2 ALARA Requirements for Power Reactors

In addition to limitations on releases of airborne radioactive materials to the environment, 10 CFR Part 20 states that releases of radioactive materials should be "as low as is reasonably achievable" (ALARA). Implementation by regulatory authorities generally involves a qualitative approach describing dose-reducing considerations. However, for nuclear power reactors, the NRC has developed specific quantitative ALARA criteria in 10 CFR Part 50, "Domestic Licensing of Production and Utilization Facilities," Appendix I. This regulation establishes design objectives and limiting conditions for operation of power reactors to ensure that releases to the environment comply.

Table 12.7 characterizes these design objectives. They are not operating limits; there is flexibility allowed in operation. Doses may be up to twice as high as the design objectives before corrective action is required.

In addition to giving the dose objectives to be met, Appendix I specifies that licensees must augment their effluent control systems to reduce actual doses below the design objective whenever the cost-benefit ratio is favorable. A favorable cost-benefit ratio would be defined as a situation in which population doses can be reduced at a cost of $1000/man-rem or less. However, experience

Table 12.5. A summary guide to radiation protection requirements for the public in 10 CFR Part 20—Standards for Protection Against Radiation

1. Whole-body dose not to exceed 0.5 rem per calendar year.

2. Concentration of radioactive materials in air or water not to exceed levels in Table II of Appendix B of 10 CFR Part 20.

   As per the provisions of Sect. 20.106(e), the Commission may limit quantities of radioactive materials released in air or water if it appears that the daily intake of radioactivity by a suitable sample of the exposed population will exceed the daily intake equivalent to one-third of intake from continuous exposure, averaged over a year, to the concentrations specified in Appendix B, Table II.

3. Disposal into sanitary systems:

   (a) Material must be readily soluble or dispersible in water; and

   (b) the gross quantity of licensed and other radioactive waste (excluding ^{14}C and tritium) released into the sewage system does not exceed 1 Ci/y; the quantity of ^{14}C and tritium released does not exceed 5 Ci/y; and

   (c) the quantity of any licensed or other radioactive material released in any one month divided by the average monthly quantity of water released does not exceed the limits specified in Appendix B, Table I, Column 2 or 10 CFR Part 20; and

   (d) the quantity released in any one day does not exceed the larger of (1) ten times the quantity specified in Appendix C of 10 CFR Part 20 or (2) the concentration specified in Appendix B, Table I, Column 2 of 10 CFR Part 20 when diluted by the average daily quantity of sewage discharged by the licensee.

5. Maintaining effluents "as low as is reasonably achievable."

   Section 20.1 of 10 CFR Part 20 specifies that licensees should make every reasonable effort to maintain radiation exposures and releases of radioactive materials in effluents to unrestricted areas "as low as is reasonably achievable."

has shown that additional dose reductions below the design objectives are generally not feasible at $1000/man-rem.

12.5.3.3 Regulatory Guides

In most cases, regulations require specific performance criteria but do not go into technical background details. In addition to regulatory requirements, the NRC may incorporate license conditions or "technical specifications" into

Table 12.6. Summary guide for NRC notification requirements pertaining to radiation exposures or releases of radioactive materials

1. Immediate notification:	Incidents or conditions which may have caused or threaten to cause:
	(1) Exposure of any individual in excess of
[Sect. 20.403(a) of 10 CFR Part 20]	(a) 25 rem or more to the whole body, or (b) 150 rem or more to the skin, or (c) 375 rem or more to the feet, ankles, hands, or forearms.
	(2) Release of radioactive materials in concentrations which, if averaged over 24 h, would exceed 5000 times the limits specified in Table II, Appendix B of 10 CFR Part 20.
[Sect. 50.72 of 10 CFR Part 50]	(3) For power reactors, any accidental, unplanned, or uncontrolled radioactive release.
2. 24-h notification:	Incidents or conditions which may have caused or threaten to cause:
	(1) Exposure of any individual in excess of
[Sect. 20.403(b) of 10 CFR Part 20]	(a) 5 rem or more to the whole body, or (b) 30 rem or more to the skin, or (c) 75 rem or more to the feet, ankles, hands, or forearms;
	(2) Release of radioactive materials in concentrations which, if averaged over 24 h, would exceed 500 times the limits specified in Table II, Appendix B of 10 CFR Part 20; or
	(3) Loss of one day or more of the operation of any facilities affected; or
	(4) Damage to property in excess of $1000.

Table 12.6 (continued)

3. 30-d notification:	
A. [Sect. 20.405 of 10 CFR Part 20]	(1) Each exposure of an individual to radiation or concentration of radioactive material in excess of any applicable limit to 10 CFR Part 20 or in the licensee's license;
	(2) Any incident covered by Sect. 20.403 of 10 CFR Part 20;
	(3) Levels of radiation or concentrations of radioactive material (not involving excessive exposure of any individual) in an unrestricted area in excess of ten times any applicable limit in 10 CFR Part 20 or in the licensee's license;
	(4) Radiation levels or releases in excess of those specified in 40 CFR Part 190.
B. [10 CFR Part 50, Appendix I]	(1) Releases of radioactive materials in LWR effluents in any quarter which would result in calculated exposures in excess of one-half the design objectives of Sects. I and II of Appendix I.
4. Reporting effluent releases:	Section 50.36a of 10 CFR Part 50 requires that a licensee submit semiannual reports to NRC specifying the quantity of each of the principal radionuclides in liquid or gaseous effluents during the preceding six-month period. Section 40.65 of 10 CFR Part 40 requires that source material licensees for uranium milling or production of uranium hexafluoride file semiannual reports of the principal radionuclides released to unrestricted areas as liquid or gaseous effluents. Section 70.59 of 10 CFR Part 70 requires that special nuclear material licensees engaged in processing, fuel fabrication, scrap recovery, or conversion of uranium hexafluoride report semiannually the quantity of the principal radionuclides released to unrestricted areas in gaseous or liquid effluents.

Table 12.7. Provisions of Appendix I of 10 CFR Part 50 defining numerical guides for "as low as is reasonably achievable" levels of radioactive materials in light-water-cooled nuclear power plant effluents

Exposure mode	Design objective
Liquid effluents	
Dose to the total body from all pathways	3 mrem per year per reactor
Dose to any organ from all pathways	10 mrem per year per reactor
Gaseous effluents	
Gamma dose in air	10 mrad per year per reactor
Beta dose in air	20 mrad per year per reactor
Dose to the total body of an individual	5 mrem per year per reactor
Dose to the skin of an individual	15 mrem per year per reactor
Radionuclides and particulate matter released to the atmosphere	
Dose to any organ from all pathways	15 mrem per year per reactor

individual licenses. These conditions are detailed requirements, designed to ensure compliance with regulations. For example, short-term release limits or monitoring programs may be specified.

The NRC supplements its regulations further by issuance of Regulatory Guides (see the chapter's bibliography). These guides describe acceptable methods for compliance with regulations at appropriate levels of detail. Regulatory Guides have been published on all aspects of compliance with 10 CFR Part 50, Appendix I, as well as on monitoring of radioactive effluents from various facilities.

As noted, Regulatory Guides do not have the force of law; compliance is not required. However, if a Regulatory Guide is not followed, alternative actions that provide the same degree of public protection must be taken.

12.5.4 DOE Standards

The DOE Policy Manual (USDOE 1978) includes radiation protection standards applicable to DOE facilities, which also apply to contractor-operated national laboratories. DOE standards have generally been consistent with the recommendations of FRC, ICRP, and NCRP and the regulations of NRC.

12.5.5 NCRP Recommendations

NCRP recommendations (NCRP 1971) specify dose criteria for individual members of the public (0.5 rem/y) and for the average dose to a most highly

exposed group (0.17 rem/y). These recommendations do not have the force of law. They have, however, provided the basis for FRC radiation protection guidance and the NRC regulations discussed above.

12.5.6 ICRP Recommendations

As mentioned above, ICRP recommendations have formed the basis for radiation protection standards in most countries of the world, although they do not have the force of law.

The recommendations in ICRP Publication 26 (ICRP 1977) represent a new approach to assessing risks associated with multiple organ doses. Previous recommendations (ICRP 1959b) generally addressed doses to the whole body and to critical organs. The new ICRP recommendations retain the annual whole-body criterion of 0.5 rem. However, in Publication 26, the "critical organ approach" has been replaced with a new approach, which takes into account evaluation and summation of the risks associated with internal doses to all organs at risk. Internal organs have been assigned "weighting factors" (Table 12.8). Total risk incurred by an exposed individual is determined by summing the risks associated with the weighted doses to each exposed organ, as shown in Table 12.8. The result is a "risk equivalent dose."

Table 12.8. ICRP Publication 26 weighting factors

Organ	Weighting factor
Gonads	0.25
Breasts	0.15
Red bone marrow	0.12
Lung	0.12
Thyroid	0.03
Bone surfaces	0.03
Other organs[a]	0.06
Total body	1.0

[a]If more than five other organs, use the five receiving the highest dose equivalent.

If only one organ is exposed (an unlikely circumstance), ICRP Publication 26 recommends that individual organ doses be obtained by dividing the annual whole-body dose criterion (0.5 rem) by the appropriate factor in Table 12.8. Thus, the annual dose criterion for the lung would be 0.5/0.12, or 4.2 rem. Publication 26 includes a criterion limit of 5.0 rem to any organ, as protection against nonstochastic or "acute" effects.

The impact that would result from implementation of ICRP Publication 26 recommendations regarding control of multiple organ doses is not yet clear. The NRC has announced its intent to revise 10 CFR Part 20 (USNRC 1980); the EPA has prepared draft guidance that would adopt a modification of the ICRP Publication 26 model. Decisions regarding U.S. implementation have not yet been determined.

12.6 PROBLEMS

1. What Federal laws form the basis for Federal regulation of radioactive materials in the United States?

2. What major activities involving use of radioactive material are not subject to regulation by the U.S. Nuclear Regulatory Commission?

3. What Federal agencies have responsibility for regulation of radioactive material in the United States? What Federal agency has responsibility for providing radiation protection guidance to other Federal agencies?

4. What different types of standards are promulgated by the U.S. Nuclear Regulatory Commission? Which standards have the force of law?

5. Describe the Agreement State program for regulating radioactive materials.

6. What are the two major advisory organizations that promulgate radiation protection standards? Do their standards have the force of law in the United States?

7. What radiation protection standards have been promulgated by the Federal Radiation Council and the U.S. Environmental Protection Agency?

8. What authority over radioactive materials is given to the U.S. Environmental Protection Agency by the Clean Air Act?

9. What standards have been promulgated applicable to environmental releases of radioactive materials from nuclear power reactors?

REFERENCES

10 CFR Pts. 0–199 Jan. 1, 1982. Revised.

International Commission on Radiological Protection (ICRP) 1959a. *Recommendations of the International Commission of Radiological Protection (Adopted September 9, 1958)*, ICRP Publication 1, Pergamon, Elmsford, N.Y.

International Commission on Radiological Protection (ICRP) 1959b. *Report of Committee II on Permissible Dose for Internal Radiation*, ICRP Publication 2, Pergamon, Elmsford, N.Y.

International Commission on Radiological Protection (ICRP) 1977. *Recommendations of the International Commission on Radiological Protection (Adopted January 17, 1977)*, ICRP Publication 26, Pergamon, Elmsford, N.Y.

National Council on Radiation Protection and Measurements (NCRP) 1971. *Basic Radiation Protection Criteria*, NCRP Report 39.

Peterson, H. T., Jr., and Mattson, R. J. 1978. "Laws, Regulations, and Standards," pp. 99–166 in *Nuclear Power Waste Technology*, ed. A. A. Moghissi et al., American Society of Mechanical Engineers, New York.

U.S. Department of Energy (USDOE) Dec. 15, 1978. "Policy Manual," *Fed. Regist.* **43,** 58790.

U.S. Environmental Protection Agency (USEPA) Jan. 23, 1981. "Federal Radiation Protection Guidance for Occupational Exposures: Proposed Recommendations—Request for Written Comments and Public Hearings," *Fed. Regist.* **46,** 7836.

U.S. Nuclear Regulatory Commission (USNRC) Mar. 20, 1980. "Nuclear Regulatory Commission, 10 CFR Part 20: Standards for Protection Against Radiation; Advance Notice of Proposed Rulemaking," *Fed. Regist.* **45,** 18023.

BIBLIOGRAPHY

American National Standards Institute (ANSI) (Standards available for sale from ANSI, 1430 Broadway, New York, N.Y. 10018).

N13.1-1969, *Guide to Sampling Airborne Radioactive Materials in Nuclear Facilities.*

N13.2-1969, *Administrative Practices in Radiation Monitoring (A Guide for Management).*

N13.10-1974, *Specification and Performance of On-Site Instrumentation for Continuously Monitoring Radioactivity in Effluents.*

Code of Federal Regulation, Title 10: "Energy," Chap. 1: "Nuclear Regulatory Commission," rev. January 1982 (available for sale from U.S. Government Printing Office, Washington, DC 20402).

Code of Federal Regulations, Title 40: "Protection of Environment," Chap. 1: "Environmental Protection Agency," rev. July 1981 (available for sale from U.S. Government Printing Office, Washington, DC 20402).

International Atomic Energy Agency (publications available for sale from UNI Publications, P.O. Box 433, Murray Hill Station, New York, NY 10016).

STI/PUB/147, *Basic Safety Standards for Radiation Protection,* 1967.

STI/PUB/98, *Manual on Environmental Monitoring in Normal Operation,* 1966.

International Commission on Radiological Protection (publications available for sale from Pergamon Press, Elmsford, NY 10523).

Publication 2, *Report of Committee II on Permissible Dose for Internal Radiation*, 1959.

Publication 7, *Principles of Environmental Monitoring Related to the Handling of Radioactive Materials*, 1965.

Publication 23, *The Reference Man*, 1975.

Publication 26, *Recommendations of the International Commission on Radiological Protection (Adopted January 17, 1977)*, 1977.

National Council on Radiation Protection and Measurements (publications available for sale from National Council on Radiation Protection, P.O. Box 30175, Washington, DC 20014).

Report 10, *Radiological Monitoring Methods and Instruments*, 1952.

Report 39, *Basic Radiation Protection Criteria*, 1971.

Report 50, *Environmental Radiation Measurements*, 1976.

Peterson, H. T., Jr. and Mattson, R. J. 1978. "Laws, Regulations, and Standards," pp. 99–166 in *Nuclear Power Waste Technology*, ed. A. A. Moghissi et al., American Society of Mechanical Engineers, New York, NY.

U.S. Government agencies (Federal Radiation Council/Environmental Protection Agency) publish federal radiation protection guidance in the *Federal Register*, and background material is published separately as cited below. The documents may be purchased from the U.S. Government Printing Office, Washington, DC 20402.

Federal Radiation Council, "Report 1, Background Material for the Development of Radiation Protection Standards," *Fed. Regist.*, May 18, 1960.

Federal Radiation Council, "Report 2, Background Material for the Development of Radiation Protection Standards," *Fed. Regist.*, Sept. 26, 1961.

Federal Radiation Council, "Report 5, Background Material for the Development of Radiation Protection Standards," *Fed. Regist.*, Aug. 22, 1964.

Federal Radiation Council, "Report 7, Background Material for the Development of Radiation Protection Standards—Protective Action Guides for Strontium-89, Strontium-90, and Cesium-137," *Fed. Regist.*, May 22, 1965.

U.S. Nuclear Regulatory Commission Regulatory Guides (inquiries regarding subscriptions or purchase of individual copies should be addressed to Publication Sales Manager, U.S. Nuclear Regulatory Commission, Washington, DC 20555).

Regulatory Guide 1.21, *Measuring, Evaluating, and Reporting Radioactivity in Solid Wastes and Release of Radioactivity in Liquid and Gaseous Effluents from Light-Water-Cooled Nuclear Power Plants*, June 1974.

Regulatory Guide 1.97, *Instrumentation for Light-Water-Cooled Nuclear Power Plants to Assess Plant and Environs Conditions During and Following Accident*, August 1981.

Regulatory Guide 1.109, *Calculation of Annual Doses to Man from Routine Releases of Reactor Effluents for the Purpose of Evaluating Compliance with 10 CFR Part 50, Appendix I*, October 1977.

Regulatory Guide 1.110, *Cost-Benefit Analysis for Radwaste Systems for Light-Water-Cooled Nuclear Power Reactors*, March 1976.

Regulatory Guide 1.111, *Methods for Estimating Atmospheric Transport and Disperson of Gaseous Effluents in Routine Releases from Light-Water-Cooled Reactors*, July 1977.

Regulatory Guide 1.112, *Calculation of Releases of Radioactive Materials in Gaseous and Liquid Effluents from Light-Water-Cooled Power Reactors*, May 1977.

Regulatory Guide 1.113, *Estimating Aquatic Dispersion of Effluents from Accidental and Routine Reactor Releases for the Purpose of Implementing Appendix I*, April 1977.

Regulatory Guide 4.13, *Performance, Testing, and Procedural Specifications for Thermoluminescence Dosimetry: Environmental Applications*, August 1977.

Regulatory Guide 4.14, *Radiological Effluent and Environmental Monitoring at Uranium Mills*, April 1980.

Regulatory Guide 4.15, *Quality Assurance for Radiological Monitoring Programs (Normal Operations)—Effluent Streams and the Environment*, February 1979.

Regulatory Guide 4.16, *Measuring, Evaluating, and Reporting Radioactivity in Releases of Radioactive Materials in Liquid and Airborne Effluents from Nuclear Fuel Processing and Fabrication Plants*, March 1978.

13 Development of Computer Codes for Radiological Assessments

By C. A. LITTLE*

13.1 INTRODUCTION

Virtually every field of science and engineering has found an application for modeling. Aeronautical engineers rely on models of wing and fuselage structures to design new aircraft. Hydrologists use models to predict the ability of aquifers to supply communities with adequate drinking water. As evidenced by this book, regulation of the nuclear industry has led to the increasing use of models to estimate radionuclide environmental transport and subsequent dose to humans.

In contrast to the hand calculations that can be done within the framework of a given model, many models have been coded into computer language. This practice allows many model calculations in a short time with little or no computational error. The use of computers has become so widespread that the term "model" has at times come to be used interchangeably with "computer code."

Earlier chapters have discussed types and amounts of materials released from nuclear facilities and detailed the methods employed to estimate the transport of these materials in the atmosphere, in surface and groundwaters, and through terrestrial food chains to man. Models to calculate internal and external radiological dose and the possible risk to humans from exposure to these radionuclides have also been discussed. This chapter deals with some of the important characteristics of computer programs designed to implement these transport, dose, and risk models.

*Health and Safety Research Division, Oak Ridge National Laboratory.

This chapter is not intended either to describe the many existing codes or to provide an instruction manual for developing a computer code for environmental assessment purposes. Rather, the purpose is to describe some of the important characteristics of codes used for environmental assessments. This information will be helpful to potential code users.

13.2 MODELS AND COMPUTER CODES

A model can be defined as any representation of reality; therefore, it can be physical (toy train, soil column in a laboratory) or mathematical (the diffusion equation). The topics considered in the previous chapters involve mathematical models of one form or another.

Computers and models become associated when one wishes to make repeated calculations using a model but prefers to spend a minimum amount of time and effort. This gives rise to the computer model or, more precisely, the representation of the mathematical model in computer language. Therefore, the computer model is not a model at all but simply a translation into computer language of an existing mathematical model, equation, or group of equations. For example, in Fig. 13.1, both hypothetical programs DISPERSE and BREATHE are codifications of the Gaussian plume model (see Chapter 2).

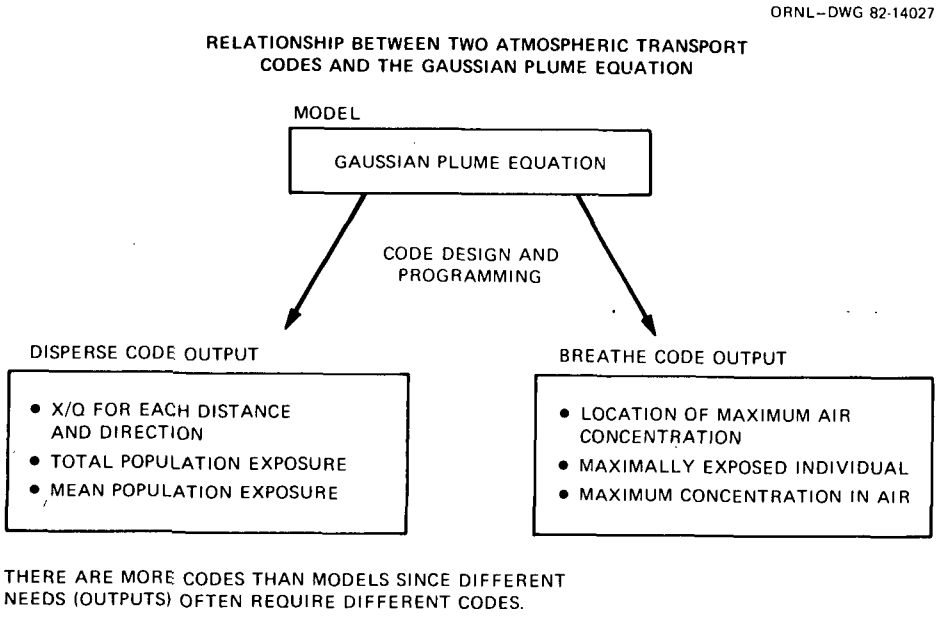

Figure 13.1. Relationship between two atmospheric transport codes (DISPERSE and BREATHE) and the Gaussian Plume equation.

The two codes produce different output and differ in language, machine of usage, and operating mode. Since the mathematics of a given model can be programmed in numerous ways to achieve the same result, there are likely to be many more codes than models. This is certainly the case.

One should not be confused into thinking that all computer codes are associated with models. Some codes are used for bookkeeping (i.e., efficient storage and easy retrieval of large amounts of data). To avoid confusion in this chapter, the following definitions and descriptions will apply: a model is an equation or series of equations or expressions that describe some process of interest; a computer code, or program, is a representation in computer language of some model; and a computer model is synonymous with a model that has been coded into a useful computer package.

13.3 IMPORTANT PROGRAM CHARACTERISTICS

Whether using an existing code or devising a new one, the programmer or user should bear in mind several characteristics. Some of these characteristics are so important as to preclude usability, whereas others merely facilitate use of a code or promote confidence in its use. As Kernighan and Plauger (1978) state in the preface to their excellent book *The Elements of Programming Style*:

> Good programming cannot be taught by preaching generalities. The way to learn to program well is by seeing, over and over, how real programs can be improved by the application of a few principles of good practice and a little common sense. Practice in critical reading leads to skill in rewriting, which in turns leads to better writing.

This chapter stops considerably short of teaching the reader how to program but examines instead some of the practices that constitute well-written programs and some facets of codes that make them more or less usable for a given environmental assessment problem. No matter what type of transport is being modeled, it is important that the code selected suit the application. For whatever reason—lack of resources, lack of alternatives, etc.—codes are often applied to situations for which they are not intended. In such situations, it should be the user, not the developer of the code/model, who bears the responsibility for inaccurate or misleading results.

13.3.1 Computer Language

The language in which a code is written is an important consideration when a new code is being developed or a program written elsewhere is being used.

Obviously, a code developed for one's own use or acquired from another site is constrained by the capabilities of the computer at the user's site. A code developed for users other than the author of the code should be written in a well-known language, or it may not be well accepted.

Numerous computer languages are available, and more are currently being devised. However, among scientific personnel, including those involved in environmental assessments, FORTRAN, introduced in 1956, is probably the most commonly utilized language. Most institutions where assessment codes are used or developed have access to a FORTRAN compiler on their computer system. Other languages that are relatively familiar and powerful enough for use with environmental assessment codes include BASIC, PL/1, PASCAL, and ALGOL. Most of these languages have energetic proponents and well-defined ranges of application. PL/1 was introduced in the 1960s as an all-purpose language which the designers hoped would replace FORTRAN and its business counterpart COBOL (McCracken 1974). It has replaced neither, but it is popular in some circles.

Each of these languages also has its own set of peculiarities and difficulties. BASIC, for example, is greatly limited in the length of variable names. This may seem trivial until one tries to program a problem with many variables; then, the name of the variable may not connote the sense of the variable as it might in FORTRAN. PL/1, PASCAL, and ALGOL, "whose control structures encourage a natural 'top-down' description of a program" (Conway and Gries 1975), are higher-level languages than FORTRAN IV. In most ways, PL/1 is less attractive than ALGOL or PASCAL, but it is also more widely used. However, none of the three is as commonly used as FORTRAN.

To complicate matters, there is more than one version of some languages (e.g., FORTRAN IV, FORTRAN FF; PL/1, PL/C). The different varieties of a language have come into existence as the technology progresses. Previous versions of a language may not be compatible with compilers designed for a newer version. For instance, some of the FORTRAN implementations vary in such traits as permissible size of number and the presence or absence of some operators, such as logical IF or mixed-mode arithmetic expressions (McCracken 1965). Later versions of FORTRAN (FORTRAN IV) will probably not operate on a FORTRAN II compiler (Hoffman et al. 1977), but it is less likely that problems will be encountered when a lower-order FORTRAN code is run on a higher-order compiler of the same language.

No matter what language is employed, one should try to anticipate any possible problems with the language of the code. This is true whether one is acquiring a code developed elsewhere or devising a new code.

13.3.2 Computer Type

Developers and users of codes should be aware of the type of machine for which a code was originally produced because a code written for one type of

machine may not run on another model of the same machine or one of different manufacture. For example, a program written for an International Business Machines (IBM) computer may not operate on a Control Data Corporation (CDC) machine or even on another IBM system. The reasons for computer incompatibility are not within the scope of this chapter; however, some specific incompatibilities will be listed.

For programs written in FORTRAN, some of the characteristics that may preclude proper execution of a program are given in Table 13.1. Although the list is somewhat dated, it gives an idea of the range of possible differences between machines. Differences not listed in the table include such things as disparate approaches to variable initialization, dissimilar job control statements, diverse treatments of machine language utility programs, contrasting methods of transmitting literal strings, and unmatched word length (McCracken 1965). Various incompatibilities exist for other languages, but these will not be explored here.

Table 13.1. Characteristics of FORTRAN that may vary between various manufacturer's computers

Must specification statement precede first executable statement?
Maximum statement identification number.
Maximum number of continuation cards.
INTEGER constant, maximum digits.
INTEGER, maximum magnitude.
REAL constant, maximum digits.
DOUBLE PRECISION constant, number digits.
REAL, double precision magnitude.
Variable name, maximum characters.
Mixed mode arithmetic permitted?
Assigned GO TO permitted?
Logical IF permitted?
DOUBLE PRECISION permitted?
COMPLEX operations permitted?
LOGICAL operations permitted?
Dimensional data in PRINT statements?
Labeled COMMON?
Maximum array dimensions.
Adjustable dimensions permitted?
Zero or negative subscripts permitted?
Subscripted variables allowed as subscripts?
Multiple entry into subroutines?
DATA statements allowed?
Object time FORMAT permitted?

Source: Adapted from McCracken, D. D. (1965). *A Guideline to FORTRAN IV Programming,* Wiley, New York.

Any two computers are likely to have many commonalities, and many differ in only a few of the listed characteristics. Also, some of these differences are more difficult to reconcile. For instance, if a code written for a CDC machine has 50 continuation cards for a particular FORTRAN statement (CDC has no limit), then a user wishing to run that code on an IBM machine would need to rewrite the offending statement into at least six separate statements because IBM allows only nine continuation cards per statement. Such a modification, although tedious, would not prevent the use of the code on an IBM machine.

Other disparities might not be so simple to correct. For some codes a problem may arise regarding the maximum number of digits allowed in a real constant, which may vary from as low as 7 to as high as 20. A code written for and operated successfully on a higher-capacity machine may occasionally fail to run on a lower-capacity machine simply because of the size of the numbers. Except for scaling down the entire problem, little can be done to remedy such a situation.

The best general advice for one wishing to use a code on a machine other than that for which it was written is to know both machines. The characteristics of the original machine and the new machine may not be radically different, and the code may be easily adaptable. If not, other codes to accomplish the same task may be available. Section 13.5 contains information about obtaining codes.

13.3.3 Code Size and Efficiency

Potential users or developers of codes should also consider the size of the code in terms of memory storage. Codes that require memory exceeding that provided by a user's computer system will be of little value. Depending on the size of the problem being coded, it may or may not be possible to decrease the size of a code substantially. The number of statements is not in itself an accurate indicator of the necessary core storage. This is especially true of comment cards, which are ignored in the "compile" and "load" steps of computer program execution (see also Sect. 13.3.4, "Mode of Code Operation").

A related quality, one more difficult to determine, is code efficiency. Computer run time is an important (but not the only) measure of efficiency, especially in this age of relatively cheap computer time. The time spent by code users is another important aspect of code efficiency. Both of these are discussed briefly below.

A commonly listed statistic is the running time in terms of central processing unit (CPU) seconds. Although not a direct indicator of efficiency, CPU time can be a helpful barometer when similar codes are compared. When using a code designed by another person, it is unlikely that one would wish to modify the statements within the code to attempt an increase in efficiency. As Kernighan and Plauger (1978) point out in their chapter on efficiency, unless the

inefficiency is extreme, "the programmer time needed to make a noticeable improvement in speed is certainly more valuable than a few minutes of machine 'time.'"

Someone wishing to modify an existing code or develop their own code would be well served to read Chapter 7, "Efficiency and Instrumentation," of Kernighan and Plauger (1978). The authors give a number of simple rules to follow with regard to efficiency when programming. Among their comments are several that are especially important in the context of environmental assessment models and codes. First, if a code does not work, its efficiency is unimportant. All codes should be verified and, if possible, validated (see Sect. 13.4). Second, in modifying existing codes, one should not sacrifice clarity and accuracy for supposed efficiency, especially when human time is considered. Finally, before coding for special cases, the user should verify that the cases are really special. This last caveat may be useful in environmental assessment codes that attempt to include many processes within a structure of various scenarios of release or exposure. An example of a truly special case is the calculation of ^{3}H concentration in foods by the specific activity model following an atmospheric release (see Chapter 9).

As stated above, a discussion of efficiency should include not only computer efficiency, but also efficiency in the use of human time. The most obvious case involves the input requirements of the code. An example will help illustrate the importance of this point. Consider two computer programs, code A and code B to calculate ground-level, centerline air concentrations using the Gaussian plume model.

Code A requires input of annual-average meteorological data in the form of a STAR (STability ARray) data set, as shown condensed (zeros removed) in Table 13.2. These data are easily attainable on cards or tape in the format shown from the Environmental Data Service of the National Climatic Center in Asheville, North Carolina. The full STAR data set consists of 96 cards, each of which has information for 1 of 16 compass directions and 1 of 6 stability categories. The data on each card are the frequencies for wind blowing in 6 wind speed categories; that is, in Table 13.2, the wind in stability class A was from the north, and wind speed was less than 1.5 m/s only 0.038% of the year.

Contrast code A input data with the input meteorology data set of code B shown in Table 13.3. This data set includes input of values for each of four variables on a total of 29 cards: DIRFRQ, the frequency the wind blows from each direction; RAVSPD, the reciprocal-averaged wind speed for each stability category and direction; TAVSPD, the true-averaged wind speed for each stability and direction; and STBFRQ, the fraction of time that the wind blows in each wind speed and direction.

A question arises: Which method of inputting the meteorological data is more efficient? In terms of computer time, code B is probably more efficient; only 304 values on 29 cards are read into the computer by code B, whereas

Table 13.2. Representation of a STAR data set of annual meteorology as used by code A

Direction	Stability	Fraction of year wind blows in given direction and stability class, by speed category (m/s)					
		<1.5	<3.1	<5.1	<8.2	<10.8	>10.8
N	A	0.00038	0.00021	0	0	0	0
NNE	A	0.00007	0.00014	0	0	0	0
NE	A	0.00015	0.00017	0	0	0	0
ENE	A	0.00005	0	0	0	0	0
E	A	0.00009	0.00007	0	0	0	0
ESE	A	0.00006	0.00010	0	0	0	0
SE	A	0.00007	0.00003	0	0	0	0
SSE	A	0.00004	0.00007	0	0	0	0
S	A	0.00013	0.00014	0	0	0	0
SSW	A	0.00006	0.00010	0	0	0	0
SW	A	0.00006	0.00010	0	0	0	0
WSW	A	0.00002	0.00003	0	0	0	0
W	A	0.00007	0.00003	0	0	0	0
WNW	A	0.00006	0.00010	0	0	0	0
NW	A	0.00011	0.00010	0	0	0	0
NNW	A	0.00011	0.00010	0	0	0	0
N	B	0.00072	0.00103	0.00051	0	0	0
NNE	B	0.00036	0.00069	0.00034	0	0	0
NE	B	0.00039	0.00065	0.00058	0	0	0
WNW	E	0	0.00130	0.00319	0	0	0
NW	E	0	0.00134	0.00202	0	0	0
NNW	E	0	0.00154	0.00202	0	0	0
N	F	0.00239	0.00284	0	0	0	0
NNE	F	0.00184	0.00147	0	0	0	0
NE	F	0.00284	0.00305	0	0	0	0
ENE	F	0.00198	0.00329	0	0	0	0
E	F	0.00159	0.00329	0	0	0	0
ESE	F	0.00138	0.00373	0	0	0	0
SE	F	0.00181	0.00264	0	0	0	0
SSE	F	0.00145	0.00370	0	0	0	0
S	F	0.00524	0.01576	0	0	0	0
SSW	F	0.00261	0.00695	0	0	0	0
SW	F	0.00178	0.00490	0	0	0	0
WSW	F	0.00171	0.00414	0	0	0	0
W	F	0.00134	0.00486	0	0	0	0
WNW	F	0.00088	0.00240	0	0	0	0
NW	F	0.00088	0.00271	0	0	0	0
NNW	F	0.00109	0.00253	0	0	0	0

Table 13.3. Card images for annual average meteorology data set for code B[a]

.0551.0226.0289.0394.0554.0629.0718.0596.0625.0363.0370.0462.0713.0838.0914.0552	DIRFRQ
1.1421.3711.4241.3381.2391.2441.3041.3141.2371.3111.3981.2711.3851.3621.2111.311	
1.3411.3551.5061.4981.5251.6921.6681.6301.5691.7581.7011.6911.4681.5211.5611.400	
2.3752.2512.5292.5082.6972.6732.6362.7142.8232.9203.0323.0382.7762.6962.6412.404	RAVSPD
2.9112.6062.3152.3532.3172.7432.9433.0892.8763.0763.4173.7993.6703.6733.4573.511	
2.8222.7032.7152.6782.6282.7112.9003.1163.1603.5833.1473.0553.3313.1433.0122.929	
1.2181.0881.2201.2061.1531.2311.2191.3661.4151.3611.3291.3621.3411.3241.3731.267	
1.6081.8821.9331.8491.7361.7431.8131.8231.7341.8191.9091.7741.8971.8731.7021.819	
2.1922.1742.3842.3752.4552.5532.5082.4612.4332.6832.5912.6092.3602.4542.4582.228	
3.4923.4033.5093.4633.5893.7153.6753.6513.7513.8774.0494.1353.9993.8243.7503.575	TAVSPD
4.4274.0903.5803.4763.3933.8984.1054.3204.1174.5474.9895.5955.5195.2424.8214.798	
2.9912.8232.8412.7862.7102.8353.0933.3513.3983.8003.3843.2813.5733.3803.2313.130	
1.7111.5261.7131.6951.6241.7261.7111.8771.9251.8721.8391.8731.8511.8341.8851.770	
0.0096 0.0934 0.1313 0.4246 0.1641 0.1770	
0.0150 0.1424 0.1129 0.4392 0.1424 0.1481	
0.0246 0.1411 0.1466 0.4032 0.1407 0.1438	
0.0109 0.1510 0.1868 0.4098 0.1115 0.1300	
0.0099 0.1170 0.1781 0.4709 0.1112 0.1130	
0.0107 0.0913 0.1606 0.5197 0.1067 0.1111	
0.0117 0.1012 0.1422 0.5578 0.0913 0.0958	
0.0104 0.0800 0.1244 0.5526 0.1068 0.1258	STBFRQ
0.0102 0.0917 0.1421 0.4588 0.1341 0.1632	
0.0099 0.0925 0.1559 0.4440 0.1457 0.1520	
0.0208 0.1305 0.2072 0.3884 0.1072 0.1459	
0.0089 0.0811 0.1649 0.3761 0.1211 0.2479	
0.0081 0.0688 0.1434 0.3956 0.1510 0.2330	
0.0080 0.0654 0.1465 0.3560 0.1547 0.2694	
0.0062 0.0619 0.1428 0.3929 0.1627 0.2335	
0.0065 0.0739 0.1208 0.4447 0.1552 0.1989	

[a]DIRFRQ = wind direction frequency (16 directions); RAVSRD = reciprocal-averaged wind speeds (6 stability categories, 16 directions); TAVSPD = true-averaged wind speeds (6 stability categories, 16 directions); STBFRQ = frequencies for each direction (6 stability categories, 16 directions).

code A reads 576 values from 96 cards. Code A also must manipulate the frequencies to calculate values for variables analogous to DIRFRQ, RAVSPD, TAVSPD, and STBFRQ in code B. However, in terms of human time, code A is much more efficient. The variables read in by code B were hand calculated from a STAR data set and then input to the code; the time required to calculate the values of the four variables in Table 13.3 by hand probably approaches one hour. Such a practice not only wastes staff time but also tends to introduce error into the input data set. The amount of computer time and money saved by such an input structure is small compared to the costs of having someone modify the STAR data set outside the computer. This example demonstrates that because computer time is inexpensive, it should be utilized whenever possible to lessen the potential for human error in operation of computer codes.

13.3.4 Mode of Code Operation

There are likely to be only two choices for the mode in which a code operates: conversational or batch. Both modes have distinct advantages.

Conversational codes prompt the user via statements in English (or other human language) written by the code onto a screen. In response to these prompts, the user supplies some necessary instructions or data. Table 13.4 reproduces part of a typical conversation between user and computer for a code calculating doses from radioactively contaminated drinking water.

The conversation presented in Table 13.4 illustrates some of the reasons why conversational codes are popular. For one thing, the code uses readily understandable phrases. For relatively uninitiated users, this is comforting. Data input, via response to the queries, may be accomplished by typing directly into a terminal, in some cases without concern for formatting the responses. In the illustrated conversation, the input formats for required information are indicated in the queries (e.g., E9.2, A5).

Drawbacks of the conversational mode are several. First, a conversational code for solving a problem probably uses more core storage space; and time of execution is longer because of the query statements. This is clear when one considers a conversational code as a program within a program. The problem-solving code might be similar for either the batch or conversational mode. In the latter case, the problem-solving portion is augmented by the prompting portion of the code, which assists with input/output decisions. This is illustrated by Table 13.5, which has sections from both a batch code and a conversational code to accomplish the same simple task. Both are written in FORTRAN. No job control language is included for either. The number of statements necessary to achieve the same outcome (inputting X and Y and adding to calculate Z) is much greater with the conversational code. In more complicated problems, the difference in length between the two styles is even greater.

A second drawback of some conversational codes is the necessity to repeat the same queries for each run of the code. Well-written conversational codes

Table 13.4. A typical set of prompts and responses from a conversational computer code that calculates doses from aquatic food chain transfers

```
    ENTER RELEASE IDENTIFICATION INFORMATION (14A5)
TEST CASE FOR MISSISSIPPI
    ENTER NUMBER (I5) OF NUCLIDES (20 MAX)
4
    ENTER NUCLIDE NAMES (A6 RIGHT JUSTIFIED)
   H-3
 SR-90
CS-134
PU-239
    ENTER INDIVIDUAL NUCLIDE RELEASE RATES (E9.2), MICROCURIES/CC
5.6E-11
3.5E-10
7.4E-10
2.2E-10
    ENTER FRACTION OF YEAR PERSON SUBMERGED IN WATER (E9.2)
0.25
    WISH TO MODIFY DRINKING WATER INTAKE RATE?
    ENTER Y FOR YES AND N FOR NO (A5)
Y
    ENTER NEW DRINKING WATER INTAKE RATE (E9.2, LITER/DAY)
1.5
    FRESHWATER OR MARINE BIOACCUMULATION FACTORS?
    ENTER F OR M (A5)
M
    WISH TO MODIFY INGESTION RATE?
    ENTER Y FOR YES AND N FOR NO (A5)
Y
    ENTER NEW INGESTION RATE (E9.2, G/DAY)
450.
    ANY OTHER CHANGES?
    ENTER Y FOR YES AND N FOR NO
N
    READY TO MAKE CALCULATIONS
```

Table 13.5. An example of two computer methods to accomplish the same task

```
                                  Conversational Method
001          TYPE 106
002          ACCEPT 108,(TITLE(I),I-1,14)
003          TYPE 116
004          ACCEPT 118,N
005          TYPE 120
006          ACCEPT 118,(IN(I),I=1,N)
007          TYPE 110
008          ACCEPT 112,(CI(I),I=1,N)
009          TYPE 111
010          ACCEPT 112, FY
011          TYPE 113
012          ACCEPT 124,AANS
013     106  FORMAT (5X, 'ENTER RELEASE IDENTIFICATION INFORMATION (14A5)')
014     108  FORMAT (14A5)
015     110  FORMAT (5X, 'ENTER INDIVIDUAL RADIONUCLIDE RELEASES (E9.2) IN
             &MICROCURIES/CM**3')
016     111  FORMAT (5X, 'ENTER FRACTION OF YEAR SUBMERGED IN WATER (E9.2)')
017     112  FORMAT (E9.2)
018     113  FORMAT (5X, 'WISH TO MODIFY DRINKING WATER INTAKE RATE?',/
             &,5X, 'ENTER Y FOR YES OR N FOR NO (A5)')
019     116  FORMAT (5X, 'ENTER NUMBER (I5) OF NUCLIDES (20 MAX)')
020     118  FORMAT (I5)
021     120  FORMAT (5X, 'ENTER NUCLIDE I.D. NUMBERS (I5)')
022     124  FORMAT (A5)

                                  Batch Method
001          READ (5,108) (TITLE(I),I=1,14)
002          READ (5,118) N
003          READ (5,118) (IN(I),I=1,N)
004          READ (5,112) (CI(I),I=1,N)
005          READ (5,112) FY
006          READ (5,124) AANS
007     108  FORMAT (14A5)
008     118  FORMAT (I5)
009     112  FORMAT (E9.2)
010     124  FORMAT (A5)
```

allow the user to request queries for only the variables that must be changed for that specific run. Such codes must include a default database that supplies the necessary data to solve the problem or must have in memory the data input for the previous run.

Regardless of how many queries must be answered during each run, the user of a conversational code may be required to wait for the final solution of the problem before changing conditions and running another problem. While this practice may not result in a large amount of wasted human time for each code run, it may be significant if numerous runs in conversational mode are required.

In some applications, codes may be run many times to estimate the relative importance to some output quantity by varying the values of chosen input parameters. In such situations, a code that operates in a batch mode may be more appropriate than a conversational one. Batch jobs may be run as often as the code can be read into the computer; therefore, many jobs may be submitted in a relatively short time. Long computer programs that are run strictly in the batch mode may be unwieldy, however. This is especialy true if the complete code source deck must be read into the computer as cards for each run of the code. Most substantial computer systems allow storage and referencing of the compiled source codes on disks or tapes. This method permits quicker resubmittal because only the data deck and a few job control cards need be input for each use of the code.

A common mode of operation at large institutions is the use of interactive job submittal. This method combines some of the desirable characteristics of both conversational and batch modes. An interactive system allows data and code manipulation by a computer to prepare a code to be run on the same or a more powerful computer. In this scheme, modifications via some editing system are done electronically as card images that are then forwarded to the larger computer for execution of the code. Such a method overcomes many of the drawbacks of either conversational or batch jobs but may be more intimidating than either mode to users unfamiliar with large computer systems.

13.3.5 Documentation

Documentation is one of the most important but least appreciated aspects of developing and using an environmental transport code. It is worse than worthless if wrong but precious if correct. Documentation can help the user to operate an environmental assessment code successfully. Documentation may also prevent or hinder the use of a code. Because it is tedious and troublesome, documentation of a code is less interesting than programming; but useful documentation is no less a challenge than useful programming.

This section describes some characteristics of good documentation and some of the forms it may take. Documentation should include a well-organized code structure, well-named variables, comments within the code, and an external report or user's manual.

At the outset of any discussion of documentation, it should be said that the only reliable description of the code is the code itself. This may seem to be an obvious point, but code users often forget that the documentation of a code may not be accurate. Discovering this fact may be very painful and time consuming.

Features of the code that may be helpful in furthering understanding are a well-organized code structure and meaningful variable names. Defining a well-organized structure is probably as difficult as programming one. Many users

find that a so-called "modular" code is relatively easy to understand. It consists of a relatively short main program that calls numerous specific-purpose subroutines. In such a scheme, all input statements are grouped into a single subroutine, as are output statements. Particular algorithms, equations, or subroutines may be replaced or updated fairly simply. The antithesis of a modular code would be a program having no subroutines and with input and output functions widely spaced throughout the code. Not all codes, particularly short codes, lend themselves to modular construction; but to the extent feasible, grouping input, output, and format statements will help make the code easier to understand and use.

Thoughtfully chosen variable names are another form of documentation that can ease the user's burden. Variable names that have some connotative meaning are better than names that do not. For instance, an atmospheric dispersion code might calculate the value of the annual-average dispersion coefficient χ/Q. If the statement is written $Z = Y/X$, little or no information is conveyed except that a new variable is being defined. If, however, the statement CHIQ = CHI/Q appears, the reader not only knows that CHIQ is being calculated, but also that information about the use of CHIQ is conveyed by the name.

One caveat: the ability of the programmer to create connotative variable names is limited by the length of name the language allows. Older forms of BASIC allow only two-digit variable names from A1 through Z9. PASCAL allows variable names as long as 32 characters, while FORTRAN may allow 6 or more depending on the implementation.

Another valuable form of code documentation is internal comment cards. Comments are nonprogram statements within the code that allow insertion of English wording for descriptive purposes. An example of valuable commenting is given in Table 13.6. The sample code is well-commented, and for many calculations the sources of the equations are identified. Unit conversions are also indicated. In this sample, the variable names are frequently connotative of the quantity being calculated, and they mimic the names used in the original model. Although this and most internal documentation can probably be improved, the sample in Table 13.6 gives several examples of good documentation. For a more detailed discussion of comments and internal documentation, see Chapter 8 of Kernighan and Plauger (1978).

Most code users probably associate documentation with a user's manual rather than with internal code comments. For many environmental assessment programs, the user's manual may be more important than the internal comments in understanding code operation. Although earlier comments about accuracy of documentation still apply, many environmental transport codes are large and diverse enough that they are very difficult to use without an external document to support the program. As a result, most of the codes listed in large compendia of environmental transport programs such as Mosier et al. (1980)

Table 13.6. Section of environmental assessment code to illustrate internal comment documentation

```
C CALCULATE MLKDOS(J)=ANNUAL DOSE TO ORGAN J FROM INGESTION OF
C RADIONUCLIDES IN MILK USING EQ C-13, REG GUIDE 1.109-28.
C
     IF (I1.NE.0.AND.REL(1,I).NE.0.) D4=F1M+F2M*(MAGCON(I)/
    1 (GCON(I,NO,NR)+RATUA*GCI))
     IF (I1.NE.0.AND.REL(1,I).NE.O.) D3=F1B+F2B*(BAGCON(I)/
    2 (GCON(I,NO,NR)+RATUA*GCI))
     MLKDOS(J)=DFIJ*UM*CIM*D4
C
C THE NRC MODEL GIVES DOSES IN MREM/YR. TO CONVERT TO REM/YR,
C MULTIPLY BY 0.001
C
     MLKDOS(J)=MLKDOS(J)*.001
C
C CALCULATE CIF=NUCLIDE CONCENTRATION IN MEAT USING EQ C-12,
C REG GUIDE 1.109
C
     CIF=FSUBFI*CIV*QSUBF*EXP(-LAMRR*TSUBS)
C
C CALCULATE BEFDOS(J)=ANNUAL DOSE TO ORGAN J FROM INGESTION OF
C RADIONUCLIDE I IN MEAT. (REG GUIDE 1.109-28, EQ C-13)
C
     BEFDOS(J)=DFIJ*UF*CIF*D3
     BEFDOS(J)=BEFDOS(J)*.001
C
C CALCULATE CIVP=CONCENTRATION OF RADIONUCLIDE IN PRODUCE CONSUMED
C BY MAN. USE PARAMETERS FOR CROP/VEGETATION-MAN PATHWAY, AND
C USE TSUBB FOR PRODUCE.
C
     TSUBE=TSUBE2
     YSUBV=YSUBV2
     TSUBH=TSUBH4
     BSUBV=BSUBV2
     DR=DD1
     MODE=1
     CALL RVALUE(IFLAG,MODE,I,NO,NR.R)
     CIVP=CV(I,LAMI,DEPRAT,GCRU,TSUBE,YSUBV,TSUBH,R)
```

and Owen et al. (1979) have not been used outside their founding institutions. In many cases, this is because they were poorly documented.

The best external documentation reports, or users's manuals, contain at least the following: theory of the model(s) used within the code, description of code structure, necessary job control language, a sample problem, and a code listing. Each of these is discussed briefly below.

The user's manual can explain the theory of model development and describe the selected equations better than internal commenting because the amount of internal commenting is limited, in a practical sense, to some fraction of the total code length. In contrast, the user's manual may trace the

development of each model coded and may identify specific subroutines or code sections as solving particular models. While the derivation of each code equation need not be included in the user's manual, enough information should be presented so that the reader understands what assumptions were made and why equations are included in the program.

The user's manual should also include a description of the structure of the program. If the code contains numerous subroutines, a table indicating which subroutines call each other and what variable quantities are calculated may be useful. A diagram that describes flow of information throughout the program may serve the same purpose. A discussion of the purpose and intended use of the code will be valuable to potential code users who are examining a program. It is also important that the structure of the input data file be clearly described in the user's manual. Examples of a format for describing input data are shown in Tables 13.7a and 13.7b. These two tables define the necessary variables for code operation and describe their placement within the input data deck. The information may be presented in a single large table or several smaller ones. It is paramount that the necessary data and their formats be identified for the user.

Manuals for codes developed at one institution for purposes of dissemination should have a description of the necessary job control language (JCL) and characteristic operating parameters. While the same JCL may not apply at another institution with the same or another type of computer, a JCL listing and description of its purpose will assist new users to installing the code on their computer system. A tabulation of characteristic core size requirements and run times may caution a user attempting to install too large a program and subsequently spending time and money in vain.

An extremely important part of any code manual is the sample problem. Briefly, a sample problem is an example run of the program, including the input data and the resultant output from the code. The sample problem serves two purposes. First, by examining the sample problem, a potential user can begin to grasp how the code operates and what its products may be. In the case of a conversational code, the sample problem may take the form of an example session between user and computer, complete with prompting statements and responses. Second, and more valuable, the sample problem functions as the check of code operations. If the user's code can generate the same output after reading the same input data, the program is working correctly. Two caveats should be mentioned: (1) Many environmental assessment codes contain several optional methods of calculation. In such a case, it is probably not feasible to include sample problems for each option. (2) As with the rest of the documentation, the sample problem is a potential source of error. If the author of the code attends to detail, the example problem can be very useful. However, if for some reason the example contains input or output for an incorrect or another version of the code, the illustration will be of little value.

Table 13.7a. Example of input parameter definitions

Name	Number of values	Definition	Units
NOL	1	Lower grid limit (abscissa)	
NOU	1	Upper grid limit (abscissa)	
NRL	1	Lower grid limit (ordinate)	
NRU	1	Upper grid limit (ordinate)	
PR	7	Specific plume rise for each Pasquill category	m
IDIST	20	Distances from plant to be used with circular option	m
LIDAI (L)	1	Height of lid	m
RR	1	Rainfall rate in area	cm/y
TA	1	Average air temperature in area	°K
TG	3	Vertical temperature gradient for Pasquill categories E, F, and G	°K/m
PERD	16	Wind direction frequency (16 directions)	

Table 13.7b. Example of card deck descriptions (format) from an environmental assessment code

Parameters	Number of values	Number of cards	Data type	Format
NOL, NOU, NRL, NRU	1 for each parameter	1	Integer	8I10
PR	7	1	Fixed point	8F10.0
IDIST	20	3	Integer	8I10
LIDA1	1	1	Integer	8I10
RR, TA, TG	1 for RR, 1 for TA, 3 for TG	1	Fixed point	8F10.0
PERD	16	1	Fixed point	16F5.0

Although somewhat bulky in the case of large codes, a complete program listing is often useful when placed in the user's manual. The listing may serve two primary purposes. First, because the code itself is the ultimate documentation, the listing will help to resolve any discrepancies or inaccuracies in the program description. Second, rather than transmit the program to other users via tape, disk, or cards, the code may be keypunched from the listing. In the case of large codes, this is not likely to be a satisfying method of transmittal

and will probably generate errors. Nevertheless, the listing may be of value. To save printing costs and paper, manuals for large assessment codes may include the code listing on microfiche, which are useful but less accessible than the printed page.

13.4 VERIFICATION AND VALIDATION

Very few terms in modeling spark as much debate as validation and verification. Although there seems to be no commonly accepted definition of the two words, there is agreement that both are important. The relationships may be clarified by examining Fig. 13.2.

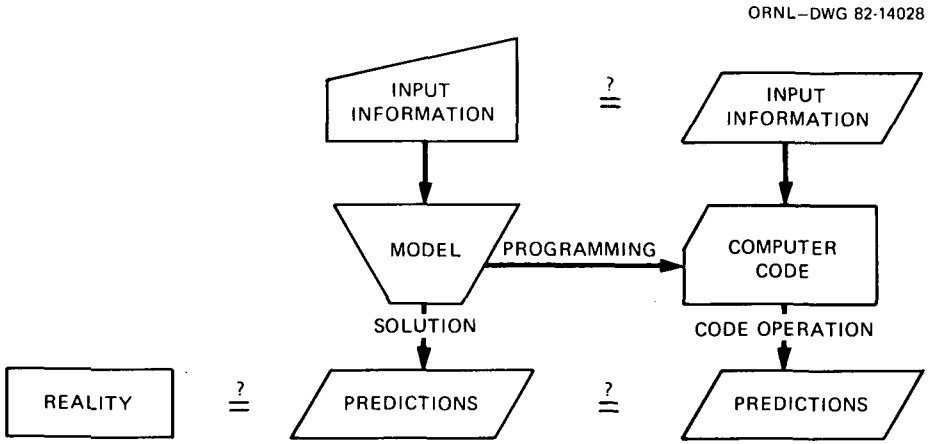

Figure 13.2. Relationship between model validation and code verification.

We begin with a model. The model can be used (solved) to generate predictions of some phenomenon of interest. If the model is reasonable and if we have appropriate input information, the model's predictions may adequately simulate reality. The process of comparing model predictions with reality is often considered model validation. When a model has been shown to produce reasonable results, it may be termed validated. Unfortunately, the determination of what are reasonable results varies from person to person and from one situation to another.

Particularly with environmental transport models, validation is probably a continuous process because of the variety of applications. For instance, results of the Gaussian plume model have been compared with field observations of several well-instrumented, flat sites with relatively simple meteorology. These comparisons indicate that the model often predicts the correct air concentrations within a factor of 2. For many uses, such a result means that the Gaus-

sian plume model has been validated. However, for other cases, the model may not be considered to be either useful or validated.

Validation should not be confused with calibration, which may also be known as "tuning" of the model. When calibrating a model, the researcher will make predictions and compare them with field data, then adjust the model and again compare the predictions with field data. This is a useful process for a model that will be used repeatedly for the same site or situation, but beyond the first model run, calibration may not provide useful information for other sites or applications.

But how does validation relate to verification? Referring back to Fig. 13.2, we see that a model may be translated into a computer code. The resulting code, when executed, should provide predictions that are similar to the model predictions. A code may be seen to be verified if, given the same inputs as the model, it produces the same predictions. Verification, then, simply indicates whether or not the code mimics the model, but has nothing to do with comparison to the real world. Therefore, verification and validation are not necessarily related. If a code is verified and the model on which it is based is validated, then the code should make reasonable predictions of reality. Lack of either validation or verification may render a code useless.

Verification may seem at first glance to be a relatively simple process. For some codes, especially those which are deterministic and analytic in nature, verification is merely a matter of time and effort. Using a hand calculator, one makes all the calculations that are made by the code. If the hand calculation gives the same results for the same inputs as the code, the code would be verified.

There are complicating factors, however. First, most hand calculators carry only about 10 decimal places, while many computers carry 16 or more. In a calculation, this difference in capability may noticeably affect the result of the hand calculation. It may help, when performing a verifying hand calculation, to use inputs that will result, if possible, in simple solutions.

The process of verifying that a code reproduces a model is more difficult when dealing with a model that is probabilistic or numerical. Probabilistic (or stochastic) codes are those that make choices of paths to follow or results to be calculated based on random choices within some statistical distribution, such as the normal distribution. Figure 13.3 compares the operation of a deterministic code with that of a probabilistic code and is based on the simple model $z = x + y$.

When using the deterministic code, one simply chooses values of x and y, and the code calculates a single output value of z. In a probabilistic code, the user chooses control parameters that specify the distribution of each variable (e.g., mean value and variance). The code then "samples" the distribution (of x and y) n times to generate a distribution of z. Using a calculator, the user can

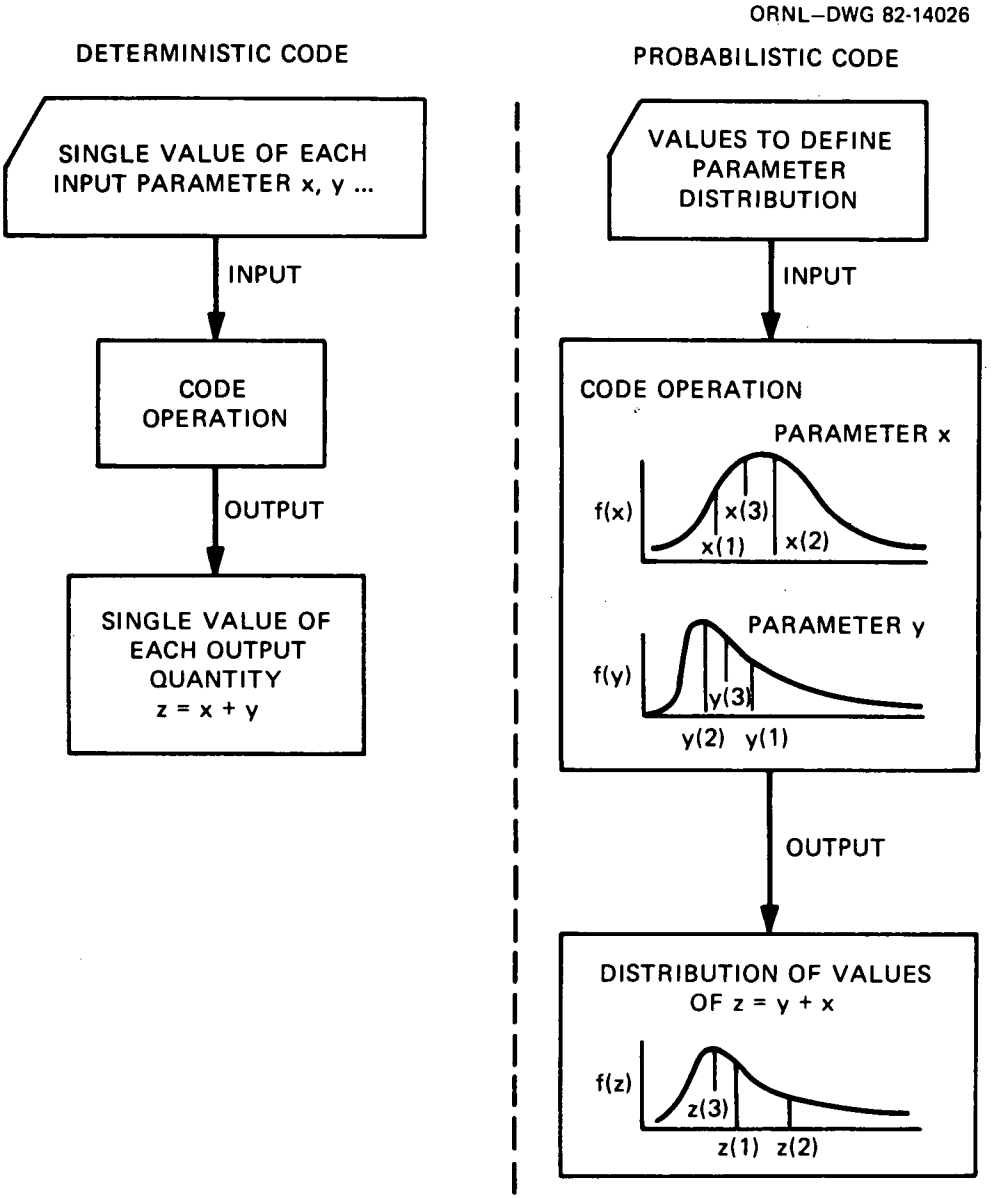

Figure 13.3. Comparison of a deterministic code and a probabilistic code.

easily verify that a deterministic code operates correctly, but it is difficult for a hand calculation to reproduce the choices that a probabilistic code might make. Therefore, such a code might be verified in separate parts, with all of the analytic sections reproduced by hand calculation. The probabilistic aspects of the code could then be assumed to be verified; this is a reasonable assumption, especially if the probabilistic subroutines or algorithms are from some reputable program library.

When a code contains numeric, as opposed to analytic, algorithms, verification must proceed much as for a stochastic code. Codes often contain a few special-purpose numeric sections, such as solving an integral, but may remain largely analytic. Verification of each part of the code could then proceed separately, with the numeric portions being verified by the original author or assumed verified after examination.

As one might expect, verification, though time consuming and tedious, is still more achievable than validation because validation deals with the model and verification deals with the code. While the code may be verified by comparing its predictions with those produced by the model, the model may only be validated by comparing its predictions with reality. This means one must either design and perform experiments to estimate a predictable quantity, or use the results of previous experiments for validation. Such experimental data are few in number, particularly for environmental transport models. Having found such suitable data and compared them with model output, one must still be aware that the model is not validated for other applications. Only after repeated validating exercises in various circumstances should a model be termed validated.

13.5 SOURCES OF CODES

There are two ways to obtain a computer code for a particular application. First, one can write it, in which case one may be more or less interested in some of the previous topics. In particular, the author of a code will need to decide which of the many available models is best suited to the problem. Questions of documentation, verification, and validation will need to be addressed, as well as appropriate tailoring of the output.

The second alternative is to use a code designed and published by someone else. There are hundreds of such codes designed for various environmental assessment applications. This section briefly describes the sources of information about environmental transport and sources of the codes themselves.

Information about the numerous environmental transport codes can be found in several documents published in recent years. Reports by Owen et al. (1979) and Mosier et al. (1980) are examples of compendia published with particular goals in mind (i.e., environmental impact and low-level radioactive waste management respectively). The report by Owen et al. lists information in up to 31 different categories for each of 821 models. Information categories

include the model title and acronym; the name, address, organization, and telephone number of the contact person; and selected information about computerization. A complete list of information categories listed by Owen et al. (1979) is shown in Table 13.8. Owen et al. also include indices for contact persons, titles, model acronyms, and keywords to assist their readers to locate suitable codes. Additionally, the models are grouped into 15 categories of subjects, including atmospheric transport, aquatic transport, soil transport, and food chains.

The report by Mosier et al. (1980) is, in some respects, similar to that by Owen et al. but includes far fewer codes and less information for each code. Many of the programs listed by Mosier et al. are also included in the report by Owen et al., but a few are not. Information fields given for each code are the model name or acronym, its purpose, a short description, a contact person, and

Table 13.8. Data fields used by Owen et al. (1979) to describe environmental impact models

<CONT>	Contact person for questions concerning model
<TITLE>	Name of model or title of model documentation
<ACRO>	Acronym of model
<ADDR>	Contact person's mailing address and organizational affiliation
<CITY>	City where organization is located
<STATE>	State where organization is located
<ZIP>	Zip code of organization
<COUNTRY>	Country where organization is located
<PHONE>	Telephone number of contact person
<SOURCE>	Name of person or institution from which documentation is available
<DOC>	Bibliographic citation of documentation or references relating to model
<SUB>	Brief statement of general subject coverage of model
<ABST>	Brief description of model
<GEO>	Geographical area to which model applies
<TIME>	Time span of data utilized
<STATUS>	Status of model
<MEDIA>	Type of media employed
<SIZE>	Indication of size of model
<COMP>	Abbreviation of computer manufacturer
<CONFIG>	Minimum hardware configuration necessary to execute model
<LANG>	Software language or data base management system utilized by the model
<CHAR>	Character set used by model
<ALGO>	General statement of algorithms, computational methods, or theories used
<CLAS>	Descriptive model classifications
<APPL>	General problem area to which model can be applied
<USERS>	Organizations using model (1979)
<SMD>	Source(s) of data utilized by model
<MVAL>	Model validation methods, sensitivity analysis, or other related procedures
<COM>	Additional comments not stated above
<UPDATE>	Date information was input last entered

references for the code. Codes are listed in the following categories: groundwater transport, soil transport, surface water transport, and other low-level waste models.

Several other published reports either compile, review, or tabulate codes designed for a particular purpose. Winton (1969, 1971, and 1974) compiled codes for dealing with analyses of nuclear accidents; however, very few of the programs compiled by Winton include environmental transport or dosimetry of radionuclides.

Strenge, Watson, and Droppo (1976) published a more detailed review of 32 dosimetry and environmental transport codes, most of which were designed for atmospheric release simulations. For each code surveyed, the language, computer of origin, pathways of transport, and exposure modes were tabulated. Further, operating experience for each acquired code was described briefly, with special notation for potential problem areas.

Hoffman et al. (1977) published a compilation of 83 computer codes for assessment of radiological consequences of discharge from nuclear facilities. This compendium listed models of atmospheric transport, surface water transport, and food chain transfer. Computer characteristics and an evaluation of the status of code documentation were included for each program listed. The processes for which calculations were made were also listed for each code.

Onishi et al. (1981) authored a critical review of about 70 surface water transport codes. The models they reviewed included processes for dissolved pollutant transport, sediment transport, water quality, and radionuclide adsorption/desorption processes. The level of detail of this work is much greater than that found in the other reviews mentioned above. The report investigates not only the models, but also the information necessary to support and establish the parameters for the codes; in particular, data that influence the estimation of adsorption/desorption mechanisms and the distribution coefficient k_d are reviewed in detail.

Other reviews and compilations of transport models have also been published. A bibliography of such reports is included in Appendix A of this chapter.

In addition to published sources of information about existing codes, there are several formalized, institutional sources of codes, code documentation, or code descriptions. The International Clearinghouse for Groundwater Models, which is housed at the Holcomb Research Institute on the campus of Butler University, Indianapolis, Indiana, provides facilities for holding seminars and workshops, furnishes consulting services, and maintains a Model Annotation Retrieval Service (MARS). The MARS system indexes nearly 400 groundwater models by such characteristics as aquifer conditions, fluid conditions, model processes, solution technique, geometry, etc. Output from MARS to a requestor includes a description of all models that meet the requestor's needs and the address of a custodian of the code. A full address of the clearinghouse is included in Appendix B of this chapter.

Two other excellent sources of both codes and documentation are the National Energy Software Center (NESC) located at Argonne National Laboratory, Argonne, Illinois, and the Radiation Shielding Information Center (RSIC), located at Oak Ridge National Laboratory, Oak Ridge, Tennessee. In contrast to the information provided by MARS, both NESC and RSIC provide not only information on available codes but also full documentation and copies of the code source decks or code tapes.

The RSIC was established in 1962 by the U.S. Atomic Energy Commission to collect and maintain radiation shielding codes. The NESC was established to handle all other types of codes, including environmental transport codes. In recent years, RSIC, supported by the U.S. Department of Energy (DOE), U.S. Defense Nuclear Agency, and the U.S. Nuclear Regulatory Commission (NRC), has expanded its scope to include environmental transport, resulting in an overlap between the code inventories of the two centers.

In general, NESC and RSIC work in the same manner to supply codes to users. A potential user should contact the centers listed in Appendix B of this chapter for detailed information about using their services. The potential user can request a listing of the available codes and hopefully find a code that meets his/her needs. If a suitable code is found, the software package can be requested that includes all the elements necessary to use the software or to implement the code on a computer. The software package includes both documentation and the source code on some computer medium such as cards or tape. An important difference between NESC and RSIC is that the latter will provide codes to virtually any user, private or public, for no fee, although a requestor is asked to provide a tape on which the code can be written. NESC charges a subscription fee for nongovernment agencies and for writing the tapes and preparing the package, with costs varying from package to package.

Services provided by RSIC include: (1) a monthly newsletter; (2) packaging and distribution of digital computer codes; (3) packaging and distribution of computer-readable data libraries useful for radiation transport calculations; (4) specific literature searches of the RSIC information retrieval system; (5) publication of reports on special topics; and (6) sponsorship of seminars or workshops related to computer codes or other topics.

NESC, supported by both DOE and NRC, provides many of the same services as RSIC, but the scope of software dealt with by NESC is larger than that handled by RSIC. Both centers check their code packages before distribution to make certain that they operate as described by the documentation. NESC may also summarize existing software not included in their collection or may assist a user in obtaining a needed code from commercial sources. More detailed information on both centers may be obtained by contacting these centers (see Appendix B of this chapter for addresses).

13.6 PATHWAYS OR PROCESSES MODELED BY SELECTED CODES

Four major types of codes may be found in the environmental assessment literature: atmospheric transport codes, surface water transport codes, groundwater codes, and food chain codes. In existing programs, there are numerous combinations of these four types of codes. Additionally, a few codes include all of these pathways of transport to humans. The following four sections will examine the types of pathways one might expect to find in each of these four types of codes. Examples of each type are given so that interested readers may acquire and examine the programs. This listing is neither exhaustive nor an endorsement of the tabulated codes but merely serves as an example of the variety of codes and pathway combinations available.

13.6.1 Atmospheric Transport

Published codes for atmospheric transport calculations usually are implementations of one of three types of dispersion models: Gaussian plume model, trajectory model, or particle-in-cell model. Of the three, the Gaussian plume model is by far the most common because of its simplicity, relative ease of implementation, and relatively small input data requirements. Each of these three is implemented by at least one code listed in Table 13.9.

Regardless of the model used to estimate transport of materials in air from a source to some receptor, there are processes besides dispersion that may be of importance in given situations to which the programs are applied. If particulate materials are contained in the effluent releases (source term), the effect of deposition may be accounted for in the code. Deposition refers to the accelerated accumulation of suspended materials onto receptor surfaces as a result of gravity, etc; and it is often accounted for by using a deposition velocity or fractional rate. Deposition may be either wet or dry, and separate computational schemes are used for each type.

Once material has been deposited onto a receptor surface such as the ground, it may be resuspended by turbulent air and be redeposited further downwind. Although this may be an important mode of transport, particularly of materials that attach to soil particles in arid climates, few atmospheric transport codes include resuspension computations. This is not surprising given the high site-specificity of the process and empirical nature of most of the existing models of resuspension (Anspaugh et al. 1975; Healy 1980; Healy 1981).

Two other attributes to consider in programs of atmospheric transport are the type of grid and the downwind range. Either a Cartesian or a polar grid is employed in codes of atmospheric dispersion; both may be available, and the choice of which grid to employ is left to the code user. The range of downwind distance may also influence which code is used for a given application. Many codes are intended for use at distances of 100 km or less, although the distances may be changed by the user. Codes of the Gaussian plume model prob-

Table 13.9. A listing of atmospheric transport codes and their characteristics

Code	Release Type[a]	Model Type[b]	Deposition		External Dosimetry		Terrrestrial Foods	Human Behavior	Internal Dosimetry		Computerization				Reference
			Wet	Dry	Air Exposure	Ground Exposure			Inhalation	Ingestion	Language	Computer[c]	Documentation	Sample Problem	
ACRA-II	A	GP	•	•	•				•		FORTRAN	IBM	Partial	•	Stallman and Kam 1973; McGill et al., 1976
ADPIC	A, R	PC									FORTRAN	CDC	Partial		Lange 1973
AIRDOS-EPA	R	GP	•	•	•	•	•	•	•	•	FORTRAN	IBM	Extensive	•	Moore et al. 1979
COMRADEX I, II, III	A	GP			•				•		FORTRAN		Extensive	•	Willis et al. 1970; Specht et al. 1975; Otter and Conners 1975
DWNWND	R	GP		•							FORTRAN	IBM	Extensive	•	Fields and Miller 1980
EXDOSE	A	GP		•	•						FORTRAN		Extensive	•	Hendrickson 1966
GADOSE/DOSET	A		•	•	•			•	•		FORTRAN	CDC	Sparse	•	Lee et al. 1966
GRONK	R	GP	•	•			•	•	•	•	BASIC	CDC	Extensive	•	Soldat et al. 1974
Heffter et al.	A, R	T	•	•									Partial		Heffter et al. 1975
HERMES	R	GP	•	•	•	•	•	•	•	•	FORTRAN	CDC	Extensive		Fletcher and Dotson 1971; Soldat 1971
INDOS2	A, R		•	•					•				Sparse		Thykier-Nielsen 1974
INREC	A, R				•				•		FORTRAN	IBM	Extensive	•	MacKay and Ely 1974
ISOLA II	R	GP			•						FORTRAN		Partial	•	Hübschmann and Nagel 1975
ISCLT	R	GP	•	•							FORTRAN	UNI	Extensive	•	Bowers, Bjorklund, and Cheney 1979
RSAC-2	A, R	GP	•	•	•	•			•		FORTRAN	IBM	Sparse		Wenzel 1974
SEP	A, R										FORTRAN	IBM	Partial		Sagendorf 1974
STAREL	R	GP									FORTRAN	IBM	Extensive	•	Binford et al. 1970
SUBDOSA	A	GP			•							CDC	Extensive	•	Strenge et al. 1975
TIRION	A	GP		•		•	•		•		FORTRAN	ICL	Partial	•	Kaiser 1976
WEERIE	A, R	GP		•	•				•		FORTRAN	IBM	Partial		Clarke 1973

[a] A = accidental; R = routine or chronic.
[b] GP = Gaussian plume; PC = particle in cell; T = trajectory.
[c] CDC = Control Data Corporation; IBM = International Business Machines; ICL = Risley ICL 4-72; UNI = Univac.

ably fall into this category. Codes that incorporate other models, such as a long-term trajectory or particle-in-cell models, would be more suitable to regional applications.

Some atmospheric codes include external dosimetry calculations from immersion in contaminated air or exposure to contaminated surfaces. For air exposures to beta radiation, virtually all existing codes consider the contaminant cloud to be infinite or semi-infinite; many codes assume the cloud to be finite for photon doses. Codes that include ground exposure calculations usually assume the contaminated surface to be a flat plane of infinite extent.

Some existing atmospheric transport codes include some calculations of radionuclide transport through terrestrial food chains following direct deposition onto plant surfaces or deposition onto soil surfaces and subsequent uptake into plant roots and upward. Some of these codes may include information about human dietary and behavioral factors to calculate internal doses from radionuclides received through the food chain. Internal doses from inhalation of the contaminated plume by a human receptor may be calculated with an atmospheric transport code. Existing codes generally use dose conversion factors for both inhalation and ingestion that derive from recommendations made by the International Commission on Radiological Protection (ICRP 1959; ICRP 1966; ICRP 1968; ICRP 1971).

13.6.2 Surface Water Transport

The complexity of methods of calculating a concentration of radionuclides in a stream or river some distance downstream from a release point ranges from a simple dilution factor to solving the convection/dispersion equation. The latter case may be for one, two, or three dimensions. Two-dimensional transport models may be either longitudinal-transverse or longitudinal-vertical depending on the application. Table 13.10 lists some of the many available surface water codes with some of their characteristics.

Some existing surface water codes have provisions for the calculation of particulate transport, which may include sediment transport, particulate pollutant transport, and contaminated sediment transport. These phenomena are more complex than solute transport, the movement of dissolved materials in flowing water. In most of the codes, the solute is considered to be conservative (i.e., nonreactive); but some codes may calculate chemical reactions that occur between the materials and the water as they flow downstream.

Again, the problem to which a surface water code is to be applied should be the prime determining factor in the number of dimensions and complexity of the code. The more dimensions, the more data that are needed to drive the code. Particulate transport requires specification of particle sizes and associated functions that are not necessary for solute transport alone.

Table 13.10. A listing of surface water codes and their characteristics

Code/Authors	Release Type[a]	Dimensions		Particulate Transport	Solute Transport	Time Dependence[b]	Solution Techniques[c]	Irrigation	Food Chains	Human Dietary Habits	External Dosimetry		Drinking Water	Computerization			
		1	2								Shoreline	Submersion		Language	Computer[d]	Documentation	Sample Problem
AQUAMAN (Shaeffer and Etnier 1979)	R					SS			•	•		•	•	FORTRAN	PDP	Extensive	•
Armstrong and Gloyna 1968	A, R	•				D	FD							FORTRAN	CDC	Partial	
AARG (Soldat et al. 1974)	R					SS				•	•	•	•	BASIC	UNI	Extensive	•
CARDOCC (Watts 1976)	R	•			•	SS			•	•			•	FORTRAN	IBM	Partial	
CHNSED (Fields 1976a)	R	•		•	•	SS	FD							FORTRAN	IBM	Extensive	•
COLHEAT (Daniels et al. 1970)	A, R	•			•	D										Sparse	
FETRA (Onishi et al. 1976)	A, R		•		•	D, SS	FE							FORTRAN	CDC	Partial	
HERMES (Fletcher and Dotson 1971; Soldat 1971)	R	•			•	D	FD	•	•	•	•	•	•	FORTRAN	UNI	Extensive	
LADTAP II (Simpson and McGill 1980)	R		•		•	D, SS		•	•	•	•	•	•	FORTRAN	IBM/CDC	Extensive	•
LINSED (Fields 1976b)	R	•		•		D	FD							FORTRAN	IBM	Partial	•
RVRDOS (Onishi et al. 1976)	A, R	•			•	D			•	•			•	FORTRAN		Partial	•
SERATRA (Onishi et al. 1976)	A, R		•	•	•	D	FE							FORTRAN	CDC	Partial	•
Shih and Gloyna 1967	A, R	•			•	D	A							FORTRAN	CDC	Partial	

[a] R = routine; A = accidental.
[b] SS = steady state; D = dynamic.
[c] FD = finite difference; FE = finite element; A = analytical.
[d] CDC = Control Data Corporation; IBM = International Business Machines; PDP = Digital Equipment Corporation; UNI = Univac.

As with atmospheric transport codes, a surface water code may include calculations of radiological dose via the human food chain. It may include appropriate bioaccumulation of radioactivity in fish eaten by humans or may allow contaminated irrigation water to be ingested by humans or to enter the terrestrial food chain. External doses to humans, which may occur during swimming in contaminated water or by exposure to shorelines contaminated by such water, may also be included in a suface water code.

In the case of more complex surface water codes (e.g., two-dimensional transport simulation), there is no simple analytical solution to the partial differential equations that represent convection and dispersion. In such cases, the solution must be approximated by some numerical method within the code. The two most common numerical methods for surface water flow problems are the finite-difference (FD) and the finite-element (FE) methods. The FD method is relatively easy to program because FD spatial grids are rectangular and often regularly spaced. Such codes are usually relatively short in length. The FE method is more difficult to program because the spatial grid that represents the flow field is composed of irregularly shaped boxes of three or more sides. In terms important to a code user, the FD method is easier to input, probably more efficient to run on the computer, but not as accurate for transport problems. When compared with the FD method, the FE method has the added advantage of having more flexible boundary conditions. Nevertheless, both methods are suitable for many applications.

13.6.3 Groundwater Transport

Several programs that address transport of materials through an aquifer are listed in Table 13.11. Methods of simulating flow of water and transport of pollutants through aquifers may range from very simplistic to very complex. In the simplest approach to groundwater transport, the modeler assumes (1) that no dispersion occurs as the materials are transported from their point of entry into the aquifer and (2) that the transport velocity is known and constant. More complex approaches may assume net convection (transport) in one direction but dispersion in all three dimensions. Further, the dispersion or velocity of transport may vary through both time and space. Many existing groundwater codes are designed only for estimating flows for the purpose of calculating aquifer usage. Fewer codes are designed to predict the transport of pollutants away from some source, and most of these codes assume the pollutant is nonreactive.

In the above paragraph and in Table 13.11, the transport medium being considered was constantly saturated with water. However, saturated conditions may be an unrealistic assumption for some modeling applications (e.g., shallow land disposal of low-level radioactive waste at an arid site with a deep aquifer). For this reason, a few codes have been developed to model flow and subsequent transport through soil zones variably saturated with moisture. Modeling water

Table 13.11. A listing of selected groundwater codes and their characteristics[a]

Code/Authors[a]	Groundwater Flow	Solute Transport	Heat Transport	Dimensions			Conditions		Computerization			
				1	2	3	Saturated	Unsaturated	Solution Technique[b]	Data Preparation[c]	Documentation	Sample Problem
BURYIT (Lester et al. 1981)	*	*		*			*	*	FD	M	Extensive	*
CCC (Mangold, Lippman, and Bodvarsoon 1980)	*	*	*	*			*		FD	M	Extensive	*
Cole and Gupta 1979	*					*	*		FE		Partial	
DPRWGW (Ahlstrom and Foote 1976)	*	*							FE		Partial	
Duguid and Reeves 1976	*	*				*	*	*	FE	M	Partial	*
CARD2 (Rosinger and Tremaine 1980)		*		*		*	*		A	E	Extensive	*
HERMES (Fletcher and Dotson 1971; Soldat 1971)		*				*	*			M	Partial	
INTERCOMP 1976	*	*	*		*	*	*		FD	D	Extensive	*
Konikow and Bredehoeft 1978	*	*			*		*		FD, MC	M	Extensive	*
Larson and Reeves 1976	*	*		*				*	A	M	Extensive	*
Prickett and Lonnquist 1976	*				*	*	*		FD	E	Extensive	*
SWIFT (Dillon, Lantz, and Pahwa 1978)	*	*			*		*		FD	E	Extensive	*
Trescott and Larson 1975	*		*		*		*		FD	M	Extensive	*
Trescott, Pinder and Larson 1976	*			*			*		FD	E	Extensive	*

[a]Partially adapted from Faust and Mercer (personal communication).
[b]A = analytic solution; FD = finite difference; FE = finite element; MC = method of characteristics (particle-in-cell).
[c]D = difficult; E = easy; M = moderately difficult.

behavior in these regions is "a very difficult mathematical problem" (Larson and Reeves 1976) that must be confined to a small-scale, physics-based approach limited by both the core storage and time capacity of the computer.

Only the simpler groundwater flow codes are amenable to analytic solutions of the equations. Most two-dimensional transport and flow systems are not suited to analytical solutions and must be approximated numerically. The most common numerical method in groundwater codes seems to be the FE and FD methods.

In certain applications (e.g., burial of radioactive waste), the groundwater code may include provisions for calculating entry of radionuclides into the food chain via irrigation or drinking water from a well in the aquifer. Such formulations, with some modification, may be useful for assessments of areas around waste repositories or even chemical dumps.

Input data requirements increase with code complexity. In some simpler codes, an important flow parameter is water velocity (length/time). This constant value may be input once and used in conjunction with the length of the path to calculate the time it takes for buried radionuclides to reach a potable well. In contrast, the important aquifer parameters for a more complex code may include the hydraulic conductivity (length/time), depth to the aquifer, storage coefficient, and specific yield for each node in the FD or FE grid. Before acquiring a large code, a user should examine the documentation to determine whether or not the required data will be available for the specific application in question.

13.6.4 Food Chain Transfer

Most existing food chain codes are programmed in conjunction with codes of some specific pathway of transport (e.g., atmospheric transport, surface water transport); that is, few stand-alone food chain codes exist. Most terrestrial food chain codes are programmed in conjunction with atmospheric transport codes. Historically, this is so because atmospheric releases from nuclear facilities were seen as the most likely source of radionuclide entry of into the terrestrial food chain. Hence, many atmospheric dispersion codes have provisions for calculating radionuclide concentrations in foodstuffs following their transport downwind. Similarly, there are few aquatic food chain codes that are not associated with some program of aquatic dispersion or transport. Some existing codes include provisions for calculating food chain transfers associated with irrigation with contaminated water.

Many existing terrestrial food chain codes are based on the assumption that the transfers between compartments (the transfer coefficients), such as from soil to plants, are constant through time (see Chapter 5). These are sometimes known as steady-state or equilibrium models and are intended for chronic release situations, not accidents. One such model is presented in the NRC Regulatory Guide 1.109 (USNRC 1977). Recently, several codes have been

developed that supposedly are more dynamic than steady-state, constant-deposition food chain codes (e.g., Simmonds, Linsley, and Jones 1979; Pleasant, McDowell-Boyer, and Killough 1981). These codes, and perhaps others, allow the inclusion of time-dependent, rather than constant, transfer coefficients. This distinction equips these codes for use in acute-release, or accident, scenarios if the appropriate deposition pulses are available.

13.7 PROBLEMS

1. Discuss additional advantages or disadvantages between batch and conversational codes.
2. Design a verification exercise for any atmospheric dispersion code.
3. Design a validation experiment for an environmental transport code.
4. Compare the input file structures of ISCLT and AIRDOS-EPA (Table 13.9). Which is simpler and more efficient?
5. Repeat problem 4 using two food chain codes or surface water dispersion codes.
6. Discuss additional reasons why so many codes exist in the literature.

REFERENCES

Anspaugh, L. R., Shinn, J. H., Phelps, P. L., and Kennedy, N. C. 1975. "Resuspension and Redistribution of Plutonium in Soils," *Health Phys.* **29**, 571–82.

Armstrong, N. E., and Gloyne, E. F. 1968. *Radioactive Transport in Water. Numerical Solutions of Radionuclide Transport Equations and Role of Plants in SR-85 Transport,* EHE-12-6703, Austin, Texas.

Binford, F. T., Hamrick, T. P., and Cope, B. H. 1970. *Some Techniques for Estimating the Results of the Emission of Radioactive Effluent from ORNL Stacks,* ORNL/TM-3187, Union Carbide Corp., Nuclear Div., Oak Ridge Natl. Lab.

Bowers, J. F., Bjorklund, J. B., and Cheney, C. S. 1979. *Industrial Source Complex (ISC) Dispersion Model User's Guide,* EPA-45014-79-030, H. E. Cramer Co., Salt Lake City.

Clarke, R. H. 1973. "The WEERIE Program for Assessing the Radiological Consequences of Airborne Effluents from Nuclear Installations," *Health Phys.* **25**, 267–80.

Cole, C. R., and Gupta, S. K. 1979. *A Brief Description of Three-Dimensional Finite Element Ground-Water Flow Model Adapted for Waste Isolation Safety Assessments,* PNL-2652, Battelle Pacific Northwest Labs., Richland, Wash.

Conway, R., and Gries, D. 1975. *An Introduction to Programming: A Structural Approach Using PL/1 and PL/C-7,* Winthrop Publishers, Cambridge, Mass.

Daniels, D. G., Sonnichsen, J. C., and Jakes, R. T. 1970. *The Estuarine Version of the COLHEAT Digital Simulation Model,* BNWL-1342, Battelle-Northwest, Richland, Wash.

Dillon, R. T., Lantz, R. B., and Pahwa, S. B. 1978. *Risk Methodology for Geologic Disposal of Radioactive Waste: The Sandia Waste Isolation Flow and Transport (SWIFT) Model,* SAND78-1267, Sandia Labs., Albuquerque, N.Mex.

Duguid, J. O., and Reeves, M. 1976. *Material Transport through Porous Media: A Finite-Element Galerkin Model,* ORNL-4928, Union Carbide Corp., Nuclear Div., Oak Ridge Natl. Lab.

Faust, C. and Mercer, J. W., GEOTRANS, INC., Herndon, Va., personal communication.

Fields, D. E. 1976a. *CHNSED—Simulation of Sediment and Trace Contaminant Transport with Sediment/Contamination Interaction,* ORNL/NSF/EATC-19, Union Carbide Corp., Nuclear Div., Oak Ridge Natl. Lab.

Fields, D. E. 1976b. *LINSED—A One Dimensional Multireach Sediment Transport Model,* ORNL/CSD-15, Union Carbide Corp., Nuclear Div., Oak Ridge Natl. Lab.

Fields, D. E., and Miller, C. W. 1980. *User's Manual for DWNWND—An Interactive Gaussian Plume Atmospheric Transport Model with Eight Dispersion Paramerer Options,* ORNL/TM-6874, Union Carbide Corp., Nuclear Div., Oak Ridge Natl. Lab.

Fletcher, J. F., and Dotson, W. L., comps. 1971. *HERMES—A Digital Computer Code for Estimating Regional Radiological Effects from the Nuclear Power Industry,* HEDL-TME-71-168, Hanford Engineering Dev. Lab., Richland, Wash.

Healy, J. W. 1980. "Review of Resuspension Models," pp. 209–35 in *Transuranic Elements in the Environment,* DOE/TIC-22800, ed. W. C. Hanson, Tech. Inf. Cent., U.S. DOE, Oak Ridge, Tenn.

Healy, J. W. 1981. "An Overview of Resuspension Models: Application to Low-Level Waste Management," pp. 273–82 in *Modeling and Low-Level Waste Management: An Interagency Workshop,* ORO-821, comp. C. A. Little and L. E. Stratton, Natl. Tech. Inf. Serv., Springfield, Va.

Heffter, J. L., Taylor, A. D., and Ferber, G. J. 1975. *A Regional-Continental Scale Transport, Diffusion and Deposition Model,* NOAA Technical Memorandum ERL ARL-50, Air Resour. Labs., Silver Spring, Md.

Hendrickson, M. M. 1968. *A Computer Program for Calculating the External Gamma Dose from Airborne Fission Products,* BNWL-811, Battelle-Northwest, Richland, Wash.

Hoffman, F. O., Miller, C. W., Shaeffer, D. L., Garten, C. T., Jr., Shor, R. W., and Ensminger, J. T. 1977. *A Compilation of Documented Computer Codes Applicable to Environmental Assessment of Radioactivity Releases,* ORNL/TM-5830, Union Carbide Corp., Nuclear Div., Oak Ridge Natl. Lab.

Hübschmann, W., and Nagel, D. 1975. *ISOLA II—A FORTRAN IV Code for the Calculation of the Long-Term Alpha and Beta Dose Distributions in the Vicinity of Nuclear Installations,* ORNL-tr-4295, Union Carbide Corp., Nuclear Div., Oak Ridge Natl. Lab.

International Commission on Radiological Protection (ICRP) 1959. *Report on Committee 2 on Permissible Dose for Internal Radiation,* ICRP Publication 2, Pergamon, London.

International Commission on Radiological Protection (ICRP) 1968. *Report of Committee 4 on Evaluation of Doses to Body Tissues from Internal Contamination Due to Occupational Exposure,* ICRP Publication 10, Pergamon, London.

International Commission on Radiological Protection (ICRP) 1971. *Report of Committee 4 on the Assessment of Internal Contamination Resulting from Recurrent or Prolonged Uptakes,* ICRP Publication 10A, Pergamon, London.

International Commission on Radiological Protection, Task Group of Committee II, (ICRP) 1966. "Task Group on Lung Dynamics for Committee II of the ICRP," *Health Phys.* **12,** 173.

Kaiser, G. D. 1976. *A Guide to the Use of TIRION—A Computer Program for the Calculation of the Consequences of Releasing Radioactive Material to the Atmosphere,* SRD-R-62, Safety and Reliability Directorate, United Kingdom Atomic Energy Authority, Culcheth, Warrington, Lancashire, United Kingdom.

Kernighan, B. W., and Plauger, P. J. 1978. *The Elements of Programming Style,* 2d ed., McGraw, New York.

Konikow, G. F., and Bredehoeft, J. D. 1978. *Computer Model of Two-Dimensional Solute Transport and Dispersion in Ground Water,* U.S. Geological Survey Techniques of Water Resources Investigations 7, U.S. Geol. Surv., Reston, Va., Chap. C2.

Lange, R. 1973. *ADPIC: A Three-Dimensional Computer Code for the Study of Pollutant Dispersal and Deposition Under Complex Conditions,* UCRL-51462, Lawrence Livermore Lab., Livermore, Calif.

Larson, N. M., and Reeves, M. 1976. *Analytical Analysis of Soil-Moisture and Trace-Contaminant Transport,* ORNL/NSF/EATC-12, Union Carbide Corp., Nuclear Div., Oak Ridge Natl. Lab.

Lee, R., Mack, J., and Sedgley, D. B. 1966. *GADOSE and DOSET: Programs to Calculate Environmental Consequences of Radioactivity Release,* GA-6511, Gen. Atomic, San Diego.

Lester, D., Buckley, D., and Donelson, S. 1981. *System Analysis of Shallow Land Burial,* SAI-01380-652LJ, collective vols. 1–3, Science Applications, La Jolla, Calif.

MacKay, T. F., and Ely, R. F., Jr. 1974. *Computation of Radiological Consequences Using INHEC Computer Program,* GAI-TR-101P, Gilbert Associates, Reading, Pa.

Mangold, D. C., Lippman, M. J., and Bodvarsson, G. S. 1980. *Draft CCC User's Manual,* version 2, LBL-10909, Lawrence Berkeley Lab., Univ. California, Berkeley.

McCracken, D. D. 1965. *A Guideline to FORTRAN IV Programming,* Wiley, New York.

McCracken, D. D. 1974. *A Simplified Guide to FORTRAN Programming,* Wiley, New York.

McGill, B., Maskewitz, B. F., Anthony, C. M., Commolander, H. E., and Hendrickson, H. R. 1976. *Abstracts of Digital Computer Code Packages Assembled by the Radiation Shielding Information Center,* ORNL/RSIC-13, vol. 4, Union Carbide Corp., Nuclear Div., Oak Ridge Natl. Lab.

Moore, R. E., Baes, C. F., III, McDowell-Boyer, L. M., Watson, A. P., Hoffman, F. O., Pleasant, J. C., and Miller, C. W. 1979. *AIRDOS-EPA: A Computerized Methodology for Estimating Environmental Concentrations and Dose to Man from Airborne Releases of Radionuclides,* ORNL-5532, Union Carbide Corp., Nuclear Div., Oak Ridge Natl. Lab.

Mosier, J. E., Fowler, J. R., Barton, C. J., Tolbert, W. W., Myers, S. C., Vanci, J. E., Price, H. A., Vasko, M. J. R., Rutz, E. E., Wendeln, T. X., and Rickertsen, L. D. 1980. *Low-Level Waste Management: A Compilation of Models and Monitoring Techniques,* ORNL/SUB-79/13617/2, Science Applications, Oak Ridge, Tenn.

Onishi, Y. P. A., Johanson, R. B., Baca, and Hilty, E. L. 1976. *Studies of Columbia River Water Quality, Development of Mathematical Models for Sediment and Radionuclide Transport Analysis,* BNWL-B-452, Battelle-Nothwest, Richland, Wash.

Onishi, Y., Serne, R. J., Arnold, E. M., Cowan, C. E., and Thompson, F. L. 1981. *Critical Review: Radionuclide Transport, Sediment Transport and Water Quality Management Modeling; and Radionuclide Sorption/Desorption Mechanisms,* PNL-2901, Pacific Northwest Lab., Richland, Wash.

Otter, J. M., and Conners, P. A. 1975. *Description of the COMRADEX—III Code,* Tl-001-130-053, Atomics Int., Canoga Park, Calif.

Owen, P. T., Dalle, N. S., Johnson, C. A., and Martin, F. M., eds. 1979. *An Inventory of Environmental Impact Models Related to Energy Technologies,* ORNL/EIA-147, Union Carbide Corp., Nuclear Div., Oak Ridge Natl. Lab.

Pleasant, J. C., McDowell-Boyer, L. M., and Killough, G. G. 1980. *RAGTIME: A FORTRAN IV Implementation of a Time-Dependent Model for Radionuclides in Agricultural Systems,* ORNL/NUREG/TM-371, Union Carbide Corp., Nuclear Div., Oak Ridge Natl. Lab.

Prickett, T. S., and Lonnquist, C. G. 1971. *Selected Digital Computer Techniques for Ground-Water Resource Evaluation,* Illinois State Water Survey Bul. 55, Illinois State Geological Survey, Urbana, Ill.

Rosinger, E. L. J., and Tremaine, K. K. R. 1980. *GARD2: A Computer Program for Geosphere Systems Analysis,* AECL-6423, Atomic Energy Canada, Whiteshell Nuclear Res. Establishment, Pinawa, Manitoba ROE ILO, Canada.

Sagendorf, J. F. 1974. *A Program for Evaluating Atmospheric Dispersion from a Nuclear Power Station,* NOAA Technical Memorandum ERL ARL-42, Air Resour. Lab., Idaho Falls, Idaho.

Shaeffer, D. L., and Etnier, E. L. 1979. *AQUAMAN—A Computer Code for Calculating Dose Commitment to Man for Aqueous Releases of Radionuclides,* ORNL/TM-6618, Union Carbide Corp., Nuclear Div., Oak Ridge Natl. Lab.

Shih, C. S., and Gloyna, E. F. 1967. *Radioactivity Transport in Water-Mathematical Model for the Transport of Radionuclides,* EHE-04-6202, Univ. Texas, Austin.

Simmonds, J. R., Linsley, G. S., and Jones, J. A. 1979. *A General Model for the Transfer of Radioactive Materials in Terrestrial Food Chains,* NRPB-R89, Natl. Radiological Protection Board, Harwell, Didcot, United Kingdom.

Simpson, D. B., and McGill, B. L. 1980. *User's Manual LADTAP II—A Computer Program for Calculating Radiation Exposure to Man from Routine Releases of Nuclear Reactor Liquid Effluents,* NUREG/CR-1276, Natl. Tech. Inf. Cent., Springfield, Va.

Soldat, J. K. 1971. *Modeling of Environmental Pathways and Radiation Doses from Nuclear Facilities,* BNWL-SA-3939, Battelle-Northwest, Richland, Wash.

Soldat, J. K., Robinson, N. M., and Barer, D. A. 1974. *Models and Computer Codes for Evaluating Environmental Radiation Doses,* BNWL-1754, Battelle-Northwest, Richland, Wash.

Specht, E., Martin, C., Otter, J., and Hart, R. 1975. *Description of COMRADEX-II Code,* TI-001-130-048, Atomics Int., Canoga Park, Calif.

Stallman, F. W., and Kam, F. B. K. 1973. *ACRA—A Computer Program for the Estimation of Radiation Doses Caused by a Hypothetical Reactor Accident,* ORNL/TM-4082, Union Carbide Corp., Nuclear Div., Oak Ridge Natl. Lab.

Strenge, D. L., Watson, E. C., and Droppo, J. G. 1976. *Review of Calculational Models and Computer Codes for Environmental Dose Assessment of Radioactive Releases,* BNWL-B-454, Battelle Pacific Northwest Labs., Richland, Wash.

Strenge, D. L., Watson, E. C., and Houston, J. R. 1975. *SUBDOSA—A Computer Program for Calculating External Doses from Accidental Atmospheric Releases of Radionuclides,* BNWL-B-264, Battelle-Northwest, Richland, Wash.

Thykier-Nielsen, S. 1974. *Models for Calculation of External Gamma Doses and Inhalation Doses from Releases of Radioactive Isotopes to the Atmosphere,* RISO-M-1725, Danish Atomic Energy Commission, Riso Research Establishment, Demark.

Trescott, P. C., and Larson, S. P 1975. *Documentation of Finite-Difference Model for Simulation of Three-Dimensional Ground-Water Flow,* Open File Report 75-438, U.S. Geol. Surv., Reston, Va.

Trescott, P. C., Pinder, G. F., and Larson, S. P., *Finite-Difference Model for Aquifer Simulation in Two Dimensions with Results of Numerical Experiments,* U.S. Gelogical Survey Techniques of Water Resources Investigations 7, U.S. Geol. Surv., Reston, Va., Chap. 1.

U.S. Geological Survey 1976. *INTERCOMP, A Model for Calculating Effects of Liquid Waste Disposal in Deep Saline Aquifers,* Water Resources Inv. 76-61

U.S. Nuclear Regulatory Commission, Office of Standards and Development (USNRC) 1977. *Calculation of Annual Doses to Man from Routing Releases of Reactor Effluents for the Purpose of Evaluating Compliance with 10 CFR Part 50, Appendix I,* Regulatory Guide 1.109.

Watts, J. R. 1976. *Modeling of Radiation Doses from Chronic Aqueous Releases,* DP-MS-75-126, Savannah River Lab., Aiken, S.C.

Willis, C. A., Spangler, G. A., and Rhoades, W. A. 1970. "A New Technique for Reactor Siting Dose Calculations," *Health Phys.* **19**, 47–54.

Winton, M. L. 1969. "A Compilation of Computer Codes for Nuclear Accident Analysis," *Nucl. Saf.* **10**(2), 131–47.

Winton, M. L. 1971. "Computer Codes for Analyzing Nuclear Accidents," *Nucl. Saf.* **12**(5), 461–87.

Winton, M. L. "Computer Codes for Analyzing Nuclear Accidents," *Nucl. Saf.* **15**(5), 535–53.

Appendix 13A

Bibliography of Model and Code Compilations and Reviews

Benedict, B. A. November 1978. *Review of Toxic Spill Modeling,* AD-A073 222/2ST, Tulane Univ., Department Civil Engineering, New Orleans.

Benedict, B. A., Jones, L. T., and Chow, V. T., eds. 1973. "Review of Heated Surface Discharge Models Applicable to Rivers," pp. 194–203 in *Water for the Human Environment,* vol. 4, Intl. Water Resour. Association, Champaign, Ill.

Bloom, S. G., Cornaby, B. W., and Martin, W. E. February 1978. *A Guide to Mathematical Models Used in Steam Electric Power Plant Environmental Impact Assessment,* FWS/OBS-7801, U.S. Department Interior.

Carrigan, B. June 1980a. *Atmospheric Modeling of Air Pollution. 1979–May, 1980 (A Bibliography with Abstracts),* Natl. Tech. Inf. Serv., Springfield, Va.; PB 80-811631.

Carrigan, B. June 1980b. *Atmospheric Modeling of Air Pollution. 1977–1978 (A Bibliography with Abstracts),* Natl. Tech. Inf. Serv., Springfield, Va.; PB 80-811623.

Cushman, J. H. October 1980. "Completion of the List of Analytical Solutions for Nutrient Transport to Roots. 1. Exact Linear Models (Soil-Water Systems)," *Water Resour. Res.* **16**(5), 891.

Darling, E. M., Jr., and Garlitz, J. D. March 1978. *Computer Modeling of Transportation-Generated Air Pollution. State-of-the-Art Survey. II. Final Report, July 1976–June 1977,* DOT-TSC-OST-78-6, DOT-TSC-RSPD-78-1, Transportation Syst. Cent., U.S. Department Transportation, Cambridge, Mass.; PB 280109.

Dionne, P. J., and Mathisen, D. I. October 1978. *Inventory of Data Bases, Models, and Graphics Packages at the Pacific Northwest Laboratory,* PNL-2560, Batelle Pacific Northwest Labs, Richland, Wash.

Eliassen, A. March 1980. "Review of Long-Range Transport Modeling," J. Appl. Meteorol. **19**(3), 231–40.

Eschenroeder, A. 1977. "An Overview of Atmospheric Reactive Pollutant Models," presented at ASTM Air Quality Meteorology and Atmospheric Ozone Symposium, Boulder, Colorado, July 31–Aug. 6, 1977, American Society for Testing and Materials.

Ferris, G., and Mason, B. June 1979. *Review of Regional Economic Models with Special Reference to Labor Impact Assessments,* SERI/TR-53-100, Solar Energy Res. Institute, Goldon, Colo.

Gardner, R. H., and O'Neill, R. V. 1979. "Parameter Uncertainty and Model Predictions: A Review of Monte Carlo Results," in *Symposium on Error Analysis of Ecological Models, Vienna, Austria,* CONF-791136-1, Union Carbide Corp., Nuclear Div., Oak Ridge Natl. Lab.

Hanna, S. R. Mar. 5, 1981. *Handbook on Atmospheric Diffusion Models,* ATDL-81/5, Natl. Oceanic and Atmospheric Administration, Oak Ridge, Tenn.

Harrison, E. A. November 1979. *Ecosystem Models. Volume 3. November 1977–November 1979 (A Bibliography with Abstracts),* Natl. Tech. Inf. Serv., Springfield, Va.; PB 80-801053.

Harrison, E. A. November 1977. *Ecosystem Models. Volume 2. November 1975–November 1977 (A Bibliography with Abstracts),* NTIS/PS-77/1011/4ST, Natl. Tech. Inf. Serv., Springfield, Va.

Harrison, E. A. November 1976. *Ecosystem Models. Volume 2. November 1975–November 1976 (A Bibliography with Abstracts),* NTIS/PS-76/0904/3ST, Natl. Tech. Inf. Serv., Springfield, Va.

Harrison, E. A. November 1975. *Ecosystem Models. (A Bibliography with Abstracts),* NTIS/PS-75/846/6ST, Natl. Tech. Inf. Serv., Springfield, Va.

Healy, J. W., and Hanson, W. C., eds. 1980. *Review of Resuspension Models,* Tech. Inf. Cent., Oak Ridge, Tenn.

Hildreth, W. W. April 1978. *Soil Moisture Modeling Review,* N78-23646/OST, Aerospace Syst. Div., Lockheed Electronics Co., Houston, Tex.

Hoffman, F. O., Miller, C. W., Shaeffer, D. L., Garten, C. T., Jr., Shor, R. W., and Ensminger, J. T. April 1977. *Compilation of Documented Computer Codes Applicable to Environmental Assessment of Radioactivity Releases (Nuclear Power Plants),* ORNL/TM-5830, Union Carbide Corp., Nuclear Div., Oak Ridge Natl. Lab.

Horst, T. W. 1979. "Review of Gaussian Diffusion-Deposition Models," in *Symposium on Potential Environmental and Health Effects of Atmospheric Sulfur Deposition, Gatlinburg, Tennessee,* PNL-SA-8009, CONF-791090-9, Natl. Tech. Inf. Serv., Springfield, Va.

Jenne, E. A. June 1981. *Geochemical Modeling: A Review,* PNL-3574, Battelle Pacific Northwest Labs., Richland, Wash.

Lee, S. S., and Sengupta, S. May 1978. *Three Dimensional Thermal Pollution Models. Volume 1: Review of Mathematical Formulations,* NASA-CR-154624-V-1, Natl. Aeronautics and Space Administration.

Lehmann, E. J. 1974. *Water Quality Modeling. A Bibliography with Abstracts,* U.S. Department Commerce.

Lehmann, E. J. June 1975. *Atmospheric Modeling of Air Pollution. A Bibliography with Abstracts,* NTIS/PS-75/476, Natl. Tech. Inf. Serv., Springfield, Va.

Meyers, C. R., Jr. June 1973. *Regional Modeling Abstracts. A Bibliography of Regional Analysis. Volume V,* ORNL-EIS-73-61, Union Carbide Corp., Nuclear Div., Oak Ridge Natl. Lab.

Miller, C. July 1978. *Exposure Assessment Modeling: A State-of-the-Art Review,* Office Res. and Dev., U.S. Environ. Protection Agency, Athens, Ga.

Molz, F. J. October 1981. "Models of Water Transport in the Soil-Plant System: A Review," Water Resour. Res. 17(5), 1245–60.

Mosier, J. E., Fowler, J. R., and Barton, C. J. April 1980. *Low Level Waste Management: A Compilation of Models and Monitoring Techniques. Volume 1,* SAI/OR-565-2, Science Applications, Oak Ridge, Tenn.

National Technical Information Service 1982. *Mathematical Modeling and Computerized Simulation of Atmospheric Aerosols. 1970–January 1982 (Citations from the Engineering Index Data Base),* Springfield, Va.; PB 80-860255.

O'Neill, R. V. Gerguson, N., and Watts, J. A. 1975. *Bibliography of Mathematical Modeling in Ecology,* EDFB/IBP-75/5, Union Carbide Corp., Nuclear Div., Oak Ridge Natl. Lab.

Onishi, Y. 1981. *Critical Review. Radionuclide Transport, Sediment Transport, and Water Quality Mathematical Modeling, and Radionuclide Adsorption/Desorption Mechanisms,* NUREG/CR-1322, Div. Safeguards, Fuel Cycle, and Environ. Res., U.S. Nuclear Regulatory Commission.

Owen, P. T., Dailey, N. S., Johnson, C. A., and Martin, F. M., eds. February 1979. *Inventory of Environmental Impact Models Related to Energy Technologies,* ORNL/EIS-147, Union Carbide Corp., Nuclear Div., Oak Ridge Natl. Lab.

Policasto, A. J., Dunn, W. E., and Zaric, Z. P., eds. 1978. "Numerical Modeling of Surface Thermal Plumes," in *Thermal Effluent Disposal from Power Generation,* CONF-7608130, Argonne Natl. Lab., Argonne, Ill.

Randerson, D. July 1976. "Overview of Regional-Scale Numerical Models," *American Meteorological Society B* 57(7), 797.

Rose, K. A., and Swartzman, G. L. May 1981. *A Review of Parameter Sensitivity Methods Applicable to Ecosystem Models,* NUREG/CR-2016, Office Nuclear Regulatory Res., U.S. Nuclear Regulatory Commission.

Rupp, E. M., Luxmoore, R. J., and Parzyck, D. C. September 1979. *Energy Technology Impacts on Agriculture with a Bibliography of Models for Impact Assessment on Crop Ecosystems,* ORNL/TM-6694, Union Carbide Corp. Nuclear Div., Oak Ridge Natl. Lab.

Strenge, D. L., Watson, E. C., and Droppo, J. G. June 1976. *Review of Calculational Models and Computer Codes for Environmental Dose Assessment of Radioactive Releases,* BNWL-B-454, Battelle Pacific Northwest Labs., Richland, Wash.

Tracy, J. June 1979. *Review of Hydrodynamic Dispersion in Transport Models,* CONF-790602-(Summary), *Trans. Am. Nucl. Soc.*

Trubey, D. K., and Comolander, H. E. May 1972. *Review of Calculations of Radiation Transport in Air-Theory, Techniques, and Computer Codes. Proceedings of a Seminar, November 15–17, 1971,* CONF-711125, Union Carbide Corp. Nuclear Div., Oak Ridge Natl. Lab.

Turner, D. B. May 1979. "Atmospheric Dispersion Modeling: A Critical Review," *APCA J.* **29**(5), 502.

Appendix 13B

Sources of Codes or Code Information

Hazardous Materials Information Center
Oak Ridge National Laboratory
P.O. Box X, Building 2029
Oak Ridge, Tennessee 37830

International Clearinghouse for Groundwater Models
Model Annotation Retrieval System
Holcomb Research Institute
Butler University
Indianapolis, Indiana 46208

National Energy Software Center
Argonne National Laboratory
9700 South Cass Avenue
Argonne, Illinois 60439

Radiation Sheilding Information Center
Oak Ridge National Laboratory
P.O. Box X, Building 6025
Oak Ridge, Tennessee 37830

14 Assessment of Accidental Releases of Radionuclides

By H. R. MEYER,* C. W. MILLER,* A. E. DESROSIERS,†
G. A. STOETZEL,† D. L. STRENGE,† *and* R. E. SWAJA*

14.1 INTRODUCTION

Assessment of the radiological impact of accidental releases of radionuclides from power reactors involves the use of models and assumptions similar to those described in previous chapters. However, there are some important differences in the requirements of models that estimate releases under accident conditions, involving the need for the following:

1. *Site-specific analysis.* Local meteorological, population, crop, and terrain data may be required in analyses involving the real-time estimation of accident sequence consequences.

2. *Probabilistic analysis.* Commercial power reactors are designed with multiple levels of protection against failures with the potential for significant releases of radionuclides. Therefore, reactor design engineers estimate that such accidents have very low probabilities of occurring. For example, the most significant study to date of reactor accident probabilities and consequences, the *Reactor Safety Study* (USNRC 1975), estimates probabilities of occurrence of various accidents ranging from 10^{-4} to 10^{-6} per reactor-year, with the high-consequence accident sequences linked to the lowest probabilities. While routine release assessments are typically based on continuous, predictable releases, accident assessments must account for the extremely low probabilities of high-consequence releases in order to fairly compare risks both within nuclear systems and between alternative types of energy-producing systems.

*Oak Ridge National Laboratory.
†Pacific Northwest Laboratory.

While a large body of data and modeling techniques have evolved over the years with respect to accident consequence analysis, the U.S. Nuclear Regulatory Commission (NRC) is currently evaluating probabilistic risk assessment procedures. The reader is referred to the following documents for a detailed appraisal of current thinking on the topic.

PRA Procedures Guide—an NRC-sponsored guide to the performance of probabilistic risk assessment for nuclear power plants (USNRC 1983).

Models Selected for Calculation of Doses, Health Effects and Economic Costs Due to Accidental Radionuclide Release from Nuclear Power Plants (Strenge 1980)—an NRC-sponsored report describing available or desired models for accident consequence analysis and the basis for the atmospheric and terrestrial transport model discussions in this chapter.

Criteria for Preparation and Evaluation of Radiological Emergency Response Plans and Preparedness in Support of Nuclear Power Plants (USNRC 1980)—a summary of reactor emergency planning requirements prepared jointly by the NRC and the Federal Emergency Management Agency.

This chapter provides summarized descriptions of some of the models available for predicting the atmospheric and terrestrial transport of accidental releases of radionuclides to man. For an accident releasing significant quantities of, for example, $^{131-135}I$, ^{131m}Te, ^{132}Te, ^{89}Sr, ^{140}Ba, ^{134}Cs, and ^{88}Kr, the atmospheric pathway (including gamma and beta exposure from the passing cloud and ground deposition and internal dose from inhalation) would be expected to dominate short-term human health risk (USNRC 1983).

The magnitudes of accident dose estimates are subject to considerable uncertainties, which were considered at a recent international workshop in the Federal Republic of Germany.* Key uncertainties involve reactor operator estimates as to radionuclide source term composition and magnitude of releases, errors in predictive accuracy of environmental transport codes, and difficulties in predicting population responses to evacuation or sheltering orders from local authorities. These considerations are also discussed in this chapter. Not discussed are uncertainties associated with age dependency in dose calculation, an area in which significant research and modeling remains to be done. A discussion of instrument and operator requirements to provide adequate monitoring data completes the chapter's discussion of accident modeling and monitoring requirements.

*Technical University of Aachen and Bonnenberg and Drescher Ingienieurgesellschaft, Federal Republic of Germany, unpublished data, 1982.

14.2 ATMOSPHERIC AND TERRESTRIAL FOOD CHAIN TRANSPORT

14.2.1 Background

The purpose of this section is to present methods for estimating air concentrations (at ground level) and ground contamination concentrations at off-site locations as a result of accidental release of radionuclides to the atmosphere. Such releases can lead to exposures to man via four principal pathways (USNRC 1978): (1) whole-body external exposures from the passing cloud, (2) whole-body external exposure from deposited material, (3) internal exposure from inhalation of radionuclides in the passing cloud, and (4) internal exposure from ingestion of farm products contaminated by deposited radionuclides. Exposures due to the first three pathways are of primary concern during the first several hours following the release, while exposure from ingestion of farm products is a longer-term concern. Not considered in the context of this chapter are the long-term social and economic costs associated with interdiction of contaminated property. For power reactors located near cities or productive farmlands, as is the case in much of central Europe, for example, these costs may dominate the overall consequence analysis.

The methods presented in this section for calculating atmospheric dispersion and deposition are based primarily on the straight-line Gaussian plume atmospheric dispersion model. This model is described in Chapter 2. When used for routine radionuclide releases, the model employs frequency-of-occurrence data for wind speed, atmospheric stability, and wind direction to produce annual average air concentration and deposition rates as a function of direction and distance (USNRC 1977). Also, this model assumes that the plume continually travels in a straight line. Variations on this basic technique may be appropriate for performing assessments of potential accident consequences. However, this basic approach may not always be applicable for real-time, site-specific atmospheric dispersion estimates when accidental radioactive releases occur. Under these circumstances spatial and temporal variations in meteorological, terrain, and release conditions often must be taken into account.

Radionuclides deposited on farmland can result in human radiation exposure through farm product pathways. These pathways are illustrated in Chapter 5 and include food crops (vegetables, grain, fruit, etc.) and animal products (meat, milk, eggs, etc.). Under accidental release situations the amount of activity ingested through these pathways is difficult to assess. The annual average parameter values and equilibrium bioaccumulation factors used in the chronic pathway analysis models are not directly applicable in describing radionuclide behavior during the short time periods considered in accidental

release situations, but may be more useful for initial estimation of time-integrated dose. More attention must be given to transient behavior during transport through the food chains and uptake by humans.

14.2.2 Potential Accident Assessments

The NRC has published guidance as to the atmospheric dispersion models acceptable for assessing the consequences of potential accidents at nuclear power plants (USNRC 1977). As suggested above, this guidance uses a bivariate straight-line Gaussian expression and Pasquill atmospheric stability classes. The model considers building wake effects, ambient plume meander, and directional dependence of dispersion conditions.

Regulatory Guide 1.145 (USNRC 1979a) includes different equations for ground-level and elevated releases. At a nuclear reactor, a release is considered to be elevated if the point of release is more than 2-1/2 times the height of any structure close enough to affect the dispersion of the plume (USAEC 1973; USAEC 1974). If the point of release is lower, it is categorized as a ground-level release.

In an accident situation, releases from a pressurized-water reactor (PWR) would be generally through a vent or other building penetration and considered a ground-level release. Releases from boiling-water reactors (BWRs) are normally elevated releases if they go through the main stack and ground-level releases if they go through building vents. The location of reactors can have a bearing on whether releases will go through elevated stacks (elevated release) or building vents (ground-level release). If the reactor is located near a highly populated area, elevated stacks will most likely be present to allow greater dispersion of any releases. Millstone 2 (a PWR located in a populated area) has such an elevated stack, which will take advantage of the additional dispersion should an accidental release occur.

14.2.2.1 Ground-Level Release Model

Use of the ground-level-release equations will allow calculation of the ground-level relative concentration at the plume centerline for a specified downwind distance. The basic ground-level-release equation (USNRC 1979a) is

$$\chi/Q = \frac{1}{\pi \bar{u} \sigma_y \sigma_z} , \tag{14.1}$$

where

χ = ground-level concentration (Ci/m^3) at the downwind location of interest,

Q = release rate of material from the accident site (Ci/s),

$\bar{u}$ = wind speed (m/s),

σ_y = lateral plume spread (m), a function of atmospheric stability and distance (see Fig. 14.1),

σ_z = vertical plume spread (m), a function of atmospheric stability and distance (see Fig. 14.2).

Equation 14.1 may be modified to consider the effects of building wake mixing and ambient plume meander on atmospheric dispersion. The resulting equations (USNRC 1979a) are

$$\chi/Q = \frac{1}{\bar{u}_{10}(\pi\sigma_y\sigma_z + A/2)}, \tag{14.2}$$

$$\chi/Q = \frac{1}{\bar{u}_{10}(3\pi\sigma_y\sigma_z)}, \tag{14.3}$$

$$\chi/Q = \frac{1}{\bar{u}_{10}\pi\Sigma_y\sigma_z)}, \tag{14.4}$$

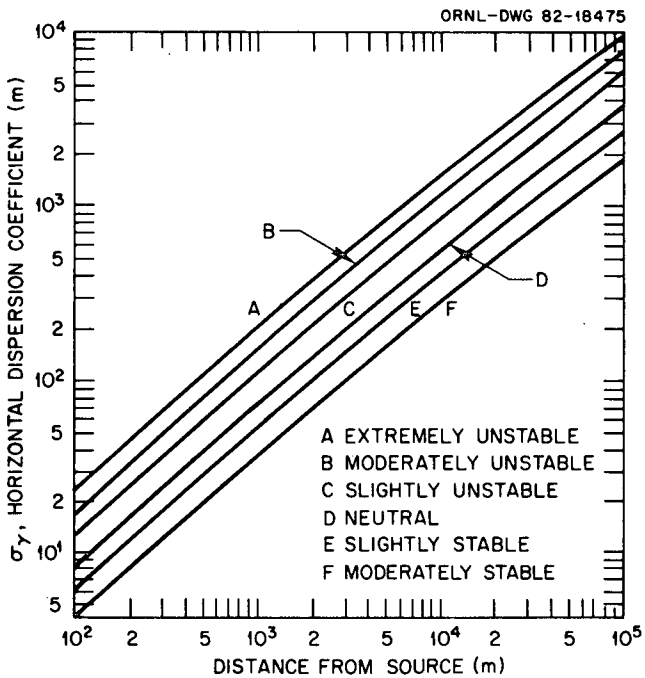

Figure 14.1. Lateral diffusion σ_y versus downwind distance from source for Pasquill's turbulence types. Source: Gifford, F. A., Jr. 1968. "An Outline of Theories of Diffusion in the Lower Atmosphere," in *Meteorology and Atomic Energy—1968,* TID-24190, ed. D. Slade, Tech. Inf. Center, U.S. Department of Energy, Oak Ridge, Tenn.

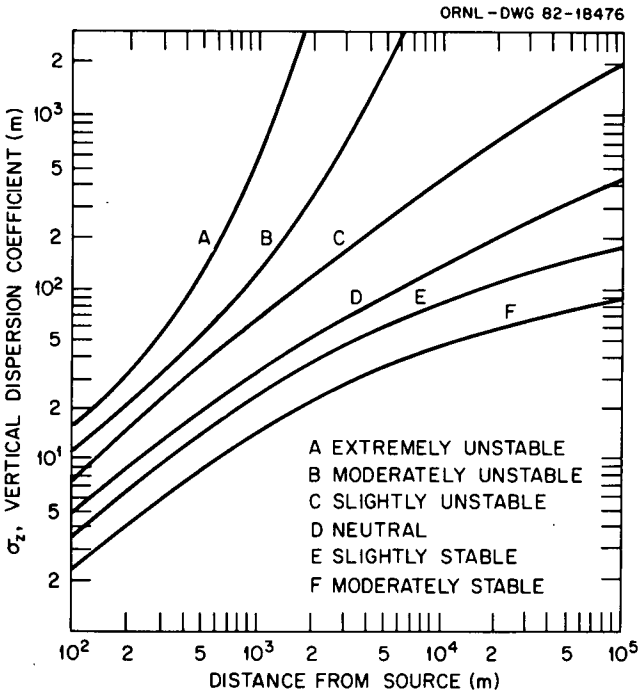

Figure 14.2. Vertical diffusion σ_z versus downwind distance from source for Pasquill's turbulence types. Source: Gifford, F. A., Jr. 1968. "An Outline of Theories of Diffusion in the Lower Atmosphere," in *Meteorology and Atomic Energy—1968,* TID-24190, ed. D. Slade, Tech. Inf. Center, U.S. Department of Energy, Oak Ridge, Tenn.

where

$\bar{u}_{10}$ = mean wind speed at 10 m above plant grade (m/s),

A = smallest vertical-plane cross-sectional area of the reactor building (m^2),

Σ_y = lateral plume spread with meander and building wake effects (m)—a function of atmospheric stability, wind speed $\bar{u}_{10}$, and distance. For downwind distances of 800 m or less, $\Sigma_y = M\sigma_y$ (where M is determined from Fig. 14.3). For downwind distances greater than 800 m, $\Sigma_y = (M - 1)\sigma_{y_{800m}} + \sigma_y$.

It is recommended (USNRC 1979a) that horizontal (lateral) plume meander be considered during neutral (D) or stable (E, F, or G) atmospheric stability conditions when the wind speed at the 10-m level is less than 6 m/s. During unstable atmospheric conditions (A, B, or C) and/or 10-m-level wind speeds of 6 m/s or more, plume meander should not be considered, because

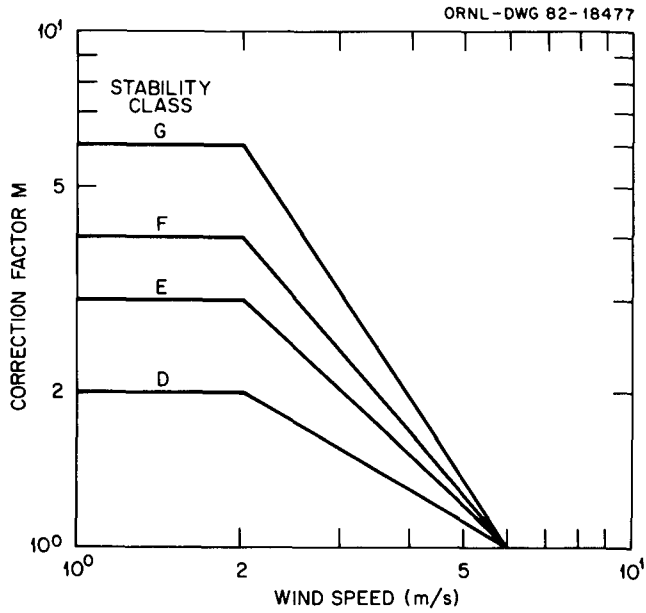

Figure 14.3. Correction factors for Pasquill-Gifford σ_y values by atmospheric stability class. Source: U.S. Nuclear Regulatory Commission 1979a. *Atmospheric Dispersion Models for Potential Accident Consequence Assessments at Nuclear Power Plants,* Regulatory Guide 1.145.

building wake mixing becomes more effective in dispersing effluents than meander effects as the wind speed increases and atmospheric conditions become more unstable.

For neutral or stable atmospheric conditions, Regulatory Guide 1.145 suggests that χ/Q values be calculated using Eqs. 14.2, 14.3, and 14.4, with the higher of the values calculated from Eqs. 14.2 and 14.3 compared to the value from Eq. 14.4 and the lower of these two values selected as the appropriate χ/Q. For unstable conditions, it is suggested that the appropriate χ/Q value is the higher value calculated from Eqs. 14.2 and 14.3.

The plume meander factor M associated with Eq. 14.4 is based on NRC staff analysis of results from atmospheric diffusion experiments conducted at the Rancho Seco nuclear power plant (Start et al. 1978). Figure 14.4 illustrates that this NRC methodology overpredicts the values actually observed during the Rancho Seco tests (Miller 1981). However, the amount of overprediction obtained using this method is markedly less than that found when the standard Pasquill-Gifford (PG) values of σ_y and σ_z are used (Eq. 14.1).

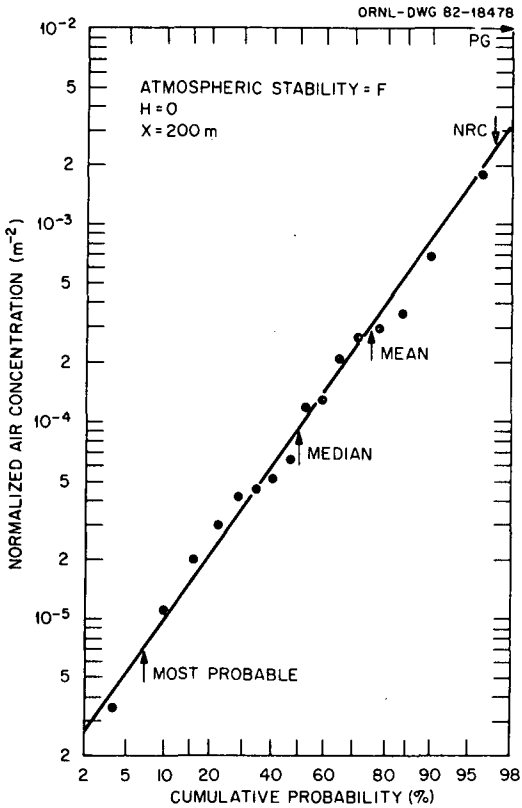

Figure 14.4. Percentiles of predicted air concentrations and cumulative probability distribution of air concentrations observed at Rancho Seco Nuclear Generating Station for one set of release and meteorological conditions. Source: Adopted from Miller, C. W. 1981. "Comparison of Methods for Predicting Air Concentrations Near Reactor Complexes," *Trans. Am. Nucl. Soc.* **39,** 125–26.

14.2.2.2 Elevated Release Model

The basic equation for determining a downwind ground-level concentration at the plume centerline for an elevated release is

$$\chi/Q = \frac{1}{\pi \bar{u} \sigma_y \sigma_z} \exp\left[\frac{-h^2}{\sigma_z^2}\right], \tag{14.5}$$

where h = effective height of release.

Regulatory Guide 1.145 (USNRC 1979a) discusses equations for nonfumigation and fumigation conditions. Fumigation conditions occur when a

temperature inversion occurs above the stack, limiting the vertical dispersion of the plume and resulting in greater ground-level concentrations closer to the stack.

The nonfumigation equation is

$$\chi/Q = \frac{1}{\pi \bar{u}_h \sigma_y \sigma_z} \exp\left[\frac{-h_e^2}{2\sigma_z^2}\right], \tag{14.6}$$

where

$\bar{u}_h$ = wind speed representing conditions at the release height,

h_e = effective stack height (m): $h_e = h_s - h_t$,

h_s = physical height of the stack above plant grade (m),

h_t = maximum terrain height (m) above plant grade between the release point and the point for which the calculation is made: h_t cannot exceed h_s.

If h_t is equal to or greater than h_s, then $h_e = 0$, and the nonfumigation equation becomes a ground-level release equation.

The fumigation equation is

$$\chi/Q = \frac{1}{(2\pi)^{1/2} \bar{u}_{h_e} \sigma_y h_e}, \quad h_e > 0, \tag{14.7}$$

where

$\bar{u}_{h_e}$ = wind speed representative of the layer of depth h_e (m/s),

σ_y = lateral plume spread (m) [a moderately stable (F) atmospheric stability condition is usually assumed],

h_e = effective stack height (m).

This equation cannot be used when h_e becomes small (on the order of 10 m), as calculated χ/Q values will become unrealistically large.

As previously mentioned, elevated releases will result in additional dispersion compared to equivalent ground-level releases. Figure 14.5 is a plot of atmospheric dispersion factors (χ/Q values) versus distance from the release point for ground-level and elevated releases, assuming a Pasquill F stability class. The basic dispersion equations (Eqs. 14.1 and 14.5) were used to calculate χ/Q values assuming a 1-m/s wind speed and a 75-m release height. This example shows the additional dilution effect of the elevated release. Also, note that the maximum downwind concentration (equivalent to the highest χ/Q value) occurs at approximately 6 km. As stack height increases, the

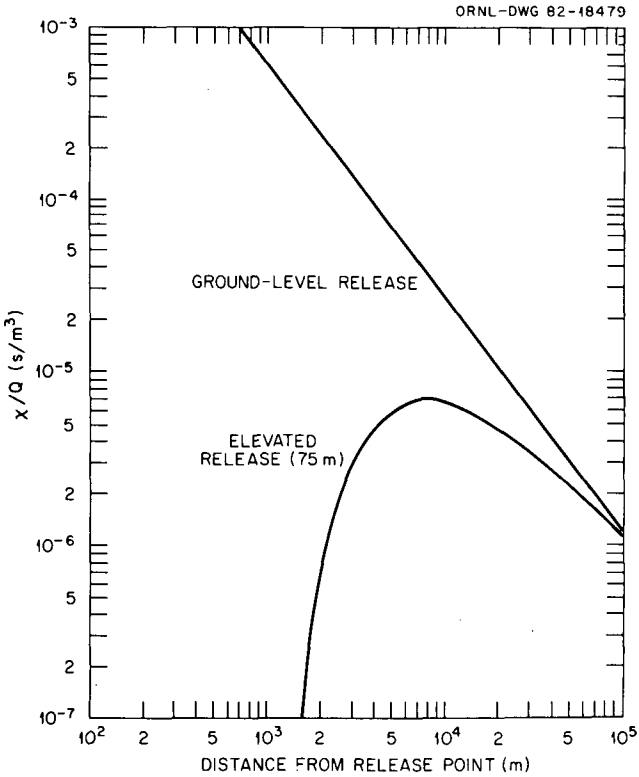

Figure 14.5. Atmospheric dispersion factors versus downwind distance for Pasquill Class F.

dilution effect will be greater and maximum downwind ground concentrations will occur further downwind (see Fig. 14.6).

14.2.2.3 Special Considerations

As noted above, plume meander and building wake effect considerations have been included in the methodology represented by Eqs. 14.2, 14.3, and 14.4. However, a number of other considerations, discussed below, have not been included in any of the preceding equations.

Plume rise. During an accident, radioactive material may be released to the atmosphere at an elevated temperature and with a vertical velocity. The effective stack height may be higher than the physical height because of the combined effects of buoyancy (dependent on temperature of released material) and momentum (dependent on velocity of released material). Plume buoyancy is a function of atmospheric stability, wind speed, source heat content, and downwind distance. Plume momentum is a function of atmospheric stability, stack exit velocity, and internal diameter of the stack.

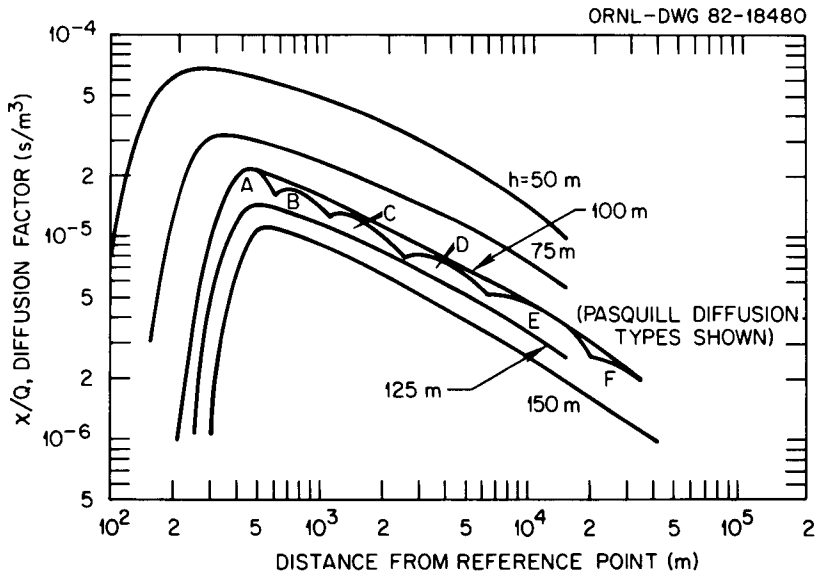

Figure 14.6. Atmospheric diffusion factors for elevated releases, 0- to 8-h release times. Source: U.S. Atomic Energy Commission 1973. *Assumptions Used for Evaluating the Potential Radiological Consequences of a Loss-of-Coolant Accident for Boiling-Water Reactors,* Regulatory Guide 1.3.

Terrain effects. Terrain features such as mountains can also have an effect on the dispersion of the plume. The effect of most elevated terrain features would be to limit or divert dispersion. One model to describe terrain effects has been incorporated into Eqs. 14.6 and 14.7 (USNRC 1979a). This model suggests subtracting a terrain elevation value from the physical stack height. As discussed by Strenge, Soldat, and Watson (1978), other methods of correcting for terrain effects are available. The plume model for terrain correction incorporated into Eqs. 14.6 and 14.7 is often used because it is expected to produce conservative results (i.e., overestimate ground-level air concentrations). Also, more complex models may not be practical to implement (Strenge, Soldat, and Watson 1978).

Deposition and resuspension. Radioactive particles and reactive gases and vapors may be removed from the atmosphere and deposited on the surface of the earth through the processes of dry and wet deposition. These processes affect subsequent human exposure in two ways:

1. Deposited material serves as a source of surface and/or food chain exposure and as a source of inhalation explosure via wind-driven resuspension.
2. Plume depletion results in a reduction in the amount of material transported downwind.

Dry deposition is the process by which particles and reactive gases are deposited on various surfaces (soil, grass, leaves, etc.) via impingement, electrostatic interactions, chemical reactions, biological uptake, and other mechanisms; hence, it is a continuous process in the atmosphere. These processes are often described in terms of a dry deposition velocity V_d. This parameter may be defined as the deposition flux to the ground surface divided by the airborne concentration of the same material; see, for example, Van der Hoven (1968).

Sehmel (1980) presented a review of many field experiments conducted to determine V_d for various particles and gases. He was unable to generalize these results even to within an order of magnitude because of experimental uncertainties and limited data. He found that the V_d values he reviewed are an unknown function of experimental conditions and show a wide numerical range even for the same type of deposition surface. He also found that in some individual experiments, V_d ranges over at least one order of magnitude. For all experiments reviewed by Sehmel, the range in V_d for gases was more than four orders of magnitude, and the range for particles was more than three orders of magnitude.

Wet deposition or precipitation washout of airborne material includes washout processes within the cloud or below the cloud. In the in-cloud washout process, the airborne material stimulates or even initiates precipitation by increasing condensation. The below-cloud washout process occurs when precipitation falling through the plume impacts upon and collects the airborne material. Several good references on the subject of wet deposition are available in the literature [e.g., Engelmann (1968)]. In the *Reactor Safety Study* (USNRC 1975), the consequence model assumes the plume concentration to decrease from precipitation washout according to

$$\exp[\Lambda(t - t_0)] ,$$

where $(t - t_0)$ is the time since the onset of precipitation and Λ is the wet removal rate. The removal rate Λ is taken to be 10^{-4}/s under stable conditions and 10^{-3}/s under unstable conditions. Particles and gases are treated identically, and noble gases are assumed to be insoluble and not removed by precipitation. Precipitation at the time of an accident will result in a greater deposition at the precipitation site. At greater distances from the precipitation site, doses will be reduced.

Resuspension and transport of particles by the wind is a topic covered by a large body of literature. Data available ranges from erosion of agricultural soils to resuspension of fallout particles. Numerous models have been developed to estimate resuspension from various substrates; the models and their implementations range from simple mass loading or resuspension factor approaches based on measured ratios of surface vs air concentrations to more

complex models based on theoretical considerations. Applicability of these models is usually quite limited, although the extent of a specific model's limitations is often not recognized by a potential user or emphasized by its developer. Smith et al. (1982) have published a useful intercomparison of fifteen resuspension models and their computer implementations where appropriate. The interested reader is referred to that review as an entry point into the literature.

14.2.3 Post-Release Assessments

The NRC has published guidance for performing post-release assessments (USNRC 1980). This guidance calls for the use of real-time, site-specific atmospheric transport and diffusion models when accidental airborne radioactive releases occur. Two classes of models are suggested: (1) Class A model, which must produce initial transport and diffusion estimates of the plume exposure for an emergency planning zone (EPZ) distance of approximately 10 miles within 15 min following the classification of an incident, and (2) Class B model, a numerical model which can represent the actual spatial and temporal variations of plume distribution and can provide estimates of deposition and relative concentration of radioactivity within the plume exposure and ingestion EPZs for the duration of the release.

14.2.3.1 Class A Models

The purpose of a Class A model is to provide data that can be used for an immediate informed response in the event of an emergency. As a result, it has been recommended that the output of a Class A model be routinely and automatically available at all times in a simple and easily understood form (USNRC 1980). Hand-calculation, nomogram, or plume-overlay methods should be available as backup if the automatic system should fail.

A number of different models and computer codes have been identified for potential use to satisfy Class A modeling requirements (Bass and Smith 1981). It has been recommended, however, that model complexity be minimized because of the many demands that are likely to be placed on on-site personnel during the early stages of any emergency. For many sites an automated version of a simple straight-line Gaussian plume model (Eqs. 14.1 to 14.7) may be quite adequate for Class A requirements. For sites characterized by spatial variations in terrain and/or spatial and temporal changes in meteorology, however, such a model may not be sufficient. In such cases, some kind of a variable trajectory model adjusted to the particular site in question may be required (Bass and Smith 1981; USNRC 1980).

Any model chosen for estimating atmospheric dispersion requires the input of various site-specific meteorological data. The most important data required for Class A purposes is wind direction and wind speed (USNRC 1980). Wind direction changes that alter the plume's path can occur during the release, and

these changes must be accounted for in the assessment of accident consequences. Wind speed determines the initial volume of air in which releases are diluted and the plume transport time to populated areas. In general, the higher the wind speed, the greater the dispersion and the lower the off-site doses, but the shorter the travel time to populated areas.

14.2.3.2 Class B Models

The purpose of a Class B model is to provide estimates of plume behavior that are more refined than those provided by a Class A model. Basically, a Class B model should (1) describe plume transport over distances corresponding to the ingestion EPZ (typically <50 miles), (2) use a dispersion model that is compatible with multi-station wind data or derived wind field models, and (3) provide near-field estimates that are compatible with Class A model estimates (Bass and Smith 1981).

Bass and Smith (1981) have also examined a number of Class B models. These ranged from relatively complicated Eulerian or hybrid models, "true" Class B models, to simpler segmented-plume or puff models. These latter two types of models in even simpler form have already been suggested for possible use as Class A models, too. In general, when compared to Class A models, Class B models (1) require more computer capacity, (2) require more computer time to run, (3) are more difficult to run, (4) require more extensive meteorological data as input, and (5) require extensive site-specific topography and source geometry.

Bass and Smith (1981) emphasize that a Class B model is no better than the wind field module used in the model. Extensive site-specific field tests will most likely be needed to verify the wind field modules, as well as the diffusion portions, of any Class B model chosen for a particular reactor site. In general, when selecting a Class B model, one must balance the increased versatility expected from the model against the time necessary to implement and verify the model at a given site and the increased meteorological data needs, as compared to most Class A models.

14.2.3.3 Other Approaches

Approaches other than the use of Class A and Class B models may at times be appropriate for estimating atmospheric dispersion during accidental radionuclide releases. Nearly all potential Class A and Class B models suffer from inadequate validation. As a result, site-specific field tests may be required before any model can be fully implemented at a given reactor location. Such tests will be especially necessary at sites dominated by complex terrain or meteorological conditions (e.g., coastal locations). However, such field results can be used not only for model verification but also for development of site-specific dispersion estimation systems that do not depend on running the model

itself. If developed properly, such a system would be a relatively quick and accurate way of estimating dispersion under emergency release conditions.

Modeling results can also be supplemented by releasing tracers and making real-time dispersion measurements during the emergency situation. If an actual release is expected sometime after the occurrence of an initiating event, a tracer could be released even before the radionuclide emission occurs. Tracer balloons (tetroons; tetrahedral-shaped constant-volume balloons set to float at a predetermined pressure height) could be released and followed by remote sensing to estimate potential plume trajectories. Inert gases would require more extensive monitoring efforts, but they would provide information with regard to both diffusion and dispersion of the radioactive material. Because of economic and logistical considerations, it is unlikely that such systems would be feasible or necessary at all operating nuclear reactors. However, the use of some kind of real-time dispersion estimates may be needed at those reactor sites dominated by complex terrain or meteorology.

14.2.4 Terrestrial Food Chain Models

The model presented in this section can be used to estimate the amount of radioactive material that will reach humans through farm product pathways. These models are applicable to the period immediately following the accident and for about 1 y thereafter. For succeeding years, the human exposure resulting from residual contamination can be estimated using the chronic release models described in Chapter 5.

Estimating near-term transport of radionuclides through terrestrial food chains following acute releases is complicated by the need to consider the temporal relationship of many parameters. These parameters include time of deposition with respect to growing season, time of planting, time of harvest, plant growth cycle, consumption period, and other factors affecting the concentration of radionuclides in the edible portions of plants. For animal product pathways, the parameters of interest include feeding habits, transfer to animal product, production period, and consumption period. Other considerations could also be mentioned. The long-term averaged values used for chronic contamination situations may not be appropriate for accidental releases. Equilibrium will not necessarily be attained in all phases of the food chain transport. Three models are described in the following discussion: (1) a simple crop ingestion model for estimating consumption by humans over a prolonged period, (2) a dynamic plant growth model for describing the root uptake pathway, and (3) a compartmental model that attempts to describe the transient behavior throughout the terrestrial food chain.

14.2.4.1 Simple Food Chain Model

Deposition of airborne contamination onto farmland can lead to plant contamination through direct deposition onto plant surfaces and through

deposition onto soil with subsequent uptake by roots. Root uptake is generally slow and relatively unimportant compared to the direct deposition pathway when deposition occurs during the growing season. The model presented here can be used to estimate uptake by humans for the direct deposition pathway and for certain animal products where the product is formed quickly within the animal (such as milk and eggs). This model was developed by Napier et al. (1980) for the PABLM computer program.

The direct deposition pathway is important when deposition occurs during the plant growing season, prior to harvest. The deposition must also be on edible parts of the plant (or easily transferred to edible parts). The important events to consider are the times of deposition, harvest, and consumption. The initial concentration on the plant can be estimated as

$$C(0) = R \cdot G \cdot T / Y , \tag{14.8}$$

where

$C(0)$ = initial concentration of radionuclide on edible portions of the plant (Ci/kg),

R = fraction of initial deposition retained on the plant,

G = ground concentration due to air deposition (Ci/m^2),

T = translocation factor for transfer from plant leaves to edible parts of the plant (dimensionless),

Y = crop yield (kg/m^2).

The initial plant concentration is reduced with time by radiological decay and removal by weathering. These processes are assumed to occur continuously from deposition until harvest. The plant concentration at harvest is calculated as

$$C(T_h) = C(0) \cdot \exp(-\lambda_e \cdot T_h \cdot 86400) , \tag{14.9}$$

where

$C(T_h)$ = plant concentration at time of harvest (Ci/kg),

λ_e = effective removal rate constant (s^{-1}),

T_h = time between deposition and harvest (d),

$\lambda_e = \lambda_r + \lambda_w$,

λ_r = radiological decay constant (s^{-1}),

λ_w = weathering removal rate constant (s^{-1}),

86,400 = s/d.

The weathering rate constant is usually based on a half-time of 14 d.

After harvest, there is usually a delay period before consumption of the food product begins. During this period additional radiological decay may occur as described by

$$C(T_c) = C(T_h)\cdot\exp(-\lambda_r\cdot T_p\cdot 86400)\,, \tag{14.10}$$

where

$C(T_c)$ = plant concentration at the beginning of the consumption period (Ci/kg),

T_c = time after initial deposition when consumption begins (d),

T_p = time between harvest and start of consumption (d).

For some crops, the consumption period may last for weeks or months. To estimate uptake during this period, it is assumed that consumption is at a uniform rate. The total intake is then given by a time integral over the consumption period

$$I(T_f) = \int_{T_c}^{T_c+T_f} C(T_c)\cdot U\cdot\exp(-\lambda_r\cdot t)\,dt \tag{14.11}$$

or

$$I(T_f) = U\cdot C(T_c)\cdot[1-exp(-\lambda_r\cdot T_f\cdot 86{,}400)]/(\lambda_r\cdot 86{,}400)\,, \tag{14.12}$$

where

$I(T_f)$ = total activity of a radionuclide ingested over a consumption period T_f (Ci),

T_f = length of consumption period (d),

U = average daily intake rate of crop over the consumption period (kg/d).

The radiation dose received by a person ingesting this amount of activity can be found using appropriate ingestion dose conversion factors for the given radionuclide.

The model defined by Eq. 14.12 is for describing ingestion of food crops. To extend it for use with animal products, the animal is assumed to eat contaminated crops and produce contaminated products continuously over the consumption period defined for humans. The delay time between harvest and consumption may be extended slightly to account for holdup within the animal. The animal product concentration at the time of consumption is then given by

$$C_a(T_c) = C(T_h)\cdot B\cdot U\cdot exp(-\lambda_r\cdot T_a\cdot 86{,}400)\,, \tag{14.13}$$

where

$C_a(T_c)$ = concentration in animal product at the start of the consumption period (Ci/kg),

B = bioaccumulation factor for the radionuclide and animal product of interest (Ci/kg per Ci/d ingested),

T_a = delay time in animal product production (d),

U = ingestion rate of food crop by animal (kg/d).

The animal product concentration is used in Eq. 14.12 to estimate the total radionuclide intake by an individual consuming the particular animal product. As mentioned above, this model can be used only for animal products wherein the radionuclide concentration within the animal comes to rapid equilibrium, such as for milk and eggs. For meat-type animal products, the long-term bioaccumulation factors do not adequately represent the acute transfer of radionuclides from feed to animal product.

14.2.4.2 Nutrient-Contaminant Plant Accumulation Model

Transport of contaminants from the soil via root uptake to edible parts of the plant can be overestimated in some cases if the plant concentration is based strictly on equilibrium bioaccumulation factors. The model described in this section is presented as an example of a dynamic plant growth model used to estimate the time dependence of plant root uptake.

Cowan et al. (1981) have developed a model based on known plant physiological processes to describe uptake of a contaminant through the plant nutrient transport system. The model was exercised using experimental data on plutonium uptake by soybean plants. The model considers four plant components: roots, stems, branches, leaves, and reproductive parts (edible portions such as seeds). Two parallel submodels are used. First, there is a biomass submodel that describes the growth of each plant component during the growing season. The logistic growth equations (sigmoid shaped) are based on data collected for soybeans grown in the split root system described by Garland et al.* The second submodel describes the nutrient transport and accumulation in each plant component. This submodel uses a set of linear differential equations with time invariant coefficients.

The model was exercised by Cowan et al. (1982) to study the effect of varying the time of contamination with respect to the growing season. The soybean matures in approximately 95 d. By assuming that soil contamination occurred at several different times, they found that the contamination level in

*Garland, T. R., Cataldo, D. A., and Wildung, R. E. 1981. Unpublished data.

seeds was nearly constant except when contamination occurred very late in the growing season. This implies that use of equilibrium bioaccumulation values may be adequate, provided contamination occurs before the beginning of seed development. When contamination of soil occurs after seed development has begun, the contamination level in seeds at harvest may be significantly below the equilibrium value.

14.2.4.3 Compartmental Food Chain Model

An estimate of radionuclide transport to man via the terrestrial food chain, for processes not properly described by equilibrium models, can be made using transient behavior compartment models such as the TERMOD (Booth et al. 1971; Killough and McKay 1976) or the RAGTIME (Pleasant et al. 1980) computer programs. These models describe the various segments of the food chain as compartments that exhibit exponential uptake and clearance.

RAGTIME is written in FORTRAN IV and estimates crop, beef, and milk contamination from radionuclide deposition. Pathways include deposition on above-ground crops and pasture grass and the soil surface, with ingrowth of daughters also calculated. Input may be prescribed as a step function for each radionuclide in the chain. Deposition is specified as time-dependent interception fractions for food crops; pasture grass or soil interception may also be specified as time-dependent. Emergence and harvest times of crops are explicitly considered. Total radioactivity moving through the system is estimated via discrete-variable numerical integration; the total estimates are verified by solution of the Bateman equations.

14.2.5 Example Problems

Example 14.1. A unit of radioactivity is accidentally released from the building vent of a BWR under atmospheric stability category F and a wind speed of 2 m/s. The cross-sectional area of the building is 2000 m^2. What is the diffusion factor (χ/Q) at 100 m, 500 m, and 1000 m downwind of this BWR?

Solution. Since this release is from a building vent, it is considered to be a ground-level release for calculational purposes (Sect. 14.2.2). Since the release occurs under stable conditions with a wind speed of less than 6 m/s, Eqs. 14.2, 14.3, and 14.4 must be used in the calculation. For a downwind distance of 100 m,

$$\begin{aligned} \sigma_y &= 4 \text{ m (Fig. 14.1)}, \\ \sigma_z &= 2.4 \text{ m (Fig. 14.2)}, \\ \bar{u}_{10} &= 2 \text{ m/s}, \\ M &= 4 \text{ (Fig. 14.3)}, \\ \Sigma_y &= M\sigma_y = 16 \text{ m}, \\ A &= 2000 \text{ m}^2. \end{aligned}$$

Using these values,

$$\chi/Q = \frac{1}{\bar{u}_{10}(\pi\sigma_y\sigma_z + A/2)}$$

$$= \frac{1}{(2\text{ m/s})[\pi(4\text{ m})(2.4\text{ m}) + (2000\text{ m}^2/2)]}$$

$$= 4.9\times10^{-4}\text{ s/m}^3,$$

$$\chi/Q = \frac{1}{\bar{u}_{10}(3\pi\sigma_y\sigma_z)}$$

$$= \frac{1}{(2\text{ m/s})[(0.3)(\pi)(4\text{ m})(2.4\text{ m})]}$$

$$= 5.5\times10^{-3}\text{ s/m}^3,$$

$$\chi/Q = \frac{1}{\bar{u}_{10}\pi\Sigma_y\sigma_z}$$

$$= \frac{1}{(2\text{ m/s})[(\pi)(16\text{ m})(2.4\text{ m})]}$$

$$= 4.1\times10^{-3}\text{ s/m}^3.$$

Comparing these values in the prescribed manner results in the selection of the value from Eq. 14.4—$\chi/Q = 4.1 \times 10^{-3}$ s/m^3. Similar calculations for 500 m and 1000 m will yield the additional values shown below.

Quantity	Downwind distance		
	100 m	500 m	1000 m
σ_y (Fig. 14.1)	4 m	20 m	40 m
σ_z (Fig. 14.2)	2.4 m	8 m	14 m
M (Fig. 14.3)	4	4	4
Σ_y	16 m	80 m	130 m

	Calculated χ/Q values for three downwind distances		
	100 m	500 m	1000 m
Eq. 14.2	4.9×10^{-4} s/m^3	3.3×10^{-4} s/m^3	1.8×10^{-4} s/m^3
Eq. 14.3	5.5×10^{-3} s/m^3	3.3×10^{-4} s/m^3	9.5×10^{-5} s/m^3
Eq. 14.4	4.1×10^{-3} s/m^3	2.5×10^{-4} s/m^3	8.7×10^{-5} s/m^3
Selected χ/Q	4.1×10^{-3} s/m^3	2.5×10^{-4} s/m^3	8.7×10^{-5} s/m^3

Example 14.2. If the release considered in Example 14.1 occurs under stability category D instead of category F, what would be the χ/Q at 100 m?

Solution. Again, for a downwind distance of 100 m,

$$\begin{aligned} \sigma_y &= 8 \text{ m (Fig. 14.1)}, \\ \sigma_z &= 5 \text{ m (Fig. 14.2)}, \\ \bar{u}_{10} &= 2 \text{ m/s}, \\ M &= 2, \\ \Sigma_y &= M\sigma_y = 16 \text{ m}, \\ A &= 2000 \text{ m}^2. \end{aligned}$$

Using these values, Eq. 14.2 = 4.4×10^{-4} s/m^3, Eq. 14.3 = 1.3×10^{-3} s/m^3, and Eq. 14.4 = 2.0×10^{-2} s/m^3; selected $\chi/Q = 1.3 \times 10^{-3}$ s/m^3.

Note that under these release conditions, Eq. 14.3 is used to calculate the selected value of χ/Q instead of Eq. 14.4, as was the case under the original release conditions.

Example 14.3. If the release considered in Example 14.1 occurs under stability category A, what would be the χ/Q at 100 m?

Solution. Since this release now occurs under unstable conditions, Eq. 14.1 is used in the calculation:

$$\bar{u} = 2 \text{ m/s},$$

$$\sigma_y = 24 \text{ m (Fig. 14.1)},$$

$$\sigma_z = 17 \text{ m (Fig. 14.2)},$$

$$\frac{\chi}{Q} = \frac{1}{\pi \bar{u} \sigma_y \sigma_z}$$

$$= \frac{1}{\pi(2 \text{ m/s})(24 \text{ m})(17 \text{ m})}$$

$$= 3.9 \times 10^{-4} \text{ s/m}^3.$$

Example 14.4. A unit of radioactivity is accidentally released from a 100-m-tall stack of a BWR under stability category F and a wind speed of 5 m/s. Assuming nonfumigation conditions, what is the diffusion factor (χ/Q) 3000 m downwind if the receptor is located 30 m above plant grade?

Solution. Applying Eq. 14.6 to this problem,

$\bar{u}_h = 5$ m/s,
$\sigma_y = 100$ m (Fig. 14.1),
$\sigma_z = 280$ m (Fig. 14.2),
$h_s = 100$ m,
$h_t = 30$ m,
$h_e = h_s - h_t = 100\text{ m} - 30\text{ m} = 70\text{ m}$.

$$\chi/Q = \frac{1}{\pi \bar{u}_h \sigma_y \sigma_z} \exp(-h_e^2/2\sigma_z^2)$$

$$= \frac{1}{\pi(5\text{ m/s})(100\text{ m})(280\text{ m})} \exp\left[\frac{-(70\text{ m})^2}{2(280\text{ m})^2}\right]$$

$$= 2.2\times10^{-6}\text{ s/m}^3.$$

Example 14.5. Assume that the release considered in Example 14.4 occurs under fumigation conditions. If a wind speed of 2 m/s is representive of the fumigation depth, what is now the χ/Q at the same receptor?

Solution. Applying Eq. 14.7 to this revised problem,

$\bar{u}_h = 2$ m/s,
$\sigma_y = 100$ m (Fig. 14.1),
$h_e = 70$ m (from Example 14.4).

$$\chi/Q = \frac{1}{(2\pi)^{1/2}\bar{u}_h \sigma_y h_e}$$

$$= \frac{1}{(2\pi)^{1/2}(2\text{ m/s})(100\text{ m})(70\text{ m})}$$

$$= 2.8\times10^{-5}\text{ s/m}^3.$$

Note that, as expected, the diffusion factor calculated here is larger than the value calculated in Example 14.4 for nonfumigation conditions.

14.3 INFORMATION NEEDS IN EMERGENCY PLANNING

Emergency planning is intended to ensure timely and efficient response by the reactor operator and government organizations to mitigate the potential consequences of a reactor accident. To this end, the following actions must be taken:

- A plan outlining responsibilites, duties, and actions for the major response organizations must be prepared.
- Each organization must fully implement the plan.
- The plan must be periodically tested, critiqued, and improved as feasible.

The operating organization is responsible for detecting an incident with potential for off-site consequences, assessing or classifying its significance, notifying the proper authorities of the reactor's condition, analyzing potential or actual off-site impacts, and recommending appropriate actions. Off-site authorities must make decisions regarding protective actions, notification of the public, and implementation of protective actions and must assist in environmental monitoring.

A typical progression might be as follows: Following an incident, initial notification to the authorities will be made by the senior reactor operator or supervisor. Available data will initially consist of plant status parameters and meteorological data. Simple dose calculations, based on available χ/Q values, could be employed using actual release data or estimates of potential release magnitudes. A recent USNRC report (Pasciak et al. 1983) presents a set of dose-calculation nomograms suitable for such application. Environmental survey data may or may not be initially available.

The reactor supervisor, however, must use the available information to classify the incident as having potential off-site consequences and recommend protective action to be taken. The government authorities must make decisions based on this preliminary information. The following data should be transmitted to permit informed decision-making by off-site authorities: (1) description of the accident, (2) status of releases, (3) status of the plant and safety systems, (4) projected dose via air and amount of time until a protective action level is reached, (5) meteorological data, (6) emergency operations in progress, and (7) recommended protective actions. These data must be periodically updated and expanded to include environmental monitoring results when available.

If the incident is potentially significant, the operator and the authorities will activate their emergency organizations. Within 2 to 3 h, a large body of environmental measurements, dose predictions, and engineering analyses should be available. This subsequent information will be used to refine the initial estimates and recommendations.

It is clear that engineering data, dose projections, and environmental measurements are not substituted for each other. Rather, they constitute a

body of information that must be analyzed competently and combined skillfully to produce the most accurate picture of the status of the reactor, the potential off-site impact, and the need for protective actions. Emergency planning must emphasize the fact that protective actions require time for implementation and that criteria for decisions should be based on the type of information that will be available at the time when a decision is necessary. Protective actions are possible only if early warnings and decisions are possible.

Various factors contribute to uncertainties in the information provided by the operator to outside authorities and in the methodologies employed by both the operator and outside authorities to estimate consequences. In the remainder of this section, we will consider the major sources of uncertainty impacting the accident situation and recommend methods by which these uncertainties may be reduced in practice.

Two possible situations may exist at a reactor site during an emergency condition: (1) an accident sequence with no immediate release of radionuclides to the environment or (2) an accident sequence followed immediately (within minutes) by measurable release of radioactivity.

For a category 1 sequence, the major source of uncertainty influencing the accuracy of consequence estimates involves predicting and measuring the quantity and type of radionuclides to be released (if any). Due to problems in measuring types and quantities of radionuclides released from the core into the containment and in distinguishing between plated-out materials vs suspended materials (available for release), engineering estimates of the material potentially capable of release may be in error by many orders of magnitude. Decisions to evacuate or shelter populations would be dominantly affected by these uncertainties.

For a category 2 sequence, immediate releases can be measured both on- and off-site as the radioactive plume disperses. Therefore, the radionuclide release rate estimates will be subject to far less uncertainty than for category 1 situations. In this case, atmospheric dispersion modeling will most greatly influence uncertainties in predicted population exposure rates.

The above information may be employed under three very different sets of conditions:

1. before release, to forecast dose rates, time remaining until protective action levels would be exceeded, location of maximum dose rates and doses, regions of interest in terms of preparation for monitoring activities, etc.;
2. during release, to estimate impacts on the public and to provide direction for surveillance and evacuation/sheltering responses;
3. after release, to define regions of potential contamination to focus monitoring and interdiction plans.

14.4 MONITORING REQUIREMENTS

Data concerning the characteristics of potential and actual releases of radionuclides are needed to determine emergency action levels, to recommend protective action, and to identify critical exposure modes. Although models used for transport predictions and dose projections can approximate some of this information, measured data based on environmental monitoring must also be considered in the overall evaluation. At a minimum, monitoring results can be used to verify that a release has occurred, provide data for input to analytic models, and define affected areas. Measured data can also be used to calibrate calculated results and estimate hazards to the public. The required information can be obtained by monitoring geophysical and radiological characteristics of the environment.

Effective evaluation of reported information and coordination of monitoring activities require the establishment of a facility staffed by personnel capable of directing field operations and interpreting analytic and measured results. This facility must have reliable communications capability to primary and backup monitoring personnel, emergency directors, laboratory facilities, transportation agencies, and weather services. Required equipment includes computers or calculators necessary to implement analytic models, area maps with coordinates corresponding to those used by field personnel, geophysical monitoring equipment, and technical reference data. The coordination and evaluation facility must be located in an area where the probability of evacuation is low.

14.4.1 Geophysical Monitoring

The most important geophysical parameters used to describe release characteristics are related to meteorological conditions—wind speed, wind direction, variability, and weather conditions. Nuclear facilities should have a primary measurement system that records current and historical local wind data. This information is required to predict atmospheric dispersion properties of the release and to make field assignments for radiological monitoring teams. Smoke bombs or other visible tracers can also be used to follow atmospheric effluent transport in the atmosphere. Existing and forecast weather conditions, which can affect radioactive material dispersion and deposition, can be obtained by direct observation and contact with local weather service agencies. These agencies could also be used to replace meteorological measurement systems in the event of primary instrumentation failure.

Other geophysical parameters that require monitoring are related to seismic and various catastrophic events that could initiate or complicate accident conditions. Seismic monitoring to detect earthquakes or massive landslides can be performed at local university or government facilities. These facilities should have direct communication capability with emergency

coordination and evaluation centers. Other catastrophic events that require monitoring are fires or explosions. These events may initiate radiological accident conditions, provide driving forces for atmospheric releases of radioactive effluents, or cause loss of containment integrity.

14.4.2 Radiological Monitoring

Although radiological measurements are not prerequisites for classifying an emergency, they are important for verifying that a release has occurred, providing input for analytic models, estimating the hazards associated with various exposure pathways, and determining mitigating measures. Information concerning the release can be obtained by monitoring in-plant and environmental conditions using fixed or portable equipment. Fixed instruments include devices that provide continuous indication or time integral measurement of radiological parameters. Portable equipment includes sampling devices, radiation survey instruments, and associated analysis and power systems.

14.4.3 In-Plant Monitoring

Radiological conditions inside the plant can be monitored by fixed instruments located in the containment and in the atmospheric release (stack) and liquid effluent release systems. The quantity of noble gases available for release can be estimated using measured radiation levels obtained from detectors, such as ionization chambers, inside the containment. These detectors must be positioned in such a way that the sensitive regions are not shielded by physical protrusions and the ensemble of instruments monitors all critical areas of the containment. To minimize contributions from fission products in the reactor core, the detectors must be shielded from the core by the biological shield. The effective measurement range of the survey instruments must extend over about seven orders of magnitude, and the detectors must be able to withstand the extremes of temperature and humidity associated with the particular monitoring locations in the containment structure. Indication of airborne contamination can be obtained using fixed monitors that continuously sample air inside the containment. Structural integrity can be monitored by measuring pressure and penetration status (isolation, relief valve position, etc.) inside the building.

In addition to radiological instrumentation inside the containment structure, atmospheric and liquid effluent release pathways must be continuously monitored using fixed equipment. Continuous air monitors can be used to measure the levels of radioactive iodine and airborne particulates and iodines released through stack or other plant vents. Particulate activity can be measured using standard air filters, while iodine detection requires charcoal or silver-activated filters. Monitoring of liquid effluent activity requires installa-

tion of fixed radiation detectors, which must be effectively protected from moisture or temperature influences.

The data obtained from containment and effluent monitoring can be used to estimate releases and projected radiological hazards. Estimation of these release parameters requires the previous development, by facility personnel, of correlations between measured radiation levels based on fixed in-plant instrumentation and the types, quantity, and form of materials available for release. To facilitate accident characterization and protective action decisions, the relationships between effluent monitor readings and resulting personnel exposures and contamination must also be developed for various meteorological conditions. Evaluation personnel must be familiar with these correlations and must be able to modify existing data to account for actual accident or geophysical characteristics.

14.4.4 Environmental Monitoring

Depending on the nature of the release, both short-term and long-term environmental monitoring may be necessary. Short-term measurements, which are performed by emergency personnel during the period of initial emergency response, are primarily aimed at providing input for analytic models and data for determining appropriate action levels and mitigating measures. Long-term monitoring is generally conducted by support or consulting personnel after the release is terminated and is performed to provide detailed analyses of radiological hazards and accident consequences.

Initial environmental measurements are made by facility emergency response personnel using portable instruments at locations assigned by a central coordinating facility. These persons are usually organized as teams whose members must be capable of performing required radiological surveys, calibrating and operating instrumentation, and transporting the portable equipment. Each team must be capable of communicating with the coordinating facility and must have independent transportation. Teams must also have local maps with the same coordinates used by evaluation personnel to ensure proper correlation of measured data with monitoring locations.

For airborne releases, measurements to be made by initial environmental monitoring teams include dose rate in air, airborne particulate activity, and airborne iodine activity. Dose rate can be measured using a standard radiation survey detector (movable window ionization detector) held at waist height. This measurement provides an indication of the radiological hazard resulting from whole-body exposure to external gamma rays from immersion in the plume and from ground contamination. These data can be correlated with atmospheric transport predictions based on analytic models, meteorological conditions, and in-plant monitoring information. Airborne particulate activity can be measured using high-volume, high-efficiency filtered or impact air

samplers. Particulate samples can be evaluated in the field for alpha and beta-gamma activity using standard survey meters. Care must be taken to note the time and place of sample collection, to accurately determine the volume of sampled air, to evaluate the sample medium in a low-background area, and to ensure that the medium is not contaminated prior to evaluation. Airborne iodine activity should be measured using air samplers with silver-activated filters as previously described. Sampling media with low affinities for other airborne radioactive elements (such as xenon) must be used to preclude erroneous indications of high iodine activity. The portable instruments used to make these measurements must be frequently calibrated and carefully packaged and transported to ensure proper operation and to avoid mechanical shock. Field and facility evaluation personnel must be familiar with local background radiation.

Fixed instruments used for airborne environmental monitoring include passive dosimeters (thermoluminescent or film), airborne particulate filters, and iodine absorber cannisters, which measure the time integral of direct radiation dose or airborne activity. Passive dosimeters can be mounted at fixed locations around the facility and periodically collected to determine direct radiation doses accumulated over the exposure period. Continuous air and iodine monitors can be placed at effluent release locations at the facility and at fixed positions in the surrounding environment. Following an accidental release of radionuclides, the fixed monitors should be collected and returned to a laboratory for analysis to verify the existence of an abnormal situation and to estimate integral dose commitments.

To define the spatial extent and magnitude contours of a radiation field resulting from an atmospheric release, ground-level measurements can be supplemented by aerial surveys performed with a helicopter or fixed-wing aircraft. The former aircraft is preferred because it can operate close to the ground where standard portable instruments can be used to detect effects from both airborne and deposited contaminants. Above a height of approximately 200 m, radiation levels from significant ground deposits may be of the same order of magnitude as variations in count rate attributable to different geological formations. High-sensitivity detectors, such as large inorganic crystal scintillators, provide adequate monitoring capability for airborne surveys of ground contamination. Monitoring personnel must have communications capability with coordinating facilities and maps with coordinates consistent with those used by evaluation personnel.

In the event of a liquid effluent release, hydrological monitoring may be necessary to determine activities of fission products and other beta-gamma emitters in rivers, lakes, or reservoirs. A rapid field estimate of radionuclide activity can be obtained by immersing the probe of a beta-gamma survey instrument into a sample of the liquid. The probe must be wrapped in a very thin waterproof covering to prevent damage or contamination. Surveys to

determine plume magnitude contours and local radionuclide activity for large bodies of water can be taken from a boat using portable equipment. These rapid field estimates must be augmented by detailed laboratory analysis of periodic effluent samples (usually 1-L samples). This analysis is particularly important if alpha emitters are present among the contaminants. Fixed continuous monitoring equipment at liquid effluent release locations can provide initial indications of high beta-gamma activity.

Long-term environmental monitoring requirements depend on the characteristics of the radionuclide release. For atmospheric releases, long-term monitoring involves measurement of activities in soil, vegetation, milk, food, and water samples taken periodically until no radiological hazard is indicated. Periodic measurements of air and ground contamination must also be conducted if these transport pathways are associated with the release. Evaluation and performance of long-term measurements requires establishing sample collection points, maintaining laboratory facilities, and staffing the field monitoring teams for potentially long periods of time. To properly interpret measured data, evaluators must be familiar with the normal levels of background radiation for the monitoring locations prior to the release. Thus, routine environmental monitoring must be performed periodically to determine normal radioactivity levels associated with the local area.

Laboratory facilities to analyze environmental samples should include a gamma ray spectrometer for identification of individual radionuclides. With this instrument the composite spectrum of gamma energy emission from a radioactive sample can be analyzed to determine contributor isotopes and associated activities. Portable spectrometers are also available for field analysis in areas of low background radiation.

14.4.5 Personnel Monitoring

Monitoring of emergency personnel can provide indications of ingested radionuclides and estimates of resulting dose commitments. Applicable measurement techniques include whole-body counting and bioassay, which can be performed at local laboratory or hospital facilities. Emergency personnel must also be monitored for direct radiation exposure and transferable contamination. Direct exposure can be measured using passive personnel dosimeters such as thermoluminescent materials or film badges and direct-reading devices, such as ionization chambers or electronic devices. Personnel should be surveyed for transferable alpha and beta-gamma contamination using standard monitoring methods in low-background areas that are certified to be free of radioactive contaminants. When performing field measurements, emergency personnel should take appropriate protective action such as wearing shoe covers, anticontamination clothing, and filtered respirators to minimize potential radiological hazards, where appropriate. Potassium iodide should be available in case of need.

14.5 PROBLEMS

1. A reactor building is 50 m high and 30 m wide. An accidental release occurs from a stack located 70 m above plant grade on the top of the reactor building under stability category D with a wind speed of 3 m/s. What is the ground-level value of χ/Q 800 m downwind of this plant?

2. Assume that the release considered in problem 1 occurs from a stack 150 m above plant grade. What is now the χ/Q value at the same receptor point, assuming nonfumigation conditions?

REFERENCES

Bass, A., and Smith, D. G. 1981. *Atmospheric Dispersing Modeling for Emergency Preparedness,* AIF/NESP-022, Atomic Industrial Forum, Washington, D.C.

Booth, R. S., Kaye, S. V., and Rohwer, P. S. 1971. "A Systems Analysis Methodology for Predicting Dose to Man from a Radioactively Contaminated Terrestrial Environment," in *Proceedings of the Third Symposium on Radioecology,* AEC-CONF-710501, U.S. Atomic Energy Commission.

Cowan, C. E., Jenne, E. A., Simpson, J. C., and Cataldo, D. A. 1982. "Nutrient Contaminant (Pu) Plant Accumulation Model," in *Biological Availability of Trace Metals,* CONF-811035, Elsevier, Amsterdam.

Engelmann, R. J. 1968. "The Calculation of Precipitation Scavenging," pp. 208–21 in *Meteorology and Atomic Energy—1968,* TID-24190, ed. D. Slade, Tech. Inf. Center, U.S. Department of Energy, Oak Ridge, Tenn.

Gifford, F. A., Jr. 1968. "An Outline of Theories of Diffusion in the Lower Atmosphere," Chap. 3 in *Meteorology and Atomic Energy—1968,* TID-24190, ed. D. Slade, Tech. Inf. Center, U.S. Department of Energy, Oak Ridge, Tenn.

International Atomic Energy Agency (IAEA) 1966. *Environmental Monitoring in Emergency Situations,* IAEA Safety Series No. 18, Vienna.

International Atomic Energy Agency (IAEA) 1974. *Evaluation of Radiation Emergencies and Accidents,* IAEA Safety Series No. 152, Vienna.

Killough, G. G., and McKay, L. R. 1976. *A Methodology for Calculating Radiation Doses from Radioactivity Released to the Environment,* ORNL-4992, Union Carbide Corp., Nuclear Div., Oak Ridge Natl. Lab., Oak Ridge, Tenn.

Los Alamos Scientific Laboratory 1958. *Los Alamos Handbook of Radiation Monitoring,* LA-1835, Los Alamos, N. Mex.

Miller, C. W. 1981. "Comparison of Methods for Predicting Air Concentrations Near Reactor Complexes," *Trans. Am. Nucl. Soc.* **39,** 125–26.

Napier, B. A., Kennedy, W. E., Jr., and Soldat, J. K. 1980. *PABLM—A Computer Program to Calculate Accumulated Radiation Doses from Radionuclides in the Environment,* PNL-3209, Pacific Northwest Lab., Richland, Wash.

Pasciak, W. J., Fairobent, L. A., Wangler, M. E., and Mo, T. 1983. *Nomograms for Evaluation of Doses from Finite Noble Gas Clouds,* NUREG-0851, USNRC, Washington, D.C.

Pleasant, J. C., McDowell-Boyer, L. M., and Killough, G. G. 1980. *RAGTIME: A FORTRAN IV Implementation of a Time-Dependent Model for Radionuclides in Agricultural Systems—First Progress Report,* NUREG/CR-1196, USNRC, Washington, D.C.

Sehmel, G. A. 1980. "Particle and Gas Dry Deposition: A Review," *Atmos. Environ.* **14,** 983–1011.

Smith, W. J. II, Whicker, F. W., and Meyer, H. R. 1982. "A Review and Categorization of Saltation, Suspension and Resuspension Models," *Nucl. Saf.* **23**(6).

Start, G. E., Cate, J. H., Dickson, C. R., Ricks, N. R., Ackerman, G. R., and Sagendorf, J. F. 1978. *Rancho Seco Building Wake Effects on Atmospheric Diffusion,* NUREG/CR-0456.

Strenge, D. L. 1980. *Models Selected for Calculation of Doses, Health Effects and Economic Costs Due to Accidental Radionuclide Releases from Nuclear Power Plants,* NUREG/CR-1021, PNL-3108, Pacific Northwest Lab., Richland, Wash.

Strenge, D. L., Soldat, J. K., and Watson, E. C. 1978. *A Review of Methodology for Accident Consequence Assessment,* NUREG/CR-0545, PNL-2633, Pacific Northwest Lab., Richland, Wash.

U.S. Atomic Energy Commission (USAEC) 1973. *Assumptions Used for Evaluating the Potential Radiological Consequences of a Loss-of-Coolant Accident for Boiling-Water Reactors,* Regulatory Guide 1.3.

U.S. Atomic Energy Commission (USAEC) 1974. *Assumptions Used for Evaluating the Potential Radiological Consequences of a Loss-of-Coolant Accident for Pressurized-Water Reactors,* Regulatory Guide 1.4.

U.S. Environmental Protection Agency (USEPA) 1980. *Manual of Protective Action Guides and Protection Actions for Nuclear Accidents,* EPA-520/1-75-001, rev.

U.S. Nuclear Regulatory Commission (USNRC) 1975. *Reactor Safety Study, Appendix VI—Calculation of Reactor Accident Consequences,* WASH-1400.

U.S. Nuclear Regulatory Commission (USNRC) 1977. *Methods for Estimating Atmospheric Transport and Dispersion of Gaseous Effluents in Routine Releases from Light-Water-Cooled Reactors,* Regulatory Guide 1.111, rev. 1.

U.S. Nuclear Regulatory Commission (USNRC) 1978. *Planning Basis for the Development of State and Local Government Radiological Emergency Response Plans in Support of Light-Water Nuclear Power Plants,* NUREG-0396.

U.S. Nuclear Regulatory Commission (USNRC) 1979a. *Atmospheric Dispersion Models for Potential Accident Consequence Assessments at Nuclear Power Plants,* Regulatory Guide 1.145.

U.S. Nuclear Regulatory Commission (USNRC) September 1979b. *Draft Emergency Action Level Guidelines for Nuclear Power Plants,* NUREG-0610.

U.S. Nuclear Regulatory Commission (USNRC) 1980. *Criteria for the Preparation and Evaluation of Radiological Emergency Response Plans and Preparedness in Support of Nuclear Power Plants,* NUREG-0654/FEMA-RFP-1, rev. 1.

U.S. Nuclear Regulatory Commission (USNRC) 1981a. *PRA Procedures Guide* (Draft), NUREG/CR-2300.

U.S. Nuclear Regulatory Commission (USNRC) 1981b. Proceedings of a Workshop on Meteorological Aspects of Emergency Response Plans for Nuclear Power Plants, Menlo Park, California, December 1–3, 1981; to be published.

Van der Hoven, I. 1968. "Deposition of Particles and Gases," pp. 202–8 in *Meteorology and Atomic Energy—1968,* TID-24190, ed. D. Slade, Tech. Inf. Center, U.S. Department of Energy, Oak Ridge, Tenn.

Glossary

Abiotic substances: Inorganic or organic, nonliving substances in the environment.

Absolute humidity: Vapor content of water in air expressed as g/m^3. A key parameter in the calculation of dose from tritium released to the atmosphere.

Absorbed dose: The energy deposited in matter by ionizing radiation per unit mass of irradiated material. The unit of absorbed dose is the rad [the SI unit is the gray (Gy), where 100 rad = 1 Gy].

Absorbed fraction: The ratio of the energy absorbed by a target organ to the energy emitted by a source organ (or region) within the body.

Acceptable degree of accuracy: The amount of error or uncertainty in model predictions tolerated for any given assessment situation. Usually, a greater degree of accuracy is required for potential outcomes involving high risks as well as economic costs.

Accuracy: As applied to environmental assessment models, accuracy implies agreement between the model prediction and actual events. An "accurate" model should be precise and unbiased. However, because of the stochastic nature of environmental processes, all deterministic models are inherently inaccurate.

Algorithm: An explicit step-by-step procedure for producing a solution to a given problem. In a computer model, an algorithm may be any statement or set of statements expressing the functional operation of a model which enables a set of inputs to produce a given output.

Aquifer: A formation (or group of formations) of water-bearing stratum that contains sufficient permeable rock, sand, or gravel to yield significant quantities of water to wells and springs.

As low as reasonably achievable (ALARA): A conceptual radiation exposure guideline with the intent to encourage protection practices that are better than any prescribed standard. This is the basic criterion for all cases in which a nonthreshold dose-effect relationship either exists or has to be assumed.

Batch mode: An older, traditional method of processing in which transactions are collected and prepared for computer input to process as a single unit.

Benthic: Relating to or occurring at the bottom of a body of water.

Bias: The tendency for an estimate to deviate from an actual or real event. Bias may be the tendency for a model to over- or underpredict.

Bioaccumulation factor: The ratio of radionuclide concentration in an organism to that in water.

Biosphere: That part of the earth which contains living organisms and in which ecosystems exist.

Buildup factor: The ratio of the intensity of X or gamma radiation (both primary and scattered) at a point in an absorbing medium to the intensity of only the primary radiation.

Cladding: A metal encasement surrounding the fuel in a nuclear reactor. The purpose of cladding is to provide a structure for the fuel material, to efficiently conduct the heat generated during fission away from the fuel, and to contain the fission products.

Collective dose equivalent: The sum of per capita dose equivalent for a given organ over the number of individuals exposed.

Committed dose equivalent: The dose equivalent that will be accumulated by a specific organ over a specified period (often 50 y) following intake.

Concentration ratio: Ratio of radionuclide activity per unit mass of plant to that in soil, often expressed on a dry-weight basis.

Conservative bias: Intentional bias toward dose overestimation.

Conversational mode: A computer code which prompts the user via questions. In response to the prompts, the user supplies instructions or data.

Default values: Parameter values that are used in radiological assessment models when site-specific values cannot be obtained.

Demineralizer bed: A mechanical component in a reactor system that selectively removes fission and activation products and other unwanted contaminants from the primary coolant. Demineralizers generally work on the principle of ion exchange, using a chemical resin bed to accumulate materials as they pass through.

Deposition velocity: An empirical rate constant that relates the concentration of a radionuclide in air to that on ground or plant surfaces.

Deterministic model: A model whose output is fixed by the mathematical form of its equations and the selection of a single value for each input parameter; nonstochastic model.

Diffusion category (stability classes): A category which describes an atmospheric turbulence condition in terms of boundary layer atmospheric stability. Diffusion categories are generally grouped into six classes, ranging from class A, very unstable, through class F, very stable.

Distribution coefficient: The quantity of radionuclide sorbed by a solid per unit weight of the solid, divided by the concentration of the radionuclide dissolved in water.

Documentation: Description of what a computer program does and how it does it, its assumptions, and its possible applications. An "owners' and operators' manual" for a program.

Dose equivalent: The quantity that expresses the effects of all radiations on a common scale for calculating the effective absorbed dose. It is defined as the product of the absorbed dose, the quality factor, and other modifying factors. The unit of dose equivalent is the rem [the SI unit is the sievert (Sv), where 100 rem = 1 Sv].

Dose equivalent commitment: The time integral of the per capita dose equivalent rate.

Dose reduction factor: The ratio of the dose rate inside a building to the corresponding dose rate outdoors.

Dry deposition: The process of deposition of airborne radioactive materials due to gravitational and surface processes.

Ecosystem: A basic functional unit in ecology. An area which includes living organisms and nonliving substances interacting to produce an exchange of materials and which is self-sustaining with the exception of energy.

Effective source height: A mathematical approximation of the height at which the source term is released to the atmosphere, taking into account the initial buoyancy and momentum created by the emission of radioactive gases at high temperature or velocity.

Error propagation: The translation of input errors into estimates associated with assessment modeling; in this context, statistical and numerical error propagation techniques are the fundamental methods used to combine parameter uncertainties into an estimate of the overall uncertainty in model predictions. This process is referred to in this book as "parameter uncertainty analysis."

External dose rate conversion factor: A factor which when multiplied by the radionuclide concentration in air or on a contaminated surface gives the dose rate from external sources to a specific organ in the body.

External dosimetry: Deals with the calculation of absorbed dose from radiation that originates outside the body.

Far field: That area where natural phenomena dominate in the groundwater transport of radionuclides.

Fission-product inventory: The quantity and type of fission products generated during reactor operation and contained in the core of the reactor. The fission-product inventory will increase as fuel burnup proceeds and can be estimated at any point in the life of a reactor if the power history is known.

Fracture flow: Groundwater flow through a fractured medium. The medium itself may be porous and permeable, but the flow would be dominated by fractures, cracks, or solution cavities.

Gaussian plume model: Commonly used mathematical model to predict atmospheric diffusion of particulates and gases. Based on assumptions of statistically "normal" or Gaussian plume dispersion, modified by empirical dispersion coefficients.

Genetic (hereditary) effects: Those effects of radiation that may be transmitted to the progeny of exposed individuals.

Hydraulic conductivity (permeability): The volume of water that will move per unit time under a unit gradient through a unit cross-sectional area perpendicular to the direction of flow.

Integrating exposure pathway: A pathway in which the radionuclide concentration increases with continuing release of materials into the environment and may persist beyond the cessation of these releases.

Internal dose rate conversion factor: A factor which when multiplied by the quantity of radionuclide ingested, inhaled, or injected gives the steady-state, or maximum internal dose rate to a specific organ of the body.

Intrinsic permeability: The measure of the ability of a rock or soil to transmit fluid under a fluid potential gradient (see **hydraulic conductivity**).

Maximum permissible dose: The dose which, in the light of present knowledge, carries a negligible probability of severe somatic or genetic injuries and such that any effects that occur more frequently are limited to those of a minor nature that would be considered acceptable by the exposed individual and by competent medical authority.

Model: A physical or mathematical representation of reality.

Model prediction: The result or dependent variable produced by a model calculation.

Model structure: The conceptual design, mathematical equations, and set of algorithms that control the results or predictions produced from a given set of input.

Model validation: Documentation of the difference between model predictions and actual events through comparison of predicted values with measured field data obtained over the range of conditions representing the extent of intended application of the model.

Model verification: An indication of whether or not a computer code accurately mimics a given model.

Near field: Region in which waste characteristics and repository phenomena dominate the transport of radionuclides in groundwater.

Nonstochastic effects: Health effects exhibiting a radiation dose threshold.

Nuclear fuel cycle: All aspects of the industry involved in the generation of electricity from nuclear energy, from mining of raw materials for fuel to disposal of nuclear waste. Those steps preceding power generation constitute the front end of the cycle.

Observed ratio: The ratio of the radionuclide:stable-element-concentration in one medium to the radionuclide:stable-element-concentration in a precursor pathway.

Parameter: Any one of a set of variables in a model whose values determine model predictions.

Parameter imprecision analysis: An analysis of uncertainty in deterministic models, using error propagation techniques to produce a stochastically variable prediction as a function of stochastically variable parameters.

Point isotropic specific absorbed fraction: The fraction of the energy emitted by a point isotropic source that is absorbed per gram at a distance from the source.

Porosity: Total porosity is expressed as the ratio of the volume of interstices to total volume.

Primary coolant: The liquid or gas that flows over the reactor core, removing heat generated during the fission process.

Quality factor: The linear-energy-transfer-dependent factor by which absorbed doses are multiplied to give dose equivalent.

Reference Man: A hypothetical individual whose characteristics are often used to estimate radiation dose. Reference Man is assumed to be 20—30 years of age, 170 cm in height, weighing 70 kg, and living in a climate with an average temperature of from 10° to 20°C. Reference man is a Caucasian and is Western European or North American in habitat and custom.

Relative risk: The ratio of risk from radiation in an irradiated population to the risk in a comparable nonirradiated population.

Research model: Any model developed to fulfill research objectives. Usually, research models are developed to provide insight into explicit processes and mechanisms and thus are mathematically more complex than assessment models.

Resuspension: Wind blown reintroduction to the atmosphere of material originally deposited onto surfaces from a particular source.

Retardation coefficient: A measure of the capability of porous media to impede the movement of a particular radionuclide being carried by the fluid.

Saturated zone: That portion of porous ground media in which the interconnecting interstices are filled with water.

Screening: The process of rapidly identifying potentially important radionuclides and exposure pathways by eliminating those of probable lesser significance.

Screening models: Simple models employing conservative assumptions, used to exclude radionuclides and exposure pathways of negligible importance.

Site-specific data: Data, collected for use in radiological assessment models, applicable to the particular location for which the assessment is being performed.

Soil-to-plant transfer factor: Ratio of radionuclide activity per unit mass of plant tissue to activity per unit mass of soil (often expressed on a wet-weight basis).

Somatic effects: Those effects of radiation that are expressed during the lifetime of an individual and are not passed along to future generations.

Sorption: In groundwater transport, interactions that cause radionuclides to migrate at a slower rate than the groundwater itself.

Source term: The quantity of radioactive material released to the biosphere, usually expressed as activity per unit time. Source terms should be characterized by the identification of specific radionuclides and their physical and chemical forms.

Specific absorbed fraction: Fraction of emitted energy E absorbed per gram of material at a distance from an isotropic point source.

Specific activity model: A model which estimates dose from a radionuclide by assuming that the specific activity in food or water is equal to that in air for a given location. This approach bypasses the steps normally used in radionuclide transport models; it is primarily applicable to radionuclides that have an abundant stable element carrier in nature, such as tritium/water and carbon-14/carbon dioxide.

Stability classes: See **diffusion category.**

Stochastic effects: Those health effects for which the probability of an occurrence, rather than the severity, is considered to be a function of dose without threshold.

Stochastic model: A model whose output is expressed as a range or distribution. Compare with deterministic model.

Tolerance dose: An early standard for radiation protection based upon the dose that could be "tolerated" without serious harm to humans.

Transfer coefficient to milk: The fraction of an element ingested daily by a cow that is secreted in milk at steady state or equilibrium.

Transfer coefficient to other animal products: The fraction of an element ingested daily by a herbivore that can be measured per unit mass of animal product at steady state or equilibrium.

Transitory exposure pathways: A pathway in which the radionuclide concentration is directly proportional to the rate of release of the radionuclide into the environment.

Unsaturated zone: The portion of porous media in the ground where the interconnecting interstices are only partially filled with fluid.

Washout coefficient: A measure of wet deposition per unit air concentration integrated over the entire height of the air column affected by washout.

Wet deposition: The deposition resulting from the scavenging of particles and gases by precipitation.

Index